

Advances in Experimental Medicine and Biology 1379

David Caballero
Subhas C. Kundu
Rui L. Reis *Editors*

Microfluidics and Biosensors in Cancer Research

Applications in Cancer Modeling and
Theranostics

 Springer

Advances in Experimental Medicine and Biology


Volume 1379

Series Editors

Wim E. Crusio, Institut de Neurosciences Cognitives et Intégratives d'Aquitaine, CNRS and University of Bordeaux, Pessac Cedex, France

Haidong Dong, Departments of Urology and Immunology, Mayo Clinic, Rochester, MN, USA

Heinfried H. Radeke, Institute of Pharmacology & Toxicology, Clinic of the Goethe University Frankfurt Main, Frankfurt am Main, Hessen, Germany

Nima Rezaei , Research Center for Immunodeficiencies, Children's Medical Center, Tehran University of Medical Sciences, Tehran, Iran

Ortrud Steinlein, Institute of Human Genetics, LMU University Hospital, Munich, Germany

Junjie Xiao, Cardiac Regeneration and Ageing Lab, Institute of Cardiovascular Science, School of Life Science, Shanghai University, Shanghai, China

Advances in Experimental Medicine and Biology provides a platform for scientific contributions in the main disciplines of the biomedicine and the life sciences. This series publishes thematic volumes on contemporary research in the areas of microbiology, immunology, neurosciences, biochemistry, biomedical engineering, genetics, physiology, and cancer research. Covering emerging topics and techniques in basic and clinical science, it brings together clinicians and researchers from various fields.

Advances in Experimental Medicine and Biology has been publishing exceptional works in the field for over 40 years, and is indexed in SCOPUS, Medline (PubMed), EMBASE, BIOSIS, Reaxys, EMBiology, the Chemical Abstracts Service (CAS), and Pathway Studio.

2020 Impact Factor: 2.622

David Caballero • Subhas C. Kundu •
Rui L. Reis
Editors

Microfluidics and Biosensors in Cancer Research

Applications in Cancer Modeling
and Theranostics

 Springer

Editors

David Caballero
3B's Research Group, I3Bs - Research
Institute on Biomaterials, Biodegradables
and Biomimetics at the University of
Minho, Headquarters of the European
Institute of Excellence on Tissue
Engineering and Regenerative Medicine
ICVS/3B's – PT Government Associate
Laboratory
Braga/Guimarães, Portugal

Subhas C. Kundu
3B's Research Group, I3Bs - Research Institute
on Biomaterials, Biodegradables and
Biomimetics at the University of Minho,
Headquarters of the European Institute of
Excellence on Tissue Engineering and
Regenerative Medicine
ICVS/3B's – PT Government Associate
Laboratory
Braga/Guimarães, Portugal

Rui L. Reis
3B's Research Group, I3Bs - Research
Institute on Biomaterials, Biodegradables
and Biomimetics at the University of
Minho, Headquarters of the European
Institute of Excellence on Tissue
Engineering and Regenerative Medicine
ICVS/3B's – PT Government Associate
Laboratory
Braga/Guimarães, Portugal

ISSN 0065-2598

ISSN 2214-8019 (electronic)

Advances in Experimental Medicine and Biology

ISBN 978-3-031-04038-2

ISBN 978-3-031-04039-9 (eBook)

<https://doi.org/10.1007/978-3-031-04039-9>

© The Editor(s) (if applicable) and The Author(s), under exclusive license to Springer Nature Switzerland AG 2022, corrected publication 2022

This work is subject to copyright. All rights are solely and exclusively licensed by the Publisher, whether the whole or part of the material is concerned, specifically the rights of translation, reprinting, reuse of illustrations, recitation, broadcasting, reproduction on microfilms or in any other physical way, and transmission or information storage and retrieval, electronic adaptation, computer software, or by similar or dissimilar methodology now known or hereafter developed.

The use of general descriptive names, registered names, trademarks, service marks, etc. in this publication does not imply, even in the absence of a specific statement, that such names are exempt from the relevant protective laws and regulations and therefore free for general use.

The publisher, the authors and the editors are safe to assume that the advice and information in this book are believed to be true and accurate at the date of publication. Neither the publisher nor the authors or the editors give a warranty, expressed or implied, with respect to the material contained herein or for any errors or omissions that may have been made. The publisher remains neutral with regard to jurisdictional claims in published maps and institutional affiliations.

This Springer imprint is published by the registered company Springer Nature Switzerland AG
The registered company address is: Gewerbestrasse 11, 6330 Cham, Switzerland

Preface

Microfluidics and biosensors have been massively utilized in biomedical research. During the last decade, they have reached a high degree of performance offering unprecedented opportunities for the investigation of pathophysiological processes and with an enormous potential to improve patient prognosis. As a result, the scientific community has adopted the use of microfluidic devices and analytical biosensing tools as a routine practice for their investigations. The synergistic combination of both technologies can provide revolutionary approaches in the clinic, particularly in the oncology field, where novel technologies and medical practices are always demanded. As such, biosensors-integrated microfluidic systems offer unique advantages in the area of cancer diagnosis and drug screening by providing accurate sensing tools for detecting the onset of the disease or realistic microenvironments for assessing the efficacy of drugs. Additionally, the high sophistication of this type of technology also enables their use for other applications, such as for developing advanced drug delivery systems or as innovative biofabrication tools, thus expanding the conventional range of applications of this type of technology. Therefore, microfluidics and biosensors can provide to physicians and researchers innovative tools and procedures for unraveling unknown mechanistic determinants of cancer dissemination or the mechanism of action of drugs, and for improving the discovery and screening of drugs in a rapid, efficient, and minimally-invasive manner. In this regard, this point-of-care technology can undoubtedly boost the field of personalized and precision cancer medicine leading to a new paradigm in cancer research.

This book focuses on the critical use of biosensors and microfluidics, either individually or in combination, to develop advanced lab-on-a-chip systems for cancer research applications. For this, we have gathered the contributions of world-recognized experts in cancer biology, microfluidics, nanotechnology, biosensors, biofabrication, and tissue engineering from academia, industry, and clinic, describing the latest developments, innovations, and applications on this area. Notably, the book includes looking-forward visions and opinions from experts about the future of this new generation of miniaturized diagnostic, screening, and biofabrication methods in oncology. Finally, we hope that this book will prove helpful in illustrating the potential of microfluidics and biosensors in cancer research as well as in other fields of study, and in particular, for designing new experiments to

answer some of the essential questions related to crucial mechanisms involved in cancer metastasis or the efficacy of drugs, among others.

Braga/Guimarães, Portugal
June 2022

David Caballero
Subhas C. Kundu
Rui L. Reis

Acknowledgments

The editors acknowledge the financial support from the FCT – Portuguese Foundation for Science and Technology (FCT) under the programs/projects CEECIND/00352/2017, PTDC/BTM-ORG/28070/2017, and PTDC/BTM-ORG/28168/2017 funded by the Programa Operacional Regional do Norte supported by European Regional Development Funds (ERDF). The editors also thank the financial support from the European Union Framework Program for Research and Innovation Horizon 2020 on FoReCaST project (668983), and the Institution of Engineering and Technology (IET) for the funding provided under the ENG The CANCER project.

Contents

Part I Fundamentals of Microfluidics and Biosensors

- 1 Fundamentals of Biosensors and Detection Methods** 3
Marília Barreiros dos Santos, Laura Rodriguez-Lorenzo,
Raquel Queirós, and Begoña Espiña
- 2 How to Get Away with Gradients** 31
Jordi Comelles, Óscar Castillo-Fernández, and Elena Martínez
- 3 Sensors and Biosensors in Organs-on-a-Chip Platforms** 55
Gerardo A. Lopez-Muñoz, Sheeza Mughal, and Javier Ramón-Azcón
- 4 Current Trends in Microfluidics and Biosensors for Cancer
Research Applications** 81
David Caballero, Rui L. Reis, and Subhas C. Kundu

Part II Modelling the Tumor Microenvironment and Its Dynamic Events

- 5 The Tumor Microenvironment: An Introduction to the
Development of Microfluidic Devices** 115
B. Kundu, D. Caballero, C. M. Abreu, R. L. Reis, and S. C. Kundu
- 6 Biomaterials for Mimicking and Modelling Tumor
Microenvironment** 139
Rupambika Das and Javier G. Fernandez
- 7 Advancing Tumor Microenvironment Research by Combining
Organs-on-Chips and Biosensors** 171
Isabel Calejo, Marcel Alexander Heinrich, Giorgia Zambito,
Laura Mezzanotte, Jai Prakash, and Liliana Moreira Teixeira
- 8 Microfluidic-Driven Biofabrication and the Engineering of
Cancer-Like Microenvironments** 205
Carlos F. Guimarães, Luca Gasperini, and Rui L. Reis

9	Advances in 3D Vascularized Tumor-on-a-Chip Technology	231
	Sangmin Jung, Hyeonsu Jo, Sujin Hyung, and Noo Li Jeon	
Part III Cancer Detection and Diagnosis		
10	Biosensors Advances: Contributions to Cancer Diagnostics and Treatment	259
	Ana I. Barbosa, Rita Rebelo, Rui L. Reis, and Vitor M. Correlo	
11	Flexible Sensing Systems for Cancer Diagnostics	275
	Anne K. Brooks, Sudesna Chakravarty, and Vamsi K. Yadavalli	
12	Coupling Micro-Physiological Systems and Biosensors for Improving Cancer Biomarkers Detection	307
	Virginia Brancato, Rui L. Reis, and Subhas C. Kundu	
13	Microfluidic Biosensor-Based Devices for Rapid Diagnosis and Effective Anti-cancer Therapeutic Monitoring for Breast Cancer Metastasis	319
	V. S. Sukanya and Subha Narayan Rath	
14	Liquid Biopsies: Flowing Biomarkers	341
	Vincent Hyenne, Jacky G. Goetz, and Naël Osmani	
15	From Exosomes to Circulating Tumor Cells: Using Microfluidics to Detect High Predictive Cancer Biomarkers	369
	Catarina M. Abreu, David Caballero, Subhas C. Kundu, and Rui L. Reis	
16	Microfluidics for the Isolation and Detection of Circulating Tumor Cells	389
	Jessica Sierra-Agudelo, Romen Rodriguez-Trujillo, and Josep Samitier	
17	Evolution in Automatized Detection of Cells: Advances in Magnetic Microcytometers for Cancer Cells	413
	Alexandre Chícharo, Diogo Miguel Caetano, Susana Cardoso, and Paulo Freitas	
18	Droplet-Based Microfluidic Chip Design, Fabrication, and Use for Ultrahigh-Throughput DNA Analysis and Quantification	445
	Stéphanie Baudrey, Roger Cubi, and Michael Ryckelynck	
19	Emerging Microfluidic and Biosensor Technologies for Improved Cancer Theranostics	461
	David Caballero, Catarina M. Abreu, Rui L. Reis, and Subhas C. Kundu	

Part IV Clinical Applications: Towards Personalized Medicine

20 Microfluidics for Cancer Biomarker Discovery, Research, and Clinical Application	499
Justina Žvirblytė and Linas Mažutis	
21 Methods for the Detection of Circulating Biomarkers in Cancer Patients	525
Patricia Mondelo-Macía, Ana María Rodríguez-Ces, María Mercedes Suárez-Cunqueiro, and Laura Muínelo Romay	
22 Advances in Microfluidics for the Implementation of Liquid Biopsy in Clinical Routine	553
Alexandra Teixeira, Adriana Carneiro, Paulina Piairol, Miguel Xavier, Alar Ainla, Cláudia Lopes, Maria Sousa-Silva, Armando Dias, Ana S. Martins, Carolina Rodrigues, Ricardo Pereira, Líliliana R. Pires, Sara Abalde-Cela, and Lorena Diéguez	
Correction to: Sensors and Biosensors in Organs-on-a-Chip Platforms	C1
Gerardo A. Lopez-Muñoz, Sheeza Mughal, and Javier Ramón-Azcón	

Editors and Contributors

About the Editors

David Caballero is an experienced biophysicist with a MSc and PhD in Nanoscience from the University of Barcelona (Spain). Currently, Dr. Caballero is a senior Assistant Researcher at the 3B's Research Group, I3Bs – Research Institute on Biomaterials, Biodegradables and Biomimetics from the University of Minho (Portugal) working in the field of *Physics of Cancer*. His research is focused on unraveling the mechano-chemical mechanisms of cancer dissemination. For this, Dr. Caballero is using microfluidics, microfabrication tools, and cutting-edge screening technologies for his experiments that are the interface between cell biology and physics.

Subhas C. Kundu received his PhD in Genetics from Banaras Hindu University (India). His area of interest includes biomaterials for 3D cancer modelling and drug screening. Currently, Prof. Kundu is a Research Coordinator at the 3B's Research Group, I3Bs – Research Institute on Biomaterials, Biodegradables and Biomimetics of the University of Minho, where he leads a multidisciplinary team dedicated to developing a new generation of predictive *in vitro* 3D tumor models using engineered biomaterials.

Rui L. Reis is the Dean/President of I3Bs – Research Institute for Biomaterials, Biodegradables and Biomimetics, founding Director of the 3B's Research Group at the University of Minho, Full Professor of Tissue Engineering, Regenerative Medicine, Biomaterials and Stem Cells, the CEO of the European Institute of Excellence on Tissue Engineering and Regenerative Medicine, and the Director of the PT Government Associate Laboratory ICVS/3Bs from the University of Minho (Portugal). Prof. Reis was awarded with the IET Harvey Engineering Research Prize to create reliable breakthrough 3D engineered functional cancer disease models for an improved prediction and efficacy of cancer drugs.

Contributors

Sara Abalde-Cela International Iberian Nanotechnology Laboratory, Braga, Portugal

Catarina M. Abreu 3B's Research Group, I3Bs - Research Institute on Biomaterials, Biodegradables and Biomimetics of University of Minho, Guimaraes, Portugal

LA ICVS/3B's, Braga, Portugal

Alar Ainla International Iberian Nanotechnology Laboratory, Braga, Portugal

Ana I. Barbosa 3B's Research Group, I3Bs – Research Institute on Biomaterials, Biodegradables and Biomimetics, University of Minho, Headquarters of the European Institute of Excellence on Tissue Engineering and Regenerative Medicine, Braga, Guimarães, Portugal

ICVS/3B's – PT Government Associate Laboratory, Braga/Guimarães, Portugal

Stéphanie Baudrey Université de Strasbourg, CNRS, Architecture et Réactivité de l'ARN, Strasbourg, France

Virginia Brancato 3B's Research Group, I3Bs - Research Institute on Biomaterials, Biodegradables and Biomimetics of University of Minho, Guimaraes, Portugal

LA ICVS/3B's, Braga, Portugal

Anne K. Brooks Department of Chemical and Life Science Engineering, Virginia Commonwealth University, Richmond, VA, USA

David Caballero 3B's Research Group, I3Bs - Research Institute on Biomaterials, Biodegradables and Biomimetics of University of Minho, Guimaraes, Portugal

LA ICVS/3B's, Braga, Portugal

Diogo Caetano Instituto de Engenharia de Sistemas e Computadores – Microsistemas e Nanotecnologias, INESC-MN, Lisbon, Portugal

Isabel Calejo Department of Developmental Bioengineering, Technical Medical Centre, University of Twente, Enschede, The Netherlands

Susana Cardoso Instituto de Engenharia de Sistemas e Computadores – Microsistemas e Nanotecnologias, INESC-MN, Lisbon, Portugal

Adriana Carneiro International Iberian Nanotechnology Laboratory, Braga, Portugal

IPO Experimental Pathology and Therapeutics Group, Research Center of IPO Porto (CI-IPOP)/RISE@CI-IPOP (Health Research Network); Portuguese Oncology Institute of Porto (IPO Porto)/Porto Comprehensive Cancer Center (Porto.CCC), Porto, Portugal

Óscar Castillo-Fernández Biomimetic Systems for Cell Engineering Laboratory, Institute for Bioengineering of Catalonia (IBEC), The Barcelona Institute of Science and Technology (BIST), Barcelona, Spain

Sudesna Chakravarty Department of Chemical and Life Science Engineering, Virginia Commonwealth University, Richmond, VA, USA

Alexandre Chicharo International Iberian Nanotechnology Laboratory, Braga, Portugal

Jordi Comelles Institute for Bioengineering of Catalonia, Barcelona, Spain

Vitor M. Correlo 3B's Research Group, I3Bs - Research Institute on Biomaterials, Biodegradables and Biomimetics of University of Minho., Guimaraes, Portugal
LA ICVS/3B's, Braga, Portugal

Roger Cubi Université de Strasbourg, CNRS, Architecture et Réactivité de l'ARN, Strasbourg, France

Rupambika Das The Francis Crick Institute, London, UK

Armando Dias International Iberian Nanotechnology Laboratory, Braga, Portugal
Escola de Ciências, Campus de Gualtar, Universidade do Minho, Braga, Portugal

Lorena Diéguez International Iberian Nanotechnology Laboratory, Braga, Portugal

Begoña Espiña INL, International Iberian Nanotechnology Laboratory, Braga, Portugal

Javier G. Fernandez Singapore University of Technology and Design, Singapore, Singapore

Paulo Freitas International Iberian Nanotechnology Laboratory, Braga, Portugal
Instituto de Engenharia de Sistemas e Computadores – Microsistemas e Nanotecnologias, INESC-MN, Lisbon, Portugal

Luca Gasperini 3B's Research Group, I3Bs – Research Institute on Biomaterials, Biodegradables and Biomimetics, University of Minho, Headquarters of the European Institute of Excellence on Tissue Engineering and Regenerative Medicine, Braga, Guimarães, Portugal
ICVS/3B's – PT Government Associate Laboratory, Braga/Guimarães, Portugal

Jacky G. Goetz INSERM UMR_S1109, Strasbourg, France
Université de Strasbourg, Strasbourg, France
Fédération de Médecine Translationnelle de Strasbourg, Strasbourg, France
Equipe Labellisée Ligue Contre le Cancer, Paris, France

Carlos Guimarães 3B's Research Group, I3Bs - Research Institute on Biomaterials, Biodegradables and Biomimetics of University of Minho, Guimaraes, Portugal
LA ICVS/3B's, Braga, Portugal

Marcel Alexander Heinrich Department of Advanced Organ Bioengineering and Therapeutics, Section: Engineered Therapeutics, Technical Medical Centre, University of Twente, Enschede, The Netherlands

Vincent Hyenne INSERM UMR_S1109, Strasbourg, France
Université de Strasbourg, Strasbourg, France
Fédération de Médecine Translationnelle de Strasbourg, Strasbourg, France
Equipe Labellisée Ligue Contre le Cancer, Paris, France
CNRS, SNC5055, Strasbourg, France

Sujin Hyung Innovative Institute for Precision Medicine, Samsung Medical Center, Seoul, South Korea

Noo Li Jeon Seoul National University, Seoul, South Korea

Hyeonsu Jo Innovative Institute for Precision Medicine, Samsung Medical Center, Seoul, South Korea

Sangmin Jung Innovative Institute for Precision Medicine, Samsung Medical Center, Seoul, South Korea

Banani Kundu 3B's Research Group, I3Bs - Research Institute on Biomaterials, Biodegradables and Biomimetics of University of Minho, Guimaraes, Portugal
LA ICVS/3B's, Braga, Portugal

Subhas C. Kundu 3B's Research Group, I3Bs - Research Institute on Biomaterials, Biodegradables and Biomimetics of University of Minho, Guimaraes, Portugal
LA ICVS/3B's, Braga, Portugal

Cláudia Lopes International Iberian Nanotechnology Laboratory, Braga, Portugal

Gerardo A. Lopez-Muñoz Institute for Bioengineering of Catalonia (IBEC), The Barcelona Institute of Science and Technology (BIST), Barcelona, Spain

Elena Martínez Biomimetic Systems for Cell Engineering Laboratory, Institute for Bioengineering of Catalonia (IBEC), The Barcelona Institute of Science and Technology (BIST), Barcelona, Spain
Department of Electronics and Biomedical Engineering, University of Barcelona (UB), Barcelona, Spain

Ana S. Martins International Iberian Nanotechnology Laboratory, Braga, Portugal
Escola de Ciências, Campus de Gualtar, Universidade do Minho, Braga, Portugal

Linus Mazutis Vilnius University, Vilnius, Lithuania

Laura Mezzanotte Department of Radiology and Nuclear Medicine, Erasmus Medical Center, Rotterdam, The Netherlands
Department of Molecular Genetics, Erasmus Medical Center, Rotterdam, The Netherlands

Patricia Mondelo-Macia Translational Medical Oncology Group (Oncomet), Health Research Foundation Institute of Santiago (IDIS), Complejo Hospitalario Universitario de Santiago de Compostela (SERGAS), Santiago de Compostela, Spain

Department of Surgery and Medical-Surgical Specialties, Medicine and Dentistry School Universidade de Santiago de Compostela (USC), Santiago de Compostela, Spain

Translational Medical Oncology Group (Oncomet), Health Research Foundation Institute of Santiago (IDIS), Complejo Hospitalario Universitario de Santiago de Compostela (SERGAS), Santiago de Compostela, Spain

Centro de Investigación Biomédica en Red en Cáncer (CIBERONC), Instituto de Salud Carlos III, Madrid, Spain

Sheeza Mughal Institute for Bioengineering of Catalonia (IBEC), The Barcelona Institute of Science and Technology (BIST), Barcelona, Spain

Laura Muínelo Health Research Institute of Santiago de Compostela (IDIS), Complejo Hospitalario Universitario de Santiago de Compostela (SERGAS), Santiago de Compostela, Spain

Naël Osmani Université de Strasbourg and INSERM, Strasbourg, France

Ricardo Pereira International Iberian Nanotechnology Laboratory, Braga, Portugal

Escola de Ciências, Campus de Gualtar, Universidade do Minho, Braga, Portugal

Paulina Piairo International Iberian Nanotechnology Laboratory, Braga, Portugal

Liliana R. Pires RUBYnanomed Lda, Braga, Portugal

Jai Prakash Department of Advanced Organ Bioengineering and Therapeutics, Section: Engineered Therapeutics, Technical Medical Centre, University of Twente, Enschede, The Netherlands

Raquel Queirós INL, International Iberian Nanotechnology Laboratory, Braga, Portugal

Javier Ramón-Azcón Institute for Bioengineering of Catalonia, ICREA-Institució Catalana de Recerca i Estudis Avançats, Barcelona, Spain

Subha Rath Indian Institute of Technology Hyderabad, Sangareddy, Telangana, India

Rita Rebelo 3B's Research Group, I3Bs – Research Institute on Biomaterials, Biodegradables and Biomimetics, University of Minho, Headquarters of the European Institute of Excellence on Tissue Engineering and Regenerative Medicine, Braga, Guimarães, Portugal

ICVS/3B's – PT Government Associate Laboratory, Braga/Guimarães, Portugal

Rui L. Reis 3B's Research Group, I3Bs – Research Institute on Biomaterials, Biodegradables and Biomimetics, University of Minho, Headquarters of the

European Institute of Excellence on Tissue Engineering and Regenerative Medicine,
Braga, Guimarães, Portugal

ICVS/3B's – PT Government Associate Laboratory, Braga/Guimarães, Portugal

Carolina Rodrigues International Iberian Nanotechnology Laboratory, Braga,
Portugal

Escola de Ciências, Campus de Gualtar, Universidade do Minho, Braga, Portugal

Ana María Rodríguez-Ces Translational Medical Oncology Group (Oncomet),
Health Research Foundation Institute of Santiago (IDIS), Complejo Hospitalario
Universitario de Santiago de Compostela (SERGAS), Santiago de Compostela,
Spain

Department of Surgery and Medical-Surgical Specialties, Medicine and Dentistry
School Universidade de Santiago de Compostela (USC), Santiago de Compostela,
Spain

Translational Medical Oncology Group (Oncomet), Health Research Foundation
Institute of Santiago (IDIS), Complejo Hospitalario Universitario de Santiago de
Compostela (SERGAS), Santiago de Compostela, Spain

Centro de Investigación Biomédica en Red en Cáncer (CIBERONC), Instituto de
Salud Carlos III, Madrid, Spain

Laura Rodriguez-Lorenzo INL, International Iberian Nanotechnology Labora-
tory, Braga, Portugal

Romén Rodríguez Institute for Bioengineering of Catalonia and Universitat de
Barcelona, Barcelona, Spain

Laura Muínelo Romay Translational Medical Oncology Group (Oncomet),
Health Research Foundation Institute of Santiago (IDIS), Complejo Hospitalario
Universitario de Santiago de Compostela (SERGAS), Santiago de Compostela,
Spain

Michael Ryckelnyck Université de Strasbourg, Strasbourg, France

Josep Samitier Nanobioengineering Group, Institute for Bioengineering of
Catalonia (IBEC), Barcelona Institute of Science and Technology (BIST),
Barcelona, Spain

Department of Electronics and Biomedical Engineering, University of Barcelona,
Barcelona, Spain

Centro de Investigación Biomédica en Red en Bioingeniería, Biomateriales y
Nanomedicina (CIBER-BBN), Madrid, Spain

Marilia Santos International Iberian Nanotechnology Laboratory, Braga, Portugal

Jessica Sierra Nanobioengineering Group, Institute for Bioengineering of
Catalonia (IBEC), Barcelona Institute of Science and Technology (BIST),
Barcelona, Spain

Maria Sousa-Silva International Iberian Nanotechnology Laboratory, Braga, Portugal

Escola de Ciências, Campus de Gualtar, Universidade do Minho, Braga, Portugal

María Mercedes Suárez-Cunqueiro Translational Medical Oncology Group (Oncomet), Health Research Foundation Institute of Santiago (IDIS), Complejo Hospitalario Universitario de Santiago de Compostela (SERGAS), Santiago de Compostela, Spain

Centro de Investigación Biomédica en Red en Cáncer (CIBERONC), Instituto de Salud Carlos III, Madrid, Spain

V. S. Sukanya Regenerative Medicine and Stem Cell Laboratory (RMS), Department of Biomedical Engineering, Indian Institute of Technology Hyderabad, Sangareddy, Telangana, India

Alexandra Teixeira International Iberian Nanotechnology Laboratory, Braga, Portugal

Life and Health Sciences Research Institute (ICVS), School of Health Sciences, University of Minho, Braga, Portugal

Liliana Teixeira Twente University, Enschede, The Netherlands

Miguel Xavier International Iberian Nanotechnology Laboratory, Braga, Portugal

Vamsi Yadavalli Virginia Commonwealth University, Richmond, VA, USA

Giorgia Zambito Department of Radiology and Nuclear Medicine, Erasmus Medical Center, Rotterdam, The Netherlands

Department of Molecular Genetics, Erasmus Medical Center, Rotterdam, The Netherlands

Justina Žvirblytė Institute of Biotechnology, Life Sciences Center Vilnius University, Vilnius, Lithuania

Part I

Fundamentals of Microfluidics and Biosensors



Fundamentals of Biosensors and Detection Methods

1

Marília Barreiros dos Santos, Laura Rodriguez-Lorenzo,
Raquel Queirós, and Begoña Espiña

Abstract

Biosensors have a great impact on our society to enhance the life quality, playing an important role in the development of Point-of-Care (POC) technologies for rapid diagnostics, and monitoring of disease progression. COVID-19 rapid antigen tests, home pregnancy tests, and glucose monitoring sensors represent three examples of successful biosensor POC devices. Biosensors have extensively been used in applications related to the control of diseases, food quality and safety, and environment quality. They can provide great specificity and portability at significantly reduced costs. In this chapter are described the fundamentals of biosensors including the working principles, general configurations, performance factors, and their classifications according to the type of bioreceptors and transducers. It is also briefly illustrated the general strategies applied to immobilize biorecognition elements on the transducer surface for the construction of biosensors. Moreover, the principal detection methods used in biosensors are described, giving special emphasis on optical, electrochemical, and mass-based methods. Finally, the challenges for biosensing in real applications are addressed at the end of this chapter.

Keywords

Biosensors · Bioreceptors · Transducers · Immobilization strategies

M. Barreiros dos Santos (✉) · L. Rodriguez-Lorenzo · R. Queirós · B. Espiña
INL, International Iberian Nanotechnology Laboratory, Braga, Portugal
e-mail: marilia.santos@inl.int

© The Author(s), under exclusive license to Springer Nature Switzerland AG 2022
D. Caballero et al. (eds.), *Microfluidics and Biosensors in Cancer Research*,
Advances in Experimental Medicine and Biology 1379,
https://doi.org/10.1007/978-3-031-04039-9_1

3

1.1 Biosensors

Biosensors are flexible analytical tools of enormous importance, being able to resolve a potential number of problems and challenges in diverse areas like homeland security, defence, medicine and pharmacology, environmental monitoring, and food safety, among others [1]. They have a great impact on our society and are expected to improve life quality, regarding the control of diseases, food quality and safety, and the quality of our environment [2]. For instance, the earlier detection of diseases and disease screening may be improved using biosensor-based diagnostics. These analytical tools may monitor the disease progression and treatment, being extremely appropriate to improve the related prognosis and enhance healthcare delivery in the community [3, 4].

Biosensors are used to investigate the presence of target analytes in a variety of samples, including body fluids (urine, blood, saliva, tears, and sweat), food samples, cell cultures, and environmental samples [5–7]. Numerous potential advantages can be found in biosensors compared with other biodetection methods, such as the increase in assay speed and flexibility, rapid and real-time analysis, multi-target analyses, automation, and reduction of costs [4].

Biosensor is defined by the International Union of Pure and Applied Chemistry (IUPAC) as “a device that uses specific biochemical reactions mediated by isolated enzymes, immunosystems, tissues, organelles, or whole cells to detect chemical compounds usually by electrical, thermal, or optical signals” [8, 9]. A schematic diagram of the building blocks comprising a typical biosensor is shown in Fig. 1.1.

A biosensor consists of two main components: a biorecognition element or bioreceptor (Fig. 1.1a) and a transducer (Fig. 1.1b). The bioreceptor, which specifically recognizes the target analyte, is generally an immobilized biological system or component among many others (impurities). The transducer converts the biological response into a measurable signal. The small input signal from the transducer is amplified (Fig. 1.1c) to a large output signal, which contains the essential waveform

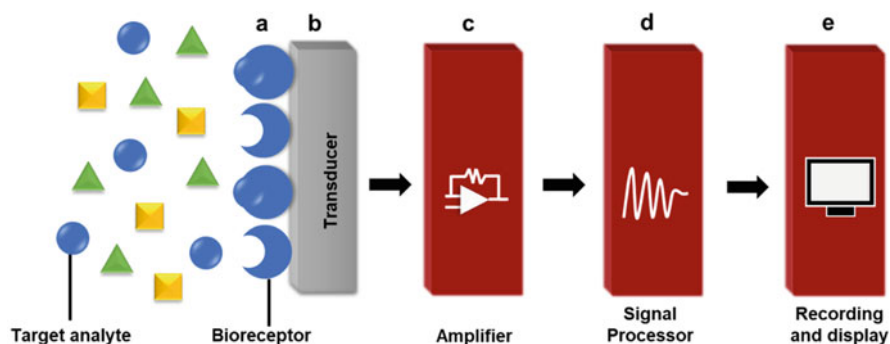


Fig. 1.1 Schematic diagram of a biosensor with the different building blocks: (a) bioreceptor, (b) transducer, (c) amplifier, (d) signal processor, and (e) recording and display

characteristics of the input signal. Then, the signal processor processes the amplified signal (Fig. 1.1d) that can be stored, displayed, and analyzed (Fig. 1.1e) [4].

The biorecognition layer must be highly specific to the analyte in a successful biosensor and the reaction must be independent of several physical parameters like pH, stirring, and temperature. Moreover, the biosensor signal must be stable and without electrical noise and the sensor response should be linear over a useful analytical range, accurate, precise, and reproducible [10–12], preferentially without sample dilution or pre-concentration. The biosensor should be portable, fast, inexpensive, manageable, and adaptable to be used by an unskilled operator. A non-invasive monitoring must be employed in clinical situations and the biosensors should be small and biocompatible [7, 13]. The sensitivity and selectivity of the biosensor is critically affected by the selection of a suitable bioreceptor with a high affinity for the analyte, the right transducer, and a feasible method to immobilize the bioreceptor onto the transducer surface [4]. For this reason, these important factors involved in the biosensor design will be further discussed in detail. This chapter will be mainly focused on affinity or bioreceptor-based biosensors, even though other types of biosensors based on non-affinity sensors have been widely investigated [14].

1.1.1 Bioreceptors

A bioreceptor is a biological molecular specie or living biological system that uses a biochemical mechanism for recognition [15]. Bioreceptors, crucial for the specificity of the biosensor, are generally classified into four major categories: antibody, enzymes, nucleic acids, and cellular structures/cells. Nevertheless, other bioreceptors, such as aptamers, biomimetic receptors, peptides, and bacteriophage, have been widely used in the last years [6, 10, 16–18]. A detailed description of the most used bioreceptors will be presented in the next sections.

1.1.1.1 Antibody

Antibodies are the most widely used biorecognition elements due to the high antibody-antigen binding specificity. The three-dimensional structures of antigen and antibody molecules match in a highly specific manner. For this reason and due to the diversity inherent in individual antibody make-up, it is possible to find an antibody that can recognize and bind to any antigen of a large variety of molecular shapes [6, 17]. Biosensors that use antibodies as biorecognition elements are termed *immunosensors*, and they are usually used because antibodies are highly specific, versatile, and bind strongly to the antigen. The main advantages of using antibodies are their high sensitivity and selectivity. Long-term stability and manufacturing costs, especially when many ligands are needed for multi-target biosensor applications, are some of the limitations of this type of biosensors [3, 4].

Antibodies can recognize and bind to an analyte within a large number of other chemical substances, even in very small amounts. The antibodies can be immobilized onto a surface of the transducer to specifically capture the antigens,

being antibody-antigen reactions highly compatible with known conjugation chemistries [4, 19]. All these antibodies properties make the immunosensors a great analytical tool to detect cancer biomarkers [20], chemicals [21], biomolecules [22], and microorganisms [23, 24], among others [25, 26].

1.1.1.2 Cells

Cell-based biosensors use living cells as bioreceptor to acquire information from an external physical or chemical stimulus [27]. The application of cell-based biosensors ranges from environmental monitoring to pharmaceutical research areas, in which significant accomplishments have been achieved for pathogens detection [28] and early diagnosis of oral cancer [29]. For instance, toxicity assessment and water quality monitoring have used different cell types (bacteria, yeast, fungi, algae), while the study of disease pathogenesis and basic cellular functions have used eukaryotes cells (fish, rat, and human cells) [30].

Cell-based biosensor present several advantages in terms of long-term recording in non-invasive ways, fast response, and the biosensor fabrication process is relatively simple and inexpensive compared to pure enzymes, nucleic acids, and antibodies [27]. In the past few years, more sensitive, accurate, and efficient cell-based biosensing technologies have been created by emerging microfluidics, 3D bioprinting, and microarray technology [30]. The main limitation of this type of biosensors is that the cell viability is affected by factors like the lifetime of cells, sterilization, and biocompatibility issues of the device [27].

1.1.1.3 Enzymes

Enzymes are frequently chosen as bioreceptors due to their specific binding capabilities and their catalytic activity [15]. Several possible mechanisms have been used for analyte recognition: (a) the sensor detects a product that was produced by the enzyme conversion of the analyte, (b) the enzyme inhibition or activation by the analyte is detected, or (c) the interaction of the analyte with the enzyme results on enzyme properties modification of that can be monitored [31]. Even though enzymes are considered one category of the biorecognition elements, they are frequently used as labels instead of bioreceptors. Enzymes have gained popularity as labels in immunoassay detection like Enzyme-Linked ImmunoSorbent Assay (ELISA), in which three enzymes are generally: alkaline phosphatase, horseradish peroxidase (HRP), and beta-galactosidase [4, 32].

Enzyme-based biosensors can be used to detect cancer biomarkers [33], cholesterol [34], food safety and environmental monitoring [35], heavy metals [36] and pesticides [37]. Enzymes offer several advantages in terms of high sensitivity, long stability and direct visualization possibility, eliminating the need for expensive and complicated equipment. Some disadvantages found when using enzymes as labels include the multiple assay steps and the possibility of interference from endogenous enzymes [6].

1.1.1.4 Nucleic Acids

In nucleic acid biosensors, complementary strands of nucleic acids are used as biological recognition elements and the identification of a target analyte nucleic acid is based on the natural affinity of matching the complementary base pairs of adjacent strands, forming a double helix of deoxyribonucleic acid (DNA) through stable hydrogen bonds [31, 38]. In classic nucleic acid biosensors is measured the hybridization of a single strand DNA strand immobilized onto the sensor surface with its complementary strand in the samples. Moreover, intercalating agents can be inserted in the helical structure of a double-stranded oligonucleotide and be used in a nucleic acid biosensor [39].

Biosensors based on nucleic acid are highly stable, simple, rapid, inexpensive, and easily reusable by thermal melting of the DNA duplex. This type of biosensor possesses a remarkable specificity that can be found in this type of biosensor and the presence of a single molecule species can measure in a complex mixture. Moreover, the nucleic acid recognition layers can be regenerated and readily synthesized in comparison with enzymes or antibodies. One of the most important factors for nucleic acid bioreceptor is DNA damage. Detection of chemicals may cause irreversible damage to DNA by changing the structure of DNA and the base sequence, which in turn disturbs the DNA replication [4, 6, 40].

Applications of nucleic acids as biorecognition elements are numerous and DNA-based biosensors have potential applications in clinical diagnostics for virus and disease detection [41, 42]. Moreover, several applications of DNA microarrays have been found in the last decades for, among others, the detection and characterization of pathogens and genotyping, and the profiling of gene expression [43, 44].

1.1.1.5 Aptamers

Aptamers are single-stranded oligonucleotides of DNA or Ribonucleic acid (RNA) sequences, usually 25–80 bases long [45], produced by an *in vitro* selection process called *systematic evolution of ligands by an exponential enrichment* (SELEX). This process identifies a monomer sequence and strongly binds the target from a large library of random sequences [39, 46]. The main characteristics of aptamers include small size, cost efficiency, chemical stability, and once selected, can be synthesized with high reproducibility and purity from commercial sources. Moreover, aptamer provides remarkable flexibility and convenience in the design of their structures [47]. Aptamers are more stable than antibodies and the biosensors using aptamers, termed *aptasensors*, can be regenerated [39]. The structural pleomorphic and chemical simplicity of nucleic acids is a common challenge of aptasensors that reduce the assay efficiency and increase its production cost [4, 40].

Aptamers can be chemically modified by biotin, thiol or amino groups, allowing them to be immobilized on various solid supports [48]. They possess a high recognition ability toward specific molecular targets ranging from small molecules to proteins and even cells [49]. Aptasensor's applications include the detection of biomarkers like thrombin [50], clinical testing of cancer-related markers [51, 52], and also detection of microorganisms and viruses [53].

1.1.2 Immobilization Strategies in Biosensors

A wide variety of different materials and modification methods have been used in the design of biosensor surfaces to obtain efficient biosensing devices with oriented biomolecules. The typical materials used include gold (Au), silicon, silicon oxide, silicon nitride, graphite, glass carbon, and Indium Tin Oxide (ITO), among others [7]. Moreover, the surfaces may need to fulfill specific requirements depending on the measurement technique, for example, electrical conductivity for electrochemical measurements or transparency for optical devices.

The modification of the sensing surface to integrate the selected biorecognition elements is one of the most critical steps in biosensor development because biosensor performance (sensitivity, response time, dynamic range, and reproducibility) depends on how the original properties of the bioreceptor are kept after its immobilization. The immobilization strategies include adsorption (Fig. 1.2a), entrapment and encapsulation into polymers or membranes (Fig. 1.2c, respectively), cross-binding or covalent binding of a biomolecule to a silane or self-assembled monolayers (SAM) (Fig. 1.2d) [4, 48, 54].

The immobilization of the bioreceptor must be stable and the accessibility of the target molecule and its recognition ability must be guaranteed. Moreover, the modified surface needs to be inert and biocompatible in a way that it does not affect the sample composition or its integrity, and a constant signal baseline should ensure. The different biomolecule immobilization strategies mentioned are described in more detail above.

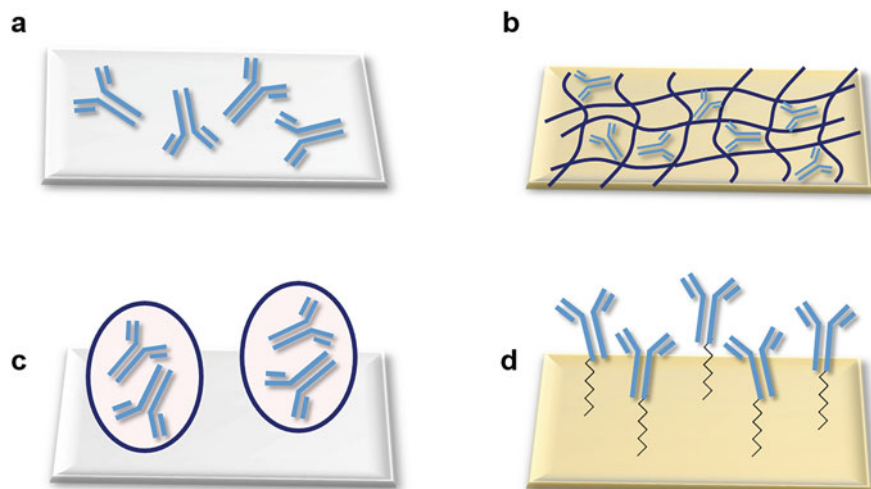


Fig. 1.2 Different examples of biomolecule immobilization strategies: (a) adsorption, (b) entrapment (c) encapsulation, and (d) cross-linking to a pre-assembled SAM

1.1.2.1 Adsorption

Non-specific adsorption (Fig. 1.2a) is based on the deposition of biomolecules on the surface that interact in a completely random way. At an initial stage, the driving forces may be hydrophobic or electrostatic, then the protein adsorption is stabilized by a combination of hydrophobic interactions, hydrogen bonding, and/or *Van der Waals* forces [55]. The resulting behavior is highly dependent on each protein surface involved, as well as a highly stable product [56, 57]. This method is one of the easiest ways to modify the surface and presents some advantages, such as simplicity, a cost-effective process, and no modification of the bioreceptors is required [10]. In terms of limitations, proteins may partly denature as a consequence of adsorption and thus lose structure and/or function [58]. Moreover, the adsorption process is difficult to control and the amount of protein adsorbed to most solid surfaces is usually below a close-packed monolayer. In addition, the exposure of internal hydrophilic groups of proteins to hydrophobic surfaces during the adsorption causes a decrease in the activity and specificity of the protein/target interactions [4, 48].

1.1.2.2 Entrapment

Biomolecules can be entrapped within organic or inorganic polymer matrices during the matrix polymerization (Fig. 1.2b) and their integrity is not affected since there is no chemical modification during the process. The proteins are stabilized by the confinement into small inert spaces, being this method easy and cheap [55, 59]. The main drawbacks associated with this strategy include the requirement of high concentrations for both monomers and biomolecules, poor accessibility to certain target molecules, lack of reproducibility and sensibility to the polymerization conditions and/or polymer components [4, 60].

1.1.2.3 Microencapsulation

Microencapsulation (Fig. 1.2c) involves the entrapment of molecules within micro/nano-capsules with different compositions (particles, spheres, tubes, fibers, vesicles; made of hydrogel, polymer, carbon, silica, lipids, etc.) that can be formed by different strategies (via template molding, polymerization, self-assembly, emulsification, etc). Encapsulation has been reported to protect proteins from unfolding and degradation, ensuring longer activity times. On the other hand, microencapsulation requires relatively high biocomponent concentrations and generates longer response times over the biocomponent is free in solution [4, 48].

1.1.2.4 Self-Assembled Monolayers

SAM are well-defined organic surfaces formed by the spontaneous organization of thiolated molecules on metal surfaces [61]. SAMs are easy to prepare and functionalize in an ordinary chemistry laboratory, can be formed on surfaces of any size and it is possible to link molecular-level structures to macroscopic interfacial phenomena. SAMs are often the basis for the subsequent immobilization of the biorecognition elements since the functional groups provided by the SAM layer termination can be personalized to suit any specific requirement [4, 56].

1.1.2.5 Silanization

Silanes have the general chemical composition formula RSiX_3 , where R is an organofunctional group selected according to the desired surface properties; and X is a hydrolyzable group, typically an alkoxy group (alkyl group linked to oxygen). They are capable of reacting with different substrates such as silica, silicon, silicon oxide, silicon nitride, glass, cellulose, and metal oxide surfaces. Silanization is a SAM substitute and hydroxyl-terminated substrates are one of the most frequently and effectively used procedures for the chemical and physical properties modification of the substrate. Silanes are normally hydrolyzed at some stage in the coating process, allowing interaction with the substrate either via hydrogen or covalent bonds [4, 48].

1.1.2.6 Chemical Conjugation

The most commonly used strategy of chemical conjugation consists in cross-binding between carboxylic ($-\text{COOH}$) and amine groups ($-\text{NH}_2$), exploiting the carbodiimide chemistry (i.e. 1-ethyl-3-(3-dimethylaminopropyl)carbodiimide (EDC)/N-hydroxysuccinimide (NHS)). The COOH group can be situated either on the termination of the SAM or on the (bio) component to be immobilized. The use of glutaraldehyde allows the reaction of two amino groups. Thiols can be coupled to amino groups using heterofunctional cross-linkers such as succinimidyl 4-(N-maleimidomethyl)-cyclohexane-1-carboxylate (SMCC) or N-succinimidyl S-acetylthioacetate (SATA). The polysaccharides present in some proteins can be oxidized with sodium periodate and later conjugated to amine or hydrazide groups in the SAM by reductive amination. Hydroxyl groups on a SAM can be treated the same way [62]. In addition, the recognition element may also be self-assembled. For example, a modified nucleic acid fragment incorporating an $-\text{SH}$ terminal group is directly self-assembled on the metal surface [4, 48].

1.1.3 Transducers

The transducer has an important role in the detection process of a biosensor. Biosensors can be classified based on the transduction methods used, which include electrochemical, optical, magnetic, mass sensitive, and thermal. In the past years, the transduction mechanism has been improved significantly by using nanomaterials that can provide them different characteristics in biosensors, such as greater sensitivity, faster detection, shorter response time, and reproducibility [10]. The different nanomaterials include nanoparticles (NPs), nanorods (NRs), nanowires (NWs), carbon nanotubes (CNTs), quantum dots (QDs), graphene (G), graphene oxide (GO), carbon dots (CD), metal-organic frames (MOFs) and dendrimers. For example, metallic NPs are usually employed in biosensor as enhancers of biochemical signals. For instance, NWs are used as charge transport and carriers, while the CNTs are used as enhancers of reaction specificity and efficiency. QDs may be employed in biosensor as contrast agents for improving optical responses [10]. There are some

reviews available with an in-depth description of the most recent advances of nanomaterials in biosensors [10, 55, 63–69].

Optical, electrochemical, and mass-based transducers are the most popular and common methods used [6, 70]; for this reason, they are given more importance in this chapter. These transducers can be categorized into two groups: (1) direct recognition and (2) indirect detection biosensors. For instance, the direct detection biosensors exploit the direct measurements of the phenomenon occurring during the biochemical reactions on a transducer surface and no requirements of labeling for detection are needed (i.e., label-free). In the case of indirect detection biosensors, the detection is enhanced by secondary elements (labels), such as enzymes, fluorophores, and nanoparticles [3, 65, 71].

1.1.3.1 Optical-Based Biosensors

Optical-based biosensors have been commonly employed due to the numerous different types of spectroscopy measurements available (e.g., fluorescence, Raman, refraction, phosphorescence, absorbance, dispersion spectrometry, etc.) [15, 17]. The optical biosensors are probably the most popular especially because of their sensitivity, high specificity, cost-effectiveness, and small size. These types of transducers also permit direct, real-time, and label-free detection [72].

Figure 1.3 shows some examples of the most common optical detection methods used in the biosensors field: (a) fluorescence and chemiluminescence, (b) surface plasmon resonance (SPR), (c) surface-enhanced Raman scattering (SERS), and (d) colorimetric.

Fluorescence-Based Biosensors

Fluorescence biosensors can detect the concentration, location, and dynamics of biomolecules based on a fluorescent phenomenon. This phenomenon occurs when electromagnetic radiation is absorbed by fluorophores or fluorescently labeled molecules, in which the energy is converted into fluorescence emission [73] (Fig. 1.3a). The fluorophore molecules that label target biomolecules can be dyes, fluorescent proteins, or QDs. These types of biosensors usually embrace three main approaches: (a) Fluorescent quenching (turn-off), (b) fluorescent enhancement (turn-on), and (c) fluorescence resonance energy transfer (FRET) [10, 74]. Fluorescence biosensors often includes: excitation light source (e.g. LEDs (light-emitting diodes), lasers, fluorophore molecules, and photodetector that records changes in the fluorescence intensity [73, 75].

Fluorescence-based biosensors combine high sensitivity, sensitivity, and short response time, being widely employed in medical diagnosis [76], environment and food quality monitoring applications [63]. FRET-based optical sensors also have drawn much attention in clinical applications, such as cancer therapy and aptamers analysis, since they can detect changes in angstroms to nanometers [10, 77]. As for disadvantages, fluorescent molecules (i.e., organic dyes) can be often toxic and easily photobleached. The use of nanomaterials has introduced an interesting approach to the development of low-cost and portable fluorescent devices, in

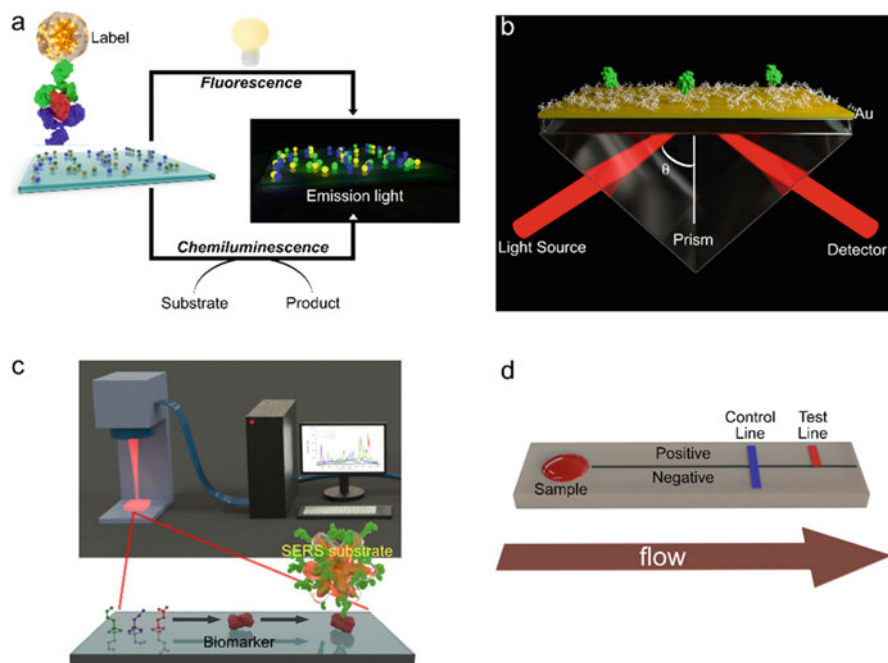


Fig. 1.3 Schematic overview of optical-based biosensors: (a) fluorescence and chemiluminescence-based biosensors, (b) Surface Plasmon Resonance, (c) Surface-enhanced Raman scattering, and (d) colorimetric

which nanostructures that enhance the fluorescence signal has been used to construct remarkable fluorescent sensors [66, 78].

Chemiluminescence-Based Biosensors

Chemiluminescence is a phenomenon in which light energy is released due to a chemical reaction [10] (Fig. 1.3a). Certain substances (reactants, intermediates, and fluorophores) are activated by oxidation to form an oxidized high-energy intermediate, generating luminescence by the decomposition or transference of this intermediate energy to nearby fluorophores that return to its ground state. Chemiluminescence can generally be divided into direct chemiluminescence and indirect chemiluminescence strategies, depending on the different chemical energy conversion mechanisms [79]. The intensity of emitted light can be measured by three different means: (a) in static, the mixture of reagents is done in front of the detector; (b) the interaction of chemiluminescent reagents with the analyte occurs by diffusion or convection when reagents are immobilized on a solid support (e.g., filter paper); and (c) inflow measurement systems [80].

The instrumentation for chemiluminescence measurements consists of a mixing device and a detection system. The affordable instrumentation, simplicity, low detection limit, and wide calibration limit are some of the advantages of

chemiluminescence-based biosensors [10]. Nevertheless, poor sensitivity and limited selectivity of analysis, unless coupled to a powerful separational set-up, are some of the main drawbacks [81]. Electrogenerated chemiluminescence sensors, a kind of chemiluminescence phenomenon, have been attracting much attention in the last years due to the possible unusually high sensitivity, extremely wide dynamic range, and excellent controllability [82]. The application of chemiluminescence-based biosensors includes the detection of biomarkers [83], toxins [84, 85], metal ions, viruses, and bacteria [82]. Nowadays, new applications had been extended by using nanomaterials that have been employed to improve the sensitivity [86].

Plasmon-Based Biosensors

Surface Plasmon Resonance

SPR is a powerful technique to measure biomolecular interactions in real-time and label-free environment [87]. The changes in the refractive index in the metal surface vicinity are measured by SPR that create a change in the resonance angle [88, 89]. A scheme showing the working principle of a SPR biosensor is shown in Fig. 1.3b. A sensor chip with a thin Au layer on the top is irradiated from the backside by p-polarized light (from a laser) via a hemispherical prism, and the light is reflected by the metal film acting as a mirror. The change in the angle of incidence, θ , can be monitored providing the intensity of the reflected light. The intensity of the reflected light passes through a minimum and at this angle of incidence, the light will excite surface plasmons, inducing a surface plasmon resonance, and a dip in the intensity of the reflected light is caused. The properties of the gold-solution interface can determine the angle position of this minimum. Later, adsorption phenomena and even reaction kinetics can be monitored using this sensitive technique [4, 89].

In addition to the high sensitivity and temporal resolution offered by SPR, the main advantage of this technique is that labeling is not needed on target molecules. This has a direct impact on time and cost, as well as can avoid possible perturbations during the biorecognition studies due to this additional step. The main drawbacks of this technique lay in its complexity (specialized staff is required), high cost, and large size of most currently available instruments [4, 88, 90]. SPR has been widely used in cancer research [66] and monitoring of contaminants in food and environment [39].

Localized Surface Plasmon Resonance

Another plasmon-based biosensor of great interest is localized surface plasmon resonance (LSPR)-based biosensors due to their potential of label-free and multiplexing, portability, low-cost, and real-time monitoring of diverse target [91]. This type of biosensor is based on the LSPR properties of certain metal nanostructures (e.g. Au, Ag, Cu), which is generated by the collective oscillation of conduction electron upon excitation with the appropriate light (e.g., a laser beam). As a consequence of this excitation, an absorbance band(s) can be acquired by using UV-Vis spectroscopy. The energy window of LSPRs in gold and silver NPs lies typically within the visible NIR and depends on the size, shape, and composition of

the NPs, as well as on the orientation of the electric field relative to the NP and the dielectric properties of the surrounding medium [92]. This allows for designing biosensor based on the LSPR variation when a biomarker is adsorbed/attached on the metal surface. However, their fabrication presents significant challenges, including the elimination of probe set—target set cross-reactivity, selection of well-characterized bioreceptors, minimization of non-specific binding, and synthesis of stable nanoparticles.

Few examples of multiplexed detection have been reported [93]. These assays were based on mixtures of functionalized gold nanorods in an aqueous solution; and subsequent detection of targets through changes, both at intensity and shifted, of the longitudinal surface plasmon band. These LSPR changes are generated by means of dependent-response to binding events (i.e. biorecognition antibody-antigen). These studies demonstrate that it is possible to detect multiple analytes within a single assay, but this still requires large improvement regarding reproducibility, limit of detection, and spatial resolution. This could be possible by using detectors with better signal-to-noise ratio or higher resolution [94], and increasing the intrinsic biosensor's sensitivity [95]. The utilization of different nanoparticle shapes may be a good alternative or the detection of single NPs [96], which may help to improve sensitivity through narrower plasmon bands, but the lower signal-to-noise ratio could be a limiting factor.

Surface-Enhanced Raman Scattering

SERS offers unique advantages as an analytical tool with a high selectivity and sensitivity without matrix interference and minimum sample preparation. It can provide high throughput chemical information (unique fingerprints containing vibrational information) on particles with sizes down to the nanometric scale [97] (Fig. 1.3c). SERS is based on the enhancement of the Raman signal by several orders of magnitude for molecules adsorbed on a noble metal nanostructured surface (e.g. gold and silver). This enhancement is principally caused by the LSPR in a metal nanostructure. Excitation of the LSPR results in the enhancement of the local field experienced by a molecule adsorbed on the nanostructure surface [98]. This together with the recent advances in nanofabrication techniques [99], which fuel the development of a large variety of rationally designed SERS substrates with optimized, uniform, and reproducible responses, pave finally the way for the successful translation of the great analytical potential of SERS to reliable, widely accepted and commercially viable sensing applications, addressing several limitations posed by conventional analytical techniques [100]. SERS-based biosensors offer two detection design approaches:

- *Direct SERS*. The detection is obtained by monitoring the characteristic changes of the vibrational profile of bioreceptors, bound to the metal surface, when complexed with the target species [101]. However, direct detection is not the best option due to the complexity of detecting simultaneously multicomponent mixtures of biological fluids. If the number of molecules, including targets and background species, is high, the overlapping of vibrational modes of different

molecules is very likely. In this situation, the interpretation of the vibrational spectrum becomes difficult or nearly impossible. One solution consists of the application of chemometric deconvolution algorithms such as partial least squares regression, principal component analysis, or hierarchical cluster analysis [102].

- *Indirect SERS*. In this case, the plasmonic substrate is encoded with a good Raman reporter which acts as a source of strong and distinctive SERS signature whose intensity has been designed to selectively vary according to the biomarkers concentration. This strategy is usually employed in those cases where the direct approach yields low Raman signatures or for the multiplex analysis of big analytes in very complex fluids [100].

Importantly, the availability of a large library of SERS fingerprints allows the simultaneous detection of a set of biomarkers with high selectivity enabling an accurate diagnosis of a complex disease. Moreover, the development of the multiplexed SERS-based sensors allows also for expanding the number of potential biomarkers, including new small peptides/molecules that cannot be employed with the current technology because of sensitivity limitations. Finally, the introduction of nano-enabling SERS sensing technology could enable rapid detection of multiple biomarkers at point-of-care and may facilitate fast personalized healthcare delivery.

Colorimetric-Based Biosensor

Colorimetry is a well-known sensing principle that is widely, maybe the most, used in commercial biosensors (e.g., ALS SARS-CoV-2 RT-LAMP kit [103]). It determines the concentration of an analyte by detecting a color change easily by naked eyes or simple portable optical detector, which is associated with a specific (bio) chemical reaction. These types of biosensors have been developed for a wide type of bioreceptor such as antibody, enzymes, and nucleic acids [104]. Colorimetric biosensors can be also designed using metal nanoparticles, which may cover the need for label-free and high-throughput analysis in diagnostics.

Lateral flow assay is one of the most popular colorimetric biosensors (Fig. 1.3d). This is a simple, specific, portable, and low-cost diagnostic device used to detect an analyte such as pathogens or cancer biomarkers and is currently used for PoC detection. Numerous labels are used in lateral flow biosensors, AuNPs being the most widely used. Lateral flow biosensors traditionally involve the use of antibodies, but aptamers or/and nucleic acid have also been implemented. The home pregnancy test is an excellent example of how to work a lateral flow using the optical properties of AuNPs to provide practical solutions to real problems. The concept of this pregnancy lateral-flow test is based on the presence in pregnant women's urine of an important excess of human gonadotropic hormone (HcG). HcG presents a specific protein structure that binds to a complementary DNA sequence. AuNPs are then functionalized with this complementary sequence. AuNPs also provide red color. Therefore, if HcG is detected, the spot or line of the dipstick shows red; if not, blue color is observed [105].

Despite all the advantages of the colorimetric biosensors, there are some limitations on their implementation such as (1) excellent bioreceptor preparation is

obligatory; (2) analysis time is sample-dependent; (3) inaccurate sample volume can reduce sensitivity and precision; and (4) sample preparation is needed for many of non-liquid samples [103].

1.1.3.2 Electrochemical-Based Biosensors

In the electrochemical-based biosensors, an important subclass of biosensors, an electrode is used as a transduction element [40]. Electrochemical biosensors can be classified into several categories such as amperometric, potentiometric, and impedimetric based on the measured parameter: current, potential or impedance (Z), respectively (Fig. 1.4) [88]. Electrochemical biosensors hold great potential as the next-generation detection systems due to their high sensitivity, portability, low cost, low-power instrumentation required, ease of operation, and high compatibility of integration into miniaturized devices [64, 106]. However, their sensitivity and selectivity can be slightly limited [4, 6]. The integration of nanomaterial in electrochemical biosensors, such as G, GO, and CNTs (single or multiple one atom-thick carbon concentric tubes) as well as NPs and NWs of different materials, can nowadays allow limits of detection lower than previously possible, enabling even single-molecule detection [11, 64, 67].

Electrochemical sensing usually requires a reference electrode (RE), a counter (CE) or auxiliary electrode, and a working electrode (WE), also known as the sensing or redox electrode. The RE , being the most conventional silver/silver chloride

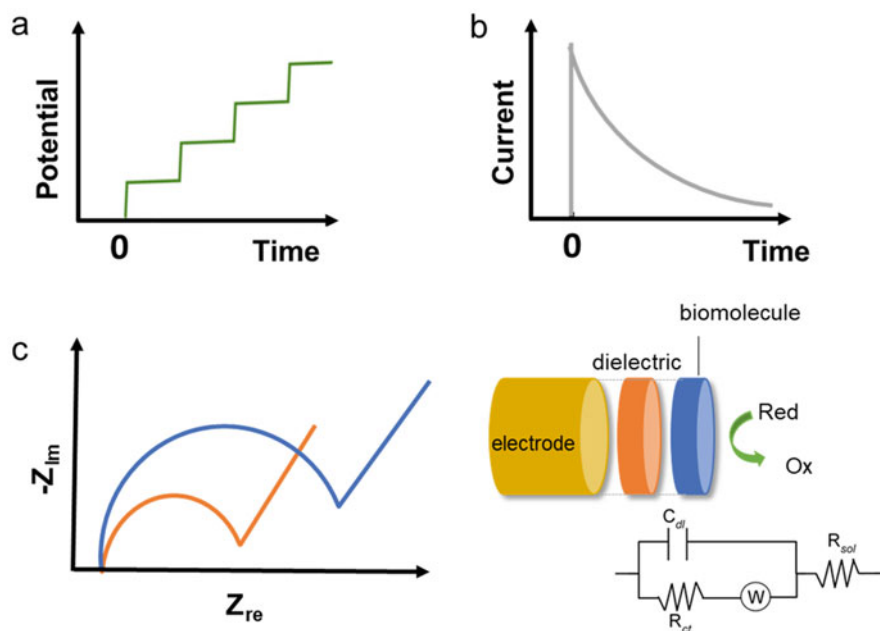


Fig. 1.4 Schematic overview of some electrochemical detection methods: (a) potentiometry, (b) amperometry, and (c) electrochemical impedance spectroscopy, based on faradaic measurements

(Ag/AgCl), is kept at a fixed distance from the reaction site in order to maintain a known fixed and stable potential. The CE usually uses an inert conducting material, such as platinum (Pt) or graphite, and establishes a connection to the electrolytic solution so that an excitation can be applied to the *WE*. Finally, the *WE*, is employed as a solid support for the immobilization of the biomolecules and it serves as the transduction element from the biochemical reaction to the electrical signal. Therefore, the *WE* should be both conductive and chemically stable [4, 67]. The materials most commonly used are Au, Pt, ITO, and carbon-based [7, 40, 107].

Potentiometric Biosensors

Potentiometry is the electrochemical measurement of an electrical potential difference between two electrodes, known as the *indicator* and *reference* electrodes, when the electrochemical cell current is zero. The reference electrode provides a constant half-cell potential, while the indicator electrode develops a variable potential, which is dependent on the activity or concentration of a specific analyte in solution. The change in potential E is plotted as a function of time (Fig. 1.4a) and is related to analyte concentration in a logarithmic mode, allowing the detection of extremely small concentration changes [4, 6, 7].

Potentiometric biosensors rely on the use of an ion-selective electrode (ISE) and ion-sensitive field effect transistor for obtaining the analytical information. The pH sensor is the most well-known example of an ISE [108]. The specificity of the device is conferred by a selective membrane, which may be formed from metal salts or polymeric membranes containing ion-exchangers or neutral carriers. Up to the present, there is a range of commercially available ISEs that can detect specific ions such as calcium, potassium, copper, barium, chloride, etc. [108]. Likewise, it can also be used to detect cancer biomarkers and other crucial biological compounds [109, 110]. The potentiometric biosensors are very attractive because they are simple, low cost, selective, and provide a fast analysis time. Nevertheless, these devices are still less sensitive than other electrochemical techniques and often present a slow response to a steady-state potential value [12, 35, 44].

Amperometric Biosensors

Amperometric sensors measure the current as a function of time, at a constant potential, Fig. 1.4b, resulting from the oxidation and reduction of an electroactive specie in a biochemical reaction that mainly depends on the concentration of an analyte [7, 40]. The applied potential serves as the driving force for the electron transfer reaction, and the current produced is a direct measure of the rate of electron transfer [6]. The peak current value acquired is directly proportional to the electroactive specie concentration. In the case of biosensors, where direct electron exchange between the electrode and either the analyte or the biomolecule is not permitted, redox mediators are required. Redox mediators are small size compounds able to reversibly exchange electrons between the electrode surface and the biological recognition molecule (e.g., ferricyanide, osmium or ruthenium complexes, dyes, etc.) [4, 88, 111].

The amperometric devices often use an indirect sensing system, however their sensitive is usually superior to potentiometric devices [7]. Amperometric biosensors were the first type to be developed and have been widely combined with different biorecognition molecules and used for various applications, from health, food safety, and environmental monitoring [112]. An example of an amperometric device is the well-known glucose biosensor, which is based on the amperometric detection of hydrogen peroxide. The enzyme, glucose oxidase, is immobilized onto the electrode surface and it catalyzes the conversion of glucose to gluconic acid and hydrogen peroxide [113, 114]. Nevertheless, amperometric biosensors show some drawbacks that limit their use, like the presence of electroactive interference in the sample matrix can cause the transducer to generate a false current reading. Although, there are various methods proposed to overcome this constraint such as sample dilution, coating of the electrode with polymers, changing the medium of analyte, and/or adding a mediator [4, 40].

Voltammetry is a form of amperometry, through which information about an analyte is obtained by determining the change in current as a function of applied potential. A potential between the WE and the RE is applied and the current generated externally from the CE to the WE is measured, also classified as an electro-analytical technique. The peak current value is used for identification, while the peak current density is proportional to the concentration of the corresponding species. The advantages of this type of electrochemical biosensor are highly sensitive measurements and simultaneous detection of multiple analytes [115]. Different voltammetric techniques such as linear sweep, differential staircase, differential pulse, normal pulse, reverse pulse, and polarography among others can be used, according to the way that the potential is scanned [116]. The first work addressing voltammetric immunosensors was published by Weber and Purdy (1979) [117], reporting the detection of an antigen in the presence of a bound antigen. Since then, an immeasurable amount of voltammetric detection schemes have been reported for different applications from cancer diagnosis to food and environmental fields [40, 118, 119].

Electrochemical Impedance Spectroscopy Biosensors

Electrochemical impedance spectroscopy (EIS) is a suitable technique for the detection of binding events that occurs on the transducer surface and a valued tool for characterizing surface modifications [120]. This versatile electrochemical tool characterizes the intrinsic electrical properties of any material or solution and its interface. The impedance Z of a system is generally determined by applying a voltage perturbation with small amplitude (between 5 and 10 mV) and detecting the current response. The impedance measures the voltage–time function $V(t)$ and the resulting current–time function $I(t)$, and thus is expressed in terms of a magnitude, Z and a phase shift, ϕ :

$$Z = \frac{V(t)}{I(t)} = \frac{V_0 \sin(2\pi ft)}{I_0 \sin(2\pi ft + \phi)} = \frac{1}{Y} \quad (\omega = 2\pi f)$$

where V_0 and I_0 are the maximum voltage and current signals, respectively, f is the frequency (angular frequency ω), t the time, ϕ the phase shift between the voltage–time and current–time functions, and Y is the complex conductance or admittance. The result of an impedance measurement can be illustrated using a *Bode plot* that plots $\log|Z|$ and ϕ as a function of ω (or f) or using a *Nyquist plot* which represents Z_{Re} and Z_{Im} (Fig. 1.4c) [4, 56, 107, 120].

EIS data is commonly modeled using an equivalent electrical circuit model that characterizes the different physicochemical properties of the system and usually consists of resistances and capacitances. Equivalent circuits are used to correlate the experimental data with the modeled curve [103]. The four elements usually used to describe the impedance behavior of EIS biosensors are: ohmic resistance of the electrolyte (R_s), capacitance (double layer) (C_{dl}), constant phase element (*CPE*), electron transfer resistance (R_{ct}), and Warburg impedance (Z_w) [46, 48, 107]. The R_{ct} is the electron transfer resistance across the electrode–electrolyte interface. The C_{dl} gives the specific capacitance at the interface of the electrolyte with the electrode and is characterized by the non-faradaic charge that arises from the surface, from the solid/liquid interface. C_{dl} is sometimes substituted with a *CPE*, to compensate for non-ideal capacitor behavior that occurs due to non-homogeneity of the surface at the double-layer interface. Z_w is called the impedance of diffusion and is a parameter that becomes significant in magnitude when a diffusion-controlled electron transfer process is present [121]. The most popular equivalent electrical circuit is the Randles equivalent circuit model, Fig. 1.4c, which includes R_s , R_{ct} , C_{dl} , and Z_w . From the Randles circuit model, the magnitude of the previously introduced circuit elements can be extracted and provide unique information about the conductive material under investigation, as well as about the biochemical reaction that is taking place on the surface of the electrode. It also serves to evaluate the suitability of the experimental operating conditions and design of the EIS system [103].

EIS can be divided into Faradaic and non-Faradaic, depending on whether there is a redox-related charge transfer across the electrode interface during measurement. In faradaic EIS, a redox specie is alternately oxidized and reduced by the transfer of an electron to and from the metal electrode (Fig. 1.4c). Faradaic EIS approaches are widely used in biosensors [122–124] and a typical redox probe used is ferricyanide $[\text{Fe}(\text{CN})_6]^{3-/4-}$. In non-Faradaic EIS, no redox process occurs and *capacitive biosensor* is the term usually designated [4, 46, 107]. Impedimetric biosensors have been received incredible attention from the research community, with a large number of publications in different areas, ranging from food quality control [125, 126] and environmental monitoring [127] to clinical diagnostics [128] due to their high sensitivity, portability, low cost, simplicity of instrumentation, label-free and ease of operation [64]. Some limitations include the susceptibility to non-specific binding and reusability of the electrodes.

1.1.3.3 Mass-Based Biosensors

Mass-based biosensors are another form of transduction used for biosensors that measures small changes in mass. The mass analysis usually depends on the use of piezoelectric crystals that can be made to vibrate at a specific frequency with the application of an electrical signal of a specific frequency. The frequency of oscillation is dependent on the applied electrical frequency to the crystal and the mass of the crystal. Therefore, the mass increases with the frequency of oscillation of the crystal changes due to the binding of chemicals. This resulting change can be measured electrically and to determine the additional mass of the crystal [6, 17]. Quartz is being used as a common piezoelectric material and the two types of mass-based sensors are bulk wave (BW) or quartz crystal microbalance (QCM) and surface acoustic wave (SAW) [6, 16, 129]. The main advantages of using mass-based include real-time monitoring, label-free detection, and simplicity of use. Nevertheless, some important drawbacks are lack of specificity and sensitivity, and excessive interference [4, 40].

1.2 Challenges in Biosensing

Biosensors are expected to play a very important role in “the medicine of the future” or “P4 medicine,” which is predictive, personalized, preventative, and participatory [130]. One of the best examples is the huge development in wearable biosensors (Table 1.1). Despite these advances, extensive efforts are still required to realize their full diagnostic potential. In this section, we will briefly discuss the main barriers for biosensors’ full transference and passing the “valley of death” in real application and market and the most recent developments to overcome them.

1.2.1 Market Barriers

1. Scalability:

Cost-affordability and reproducibility of biosensors in production highly depend on the industry capability to increase the number of devices per batch. With the ever-growing complexity of biosensors (many times depending on biomolecules, NPs or nano/microfabricated devices), their reproducible scalability is highly difficult. Reducing the dependence on highly complex systems and increasing the number of specialized pilot plants for production will increase the success of overcoming this issue.

2. Certification:

There are high regulatory barriers due to the strict international healthcare standards. Apart from the need for licenses on genes and molecules, new regulations are released. In Europe, Regulation (EU) 2017/745 establishes the frame on the clinical investigation and sale of medical devices for human use and it is full into force since 26 May 2021. This regulation included a stricter premarket review of high-risk devices, strengthened designation criteria for

Table 1.1 Examples of wearable biosensors. Adapted from [107]

Product	Company	Analyte/sample	Wearable platform	Monitoring mechanism	Current stage	Website
Smart contact lens	Google and Novartis	Glucose in tears	Contact lens	Electrochemistry	Last update in 2018; this project is now on hold	–
GlucoWatch	Cygnus Inc.	Glucose in ISF	Watch type	Electrochemistry	FDA approved but retracted from market	–
BioMKR,	Prediktor medical	Blood glucose	Wrist strap similar to a smart watch	Near infrared spectroscopy, bioimpedance	Last update in 2019; this project is now on hold	–
GlucoWise	MediWise	Blood glucose	Finger clip	Radio frequency	Two small-scale human studies recently carried out; more human tests ongoing	http://www.gluco-wise.com/
Freestyle libre	Abbott	Glucose in ISF	Patch	Electrochemistry	Commercially available and approved as well in US and EU; second version Freestyle Libre2 available	https://www.freestylelibre.us/
Dexcom G6 CGM	Dexcom	Glucose in ISF	Patch	Electrochemistry	Approved and commercialized in US and EU	https://www.dexcom.com/
GlucoTrack	Integrity applications	Blood glucose	Ear clip	Ultrasonic, electromagnetic, thermal waves	Type 2 diabetes, approved in EU	https://www.glucotrack.com/
Eversense	Senseonics	ISF glucose	Subcutaneous small stick implant	Fluorescence	Approved in EU and US	https://www.eversensedabetes.com/
NovioSense tear glucose sensor	NovioSense	Tear glucose	Small stick (spiral type) placed under the lower eyelid	Electrochemistry	Phase 2 clinical trials passed	http://noviosense.com/

notified bodies, improved traceability, as well as a risk-based classification system for In Vitro Diagnostic systems (IVDs). Time and budget investment needed to obtain those licenses and certifications are many times the biggest barrier to the full implementation of biosensors.

1.2.2 Technical Barriers

– Robustness:

Biosensors depend on a biorecognition element that binds to the target analyte. Those biomolecules are typically highly sensitive to pH, temperature, and salinity among other parameters that are highly variable in a human fluid or at POC. Over the years, this fact has greatly limited the robustness of biosensors and their transference to market. Recently, the development of biomimetic recognition elements has enabled great advances in this issue [131]. Nanozymes, synzymes, molecularly imprinted polymers (MIPs), nanochannels, and metal complexes such as metal-organic frameworks, with selective recognition capability but improved resistance and recyclability have been developed and integrated, mainly in electrochemical sensors to improve their robustness.

– Sample interference:

Typically, biological fluids composition is complex and the presence of a high concentration of salts, proteins, carbohydrates, and nucleic acids can compromise the biosensors' sensitivity, selectivity, and robustness. However, POC devices should be independent of complex sample preparation procedures such as centrifugation, filtration, or solid-phase extraction. Microfluidics have been applied to address the challenges of sampling and sample interference. Integration of sample preparation steps in modules that are compatible with automation or the same sensing device has been one of the raising trends in the last decades [132]. The incorporation of magnetic beads or nanoparticles for analyte preconcentration or solid-phase microextraction are clear examples of how miniaturization and automatization of processes can help to address the sample interferences.

– Power:

- Power consumption. Another important problem to face to use biosensors for innovative IoT and Big Data applications is to have energetically autonomous sensors for improving the accuracy/resolution of the measurement for given power consumption, to increase their operation time or allowing a “perpetual” operation. So, electronic sensors and their electronic interfaces need to be able to operate autonomously and wirelessly during a relatively long period of time from an embedded local power source. Unfortunately, batteries are most commonly based on lithium, which is scarce (particularly in Europe) and highly demanded, and systems for energy harvesting are still obsolete.
- Autonomy (energy harvesting systems and batteries). In relation to power consumption, the autonomy and the power consumption will define the power storage and/or supply requirements. POC biosensors consume energy in the sensing process (directly related to the number of measurements or

analytes detected), but as well in data processing and communication. Power sources can be based on batteries, and/or energy harvesting and storage devices such as biofuel cell or solar cells, and more recently based on a combination of sources [106, 133, 134]. Energy can be transferred wireless but biosensors can be designed to be self-sustainable incorporating their own biofuel cells based on the target analyte. A better energy-efficient biosensor can be also obtained by the optimization of the sampling frequency, data storage, processing, and communication.

– Fouling:

Unspecific adsorption of biomolecules and subsequent layers of biofluid components and/or microorganisms is one of the main reasons for decreased robustness and reliability of biosensors in a real scenario. For instance, the high concentrations of protein in saliva, including mucins and proteolytic enzymes, along with food debris, can lead to rapid biofouling of the oral cavity sensor through nonspecific adsorption at the transducer surface. These challenges can be addressed by developing perm-selective protective coatings that exclude macromolecules from the surface [106]. Recent advances have been applied for surface modification which minimizes surface fouling, including immobilization of polymers, self-cleaning coatings, incorporation of biocidal agents, and surface structuring. Surface functionalization, however, sometimes hinders or interferes with the sensor sensitivity. Recent reports include a new generation of surface functionalization that avoids fouling formation without compromising sensor signal, such as the use of zwitterionic-based materials [128].

1.3 Conclusions

In this chapter, we have discussed the fundamentals of biosensors focused on receptors (enzymes, antibodies, nucleic acid, cell, and aptamers), transducers (electrochemical, optical, and mass sensitive), and the main strategies for the immobilization of biomolecules onto surfaces. In the recent decade, a rapid growth in biosensing technology has been observed, at the research and product development level, becoming more versatile, robust, and dynamic. This growth has been produced mainly due to the development of new biorecognition elements and transducers, progress in miniaturization, the introduction of novel nanomaterials and nanostructured devices, microfluidics, on-chip electronics, sampling techniques, and novel anti-fouling surface chemistries, among others. Biosensors are versatile and powerful tools for POC applications, such as for the monitoring of treatment efficacy and disease progression, food control, drug discovery, environmental monitoring, and biomedical research. For instance, biosensors can be of most importance for POC testing, providing quick results in a cost-effective manner and allowing the rapid diagnostics of disease condition. In this regard, lab-on-a-chip technology has an important role in the development of POC and cancer biomarkers multi-target analysis, maintaining the precision and reliability of a laboratory analysis.

Acknowledgments The authors acknowledge the financial support from the Scientific and Technological Research Support System (SAICT)—Scientific Research and Technological Development Projects (IC&DT) from the Foundation for Science and Technology (FCT) and the Competitiveness and Internationalization Operational Program under Grant Agreement No. 030881 (POCI-01-0145-FEDER-029547). This work was supported by NANOCULTURE Interreg Atlantic Area project (EAPA_590/2018); ACUINANO Interreg POCTEP project (code 1843); Horizon 2020 project LABPLAS—Land-Based Solutions for Plastics in the Sea (101003954); SbDToolBox- Nanotechnology-based tools and tests for Safe-by-Design nanomaterials (NORTE-01-0145-FEDER-000047) supported by the North Portugal Regional Operational Programme (NORTE2020) under the PORTUGAL 2020 Partnership Agreement through the European Regional Development Fund (ERDF). LR-L acknowledges funding from FCT (Fundação para a Ciência e Tecnologia) for the Scientific Employment Stimulus Program (2020.04021.CEECIND). We would like to thank Dr. Miguel Spuch-Calvar for preparing the 3D illustrations used in Fig. 1.3.

References

1. Kirsch J, Siltanen C, Zhou Q, Revzin A, Simonian A (2013) Biosensor technology: recent advances in threat agent detection and medicine. *Chem Soc Rev* 42:8733–8768. <https://doi.org/10.1039/c3cs60141b>
2. Castillo J et al (2004) Biosensors for life quality design, development and applications. *Sensors Actuators B* 102:179–194
3. Walker JM, Rasooly A, Herold KE (2009) *Biosensors and biodetection*, vol 503. Humana Press
4. Barreiros dos Santos M (2014) Development of a multi-electrode impedimetric biosensor: detection of pathogenic bacteria and mycotoxins. University of Barcelona
5. Mallotra BD, Turner APF (2003) Advances in biosensors perspectives in biosensors, vol 5. Elsevier Science B.V
6. Velusamy V, Arshak K, Korostynska O, Oliwa K, Adley C (2010) An overview of foodborne pathogen detection: in the perspective of biosensors. *Biotechnol Adv* 28:232–254
7. Grieshaber D (2008) Electrochemical biosensors - sensor principles and architectures. *Sensors* 8:1400–1458
8. Nayak M, Kotian A, Marathe S, Chakravorty D (2009) Detection of microorganisms using biosensors - a smarter way towards detection techniques. *Biosens Bioelectron* 25:661–667
9. Rasooly A, Prickril B (2009) *Biosensors and biodetection methods and protocols*. Methods. Springer Protocols
10. Naresh V, Lee N (2021) A review on biosensors and recent development of nanostructured materials-enabled biosensors. *Sensors (Switzerland)* 21:1–35
11. Bhalla N, Jolly P, Formisano N, Estrela P (2016) Introduction to biosensors. *Essays Biochem* 60:1–8
12. Metkar SK, Girigoswami K (2019) Diagnostic biosensors in medicine – a review. *Biocatal Agric Biotechnol* 17:271–283
13. Sharma H, Mutharasan R (2013) Review of biosensors for foodborne pathogens and toxins. *Sensors Actuators B Chem* 183:535–549
14. Domínguez E, Narváez A (2005) Chapter 10. Non-affinity sensing technology: the exploitation of biocatalytic events for environmental analysis. In: *Biosensors and modern biospecific analytical techniques*, vol 44. Elsevier, pp 429–537
15. Vo-Dinh T (2008) *Micro and nanoscale biosensors and materials: biosensors and biochips*. Springer
16. Shinde SB, Fernandes CB, Patravale VB (2012) Recent trends in in-vitro nanodiagnostics for detection of pathogens. *J Control Release* 159:164–180

17. Vo-Dinh T, Cullum B (2008) Biosensors and biochips: advances in biological and medical diagnostics. *Fresenius J Anal Chem* 366:540–551
18. Zamora-Gálvez A, Morales-Narváez E, Mayorga-Martinez CC, Merkoçi A (2017) Nanomaterials connected to antibodies and molecularly imprinted polymers as bio/receptors for bio/sensor applications. *Appl Mater Today* 9:387–401
19. Hall RH (2002) Biosensor technologies for detecting microbiological foodborne hazards. *Microbes Infect* 4:425–432
20. Sinha A, Mugo SM, Zhao H, Chen J, Jain R (2019) Electrochemical immunosensors for rapid detection of breast cancer biomarkers. In: *Advanced biosensors for health care applications*. Elsevier. <https://doi.org/10.1016/B978-0-12-815743-5.00005-6>
21. Ragavan KV, Rastogi NK, Thakur MS (2013) Sensors and biosensors for analysis of bisphenol-A. *Trends Anal Chem* 52:248–260
22. Moína C, Ybarra G (2012) Fundamentals and applications of immunosensors. In: Chiu NHL (ed) *Advances in immunoassay technology*. IntechOpen
23. Skottrup PD, Nicolaisen M, Justesen AF (2008) Towards on-site pathogen detection using antibody-based sensors. *Biosens Bioelectron* 24:339–348
24. Byrne B, Stack E, Gilmartin N, O’Kennedy R (2009) Antibody-based sensors: principles, problems and potential for detection of pathogens and associated toxins. *Sensors (Basel)* 9: 4407–4445
25. Medyantseva EP, Khaldeeva EV, Budnikov GK (2001) Immunosenors in biology and medicine: analytical capabilities, problems, and prospects. *J Anal Chem* 56:886–900
26. Zhang X, Ju H (2008) Electrochemical sensors, biosensors and their biomedical applications. *Biosensors*. Elsevier
27. Ziegler C (2000) Cell-based biosensors. *Fresenius J Anal Chem* 366:552–559
28. Banerjee P, Bhunia AK (2009) Mammalian cell-based biosensors for pathogens and toxins. *Trends Biotechnol* 27:179–188
29. Weigum SE, Floriano PN, Christodoulides N, McDevitt JT (2007) Cell-based sensor for analysis of EGFR biomarker expression in oral cancer. *Lab Chip* 7:995–1003
30. Gupta N, Renugopalakrishnan V, Liepmann D, Paulmurugan R, Malhotra BD (2019) Cell-based biosensors: recent trends, challenges and future perspectives. *Biosens Bioelectron* 141: 111435
31. Marazuela D, Moreno-Bondi MC (2002) Fiber-optic biosensors—an overview. *Anal Bioanal Chem* 372:664–682
32. Yolken RH (1980) Enzyme-linked immunosorbent assay (ELISA): a practical tool for rapid diagnosis of viruses and other infectious agents. *Yale J Biol Med* 53:85–92
33. Mani V, Chikkaveeraiiah BV, Patel V, Gutkind JS, Rusling JF (2013) Ultrasensitive immunosensor for cancer biomarker proteins using gold nanoparticle film electrodes and multienzyme-particle amplification. *ACS Nano* 83:1–11
34. Ohnuki H, Honjo R, Endo H, Imakubo T, Izumi M (2009) Amperometric cholesterol biosensors based on hybrid organic–inorganic Langmuir–Blodgett films. *Thin Solid Films* 518:596–599
35. Amine A, Mohammadi H, Bourais I, Palleschi G (2006) Enzyme inhibition-based biosensors for food safety and environmental monitoring. *Biosens Bioelectron* 21:1405–1423
36. Malitesta C, Guascito MR (2005) Heavy metal determination by biosensors based on enzyme immobilised by electropolymerisation. *Biosens Bioelectron* 20:1643–1647
37. Zapp E et al (2011) Biomonitoring of methomyl pesticide by laccase inhibition on sensor containing platinum nanoparticles in ionic liquid phase supported in montmorillonite. *Sensors Actuators B Chem* 155:331–339
38. Liu H, Ge J, Ma E, Yang L (2018) Advanced biomaterials for biosensor and theranostics. In: *Biomaterials in translational medicine: a biomaterials approach*. Elsevier. <https://doi.org/10.1016/B978-0-12-813477-1.00010-4>
39. Van Dorst B et al (2010) Recent advances in recognition elements of food and environmental biosensors: a review. *Biosens Bioelectron* 26:1178–1194

40. Perumal V, Hashim U (2014) Advances in biosensors: principle, architecture and applications. *J Appl Biomed* 12:1–15
41. Lui C, Cady NC, Batt C, a. (2009) Nucleic acid-based detection of bacterial pathogens using integrated microfluidic platform systems. *Sensors* 9:3713–3744
42. Chua A, Yean CY, Ravichandran M, Lim B, Lalitha P (2011) A rapid DNA biosensor for the molecular diagnosis of infectious disease. *Biosens Bioelectron* 26:3825–3831
43. Bang J et al (2013) Development of a random genomic DNA microarray for the detection and identification of listeria monocytogenes in milk. *Int J Food Microbiol* 161:134–141
44. Trevino V, Falciani F, Barrera-saldaña HA (2007) DNA microarrays: a powerful genomic tool for biomedical and clinical research. *Mol Med* 13:527–541
45. Yang X-H, Kong W-J, Yang M-H, Zhao M, Ouyang Z (2013) Application of aptamer identification technology in rapid analysis of mycotoxins. *Chin J Anal Chem* 41:297–306
46. Luo X, Davis JJ (2013) Electrical biosensors and the label free detection of protein disease biomarkers. *Chem Soc Rev* 42:5944–5962
47. Song S, Wang L, Li J, Zhao J, Fan C (2008) Aptamer-based biosensors. *Trends Anal Chem* 27:108–117
48. Zourob M, Elwary S, Turner A (2008) Principles of bacterial detection: biosensors, recognition receptors and microsystems. Consultant. Springer
49. Zhang Z et al (2009) A sensitive impedimetric thrombin aptasensor based on polyamidoamine dendrimer. *Talanta* 78:1240–1245
50. Yang H, Ji J, Liu Y, Kong J, Liu B (2009) An aptamer-based biosensor for sensitive thrombin detection. *Electrochem Commun* 11:38–40
51. Wochner A et al (2008) A DNA aptamer with high affinity and specificity for therapeutic anthracyclines. *Anal Biochem* 373:34–42
52. Zhao J, Zhang L, Chen C, Jiang J, Yu R (2012) A novel sensing platform using aptamer and RNA polymerase-based amplification for detection of cancer cells. *Anal Chim Acta* 745:106–111
53. Lee YJ, Han SR, Maeng J-S, Cho Y-J, Lee S-W (2012) In vitro selection of Escherichia coli O157:H7-specific RNA aptamer. *Biochem Biophys Res Commun* 417:414–420
54. D’Orazio P (2003) Biosensors in clinical chemistry. *Clin Chim Acta* 334:41–69
55. Saletti-cuesta L et al (2020) Nanomaterials in biosensors: fundamentals and applications. *Sustain (Switz)* 4 64–69
56. Wang Y, Ye Z, Ying Y (2012) New trends in impedimetric biosensors for the detection of foodborne pathogenic bacteria. *Sensors* 12:3449–3471
57. Parida SK, Dash S, Patel S, Mishra BK (2006) Adsorption of organic molecules on silica surface. *Adv Colloid Interf Sci* 121:77–110
58. Heitz F, Van Mau N (2002) Protein structural changes induced by their uptake at interfaces. *Biochim Biophys Acta* 1597:1–11
59. Zhou H, Dill KA (2001) Stabilization of proteins in confined spaces. *Biochemistry* 40:1–5
60. Cosnier S (2003) Biosensors based on electropolymerized films: new trends. *Anal Bioanal Chem* 377:507–520
61. Love JC, Estroff LA, Kriebel JK, Nuzzo RG, Whitesides GM (2005) Self-assembled monolayers of thiolates on metals as a form of nanotechnology. *Chem Rev* 105:1103–1169
62. Hermanson GT (2008) Bioconjugate techniques. Academic Press
63. Gaviria-arroyave MI, Cano JB, Peñuela GA (2020) Nanomaterial-based fluorescent biosensors for monitoring environmental pollutants: a critical review. *Talanta Open* 2:100006
64. da Silva ETSG et al (2017) Electrochemical biosensors in point-of-care devices: recent advances and future trends. *ChemElectroChem* 4:778–794
65. Malekzad H, Sahandi Zangabadi P, Mirshekari H, Karimi M, Hamblin MR (2017) Noble metal nanoparticles in biosensors: recent studies and applications. *Nanotechnol Rev* 6:301–329
66. Zhang Y, Lyu H (2021) Application of biosensors based on nanomaterials in cancer cell detection. *J Phys Conf Ser* 1948:012149

67. Cho IH, Kim DH, Park S (2020) Electrochemical biosensors: perspective on functional nanomaterials for on-site analysis. *Biomater Res* 24:1–12
68. Holzinger M, Le Goff A, Cosnier S (2014) Nanomaterials for biosensing applications: a review. *Front Chem* 2:1–10
69. Su H et al (2017) Nanomaterial-based biosensors for biological detections. *Adv Heal Care Technol* 3:19–29
70. Wark AW, Lee J, Kim S, Faisal SN, Lee HJ (2010) Bioaffinity detection of pathogens on surfaces. *J Ind Eng Chem* 16:169–177
71. Sobiepanek A, Kobiela T (2018) Application of biosensors in cancer research. *Rev Res Cancer* 4:4–12
72. Damborský P, Švitel J, Katrlík J (2016) Optical biosensors. *Essays Biochem* 60:91–100
73. Chen YT et al (2020) Review of integrated optical biosensors for point-of-care applications. *Biosensors* 10:1–22
74. Kudlacek O, Gsandtner I, Ibršimović E, Nanoff C (2008) Fluorescence resonance energy transfer (FRET) sensors. *BMC Pharmacol* 8:A44
75. Tainaka K et al (2010) Design strategies of fluorescent biosensors based on biological macromolecular receptors. *Sensors* 10:1355–1376
76. Nawrot W, Drzozga K, Baluta S, Cabaj J, Malecha K (2018) A fluorescent biosensors for detection vital body fluids' agents. *Sensors (Switzerland)* 18:1–21
77. Shaoying L, Wang Y (2011) FRET biosensors for cancer detection and evaluation of drug efficacy. *Clin Cancer Res* 16:3822–3824
78. Girigoswami K, Akhtar N (2019) Nanobiosensors and fluorescence based biosensors: an overview. *Int J Nano Dimens* 10:1–17
79. Yang M et al (2020) Chemiluminescence for bioimaging and therapeutics: recent advances and challenges. *Chem Soc Rev* 49:6800–6815
80. Fereja TH, Hymete A, Gunasekaran T (2013) A recent review on chemiluminescence reaction, principle and application on pharmaceutical analysis. *ISRN Spectrosc* 2013:1–12
81. García-Campaña AM, Baeyens WRG (2000) Principles and recent analytical applications of chemiluminescence. *Analisis* 28:686–698
82. Babamiri B, Bahari D, Salimi A (2019) Highly sensitive bioaffinity electrochemiluminescence sensors: recent advances and future directions. *Biosens Bioelectron* 142:111530
83. Choi G, Kim E, Park E, Lee JH (2017) A cost-effective chemiluminescent biosensor capable of early diagnosing cancer using a combination of magnetic beads and platinum nanoparticles. *Talanta* 162:38–45
84. Zakir Hossain SM (2016) Enzyme-luminescence method: tool for real-time monitoring of natural neurotoxins in vitro and l-glutamate release from primary cortical neurons. *Biotechnol Rep* 9:57–65
85. Vdovenko MM, Hung CT, Sakharov IY, Yu FY (2013) Determination of okadaic acid in shellfish by using a novel chemiluminescent enzyme-linked immunosorbent assay method. *Talanta* 116:343–346
86. Calabretta MM et al (2021) Paper-based immunosensors with bio-chemiluminescence detection. *Sensors* 21:4309
87. Long F, Zhu A, Gu C, Shi H (2013) Recent Progress in optical biosensors for environmental applications. In: *State of the art in biosensors*. IntechOpen
88. Lazcka O, Del Campo FJ, Muñoz FX (2007) Pathogen detection: a perspective of traditional methods and biosensors. *Biosens Bioelectron* 22:1205–1217
89. Tudos AJ, Schasfoort RBM (1968) Introduction to surface plasmon resonance. *Time*
90. Konradi R, Textor M, Reimhult E (2012) Using complementary acoustic and optical techniques for quantitative monitoring of biomolecular adsorption at interfaces. *Biosensors* 2:341–376
91. Kim DM, Park JS, Jung SW, Yeom J, Yoo SM (2021) Biosensing applications using nanostructure-based localized surface plasmon resonance sensors. *Sensors* 21:1–27

92. Zhao J, Zhang X, Yonzon CR, Haes AJ, Van Duyne RP (2006) Localized surface plasmon resonance biosensors. *Nanomedicine* 1:219–228
93. Wang Y, Tang L (2015) Multiplexed gold nanorod array biochip for multi-sample analysis. *Biosens Bioelectron* 67:18–24
94. Dahlin AB, Tegenfeldt JO, Höök F (2006) Improving the instrumental resolution of sensors based on localized surface plasmon resonance. *Anal Chem* 78:4416–4423
95. Guo L et al (2015) Strategies for enhancing the sensitivity of plasmonic nanosensors. *Nano Today* 10:213–239
96. Sannomiya T, Vörös J (2011) Single plasmonic nanoparticles for biosensing. *Trends Biotechnol* 29:343–351
97. Li P et al (2020) Fundamentals and applications of surface-enhanced Raman spectroscopy-based biosensors. *Curr Opin Biomed Eng* 13:51–59
98. Szaniawska A, Kudelski A (2021) Applications of surface-enhanced Raman scattering in biochemical and medical analysis. *Front Chem* 9:296
99. George SD (2020) Surface-enhanced Raman scattering substrates: fabrication, properties, and applications. In: Inamuddin, Boddula R, Asiri AM (eds) *Self-standing substrates: materials and applications*. Springer International Publishing, pp 83–118. https://doi.org/10.1007/978-3-030-29522-6_3
100. Quarin S, Strobbia P (2021) Recent advances towards point-of-care applications of surface-enhanced Raman scattering sensing. *Front Chem* 9:714113
101. Abalde-Cela S et al (2010) Surface-enhancement Raman scattering biomedical applications of plasmonic colloidal particles. *J R Soc Interface* 7:S435–S450
102. Wang J, Chen Q, Belwal T, Lin X, Luo Z (2021) Insights into chemometric algorithms for quality attributes and hazards detection in foodstuffs using Raman/surface enhanced Raman spectroscopy. *Compr Rev Food Sci Food Saf* 20:2476–2507
103. ALS. ALS obtains FDA registrations. https://www.alsglobal.pt/noticias/ALS-obtains-FDA-registrations_1455
104. Pohanka M (2020) Colorimetric hand-held sensors and biosensors with a small digital camera as signal recorder, a review. *Rev Anal Chem* 39:20–30
105. Tanaka R et al (2006) A novel enhancement assay for immunochromatographic test strips using gold nanoparticles. *Anal Bioanal Chem* 385:1414–1420
106. Kim J, Campbell AS, de Ávila BEF, Wang J (2019) Wearable biosensors for healthcare monitoring. *Nat Biotechnol* 37:389–406
107. Daniels JS, Pourmand N (2007) Label-free impedance biosensors: opportunities and challenges. *Electroanalysis* 19:1239–1257
108. Tothill IE, Turner APF (2003) Biosensors. In: *Encyclopedia of food sciences and nutrition*, 2nd edn. Academic Press, pp 41–46
109. Karimi-Maleh H et al (2021) A critical review on the use of potentiometric based biosensors for biomarkers detection. *Biosens Bioelectron* 184:113252
110. Pisoschi AM (2016) Potentiometric biosensors: concept and analytical applications-an editorial. *Biochem Anal Biochem* 5:19–20
111. Vanarsdale E, Pitzer J, Payne GF, Bentley WE (2020) Redox electrochemistry to interrogate and control biomolecular communication. *ISCIENCE* 23:101545
112. Fang C, He J, Chen Z (2011) A disposable amperometric biosensor for determining total cholesterol in whole blood. *Sensors Actuators B Chem* 155:545–550
113. Yoo E, Lee S (2010) Glucose biosensors: an overview of use in clinical practice. *Sensors* 10: 4558–4576
114. Weibel MK, Bright HJ (1971) The glucose oxidase mechanism. *J Biol Chem* 246:2734–2744
115. Srivastava KR, Awasthi S, Mishra PK (2020) Biosensors/molecular tools for detection of waterborne pathogens. In: *Waterborne pathogens: detection and treatment*. Elsevier. <https://doi.org/10.1016/B978-0-12-818783-8.00013-X>
116. Materials I, Heidelberg SB (2012) Electrochemical methods. In: *Electrochemistry of insertion materials for hydrogen and lithium*. Springer. <https://doi.org/10.1007/978-3-642-29464-8>

117. Weber SG, Purdy WC (1979) Homogeneous voltammetric immunoassay: a preliminary study. *Anal Lett* 12:1–9
118. Felix FS, Baccaro ALB, Angnes L (2018) Disposable voltammetric immunosensors integrated with microfluidic platforms for biomedical, agricultural and food analyses: a review. *Sensors (Basel)*. 18:4124
119. Wang J (2006) Electrochemical biosensors: towards point-of-care cancer diagnostics. *Biosens Bioelectron* 21:1887–1892
120. Lisdat F, Schäfer D (2008) The use of electrochemical impedance spectroscopy for biosensing. *Anal Bioanal Chem* 391:1555–1567
121. Laschuk NO, Easton EB, Zenkina OV (2021) Reducing the resistance for the use of electrochemical impedance spectroscopy analysis in materials chemistry. *RSC Adv* 11:27925–27936
122. Guo X et al (2012) Carbohydrate-based label-free detection of *Escherichia coli* ORN 178 using electrochemical impedance spectroscopy. *Anal Chem* 84:241–246
123. Chen H et al (2005) Detection of immobilized on self-assembled monolayer (SAM) of alkanethiolate using electrochemical impedance spectroscopy. *Anal Chim Acta* 554:52–59
124. Escamilla-Gómez V, Campuzano S, Pedrero M, Pingarrón JM (2009) Gold screen-printed-based impedimetric immunobiosensors for direct and sensitive *Escherichia coli* quantisation. *Biosens Bioelectron* 24:3365–3371
125. Barreiros dos Santos M et al (2015) Label-free ITO-based immunosensor for the detection of very low concentrations of pathogenic bacteria. *Bioelectrochemistry* 101:146–152
126. Barreiros dos Santos M et al (2013) Highly sensitive detection of pathogen *Escherichia coli* O157: H7 by electrochemical impedance spectroscopy. *Biosens Bioelectron* 45:174–180
127. Barreiros dos Santos M et al (2019) Portable sensing system based on electrochemical impedance spectroscopy for the simultaneous quantification of free and total microcystin-LR in freshwaters. *Biosens Bioelectron* 142:111550
128. Zou Y et al (2021) Anti-fouling peptide functionalization of ultraflexible neural probes for long-term neural activity recordings in the brain. *Biosens Bioelectron* 192:113477
129. Leonard P (2003) Advances in biosensors for detection of pathogens in food and water. *Enzym Microb Technol* 32:3–13
130. Hood L, Friend SH (2011) Predictive, personalized, preventive, participatory (P4) cancer medicine. *Nat Rev Clin Oncol* 8:184–187
131. Romanholo PVV et al (2021) Biomimetic electrochemical sensors: new horizons and challenges in biosensing applications. *Biosens Bioelectron* 185:113242
132. Van Nguyen H et al (2019) Nucleic acid diagnostics on the total integrated lab-on-a-disc for point-of-care testing. *Biosens Bioelectron* 141:111466
133. Falk M, Shleev S (2019) Hybrid dual-functioning electrodes for combined ambient energy harvesting and charge storage: towards self-powered systems. *Biosens Bioelectron* 126:275–291
134. Kim H et al (2020) Electrical energy harvesting from ferritin bisrolled carbon nanotube yarn. *Biosens Bioelectron* 164:112318



How to Get Away with Gradients

2

Jordi Comelles, Óscar Castillo-Fernández, and Elena Martínez

Abstract

Biomolecular gradients are widely present in multiple biological processes. Historically they were reproduced in vitro by using micropipettes, Boyden and Zigmond chambers, or hydrogels. Despite the great utility of these setups in the study of gradient-related problems such as chemotaxis, they face limitations when trying to translate more complex in vivo-like scenarios to in vitro systems. In the last 20 years, the advances in manufacturing of micromechanical systems (MEMS) had opened the possibility of applying this technology to biology (BioMEMS). In particular, microfluidics has proven extremely efficient in setting-up biomolecular gradients which are stable, controllable, reproducible and at length scales that are relevant to cells. In this chapter, we give an overview of different methods to generate molecular gradients using microfluidics, then we discuss the different steps of the pipeline to fabricate a gradient generator microfluidic device, and at the end, we show an application example of the fabrication of a microfluidic device that can be used to generate a surface-bound biomolecular gradient.

J. Comelles (✉) · E. Martínez (✉)

Biomimetic Systems for Cell Engineering Laboratory, Institute for Bioengineering of Catalonia (IBEC), The Barcelona Institute of Science and Technology (BIST), Barcelona, Spain

Department of Electronics and Biomedical Engineering, University of Barcelona (UB), Barcelona, Spain

e-mail: jcomelles@ibecbarcelona.eu; emartinez@ibecbarcelona.eu

Ó. Castillo-Fernández

Biomimetic Systems for Cell Engineering Laboratory, Institute for Bioengineering of Catalonia (IBEC), The Barcelona Institute of Science and Technology (BIST), Barcelona, Spain

© The Author(s), under exclusive license to Springer Nature Switzerland AG 2022

31

D. Caballero et al. (eds.), *Microfluidics and Biosensors in Cancer Research*,

Advances in Experimental Medicine and Biology 1379,

https://doi.org/10.1007/978-3-031-04039-9_2

KeywordsMicrofabrication · Gradient · Microfluidics · bioMEMS · Nanotechnology

2.1 Introduction

Gradients are defined as “an increase or decrease in the magnitude of a property (e.g. temperature, pressure, or concentration) observed in passing from one point or moment to another” by The Oxford online dictionary [1]. Thus, gradients are all around in nature and, in particular, in living organisms. Biomolecular gradients are an important, evolutionarily conserved signaling mechanism to guide cell growth, migration, and differentiation within the dynamic, three-dimensional environment of living tissues. Gradients direct many biological processes such as cancer metastasis [2, 3], immune response [4], and neuronal growth [5].

Historically, various *in vitro* assays were developed to study the effects of biochemical gradients on cell behavior. For example, micropipettes, Boyden and Zigmond chambers, and hydrogels have been used to generate concentration gradients of soluble factors [6]. These gradient generation setups were and still are incredibly useful in multiple applications, such as understanding immune cell response to pathogens or screening the efficiency of antimetastatic drugs. However, these gradients are limited to soluble factors, they have short-range spatial action, and some of them are not fully compatible with microscopy techniques. These limitations hamper the amount of biological questions that can be addressed by such techniques [7].

Later, other methods to create biomolecular gradients, both on surfaces and in solutions, emerged. These include vapor diffusion [8], immersion technique applied to self-assembled monolayers [9], and microfluidics [10]. These techniques have the advantage of allowing a better control of the gradient length and shape, which is crucial in the development of graded interfacial zones that mimic transitions in heterogeneous tissues. The length scale over which a surface physicochemical property changes gradually characterizes each gradient. To this end, each gradient can be viewed as having a dual character. First, the length scale that is associated with the overall gradual variation of a given property on the sample: the inherent gradient length scale. And second, at length scales significantly smaller than the inherent length scale, the sample appears to exhibit a uniform property. The overall sample can then be considered as a collection or library of individual homogeneous specimens, each having a discrete value of a given property. This dual nature (discrete at the nano/microscale and continuous at the mesoscale) makes gradients a powerful tool for systematically studying various physicochemical phenomena, and, on the other hand, driving certain phenomena [11].

Therefore, if a gradient is envisioned as a drug screening platform, the sample must be large enough, and the gradient slope must be small enough so that the library possesses a uniform property at the size of an individual cell. Moreover, it is imperative that the characteristics of the individual library elements remain uniform

at the scale of the cell to obtain an acceptable uncertainty in the measured effect [12]. However, if one aims to use a gradient to drive a phenomenon that takes place at micrometric length scales, like cell migration, then the sample must change its properties at this very same length scale.

In this chapter, we will focus on the development of gradients with a length scale closer to the cell size using microfluidic technology. We will briefly cover the fundamentals of microfluidics, discuss the key aspects to consider when designing the device, introduce the different technical approaches, and finally present a step-by-step process to fabricate a fully functional microfluidic device to generate protein gradients.

2.2 Microfluidics to Generate Gradients

2.2.1 BioMEMS

Microelectromechanical systems (MEMS) are a collection of devices manufactured using techniques similar to those used to produce integrated circuits in microelectronics. MEMS cover a vast zoology of devices such as channels, valves, microreservoirs, micropumps, cantilevers, rotors, and sensors, among others [13]. These devices comprise dimensions ranging from hundreds of microns down to few micrometers and below, which are matching the length scale of cells and subcellular structures. Therefore, MEMS gave access to interact with biological process at a scale that was not possible before their appearance, giving rise to a completely new field known as BioMEMS.

BioMEMS devices have been applied to a wide range of applications, ranging from the measurement of the force exerted by a cell [14] to the sequencing of DNA [15] or measuring the mechanical properties of single molecules [16]. In particular, BioMEMS have fostered the appearance and growth of a whole new scientific and technological field such as microfluidics. Applications of microfluidics in biology, medicine, or chemistry have been developed; and it can be used for sorting, counting, labeling, mixing, and culturing cells or a combination of these functions in devices known as lab-on-a-chip [17, 18]. Microfluidic applications take advantage of the basic driving forces, mechanisms, and properties of microflows, which are very useful to perform the tasks listed above and to obtain molecular gradients with controlled shape at scales relevant to the cells.

2.2.2 Fundamentals of Microfluidics

The mechanical aspect of the flow, which is the motion of a liquid, is described by classical mechanics and hydrodynamics. For solid objects, their position and velocity are used to describe motion, while for fluids the velocity field becomes a more convenient quantity. This means that we are not looking at the velocity of one particular “fluid particle,” but instead we look at the velocity of the fluid at a certain

region in space. If we imagine a constant flow rate within a tube, the velocity field should be also constant. But if the tube has a narrow region, the liquid needs to accelerate to go through it, in order to maintain an overall constant flow rate. Therefore, a particular fluid particle, which would always be subjected to Newton's second equation, may experience acceleration, even if the velocity field is steady. The acceleration in a steady flow experienced by the fluid particles is the result of forces acting among them. These forces are usually caused by the pressure and the viscosity of the fluid. The equation that relates these elements (velocity fields \vec{v} , pressure P , and viscosity η) is the Navier–Stokes' equation.

$$\rho \left(\frac{\partial \vec{v}}{\partial t} + \vec{v} \cdot \nabla \vec{v} \right) = -\nabla P + \eta \nabla^2 \vec{v}$$

When the Navier–Stokes' equation is rearranged in its dimensionless form, it only depends on one parameter,

$$\frac{\rho v_0 L_0}{\eta} \left(\frac{\partial \vec{v}}{\partial t} + \vec{v} \cdot \tilde{\nabla} \vec{v} \right) = -\nabla \tilde{P} + \tilde{\nabla}^2 \vec{v}$$

with, $Re = \frac{\rho v_0 L_0}{\eta}$ called the Reynolds number.

If the Reynolds number is large ($Re \gg 1$), the equation is dominated by the left side, which describes inertia. Due to the non-linear term $\vec{v} \cdot \tilde{\nabla} \vec{v}$, the behavior of the flow in a “high Reynolds number mode” is chaotic (turbulent flow). Alternatively, if Re is low ($Re \ll 1$), the contribution of the inertial part can be neglected, and the equation is dominated by pressure and viscosity terms, which correspond to the laminar flow regime. In the case of microfluidic channels, because of their small dimensions, the Reynolds numbers are typically much smaller than 1. Then, the system presents no turbulence, and it is in the *laminar regime*. This fact has important consequences that impact directly on the potential applications of microfluidic systems: mixing between two fluids only happens due to diffusion, which is a slow process. As a consequence, different fluids do not initially mix in a microfluidic channel, since mixing only occurs by diffusion at the interface between them. Mixing will only appear when advancing along the length of the channel, and to accelerate this process, long microfluidic channels with serpentine shapes are needed.

In a microfluidic channel, under certain conditions, the flow rate is proportional to the pressure difference at the channel ends and to a parameter depending on the channel geometry and viscosity. The relation between the flow and pressure difference is analogous to the Ohm's law in electronics, which describes the proportionality between current and a voltage difference, and the proportionality parameter is called “hydrodynamic resistance.” Also, the solution of the Navier–Stokes' equation under these circumstances results in a parabolic velocity profile, with velocity close to zero next to the channel walls. Therefore, at low Reynolds number, laminar regime with limited diffusion, and parabolic velocity profiles with

velocity close to zero next to the walls, two streams introduced into a microfluidic channel will flow side by side and the width of each stream will be proportional to their respective flows.

All these properties of microflows will be of paramount importance to apply microfluidics to obtain molecular gradients. Below, we describe the most common microfluidic platforms to generate gradients.

2.2.3 Gradient Generation Platforms

Several microfluidic devices have been used to generate gradients suitable for cell biology experiments. The three most common are the (1) convection mixing-based gradient generators, (2) the laminar flow diffusion-based gradient generators, and (3) the static diffusion-based gradient generators.

In convection mixing-based gradients, a network of serpentine-shaped microchannels with multiple junctions is used to create a series of mixtures between a reagent and a buffer solution (Fig. 2.1a). First introduced by Jeon [10], it relies on the mixing of the two solutions in serpentine-shaped channels, the even distribution

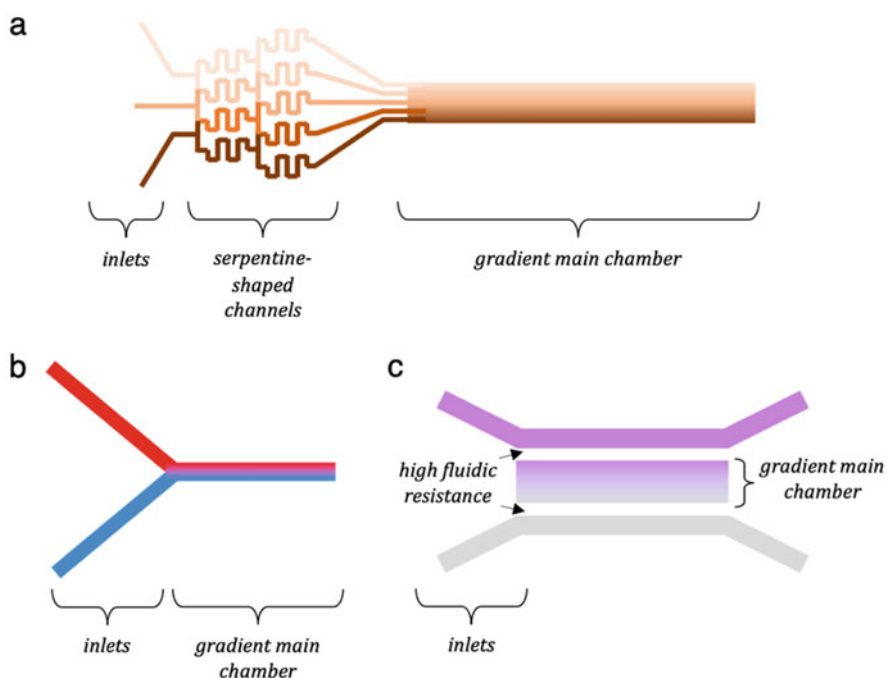


Fig. 2.1 Schematics of the most common microfluidic gradient generator devices. **(a)** Convection mixing-based gradient generator with the inlet, the serpentine and the main channel indicated. **(b)** Laminar flow diffusion-based gradient generator. **(c)** Static diffusion-based gradient generator with the two lateral channels and the gradient chamber where no shear stress is present

of flows due to equivalent hydrodynamic resistance in the joint points, and the laminar regime of the fluid when entering the main chamber. The gradient created is perpendicular to the direction of the flow.

Laminar flow diffusion-based gradient generators use simple Y-shaped channel structures (Fig. 2.1b) to flow two different solutions that conflate side by side in the main channel due to the effect of the laminar regime [19]. It relies on the slow diffusion-driven mixing at the interface of the two liquids to generate a gradient at a distant region of the joint of the Y-shaped channel. The gradient created is perpendicular to the direction of the flow as well. This gradient generation platform has a simple structure and is very easy to fabricate. Moreover, the length of the gradient generated can be established at the length scale of single cells and the gradient shape is very stable over time and controllable. However, since it requires constant flow to be maintained, a shear stress is created, and it will affect cells in the channel during the experiment. These limitations can be overcome by using Y-shaped channels and laminar flow regime to create gradients of surface-bound proteins [20, 21], as we will discuss later in the final section of this chapter.

Finally, static diffusion-based gradient generators can also generate a stable gradient while avoiding the undesired effects of shear stress on cells [22]. These systems consist of two external channels, one for the solution 1 and one for the solution 2, which are connected by a section with high fluidic resistance (a set of narrow channels, a membrane, or a hydrogel) (Fig. 2.1c). This design reduces the effects of shear stress and can generate a wide range of gradient profiles and shapes; however, it has limited dynamic control of the gradient since it relies on passive diffusion through the high resistance section.

Altogether, there are multiple designs and approaches to generate molecular gradients using microfluidic devices. Which of them will be more suitable will depend on the application envisioned.

2.3 Things to Consider when Planning your Chip

There are different approaches to obtain functional microfluidic devices for gradient generation and characterization. One direct way is the *layer-by-layer approach*, to obtain a microfluidic device by the addition in a stack, of different elements combined [23]. Each layer consists of a material with a specific hollow design and a given thickness that could be performed by using cutting tools. Then, by stacking all the layers together, the complete chip is assembled (Fig. 2.2a). Another approach is the *replica molding* [24]. The typical pipeline to produce a microfluidic chip to generate gradients with this method follows the subsequent steps: (1) chip design, (2) mold production, (3) replica molding and (4) bonding (Fig. 2.2b). To select one of these approaches, there are several aspects that need to be considered before generating a molecular gradient: what application is it intended for, which are the equipment and facilities that are available, what materials will suit the best for the intended application, and in which conditions the experiment will be performed, among them.

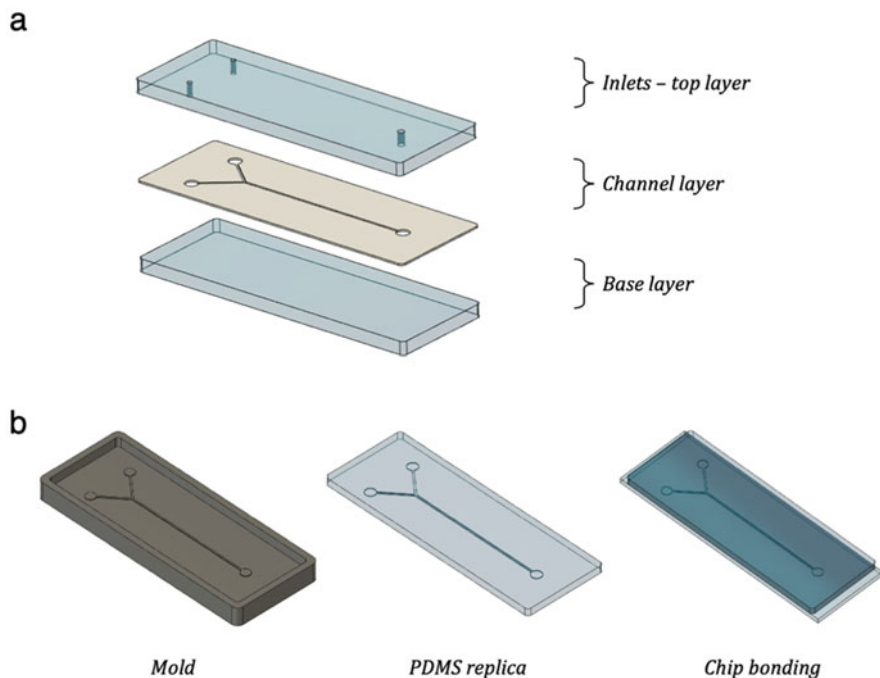


Fig. 2.2 Approaches to obtain a functional microfluidic device. (a) Layer-by-layer approach and (b) traditional replica-molding approach

In terms of protein or molecular gradients, we can think of two main categories: soluble gradients or surface-bound gradients. This first choice will have an important impact on the *chip design*. If the biological question that we want to address involves a gradient of *soluble molecules*, we should select a chip design that generates such type of gradient. Convection mixing-based, laminar flow diffusion-based, and static diffusion-based gradient generators can be used. Among them, we may favor one or another depending on the degree of dynamic control we aim at, and the amount of shear that can be present in the experiment. Lately, static diffusion-based devices are becoming the gold standard, moreover since commercial products are available [25]. In case we envision a *surface-bound gradient*, such as the ones that lead to *haptotaxis*, also all the types of gradient generators listed above can be used, although a more detailed knowledge about the kinematics of protein or molecule adsorption will be required [20, 21]. Moreover, for this type of gradients, shear stress will not be an issue, since the gradient can be formed prior to cell seeding, and the fluid flow can be stopped after it is formed.

The second thing that we must take into consideration when planning a microfluidic chip to generate a gradient is what resources we do have available. Those resources will constrain the method of choice to fabricate the *mold*. Traditionally, molds for gradient generators were fabricated using microfabrication

techniques. This involved the usage of specialized equipment and facilities (clean rooms and mask aligners). However, rapid prototyping systems such as milling machines can be used if the design has the smallest features at the $\approx 100 \mu\text{m}$ range. Currently, the widespread use of 3D printers has opened the possibility of producing fast and cheap molds for microfluidics.

Once the mold is obtained, we will have to select the material to use for the microfluidic chip. The most common material employed is the polydimethylsiloxane (PDMS) elastomer. It is biocompatible and it can faithfully replicate sub-micrometric features with no need of specialized equipment. Alternatively, thermoplastics can be used. However, to conform the thermoplastic with the mold, we will need to use specialized embossing equipment. Due to its simplicity of usage and handling, PDMS is the most popular material for the fabrication of microfluidic chips.

Finally, the different options to seal the chip should be considered. Which one is the best will depend on the application and the materials chosen. PDMS microfluidic chips are normally irreversibly bonded to the underlying glass substrate after oxygen plasma or Corona activation. This type of bonding is especially advantageous when the experiment is performed inside the chip. When alternative materials are used (either for the chip or the substrate) or when a reversible bonding is required (the need of detaching the substrate from the chip after the gradient is formed), alternative methods must be considered. Several options are available: irreversible thermal bonding (when the chip and the substrate are made of thermoplastics) or reversible mechanical bonding (when the chip and the substrate are sealed mechanically).

In the next sections, the different options that have been succinctly described above will be discussed in detail.

2.4 Chip and Mask Design

The first stage of the process to fabricate a microfluidic gradient generator is the design of the chip. Here we will define the *shape* of the chip, the different *inlets and outlets* of the device, and the *sizes for each channel*. In addition, we will make sure that the *hydrodynamic resistances* drive the flow according to what we aim. At this stage, it can be extremely useful to use a software to simulate the behavior of the chip. There we can typically load the chip design, define the inlets, outlets, and walls, the equations that rule the dynamics of the flow, the diffusion of the species, and introduce the physical parameters that match the ones in our experiments. As result of the simulation, we will obtain the predicted velocity fields and concentration profiles at different positions inside the chip (Fig. 2.3a). By doing so, we can easily readjust the chip design to obtain the desired outcome if needed.

Once we settle the chip design, we will generate a CAD (or equivalent) version. At this point, we should take into consideration some basic rules to finalize the design:

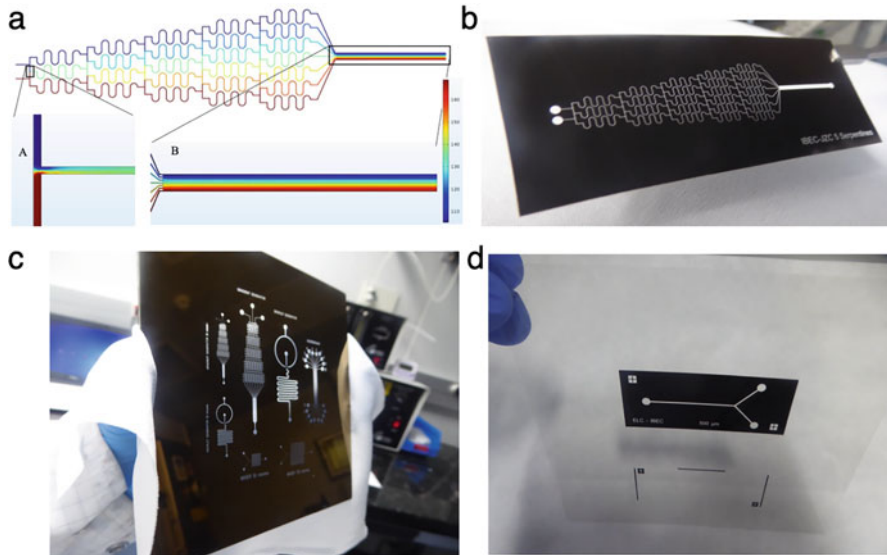


Fig. 2.3 Chip and mask design. (a) COMSOL simulation of a mixing-based gradient generator. (b) Acetate mask of a mixing-based gradient generator. (c) Chromium mask with multiple microfluidic device designs to optimize processes and reduce costs. (d) Masks with positive and negative polarity printed on the same acetate film

1. We must ensure that we add *alignment motifs* to the design to align the different layers of the chip, if needed.
2. We will check that the *inlet* and *outlet* channels have enough room to punch the holes to allow the tubing connections. This is typically done by adding a circular reservoir at the end of the inlet (outlet) channel. Such circular region should be large enough to allow the punching of a hole where the tubes for inflow (outflow) will be connected.
3. *Aspect ratios* lower than 1:10 (height:width) should be avoided. If we generate channels that are more than 10 times wider than taller, they may collapse (the roof of the channel will attach to the substrate). This applies mainly to PDMS microfluidic chips.
4. Adding *tolerances* to the design is highly recommended. By incorporating sufficient tolerances, we will ease the alignment among the motifs at the different layers. This means that the device should be designed to function properly despite certain alignment errors in all directions.

When the chip design is finalized, it is ready to be loaded into the 3D printer or the rapid prototyping device to generate the mold. On the contrary, if we use photolithography to generate the mold, the design of the chip must be translated into a mask.

The mask is the element that will let you imprint the chip design on the photosensitive resist used during photolithography. The shape of the design on the photomask will be transferred to a thin film of a light-sensitive chemical material

(Fig. 2.3b). The dark regions of the mask will prevent the light to pass through (UV light is typically used and the process is known as UV-photolithography), while the transparent regions will allow it. The resist will undergo a different chemical alteration depending on whether it has been exposed to light or not. Then, a series of chemical treatments etches the exposed/non-exposed part of the positive/negative resist. Through this process, it is possible to obtain a well-defined mold with motifs in the micrometric range.

There are two main options for UV-photolithography masks: *chromium masks* and *plastic masks*. The first type consists of a quartz glass covered with a thin chromium layer. Through a series of technical processes, the design is transferred to the chromium layer creating transparent and opaque regions on it. Chromium masks have an excellent spatial resolution but are significantly more expensive than plastic masks. This second type of masks consist of transparent plastic sheets with the design printed on them with black ink. They are fairly affordable and sufficiently resolved for features $\approx 10 \mu\text{m}$.

When preparing the file with the mask design to be submitted to the company that will print it, there are few things that should be taken into account.

1. Prepare the mask in a file format accepted by the supplier. CAD files or CleWin files are generally accepted.
2. The motifs of the mask will be transferred to a silicon wafer. Try to use a layout that has the size of the wafer that will be used. Dedicated software has pre-established templates for wafers of standard sizes.
3. Use a resolution (dots per inch) according to the one set by the supplier.
4. Try to fit as much designs as possible in one wafer, while leaving enough space between them to safely retrieve their replicas (Fig. 2.3c). Also, make sure that your designs do not overlap the outer region of the wafer (around 5 mm next to the edge), since defects may appear during spin coating of the photoresist in this area.
5. Make sure that your mask polarity (positive or negative masks (Fig. 2.3d)) matches the needs of the resist that will be used in the microfabrication process (positive or negative resist).

2.5 Fabrication of the Mold

The first step to produce a microfluidic chip is the *fabrication of the mold*. As mentioned in the previous section, there are three main approaches: UV-photolithography, 3D printing, and micro milling.

In *UV-photolithography*, a photosensitive resist is spun coated over a substrate, typically a silicon wafer. The spin coating process will define the thickness of the resist coating and therefore the heights of the structures on the mold. Then, by using a mask aligner, the resist is exposed to UV light. Exposure is not even, since the light passes through the mask that contains the chip design. The resist undergoes a series of chemical reaction upon light exposure, and the shape of the mask will be

transferred to it. For a negative resist, the exposed regions will crosslink and remain on the mold. On the contrary, for positive resists the exposed regions will be removed after the application of a developer. As a result, a mold with the shape of the mask and the thickness of the resist layer will be obtained.

3D printers, as mentioned above, can be used as well to fabricate molds. There are two main 3D printer approaches, which are both additive manufacturing approaches: (1) Fused Deposition Modeling (FDM) and (2) stereolithographic techniques. FDM printers consist in the controlled and continuous deposition of a fused filament, generally thermoplastic. The position on the x , y , and z coordinates and the displacement of the extruder head allow the control of the filament deposition. The addition of several filaments creates the 3D model. Among stereolithographic techniques, the most common is the Digital Light Processing (DLP) technique. DLP printers produce the solidification of thin layers of a photo-sensitive resist in a layer-by-layer process. Each of these solid layers can have a specific and independent appearance by the digital control of the light exposure. The additive sum of different layers gives shape to 3D objects. Both techniques are suitable to build a mold, however, the DLP printers generate smoother surfaces than FDM printers.

In the case of *Computer Numeric Control (CNC) micro milling*, it is a subtractive process that consists of removing material from a thermoplastic or metallic bulk with the shape of the negative of our design. In the case of a microfluidic chip, the micro milling process would remove most of the material, resulting in a flat surface with the topographical shape of the channels.

2.6 Fabrication of the Microfluidic Chip

As mentioned in Sect. 2.3, there are two main strategies that can be used to fabricate a fluidic device. The first one is the replica-molding approach: by using a mold where the channels are defined, the design can be replicated as many times as we want. The second one is a mold-less approach: the addition, layer by layer, of different sheets which combined to generate a microfluidic device, with each layer consisting of a material that could be shaped by using machining techniques or molding processes. In this section, we discuss these two approaches with more detail.

2.6.1 Replica-Molding Techniques

Once we get the mold, which approach is the optimal to fabricate the microfluidic chip will depend on the materials selected, and the equipment we do have available. Below, we describe in more detail two replica-molding techniques, focusing specifically on the strategies employing optically transparent materials. These materials are compatible with standard microscopy techniques, which is of paramount importance in biology-related applications.

2.6.1.1 Hot Embossing of Thermoplastics

Thermoplastics are polymeric materials that become adaptable above a specific temperature, named as glass transition temperature (T_g), and when cooling down below T_g they become solid again. This property makes these materials very suitable for microfluidic applications. Moreover, thermoplastics such as polystyrene (PS) or poly(methyl methacrylate) (PMMA) are optically transparent, cheap, chemically stable, and biocompatible, which make them a solid option to be used for BioMEMS applications. Because of their mechanical properties, the features of a mold can be easily and faithfully transferred to the surface of these materials. Therefore, they are good candidate materials for the fabrication of microfluidic chips using hot embossing in a rapid prototyping manner.

The method of fabricating microfluidic channels by hot embossing consists in the transfer of a structure from a hard mold onto the surface of the polymer using an equipment that controls the temperature and the pressure necessities for the printing procedure. The surface of the thermoplastic polymer is brought into contact to the structured mold. Then, the mold-substrate sandwich is heated above the glass transition temperature of the polymer, so that its Young's modulus and viscosity decrease and it can flow. Simultaneously the pattern on the mold is pressed into the softened polymer, filling the gaps on the mold surface. After cooling the whole system and releasing the pressure, the replica can be peeled off the mold.

2.6.1.2 Micro Molding with PDMS

PDMS is a hydrophobic material widely used in the BioMEMS field. Among many reasons, it is gas permeable, biocompatible, and transparent. PDMS is a stable silicone elastomer that behaves as an elastic material at physiological temperatures ($\approx 37^\circ\text{C}$) because its glass transition temperature is very low ($T_g \approx -120^\circ\text{C}$). It is suitable to replicate microstructures from molds generated by soft lithography, which consists of casting PDMS against a patterned mold.

For soft lithography applications, the PDMS pre-polymer is mixed with a cross-linker (typically in a ratio 1:10 cross-linker: pre-polymer), degassed, and poured onto the mold. The pre-polymer/cross-linker mixture will fill all the cavities of the mold easily, thanks to its viscous nature and the slow dynamics of the cross-linking process. Eventually, the polymer crosslinks and achieves its characteristic elastic nature. The PDMS can then be peeled off the mold, resulting in an elastic solid material that is shaped complementary to the structures presented on the surface of the mold.

PDMS can be easily cut and punched, which makes it very convenient for the setup of microfluidic chips. In addition, PDMS can faithfully replicate submicron structures, so it has many applications beyond the production of microfluidic chips.

PDMS, SYLGARD[®] 184 Silicone, can be found in most distributors of chemical products. Regarding punchers, they can be found in different suppliers, we recommend to use *Biopsy Punches*, which are available in a large variety of sizes and are very robust.

2.6.2 Mold-Less Technique: Layer-by-Layer

A microfluidic channel can be seen as a stack of layers, the layer with the base of the channel, the layer with the lateral walls of the channel and the layer with the roof of the channel. Thus, a chip can be built by stacking several layers that, if designed appropriately, results in a device through which liquids can be perfused. This approach does not require the use of molds and relies on rapid prototyping techniques, such as micro milling and cutting tools, which are described next.

Through laser cutting, parts of the bulk materials are removed from a thermoplastic sheet, creating holes with the shapes needed (for example, the microfluidic channel). Then, this layer is stacked with additional sheets acting as the base or the roof of the microchannel, which can also contain hollow structures (inlet and outlet reservoirs, for example). The assembled structure forms the final chip. A similar procedure, known as *xurography*, is followed using a cutter plotter. In this case, a razor, which is more suitable for silicone materials and paper, is used instead of a laser.

This approach has the advantage of skipping the mold fabrication. However, how the stack is assembled to seal the channel without leakage is a very important step to be considered in these fluidic devices. It will be critical to select properly the materials to use, how the different layers will bond together, and which are the chemical requirements to do so. Moreover, this approach brings along a higher complexity in the mask design, since a single mask may need to be prepared for each layer, a precise alignment may also be required for the correct function of the microfluidic gradient generator.

2.7 Bonding

The channels obtained, whether from replica molding or through layer-by-layer, are open structures that need to be closed to function as microfluidic channels. This sealing process should ensure that the dimensions and shape of the channels are not altered and that no clogging is produced. Therefore, this is a critical step, and the best approach will depend again on the needs of our device, the materials used, and the equipment that we have available.

We can define two main bonding categories: reversible and irreversible bonding. Reversible bonding implies that the different elements can be separated again without damaging any of them, contrary to irreversible bonding, where some potential damage might happen. Therefore, if we aim at creating a surface-bound gradient to be used outside the chip, we will need to choose a reversible bonding. On the contrary, if the whole experiment is going to take place inside the chip, an irreversible bonding can be used. Below, we review the most common bonding strategies.

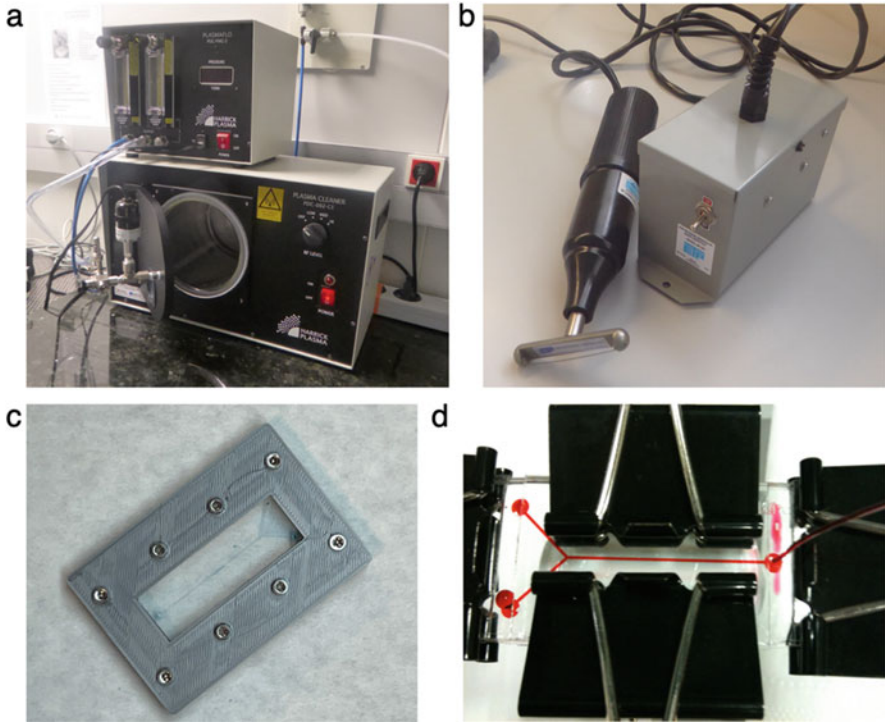


Fig. 2.4 Bonding methods. (a) O_2 plasma equipment and (b) corona device for irreversible PDMS—glass bonding. (c) 3D printed clamping setup and (d) paper clip arrangement for reversible PDMS—glass bonding

- *Oxygen Plasma*

One of the most common approaches in microfluidics is using a glass substrate to seal a PDMS chip. The elastomer adheres reversibly to the glass; however, this adhesion is weak and cannot sustain high flow rates. To create stronger adhesions, both the glass and the PDMS can be transiently activated with oxygen plasma treatment (Fig. 2.4a). This will generate Si-OH groups on both surfaces that, when brought together, will react forming Si-O-Si covalent bonds. It is an easy method to produce channels that can sustain high flow rates without leakage.

- *Corona Treatment*

The working principle of the corona treatment is the same as the oxygen plasma, creating the same type of irreversible bonding. In this case, the equipment needed is simpler (Fig. 2.4b), but the activation of the surfaces is less even than the one achieved with plasma treatments. This results in a higher uncertainty in the outcome.

- *Solvent Bonding*

In case the chip is not fabricated with PDMS and glass but formed by two parts made of thermoplastic polymers, we can use solvent bonding. This approach

takes advantage of the solubility of some thermoplastics to specific solvents. The polymeric chains at the chip surfaces interpenetrate through diffusion at the interface, thus resulting in a strong irreversible bonding between the two parts of the chip after solvent evaporation. However, this technique has the drawback of potential breakage points if the solvents do not completely evaporate.

- *Adhesives*

Bonding can be achieved by placing an adhesive sheet in between the two layers that need to be attached. These adhesive layers can be activated by pressure or temperature. For example, polyethylene terephthalate foils covered with acrylic glues at both sides become activated by pressure and are very useful to bind different layers of a chip.

- *Glues*

Glues are based on chemical reactions at the interface between the two parts of the chip. The gluing substance is placed at the interface and the reaction can be mediated by evaporation, temperature, or UV light. It is mainly an irreversible approach, although it may change depending on the type of glue selected. Typical glues are epoxy resist or acrylates.

- *Thermal Bonding*

When thermoplastics are used to build the microfluidic chip, direct thermal bonding is a suitable option. It is an irreversible method that follows the same principle that hot embossing technique: above the glass transition temperature, thermoplastics become liquid. So, the two sides of the interface are heated up to the T_g while controlled pressure is applied. This process leads to the interpenetration of polymer chains of the two bulks that become interconnected when the thermoplastic re-solidify as the temperature decreases. However, it requires a fine-tuning of the parameters of the process to avoid the appearance of defects in the shape of the channel or clogging.

- *Clamping*

The most common reversible bonding is clamping. In this approach, the two sides of the interface are held in contact and sealed by using mechanical force. It can be performed by using screws (Fig. 2.4c) or simple paper clips (Fig. 2.4d). The critical point in this approach is to ensure the even distribution of pressure over the interface to avoid non-uniform deformations of the channels or leakage due to low stress resistance.

2.8 Tube Connections

To flow liquid through the microfluidic chip, we must set up proper fluidic connections between the chip inlets and the syringes or fluid reservoirs. Although the type of connection will depend on the material used to produce the chip, the tubing used is usually made of a material compatible with autoclave.

Typical tubing materials are platinum-cured silicone, peroxide doped silicone or polytetrafluoroethylene (PTFE), which are transparent or translucent materials that can sustain autoclave process.

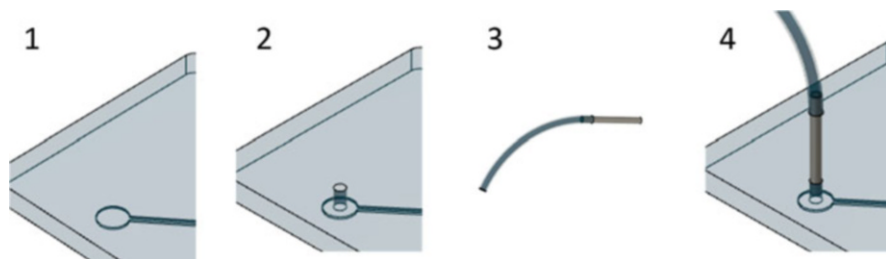


Fig. 2.5 Typical steps for tube connection. First, a hole is punched on the reservoir (1, 2), then the metallic cannula is applied inside the silicone tube (3), and finally, the cannula is inserted in the hole drilled on the PDMS (4)

Table 2.1 Relation of different cannula sizes with the recommended internal tube diameter and punches. (OD: outer diameter; ID: inner diameter)

Needle gauge	Cannula OD	Tube ID HelixMark [®] /Masterflex [®]	Punch
16G	1.65 mm	1.47 mm / 1.42 mm	1.5 mm
18G	1.27 mm	1.02 mm / 1.14 mm	1 mm
20G	0.9 mm	0.76 mm / 0.89 mm	0.75 mm
23G	0.64 mm	0.51 mm / 0.51 mm	0.5 mm

To set the tube connections, the inlet hole must have a diameter smaller than the outer diameter of tube selected, this difference depending on the materials used. Typically, we will proceed following the next steps: (1) drill a hole on the chip, (2) apply a metallic cannula inside the silicone or PTFE tube, and (3) apply the cannula to the hole on the chip (Fig. 2.5).

To create a hole on the chip, we can use different options depending on the material of the chip. For PDMS devices, a puncher can be used. For PMMA devices, holes can be drilled on the chip surfaces using drillers. As mentioned above, the diameter of these holes must be in accordance with the outer diameters of the cannulas and the tubes. In Table 2.1, we present a short relation of different cannula sizes with the recommended internal tube diameter and punches to perform on the PDMS insert.

For PDMS devices, we can take advantage of their elastomeric nature to tighten the tubing connection without any adhesive, simply by introducing the tube a few millimeters inside the PDMS body. That kind of connections are the simplest ones and can resist high local pressure if the PDMS device is thick enough. Moreover, using PTFE tubes, we could directly apply the tube on the PDMS skipping the metallic cannula as PTFE is rigid enough to sustain the forces applied by the PDMS [26]. In this case, the outer diameter of the tube rather than the one of the cannula should be larger than the diameter of the hole.

Tubes mentioned in Table 2.1 are *HelixMark[®]* and *MasterFlex[®]*. They are available at several distributors and providers such as: *Cole-Parmer[®]*, *IDEX Health and Science*, *Nordson Medical*, or *Freudenberg Medical*. The cannula, different

connectors and other elements can be found in the catalog of those providers as well. The different punch sizes are available as Biopsy Punches on different distributors, as mentioned above. There are some companies with a specific catalog of accessories and tools dedicated to microfluidics and related: *Darwin microfluidics* and *Microfluidic Chip-Shop*.

2.9 Application Example

In this final section, we will describe the process to fabricate a Y-shaped microfluidic device that can be used to generate diffusion gradients [19] or surface-bound gradients [20, 21]. We will fabricate the chip with PDMS replica molding and use mechanical bonding to seal it. For this example, we selected this approach since it is simple, versatile and it does not require complex equipment or specialized infrastructure (such as the one found in a clean room).

The microfluidic channels will be 500 μm in width and 200 μm in height. Since these dimensions are faithfully achieved by 3D printing, we will use this method to generate the mold. The mechanical bonding will be performed by screwing two 3D printed holding pieces, such as the one depicted in Fig. 2.4c, which were designed with the dimensions of a multi-well plate to fit a microscope stage. Finally, the tubing and their connection to the chip and to the syringes will be performed with metallic cannulas and luer connectors, respectively.

The 3D designs for the mold and the mechanical bonding presented in this example can be downloaded at: <https://github.com/BiomimeticsLab/Chapter-Gradients>.

2.9.1 Chip Design

As mentioned above, for this example we selected a simple Y-shaped microfluidic channel. We generated a 3D model of the chip using *FUSION 360 (AutoDesk)* software.

Our design consists of two inlet channels of 500 μm in width and 9 mm in length that converge into a main channel with an angle of 40 degrees. The main channel has 500 μm in width and 70 mm in length. At the end of each channel, we placed circular reservoirs to host the tubing connections for the inlets and outlets. These reservoirs are 2 mm in diameter.

Since the minimum dimensions of this design are compatible with the lateral resolution limit of a digital light processing (DLP) 3D printer, we decided to use this technique to produce the mold. Because of this, we had to define the height of the channels in the design as 200 μm (in classical microfabrication, the height is set during the spin coating steps of the UV-photolithographic process). Note that vertical resolution for the DLP 3D Printer technology strongly depends on the relation between the resist and the energy dose for cross-linking. Therefore, a previous characterization process is needed.

It is important that this height fulfills the criteria for aspect ratios defined in Sect. 2.4. In the present example, the wider structure will be the diameter of the inlet/outlet reservoir, which should be not more than ten times the height of the chip (2 mm: 200 μm). However, experimentally, the final aspect ratio achieved was close to 15 due to the variability of the vertical resolution in the 3D printer. To solve this problem, we decided to prepare a thicker PDMS chip (increasing the thickness between the roof of the channel and the upper surface of the chip), which will prevent the roof of the channels from collapsing.

We added walls at the edge of the mold so the whole dimensions of the microfluidic chip will be already set, and we can ensure that the thickness of the chip is sufficient to prevent any collapsing of the channels. This edge will contain the uncross-linked PDMS when poured onto the mold. Since this wall is 3 mm high, the thickness of the PDMS chip above the channel will be more than 2 mm, ensuring as well that when the metallic cannula is introduced into the PDMS body, it will be tightened because of the elastomeric nature of the PDMS. We could implement this feature because we use a 3D printer to fabricate the mold. In traditional molds prepared on silicon wafers, the total thickness of the chip will be set by the amount of PDMS poured in the dish containing the mold.

2.9.2 Mold Fabrication

To generate the mold for the microfluidic channel, we have used an *ABS-like commercial resist*, from *Phrozen*. As mentioned above, we selected a DLP 3D printer, which has sufficient lateral resolution for the design we have prepared. The printer is a *Solus* platform connected to a *Vivitek h1188 DLP* projector system (1920 \times 1080 pixels). In this case, the light source is a halogen bulb with homogeneous light distribution and high luminosity. The choice of the *ABS-like resist* in combination with this *Solus* configuration aimed to maximize the resolution offered by both elements. As a result, we can reduce the roughness on the surfaces of the mold.

After the printing process, we cleaned the mold by rinsing it with the *Resinaway* solution. This process removes the resist leftovers that did not solidify. Then we put the mold under UV light for 5 min for a post-curing step to ensure the complete solidification of the mold. Finally, we cleaned and removed any solvent remaining by washing the mold with water and soap. To do so, we kept the mold in a solution of water and soap on an orbital shaker for 24 h.

This final process is critical to guarantee the correct cross-linking of PDMS in the following steps. The solvent extraction strategy depends on the type of solvent used (usually organic solvents such as isopropanol alcohol are employed) [27].

2.9.3 Chip Fabrication

The PDMS chip was obtained by replica molding. First, 10 mL of a 10:1 mixture of *PDMS pre-polymer* and *cross-linker* was thoroughly mixed. The uncured PDMS was then poured on the 3D printed mold and kept under vacuum for 45 min to remove air bubbles. Once all the air was removed, the mold with PDMS was cured in two steps, first overnight on a flat surface to prevent tilting, and then in the oven at 65 °C for 4 h. Once cross-linked, the PDMS was peeled off the mold and stored in a plastic petri dish until use.

As we described above, the 3D printed mold was shaped to obtain a PDMS chip with the desired size and thickness (Fig. 2.6). In the present example, the size of the chip matches a microscope glass slide and it is thick enough to ensure proper tubing connection and preventing the collapse of the reservoirs.

2.9.4 Mechanical Bonding Setup

Here we aim at having a chip that has a reversible bonding, thus the substrate enclosing the channel can be separated from the PMDS chip. To do so, we have designed a holder that keeps the channel closed mechanically, considering that we will close the fluidic chip using a microscope glass slide and that we will place the holder on a microscope to image some parts of the process.

The holder has two elements, a bottom part and a top that are kept together by screws. The size of the holder is compatible with standard microscope stages. The bottom part has a cavity 4.5 mm deep to accommodate the glass slide (25 mm × 70 mm area, ≈1.5 mm thick) with the PDMS chip (3 mm thick). We also include a large aperture to allow the visualization in different optical configurations (upright, inverted, transmission, reflection). We have placed four screw holes for *M3 screws* at each side. This allows to close the holder and apply the force needed to ensure the bonding and avoid leakage. The top part has the same

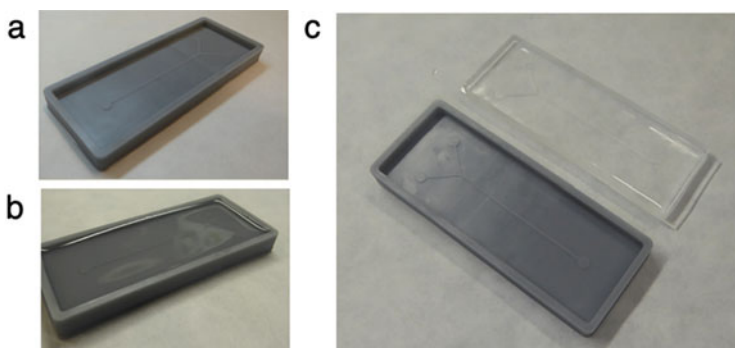


Fig. 2.6 Fabrication of the PDMS chip. (a) 3D printed mold. (b) PDMS is poured on the channel structure. (c) The cross-linked PDMS is peeled off the mold

aperture for visualization and the same holes for the screws. Moreover, the top part of the holder has an extruded volume facing the chip, this ensures the pressure over the PDMS surface.

2.9.5 Tubing

In this example, we used a tubing setup consisting of *metallic cannula—silicone tube—female luer connector*. As explained before, the diameters of the different elements of the tubing setup are selected to ensure tight connections. The outer diameter of the metallic cannula (0.9 mm/20G) is larger than the inner diameter of the silicone tube (0.76 mm), which in turn is smaller than the outer diameter of the luer connector. This connector is shaped in a way that maximized its capacity to sustain high flow rates. Finally, the connection of the cannula to the chip is made by taking advantage of the elastomeric nature of the PDMS. We drilled a hole onto the PDMS using a puncher to hold the cannula tightly.

By selecting this configuration, we have a tubing setup that can be autoclaved, which can be easily connected to syringes through the standard luer connectors, and that can be closed if we use luer caps.

2.9.6 Chip Assembly and Fluidic Experiment

To assemble the microfluidic chip, we first made on the PDMS the holes that will host the tubing connections. To do so, we used a punch with a diameter of 0.75 mm at the reservoirs (Fig. 2.7a), making sure that no leftovers that could potentially block the flow remained. It is advised to drill from the channel side towards the outer side, to avoid PDMS residues being left inside the chip.

Once the holes were drilled, we placed the PDMS chip onto a glass substrate to close the microchannels (Fig. 2.7b). The PDMS chip sticks to the glass substrate easily. This facilitates this step but has the drawback of difficulting the alignment of the channel with the motifs of the substrate, if any.

We then placed the chip on the 3D printed holder (Fig. 2.7c) and closed it by tightening the screws (Fig. 2.7d).

Next, we assembled the tubing system. First, we inserted the metallic cannula into the silicone tube (Fig. 2.7e). Second, we inserted the silicone tube into a female luer connector (Fig. 2.7f). Then, we connected a syringe to the luer and filled it with the solution through the metallic cannula (Fig. 2.7g). Finally, we removed the air bubbles from the system. Last, we inserted the metallic cannula into the holes performed on the reservoirs (Fig. 2.7h).

At this point, the syringes were mounted onto the syringe pumps, and we could start flowing the solutions to the chip. Figure 2.7i shows blue ink and water flowing through the chip and defining an interface at the point where the two inlets met.

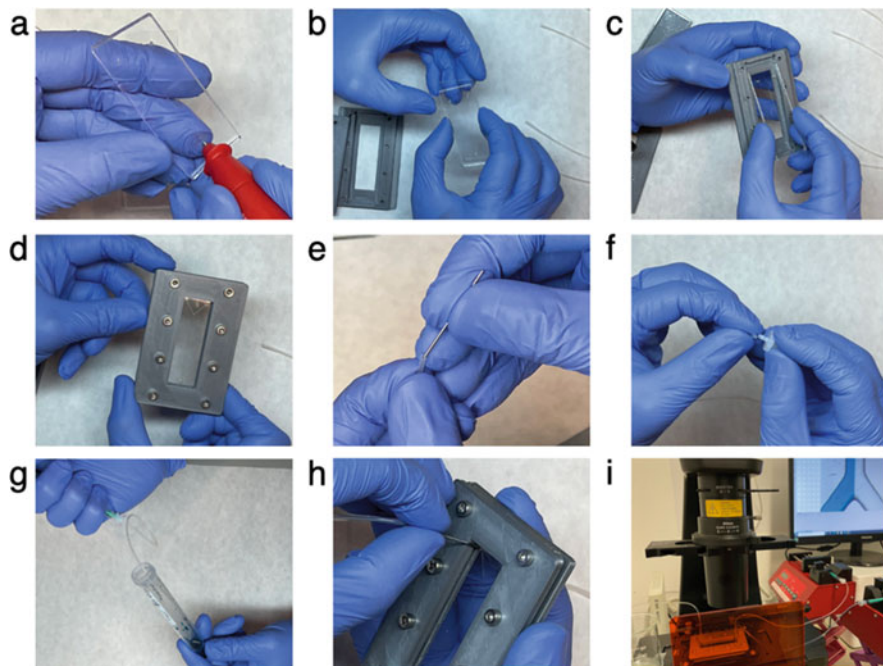


Fig. 2.7 Steps to assemble the chip. Overview of the different steps undertaken to assemble the microfluidic device

2.9.7 Gradient Generation

Using this simple Y-shaped microfluidic chip, we can follow two strategies to generate molecular gradients: by diffusion [19], or by progressively exposing the substrate to the molecule of interest [20]. The first approach generates a gradient in solution, while the second one generates a gradient on the surface of the channel.

The *classical diffusion gradient* is generated by the lateral diffusion of the two solutions at the interface. While near the region where the two inlets merge, there is a well-defined interface between the two fluids, further into the main channel this interface blurs due to passive diffusion. The shape of the gradient generated is fairly stable and can be modulated by adjusting the flow rates of the two inlets. However, the experiment (such as the study of chemotactic effects on cells, for example) has to be performed inside the chip and while the solutions are flowing, thus in the presence of shear stress.

We encourage the reader to explore this approach by using inks to easily visualize how the gradient behaves before the actual cellular experiments. Food colorings are very useful for this test phase. Then, a subsequent step would be to use fluorescently-labeled molecules, such as dextran. By selecting such a fluorescent probe with a molecular weight similar to the one of the “molecule of interest,” one can fairly model the profile of the gradient that the final experiment should have.

Alternatively, we can generate *surface-bound gradients* if we progressively expose the substrate to the protein of interest. With this strategy, we take advantage of the well-defined interface between the two solutions in the region of the main channel closer to the intersection between the two inlets. Since we can control the position of the interface by changing the ratios between the flow rates of the two inlets, we can in fact control what region of the surface is exposed to a certain solution at every time. This process is equivalent to progressively incubate the substrate with the molecule of interest. Therefore, if we know the adsorption dynamics of the molecule on the substrate, we can control the amount of protein that will adsorb on each region. When this progressive incubation is finished, the flows can be stopped and we can either detach the microfluidic chip (if the bonding was reversible) and use the substrate as in any other experiment, or flow cells into the channel and when adhered and spread, perform the experiment in static conditions preventing the effects of shear.

If selecting this approach, it is extremely important that (1) the adsorption kinetics of the molecule that is used is well-characterized and that (2) the region where the interface is well defined without diffusion is well-known. Thus, as before, some “calibration” is needed. Some relations between flow rate and incubation times can be found in the literature [26].

2.10 Conclusions

In this chapter, we have given an overview of the different steps needed to design and fabricate a microfluidic chip to generate biomolecular gradients. We have discussed (1) 3 different gradient generators and their working principles, (2) important aspects when designing the chip, (3) different methods to fabricate the mold and the chip, (4) different bonding strategies and (5) the most common methods to connect the chip to the tubing system. Finally, we have shown an application example to illustrate the complete process. Overall, we have seen that it is of paramount importance to define the type of experiment that we want to perform and to identify the resources that we have available, before starting the process of designing and fabricating the chip. The experiment will define a set of requirements for the device, and the resources will drive us through the different methodologies that are currently available for fabricating microfluidic devices. The widespread of 3D printing technologies has opened the possibility to obtain molds fast, fairly unexpensive and without the need of specialized facilities such as cleanrooms. Therefore, we believe it is now time for microfluidics to become a common resource of cell biology labs.

Acknowledgments We thank the Martinez Lab members for their discussions and help. Funding was provided by a European Union Horizon 2020 ERC grant (agreement no. 647863—COMIET), ‘La Caixa’ Foundation (grant no. LCF/PR/HR20/52400011), the CERCA Programme/Generalitat de Catalunya (2017-SGR-1079), and the Spanish Ministry of Economy and Competitiveness (Severo Ochoa Program for Centers of Excellence in R&D 2016-2019). The results presented

here only reflect the views of the authors; the European Commission is not responsible for any use that may be made of the information it contains.

References

1. Pearsall J et al (2012) Oxford dictionaries online. Oxford Univ. Press
2. Bogenrieder T, Herlyn M (2003) Axis of evil: molecular mechanisms of cancer metastasis. *Oncogene* 22:6524–6536
3. Wang S-J et al (2004) Differential effects of EGF gradient profiles on MDA-MB-231 breast cancer cell chemotaxis. *Exp Cell Res* 300:180–189
4. Janeway CA, Travers P, Walport M, Shlomchik MJ (2001) *Immunobiology: the immune system in health and disease*, 5th edn. Garland
5. Goodman CS (1996) Mechanisms and molecules that control growth cone guidance. *Annu Rev Neurosci* 19:341–377
6. Stossel TP (1993) On the crawling of animal cells. *Science* 260:1086–1094
7. Redd MJ, Kelly G, Dunn G, Way M, Martin P (2006) Imaging macrophage chemotaxis in vivo: studies of microtubule function in zebrafish wound inflammation. *Cell Motil Cytoskeleton* 63: 415–422
8. Chaudhury MK, Whitesides GM (1992) How to make water run uphill. *Science* 256:1539–1541
9. Morgenthaler S, Lee S, Zürcher S, Spencer ND, Zu S, Simple A (2003) Reproducible approach to the preparation of surface-chemical gradients. *Langmuir* 19:988–989
10. Jeon NL et al (2000) Generation of solution and surface gradients using microfluidic systems. *Langmuir* 16:8311–8316
11. Genzer J, Bhat RR (2008) Surface-bound soft matter gradients. *Langmuir* 24:2294–2317
12. Meredith JC, Karim A, Amis EJ (2002) Combinatorial methods for investigations in polymer materials science. *MRS* 27:330–335
13. Grayson ACR et al (2004) A BioMEMS review: MEMS technology for physiologically integrated devices. *Proc IEEE* 92:6–21
14. Trichet L et al (2012) Evidence of a large-scale mechanosensing mechanism for cellular adaptation to substrate stiffness. *Proc Natl Acad Sci* 109:6933–6938
15. Lin B, Hui J, Mao H (2021) Nanopore technology and its applications in gene sequencing. *Biosensors* 11:214
16. Heller I, Hoekstra TP, King GA, Peterman EJG, Wuite GJL (2014) Optical tweezers analysis of DNA-protein complexes. *Chem Rev* 114:3087–3119
17. Rigat-Brugarolas LG et al (2014) A functional microengineered model of the human splenon-on-a-chip. *Lab Chip* 14:1715–1724
18. Castillo-Fernandez O, Rodríguez-Trujillo R, Gomila G, Samitier J (2014) High-speed counting and sizing of cells in an impedance flow microcytometer with compact electronic instrumentation. *Microfluid Nanofluidics* 16:91–99
19. Holden MA, Kumar S, Castellana ET, Beskok A, Cremer PS (2003) Generating fixed concentration arrays in a microfluidic device. *Sensors Actuators B Chem* 92:199–207
20. Georgescu W et al (2008) Model-controlled hydrodynamic focusing to generate multiple overlapping gradients of surface-immobilized proteins in microfluidic devices. *Lab Chip* 8: 238–244
21. Comelles J, Hortigüela V, Samitier J, Martínez E (2012) Versatile gradients of covalently bound proteins on microstructured substrates. *Langmuir* 28:13688–13697
22. Keenan TM, Hsu C-H, Folch A (2006) Microfluidic “jets” for generating steady-state gradients of soluble molecules on open surfaces. *Appl Phys Lett* 89:114103
23. Cosson S, Aeberli LG, Brandenberg N, Lutolf MP (2015) Ultra-rapid prototyping of flexible, multi-layered microfluidic devices via razor writing. *Lab Chip* 15:72–76

-
24. Duffy DC, McDonald JC, Schueller OJA, Whitesides GM (1998) Rapid prototyping of microfluidic systems in poly(dimethylsiloxane). *Anal Chem* 70:4974–4984
 25. Ibidi (2021) μ -Slide chemotaxis
 26. Comelles J, Hortigüela V, Martínez E, Riveline D (2015) Methods for rectifying cell motions in vitro: breaking symmetry using microfabrication and microfluidics. In: Paluch E (ed) *Biophysical methods in cell biology*. Elsevier Inc., pp 437–452
 27. Hollingsworth K (2020) *Chips and tips*. Solvent extraction of 3D printed molds for soft lithography. Royal Society Chemistry



Sensors and Biosensors in Organs-on-a-Chip Platforms

3

Gerardo A. Lopez-Muñoz, Sheeza Mughal, and Javier Ramón-Azcón

Abstract

Biosensors represent a powerful analytical tool for analyzing biomolecular interactions with the potential to achieve real-time quantitative analysis with high accuracy using low sample volumes, minimum sample pretreatment with high potential for the development of in situ and highly integrated monitoring platforms. Considering these advantages, their use in cell-culture systems has increased over the last few years. Between the different technologies for cell culture, organs-on-a-chip (OOCs) represent a novel technology that tries to mimic an organ's functionality by combining tissue engineering/organoid with microfluidics. Although there are still challenges to achieving OOC models with high organ mimicking relevance, these devices can offer effective models for drug treatment development by identifying drug targets, screening toxicity, and determining the potential effects of drugs in living beings. Consequently, in the future, we might replace animal studies by offering more ethical test models. Considering the relevance that different physiological and biochemical parameters have in the correct functionality of

The original version of the chapter has been revised. A correction to this chapter can be found at https://doi.org/10.1007/978-3-031-04039-9_23

G. A. Lopez-Muñoz · S. Mughal

Institute for Bioengineering of Catalonia (IBEC), The Barcelona Institute of Science and Technology, Barcelona, Spain

J. Ramón-Azcón (✉)

Institute for Bioengineering of Catalonia (IBEC), The Barcelona Institute of Science and Technology, Barcelona, Spain

ICREA-Institució Catalana de Recerca i Estudis Avançats, Barcelona, Spain

e-mail: jramon@ibecbarcelona.eu

© The Author(s), under exclusive license to Springer Nature Switzerland AG 2022, corrected publication 2022

D. Caballero et al. (eds.), *Microfluidics and Biosensors in Cancer Research*, Advances in Experimental Medicine and Biology 1379, https://doi.org/10.1007/978-3-031-04039-9_3

cells, sensing and biosensing platforms can offer an effective way for the real-time monitoring of physiological parameters and, in our opinion, more relevant, the secretion of biomarkers such as cytokines, growth factors, and others related with the influence of drugs or other types of stimulus in cell metabolism. Keeping this concept in mind, in this chapter, we focus on describing the potential use of sensors and biosensors in OOC devices to achieve fully integrated platforms that monitor physiological parameters and cell metabolism.

Keywords

Sensors · Biosensors · Organ-on-a-chip · Screening · Pre-clinical platforms

3.1 Biosensors

According to market projections, the biosensors market is valued at USD 25.5 billion in 2021 and can reach USD 36.7 billion by 2026 [1]. Between the different applications, point-of-care (i.e., insulin monitoring, pregnancy test) represents the main segment of the market (about 57%); however, there is a remarkable increase in biosensors for nonmedical applications, for example, in the development of cell-culture systems. Among the different biosensors suitable for cell-culture systems, electrochemical biosensors are still the most relevant due to their high-throughput quantification and analysis of biochemical interactions. However, optical biosensors have emerged with the fastest growth over recent years. This rise in optical biosensing technology is related to a wide analytical coverage [1].

3.1.1 Definition of a Biosensor and Classification

How can a biosensor be described? The International Union of Pure and Applied Chemists (IUPAC) describes a biosensor as “a device that uses specific biochemical reactions mediated by isolated enzymes, immunosystems, tissues, organelles or whole cells to detect chemical compounds usually by electrical, thermal or optical signals” [2]. From this description, we can define two main features: a biosensor device requires a biological recognition element in direct contact with a transducer and transforms a biorecognition or biophysical event mainly into a signal that later can be measured. Although there are many aspects involved in the design of a biosensor, we can describe three main parts: the first part is the biorecognition material (i.e., antibody, aptamer, or enzyme) that gives the potential to detect the analyte with high specificity and selectivity; the second part is the transducer (i.e., optical, electrochemical, mechanical) that transforms the biorecognition event in a physical quantity, which later can be measured and analyzed by an electronic device that monitors the results for the final user (see Fig. 3.1) [3].

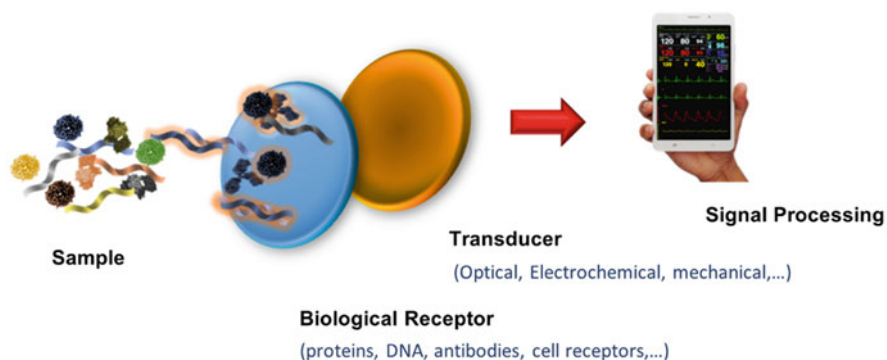


Fig. 3.1 Representation of the main parts of a biosensor device. The analyte, the biorecognition material, the transducer, and the signal processing system

On the other hand, there are expected attributes from a biosensor. These attributes range from the potential to detect and quantify biomolecular interactions in minutes, using minimum sample pretreatment and reagents, to the potential to be portable and used by non-trained personnel. Biosensors are considered as analytical tools with a high potential to achieve miniaturized and integrated Lab-on-a-Chip (LOC) platforms and end-user devices [4]. As a consequence of these potential attributes, the biosensors field has been extensively investigated and developed over the recent few years and, year-to-year emerge novel point-of-care and end-user devices.

There are different transduction methods for biosensors; however, only three technologies have relevance in the market [5]: electrochemical, mechanical, and optical biosensors.

Electrochemical biosensors have been the gold standard over the years in biosensing. The working principle of these biosensors is to detect electrochemical changes with biorecognition events. When the biorecognition layer covers the working electrode and an electric potential is applied, electroactive species conversion into electrical changes can be quantified (see Fig. 3.2a). Electrochemical biosensors allow simple and high-throughput fabrication with compact instrumentation [8].

The principal example of this technology in our lives is the glucose biosensor. This biosensor emerged in 1962 and is based on the amperometric detection of an enzymatic reaction related to hydrogen peroxide generation [8]. Over the last years, there have been significant improvements in electrochemical biosensors. However, there are still many changes to overcome, most of them related to novel materials that improve the limited sensitivity of the biosensors and their stability [9, 10].

Mechanical biosensors also have been widely reported and employed. The working principle of mechanical biosensors is to detect the biorecognition events as superficial mass changes. Between the different mechanical biosensors, the quartz crystal microbalance (QCM) biosensor is the most representative. QCM has a native resonant frequency. This frequency changes with mass changes in their surface, in this case, when the analyte binds to the biorecognition molecule (see Fig. 3.2b). This change in resonant frequency is proportional to the amount of analyte bound [11]. Among their main advantages is the possibility to achieve label-free and

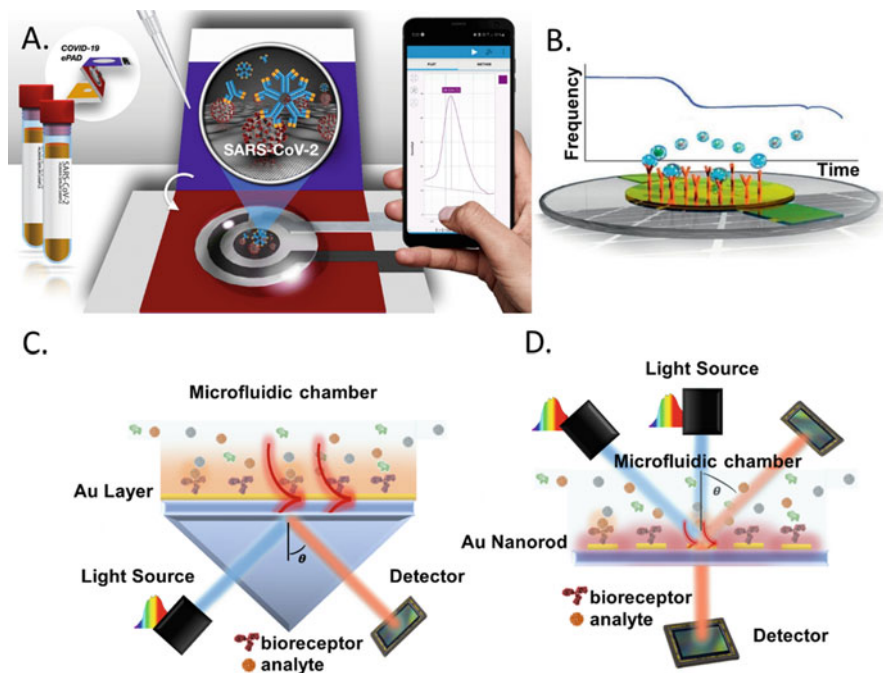


Fig. 3.2 Schematic illustration of the working principles of the three leading biosensing technologies in the market: (a) electrochemical (Adapted and reprinted with permission from [6]. © Copyright 2021, Elsevier Inc.), (b) mechanical quartz crystal microbalance (Adapted and reprinted with permission from [7]. © Copyright 2015, Elsevier Inc.), and optical (c) prism coupled SPR and (d) transmission/reflection LSPR

multiplexed biodetection. However, the mechanical nature of their working principle decreases their sensitivity and potential uses; between them in the biodetection of bacteria and cells [12]. Also, liquid environments without thermal control lead to erroneous readings [13, 14].

Although optical biosensors have been widely studied over the last decades, the last advances in nanomaterials boosted their growth in recent years. These biosensors detect variations in intensity, wavelength, and refractive index between others of the propagated light with biointeractions [15]. Between the different detection mechanisms, most optical biosensors measure refractive index changes [16]. Refractometric biosensing uses the evanescent field, which acts as a probe to detect refractive index changes near the surface [17]. The amount of analyte in the biorecognition event is proportional to the optical changes [18]. As mentioned before, these biosensors only detect superficial changes and, as a consequence, there is a limited interference of other compounds of the media [19]. Unlike electrochemical and mechanical biosensors, optical biosensors have a high sensitivity and do not suffer from electronic or mechanical interferences. Although there are different optical biosensors, we can summarize two principal technologies: those

based on dielectric waveguides like interferometers [20] and resonators [19], and those based on plasmonic modes. Plasmonic biosensors are the most widely used optical sensors to study multiple biorecognition events in the last decades [21]. Unlike semiconductor materials, noble metals (mainly gold) have a well-established surface biofunctionalization based on thiol-based surface chemistry with high chemical stability [15].

Contemporary biosensing techniques have sought through years to achieve favorable figures of merit such as high sensitivity, limits of detection, signal-to-noise ratio, specificity, and binding capacity by employing different techniques to design integrated biosensors. Attempts to design an all-encompassing biosensor have been futile and instead took recourse to focus on achieving at least one of these facets of device performance. Revolution in immunochemistry and biomarker detection began in the 1970s when Faulk and Taylor conjugated an antibody to gold nanoparticles to visualize salmonella antigens in direct electron microscopy. After Seeman presented DNA as a structural molecule in 1980, Mirkin and Alivisatos explored the possibility of using DNA to produce aggregated gold nanoclusters. Taking inspiration, Boal explored the utility of 2 nm gold nanoparticles protected by self-assembled monolayers to serve as building blocks for micro and eventually macro-scale constructs. Multiple studies, henceforth, used controlled and self-assembly of gold nanostructures to develop different types of biosensors, including the electrochemical and optical types. These devices work by amplifying the optical or electrical signal generated of the interaction within gold and the biorecognition elements. Therefore, two properties of gold nanoparticles have mainly been interesting; surface plasmon resonance and electrical conductivity. For optical biosensors, multiple factors allowed for accounting and tuning the sensor's performance. These included the particles' size and shape, interparticle distance, and the refractive index of the surrounding media/environment. In 1983, Lieberg, for the first time, used surface plasmon resonance (SPR) for label-free detection of biomolecular interactions and gas sensing. The technique was presented as a hassle-free, cheap way to detect analytes without any expensive machinery. Biacore™'s optical sensors deserve a special mention in the SPR optical sensor field [22]. They have various options that allow measuring the specificity, affinity, thermodynamic parameters, biologically active concentration of the analyte, and the association and dissociation constants. Their technology couples a microfluidic system with an exchangeable sensor chip. Biacore™'s optical SPR sensors have been in use since the 1990s to answer questions about bio-specific interactions [22].

The working principle of plasmonic biosensors, also called SPR biosensors, can be summarized. SPR is an electromagnetic (EM) wave that occurs when incident light hits a noble metal surface. At specific conditions in momentum or wavelength between others, a portion of the light energy couples with the surface electrons of the metallic layer, which move due to excitation [23]. The electrons' oscillation generates an exponentially decaying evanescent field which is highly sensitive to refractive index changes, especially near the surface. Consequently, the biorecognition events close to the surface generate variations of the different optical properties of the propagated light, such as intensity, wavelength, or phase, which can

be monitored and quantified. Plasmonic phenomena can be generated through grating couplers [24] or by waveguides [25], although the most common way is using a coupling prism, usually known as Kretschmann configuration (see Fig. 3.2c). However, this configuration considerably reduces the potential for multiplexing and miniaturization of plasmonic sensors [15].

The need for “bulky” coupling elements for SPR generation can be overcome using metallic nanostructures in the sub-wavelength size range instead of thin metallic films (see Fig. 3.2d), generating the so-called localized surface plasmon resonance (LSPR) [15]. Meanwhile, plasmonic waves propagate through the surface of a continuous metallic film; localized surface plasmons are confined excitations of the conduction electrons of metallic nanostructures. These modes arise naturally from the light scattering of sub-wavelength conductive nanostructures in an oscillating electromagnetic field. Another consequence of the nanostructured surfaces is that plasmon resonances can be excited by direct light illumination than conventional SPR [26]. The presence of edges in nanostructures strongly scatters light at a specific wavelength range. Analogous to conventional SPR, LSPR can be exploited for biosensing applications, as the wavelength depends on the surrounding media’s refractive index. The binding on the surface of the nanostructures results in a refractive index change, causing a shift in the extinction peak wavelength, which can be maximized by optimizing the nanostructure characteristics (i.e., metal type and geometry).

Table 3.1 summarizes relevant emerging examples of different biosensors based on the leading transduction technologies (optical, mechanical, and electrochemical).

Table 3.1 Examples of emerging biosensing technologies applied to relevant clinical diagnosis

Type of Biosensor	Material	Biomarker	Limit of detection	Application
Electrochemical [27]	Au nanoparticles /graphene modified carbon electrodes	microRNA (21,155, and 210)	Up to 0.04 fM in serum	Breast cancer
Electrochemical [28]	ZnO/Au electrodes	Cytokines (IL-6, IL-8, IL-10, TRAIL, and IP-10)	Up to 1 pg/mL in plasma	Sepsis
Optical [29]	Au nanopillars	SARS-CoV-2 virus particles	370 virus/mL in PBS	SARS-CoV-2
Optical [30]	Au nanoprisms	microRNA (10b,64,145,143 and 490-5p)	100 aM in plasma	Bladder cancer
Mechanical [31]	Au electrodes	MDA MB 231 human breast cancer cells	12 cells/mL	Breast cancer
Mechanical [32]	Graphene oxide/ Au nanoparticles coated Au electrodes	Carcinoembryonic antigen	Up to 0.06 ng/mL in serum	Colorectal, ovarian, and breast cancer

Most of the presented examples directly detect human fluids and present relevant clinical diagnosis applications, including cancer diagnosis.

3.1.2 Biosensors and Cancer Research

Multiple biomarkers have been considered for cancer detection, such as circulating tumor cells (CTCs), circulating DNAs and micro RNAs, proteins, and exosomes. Of these, the CTCs and protein biomarkers have been utilized in the design of multiple biosensor devices. Current techniques popularly used for detecting and quantifying these markers include ELISA and sequencing kits commercially available, such as SafeSeqS, PCR, and TamSeq (Tagged Amplicon Sequencing) [33]. While these techniques are reliable, they have considerable limitations such as a lengthy multi-step protocol, impossibility to achieve device miniaturization, integration, and multiplex detection. Other techniques such as FACS, Dynamic Light Scattering (DLS), and NTA require complex machinery and are, therefore, restricted to the laboratory. Nanoplasmonic sensing techniques such as SPR and LSPR, therefore, present viable solutions to these issues. These optical sensing techniques depend on the optical shift observed as a change in local refractive index within a comparatively small sample size. They are label-free and can provide measurements free from the interference of the surrounding medium, particularly LSPR. SPR presents the capability to measure surface depths between 100–200 nm suitable for detecting circulating tumors cells, proteins, and exosomes but not nucleic acids, while the LSPR technique has a sensing depth of 5–20 nm, thereby providing the opportunity to detect nucleic acids directly. Both SPR and LSPR are capable of detecting low concentrations of the sample analyte. One of their key differences is that while the interaction of monochromatic light source on planar conductive thin film creates an evanescent wave as observed in SPR [34], the interaction of the electromagnetic light source with conductive metallic nanoparticles with sizes smaller than the wavelength of incident light causes localized surface plasmon resonance, which is a collective, non-propagative oscillation of the conduction band free electrons [33]. This enhances the local electromagnetic field in the vicinity of the particle surface. In other words, any change in the local environment of the dielectric will directly affect the nanoparticle's polarizability and the optical extinction spectrum [35]. Such changes will alter the electron wave function delocalization of the nanoparticles, resulting in proportional changes to the LSPR pattern, allowing the opportunity to quantify biorecognition events [36].

The thermal convection method was used to deposit gold nanoislands from a colloidal gold solution on a glass slide [37]. Their design allowed the detection of exosomes via vn96 polypeptide through LSPR in an MCF7 conditioned cell-culture media. Nevertheless, the binding capacity was only theoretically, and not practically, proved.

A parallel gold nanorod LSPR, microfluidic-based, portable lab-on-a-chip sensor was developed with eight channels and 32 sensing sites for real-time detection of four cancer biomarkers, including alpha-fetoprotein (AFP) and prostate-specific antigen [38]. The device can simultaneously measure analyte concentrations as low as 500 pg/mL in a solution with 50% human serum in all eight channels. This design bridges substantial gaps in sensors miniaturization, reliability, sensitivity, integration, and compactness. The researchers claimed the device to be ready for the transition from lab to market. There are, however, noticeable differences between LOD values for different biomarkers attributed to the uneven and different performance of antibody pairs.

Like proteins and exosomes, miRNAs continue to hold great promise for the non-invasive detection of cancer. An ssDNA functionalized gold nano prism-based LSPR sensor capable of achieving sensitivity as low as 140 zp/M was also developed [36]. Their design could detect a single base-pair mismatch in the ssDNA and miRNA duplex by sensing a significant change in the LSPR properties. The researchers assayed four types of miRNAs obtained from 50 uL of bladder cancer patients' plasma, namely microRNA-10b, -182, -143, and -145. This work substantiated the utility of noble metallic nanoparticles to achieve device miniaturization, particularly for cancer detection [36].

3.2 Sensors and Biosensors in Organs-on-a-Chip Platforms

3.2.1 Organs-on-a-Chip Definition

Studies on two-dimensional *in vivo* cell cultures and animal models have contributed to significant cellular and molecular biology accomplishments, but the progress has been slow. The ratio of FDA-approved drugs to the billions of dollars spent on research development programs is unprofitably low and decreases monotonically. To curtail this drop, contemporary drug development approaches require substantial advancements in tools and techniques to achieve efficiency with cost-effectiveness. The role played by animal models in drug development to unveil essential aspects of physiology and biochemistry has been pivotal to evaluate drug response. Nevertheless, the anatomic and physiologic difference between humans and animal models is hard to ignore and often becomes a bone of contention to predict a patient's response. This is evidenced by the fact that from the drugs that fail in the clinical trials, 60% are inefficacious and 40% are due to toxicity. It is therefore impractical and illogical to use animal models for developing a patient-specific personalized treatment. Currently, efforts are in place to get the organs-on-a-chip (OOCs) (see Fig. 3.3) approved by the National Institute of Health Sciences for clinical research and translation [40].

An OOC device has cells harvested from the patient or a healthy donor in a 3-dimensional microfluidic cell-culture platform to the input culture medium, drug of choice, and harvest the products of cellular metabolism. The output can then be tested either with sensors integrated into the chip or by off-chip analyses. These

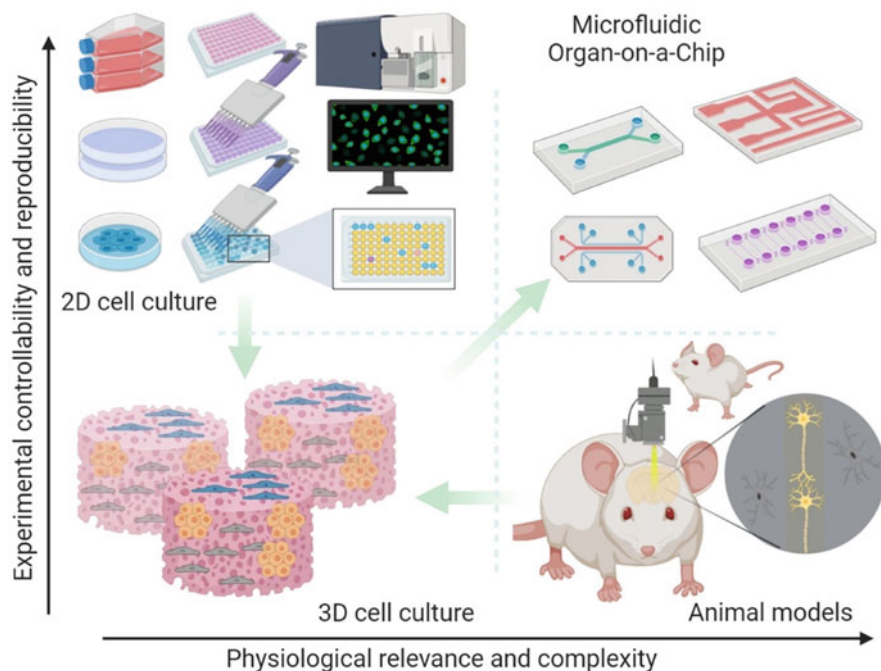


Fig. 3.3 Relevance of OOC devices as platforms to controllably and systematically interrogate human biology. Adapted and reprinted with permission from [39]. © Copyright 2021, Elsevier Inc.

microfluidic chips allow growing the organs in an environment mimicking the microenvironment within the human body. The organs or organoids are allowed to culture in a hydrogel, exchanging nutrients and metabolites, thereby monitoring drug response in situ. Therefore, choosing the biomaterial to encapsulate the organs/organoids of choice is essential to design a platform similar to the patient's or model's microenvironment.

3.2.2 Clinical Applications

After developing lung-on-a-chip as the first OOC model, many OOC platforms were developed for disease modeling, toxicology studies, pathophysiological evaluation, drug response testing under varying external and internal conditions (see Fig. 3.4).

3.2.2.1 Pancreas-on-a-Chip

Type 2 Diabetes caused 1.5 million deaths in 2019 alone. While the cause of type 1 diabetes is a genetic predisposition to the disease, the leading cause of type 2 diabetes is excess body weight, lack of exercise, and unchecked dietary intake. Islets of Langerhans or beta cells play a pivotal role in regulating glucose metabolism. However, static culture techniques do not bode well with the Islet functionality

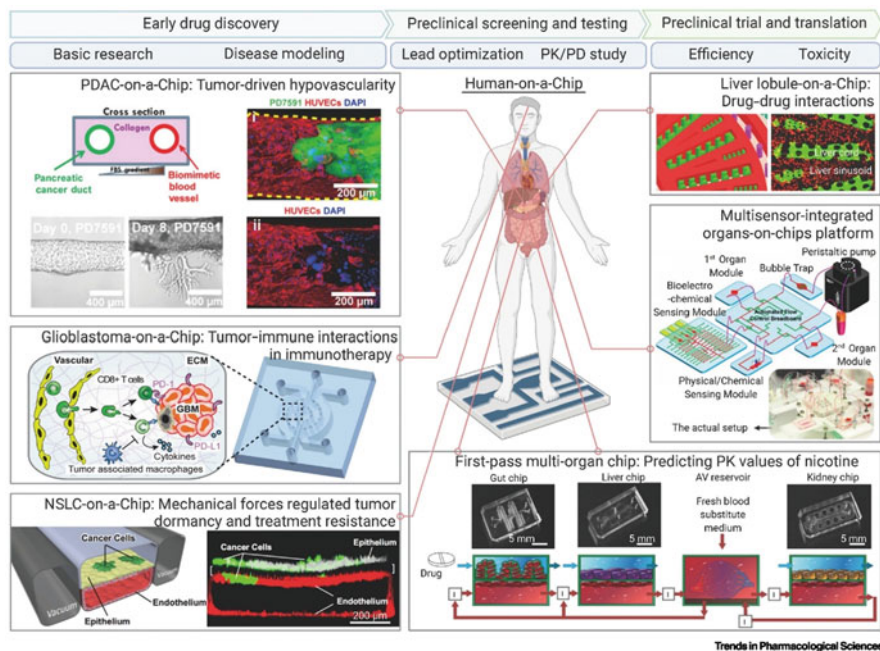


Fig. 3.4 The prospective multi-functional utility of OOC platforms disease modeling in drug development and as an alternative of research with animal models. Adapted and reprinted with permission from [39]. © Copyright 2021, Elsevier Inc.

because they cannot mimic the *in vivo* physiology and the continuous perfusion offered by microfluidic platforms to the 3-dimensional organs or organoids. Therefore, the Islets of Langerhans mounted on microfluidic platforms are the culture of choice for studying disease pathology and drug response. The cells can be harvested from diseases and healthy donors. At present, glucose-stimulated insulin secretion (GSIS) assays which are primarily enzymatic in nature, are conducted to evaluate islet functionality. However, the OOC technology offers the opportunity to integrate detection of *in situ* response with different types of sensors. Numerous research teams have come up with varied designs to address complexities about organ growth and detection mechanisms. In 2009, Mohammed et al. came up with the first microfluidic perfusion design to achieve multimodal characterization, which included functionality analysis of mitochondrial potential and simultaneous quantification of insulin production through ELISA under a glucose challenge [41]. Their chosen combination of analyses provided a more reliable course for assessing islet quality before transplantation than the standard assays in practice at the time. Over time the integration and real-time evaluation of islet cell integrity and functionality have continued to improve. Perrier used integrated electrochemical biosensors based on a microarray of platinum black electrodes to study ionic fluxes generated with variable glucose concentrations [42]. This approach allowed to detect changes in

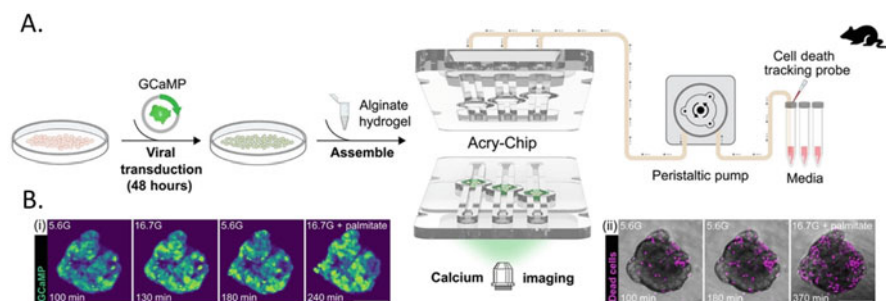


Fig. 3.5 Scheme of the monitoring of glucolipotoxicity stimuli on in situ Ca^{2+} signaling and viability of hydrogel-embedded pancreatic islets. (a) Schematic representation of the experimental workflow. (b) Time-course snapshots of a representative (i) GCaMP islet and (ii) accumulated dead. Adapted and reprinted with permission from [44]. © Copyright 2021, American Association for the Advancement of Science

islet function proportional to glucose within only 40 μs . The integrated islet-on-a-chip with an LSPR sensor device developed in 2021 allows studying in situ response of the microtissues or islets-on-a-chip to external stimuli [43]. Moreover, the GSIS assays are now acknowledged to have low potency to predict islet cell potency in insulin production. In another example, a microfluidic device has been used to test the glucolipotoxicity stimuli on in situ Ca^{2+} signaling and the viability of the cells embedded in a hydrogel has been tested (see Fig. 3.5) [44].

Another critical concern while designing the islet or pancreas on a chip is to control differentiation, optimize culture and flow conditions to minimize shear stress, and improve the exchange of nutrients. Multiple researchers have attempted to address these complications by approaches such as dynamic culturing to achieve matrix reconstitution [45], employing a multilayer perfusion system to optimize differentiation of pluripotent stem cells (iPSCs) [46], developing a system with self-guided trapping sites to optimize both real-time monitoring and functionality analyses [47] and using scaffolds based on the right biomaterial such as cellulose to enhance the differentiation, formation, and functionality of pancreatic pseudo-islets [48].

Researchers from the Edmonton group [49] demonstrated that islet transplantation in 7 patients allowed them to achieve significant insulin independence coupled with steroid-free immunosuppression. After that, islet cell transplantation has been considered to be a promising approach, particularly for type 1 diabetes. However, the transplantation process requires manual handling and is often coupled with pro-inflammatory signals and ischemic damage. Pancreas-on-a-chip allows not only to precisely control the flow conditions but also to check the vitality of islets post-isolation. They also provide an opportunity to assess the growth and function of stem cell-derived beta cell function. Other checks against size heterogeneity prevalent between different islets, physical protection, and control of nutrient flow can also be controlled within the platform to achieve standardization (Table 3.2).

Table 3.2 Pancreas-on-a-chip models with their fabrication technology

Objective	Technique
Multimodal characterization	Functionality analysis of mitochondrial potential and a simultaneous quantification of insulin production through ELISA under glucose changes [41].
To study islet ionic fluxes in response to nutrient stimulation	Array of platinum black electrodes to detect changes in islet function proportional to glucose within only 40 μ s [42].
To optimize matrix reconstitution	Dynamic culturing [45].
To optimize differentiation of iPSCs to organoids	A multilayer perfusion system [46].
To achieve real-time monitoring and functionality evaluation	Development of self-guided trapping sites [47].
To optimize the formation and function of pseudo-islets	Using scaffolds based on cellulose [48].
To study in situ response of islet cells to external stimuli	Integration of an LSPR sensor [43].

3.2.2.2 Muscle-on-a-Chip (Muscular Dystrophy)

Muscle-on-a-chip models have been developed to study the underlying pathologies of progressively degenerative diseases such as Duchenne Muscular Dystrophy, amyotrophic lateral sclerosis (ALS), diabetes mellitus, endothelial inflammation, and atherosclerosis. These models provide an opportunity to develop personalized treatment options alongside studying the underlying biochemical pathologies by detecting cytokines, transcription factors, and other relevant biomarkers such as dystrophin. While immunostaining allows for studying immunohistochemistry, electrical stimulation allows evaluating contractile muscle response under multiple external stimuli, ranging from chemical to electrical impulses.

To achieve these objectives, contemporary research on muscle-on-a-chip has aimed to find the right biomaterial, perfusion strategies to enhance organoid formation and function, and integration with sensors to achieve real-time monitoring. The cells used can be both myoblasts and satellite cells harvested from both human donors and mice. Human amniotic mesenchymal stem cells (hAMCs) have also recently shown potential for myogenic differentiation [50]. There are, however, specific differences in the culture or encapsulation protocols and components of the growth/differentiation medium to be used for each of these cell types. There are also innate differences in the functionality of these cells. For example, skeletal muscle tissue organoids made from mice C2C12 cells show spontaneous contractions instead of those harvested from human cells, which show stimulated or induced contractions.

The applicability of PEG-DA and GelMA was proved as promising biomaterials for dielectropatterning of cells [52] (see Fig. 3.6), after which a nano-biosensor was developed to evaluate glucose consumption by GelMA hydrogel encapsulated skeletal muscle models under electrical stimulation at different time durations [53]. They found that skeletal muscle organoids exhibited maximum glucose

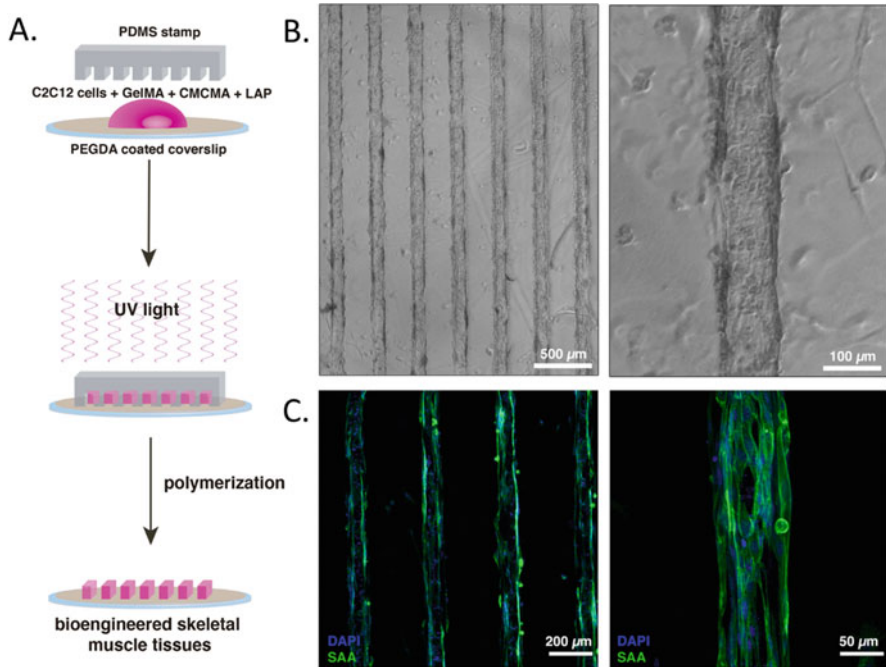


Fig. 3.6 Bioengineered 3D skeletal muscles in GelMA hydrogels. (a) Fabrication protocol to obtain 3D skeletal muscle tissues hydrogels. (b) Microscope images of cell-laden micropatterned hydrogels. (c) Representative confocal microscopy images of 3D skeletal muscle microtissues stained for the muscle maturation marker sarcomeric α -actinin (SAA, green) and nuclei (DAPI, blue). Adapted and reprinted with permission from [51]. © Copyright 2021, Walter de Gruyter GmbH

consumption in the initial 3 h, and the chosen biomaterial offered low viscosity and helped maintain cell viability [53]. Geometric orientation and alignment have been found to be extremely important for the proper development of myotubes. Towards this end, extracellular matrix conditions, type of scaffold, and patterning techniques play an essential role. Components in the chosen biomaterial act as geometric cues to achieve proper alignment, as observed in Matrigel, which has Collagen I, II, and these components create a tensile stretch necessary to achieve cell alignment into tubules and elasticity [54]. The fabrication approaches to achieve this alignment are also multiple such as 3D printing (bioprinting) [55], microfluidic extrusion/electrospinning [55, 56], bio-casting, 3-D and 2-D bioprinting [57], thermal gelation, micro-molding [58], photo mold patterning [59], micropatterning (3D and 2D), dielectropatterning [52], droplet-emulsion assisted patterning, e-field assisted printing [55], cryogelation and hydrogelation. All these techniques facilitate alignment and cell orientation and help identify biochemical, micromechanical, and geometric cues to enhance myotubes' differentiation, maturation, growth, and regeneration (Table 3.3).

Table 3.3 Skeletal muscle-on-a-chip models with their biofabrication technology

Objective	Technique
To identify the biochemical and microphysical cues involved in myoblast alignment	Electrospinning and 3-D printing to co-culture HUVECs and myoblasts [55].
To induce morphological retention and stimulate cellular alignment in myoblasts	Thermogel-assisted bioprinting [57].
To test the applicability of PEG-DA and GelMA for cell-patterning	Dielectropatterning [52].
To evaluate glucose consumption, GelMA encapsulated myoblasts under electrical stimulation	Nano-biosensor integrated with GelMA hydrogel encapsulated myoblasts coupled with electrical stimulation [53].
To bioengineer an all-encompassing 3-D skeletal muscle model of myotonic dystrophy type 1 and subsequent drug testing	Photomold patterning of GelMA and CMCMA hydrogel laden with cells [59].
To develop a new approach for vascularization of in vitro synthetic tissues	Micromilling-molding [58].
To enhance skeletal muscle development and evaluate the effect of agrin treatment on growth dynamics	Microfluidic extrusion and photo-crosslinking [56].
To design a new process to achieve better alignment and differentiation	E-field assisted printing [60].

3.2.2.3 Liver-on-a-Chip

The liver is not only the largest but also the most important internal organ of the human body. Its primary functions include detoxification, metabolism of macronutrients, drugs, and hormones, glycogenesis, bile production, and inflammatory response control. This organ is known for its regenerative capacity but is sufficiently vulnerable to drug toxicity. Liver-on-a-chip platforms allow mimicking the spatiotemporal characteristics and subsequently evaluating drug response outside the actual human body. At present, there are three primary research paradigms: disease modeling, drug toxicology, and organ physiology and regenerative capacity.

Current approaches involve multiple strategies to fabricate liver-on-a-chip devices. Among these, a few studies have even attempted to synergistically associate artificial intelligence with OOC to study disease pathology, such as that for NAFLD [62] (see Fig. 3.7). A few of these have been summarized in Table 3.4.

Similarly, OOCs for other organs such as the lung [65, 66], heart [67], gut [68, 69], kidney [70], and brain [71] also exist, as do the co-culture and multiple organ systems. There is, at present, exhaustive literature evidencing research undertaken using different approaches to elucidate drug responses, toxicology, physiology, biochemistry, regenerative capacity, and inter-organ communication.

3.2.2.4 Tumor-on-a-Chip

Billions of dollars are spent every year in research and development for unmasking underlying disease pathology in cancer and the development of viable drug targets. Conventional techniques, such as 2-D and 3-D cell cultures and animal models, are unsuitable as they cannot precisely replicate the tumor microenvironment, notably

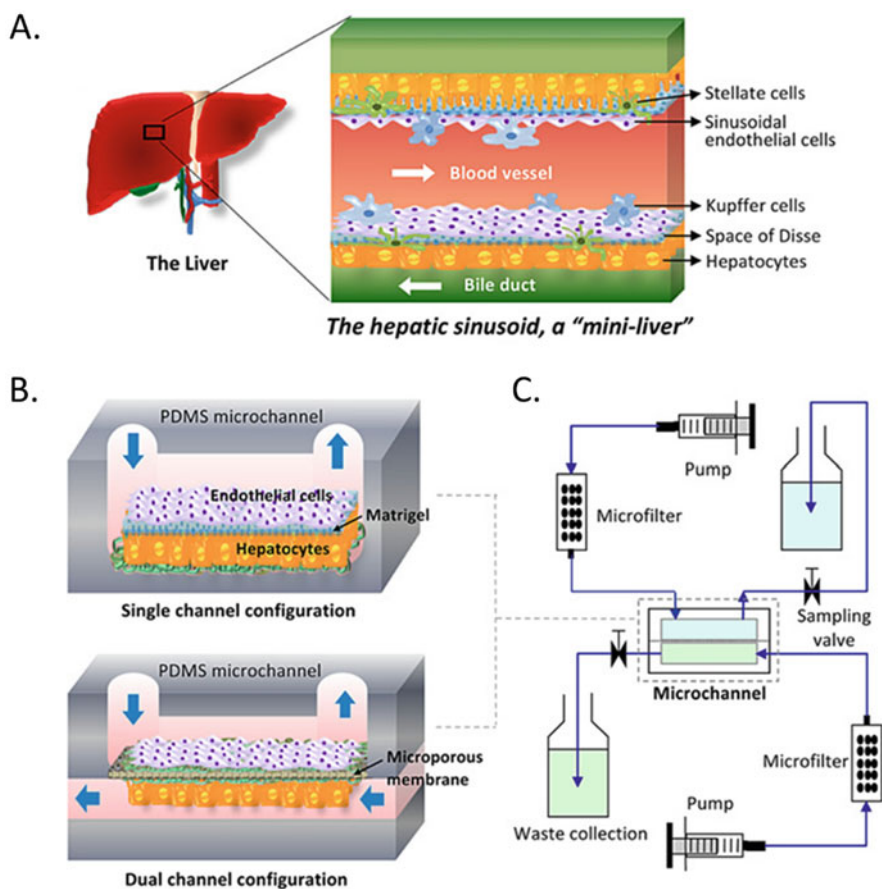


Fig. 3.7 Design of a microfluidic platform for the liver sinusoid model. (a) The liver sinusoid functional unit, (b) two proposed microfluidic configurations; and (c) bioreactor circuit for continuous perfusion of media and waste collection. Adapted and reprinted with permission from [61]. © Copyright 2015, John Wiley & Sons

Table 3.4 Liver-on-a-chip models with their biofabrication technology

Objective	Technique
To fabricate in vitro integrated models for evaluation of hepatic safety and metabolism of drugs	3-D liver OOC and spheroid culture for hepatotoxic screening and metabolic profiling using PDMS based microchannels [63].
To model the first-pass metabolism of a flavonoid using a co-culture model	Soft-lithography to model to develop a live co-culture first-pass metabolism [64].
To model liver sinusoid	Soft-lithography (single and dual-channel designs) to support long-term primary liver cultures [61].

Table 3.5 Tumor-on-a-chip models with their biofabrication technology

Objective	Technique
To evaluate the possibility of 3D multicellular structure bioprinting for investigating the response of paclitaxel on breast cancer spheroids	A dual nozzle bio-deposition system to bioprint cells and spheroids using different bioinks based on matrigel, gelatin, alginate, and collagen [73].
To address obstacles to high-throughput screening assays	Production of tumor spheroids using ultra low-attachment microplates and microwell arrays of hydrogels [74].
To precisely model complexity of in vivo pathophysiology of colorectal cancer and efficacy of drug loaded nanoparticles in a dose-dependent regime	A PDMS microfluidic platform fabricated by photolithography. The endothelial invasion of the core was quantified using bright-field microscopy followed by gene expression studies [75].

the extracellular matrix. The tumor microenvironment plays an essential role in cancer progression. This is where tumor-on-chip devices provide the opportunity and flexibility to replicate tumor microenvironment as close as possible to the in vivo environment, such as creating biomimetic microfluidic channels to mimic the oxygen gradients with spatial and temporal resolution. This oxygen gradient is known to be pivotal for metastasis. Therefore, the tumor-on-chip models can be used to mimic angiogenesis, metastasis, and transition from early to advanced forms by epithelial to mesenchymal transition [72]. A few models of tumor-on-chip are tabulated below (Table 3.5).

3.2.3 Drugs/Dosage Tested on Organs-on-a-Chip Technology

As previously stated, one of the purposes of developing OOCs is to model disease phenotype for drug development. Table 3.6 shows a few examples of drugs that have been tested for their response in different organ systems. A database by The North Columbian 3R's Collaborative (<https://www.na3rsc.org/mps-tech-hub/>) provides easy access to commercially available OOC platforms along with exhaustive literature and previous studies.

3.2.4 Integration of Biosensors in OOC Platforms

Although the number of examples applying different biosensors to detect relevant biomarkers in OOC devices is steadily increasing, there are limited advances in the achievement of fully integrated and self-operative devices, with complete integration in compact autonomous platforms and their validation in real environments.

Integration and high-throughput analysis are required to succeed in the development of relevant biosensor devices for OOC platforms. Microfluidics is, in this sense, an indispensable module to provide simultaneous analysis and assure low

Table 3.6 Commercially available OOC systems used in drug assays

Drug	Model	Objective
Aurora B kinase AZD2811 inhibitor	Bone marrow-on-chip	To elucidate the clinical toxicity profile of the drug in question [40].
Cisplatin and cyclosporine	Kidney-on-chip	Drug-induced nephrotoxicity and linkage with glucose accumulation [76].
AntagomiR-23b	DM1 skeletal-muscle-on-chip	Protects and helps in restoring both molecular and structural characteristics of DM1 myotubes [59].
Inhibitor empagliflozin	Kidney-on-chip	Significantly reduced cisplatin and cyclosporine-mediated kidney damage due to glucose accumulation [40].
Nimesulide and troglitazone	Liver-on-chip	To evaluate toxicity dose-dependent profiles of nimesulide and troglitazone (direct hepatotoxic agents) [77].
Trovafloxacin	Liver-on-chip	To evaluate indirect immune-mediated hepatotoxicity [78].
Acetaminophen, amiodarone, troglitazone, and rotenone	Liver-on-chip	To evaluate drug-induced hepatotoxicity by disruption of mitochondria [79].
Fialuridine and acetaminophen	Liver-on-chip and 3D hepatic spheroids	To analyze and compare model sensitivities of two drugs by measuring cytotoxic profiles [63].
Apigenin	Gut-on-chip	To verify the success of first-pass metabolism by analyzing the metabolites [64].

sample and reagent consumption. Appropriate dimensions and geometries in microfluidic pathways can enhance the diffusive mixing and, consequently, the speed and accuracy of reactions. Performance improvements like reduced measurement times, improved sensitivity, higher selectivity, and parallelism can be obtained by integrating an appropriate microfluidic system. On the other hand, the appropriate surface biofunctionalization that allows sensitive and selective biorecognition while minimizing non-specific adsorptions from cell-culture media is highly desirable. Also, it is necessary to remark that most of the proposed surface biofunctionalization methods are based on single-use/detection, limiting the platforms' capability. New surface functionalization methods that allow biosensor regeneration for several biodetection cycles would be ideal.

The impact of external stimuli or internal abnormalities manifests in multiple ways: changes in temperature, the optical density of the extracellular media, pH, levels of oxygen and carbon dioxide, metabolites such as glucose and lactate, and chemicals such as hormones and cytokines, and changes in the cell behavior. Table 3.7 shows only a few different techniques adopted to monitor these parameters for multiple objectives.

Over the last years, there have been limited examples of integrated biosensing systems for in situ biodetection of segregated biomarkers from OOC devices. Considering the high availability of commercial electrodes for the development of

Table 3.7 Integrated sensors for respective culture parameters

Parameter	Technique
Temperature	To monitor any physiologic changes in iPSC culture medium using an integrated CMOS smart sensor [80].
pH	To measure temperature, oxygen, and pH simultaneously using a combination of silica beads and fluorescent dyes for fluorescent based sensing [81].
pH	To measure carbon dioxide and oxygen using a pH sensitive fluorescent indicator within ethyl-cellulose [82].
pH	To dynamically measure cancer metabolism based on potentiostatic analysis [83].
O ₂	To study the respiratory kinetics in adherent (HeLa) cells using a Clark-type oxygen chip [84].
O ₂	To develop sensitive miniaturized amperometric oxygen sensors [85].
O ₂	To study hepatocyte polarization and metabolic function based on the involvement of non-parenchymal cells (NPCs) using luminescence-based sensor spots (building on the ability of oxygen to quench luminescence) [86].
O ₂	To study oxygen gradients and oxygen consumption in 2-D and 3-D hydrogel cultures using amine functionalized polystyrene bead-based oxygen sensor. Monitoring was performed using FireStingO2 optical sensor at 1 Hz [87].
CO ₂	To measure temperature, oxygen, and pH simultaneously using a combination of silica beads and fluorescent dyes for fluorescent based sensing [81].
CO ₂	To measure carbon dioxide and oxygen using pH sensitive fluorescent indicator within ethyl-cellulose [82].
Metabolites:	
Glucose and lactate	To dynamically measure cancer metabolism using an enzyme immobilized hydrogel for amperometric measurements [83].
Glucose and lactate	To measure mitochondrial function in liver-on-a-chip model using imbedded amperometric sensors for glucose and lactate [79].
Glucose and lactate	To selectively detect ascorbate, glucose, and lactate using dehydrogenase based sensing mechanism adsorbed onto single-walled carbon nanotubes [88].
Calcium	To study activity dynamics and electrical activity in neurons using a microfluidic/microelectrode array [89].

electrochemical biosensors, most of the developed biosensing systems are based on this technology. Recently, Ramon-Azcon research group presented a multiplexed integrated platform based on electrochemical biosensors for high sensitivity biodetection of IL-6 and TNF- α in a muscle-on-chip model platform with electrical stimulation [90]. Although they reach a sensitivity in the order of ng/mL, it is based on an amplified biodetection (sandwich assay) using a secondary recognition antibody, increasing the complexity of the bioassay. Other examples of electrochemical-based biosensing devices have been developed by Khademhosseini research group (see Fig. 3.8). The first device was based on the multiplexed monitoring of creatine kinase, albumin, and GST- α in a Heart-Liver-on-Chip model using monoclonal antibodies [92]. The system was able to detect changes of the biomarkers with a sensitivity of ng/mL produced by the presence of acetaminophen as a model for liver toxicity. The second device was based on the single monitoring of creatine kinase in a heart-on-chip model using biorecognition based on aptamers [93]. The system

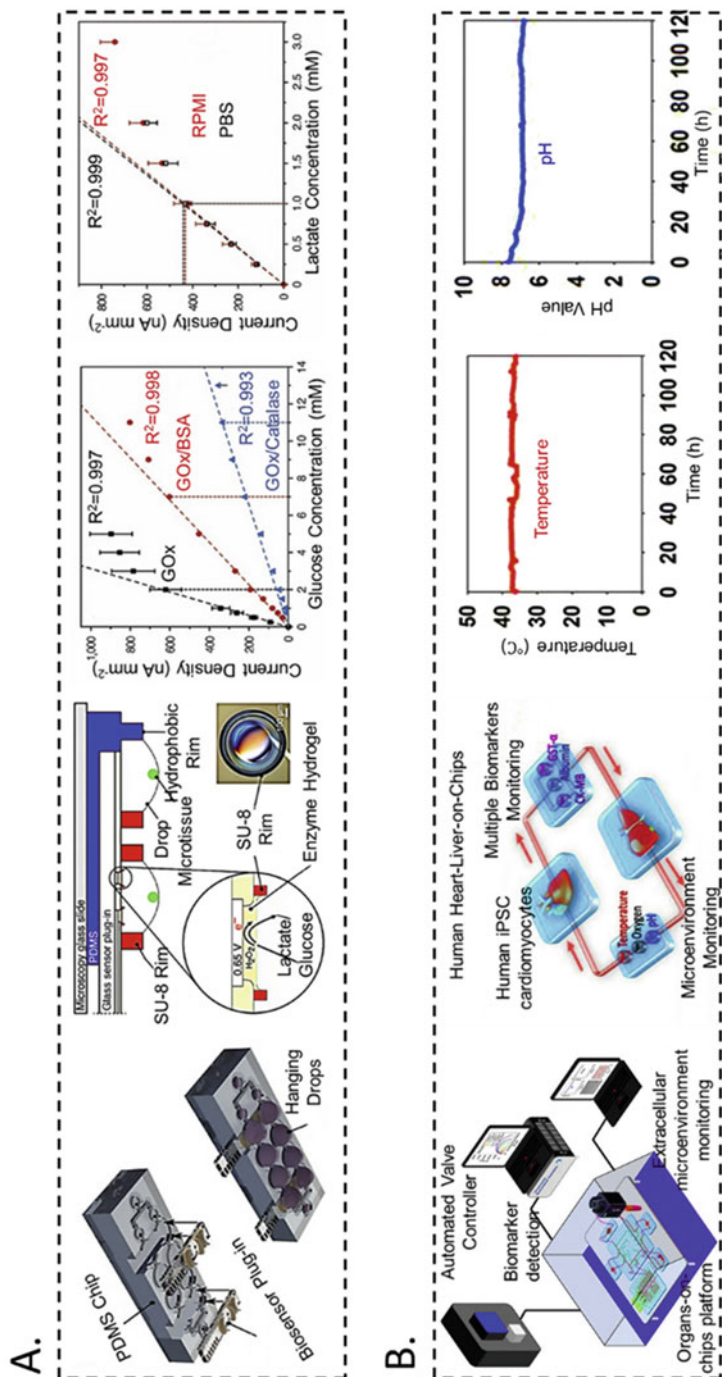


Table 3.8 Examples of emerging biosensing systems in the monitoring of relevant biomarkers in OOC devices

Type of biosensor	OOC	Biomarker	Limit of detection
Electrochemical [90]	Muscle	IL-6 and TNF- α	ng/mL
Electrochemical [92]	Liver/heart	Creatine kinase, albumin, and GST- α	ng/mL
Electrochemical [93]	Heart	Creatine kinase	pg/mL
Optical [43]	Pancreas	Insulin	μ g/mL

based on aptamers shows a high shelf life for up to 7 days while antibodies biosensing performance decreases over time. Even more, the aptamer biosensor showed a superior biosensing performance with a sensitivity in the order of pg/mL in cell-culture media. The heart model was based on the secretion of creatine kinase under doxorubicin, an anticancer drug used as a model to induce cardiac injury.

Finally, a novel optical biosensing platform has recently been presented by Ramon-Azcón group based on nanoplasmonic biosensors for monitoring insulin secretion from pancreatic islets spheroids under the presence of different concentrations of glucose in a Pancreas-on-Chip model [43]. The nanoplasmonic biosensor based on gold rod-shaped nanoantennas allows multiplexed monitoring of insulin secretion with a sensitivity of 0.85 μ g/mL. Although the sensitivity is worst compared to other biosensors, the system allows label-free real-time monitoring without sample pretreatment and amplification. The optical readout is based on simple transmission configuration, increasing the potential for highly integrated monitor systems. Table 3.8 summarizes the most relevant emerging examples of different biosensing platforms applied to OOC devices. On the other hand, in Fig. 3.9, we present the schemes of two examples of all integrated OOC/biosensing platforms.

3.3 Conclusion and Perspectives

Biosensors are a rising technology in their integration with OOC devices to achieve fully operative and autonomous platforms that can effectively monitor physiological parameters and the secretion of biomarkers by the cell to a physical and chemical stimulus. Although there are still challenges to surpass, mainly related to the integration and multiplexing biosensing, the new advances in surface biofunctionalization can minimize cross-reactivity, non-specific adsorption and allow biosensors regeneration for real-time multiplexed detection. On the other hand, effective microfluidic designs with the correct flow components can create compact and modular systems. Due to its high versatility and straightforward integration in OOC platforms, biosensors technology is an exciting candidate for developing sensing platforms for real-time cell monitoring in OOC devices.

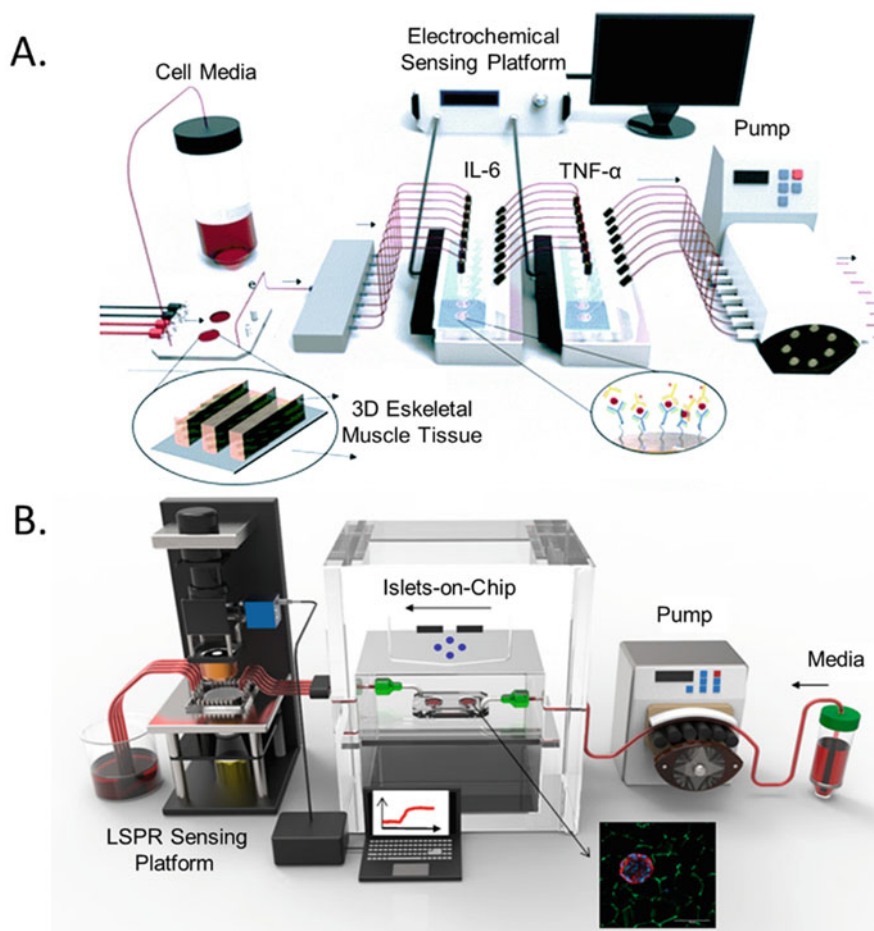


Fig. 3.9 Schematic illustration of OOC systems with integrated biosensing platforms based on (a) electrochemical (Adapted and reprinted with permission from [90]. © Copyright 2019, Royal Society of Chemistry) and (b) optical (Adapted and reprinted with permission from [43]. © Copyright 2021, MDPI) detection

Acknowledgments This project received financial support from the European Research Council program under grants ERC-StG-DAMOC (714317), the European Commission under FET-open program BLOC project (GA-863037), the Spanish Ministry of Economy and Competitiveness, through the “Severo Ochoa” Program for Centres of Excellence in R & D (SEV-2016–2019) and “Retos de investigación: Proyectos I+D+i” (TEC2017-83716-C2-2-R), the CERCA Programme/ Generalitat de Catalunya (2017-SGR-1079) and Fundación Bancaria “la Caixa”- Obra Social “la Caixa” (project IBEC-La Caixa Healthy Ageing) to Javier Ramón-Azcón. Gerardo A. Lopez-Muñoz acknowledges SECTEI (Secretaría de Educación, Ciencia, Tecnología e Innovación de la Ciudad de México) for Postdoctoral Fellowship SECTEI/143/2019 and CM-SECTEI/013/2021.

References

1. Biosensors market by type, product, technology, application. COVID-19 impact analysis. MarketsandMarkets™. <https://www.marketsandmarkets.com/Market-Reports/biosensors-market-798.html>. Accessed 27 Aug 2021
2. IUPAC - biosensor (B00663). <https://goldbook.iupac.org/terms/view/B00663>. Accessed 27 Aug 2021
3. Kaur H, Shorie M (2019) Nanomaterial based aptasensors for clinical and environmental diagnostic applications. *Nanoscale Adv* 1(6):2123–2138. <https://doi.org/10.1039/C9NA00153K>
4. Dahlin AB, Tegenfeldt JO, Höök F (2006) Improving the instrumental resolution of sensors based on localized surface plasmon resonance. *Anal Chem* 78(13):4416–4423. <https://doi.org/10.1021/AC0601967>
5. Vigneshvar S, Sudhakumari CC, Senthilkumaran B, Prakash H (2016) Recent advances in biosensor technology for potential applications – an overview. *Front Bioeng Biotechnol* 4:11. <https://doi.org/10.3389/FBIOE.2016.00011>
6. Yakoh A, Pimpitak U, Rengpipat S, Hirankarn N, Chailapakul O, Chaiyo S (2021) Paper-based electrochemical biosensor for diagnosing COVID-19: detection of SARS-CoV-2 antibodies and antigen. *Biosens Bioelectron* 176:112912. <https://doi.org/10.1016/J.BIOS.2020.112912>
7. Bragazzi NL, Amicizia D, Panatto D, Tramalloni D, Valle I, Gasparini R (2015) Quartz-crystal microbalance (QCM) for public health: an overview of its applications. *Adv Protein Chem Struct Biol* 101:149–211. <https://doi.org/10.1016/BS.APCSB.2015.08.002>
8. da Silva ETSG, Souto DEP, Barragan JTC, de F Giarola J, de Moraes ACM, Kubota LT (2017) Electrochemical biosensors in point-of-care devices: recent advances and future trends. *ChemElectroChem* 4(4):778–794. <https://doi.org/10.1002/CELC.201600758>
9. Zhu C, Yang G, Li H, Du D, Lin Y (2014) Electrochemical sensors and biosensors based on nanomaterials and nanostructures. *Anal Chem* 87(1):230–249. <https://doi.org/10.1021/AC5039863>
10. Wang J (2006) Electrochemical biosensors: towards point-of-care cancer diagnostics. *Biosens Bioelectron* 21(10):1887–1892. <https://doi.org/10.1016/J.BIOS.2005.10.027>
11. Deng X et al (2016) A highly sensitive immunosorbent assay based on biotinylated graphene oxide and the quartz crystal microbalance. *ACS Appl Mater Interfaces* 8(3):1893–1902. <https://doi.org/10.1021/ACSAMI.5B10026>
12. Atay S, Pişkin K, Yılmaz F, Çakır C, Yavuz H, Denizli A (2015) Quartz crystal microbalance based biosensors for detecting highly metastatic breast cancer cells via their transferrin receptors. *Anal Methods* 8(1):153–161. <https://doi.org/10.1039/C5AY02898A>
13. Dubiel EA, Martin B, Vigier S, Vermette P (2017) Real-time label-free detection and kinetic analysis of etanercept—protein interactions using quartz crystal microbalance. *Colloids Surf B Biointerfaces* 149:312–321. <https://doi.org/10.1016/J.COLSURFB.2016.10.036>
14. Reviakine I, Johannsmann D, Richter RP (2011) Hearing what you cannot see and visualizing what you hear: interpreting quartz crystal microbalance data from solvated interfaces. *Anal Chem* 83(23):8838–8848. <https://doi.org/10.1021/AC201778H>
15. Lopez GA, Estevez M-C, Soler M, Lechuga LM (2017) Recent advances in nanoplasmonic biosensors: applications and lab-on-a-chip integration. *Nano* 6(1):123–136. <https://doi.org/10.1515/NANOPH-2016-0101>
16. Garland PB (1996) Optical evanescent wave methods for the study of biomolecular interactions. *Q Rev Biophys* 29(1):91–117. <https://doi.org/10.1017/S0033583500005758>
17. Hutchinson AM (1995) Evanescent wave biosensors. *Mol Biotechnol* 3(1):47–54. <https://doi.org/10.1007/BF02821334>
18. Fan X, White IM, Shopova SI, Zhu H, Suter JD, Sun Y (2008) Sensitive optical biosensors for unlabeled targets: a review. *Anal Chim Acta* 620(1–2):8–26. <https://doi.org/10.1016/J.ACA.2008.05.022>

19. Vollmer F, Arnold S (2008) Whispering-gallery-mode biosensing: label-free detection down to single molecules. *Nat Methods* 5(7):591–596. <https://doi.org/10.1038/nmeth.1221>
20. Kozma P, Kehl F, Ehrentreich-Förster E, Stamm C, Bier FF (2014) Integrated planar optical waveguide interferometer biosensors: a comparative review. *Biosens Bioelectron* 58:287–307. <https://doi.org/10.1016/J.BIOS.2014.02.049>
21. Nguyen HH, Park J, Kang S, Kim M (May 2015) Surface plasmon resonance: a versatile technique for biosensor applications. *Sensors* 15(5):10481–10510. <https://doi.org/10.3390/S150510481>
22. Jason-Moller L, Murphy M, Bruno JA (2006) Overview of Biacore systems and their applications. *Curr Protoc Protein Sci* 19:1–14. <https://doi.org/10.1002/0471140864.ps1913s45>
23. Homola J (2003) Present and future of surface plasmon resonance biosensors. *Anal Bioanal Chem* 377(3):528–539. <https://doi.org/10.1007/S00216-003-2101-0>
24. Long S et al (2020) Grating coupled SPR sensors using off the shelf compact discs and sensitivity dependence on grating period. *Sens Actuators Rep* 2(1):100016. <https://doi.org/10.1016/J.SNR.2020.100016>
25. Peng W, Liu Y (2021) Fiber-optic surface plasmon resonance sensors and biochemical applications: a review. *J Light Technol* 39(12):3781–3791. <https://www.osapublishing.org/abstract.cfm?uri=jlt-39-12-3781>
26. Mayer KM, Hafner JH (2011) Localized surface plasmon resonance sensors. *Chem Rev* 111(6):3828–3857. <https://doi.org/10.1021/CR100313V>
27. Pothipor C, Jakmunee J, Bamrungsap S, Ounnunkad K (2021) An electrochemical biosensor for simultaneous detection of breast cancer clinically related microRNAs based on a gold nanoparticles/graphene quantum dots/graphene oxide film. *Analyst* 146(12):4000–4009. <https://doi.org/10.1039/D1AN00436K>
28. Tanak AS, Muthukumar S, Krishnan S, Schully KL, Clark DV, Prasad S (2021) Multiplexed cytokine detection using electrochemical point-of-care sensing device towards rapid sepsis endotyping. *Biosens Bioelectron* 171:112726. <https://doi.org/10.1016/J.BIOS.2020.112726>
29. Huang L et al (2021) One-step rapid quantification of SARS-CoV-2 virus particles via low-cost nanoplasmonic sensors in generic microplate reader and point-of-care device. *Biosens Bioelectron* 171:112685. <https://doi.org/10.1016/J.BIOS.2020.112685>
30. Masterson AN, Liyanage T, Kaimakliotis H, Derami HG, Deiss F, Sardar R (2020) Bottom-up fabrication of plasmonic nanoantenna-based high-throughput multiplexing biosensors for ultrasensitive detection of microRNAs directly from cancer Patients' plasma. *Anal Chem* 92(13):9295–9304. <https://doi.org/10.1021/ACS.ANALCHEM.0C01639>
31. Bakhshpour M, Piskin AK, Yavuz H, Denizli A (2019) Quartz crystal microbalance biosensor for label-free MDA MB 231 cancer cell detection via notch-4 receptor. *Talanta* 204:840–845. <https://doi.org/10.1016/J.TALANTA.2019.06.060>
32. Jandas PJ, Luo J, Quan A, Li C, Chen F, Fu YQ (2020) Graphene oxide-au nano particle coated quartz crystal microbalance biosensor for the real time analysis of carcinoembryonic antigen. *RSC Adv* 10(7):4118–4128. <https://doi.org/10.1039/C9RA09963H>
33. Ferhan AR, Jackman JA, Park JH, Cho NJ (2018) Nanoplasmonic sensors for detecting circulating cancer biomarkers. *Adv Drug Deliv Rev* 125:48–77. <https://doi.org/10.1016/j.addr.2017.12.004>
34. Stewart ME et al (2008) Nanostructured plasmonic sensors. *Chem Rev* 108(2):494–521. <https://doi.org/10.1021/cr068126n>
35. Yang J, Giessen H, Lalanne P (2015) Simple analytical expression for the peak-frequency shifts of plasmonic resonances for sensing. *Nano Lett* 15(5):3439–3444. <https://doi.org/10.1021/acs.nanolett.5b00771>
36. Liyanage T, Masterson AN, Oyem HH, Kaimakliotis H, Nguyen H, Sardar R (2019) Plasmo-electronic-based ultrasensitive assay of tumor suppressor microRNAs directly in patient plasma: design of highly specific early cancer diagnostic technology. *Anal Chem* 91(3):1894–1903. <https://doi.org/10.1021/acs.analchem.8b03768>

37. Bathini S et al (2018) Nano-bio interactions of extracellular vesicles with gold nanoislands for early cancer diagnosis. *Research* 2018. <https://doi.org/10.1155/2018/3917986>
38. Yavas O et al (2018) Self-calibrating on-chip localized surface plasmon resonance sensing for quantitative and multiplexed detection of cancer markers in human serum. *ACS Sens* 3(7): 1376–1384. <https://doi.org/10.1021/acssensors.8b00305>
39. Ma C, Peng Y, Li H, Chen W (2021) Organ-on-a-chip: A new paradigm for drug development. *Trends Pharmacol Sci* 42(2):119–133. <https://doi.org/10.1016/J.TIPS.2020.11.009>
40. Clapp N, Amour A, Rowan WC, Candarlioglu PL (2021) Organ-on-chip applications in drug discovery: an end user perspective. *Biochem Soc Trans* 49(4):1881–1890. <https://doi.org/10.1042/bst20210840>
41. Mohammed JS, Wang Y, Harvat TA, Oberholzer J, Eddington DT (2009) Microfluidic device for multimodal characterization of pancreatic islets. *Lab Chip* 9(1):97–106. <https://doi.org/10.1039/B809590F>
42. Perrier R et al (2018) Bioelectronic organ-based sensor for microfluidic real-time analysis of the demand in insulin. *Biosens Bioelectron* 117:253–259. <https://doi.org/10.1016/j.bios.2018.06.015>
43. Ortega MA et al (2021) In situ LSPR sensing of secreted insulin in organ-on-chip. *Biosens* 11(5):138. <https://doi.org/10.3390/BIOS11050138>
44. Patel SN et al (2021) Organoid microphysiological system preserves pancreatic islet function within 3D matrix. *Sci Adv* 7(7). <https://doi.org/10.1126/SCIADV.ABA5515>
45. Jun Y et al (2019) In vivo-mimicking microfluidic perfusion culture of pancreatic islet spheroids. *Sci Adv* 5(11). <https://doi.org/10.1126/sciadv.aax4520>
46. Tao T et al (2014) Engineering human islet organoids from iPSCs using an organ-on-chip platform. *Lab Chip* 24(iii):1381–1388. <https://doi.org/10.1039/C8LC01298A>. Volume
47. Zbinden A et al (2020) Non-invasive marker-independent high content analysis of a microphysiological human pancreas-on-a-chip model. *Matrix Biol* 85–86:205–220. <https://doi.org/10.1016/j.matbio.2019.06.008>
48. Velasco-Mallorquí F, Rodríguez-Comas J, Ramón-Azcón J (2021) Cellulose-based scaffolds enhance pseudoislets formation and functionality. *Biofabrication* 13(3):035044. <https://doi.org/10.1088/1758-5090/ac00c3>
49. Edmonton protocol. Alberta Diabetes Institute. <https://www.ualberta.ca/alberta-diabetes/about/edmonton-protocol.html>. Accessed 30 Sep 2021
50. Zhang D et al (2019) Myogenic differentiation of human amniotic mesenchymal cells and its tissue repair capacity on volumetric muscle loss. *J Tissue Eng* 10. <https://doi.org/10.1177/2041731419887100>
51. Lopez-Muñoz GA, Fernández-Costa JM, Ortega MA, Balaguer-Trias J, Martín-Lasierra E, Ramon-Azcon J (2021) Plasmonic nanocrystals on polycarbonate substrates for direct and label-free biodetection of Interleukin-6 in bioengineered 3D skeletal muscles. *Nano* 10(18): 4477–4488
52. Ramón-Azcón J et al (2012) Gelatin methacrylate as a promising hydrogel for 3D microscale organization and proliferation of dielectrophoretically patterned cells. *Lab Chip* 12(16): 2959–2969. <https://doi.org/10.1039/c2lc40213k>
53. Obregón R et al (2013) Non-invasive measurement of glucose uptake of skeletal muscle tissue models using a glucose nanobiosensor. *Biosens Bioelectron* 50:194–201. <https://doi.org/10.1016/j.bios.2013.06.020>
54. Fernández-Costa JM, Fernández-Garibay X, Velasco-Mallorquí F, Ramón-Azcón J (2021) Bioengineered in vitro skeletal muscles as new tools for muscular dystrophies preclinical studies. *J Tissue Eng* 12:10–12. <https://doi.org/10.1177/2041731420981339>
55. Yeo M, Kim GH (2020) Micro/nano-hierarchical scaffold fabricated using a cell electrospinning/3D printing process for co-culturing myoblasts and HUVECs to induce myoblast alignment and differentiation. *Acta Biomater* 107:102–114. <https://doi.org/10.1016/j.actbio.2020.02.042>

56. Ebrahimi M, Ostrovidov S, Salehi S, Kim SB, Bae H, Khademhosseini A (2018) Enhanced skeletal muscle formation on microfluidic spun gelatin methacryloyl (GelMA) fibres using surface patterning and agrin treatment. *J Tissue Eng Regen Med* 12(11):2151–2163. <https://doi.org/10.1002/term.2738>
57. Mozetic P, Giannitelli SM, Gori M, Trombetta M, Rainer A (2017) Engineering muscle cell alignment through 3D bioprinting. *J Biomed Mater Res Part A* 105(9):2582–2588. <https://doi.org/10.1002/jbm.a.36117>
58. Wan L, Flegle J, Ozdoganlar B, Leduc PR (2020) Toward vasculature in skeletal muscle-on-a-chip through thermo-responsive sacrificial templates. *Micromachines* 11(10):1–13. <https://doi.org/10.3390/mi11100907>
59. Fernández-Garibay X et al (2021) Bioengineered in vitro 3D model of myotonic dystrophy type 1 human skeletal muscle. *Biofabrication* 13(3):035035. <https://doi.org/10.1088/1758-5090/abf6ae>
60. Kim JY, Kim WJ, Kim GH (2020) Scaffold with micro/nanoscale topographical cues fabricated using E-field-assisted 3D printing combined with plasma-etching for enhancing myoblast alignment and differentiation. *Appl Surf Sci* 509:145404. <https://doi.org/10.1016/j.apsusc.2020.145404>
61. Kang YBA et al (2015) Liver sinusoid on a chip: Long-term layered co-culture of primary rat hepatocytes and endothelial cells in microfluidic platforms. *Biotechnol Bioeng* 112(12):2571–2582. <https://doi.org/10.1002/bit.25659>
62. De Chiara F, Ferret-Miñana A, Ramón-Azcón J (2021) The synergy between organ-on-a-chip and artificial intelligence for the study of NAFLD: from basic science to clinical research. *Biomedicine* 9(3):1–16. <https://doi.org/10.3390/biomedicines9030248>
63. Foster AJ et al (2019) Integrated in vitro models for hepatic safety and metabolism: evaluation of a human Liver-Chip and liver spheroid. *Arch Toxicol* 93(4):1021–1037. <https://doi.org/10.1007/s00204-019-02427-4>
64. Choe A, Ha SK, Choi I, Choi N, Sung JH (2017) Microfluidic Gut-liver chip for reproducing the first pass metabolism. *Biomed Microdevices* 19(1):1–11. <https://doi.org/10.1007/s10544-016-0143-2>
65. Huh D (2015) A human breathing lung-on-a-chip. *Ann Am Thorac Soc* 12(3):S42–S44. <https://doi.org/10.1513/AnnalsATS.201410-442MG>
66. Zamprogno P et al (2021) Second-generation lung-on-a-chip with an array of stretchable alveoli made with a biological membrane. *Commun Biol* 4(1):1–10. <https://doi.org/10.1038/s42003-021-01695-0>
67. Kitsara M, Kontziampasis D, Agbulut O, Chen Y (2019) Heart on a chip: micro-nanofabrication and microfluidics steering the future of cardiac tissue engineering. *Microelectron Eng* 203–204:44–62. <https://doi.org/10.1016/j.mee.2018.11.001>
68. Xiang Y, Wen H, Yu Y, Li M, Fu X, Huang S (2020) Gut-on-chip: recreating human intestine in vitro. *J. Tissue Eng.* 11. <https://doi.org/10.1177/2041731420965318>
69. de Haan P, Santbergen MJC, van der Zande M, Bouwmeester H, Nielen MWF, Verpoorte E (2021) A versatile, compartmentalised gut-on-a-chip system for pharmacological and toxicological analyses. *Sci Rep* 11(1):1–13. <https://doi.org/10.1038/s41598-021-84187-9>
70. Yin L et al (2020) Efficient drug screening and nephrotoxicity assessment on co-culture microfluidic kidney chip. *Sci Rep* 10(1):1–11. <https://doi.org/10.1038/s41598-020-63096-3>
71. Raimondi I, Izzo L, Tunesi M, Comar M, Albani D, Giordano C (2020) Organ-on-a-chip in vitro models of the brain and the blood-brain barrier and their value to study the microbiota-gut-brain axis in neurodegeneration. *Front Bioeng Biotechnol* 7. <https://doi.org/10.3389/fbioe.2019.00435>
72. Liu X et al (2021) Tumor-on-a-chip: from bioinspired design to biomedical application. *Microsyst Nanoeng* 7(1). <https://doi.org/10.1038/s41378-021-00277-8>
73. Swaminathan S, Hamid Q, Sun W, Clyne AM (2020) Bioprinting of 3D breast epithelial spheroids for human cancer models. 11(2). <https://doi.org/10.1088/1758-5090/aafc49>. [Bioprinting](https://doi.org/10.1088/1758-5090/aafc49)

74. Shan S, Johnston AP (2017) The production of 3D tumor spheroids for cancer drug discovery. *Physiol Behav* 176(12):139–148. <https://doi.org/10.1016/j.ddtec.2017.03.002>.The
75. Carvalho MR et al (2019) Colorectal tumor-on-a-chip system: A 3D tool for precision onconanomedicine. *Sci Adv* 5(5):1–12. <https://doi.org/10.1126/sciadv.aaw1317>
76. Cohen A et al (2021) Mechanism and reversal of drug-induced nephrotoxicity on a chip. *Sci Transl Med* 13(582). <https://doi.org/10.1126/SCITRANSLMED.ABD6299>
77. Vernetti LA et al (2015) Original research. A human liver microphysiology platform for investigating physiology, drug safety, and disease models. *Exp Biol Med* 241:101–114. <https://doi.org/10.1177/1535370215592121>
78. Moradi E, Jalili-Firoozinezhad S, Solati-Hashjin M (2020) Microfluidic organ-on-a-chip models of human liver tissue. *Acta Biomater* 116:67–83. <https://doi.org/10.1016/j.actbio.2020.08.041>
79. Bavli D et al (2016) Real-time monitoring of metabolic function in liver-onchip microdevices tracks the dynamics of Mitochondrial dysfunction. *Proc Natl Acad Sci U S A* 113(16):E2231–E2240. <https://doi.org/10.1073/pnas.1522556113>
80. da Ponte RM et al (2021) Monolithic integration of a smart temperature sensor on a modular silicon-based organ-on-a-chip device. *Sensors Actuators A Phys* 317:112439. <https://doi.org/10.1016/j.sna.2020.112439>
81. Wang C, Otto S, Dorn M, Heinze K, Resch-Genger U (2019) Luminescent TOP nanosensors for simultaneously measuring temperature, oxygen, and pH at a single excitation wavelength. *Anal Chem* 91(3):2337–2344. <https://doi.org/10.1021/acs.analchem.8b05060>
82. Chu C-S, Syu J-J (2017) Optical sensor for dual sensing of oxygen and carbon dioxide based on sensing films coated on filter paper. *Appl Opt* 56(4):1225. <https://doi.org/10.1364/ao.56.001225>
83. Weltin A et al (2014) Cell culture monitoring for drug screening and cancer research: a transparent, microfluidic, multi-sensor microsystem. *Lab Chip* 14(1):138–146. <https://doi.org/10.1039/c3lc50759a>
84. Wu CC, Luk HN, Lin YTT, Yuan CY (2010) A Clark-type oxygen chip for in situ estimation of the respiratory activity of adhering cells. *Talanta* 81(1–2):228–234. <https://doi.org/10.1016/j.talanta.2009.11.062>
85. Oomen PE, Skolimowski MD, Verpoorte E (2016) Implementing oxygen control in chip-based cell and tissue culture systems. *Lab Chip* 16(18):3394–3414. <https://doi.org/10.1039/c6lc00772d>
86. Rennert K et al (2015) A microfluidically perfused three dimensional human liver model. *Biomaterials* 71:119–131. <https://doi.org/10.1016/j.biomaterials.2015.08.043>
87. Zirath H et al (2018) Every breath you take: non-invasive real-time oxygen biosensing in two- and three-dimensional microfluidic cell models. *Front Physiol* 9(JUL):1–12. <https://doi.org/10.3389/fphys.2018.00815>
88. Lin Y, Yu P, Hao J, Wang Y, Ohsaka T, Mao L (2014) Continuous and simultaneous electrochemical measurements of glucose, lactate, and ascorbate in rat brain following brain ischemia. *Anal Chem* 86(8):3895–3901. <https://doi.org/10.1021/ac4042087>
89. Moutaux E, Charlot B, Genoux A, Saudou F, Cazorla M (2018) An integrated microfluidic/microelectrode array for the study of activity-dependent intracellular dynamics in neuronal networks. *Lab Chip* 18(22):3425–3435. <https://doi.org/10.1039/C8LC00694F>
90. Ortega MA et al (2019) Muscle-on-a-chip with an on-site multiplexed biosensing system for: in situ monitoring of secreted IL-6 and TNF- α . *Lab Chip* 19(15):2568–2580. <https://doi.org/10.1039/c9lc00285e>
91. Zhu Y et al (2021) State of the art in integrated biosensors for organ-on-a-chip applications. *Curr Opin Biomed Eng* 19:100309. <https://doi.org/10.1016/j.cobme.2021.100309>
92. Zhang YS et al (2017) Multisensor-integrated organs-on-chips platform for automated and continual in situ monitoring of organoid behaviors. *Proc Natl Acad Sci* 114(12):E2293–E2302. <https://doi.org/10.1073/PNAS.1612906114>
93. Shin SR et al (2016) Aptamer-based microfluidic electrochemical biosensor for monitoring cell-secreted trace cardiac biomarkers. *Anal Chem* 88(20):10019–10027. <https://doi.org/10.1021/ACS.ANALCHEM.6B02028>



Current Trends in Microfluidics and Biosensors for Cancer Research Applications

4

David Caballero, Rui L. Reis, and Subhas C. Kundu

Abstract

Despite the significant amount of resources invested, cancer remains a considerable burden in our modern society and a leading cause of death. There is still a lack of knowledge about the mechanistic determinants of the disease, the mechanism of action of drugs, and the process of tumor relapse. Current methodologies to study all these events fail to provide accurate information, threatening the prognosis of cancer patients. This failure is due to the inadequate procedure in how tumorigenesis is studied and how drug discovery and screening are currently made. Traditionally, they both rely on seeding cells on static flat cultures and on the immunolabelling of cellular structures, which are usually limited in their ability to reproduce the complexity of the native cellular habitat and provide quantitative data. Similarly, more complex animal models are employed for—unsuccessfully—mimicking the human physiology and evaluating the etiology of the disease or the efficacy/toxicity of pharmacological compounds. Despite some breakthroughs and success obtained in understanding the disease and developing novel therapeutic approaches, cancer still kills millions of people worldwide, remaining a global healthcare problem with a high social and economic impact. There is a need for novel integrative methodologies and technologies capable of providing valuable readouts. In this regard, the combination of microfluidics technology with miniaturized biosensors offers unprecedented advantages to

D. Caballero (✉) · R. L. Reis · S. C. Kundu

3B's Research Group, I3Bs – Research Institute on Biomaterials, Biodegradables and Biomimetics, University of Minho, Headquarters of the European Institute of Excellence on Tissue Engineering and Regenerative Medicine, AvePark, Parque de Ciência e Tecnologia, Zona Industrial da Gandra, Guimarães, Portugal

ICVS/3B's – PT Government Associate Laboratory, Braga/Guimarães, Portugal
e-mail: dcaballero@i3bs.uminho.pt

accelerate the development of drugs. This integrated technology have the potential to unravel the key pathophysiological processes of cancer progression and metastasis, overcoming the existing gap on in vitro predictive platforms and in vivo model systems. Herein, we discuss how this combination may boost the field of cancer theranostics and drug discovery/screening toward more precise devices with clinical relevance.

Keywords

Biosensors · Cancer · Drug screening · Microfabrication · Microfluidics

4.1 Introduction

Cancer is a leading cause of death worldwide, responsible for about 10 million deaths in 2020 [1]. Breast, lung, colorectal, prostate, stomach, skin, and liver are the most common cancer cases. Cancer mortality can be significantly reduced by early detection and improved treatment of the disease and before the appearance of any evident symptoms. During the last years, the cancer research community has demanded more sophisticated technologies that overcome the intrinsic limitations of traditional screening and modeling methods to study the effect of drugs better and reproduce key cancer-related events [2]. These are based on regular—flat—tissue culture dishes, which fail to reproduce the biological, rheological, and structural complexities of the native scenario, and where cells react to drugs very differently compared to what happens during systemic delivery.

Additionally, conventional screening methods are, in general, too laborious, and some of them require a myriad of pre-treatment steps and high sample volumes. More sophisticated in vitro systems include three-dimensional tumor spheroids or semi-permeable membrane assays, with or without ECM, and other cell types. However, these approaches lack, in general, fluid flow, may be incompatible with live imaging, and cannot recapitulate the metastatic cascade [2]. Similarly, animal experimentation cannot reproduce the human condition, particularly the immune system, and therefore, are poor predictive models of human cancer. Additionally, and in general, animal models do not permit the identification of the individual factors from the tumor microenvironment (TME) responsible for tumor growth and progression. Overall, all the mentioned above causes that about 90% of the (oncology) drugs developed by the pharmaceutical industry that successfully reach the clinical assay stage fail when tested in humans due to lack of efficacy and/or safety.

More integrative technologies capable of providing more valuable readouts during drug discovery and screening and new insights into cancer pathogenesis are needed. The combination of biosensors and microfluidic technologies can provide unprecedented opportunities in cancer theranostics by merging their unique properties in terms of accuracy, real-time detection, lower consumption of reagents, portability, or high-throughput [3, 4]. This integration will improve the predictability of drug screening by evaluating their efficacy (or toxicity) in a realistic

microenvironment and help physicians decide about the use of the right drug and dose for each patient. It will also enable early tumor diagnosis by detecting and analyzing predictive biomarkers in real-time [5]. Additionally, this leading technology will gather more robust and reliable data about the mechanism of action of drugs and the pathophysiology of the disease while reducing animal experimentation. Finally, their low fabrication costs associated with the microfabrication technology inherited from the microelectronics industry and the capability of automation and parallelization of experiments make the combination of biosensors and microfluidics a robust methodology to address the demands mentioned above. This will univocally result in better point-of-care platforms for improved cancer diagnosis and treatment, with promising applications in the clinics [6].

This chapter introduces the fundamental fields of biosensors and microfluidics applied to cancer research and illustrates how their combination can boost drug discovery and screening and improve cancer diagnosis and therapy. We first introduce both topics separately and the most relevant concepts involved, and next, discuss the advantages of merging both technologies with some clarifying examples.

4.2 The Tumor Microenvironment: An Overview

The TME is a highly rich, complex, and dynamic habitat where a diverse population of—malignant and non-malignant—cells interact with each other, with the ECM network, and with a complex repertoire of cytokines, chemokines, growth factors (e.g., pro-angiogenic factors), signaling molecules, and enzymes (e.g., matrix metalloproteinases—MMPs), among others, located at the center or periphery of the tumor region (Fig. 4.1). Besides the cancer cells, the TME includes the microvasculature (vascular and lymphatic vessels), cancer-associated fibroblasts (CAFs), immune cells (T and B lymphocytes, NK and NKT cells, macrophages, dendritic cells, etc.), stem cells, adipocytes, and others [7]. The ECM of the TME is not just a physical scaffold to provide support to cells, but it has an active function in the spreading of the tumor. In brief, CAFs and tumor-associated macrophages (TAMs) are responsible for reorganizing the ECM into aligned bundles that, together with the generation of biochemical gradients, guide the locomotion of cancer cells toward the microvasculature that transport the cancer cells to distant tissues for their colonization. The ECM is typically more rigid than the standard healthy counterpart due to increased proteins, mainly collagen and elastin [8, 9].

The ECM has a fundamental role in tumor growth and metastasis. Indeed, several pre-clinical approaches have aimed at targeting (or replicating) different aspects of the TME. In particular, the specific aligned architecture of the ECM can be easily replicated *in vitro* (or on-chip). By culturing fibroblasts in an environment that orients their adhesion, polarization, and motion, it is possible to control the deposition of ECM that is rich in collagen, fibronectin, and elastin, among other components, and with an aligned tumor-like orientation. Methods to do this include the use of topographical templates for the contact guidance of cells [10, 11], haptotactic gradients [12], mechanical gradients [13], or shear stress

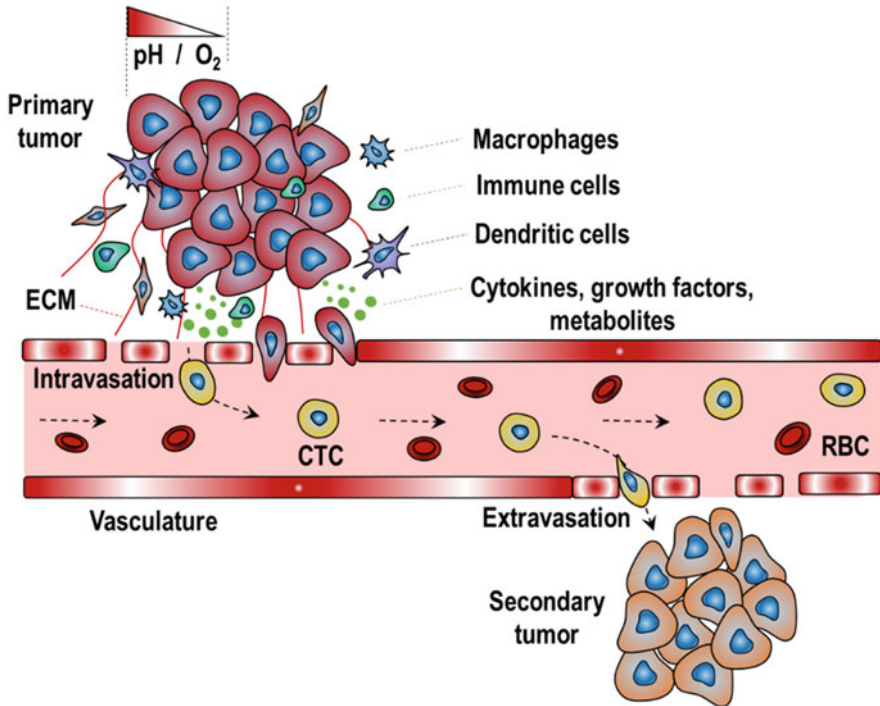


Fig. 4.1 The complexity of the tumor microenvironment. The voyage of cancer cells during tumor dissemination includes a multitude of events that starts with the tumor growth and is followed by the invasion in the surrounding stroma, the intravasation into the microvasculature, the transit of circulating tumor cells, their extravasation in a distant region, and the formation of a secondary metastatic niche

[14]. Alternatively, CAFs can be encapsulated within a 3D hydrogel of natural- (e.g., Matrigel™ or collagen I) or synthetic- (e.g., poly(ethylene glycol)—PEG) origin to re-organize the polymeric network into aligned, cross-linked, and rigid fibers by the sustained release of MMPs [15]. One of the main advantages of this approach is that the rigidity of the hydrogel can be modulated to mimic the higher stiffness of the tumor ECM.

As mentioned above, within the TME, there is a cocktail of chemokines,—pro-angiogenic—growth factors, and inflammatory enzymes, among other cues, with acidic pH and hypoxic niche (low O₂ levels) that influence the activity of cells and upon which the ECM can be remodeled. These are, in part, responsible for the formation of newly formed vascular (angiogenesis) and lymphatic (lymphangiogenesis) vessels, which play a fundamental role in the growth of the tumor and its dissemination, and are involved in the generation of an elevated interstitial fluid pressure that contributes to driving the migration of cancer cells (and other tumor-related compounds) toward the lymphatic and vascular vessels. These vessels become highly fenestrated and leaky, facilitating the invasion

(intravasation) of tumor cells, extracellular vesicles, and other types of tumor-related compounds into the microcirculation system [16]. This enhanced permeability is known as the EPR effect, that is, *enhanced permeability and retention* effect, and it is used as a therapeutic strategy to precisely deliver drugs into tumors. In addition to this permeability, the (micro) vasculature around the TME also displays a significant alteration in their architecture, dimension, and flow rate, which is very heterogeneous (i.e., from almost null to important flow values).

Overall, the TME is a highly heterogeneous, complex, and dynamic ecosystem comprising many constituents that interact among them. Accumulating evidence has shown its importance for the initiation, progression, and invasion of the tumor, and its response to therapies. For this reason, modern therapeutic approaches need to switch from a tumor-centric system to a more TME-oriented one [17]. In this regard, the use of integrative technologies capable of reproducing the native habitat of cells with better accuracy can greatly benefit further investigations about the mechanism of action of drugs, contributing to improving the unsatisfactory efficiency of drugs when developed using traditional culturing approaches. In this regard, microfluidics offers multiple advantages to mimic the cellular, biochemical, mechanical, and dynamical events of the TME, including cancer metastasis.

4.3 Microfluidics

4.3.1 Introduction to Microfluidics

Microfluidics is defined as the manipulation of minute amounts of fluid (from few μL to pL) using channels and chambers of micrometric size [18]. This technology originated from the so-called *Micro Total Analytical Systems*, or μTAS , which aimed at integrating all the lab equipment and functions into a microfabricated chip of tens of millimeters in size to carry out the microprocessing and microanalysis of compounds with high resolution and sensitivity at a meager cost and short time of analysis. As mentioned above, microfluidics and μTAS exploit the technology initially developed by the microelectronics industry to fabricate integrated circuits. This enables the mass production of chips, a crucial factor in developing cheap point-of-care products addressed to the healthcare market. A subset of μTAS systems are lab-on-a-chip (LoC); these are microfluidic platforms where only a few lab processes are employed for manipulating biological material, such as fluids from patients, or for modeling in vitro specific tissues from the human body.

The design and fabrication of the LoC microfluidic devices rely on a wide range of scientific and technical aspects. In particular, recapitulating on-chip the architecture and the physiology of a specific tissue requires the computed-assisted design of a photomask containing all the essential features of the chip (e.g., reservoirs, channels, microstructures, and others). Then, microfabrication technologies, typically UV-photolithography, are used to transfer the chip design to a photosensitive polymer (photoresist) by controlled UV exposure through the photomask [4]. After some steps of curing and developing, the resulting molds are replicated in a

polymeric and biocompatible biomaterial, typically an elastomer, by soft lithography and sealed with a glass slide. Finally, after perforating the inlets/outlet to permit the perfusion of fluids, the chip is ready (e.g., to encapsulate the cells).

In some cases, very versatile chip designs can reproduce the tissue of interest and recapitulate physiological responses with high precision. Indeed, some of these chips are commercially available and utilized by many laboratories for their experiments [4]. In addition to these technical aspects, the use of adequate cells (primary cells or cell lines) and engineering ECMs with native-like structural properties (e.g., hydrogels with well-controlled stiffness and biochemical cues) are also major scientific concerns. Next, fluid flow (and shear stress) within the chip must be accurately simulated and experimentally validated to mimic that from the actual tissue to provide the cells with the hydrodynamic cues encountered *in vivo*. This is particularly important to investigate the flow of drug-loaded carriers in endothelial-coated channels and investigate their interaction with the endothelial wall. Finally, the material used to fabricate the chip has a significant impact on the behavior of cells. Typically, polydimethylsiloxane (PDMS) is employed due to its superior properties (e.g., good optical properties, biocompatible, tunable, etc.). Other biocompatible polymeric materials used for microfluidic chip fabrication include polymethyl methacrylate, polycarbonate, or polystyrene, among others. However, these materials cannot reproduce the soft cellular environment. Cytocompatible hydrogel-based microfluidic devices have been developed during the last years by traditional replica molding or more sophisticated biofabrication methods, such as 3D bioprinting [19]. These are more physiologically relevant than the PDMS-based counterparts. Still, it is vital to avoid the inherent swelling of hydrogels that can lead to a deformation of the embedded structures and channels and decreased mechanical strength. In this regard, hydrogels made of silk fibroin [20], (methacrylated-) gelatin [19, 21], di-acrylated poly(ethylene glycol) [22], or Pluronic F127 [19], offer advanced performance in terms of mechanical and cellular stability, and powerful alternative to conventional PDMS.

In some cases, though, framing the hydrogel with a more rigid material (e.g., acrylic or PDMS) is necessary to provide extra mechanical support to avoid their collapse or deformation [23]. Finally, an essential challenge of LoC systems is their compatibility with existing characterization and analytical technologies, such as optical microscopy and biosensors, among others. This makes LoC technology very attractive for the biomedical sector, including R & D laboratories, big pharma, and hospitals. Indeed, significant efforts have been invested in studying tumor growth and metastasis using biomimetic LoC models of tissue and organs due to its superior capacity to culture different tissue types under physiological conditions [2, 4, 11, 24–29]. Moreover, LoC also enables the real-time and high-resolution imaging of living cells and the well-controlled perfusion of cell culture media under physiological conditions. Similarly, microfluidics has also found vast applications in the field of diagnosis and therapeutics, in particular in cancer research (Fig. 4.2). In the following, we comment on how microfluidics can be employed to investigate different events of cancer metastasis as well as for drug development and therapeutics.

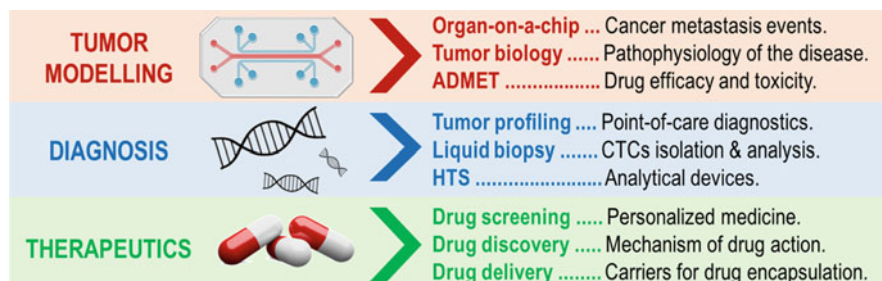


Fig. 4.2 Primary applications of microfluidics in cancer research. Microfluidic systems are mainly employed in tumor modeling, therapeutics, and diagnosis, with many different uses. *ADMET* Administration, distribution, metabolism, excretion, and toxicity, *HTS* High-throughput screening

4.3.2 Microfluidics in Cancer Research

4.3.2.1 Tumor Modeling

LoC technology can be applied to develop biomimetic microfluidic devices for identifying essential factors involved in the pathogenesis of the disease, novel therapeutic targets and drugs, or their mechanism of action [4]. For this, microfluidic chips can be combined with the culture of human cells arranged to simulate fundamental units of human organs and tissues, resulting in the so-called *organ-on-a-chip* (OoC) models [30]. This type of biomimetic platform is capable to faithfully recapitulate the multi-cellular composition, architectures, interfaces, biochemistry, and vascular perfusion of the human body not possible with traditional culture systems. This makes the cells embedded within the chip show phenotypes, dynamics, and gene expressions similar to those encountered *in vivo*, and therefore, provides a more realistic scenario to investigate the etiology of diseases and for the discovery of drugs. These superior characteristics (compared to traditional culture platforms) made OoC receive significant attention from the cancer research community due to its high potential to reproduce key events of the metastatic cascade and for identifying novel biomarkers or therapeutic targets; in this case, they have been denoted as *cancer-*, *tumor-*, or *metastasis-on-a-chip* platforms. Indeed, tumor modeling using OoC platforms has enormously progressed during the last decade and big pharmaceutical and biotechnological industries have invested in this technology to discover and screen novel pharmacological compounds [25] (Fig. 4.2).

Multiple works have shown how OoC can contribute to understanding characteristic features of tumor progression [2, 4, 16, 31–34]. For this, the structural (i.e., mechanical and architecture), biochemical (i.e., growth factor gradients, chemokines), rheological (i.e., shear stress, fluid flow), and multi-cellular properties and content of the native scenario need to be accurately reproduced on-chip. A myriad of OoC models has been fabricated so far, including the seminal work on lung-on-a-chip, and follow-up publications, which paved the way for the development of this technology [35–37]. Other organs- and tissues-on-a-chip include the heart [38], spleen [39], gut [40], liver [24], kidney [41], brain [25], and vasculature

[16, 33], among many others [42]. These models have been utilized for various applications ranging from mechanistic studies to more applied uses, such as drug discovery and screening [43–45]. This versatility has contributed to OoC having reached a significant degree of maturity in the academic field. Similarly, the interest in this technology by the end-users is advancing at a good pace, as demonstrated by the adoption of OoC by certain industrial stakeholders (e.g., pharmaceutical and biotech companies) and regulatory agencies (e.g., the U.S. Food and Drug Administration—FDA) [2, 46, 47].

OoC models of cancer enable the real-time monitoring of tumor progression with high control over the molecular, cellular, biochemical, and structural (mechanical and architecture) parameters of the TME, particularly the formation of chemokine gradients. This is fundamental to accurately reproduce all the cascade of events occurring during metastasis, namely (1) tumor growth and invasion, (2) angiogenesis/lymphangiogenesis, (3) intravasation, (4) transit of cancer cells in the vasculature, (5) extravasation, and (6) secondary organ invasion. These events can be reproduced either in conjunction or independently, thus helping to uncouple the mechanistic determinants responsible for each event. In the following, we briefly comment on how these different events can be reproduced and studied using OoC technology. For more detailed information or examples on each case, the readers are referred to specialized reviews on the topic [2, 32, 34, 45].

1. *Tumor growth and invasion-on-a-chip*: The uncontrolled growth of the tumor is the first event of the cancer metastasis cascade prior to the invasion of tumor cells in the surrounding stroma. During this event, the tumor grows, and eventually, one or several cells perform an epithelial-to-mesenchymal transition (EMT) and start to migrate directionally along the re-arranged fibers of the ECM. This is one of the most specific events to model within a microfluidic device, which mainly requires a 3D chamber where to seed the tumor cells, and a microfluidic channel (coated or not with endothelial cells) mimicking the native microvasculature for perfusion. A co-culture with other types of cells can also be performed to investigate the cross-talk among the different cells or evaluate their influence on the addition of anti-cancerous drugs. Other features to be explored include the impact of the rigidity or architecture of the ECM in tumor growth and invasion of the surrounding microenvironment. Similarly, the levels of hypoxia or the presence of cytokines or growth factors can be quickly investigated.
2. *Angiogenesis- and lymphangiogenesis-on-a-chip*: This is the growth of newly formed blood and lymphatic microvasculature from pre-existing ones to support the development of the tumor with nutrients and oxygen supply (angiogenesis) and to release the excess of interstitial fluid within the TME (lymphangiogenesis). In both cases, the vasculature is chaotic, highly fenestrated, and with a heterogeneous flow. All these factors favor the directed locomotion of cells toward the vessels in response to chemokine and growth factor gradients (e.g., the vascular endothelial growth factor—VEGF), and second, their intravasation within the vessels [16, 31, 48, 49]. Typical microfluidic chips employed to recapitulate this phenomenon use a central 3D tumor chamber containing the tumor (typically, a

spheroid) embedded within a hydrogel matrix interconnected by micro-slits or micro-posts to lateral channels coated with—blood or lymphatic—microvascular cells, which initiate sprouting toward the tumor.

3. *Intravasation-on-a-chip*: It is defined as the invasion of cancer cells into the blood or lymphatic vasculature due to its fenestrated phenotype. This high permeability facilitates the transendothelial invasion of cancer cells into the bloodstream, where they become circulating tumor cells (CTCs). This event can be reproduced using a reductionistic approach with only two cell types: the tumor cells and the endothelial (blood or lymphatic), and a simple design. Typically, two main techniques are used. The first is based on a 3D chamber containing the tumor cells interconnected through a porous membrane or micro-slits to a hollow microchannel coated with endothelial cells mimicking the native vasculature. The second one is based on building a vascular network within a tumor cell-laden 3D hydrogel matrix by direct self-assembly and monitoring the intravasation of the tumor cells. In this case, though, the presence of tumor cells may impact the interconnectivity of the generated network [50].
4. *Transit of cancer cells on-a-chip*: During this event, the intravasated CTCs transit along the vasculature, and eventually, arrest under certain favorable conditions (e.g., adhesion to the vessel wall, physical entrapment, flow patterns). Typically, this event is modeled together with intra- or extravasation phenomena. Therefore, a chip containing a primary and/or secondary tumor reservoir and a hollow channel coated (or not) with endothelial cells is needed.
5. *Extravasation-on-a-chip*: This is the opposite event of intravasation, that is, the transendothelial migration of CTCs off the vasculature. The location of extravasation is a crucial factor, which determines the organ specificity of cancer metastasis. The “seed & soil” theory determines, among other factors, that this location is determined by the morphological and hydrodynamic properties of the vessel. Upon favorable conditions, the CTCs adhere and arrest in the walls of the endothelium, where they mature a diverse repertoire of adhesion molecules that, in the end, allows their invasion in the surrounding stroma [51]. The basic design may be similar to the intravasation counterpart: a hollow channel coated with endothelial cells interconnected to a metastatic niche chamber through micro-slits or porous membrane. Alternatively, extravasation can also be studied using a self-assembled network of vessels within a 3D matrix [52].
6. *Secondary organ invasion (metastasis-on-a-chip)*: This is the last and most critical step of the metastatic cascade, where cancer cells extravasate off the vasculature, form a pre-metastatic niche, and proliferate, invading a specific tissue/organ forming a secondary tumor. Strikingly, it is not known why a particular tumor invades specific tissues in contrast to others. Intense research has been focused on understanding this organ specificity, and OoC is the ideal platform to unravel its mechanism of action due to the high control over the involved parameters, that is, the structural composition, the biological content, and the hydrodynamic properties. This has led to the development of multi-organ-on-a-chip (multi-OoC) devices where cancer cells have been seeded together with cells from different tissues or organs. Due to the particularity of the various

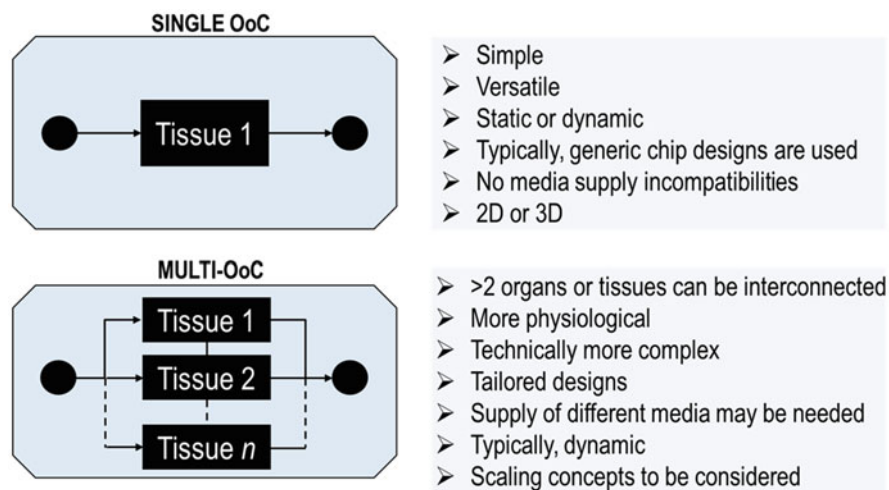


Fig. 4.3 (Multi-) organ-on-a-chip technology. (Left) Scheme showing the rationale of using OoC technology either as a single or in combination. (Right) Summary of the characteristics of single vs multi-OoC

tissues, these have been seeded in separate chambers, and in some cases, following a physiological distribution. This more complex platform is denoted as *metastasis-on-a-chip* and has provided vital insights into the physiopathology of the disease, particularly the biophysical rules governing organ specificity [2].

Undoubtedly, OoC has enormous potential, as showcased by its properties and applications described above. However, this type of single-organ model cannot recapitulate certain conditions of human physiology, particularly the interaction between different tissues and organs. This is of utmost importance for particular applications, such as drug screening, where the effect of drug metabolites or their potential toxicity must be considered [5, 53, 54]. With this in mind, several OoC can be interconnected following a physiological configuration resulting in multi-OoC platforms (Fig. 4.3). These more advanced multi-organ microfluidic models can recapitulate with higher fidelity the native scenario, providing a more realistic environment for testing drugs and unraveling the mechanistic determinants of pathologies. Indeed, many multi-OoC have been reported during the last years [32, 53, 54] (Table 4.1). They differ in their complexity, tissues and organs modeled, and the scientific question addressed. The simplest models include two organs/tissues interconnected through a microfluidic channel coated with endothelial cells to reproduce the native (micro-) vasculature. This is of particular interest for cancer dissemination studies to investigate organ specificity during metastasis or to evaluate the toxicity of a drug using a *heart* model (i.e., cardiotoxicity) or the effect of drug metabolites in a secondary tissue using a *liver* model [65, 66]. Undoubtedly, increasing the number of interconnected organs also increases the complexity of the

Table 4.1 Examples of multi-organs-on-a-chip models

Multi-organs/tissues	Num. organs	Applications	Ref.
• Liver—Heart	2	Drug screening and cardiotoxicity evaluation of drugs	[55]
• Liver tumor—Heart	2	Cardiotoxicity of anticancer drug resulting from toxic metabolites produced in the liver	[56]
• Gut—Liver	2	Drug screening and metastasis studies	[57]
• Liver—Heart—Lung	3	Screening of drug toxicology; disease modeling	[58]
• Intestine—Liver—Skin—Kidney	4	Evaluation of the long-term ADMET of drugs	[59]
• Lung tumor—Brain—Bone—Liver	4	Study of organ specificity of lung cancer metastasis	[60]
• Cardiac—Muscle—Brain—Liver	4	Long-term investigation of the effect of different drugs with well-known toxicity	[26]
• Intestine—Liver—Colorectal tumor—Connective tissue	4	Evaluating the efficacy and toxicity of anti-cancerous drugs and their metabolites	[61]
• Intestine—Lung—Liver—Bone marrow—Kidney	5	Evaluating the cross-talk among the different organs; drug ADMET; screening of cellular biomarkers and gene expression	[62]
• Intestine—Liver—Kidney—BBB—Muscle	5	Studies of drug ADMET, organ-specificity, and PK/PD	[63]
• Intestine—Liver—Kidney—Heart—Lung—Skin—BBB—Brain	8	Human body mimicry of physiological functions; PK/PD of drugs; drug discovery	[64]

microfluidic model. A particular bottleneck is the need for a common cell culture media for the different types of cells. In some cases, such as when using stem cells or primary cells, this is not possible, and therefore, alternative strategies are employed to separate the different tissues. One option is mixing culture media at specific ratios [55], even though this becomes challenging when increasing the number of organs interconnected. Another option is using different chambers interconnected through micro-slits or porous membranes that physically separate tissues with distinct requirements of media; however, this is associated with some technical challenges. Intense efforts have therefore been focused on the development of a universal media suitable for different multi-cellular tissues. Such utopic achievement would boost even more the applicability of OoC in all the biomedical fields, and in particular, in oncology.

4.3.2.2 Tumor Diagnosis

Microfluidics has considerable potential for isolating, enriching, and molecular characterizing cellular and molecular markers, such as CTCs, extracellular vesicles (e.g., exosomes), or ctDNA/RNA, from peripheral blood. These biomarkers can provide critical information about the pathophysiology of the primary tumor. Their levels in metastatic cancer patients are related to their clinical progression, and

therefore, can help physicians on therapy decision-taking (Fig. 4.2). This assay is reminiscent of analyzing the genetic content of a solid tumor biopsy, and therefore, the characterization of CTCs is known as *liquid biopsy*. In this regard, the isolation and analysis of tumor biomarkers within a microfluidic device have been coined *liquid biopsy-on-a-chip*. Besides pure isolation and enrichment of tumor-associated biomarkers, their molecular characterization and analysis can also be performed on-chip by standard immunolabelling assay. Similarly, CTCs can be automatically detected, enumerated, and profiled on-chip by integrating miniaturized electrodes that work as high-speed and label-free micro-Coulter counters or analytical biosensors [67].

The presence and number of CTCs in the bloodstream are associated with a poor outcome in the prognosis of cancer patients and indicate that the tumor has started to disseminate (i.e., metastasize) throughout the body. Therefore, their early detection and analysis could be advantageous for initiating the most appropriate treatment adjusted to the genetic profile of the primary tumor, thus enabling personalized medicine and improving the recovery of patients. However, their isolation is indeed very challenging. This is because their number in peripheral blood is very scarce (1–10 CTCs in 1 mL of blood) compared to the vast amount of other cells present in the blood ($\sim 10^9$ cells). Traditional isolation methods to collect CTCs, such as immune-capture or flow cytometry, are not efficient enough. Microfluidics can improve the detection and capture of CTCs and other types of tumor-associated biomarkers, such as ctDNA/RNA, extracellular vesicles (e.g., exosomes), or antibodies from peripheral blood. The advanced capabilities of microfluidic systems for the separation of particles of different sizes, shapes, or rigidity can be exploited as a liquid biopsy-on-a-chip approach for the isolation and capture of tumor biomarkers [27]. Most of these microfluidic systems are related to the capture and isolation of CTCs, most likely due to the difficulty to capture the other ones (lower presence and smaller size compared to CTCs). Typical isolation methods include the use of affinity-based techniques for their entrapment. For this, microfluidic channels containing micro-sized posts functionalized with specific biorecognition elements (e.g., antibodies) specific to the epithelial surface markers of CTCs—whose presence showcases its foreign origin—, such as the epithelial cellular adhesion molecule—EpcAM, E-Cadherin, vimentin or cytokeratins, are employed. Some of these affinity methods can also target non-CTCs cells to purify or enrich the CTCs content. For this, herringbone structures can be created within a microfluidic channel coated with antibodies specific to white blood cells (e.g., anti-CD45). The herringbone promotes the mixing of cells within the channel and their physical interaction with the functionalized structures.

Unfortunately, CTCs can be very heterogeneous and do not always present the markers mentioned above on the membrane surface as they may gain more mesenchymal-like properties [68]. Alternatively, label-free methods can be used to isolate the CTCs. Microfiltration uses physical trapping to isolate CTCs taking advantage of their larger size (15–20 μm) compared to other type of cells present in peripheral blood (in average, red blood cells: 5–8 μm ; white blood cells: 12–16 μm). Despite its simplicity, this method is limited to manipulating low

volumes of samples due to the risk of clog. Other approaches include magnetic isolation or the use of spiral—inertial—microfluidic channels for their hydrodynamic separation, among others (e.g., deterministic lateral displacement, centrifugation, inertial focusing). All these methods can be further combined with affinity-based isolation to boost the efficiency of the isolation. A fascinating way used for CTCs isolation is inertial microfluidics, which exploits the hydrodynamic forces at the microscale to sort the cells according to their physical properties (size and deformability) without the need for labeling. This method operates in an intermediate Re number (1 to ~ 100), where the inertial effects start to be relevant, and cells can move transversal to the direction of the fluid flow; the separation is again based on the difference in cell size. This approach, when mastered, is capable of achieving high throughputs. Indeed, several spiral devices have been utilized to isolate CTCs directly from peripheral blood, which are then employed for further molecular analysis [28, 29, 69].

Altogether, liquid biopsy-on-a-chip is a robust methodology for detecting, isolating, and analyzing CTCs and other tumor-derived biomarkers. It provides multiple advantages compared to traditional methods based on collecting a biopsy of the tissue or imaging approaches, which are invasive or not very sensitive. Finally, it is worth noting that this advanced performance can further be boosted by integrating miniaturized biosensors into the chips (see below), which may help their rapid identification and analysis.

4.3.2.3 Tumor Therapeutics

One of the main advantages of microfluidic devices is their capability to reproduce dynamic physiological events and key features characteristic of the native tumor scenario. Of great interest is the generation of (bio) chemical gradients, which have been demonstrated to have a fundamental role in the initial stage of tumor dissemination by favoring the invasion of tumor cells [70]. For this, a myriad of microfluidic designs is available for the generation of growth factors and chemokines gradients, namely cascade-based, Y-shaped, membrane-based, or pressure-balanced methods [4]. In all these cases, the flow properties of fluids at the microscale are exploited to generate gradients with high precision. At this scale, the fluid shows a laminar flow within the microchannel where viscous forces dominate over the inertial ones. A dimensionless parameter coined *Reynolds number* (Re), quantifies this ratio. It is defined as $Re = (\rho \cdot l \cdot v) \cdot \eta^{-1}$, where ρ , l , v , and η are the fluid density ($\text{kg} \cdot \text{m}^{-3}$), the length scale (m), the flow velocity ($\text{m} \cdot \text{s}^{-1}$), and the fluid viscosity ($\text{kg} \cdot \text{m}^{-1} \cdot \text{s}^{-1}$), respectively. Values of $Re \leq 2000$ correspond to a laminar flow where the fluid streamlines flow in parallel and display a Gaussian profile with a null flow at the walls of the channel. In contrast, if $Re > 2000$ the flow of the fluid is turbulent.

A key advantage of generating gradients using microfluidic chips is the possibility to evaluate the correct dose regime of therapeutic drugs in a genuinely physiological and multi-cellular microenvironment, saving a lot of effort and resources [71]. Along the same line, microfluidic OoC systems can also be employed to evaluate their pharmacokinetics and pharmacodynamics (PK/PD) (Fig. 4.2). More specifically, multi-OoC platforms can be utilized to assess the so-called ADMET of

drugs, their *administration, distribution, metabolism, excretion* and *toxicity* [5, 26, 54]. This is fundamental to evaluating which drugs are more efficient in treating an individual patient's tumor while reducing potential toxicity events. The latter is of utmost importance since most of the drugs that have been released from the market are related to cytotoxicity, which has not been observed when tested on traditional screening platforms. Finally, microfluidic OoC can also be utilized to investigate the mechanism of systemic drug administration [31]. In particular, the development of *vessel-on-a-chip* devices emulating the cellular composition and architecture of the native microvasculature can provide critical insights into the microvascular transport of drugs or drug-loaded carriers, their interaction with the endothelial wall, and even the mechanism of corona formation [16, 33, 72].

4.4 Biosensors

4.4.1 Introduction to Biosensors

Biosensors are miniaturized analytical devices designed to detect a specific analyte, or group of analytes, by converting the detected biological or chemical response into a readable signal proportional to the analyte content [73]. Biosensors are nowadays omnipresent in a multitude of research fields, in particular, in biomedical research (pharmacology, medicine, etc.) for drug discovery, disease diagnosis, or monitoring its progression and response to treatment [73–77]. Other areas where biosensors are being utilized are food control (e.g., detection of micro-organisms [78, 79]) or environmental monitoring (e.g., detection of pollutants [80, 81]), among others. In this regard, biosensors offer unprecedented capabilities to assess the health status (as external point-of-care systems; or implantable devices, e.g., pacemakers) and disease progression, with attractive applications for the academic, clinical, and industrial sectors. Indeed, the significant growth in cancer cases resulting from the aging of the population, pollution, and unhealthy lifestyle, has increased the demand for point-of-care devices for the early detection, routine check-ups, and continuous monitoring of patient healthcare status in a rapid, precise, and effective manner.

Biosensors are characterized for displaying specific attributes that determine their final performance. These include a high sensitivity (i.e., low limit of detection, that is, the minimum amount of analyte that can be measured), specificity (i.e., response to a single analyte without interference from other elements), reproducibility (i.e., generation of identical responses in different experiments), stability (i.e., the reaction from the biosensor is not affected by ambient disturbances), and working in a linear range (i.e., the biosensor output signal changes linearly with the analyte concentration). Mathematically, this linearity can be expressed as: $[\text{output signal}] = k \cdot [\text{concentration analyte}]$, where k is the sensitivity of the biosensor and the slope of the graphic representation within the linear range. In general, biosensors can be classified according to their transducer type. Most types of biosensors contain three main components (Fig. 4.4):

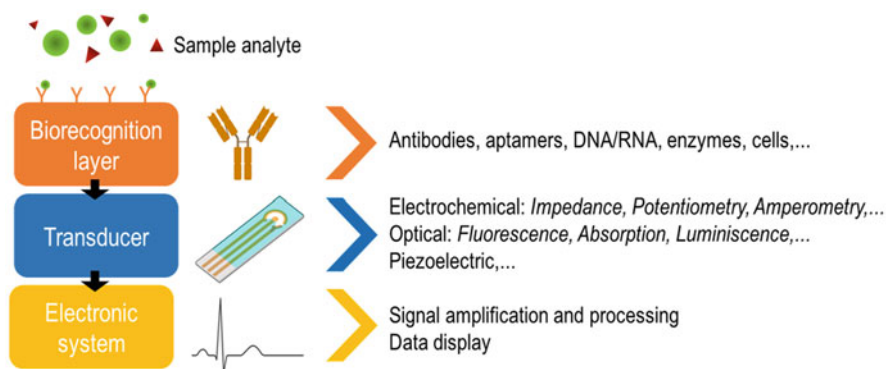


Fig. 4.4 Typical build-up and components of a biosensor

1. A *biorecognition layer* containing the biological-based high-affinity detection elements, such as antibodies, aptamers, DNA/RNA strands, peptides, molecularly imprinted polymers, cells, or similar, on top of the sensor transducer. The specific coupling between the detection element and the analyte is denoted as “biorecognition.” Depending on the type of biorecognition elements used, biosensors are classified as immunosensors (for antibodies), aptasensors (for aptamers), or enzymatic biosensors (for enzymes), among others.
2. A physicochemical *transducer* converts the detection signal of a biological/chemical substance, or analyte, into a quantitatively measurable signal (the biorecognition reaction determines the selectivity and sensitivity of the transducer). The produced signal is typically proportional to the amount of analyte-bioreceptor interactions [73].
3. An *electronic system* device is used to read, amplify, process, and digitalize the physicochemical output signal from the transducer. Then, the output signal is shown using a readable display and especially dedicated software. This readout can be in the form of a table, graphic, or image.

The most typical detection signals are *optical* (e.g., surface plasmon resonance—SPR) and *electrochemical* (e.g., cyclic voltammetry, electrochemical impedance spectroscopy), even though other types of signals, such as *magnetic* (e.g., magneto-resistance), *thermal* (e.g., thermistor), or *mass sensitive*—acoustic/piezoelectric (e.g., quartz crystal microbalance—QCM) are also available (Fig. 4.4). Optical-based biosensors, particularly those based on the emission of fluorescence, are undoubtedly very popular and efficient. However, one of their main disadvantages is that, in general, they are non-label free, which may threaten specific measurements (e.g., the biorecognition of low analyte concentrations may not be readable by fluorescence), alter the properties of the analyte to be detected, or generate interferences. In contrast, label-free methods are more convenient considering the limitations mentioned above. Techniques such as SPR (changes in the refractive index), or QCM and microcantilevers (variation in resonant frequency due to mass

changes) permit the quantitative detection of minute amounts of analyte without the need for labeling and in real-time. Despite their performance, one limiting factor of these biosensors is their difficulty to be miniaturized and integrated within point-of-care devices to improve their signal-to-noise ratio. In this regard, electrochemical biosensors are more advantageous due to their high degree of integration capacity (i.e., miniaturization), selectivity, sensitivity, fast response, and low detection limit. This versatility has made electrochemical biosensors one of the most employed detection methods. They are also low cost, simple to operate, and require no expensive equipment besides a standard potentiostat.

Electrochemical biosensors began in the 1950s by Leland C. Clark Jr. with the invention of an electrode to measure the dissolved O_2 in the blood of patients undergoing surgery [82, 83]. A modification of this system led to the first blood glucose biosensor containing an oxygen electrode, an inner membrane semipermeable to O_2 , a thin GOx layer, and an outer dialysis membrane [83]. An electrochemical transducer was used to immobilize enzymes, and a decrease in O_2 was proportional to the glucose concentration. This type of glucose oxidase sensor is still widely used, even though significant improvements have been made to increase its performance. Next, almost two decades later, the first urea biosensor was developed by Guilbault and Montalvo, Jr. [84], and in 1975 the first commercial biosensor was launched into the market by Yellow Spring Instruments for the detection of glucose. Nowadays, many other types of biosensors are widely available for various applications, including well-recognized pregnancy tests, (illegal) drug testing, cholesterol measurement, or, more recently, COVID-19 tests, among many others. A particular area of interest of biosensors is cancer research. They could be massively utilized to detect disease onset early, monitor its progression and therapy efficacy, or identify novel therapeutic targets. By doing this, the patient prognosis would be univocally improved. Overall, biosensors are expected to boost the development of novel anti-cancer drugs, unravel the mechanism of key pathophysiological processes, and therefore, helping physicians in taking appropriate interventions.

4.4.2 Biosensors in Cancer Research

The early diagnosis and subsequent treatment of cancer can significantly improve the prognosis of cancer patients. Typically, the identification of mutations in the DNA/RNA of cancer patients through biopsies or detecting changes in protein levels, together with imaging methods (MRI or ultrasounds), are the strategies employed in the clinics to detect tumors. In particular, polymerase chain reaction (PCR), Western Blot, enzyme-linked immunosorbent assay (ELISA), or immunohistochemistry are the most common screening techniques used. However, and despite being quite efficient, usually, these methodologies are incapable of detecting the presence of the tumor at a very early stage but only after the appearance of related symptoms. In addition, these methods may not allow grading the tumor and indicate the most effective treatments, besides being invasive (which is inconvenient for the patient), time-consuming, costly, tedious, and requiring expensive reagents,

facilities, and trained personnel. In contrast, biosensors are emerging as a powerful alternative to standard analytical methods for the detection of cancer biomarkers. Biosensors are rapidly expanding in the medical field, with the significant impetus coming from the healthcare, diagnosis, and biotechnology industry.

Biosensors have already been applied in clinics to detect cancer biomarkers in body fluids (e.g., blood, serum, urine, saliva, or cerebral spinal fluid, among others). Among all the types of biomarkers, molecular ones are the most common types. They include (onco-) genes, growth factors receptors, proteins, or other classes of tumor-specific compounds (Table 4.2). There are +160 types of biomarkers related to different types of cancer [85]. This requires the biosensor to be specific and exclusively recognize the analyte of interest, avoiding interference with other molecules or compounds present in the sample.

Similarly, non-specific adsorption of compounds must be avoided to reduce signal noise or false positives. In this regard, typical methods include a washing step with a buffer to remove weakly adhered molecules. Next, the developed biosensors must be robust and reproducible. This means that the functionalization protocols should be easily reproduced to provide always the same response independently of the operator. For this, integrating controls is imperative to ensure that the device is working as it should. Next, sensors must be capable of working with shallow volumes of samples, particularly in the clinics. In this regard, their integration within lab-on-a-chip platforms provides the perfect technological environment to fulfill this requirement.

Perturbation of an individual molecular biomarker's levels does not univocally determine the presence of a tumor, since this alteration may arise from other disorders (e.g., inflammation, cardiovascular disease, infection, and others). In contrast, an alteration of a panel of different markers may be specific to a particular type of tumor and, therefore, may constitute a molecular signature of that specific tumor. Finally, the type and design of the biosensor may differ according to the specific biomarker (or repertoire of biomarkers) to be detected.

4.5 Integration of Biosensors Within Microfluidic Devices

Despite the myriad of publications and success of human OoC, very few works have been reported of OoC integrating biosensors for the real-time measurement of pathophysiological parameters and the dynamic responses of tissues to drugs. However, the compatibility of biosensors with cutting-edge microfabrication technologies has enabled their integration within microfluidics systems for the continuous, in situ, and non-invasive quantification of soluble biomarkers, boosting their diagnostic applications. Typically, integrated sensors are based on the use of electrochemical transducers. These provide multiple advantages compared to optical-based readouts, which cannot quantify the released levels of a specific chemokine; for this, the medium needs to be collected at desired time points and analyzed outside the chip by traditional analytical methods, such as ELISA. Other advantages include a high degree of portability (enabling in-field applications), easy

Table 4.2 Tumor markers in everyday use

Cancer type	Biomarker	Source
Bladder	BTA—Bladder tumor antigen	Urine
	CEA—Carcinoembryonic antigen	Urine
	Chromosomes 3, 7, 17, 9p21	Urine
	Fibrin/fibrinogen	Urine
	NMP-22—Nuclear matrix protein 22 (NMP22)	Urine
Breast	BRCA 1/2	Serum/tissue
	CA15–3 and 27–29—Cancer antigen 15–3 and 27–29	Serum
	CEA	Serum
	C-reactive protein—CRP	Blood
	CTCs—Circulating tumor cells	Blood
	Cytokeratins	Blood
	ER—Estrogen receptor	Tissue
	HER-2/neu—Human epidermal growth factor receptor 2	Tissue
	P53 antibodies	Tissue
Colorectal	ANXA3	Urine/serum
	BMP4	Serum
	CA19–9 and 72–4—Cancer antigen 19–9 and 72–4	Serum
	CEA	Serum
	CTCs—Circulating tumor cells ^a	Blood
	Epidermal growth factor receptor—EGFR	Tissue
	MMP7 and MMP11	Serum
Gastric	CEA	Serum
	CA19–9	Serum
Liver	AFP— α -fetoprotein	Serum
	CEA	Serum
Lung	ALK—Anaplastic lymphoma kinase	Tissue
	CRP	Serum
	CEA	Serum
	PD-L1	Blood
Melanoma	S100 protein	Tissue/serum
	CEA	Serum
Ovarian	CA-125	Serum
	CEA	Serum
	BRCA genes	Serum/tissue
	hCG—Human chorionic gonadotropin	Serum
Pancreas	CRP	Serum
	CEA	Serum
	CA19–9	Serum
	PIGR—Polymeric immunoglobulin receptor	Tissue
Prostate	CTCs—Circulating tumor cells	Blood
	Prostate-specific antigen—PSA	Serum

^aThrough the CellSearch™ system

manipulation (for being utilized by non-skilled personnel), rapid detection (for starting the necessary treatment), reduced perturbation/disturbance of the microtissue due to continuous sampling of large volumes, or a high-throughput production (reducing its cost). Undoubtedly, the main attribute of microfluidics-

integrated biosensors is the possibility to provide quantitative and accurate information about the biological and biochemical events occurring within the chip, and therefore, can have an instrumental role not only for the diagnosis of cancer but also for its prevention, treatment evaluation, and drug discovery/screening.

The high performance of microfluidic-integrated biosensors is, in particular, given by their reduced sensing area. They are typically made of conductive material, such as metals (e.g., gold, platinum, ITO, etc.) fabricated by conventional photolithography, where photoresists are used as sacrificial layers before metal deposition [78, 79, 86]. Then, a solvent (typically, acetone) is employed to dissolve the non-desired photoresist underneath the deposited metal during the lift-off, releasing the sensing electrodes. The patterned metallic microelectrodes can further be coated with conductive polymers (e.g., polypyrrole) to increase the biocompatibility and/or sensitivity [87]. The size of the generated electrodes impacts the sensitivity of the biosensors. In general, the smaller the electrode, the higher the sensitivity. However, the dimensionality depends on the fabrication methodology employed. With UV-photolithography, this is about 1–5 μm . The fabrication of nanoelectrodes may require the use of alternative fabrication technologies, such as e-beam (~ 10 nm), nano-imprint lithography (< 100 nm), or focused ion beam (~ 10 nm), among others. As a drawback, these techniques are costly and show a low throughput.

Integrating several microelectrodes in the chip (microarrays) permits the high-throughput detection of multiple analytes simultaneously. This multiplexing ability is fundamental for screening biomarkers that work as the tumor's "signature" (or indicator) or for the rapid screening of drugs. One limitation of (micro-) electrode integration within microfluidic devices is the effect of shear stress, which can detach (or inhibit) the binding between the biorecognition element and the analyte of interest due to the planar configuration of the electrodes. To solve this, a new generation of biosensors has emerged to improve capture efficiency and sensitivity. These are 3D biosensors, which typically display an enhanced roughness, porosity, or 3D topography, enhancing the amount of captured analyte and, similar to the use of herringbone in CTCs discussed above, promote their interaction with the capture probes [3]. Indeed, CTCs and a diverse repertoire of tumor biomarkers have been detected (and analyzed) by microfluidic-integrated biosensor devices [88].

External electrodes can also be used in combination with microfluidic devices [89], despite impacting on the overall sensing performance (e.g., sensitivity, portability, and others). Either way, this combination allows developing more sophisticated point-of-care systems capable of detecting or monitoring the analytes of interest in biological fluids with improved sensitivity (several orders of magnitude) compared to traditional assays. Similarly, they are advantageous to analyze specific metabolic parameters of living cancer cells, which are critical to monitoring tumor evolution. In particular, oxygen concentration [90], lactate production, glucose consumption, oxygen peroxide levels, or pH value are among the critical parameters directly associated with the growth of the tumor and its dissemination. Therefore, they can provide essential information about the metabolic characteristics or its response to drugs. In the following, we briefly comment on the aspects of these biomarkers and how they can be detected.

- *H₂O₂ detection*: Hydrogen peroxide (H₂O₂) is a reactive oxygen species that play an essential role in cells' physiological functioning. At high levels, it can cause cell damage, and it is associated with tumor growth and progression. Diverse methods have been used to measure H₂O₂ (enzymatic, fluorescent, luminescent), but the most efficient ways to detect and quantify H₂O₂ are based on electrochemistry. H₂O₂ is reduced or oxidized at various electrode materials, such as Au, Ag, and Pt, a specific catalyst for H₂O₂ redox reactions. Methods to detect hydrogen peroxide include:
 - *Potentiometry* measures the voltage between two electrodes (a working and a reference electrode—WE and RE, respectively) at zero current. The WE has to be functionalized with H₂O₂-sensitive moieties to correlate changes in voltage to changes in H₂O₂ concentration.
 - *Voltammetry* estimates the current resulting from oxidation/reduction reactions occurring at WE of a given electroactive species, typically dissolved in an electrolyte solution. The potential difference then drives redox reactions at the electrode/electrolyte interface vs a RE. Increasing [H₂O₂] changes the cathodic and/or anodic current at a particular potential, depending on the reduction or oxidation of the analyte, respectively.
 - *Amperometry* measures the changes in current at constant voltage resulting from the oxidation or reduction of an electroactive species.
- *O₂ detection*: Hypoxia is a hallmark of tumor development resulting from the disorganized vasculature. Low pO₂ levels impact the dissemination of cancer cells by promoting EMT and their resistance to radiotherapy. In this regard, the measurement of pO₂ levels is critical. The detection is based on the so-called “Clark electrode,” which employs a Pt electrode and amperometry to measure, via a reduction reaction, a current proportional to the pO₂ levels.
- *Lactate detection*: Typically, there is an increase in lactate concentration in oxygen debt situations (from 0.5–1 mM in healthy individuals to >4 mM in sick patients) [91]. Typically, electrochemical sensors are employed to detect lactate through the translation of enzymatic reactions into an electric signal in the presence of its specific enzyme. For this, the enzymes, such as lactate oxidase (LOX) or lactate dehydrogenase (LDH), are immobilized on the surface of an electrode as the biorecognition elements. The most typical electrochemical methods for lactate measurements are amperometry and potentiometry.
- *Glucose detection*: Similarly, glucose detection is mainly performed using electrochemical sensors by transforming the detection of the enzymatic reaction into an electric signal. For this, enzymes, such as glucose oxidase (GOx), immobilized on the electrode's surface, are employed. However, this strategy is associated with some challenges, such as low stability and performance (e.g., interferences). Non-enzymatic detection of glucose has been explored for its direct electro-oxidation in the absence of GOx to solve. In particular, the use of Cu NPs-based biosensors has shown a sensitivity equivalent or superior to those based on GOx [92].
- *pH detection*: Acidic pH is another hallmark of the TME. Its detection can be performed either by optical, chemical or electrochemical sensors. The former

includes the immobilization within the microfluidic device of materials sensitive to pH values, such as a molecular probe with a chromophore that reacts to the different protonation levels having a pH-dependent behavior. Alternative, more simple color-coded pH-sensitive strips can be utilized. These are sensitive materials in the entire range of 1–14 values but not very sensitive. More sophisticated optical biosensors use chemical species that modify their optical properties when reacting with acidic/basic solutions, such as the index of refraction or absorbance [93]. An advantage of optical transducers is their simple read-out, but leakage coming from the medium must be considered. In contrast, electrochemical-based pH sensors are susceptible to the entire range of values. They are mainly potentiometric and voltammetric. The working mechanism measures the voltage between the WE and RE (potentiometry) and current during the redox process (voltammetry) and correlates it with pH. Typically, these approaches require the functionalization of the electrodes with molecules that react to the pH level, such as polymeric membranes, even though metallic-based pH sensors have been described [94]. A particular type of electrochemical sensor that does not require pH-sensitive molecules is ISFETs (ion-sensitive field-effect transistors). Different pH values alter the electrical current that flows via the field effect between the source and the drain through the H⁺-sensitive gate [95]. A clear advantage of electrochemical biosensors, in particular ISFETs, is their easy miniaturization and integration within a microfluidic chip, as well as their high reproducibility and reusability [96].

Finally, the next generation of clinically-oriented point-of-care microfluidic devices needs to fulfill rigid requirements if they are intended to be adopted by the clinics. In particular, they need to be portable and require minimal manipulation. Other key elements must also be integrated on-chip to perform all the required operations, such as micro-sized pumps and valves (to drive the fluid toward the sensing elements) and multiple reservoirs and channels (for the processing of the sample) [97, 98]. Next, if unprocessed specimens are utilized, such as raw human fluids, the injection, filtration, pre-treatment, and sample processing must also be carried out on-chip. Additionally, this diagnostic device must ensure a proper habitat for cells, with controlled physiological (flow, temperature, humidity, etc.) and structural (rigidity, architecture, chemical composition, etc.) conditions to mimic the native human condition. This biomimicry provides improved sensitivity and reliability to the measurement, reduces the sensing time and the volume of reagents employed, and the overall cost of the assay.

A recent example of microfluidics-integrated biosensors includes the development of a multi-sensor fully-integrative microfluidic modular platform for the in situ, continuous, and automated sensing of biophysical microenvironmental parameters, such as pH, O₂, and temperature through physical sensors, and quantification of soluble protein biomarker levels through electrochemical-integrated sensors [55]. However, the high versatility and modularity of this approach enables its use for a diverse variety of applications, such as drug screening applications, as recently described (Fig. 4.5A) [99]. The system was employed, among other applications, to

assess short-term acute toxicity using liver cancer- and heart-on-a-chip model systems. A relevant feature of this approach was the possibility of regeneration of the microelectrodes, a limiting factor of most of the sensing devices, even though the procedure was significantly slow (around 4 h). Other limitations include using traditional PDMS, which is associated with several drawbacks, as discussed below. Finally, the number of available antibodies is limited; however, the use of aptamers is proposed as a feasible alternative (Fig. 4.5A). A similar multi-parametric microfluidic device capable of measuring pH and O₂ of the TME and the lactate and glucose levels was reported using a modular chip with miniaturized integrated microsensors [100]. Human brain tumor cells were seeded into the chip to demonstrate the performance of the device (Fig. 4.5B). By periodically stopping the flow, the media's acidification, O₂ levels, glucose consumption, and lactate production were continuously monitored, showing a high sensitivity within the desired linear range. All the electrochemical sensor electrodes (WE, RE, and CE) were integrated within the chip for amperometric measurements. It is worth mentioning that the developed chip was also transparent, which permitted the optical observation of the cultured cells. Finally, the pharmacokinetics and overall responses of the device were tested after the addition of cytochalasin B. It was found that the altered metabolism and recovery of the cells could be detected. Overall, and despite being developed a while ago, this work is still a reference about how microfluidics and biosensors can be combined for the on-chip monitoring of human cancer cell metabolism.

Finally, and as described above, the microfluidic isolation and enumeration of CTCs from unprocessed peripheral blood is of utmost importance due to their significance in early cancer diagnosis and personalized medicine [101]. Indeed, a large variety of microfluidic-based methods have been reported so far [102]. Most of them are based on the physical/antibody capture and identification of phenotypic surface CTCs markers by fluorescence immunostaining [103, 104], where a more detailed analysis of the genetic content and subtype classification of the cells is typically performed either inside or outside the chip [105]. However, this approach does not fully benefit from microfluidics' sensing and analytical capabilities to screen the phenotypic distribution of CTCs on-chip to predict disease tumors and therapy efficiency better. Despite the obtained insights, these approaches are limited to the standard surface markers (typically, one), which have been demonstrated to be inadequate to differentiate CTCs sub-types in particular through fluorescence means, which lack specificity and are associated to background noise. To solve this limitation, a new microfluidic device was recently developed for the isolation and profiling of CTCs using surface-enhanced Raman scattering (SERS) spectroscopy as an—optical-based—sensing method (Fig. 4.5C) [101]. As a proof-of-concept, three subtypes of breast cancer cells with different metastatic potential (as CTCs) were injected into the chip and captured explicitly through a porous membrane based on their large size. Next, a cocktail of multiple SERS aptamer vectors, namely HER2, EpCAM, and EGFR, was injected to recognize the different subtypes through the SERS spectrum. This “signature” was used to profile and classify the content of the sample. Altogether, this SERS-based liquid biopsy-on-a-chip provided a new

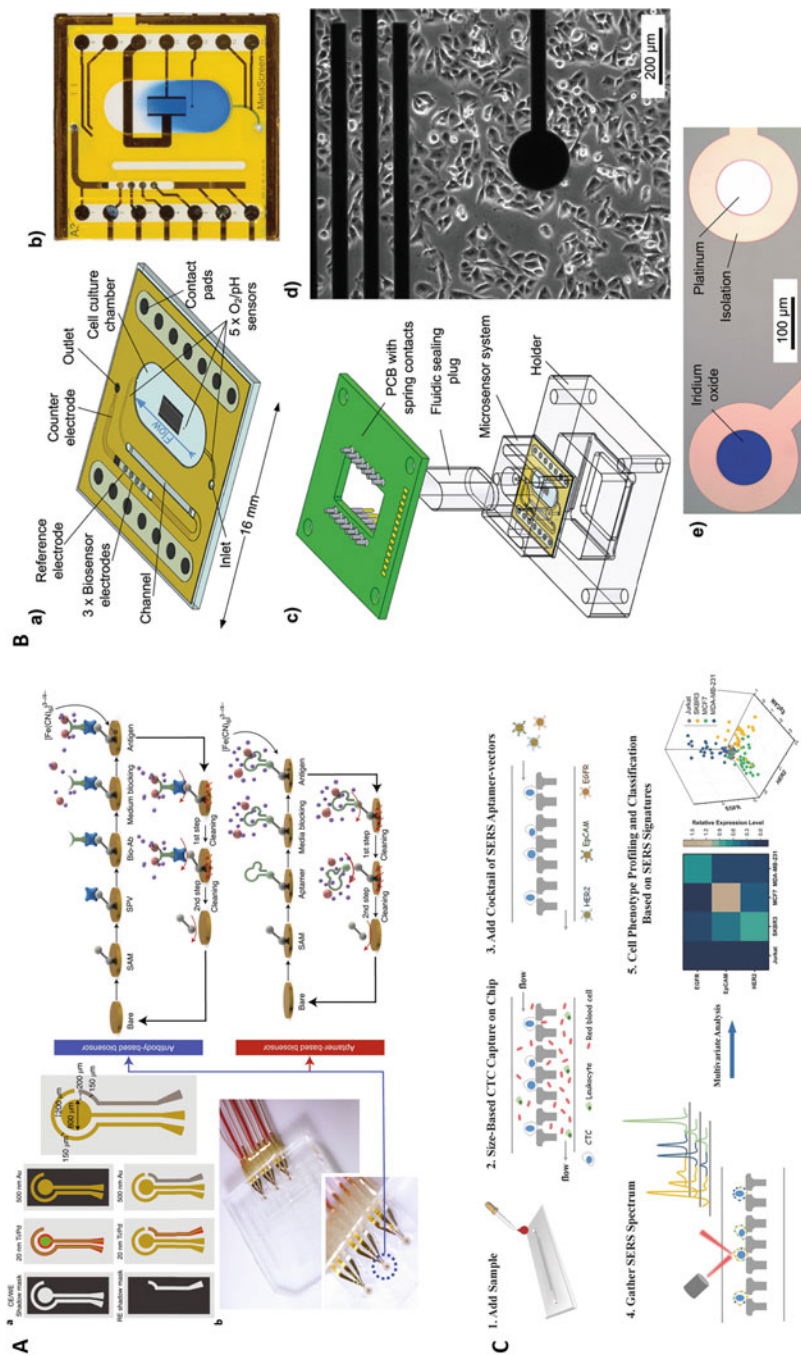


Fig. 4.5 Microfluidic-integrated biosensors for real-time and in-situ monitoring of cancer biomarkers. (A) Microelectrode fabrication procedure; (b) Picture of the microfabricated electrodes (WE and CE, in Au; RE, in Ag), and step-by-step functionalization and regeneration protocol for antibody-based and aptamer-based biosensing of soluble antigens [99]. (B) (a–c) Layout and main components of the microfluidic chip and electric interface; (d) T98G human brain cancer cells seeded in the cell culture chamber next to a sensing electrode; (e) pH and O₂ sensor electrodes [100]. (C) The working mechanism of the microfluidic device for the capture, profiling, and classification of CTCs based on SERS signatures [101]. Figure panels reproduced with permission from the publishers

quantitative approach for the in situ isolation, detection, and profiling of a heterogeneous population of CTCs, and therefore, may have clinical utility for the diagnosis of cancer.

Overall, this new paradigm in point-of-care devices can fulfill the demand of the cancer research community for high-performance instruments capable of providing accurate results while being—relatively—automated and cheap. This is of utmost importance for cancer diagnosis since the early detection of prognostic biomarkers can initiate sooner the treatment and provide critical information about the tumor.

4.5.1 Challenges of Microfluidics-Integrated Biosensor for Point-of-Care Applications

Even though the use of microfluidics-integrated biosensors has exponentially grown during the last decade for cancer research applications, their adoption by the clinics, who aim for simple, robust, and multi-functional devices capable of providing a helpful readout, is still minimal. The reasons for this may be very heterogeneous but are mainly related to the current level of development of most microfluidic devices. In the following, we comment on the technological and biologically-related challenges that this type of technology must face to overcome this lack of attention.

4.5.1.1 Technological Challenges

- *Low high-throughput characteristics:* Current microfluidic-integrated biosensor devices lack HTS characteristics and are mainly based on single sensing electrodes. Integrating an array of microelectrodes may permit the realization of multiple assays in parallel (i.e., multiplexing). This will enable the screening of a large battery of anti-cancerous compounds for ADMET studies and detect tumor-associated biomarkers characteristic of a particular type of tumor rapidly and efficiently. Alternatively, the development of multi-well plates (which are compatible with a large plethora of laboratory equipment) containing an array of microfluidic chips together with electrodes may raise the interest of clinics and the industrial healthcare sector.
- *Current microfluidic chips are difficult to manipulate and fragile:* This complexity originates from its development by academic labs with no focus on translating the chips to the market. However, if intended to be used by the non-trained clinical users, they should be simpler to manipulate and robust. For this, the automation of chip manipulation would boost their adoption by the clinics. Indeed, some companies are working in this direction where all the seeding, perfusion, and monitoring are done within a single piece of equipment.
- *Lack of well-established protocols for manipulating patient cells into microfluidic chips:* This is a significant issue for applying microfluidics in clinics. This type of device must be developed under the so-called GMP conditions (i.e., good manufacturing practices) using protocols and biomaterials approved by the regulatory agencies with rigid requirements in terms of biocompatibility. Similarly,

strict protocols about the isolation, manipulation, and integration of cells from patients inside the chips must also be developed.

- *Lack of standardization of microfluidic chips and biosensors and compatibility with existing technologies:* Typically, microfluidic chips are not generic, but their design is “fit-for-purpose”, that is, different laboratories have developed their own microfluidic devices. First of all, this approach is not compatible with mass production and is not cost-effective. Second, this diversity is univocally associated with a large variability of results from lab to a lab. Moreover, and in general, these custom-made systems are not compatible with other analytical technologies typically used in the clinics (e.g., plate reader) besides standard optical microscopy. One solution would be to fabricate universal units that recapitulate each tissue, which can be interconnected following a Lego™-like—modular—approach; this would be a step toward the universalization of this technology. Alternatively, highly versatile commercial devices have emerged (e.g., Mimetax™, Emulate™, AIM Biotech™, Cherry Biotech™, ChipShop™, etc.), which can be employed for various applications [2]. However, few of them integrate electrodes on-chip (e.g., Micronit™, Darwin Microfluidics™, Micrux™). Some others integrate the sensing unit outside the chip, which may be enough for certain applications (e.g., Elveflow™, Dropsens™, etc.). Clinical applications of these devices may include the accurate screening of released compounds (e.g., analytes, metabolites, cells, etc.) or evaluating the efficacy of new drugs or drug combinations.
- *Increase sensitivity of integrated electrodes:* The gold-standard biomaterial in biosensors is gold. Other materials, such as Pt, ITO, conducting polymers, and others, are also widely utilized due to the easy manufacturing, compatibility with microfabrication techniques, or integration. Under certain circumstances, these materials do not show the desired signal-to-noise ratio hampering the detection of expected biochemical or biological events. In this regard, using materials with advanced physical and chemical properties, such as carbon nanotubes or graphene (and its derivatives, such as graphene oxide), can provide lower detection limits, enabling single-molecule detection.
- *Incapacity to translate the developed products into the market:* Unfortunately, very few biosensors or microfluidic-integrated biosensors have reached the market (e.g., pregnancy tests, glucose, illegal drugs, or COVID-19, among few others). The main reasons behind this difficulty are complex regulatory laws, lack of performance compared to existing methods, high complexity of the biosensor, or lack of market to generate a profit for the industry.

4.5.1.2 Biological Challenges

- *Reproducing the complexity of the native TME from each patient:* It is challenging to collect the different types of cells (tumoral and non-tumoral) from each patient (e.g., for metastasis or drug screening studies), keep the cells alive for long periods, and seed them within the chip. Protocols should be clear for combining microfluidics and cells from patients, which are non-complex and less time-consuming. In this regard, applications should be focused on culture tissue

biopsies on the chip to evaluate the efficacy of drugs in a more predictable environment. Chips with (non-essential) pre-seeded cells would also be advantageous.

- *Isolation of different cell types and use of animal-origin materials/reagents:* This may also be considered a technological challenge since collecting different cells (tumoral, stromal, endothelial, immune cells, and others) from the same patient is highly complex. In addition to this, seeing the purified cells within the chip in the correct proportion and location keeping them alive for an extended time using adequate cell culture media with serum from animal origin (e.g., FBS) and/or biomaterials for cell encapsulation (e.g., Matrigel™) is a significant challenge. The use of scaling concepts may help in selecting the proper cell ratio. Finally, the use of alternative xeno-free biomaterials substituting Matrigel™, such as platelet lysates or silk fibroin, may solve a multitude of problems.
- *Addition of actuators to mimic dynamic events and rhythms:* The body is not static but in movement. Besides the continuous flow of fluid and/or blood, microfluidic devices must integrate miniaturized actuators to reproduce specific physiological activities. A clear example is a lung, where the action of breathing inflates and deflates the alveoli. Mimicking this mechanical stretching is, therefore, of utmost importance to understand critical events associated to it, such as the capacity of cancer cells to invade the surrounding stroma resulting from this cue. Similarly, Circadian rhythms are typically overlooked on-chip, and reproducing them would make the models more realistic and predictable.

A recent set of articles with researchers from academia, clinicians, industry, and policymakers reported on the challenges and requirements that microfluidic chips must address to be adopted by the healthcare market and clinics [106]. Among all the discussed topics, the use of human-induced pluripotent stem cells, the need to characterize the genetic and functional cell state within the chip, and the need to respect physiological scaling rules, were some of the main conclusions obtained. If these and the challenges mentioned above are addressed (and others non-mentioned here), it is expected that microfluidics-integrated biosensors will become a standard tool used in clinics to evaluate cancer onset, progression, and response to medication in a better, safer, and more accurate way. This statement is supported by the inclusion in 2016 of OoC technology as one of the ten most promising technologies by the World Economic Forum with the potential to improve lives and transform industries. Indeed, some microfluidic companies, some of them already introduced above, have emerged and already reached their maturity. The fabricated chips are being employed by several pharmaceutical companies and regulatory agencies, such as the FDA in the USA, e.g., to assess the toxicity of compounds. Several market studies have valued the microfluidics market at \$44 billion by 2025, growing at a CAGR of 22.9% [107], and the biosensors one at around \$38,600 million by 2026, with a CAGR of 10.4% [108]. Overall, combining both technologies will univocally accelerate the transfer of microfluidics from the bench to the bedside, paving the way toward developing a highly profitable market.

4.6 Discussion and Future Directions

There is a growing clinical and societal demand for novel technologies for the routine monitoring of cancer patients, which are more reliable, inexpensive, and capable of delivering results with better specificity, sensitivity, and immediacy. In this regard, the integration of miniaturized biosensors within microfluidic chips is essential for the early detection of a broad spectrum of biomarkers indicative of tumor onset, thus helping oncologists treat the patient very early. Similarly, this integrative technology is opening new avenues for the improved discovery and screening of drugs, and their mechanism of action, due to the lack of predictive power of traditional *in vitro* and *in vivo* models. Importantly, key events of the metastatic cascade can be modeled with high accuracy and released compounds detected and analyzed in real-time. However, as mentioned above, this technology is still far from being adopted by the clinics and the healthcare market. To this aim, this type of point-of-care devices must demonstrate that they are safe and their performance is similar (or superior) to those obtained by regular clinical laboratory tests before receiving approval by the regulatory agencies; this would allow their use by healthcare professionals in patients with total confidence.

Additionally, current microfluidic systems and biosensors must overcome other bottlenecks. This includes their lack of portability, low mixing capacity due to laminar flow, or surface effects. Another improvement may be devoted to finding alternatives to the widely used PDMS. Despite being considered a biocompatible biomaterial, optically transparent, flexible, gas permeable, and—relatively—cheap, PDMS can also absorb small molecules, such as drugs, that may hamper certain studies about the PK/PD of therapeutic compounds. More investigation into material science is necessary to provide an alternative to PDMS. An additional advantage of microfluidics and biosensors integration is the capacity to generate wearable sensing systems with the potential to revolutionize the canonical medical diagnosis of cancer, treatment follow-up, and tumor relapse. Together with the Internet-of-Things (IoT) and artificial intelligence, this type of healthcare approach is expected to change the medical policy to this and other diseases and, therefore, reduce the associated costs to the national healthcare systems.

4.7 Conclusions

The combined characteristics and advantages of microfluidics (for manipulating biological fluids) and biosensors (for the specific detection and analysis of the analytes of interest) have made microfluidic-based systems ideal platforms for cancer research and improved healthcare. Indeed, an extensive portfolio of applications combining microfluidics and biosensor technologies have been reported, ranging from realistic tumor modeling to drug discovery and screening. Even though most of these applications have been developed for fundamental applications, this technology has a promising future in the clinics to help physicians in decision-making. Therefore, microfluidics-integrated biosensors can have a very

influential role in the clinics and biomedical industry. Early cancer detection, selection of the most appropriate drug, monitoring therapy efficiency in real-time, or evaluation of side effects are only a few of the applications where microfluidics and biosensors can significantly improve the prognosis of cancer patients.

Acknowledgments D.C. acknowledges the financial support from the Portuguese Foundation for Science and Technology (FCT) under the program CEEC Individual 2017 (CEECIND/00352/2017). We also thank the support from the FCT under the scope of the projects 2MATCH (PTDC/BTM-ORG/28070/2017) to D.C. and S.C.K, and BREAST-IT (PTDC/BTM-ORG/28168/2017) to S.C.K, funded by the Programa Operacional Regional do Norte supported by European Regional Development Funds (ERDF). All the authors acknowledge the financial support from the EU Framework Programme for Research and Innovation Horizon 2020 on Forefront Research in 3D Disease Cancer Models as in-vitro Screening Technologies (FoReCaST—no. 668983).

Conflicts of Interest None.

References

1. Ferlay J et al (2020) Global cancer observatory: cancer today. Lyon, International Agency for Research on Cancer. <https://gco.iarc.fr/today>. Accessed 16 Aug 2021
2. Caballero D et al (2017) Organ-on-chip models of cancer metastasis for future personalized medicine: from chip to the patient. *Biomaterials* 149:98–115
3. Rebelo R et al (2019) 3D biosensors in advanced medical diagnostics of high mortality diseases. *Biosens Bioelectron* 130:20–39
4. Caballero D et al (2020) Chapter 15 - microfluidic systems in cancer research. In: Kundu SC, Reis RL (eds) *Biomaterials for 3D tumor modeling*. Elsevier, pp 331–377
5. Ma C et al (2021) Organ-on-a-Chip: a new paradigm for drug development. *Trends Pharmacol Sci* 42(2):119–133
6. Peck RW, Hinojosa CD, Hamilton GA (2020) Organs-on-chips in clinical pharmacology: putting the patient into the center of treatment selection and drug development. *Clin Pharmacol Ther* 107(1):181–185
7. Balkwill FR, Capasso M, Hagemann T (2012) The tumor microenvironment at a glance. *J Cell Sci* 125(23):5591–5596
8. Weigelt B, Bissell MJ (2008) Unraveling the microenvironmental influences on the normal mammary gland and breast cancer. *Semin Cancer Biol* 18(5):311–321
9. Levental KR et al (2009) Matrix crosslinking forces tumor progression by enhancing integrin signaling. *Cell* 139(5):891–906
10. Caballero D et al (2017) An interplay between matrix anisotropy and actomyosin contractility regulates 3D-directed cell migration. *Adv Func Mater* 27(35):1702322
11. Caballero D, Samitier J (2017) Topological control of extracellular matrix growth: a native-like model for cell morphodynamics studies. *ACS Appl Mater Interf* 9(4):4159–4170
12. Comelles J et al (2015) Cells as active particles in asymmetric potentials: motility under external gradients. *Biophys J* 108(2):456a
13. Espina JA, Marchant CL, Barriga EH Durotaxis: the mechanical control of directed cell migration. *FEBS J*. <https://doi.org/10.1111/febs.15862>
14. Lee HJ et al (2017) Fluid shear stress activates YAP1 to promote cancer cell motility. *Nat Commun* 8(1):14122

15. Lutolf MP et al (2003) Synthetic matrix metalloproteinase-sensitive hydrogels for the conduction of tissue regeneration: engineering cell-invasion characteristics. *Proc Natl Acad Sci U S A* 100(9):5413–5418
16. Luque-González MA et al (2020) Human microcirculation-on-chip models in cancer research: key integration of lymphatic and blood vasculatures. *Adv Biosys* 4(7):2000045
17. Jin M-Z, Jin W-L (2020) The updated landscape of tumor microenvironment and drug repurposing. *Sig Transduct Target Ther* 5(1):166
18. Whitesides GM (2006) The origins and the future of microfluidics. *Nature* 442(7101):368–373
19. Shen C et al (2019) Non-swelling hydrogel-based microfluidic chips. *Lab Chip* 19(23):3962–3973
20. Bettinger CJ et al (2007) Silk fibroin microfluidic devices. *Adv Mater (Deerfield Beach, FL)* 19(5):2847–2850
21. Zhao X et al (2016) Photocrosslinkable gelatin hydrogel for epidermal tissue engineering. *Adv Healthc Mater* 5(1):108–118
22. Gjorevski N, Lutolf MP (2017) Synthesis and characterization of well-defined hydrogel matrices and their application to intestinal stem cell and organoid culture. *Nat Protoc* 12(11):2263–2274
23. Zhao S et al (2016) Bio-functionalized silk hydrogel microfluidic systems. *Biomaterials* 93:60–70
24. Ma L-D et al (2018) Design and fabrication of a liver-on-a-chip platform for convenient, highly efficient, and safe in situ perfusion culture of 3D hepatic spheroids. *Lab Chip* 18(17):2547–2562
25. Kilic O et al (2016) Brain-on-a-chip model enables analysis of human neuronal differentiation and chemotaxis. *Lab Chip* 16(21):4152–4162
26. Oleaga C et al (2016) Multi-organ toxicity demonstration in a functional human in vitro system composed of four organs. *Sci Rep* 6(1):20030
27. Jeffrey SS, Toner M (2019) Liquid biopsy: a perspective for probing blood for cancer. *Lab Chip* 19(4):548–549
28. Kalyan S et al (2021) Inertial microfluidics enabling clinical research. *Micromachines* 12(3):257
29. Yang DK, Leong S, Sohn LL (2015) High-throughput microfluidic device for circulating tumor cell isolation from whole blood. *Micro Total Anal Syst* 2015:413–415
30. Bhatia SN, Ingber DE (2014) Microfluidic organs-on-chips. *Nat Biotechnol* 32(8):760–772
31. Caballero D et al (2017) Tumour-vessel-on-a-chip models for drug delivery. *Lab Chip* 17(22):3760–3771
32. Caballero D, Reis RL, Kundu SC (2020) Engineering patient-on-a-chip models for personalized cancer medicine. In: Oliveira JM, Reis RL (eds) *Biomaterials- and microfluidics-based tissue engineered 3D models*. Springer International Publishing, Cham, pp 43–64
33. Llenas M et al (2021) Versatile vessel-on-a-chip platform for studying key features of blood vascular tumors. *Bioengineering* 8(6):81
34. Sontheimer-Phelps A, Hassell BA, Ingber DE (2019) Modelling cancer in microfluidic human organs-on-chips. *Nat Rev Cancer* 19(2):65–81
35. Huh D et al (2010) Reconstituting organ-level lung functions on a chip. *Science* 328(5986):1662–1668
36. Benam, K.H., et al., Human lung small airway-on-a-chip protocol, in 3D cell culture: methods and protocols, Z. Koledova, Editor 2017, Springer, New York. p. 345–365
37. Hassell BA et al (2017) Human organ chip models recapitulate orthotopic lung cancer growth, therapeutic responses, and tumor dormancy in vitro. *Cell Rep* 21(2):508–516
38. Gaudriault P, Fassini D, Homs-Corbera A (2020) Chapter 8 - heart-on-a-chip. In: Hoeng J, Bovard D, Peitsch MC (eds) *Organ-on-a-chip*. Academic Press, pp 255–293
39. Rigat-Brugarolas LG et al (2014) A functional microengineered model of the human splenon-on-a-chip. *Lab Chip* 14(10):1715–1724

40. Kim HJ et al (2016) Contributions of microbiome and mechanical deformation to intestinal bacterial overgrowth and inflammation in a human gut-on-a-chip. *Proc Natl Acad Sci U S A* 113(1):E7–E15
41. Wilmer MJ et al (2016) Kidney-on-a-chip technology for drug-induced nephrotoxicity screening. *Trends Biotechnol* 34(2):156–170
42. Ronaldson-Bouchard K, Vunjak-Novakovic G (2018) Organs-on-a-chip: A fast track for engineered human tissues in drug development. *Cell Stem Cell* 22(3):310–324
43. Ingber DE (2018) Developmentally inspired human ‘organs on chips’. *Development* 145(16):156125
44. Kim S et al (2016) Pharmacokinetic profile that reduces nephrotoxicity of gentamicin in a perfused kidney-on-a-chip. *Biofabrication* 8(1):1758–5090
45. Esch EW, Bahinski A, Huh D (2015) Organs-on-chips at the frontiers of drug discovery. *Nat Rev Drug Discov* 14(4):248–260
46. Zhang B, Radisic M (2017) Organ-on-a-chip devices advance to market. *Lab Chip* 17(14):2395–2420
47. Low LA et al (2021) Organs-on-chips: into the next decade. *Nat Rev Drug Discov* 20(5):345–361
48. Pisano M et al (2015) An in vitro model of the tumor-lymphatic microenvironment with simultaneous transendothelial and luminal flows reveals mechanisms of flow enhanced invasion. *Integr Biol* 7(5):525–533
49. Fathi P et al (2020) Lymphatic vessel on a chip with capability for exposure to cyclic fluidic flow. *ACS Appl Bio Mater* 3(10):6697–6707
50. Zervantonakis IK et al (2012) Three-dimensional microfluidic model for tumor cell intravasation and endothelial barrier function. *Proc Natl Acad Sci U S A* 109(34):13515–13520
51. Osmani N et al (2019) Metastatic tumor cells exploit their adhesion repertoire to counteract shear forces during intravascular arrest. *Cell Rep* 28(10):2491–2500
52. Jeon JS et al (2015) Human 3D vascularized organotypic microfluidic assays to study breast cancer cell extravasation. *Proc Natl Acad Sci U S A* 112(1):214–219
53. Wang YI et al (2018) Multiorgan microphysiological systems for drug development: strategies, advances, and challenges. *Adv Healthc Mater* 7(2):1701000
54. Lee SH, Sung JH (2018) Organ-on-a-chip technology for reproducing multiorgan physiology. *Adv Healthc Mater* 7(2):1700419
55. Zhang YS et al (2017) Multisensor-integrated organs-on-chips platform for automated and continual in situ monitoring of organoid behaviors. *Proc Natl Acad Sci U S A* 114(12):E2293–E2302
56. Kamei K-i et al (2017) Integrated heart/cancer on a chip to reproduce the side effects of anti-cancer drugs in vitro. *RSC Adv* 7(58):36777–36786
57. Skardal A et al (2016) A reductionist metastasis-on-a-chip platform for in vitro tumor progression modeling and drug screening. *Biotechnol Bioeng* 113(9):2020–2032
58. Skardal A et al (2017) Multi-tissue interactions in an integrated three-tissue organ-on-a-chip platform. *Sci Rep* 7(1):017-08879
59. Maschmeyer I et al (2015) A four-organ-chip for interconnected long-term co-culture of human intestine, liver, skin and kidney equivalents. *Lab Chip* 15(12):2688–2699
60. Xu Z et al (2016) Design and construction of a multi-organ microfluidic chip mimicking the in vivo microenvironment of lung cancer metastasis. *ACS Appl Mater Interfaces* 8(39):25840–25847
61. Satoh T et al (2018) A multi-throughput multi-organ-on-a-chip system on a plate formatted pneumatic pressure-driven medium circulation platform. *Lab Chip* 18(1):115–125
62. Miller PG, Shuler ML (2016) Design and demonstration of a pumpless 14 compartment microphysiological system. *Biotechnol Bioeng* 113(10):2213–2227
63. Verneti L et al (2017) Functional coupling of human microphysiology systems: intestine, liver, kidney proximal tubule, blood-brain barrier and skeletal muscle. *Sci Rep* 7(1):42296

64. Novak R et al (2020) Robotic fluidic coupling and interrogation of multiple vascularized organ chips. *Nat Biomed Eng* 4(4):407–420
65. Jellali R et al (2016) Long-term human primary hepatocyte cultures in a microfluidic liver biochip show maintenance of mRNA levels and higher drug metabolism compared with Petri cultures. *Biopharm Drug Dispos* 37(5):264–275
66. Oleaga C et al (2018) Investigation of the effect of hepatic metabolism on off-target cardiotoxicity in a multi-organ human-on-a-chip system. *Biomaterials* 182:176–190
67. Kong C et al (2020) Label-free counting of affinity-enriched circulating tumor cells (CTCs) using a thermoplastic micro-coulter counter (μ CC). *Analyst* 145(5):1677–1686
68. Barriere G et al (2014) Circulating tumor cells and epithelial, mesenchymal and stemness markers: characterization of cell subpopulations. *Ann Transl Med* 2(11):109–109
69. Farahinia A, Zhang WJ, Badea I (2021) Novel microfluidic approaches to circulating tumor cell separation and sorting of blood cells: a review. *J Sci Adv Mater Dev* 6(3):303–320
70. Wang X, Liu Z, Pang Y (2017) Concentration gradient generation methods based on microfluidic systems. *RSC Adv* 7(48):29966–29984
71. Miller OJ et al (2012) High-resolution dose–response screening using droplet-based microfluidics. *Proc Natl Acad Sci* 109(2):378–383
72. Weiss ACG et al (2019) In situ characterization of protein corona formation on silica microparticles using confocal laser scanning microscopy combined with microfluidics. *ACS Appl Mater Interf* 11(2):2459–2469
73. Bhalla N et al (2016) Introduction to biosensors. *Essays Biochem* 60(1):1–8
74. Caballero D et al (2012) Impedimetric immunosensor for human serum albumin detection on a direct aldehyde-functionalized silicon nitride surface. *Anal Chim Acta* 720:43–48
75. Diéguez L et al (2012) Optical gratings coated with thin Si₃N₄ layer for efficient immunosensing by optical waveguide lightmode spectroscopy. *Biosensors* 2(2):114–126
76. Baccar ZM et al (2012) Development of an impedimetric DNA-biosensor based on layered double hydroxide for the detection of long ssDNA sequences. *Electrochim Acta* 74:123–129
77. Darwish N et al (2010) Multi-analytic grating coupler biosensor for differential binding analysis. *Sens Act B Chem* 144(2):413–417
78. Barreiros dos Santos M et al (2015) Label-free ITO-based immunosensor for the detection of very low concentrations of pathogenic bacteria. *Bioelectrochemistry* 101:146–152
79. Barreiros dos Santos M et al (2013) Highly sensitive detection of pathogen *Escherichia coli* O157:H7 by electrochemical impedance spectroscopy. *Biosens Bioelectron* 45:174–180
80. Justino CIL, Duarte AC, Rocha-Santos TAP (2017) Recent progress in biosensors for environmental monitoring: a review. *Sensors (Basel, Switz)* 17(12):2918
81. Zazoua A et al (2009) Characterisation of a Cr(VI) sensitive polysiloxane membrane by X-ray photoelectron spectrometry and atomic force microscopy. *Sens Lett* 7(5):995–1000
82. Clark LC Jr et al (1953) Continuous recording of blood oxygen tensions by polarography. *J Appl Physiol* 6(3):189–193
83. Clark LC Jr, Lyons C (1962) Electrode systems for continuous monitoring in cardiovascular surgery. *Ann N Y Acad Sci* 102:29–45
84. Guilbault GG, Montalvo JG Jr (1969) A urea-specific enzyme electrode. *J Am Chem Soc* 91(8):2164–2165
85. Kumar S et al (2013) Microfluidic-integrated biosensors: prospects for point-of-care diagnostics. *Biotechnol J* 8(11):1267–1279
86. Park BY, Zaouk R, Madou MJ (2006) Fabrication of microelectrodes using the lift-off technique. In: Minter SD (ed) *Microfluidic techniques: reviews and protocols*. Humana Press, Totowa, NJ, pp 23–26
87. Caballero D et al (2013) Directing polypyrrole growth by chemical micropatterns: a study of high-throughput well-ordered arrays of conductive 3D microrings. *Sens Act B Chem* 177:1003–1009
88. Xie Y et al (2015) A novel electrochemical microfluidic chip combined with multiple biomarkers for early diagnosis of gastric cancer. *Nanoscale Res Lett* 10(1):477

89. Ortega MA et al (2019) Muscle-on-a-chip with an on-site multiplexed biosensing system for in situ monitoring of secreted IL-6 and TNF- α . *Lab Chip* 19(15):2568–2580
90. Marland JRK et al (2020) Real-time measurement of tumour hypoxia using an implantable microfabricated oxygen sensor. *Sens Bio-Sens Res* 30:100375
91. Alam F et al (2018) Lactate biosensing: the emerging point-of-care and personal health monitoring. *Biosens Bioelectron* 117:818–829
92. Juska VB, Walcarius A, Pemble ME (2019) Cu Nanodendrite foams on integrated band Array electrodes for the nonenzymatic detection of glucose. *ACS Appl Nano Mater* 2(9):5878–5889
93. Wencel D, Abel T, McDonagh C (2014) Optical chemical pH sensors. *Anal Chem* 86(1):15–29
94. Eftekhari A (2003) pH sensor based on deposited film of lead oxide on aluminum substrate electrode. *Sensors Actuators B Chem* 88(3):234–238
95. Sinha S et al (2019) Fabrication, characterization and electrochemical simulation of AlN-gate ISFET pH sensor. *J Mater Sci Mater Electron* 30(7):7163–7174
96. Vivaldi F et al (2021) Recent advances in optical, electrochemical and field effect pH sensors. *Chemosensors* 9(2):33
97. Castanheira A et al (2021) A novel microfluidic system for the sensitive and cost-effective detection of okadaic acid in mussels. *Analyst* 146(8):2638–2645
98. Barreiros Dos Santos M et al (2019) Portable sensing system based on electrochemical impedance spectroscopy for the simultaneous quantification of free and total microcystin-LR in freshwaters. *Biosens Bioelectron* 142(111550):30
99. Aleman J et al (2021) Microfluidic integration of regeneratable electrochemical affinity-based biosensors for continual monitoring of organ-on-a-chip devices. *Nat Prot* 16(5):2564–2593
100. Weltin A et al (2014) Cell culture monitoring for drug screening and cancer research: a transparent, microfluidic, multi-sensor microsystem. *Lab Chip* 14(1):138–146
101. Zhang Y et al (2018) Combining multiplex SERS nanovectors and multivariate analysis for in situ profiling of circulating tumor cell phenotype using a microfluidic chip. *Small* 14(20):1704433
102. Farshchi F, Hasanzadeh M (2021) Microfluidic biosensing of circulating tumor cells (CTCs): recent progress and challenges in efficient diagnosis of cancer. *Biomed Pharmacother* 134:111153
103. Poudineh M et al (2017) Tracking the dynamics of circulating tumour cell phenotypes using nanoparticle-mediated magnetic ranking. *Nat Nanotech* 12(3):274–281
104. Ahmed MG et al (2017) Isolation, detection, and antigen-based profiling of circulating tumor cells using a size-dictated immunocapture chip. *Angew Chem Int Ed* 56(36):10681–10685
105. Poudineh M et al (2017) Profiling functional and biochemical phenotypes of circulating tumor cells using a two-dimensional sorting device. *Angew Chem Int Ed* 56(1):163–168
106. Watson DE, Hunziker R, Wikswo JP (2017) Fitting tissue chips and microphysiological systems into the grand scheme of medicine, biology, pharmacology, and toxicology. *Exp Biol Med* 242(16):1559–1572
107. Markets and Markets Microfluidics market by product (devices, components (chips, sensors, pump, valves, and needles)), application (IVD [POC, clinical, veterinary], research, manufacturing, therapeutics), end user and region - global forecast to 2025. *Markets and Markets*
108. Manjrekar S, Sumant O (2020) Biosensors market by product (wearable biosensors and non-wearable biosensors), technology (electrochemical biosensors, optical biosensors, piezoelectric biosensors, thermal biosensors, and nanomechanical biosensors): global opportunity analysis and industry forecast, 2019–2026. *Allied Market Research*, p 163

Part II

Modelling the Tumor Microenvironment and Its Dynamic Events



The Tumor Microenvironment: An Introduction to the Development of Microfluidic Devices

5

B. Kundu, D. Caballero, C. M. Abreu, R. L. Reis, and S. C. Kundu

Abstract

The tumor microenvironment (TME) is like the *Referee* of a soccer match who has constant eyes on the activity of all players, such as cells, acellular stroma components, and signaling molecules for the successful completion of the game, that is, tumorigenesis. The cooperation among all the “team members” determines the characteristics of tumor, such as the hypoxic and acidic niche, stiffer mechanical properties, or dilated vasculature. Like in soccer, each TME is different. This heterogeneity makes it challenging to fully understand the intratumor dynamics, particularly among different tumor subpopulations and their role in therapeutic response or resistance. Further, during metastasis, tumor cells can disseminate to a secondary organ, a critical event responsible for approximately 90% of the deaths in cancer patients. The recapitulation of the rapidly changing TME in the laboratory is crucial to improve patients’ prognosis for unraveling key mechanisms of tumorigenesis and developing better drugs. Hence, in this chapter, we provide an overview of the characteristic features of the TME and how to model them, followed by a brief description of the limitations of existing in vitro platforms. Finally, various attempts at simulating the TME using microfluidic platforms are highlighted. The chapter ends with the concerns that need to be addressed for designing more realistic and predictive tumor-on-a-chip platforms.

B. Kundu (✉) · D. Caballero · C. M. Abreu · R. L. Reis · S. C. Kundu
3B’s Research Group, I3Bs—Research Institute on Biomaterials, Biodegradables and Biomimetics,
University of Minho, Headquarters of the European Institute of Excellence on Tissue Engineering
and Regenerative Medicine, AvePark, Parque de Ciência e Tecnologia, Zona Industrial da Gandra,
Barco, Guimarães, Portugal

ICVS/3B’s—PT Government Associate Laboratory, Braga/Guimarães, Portugal

© The Author(s), under exclusive license to Springer Nature Switzerland AG 2022
D. Caballero et al. (eds.), *Microfluidics and Biosensors in Cancer Research*,
Advances in Experimental Medicine and Biology 1379,
https://doi.org/10.1007/978-3-031-04039-9_5

115

Keywords

Tumor microenvironment · Three-dimensions · Microfluidics · In vitro tumor models · Metastasis

5.1 Introduction

The cell is the basic unit of human life and the building block of tissues and organs. Cell proliferation is involved in fundamental physiological processes, such as embryonic development, tissue repair, or wound healing. In normal conditions, cell division is tightly controlled by several regulators to maintain tissue homeostasis. But when this control system collapses, cells start dividing uncontrollably, resulting in a mass of cells often called *tumors*. Yet, a tumor is not simply a group of uncontrollably dividing cells. It is instead a heterogeneous crowd of resident and infiltrating host cells that secrete various signaling molecules such as cytokines and chemokines and produce extracellular matrix (ECM), all of which together form the tumor microenvironment (TME) [1, 2]. The precise composition of TME varies between types of tumors. Still, it is well accepted that the “*tumor microenvironment is not just a silent bystander, but rather an active promoter of cancer progression*” [3]. Apart from cancer cells, the TME also hosts non-tumorigenic healthy cells, including fibroblasts, endothelial cells, pericytes, a diverse repertoire of immune cells, stem cells, and neurons. Tumor cells are adept at deceiving these cells to join hand with them to bypass the body’s immune surveillance. Hence, the components of TME can be broadly classified into two categories: cellular and acellular. In the following, we discuss the main features and functions of these two building blocks of the TME.

5.1.1 Cells in the TME

TME contains the tumor vasculature and lymphatics, immune cells, fibroblasts, stromal cells, and occasionally adipocytes along with tumor cells [4, 5]. These cells comprise more than 50% of the primary mass of the tumor and have a dynamic and tumor-promoting function during its development (Fig. 5.1). Intercellular communication occurs through the well-controlled release of cytokines, chemokines, matrix remodeling enzymes, inflammatory mediators, and growth factors. Macrophages are also occasionally found in TME and are associated with immune suppression, angiogenesis, migration, invasion, and recruitment of other immune cells [6]. Macrophages and innate immune system cells serve as the first line of defence against infection and tissue damage [7]. Macrophages get activated under the influence of the local ECM or cytokine milieu. In a tumor, chemokines such as C-C motif chemokine ligand 2 (CCL2), C-X-C motif chemokine ligand 10 (CXCL10), and cytokines like interleukin-34 (IL-34), IL-6, colony-stimulating factor I (CSF-1)—together activate macrophages. Once activated, macrophages

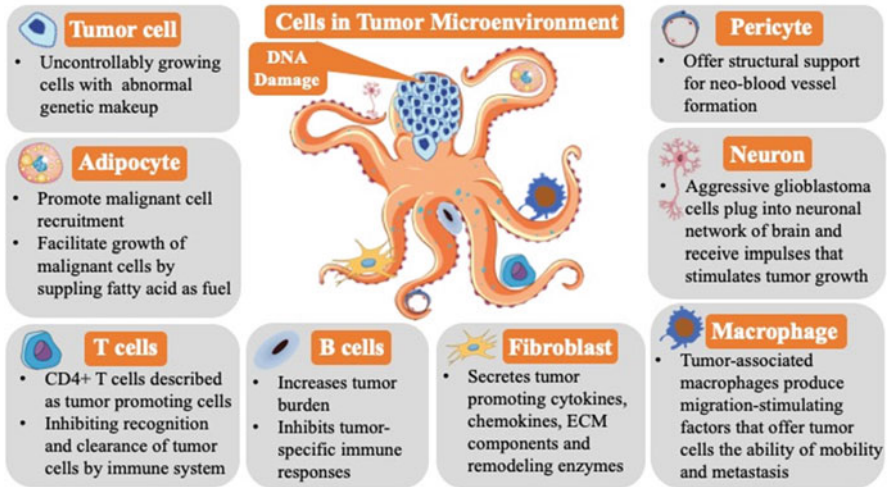


Fig. 5.1 The TME and its complex cellular content. Illustration summarizing the different types of cells present in the TME and their central role. Like the arms of an octopus, tumor cells have various “tricks” to deceive healthy cells in their microenvironment to help the tumors grow

either exhibit an M1 state, responsible for inflammation, or an M2 state, involve in tissue homeostasis and regeneration. The M2 macrophages lack tumor antigens and are called tumor-associated macrophages (TAMs) [8]. TAMs secrete IL-10, fibroblast growth factor (FGF), epidermal growth factor (EGF), vascular endothelial growth factor (VEGF), matrix metalloproteinases (MMPs), chemokines (CCL-2, -5, -8, -22) and also regulate aerobic glycolysis and apoptotic resistance in tumor cells, thus promoting malignancy [9]. When a pathogen or foreign antigen enters the body, the immune cells such as T- (or B-) cells become active. But the rate of activation of these immune cells is much lower than the rate of infection. Hence, macrophages rush to the site to manage the situation and instruct the T cells to produce Th-1 or Th-2-type response [10]. The M1-Th-1 contributes to antitumor defence [11]. The presence of tumoral macrophages is associated with unfavorable prognosis.

Apart from macrophages, the other types of immune cells recruited by the tumor are neutrophils, eosinophils, CD8⁺ cytotoxic tumor cells (the major anti-tumoral component in TME), antigen-presenting cells (APCs), CD4⁺ T helper 2 cells (Th-2), and regulatory T cells (Tregs). Lesser in number than macrophages, neutrophils are drawn to the TME by IL-8 secretion. The neutrophils take part in two opposite activities: (1) pro-tumorigenic activity (N2) by facilitating angiogenesis, ECM degradation, and immune suppression and (2) tumor inhibiting activity (N1) [12]. Interferon-gamma (IFN- γ) turns neutrophils into tumoricidal N1 cells. The neutrophil infiltration is associated with a poor prognosis. Next, eosinophils participate in Th-2 type immune responses and become tumoricidal in certain tumors [13]. The presence of eosinophils is associated with a good prognosis. During the

early stages of tumor development, CD8⁺ T lymphocytes are active in the TME. These cells, along with CD4⁺ T helper cells, promote the production of IL-2, IFN- γ , and induce the arrest of the cell cycle, apoptosis, and necrosis [14]. The APCs in TME phagocytose the proteinous debris of apoptotic cells. The Tregs augment CD8⁺ cell proliferation while inhibiting macrophages and APCs' activity. Other CD4⁺ T cells like Th-2 produce IL-4, IL5, and IL-13, favoring tissue inflammation and tumor growth [15]. CD4⁺ T cells are most commonly known as "Tregs", which inhibit the immune system's identification and clearance of tumor cells [16]. In the TME, the presence of Tregs is correlated with the worst type of prognosis, whereas CD8⁺ T cells are associated with good prognosis.

The TME also contains endothelial cells, mesenchymal stem cells (MSCs), and cancer-associated fibroblasts (CAFs). Tumor cells secrete basic fibroblast growth factors (bFGFs) and VEGF to induce angiogenesis via Akt and NF- κ B pathways [17]. The endothelial cells of the TME further release angiocrine factors, such as chemokines and adhesion molecules, which are essential for metastasis [18]. Additionally, MSCs migrate toward inflammatory sites, such as tumor, and incorporate with it. In the TME, MSCs assist the tumor in multi-stage disease progression, including epithelial-to-mesenchymal transition (EMT) and metastasis [19]. These MSCs are of bone marrow or fat tissue origins, stimulating tumor cell quiescence and drug resistance [19]. Lastly, CAFs are one of the most important cellular components of the TME, being the largest population of tumor stroma cells that secrete the ECM components [20]. The origin and functional heterogeneity of CAFs are not entirely understood, despite their potential as therapeutic targets [21]. CAFs secrete VEGF-A, CXCL12, IL-6 and remodel the ECM that, together, promote the invasion of cancer cells that result in metastasis [22]. Finally, CAFs also regulate the plasticity of cancer stem cells [23] and alter the metabolism of epithelial tumor cells [24].

Finally, non-tumorous cells, such as normal fibroblasts, are also present in the TME. Their primary function is to deposit the interstitial ECM. Once activated by the tumor cells, they enable the mechanical alteration of ECM topology. Activated myofibroblasts trigger the secretion of pro-inflammatory factors such as Transforming Growth Factor β (TGF- β), TGF- α , Fibroblast Growth Factors (FGFs), leading to the creation of a cytokine and chemokine storm. Furthermore, macrophages recruited into TME secrete TGF- β , which collaborates with myofibroblast secretion to produce dysregulated, overactive, and highly proliferative myofibroblasts [25].

5.1.2 The ECM as a Multi-Functional Regulator of Cell Activity

Based on its location, function, and composition, the ECM can be classified as (1) the interstitial matrix—a 3D porous and interconnected network located around the cells connecting the cellular stroma to the basement membrane and (2) the basement membrane—a sheet-like and dense membranous structure lining the basal surface. In the TME, the ECM is composed of a complex network of

macromolecules, mainly collagen, laminin, fibronectin, and elastin. Proteoglycans are also key players in the ECM, and among other functions, they are directly involved in regulating cell signaling properties, particularly in growth control [26, 27]. All these ECM components form the acellular part of the TME, which, when organized normally, provides physical support to the cells. The ECM not only serves as a scaffolding material to embed the cells of a given tissue, but it also functions as a reservoir of growth factors and cytokines to regulate cell behavior. As such, it plays a crucial active role in tumor cell dissemination [28].

During tumorigenesis, four fundamental mechanisms are involved in ECM remodeling, which also affects its mechanical, biophysical, and biochemical properties:

1. Deposition of neo-ECM components (predominantly, fibrillary collagen, which represents ~60% of the tumor mass) by CAFs [29], making the tumors stiffer than the surrounding tissues;
2. Post-translational modifications of ECM components;
3. Proteolytic degradation of ECM, which not only releases bioactive fragments but also creates space for cellular migration;
4. Force-mediated ECM reorganization [30].

Tumor cells deposit collagen type I, collagen type III, and ECM modifying enzymes, namely lysyl oxidases (LOX) and LOX-like proteins [31]. LOX cross-links the collagen fibers and, together with the action of stromal cells, an abundant collagen-rich ECM with increased rigidity is formed with a minimum number of cells, mainly fibroblasts and myofibroblasts. This is known as *desmoplasia* and has been associated with a poor prognosis. Desmoplastic tissues also include those with an abundant presence of cells, such as fibroblasts, endothelial cells, or immune cells with little ECM [32]. In both cases, the increased stiffness alters the expression of cell surface markers. For example, integrin expression is upregulated, triggering integrin-mediated mechano-signaling in TME.

The ECM can be degraded by proteases, such as MMPs and disintegrins, secreted by the tumor and other recruited cells (e.g., stem cells), causing basement membrane breakage. This proteolytic degradation leads to a sequence of events characteristic of cancer progression [30, 33]:

1. Replacement of the degraded ECM by a new tumorous one;
2. Migration of tumor cells, which form invadopodia (a specific type of invasive protrusions) that express integrins for binding and invading the ECM;
3. The release of soluble molecules promotes tumor cell proliferation, angiogenesis, and invasion.

The migration of tumor cells can be categorized into (1) single-cell migration (amoeboid or mesenchymal locomotion mode) and (2) collective migration in the form of cell sheets. The type of migration exhibited by the tumor cells is influenced by the physical properties of the TME, such as the porosity of the TME, which

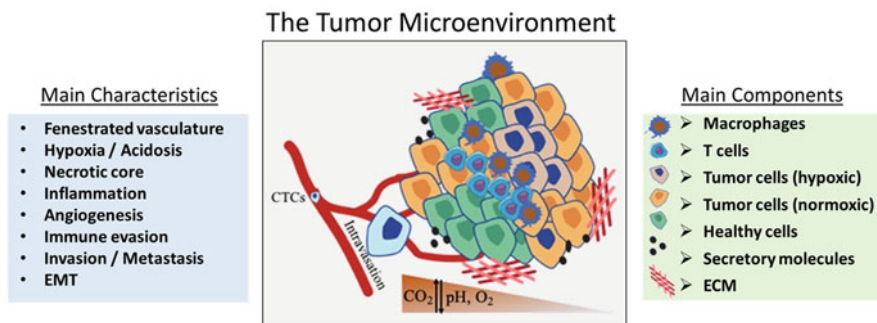


Fig. 5.2 The TME and its main characteristic features. The acidic pH in the TME acts as a shield for tumor cells, protecting them from the body's immune surveillance. The low pH washes out all the antitumor immune effectors, such as T cells and antigen-presenting immune cells, by inducing the onset of a negative feedback mechanism involving the reprogramming of a subset of the regulatory T cells and myeloid cells into pro-tumor cells, or immunosuppressors. Simultaneously, the acidification of TME upregulates the HIF-1 α that promotes the activation of pH regulator genes, leading to a further decrease in pH. The low pH additionally traps ions that retain drugs in the ECM

promotes single-cell migration. In contrast, low porosity supports the migration of cell sheets [34]. During mesenchymal migration, cells form a rich repertoire of protrusions to optimize their invasion efficiency, including actin-rich protrusions called lamellipodia, filopodia, invadopodia, lobopodia, and others. At this stage, the tumor cells become more deformable than healthy cells, allowing them to squeeze through the rigid ECM pores. This, together with the aligned architecture of the ECM, enables the directed migration of cancer cells toward the microvasculature. Therein, the tumor cells can intravasate, becoming circulatory tumor cells (CTCs). Then, the CTCs transit along the vessels and eventually attach to the vascular wall before extravasating and invading a secondary site, forming a secondary tumor. This invasion is facilitated by the previous remodeling of the ECM. This increases the activity of MMPs, causing a leaky vasculature that facilitates the extravasation of CTCs [35].

The dynamics of ECM during tumor progression also generates spatiotemporal gradients, which are chiefly of different types: (1) chemical, (2) mechanical, and (3) electrical gradients. For the latter, each cell possesses an electric potential across the plasma membrane, which is regulated through ion channels, the ionic composition of the ECM, and the bi-electric gradient within a tissue. Tumor cells exhibit a comparatively higher positive membrane potential than healthy cells, similar to multipotent stem cells [36]. The growth of tumor cells encounters interference with membrane and trans-epithelial potential, local ionic environments,—together, readjust the localized ionic setting. This physiological electric field guides the migration of metastatic tumor cells through TME, known as electrotaxis or galvanotaxis.

An additional characteristic feature of the TME is the lack of oxygen (and nutrients) needed to maintain adequate tissue homeostasis resulting from the lack of vascularization. This is known as *hypoxia*, which generates a necrotic core in the

tumor [37] (Fig. 5.2). For survival, tumor cells undergo metabolic reprogramming and overexpress glycolysis-related surface proteins, including glucose transporter 1 (GLUT1), GLUT3, pyruvate kinase M2 (PKM2), and lactate dehydrogenase-A (LDHA) to increase glucose uptake [38]. LDHA catalyzes pyruvate to lactic acid, thus turning the tumor ECM acidic. Hypoxia promotes EMT of tumor cells by down-/up-regulating the expression of N-cadherin, E-cadherin, slug, and/or vimentin, among others, with a rise in the production of MMPs [39]. This further facilitates the migration of tumor cells, allowing them to invade the surrounding stroma. In hypoxia, cells overexpress hypoxia-inducible factor-1 (HIF-1), which in turn drives the process of new blood vessel formation (i.e., angiogenesis) by upregulating the VEGF protein [40]. Tumor neovascularization inhibits the maturation of dendritic cells (DCs) and the presentation of antigens on the cell surface. It inhibits the activity of cytotoxic T cells through angiogenic factors while recruiting immunosuppressive cells [41]. However, the new blood vessels formed are leakier and dilated, challenging the delivery of oxygen and the removal of metabolites. As a result, the TME becomes highly acidic and hypoxic. Additionally, the fenestrated endothelium also threatens the effective delivery of chemotherapeutics [42]. Further, a VEGF chemoattractant is formed, increasing the infiltration of tumor-associated macrophages, which constitute nearly 50% of the entire cellular mass of TME [43].

Finally, the degree of TME heterogeneity is different among individuals or even at various sites of an individual's body. This heterogeneity is manifested both biologically and chemically. For this reason, it needs to be taken into consideration in cancer theranostics for personalized medicine and for designing screening models with improved predictive power. In this regard, the overview of ECM remodeling and its impact on cell behavior will enable a better understanding of how to design more realistic pre-clinical tumor models (Fig. 5.3).

5.2 Capturing the Complexity of the 3D TME In Vitro: Existing Models and Limitations

A myriad of 3D in vitro models of the TME have been developed, overcoming the limitations of traditional 2D platforms. These advanced systems provide a more realistic scenario for investigating the complexity of cell–cell and cell–ECM interactions [44]. These models include the culture of cancer (and other) cells in biomimetic hydrogels, scaffolds, transwell membranes, and microcarriers, or the use of tumor spheroids (fabricated by traditional hanging drop, forced floating, or agitation-based methods) that recapitulate the native tumor architecture and micro-environment complexity [45] (Table 5.1). Even though conventional 3D in vitro models offer a good platform for identifying prognostic biomarkers and screening potential anti-cancer drugs, there are still several unmet needs threatening their adoption by the cancer research community. Among all of them, the 3D models are typically static. They can barely recapitulate some of the dynamic physiological events occurring during tumorigenesis and cancer cell dissemination, such as fluid flow, biochemical gradient formation, or specific events of the metastatic cascade

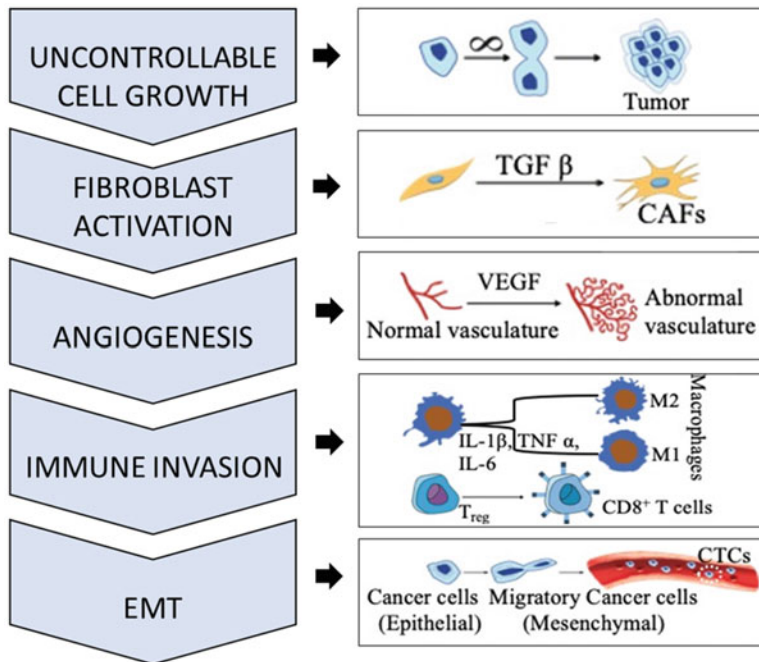


Fig. 5.3 Summary of the main events taking place in the TME during tumorigenesis

[55]. As an example, the transwell inserts allow the study of endothelium adhesion and transendothelial migration. But, they fail to reproduce the dynamic condition of the extravasation process and the endothelial junction architecture [56].

Three-dimensional *in vitro* models also suffer from additional limitations. This may include the use of large volumes of sample and reagents, which is also associated with a high economic burden. Similarly, using “big” scaffolds may limit the integration and compatibility with traditional analytical techniques and high-throughput screening (HTS) platforms. Hence, there is an immense interest in bridging the gap between 3D *in vitro* models and existing HTS platforms. This is particularly relevant for the pharmaceutical industry, which is continuously pursuing innovative, efficient, cost-effective, automated, quantitative, and, importantly, highly predictive technologies [57]. In this regard, microfluidic platforms appear as the best-suited, rational alternative option over traditional systems, and discussed below.

Table 5.1 Conventional 3D in vitro tumor models

Techniques	Process	Advantages	Limitations	References
Spheroid—hanging-drop method	A drop of single-cell suspension is pipetted into a surface (plate/tray). The surface is then inverted, which turns the drop into a hanging droplet. The cells aggregate at the tip of the drop due to surface tension–gravity	<ul style="list-style-type: none"> • A small volume of sample (20–50 μl) • Inexpensive • Uniform sizes of the spheroids 	<ul style="list-style-type: none"> • Lack of extracellular matrix • Inappropriate for migration assays • The spheroids are not transferrable to another surface or molds • Fail to create the different gradients of TME • Difficulty in maintaining the long-term culture 	[46–48]
Spheroid—forced-floating method	Cells are cultured using non-adhesive surfaces like poly-hydroxyethylmethacrylate (poly-HEMA), agarose-coated surfaces, and commercially available PrimeSurface, Lipidure, and Sumitomo Bakelite. The non-adhesive surfaces forcefully enhance the cell–cell interaction and spheroid formation	<ul style="list-style-type: none"> • Inexpensive • Simple, but the commercial surfaces are costly 	<ul style="list-style-type: none"> • Fail to create the different gradients of TME • Difficulty in maintaining the long-term culture 	[46–48]
Spheroid—agitation-based approaches	In this case, the cells are maintained in solution either by the continuous stirring of the cell suspension (by using spinner flask bioreactors) or rotating the whole container (by using rotating cell culture bioreactors) or consistent feeding of the cell chamber from external flow to promote cell–cell interaction and formation of cellular aggregates	<ul style="list-style-type: none"> • Simple, easy handling, and long-term maintenance of the spheroids in culture • Low shear force in rotating bioreactors • The fluid motion facilitates nutrient supply and waste removal • Controllable mechanical cues can be provided using a compression bioreactor 	<ul style="list-style-type: none"> • No control over spheroid sizes • Spinner systems alter cellular physiology by shear force of stirring bar • A larger amount of culture medium is needed 	[49–51]
Matrices and scaffolds	Cells are either seeded on the top of matrices or encapsulated within the gel-like substances and cultured over time. The cell–cell and cell–matrix interactions lead to the development of solid	<ul style="list-style-type: none"> • Recapitulation of ECM component in TME and the cross-talk between cells and ECM • Able to 	<ul style="list-style-type: none"> • Nonuniformity in the sizes of the spheroids • Expensive for scale-up • Batch-to-batch 	[48, 52]

(continued)

Table 5.1 (continued)

Techniques	Process	Advantages	Limitations	References
	tumors. Natural biopolymers such as collagen, laminin, alginate, silk fibroin, gellan gum, or commercially available ECM materials such as Matrigel, basement membrane extract (BME) are popular scaffolding materials for tumor modeling	investigate the matrix remodeling curing disease progression <ul style="list-style-type: none"> • The balance between disease complexity and experimental control 	variability of ECM material <ul style="list-style-type: none"> • Usually lack vasculature 	
3D bioprinting	Offers simultaneous deposition of cells, signaling factors, and biomaterials using computer-aided design to generate highly controlled architecture	<ul style="list-style-type: none"> • Allow the incorporation of perfusable vascular networks • Readily integrated with an automated platform • Offer high-throughput fast testing • Allow the creation of complex structure 	<ul style="list-style-type: none"> • Expensive • Required sophisticated equipment and skilled personnel • Limited choice of materials as bioink • Reduced printing speed • Resolution is compromised in certain types of printers 	[53, 54]

5.3 Investigating the Hallmarks of Cancer Metastasis Using Microfluidics

With a length scale comparable to that of cells and tissues, microfluidic platforms offer immense opportunities to investigate some of the—dynamic—events occurring during tumor progression, from cellular to subcellular level [58]. The narrow microchannels of the microfluidic systems can reproduce the rheological forces and shear stress experienced by cells and tissues in the circulatory system [59, 60]. A key feature of microfluidic platforms is their ability to reproduce the main events occurring in the metastatic cascade, which allows further unraveling of unknown fundamental mechanisms. For example, a critical event in the dissemination of cancer is the extravasation of CTCs. In a microfluidic assay, it has been shown that cell stiffness is a critical determinant of their retention time in the circulatory system [61]. Stiffer cells revealed a prolonged transit time in the vasculature compared to softer cells, a characteristic feature of metastatic tumor cells.

Microfluidic devices are especially well-suited for investigating how cancer cells respond to external mechanical cues, in particular during their metastatic dissemination, where migratory metastatic tumor cells usually experience higher axial strain compared to their healthy counterparts [62]. To study the effect of mechanical constraint on CTCs' migration, Irimia and Toner [63] proposed a microfluidic platform containing microchannels with dimensions comparable to the cell's size. This work revealed that cancer cells spontaneously migrate when subjected to mechanical constraint. Similarly, Mak and colleagues used a device known as *Multi-staged Serial Invasion Channels* (MUSIC) to investigate how the mechanical confinement at sub-nuclear scale could cause phenotypic changes in migratory tumor cells as well as the dynamics of their mobility [64]. Finally, the mechanical properties of a single deformed cell in suspension could be determined using optical laser-induced deformation in a microfluidic optical stretcher [65]. However, this approach failed to recapitulate the mechanical dynamics experienced by migratory—adherent—cells under physiological conditions [66].

The characteristic (bio) chemical gradients of the TME can be easily reproduced within a microfluidic chip, taking advantage of the unique properties of fluid flow (laminar) at this length scale [67]. For example, gradients can be generated by mixing (by diffusion) different concentrations of biomolecules using cascade microfluidic channels, which create star-shaped chemical gradients [68]. However, this approach requires a relatively large amount of solution to preserve the gradient, and cells can experience shear stress, affecting their mobility and viability. To overcome this, microchannels have been fabricated with relatively small diameters or filled with hydrogels that create chemical gradients by passive diffusion [69]. The hydrogel packed channels recapitulated the TME more closely. In this case, the selection of an appropriate hydrogel material determines the success of these microfluidic platforms. Table 5.2 details the different hydrogel systems that are used in microfluidic channels, along with their advantages and limitations.

Overall, the versatility in the design of microfluidic platforms and the associated advantages of operating at the microscale serve as a good toolbox for the recapitulation of the TME *in vitro*. Besides the aforementioned features, other properties of the TME can also be reproduced on-chip, including electrical fields or gradient-free locomotion, mimicking the native *electrotaxis* or *ratchetaxis* of migratory tumor cells [78–80]. This versatility of microfluidic chips may boost the discovery of unknown mechanisms involved in tumorigenesis, the reproduction of patient-specific *in vitro* models for individualized drug screening, or the early diagnosis of the pathology. In the following section, some examples of microfluidic-based platforms are described to highlight their importance for understanding the disease's etiology and improving anti-cancer drug discovery and treatments.

Table 5.2 ECM hydrogels used in microfluidic platforms (adapted from [70])

Hydrogel material	Chemical nature	Gelation mechanism	Advantageous features	Limitations	References
Fibrin	Protein-natural biomacromolecules -ECM components	Enzymatic	<ul style="list-style-type: none"> • Biocompatible • Biodegradable • Easily tunable • Ease in chemical or physical modification. For example, silk fibroin is mixed with Col I in different ratios to improve its mechanical and biological property 	<ul style="list-style-type: none"> • Poor mechanical properties • Susceptible to enzymatic degradation • Batch-to-batch variation • Fail to support long-term culture 	[70]
Collagen type I		Thermoresponsive			[70, 71]
Gelatin					[70]
Hyaluronic acid	Polysaccharide-natural biomacromolecules		<ul style="list-style-type: none"> • Biocompatible • Nonimmunogenic • Easy chemical modifications • Enzymatic degradability 	<ul style="list-style-type: none"> • Considerable variation in properties with a molecular weight • Non-adhesive 	[72]
Agarose					<ul style="list-style-type: none"> • Biocompatible • Easily tunable gelling and melting conditions • Mechanical robustness
Chitosan		pH-responsive	<ul style="list-style-type: none"> • Biocompatible • Biodegradable • Bioadhesive • Easily tunable mechanical property and structure 	<ul style="list-style-type: none"> • No control over the process of fabrication • High batch-to-batch variation • Complex processing results in difficulty in scaling up 	[70, 74]

Alginate		Ionotropic	<ul style="list-style-type: none"> • Inexpensive • Low cytotoxicity • Bioinert • Low foreign body reaction 	<ul style="list-style-type: none"> • Limited control over mechanical properties • Instability due to ion-leaching • The fall of pH during gelation reduces cell viability 	[75]
Polyacrylamide	Synthetic		<ul style="list-style-type: none"> • Structural stability • Offers constant spatiotemporal microenvironment to cells • Fine-tune hydrogel stiffness 	<ul style="list-style-type: none"> • Chemical cross-linkers used results cytotoxicity • Fine-tune the stiffness • Non-degradable • Absence of cell adhesive motifs 	[76]
Poly(ethylene glycol)			<ul style="list-style-type: none"> • Readily tunable mechanical properties • Low cytotoxicity • Reproducibility • Easy incorporation of cell adhesive motives 	<ul style="list-style-type: none"> • Absence of bioadhesive motifs • Non-biodegradable 	[77]

5.3.1 Microfluidic Cancer Cell Sorter: Liquid Biopsy

5.3.1.1 Molecular Surface Markers

As previously described, the first stage of metastasis is the detachment of cancer cells from the primary tumor before their dissemination to distant sites through the vasculature as CTCs. The presence of CTCs in the bloodstream permits the early detection of the disease and improves therapeutic success by analyzing the genetic background of the captured cells. This can provide critical information about the tumor origin and etiology, and therefore, more specific and individualized therapies can be applied, improving their efficacy. However, the detection and capture of CTCs are challenging due to their low availability (1–10 CTCs in 1 ml of blood) [67]. In this regard, microfluidics offers a considerable potential for detecting and isolating CTCs.

CTCs of epithelial origin express epithelial cell adhesion molecules (EpCAM) on their surfaces. Typical strategies employed for their capture are based on recognizing these (and other) molecules. This is indeed the approach used by the commercial CellSearch™ system developed by Veridex [81, 82], a pioneering microfluidic-based platform approved by the US Food and Drug Administration (FDA) for the detection of CTCs in different cancers, such as breast or lung. This platform uses ferrofluid containing magnetic particles coated with antibodies targeting EpCAM [83]. The sample volume needed is approximately 7.5 ml of blood, and the capturing efficacy is reported to be around 85% [82]. The CellSearch™ based isolation of CTCs is a quantitative approach, and typically, the isolated cells cannot be used for further investigations.

Other microfluidic platforms have been reported for the purification and isolation of CTCs. For example, in iCHIP, the CTCs specifically bound to EpCAM-magnetic beads were separated from platelets and non-nucleated blood cells, such as red blood cells, using inertial focusing and magnetic capture [84]. Following isolation, the CTCs could be further characterized by PCR or immunohistochemistry. As the CTCs were not physically bound to the microfluidic device, this magnetophoretic separation method outperformed the CellSearch™ platform in terms of throughput (97% capturing efficacy).

Micro- and nanostructured surfaces further improve the efficiency of CTC sorting within microfluidic chips. Different microfluidic platforms with geometrically enhanced microstructures have been developed. For example, Kirby et al. [85] developed a geometrically enhanced differential immunocapture (GEDI) chip that improved the collision frequency between the antibody-coated micro-posts (specifically, anti-prostate-specific membrane antigen—PSMA) and the target cells (prostate CTCs), resulting in CTC enrichment. Another commercially available similar platform is the Cell Enrichment and Extraction™ (CEE) microfluidic chip developed by Biocept™ [86]. Finally, it is worth mentioning that besides antibodies, surface functionalization with aptamers can closely mimic the basement membrane and further help in CTC isolation [87].

5.3.1.2 Physical Properties

Apart from surface markers, the physical characteristics of CTCs, such as size, stiffness, density, metabolism, electrical and magnetic properties, can also be exploited to sort them out using microfluidic platforms. Size-based platforms like the commercially available ISET (Rarecells™, Paris, France) and ScreenCell™ employ membranes with uniform pores (6–10 μm in diameter) for cell sorting [88], while others use laminar flow within precisely controlled microtextured microchannels [89]. For example, crescent-shaped pillars [90] or wire-shaped barriers [91] trap the CTCs from whole blood. Similarly, a trapezoidal cross-section spiral microfluidic chip reported an 80% efficacy in CTC sorting in less than 10 min with a minimal sample volume (<7.5 ml) and without affecting the viability of isolated CTCs [92].

Finally, it is worth mentioning that combining size-based microfluidic sorting systems with dielectrophoretic (DEP) technologies can result in more advanced platforms with enhanced purification performance [93]. For example, in DEP-field flow fractionation (FFF) microfluidics, the continuous-flow dielectric field-flow fraction-hydrodynamic lift is combined with sedimentation force [94]. As a result, different blood components can simultaneously be separated and collected into distinct chambers located at different heights.

5.3.1.3 Metabolic Properties

Tumor cells use glycolysis as a chief metabolic pathway, which results in acidification of the TME due to the secretion of lactate. Therefore, the metabolic status of tumor cells can also be exploited for their detection using microfluidics. Indeed, a micro-droplet emulsion microfluidic device was recently developed for the metabolic detection of CTCs [95]. Each droplet contained a pH-sensitive dye, which changed its color in response to lactate produced by the encapsulated CTCs within 20 min after encapsulation. A vital feature of this high-throughput liquid biopsy approach is that the CTC-laden droplets can be retrieved and used for further analysis.

5.3.2 Modeling Hypoxia

Oxygen concentration gradients have also been created in microfluidic channels. The typical approaches that are employed to develop such concentration gradients include [96]:

1. *Control of gas supply within the microchannels:* The microfluidic platforms in this approach have multi-layered channels. Their optimal positioning over or under the cell layer allows tight control over oxygen diffusion [97, 98]. In advanced devices, channels are created above and below the cell chamber [97]. In some cases, aqueous solutions or culture media are pre-equilibrated with oxygen to reduce the variations in oxygen concentration [98]. However, oxygen fails to equilibrate equally in all the sample volumes.

2. *Injection of oxygen scavenging chemicals:* Injecting oxygen-scavenging chemicals is a popular method for controlling the level of oxygen in microfluidic channels. The oxygen concentration gradient is created by placing oxygen-generating reaction on one side and oxygen-scavenging material on the other side of the channel [99]. Airflow is continuously injected using either a syringe pump or passive pumping techniques to maintain the oxygen gradient.
3. *Oxygen impermeable materials:* The traditional material employed for microfluidic chip fabrication, i.e., polydimethylsiloxane (PDMS), is replaced by other oxygen non-permeable materials, such as polymethylmethacrylate (PMMA) in this approach to prevent the diffusion of oxygen from the atmosphere [100]. This approach enables to conduct investigations under micro-aerobic and anaerobic conditions. Importantly, partial oxygen permeability can be incorporated into this system by blending the oxygen impermeable material with PDMS [101]. However, the fabrication of channels using the non-permeable material is time-consuming. The incorporation of these channels into ancillaries is challenging too.

5.3.3 Modeling the Tumor Microvasculature

The vasculature is a crucial component of the TME necessary to maintain the supply of nutrients and gases. It is also a vital element of the metastatic cascade to disseminate cancer cells to distant tissues and organs. Microfluidics technology can be used to engineer on-chip perfusable vascular network structures that mimic the TME microvasculature and investigate the mechanism(s) involved in these critical processes [102, 103]. Typically, two strategies are followed to generate vascular networks within a microfluidic chip: (1) self-organization of endothelial cells and (2) cell coating of micro-engineered channels. Self-organization takes advantage of the self-assembly properties of (micro-) vascular cells. For this, endothelial cells are typically cultured on 3D hydrogels (e.g., Matrigel™). The necessary nutrients and/or vasculogenic or pro-angiogenic factors are injected to promote vessels formation and maturation. Next, many methods have been reported to fabricate microchannels for endothelial cells coating. Traditional methods like molding capillaries in hydrogels using rods or needles, sacrificial templates, replica molding, 3D bioprinting, or viscous fingering instabilities have been used to create simple and more complex vascular structures [104, 105]. Alternatively, a pressurized air stream can be used to form hollow tubes of diverse diameters in partially solidified microchannels filled with non-crosslinked silicone [106, 107]. The diameter of these hollow tubes can be controlled by employing the double templating strategy [108]. In double templating, the inner open chamber is created using airflow or rod templates, while the outer layer uses plastic as a template. The resultant PDMS vasculature is optically transparent, permeable to gas, and possesses elasticity like that of native blood vessels.

Overall, microfluidic perfusable platforms provides the opportunity to investigate dynamic events of cancer metastasis, such as angiogenesis, intra/extravasation, etc., in a well-controlled environment.

5.3.4 Modeling Critical Events of Cancer Metastasis On-Chip: Tumor-on-a-Chip

A tumor-on-a-chip is a microfluidic device that reproduces the functional units of a tumor, including the cellular and non-cellular content. It is typically made of optically transparent material containing perfusable microchannels and 3D chambers bearing the living cells, including the tumor cells. These are spatiotemporally arranged like the native physiological environment [109]. The viability of the cells is continued over several days, or even weeks, by the continuous supply of nutrients through endothelium-lined or parenchymal-lined vascular channels. In addition, the endothelialized microchannels can also support the flow of whole blood for a while recapitulating more realistically the circulatory system [110].

The typical tumor-on-chip device is compartmentalized, containing a tumor (3D chamber) and endothelial (microchannels) regions interconnected by micro-posts or through porous membranes. The tumor cells are typically seeded in a 3D ECM material and can be co-cultured with stromal cells, such as fibroblasts, endothelial cells, stem cells, or immune cells, to study their cross-talk and involvement in cancer progression [45]. The hollow microchannels are typically coated with endothelial cells, such as HUVEC, to mimic the vasculature. These endothelial cells can be stimulated to sprout toward the tumor, thus mimicking physiological angiogenesis. These platforms can also exhibit air–liquid interfaces, fluid flow, and shear stresses.

The tumor-on-a-chip can be customized to study the cross-talk between cancer cells and the heterocellular TME [111]. In 2008, Walsh and colleagues developed one of the first-ever tumor-on-a-chip devices that reproduced the microenvironment gradients occurring during tumorigenesis [112]. Later, more complex designs were adapted, such as incorporating multiple parallel channels loaded with tumor spheroids, allowing us to explore the role of soluble factors in EMT without the direct contact of cells [113, 114]. Finally, the presentation of specific ligands of TME, such as CXC-chemokine ligand-12 (CXCL-12), the higher expression of which in the endothelium is linked with preferential adhesion of CTCs [115], can also be incorporated into the microfluidic device using a multi-layer approach [116].

Microfluidic platforms offer a unique performance to reproduce many of the—dynamic—phenomena occurring during cancer dissemination in a well-controlled manner. For this, microfluidics also takes advantage on the high control over fluid flow using perfusion (continuous, intermittent, or cyclic) and pneumatic micro-valves, which is a major advancement over the traditional static culture methods enables also the investigation of, e.g., paracrine loops [117]. The incorporation of perfused endothelium-lined vasculature provides better clinical relevance to investigate the delivery of therapeutics and modeling pharmacodynamics and

pharmacokinetics [118]. In addition, the establishment of chemical and physical gradients, air–liquid interfaces, and the mechanical environment (shear stresses and hydrostatic pressures) are additional advantages offered by the microfluidic platform. Finally, the effect of mechanical forces or chemical cues on cancer dissemination can be easily investigated by integrating flexible structures [119] and biosensors [120] on-chip.

5.4 Concluding Remarks and Prospects

The TME is a highly complex, dynamic, and rapidly changing microenvironment with an active role in cancer progression. The recapitulation of the main features of the TME *in vitro* is crucial for investigating the critical mechanisms of tumorigenesis and developing better drugs. In this regard, microfluidic platforms offer a more realistic recapitulation of the TME complexity. Microfluidic devices are envisioned as revolutionary platforms to improve healthcare diagnosis and precision cancer medicine. However, its success largely depends on our understanding of the TME properties and dynamics, which unwinds the interplay between tumor cells and stroma. The current research goal is to gain a more realistic mechano-biological insight of these cross-talks, which improves the performance of the microfluidic devices and leads to new therapeutic interventions. The most-reported tumor models, including the microfluidic ones, typically lack immune cells, such as macrophages and T lymphocytes. But the immune landscape of the tumor is more significant and closely regulates the behavior of stromal cells. These hurdles need to be overcome to mimic the TME. Next, cellular heterogeneity is also a hallmark of the TME. To recapitulate it, *in vitro* co-culture models need to be established involving different media cocktails. The composition of these media cocktails and the optimum ratios of other cells are also critical in faithfully recapitulating cancer progression in microfluidic platforms. Finally, a key challenge of most pre-clinical models is their predictability. Typically, cell lines are employed to investigate a large plethora of cancer-related events and drug screening, despite the limited relevancy of the obtained data. In this regard, the use of patient-derived cells on-chip is considered a significant milestone. To do this, the isolation, manipulation, and culturing conditions of these cells need to be well defined to ensure the reproducibility of the investigations.

Acknowledgements The work was supported by the European Union Framework Programme for Research and Innovation Horizon 2020 under grant agreement no. 668983—FoReCaST and the Portuguese Foundation for Science and Technology (FCT) under the BREAST-IT project (PTDC/BTM-ORG/28168/2017) to SCK, 2MATCH project (PTDC/BTM-ORG/28070/2017) to D.C., C. M.A., and S.C.K, and OncoNeoTreat (PTDC/CTM-REF/0022/2020) to C.M.A. D.C. also thanks the financial support from FCT for the CEEC Individual 2017 (CEECIND/00352/2017).

References

1. Carter EP, Roozitalab R, Gibson SV, Grose RP (2021) Tumour microenvironment 3D-modelling: simplicity to complexity and back again. *Trends Cancer* 7(11):1033–1046
2. Hinshaw DC, Shevde LA (2019) The tumor microenvironment innately modulates cancer progression. *Cancer Res* 79(18):4557–4566
3. Truffi M, Sorrentino L, Corsi F (2020) Fibroblasts in the tumor microenvironment. *Adv Exp Med Biol* 1234:15–29
4. Balkwill FR, Capasso M, Thorsten Hagemann T (2012) The tumor microenvironment at a glance. *J Cell Sci* 125:5591–5596
5. Baghban R, Roshangar L, Jahanban-Esfahlan R, Seidi K, Ebrahimi-Kalan A, Jaymand M, Kolahian S, Javaheri T, Zare P (2020) Tumor microenvironment complexity and therapeutic implications at a glance. *Cell Commun Signal* 18:59
6. Aras S, Zaidi MR (2017) TAMEless traitors: macrophages in cancer progression and metastasis. *Br J Cancer* 117:1583–1591
7. Murphy K, Weaver C (2017) *Janeway's immunobiology*, 9th edn. Garland Science, New York
8. Shapouri-Moghaddam A, Mohammadian S, Vazini H, Taghadosi M, Esmaeili SA, Mardani F, Seifi B, Mohammadi A, Afsharu JT, Sahebkar A (2018) Macrophage plasticity, polarization, and function in health and disease. *J Cell Physiol* 233:6425–6440
9. Chen F, Chen J, Yang L, Liu J, Zhang X, Zhang Y, Tu Q, Yin D, Lin D, Wong PP, Huang D, Xing Y, Zhao J, Li M, Liu Q, Su F, Su S, Song E (2019) Extracellular vesicle-packaged HIF-1 α -stabilizing lncRNA from tumour-associated macrophages regulates aerobic glycolysis of breast cancer cells. *Nat Cell Biol* 21:498–510
10. Mills CD (2015) Anatomy of a discovery: M1 and M2 macrophages. *Front Immunol* 6:212
11. Kawai O, Ishii G, Kubota K, Murata Y, Naito Y, Mizuno T, Aokaje K, Saijo N, Nishiwaki Y, Gemma A, Kudoh S, Ochiai A (2008) Predominant infiltration of macrophages and CD8(+) T cells in cancer nests is a significant predictor of survival in stage IV nonsmall cell lung cancer. *Cancer* 113:1387–1395
12. Fridlender ZG, Sun J, Kim S, Kapoor V, Cheng G, Ling L, Worthen GS, Albelda SM (2009) Polarization of tumor-associated neutrophil phenotype by TGF-beta: 'N1' versus 'N2' TAN. *Cancer Cell* 16:183–194
13. Carretero R, Sektioglu IM, Garbi N, Salgado OC, Beckhove P, Hämmerling GJ (2015) Eosinophils orchestrate cancer rejection by normalizing tumor vessels and enhancing infiltration of CD8(+) T cells. *Nat Immunol* 16:609–617
14. Matsushita H, Hosoi A, Ueha S, Abe J, Fujieda N, Tomura M, Maekawa R, Matsushima K, Ohara O, Kakimi K (2015) Cytotoxic T lymphocytes block tumor growth both by lytic activity and IFN γ -dependent cell-cycle arrest. *Cancer Immunol Res* 3:26–36
15. Fridman WH, Page's F, Saute's-Fridman C, Galon J (2012) The immune contexture in human tumours: impact on clinical outcome. *Nat Rev Cancer* 12:298–306
16. Campbell DJ, Koch MA (2011) Treg cells: patrolling a dangerous neighborhood. *Nat Med* 17: 929–930
17. Ferrara N (2002) VEGF and the quest for tumour angiogenesis factors. *Nat Rev Cancer* 2:795–803
18. Maishi N, Hida K (2017) Tumor endothelial cells accelerate tumor metastasis. *Cancer Sci* 108: 1921–1926
19. Ridge SM, Sullivan FJ, Glynn SA (2017) Mesenchymal stem cells: key players in cancer progression. *Mol Cancer* 16:31
20. Nurmik M, Ullmann P, Rodriguez F, Haan S, Letellier E (2019) In search of definitions: cancer-associated fibroblasts and their markers. *Int J Cancer* 146:895–905
21. Sahai E, Astsaturov I, Cukierman E, DeNardo DG, Egeblad M, Evans RM, Fearon D, Greten FR, Hingorani SR, Hunter T, Hynes RO, Jain RK, Janowitz T, Jorgensen C, Kimmelman AC, Kolonin MG, Maki RG, Powers RS, Puré E, Ramirez DC, Scherz-Shouval R, Sherman MH, Stewart S, Tlsty TD, Tuveson DA, Watt FM, Weaver V, Weeraratna AT, Werb Z (2020) A

- framework for advancing our understanding of cancer-associated fibroblasts. *Nat Rev Cancer* 20:174–186
22. Orimo A, Weinberg RA (2006) Stromal fibroblasts in cancer: a novel tumor-promoting cell type. *Cell Cycle* 5:1597–1601
 23. Lau EYT, Lo J, Cheng BYL, Ma MKF, Lee JMF, Ng JKY, Chai S, Lin CH, Tsang SY, Ma S, Ng IOL, Lee TKW (2016) Cancer-associated fibroblasts regulate tumor-initiating cell plasticity in hepato-cellular carcinoma through c-Met/FRA1/HEY1 signaling. *Cell Rep* 15:1175–1189
 24. Su S, Chen J, Yao H, Liu J, Yu S, Lao L, Wang M, Luo M, Xing Y, Chen F, Huang D, Zhao J, Yang L, Liao D, Su F, Li M, Liu Q, Song E (2018) CD10+GPR77+ cancer-associated fibroblasts promote cancer formation and chemoresistance by sustaining cancer stemness. *Cell* 172:841–856
 25. Barbazán J, Vignjevic DM (2019) Cancer associated fibroblasts: is the force the path to the dark side? *Curr Opin Cell Biol* 56:71–79
 26. Barkovskaya A, Buffone A, Židek M, Weaver VM (2020) Proteoglycans as mediators of cancer tissue mechanics. *Front Cell Dev Biol* 8(569377):1–21
 27. Kresse H, Schönherr E (2001) Proteoglycans of the extracellular matrix and growth control. *J Cell Physiol* 189:266–274
 28. Anderson NM, Simon MC (2020) The tumor microenvironment. *Curr Biol* 30:R921–R925
 29. Weigelt B, Bissell MJ (2008) Unraveling the microenvironmental influences on the normal mammary gland and breast cancer. *Semin Cancer Biol* 18:311–321
 30. Winkler J, Abisoye-Ogunniyan A, Metcalf KJ, Werb Z (2020) Concepts of extracellular matrix remodelling in tumour progression and metastasis. *Nat Commun* 11:5120
 31. Kai FB, Drain AP, Weaver VM (2019) The extracellular matrix modulates the metastatic journey. *Dev Cell* 49:332–346
 32. DeClerck YA (2012) Desmoplasia: a response or a niche? *Cancer Discov* 2(9):772–774
 33. Kundu B, Reis RL, Kundu SC (2020) Metastasis in 3D biomaterials. In: Kundu SC, Reis RL (eds) *Biomaterials for 3D tumor modelling*. Elsevier, London, pp 191–210
 34. Haeger A, Krause M, Wolf K, Friedl P (2014) Cell jamming: collective invasion of mesenchymal tumor cells imposed by tissue confinement. *Biochim Biophys Acta* 1840:2386–2395
 35. Quintero-Fabián S, Arreola R, Becerril-Villanueva E, Torres-Romero J, Arana-Argáez V, Lara-Riegos J, Ramírez-Camacho MA, Alvarez-Sánchez ME (2019) Role of matrix metalloproteinases in angiogenesis and cancer. *Front Oncol* 9:1370
 36. Payne SL, Levin M, Oudin MJ (2019) Bioelectric control of metastasis in solid tumors. *Bioelectricity* 1:114–130
 37. Shang M, Soon RH, Lim CT, Khoo BL, Han J (2019) Microfluidic modelling of the tumor microenvironment for anti-cancer drug development. *Lab Chip* 19:369–386
 38. Semenza GL (2011) Regulation of metabolism by hypoxia-inducible factor 1. *Cold Spring Harb Symp Quant Biol* 76:347–353
 39. Azab AK, Hu J, Quang P, Azab F, Pitsillides C, Awwad R, Thompson B, Maiso P, Sun JD, Hart CP, Roccaro AM, Sacco A, Ngo HT, Lin CP, Kung AL, Carrasco RD, Vanderkerken K, Ghobrial IM (2012) Hypoxia promotes dissemination of multiple myeloma through acquisition of epithelial to mesenchymal transition-like features. *Blood* 119:5782–5794
 40. Lin C, McGough R, Aswad B, Block JA, Terek R (2004) Hypoxia induces HIF-1 α and VEGF expression in chondrosarcoma cells and chondrocytes. *J Orthop Res* 22:1175–1181
 41. Martin JD, Seano G, Jain RK (2019) Normalizing function of tumor vessels: progress, opportunities, and challenges. *Annu Rev Physiol* 81:505–534
 42. Farnsworth RH, Lackmann M, Achen MG, Stacker SA (2014) Vascular remodeling in cancer. *Oncogene* 33:3496–3505
 43. Murdoch C, Giannoudis A, Lewis CE (2004) Mechanisms regulating the recruitment of macrophages into hypoxic areas of tumors and other ischemic tissues. *Blood* 104:2224–2234
 44. Brancato V, Oliveira JM, Correlo VM, Reis RL, Kundu SC (2020) *Biomaterials* 232:119744

45. Sung KE, Yang N, Pehlke C, Keely PJ, Eliceiri KW, Friedl A, Beebe DJ (2011) Transition to invasion in breast cancer: a microfluidic in vitro model enables examination of spatial and temporal effects. *Integr Biol* 3:439–450
46. Gupta N, Liu JR, Patel B, Solomon DE, Vaidya B, Gupta V (2016) Microfluidics-based 3D cell culture models: utility in novel drug discovery and delivery research. *Bioeng Transl Med* 1:63–81
47. Fontana F, Marzagalli M, Sommariva M, Gagliano N, Limonta P (2021) In vitro 3D cultures to model the tumor microenvironment. *Cancer* 13:2970
48. Kundu B, Reis RL, Kundu SC (2021) Polysaccharides in cancer therapy. In: Oliveira JM, Radhouani H, Reis RL (eds) *Polysaccharides of microbial origin: biomedical applications*. Springer, Cham
49. Gaspar DA, Gomide V, Monteiro FJ (2012) The role of perfusion bioreactors in bone tissue engineering. *Biomatter* 2:167–175
50. Barrila J, Radtke AL, Crabbe A, Sarker SF, Herbst-Kralovetz MM, Ott CM, Nickerson CA (2010) Organotypic 3D cell culture models: using the rotating wall vessel to study host-pathogen interactions. *Nat Rev Microbiol* 8:791–801
51. Lin RZ, Chang HY (2008) Recent advances in three-dimensional multicellular spheroid culture for biomedical research. *Biotechnol J* 3:1172–1184
52. Kundu B, Bastos ARF, Brancato V, Cerqueira MT, Oliveira JM, Correlo VM, Reis RL, Kundu SC (2019) Mechanical property of hydrogels and the presence of adipose stem cells in tumor stroma affect spheroid formation in the 3D osteosarcoma model. *ACS Appl Mater Interfaces* 11:14548–14559
53. Augustine R, Kalva SN, Ahmad R, Zahid AA, Hasan S, Nayeem A, McClements L, Hasan A (2021) 3D bioprinted cancer models: revolutionizing personalized cancer therapy. *Transl Oncol* 14:101015
54. Kapałczyńska M, Kolenda T, Przybyła W, Zajaczkowska M, Teresiak A, Filas V, Ibbs M, Bliźniak R, Łuczewski L, Lamperska K (2016) 2D and 3D cell cultures—a comparison of different types of cancer cell cultures. *Arch Med Sci* 12:910–919
55. Sleeboom JFF, Amirabadi HE, Nair P, Sahlgren CM, den Toonder JMJ (2018) Metastasis in context: modeling the tumor microenvironment with cancer-on-a-chip approaches. *Dis Model Mech* 11:dmm033100
56. Kim Y, Williams KC, Gavin CT, Jardine E, Chambers AF, Leong HS (2016) Quantification of cancer cell extravasation in vivo. *Nat Protoc* 11:937–948
57. Mondadori C, Crippa M, Moretti M, Candrian C, Lopa S, Chiara Arrigoni C (2020) Advanced microfluidic models of cancer and immune cell extravasation: a systematic review of the literature. *Front Bioeng Biotechnol* 8:907
58. Chaudhuri PK, Warkiani ME, Jing T, Kenryd LCT (2016) Microfluidics for research and applications in oncology. *Analyst* 141:504–524
59. Byun S, Son S, Amodei D, Cermak N, Shaw J, Kang JH, Hecht VC, Winslow MM, Jacks T, Mallick P, Manalis SR (2013) Characterizing deformability and surface friction of cancer cells. *Proc Natl Acad Sci U S A* 110:7580–7585
60. Lim M, Park J, Kim T-H, Cho Y-K (2016) Analysis of circulating tumor cells from lung cancer patients. The Korean BioChip Society, Seoul
61. Adamo A, Sharei A, Adamo L, Lee B, Mao S, Jensen KF (2012) Microfluidics-based assessment of cell deformability. *Anal Chem* 84:6438–6443
62. Lincoln B, Schinking S, Travis K, Wottawah F, Ebert S, Sauer F, Guck J (2007) Reconfigurable microfluidic integration of a dual-beam laser trap with biomedical applications. *Biomed Microdevices* 9:703–710
63. Irimia D, Toner M (2009) Spontaneous migration of cancer cells under conditions of mechanical confinement. *Integr Biol* 1:506–512
64. Mak M, Reinhart-King CA, Erickson D (2013) Elucidating mechanical transition effects of invading cancer cells with a subnucleus-scaled microfluidic serial dimensional modulation device. *Lab Chip* 13:340–348

65. Guck J, Schinkinger S, Lincoln B, Wottawah F, Ebert S, Romeyke M, Lenz D, Erickson HM, Ananthakrishnan R, Mitchell D, Kas J, Ulvick S, Bilby C (2005) Optical deformability as an inherent cell marker for testing malignant transformation and metastatic competence. *Biophys J* 88:3689–3698
66. Suresh S (2007) Biomechanics and biophysics of cancer cells. *Acta Mater* 55:3989–4014
67. Caballero D, Luque-González MA, Reis RL, Kundu SC (2020) Chapter 15—microfluidic systems in cancer research. In: Kundu SC, Reis RL (eds) *Materials today, biomaterials for 3D tumor modeling*, pp 331–377
68. Li Jeon N, Baskaran H, Dertinger SK, Whitesides GM, Van de Water L, Toner M (2002) Neutrophil chemotaxis in linear and complex gradients of interleukin-8 formed in a microfabricated device. *Nat Biotechnol* 20:826–830
69. Zhang Y, Zhang W, Qin L (2014) Mesenchymal-mode migration assay and Antimetastatic drug screening via high throughput microfluidics channel networks. *Angew Chem Int Ed* 53: 2344–2348
70. Akther F, Little P, Li Z, Nguyen N-T, Ta HT (2020) Hydrogels as artificial matrices for cell seeding in microfluidic devices. *RSC Adv* 10:43682–43703
71. Buitrago JO, Patel KD, El-Fiqi A, Lee JH, Kundu B, Lee HH, Kim HW (2018) Silk fibroin/collagen protein hybrid cell-encapsulating hydrogels with tunable gelation and improved physical and biological properties. *Acta Biomater* 69:218–233
72. Amorim S, da Costa DS, Pashkuleva I, Reis CA, Reis RL, Pires RA (2020) Hyaluronic acid of low molecular weight triggers the invasive “Hummingbird” phenotype on gastric cancer cells. *Adv Biosyst* 4:e2000122
73. Li Y, Yan X, Feng X, Wang J, Du W, Wang Y, Chen P, Xiong L, Liu B-F (2014) Agarose-based microfluidic device for point-of-care concentration and detection of pathogen. *Anal Chem* 86:10653–10659
74. Gao Y, Ma Q, Cao J, Wang Y, Yang X, Xu Q, Liang Q, Suna Y (2021) Recent advances in microfluidic-aided chitosan-based multifunctional materials for biomedical applications. *Int J Pharm* 600:120465
75. Sahoo DR, Biswal T (2021) Alginate and its application to tissue engineering. *SN Appl Sci* 3: 30
76. Nghe P, Boulineau S, Gude S, Recouvreux P, van Zon JS, Tans SJ (2013) Microfabricated polyacrylamide devices for the controlled culture of growing cells and developing organisms. *PLoS One* 8:e75537
77. Liu Z, Xiao L, Xu B, Zhang Y, Mak AFT, Li Y, Man W-y, Yang M (2012) Covalently immobilized biomolecule gradient on hydrogel surface using a gradient generating microfluidic device for a quantitative mesenchymal stem cell study. *Biomicrofluidics* 6: 024111–024112
78. Caballero D, Kundu SC, Reis RL (2020) The biophysics of cell migration: biasing cell motion with Feynman ratchets. *Biophysicist* 1(2):1–19
79. Huang CW, Cheng JY, Yen MH, Young TH (2009) Electrotaxis of lung cancer cells in a multiple-electric-field chip. *Biosens Bioelectron* 24:3510–3516
80. Mahmud G, Campbell CJ, Bishop KJM, Komarova YA, Chaga O, Soh S, Huda S, Kandere-Grzybowska K, Grzybowski BA (2009) Directing cell motions on micropatterned ratchets. *Nat Phys* 5:606–612
81. Allard WJ, Matera J, Miller MC, Repollet M, Connelly MC, Rao C, Tibbe AGJ, Uhr JW, Terstappen LWMM (2004) Tumor cells circulate in the peripheral blood of all major carcinomas but not in healthy subjects or patients with nonmalignant diseases. *Clin Cancer Res* 10:6897–6904
82. Mathur L, Ballinger M, Utharala R, Merten CA (2020) Microfluidics as an enabling technology for personalized cancer therapy. *Small* 16:1904321
83. Tandon AK, Clark GM, Chamness GC, Mcguire WL (1990) Association of the 323/A3 surface glycoprotein with tumor characteristics and behavior in human breast cancer. *Cancer Res* 50:3317–3321

84. Ozkumur E, Shah AM, Ciciliano JC, Emmink BL, Miyamoto DT, Brachtel E, Yu M, Chen PI, Morgan B, Trautwein J, Kimura A, Sengupta S, Stott SL, Karabacak NM, Barber TA, Walsh JR, Smith K, Spuhler PS, Sullivan JP, Lee RJ, Ting DT, Luo X, Shaw AT, Bardia A, Sequist LV, Louis DN, Maheswaran S, Kapur R, Haber DA, Toner M (2013) Inertial focusing for tumor antigen-dependent and -independent sorting of rare circulating tumor cells. *Sci Transl Med* 5:179ra47
85. Kirby BJ, Jodari M, Loftus MS, Gakhar G, Pratt ED, Chanel-Vos C, Gleghorn JP, Santana SM, Liu H, Smith JP, Navarro VN, Tagawa ST, Bander NH, Nanus DM, Giannakakou P (2012) Functional characterization of circulating tumor cells with a prostate-cancer-specific microfluidic device. *PLoS One* 7:e35976
86. Nora Dickson M, Tsinberg P, Tang Z, Bischoff FZ, Wilson T, Leonard EF (2011) Efficient capture of circulating tumor cells with a novel immunocytochemical microfluidic device. *Biomicrofluidics* 5:34119–3411915
87. Wan Y, Mahmood M, Li N, Allen PB, Kim YT, Bachoo R, Ellington AD, Iqbal SM (2012) Nano-textured substrates with immobilized aptamers for cancer cell isolation and cytology. *Cancer* 118:1145–1154
88. Warkiani ME, Bhagat AAS, Khoo BL, Han J, Lim CT, Gong HQ, Fane AG (2013) Isoporous micro/nanoengineered membranes. *ACS Nano* 7:1882–1904
89. Bhagat A, Bow H, Hou H, Tan S, Han J, Lim C (2010) Microfluidics for cell separation. *Med Biol Eng Comput* 48:999–1014
90. Tan SJ, Yobas L, Lee GYH, Ong CN, Lim CT (2009) Microdevice for the isolation and enumeration of cancer cells from blood. *Biomed Microdevices* 11:883–892
91. Chung J, Shao H, Reiner T, Issadore D, Weissleder R, Lee H (2012) Microfluidic cell sorter (μ FCS) for on-chip capture and analysis of single cells. *Adv Healthc Mater* 1:432–436
92. Warkiani ME, Guan G, Luan KB, Lee WC, Bhagat AA, Chaudhuri PK, Tan DS, Lim WT, Lee SC, Chen PC, Lim CT, Han J (2014) Slanted spiral microfluidics for the ultra-fast, label-free isolation of circulating tumor cells. *Lab Chip* 14:128–137
93. Moon HS, Kwon K, Kim SI, Han H, Sohn J, Lee S, Jung HI (2011) Continuous separation of breast cancer cells from blood samples using multi-orifice flow fractionation (MOFF) and dielectrophoresis (DEP). *Lab Chip* 11:1118–1125
94. Shim S, Stemke-Hale K, Tsimberidou AM, Noshari J, Anderson TE, Gascoyne PR (2013) Antibody-independent isolation of circulating tumor cells by continuous-flow dielectrophoresis. *Biomicrofluidics* 7:011807
95. Schutz SS, Beneyton T, Baret JC, Schneider TM (2019) Rational design of a high-throughput droplet sorter. *Lab Chip* 19:2220–2232
96. Byrne MB, Leslie MT, Rex Gaskins H, Kenis PJA (2014) Methods to study the tumor microenvironment under controlled oxygen conditions. *Trends Biotechnol* 32:556–563
97. Oppgard SC, Eddington DT (2013) A microfabricated platform for establishing oxygen gradients in 3-D constructs. *Biomed Microdevices* 15:407–414
98. Thomas PC, Raghavan SR, Forry SP (2011) Regulating oxygen levels in a microfluidic device. *Anal Chem* 83:8821–8824
99. Chen YA, King AD, Shih HC, Peng CC, Wu CY, Liao WH, Tung YC (2011) Generation of oxygen gradients in microfluidic devices for cell culture using spatially confined chemical reactions. *Lab Chip* 11:3626–3633
100. Abaci HE, Devendra R, Smith Q, Gerecht S, Drazer G (2012) Design and development of microbioreactors for long-term cell culture in controlled oxygen microenvironments. *Biomed Microdevices* 14:145–152
101. Funamoto K, Zervantonakis IK, Liu Y, Ochs CJ, Kim C, Kamm RD (2012) A novel microfluidic platform for high resolution imaging of a three-dimensional cell culture under a controlled hypoxic environment. *Lab Chip* 12:4855–4863
102. Hasan A, Paul A, Vrana NE, Zhao X, Memic A, Hwang YS, Dokmeci MR, Khademhosseini A (2014) Microfluidic techniques for development of 3D vascularized tissue. *Biomaterials* 35:7308–7325

103. Luque-González MA, Reis RL, Kundu SC, Caballero D (2020) Human microcirculation-on-chip models in cancer research: key integration of lymphatic and blood vasculatures. *Adv Biosys* 4(7):2000045
104. Caballero D, Blackburn SM, de Pablo M, Samitier J, Albertazzi L (2017) Tumour-vessel-on-a-chip models for drug delivery. *Lab Chip* 17:3760–3771
105. Tsai H-F, Trubelja A, Shen AQ, Bao G (2017) Tumour-on-a-chip: microfluidic models of tumour morphology, growth and microenvironment. *J R Soc Interface* 14:20170137
106. Abdelgawad M, Wu C, Chien WY, Geddie WR, Jewett MA, Sun Y (2011) A fast and simple method to fabricate circular microchannels in polydimethylsiloxane (PDMS). *Lab Chip* 11: 545–551
107. Wang X, Sun Q, Pei J (2018) Microfluidic-based 3D engineered microvascular networks and their applications in vascularized microtumor models. *Micromachines (Basel)* 9:493
108. Zhang W, Zhang YS, Bakht SM, Aleman J, Shin SR, Yue K, Sica M, Ribas J, Duchamp M, Ju J, Sadeghian RB, Kim D, Dokmeci MR, Atala A, Khademhosseini A (2016) Elastomeric free-form blood vessels for interconnecting organs on chip Systems. *Lab Chip* 16:1579–1586
109. Bhatia SN, Ingber DE (2014) Microfluidic organs-on-chips. *Nat Biotechnol* 32:760–772
110. Jain A, Barrile R, van der Meer AD, Mammoto A, Mammoto T, De Ceunynck K, Aisiku O, Otieno MA, Loudon CS, Hamilton GA, Flaumenhaft R, Ingber DE (2018) Primary human lung alveolus-on-a-chip model of intravascular thrombosis for assessment of therapeutics. *Clin Pharmacol Ther* 103:332–340
111. Montanez-Sauri SI, Sung KE, Berthier E, Beebe DJ (2013) Enabling screening in 3D microenvironments: probing matrix and stromal effects on the morphology and proliferation of T47D breast carcinoma cells. *Integr Biol* 5:631–640
112. Walsh CL, Babin BM, Kasinskas RW, Foster JA, McGarry MJ, Forbes NS (2009) A multipurpose microfluidic device designed to mimic microenvironment gradients and develop targeted cancer therapeutics. *Lab Chip* 9:545–554
113. Jeong SY, Lee JH, Shin Y, Chung S, Kuh HJ (2016) Co-culture of tumor spheroids and fibroblasts in a collagen matrix-incorporated microfluidic chip mimics reciprocal activation in solid tumor microenvironment. *PLoS One* 11:e0159013
114. Lee JH, Kim SK, Ali Khawar I, Jeong SY, Chung S, Kuh HJ (2018) Microfluidic co-culture of pancreatic tumor spheroids with stellate cells as a novel 3D model for investigation of stroma-mediated cell motility and drug resistance. *J Exp Clin Cancer Res* 37:4
115. Sontheimer-Phelps A, Hassell BA, Ingber DE (2019) Modelling cancer in microfluidic human organs-on-chips. *Nat Rev Cancer* 19:65–81
116. Song JW, Cavnar SP, Walker AC, Luker KE, Gupta M, Tung YC, Luker GD, Takayama S (2009) Microfluidic endothelium for studying the intravascular adhesion of metastatic breast cancer cells. *PLoS One* 4:e5756
117. Hsu TH, Xiao JL, Tsao TW, Kao YL, Huang SH, Liao WY, Chau-Hwang Lee CH (2011) Analysis of the paracrine loop between cancer cells and fibroblasts using a microfluidic chip. *Lab Chip* 11:1808–1814
118. Prantil-Baun R, Novak R, Das D, Somayaji MR, Przekwas A, Ingber DE (2018) Physiologically based pharmacokinetic and pharmacodynamic analysis enabled by microfluidically linked organs-on-chips. *Annu Rev Pharmacol Toxicol* 58:37–64
119. Ao M, Brewer BM, Yang L, Coronel OEF, Hayward SW, Webb DJ, Li D (2015) Stretching fibroblasts remodels fibronectin and alters cancer cell migration. *Sci Rep* 5:8334
120. Rebelo R, Barbosa AI, Caballero D, Kwon IK, Oliveira JM, Kundu SC, Reis RL, Correlo VM (2019) 3D biosensors in advanced medical diagnostics of high mortality diseases. *Biosens Bioelectron* 130:20–39



Biomaterials for Mimicking and Modelling Tumor Microenvironment

6

Rupambika Das and Javier G. Fernandez

Abstract

This chapter summarizes the current biomaterials and associated technologies used to mimic and characterize the tumor microenvironment (TME) for developing preclinical therapeutics. Research in conventional 2D cancer models systematically fails to provide physiological significance due to their discrepancy with diseased tissue's native complexity and dynamic nature. The recent developments in biomaterials and microfabrication have enabled the popularization of 3D models, displacing the traditional use of Petri dishes and microscope slides to bioprinters or microfluidic devices. These technologies allow us to gather large amounts of time-dependent information on tissue–tissue, tissue–cell, and cell–cell interactions, fluid flows, and biomechanical cues at the cellular level that were inaccessible by traditional methods. In addition, the wave of new tools producing unprecedented amounts of data is also triggering a new revolution in the development and use of new tools for analysis, interpretation, and prediction, fueled by the concurrent development of artificial intelligence. Together, all these advances are crystalizing a new era for biomedical engineering characterized by high-throughput experiments and high-quality data.

Furthermore, this new detailed understanding of disease and its multifaceted characteristics is enabling the long searched transition to personalized medicine.

R. Das

The Francis Crick Institute, London, UK

e-mail: rupambika.das@crick.ac.uk

J. G. Fernandez (✉)

Singapore University of Technology and Design, Singapore, Singapore

e-mail: javier.fernandez@sutd.edu.sg

© The Author(s), under exclusive license to Springer Nature Switzerland AG 2022

139

D. Caballero et al. (eds.), *Microfluidics and Biosensors in Cancer Research*,

Advances in Experimental Medicine and Biology 1379,

https://doi.org/10.1007/978-3-031-04039-9_6

Here we outline the various biomaterials used to mimic the extracellular matrix (ECM) and redesign the tumor microenvironment, providing a comprehensive overview of cancer research's state of the art and future.

Keywords

Tumor micro environment (TME) · Biomaterials · Microfluidics · Extra cellular matrix (ECM) · 3D models · Cancer

6.1 Introduction

The disease cancer was named after the word crab by the father of medicine, Hippocrates, is caused by consecutive mutations in the DNA sequence initiating from a single abnormal cell. The progressive gene instability with a few rounds of selective mutation leads to the formation of a tumor mass [1]. After several cycles of cell division, the expanded mass of neoplastic cells breaks open the basal membrane to invade locally by metastasizing and eventually causing fatality. The nature of the tumor and its progression depend on external and internal environmental factors. The contributing factors occur in parallel or sequence, leading to a massively growing lump of cells showing abnormal and uncontrolled clonal expansion [2]. Other important aspects like cell adhesion, secretion of proteolytic enzymes, tumor angiogenic factors, etc., are increasingly studied to understand the nature of tumor progression and its ability to escape the immune system and resist drug therapies [3]. The most common therapies to treat cancer consists of chemo and radiotherapy along with checkpoint inhibitor drugs. The drugs have shown efficacy but with many side effects on healthy cells, highlighting the central role of biomaterial research in providing better models for more targeted and personalized therapies [4, 5].

In this context, materials with tunable properties matching tissue stiffness give us a fair chance to study cancer cell development, progression, and infiltration properties in real-time outside the “noisy” in vivo environment. Here we cover the biomimetic use of biomaterials to reproduce the tumor microenvironment for the study of tumoral development and immunotherapy.

6.2 Cancer Pathology and Progression

Despite the vast number of open questions related to cancer, its conceptualization as a genetic disorder and a somatic mutation was established more than a century ago [6]. Due to the shift in the chromosomal stability, the transition from normal to malignant tumor is witnessed. Nonetheless, be it malignant or benign still ends up killing their host. Therefore, understanding the mechanisms behind the disease development and progression is central to developing new therapies. In particular, the prevention of tumor dissemination from the origin to distant sites, which might

occur before diagnosis, is necessary to enable targeted treatments [7, 8]. The tumoral extravasation to distant sites starts with an epithelial to mesenchymal transition, followed by the invasion into the new site by degrading the basal lamina of the ECM. In the new site, the cells are characterized by their reliance, enabling them to survive long enough to promote angiogenesis and start expanding. After the process is complete, the new tumor will continue developing while evading the immune system [9].

In the following section, we describe the complexity of the tumoral niche and the complex relations with the microenvironment enabling cancer persistence.

6.2.1 Cancer Complexity and Dynamics

The robustness of tumors results from complex functionalities and synergetic mechanisms, enabling cells to continue proliferating against checkpoints and anti-cancer therapies. This robustness is theorized to be connected to an outstanding feedback control system that allows rapid adaptation and functional redundancy to replace compromised functionalities.

6.2.1.1 Functional Redundancy

Cellular redundancy plays an essential role in maintaining cancer cells' robustness, a strategy used in cellular biology at many levels [10]. For example, it has been seen that the transcription factor E2F1-3 is involved in many functions like DNA replication, mitosis, DNA repair, differentiation, etc., and also restricts the mammalian cells from entering the S-phase [11]. Additionally, Cdk2 compensates for Cdk-4, -6, and -1 due to their redundancy in governing the cell cycle [12]. In the case of cancer cells, numerous overlapping changes in their genes ensure their survival and resistance to drugs through the escape of cell cycle checkpoints, uncontrolled growth, dodging apoptosis, etc. These mechanisms effectively enable, among others, high drug efflux, decreased drug uptake, and very efficient DNA repair. This sophisticated, rapid, and mostly unknown response to external factors makes the treatment of advanced cancer largely ineffective [13]. The concept of biological redundancy is always neglected while drug designing procedure which thereby leads to the development of multidrug-resistant cells due to the dysfunctional cell cycle mechanism [14]. This translates into an acquired cancer cell resistance, even before their exposition to a new treatment.

6.2.1.2 Feedback Control System

The feedback loop mechanism and associated genes synchronously preserve the redundancy and robustness of the neoplastic cells [15]. When the feedback control is triggered, a cascade of reactions occurs to ensure the survival of cells. A paradigmatic example of this system is the lowering of cytotoxin levels in the tumor cells, maintained by the upregulation of the multidrug-resistance 1 gene (MDR1) through a positive feedback mechanism. In this state, cells export drugs out of the cytoplasm through an ATP-dependent efflux pump [16]. Similarly, the

overexpression of the MDM2 gene due to internal changes causes degradation of the p53 gene, thereby blocking apoptosis of the cancer cell. MDM2-p53 interaction is generally enhanced once the DNA is seriously damaged, and the feedback control loop mechanism contributes to the robustness [17]. The feedback loops maintain the cell cycle against cellular perturbations, enabling the continuous proliferation of the neoplastic cells after therapy.

Along with the intracellular feedback loops, tumor cells also initiate these feedback mechanisms in response to the environmental cues. When the tumor cells harmonize with the extracellular matrix and the immune cells, they adapt to the innate tumor-suppression mechanism and cope with its environment. In instances of stress, such as nutrient deprivation or low oxygen concentration, tumor cells acclimatize to the change by either taking advantage of the swapped condition or migrating to a distant location, thereby starting the process of metastasis [18].

6.2.2 Tumor Microenvironment

The tumor microenvironment (TME) is one of the regulatory factors for tumor formation and progression. Therefore, monitoring the surrounding microenvironment, along with the genetic factors, is required to understand the dynamics of the neoplastic cells. The TME comprises the tumor cells, fibroblasts, endothelial cells, adipose tissue, specific immune cells, and proteins making up the extracellular matrix (ECM) [19]. The cancer cells use healthy cells to their advantage, signaling cross-talk mechanism to initiate and maintain tumorigenesis, metastasize and develop an effective resistance against therapeutic drugs [20].

6.2.2.1 Cancer-Associated Fibroblasts

Cancer-associated fibroblasts (CAFs) are healthy (i.e., non-cancerous) cells that are generally activated and rapidly multiply in wounds. However, in the case of a tumor, they are perpetually activated as a mechanism for the tumor to grow [21].

The activation is maintained by the plethora of secreted growth factors and chemokines, playing a crucial role in cancer progression and ECM remodelling. For example, CAFs have overexpression of Galectin-1 protein, which leads to a poor prognosis of the disease [22]. Additionally, it was seen that MMP-2 was a major remnant from the CAF-CM (conditioned media) derived from oral squamous cancer cell culture and thereby, leading to keratinocyte dis-cohesion and invasion into the epithelium when studied in collagen gel [23].

6.2.2.2 Immune and Inflammatory Cell

Immune cells are programmed to survey and defend bodily functions, eliminating invading foreign pathogens. During a typical (i.e., non-cancerous) illness, the immune cells do not persist at the site of inflammation, avoiding the creation of downstream pathologies. However, the immune-inflammatory cells linger in the inflammation site in abnormal cases, leading to neoplasia and angiogenesis, signaling the initial cancer stage [24]. After that, these cancer cells will transit through

three stages in coordination with the immune cells (i.e., elimination, equilibrium, and escape) [25]. In the initial elimination stage, the immune cells mitigate the diseased cells to defeat the budding neoplastic cells. However, in the consecutive stages, the cancer cells evolve phenotypic changes to continue growth and progression. In this limited environment, cancer cells continue developing using the support of the immune cells to escape and promote invasion. The interaction of various cell types with the inflammatory cells in the TME results in the immune cells behaving erratically, producing numerous cytokines and other proteins, thereby challenging the design of uniform drugs for therapy. Similarly, healthy granulocytes can contribute to cancer development by producing cytokines-like hematopoietic growth and granulocyte colony-stimulating factors [26].

6.2.2.3 Lymphatic Networks

The blood and the lymphatic networks are the major components helping the tumor progress and escape the defense mechanism [27]. This process happens in two main ways. First, a tumor surrounded by new blood vessels is generally leaky, twisted, and inefficiently retains its cells, leading to quick metastasis [28]. Second is the angiogenesis process, an omnipresent and necessary factor of tumorigenesis. The new vasculature significantly increments the complexity of the tumoral site, a drawback overshadowed by the provided ability to access oxygen from the surrounding environment [29]. Therefore, the new or primary tumor cells find it easy to adapt to hypoxic conditions with the help mainly of the blood system.

Similarly, the lymphatic system excludes the immune cells not to affect the survival of the tumor cells. The myeloid-derived suppressor cells (MDSCs) and the immature dendritic cells restrict T-cells' normal function to clear out the mutated cells [30]. Additionally, the lymphatic vessel forms a physical link between the sentinel lymph nodes and the primary tumor. This connection, in turn, creates the primary direct path for the tumor cells to spread to all possible other locations.

6.2.2.4 ECM in the Microenvironment

The extracellular matrix is made from various proteins such as collagen, laminin, and fibronectin and secretes multiple growth factors and cytokines, which contribute to cancer development and metastasis [31]. The extra cellular secretions affect the tumor progression by altering the phenotype of the stromal cells, causing many oncogenic mutations providing enhanced survival capacity in hypoxic or acidic environments. After these ECM-induced mutations, tumoral cells tend to express markers like TGF- β 1 and IL-6, which makes them escape the detrimental effect from the macrophages and results in a high rate of angiogenesis [32] (Fig. 6.1).

6.2.3 Emerging Biomaterials for Cancer Models

One of the critical aspects of cancer survival and development is its microenvironment. Understanding the tumor microenvironment and replicating it *in vitro* allows rapid and efficient designing of drugs for preclinical trials, providing a controlled

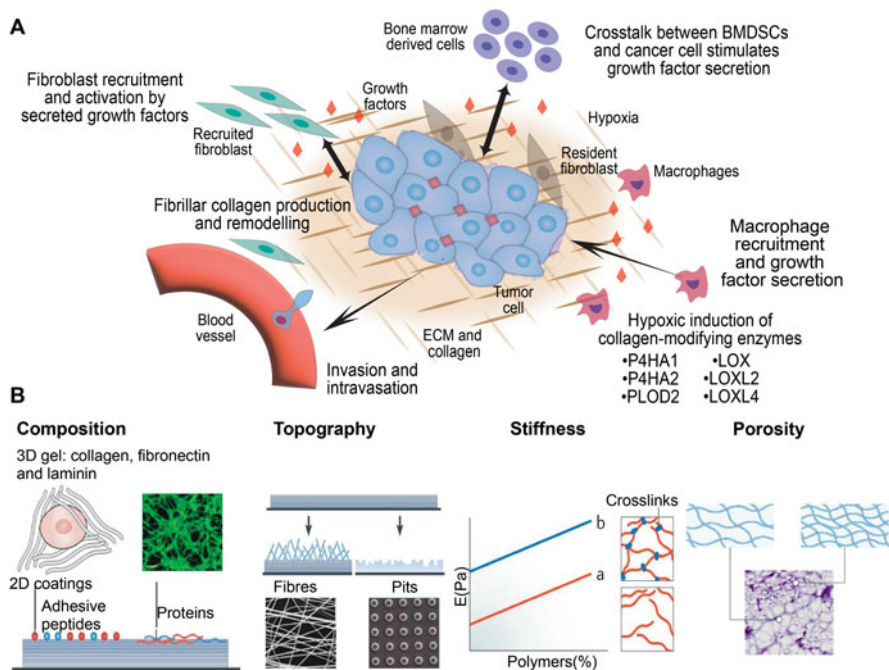


Fig. 6.1 Representation of the dynamic tumor microenvironment (TME). (A) The illustration represents the cross-talk that takes between the normal cells and the mutated cells. Several growth factors are involved in the process and interplay of the microenvironment for tumor development and metastasis. (B) Modelling the TME by using materials to mimic the ECM composition, stiffness, topography to study cancer development (Reproduced with permission from [33])

environment for testing. This enhanced control is critical, as tumors are characterized by changing behavior and a heterogeneous population of cells, difficulty the inter-connection between genetic and phenotypic observations. Among all the engineering tools developed to understand the disease progression, biomaterials have played a central role in the past two decades as vehicles to replicate and manipulate the cancer TME. The broad number of materials developed to encapsulate and maintain cells can be logically divided between those using the native components of organisms (i.e., natural) and those synthesized for the task (i.e., synthetics). The following section is a general overview of the main materials to engineer cell encapsulations and their use as scaffolds to study cancer.

6.2.3.1 Natural Matrix

Two-dimensional (2D) cell cultures are prevalent, and they are the first approach to model disease due to their simplicity in producing and characterizing cell populations [34]. However, this straightforwardness comes with the trade-off of a poor ability to replicate physiological behaviors and disease mechanisms. In that aspect, three-dimensional (3D) models significantly outperform their flat

counterparts. This ability to reproduce physiological mechanisms is greatly enhanced when in addition to reproducing the 3D geometry, the model is developed using native and naturally derived biomaterials replicating the composition.

Matrigel is one of the first commercial natural 3D models for cell culturing and still being among the most popular ones. Matrigel is a combination of collagen IV, entactin, perlecan, laminin, and other growth factors, and while it has broad use, it has gained special attention in cancer for the specific culture pancreatic cells. However, the main limitation of Matrigel, arising from its natural origin, is the batch-to-batch variation, constraining the reliability of its results when mimicking the ECM [35, 36]. Another popular option to study cancer cell migration in an environment close to the native one is the direct use of collagen type I and IV, the abundant protein molecule in the interstitial stroma [4, 37]. Collagen is denser than normal tissue and linearly organizes to provide an appropriate and tuneable matrix stiffness to culture cancer cells. It also allows secretion of MMPs by the cells, further influencing downstream cell–cell communication for cell migration, and promoting cell adhesion, thereby excluding the requirement to functionalize the matrix artificially [38].

An equally popular natural approach is the use of fibronectin, a cell surface glycoprotein binding to integrins. It supports cell invasion and metastasis, and it is known for having pro-tumorigenic factors. In a 3D cell culture setup, fibrillar fibronectin closely mimics the natural ECM, supporting spheroid cell cultures and cell migration [39].

Hyaluronic acid (HA), a glycosaminoglycan, has also been demonstrated to provide a very stable platform to culture cancer cells. HA binds to the receptor CD44, which encourages cancer cell proliferation. The material has been extensively used to explore the behavior of pancreatic carcinoma cells. Other properties of HA include initiating cell invasiveness, supporting spheroid formations, and enabling tweaking the scaffold stiffness [40].

Among other native materials with growing use as artificial scaffolds, laminin, and fibrinogen are rapidly gaining interest, as they have a demonstrated ability to mimic the properties of basement membrane along with enhancing cell invasiveness.

6.2.3.2 Synthetic Matrix

Synthetically designed polymers offer a broader range of biochemical and biomechanical properties over naturally occurring ones [41]. However, since they generally lack the moieties required for cell adhesion, invasion, and migration, they demand many added chemical modifications. In this category, the most popular options are polyethylene glycol (PEG), poly (vinyl alcohol) PVC, and polyacrylamide (PAAm). These molecules are conjugated with RGD groups or with MMPs to enhance their susceptibility to cells.

Modifying the matrix with peptides makes the material suitable to study the growth and morphogenesis of cancer cells. The degree of customization of synthetic polymers enables PEG-based hydrogels and oligopeptides-derived hydrogels with specific amino acid sequences. This customization enables the accurate mimicking of the TME for cancer research using chemically stable and versatile peptides. A

common example is the antiparallel organized peptide RADA-16, which has great implications in studying anticancer drug resistance [42].

A common approach to simultaneously have the customizability of synthetic polymer and the accuracy of natural ones is using hybrid hydrogels, developed by combining natural and synthetic polymers. The natural polymers act as the bioactive part, taking care of the cell adhesion and other biological phenomena. In contrast, synthetic polymers help regulate the mechanical properties, enabling the replica of the tissue counterpart. For example, norbornene modified gelatin and thiolated hyaluronic acid were cross-linked in the presence of white light with eosin-Y and used to culture pancreatic cancer cells [43]. The gel's stiffness is managed by controlling the cross-linking (resulting in the desired modulus). Similarly, collagen fibers chemically linked to (PEG-diNHS) alter collagen's stiffness without altering the space between the adjacent fibers, preserving the similitude with natural tissue. With a tensile modulus between 0.7 and 4.0 kPa, these models succeed in mimicking soft tissue stiffness and the suitability to model hepatocellular carcinoma [44]. Therefore, by modulating the material stiffness properties of the hepatocytes vary. Polyurethane is also emerging as a suitable material for culturing cancer cells but upon fibronectin coating modification which allows cells to attach and proliferate [45]. Polyurethane coated with fibronectin to enable cellular attachment and proliferation is an emerging material for culturing cancer cells. Similarly, hybrid hydrogels prepared from chitosan and poly (γ -glutamic acid) have shown promising results for pancreatic cancer studies [46].

In addition to being biocompatible, these hybrid polymeric materials can produce scaffolds of controlled and highly interconnected micro-porosity and abnormally long degradation rates [47]. These properties have enabled recently culturing oral squamous carcinoma cells during 3 weeks, without significant changes in the scaffold, establishing the link between the size of the tumor with the production of specific angiogenic factors [48]. Additionally, cells cultured in these 3D systems generally possess higher invasion rates than those cultured in 2D and are characterized by the expression of specific epithelial and mesenchymal markers. The stable sponge-like environment enables cancer cells to grow and develop, recreating an *in vivo*-like atmosphere and promoting clusters with physiological morphology and chemokine secretion.

6.2.4 Tumor and Drug Response

Tumor response to drugs has classically been studied by investigating the molecular mechanism of the cells. These studies are critical in understanding the drug resistance mechanism that the cells develop over time [49]. Apart from cellular processes, the TME also plays a role in developing drug resistance [50]. Cancer cells generally adopt two distinct mechanisms to establish a protective action against drugs. First, an interplay between various interleukins secreted by non-tumor cells support cancer cell survival and block apoptosis. Second, an interaction mediated by the TME upregulates integrins to activate signaling cascade to stop the induced apoptosis.

6.2.4.1 Influence of Interleukins on Drug Response

Interleukins (IL-1, 4 and 6) are the pro-inflammatory cytokines that mediate the proliferation of cancer cells and help them escape the defense surveillance of the immune cells [51].

There are two types of IL-1, i.e., IL-1 β and IL-1 α . In general, IL-1 is tracked in all cancer development stages and is responsible for protecting the cells from therapeutic drugs [52]. This is carried out by the secretion of inflammatory molecules like MMPs, VEGF, chemokines, integrins, etc., which block the drug receptors. IL-4 is an indicator of tumor aggressiveness and invasiveness. Cancer cells produce IL-4 for the upregulation of cathepsin production, which is critical for metastasis, growth, invasion, and angiogenesis [53]. IL-4 also increases drug resistance by expressing CD133 cell surface markers and establishing an anti-apoptotic pathway in the cells, protecting them from chemo radiations [54].

IL-6 is predominantly produced by bone marrow stromal cells and indicates the growth and development of myeloma cells. IL-6 enhances cells to become resistant against the apoptotic stimuli from drugs such as dexamethasone or vitamin D3. Additionally, IL-6 is known to activate the MAPK and JAK/STAT pathways, which are prime in blocking cell-mediated apoptosis in the presence of drugs. This activation results in the regulation of the STAT3 dimerization and production of the anti-apoptotic protein Bcl-xl, enabling cells to avoid chemotherapeutic drugs [55].

6.2.4.2 Cell Adhesion-Dependent Drug Resistance

Cell adhesion-dependent drug resistance (CAM-DR) occurs when the cancer cell interacts with specific receptors of the microenvironment or other cells. These established contacts lead to upregulation of p27 $kip1$ and drug resistance. Along with the abovementioned proteins, integrins are the major players in the drug resistance mechanisms of cancer [56]. Integrins participate in the intracellular signal transduction mechanism giving higher survival opportunities to cancer cells. For instance, integrin $\beta1$ and fibronectin cause suppression of apoptosis and are indicative of high cell survival rates against treatment. Furthermore, VLA-4 and VLA-5 specifically have been highlighted as the most critical integrin receptors giving rise to resistance against popular anticancer drugs, such as Doxorubicin or Melphalan. The role of cell-mediated drug resistance comes into play when the integrins and fibronectin bind their respective receptors, leading to the phosphorylation of the Bcl-2 family of protein. This process triggers a cascade of reactions initiated by the PI3 kinase/AKT pathway, which is well known to play a central role in cell survival and drug efflux strategies [57].

6.2.5 Engineered 3D Matrix to Study Tumor-Associated ECM Alterations

Tumoral tissue strongly affects and is in continuous communication with the surrounding ECM. The secreted MMPs and growth factors change the behavior of the ECM, helping the cells proliferate, invade, and metastasize. During the entire

process of tumor development and progression, the matrix keeps on altering. Detailed characterization of the changing ECM has been performed in stand-alone studies, exploring various molecules that make up the matrix. For example, collagen I levels are elevated in primary breast, liver, and lung cancer [58].

Similarly, HA is overexpressed in breast, prostate, colon cancer resulting in poor prognosis and metastasis [59]. Variations of laminin production, where laminin-111 decreases and laminin-332 increases, are common in breast cancer. However, all these factors have not been aggregated into a comprehensive disease model because of the matrix's complexity. As an alternative, genetically modified models such as Cre/Lox are now a popular platform for studying cancer. This section analyses the various engineered models to study cancer progression and the methodologies to recreate the microenvironment [60, 61].

6.2.5.1 Engineered ECM Models

In multicellular organizations, cellular mutations trigger changes in both the cells and their interaction with the environment. The disease progression strongly impacts the cell-matrix biology, a process often studied by mimicking the ECM on a chip using biomaterials. For example, the complex intravasation and extravasation of cancer have been studied on endothelial cells in fibrin gels. The model was later enhanced by incorporating other patterned growth factors and chemokines, enabling a step-by-step controlled replication of tumoral complexity. However, the model was time-limited by the biomaterial. While fibrin is a good model at the early stages of development, as the tumor grows tends to become more fibrous, diverging from fibroin. In later stages, collagen hydrogels provide a more physiologically relevant replica of the ECM, highlighting the importance of choosing the right biomaterial for the study. Additionally, collagen is suitable for patterning structures and topographies, enabling the incorporation of geometrical cues [62, 63]. Lumens of a specific diameter, for example, help aligning epithelial cells and produce tubular structures of cancer cells, closely mimicking fallopian tubes and enabling the study of ovarian cancer [64, 65].

6.2.5.2 Biomaterial Approach

To better understand the influence of ECM on tumor progression, the native biomaterials of the ECM have been used to reconstruct the tumor microenvironment. This reconstruction of the ECM in artificial scaffolds is accomplished either using the whole ECM (e.g., decellularized matrix) or individual ECM components [66]. Decellularized scaffolds are extracted from native tissue and considered to retain the chemical cues required for cell function. In the case of cancerous tissue, proper decellularization of the ECM has been demonstrated to retain factors leading to high chances of developing cancer. Additionally, the patient-derived tumor-affected ECM shows increased migration of cells when compared to the healthy decellularized ECM [67]. Similarly, spheroids made from colon cancer grow faster on cancer-derived ECM when compared to a healthy ECM. Similarly, spheroids made from colon cancer grow faster on cancer-derived ECM compared to a healthy ECM [68]. While decellularized cancer-derived ECM is one of the best platforms to

study cancer progression and probably the closest possible composition of the tissue matrix, sourcing, preparation, and consistency are of extreme complexity. A more reliable solution (at the expense of significance) is the fabrication of scaffolds from the matrix protein. Gels based on Collagen I from explants are primarily used to produce breast cancer models. Recently, these scaffolds have gained popularity as platforms to add other ECM components [69]. Similarly, native fibronectin and collagen I combinations are popular models to study breast cancer invasion, migration, and MMP production [70].

6.3 Tumor on a Chip

Tumor-on-a-chip models have soared in the last decade because of the inflection point they represent in the field of *in vitro* experimentation. Tumor-on-a-chip are: (1) relatable to *in vivo* 3D tissue, (2) enabled for dynamic studies because of their microfluidic component, (3) easy to monitor compared to animal and patient models [71].

Conventional platforms have set credible benchmarks to study and understand the biology and mechanism the cancer cell plays in the presence of various cues. However, their 2D design (i.e., monolayer) strongly differs from the three-dimensional physiological tissue. While 2D systems have been the base of modern cancer research since its inception, nowadays, their limitations have set a glass ceiling in the field, limiting the development of models to carry out pharmaceutical and industrial-level drug testing. Those limitations are triggering a fast transition to standardized 3D tumor models, enabling the acquisition of the relevant information unreachable by 2D setups. In this transition, tumor-on-a-chip models have emerged as promising platforms to mimic the ECM in a controlled fashion to study cancer progression, including the complexity and dynamics of tumor niches [72].

6.3.1 Microfluidic Platform to Model Cancer

Organ-on-a-chip setups are microfluidic devices fabricated from glass, rigid plastics, or flexible polymeric materials, such as PDMS, to culture cells in micro-channels replicating some of the physiological and pathophysiological complexity of an *in vivo* system. They are named “chips” because, in the absence of custom methods, the initial fabrication processes were borrowed from the micro-manufacturing field (Fig. 6.2).

6.3.1.1 Organ on Chip Technology

The central and common element to most organs-on-a-chip is one or several channels, populated with various cell types, and designed to replicate the complexity of a tissue. These channels are coated or incorporate a biomaterial mimicking the ECM. Additionally, the “chip” configuration allows a dynamic manipulation of parameters such as mechanical stiffness, chemical cues, and cell density

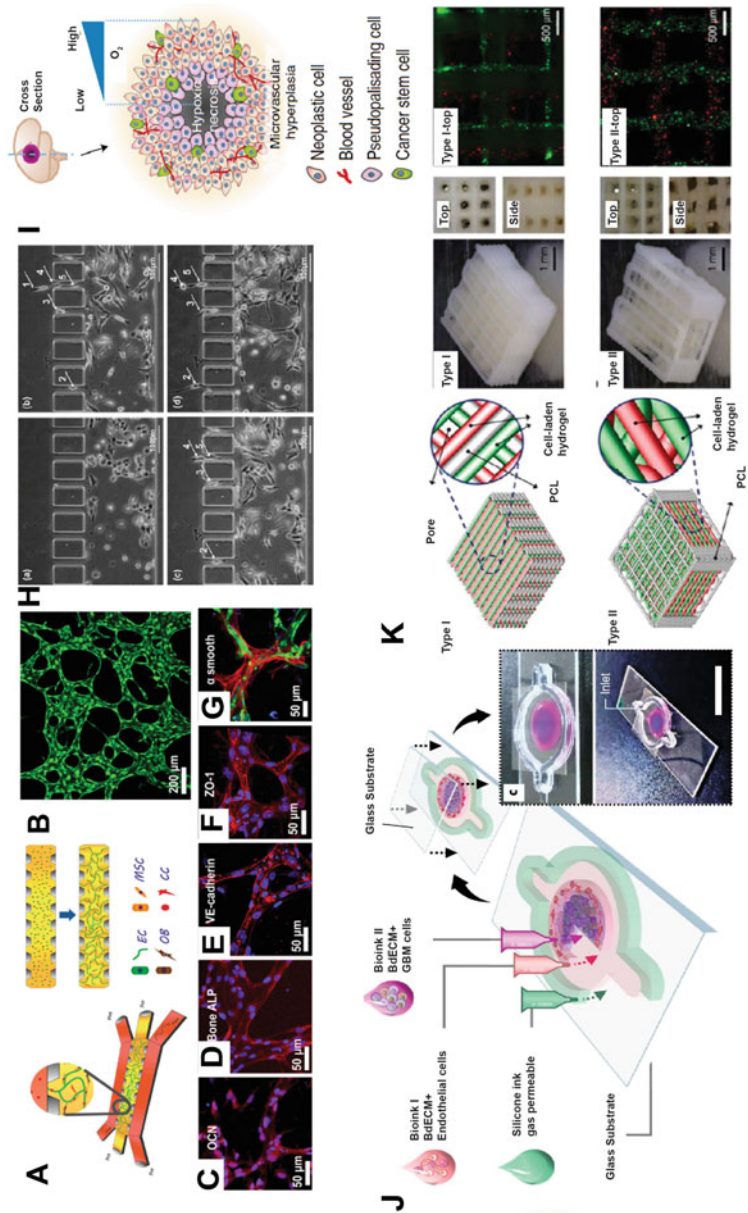


Fig. 6.2 Fabrication of microfluidic devices and adopting 3D printing technology to mimic cancer model. **(A)** Overall depiction of the microfluidic channel used to study breast cell extravasation. **(B)** Microvasculature formed by using endothelial cells in the microfluidic channel as shown in green as they were transfected with GFP. **(C–G)** Staining the fabricated microenvironment with osteocalcin, alkaline phosphatase, VE-cadherin, and smooth muscle cells which are secreted by the cells. The cancer cells extravasate through this formed microenvironment. **(H)** Microfluidic device designed to study the migration of breast

Fig. 6.2 (continued) cancer cell (MDA-MB-435S) as seen in the figure. **(I, J)** Using bioprinting strategies to print TME. Silicone ink is used to print the boundary, and the cells are encapsulated in the bioink derived from decellularized pig tissue. This model is also validated by computer simulations and to understand the response of the diseased cells to chemotherapy. **(K)** 3D bioprinted model using collagen hydrogel to study the cancer cell migration in a highly vascularized system (Reproduced with permission from [73–76])

[77]. These characteristics enable an unprecedented characterization of the cell-matrix interactions in both diseased and normal conditions [78].

The segregated design of organs-on-a-chip platforms enables multicellular architectures, a feature unachievable in 2D culture platforms. Furthermore, cell viability is maintained for an extended time in these architectures without disrupting the population, thanks to the constant circulation of nutrients and gases. Recent advances have shown the establishment of various organs on chip format and their use to perform tests on drugs, toxins, inflammatory cytokines, or radiation. These complex analyses include mapping the cancer cascade, enabled by framing up the disease in a chip format [9].

6.3.1.2 Growth and Neovasculature

The growth of the tumor cells is vastly regulated by their interaction with the surrounding healthy cells. Breast carcinoma cells T47D, for example, when cultured with human mammary fibroblast cells (HMFs) with various proteins forming the ECM, change their growing pattern to form clusters. Included in a cancer-on-a-chip configuration, the MMPs involved in this change and the influence of the ECM composition were mapped. The precise control of the media enabled by the microfluidic platform enabled the identification of the downregulation of estrogen receptor- α in cancer, which is now exploited to develop hormonal therapies to treat cancer [79].

The freedom to incorporate various cell types, enabled by organ-on-a-chip platforms, has helped establish models addressing the role of cytokines and other paracrine signaling processes in cancer growth, beyond breast cancer. For example, lung cancer cells follow very distinct development patterns when they grow alone or in the presence of healthy lung cells. In the former case, cancer cells fail to proliferate in standard conditions. This result set the ground for finding the specific growth factors secreted by the healthy cell that are prime for the tumor cells to survive and develop.

As mentioned above, the survival, proliferation, and extravasation of cancer cells—and their progression from hyperplasia to neoplasia—are strongly linked to the neovascularization of the tumor site [80]. This critical role has motivated the development of several microfluidic platforms recreating the micro-vessels and capillary sprouting design of tumoral vasculature [81]. Due to their hollow architecture, sacrificial 3D printing is one of the preferred methods to design and produce micro-channels. These structures are transformed into hollow structures, suitable to harbor endothelial cells, by the solubilization of the sacrificial material [82]. The monolithic close design enables continuous media perfusion with leakage, closely mimicking the design of blood vessels [83]. These platforms have enabled, among others, the demonstration of a consistent cell sprouting from the vessel in response to the perfusion of tumor angiogenic factors. Furthermore, the suitability of these systems to rapidly compare cellular responses to changes in the media has enabled the evaluation of those results in the presence of a library of various growth factors and concentrations (e.g., VEGF, HGF, and bFGF).

Another popular design for microfluidic devices modelling vasculogenesis is the fabrication of ECM gel-filled chambers containing endothelial cells within a cell-free environment. Because of their relative simplicity, these models are broadly used to study interactions between cancer and endothelial cells in varied conditions [84].

6.3.2 3D Printing Cancer Models

Because of the extraordinary complexity of cancer and its metastasis process, their interpretation using 2D and animal models is cumbersome, expensive, and prone to fail to capture the critical aspect of disease progression. This lack of suitable models is resulting in a decreasing efficiency of the drug discovery process. Animal models permit systematic investigation for understanding cancer progressing. However, due to new ethical concerns and regulatory policies, the use of animals is nowadays the last resource, rather than the traditional primary approach to study processes such as ECM-cell interactions, cell proliferation, and migration.

In the last decade, the field of physiological models has branched out towards the advancement in tissue engineering, aiming to substitute animal models with equally relevant and less unethical options. This approach is giving a significant boost to the replication of the matrix-cell paradigm, closely studying the mechano-chemical properties of the cancer cells with the help of biomaterials [85]. These biomaterials can mimic the organization of the ECM and precisely recapitulate the tumor microenvironment [86]. When incorporated in bioreactors, they overcome the limitations of current models reproducing physiological conditions, emerging as strong candidates to revolutionize medical cancer research [87].

3D printing has advanced to the levels of minutely incorporating polymer and cells to fabricate a replica of an organ of interest with proper nutrient and oxygen diffusion, provided by micro-channels printed simultaneously during the manufacturing process [88]. The entire systematic process of designing, fabricating, and modelling tumors with 3D bioprinters is very detailed, and the hopes for leading future drug innovation are very high [89].

In 3D bioprinting, the traditional extrusion-based technique gives control over porosity and produces mechanically robust constructs [90]. However, direct and inkjet printing are better fitted for incorporating cells while printing with a reasonably defined resolution [91, 92]. These techniques allow the usage of a broader range of cell-friendly polymers and can be incorporated into the ink while printing. Recent advances in using decellularized scaffold-derived inks have brought together a heterogenous protein composition and intricate geometry similar to the tumor microenvironment [93].

The manufacturability of the bio-inks can be enhanced by chemical modifications, becoming photocurable materials suitable for more complicated architectures [94]. This enhanced manufacturability has enabled, for example, the production of 3D spheroids with MCF-7 breast cancer cells with a hypoxic core using gelation and PEGDMA hydrogels [95]. Similar results have been produced with the direct extrusion of PEG-based hydrogels, which are employed to create

microstructures enabling the formation and long-term culture of cancerous spheroids. Later on, these spheroids are used to investigate drug resistance and malignancy hallmarks in the tumor cells, providing new insights into the proteins secreted in hypoxic conditions enabling drug resistance. This mechanism, for example, is absent in 2D platforms.

3D printing enables printing intricate and defined structures, such as vasculatures, comparable to those *in vivo*. However, in addition to producing complex geometries, 3D printing also enables tweaking the micro-architectures and stiffness of the matrix and their influence on cell migration and proliferation [96]. This versatility opens a new venue to study crucial parameters in understanding cancer cell behavior that are often overlooked on 2D systems, such as cell displacement, velocity, and path straightness.

The geometrical and mechanical advantages of bioprinting add to the versatility of the cell population. This versatility is apparent in co-culture studies, such as the recent printing of OVCAR-5 ovarian cancer cells with MRC-5 fibroblasts on Matrigel, to understand the synergies between both to promote proliferation and migration [97]. The model also incorporated drug candidates to study their efficacy to prevent tumor progression. Similar studies using fused-filament 3D printing have been performed to study the influence of a bone-like microenvironment in the proliferation and migration of breast cancer.

While most studies in 3D printed models performed to date have been conducted using immortalized cell lines, the field is rapidly moving toward the use of patient-derived cells. This transition is a significant step toward drug discovery and critical in the development of personalized medicine.

6.3.3 Towards Personalized Medicine

The traditional “one-size-fits-all” idea of medicine is rapidly adapting to incorporate the heterogeneity and variability of human biology [98]. Each individual’s biology is different, even the biology of one individual at different time points changes. However, the precision achieved in many medical procedures enables their accommodation to this conventionally overlooked variability. The type of drug used in cancer treatment is as critical in its performance as the procedure and dose employed. However, the correct dose is a moving target, depending on the patient’s metabolism and situation, and usually aimed through a trial and error process. The new generation of medical procedures aims to diversify the process of drug discovery and utilization. Instead of using a generic model, perform the development process focused on the patient’s specific biology. The main barriers to achieving personalized medicine’s ambitious and logical goals are the cost, sample preparation, and delivery system required for such development [99]. Moving the medicine out of the patient to overcome these barriers requires the development of biomaterials and devices designed and fabricated customized for patient-specific analyses.

6.3.3.1 Device Fabrication Based on Patient Information

Mass manufacturing is based on the parallel replication of a single process, enabling a theoretically infinite scaling of the process and its efficiency [100]. The same approach is also the base for fabricating and using biomaterial-based devices for patient-specific medicine. The idea is to fabricate a series of devices with physiological relevance for a particular patient and disease. Therefore, these devices have a set (but modifiable) biological, chemical, and mechanical configuration, enabling the study of the effect of a specific treatment. Furthermore, by parallelizing different conditions and treatments, such devices aim to identify the best approach for the case. Technologies such as additive manufacturing, photolithography, and direct ink writing are the main in the device manufacturing process for their combination of versatility and high throughput [101]. Combined with the recent advancements in material chemistry, they are being used to produce devices focused on recording and analyzing patient-specific data in real-time. Biopsy tumor testing kits offer a different approach to producing patient-specific information but are hampered by labor-intensive procedures [102]. They use immunohistochemistry (IHC) or in situ hybridization (ISH) to identify the relevant genes involved in developing a specific tumor. In order to access similar information but without lengthy laboratory procedures, the method is being substituted by a combination of qPCR and microfluidic devices. The microfluidic platforms are designed to recognize the exact gene mutation (e.g., Her2 or KRAS) and, therefore, provide valuable information to narrow down possible drugs for the treatment [103]. These microfluidic platforms are coated with various types of matrix proteins to enhance the quality of the data acquired [104]. The cell-friendly surface enhances the integration of the cells from the biopsies, resulting in better characterizations and, ultimately, higher quality data, suitable for machine-aided algorithms and computational analysis. Additionally, the data can also be used in reverse to identify patients that would require treatment. Patient-specific circulating cancer cells, which often branch out from the primary cancer site into the bloodstream, have also been extracted in microfluidic devices to formulate drugs and design therapies. The most well-established system using this approach isolates CTCs escaping from breast, colorectal, and prostate cancer [105]. It utilizes the EpCAM markers expressed by epithelial cells to separate the CTCs from the remaining cell population.

6.3.3.2 Enhanced Drug Delivery to Tumor

Drugs administered into a living host will immediately be coated by various biomolecules, predominately proteins, significantly affecting their activity [106]. Critical parameters such as stability, size, and adsorption get impacted, significantly modifying the original pharmacokinetics [107, 108]. This modification can happen in any direction. For instance, when the nanoparticle-loaded drugs are covered with albumin or apolipoprotein, their activity is greatly reduced, but their encapsulation by plasma membrane proteins will enhance it [109]. Therefore, the right drug may be unusual if it cannot perform in this environment. Because of this, the nanoparticles used as drug carriers with physicochemical properties suitable to adapt to these varying conditions are critical to drug delivery.

The relation between blood circulation and drug circulation half-life is as crucial as drug adaptation to encapsulating proteins [110]. A significant downside of this approach is the encapsulation of the drugs with surrounding proteins. The functionalization of the particles to promote their hydrophilicity has traditionally been used to improve the process, and recent technologies, such as pegylation of the carrier, have shown enrichment of the protein clustering and an associated non-specific macrophage drug uptake [111]. Similarly, modifications of the nanoparticles with proteins targeting the inhibition of phagocytosis (e.g., CD47) are also producing positive results [112].

After the delivery profile and the drug half-life, drug penetration into the tumor site is the last crucial controllable aspect defining the outcome of a drug. The diffusion kinetics of a drug is a consequence of its size and binding affinity [113]. Molecules with high binding affinity are characterized by short penetration distances, while those characterized by weaker interactions with the tissue are prone to traverse it. Similarly, large drugs and drug carriers, independently of their nature, are more susceptible to entangle in the tumor microenvironment than their small counterpart. As a result, fewer amounts extravasate to the target site [114].

The use of drug carriers enables an independent control of such parameters without affecting the chemistry of the drug. For example, drug carriers of about 15 nm and a surface functionalized with cyclic peptides are considered ideal for rapid tumor penetration. Similarly, 10 nm quantum dots loaded in 100 nm spherical nanoparticles are becoming a standard for rapidly reaching a tumor and diffusing a drug [115].

6.3.3.3 Challenges in Clinical Translation

The rapid emergence of novel techniques to design and fabricate tools in the last two decades has enabled a significant leap in the development of therapeutics and the understanding of the environmental factors playing a role in cancer cell progression and extravasation. However, the large-scale screening of therapies is still hindered by suboptimal reproducibility and precision [116]. The current strategy to improve the screening efficiency and make it high throughput goes through the substitution of traditional 2D cultures by 3D organoid culture systems. Forming embryoid bodies can be routinely done by various methods (e.g., digital manufacturing and microfluidic platforms), enabling the upscaling of the testing pipeline and enhancing its physiological relevance [117]. In addition to the incorporation of patient-specific samples, this efficiency is a critical step to generalize the production of customized treatments, which requires studies on a genetic level, running numerous trials, and low-profit margin.

6.3.4 Contribution of AI in Cancer Biology

Years of documented medical cancer research have produced outstanding amounts of data. This data is not only abundant but also unstructured and, in many cases, contradictory due to the disease's dynamic nature. Although this knowledge banked

through years of research has made enormous contributions to advancing medical treatments, its complexity prevents its efficient use by physicians to predict prognosis accurately. Machine learning has emerged as a promising tool to overcome human analytical limitations in cancer research [118]. These algorithms are discovering unobvious patterns and finding out relations between the disease onset and its future development. Therefore, machine learning complements the new physical tools and devices for personalized medicine, providing the tools to handle the unprecedented amount of data collected.

6.3.4.1 Machine Learning in Cancer Prediction and Survival

Machine learning algorithms predict the prognosis of the disease by mapping it, using modelling tools based on supervised and unsupervised learning [119]. These tools can identify and isolate unobvious parameters related to cancer susceptibility, survival, and relapse rate. Beyond predictions associated with cancer properties, machine learning algorithms have proven useful linking phenomena at very different scales, such as the properties of a specific tumor and its diagnosis [120]. Deep learning tools can infer, from biopsies, patient-specific information such as life expectancy, survivability, and treatment sensitivity [121].

Similarly, due to the human analytical limits and time availability of physicians, the usual diagnosis is based on histological and clinical data [122]. It rarely covers in-depth features like family background, diet, or habits that play a role in predicting cancer development. With swift improvement in analytical techniques, such as microscopy, physicians now have access to much more valuable data, yet its greater complexity results in even more challenging predictions. Therefore, machine learning tools are becoming increasingly popular tools for physicians to predict disease progression [123].

6.3.4.2 Clinical Application of the Prediction

The use of machine learning in health care was nominal only 10 years ago [124]. Since then, it has rapidly developed, being ubiquitous in imaging platforms and analytical tools, revolutionizing the treatment paradigm. In radiology, machine learning gives radiologists an upper hand by providing them with tokens of digital knowledge, which adds to the clinical data they already have access to [125]. Incorporating artificial intelligence into medicine does not aim to replace radiologists but rather help them use amounts of data that would otherwise be unmanageable. The algorithms help run analyses with great accuracy and precision, helping, for example, enhance images or generate results useful in the treatment process.

In oncology, the heterogeneity of the tumor requires analyses based on cells at the individual, or close to the individual, level. The genomic and proteomic data, necessary to produce custom and personalized drugs, occur at that level. However, the vast and complex data generated by next generation sequencing makes the analysis unreachable without the use of artificial intelligence algorithms. Therefore, with a future medicine based on genetic information, artificial intelligence plays a critical role in the future of therapeutics [126, 127].

6.4 Cancer Vaccines

Cancer disease most probably is the therapeutic medical field that has advanced the most since its inception. Its parallel progression improving technology, specificity, deep learning methods for diagnostics and radiology, specific target selection, and developing checkpoint inhibitors are unmatched. The field's focus on eradicating cancer is equally absolute and ambitious and has triggered the development of new fields focused on that goal. Cancer vaccines, for example, aim to induce tumor regression with zero relapse tendency, eliminate the adverse effect of drugs, and produce memory cells preventing any relapse.

6.4.1 Types of Cancer Vaccines

Cancer vaccines aim to create a specific response to tumor antigens. Tumor antigens are proteins overexpressed in cancer and playing a role in its initiation and progression [128]. Therefore, the choice of antigen is the single most crucial component of cancer vaccine design. Since protein production is ubiquitous in normal and diseased cells, the challenge is to isolate those produced by cancer cells for survival and not by normal cells (Fig. 6.3).

6.4.1.1 Virus Based

Our body has evolved complex and efficient mechanisms to respond against viruses, and various viruses are studied as candidates for a cancer vaccine making use of those mechanisms. When a viral pathogen invades our immune system, it causes the activation of antigen-presenting cells (APCs), which is triggered by the interaction of the viral antigens with pattern recognition receptors [133]. Exploiting these interactions, viral vaccine vectors, such as poxviruses and adenoviruses, have been used for therapeutic applications in cancer.

The main drawback of using virus antigens to tag cancer cells is the neutralization effect of the viral vectors by the body, difficulting the use of booster doses. However, this limitation can be circumvented in some cases. For example, PROSTVAC-VF/Tricom, a virus-based vaccine for prostate cancer, is designed to dodge the immune system with booster shots containing the same tumor antigen but different viral vector or vector type [134]. Additionally, the activity of the vaccine can be enhanced with virus-based immunotherapy regimens, which are primed with checkpoint inhibitors—this therapy with prostate-specific membrane antigen is under clinical trials. The therapy is further enhanced by coupling it with subcutaneous injections of antibodies, such as CTLA-4 antagonist or tremelimumab [135].

6.4.1.2 Tumor Based

Vaccines carrying either killed cancer cells or patient-specific antigen-presenting cells (APCs) with cancer antigens are developed to have specificity against the disease and are irradiated to restrict further cell division [136]. Some of these vaccines, for example, are prepared using whole tumors explants that are genetically

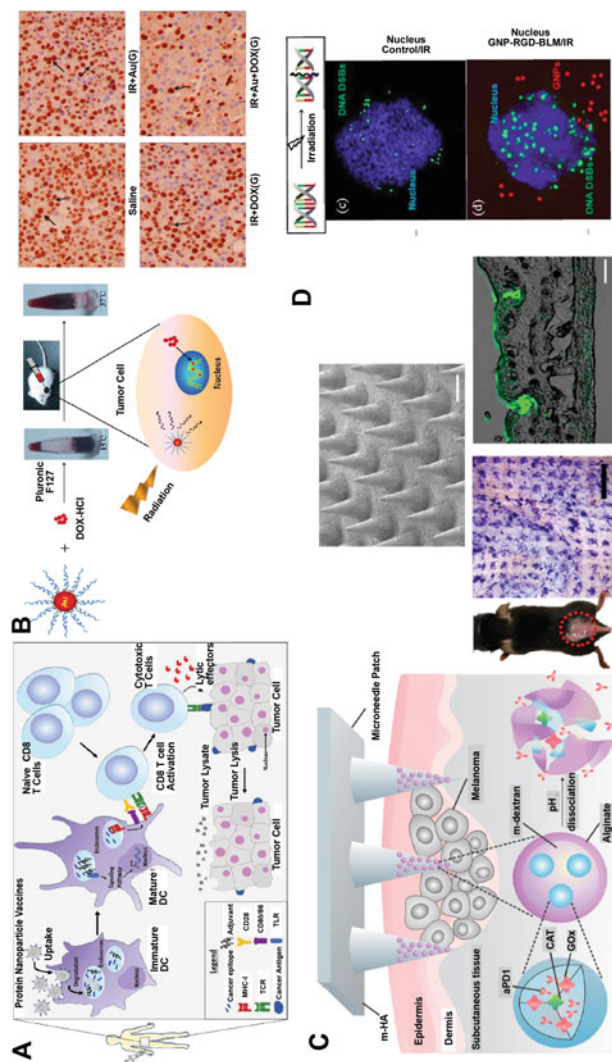


Fig. 6.3 Cancer therapeutics in using biomaterials as drug vehicle. (A) Depiction of cancer elimination from the system by using protein nanoparticles as cancer vaccine. (B) Combinational therapy using both nanoparticles and radiation therapy. Pluronic hydrogel is loaded with both gold nanoparticles and Doxorubicin, followed by exposure to IR radiation. As seen from the Ki-67 immunohistochemistry, the panel with radiation gold nanoparticles and Doxorubicin has higher effectiveness compared to the control sample with saline treatment. (C) Dextran nanoparticles used in microneedles to deliver drugs for melanoma treatment. The image shows the penetration of the microneedle with drugs into the mouse skin. The green signal shows FITC positive penetrated antibody loaded microneedle. (D) Cancer therapy combining gold nanoparticles with radiation therapy. As seen from the image, the cancer is highly targeted, causing DNA damage when gold nanoparticles are accompanied by IR radiation. (Reproduced with permission from [129–132])

modified to secrete cytokines and granulocyte–macrophage colony-stimulating factors. These GM-CSF play a significant role in antigen presentation and survival of dendritic cells [137]. Vaccines working on this principle have shown potent action on murine models but a low success rate in humans. However, those successful cases, such as Sipuleucel-T, which is FDA approved for prostate cancer, are hampered by costs preventing worldwide use [138].

Other cell-based vaccine preparations using bacteria and yeast have succeeded in stimulating an immune response. This approach was first demonstrated by Coley et al. using heat attenuated bacteria to treat cancer patients. Since then, many other examples have emerged [139]. For example, BCG (also heat-inactivated) is commonly used to treat bladder cancer. Other [140] species of bacteria, such as attenuated strains of *Salmonella* and *Listeria*, have also been used as cancer vaccines. These are internalized after infection and help the APCs deliver DNA-or RNA-encoded tumor antigens, followed by a robust antitumor immunity.

6.4.1.3 Peptide-Based

Peptide vaccines are based on a single antigen-based short peptide showing an immune response, potent enough to be employed for therapeutics [141]. Existing examples use short peptides and a single antigen, neglecting the heterogeneity of the pool of antigens, and are characterized by reduced immune responses [142]. This reduced response arises from the tendency of small peptide moieties to directly bind MHC class I molecules, bypassing the APCs processing and increasing T-cell dysfunction and tolerogenic signal. Efforts to improve the design of the vaccine focus on enhancing the activation of T-cell responses by incorporating peptides into constructs that are either amphiphilic or combined with inflammatory and immune modulators. Poly-IC and Poly-ICLC are ligands that have succeeded as adjuvants in peptide vaccines in experimental setups [143]. Additionally, some long peptides containing both MHC class I and II moieties have succeeded in eliciting CD8 and CD4 T-cell response through DC cell processing rather than APCs [144]. These long peptides produce a more robust T-cell response than short peptides, with the additional advantage of a simultaneous induction of memory T-cell response [145].

6.4.2 Biomaterials for Cancer Immunotherapy

Biomaterials are a necessary piece to study cancer progression by recapitulating its native microenvironment *in vitro*. In the last decade, the field has developed from the original goals focused on biocompatibility and survival of an encapsulated cell population to reproduce specific tissue properties [146]. This growing interlink between materials and biology promotes a new paradigm, where materials move beyond their support role to become essential in controlling cellular pathways [147]. This new paradigm has profound implications on the role of biomaterials in cancer drug testing and therapeutics.

6.4.2.1 Drug Delivery

Current strategies to fight the progressing disease of cancer are a combination of surgical interventions, chemotherapy, and radiation therapy. The main downside of these methods is their suboptimal specificity. They effectively block DNA synthesis and mitosis in cancer cells but also affect the functionality of healthy cells [148].

The collateral damage of cancer drugs partially results from the high doses required due to their poor accessibility to the cancer cells [149]. Therefore, there is an immediate need for therapies that actively or passively target the cancer cells only, avoiding the need to flood the system for a significant amount to reach the cancer site. Towards that objective, several materials have been developed with the specific aim to deliver drugs directly to the cancer site—synthetic and natural biopolymers, lipids, hydrogels, and nano-inorganic carriers, to name but a few. Furthermore, these carriers are in continuous enhancement by other fields, as they are designed to easily bind to ligands like DNA, RNA, and proteins, simplifying the process of drug delivery [150, 156].

Inorganic carriers (generally based on metal cores) are bringing new functionalities to the field. Quantum dots, for example, have already proven to be very effective in both drug delivery and tissue imaging. Because of its size (1–10 nm), large surface-area-to-volume ratio, photoluminescence, and uniformity, QDs have emerged as one of the best methods [164]. Their main drawback is their intrinsic hydrophobicity, resulting in a tendency to form aggregates [158]. Nevertheless, coating the QDs has proven to be an effective strategy to increase their affinity to water and bioactivity. Similarly, carbon nanotubes (CNTs) have recently found a unique application as the central element in photoablation therapy, where they transform incident light into heat, selectively raising the temperature of tumoral tissue [151, 155].

Superparamagnetic iron oxide nanoparticles (SPIONs) are another inorganic carrier that is now increasingly being used. They are characterized by magnetism, easy visualization, and biocompatibility, playing a central role in modern magnetic resonance imaging [152].

Organic carriers based on nano-size biocompatible polymers complement have also found direct application in cancer treatment and diagnostic. These polymeric vehicles can be prepared from synthetic polymers such as PCL, PLA, HPMA, and PLGA or natural polymers like chitosan, gelatin, and collagen [157, 160]. Unlike their organic counterparts, drugs encapsulated in these bioabsorbable polymer matrices are released by erosion or swelling, followed by diffusion. This process, significantly slower in synthetic polymers than in natural polymers, provides the former with the advantage of a prolonged drug release, which can be sustained for several weeks. For example, Doxorubicin is a drug used to treat solid cancer and typically encapsulated in a hydrogel by conjugating it to a sugar moiety (i.e., dextran) [165]. Similarly, PLGA has been used to embed Tamoxifen, an anticancer drug cleaving tumoral DNA [161]. Carrier and cargo are designed as part of a unique system rather than as separate parts in all cases. In the design process, factors such as the drug-to-polymer ratio, the polymer's molecular weight, and the polymer's source affect the drug's delivery and effectiveness [153].

Liposomes, lipid bilayers with enclosed aqueous centers, are an emerging carrier for hydrophilic drugs. They have unparallel biocompatibility and effectiveness but suffer from difficult clearance from the system. Midway between the polymer and the liposomes are the hydrogels, characterized by a very porous core and unmatched ability to absorb biological fluids. Hydrogels are primarily used to encapsulate hydrophilic drugs [159]. However, their susceptibility to modifications makes them suitable to carry other drugs and perform controlled drug release, targeted drug delivery, and promote bio-adhesion.

6.4.2.2 Combination Therapies

While some patients in advanced stages of cancer tend to respond more favorably to a single treatment, in the vast majority of clinical cases, combination therapeutics show higher effectiveness. For example, a combination of regulators expressed by T-lymphocytes, such as CTLA-4 and PD1 (Nivolumab), results in a synergetic effect where CTLA-4 (Ipilimumab) plays a role in dampening the T-cell priming, and PD1 blocks the effector response of T-cells [141]. The efficacy of the treatment increases by 60% when the drugs are used in combination with respect to their use in isolation. However, this increased efficacy comes at the cost of additional toxicity to non-cancerous cells, comparable to autoimmune diseases.

Combining chemotherapy and checkpoint inhibitors is also a usual strategy to lower the impact of tumor treatment in other cells. For instance, Cyclophosphamide is known to deplete T regulatory cells, and when combined with chemotherapeutic drugs like Paclitaxel, it enhances antitumor T-cell functions and initiates antitumor responses [154, 162]. However, not all combinations of drugs result in a positive effect. Several drugs have shown detrimental effects that largely overcome the possible benefits and have resulted in their discontinuation. As a result of these extreme side effects of chemotherapy and the massive damage that can cause to healthy cells, there is a growing field of research focused on developing molecularly targeted therapies. These therapies are designed to target cells with the specific genetic characteristics of cancer.

Immunostimulatory antibodies are another class of cancer therapeutics that are used as monotherapy or in combination. These are designed to target the TNF receptors in order to activate them. For example, a combination of checkpoint inhibitor anti-CTLA-4 and immunostimulatory antibodies anti-4-1BBL triggers T-cell co-inhibitory blockade in B16 melanoma and prostate tumors [163].

The combination of molecular therapeutics with immunotherapy does not, however, provide optimum results in all situations. For example, while some molecular therapies impart immunomodulatory effects, they inhibit the benefits of the mutations caused by chemotherapy, making immunotherapies less effective. Nevertheless, while current combinatorial strategies are far from perfect, modern studies have demonstrated solid advances in developing effective drug combinations that do not compromise the health of normal cells.

6.5 Summary

Even though tremendous advances have been made in the field to bridge the gap between cancer vaccine development and biomaterials, there is still much work left to translate the research from lab to bedside.

The development of better disease models is critical to remove the disagreement between the immunological response in small animals, large animals, and humans. Furthermore, these models need to be developed within the paradigm of cancer as an individual disease, with particular characteristics and exceptionalities for each patient. In developing biomaterials for cancer study and treatment, it is critical to address the native batch-to-batch variance of the material and the different responses between patients and situations. These two aspects will strongly condition the success of the field upscaling to strategies of general use.

The use of biomaterials as the primary agent for developing potent cancer immunotherapeutic is promising but still has a long path to cover before its application. All the main challenges of the field are, however, characterized by a strong multidisciplinary. Thus, succeeding on the objective of fully understanding and eradicating cancer will ultimately depend on our ability to establish collaborations between scientists from various fields, from medical and material sciences to computer and mechanical sciences.

References

1. Klein CA (2020) Cancer progression and the invisible phase of metastatic colonization. *Nat Rev Cancer* 20:681–694
2. DeVita VT, Chu E (2008) A history of cancer chemotherapy. *Cancer Res* 68:8643–8653
3. Messerschmidt JL, Prendergast GC, Messerschmidt GL (2016) How cancers escape immune destruction and mechanisms of action for the new significantly active immune therapies: helping nonimmunologists decipher recent advances. *Oncologist* 21:233
4. Campbell JJ, Husmann A, Hume RD, Watson CJ, Cameron RE (2017) Development of three-dimensional collagen scaffolds with controlled architecture for cell migration studies using breast cancer cell lines. *Biomaterials* 114:34–43
5. Hassan G, Afify SM, Kitano S, Seno A, Ishii H, Shang Y et al (2021) Cancer stem cell microenvironment models with biomaterial scaffolds in vitro. *PRO* 9:45
6. Greenman C, Stephens P, Smith R, Dalgliesh GL, Hunter C, Bignell G et al (2007) Patterns of somatic mutation in human cancer genomes. *Nature* 446:153–158
7. Kalluri R, Weinberg RA (2009) The basics of epithelial-mesenchymal transition. *J Clin Invest* 119:1420–1428
8. Vergati M, Intrivici C, Huen N-Y, Schlom J, Tsang KY (2010) Strategies for cancer vaccine development. *J Biomed Biotechnol* 2010:596432
9. Ma Y-HV, Middleton K, You L, Sun Y (2018) A review of microfluidic approaches for investigating cancer extravasation during metastasis. *Microsyst Nanoeng* 4:1–13
10. Cereda M, Mourikis TP, Ciccarelli FD (2016) Genetic redundancy, functional compensation, and cancer vulnerability. *Trends Cancer* 2:160–162
11. He S, Cook BL, Deverman BE, Weihe U, Zhang F, Prachand V et al (2000) E2F is required to prevent inappropriate S-phase entry of mammalian cells. *Mol Cell Biol* 20:363–371
12. Goel S, DeCristo MJ, McAllister SS, Zhao JJ (2018) CDK4/6 inhibition in cancer: beyond cell cycle arrest. *Trends Cell Biol* 28:911–925

13. Mansoori B, Mohammadi A, Davudian S, Shirjang S, Baradaran B (2017) The different mechanisms of cancer drug resistance: a brief review. *Adv Pharm Bull* 7:339
14. Gottesman MM, Lavi O, Hall MD, Gillet J-P (2016) Toward a better understanding of the complexity of cancer drug resistance. *Annu Rev Pharmacol Toxicol* 56:85–102
15. Rückert F, Sticht C, Niedergethmann M (2012) Molecular mechanism of the “feedback loop” model of carcinogenesis. *Commun Integr Biol* 5:506–507
16. Gottesman MM, Pastan IH (2015) The role of multidrug resistance efflux pumps in cancer: revisiting a JNCI publication exploring expression of the MDR1 (P-glycoprotein) gene. *J Natl Cancer Inst* 107:djv222
17. Moll UM, Petrenko O (2003) The MDM2-p53 interaction. *Mol Cancer Res* 1:1001–1008
18. Eltzschig HK, Carmeliet P (2011) Hypoxia and inflammation. *N Engl J Med* 364:656–665
19. Frantz C, Stewart KM, Weaver VM (2010) The extracellular matrix at a glance. *J Cell Sci* 123: 4195–4200
20. Martin TA, Ye L, Sanders AJ, Lane J, Jiang WG (2013) Cancer invasion and metastasis: molecular and cellular perspective. In: *Madame Curie Bioscience Database [Internet]*. Landes Bioscience
21. Ping Q, Yan R, Cheng X, Wang W, Zhong Y, Hou Z et al (2021) Cancer-associated fibroblasts: overview, progress, challenges, and directions. *Cancer Gene Ther*:1–16
22. Cousin JM, Cloninger MJ (2016) The role of galectin-1 in cancer progression, and synthetic multivalent systems for the study of galectin-1. *Int J Mol Sci* 17:1566
23. Hassona Y, Cirillo N, Heesom K, Parkinson E, Prime SS (2014) Senescent cancer-associated fibroblasts secrete active MMP-2 that promotes keratinocyte dis-cohesion and invasion. *Br J Cancer* 111:1230–1237
24. Grivennikov SI, Greten FR, Karin M (2010) Immunity, inflammation, and cancer. *Cell* 140: 883–899
25. Mittal D, Gubin MM, Schreiber RD, Smyth MJ (2014) New insights into cancer immunoediting and its three component phases—elimination, equilibrium and escape. *Curr Opin Immunol* 27:16–25
26. Wu L, Saxena S, Awaji M, Singh RK (2019) Tumor-associated neutrophils in cancer: going pro. *Cancer* 11:564
27. Alitalo A, Detmar M (2012) Interaction of tumor cells and lymphatic vessels in cancer progression. *Oncogene* 31:4499–4508
28. Geiger TR, Peeper DS (2009) Metastasis mechanisms. *Biochim Biophys Acta* 1796:293–308
29. Folkman J (2002) Role of angiogenesis in tumor growth and metastasis. In: *Seminars in oncology*, vol 29. Elsevier, pp 15–18
30. Gabrilovich DI, Nagaraj S (2009) Myeloid-derived suppressor cells as regulators of the immune system. *Nat Rev Immunol* 9:162–174
31. Walker C, Mojares E, del Río Hernández A (2018) Role of extracellular matrix in development and cancer progression. *Int J Mol Sci* 19:3028
32. Shi J, Feng J, Xie J, Mei Z, Shi T, Wang S et al (2017) Targeted blockade of TGF- β and IL-6/JAK2/STAT3 pathways inhibits lung cancer growth promoted by bone marrow-derived myofibroblasts. *Sci Rep* 7:1–10
33. Beri P, Matte BF, Fattet L, Kim D, Yang J, Engler AJ (2018) Biomaterials to model and measure epithelial cancers. *Nat Rev Mater* 3:418–430
34. Hudalla GH, Murphy WL (2015) Mimicking the extracellular matrix: the intersection of matrix biology and biomaterials. *Royal Society of Chemistry*
35. Hughes CS, Postovit LM, Lajoie GA (2010) Matrigel: a complex protein mixture required for optimal growth of cell culture. *Proteomics* 10:1886–1890
36. Moreira L, Bakir B, Chatterji P, Dantes Z, Reichert M, Rustgi AK (2018) Pancreas 3D organoids: current and future aspects as a research platform for personalized medicine in pancreatic cancer. *Cell Mol Gastroenterol Hepatol* 5:289–298
37. Rommerswinkel N, Niggemann B, Keil S, Zänker KS, Dittmar T (2014) Analysis of cell migration within a three-dimensional collagen matrix. *J Vis Exp*:e51963

38. Collen A, Hanemaaijer R, Lupu F, Quax PH, van Lent N, Grimbergen J et al (2003) Membrane-type matrix metalloproteinase-mediated angiogenesis in a fibrin-collagen matrix. *Blood* 101:1810–1817
39. Akiyama SK, Olden K, Yamada KM (1995) Fibronectin and integrins in invasion and metastasis. *Cancer Metastasis Rev* 14:173–189
40. Makkar S, Riehl TE, Chen B, Yan Y, Alvarado DM, Ciorba MA et al (2019) Hyaluronic acid binding to TLR4 promotes proliferation and blocks apoptosis in colon cancer. *Mol Cancer Ther* 18:2446–2456
41. Liu F, Wang X (2020) Synthetic polymers for organ 3D printing. *Polymers* 12:1765
42. Xu J, Qi G, Wang W, Sun XS (2021) Advances in 3D peptide hydrogel models in cancer research. *NPJ Sci Food* 5:1–10
43. Chang C-Y, Johnson HC, Babb O, Fishel ML, Lin C-C (2021) Biomimetic stiffening of cell-laden hydrogels via sequential thiol-ene and hydrazone click reactions. *Acta Biomater* 130:161–171
44. Liang Y, Clay NE, Sullivan KM, Leong J, Ozcelikkale A, Rich MH et al (2017) Enzyme-induced matrix softening regulates hepatocarcinoma cancer cell phenotypes. *Macromol Biosci* 17:1700117
45. Totti S, Allenby MC, Dos Santos SB, Mantalaris A, Velliou EG (2018) A 3D bioinspired highly porous polymeric scaffolding system for in vitro simulation of pancreatic ductal adenocarcinoma. *RSC Adv* 8:20928–20940
46. Chiellini F, Puppi D, Piras AM, Morelli A, Bartoli C, Migone C (2016) Modelling of pancreatic ductal adenocarcinoma in vitro with three-dimensional microstructured hydrogels. *RSC Adv* 6:54226–54235
47. Fernandez JG, Seetharam S, Ding C, Feliz J, Doherty E, Ingber DE (2016) Direct bonding of chitosan biomaterials to tissues using transglutaminase for surgical repair or device implantation. *Tissue Eng A* 23:135–142
48. Ravi M, Paramesh V, Kaviya S, Anuradha E, Solomon FP (2015) 3D cell culture systems: advantages and applications. *J Cell Physiol* 230:16–26
49. Li Y, Umbach DM, Krahn JM, Shats I, Li X, Li L (2021) Predicting tumor response to drugs based on gene-expression biomarkers of sensitivity learned from cancer cell lines. *BMC Genomics* 22:1–18
50. Qu Y, Dou B, Tan H, Feng Y, Wang N, Wang D (2019) Tumor microenvironment-driven non-cell-autonomous resistance to antineoplastic treatment. *Mol Cancer* 18:1–16
51. Briukhovetska D, Dörr J, Endres S, Libby P, Dinarello CA, Kobold S (2021) Interleukins in cancer: from biology to therapy. *Nat Rev Cancer*:1–19
52. Mantovani A, Barajon I, Garlanda C (2018) IL-1 and IL-1 regulatory pathways in cancer progression and therapy. *Immunol Rev* 281:57–61
53. Gocheva V, Wang H-W, Gadea BB, Shree T, Hunter KE, Garfall AL et al (2010) IL-4 induces cathepsin protease activity in tumor-associated macrophages to promote cancer growth and invasion. *Genes Dev* 24:241–255
54. Todaro M, Perez Alea M, Scopelliti A, Medema JP, Stassi G (2008) IL-4-mediated drug resistance in colon cancer stem cells. *Cell Cycle* 7:309–313
55. Taher MY, Davies DM, Maher J (2018) The role of the interleukin (IL)-6/IL-6 receptor axis in cancer. *Biochem Soc Trans* 46:1449–1462
56. Eymin B, Haugg M, Droin N, Sordet O, Dimanche-Boitrel M-T, Solary E (1999) p27 Kip1 induces drug resistance by preventing apoptosis upstream of cytochrome c release and procaspase-3 activation in leukemic cells. *Oncogene* 18:1411–1418
57. Damiano JS, Cress AE, Hazlehurst LA, Shtil AA, Dalton WS (1999) Cell adhesion mediated drug resistance (CAM-DR): role of integrins and resistance to apoptosis in human myeloma cell lines. *Blood* 93:1658–1667
58. Zissimopoulos A, Stellos K, Matthaïos D, Petrakis G, Parmenopoulou V, Babatsikou F et al (2009) Type I collagen biomarkers in the diagnosis of bone metastases in breast cancer, lung

- cancer, urinary bladder cancer and prostate cancer. Comparison to CEA, CA 15-3, PSA and bone scintigraphy. *J BUON* 14:463–472
59. Wu W, Chen L, Wang Y, Jin J, Xie X, Zhang J (2020) Hyaluronic acid predicts poor prognosis in breast cancer patients: a protocol for systematic review and meta analysis. *Medicine* 99: e20438
 60. Carpenter PM, Ziogas A, Markham EM, Cantillep AS, Yan R, Anton-Culver H (2018) Laminin 332 expression and prognosis in breast cancer. *Hum Pathol* 82:289–296
 61. Kim H, Kim M, Im S-K, Fang S (2018) Mouse Cre-LoxP system: general principles to determine tissue-specific roles of target genes. *Lab Anim Res* 34:147–159
 62. Fernandez JG, Mills CA, Pla-Roca M, Samitier J (2007) Forced soft lithography (FSL): production of micro- and nanostructures in thin freestanding sheets of chitosan biopolymer. *Adv Mater* 19:3696–3701
 63. Mills CA, Fernandez JG, Errachid A, Samitier J (2008) The use of high glass temperature polymers in the production of transparent, structured surfaces using nanoimprint lithography. *Microelectron Eng* 85:1897–1901
 64. Chen MB, Whisler JA, Fröse J, Yu C, Shin Y, Kamm RD (2017) On-chip human microvasculature assay for visualization and quantification of tumor cell extravasation dynamics. *Nat Protoc* 12:865–880
 65. Guthold M, Liu W, Sparks E, Jawerth L, Peng L, Falvo M et al (2007) A comparison of the mechanical and structural properties of fibrin fibers with other protein fibers. *Cell Biochem Biophys* 49:165–181
 66. Taylor DA, Sampaio LC, Ferdous Z, Gobin AS, Taite LJ (2018) Decellularized matrices in regenerative medicine. *Acta Biomater* 74:74–89
 67. Winkler J, Abisoye-Ogunniyan A, Metcalf KJ, Werb Z (2020) Concepts of extracellular matrix remodelling in tumour progression and metastasis. *Nat Commun* 11:1–19
 68. Genovese L, Zawada L, Tosoni A, Ferri A, Zerbi P, Allevi R et al (2014) Cellular localization, invasion, and turnover are differently influenced by healthy and tumor-derived extracellular matrix. *Tissue Eng Part A* 20:2005–2018
 69. Rijal G, Li W (2016) 3D scaffolds in breast cancer research. *Biomaterials* 81:135–156
 70. Ioachim E, Charchanti A, Briasoulis E, Karavasilis V, Tsanou H, Arvanitis D et al (2002) Immunohistochemical expression of extracellular matrix components tenascin, fibronectin, collagen type IV and laminin in breast cancer: their prognostic value and role in tumour invasion and progression. *Eur J Cancer* 38:2362–2370
 71. Katt ME, Placone AL, Wong AD, Xu ZS, Searson PC (2016) In vitro tumor models: advantages, disadvantages, variables, and selecting the right platform. *Front Bioeng Biotechnol* 4:12
 72. Carvalho MR, Lima D, Reis RL, Correlo VM, Oliveira JM (2015) Evaluating biomaterial-and microfluidic-based 3D tumor models. *Trends Biotechnol* 33:667–678
 73. Chaw K, Manimaran M, Tay E, Swaminathan S (2007) Multi-step microfluidic device for studying cancer metastasis. *Lab Chip* 7:1041–1047
 74. Jeon JS, Bersini S, Gilardi M, Dubini G, Charest JL, Moretti M et al (2015) Human 3D vascularized organotypic microfluidic assays to study breast cancer cell extravasation. *Proc Natl Acad Sci* 112:214–219
 75. Yi H-G, Jeong YH, Kim Y, Choi Y-J, Moon HE, Park SH et al (2019) A bioprinted human-glioblastoma-on-a-chip for the identification of patient-specific responses to chemoradiotherapy. *Nat Biomed Eng* 3:509–519
 76. Zhang YS, Duchamp M, Oklu R, Ellisen LW, Langer R, Khademhosseini A (2016) Bioprinting the cancer microenvironment. *ACS Biomater Sci Eng* 2:1710–1721
 77. Fernandez JG, Samitier J, Mills CA (2011) Simultaneous biochemical and topographical patterning on curved surfaces using biocompatible sacrificial molds. *J Biomed Mater Res A* 98A:229–234
 78. Ergir E, Bachmann B, Redl H, Forte G, Ertl P (2018) Small force, big impact: next generation organ-on-a-chip systems incorporating biomechanical cues. *Front Physiol* 9:1417

79. Aboussekhra A (2011) Role of cancer-associated fibroblasts in breast cancer development and prognosis. *Int J Dev Biol* 55:841–849
80. Kaklamanis L, Kakolyris S, Koukourakis M, Gatter K, Harris A (2000) From hyperplasia to neoplasia and invasion: angiogenesis in the colorectal adenoma-carcinoma model. In: *Angiogenesis*. Springer, pp 249–266
81. Hu C, Chen Y, Tan MJA, Ren K, Wu H (2019) Microfluidic technologies for vasculature biomimicry. *Analyst* 144:4461–4471
82. Goh WH, Hashimoto M (2018) Fabrication of 3D microfluidic channels and in-channel features using 3D printed, water-soluble sacrificial mold. *Macromol Mater Eng* 303:1700484
83. Park ES, Brown AC, DiFeo MA, Barker TH, Lu H (2010) Continuously perfused, non-cross-contaminating microfluidic chamber array for studying cellular responses to orthogonal combinations of matrix and soluble signals. *Lab Chip* 10:571–580
84. Kuzmic N, Moore T, Devadas D, Young EW (2019) Modelling of endothelial cell migration and angiogenesis in microfluidic cell culture systems. *Biomech Model Mechanobiol* 18:717–731
85. Billiet T, Vandehaute M, Schelfhout J, Van Vlierberghe S, Dubruel P (2012) A review of trends and limitations in hydrogel-rapid prototyping for tissue engineering. *Biomaterials* 33:6020–6041
86. DelNero P, Song YH, Fischbach C (2013) Microengineered tumor models: insights & opportunities from a physical sciences-oncology perspective. *Biomed Microdevices* 15:583–593
87. Martin Y, Vermette P (2005) Bioreactors for tissue mass culture: design, characterization, and recent advances. *Biomaterials* 26:7481–7503
88. Ji S, Guvendiren M (2017) Recent advances in bioink design for 3D bioprinting of tissues and organs. *Front Bioeng Biotechnol* 5:23
89. Lee JM, Yeong WY (2016) Design and printing strategies in 3D bioprinting of cell-hydrogels: a review. *Adv Healthc Mater* 5:2856–2865
90. Hwang HH, Zhu W, Victorine G, Lawrence N, Chen S (2018) 3D-printing of functional biomedical microdevices via light-and extrusion-based approaches. *Small Methods* 2:1700277
91. Li VC-F, Dunn CK, Zhang Z, Deng Y, Qi HJ (2017) Direct ink write (DIW) 3D printed cellulose nanocrystal aerogel structures. *Sci Rep* 7:1–8
92. Saunders RE, Derby B (2014) Inkjet printing biomaterials for tissue engineering: bioprinting. *Int Mater Rev* 59:430–448
93. Heath DE (2019) A review of decellularized extracellular matrix biomaterials for regenerative engineering applications. *Regen Eng Transl Med* 5:155–166
94. Das R, Fernandez JG (2020) Cellulose nanofibers for encapsulation and pluripotency preservation in the early development of embryonic stem cells. *Biomacromolecules* 21:4814–4822
95. Aggarwal V, Miranda O, Johnston PA, Sant S (2020) Three dimensional engineered models to study hypoxia biology in breast cancer. *Cancer Lett* 490:124–142
96. Wang X, Jiang M, Zhou Z, Gou J, Hui D (2017) 3D printing of polymer matrix composites: a review and prospective. *Compos Part B Eng* 110:442–458
97. Xu F, Celli J, Rizvi I, Moon S, Hasan T, Demirci U (2011) A three-dimensional in vitro ovarian cancer coculture model using a high-throughput cell patterning platform. *Biotechnol J* 6:204–212
98. Stonebraker M, Çetintemel U (2018) “One size fits all” an idea whose time has come and gone. In: *Making databases work: the pragmatic wisdom of Michael Stonebraker*, pp. 441–462
99. Belialov F (2014) Does personalized medicine have a future? *Klin Med* 92:73–74
100. She A, Zhang S, Shian S, Clarck DR, Capasso F (2018) Large area metalenses: design, characterization, and mass manufacturing. *Opt Express* 26:1573–1585
101. Tofail SA, Koumoulos EP, Bandyopadhyay A, Bose S, O’Donoghue L, Charitidis C (2018) Additive manufacturing: scientific and technological challenges, market uptake and opportunities. *Mater Today* 21:22–37

102. Clark DP (2009) Seize the opportunity: underutilization of fine-needle aspiration biopsy to inform targeted cancer therapy decisions. *Cancer Cytopathol* 117:289–297
103. Mathur L, Ballinger M, Utharala R, Merten CA (2020) Microfluidics as an enabling technology for personalized cancer therapy. *Small* 16:1904321
104. Ying L, Wang Q (2013) Microfluidic chip-based technologies: emerging platforms for cancer diagnosis. *BMC Biotechnol* 13:1–10
105. Gorges TM, Tinhofe I, Drosch M, Röse L, Zollner TM, Krahn T et al (2012) Circulating tumour cells escape from EpCAM-based detection due to epithelial-to-mesenchymal transition. *BMC Cancer* 12:1–13
106. Lehr C-M, Haas J (2002) Developments in the area of bioadhesive drug delivery systems. *Expert Opin Biol Ther* 2:287–298
107. Bischoff KB (1975) Some fundamental considerations of the applications of pharmacokinetics to cancer chemotherapy. *Cancer Chemother Rep* 59:777–793
108. Garattini S (2007) Pharmacokinetics in cancer chemotherapy. *Eur J Cancer* 43:271–282
109. Bhushan B, Khanadeev V, Khlebtsov B, Khlebtsov N, Gopinath P (2017) Impact of albumin based approaches in nanomedicine: imaging, targeting and drug delivery. *Adv Colloid Interf Sci* 246:13–39
110. Senapati S, Mahanta AK, Kumar S, Maiti P (2018) Controlled drug delivery vehicles for cancer treatment and their performance. *Signal Transduct Target Ther* 3:1–19
111. Fisher OZ, Kim T, Dietz SR, Peppas NA (2009) Enhanced core hydrophobicity, functionalization and cell penetration of polybasic nanomatrices. *Pharm Res* 26:51–60
112. Zhang YR, Luo JQ, Zhang JY, Miao WM, Wu JS, Huang H et al (2020) Nanoparticle-enabled dual modulation of phagocytic signals to improve macrophage-mediated cancer immunotherapy. *Small* 16:2004240
113. Pan AC, Borhani DW, Dror RO, Shaw DE (2013) Molecular determinants of drug–receptor binding kinetics. *Drug Discov Today* 18:667–673
114. Truong NP, Whittaker MR, Mak CW, Davis TP (2015) The importance of nanoparticle shape in cancer drug delivery. *Expert Opin Drug Deliv* 12:129–142
115. Wang Y, Chen L (2011) Quantum dots, lighting up the research and development of nanomedicine. *Nanomed Nanotechnol Biol Med* 7:385–402
116. Russo G, Zegar C, Giordano A (2003) Advantages and limitations of microarray technology in human cancer. *Oncogene* 22:6497–6507
117. Das R, Fernandez JG (2020) Additive manufacturing enables production of de novo cardiomyocytes by controlling embryoid body aggregation. *Bioprinting* 20:e00091
118. Dlamini Z, Francies FZ, Hull R, Marima R (2020) Artificial intelligence (AI) and big data in cancer and precision oncology. *Comput Struct Biotechnol J* 18:2300–2311
119. Park DJ, Park MW, Lee H, Kim Y-J, Kim Y, Park YH (2021) Development of machine learning model for diagnostic disease prediction based on laboratory tests. *Sci Rep* 11:1–11
120. Cruz JA, Wishart DS (2006) Applications of machine learning in cancer prediction and prognosis. *Cancer Inform* 2:117693510600200030
121. Adam G, Rampášek L, Safikhani Z, Smirnov P, Haibe-Kains B, Goldenberg A (2020) Machine learning approaches to drug response prediction: challenges and recent progress. *NPJ Precis Oncol* 4:1–10
122. Cui M, Zhang DY (2021) Artificial intelligence and computational pathology. *Lab Investig* 101:412–422
123. Ngiam KY, Khor W (2019) Big data and machine learning algorithms for health-care delivery. *Lancet Oncol* 20:e262–e273
124. Jain V, Chatterjee JM (2020) Machine learning with health care perspective. Springer, Cham
125. Chartrand G, Cheng PM, Vorontsov E, Drozdal M, Turcotte S, Pal CJ et al (2017) Deep learning: a primer for radiologists. *Radiographics* 37:2113–2131
126. Ahuja AS (2019) The impact of artificial intelligence in medicine on the future role of the physician. *PeerJ* 7:e7702


127. Davenport T, Kalakota R (2019) The potential for artificial intelligence in healthcare. *Future Healthc J* 6:94
128. Vigneron N (2015) Human tumor antigens and cancer immunotherapy. *BioMed Res Int* 2015: 948501
129. Cai L, Xu J, Yang Z, Tong R, Dong Z, Wang C et al (2020) Engineered biomaterials for cancer immunotherapy. *MedComm* 1:35–46
130. Li T, Zhang M, Wang J, Wang T, Yao Y, Zhang X et al (2016) Thermosensitive hydrogel co-loaded with gold nanoparticles and doxorubicin for effective chemoradiotherapy. *AAPS J* 18:146–155
131. Neek M, Kim TI, Wang S-W (2019) Protein-based nanoparticles in cancer vaccine development. *Nanomed Nanotechnol Biol Med* 15:164–174
132. Yang C, Bromma K, Ciano-Oliveira D, Zafarana G, van Prooijen M, Chithrani DB (2018) Gold nanoparticle mediated combined cancer therapy. *Cancer Nanotechnol* 9:1–14
133. Chaplin DD (2010) Overview of the immune response. *J Allergy Clin Immunol* 125:S3–S23
134. Bellmunt J, Moreno I (2017) Immunotherapy and targeted therapies in advanced castration resistant prostate cancer. In: *Management of prostate cancer*, Springer, pp 357–377
135. Drake CG (2010) Prostate cancer as a model for tumour immunotherapy. *Nat Rev Immunol* 10:580–593
136. Bou Nasser Eddine F, Ramia E, Tosi G, Forlani G, Accolla RS (2017) Tumor immunology meets. . . immunology: modified cancer cells as professional APC for priming naive tumor-specific CD4+ T cells. *Onco Targets Ther* 6:e1356149
137. Lotfi N, Thome R, Rezaei N, Zhang G-X, Rezaei A, Rostami A et al (2019) Roles of GM-CSF in the pathogenesis of autoimmune diseases: an update. *Front Immunol* 10:1265
138. Cheever MA, Higano CS (2011) PROVENGE (Sipuleucel-T) in prostate cancer: the first FDA-approved therapeutic cancer vaccine. *Clin Cancer Res* 17:3520–3526
139. McCarthy EF (2006) The toxins of William B. Coley and the treatment of bone and soft-tissue sarcomas. *Iowa Orthop J* 26:154
140. Buffen K, Oosting M, Quintin J, Ng A, Kleinnijenhuis J, Kumar V et al (2014) Autophagy controls BCG-induced trained immunity and the response to intravesical BCG therapy for bladder cancer. *PLoS Pathog* 10:e1004485
141. Hollingsworth RE, Jansen K (2019) Turning the corner on therapeutic cancer vaccines. *NPJ Vaccines* 4:1–10
142. Stephens AJ, Burgess-Brown NA, Jiang S (2021) Beyond just peptide antigens: the complex world of peptide-based cancer vaccines. *Front Immunol* 12:2629
143. Tran T, Blanc C, Granier C, Saldmann A, Tanchot C, Tartour E (2019) Therapeutic cancer vaccine: building the future from lessons of the past. In: *Seminars in immunopathology*, vol 41. Springer, pp 69–85
144. Rosendahl Huber S, van Beek J, de Jonge J, Luytjes W, van Baarle D (2014) T cell responses to viral infections—opportunities for peptide vaccination. *Front Immunol* 5:171
145. Carbone FR, Gleeson PA (1997) Carbohydrates and antigen recognition by T cells. *Glycobiology* 7:725–730
146. Sanandiya ND, Vasudevan J, Das R, Lim CT, Fernandez JG (2019) Stimuli-responsive injectable cellulose xithogel for cell encapsulation. *Int J Biol Macromol* 130:1009–1017
147. Whitesides GM, Wong AP (2006) The intersection of biology and materials science. *MRS Bull* 31:19–27
148. Shubhika K (2012) Nanotechnology and medicine—the upside and the downside. *Int J Drug Dev Res* 5:1–10
149. Chen Y, Jungsuwadee P, Vore M, Butterfield DA, St Clair DK (2007) Collateral damage in cancer chemotherapy: oxidative stress in nontargeted tissues. *Mol Interv* 7:147
150. Chao Y, Chen Q, Liu Z (2020) Smart injectable hydrogels for cancer immunotherapy. *Adv Funct Mater* 30:1902785
151. Fabbro C, Ali-Boucetta H, Da Ros T, Kostarelos K, Bianco A, Prato M (2012) Targeting carbon nanotubes against cancer. *Chem Commun* 48:3911–3926

152. Kandasamy G, Maity D (2015) Recent advances in superparamagnetic iron oxide nanoparticles (SPIONs) for in vitro and in vivo cancer nanotheranostics. *Int J Pharm* 496: 191–218
153. Kobayashi H, Turkbey B, Watanabe R, Choyke PL (2014) Cancer drug delivery: considerations in the rational design of nanosized bioconjugates. *Bioconjug Chem* 25:2093–2100
154. Laheru D, Lutz E, Burke J, Biedrzycki B, Solt S, Onners B et al (2008) Allogeneic granulocyte macrophage colony-stimulating factor–secreting tumor immunotherapy alone or in sequence with cyclophosphamide for metastatic pancreatic cancer: a pilot study of safety, feasibility, and immune activation. *Clin Cancer Res* 14:1455–1463
155. Madani SY, Naderi N, Dissanayake O, Tan A, Seifalian AM (2011) A new era of cancer treatment: carbon nanotubes as drug delivery tools. *Int J Nanomedicine* 6:2963
156. Narayanaswamy R, Torchilin VP (2019) Hydrogels and their applications in targeted drug delivery. *Molecules* 24:603
157. Neuse EW (2008) Synthetic polymers as drug-delivery vehicles in medicine. *Metal-Based Drugs* 2008:469531
158. Reshma V, Mohanan P (2019) Quantum dots: applications and safety consequences. *J Lumin* 205:287–298
159. Sharma D, Ali AAE, Trivedi LR (2018) An updated review on: liposomes as drug delivery system. *PharmaTutor* 6:50–62
160. Talebian S, Foroughi J, Wade SJ, Vine KL, Dolatshahi-Pirouz A, Mehrali M et al (2018) Biopolymers for antitumor implantable drug delivery systems: recent advances and future outlook. *Adv Mater* 30:1706665
161. Thakur CK, Thotakura N, Kumar R, Kumar P, Singh B, Chitkara D et al (2016) Chitosan-modified PLGA polymeric nanocarriers with better delivery potential for tamoxifen. *Int J Biol Macromol* 93:381–389
162. Welters MJ, van der Sluis TC, van Meir H, Loof NM, van Ham VJ, van Duikeren S et al (2016) Vaccination during myeloid cell depletion by cancer chemotherapy fosters robust T cell responses. *Sci Transl Med* 8:334ra352
163. Youlin K, Li Z, Xiaodong W, Xiuheng L, Hengchen Z (2012) Combination immunotherapy with 4-1BBL and CTLA-4 blockade for the treatment of prostate cancer. *Clin Dev Immunol* 2012:439235
164. Zhang H, Yee D, Wang C (2008) Quantum dots for cancer diagnosis and therapy: biological and clinical perspectives. *Nanomedicine (Lond)* 3(1):83–91
165. Zhao N, Woodle MC, Mixson AJ (2018) Advances in delivery systems for doxorubicin. *J Nanomed Nanotechnol* 9



Advancing Tumor Microenvironment Research by Combining Organs-on-Chips and Biosensors

7

Isabel Calejo , Marcel Alexander Heinrich , Giorgia Zambito, Laura Mezzanotte , Jai Prakash , and Liliana Moreira Teixeira 

Abstract

Organs-on-chips are microfluidic tissue-engineered models that offer unprecedented dynamic control over cellular microenvironments, emulating key functional features of organs or tissues. Sensing technologies are increasingly becoming an essential part of such advanced model systems for real-time detection of cellular behavior and systemic-like events. The fast-developing field of organs-on-chips is accelerating the development of biosensors toward easier integration, thus smaller and less invasive, leading to enhanced access and detection of (patho-) physiological biomarkers. The outstanding combination of organs-on-chips and biosensors holds the promise to contribute to more effective treatments, and, importantly, improve the ability to detect and monitor several diseases at an earlier stage, which is particularly relevant for complex diseases such as cancer. Biosensors coupled with organs-on-chips are currently being devised not only to determine therapy effectiveness but also to identify emerging cancer biomarkers and targets. The ever-expanding use of imaging modalities for

I. Calejo · L. Moreira Teixeira (✉)

Department of Developmental Bioengineering, Technical Medical Centre, University of Twente, Enschede, The Netherlands

e-mail: h.i.calejo@utwente.nl; l.moreirateixeira@utwente.nl

M. A. Heinrich · J. Prakash

Department of Advanced Organ Bioengineering and Therapeutics, Section: Engineered Therapeutics, Technical Medical Centre, University of Twente, Enschede, The Netherlands

e-mail: m.a.heinrich@utwente.nl; j.prakash@utwente.nl

G. Zambito · L. Mezzanotte

Department of Radiology and Nuclear Medicine, Erasmus Medical Center, Rotterdam, The Netherlands

Department of Molecular Genetics, Erasmus Medical Center, Rotterdam, The Netherlands

e-mail: g.zambito@erasmusmc.nl; l.mezzanotte@erasmusmc.nl

© The Author(s), under exclusive license to Springer Nature Switzerland AG 2022

171

D. Caballero et al. (eds.), *Microfluidics and Biosensors in Cancer Research*,

Advances in Experimental Medicine and Biology 1379,

https://doi.org/10.1007/978-3-031-04039-9_7

optical biosensors oriented toward on-chip applications is leading to less intrusive and more reliable detection of events both at the cellular and microenvironment levels. This chapter comprises an overview of hybrid approaches combining organs-on-chips and biosensors, focused on modeling and investigating solid tumors, and, in particular, the tumor microenvironment. Optical imaging modalities, specifically fluorescence and bioluminescence, will be also described, addressing the current limitations and future directions toward an even more seamless integration of these advanced technologies.

Keywords

Microfluidic systems · Organs-on-chips · Cancer · Tumor microenvironment · Biosensors · Imaging · Bioluminescence

7.1 Introduction

Organ-on-chip (OoC) technology, or physiological microsystems, is a rapidly emerging field, which, by extension, leads to major impacts on the development of biosensors and imaging techniques. OoCs are microfluidic living cell culture devices, comprising micrometer-sized chamber networks, and are designed to emulate (human) tissue- and organ- (patho-) physiology as well as respective key functional features [1]. The seamless integration of biosensors with OoC allows for straightforward screening of specific tissue or cellular events, or even molecular processes [2]. The combination with advanced (molecular) imaging techniques renders these state-of-the-art *in vitro* models with the unique ability to provide quantitative spatial and temporal information that can be used for investigating organ/tissue (patho-) physiological mechanisms, and/or for drug development. These new mechanistic and holistic insights are expected to lead to future advancements in personalized medicine and disease modeling.

The combination between OoC and biosensors allows for more sensitive and precise measurements over complex tissues. Furthermore, the blend of these fields is leading to the development of smaller sensors and less invasive detection methods, which results in improved access to and easier detection of (patho-) physiological markers. Together, both technologies are expected to not only lead to more effective treatments but also importantly, to improve the ability to detect several diseases at an earlier stage, which might drastically enhance patient survival. This is particularly relevant for complex diseases, such as cancer. Over 50% of cancer occurrences are only diagnosed after the malignant tumor has metastasized [3]. This late diagnosis often leads to more deadly cases and increases the difficulty of treatment. Cancer biomarkers are fundamental indicators for diagnosis, the monitoring of tumor growth and are key to defining the most suitable treatment strategy for the patient [4]. The development of advanced model systems, such as OoC, with integrated biosensors to detect cancer biomarkers, could have a major impact, allowing better prediction of disease progression and evaluation of treatment efficacy. This new

technological approach not only offers the possibility of multitarget detection of multiple biomarkers but likewise facilitates the assessment of propensity of cancer progression toward secondary tissues, enabled by multi-organ-on-chip platforms. Even though the complexity and diversity of cancer presents several challenges, biosensor and OoC technologies offer a higher degree of variable control and human specificity, while significantly less time-consuming, more cost-effective and more ethically desirable than animal alternatives. It is expected that in the upcoming 10 years, this combination of technologies will revolutionize cancer therapy development, toward a personalized medicine approach [5].

Cancer biomarkers and respective biosensors can assist on (earlier) disease detection, facilitate diagnosis/prognosis, and can improve imaging of tumors and their associated microenvironments [6]. These features can ultimately support and advance drug targeting and delivery. In more detail, biomarkers, which are molecular recognition elements or signals, are converted by different signal transducers into quantifiable/analyzable electric or digital signals. These transducers may be mass-based, calorimetric, electrochemical, or optical. The latter includes interferometry, colorimetry, fluorescence, and luminescence. When integrated into OoC, these advanced monitoring tools and coupled read-outs provide spatial-temporal information on the tumor and its microenvironment, possibly also incorporating inline detection of pharmacodynamics of anti-cancer drug responses [7]. OoC coupled biosensors permit multiplexing and online monitoring of several physico-chemical parameters associated with the tumor microenvironment (TME), including pH, osmolarity, O₂, CO₂, protein content, metabolites, and/or degree of DNA methylation, characteristically in short-time and using reduced sample volumes. In parallel, these biosensors may also offer information over biological processes, with a focus on assessing cellular behavior and their context, thus, cell–cell and cell–matrix interactions, typically using imaging-based detection [8].

The purpose of this chapter is to provide a comprehensive overview of biosensors and their integration on OoC platforms, focusing on applications toward modeling and investigating the TME. Recent advances in biosensors and innovative imaging modalities on-chip will be described, with particular emphasis on optical imaging modalities, namely fluorescence and bioluminescence techniques. Furthermore, it will provide a perspective on future directions for hybrid approaches combining OoC and biosensors, anticipated to increase predictive efficacy while decreasing time and costs associated with bringing novel cancer therapeutics or biologics toward clinical translation.

7.2 The Tumor Microenvironment

Most people are familiar with the concept, that cancer is caused by the abnormal growth of cells, called neoplasia, eventually forming a tumor [9, 10]. These tumors can be benign or malignant, and only the latter describes the situation known as “cancer” [10]. However, most solid tumors do not solely consist of these neoplastic cells but malignant tumors also gradually change the environment around them as

they develop, creating what is known as the tumor TME. Already back in 1986, Harold F. Dvorak stated correctly that tumors are “wounds that never heal” and further described the development of the TME as “wound healing gone awry” [11, 12]. Although Dvorak made this observation 35 years ago, his description still defines the underlying nature of the TME in a correct way. In the early stages of tumor development, tumor cells cause an inflammatory response in the surrounding tissue, which induces a wound healing response [9]. During the further development, however, tumor cells gradually change this surrounding tissue, which is often also referred to as the tumor stroma, the non-neoplastic parts of the TME, toward a tumor supporting environment, characterized by an in general anti-inflammatory behavior that is eventually supporting the progression and invasion of tumors as well as increasing the resistance to therapy and immune clearance. The TME in each cancer type can vary drastically depending on the surrounding environment, however, in general, tumors can be divided into fibrotic and non-fibrotic tumors.

7.2.1 The TME in Fibrotic Tumors

Due to the high prevalence and often high mortality of fibrotic tumors, such as breast, lung, or pancreatic cancer, a lot of research in recent years focused on identifying the components and underlying biological process in the TME of these tumors [13–15]. Although in general every cancer type has its own specific TME, most fibrotic cancers share similar characteristics when it comes to the cellular and acellular compositions of the TME. Fibrotic tumors are often characterized by an abundance of cancer-associated fibroblasts (CAFs), which deposit an excess amount of extracellular matrix (ECM) proteins such as collagen, fibronectin, laminin or hyaluronic acid, creating a dense and fibrotic environment, hence the definition of a fibrotic tumor [9, 15, 16]. In pancreatic ductal adenocarcinoma (PDAC), for example, CAFs account for around 80% of the tumor stroma, making it one of the most fibrotic tumors known today [17–20]. Other cellular components in the TME are tumor-associated macrophages (TAMs), neutrophils, infiltrating regulatory T cells (Treg cells), myeloid-derived suppressor cells (MDSCs), and natural killer cells (NK cells) as well as endothelial cells and pericytes forming the vasculature in tumors (Fig. 7.1) [9, 16]. The interaction of tumor cells with these stromal cells can play a significant role in the progression, metastasis, and immune evasion of tumors. In the following sections, we will briefly discuss each of these components in greater detail.

7.2.1.1 Cancer-Associated Fibroblasts (CAFs)

As aforementioned, in fibrotic tumors, CAFs are often the most prevalent cell type in the TME. In general, fibroblasts are a natural component of the wound healing response taking place in tumor development [21–24]. During that phase, fibroblasts are actively recruited by tumor cells via growth factors such as fibroblasts growth factor (FGF) or platelet-derived growth factor (PDGF) [24, 25]. The interaction of

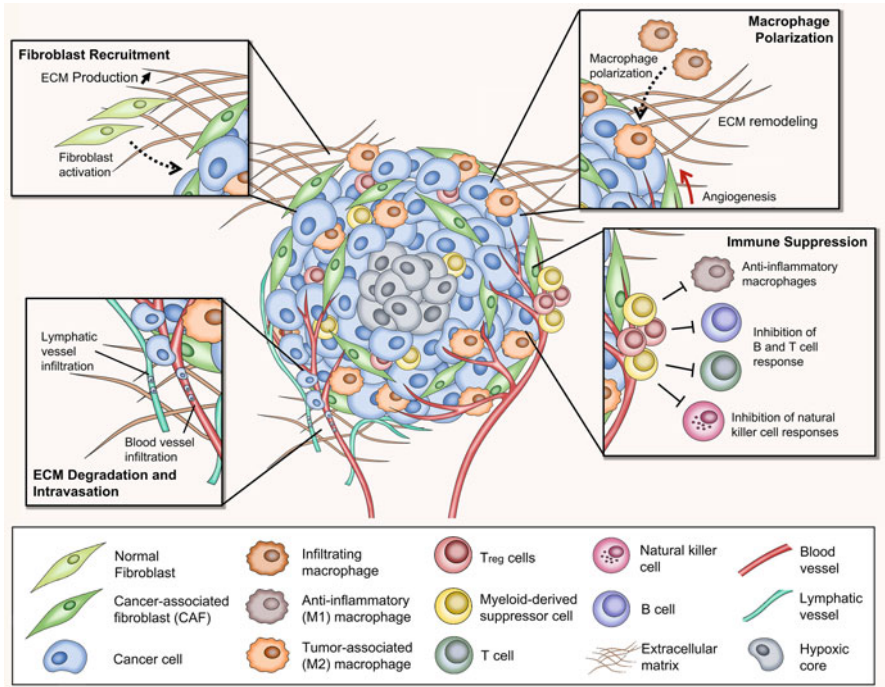


Fig. 7.1 The tumor microenvironment. Schematic representation of the TME describing different crucial processes such as the recruitment of fibroblasts, polarization of macrophages, immune suppression as well as ECM degradation allowing tumor cells to intravasate and metastasize. *ECM* Extracellular matrix, *Treg* regulatory T cell. Copyright © The author(s) 2020. Published by Elsevier Inc

these fibroblasts with tumor cells and in autocrine fashion results in an activated cancer-associated state. CAFs can originate from several different sources, including mesenchymal stromal cells, infiltrating fibroblasts, or tissue-resident fibroblasts [9, 26, 27]. For instance, in PDAC, CAFs originate from tissue-resident pancreatic stellate cells that upon crosstalk with tumor cells achieve an activated state [28, 29]. For a long time, CAFs have been thought to solely present a myofibroblast-like phenotype (myCAFs), characterized by a high expression of alpha-smooth muscle actin (α SMA) and PDGF receptor beta (PDGFR β) [30]. However, in recent years, several other subtypes of CAFs have been identified including inflammatory CAFs (iCAFs), lacking the expression of α SMA but highly express interleukin-6, or antigen-presenting CAFs (apCAFs), which highly express major histology complex II (MHCII) [31, 32]. It has been shown that the proximity to tumor cells can directly alter the phenotype of CAFs, where fibroblasts in direct contact obtain a myCAF phenotype, and distant fibroblasts an iCAF phenotype [31, 32]. As such, different subpopulations have only recently been identified, it is shown that a lot of underlying biological processes and interactions are not yet fully understood and potential other subpopulations might yet to be discovered. In

general, CAFs are known to produce an excess amount of ECM as previously mentioned. This causes a high desmoplasia in tumors creating a very dense and pressurized environment, which is hard for any anti-cancer therapeutics to overcome [9, 16]. Furthermore, this dense stromal barrier increases hypoxic and necrotic conditions in the TME, which has effects on the invasive behavior of tumor cells as well as on the immune response. CAFs have also been shown to secrete different cytokines such as stromal-derived factor (SDF), metalloproteinases (MMPs) or vascular endothelial growth factor (VEGF), actively shaping the TME and promoting the vascularization of tumors [24, 25, 33]. Furthermore, CAFs have also been shown to play a role in immune suppression by the secretion of transforming growth factor beta (TGF β) or programmed death-ligand 1 (PD-L1). Due to their abundance in fibrotic tumors, CAFs have also been the target of recently developed therapies that aim to modulate the TME to reduce the CAF-mediated growth and invasion and to increase the efficacy of conventional therapies to overcome the dense stromal barrier [26, 34, 35].

7.2.1.2 The Tumor Immune Micro-Environment (TIME)

One of the main characteristics of tumors is that they are able to escape the natural immune response, which, as part of the inflammatory response, should actively recognize and kill tumor cells. However, in recent years, it became apparent that tumors can evade the immune response and “brainwash” infiltrating immune cells to their advantage [36]. The TIME comprises several different immune cells, either resident or infiltrating, such as TAMs, T cells, neutrophils, MDSCs, and NK cells, which will be discussed in more detail in this section.

Tumor-Associated Macrophages (TAMs)

After CAFs, TAMs form the second most prevalent cell type in the TME [9, 37, 38]. Originally TAMs have been described as M2-like anti-inflammatory macrophages, opposing to M1 inflammatory macrophages. Yet, more recently, it has become clear that the classic categorization of M1 and M2 macrophages is not comprising all subsets of macrophages that have been identified [39, 40]. As a result, TAMs are often regarded a macrophage subtype on their own. The hypoxic conditions in the TME promote macrophage influx into the tumor. Furthermore, tumor cells are also known to actively recruit macrophages by the secretion of colony-stimulating factor 1 (CSF-1), IL-6 or C-C motif chemokine ligand (CCL2). Within the TME, the presence of IL-4, IL-13, IL-10, and TGF β is polarizing infiltrated macrophages toward a TAM-like phenotype. Once polarized, TAMs are actively involved in several processes such as the progression of tumor cells, recruitment of fibroblasts via FGF expression, promotion of angiogenesis via VEGF expression, remodeling of the ECM via the expression of several MMPs, as well as in the suppression of other immune components via the secretion of TGF β and IL-10 [24, 36, 39, 40]. Given their importance in several tumor-related processes, the modulation or education of TAMs has become a promising treatment strategy against several cancer types forming one of the main targets of immunotherapy.

T Cells, Neutrophils, Myeloid-Derived Suppressor Cells (MDSCs), and Natural Killer (NK) Cells

In general, the high presence of TGF β and PD-L1, mediated by tumor cells, CAFs, and TAMs in the TME create a highly immune-suppressive environment [24, 41]. While, for instance, CD8⁺ T cells, the main anti-tumor cells in the human body, are still present during the early stages of tumor development, at later stages these cells often become exhausted and the presence of PD is highly limiting their function. As a result, later-stage tumors often lack CD8⁺ T cell in their TME. Similarly, tumors lack the presence of anti-tumoral CD4⁺ T cells [41]. The lack of CD8⁺ also limits the presence of N1 neutrophils in the TME, which show anti-tumoral activity mediated by the secretion of IL-12, interferon-gamma (IFN γ) and TNF by CD8⁺ T cells [42, 43]. However, the lack of these cells, in combination with high TGF β levels, favors the presence of N2 neutrophils, which themselves are pro-tumoral by the secretion of MMP9, HFG, or VEGF [42, 43]. TGF β secretion in combination with other secreted factors, such as IL1, IL6, granulocyte macrophage-colony stimulating factor (GM-CSF) or C-X-C motif chemokine ligand 12 (CXCL12) also enhances the influx of MDSCs into the TME, which further increases the immunosuppressive characteristics [24, 44]. This highly immunosuppressive TME also prevents the presence of NK cells in the TME, which would actively kill tumor cells as via cell surface receptors such as MHCI, or natural killer group 2D (NKG2D) or induce CD8⁺ T cells by secretion of IFN γ [45, 46]. Altogether, the immunosuppressive crosstalk in the TME favors tumor progression and invasion by altering the function and efficacy of the body's own defense system. The re-activation of this defense has become an interesting and promising strategy to treat different tumors and so far it has shown promising results [36]. One of the most well-known strategies to re-activate the immune system was presented by James P. Allison and Tasuku Honjo, who received the Nobel prize in 2018 for their strategy to block the function of CTLA4 and PD-1 using specific antibodies, which eventually promoted the tumor-killing potential of the immune system [47].

7.2.1.3 The Tumor Vasculature

The vasculature in tumors displays significant differences compared to the healthy counterpart throughout the body. The often rapid and uncontrolled formation of blood vessels in the TME creates vessels that are leaky in nature presenting structural gaps in the endothelial layer [48]. As a matter of fact, the treatment of solid tumors in the last years mainly relied on this leaky vasculature as main strategy to target the tumors, as the leaky vasculature caused what is known as the enhanced permeability and retention (EPR) effect [48]. The EPR effect describes the accumulation of intravenously administered drugs in tumors. Especially drugs that present a higher circulation time in the body have a higher chance to accumulate in the tumor over time, which motivated the use of nanomedicines (therapeutics in combination with a nanocarrier system) to prolong their circulation time [48]. However, the high desmoplasia in fibrotic tumors creates a high intratumoral pressure, preventing therapeutics from extravasating despite the leaky vasculature [20, 49]. Furthermore, this desmoplasia and pressure causes the vasculature in these tumors to compress

and collapse so that therapeutics cannot reach the tumor in the first place [50, 51]. Recent studies have shown that the modulation of the TME, for instance, inhibition of CAFs, can lead to a re-opening of the vasculature, which, subsequently, enhanced the drug perfusion and efficacy [34].

7.2.2 The TME in Non-fibrotic Tumors

In general, the TME in non-fibrotic tumors is similar to the TME in fibrotic ones. The main difference derives from the typical lack of fibrosis in “non-fibrotic” tumors, based on the absence of CAFs. One of the most well-known examples of a non-fibrotic tumor is glioblastoma multiforme (GBM), the most malignant type of brain cancer [52–54]. Although the TME in glioblastoma lacks CAFs, the general immune environment in GBM is similar to the TME in fibrotic tumors, presenting the same immunosuppressive environment and properties [53, 55]. One cell type that is only present in GBM are tumor-associated astrocytes (TAAs), originating from brain resident astrocytes [56, 57]. It has been shown that these TAAs play a crucial role in the progression and invasion of GBM, as well as in the immunosuppressive and anti-inflammatory environment in GBM, based on their crosstalk with tumor-associated microglia, originating from brain-resident microglia depicting similar functions as TAMs [58, 59]. In general, the TME in GBM is less understood compared to fibrotic tumors. Nevertheless, different treatment strategies, such as the inhibition of tumor-associated microglia using immunotherapy has shown promising results in preclinical stages [60].

Altogether, the TME in fibrotic and non-fibrotic tumors displays a complex network of cellular and acellular components that are all in constant crosstalk and interaction. This often results in a very dense environment that prevents therapeutics from reaching their target as well as prevents the body’s immune systems to function properly. The modulation of the TME by either inhibiting or reducing the high desmoplasia in fibrotic tumors or by re-activating the immune system has shown promising results in recent years. Yet a lot of interactions in the TME remain to be discovered and understood, so that more efficient treatment strategies can be designed. While in the past, animal models were often used to identify such interactions, these models hardly present an optimal environment to investigate certain cell–cell or cell–ECM interactions in greater detail due to the high complexity of such models. Furthermore, animals arguably display too large differences in anatomy and physiology compared to human, which makes it difficult to translate found interactions to the human setting. Contrastively, 3D *in vitro* models, such as OoC platforms, have found wide applications to understand biological interactions in greater detail in a controlled and biologically relevant environment [61]. In this context, high-throughput and modular OoC technologies are introduced aiming at reconstructing the *in vivo* TME in a more reliable way for cancer research. Namely, tumor-on-chip systems can replicate key *in vivo* TME features, exhibiting great promise as more pragmatic and detailed platforms for studying tumor metastasis, distribution and mechanisms of growth, not withdrawing, drug toxicity, and

therapeutic efficacy. The superiority of these platforms as candidates for conventional preclinical models has attracted worldwide research attention, and great amounts of scientific progress have been made in promoting a broader adoption of these platforms.

7.3 Organs-on-Chips: Living Microfluidic Cell Platforms

The development of OoC requires the unique combination of four key components: (a) engineering approaches (microtechnology, such as microfluidics and microfabrication; tissue engineering); (b) biological methodologies (including cell biology and immunology); (c) drug delivery; and, (d) advanced biosensing and imaging technologies (Fig. 7.2a) [61]. The ultimate goal of these next-generation models is not to build a whole living organ or tissue, but rather to mimic their minimal functional units, as physical, biochemical, and biological (micro) environments. Interestingly, OoC also uniquely permit controlling basic mechanical and extracellular cues that enable the recapitulation *in vitro* of a given tissue or key organ functions. The first OoC models were initially introduced in the early 2000s [62]. These earlier models typically consist of a single, perfused microfluidic chamber containing one kind of cell, mostly exhibiting functions of one tissue type [1]. Even though these individual systems provide useful information regarding the physiological responses of the target organ, they often do not truly replicate the naturally occurring interactions between the different tissues/organs as observed in the human body [63]. Therefore, more complex designs, with two or more microchannels connected by porous membranes, lined on opposite sides by different cell types, have been devised, aiming at the recreation of interfaces between different tissues [1], as the example of blood-brain barrier-on-chip [64–66]. Additionally, different individual OoC devices can be vascularly interconnected to build multi-organs-on-chip (Fig. 7.2b), also commonly referred to as human-on-chip, to study organ–organ or tissue/tissue crosstalk [67], drugs pharmacokinetics/dynamics (ADME processes) [68], cancer metastasis [69] and development of personalized treatments [70] (Fig. 7.2c).

7.3.1 Multi-Organ-on-Chip: The Power of Inter-Organ Communication

Multi-organ-on-chip (multi-OoC) platforms have shown great potential to redefine the way in which human health research is driven. Briefly, these platforms can be divided into two main distinct types: (1) single OoC units (the “Lego-like” approach), likely to be preferred for more fundamental research in an academic setting; and (2) multi-OoC platforms that, in contrast, offer higher throughput, and, hence, are more appropriate for the identification of biomarkers, therapeutic targets, and selection of drug candidates [71]. Multi-organ disease modeling typically suffers from the poor accessibility of some organs and the fact that different cell types are

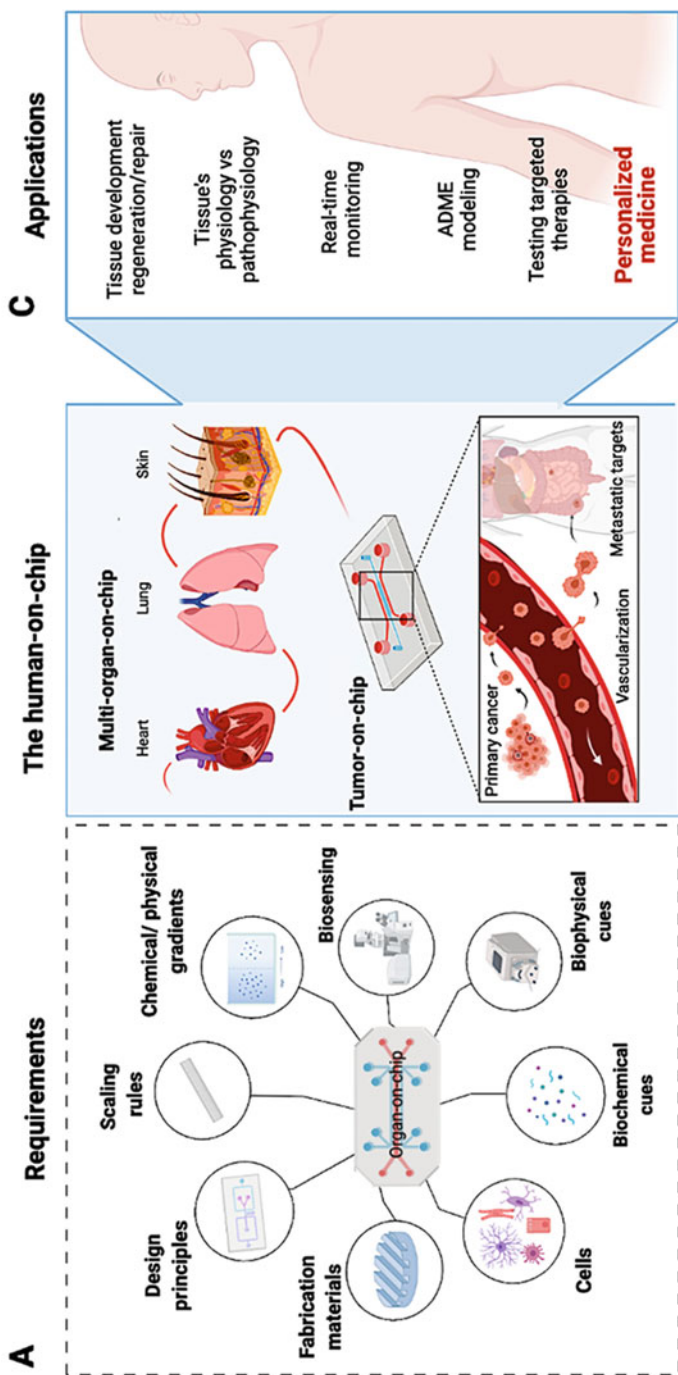


Fig. 7.2 Schematic representation of organ-on-chip devices and body-on-chip applications. (a) The incorporation of key components of tissue engineering, microfabrication, and stem cell biology techniques into organ-on-chip technology. (b) Individual OoC organ/tissue modules may be interconnected to study organ-organ or tissue/tissue crosstalk in a more systemic-like manner, also commonly referred as multi-organs-on-chip or human-on-chip, which is of particular interest to model complex diseases, such as cancer and cancer metastasis. (c) OoC systems offer myriad applications, including, but not limited to, health and disease modeling, drugs pharmacokinetics/dynamics, enabling the development/screening of personalized treatments. Created with [BioRender.com](https://www.biorender.com)

required in the overall metabolic homeostasis. In this context, multi-OoC approaches can provide more complex disease models while giving information on key molecular mechanisms [47]. Taking as an example the COVID-19, multi-organ-on-chip devices that included a lung model containing COVID-19 infected cells from patients, could be combined with other organs to evaluate possible co-effects in cardiovascular, liver, and kidney tissues, as it was already reported to occur in patients [72, 73]. Diabetes type 2 mellitus [50] have also been modeled by taking advantage of multi-OoC, using co-cultures of human pancreatic islets and liver spheroids which maintained postprandial glucose concentrations in circulation, thereby mimicking the feedback loop that controls glucose consumption and insulin secretion, while in single cultures, glucose levels remained elevated in both organ modules [74]. Another example highlights the importance of the development of multi-OoCs to understand the processes involved in cancer metastatic cascade and for the design of new treatments. These chips can replicate the complex 3D microstructure and, thus the TME or TIME, providing a better understanding of the mechanisms of tumor growth, importance of microvascularization and, consequently, metastasis. For instance, a multi-OoC model enabled the spreading of lung tumor cells into distant organs (brain, liver, and bone), all equipped with a microvasculature, and demonstrated the metastasis of cells in all three organs [75].

Nowadays, strong evidence demonstrated that organs-on-chips are capable of reproducing human organ physiology and organ-level features of disease at both, the single person to (sub-)population levels. These bioengineered systems allow the application of different features in cell culture, such as relative cell ratios, tissue's spatial arrangement and ECM (3D tissue/organ architecture and physical cues), fluid flow, defined circulating fluid (which may contain chemical cues), and mechanical cues. Altogether, these features provide unprecedented flexibility in dissecting and decoupling the cellular, molecular, chemical, and physical contributors to tissue and organ function, as well as disease development, namely cancer, as briefly discussed above.

7.3.2 Tumor and Tumor Microenvironment On-Chip Modeling

Indeed the composition of the TME and its stromal interactions are major factors that exacerbate tumor growth and metastasis, typically resulting in poor clinical outcomes [76, 77]. Over the years, increasing evidence has demonstrated that the activated stroma is a disease-defining factor, stressing it as an important player in cancer cell migration, invasion/extravasation, angiogenesis, drug resistance [78, 79], stemness of cancer cells [80], and tumor immunosurveillance evasion [81]. As explained in detail earlier in this chapter, the non-neoplastic component of the TME is composed of abundant ECM and multiple cells types, namely endothelial cells, pericytes, CAFs, immune cells, and less prevalent mesenchymal stromal cells (MSCs) and platelets [82]. Bi-directional interactions are described to actively occur between stromal cells and tumor cells, and with the ECM by the secretion of growth factors (GFs), chemokines, enzymes, extracellular vesicles, and microRNAs, known

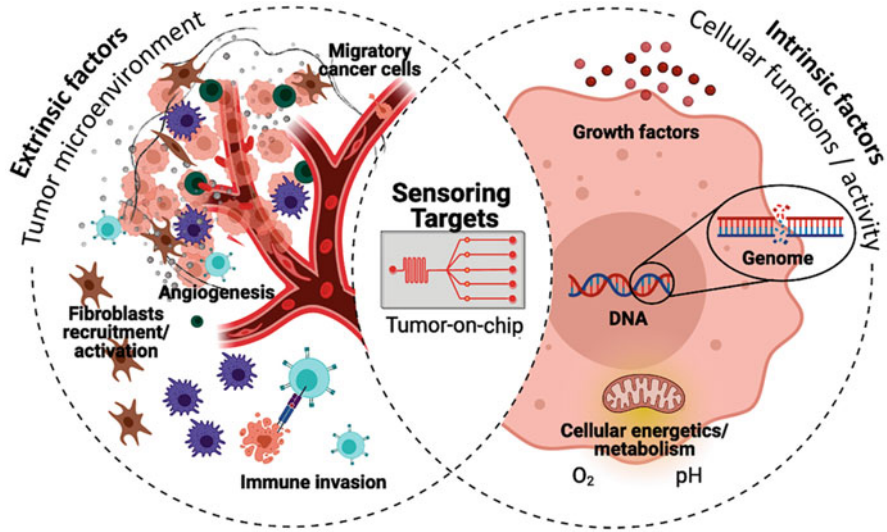


Fig. 7.3 Tumor-on-chip targets. Recent evidence has identified a multitude of cancer targets including both extrinsic and intrinsic targets, namely tumor microenvironment and intra- and inter-cellular interactions/functions. Created with [BioRender.com](https://www.biorender.com)

to regulate genes and proteins expression and to influence cancer-associated metabolic pathways [83]. Thus, much attention has been given to the accurate modeling of TME interactions *in vitro* and *in vivo*.

Over the past decades, several *in vitro* and *in vivo* cancer models have been developed aiming at understanding molecular mechanisms and cancer therapies screening. Clearly, traditional 2D *in vitro* static models, even though have been proven effective to a certain extent for studying cancer cell behavior [84], they cannot accurately recreate the level of complexity observed in the human body, namely cell–ECM and cell–cell interactions [85], or even less so at the systemic-like level, that is organ–organ or tissue–tissue interactions. Likewise, animal models have played important roles in understanding the pathobiology of cancer, drug screening, and drug discovery [86]. However, these models lack key features of human cancer, such as genomic instability, latency, tumor heterogeneity and microenvironment, limiting their ability to recapitulate the real pathobiology of human cancers [87]. Furthermore, ethical considerations and the social awareness to reduce animal experimentation have driven the development of advanced *in vitro* models toward more accurately represented stages of its human disease counterpart [88]. To date, numerous *in vitro* 3D models have been developed to bridge the gap between conventional cancer models and native human tumors [82, 89]. Among these, advanced microfluidic devices have revolutionized the ability to mimic the natural biophysical/chemical conditions of cells in *in vitro* models and target new extrinsic and intrinsic targets associated with tumor dynamics (Fig. 7.3). These systems allow a dynamic culture of multiple cell types in a microfluidic chip to analyze specific

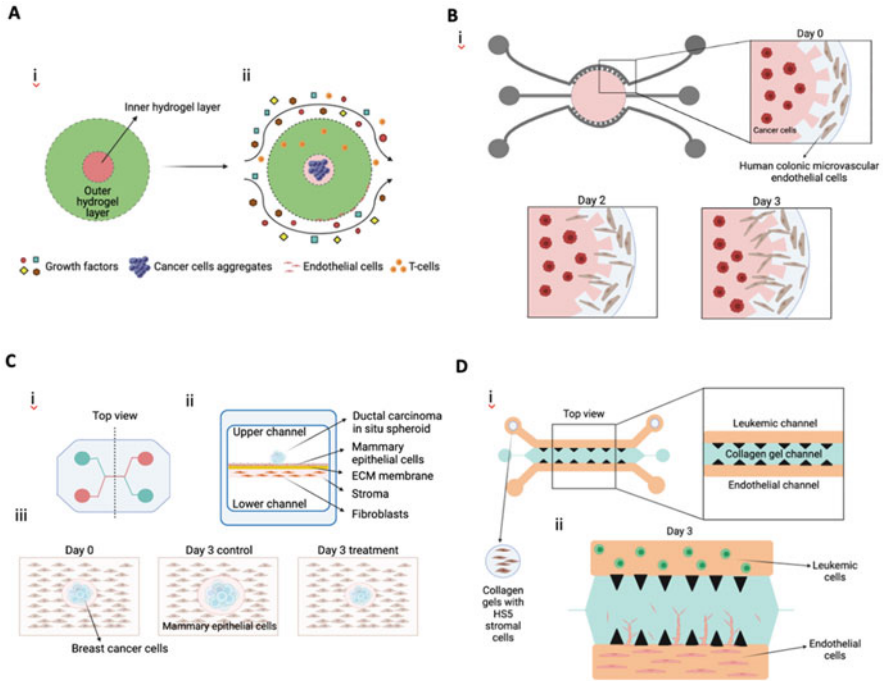


Fig. 7.4 Tumor-on-chip platforms for modeling solid and liquid tumors. **(a)** Schematic representation of the 3D photopatterning gelatin hydrogel with outer and inner GelMA hydrogels (i). Schematic of the mass transfer model demonstrating the domain geometry, boundary conditions, and position of the cell aggregates of cancer cells (MCF7), monocytes (THP-1, green), and endothelial cells (ii). **(b)** Design of colorectal tumor-on-chip model with a round microfluidic central chamber incorporating human colon cancer cell line (HCT-116 cancer cells) embedded in Matrigel and human colonic microvascular endothelial cells (HCoMECs) seeded in the side channels to form vessel-like assemblies (i). Schematics of HCoMECs invasion from the lateral to central chambers in response to VEGF presence (demonstrating the formation of endothelial sprouts (ii). **(c)** Schematic figure of primary tumor formation. Top (i) and cross-sectional (ii) views of the microfluidic OoC used to model in vitro the microarchitecture of ductal carcinoma in situ (DCIS) of the breast in vitro. Schematics of DCIS spheroids showing proliferation of cancer cells from day 0 to 3 under non-treated and treated conditions (paclitaxel) (iii). **(d)** Schematics of a biomimetic 3D angiogenesis chip to study leukemic-cell-induced bone marrow angiogenesis (i). Representative schematics of directional angiogenic sprouting toward the leukemic channel (ii). Schematic representations adapted from **(a)** [90]; **(b)** [104]; **(c)** [106] and **(d)** [122]

interactions, which renders them particularly interesting when investigating the communication between cancer and stromal cells. As an example, a perfusable multicellular tumor-on-chip platform was developed to assess breast cancer-immune cell interactions [90] (Fig. 7.4a). Breast cancer cells, monocytes, and endothelial cells were spatially confined within a gelatin hydrogel in a controlled manner by using 3D photopatterning, while human leukemic T cells (TALL-104) were dispersed within the perfused media and allowed to infiltrate. The results showed greater T cell recruitment when higher levels of hypoxia were emulated

by using tumor spheroid cultures. Moreover, the results showed that higher infiltration of the leukemic T cells occurred when monocytes were present in the culture [90]. These findings demonstrate the critical role of personalized tumor-on-chip devices in generating heterotypic 3D models where different cell types can be cultured in a dynamic microenvironment, allowing the study of specific tumor–stroma interactions.

7.3.3 On-Chip Features and Requirements

As a complex and dynamic system, the human body is composed of organs that are constantly interacting with each other. So, if emerging technology has the power to accurately capture this complexity, it will become an extremely powerful tool for disease progression analysis and drug development. However, developing such sophisticated systems poses biological and engineering challenges. Interestingly, OoC platforms have critical and defining features that make them an excellent solution to recapitulate key functional aspects of organs and tissues: (1) 3D nature and organization of the tissues inside the chips; (2) integration of multiple cell types aiming the replication of a more physiological cellular microenvironment; and (3) biomechanical forces important to the tissue’s modeling [91]. Nonetheless, the integration of emerging technologies such as OoC coupled with biosensing techniques has been revolutionizing this field (Table 7.1). The goal is to connect real-time monitoring techniques for a more mechanistic biological insight about tissue’s microenvironment interactions. At the same time, this approach enables the study and monitoring of the interactions between diseased tissues and several organs, to ultimately provide a deeper understanding about healthy and diseased tissue’s biology. In turn, this multi-disciplinary combination of efforts is expected to contribute to a faster progress in drug discovery, biomarker detection, and long-term pharmaceutical metabolism [91]. Great examples report on the use of these technologies to study tumor–stroma interactions in cancer progression, metastasis, and drug resistance [92–96].

Moreover, a major requirement for drug development advances in this area is the design of tumor-associated vasculature, which represents an important component of the TME and reliable therapeutic targets. Indeed, several anti-angiogenic drugs have been developed for use in cancer; however, not trustworthy clinical trial outcomes and oftentimes marginal survival gains have been reported [97]. Thereby, OoCs hold the promise to help elucidate the factors that contribute to therapy failure, and, ultimately, lead to more effective therapies. Furthermore, the incorporation of this feature into tumor-on-chip platforms is a breakthrough as (1) it allows the mimicry of *in vivo* structure, function, and disease processes of a vascularized tumor mass; (2) it models poorly understood key steps of metastasis, which involve tumor-stromal cell interactions and are difficult to investigate using the current preclinical models; (3) it allows a more realistic pharmaceutical screening due to the establishment of physiologically selective barriers; and, (4) drug’s anti-angiogenic and anti-metastatic efficacy can be directly assessed using these systems [98]. In this regard, several

Table 7.1 Overview of examples of integration of OoC with biosensing techniques, highlighting the biomarker assessed, the type of sensor, and the technique used for detection

Biomarker quantification	Type of biosensor	Type of used technique (examples)	Models (examples)	Reference		
<i>Oxygen</i>	Optical	Luminescence-based sensors	Microfluidically supported biochips of liver	[107]		
		Oxygen-quenched fluorescent particles	Intestine-on-chip	[108]		
		Ratiometric optical oxygen sensors	Breast tumor-on-chip	[96]		
		Oxygen-quenchable luminescent dye	Integrated human liver (cancer)- and heart-on-chips	[109]		
	Electrochemical	Amperometric	Luminescence-based sensors	Liver biochip	[107]	
			Bare platinum electrodes	Brain-cancer-on-chip	[92]	
		Optical + electrochemical	Amperometric oxygen inkjet-printed sensors	Liver-on-chip model	[110]	
			Oxygen biosensing principle of the thiol-ene epoxy biochips and electrochemical oxygen-sensing method	Blood-brain-barrier biochips	[111]	
			Optical	On-line pH monitoring through optical fibers	Lung cancer-on-chip	[93]
				Microfluidic-based optical pH sensing by detection of light absorbed by phenol red	Organ-on-chip	[130]
Physical	pH sensor detection through light absorption of phenol red	Optical filter and photodiode for media color change	Kidney-on-chip	[112]		
			Multi-organ-on-chip (liver and heart)	[109]		
<i>Glucose and/or lactate</i>	Optical	Enzyme-linked immunosorbent assay	Hanging drop chip	[113]		
		Integrated amperometric sensing electrodes	Human colon cancer microissues platform	[114]		
	Electrochemical	Off-chip electrochemical sensor unit		Liver-on-chip	[115]	
				Brain-cancer-on-chip	[92]	

(continued)

Table 7.1 (continued)

Biomarker quantification	Type of biosensor	Type of used technique (examples)	Models (examples)	Reference	
Cytokines and other metabolites	Electrochemical	Silver/silver chloride (Ag/AgCl) and platinum electrode biosensors			
	Amperometric	Superwettable biosensors	Cancer-on-chip	[94]	
		Multiplexed amperometric-based sensors	Muscle-on-chip	[116]	
		Aptamer-based biosensors	Heart-on-chip	[117]	
			Liver-injury-on-chip	[118]	
	EC impedance spectroscopy (EIS)		Electrochemical immuno-aptasensors	Heart-breast cancer-on-chip	[95]
			Functionalized screen-printed gold electrodes	Muscle-on-chip	[116]
	Trans epithelial electrical resistance (TEER)–multi-electrode array (MEA)		Label-free electrochemical immunobiosensors	Multi-organ-on-chip (liver and heart)	[109]
			In-chip integration of TEER and MEA	Heart-on-chip	[119]
		TEER	Integrated sensors	Blood-brain-barrier chip	[65]
Enzymatic		Bead-based microfluidic electrochemical immunosensors	Liver-on-chip	[120]	
	Optical	Organic-photodetector arrays	Synovium-on-chip	[121]	

groups have designed micro-vascularized on-chip constructs in which perivascular and vascular cells self-organize *de novo* into a living and perfused vascular network in response to fluid flow and shear stress [99–101].

Microfluidic devices with the ability to control multiple gradients are often employed to analyze the effect of growth factors, cytokines, and/or drugs in a biomimetic microenvironment [102, 103]. As an example, to replicate the human colorectal tumor microenvironment and reconstitute the microvascular tissue functions, a simple tumor-on-chip *in vitro* model was fabricated [104]. The platform consisted on a radial drug penetration by diffusion of small molecules from the outer boundaries into the central core of solid tumors, and it evaluated in real-time using live imaging, interactions between pre-labeled colorectal cancer cells and endothelial cells that infiltrated the vascular endothelial growth factor-infused tumor core [104] (Fig. 7.4b). Using such 3D microfluidic cell cultures, the study of phenomena such as vascularization and oncogenesis under dynamic conditions demonstrates the suitability of these models to provide a powerful insight on the cancer stage prognosis and, ultimately, on depicting a more suitable treatment option.

Given the possibility to study tumor-stroma activation that sustains cancer progression, microfluidic devices have been created to replicate the characteristic tumor stroma-ECM remodeling. As an example, Gioiella et al. [105] described a breast-cancer-microenvironment-on-chip model consisting of a stromal compartment composed by fibroblast-assembled ECM and breast cancer cells. This model elegantly replicated the interactions of breast cancer cells with the stroma and ECM activation during tumor progression. Results from inline tissue imaging (immunofluorescence-based analysis) revealed that cancer cell invasion led to the activation of cancer-associated fibroblasts, along with the overexpression of fibronectin and hyaluronic acid in the ECM [105]. Moreover, real-time analysis of collagen remodeling revealed that normal fibroblasts deposited collagen bundles that more closely resemble the native structures, when compared to CAFs, supporting earlier findings of human biopsy studies [105]. Also, similar models have been used to evaluate drug efficacy. Choi et al. [106] recently developed a micro-engineered ductal carcinoma *in situ* (DCIS)-on-chip platform (Fig. 7.4c). To mimic the surrounding matrix, an initial confluent layer consisting of human mammary epithelial cells on a porous membrane was assembled, followed by another layer of mammary fibroblast-containing hydrogel. Afterward, ductal carcinoma spheroids were inoculated on top of the epithelial cells to complete the model [106]. Using this model, the effect of paclitaxel, an anti-cancer drug, was evaluated and even though demonstrating negligible toxicity on the epithelial cells alone, it showed pronounced toxicity toward the ductal carcinoma spheroids [106]. Additionally, paclitaxel effectively inhibited the progression of the ductal carcinoma spheroids, revealed by their consisting sizes when compared with the increased tumor volume observed in the absence of the drug [106].

Interestingly, these platforms not only have been used for reproducing the solid tumor microenvironment, but they can also be adapted to liquid tumor modeling, commonly associated with hematological malignancies. Recently, Zheng et al. [122] developed a microfluidic 3D angiogenesis chip to study leukemic-cell-induced bone

marrow angiogenesis (Fig. 7.4d). By modifying a previously established angiogenesis microchip, leukemic cells were infused into one side of the chip, while endothelial cells were seeded on the other side and allowed to sprout into a middle chamber filled with collagen [122]. When needed, HS5 human bone marrow stromal cells in collagen gels were also inoculated at the two ends of the leukemic channel for co-culture establishment [122]. By both confocal and phase-contrast microscopy, the directional sprouting of endothelial cells was found to be influenced by the presence of leukemic cells, suggesting the angiogenic capacity of these leukemic cells, whereas the control group without leukemic cells revealed minimal invasion of endothelial cells [122]. Also, sprouted endothelial cells were observed to form lumen structures, which could be further enhanced by co-culturing the leukemic cells with HS5 human bone marrow stromal cells [122].

Microfluidic tumor-on-chip devices have also been used for evaluating nanomedicine, where not only the mass transport of nanoparticles (NPs) with varying parameters, namely size, shape, and surface characterizations, can be emulated, but also the geometry of the relevant architectures can be reproduced [123]. For example, Yang and co-workers customized a microfluidic 3D breast cancer model by culturing human breast cancer cells and adipose-derived stromal cells and evaluated the effectiveness of photodynamic therapy (PDT) agents, such as gold NPs [124]. Results showed that monolayer cultures were more susceptible to the photodynamic agents than the 3D cultures post-irradiation [124]. Also, in both 2D and 3D cultures, the increased rate of reactive oxygen species generation associated with the presence of NPs, demonstrated the efficacy of the photodynamic agents [124]. Using tumor-on-chip platforms for these photodynamic treatments has provided relevant insights into the advantages and drawbacks of current NP treatments, hence allowing for treatment regimens' optimization.

Recently, given the importance of rapid mutations and multidrug-resistant (MDR) phenotypes associated with an altered response to therapies, multi-organ platforms have gained attention for personalized medicine in cancer research. Over the past years, several models have been generated aiming to recapitulate human cancer phenotypes, thus, is considered as the best approximations of the human disease counterparts [125]. Even though currently used primary tumors resected from patients and derivative cell lines have been helping us to understand biomarkers and cellular phenotypes, they are not fully adequate to study early-stage cancer progression. In contrast, patient-derived induced pluripotent stem cells (iPSCs) can potentially represent the earliest stages of disease by assisting in the identification of significant molecular events responsible for disease triggering and progression [126–128]. Moreover, iPSC-based cancer models would help in the understanding of the niche in which cancers develop, enabling the re-creating of the physiological cancer-initiating context and model development [126–128]. Nonetheless, by using patient-specific *in vitro* organoids generated from cancer tissue biopsies, it is possible to create a cancer biobank, enabling an effective drug screening based on patients' genetic profile [129].

Overall, currently described and used platforms provided a unique way to monitor the switch between healthy and pathological stroma *in vitro* and represent an

alternative to currently employed *in vivo* experiments, that present limited application, namely in the prediction of treatments, human tumor progression events and response specificity and drug doses translation. In this context, the implementation of biosensors will offer the potential to better monitor the response to external stimuli and assess organotypic functionality under controlled culture conditions, while enabling a real-time monitoring of the cellular physiological microenvironment and improving the functionality of OoC models.

7.4 Biosensors and Advanced Imaging Modalities On-Chip

Biosensors are devices that allow the monitoring of physiological processes over long or short time points and in an automated manner [130]. They can be integrated into OoC platforms, rendering *in situ* and non-invasive analysis of cell behavior, tissues, and organs possible. Thus, kinetics and prognostic studies can be performed in these platforms, bypassing standard methods, such as end-point analysis, which typically requires a large volume of samples and fix time points [131]. The integrated analytical techniques implemented in OoC include electrochemical, optical, piezoelectric, thermal, magnetic, and micromechanical sensors.

7.4.1 Organs-on-Chips Integrated Analytical Techniques

The typical electrochemical biosensors integrated with OoCs are non-microscopy-based biosensors [132]. These allow the evaluation of inline cell, tissue and organ processes, the detection of cell communication/secreted signals, the formation/disruption of barrier functions, the detection of complex biotransformation processes, and the screening of absorption, distribution, metabolism, and toxicity (Fig. 7.5a). Recently, embedded electrodes have been developed to enable non-invasive and real-time detection. For instance, semi-transparent electrodes have been described for transendothelial or transepithelial electrical resistance (TEER) measurements to assess the integrity of human endothelial or epithelial barrier models [133].

The development of microfluidic co-cultures with integrated biosensors is of major significance when secreted signaling molecules, such as cytokines and growth factors, need to be studied. An example is the development of a liver-on-a chip model, where the cell signaling and communication is monitored on-chip, in co-cultures of hepatocytes and stellate cells during liver injury [118]. Similarly, sensorized on-chip systems with integrated electrothermal micropumps and sensors have been designed to study cell proliferation or adhesion, oxygen consumption, and pH detection, to prevent physiological disorders due to cellular acidification [134].

On the other hand, optical biosensors mostly involve imaging read-outs using microscopy or other imaging detection systems. In some cases, optical biosensors enable the study of the events at cellular level via sampling output media, and signal analysis is performed in a luminometer. However, most of the OoCs are analyzed by microscopy-based technologies. Optical biosensors applied as integrated detection

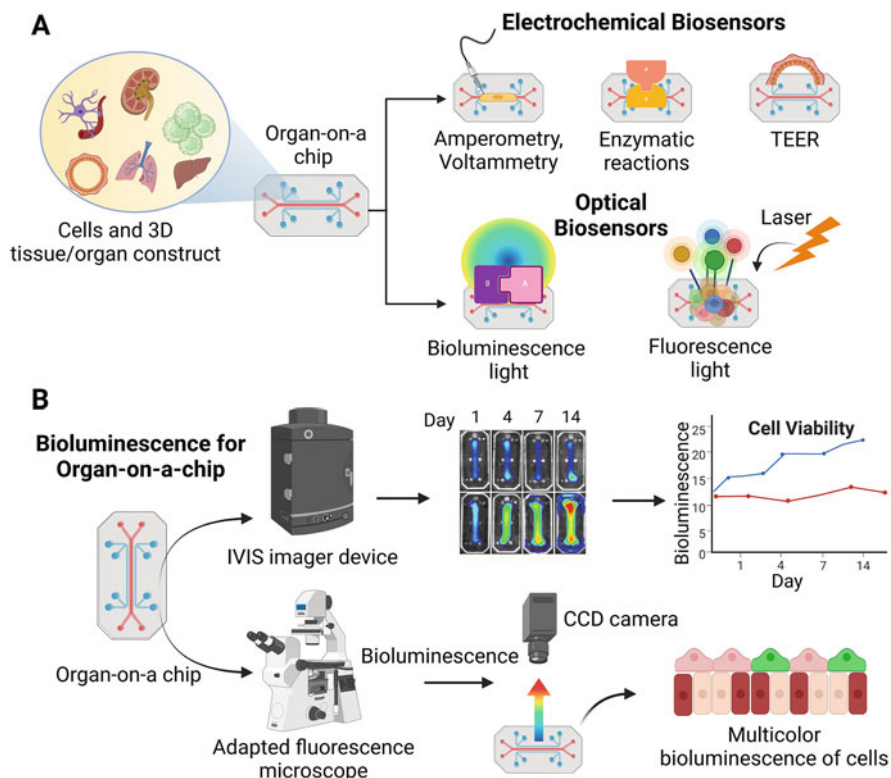


Fig. 7.5 Biosensing technologies integrated in organ-on-chip devices. (a) Electrochemical biosensors monitor physical parameters of the microenvironment (amperometry, voltammetry), enzymatic reactions like redox reaction between an enzyme and the targeted molecule, measurement of electrical resistance for cellular barrier integrity namely Transepithelial/transendothelial electrical resistance (TEER). Optical Biosensors monitor bioluminescence and fluorescence reactions. Both technologies enable multicolor imaging of cells. (b) Detection of bioluminescence from OoC. Ivis imager system has a sensitive CCD camera and detection of BL from the chip enables real-time monitoring of cell vitality and proliferation. Bright-field microscopes can be upgraded with an installed CCD camera and the detection of multicolor luciferase-expressing cells can be achieved. Created with [BioRender.com](https://www.biorender.com)

in OoCs comprise optical imaging modalities, namely fluorescence (FL) and bioluminescence (BL) techniques. Moreover, optical biosensors are typically non-destructive, robust, and compatible for in situ and inline monitoring thanks to the light emitted. Thus, the integration of optics with microfluidics is currently coining a new field named optofluidics, mainly based on label-free and label-based strategies.

The label-free strategies allow the study of cellular secreted compounds, cellular morphology, and detection of specific areas by surface plasmon resonance [135], scanning electron microscopy [136], Raman spectroscopy [137], and optical

tomography [138]. In particular, Raman spectroscopy measures the light interacting with vibrating chemical bonds of the sample and resulting in an energy shift of the backscattered light. This technique, combined with a confocal microscope to produce a better spatial resolution, can be applied to monitor insulin secretion kinetics [139] or to measure water content in a skin-on-chip [140]. Optical tomography has instead the advantage to detect the wide refractive index of cell distribution and allows label-free and 3D imaging detection. Yet quantification of specific proteins is quite limited. Nevertheless, Lee et al. successfully carried out a quantitative analysis of vasculogenesis-on-chip using optical diffraction tomography [138]. Still, some limitations of the label-free method remain related to the possible interference with the conformation of molecular structures, interaction with biological processes, and demand for bulky external equipment.

Label-based strategies, in contrast, rely on fluorescence or chemiluminescence biosensors. Successful strategies using engineered fluorescent protein/molecules have been extensively adopted for fluorescence-based analysis. A collection of fluorescent proteins includes not only the gold standard green-fluorescent protein (GFP), but also many other improved probes, such as mCherry, dsRed, mEOS, which have higher stability, brightness, and additional wavelengths. These probes enable the imaging of cellular phenotypes and detection at the single-cell level by confocal microscopy [141]. Fluorescence-based microscopy is the most commonly used to detect and visualize specific tagged proteins or molecules. Some examples can be referred to appropriate literature where confocal microscopy has been used for assessing liver, kidney, tumor, brain, and vasculature models [142–146]. To minimize process variability and user bias, fluorescent probes have been exploited for automated fluorescent workflow. Automated workflows acquire and analyze confocal images of OoC of different formats. This also allows to probe cellular phenotypes in large batches of chips, thereby increasing the throughput. Automated drug screening has been successfully implemented to assess toxicity in a liver-on-chip model [147].

Characteristically, fluorescence-based analysis requires invasive endpoint procedures, for example, cell fixation, necessary for histology and immunohistochemistry assays [148]. Recently, fluorescence microscopy has been combined with bioluminescence detection for non-terminal imaging of cell status. To study the osteogenic differentiation on bone-on-chip, Sheyn et al. elaborated a novel system for real-time monitoring of cell viability, proliferation, and differentiation while culturing cells in the bone-on-chip [149]. However, fluorescence-based sensors may also cause several technical issues due to photobleaching, phototoxicity, and autofluorescence of cells or tissues. Light-sheet microscopy offers low levels of photodamage and adequate imaging in 3D cell models as tumor spheroids, but its spatial resolution still requires some improvements [150]. Additionally, bioluminescent resonance energy transfer (BRET) technologies can also resolve undesirable outcomes due to photobleaching and allow long-term monitoring of cells. Worthy of note is the employment of microfluidic devices for the measurement of thrombin activity [151].

Another optical imaging modality used in optofluidics is bioluminescence (BL). Bioluminescent-based sensors have a higher signal-to-noise ratio than fluorescence, because a bioluminescent chemical reaction does not need an external excitation light source (Fig. 7.5b). Therefore, photobleaching does not occur in bioluminescence, in turn allowing long-term imaging and preventing phototoxicity of cells. Bioluminescent light is produced when a luciferin substrate is oxidized by a luciferase enzyme [152]. The luciferin substrates have to fulfill some chemical characteristics, such as stability, good cell membrane permeability (especially when imaging OoC models), and affinity for the luciferase enzyme [153]. The latest has been improved by site-specific engineering of the luciferase enzyme to ensure high affinity (low K_m ; measure of how easily the enzyme can be saturated by the substrate) and, therefore, less amount is needed to achieve V_{max} (maximum rate of an enzyme-catalyzed reaction i.e. when the enzyme is saturated by the substrate) and generate stronger bioluminescent signals [154]. Luciferases derived from terrestrial fireflies (FLuc), click-beetles (CBG2 and CBR2) and railroad worms (SRL) show great potential for single cells analysis and they are compatible with the standard D-luciferin substrate [155]. Synthetic substrates have also been designed to increase cell membrane permeability and to improve efficiently the performance of Fluc luciferases as CycLuc, Cybluc, and Akalumine-HCl substrates [156–158]. Optimized marine luciferases derived from copepod (GLuc) [159], or deep-sea shrimps (Nanoluc) [160] also yield bright blue BL light when paired with coelenterazine type of substrates. In particular, coelenterazine analogs, such as furimazine, and more recently Hikarazine-003, have been optimized to enhance the performance and the stability of Nanoluc, increasing the light output up to 2.5-fold [161]. There is a clear need for a more sensitive system for single-cell imaging inspired by the BRET technologies, that combines a bioluminescent donor and a fluorescent acceptor. One example is Antares, a Nanoluc enzyme fused with an orange-red fluorescent probe (CyoFp), that enables sensitive single-cell imaging due to the red-shift emission of light ($\lambda_{max} = \sim 580$ nm) [162]. Notably, multicolor-bioluminescence imaging can be also performed, where the combination of multiple luciferase-expressing cells emitting different BL lights are co-cultured on the same chip. Another strategy for non-invasive detection of enzymatic activities, small bioactive molecules, or specific uptake is represented by caged-luciferin substrate by addition of a protecting group. This has been done either to stabilize furimazine-based substrates, allowing a high signal-to-noise ratio at the single-cell level [163], or with D-luciferin analogs at its amino group, which prevents the luciferase binding and quenches the BL emission [164, 165]. Cellular events can be studied through the conversion of caged pro-luciferins in active luciferin upon the specific enzymatic event. Notably, caged D-luciferin has been employed for example to measure enzymatic processes like caspase activity or the uptake of glucose and peptides at desired time points [164, 165]. The luciferin conversion can be also easily detected by a conventional luminometer upon the addition of the specific luciferase and necessary co-factors. Noteworthy, luminescent bacterial operons can similarly be applied for heterologous engineering of organisms. The entire bacterial operon comprises the synthesis of both luciferase and substrate and can be inserted into

the genome of other organisms. The independence of the external administration of the substrate renders the bacterial system particularly attractive. Recently, iLux operon has been optimized for mammalian cell expression, thereby enabling autonomous single-cell screening [166]. However, this approach still needs some improvements mostly due to the low photon yield [167]. Nonetheless, they hold the promise to image cells on-chip without the addition of substrates.

7.4.2 Advanced Imaging Modalities for Optical Biosensors

Conventionally, luminometers equipped with photo-multiplier tubes are used for BL read-outs of *in vitro* assays. Sensitive charged-coupled device (CCD) cameras are instead required for the detection of luminescence and are usually installed in a wide-field inverted microscope. Currently, the imaging of single cells expressing the luciferase is quite challenging due to the dim light emitted. Therefore, to transmit the light from the sample to the detector, long exposure times (from seconds to minutes) are needed to enhance the detection. Thus, the development of improved microscopes for ultra-low light consists of modified imaging lenses that allow the reduction of the acquisition time for very bright luminescent systems, such as Nanoluc/furimazine [168]. Further developments in BL microscopy include the use of ultra-low-light imaging cameras, namely liquid nitrogen-cooled CCD cameras, photon-counting CCD cameras or image-intensifying CCD cameras [169–174]. To our knowledge, the newest camera commercially released is the electron-multiplying camera (EM-CCD) which provides excellent sensitivity and image quality [175, 176]. Notably, EM-CCD cameras have also been upgraded with iXon EMCCD that has a large field view (512×512 pixels) and cooled at -100 °C, allowing imaging within seconds. Dual-color imaging from two cell populations has also been attempted by installing two dichroic mirrors in an upgraded BL microscope. The collimated beam of light by the objective lens can separate green and red light reaching the EM-CCD camera [149, 177]. Another remarkable achievement allowed to exploit the detection of luciferin as a fluorescent probe. As reported by Goda et al., the possibility to select specific optical filters enabled the detection of emission spectra of both fluorescence from GFP and of BL from firefly luciferase emitted from the same sample [178]. Interestingly, promising advances in imaging hardware are represented by miniature microscopes. These optimizations yielded a miniscope (BLmini) which is lighter in weight (2.5 g only) and offers up to 15 times higher signal. The miniscope is sensitive enough to capture spatiotemporal dynamics of bioluminescence emitted by Nanoluc in the brain of mice [179]. Outstanding results are also shown by CMOS cameras of smartphones interfaced with OoC setups and can detect Nanoluc/Nanolantern expressing cells [180]. Future developments foresee the implementation of imaging devices for sensitive monitoring of single BL cells in 3D cell cultures.

7.5 Conclusions and Future Directions

While the potential of OoCs is exciting, this attractive technology is in an early phase. Although highly promising, some challenges remain to be resolved over the next decade, namely cell sourcing, platform standardization, increase in automation and throughput, non-invasive real-time imaging, and read-outs. On the other hand, while reduction and refinement of animal use is achievable, the total replacement of animals in drug and research development is still currently seen as unlikely in the very near future.

Concerning the modeling of cancer *in vitro*, it is clear that this complex field has undergone great advances, thus allowing a deeper understanding of the key molecular and cellular pathways related to tumor progression and malignancy. Namely, by the recent developments in microfabrication technologies, the creation of groundbreaking bioengineered 3D models with the potential to emulate the TME has been clearly heightened. Nevertheless, even though the current path is promising showing proof of functionality of on-chip platforms, challenges remain to be addressed, mainly regarding reproducibility and reliability, before tumor/TME-on-chip models are widely adopted into healthcare settings and drug R & D. Excellent examples of such promising trajectory are current collaborations formed between pharmaceutical companies, regulatory entities and academic centers that develop on-chip technologies. Yet, due to the complexity inherent to *in vivo* TME, OoC systems developed to mimic these, still face many challenges before their integration into practical pharmaceutical industrial and clinical applications. The list of challenges includes: (1) Optimization of biosensor detection and analysis paths to deconvolute complex signal regulation functions; (2) The industrial manufacture and standardization of microfluidic devices with biosensors, toward more user-friendly on-chip systems, so that non-experts can immediately apply these models for clinical translation; and (3) Transition to non-adsorbing materials for chip fabrication, while keeping transparency and elastic behavior. The most used material in use for chip fabrication remains polydimethylsiloxane (PDMS), which can easily adsorb hydrophobic compounds, such as drugs and proteins, and, thus, reducing the efficacy and activity of drugs, leading to experimental errors and limiting its application. As mentioned above, cell sources are another critical hindrance that remains to be addressed. Although increasing attention is being given to patient-derived cells or iPSCs, obtaining primary cells for some tumors can be difficult (e.g., pancreatic cancer). Even though it is generally accepted that primary cell sources, which can be commercially available, are more interesting for personalized medicine or to provide a better understanding of biological processes, cell lines might still continue to be used for drug screening as they are more homogenous. One should also consider that with the increased complexity derived from multi-sensor implementation on-chip, the resulting read-outs may become more convoluted and, thus, more demanding to process. Assistance from other fields such as artificial intelligence and machine learning proves to be essential for the analysis of the next generation of OoC platforms [181], which will push the field forward, as a truly multi-disciplinary effort.

Although these systems still face many challenges, they are undoubtedly promising platforms for the development of therapies. To accomplish these goals, interdisciplinary cooperation among researchers from material and biomedical sciences, biophysics, biology, and oncology is needed to achieve concerted efforts in designing and integrating read-outs, in a high-throughput manner for pathologies' research and drug discovery, finally translating bioinspired designs to clinical applications. In this context, OoC has the potential to enable a paradigm shift in clinical settings, as these technological platforms will not only help in a personalized diagnosis but also in individualized treatment, allowing a more clinically oriented, patient-centric approach.

Acknowledgments This work is financed by the Dutch Research Council (NWO), as part of the research program Incentive Grants for Women in STEM (project number 18741). The authors are also financed by the research project OA-BioDetectChips: Toward osteoarthritis fingerprinting - combining imaging biomarkers and multi-organ-on-chip technology for improved in vitro models (project number LSHM20044-SGF, Top Sector Life Sciences & Health - Top Consortia for Knowledge and Innovation - LSH-TKI).

Conflict of Interest Statement The authors have no conflicts of interest to declare.

References

1. Bhatia SN, Ingber DE (2014) Microfluidic organs-on-chips. *Nat Biotechnol* 32:760–772. <https://doi.org/10.1038/nbt.2989>
2. Kilic T, Navaee F, Stradolini F, Renaud P, Carrara S (2018) Organs-on-chip monitoring: sensors and other strategies. *Microphysiol Syst* 2
3. Seyfried TN, Huysentruyt LC (2013) On the origin of cancer metastasis. *Crit Rev Oncog* 18: 43–73. <https://doi.org/10.1615/critrevoncog.v18.i1-2.40>
4. Gion M, Trevisiol C, Fabricio ASC (2020) State of the art and trends of circulating cancer biomarkers. *Int J Biol Markers* 35:12–15. <https://doi.org/10.1177/1724600819900512>
5. Mattei F et al (2021) Oncoimmunology meets organs-on-chip. *Front Mol Biosci* 8. <https://doi.org/10.3389/fmolb.2021.627454>
6. Basil CF et al (2006) Common cancer biomarkers. *Cancer Res* 66:2953–2961. <https://doi.org/10.1158/0008-5472.can-05-3433>
7. Bohunicky B, Mousa SA (2010) Biosensors: the new wave in cancer diagnosis. *Nanotechnol Sci Appl* 4:1–10. <https://doi.org/10.2147/NSA.S13465>
8. Rudin M, Weissleder R (2003) Molecular imaging in drug discovery and development. *Nat Rev Drug Discov* 2:123–131. <https://doi.org/10.1038/nrd1007>
9. Heinrich MA, Mostafa AMRH, Morton JP, Hawinkels LJAC, Prakash J (2021) Translating complexity and heterogeneity of pancreatic tumor: 3D in vitro to in vivo models. *Adv Drug Deliv Rev* 174:265–293. <https://doi.org/10.1016/j.addr.2021.04.018>
10. Hassanpour SH, Dehghani M (2017) Review of cancer from perspective of molecular. *J Cancer Res Pract* 4:127–129
11. Dvorak HF (2015) Tumors: wounds that do not heal—redux. *Cancer Immunol Res* 3:1–11
12. Dvorak HF (1986) Tumors: wounds that do not heal. *N Engl J Med* 315:1650–1659
13. Martin-Broto J, Mondaza-Hernandez JL, Moura DS, Hindi N (2021) A comprehensive review on solitary fibrous tumor: new insights for new horizons. *Cancers (Basel)* 13:2913
14. Yamauchi M, Barker TH, Gibbons DL, Kurie JM (2018) The fibrotic tumor stroma. *J Clin Invest* 128:16–25

15. Chandler C, Liu T, Buckanovich R, Coffman LG (2019) The double edge sword of fibrosis in cancer. *Transl Res* 209:55–67
16. Rodrigues J, Heinrich MA, Moreira Teixeira L, Prakash J (2020) 3D in vitro model (R)-evolution: unveiling tumor–stroma interactions. *Trends Cancer*. Epub ahead of print
17. Bahmaee H et al (2020) Design and evaluation of an osteogenesis-on-a-chip microfluidic device incorporating 3D cell culture. *Front Bioeng Biotechnol* 8. <https://doi.org/10.3389/fbioe.2020.557111>
18. Wang S et al (2020) Tumor microenvironment in chemoresistance, metastasis and immunotherapy of pancreatic cancer. *Am J Cancer Res* 10:1937–1953
19. Murakami T et al (2019) Role of the tumor microenvironment in pancreatic cancer. *Ann Gastroenterol Surg* 3:130–137
20. Tanaka HY, Kano MR (2018) Stromal barriers to nanomedicine penetration in the pancreatic tumor microenvironment. *Cancer Sci* 109:2085–2092
21. Norton J, Foster D, Chinta M, Titan A, Longaker M (2020) Pancreatic cancer associated fibroblasts (CAF): under-explored target for pancreatic cancer treatment. *Cancers (Basel)* 12: 1347
22. Nielsen MFB, Mortensen MB, Detlefsen S (2016) Key players in pancreatic cancer-stroma interaction: cancer-associated fibroblasts, endothelial and inflammatory cells. *World J Gastroenterol* 22:2678–2700
23. Hwang RF et al (2008) Cancer-associated stromal fibroblasts promote pancreatic tumor progression. *Cancer Res* 68:918–926. <https://doi.org/10.1158/0008-5472.Can-07-5714>
24. Farc O, Cristea V (2021) An overview of the tumor microenvironment, from cells to complex networks (review). *Exp Ther Med* 21:96
25. Dumont N et al (2013) Breast fibroblasts modulate early dissemination, tumorigenesis, and metastasis through alteration of extracellular matrix characteristics. *Neoplasia* 15:249–262
26. Prakash J (2016) Cancer-associated fibroblasts: perspectives in cancer therapy. *Trends Cancer* 2:277–279
27. Hurtado P, Martínez-Pena I, Piñeiro R (2020) Dangerous liaisons: circulating tumor cells (CTCs) and cancer-associated fibroblasts (CAFs). *Cancers (Basel)* 12:2861
28. Roife D, Sarcar B, Fleming JB (2020) Stellate cells in the tumor microenvironment. *Adv Exp Med Biol* 1263:67–84
29. Vonlaufen A et al (2008) Pancreatic stellate cells: partners in crime with pancreatic cancer cells. *Cancer Res* 68:2085–2093. <https://doi.org/10.1158/0008-5472.Can-07-2477>
30. Östman A (2017) PDGF receptors in tumor stroma: biological effects and associations with prognosis and response to treatment. *Adv Drug Deliv Rev* 121:117–123
31. Öhlund D et al (2017) Distinct populations of inflammatory fibroblasts and myofibroblasts in pancreatic cancer. *J Exp Med* 214:579–596
32. Elyada E et al (2019) Cross-species single-cell analysis of pancreatic ductal adenocarcinoma reveals antigen-presenting cancer-associated fibroblasts. *Cancer Discov* 9:1102–1123
33. Gascard P, Tlsty TD (2016) Carcinoma-associated fibroblasts: orchestrating the composition of malignancy. *Genes Dev* 30:1002–1019
34. Kuninty PR et al (2019) ITGA5 inhibition in pancreatic stellate cells attenuates desmoplasia and potentiates efficacy of chemotherapy in pancreatic cancer. *Sci Adv* 5
35. Schnitter J, Heinrich MA, Kuninty PR, Storm G, Prakash J (2018) Reprogramming tumor stroma using an endogenous lipid lipoxin A4 to treat pancreatic cancer. *Cancer Lett* 420:247–258
36. Binnewies M et al (2018) Understanding the tumor immune microenvironment (TIME) for effective therapy. *Nat Med* 24:541–550
37. Valentin JE, Stewart-Akers AM, Gilbert TW, Badyal SF (2019) Macrophage participation in the degradation and remodeling of extracellular matrix scaffolds. *Tissue Eng A* 15:1687–1694
38. Kuen J, Darowski D, Kluge T, Majety M (2017) Pancreatic cancer cell/fibroblast co-culture induces M2 like macrophages that influence therapeutic response in a 3D model. *PLoS One* 12:e0182039

39. Binnemars-Postma K, Storm G, Prakash J (2017) Nanomedicine strategies to target tumor-associated macrophages. *Int J Mol Sci* 18:979
40. Aras S, Zaidi MR (2017) TAMEless traitors: macrophages in cancer progression and metastasis. *Br J Cancer* 117:1583–1591
41. Ostromov D, Fekete-Drimusz N, Saborowski M, Kühnel F, Woller N (2018) CD4 and CD8 T lymphocyte interplay in controlling tumor growth. *Cell Mol Life Sci* 75:689–713
42. Fridlender ZG et al (2009) Polarization of tumor-associated neutrophil phenotype by TGF-beta: “N1” versus “N2” TAN. *Cancer Cell* 16:183–194
43. Mócsai A (2013) Diverse novel functions of neutrophils in immunity, inflammation, and beyond. *J Exp Med* 210:1283–1299
44. Bosiljic M et al (2019) Targeting myeloid-derived suppressor cells in combination with primary mammary tumor resection reduces metastatic growth in the lungs. *Breast Cancer Res* 21:103
45. van Beek JJP, Martens AWJ, Bakdash G, de Vries IJM (2016) Innate lymphoid cells in tumor immunity. *Biomedicine* 4:7
46. Minetto P et al (2019) Harnessing NK cells for cancer treatment. *Front Immunol* 10:2836
47. Ledford H, Else H, Warren M (2018) Cancer immunologists scoop medicine Nobel prize. *Nature* 562:20–21
48. Shi Y, van der Meel R, Chen X, Lammers T (2020) The EPR effect and beyond: strategies to improve tumor targeting and cancer nanomedicine treatment efficacy. *Theranostics* 10:7921–7924
49. Brachi G, Bussolino F, Ciardelli G, Mattu C (2019) Nanomedicine for imaging and therapy of pancreatic adenocarcinoma. *Front Bioeng Biotechnol* 7
50. Katsuta E et al (2019) Pancreatic adenocarcinomas with mature blood vessels have better overall survival. *Sci Rep* 9:1310
51. Chauhan VP et al (2014) Compression of pancreatic tumor blood vessels by hyaluronan is caused by solid stress and not interstitial fluid pressure. *Cancer Cell* 26:14–15
52. Schiffer D, Annovazzi L, Casalone C, Corona C, Mellai M (2019) Glioblastoma: microenvironment and niche concept. *Cancers (Basel)* 11:5
53. Pombo Antunes AR et al (2020) Understanding the glioblastoma immune microenvironment as basis for the development of new immunotherapeutic strategies. *Elife* 9
54. Nicolò Fanelli G et al (2021) Decipher the glioblastoma microenvironment: the first milestone for new groundbreaking therapeutic strategies. *Genes (Basel)* 12:445
55. Chen Z, Hambardzumyan D (2018) Immune microenvironment in glioblastoma subtypes. *Front Immunol* 9
56. Heiland DH et al (2019) Tumor-associated reactive astrocytes aid the evolution of immunosuppressive environment in glioblastoma. *Nat Commun* 10:2541
57. Brandao M, Simon T, Critchley G, Giamas G (2019) Astrocytes, the rising stars of the glioblastoma microenvironment. *Glia* 67:779–790
58. Geribaldi-Doldán N et al (2021) The role of microglia in glioblastoma. *Front Oncol* 10
59. Quail DF, Joyce JA (2017) The microenvironmental landscape of brain tumors. *Cancer Cell* 31:326–341
60. Quail DF et al (2016) The tumor microenvironment underlies acquired resistance to CSF-1R inhibition in gliomas. *Science* 352
61. Mandenius C-F (2018) Conceptual design of micro-bioreactors and organ-on-chips for studies of cell cultures. *Bioengineering* 5. <https://doi.org/10.3390/bioengineering5030056>
62. Convery N, Gadegaard N (2019) 30 years of microfluidics. *Micro Nano Eng* 2:76–91. <https://doi.org/10.1016/j.mne.2019.01.003>
63. Park SE, Georgescu A, Huh D (2019) Organoids-on-a-chip. *Science* 364:960. <https://doi.org/10.1126/science.aaw7894>
64. Ahn SI et al (2020) Microengineered human blood–brain barrier platform for understanding nanoparticle transport mechanisms. *Nat Commun* 11:175. <https://doi.org/10.1038/s41467-019-13896-7>

65. Park T-E et al (2019) Hypoxia-enhanced blood-brain barrier chip recapitulates human barrier function and shuttling of drugs and antibodies. *Nat Commun* 10:2621. <https://doi.org/10.1038/s41467-019-10588-0>
66. Deosarkar SP et al (2015) A novel dynamic neonatal blood-brain barrier on a chip. *PLoS One* 10:e0142725. <https://doi.org/10.1371/journal.pone.0142725>
67. Maschmeyer I et al (2015) A four-organ-chip for interconnected long-term co-culture of human intestine, liver, skin and kidney equivalents. *Lab Chip* 15:2688–2699. <https://doi.org/10.1039/C5LC00392J>
68. Herland A et al (2020) Quantitative prediction of human pharmacokinetic responses to drugs via fluidically coupled vascularized organ chips. *Nat Biomed Eng* 4:421–436. <https://doi.org/10.1038/s41551-019-0498-9>
69. Caballero D et al (2017) Organ-on-chip models of cancer metastasis for future personalized medicine: from chip to the patient. *Biomaterials* 149:98–115. <https://doi.org/10.1016/j.biomaterials.2017.10.005>
70. Jalili-Firoozinezhad S, Miranda CC, Cabral JMS (2021) Modeling the human body on microfluidic chips. *Trends Biotechnol*. <https://doi.org/10.1016/j.tibtech.2021.01.004>
71. Picollet-D'hahan N, Zuchowska A, Lemeunier I, Le Gac S (2021) Multiorgan-on-a-chip: a systemic approach to model and decipher inter-organ communication. *Trends Biotechnol* 39: 788–810. <https://doi.org/10.1016/j.tibtech.2020.11.014>
72. Wang T et al (2020) Comorbidities and multi-organ injuries in the treatment of COVID-19. *Lancet* 395:e52. [https://doi.org/10.1016/S0140-6736\(20\)30558-4](https://doi.org/10.1016/S0140-6736(20)30558-4)
73. Tang H et al (2020) Human organs-on-chips for virology. *Trends Microbiol* 28:934–946. <https://doi.org/10.1016/j.tim.2020.06.005>
74. Bauer S et al (2017) Functional coupling of human pancreatic islets and liver spheroids on-a-chip: towards a novel human ex vivo type 2 diabetes model. *Sci Rep* 7:14620. <https://doi.org/10.1038/s41598-017-14815-w>
75. Xu Z et al (2016) Design and construction of a multi-organ microfluidic chip mimicking the in vivo microenvironment of lung cancer metastasis. *ACS Appl Mater Interfaces* 8:25840–25847. <https://doi.org/10.1021/acsami.6b08746>
76. Asghar W et al (2015) Engineering cancer microenvironments for in vitro 3-D tumor models. *Mater Today* 18:539–553. <https://doi.org/10.1016/j.mattod.2015.05.002>
77. Quail DF, Joyce JA (2013) Microenvironmental regulation of tumor progression and metastasis. *Nat Med* 19:1423–1437. <https://doi.org/10.1038/nm.3394>
78. McMillin DW, Negri JM, Mitsiades CS (2013) The role of tumour–stromal interactions in modifying drug response: challenges and opportunities. *Nat Rev Drug Discov* 12:217–228. <https://doi.org/10.1038/nrd3870>
79. Qin S et al (2020) Emerging role of tumor cell plasticity in modifying therapeutic response. *Signal Transduct Target Ther* 5:228. <https://doi.org/10.1038/s41392-020-00313-5>
80. Plaks V, Kong N, Werb Z (2015) The cancer stem cell niche: how essential is the niche in regulating stemness of tumor cells? *Cell Stem Cell* 16:225–238. <https://doi.org/10.1016/j.stem.2015.02.015>
81. Gonzalez H, Hagerling C, Werb Z (2018) Roles of the immune system in cancer: from tumor initiation to metastatic progression. *Genes Dev* 32:1267–1284. <https://doi.org/10.1101/gad.314617.118>
82. Rodrigues J, Heinrich MA, Teixeira LM, Prakash J (2021) 3D in vitro model (R)evolution: unveiling tumor-stroma interactions. *Trends Cancer* 7:249–264. <https://doi.org/10.1016/j.trecan.2020.10.009>
83. da Cunha BR et al (2019) Cellular interactions in the tumor microenvironment: the role of secretome. *J Cancer* 10:4574–4587. <https://doi.org/10.7150/jca.21780>
84. Katt ME, Placone AL, Wong AD, Xu ZS, Searson PC (2016) In vitro tumor models: advantages, disadvantages, variables, and selecting the right platform. *Front Bioeng Biotechnol* 4:12–12. <https://doi.org/10.3389/fbioe.2016.00012>

85. Pampaloni F, Reynaud EG, Stelzer EHK (2007) The third dimension bridges the gap between cell culture and live tissue. *Nat Rev Mol Cell Biol* 8:839–845. <https://doi.org/10.1038/nrm2236>
86. Ireson CR, Alavijeh MS, Palmer AM, Fowler ER, Jones HJ (2019) The role of mouse tumour models in the discovery and development of anticancer drugs. *Br J Cancer* 121:101–108. <https://doi.org/10.1038/s41416-019-0495-5>
87. Tammela T, Sage J (2020) Investigating tumor heterogeneity in mouse models. *Ann Rev Cancer Biol* 4:99–119. <https://doi.org/10.1146/annurev-cancerbio-030419-033413>
88. Ingle AD (2019) Alternatives and refinement for animal experimentation in cancer research. In: Kojima H, Seidle T, Spielmann H (eds) *Alternatives to animal testing*. Springer, Singapore. https://doi.org/10.1007/978-981-13-2447-5_9
89. Qiao H, Tang T (2018) Engineering 3D approaches to model the dynamic microenvironments of cancer bone metastasis. *Bone Res* 6:3. <https://doi.org/10.1038/s41413-018-0008-9>
90. Aung A, Kumar V, Theprungsirikul J, Davey SK, Varghese S (2020) An engineered tumor-on-a-chip device with breast cancer–immune cell interactions for assessing T-cell recruitment. *Cancer Res* 80:263. <https://doi.org/10.1158/0008-5472.CAN-19-0342>
91. Low LA, Mummery C, Berridge BR, Austin CP, Tagle DA (2021) Organs-on-chips: into the next decade. *Nat Rev Drug Discov* 20:345–361. <https://doi.org/10.1038/s41573-020-0079-3>
92. Weltin A et al (2014) Cell culture monitoring for drug screening and cancer research: a transparent, microfluidic, multi-sensor microsystem. *Lab Chip* 14:138–146. <https://doi.org/10.1039/C3LC50759A>
93. Khalid MAU et al (2020) A lung cancer-on-chip platform with integrated biosensors for physiological monitoring and toxicity assessment. *Biochem Eng J* 155:107469. <https://doi.org/10.1016/j.bej.2019.107469>
94. Xu T et al (2018) Superwetttable electrochemical biosensor toward detection of cancer biomarkers. *ACS Sensors* 3:72–78. <https://doi.org/10.1021/acssensors.7b00868>
95. Lee J et al (2021) A heart-breast cancer-on-a-chip platform for disease modeling and monitoring of cardiotoxicity induced by cancer chemotherapy. *Small* 17:2004258. <https://doi.org/10.1002/smll.202004258>
96. Grist SM et al (2019) Long-term monitoring in a microfluidic system to study tumour spheroid response to chronic and cycling hypoxia. *Sci Rep* 9:17782. <https://doi.org/10.1038/s41598-019-54001-8>
97. Potente M, Gerhardt H, Carmeliet P (2011) Basic and therapeutic aspects of angiogenesis. *Cell* 146:873–887. <https://doi.org/10.1016/j.cell.2011.08.039>
98. Hachey SJ, Hughes CCW (2018) Applications of tumor chip technology. *Lab Chip* 18:2893–2912. <https://doi.org/10.1039/c8lc00330k>
99. Sobrino A et al (2016) 3D microtumors in vitro supported by perfused vascular networks. *Sci Rep* 6:31589. <https://doi.org/10.1038/srep31589>
100. Hsu Y-H, Moya ML, Hughes CCW, George SC, Lee AP (2013) A microfluidic platform for generating large-scale nearly identical human microphysiological vascularized tissue arrays. *Lab Chip* 13:2990–2998. <https://doi.org/10.1039/C3LC50424G>
101. Lim J, Ching H, Yoon J-K, Jeon NL, Kim Y (2021) Microvascularized tumor organoids-on-chips: advancing preclinical drug screening with pathophysiological relevance. *Nano Convergence* 8:12. <https://doi.org/10.1186/s40580-021-00261-y>
102. Kim S, Kim HJ, Jeon NL (2010) Biological applications of microfluidic gradient devices. *Integr Biol (Camb)* 2:584–603. <https://doi.org/10.1039/c0ib00055h>
103. Boussommier-Calleja A, Li R, Chen MB, Wong SC, Kamm RD (2016) Microfluidics: a new tool for modeling cancer-immune interactions. *Trends Cancer* 2:6–19. <https://doi.org/10.1016/j.trecan.2015.12.003>
104. Carvalho MR et al (2019) Colorectal tumor-on-a-chip system: a 3D tool for precision oncology. *Sci Adv* 5:eaaw1317. <https://doi.org/10.1126/sciadv.aaw1317>

105. Gioiella F, Urciuolo F, Imparato G, Brancato V, Netti PA (2016) An engineered breast cancer model on a chip to replicate ECM-activation in vitro during tumor progression. *Adv Healthc Mater* 5:3074–3084. <https://doi.org/10.1002/adhm.201600772>
106. Choi Y et al (2015) A microengineered pathophysiological model of early-stage breast cancer. *Lab Chip* 15:3350–3357. <https://doi.org/10.1039/C5LC00514K>
107. Rennert K et al (2015) A microfluidically perfused three dimensional human liver model. *Biomaterials* 71:119–131. <https://doi.org/10.1016/j.biomaterials.2015.08.043>
108. Jalili-Firoozinezhad S et al (2019) A complex human gut microbiome cultured in an anaerobic intestine-on-a-chip. *Nat Biomed Eng* 3:520–531. <https://doi.org/10.1038/s41551-019-0397-0>
109. Xiao S et al (2017) A microfluidic culture model of the human reproductive tract and 28-day menstrual cycle. *Nat Commun* 8:14584. <https://doi.org/10.1038/ncomms14584>
110. Moya A et al (2018) Online oxygen monitoring using integrated inkjet-printed sensors in a liver-on-a-chip system. *Lab Chip* 18:2023–2035. <https://doi.org/10.1039/C8LC00456K>
111. Sticker D et al (2019) Oxygen management at the microscale: a functional biochip material with long-lasting and tunable oxygen scavenging properties for cell culture applications. *ACS Appl Mater Interfaces* 11:9730–9739. <https://doi.org/10.1021/acsami.8b19641>
112. Asif A, Kim KH, Jabbar F, Kim S, Choi KH (2020) Real-time sensors for live monitoring of disease and drug analysis in microfluidic model of proximal tubule. *Microfluid Nanofluid* 24:43. <https://doi.org/10.1007/s10404-020-02347-1>
113. Misun PM et al (2020) In vitro platform for studying human insulin release dynamics of single pancreatic islet microtissues at high resolution. *Adv Biosyst* 4:1900291. <https://doi.org/10.1002/adbi.201900291>
114. Misun PM, Rothe J, Schmid YRF, Hierlemann A, Frey O (2016) Multi-analyte biosensor interface for real-time monitoring of 3D microtissue spheroids in hanging-drop networks. *Microsyst Nanoeng* 2:16022. <https://doi.org/10.1038/micronano.2016.22>
115. Bavli D et al (2016) Real-time monitoring of metabolic function in liver-on-chip microdevices tracks the dynamics of mitochondrial dysfunction. *Proc Natl Acad Sci* 113:E2231. <https://doi.org/10.1073/pnas.1522556113>
116. Ortega MA et al (2019) Muscle-on-a-chip with an on-site multiplexed biosensing system for in situ monitoring of secreted IL-6 and TNF- α . *Lab Chip* 19:2568–2580. <https://doi.org/10.1039/C9LC00285E>
117. Shin SR et al (2016) Aptamer-based microfluidic electrochemical biosensor for monitoring cell-secreted trace cardiac biomarkers. *Anal Chem* 88:10019–10027. <https://doi.org/10.1021/acs.analchem.6b02028>
118. Zhou Q et al (2015) Liver injury-on-a-chip: microfluidic co-cultures with integrated biosensors for monitoring liver cell signaling during injury. *Lab Chip* 15:4467–4478. <https://doi.org/10.1039/c5lc00874c>
119. Maoz BM et al (2017) Organs-on-chips with combined multi-electrode array and transepithelial electrical resistance measurement capabilities. *Lab Chip* 17:2294–2302. <https://doi.org/10.1039/c7lc00412e>
120. Riahi R et al (2016) Automated microfluidic platform of bead-based electrochemical immunosensor integrated with bioreactor for continual monitoring of cell secreted biomarkers. *Sci Rep* 6:24598. <https://doi.org/10.1038/srep24598>
121. Rothbauer M et al (2020) Monitoring tissue-level remodelling during inflammatory arthritis using a three-dimensional synovium-on-a-chip with non-invasive light scattering biosensing. *Lab Chip* 20:1461–1471. <https://doi.org/10.1039/C9LC01097A>
122. Zheng Y et al (2016) Angiogenesis in liquid tumors: an in vitro assay for leukemic-cell-induced bone marrow angiogenesis. *Adv Healthc Mater* 5:1014–1024. <https://doi.org/10.1002/adhm.201501007>
123. Zhang YS, Zhang Y-N, Zhang W (2017) Cancer-on-a-chip systems at the frontier of nanomedicine. *Drug Discov Today* 22:1392–1399. <https://doi.org/10.1016/j.drudis.2017.03.011>

124. Yang Y et al (2015) Evaluation of photodynamic therapy efficiency using an in vitro three-dimensional microfluidic breast cancer tissue model. *Lab Chip* 15:735–744. <https://doi.org/10.1039/C4LC01065E>
125. Angione C (2019) Human systems biology and metabolic modelling: a review-from disease metabolism to precision medicine. *Biomed Res Int* 8304260-8304260:2019. <https://doi.org/10.1155/2019/8304260>
126. Wuputra K et al (2020) Prevention of tumor risk associated with the reprogramming of human pluripotent stem cells. *J Exp Clin Cancer Res* 39:100. <https://doi.org/10.1186/s13046-020-01584-0>
127. Kim JJ (2015) Applications of iPSCs in cancer research. *Biomark Insights* 10:125–131. <https://doi.org/10.4137/BMI.S20065>
128. Marin Navarro A, Susanto E, Falk A, Wilhelm M (2018) Modeling cancer using patient-derived induced pluripotent stem cells to understand development of childhood malignancies. *Cell Death Dis* 4:7. <https://doi.org/10.1038/s41420-017-0009-2>
129. Sachs N et al (2018) A living biobank of breast cancer organoids captures disease heterogeneity. *Cell* 172:373–386.e310. <https://doi.org/10.1016/j.cell.2017.11.010>
130. Zhang YS et al (2017) Multisensor-integrated organs-on-chips platform for automated and continual in situ monitoring of organoid behaviors. *Proc Natl Acad Sci* 114:E2293. <https://doi.org/10.1073/pnas.1612906114>
131. Zhang YS, Khademhosseini A (2015) Seeking the right context for evaluating nanomedicine: from tissue models in petri dishes to microfluidic organs-on-a-chip. *Nanomedicine (Lond)* 10:685–688. <https://doi.org/10.2217/nmm.15.18>
132. Grieshaber D, MacKenzie R, Vörös J, Reimhult E (2008) Electrochemical biosensors - sensor principles and architectures. *Sensors (Basel)* 8:1400–1458. <https://doi.org/10.3390/s80314000>
133. Henry OYF et al (2017) Organs-on-chips with integrated electrodes for trans-epithelial electrical resistance (TEER) measurements of human epithelial barrier function. *Lab Chip* 17:2264–2271. <https://doi.org/10.1039/c7lc00155j>
134. Bonk SM et al (2015) Design and characterization of a sensorized microfluidic cell-culture system with electro-thermal micro-pumps and sensors for cell adhesion, oxygen, and pH on a glass chip. *Biosensors (Basel)* 5:513–536. <https://doi.org/10.3390/bios5030513>
135. Khan NI, Song E (2020) Lab-on-a-chip systems for aptamer-based biosensing. *Micromachines* 11. <https://doi.org/10.3390/mi11020220>
136. Kasendra M et al (2018) Development of a primary human small intestine-on-a-chip using biopsy-derived organoids. *Sci Rep* 8:2871. <https://doi.org/10.1038/s41598-018-21201-7>
137. Liszka BM et al (2015) A microfluidic chip for high resolution Raman imaging of biological cells. *RSC Adv* 5:49350–49355. <https://doi.org/10.1039/C5RA05185A>
138. Lee C et al (2021) Label-free three-dimensional observations and quantitative characterisation of on-chip vasculogenesis using optical diffraction tomography. *Lab Chip* 21:494–501. <https://doi.org/10.1039/D0LC01061H>
139. Zbinden A et al (2020) Non-invasive marker-independent high content analysis of a microphysiological human pancreas-on-a-chip model. *Matrix Biol* 85–86:205–220. <https://doi.org/10.1016/j.matbio.2019.06.008>
140. Sriram G et al (2018) Full-thickness human skin-on-chip with enhanced epidermal morphogenesis and barrier function. *Mater Today* 21:326–340. <https://doi.org/10.1016/j.mattod.2017.11.002>
141. Toseland CP (2013) Fluorescent labeling and modification of proteins. *J Chem Biol* 6:85–95. <https://doi.org/10.1007/s12154-013-0094-5>
142. Jang KJ et al (2019) Reproducing human and cross-species drug toxicities using a liver-chip. *Sci Transl Med* 11. <https://doi.org/10.1126/scitranslmed.aax5516>
143. Lin NYC et al (2019) Renal reabsorption in 3D vascularized proximal tubule models. *Proc Natl Acad Sci* 116:5399. <https://doi.org/10.1073/pnas.1815208116>
144. Bischel LL, Beebe DJ, Sung KE (2015) Microfluidic model of ductal carcinoma in situ with 3D, organotypic structure. *BMC Cancer* 15:12. <https://doi.org/10.1186/s12885-015-1007-5>

145. Koo Y, Hawkins BT, Yun Y (2018) Three-dimensional (3D) tetra-culture brain on chip platform for organophosphate toxicity screening. *Sci Rep* 8:2841. <https://doi.org/10.1038/s41598-018-20876-2>
146. Costa PF et al (2017) Mimicking arterial thrombosis in a 3D-printed microfluidic in vitro vascular model based on computed tomography angiography data. *Lab Chip* 17:2785–2792. <https://doi.org/10.1039/c7lc00202e>
147. Peel S et al (2019) Introducing an automated high content confocal imaging approach for organs-on-chips. *Lab Chip* 19:410–421. <https://doi.org/10.1039/C8LC00829A>
148. Chen YY et al (2016) Clarifying intact 3D tissues on a microfluidic chip for high-throughput structural analysis. *Proc Natl Acad Sci* 113:14915–14920. <https://doi.org/10.1073/pnas.1609569114>
149. Sheyn D et al (2019) Bone-chip system to monitor osteogenic differentiation using optical imaging. *Microfluid Nanofluid* 23:99. <https://doi.org/10.1007/s10404-019-2261-7>
150. Lazzari G et al (2019) Light sheet fluorescence microscopy versus confocal microscopy: in quest of a suitable tool to assess drug and nanomedicine penetration into multicellular tumor spheroids. *Eur J Pharm Biopharm* 142:195–203. <https://doi.org/10.1016/j.ejpb.2019.06.019>
151. Kobayashi H, Bouvier M (2021) Bioluminescence resonance energy transfer (BRET) imaging in living cells: image acquisition and quantification. *Methods Mol Biol* 2274:305–314. https://doi.org/10.1007/978-1-0716-1258-3_26
152. Mirasoli M, Guardigli M, Micheli E, Roda A (2014) Recent advancements in chemical luminescence-based lab-on-chip and microfluidic platforms for bioanalysis. *J Pharm Biomed Anal* 87:36–52. <https://doi.org/10.1016/j.jpba.2013.07.008>
153. Cevenini L et al (2017) Bioluminescence imaging of spheroids for high-throughput longitudinal studies on 3D cell culture models. *Photochem Photobiol* 93:531–535. <https://doi.org/10.1111/php.12718>
154. Endo M, Ozawa T (2020) Advanced bioluminescence system for in vivo imaging with brighter and red-shifted light emission. *Int J Mol Sci* 21. <https://doi.org/10.3390/ijms21186538>
155. Kwon H et al (2010) Bioluminescence imaging of dual gene expression at the single-cell level. *Biotechniques* 48:460–462. <https://doi.org/10.2144/000113419>
156. Evans MS et al (2014) A synthetic luciferin improves bioluminescence imaging in live mice. *Nat Methods* 11:393–395. <https://doi.org/10.1038/nmeth.2839>
157. Lee KS, Levine E (2018) A microfluidic platform for longitudinal imaging in *Caenorhabditis elegans*. *J Vis Exp*. <https://doi.org/10.3791/57348>
158. Kuchimaru T et al (2016) A luciferin analogue generating near-infrared bioluminescence achieves highly sensitive deep-tissue imaging. *Nat Commun* 7:11856. <https://doi.org/10.1038/ncomms11856>
159. Tannous BA, Kim DE, Fernandez JL, Weissleder R, Breakefield XO (2005) Codon-optimized *Gaussia* luciferase cDNA for mammalian gene expression in culture and in vivo. *Mol Ther* 11:435–443. <https://doi.org/10.1016/j.ymthe.2004.10.016>
160. Hall MP et al (2012) Engineered luciferase reporter from a Deep Sea shrimp utilizing a novel imidazopyrazinone substrate. *ACS Chem Biol* 7:1848–1857. <https://doi.org/10.1021/cb3002478>
161. Yao Z et al (2021) Coumarin luciferins and mutant luciferases for robust multi-component bioluminescence imaging. *Chem Sci* 12:11684–11691. <https://doi.org/10.1039/D1SC03114G>
162. Chu J et al (2016) A bright cyan-excitable orange fluorescent protein facilitates dual-emission microscopy and enhances bioluminescence imaging in vivo. *Nat Biotechnol* 34:760–767. <https://doi.org/10.1038/nbt.3550>
163. Nomura N et al (2019) Biothiol-activatable bioluminescent coelenterazine derivative for molecular imaging in vitro and in vivo. *Anal Chem* 91:9546–9553. <https://doi.org/10.1021/acs.analchem.9b00694>
164. Maric T et al (2019) Bioluminescent-based imaging and quantification of glucose uptake in vivo. *Nat Methods* 16:526–532. <https://doi.org/10.1038/s41592-019-0421-z>

165. Mezzanotte L, An N, Mol IM, Löwik CW, Kaijzel EL (2014) A new multicolor bioluminescence imaging platform to investigate NF- κ B activity and apoptosis in human breast cancer cells. *PLoS One* 9:e85550. <https://doi.org/10.1371/journal.pone.0085550>
166. Gregor C, Gwosch KC, Sahl SJ, Hell SW (2018) Strongly enhanced bacterial bioluminescence with the *lux* operon for single-cell imaging. *Proc Natl Acad Sci* 115:962. <https://doi.org/10.1073/pnas.1715946115>
167. Gregor C et al (2019) Autonomous bioluminescence imaging of single mammalian cells with the bacterial bioluminescence system. *Proc Natl Acad Sci* 116:26491. <https://doi.org/10.1073/pnas.1913616116>
168. Kim TJ, Türkan S, Pratz G (2017) Modular low-light microscope for imaging cellular bioluminescence and radioluminescence. *Nat Protoc* 12:1055–1076. <https://doi.org/10.1038/nprot.2017.008>
169. Sternberg C, Eberl L, Poulsen LK, Molin S (1997) Detection of bioluminescence from individual bacterial cells: a comparison of two different low-light imaging systems. *J Biolumin Chemilumin* 12:7–13. [https://doi.org/10.1002/\(sici\)1099-1271\(199701/02\)12:1<7::Aid-bio427>3.0.Co;2-3](https://doi.org/10.1002/(sici)1099-1271(199701/02)12:1<7::Aid-bio427>3.0.Co;2-3)
170. Masamizu Y et al (2006) Real-time imaging of the somite segmentation clock: revelation of unstable oscillators in the individual presomitic mesoderm cells. *Proc Natl Acad Sci* 103:1313. <https://doi.org/10.1073/pnas.0508658103>
171. Ogoh K et al (2014) Bioluminescence microscopy using a short focal-length imaging lens. *J Microsc* 253:191–197. <https://doi.org/10.1111/jmi.12109>
172. Suzuki T, Kanamori T, Inouye S (2020) Novel technology for studying insulin secretion: imaging and quantitative analysis by a bioluminescence method. *Yakugaku Zasshi* 140:969–977. <https://doi.org/10.1248/yakushi.20-00012-2>
173. Hoshino H, Nakajima Y, Ohmiya Y (2007) Luciferase-YFP fusion tag with enhanced emission for single-cell luminescence imaging. *Nat Methods* 4:637–639. <https://doi.org/10.1038/nmeth1069>
174. Kim J, Grailhe R (2016) Nanoluciferase signal brightness using furimazine substrates opens bioluminescence resonance energy transfer to widefield microscopy. *Cytometry A* 89:742–746. <https://doi.org/10.1002/cyto.a.22870>
175. Tung JK, Berglund K, Gutekunst CA, Hochgeschwender U, Gross RE (2016) Bioluminescence imaging in live cells and animals. *Neurophotonics* 3:025001. <https://doi.org/10.1117/1.NPh.3.2.025001>
176. Kim TJ, Türkan S, Ceballos A, Pratz G (2015) Modular platform for low-light microscopy. *Biomed Opt Express* 6:4585–4598. <https://doi.org/10.1364/BOE.6.004585>
177. Doi M, Sato M, Ohmiya Y (2020) In vivo simultaneous analysis of gene expression by dual-color luciferases in *Caenorhabditis elegans*. *Int J Mol Sci* 22. <https://doi.org/10.3390/ijms22010119>
178. Goda K et al (2015) Combining fluorescence and bioluminescence microscopy. *Microsc Res Tech* 78:715–722. <https://doi.org/10.1002/jemt.22529>
179. Celinskis D et al (2020) Miniaturized devices for bioluminescence imaging in freely behaving animals. *bioRxiv*, 2020.2006.2015.152546. <https://doi.org/10.1101/2020.06.15.152546>
180. Hattori M, Shirane S, Matsuda T, Nagayama K, Nagai T (2020) Smartphone-based portable bioluminescence imaging system enabling observation at various scales from whole mouse body to organelle. *Sensors* 20. <https://doi.org/10.3390/s20247166>
181. Fetah KL et al (2019) Cancer modeling-on-a-chip with future artificial intelligence integration. *Small* 15:e1901985. <https://doi.org/10.1002/smll.201901985>



Microfluidic-Driven Biofabrication and the Engineering of Cancer-Like Microenvironments

8

Carlos F. Guimarães, Luca Gasperini, and Rui L. Reis

Abstract

Despite considerable advances in cancer research and oncological treatments, the burden of the disease is still extremely high. While past research has been cancer cell centered, it is now clear that to understand tumors, the models that serve as a framework for research and therapeutic testing need to improve and integrate cancer microenvironment characteristics such as mechanics, architecture, and cell heterogeneity. Microfluidics is a powerful tool for biofabrication of cancer-relevant architectures given its capacity to manipulate cells and materials at very small dimensions and integrate varied living tissue characteristics. This chapter outlines the current microfluidic toolbox for fabricating living constructs, starting by explaining the varied configurations of 3D soft constructs microfluidics enables when used to process hydrogels. Then, we analyze the possibilities to control material flows and create space varying characteristics such as gradients or advanced 3D micro-architectures. Envisioning the trend to approach the complexity of tumor microenvironments also at higher dimensions, we discuss microfluidic-enabled 3D bioprinting and recent advances in that arena. Finally, we summarize the future possibilities for microfluidic biofabrication to tackle important challenges in cancer 3D modelling, including tools for the fast quantification of biological events toward data-driven and precision medicine approaches.

C. F. Guimarães (✉) · L. Gasperini · R. L. Reis
3B's Research Group—Biomaterials, Biodegradables and Biomimetics, Headquarters of the European Institute of Excellence on Tissue Engineering and Regenerative Medicine, University of Minho, Barco, Guimarães, Portugal

ICVS/3B's—PT Government Associate Laboratory, Braga/Guimarães, Portugal
e-mail: carlos.guimaraes@i3bs.uminho.pt

© The Author(s), under exclusive license to Springer Nature Switzerland AG 2022
D. Caballero et al. (eds.), *Microfluidics and Biosensors in Cancer Research*,
Advances in Experimental Medicine and Biology 1379,
https://doi.org/10.1007/978-3-031-04039-9_8

205

Keywords

Biofabrication · Microfluidics · Tumor microenvironment · 3D bioprinting · 3D modelling

8.1 Introduction

The past couple of decades have been marked by remarkable advances in the engineering of living tissues. More than ever, it is nowadays established that the architecture of biological tissues, their physical and mechanical characteristics, are important modulators of cellular responses and contribute to the overall tissue and organ functionality—to a similar extent to that of biochemical cues [1]. This notion applies to healthy tissues, but also diseased ones, such as cancer, where changes in the architecture of the tissue, extracellular matrix composition, and consequent mechanics play critical outcomes in cellular responses, from early proliferation to late metastasis [2]. Therefore, when attempting to approach and miniaturize living tissues for creating important research models, which are capable of recapitulating critical physiological responses, it is essential to reconstruct the tissue microenvironment and approach its 3D complexity to derive relevant responses, such as predicting the outcome of a certain drug in cancer cell invasion.

In biofabrication, a more recent area of the global tissue engineering field, there has been continuous development of technologies which allow for constructing complex cell/material structures with increasing level of detail and complexity. In the field of bioprinting, for example, the latest advances have enabled the creation of human-sized organ constructs such as the heart [3], or even other 3D structures in a matter of seconds [4]. Even though bioprinting presents an important advance to recreate tissues or even approach whole organs, it entails a resolution which is not yet fine enough to reproduce the intricacies of very fine biological environments, namely those of the cancer microenvironment [5–7]. Therein, differences at the single-cell level can be found, with a variety of cellular entities and extracellular matrix components, interacting in a very small niche, which gradually grows and evolves toward a more mature cancer tissue. As such, creating smaller structures that still encompass the 3D characteristics of cancer environments can take advantage of microfluidic technologies and their finer resolution capacities.

In microfluidic conditions, liquids such as hydrogel precursors flow in very small-sized channels, where turbulence is extremely low and thus fluids tend to maintain their trajectory without typically mixing. This characteristic can be employed to translate multiple precursor flow 3D configurations into hydrogel shapes by taking advantage of crosslinking precursors upon extrusion, using a varied toolbox of hydrogel crosslinking techniques [8–12]. By manipulating materials and cells at very small scales, microfluidics enables for a whole set of possibilities for biofabrication. Unlike typical on-chip technologies that attempt at recreating the physiology of tissues and organs within plastic chips in dynamic cultures, this

chapter will mostly explore microfluidics as a direct biofabrication tool to create independent structures with advanced 3D complexity at very small scales.

Starting with an overview of how microfluidic flows can be combined with hydrogel technologies to create soft, 3D structures that can approach the mechanics of living tissues and integrate cells, within structures such as cell-laden fibers, droplets, and combinations of such. Then, we will discuss how the quick and easy manipulation of different flows can be used to create space-varying compositional characteristics within fabricated structures, such as gradient-like transitions that can approach those transitions typically found in healthy and diseased tissues, or be leveraged toward high-throughput, single-sample screening approaches. After, we will discuss how flows alone can be used to create complex 3D architectures within microfluidic-biofabricated structures, from hundreds of micrometers to near single-cell dimensions, approaching the organization of several living microenvironments, namely those of cancer in early invasive stages. We will then explore how additional complexity can be obtained by combining different technologies with microfluidic biofabrication, namely bioprinting for the gradual assembly living constructs with complex shapes due to microfluidic-enabled manufacturing.

By providing an overview of the current microfluidic biofabrication toolbox, this chapter exposes the opportunities and current needs within the field of cancer-like environment engineering. We outline a clear set of strategies that can be used to imbue purely 3D, soft, microfabricated constructs with material and cellular architectures that can approach important characteristics of living cancers. By allowing to do so in fast, standardized, and affordable ways, microfluidic biofabrication is likely to grow in the next few years and overcome other technologies when cellular-level resolution is required, such as the recreation of truly physiological cancer microenvironment models.

8.2 Microfluidics: A Versatile Tool for 3D Hydrogel Processing

Microfluidic techniques are designed to manipulate liquids of various viscosities, and different available techniques are best suited to process liquids of different nature. When the liquid is a hydrogel precursor, typically a water-based solution of specific polymers, some conditions induce its sol–gel transition or, in other terms, the crosslinking of the dissolved polymers and hardening of the liquid into a hydrogel [13]. These conditions depend on the gel-forming solution and determine which is the most suitable microfluidic technique to process them into a 3D hydrogel. These gel-forming polymers are categorized, sometimes improperly, into two main families based on their sol–gel mechanism: those that form gels physically and those that form gels chemically.

The family of polymers that physically forms gels include those polymers that do so thanks to noncovalent (ionic and weak interactions) bonds between the polymeric chains. Alternatively, chemically crosslinked polymers form a gel by strong covalent bonds between the chains. Some physically crosslinked polymers are thermoresponsive polymers that rearrange due to temperature variation into

insoluble structures. Gelatin and collagen belong to this family, and the former presents an upper critical solution temperature above which gelatin and water are miscible and the gel is formed by cooling a warm solution below the critical temperature, which is around 35 °C [14]. Collagen, regardless of being the precursor of gelatin, form gels in the opposite way and presents a low critical solution temperature close to physiological conditions, above which forms a gel. The formation of gels by temperature variation can be a relatively slow process, especially when strong cooling or heating is not allowed [15]. This limitation is particularly evident when cells are present in the solution because of their sensibility to drastic variation in temperature that affects their viability. For this reason, polymers such as collagen and gelatin are well suited for droplet-based microfluidic techniques that allow the necessary time for them to harden.

With this technique, the droplet is formed thanks to a microfluidic setup that comprises a junction of two or more channels containing different phases. The water-based droplet-forming phase is forced into the hydrophobic continuous phase at the junction, then the shear stresses applied by the continuous phase break the stream of the water-based solution, forming a droplet. This process leads to high-throughput formation of highly monodisperse and separate droplets of liquids in an immiscible phase [16]. The outlet channel can be connected to a tube of variable length and can be treated at different temperatures than the temperature of the starting solutions. The separation of the droplet is ensured by the presence of surfactants that avoid coalescence, thus allowing enough time for the gel droplet to form, and then be collected by various means such as centrifugation or filtration. A similar technique is typically used to produce droplets of photo crosslinked polymers.

Photocrosslinkable polymers are chemically crosslinkable polymers containing functional groups along the backbone that are sensible to radical chemical reactions that form covalent bonds among the polymeric chains. These polymers can be obtained by chemical modification of natural polymers, such as hyaluronic acid [17] or can naturally have this characteristic, such as collagen using riboflavin as a photoinitiator [18]. Here, the microfluidic setup for the production of 3D hydrogels is similar to the one used for the thermoresponsive polymers because also this photocrosslinking process tends to be relatively slow [19]. In fact, a light of high intensity that makes the formation of gel quicker is not optimal because it could also harm cells. The droplet-forming solution contains a photoinitiator that forms a radical reactive species when exposed to light of a specific wavelength, so the outlet channel or tube where the droplet flow is exposed to light and the hardened droplets can be collected. Here, the material that makes the outlet should be transparent to the specific wavelength that excites the photoinitiator into the radical (e.g., fluorinated ethylene propylene for UV light). While droplets based techniques are optimal for thermoresponsive and photocrosslinkable polymers, they still require a careful selection of the materials used for the microfluidic system.

For the fabrication of hydrogel droplets, the system must be hydrophobic so that the oil can efficiently wet the channels of the microfluidic setup to avoid contact between the droplets and the system. The materials that make the system should be

compatible with the oil used, a suitable and well-performing surfactant should be present, be compatible with the oil, and should favor the formation of water droplets in oil. Considering two commonly used surfactants, for example, Tween and Span, the former is characterized by a high HLB number (Hydrophilic, Lipophilic Balance, is an index of the solubilizing properties of emulsifiers) thus favoring the formation of oil in water droplets, oppositely the latter has a low HLB number and favors the formation of water droplets in oil [20, 21].

Droplet techniques, due to their nature and in particular being emulsion-based, are challenging when used to process ionically crosslinkable materials, which represent an important family of biopolymers that include alginate and gellan gum. These polymers contain carboxyl groups along their backbone that carry a net negative charge. In the presence of positive ions, they form insoluble complexes due to the complexation of those groups that are responsible for the solubility of the polymer in water. Emulsion-based microfluidic techniques are less straightforward to employ with these polymers due to the challenges in using dissolved ions in these systems. The positive ions typically derive from the dissolution of salts in water that should be placed in contact with the polymeric solution to obtain the gel. To do this, it is possible to follow a more complex approach and fabricate two different droplets, one containing the polymer and the other containing the salts, which coalesce forming a gel before collection. Another approach is to use a hardening bath containing the dissolved salts. When the suspension of water droplets and oil reaches the bath, the droplets can separate from the oil due to differences in density so that they can reach the water solution containing the salts. During this process, the droplets must pass through the oil-hardening bath interface that acts as a barrier that can deform the droplets or can block them if the difference in density is limited. Overall droplet-based techniques are interesting approaches for the fabrication of 3D hydrogels that are highly monodispersed in size. The size can vary from submicron to some hundred microns based on the viscosity of the solution used, the size of the channels, the flow rates of the oil, and the gel-forming solution. Furthermore, given their round shape and sub-needle size, the hydrogels can be easily handled with a pipette and can be injected if needed. Moreover, recent advances in microfluidic droplet fabrication are even opening new possibilities for increasing their 3D complexity, such as the creation of inner architectures using airflow (Fig. 8.1) [22].

Other than droplets, microfluidic techniques can be used to produce fibers and those techniques are generally referred to as continuous flow microfluidics. These techniques are wet spinning techniques, where a microfluidic chip is used to extrude a polymeric solution into the hardening bath. These techniques are simpler than droplet-based techniques if applied to those materials that rapidly crosslink in the presence of a hardening bath, and for this reason, they are well suited to process ionically crosslinkable materials. Here, when the solution exits the chip, the surface in contact with the bath quickly crosslinks forming a fiber, which can then sink or float based on the density ratio between gel-forming solution and bath. The fiber can be collected easier than droplets because the oil is not present and post processing steps to remove it are not needed.

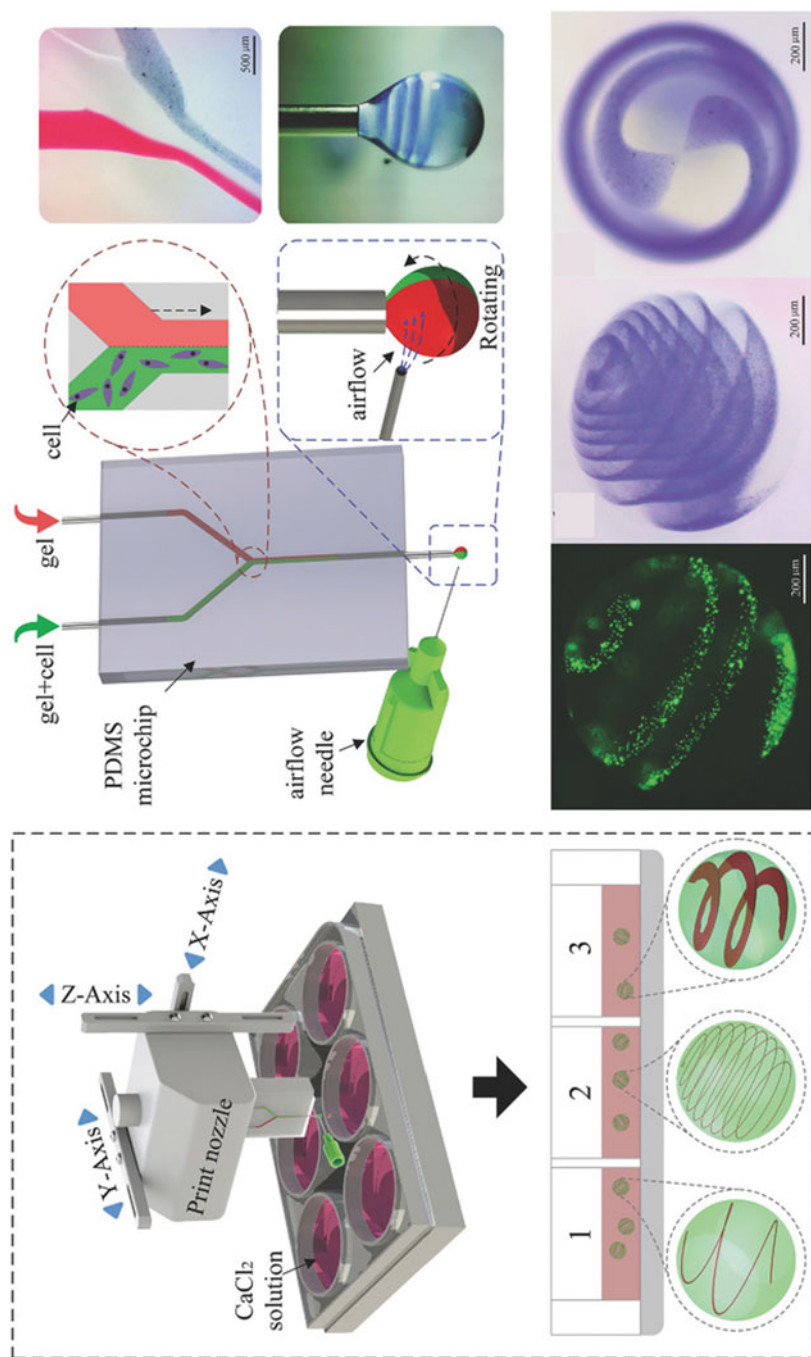


Fig. 8.1 Airflow-assisted generation of microfluidic droplets with controlled inner 3D architectures. Reprinted with permission from [22]

Oppositely to droplet techniques, continuous flow is challenging when used to process polymers that do not crosslink rapidly since the gel-forming solution does not have enough time to form the gel and ends up being dissolved into the bath. While droplet and continuous flow microfluidic are different, they share the same microfluidic concept related to how fluids behave in microchannels, that is, they flow in laminar conditions. In laminar conditions, fluids have a tendency not to mix so that it is possible to design a microfluidic chip with two inlets that meet at a junction, thus obtaining two fluids flowing side by side in the outlet. Similarly, it is possible to design a junction so that one fluid flows on the inner portion of the outlet and one on the outer part forming a coaxial flow [23].

More complex designs that encompass more fluids are possible, for example, obtaining two fluids side by side enwrapped in the third liquid. One or more fluids, e.g., the fluid generating the shell in the previous example, can be a polymeric solution that forms solid hydrogels in specific conditions. Those conditions can be triggered on-demand to solidify one or more of the streams to obtain outside the chip a micro-hydrogel with the same spatial distribution of the generating fluids. The outcome is a hydrogel fiber with different regions recognizable in its cross-section. The amount of space that these regions will occupy in the fiber is determined by the flow rate of the liquid they were made from. By changing the flow rate of the fluids, for example, one can obtain a coaxial fiber with a big core and a thin shell or a small core and a thick shell by inverting the initial flow rates. This size distribution can be obtained into a single fiber with a constant diameter using programmable flow pumps that linearly change the flow so that one side of the fiber can have a small core and the other side a bigger core with a thinner shell.

Finally, it is worth mentioning that certain approaches aim at combining discrete droplet generation with continuous hydrogel fiber spinning. A recent work has shown that GelMa droplets generated by oil–water separation could be integrated into a continuous stream of alginate, originating a hydrogel fiber with highly packed cellular spheroids (Fig. 8.2). This approach represents a very interesting alternative to fabricating single cancer cell droplets or spheroids, as the hydrogel fiber serves as a support for improving the manipulation of several droplets at once, making it easier for applying different culture treatments (e.g., anticancer drugs) as well as analyzing (e.g., fixing, staining, and imaging).

8.3 Microfluidic Real-Time Control of 3D Construct Composition

Using microfluidics-based techniques for processing hydrogel materials presents also unique opportunities to control the composition of constructs, namely, to obtain gradient-like distributions. Gradients are interesting architectures for tissue engineering and biofabrication for two main reasons. The first, is that biological tissues present natural gradients formed at interfaces such as tendon–bone or cartilage–bone interfaces [1], a characteristic which is very important when attempting to engineer, e.g., osteochondral tissues [25]. The second, is that gradients are able to integrate

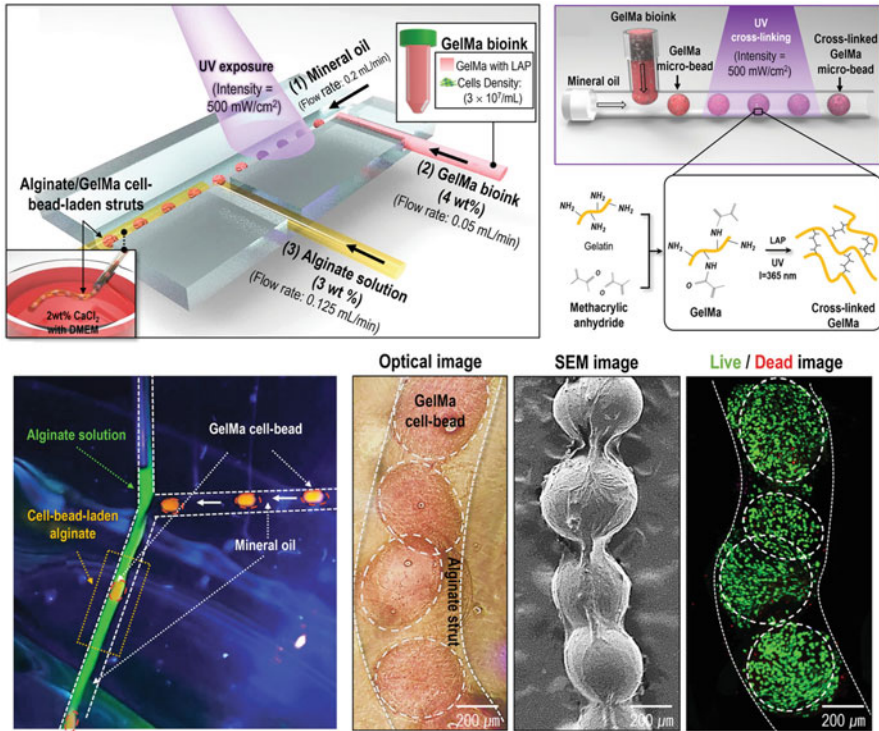


Fig. 8.2 The combination of microfluidic droplet generation and continuous flow fiber fabrication enables the creation of cell-bead-laden alginate fibers, which can transport highly cellular, packed spheroid-like structures within a single support fiber. Reprinted, with permission, from [24]

a full spectrum of conditions in a single sample, serving as very powerful platforms for high-throughput screening cell–material interactions [26]. In this regard, gradually changing material composition, cellular density, or ECM molecule distribution are important characteristics of 3D niches that must be optimized for engineering cancer microenvironments, in which microfluidic biofabrication has enabled unique advances.

For some time, microfluidic mixer chips have been used to manipulate liquid hydrogel precursors and establish gradients ranging between two extreme conditions, coupled with different crosslinking strategies, such as photopolymerization of PEG hydrogels [27]. Moreover, the manipulation of hydrogel precursors for gradient formation can be simultaneously combined with cell encapsulation in such chips, creating not just surfaces for cell adhesion but gradient-like 3D environments where cell responses can be studied, as a function of crosslinking density, polymer concentration, or even cellular density, in order to optimize the engineering of the tumor microenvironments [28]. In that work, researchers have shown that this platform was able to successfully present glioma cells with varying tumor microenvironment relevant characteristics, such as

extracellular matrix density, mechanics, and glioma cell density, where in situ analysis could be performed at the molecular and genomic levels, such as the expression of genes of interest (VEGF and HIF-1) or the secretion of MMPs. Even though these gradient-forming chips present interesting opportunities for library building and 3D biomaterial screening, the engineered environments are still confined to the chip and limited by its size and the possibilities for post-fabrication manipulation of the construct. Typically, these are also analyzed in a limited number (e.g., three or four) regions, which reduces the overall throughput of the technique. To overcome these limitations, researchers have developed techniques to fabricate 3D gradients using microfluidic biofabrication to derive individual out-of-chip constructs, which can be further manipulated and yield higher levels of throughput.

In such an approach, researchers have combined microfluidic-driven precursor mixing with wet spinning to fabricate cell-laden 3D hydrogel fibers with compositional gradients, which were able to integrate a gradient of 3D hydrogel stiffness, used to screen stem cell differentiation triggering, but representing an equally important characteristic to assess for cancer microenvironment engineering [29] (Fig. 8.3). In this work, the team has also demonstrated that a similar approach could be combined with multiple crosslinking stimuli to fabricate multi-material, multi-crosslinking gradients, where further responses ranging from adhesion to proliferation and mechanotransduction could be studied. In previous work, 3D hydrogel fibers were also shown to be interesting platforms for quickly engineering 3D tumor-like environments, where different cancer cell: macrophage ratios in proximity could be adjusted for mimicking different cancer stages [10].

Droplet-like microgels have also been explored as an alternative to continuous fibers for gradient fabrication. A team has demonstrated that droplets could be fabricated from different precursors using microfluidic water/oil emulsions and UV-crosslinking, then aggregating the resulting microgels to create patterns or gradients. By annealing the microgels, the researchers showed that a continuous 3D microgel scaffold could be deposited with gradients in stiffness or biodegradability. Mesenchymal stem cells were then cultured to screen their adhesion and morphology with the varying 3D microenvironmental characteristics [30] (Fig. 8.4). This approach may be further combined with recently developed microgel jamming and printing technologies [31], where 3D gradients can be assembled in more complex shapes for approaching the architectures of tissues or, for example, different compartments relevant to approach the cellular heterogeneity of the cancer microenvironment.

The cancer heterogeneity is not only related to architecture and mechanics but also to the presence of distinct cell populations and subpopulations, where varying numbers of cells and ratios between, e.g., cancer, stromal, and immune cells come into play as in any other functional organs [32]. In that regard, microfluidic-driven platforms have also been applied, albeit to a lower extent, to cellular and cell density gradient studies. By manipulating hydrogel precursors with suspension cells similarly to the previously discussed results, researchers have also demonstrated how intricate cellular niches, such as those of hematopoietic stem cells, can be studied in a high-throughput fashion, by creating cellular gradients ranging from pure

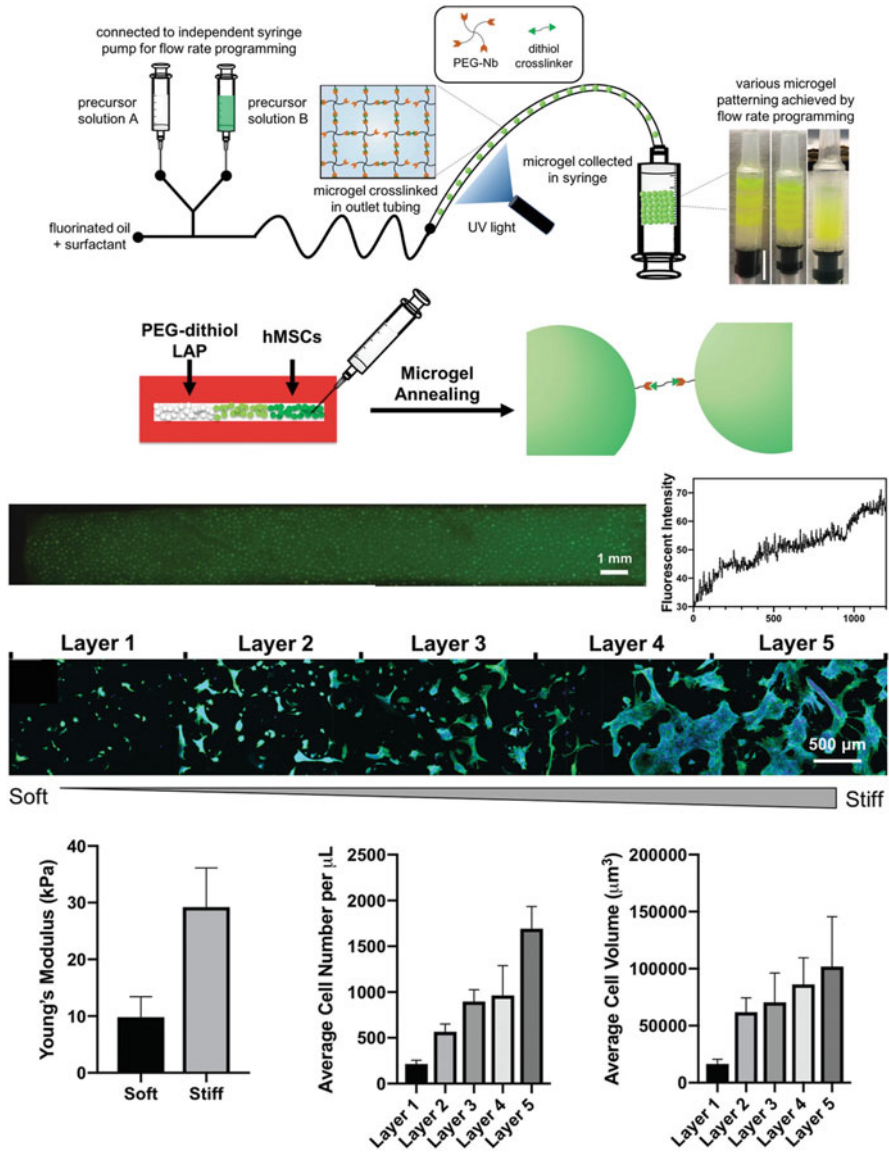


Fig. 8.4 Microfluidic-driven generation of hydrogel droplets and microgel annealing for creating 3D gradients suitable for cell culture and high-throughput screening. Adapted with permission from [30]

hematopoietic progenitor cells to pure osteoblast populations [33]. More recently, 3D gradients of vascular density were also fabricated via microfluidic mixing to study the effect of angiocrine cues on stem cell behavior [34]. Similar approaches can be leveraged to cancer microenvironment engineering, where the cancer cell

niche and cell–cell interactions can be studied and optimized quickly taking advantage of broad ranges of ratios between cancer cells, vasculature, stromal cells (e.g., cancer-associated fibroblasts), and immune cells (e.g., macrophages or T-cells).

Moreover, other types of cancer hallmarks can be approached in a high-throughput fashion for screening drugs or modelling physiologically relevant responses, such as hypoxia. Typically, cancers are characterized by highly dense environments with deficient vasculature, where certain regions of the tumor tissue experience low oxygen levels (hypoxia), which in turn lead to altered metabolism, and trigger signaling cascades such as those promoting angiogenesis [35]. Indeed, hypoxic conditions can alter the response and resistance of cancer cells to drugs, and the absence of such physiologically relevant parameters in 3D cancer models may lead to wrongful conclusions when testing new therapeutic strategies. Microfluidic chips and platforms present interesting opportunities to tackle this scenario by allowing for the creation of gradients also in oxygen concentration [36]. Researchers have shown that oxygen levels ranging from 0 to 20% could be obtained in a single chip, where cancer spheroids could be cultured in gradually changing levels of oxygen, demonstrating how varying oxygen levels could alter the metabolic activity of cancer and immune cells, as well as differences in the success of the anticancer drugs Doxorubicin and Tirapazamine [37]. The team demonstrated that lower oxygen levels (hypoxia) led to increased resistance to both drugs, highlighting the need for approaching physiological conditions when miniaturizing cancers for drug testing.

Lastly, it is important to refer that microfluidic-biofabricated gradients are not only important as fundamental and applied research tools, but these may also be more closely interfaced with clinical settings for patient-specific, personalized, and precision medicine approaches. A recent work has demonstrated how patient-derived tumor xenografts of glioblastoma could be integrated into gradients of brain-mimicking stiffness, showing how varying 3D mechanics affected cellular proliferation and, particularly, regions with increased stiffness led to increased resistance to the drug temozolomide [38]. Even though the work does not employ microfluidic techniques, it clearly demonstrates the importance of creating physiologically relevant platforms for assessing patient-derived cell responses to treatments, namely going beyond traditional 2D plates with nonphysiological stiffness. By further combining this knowledge with the high-throughput and speed of microfluidic-driven biofabrication, future platforms may enable a much faster and personalized approach to therapies, where patient cells can be quickly employed for *in vitro* therapeutical studies, also requiring lower amounts of cells and materials due to the unique microfluidic miniaturization capabilities.

8.3.1 Discrete Generation of Individual Microfluidic Segments

Even though the previous section focuses on continuous microfluidic structures, it is also important to discuss the possibility to create individualized segments within

microfluidic-fabricated structures, which can be separated by inert gaps and function as an array of 3D environments.

Indeed, the fluid tendency to not mix with microchips can be exploited to fabricate vertically segmented fibers using a microfluidic chip containing a junction. The junction can be a simple T or Y junction or can have a more advanced geometry able to connect more channels together. The junction is made in such a way that the fluids coming from different inlet channels can join in one common exit channel. By applying pressure on one or more channels, only the fluids from those channels will flow to the exit channel. By stopping the application of pressure on those channels the flow will stop. By pressurizing other channels new and different fluids will flow in the exit channel pushing forward the fluid already present in the exit channel. By repeating this process, the exit channel is filled with different fluids, such fluids do not mix (or with minimal mixing) so that different compartments along the path of the exit channel can be identified. After this, some or all the fluids composing the segments of interest are hardened so that the compartments can keep separated. The segments may not be perfectly shaped cylinders due to the rheological nature of the generating fluids. Fluids that behave as Newtonian fluids develop a parabolic speed profile inside the channel and as such the segment generated by these fluids may have a parabolic profile at the bases [39]. Oppositely, a fluid following a non-Newtonian power law model develops a different speed profile-forming cylinders with a flatter base in the middle and a parabolic profile on the sides. The final product of this technique is a fiber composed of segments that can be composed of different materials.

This feature can be exploited to obtain single segments, making this technique an oil-less alternative approach to droplet microfluidic. The advantage of this technique is the absence of oil that simplifies the fabrication (see Sect. 2) and cylinders are formed rather than spherical objects. Spheres are the geometrical shape that includes the highest amount of mass in the lowest amount of surface and this is how water-based droplets minimize the surface in contact with the oil. Oppositely, cylinders present a higher surface-to-volume ratio, which favors the diffusion of nutrients and metabolites when cells are encapsulated [40]. To obtain single segments there are two main approaches that can be followed: the use of a sacrificial gelling agent or the use of a non-gelling agent as one of the segments. In the first case, a fiber is formed and a sacrificial gelling agent can be degraded and removed. One example is a fiber composed of gellan gum and alginate segments, where the alginate can be removed by enzymatically accelerated degradation using alginase or by using chelating agents that do not affect gellan gum [41, 42]. Considering the second case, segments are formed directly by using any solution with a similar viscosity that one of the segments of interest that does not form gels in the hardening bath, such as hyaluronic acid. When extruded, the non-gelling phase dissolves in the hardening bath while the gelling phase hardens forming cylindrical gels that can be collected for further use.

8.4 Microfluidic Flow-Based Generation of 3D and Cancer-Like Architectures

As initially outlined, the shapes and architectures present within living tissues are as important as their bulk composition and play an important role in the consequent mechanical properties and biological events. Characteristics such as ECM orientation, tissue anisotropy, and the presence of multiple compartments with different cellular and ECM compositions are critical to approach and model living tissues [1]. In 2D surfaces, oriented topographies and their impact on cellular behavior have been explored for a long time [43–45], but their translation to 3D systems is not so straightforward. Typically, to introduce orientation and shape in 3D hydrogels, there is a need to use composite systems where nanoparticles [46] or microgels [47] are aligned using externally-driven methodologies such as magnetic fields, to create 3D orientation and introduce shape control in hydrogels. Alternatively, the process of hydrogel crosslinking can also be combined with the manipulation of ice crystal formation to induce a certain degree of control in pore dimension and orientation [48]. Even though the discussed technologies present high versatility and can be employed for introducing 3D shapes and topographies within constructs, these require multiple steps and component manipulation to implement and control structure within the fabricated hydrogels. However, recent studies have demonstrated that by taking advantage of microfluidic flows alone, it is possible to create organization within hydrogel precursors pre-crosslinking, which, if maintained upon crosslinking, can lead to varied and interesting architectures at very small dimensions.

One interesting approach is that of leveraging chaotic hydrogel flows with different precursors mixing and swirling together due to the presence of helical elements in microfluidic channels within a print head [49, 50]. Researchers have demonstrated how this approach could combine continuous, high-throughput wet spinning with the orientation of separate compartments of different hydrogel precursors (between alginate and alginate-gelatin methacryloyl (GelMA) blends), resulting in 3D hydrogel microfibers with intrinsic 3D architectures, generated by flows alone and without the need for any additional entities (Fig. 8.5). The researchers demonstrated that chaotic flows enabled spinning fibers with incremental numbers of semi-parallel GelMA filaments within alginate ones, and these 3D hydrogel pockets were single handedly capable of promoting muscle cell alignment and muscle fiber-like maturation [50]. Previously, the team also applied a similar strategy of chaotic flows to create densely packed cellular structures, enabling, e.g., the creation of constructs where different degrees of intimacy between cancer cells and healthy cells could be obtained [51]. The combination of both concepts presents interesting opportunities for the high-throughput fabrication of fibers where multiple compartments can mimic the interaction between cancer cells and other microenvironment entities, approaching and miniaturizing important processes and providing very interesting platforms for therapy testing.

Indeed, the creation of hydrogel microfibers is a particularly powerful approach for cancer modelling. Using less chaotic, more organized 3D flow-focusing hydrogel biofabrication, it was also demonstrated how a single microfluidic setup could be

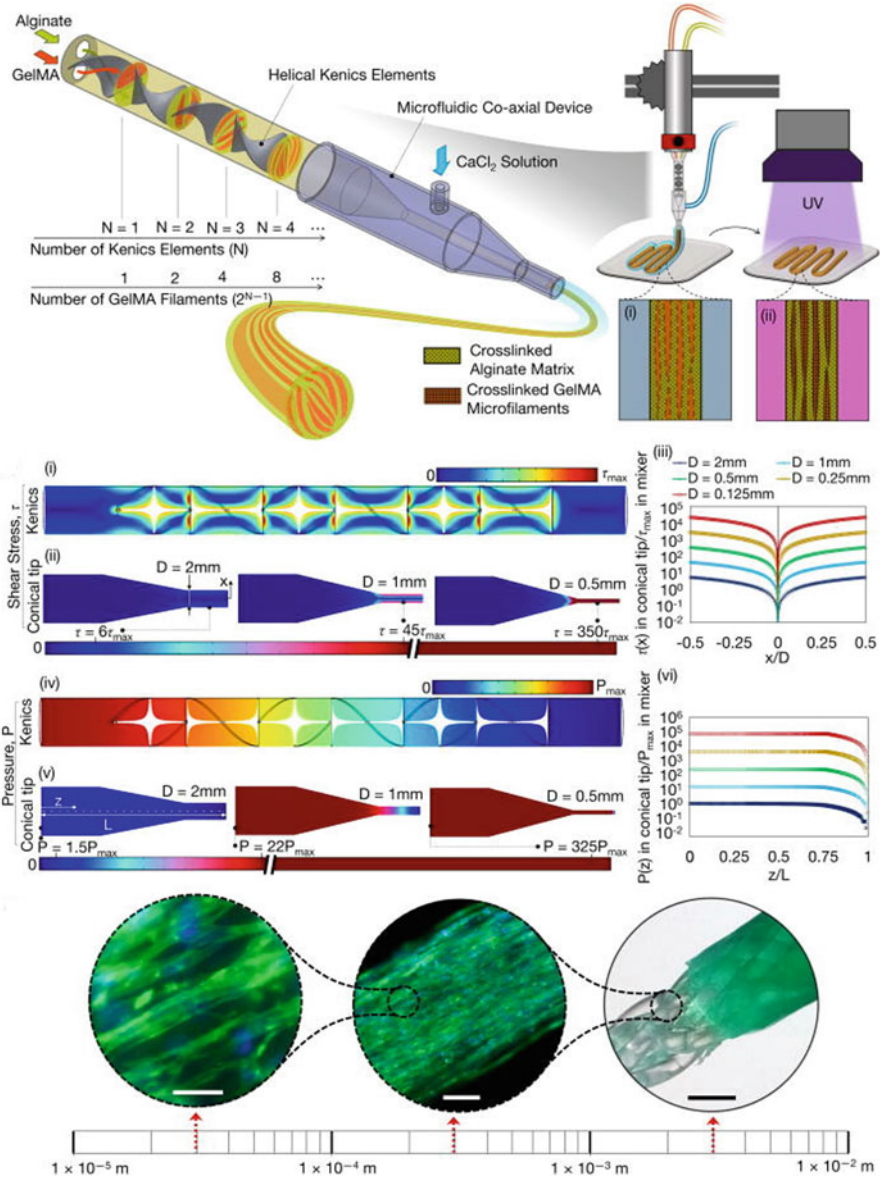


Fig. 8.5 Chaotic generation of hydrogel fiber architectures with hydrogel compartmentalization and 3D cell/hydrogel alignment. Reprinted with permission from [50]

employed together with the tuning of hydrogel precursor viscosity and the organization of flows within the chip, to create a plethora of multi-compartment hydrogel fibers with very small dimensions down to sub-50 μm diameters [52] (Fig. 8.6a). These unique microfibers were validated as suitable platforms to mimic and miniaturize important biological organizations, namely those present in cancer.

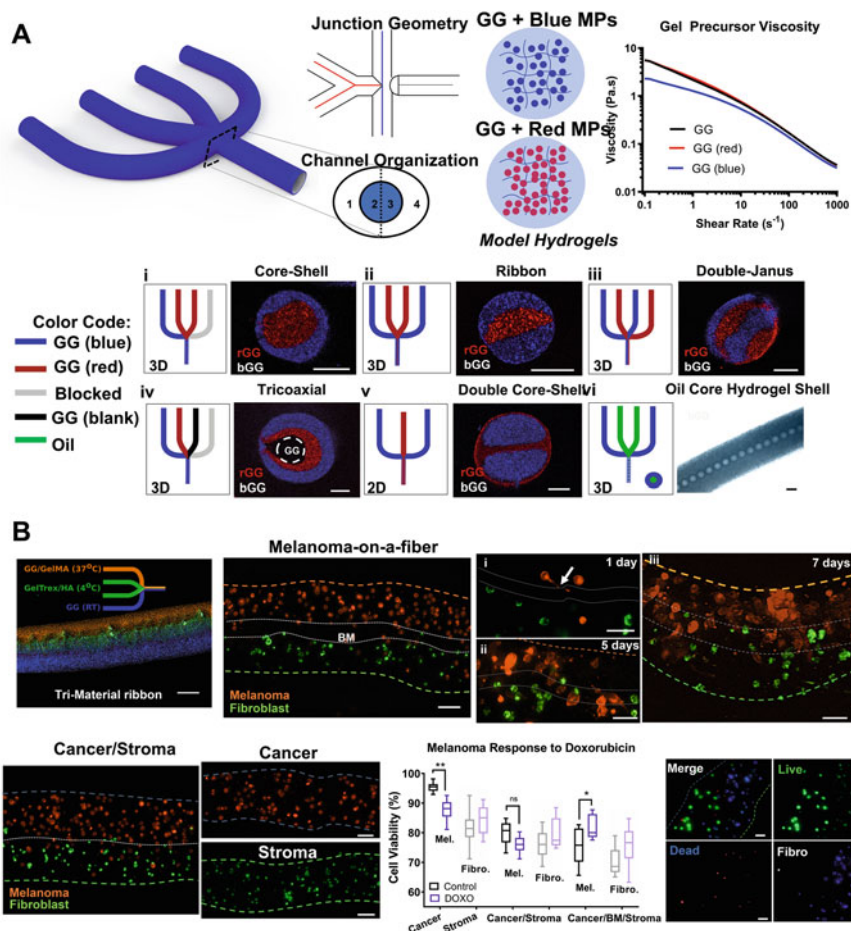


Fig. 8.6 3D Flow-focusing hydrogel biofabrication of multi-architecture hydrogel microfibers (a) and ribbon-like engineering of melanoma-on-a-fiber models (b). Adapted with permission from [52]

By exploring a specific shape, called ribbon-like, the team demonstrated that cancer/basement membrane/stroma compartments could be organized in a parallel manner, encapsulating melanoma cells in the cancer compartment, fibroblasts in the stromal one, and a thin basement membrane separating both, recreating the first steps of cancer cell invasion, potentially preceding metastasis (Fig. 8.6b). The results demonstrated that the basement membrane invasion started as early as 1-day post-fabrication, becoming more and more evident as the cancer cells overtook the construct invading toward the stroma. Furthermore, the team showed that the complexity of the 3D construct directly affected the outcome of cancer cell responses to doxorubicin, as their resistance to the drug increased with higher model complexity. These results evidence how the recapitulation of tumor microenvironments in

their multiple dimensions is important to obtain relevant responses in *in vivo* cancer models [52].

Moreover, it is also important to consider that modelling the 3D complexity of cancer microenvironments needs to be coupled with advances that enable the efficient analysis of ongoing biological processes, to derive clear and quantifiable data that can be used for next generation testing platforms and precision medicine approaches. In this regard, microfluidic biofabrication and microfiber compartment architectures may also present exciting opportunities by interfacing the engineering of 3D microtissues with advances in hydrogel optical fibers [53–56]. Very recent work has demonstrated that cytocompatible, polysaccharide-based hydrogel fibers could take advantage of co-central layers in order to clad a cell-laden fiber core with lower refractive index layers, to transport and maintain cancer cells while simultaneously enabling the guiding of light [57] (Fig. 8.7a). In these living optical fibers, the team demonstrated that light-cell interactions could transport information regarding cellular events, such as metabolic activity, proliferation, and protein expression. By taking advantage of this process, the study demonstrated how the growth of cancer fibroids (fiber-like organoids) could be tracked over time via fast, nondestructive optical analysis, directly converting the complex process of cancer 3D proliferation to directly quantifiable optical data. This quantification was then leveraged to quickly screen and identify inhibitory thresholds of the anticancer drug cisplatin, easily pinpointing the concentration level at which the drug successfully inhibited 3D cancer growth (Fig. 8.7b). The capacity to perform the digitalization of biological events presents exciting new avenues for the generation of biological data from cancer *in vitro* 3D models and paves the way for faster personalized medicine testing and precision, data-driven approaches.

Overall, microfluidic biofabrication and, particularly, the continuous, high-throughput spinning of hydrogel fibers has presented very interesting technological advances, ranging from the creation miniaturized microenvironments, with living tissue-like architectures, to the tackling of new challenges in the conversion of biological events into quantifiable data. Even though these hydrogel structures have evolved to integrate significant complexity within single fibers, the combination of microfluidic biofabrication with bottom-up, additive manufacturing approaches such as bioprinting, presents further possibilities for increasing dimensions, and obtaining further complex biological constructs and models, as discussed ahead.

8.5 Microfluidic-Enabled Bioprinting

So far, we have been discussing the possibilities for microfluidic-fabricated structures such as fibers or droplets to integrate a broad arrange of characteristics encompassing important materials, shapes, and cues within inner architectures that can mimic relevant biological environments. Even though these constructs can be seen as the final model, they can also serve as building blocks, which can further be assembled toward larger, more complex 3D structures. In particular, this process can

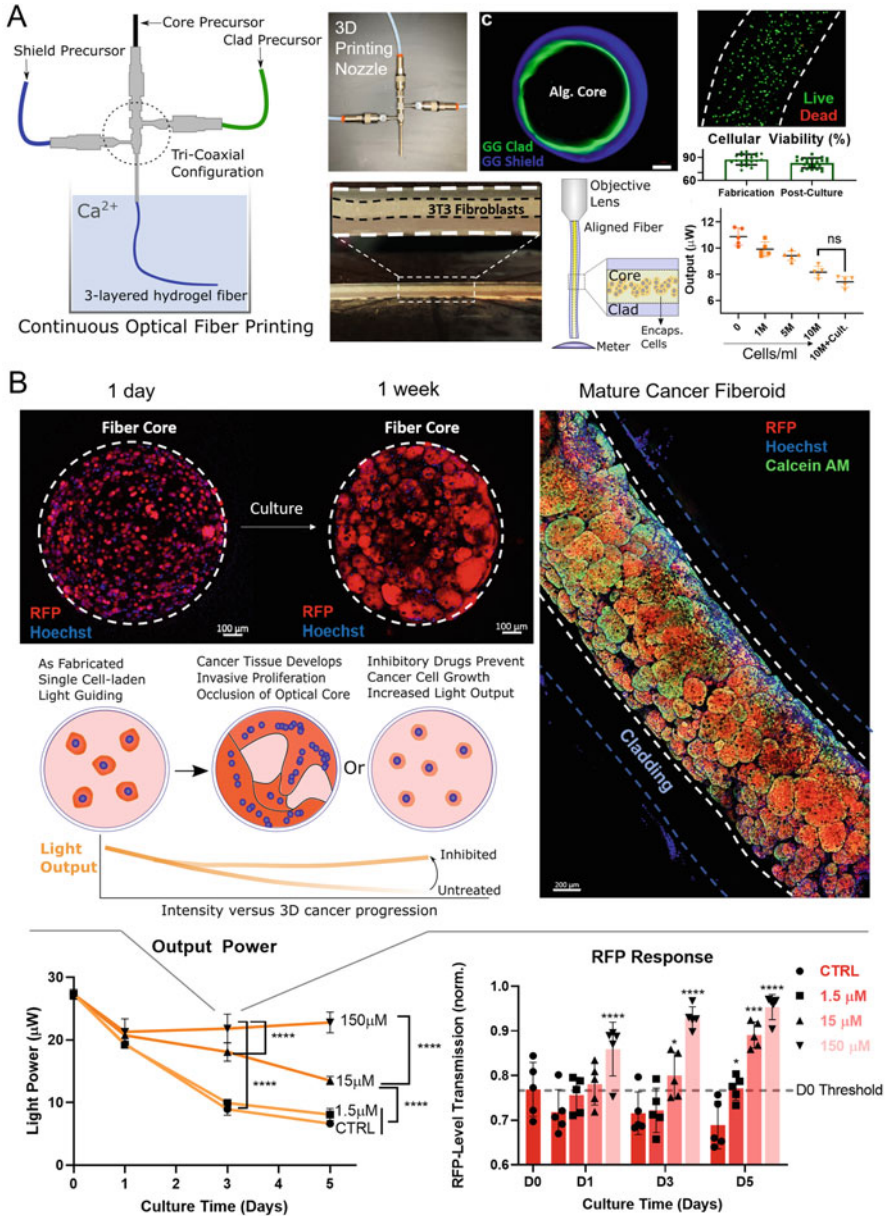


Fig. 8.7 Biofabrication of living optical fibers based on multi-layered polysaccharide hydrogel fibers (a), and the conversion of 3D cancer fibroid growth to directly quantifiable optical data for drug inhibitory threshold discovery (b). Adapted with permission from [57]

be approached by leveraging 3D bioprinting principles to deposit and assemble microfluidic biofabricated building blocks [58, 59].

An earlier example is that of using microfluidics to obtain two side-by-side, non-mixing flows, printing them as single fibers with two compartments, frequently named as Janus Fibers. This type of structure, unlike single-composition fibers, enables close contact between, e.g., different cell populations [60]. For example, researchers 3D printed constructs with dual fibers containing fibroblasts and muscle cells, each in a different Janus-fiber compartment, assembling the construct and demonstrating improved *in vivo* integration when compared to a uniform hydrogel construct [61]. With the advances in microfluidic-driven bioprinter devices, the dual inlet chips evolved to more complex configurations, where multiple materials can be controlled as well as their crosslinking, employing independent channel pressures [62]. This type of approach has been explored to create 3D muscle tissue models that responded physiologically to a variety of biochemical stimuli [63]. Similarly, microfluidic bioprinting was used to create renal models, where core-shell configurations could be manufactured to approach renal tubules, with dimension and compartment size resolutions which are typically hard to approach with classical 3D printing nozzles [62]. These technological advances may further improve previously reported multi-material 3D printing approaches, where a single nozzle connected to a variety of hydrogel precursors can be controlled to alternate between deposited material on-demand, enabling, e.g., the creation of vascularized 3D models, which would be very interesting for approaching cancer tissue vascularization modelling [64]. More recently, the integration of microfluidic-fabricated microgels within hydrogel inks has also been demonstrated as an interesting approach to obtain heterogeneous constructs with pockets of cell-laden hydrogels surrounded by an environment of a different bioink [65]. Even though the authors did not focus on cancer applications, this strategy can be very interesting to obtain micro-tumors surrounded by a distinct cellular environment in a biphasic composition that can be printed in an arbitrary shape (Fig. 8.8).

Other than taking advantage of microfluidics to create complex, multi-compartment, but continuous fiber composition, the field of bioprinting has recently explored the capacities to obtain space-varying compositions. Microfluidics has been used to combine and mix different inputs, timing it with the 3D bioprinting deposition to obtain not only single fiber gradients but gradual composition changes in whole 3D printed constructs. By developing a custom print head where a coaxial extrusion nozzle received material from a passive microfluidic mixer, which was connected to the inlets, researchers have shown how different bioinks could be deposited individually or together at the same time. By uniformly mixing inlet material before extrusion, the researchers were able to deposit layers with gradually changing composition toward approaching the osteochondral (bone cartilage) transition [66]. In a more recent work, a similar concept was explored where a custom setup connected different material inlets to a chaotic mixer, and then to an outlet [67]. Researchers demonstrated how light-based crosslinking could then be used to crosslink multiple hydrogel layers that could contain intricate gradients of composition, in different shapes (Fig. 8.9). The team then used this process to fabricate 3D

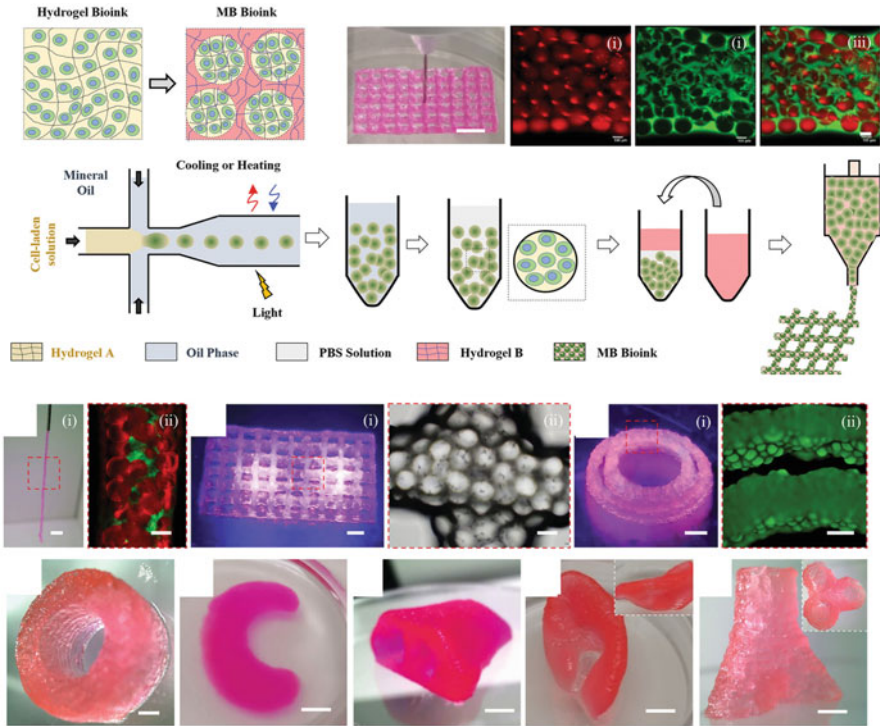


Fig. 8.8 3D Printing of heterogeneous bioinks via the combination of microfluidic biofabricated microgels within a uniform bioink blend for the integration of 3D cell-laden hydrogel depots within bioprinted constructs. Adapted with permission from [65]

cancer cell density models, where the number of cancer cells decreased radially from the center, approaching the dense characteristic of highly hypoxic tumor centers. They also demonstrated the capacity to create complex vascular structures with gradually changing configuration and channel dimensions (Fig. 8.9). The combination of both types of models would be also extremely relevant to approach cancer vascularization and the hypoxic dynamics behind angiogenesis, blood vessel growth, and potential metastatic disease.

Another interesting combination at the interface of microfluidics, bioprinting, and biofabrication, is the creation of intricate 3D architectures within chips. This can be approached through different manners, namely by bioprinting structures directly inside microfluidic chips, such as vascular channels that can then be perfused in dynamic culture conditions, among other examples [68]. However, bioprinting directly within a microfluidic chip presents limitations, as either the printing resolution is not fine enough to create complex microfluidic architectures or, alternatively, the resulting chip presents very large dimensions and diverges from the main purposes of having a microfluidic setting. To overcome this, researchers have also

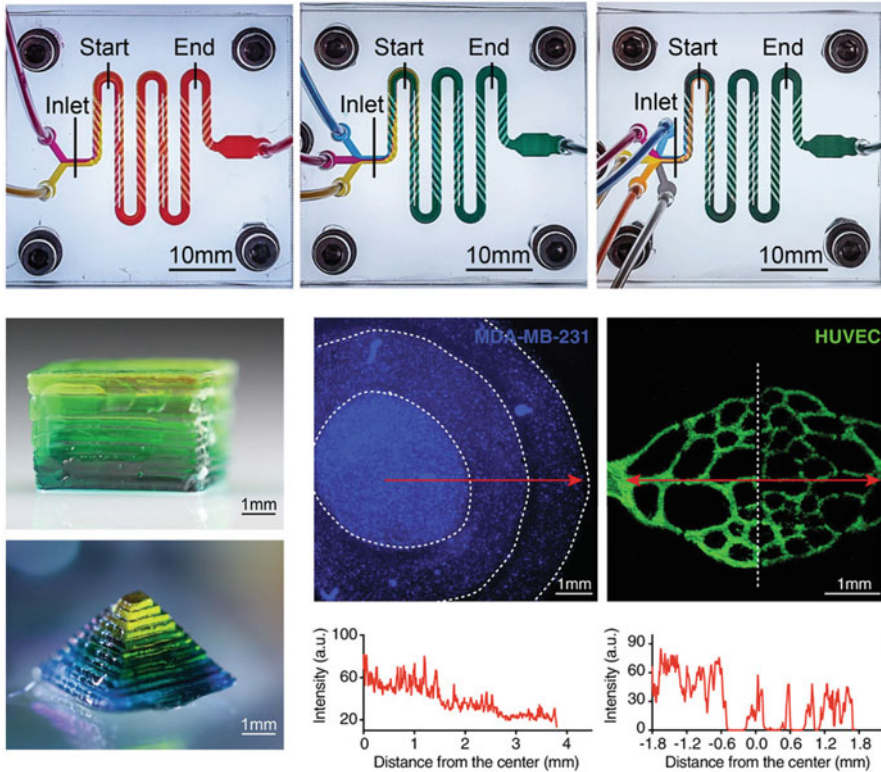


Fig. 8.9 Microfluidic-enabled bioprinting for the assembly of complex 3D constructs with gradients in layer composition, and their application to density-varying breast cancer and complex vascular networks biofabrication. Adapted with permission from [67]

developed maskless lithography, exploring the way materials flow within microfluidic conditions, and then “locking” them in a particular 3D configuration using light-based crosslinking [69]. Among other applications, this approach allowed for the creation of small tumor environments with a randomly distributed vascular-like network, all limited to an area of around 10 mm^2 , which represents a very small size within which relevant 3D shapes could be miniaturized without the restraints of having to physically print them.

Overall, microfluidics has enabled very interesting advances in the field of 3D bioprinting by allowing the controlled deposition of different fiber shapes, as well as quickly altering between different inks in real printing time to create gradients and approach important transitions of living tissues both within health and disease contexts. It will be interesting to see how some of these advances come together soon, e.g., how the combination of printed 3D cancer models may incorporate the advances in printing of blood vessel networks to recapitulate important events behind metastatic disease, which represents the highest disease burden scenario of

most cancers. Similarly, the creation of more complex, multi-cellular constructs may provide important platforms to understand the complex cancer microenvironment crosstalk, as well as model the effect of next generation, microenvironment-disruptive therapeutics.

8.6 Conclusions

Microfluidic techniques present unique opportunities to miniaturize important characteristics of biological environments in fabricated structures, ranging from individual droplets to continuous fibers. The capacity to manipulate hydrogel precursors as liquids within low turbulence settings, allied with the broad toolbox that exists in hydrogel crosslinking on-demand, microfluidic biofabrication is primed to lead the field of biofabrication at the smallest of scales and highest level of 3D resolution. Indeed, microfluidic biofabrication has enabled important advances in the miniaturization of multi-compartment 3D constructs, as well as the particularly important space-varying composition creation, either from a high-throughput screening perspective or to simply recapitulate the complexity of living tissues.

In the specific case of cancer, the complexity of the diseased tissue and its similarity to an organ on its own requires a paradigmatic shift in the way it is modelled *in vitro*, namely to integrate the multi-cellular dynamics of the microenvironment, as well as the ECM characteristics such as the typical fibrotic responses [70]. In this regard, microfluidic biofabrication has enabled important breakthroughs in the creation of complex multi-cellular, multi-material, and multi-compartment 3D architectures which can enable, e.g., closely monitoring cancer/stroma and basement membrane invasion dynamics. Indeed, the creation of 3D shapes within structures such as hydrogel fibers represents important advances to model 3D cancer environments, but a further challenge remains: the way to translate ongoing biological events into quantifiable, comparable data.

Indeed, models are only useful if their complexity can be matched by means to extract data, where advances such as the integration of optical, electrical, thermal, and similar means of analyzing biological constructs such as 3D hydrogel fibers [57] or spheroids and organoids [71] will play an ever-growing role in future *in vitro* models. As the ways to analyze engineered constructs evolve, so does the amount of data that can be generated in brief amounts of time. This data will create unique opportunities for mining, analyzing, and creating large 3D biology model databases, where its interface with machine learning and other artificial intelligence algorithms may expand *in silico* modelling informed on 3D *in vitro* constructs. Simultaneously, those technologies can also be explored to drive the optimization of microfluidic biofabrication parameters, resulting in improved models, and so on and so forth in successive synergistic iterations [72, 73].

Finally, the combination of microfluidic biofabrication with approaches that typically function at slightly different dimensions, such as 3D bioprinting, is also providing important advances where the powerful real-time material manipulation via microfluidics can be combined with 3D material deposition to create larger

constructs. Thus, characteristics such as multi-compartment fibers and space-varying compositions can be translated to 3D printed constructs. This area can still evolve toward the unique combination of multiple structures, such as cancer hypoxic 3D environments and bioprinted vascular beds, leading to a significant step forward in the understanding of multi-entity events, such as those involved in metastatic disease [74]. Furthermore, it is still important to mention that microfluidic fabrication has also been employed for some time at smaller dimensions, namely for the fast fabrication of nanoparticles of different dimensions for drug delivery purposes [70, 75, 76]. Even if not so straightforward, it would be interesting to see advances where microfluidic nanosynthesis could be combined with biofabrication platforms to assess, for example, the interaction and distribution of nanoparticles in complex 3D cancer models as well as their therapeutic efficacy. These models are primed to partially replace *in vivo* animal studies while remaining closer to human physiology using human-derived cell sources.

After decades of cancer research and the development of anticancer therapeutics, the societal burden of the disease is still among the highest, and several cancers are extremely hard to treat, especially those undergoing metastasis. Uncovering the intricate 3D complexity of the disease and the multi-entity interactions that contribute to the development and prognostics of cancer may likely hold the key for next generation therapeutics. In this context, the unique capacity of microfluidic biofabrication to miniaturize 3D biological environments in high-throughput fabrication and analysis setups is primed to open new avenues for cancer research by enabling unprecedentedly complex, easily adaptable models. Combining these models with tools for the direct quantification of biological events and data analysis is likely to unlock a whole new frontier in precision, data-driven cancer research, and medicine.

Acknowledgments CFG acknowledges support from Fundação para a Ciência e Tecnologia (FCT), grants no. PD/BD/135253/2017 and COVID/BD/152016/2021.

References

1. Guimarães CF, Gasperini L, Marques AP, Reis RL (2020) The stiffness of living tissues and its implications for tissue engineering. *Nat Rev Mater* 5:351–370
2. Kalli M, Stylianopoulos T (2018) Defining the role of solid stress and matrix stiffness in cancer cell proliferation and metastasis. *Front. Oncologia* 8
3. Mirdamadi E, Tashman JW, Shiwarski DJ et al (2020) FRESH 3D bioprinting a full-size model of the human heart. *ACS Biomater Sci Eng* 6:6453–6459
4. Bernal PN, Delrot P, Loterie D et al (2019) Volumetric bioprinting of complex living-tissue constructs within seconds. *Adv Mater* 31
5. Bakht SM, Gomez-Florit M, Lamers T et al (2021) 3D bioprinting of miniaturized tissues embedded in self-assembled nanoparticle-based Fibrillar platforms. *Adv Funct Mater* 31
6. Lee JM, Ng WL, Yeong WY (2019) Resolution and shape in bioprinting: strategizing towards complex tissue and organ printing. *Appl. Phys Rev* 6
7. Miri AK, Mirzaee I, Hassan S et al (2019) Effective bioprinting resolution in tissue model fabrication. *Lab Chip* 19:2019–2037

8. Cheng Y, Yu Y, Fu F et al (2016) Controlled fabrication of bioactive microfibers for creating tissue constructs using microfluidic techniques. *ACS Appl Mater Interfaces* 8:1080–1086
9. Cheng Y, Zheng F, Lu J et al (2014) Bioinspired multicompartmental microfibers from microfluidics. *Adv Mater* 26:5184–5190
10. Grolman JM, Zhang D, Smith AM et al (2015) Rapid 3D extrusion of synthetic tumor microenvironments. *Adv Mater* 27:5512–5517
11. Kato-Negishi M, Onoe H, Ito A, Takeuchi S (2017) Rod-shaped neural units for aligned 3D neural network connection. *Adv Healthc Mater* 6:1–7
12. Xu P, Xie R, Liu Y et al (2017) Bioinspired microfibers with embedded perfusable helical channels. *Adv Mater* 29:1–7
13. Gasperini L, Mano JF, Reis RL (2014) Natural polymers for the microencapsulation of cells. *J R Soc Interface* 11:20140817
14. Young S, Wong M, Tabata Y, Mikos AG (2005) Gelatin as a delivery vehicle for the controlled release of bioactive molecules. *J Control Release* 109:256–274
15. Caliari SR, Burdick JA (2016) A practical guide to hydrogels for cell culture. *Nat Methods* 13:405–414
16. Ushikubo FY, Birribilli FS, Oliveira DRB, Cunha RL (2014) Y- and T-junction microfluidic devices: effect of fluids and interface properties and operating conditions. *Microfluid Nanofluidics*:1–10
17. Smeds KA, Grinstaff MW, Pfister-serres A et al (2001) Photocrosslinkable polysaccharides for in situ hydrogel formation. *J Biomed Mater Res* 54:115–121
18. Heo J, Koh RH, Shim W et al (2016) Riboflavin-induced photo-crosslinking of collagen hydrogel and its application in meniscus tissue engineering. *Drug Deliv Transl Res* 6:148–158
19. Loessner D, Meinert C, Kaemmerer E et al (2016) Functionalization, preparation and use of cell-laden gelatin methacryloyl–based hydrogels as modular tissue culture platforms. *Nat Protoc* 11:727–746
20. Jiao J, Burgess DJ (2003) Rheology and stability of water-in-oil-in-water multiple emulsions containing span 83 and tween 80. *AAPS PharmSci* 5
21. Miller R (2016) Emulsifiers: types and uses. *Encycl Food Heal*:498–502
22. Zhao H, Chen Y, Shao L et al (2018) Airflow-assisted 3D bioprinting of human heterogeneous microspheroidal organoids with microfluidic nozzle. *Small* 14:1–7
23. Onoe H, Okitsu T, Itou A et al (2013) Metre-long cell-laden microfibres exhibit tissue morphologies and functions. *Nat Mater* 12:584–590
24. Kim JY, Lee H, Jin EJ et al (2021) A microfluidic device to fabricate one-step cell bead-laden hydrogel struts for tissue engineering. *Small* 2106487:1–17
25. Canadas RF, Ren T, Marques AP et al (2018) Biochemical gradients to generate 3D heterotypic-like tissues with isotropic and anisotropic architectures. *Adv Funct Mater* 28
26. Yang L, Pijuan-Galito S, Rho HS et al (2021) High-throughput methods in the discovery and study of biomaterials and materiobiology. *Chem Rev* 121:4561–4677
27. Burdick JA, Khademhosseini A, Langer R (2004) Fabrication of gradient hydrogels using a microfluidics/photopolymerization process. *Langmuir* 20:8–11
28. Pedron S, Becka E, Harley BA (2015) Spatially graded hydrogel platform as a 3D engineered tumor microenvironment. *Adv Mater* 27:1567–1572
29. Guimarães CF, Gasperini L, Ribeiro RS et al (2020) High-throughput fabrication of cell-laden 3D biomaterial gradients. *Mater Horiz* 7:2414–2421
30. Xin S, Dai J, Gregory CA et al (2020) Creating physicochemical gradients in modular microporous annealed particle hydrogels via a microfluidic method. *Adv Funct Mater*:30
31. Highley CB, Song KH, Daly AC, Burdick JA (2019) Jammed microgel inks for 3D printing applications. *Adv Sci* 6
32. Kochetkova M, Samuel MS (2021) Differentiation of the tumor microenvironment: are CAFs the organizer? *Trends Cell Biol*:1–10

33. Mahadik BP, Wheeler TD, Skertich LJ et al (2014) Microfluidic generation of gradient hydrogels to modulate hematopoietic stem cell culture environment. *Adv Healthc Mater* 3: 449–458
34. Ngo MT, Barnhouse VR, Gilchrist AE et al (2021) Hydrogels containing gradients in vascular density reveal dose-dependent role of angiocrine cues on stem cell behavior. *Adv Funct Mater*. <https://doi.org/10.1002/adfm.202101541>
35. Liao D, Johnson RS (2007) Hypoxia: a key regulator of angiogenesis in cancer. *Cancer Metastasis Rev* 26:281–290
36. Wang W, Li L, Ding M et al (2018) A microfluidic hydrogel chip with orthogonal dual gradients of matrix stiffness and oxygen for cytotoxicity test. *Biochip J* 12:93–101
37. Berger Fridman I, Ugolini GS, Vandelinder V et al (2021) High throughput microfluidic system with multiple oxygen levels for the study of hypoxia in tumor spheroids. *Biofabrication* 13
38. Zhu D, Trinh P, Li J et al (2021) Gradient hydrogels for screening stiffness effects on patient-derived glioblastoma xenograft cellfates in 3D. *J Biomed Mater Res A* 109:1027–1035
39. Suter SP, Skalak R (1993) The history of Poiseuille's law. *Annu Rev Fluid Mech* 25:1–20
40. Uludag H, De Vos P, Tresco P a (2000) Technology of mammalian cell encapsulation. *Adv Drug Deliv Rev* 42:29–64
41. Gasperini L, Maniglio D, Migliaresi C (2011) Electro hydro dynamic (EHD) encapsulation of cells in alginate based hydrogels. In: *International Journal of Artificial Organs*. Wichtig Editore s. r. l., Milano, p 685
42. Wong TY, Preston LA, Schiller NL (2000) ALGINATE LYASE: review of major sources and enzyme characteristics, structure-function analysis, biological roles, and applications. *Annu Rev Microbiol* 54:289–340
43. Kuhn PT, Zhou Q, van der Boon TAB et al (2016) Double linear gradient biointerfaces for determining two- parameter dependent stem cell behavior. *ChemNanoMat*. <https://doi.org/10.1002/cnma.201600028>
44. Zhou Q, Castañeda Ocampo O, Guimarães CF et al (2017) Screening platform for cell contact guidance based on inorganic biomaterial micro/nanotopographical gradients. *ACS Appl Mater Interfaces*:9
45. Zhou Q, Ge L, Guimarães CF et al (2018) Development of a novel orthogonal double gradient for high-throughput screening of Mesenchymal stem cells–materials interaction. *Adv Mater Interfaces* 5:4–11
46. Araújo-Custódio S, Gomez-Florit M, Tomás AR et al (2019) Injectable and magnetic responsive hydrogels with bioinspired ordered structures. *ACS Biomater Sci Eng* 5:1392–1404
47. Rose JC, Gehlen DB, Haraszti T et al (2018) Biofunctionalized aligned microgels provide 3D cell guidance to mimic complex tissue matrices. *Biomaterials*. <https://doi.org/10.1016/j.biomaterials.2018.02.001>
48. Canadas RF, Ren T, Tocchio A et al (2018) Tunable anisotropic networks for 3-D oriented neural tissue models. *Biomaterials* 181:402–414
49. Bolívar-Monsalve EJ, Ceballos-González CF, Borrayo-Montaño KI et al (2021) Continuous chaotic bioprinting of skeletal muscle-like constructs. *Bioprinting* 21
50. Samandari M, Alipanah F, Majidzadeh-A K et al (2021) Controlling cellular organization in bioprinting through designed 3D microcompartmentalization. *Appl Phys Rev* 8
51. Trujillo-De Santiago G, Alvarez MM, Samandari M et al (2018) Chaotic printing: using chaos to fabricate densely packed micro- and nanostructures at high resolution and speed. *Mater Horizons* 5:813–822
52. Guimarães CF, Gasperini L, Marques AP, Reis RL (2021) 3D flow-focusing microfluidic biofabrication: one-chip-fits-all hydrogel fiber architectures. *Appl Mater Today* 23
53. Elsharif M, Hassan MU, Yetisen AK, Butt H (2019) Hydrogel optical fibers for continuous glucose monitoring. *Biosens Bioelectron* 137:25–32
54. Guimarães CF, Ahmed R, Marques AP et al (2021) Engineering hydrogel-based biomedical photonics: design. *Adv Mater, fabrication and applications*. <https://doi.org/10.1002/adma.202006582>

55. Guo J, Liu X, Jiang N et al (2016) Highly stretchable, strain sensing hydrogel optical fibers. *Adv Mater* 28:10244–10249
56. Yetisen AK, Jiang N, Fallahi A et al (2017) Glucose-sensitive hydrogel optical fibers functionalized with phenylboronic acid. *Adv Mater*:29
57. Guimarães CF, Ahmed R, Mataji-Kojouri A et al (2021) Engineering polysaccharide-based hydrogel photonic constructs: from multiscale detection to the biofabrication of living optical fibers. *Adv Mater*:2105361
58. Ma J, Wang Y, Liu J (2018) Bioprinting of 3D tissues/organs combined with microfluidics. *RSC Adv* 8:21712–21727
59. Richard C, Richard C, Neild A et al (2020) The emerging role of microfluidics in multi-material 3D bioprinting. *Lab Chip* 20:2044–2056
60. Colosi C, Shin SR, Manoharan V et al (2016) Microfluidic bioprinting of heterogeneous 3D tissue constructs using low-viscosity bioink. *Adv Mater* 28:677–684a
61. Costantini M, Testa S, Mozetic P et al (2017) Microfluidic-enhanced 3D bioprinting of aligned myoblast-laden hydrogels leads to functionally organized myofibers in vitro and in vivo. *Biomaterials* 131:98–110
62. Addario G, Djurdjaj S, Farè S et al (2020) Microfluidic bioprinting towards a renal in vitro model. *Bioprinting* 20
63. Dickman CTD, Russo V, Thain K et al (2020) Functional characterization of 3D contractile smooth muscle tissues generated using a unique microfluidic 3D bioprinting technology. *FASEB J* 34:1652–1664
64. Liu W, Zhang YS, Heinrich MA et al (2017) Rapid continuous multimaterial extrusion bioprinting. *Adv Mater* 29
65. Fang Y, Guo Y, Ji M et al (2021) 3D printing of cell-laden microgel-based biphasic bioink with heterogeneous microenvironment for biomedical applications. *Adv Funct Mater*:2109810
66. Idaszek J, Costantini M, Karlsen TA et al (2019) 3D bioprinting of hydrogel constructs with cell and material gradients for the regeneration of full-thickness chondral defect using a microfluidic printing head. *Biofabrication*:11
67. Wang M, Li W, Mille LS et al (2021) Digital light processing based bioprinting with composable gradients. *Adv Mater*. <https://doi.org/10.1002/adma.202107038>
68. Sun H, Jia Y, Dong H et al (2020) Combining additive manufacturing with microfluidics: an emerging method for developing novel organs-on-chips. *Curr Opin Chem Eng* 28:1–9
69. Miri AK, Nieto D, Iglesias L et al (2018) Microfluidics-enabled multimaterial Maskless stereolithographic bioprinting. *Adv Mater* 30:1–9
70. Chandler C, Liu T, Buckanovich R, Coffman LG (2019) The double edge sword of fibrosis in cancer. *Transl Res* 209:55–67
71. Park Y, Franz CK, Ryu H et al (2021) Three-dimensional, multifunctional neural interfaces for cortical spheroids and engineered assembloids. *Sci Adv* 7
72. Galan EA, Zhao H, Wang X et al (2020) Intelligent microfluidics: the convergence of machine learning and microfluidics in materials science and biomedicine. *Matter* 3:1893–1922
73. Hakimi O, Krallinger M, Ginebra MP (2020) Time to kick-start text mining for biomaterials. *Nat Rev Mater* 5:553–556
74. Pape J, Magdeldin T, Ali M et al (2019) Cancer invasion regulates vascular complexity in a three-dimensional biomimetic model. *Eur J Cancer* 119:179–193
75. Gimondi S, Guimarães CF, Vieira SF et al (2022) Microfluidic mixing system for precise PLGA-PEG nanoparticles size control. *Nanomed Nanotechnol Biol Med* 40:102482
76. Karnik R, Gu F, Basto P et al (2008) Microfluidic platform for controlled synthesis of polymeric nanoparticles. *Nano Lett* 8:2906–2912



Advances in 3D Vascularized Tumor-on-a-Chip Technology

9

Sangmin Jung, Hyeonsu Jo, Sujin Hyung, and Noo Li Jeon

Abstract

Tumors disrupt the normal homeostasis of human body as they proliferate in abnormal speed. For constant proliferation, tumors recruit new blood vessels transporting nutrients and oxygen. Immune system simultaneously recruits lymphatic vessels to induce the death of tumor cells. Hence, understanding tumor dynamics are important to developing anti-cancer therapies. Tumor-on-a-chip technology can be applied to identify the structural and functional units of tumors and tumor microenvironments with high reproducibility and reliability, monitoring the development and pathophysiology of tumors, and predicting drug effectiveness. Herein, we explore the ability of tumor-on-a-chip technology to mimic angiogenic and lymphangiogenic tumor microenvironments of organs. Microfluidic systems allow elaborate manipulation of the development and status of cancer. Therefore, they can be used to validate the effects of various drug combinations, specify them, and assess the factors that influence cancer treatment. We discuss the mechanisms of action of several drugs for cancer treatment in terms of tumor growth and progression involving angiogenesis and lymphangiogenesis. Moreover, we present future applications of emerging tumor-on-a-chip technology for drug development and cancer therapy.

Sangmin Jung and Hyeonsu Jo contributed equally with all other contributors.

S. Jung · H. Jo · N. L. Jeon (✉)

Department of Mechanical Engineering, Seoul National University, Seoul, South Korea

e-mail: njeon@snu.ac.kr

S. Hyung

Innovative Institute for Precision Medicine, Samsung Medical Center, Seoul, South Korea

© The Author(s), under exclusive license to Springer Nature Switzerland AG 2022

231

D. Caballero et al. (eds.), *Microfluidics and Biosensors in Cancer Research*,

Advances in Experimental Medicine and Biology 1379,

https://doi.org/10.1007/978-3-031-04039-9_9

Keywords

Organ-on-a-chip · Tumor-on-a-chip · MPS (Microphysiological system) · Vascularized tumor microenvironment · Microfluidics

9.1 Introduction

Microfluidic technology enables researchers to bioengineer *in vitro* culture models that can replicate the physiological environments of human organs. These models more accurately describe the spatiotemporal evolution of tumor microenvironments (TMEs) than Petri dish-based traditional models [1–3]. A tumor-on-a-chip provides a means for precise monitoring of the interaction between tumor cells and surrounding cells and how this induces the formation of metastatic niches and favorable environments for the growth of the tumor. Hence, tumor-on-a-chip technology is useful for studying the complexities of cancer development and therapy. In particular, this technology enables the reconstruction of physiologically relevant three-dimensional (3D) tumor models, which can be applied for high-accuracy, rapid screening of novel biomarkers and therapeutic agents.

Moreover, a tumor-on-a-chip enables researchers to control cell patterning and self-assembly of cells in microchannels; thus, researchers can construct highly organized cultures and juxtapose stromal cells with 3D hydrogels to study tumor-induced angiogenesis and lymphangiogenesis. Several therapeutic strategies that interfere with tumor growth and metastatic spread have been investigated using such systems [4]. A tumor-on-a-chip can facilitate biomarker profiling and provide information on the effectiveness of therapeutic strategies according to structural and functional changes in the relevant vessels. Thus, it can be used to experimentally test the efficacy of therapeutic compounds in tumor models and elucidate their underlying mechanisms. Microfluidic platforms have helped advance clinical-stage research and elucidate cancer pathophysiology for precision medicine.

This chapter discusses the various types of microfluidic-based culture systems available for reconstructing angiogenesis and lymphangiogenesis, and the various factors and drugs used for inducing these processes on microfluidic platforms. It will help readers better understand vessel generation and the tumor-on-a-chip.

9.2 Angiogenesis

Blood is an important source of nutrients and oxygen for cells and helps them eliminate waste [5]. Blood mainly communicates with cells through blood vessels, which form a 3D network throughout the body. Existing blood vessels occasionally create new ones, enabling immune responses to inflammation and antigens [6]. Such formation of new blood vessels from a parental vessel is called angiogenesis [7].

9.2.1 Structure of Blood Vessels

Blood vessels include arteries, veins, and capillaries. Arteries and veins comprise three layers: tunica intima, tunica media, and tunica externa. Capillaries are the thinnest blood vessels and possess only a tunica intima layer [8–10].

Tunica externa, the outermost layer, is composed entirely of connective fibers and surrounded by an external elastic lamina. This layer may be thicker in veins because it protects vessels against external damage. Tunica media, the middle layer, is composed of smooth muscle cells, with elastic and connective tissues arranged around the vessels. Tunica intima, the thinnest and innermost layer, is composed of a single continuous layer of endothelial cells (ECs).

In vitro 3D angiogenesis models are based on various ECs such as human umbilical vein endothelial cell (HUVECs), human dermal microvascular ECs, human retinal microvascular ECs, and human brain microvascular ECs. For the formation of functional blood vessels, it is important to construct an extracellular matrix (ECM) simultaneously. Vascular smooth muscle cells (VSMCs), such as those of the human coronary artery, can be cultured with ECs for more precise vessel reconstruction [11]. ECM covers blood vessels and has morphological and functional relevance [12]. Thus far, researchers have constructed blood vessels through two main approaches, (1) self-morphogenesis: self-assembly of vasculature via communication between blood vessel cells and surrounding ECM cells (Fig. 9.1a) [13], and (2) wall patterning: the layering of ECs along a narrow, hollow space to form a single vessel (Fig. 9.1b) [14]. These methods enable the formation of 3D vascular networks and the inner lumen of blood vessels, respectively.

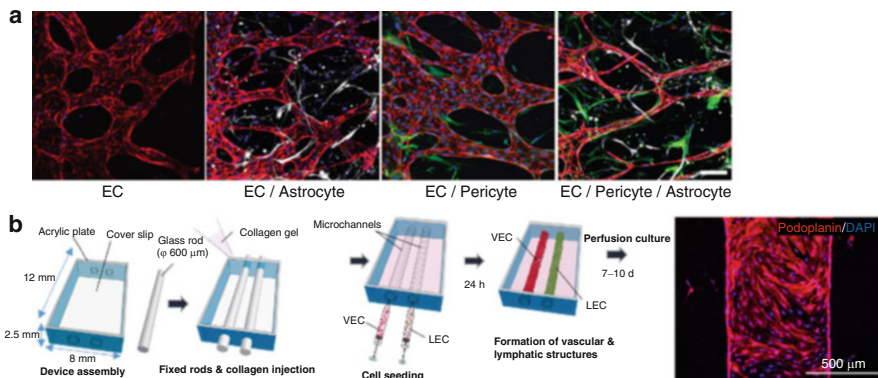


Fig. 9.1 Two main approaches to reconstruct blood vessels in vitro. (a) Self-morphogenesis method. (b) Wall patterning method (All figures are reprinted with permission from the publisher of each article)

9.2.2 Mechanism of Angiogenesis

Angiogenesis occurs through the interaction between vascular ECs and surrounding cells. A cell receives substances secreted by peripheral cells through receptors and relays a signal to ECs to promote EC proliferation and migration [15]. One of the signals triggers the differentiation of vascular ECs into tip cells and stalk cells. The cell type switches from tip to stalk or stalk to tip [16]. Tip cells release proteolytic enzymes (proteases) that degrade the basement membrane (BM) to allow ECs to escape from the parental vessel. Stalk cells proliferate behind tip cells, allowing the elongation of the capillary sprout.

Angiogenesis can be mainly divided into four stages: degradation of BM by proteases, EC migration into the interstitial space and EC sprouting, EC proliferation, and lumen formation, generation of new BM through pericyte recruitment, formation of anastomoses, and blood flow (Fig. 9.2).

After tip cells degrade the BM of parental vessels, an angiogenic sprout grows through an opening formed by EC proliferation. As stalk cells proliferate, the sprout elongates, and ECs form a tubular lumen. Angiogenesis is completed when the new vessel anastomoses with other vessels or tissues, and blood flows through the vessel after a new BM is formed via pericyte recruitment [17].

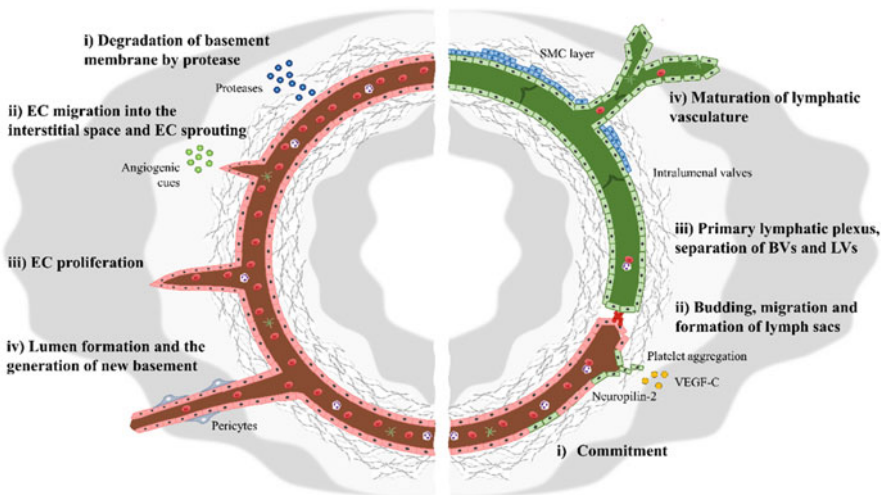


Fig. 9.2 Mechanism of angiogenesis and lymphangiogenesis. For angiogenesis, there are four stages; (i) Degradation of basement membrane by protease, (ii) EC migration into the interstitial space and EC sprouting, (iii) EC proliferation, (iv) Lumen formation and the generation of new basement. For lymphangiogenesis, there are four stages; (i) Commitment, (ii) Budding, migration, and formation of lymph sacs, (iii) Primary lymphatic plexus, separation of blood vessels and lymphatic vessels, (iv) Maturation of lymphatic vasculature

9.2.3 Effect of Angiogenic Factors

Angiogenesis is a complex process involving the constant interaction of various cells and cytokine secretions. Nevertheless, researchers have induced angiogenesis in 3D *in vitro* models using several factors such as vascular endothelial growth factor (VEGF), basic fibroblast growth factor (bFGF), angiopoietin 1 (Ang1), and tumor growth factor β (TGF- β), which are discussed below [4, 18].

There are several types of VEGFs, among which VEGF-A is known to affect angiogenesis. VEGF-A binds to VEGF receptor 2 (VEGFR-2) in ECs and activates the cells; it plays a more important role than other growth factors. VEGF-A increases the expression of B-cell lymphoma 2 (Bcl-2) and survivin through the phosphatidylinositol-3 kinase/protein kinase B (PI3k/Akt) pathway to inhibit EC apoptosis [19]; it also activates the mitogen-activated protein kinase/extracellular signal-regulated kinase (MAPK/ERK) cascade to increase EC proliferation and migration [20]. In addition, it promotes ECM degradation and matrix organization to ensure the completion of the first and second steps of angiogenesis [21].

bFGF, also known as fibroblast growth factor 2, increases the secretion of matrix metalloproteinases (MMPs) in fibroblasts to enhance ECM degradation and organization [22]. It also promotes the formation of a tubular lumen structure, similar to VEGF-A, and increases the expression of Bcl-2, which inhibits EC apoptosis [23, 24].

Ang1, similar to VEGF-A, increases the expression of survivin through the PI3k/Akt pathway, thus inhibiting EC apoptosis [25]. Similar to bFGF, Ang1 increases the expression of MMP-2, thereby enabling effective ECM degradation and organization [26].

TGF- β promotes tumor growth. Generally, tumor cells grow constantly and penetrate aggressively. The binding of TGF- β to TGF- β receptor activates MMP-2, which promotes ECM degradation. MMP-2 activation also promotes EC proliferation and migration by activating the urokinase-type plasminogen activator system [21].

9.2.4 Tumorigenesis

Tumor cells show abnormally progressive growth. They break down the systems that control cell growth and proliferation and inhibit apoptosis. Since tumor cells grow constantly, they require large amounts of nutrients for survival [27]. Tumorigenesis is the phenomenon by which tumor cells actively recruit blood vessels for abundant nutrient delivery. Tumorigenesis is mediated by tumor-secreted angiogenic growth factors that interact with surface receptors expressed on ECs [28].

Although tumor cells receive oxygen via blood, the levels can be limited in the inner part of the cell mass since the gas is delivered from the surface of the cell mass. Consequently, cells inside the tumor cell mass undergo necrosis due to a lack of oxygen, a phenomenon called hypoxia [29].

Several factors induce tumorigenesis, but VEGF-A plays the most important role, as in angiogenesis [30]. Tumor cells secrete VEGF-A via two routes: (1) activation of the Ras–Raf–MAPK pathway by excessive proliferation of tumor cells and (2) hypoxia. Increased VEGF-A secretion increases the permeability of blood vessels by activating various pathways and EC proliferation [31]. Nutrients that leak through blood vessel walls are delivered to tumor cells through the ECM surrounding tumor cells [32].

Angiogenesis occurs through repetitive tumor cell proliferation and hypoxia; when nutrient-supplied tumor cells proliferate, or the hypoxia level becomes severe, VEGF-A secretion is induced. The tumor size increases as this positive feedback is repeated. As mentioned in the previous section, inhibitors of vascular growth are used in tumor therapy.

9.2.5 Anti-angiogenic Drugs

Tumorigenesis is one of the mechanisms through which tumors survive, and several researchers and doctors worldwide have developed drugs to inhibit tumor growth by preventing tumorigenesis. Although numerous drugs have been developed, only 13 are FDA-approved (Table 9.1), and most of these function through VEGF or VEGFR inhibition. Angiogenesis plays a role in growth and healing, and several normal functions of the body depend on this process [33]; therefore, its inhibition has side effects, the likelihood of which depends on the health status of the patient [34–36]. VEGF-targeting angiogenesis inhibitors can induce hemorrhage, arterial clots (resulting in stroke or heart attack), hypertension, impaired wound healing, and protein leakage into urine. Gastrointestinal perforation and fistulas are rare side effects of certain drugs. Anti-angiogenesis agents that target VEGFR have additional side effects, such as fatigue, diarrhea, biochemical hypothyroidism, hand-foot syndrome, cardiac failure, and hair alteration.

Drugs are named according to their mechanism. The suffix -mab indicates that a drug is based on monoclonal antibodies, whereas the suffix -ib indicates that it is based on small molecules with inhibitory properties. Monoclonal antibodies act on a specific molecule or receptor, whereas -ib drugs act on multiple tyrosine kinase receptors. Axitinib, pazopanib, sorafenib, sunitinib, and vandetanib inhibit VEGFR; cabozantinib, regorafenib, and ramucirumab inhibit VEGFR-2; bevacizumab inhibits VEGF-A; and ziv-aflibercept inhibits VEGF.

Some drugs indirectly inhibit angiogenesis without directly targeting VEGF or VEGFR. Everolimus reacts specifically with mammalian target of rapamycin complex 1 (mTORC1), whereas its parent compound, rapamycin, targets both mTORC1 and mTORC2. Both lenalidomide and thalidomide bind with cereblon, an E3 ligase component, but they have opposing mechanisms. Lenalidomide activates the protein, whereas thalidomide suppresses it. Ubiquitin E3 ligase participates in various signaling pathways. When the ligase is activated by lenalidomide, ubiquitination-induced suppression of mTOR-interacting proteins or ubiquitination of hypoxia-inducible factor 1 α (HIF-1 α) suppresses VEGF expression [25]. VEGF expression

Table 9.1 Angiogenesis inhibitors approved by FDA

No.	Name	Target	Cancer type	Reference
1	Axitinib	Inhibit VEGFR	Kidney cancer	[38–40]
2	Pazopanib	Inhibit VEGFR	Kidney cancer, advanced soft tissue sarcoma	[41–43]
3	Sorafenib	Inhibit VEGFR	Kidney cancer, lung cancer, thyroid cancer	[44–46]
4	Sunitinib	Inhibit VEGFR	Kidney cancer, gastrointestinal stromal tumor (GIST), pancreatic neuroendocrine tumor (PNET)	[42, 47, 48]
5	Vandetanib	Inhibit VEGFR	Medullary thyroid cancer	[49, 50]
6	Cabozantinib	Inhibit VEGFR2	Medullary thyroid cancer, kidney cancer	[51, 52]
7	Regorafenib	Inhibit VEGFR2	Colorectal cancer, GIST	[53–55]
8	Ramucirumab	Inhibit VEGFR2	Advanced stomach cancer, colorectal cancer, gastroesophageal junction adenocarcinoma, non-small cell lung cancer	[56–58]
9	Bevacizumab	Inhibit VEGF-A	Colorectal cancer, kidney cancer, lung cancer	[59–61]
10	Ziv-aflibercept	Inhibit VEGF	Colorectal cancer	[62, 63]
11	Everolimus	Inhibit mTORC1	Kidney cancer, advanced breast cancer, PNET, mantle cell lymphoma	[64–66]
12	Lenalidomide	Activate ubiquitin E3 ligase cereblon	Multiple myeloma, mantle cell lymphoma	[67–69]
13	Thalidomide	Inhibit ubiquitin E3 ligase cereblon	Multiple myeloma	[37, 70]

can also be suppressed through the inhibition of I κ -B kinase by thalidomide, which in turn suppresses nuclear factor-kappa B (NF- κ B) production [37].

9.3 Lymphangiogenesis

Lymphatic vessels (LVs) play an important role in regulating the immune system, tissue fluid homeostasis, and absorption of dietary fat. However, under pathological conditions, such as inflammation or tumor development, LVs show abnormal function. These abnormalities can lead to lymphangiogenesis, which refers to the generation of new vessels from existing LVs.

9.3.1 Structure of Lymphatic Vessels

LVs are composed of initial lymphatics, pre-collecting lymphatics, and collecting lymphatics. Initial lymphatics contain blind-ended sacs that have gaps between lymphatic ECs (LECs) and a discontinuous BM that surrounds the LECs. In contrast to blood vessels, initial lymphatics lack pericytes and VSMCs. Instead, short anchoring filaments connect the abluminal membrane of LECs to the surrounding elastic fibers for controlling the elongation of the ECM and elastic fiber according to changes in the internal fluid pressure [71]. Using the gaps between LECs and elastic fibers, fluids and cells enter the LVs but do not leave. Fluids and cells that flow into LVs are called lymph. Lymph flows into pre-collecting lymphatics and reaches collecting lymphatics [72]. Unlike initial lymphatics, collecting lymphatics are surrounded by VSMCs and contain a valve to ensure the application of sufficient force to enable lymph flow along the entire LV in a certain direction [73]. Then, lymph flows to the bloodstream through the thoracic duct.

9.3.2 Mechanism of Lymphangiogenesis

Although the exact mechanism of lymphangiogenesis under pathological conditions is under investigation, it can be predicted based on embryonic LV formation. The mechanism of embryonic LV formation is as follows (Fig. 9.2). ECs undergo arterial-venous specification after differentiating from angioblasts [74]. Prospero homeobox protein 1 (PROX1), sex-determining region Y box (SOX)18, and chicken ovalbumin upstream promoter transcription factor II (COUP-TFII) are co-expressed in the subpopulation of venous cells. Interaction between these transcription factors causes venous ECs to differentiate into lymphatic progenitors. These lymphatic progenitors begin to express LV endothelial hyaluronan receptor 1 (LYVE-1) [75].

The lymphatic progenitors leave the cardinal vein and merge to produce the first lymph sacs [76]. This process is regulated by VEGF-C/VEGFR-3 interaction [77]. VEGF-C secreted from adjacent mesenchyme binds to VEGFR-3 expressed in the cardinal vein to promote sprouting, proliferation, and migration of LECs. Several receptors and factors also increase VEGF-C responsiveness. Typically, neuropilin (NRP)-2 is a co-receptor that reacts with VEGF-C [78].

After this stage, LECs begin to express podoplanin, which induces platelet aggregation; it blocks the lymphatic-venous connection and separates the blood and lymphatic vascular systems [79]. Finally, the lymphatics differentiate into lymphatic capillaries and collect LVs. The LVs recruit smooth muscle cells, form intraluminal valves, develop continuous inter-endothelial junctions, and produce a BM.

9.3.3 Effects of Lymphangiogenic Factors

Lymphangiogenesis depends on the balance of pro- and anti-lymphangiogenic factors. This balance is disrupted by the secretion of pro-lymphangiogenic factors from inflammatory cells, tumor cells, and stromal cells in the TME. Several studies have demonstrated that the interaction between VEGF-C and VEGFR-3 is a key regulator of lymphangiogenesis [80]. The binding of VEGF-C to VEGFR-3 causes receptor dimerization and leads to the phosphorylation of critical tyrosine residues on the cytoplasmic domains of LECs, which initiates the downstream signaling cascade. This signaling cascade initiation results in LEC proliferation, migration, and vessel dilation [81]. Additionally, VEGF-C binds to VEGFR-2 and neuropilins to enlarge LVs and modulate LEC migration, respectively [82, 83]. VEGF-D also binds to VEGFR-2 or VEGFR-3 and affects lymphatic functional capacity. Compared to wild-type mice, VEGF-D-deficient mice form initial LVs of smaller caliber, resulting in the uptake and transport of dextran. They also form highly edematous and thicker epithelium when wounded; this causes inadequate lymphatic drainage [84]. It is known that Ang-Tie interaction affects lymphangiogenesis by promoting lymphatic sprouting and growth [85]. Apart from growth factors and angiopoietins, other factors that affect lymphangiogenesis are under investigation.

9.3.4 Anti-lymphangiogenic Drugs

LVs play an important role in the TME as they act as a route for tumor cell migration, regulate tumor immunity, and provide a niche for stem-like tumor cells to induce tumor recurrence [86–88]. Thus, targeting lymphangiogenesis might be efficient for preventing tumor progression. As discussed in the previous section, lymphangiogenesis occurs through the action of various pro-lymphangiogenic factors and receptors, but it is known that VEGF-C/VEGFR-3 interaction is the dominant signaling axis in this process. Therefore, some drugs have been developed for blocking this interaction (Table 9.2). These drugs can be divided into two types: small-molecule receptor tyrosine kinase inhibitors (TKIs) that block the phosphorylation of critical tyrosine residues, and antibodies or peptides that block VEGF-C or VEGFR-3 function.

Four TKIs have been approved by the FDA: sorafenib, sunitinib, pazopanib, and axitinib. The therapeutic efficacy of TKIs has been confirmed under various tumor conditions. Sunitinib reduces the number of blood vessels and LVs around breast cancer cells, as well as tumor metastasis to lymph nodes, in mouse models [89]. As described in the section on angiogenesis, these drugs are widely used to treat angiogenesis because they respond to various receptors as well as VEGFR-3. These characteristics of low specificity and selectivity can cause adverse effects; hence, it is necessary to develop anti-VEGFR-3-specific TKIs.

Antibodies that can target specific growth factors and receptors have been developed in recent years. Some antibodies target the VEGF-C/VEGFR-3 interaction, and their therapeutic efficacy has been tested under various tumor conditions.

Table 9.2 Lymphangiogenesis inhibitors approved by FDA or in clinical testing

No.	Name	Target	Type	Current status	Reference
1	Sorafenib	Inhibit VEGFRs	Small molecule TKI	FDA-approved	[91]
2	Sunitinib	Inhibit VEGFRs	Small molecule TKI	FDA-approved	[89]
3	Pazopanib	Inhibit VEGFRs	Small molecule TKI	FDA-approved	[92]
4	Axitinib	Inhibit VEGFRs	Small molecule TKI	FDA-approved	[93]
5	Cediranib	Inhibit VEGFRs	Small molecule TKI	Phase III	[94]
6	Brivanib	Inhibit VEGFRs	Small molecule TKI	Phase III	[95]
7	VGX-100	Inhibit VEGF-C	Antibody	Phase I	[96]
8	IMC-3C5	Inhibit VEGFR-3	Antibody	Phase I	[90]
9	Anti-VEGFR3 peptide	Inhibit VEGFR-3	Peptide	Preclinical	[97]
10	Diabody	Inhibit VEGFR-2/VEGFR-3	Antibody	Preclinical	[98]

According to ClinialTrials.gov NCT01514123, VGX-100, which specifically binds to VEGF-C, is effective on metastatic solid tumors. IMC-3C5 was tested in a phase I study on colorectal cancer and showed minimal antitumor efficacy by blocking VEGFR-3 [90]. Although other antibodies or peptides that target the VEGF-C/VEGFR-3 interaction have been investigated in preclinical studies, this mechanism cannot completely block lymphangiogenesis because it cannot block the lymphangiogenesis driven by the VEGFR-2/VEGF-C pathway or other receptors. Therefore, various combination therapies are being developed to solve these problems.

Targeting tumor-associated lymphangiogenesis is considered a new therapeutic strategy to treat tumors. Recently, various anti-lymphangiogenesis drugs have been developed and some have reached the stage of clinical trials. However, there are still problems to be solved.

9.4 Vascularized Tumor-on-a-Chip

Blood vessels and LVs play a vital role in tissue regeneration, immune activity, and cell–cell communication [99–101]. Therefore, when reconstructing 3D *in vitro* models, it is important to construct not only tissues or tumors but also the ECM surrounding blood vessels [102]. Cell morphology, cell interaction, and gene expression in 3D *in vitro* models are more similar to *in vivo* behaviors than those in two-dimensional (2D) models; however, 2D cultures are still widely used because of the low cost and short experimental time involved. More *in vivo*-like

microfluidics-based 3D models, which include the surrounding ECM, can overcome the shortcomings of xenograft models such as limited accuracy and similarity to *in vivo* behavior.

9.4.1 Fabrication Approaches for Microfluidic Devices

Microfluidic devices have been studied and steadily developed since the 1950s. In particular, the emergence of soft lithography based on polydimethylsiloxane (PDMS) led to an explosion in microfluidic device research. Soft lithography can create precise microfluidic channels with high resolution [103]. However, given the time-consuming and labor-intensive nature of lithography, which is unfavorable for high-throughput experiments, and the tendency of PDMS to absorb small molecules [104], it is necessary to develop other methods for fabricating microfluidic devices. Digital lithography is a laser processing technology to create microfluidic channels on PDMS. A continuous-wave laser guides successive photothermal pyrolysis as it converts PDMS to removable silicon carbide (Fig. 9.3). Digital lithography can overcome time-consuming and labor-intensive nature of soft lithography through a fully automated process with high accuracy. However, the shortcomings associated with the PDMS material properties remain [105].

Microfluidic devices can also be fabricated via 3D printing. There are various 3D printing methods, but stereolithography apparatus (SLA) and digital light processing (DLP) are the most used (Table 9.3). Both processes share some similarities because they fabricate a sample by hardening the photopolymer using light [106]. 3D printing can be used to easily and rapidly create complex shapes owing to its high degrees of freedom; it can be utilized to prototype the designed microfluidic devices [107]. In addition, it can fabricate a large number of devices within a short time compared to soft lithography. However, the performance of 3D printer needs to be kept constantly and it has a lower resolution compared to soft lithography. In addition, material properties must be carefully considered not to be toxic to cells. Using bio-compatible polymers, some research transplanted a 3D printed structure that contains cells or tissues into a mouse [108, 109].

Injection molding is another method for the fabrication of microfluidic devices and is widely used in industries supporting mass production. Many products can be quickly fabricated from the mold and have largely uniform wells. Hence, microfluidic devices can be high-throughput and reproducible. However, the mold design process is characterized by a low degree of freedom, owing to the technical characteristics of injection molding: the upper and lower plates are repeatedly coupled and separated. Complex shapes are difficult to design and have low structural stability. In addition, one of the widely used injection molding materials, general-purpose polystyrene, limits the resolution of the technique. These limitations can be overcome by compression molding, wherein resin can be compressed through elaborate molding to create the desired shape. However, mold prices and technology costs are higher than those of injection molding; therefore, the accessibility of the technology is low. Nevertheless, compression molding seems to be the best

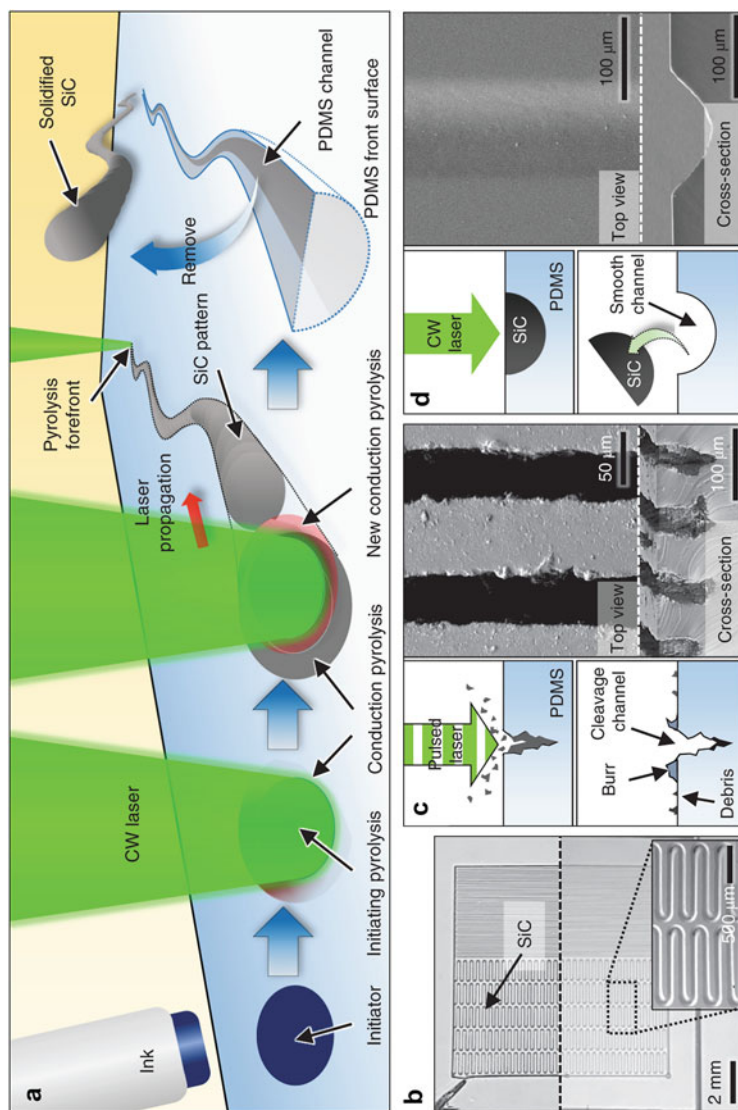


Fig. 9.3 Mechanisms of two successive laser pyrolysis (SLP). (a) The process flow of the front surface scanning (FSS); the opaque initiating point, initial laser-induced pyrolysis, successive progress of pyrolysis, and removal of silicon carbide (SiC). (b) Optical images of the SiC removal before (top) and after (bottom). (c, d) Schematics (left) and scanning electron microscopy (SEM) images (right) of the laser ablation technique using a pulsed laser (c) and the SLP (d); the SLP made the smooth inner surface. (All figures are reprinted with permission from the publisher of the article)

Table 9.3 Differences between stereolithography apparatus (SLA) and digital light processing (DLP)

Criteria	SLA	DLP
Light source	^a UV laser beam	UV light from a projector
Light movement	Point to point	Stationary
Light intensity	Invariable	Variable
Curing	High accuracy and smooth surface	Low accuracy and rough surface
Printing time	Slow	Fast
Cost	Expensive	Cheap

^a Properties are compared only between two methods

technique currently available for commercial fabrication of microfluidic devices because of high resolution as soft lithography and mass productivity.

9.4.2 Experimental Approaches of In Vitro Tumor Models

In vitro tumor models can be categorized into two experimental approaches: tumor cluster models and tumor spheroid models. Tumor clusters are the aggregation of tumor cells relatively in small size. Tumor cells can be clustered in microfluidic devices as they proliferate inside or can be introduced after they clustered elsewhere [110, 111]. Tumor spheroids are relatively bigger aggregation of tumor cells compared to tumor clusters. A U-shaped 96-well plate or a hanging droplet are utilized to form tumor spheroids [112–114]. ECMs are generally mixed with cells to assist cell adhesion proteins holding ECM and surrounding cells and keeping a spheroid-like shape. 3D bioprinting can be applied to reconstruct in vitro TME as printing cell mixtures and to form tumor spheroids. Due to 3D bio-printer continuously extruding mixture of cells and hydrogel, tumor cluster models are more dominant than a single tumor spheroid models. 3D bioprinted in vitro tumor models can be reconstructed within the microfluidic devices or printing itself [115].

9.4.3 Vascularized Tumor Models

Vessels circulate blood, oxygen, and nutrient in living organisms. Under pathological conditions like tumor, vessels undergo structural and functional changes by the factors secreted by the tumor [116]. Studies on vessel-tumor interaction and tumor therapies have been actively established with the increasing effort on anti-cancer treatment. Microfluidic based organ-on-a-chip enables to emulate more in vivo like TME.

9.4.3.1 Brain Cancer Models

The brain is the most complex organ in the human body and controls overall body functions, including emotion and physical activity. It communicates with the whole

body by transmitting electrical signals through the central nervous system (CNS). Therefore, diseases of the brain and CNS lead to lethal disorders, against which the human body has several barriers to protect itself. The blood-brain barrier (BBB) has highly selective semi-permeability and prevents macromolecules from entering the brain [117, 118]. It even disrupts drug delivery to the brain and hence causes difficulties in developing new drugs. Therefore, *in vitro* models incorporating BBB and glioblastoma have been utilized to develop effective drug delivery methods.

Chonan et al. seeded glioma-initiating cells (GICs), which are considered responsible for the therapeutic resistance and recurrence of glioma, onto a PDMS-based microfluidic chip composed of three channels: glioblastoma channel, invasion channel, and blood vessel channel [119]. They observed the interaction between GICs and HUVECs; HUVECs promoted GIC invasion and the expression of tubulin $\beta 3$ (TUBB3), a differentiated cell marker. Silvani et al. integrated a microfluidic chip and 3D bioprinting to reconstruct a glioblastoma multiforme (GBM) environment including BBB (Fig. 9.4a) [120]. They bioprinted a mixture of gelatin methacryloyl (GelMa)-alginate and GBM cells on the tissue compartment of the chip so that the GBM spheroids were formed inside the hydrogel. They showed that the BBB-surrounding tissue compartment covered by hCMEC/D3 (human cerebral microvascular endothelial cell line) cells allows no diffusion into the tissue compartment. Using the model, they observed that gravity influenced the morphology and characteristics of GBM cells such that they invaded and aggregated into the surrounding microenvironment. Cui et al. developed a microfluidics-based 3D “GBM-on-a-chip” microphysiological system with patient-derived cells from nivolumab-treated patients [121]. They distinguished immunosuppressive signatures by 6 subtypes depending on DNA methylation. They made a brain tissue-mimicking hydrogel to construct a GBM environment with interpenetrating growth-factor-reduced Matrigel matrix (Corning) and MMP-sensitive hyaluronic acid (HA) hydrogels with a volume ratio of 1:1. They showed that CD8+ T cells penetrated blood vessels toward the GBM environment and that GBM regulated immunosuppression via tumor-associated macrophages (TAMs). Finally, they suggested combo therapy with anti-PD-1 and anti-CSF1R to restore the immune system; CSF1 is a cytokine that GBM secretes to activate TAMs. Unlike monotherapy, combo therapy induced the recruitment of CD8+ T cells into the GBM environment.

9.4.3.2 Lung Cancer Models

The lung is a vital respiration organ for gas exchange. It is composed of alveoli surrounded by capillaries. The lungs are at risk of infection due to the entry of aerosols. Lung cancer is one of the major cancers with a high mortality rate and is known to metastasize to other organs. The demand for experimental models has followed the development of drugs to treat this disease, in order to improve the development of tumor therapeutics; therefore, *in vitro* microfluidics-based lung tumor models have been developed.

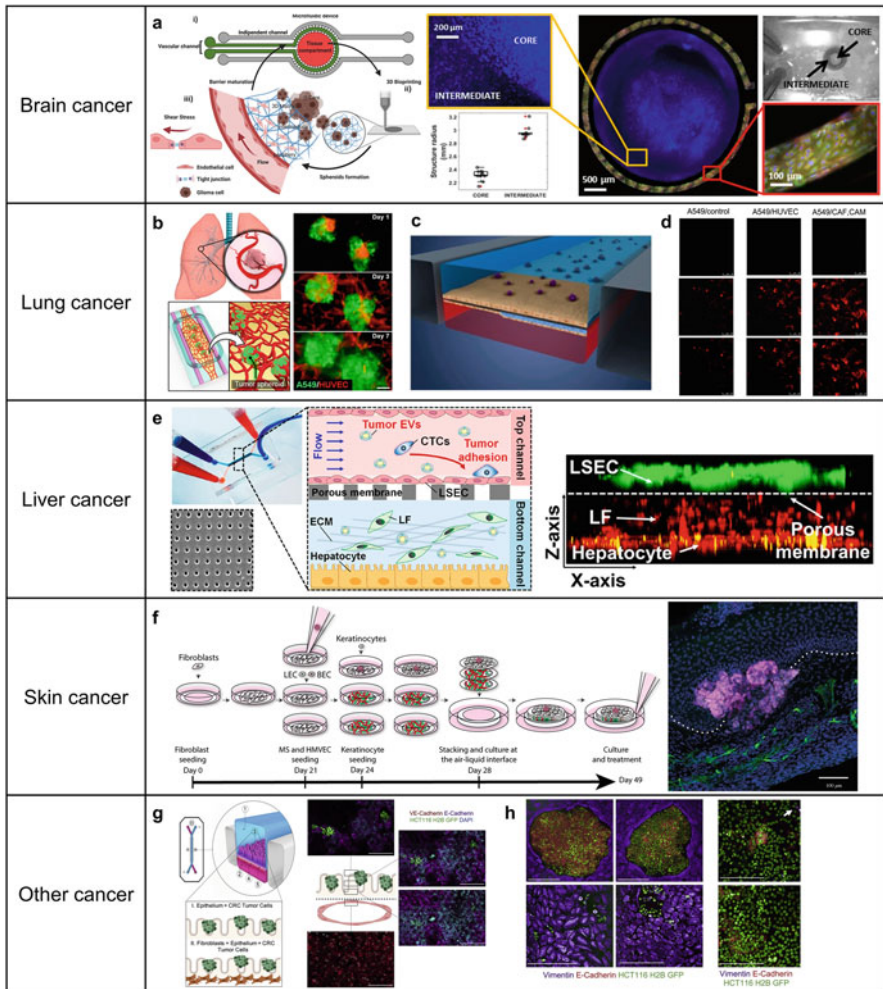


Fig. 9.4 Categorization of organ-on-a-chip models based on the organ type. **(a)** A schematic of GBM-on-a-chip. 3D bioprinting is used to cover a tissue compartment with tumor-stroma concentric structure. Shear stress is applied through flow in the vessel. Fluorescence images show separately printed structures; GBM cells inside and endothelial cells outside. **(b)** A schematic of a vascularized lung cancer-on-a-chip. The cancer spheroids composed of A549 cells (green) and RFP HUVECs (red) grow in the cell culture chamber with structural integration for 7 days. (scale bar, 50 μm). **(c)** A schematic of a multi-organ microfluidic system. Cancer and epithelial cells are cultured with exposure to air (top) and stromal cells are cultured with media (bottom). **(d)** Fluorescence images show difference in the invasion of lung cancer cells (red) by co-culture conditions. **(e)** A schematic of breast cancer-derived EVs in the liver-on-a-chip. Fluorescence image shows LSECs (top) and co-cultured hepatocytes and human LFs (bottom). **(f)** A schematic of 3D melanoma model production process. Keratinocytes and melanoma are cultured on the first sheet, and LECs, VECs, and fibroblasts were cultured on the bottom two sheets. A fluorescence image shows 70 μm transverse cryosection of 3D melanoma model. (white dot: dermo-epidermal junction, green: LEC, pink: tumor). **(g)** A schematic of colorectal cancer-on-a-chip model. Fluorescence images show EC (red), epithelial cell (purple), CRC (green), and nuclei (blue). **(h)** Fluorescence images show difference in CRC phenotypic heterogeneity when CRC cultured on chip (left) and on plastic (right). (All figures are reprinted with permission from the publisher of each article)

Using a platform with an open-top cell culture chamber, Paek et al. made a solid tumor model with a vascular network (Fig. 9.4b) [122]. They used the A549 cell line (a type of lung cancer cell) and made self-assembled perfusable vascular network-surrounding tumor spheroids. They observed the live/dead ratio of tumor cells and the condition of blood vessels with a clinical dose of paclitaxel. Paclitaxel induced an increase in caspase-3/7 expression and the production of reactive oxygen species in ECs; these can damage vasculature through apoptosis and oxidative stress, respectively. Yang et al. observed the effect of interaction between cancer cells and surrounding cells using a microfluidic device [123]. They mimicked the alveolar membrane that consists of lung cancer cells, fibroblast cells, and ECs using poly (lactic-co-glycolic acid) (PLGA) electrospun nanofibers. They showed that anti-cancer drug resistance by fibroblasts and cancer cells causes apoptosis or death of ECs, which results in cancer invasion. Hassell et al. developed orthotopic models of non-small-cell lung cancer (NSCLC) using a microfluidic device to study tumor growth/invasion patterns [124]. This chip had two channels consisting of epithelium and endothelium separated by a porous ECM-coated membrane and two parallel side chambers. To recapitulate the breathing motion, cyclic suction was applied in these chambers. It was observed that breathing motion suppresses cancer cell growth and invasion and increases drug resistance via alterations in epidermal growth factor receptor (EGFR) and MET protein kinase signaling. Recently, Xu et al. designed a multi-organ chip to study lung cancer cell metastasis to the brain, bone, and liver (Fig. 9.4c) [125]. They separated the device into three PDMS layers using a membrane. The upstream section of this device mimicked lungs, and the three downstream sections contained grown astrocytes, osteocytes, and hepatocytes. They observed lung cancer development, invasion, and metastasis in this chip by analyzing the changes in gene expression when lung cancer cells were co-cultured with other types of cells (Fig. 9.4d).

9.4.3.3 Liver Cancer Models

The liver is a metabolic organ responsible for detoxification, glycogen storage regulation, and bile synthesis. The liver is composed of hepatic sinusoids that transport nutrient-rich blood to the hepatic artery and portal vein. Since the liver is characterized by the nutrient-rich blood supply and the presence of humoral factors, it is a major tumor site. Several platforms have been developed to study the functions of the liver in tumor metastasis.

Lu et al. developed a liver tumor-on-a-chip containing decellularized liver matrix (DLM) and GelMA to screen drug toxicity [126]. This platform enhances cell viability and hepatocyte functions by preserving DLM-associated structural proteins and liver-specific growth factors. They reconstructed an *in vivo*-like TME that reflected the structural scaffold and biophysical cues. Jing et al. developed a tumor-vessel co-culture system using a microfluidic device composed of two pieces of polymethylmethacrylate frames and three layers of PDMS membranes separated by a porous membrane to study the tumor metastasis stage and test anti-tumor drugs [127]. They showed that the flow affects the stage of tumor metastasis and increases drug efficacy. Kim et al. fabricated a liver-on-a-chip that acts as a premetastatic niche

to study the effects of primary tumor-derived soluble factors on secondary organs (Fig. 9.4e) [128]. They observed that primary tumor-derived extracellular vesicles (EVs) induce the mesenchymal transition of liver sinusoidal ECs (LSECs) and destruction of vessel barriers and increase the adhesion of cancer cells in the liver microenvironment by upregulating the expression of fibronectin, an adhesive extracellular matrix protein, in LSECs.

9.4.3.4 Skin Cancer Models

The skin, as the largest organ in the body, acts as a physical and immunological barrier to the external environment. The skin is composed of three layers: epidermis, dermis, and hypodermis. The epidermis is the outermost stratum and is mainly composed of keratinocytes, which form a barrier against external matter such as pathogens. The dermis, which is underneath the epidermis, mainly comprises fibroblast-embedded collagen and contains blood vessels. This layer provides flexibility and acts as a cushion. The hypodermis, which is the deepest layer, is composed of adipocytes that store fat. Skin cancer commonly arises from squamous cells, basal cells, or melanocytes in sun-exposed areas. Various skin-on-a-chip platforms have been developed to test drugs for the treatment of skin cancer.

Skin equivalents with perfusable vessel models are essential to studying cancer. Wufuer et al. fabricated a PDMS-based three-layered chip that exchanges substances through a membrane to mimic the epidermal, dermal, and vessel layers for functional responses of human skin in inflammation, edema, and drug-based treatment [129]. Although the three cells were co-cultured, activity in the 3D environment could not be realized because each was cultured two-dimensionally. Jushoh et al. developed a 3D skin-irritation platform to test the toxicology of cosmetic compounds [130]. They showed that irritants damage keratinocytes, which results in the release of proinflammatory mediators and promotes angiogenesis. They also found that substances known as non-irritants influenced the number of sprouts, area, and length during angiogenesis. Businaro et al. developed a PDMS-based microfluidic chip consisting of two end-closed channels and two cell culture compartments to study the link between cancer and the immune system [131]. Using this platform, they co-cultured melanoma and murine spleen cells and showed that the spleen cells expressing interferon regulatory factor 8 migrate toward cancer cells and inhibit tumor cell migration and invasion. Ayuso et al. developed a microfluidic chip composed of circular chambers separated by a narrow connection channel to study the effects of epidermal keratinocytes and dermal fibroblasts (DFs) on melanoma [132]. They showed that keratinocytes and DFs change the melanoma cell morphology, secretion pattern, and metabolic phenotype. Although there is a plethora of chips that model skin and vessels separately, only a few platforms have been developed to integrate these two systems. Bourland et al. developed a 3D melanoma model with blood and lymphatic capillaries by stacking cell sheets to study the interaction between melanoma cells and the microvasculature (Fig. 9.4f) [133]. To determine the effect of the vessels in skin tumors, it is necessary to develop a microfluidic chip that can mimic the tumor and vessel environment.

9.4.3.5 Other Cancer Models

Tumors are malignant growths that mankind must overcome. Researchers and doctors worldwide have tried to elucidate the survival mechanism of tumor cells, which gain nutrients through angiogenesis or remodeling of surrounding vessels and matrices [134]. Since xenograft models require a lot of time and money, researchers have started using *in vitro* models that are high in throughput and content.

Nguyen et al. developed a pancreatic ductal adenocarcinoma (PDAC)-on-a-chip for studying the interaction between PDAC and vascular network [135]. This chip is composed of two hollow cylindrical channels surrounded by collagen gel. One channel mimics pancreatic cancer duct and the other channel mimics blood vessels. They observed the PDAC invaded into vessel lumen and ablated the ECs by the activin-ALK pathway. Strelez et al. developed colorectal cancer (CRC)-on-a-chip for studying the progression of CRC which is an early step in metastasis (Fig. 9.4g) [136]. Two channels were separated by a porous membrane with fluid flow and cyclic strain. The upstream layer comprises epithelial and cancer cells and downstream layer comprises of HUVECs. They observed that 3D tumor-on-a-chip reflect phenotypic heterogeneity more during intravasation than 2D models and coculture with stromal cell increases CRC invasion to blood vessels (Fig. 9.4h). Chen et al. made a tumor extravasation model with MDA-MB-231, a breast cancer cell line [137]. They engineered MDA-MB-231 cells to exhibit $\beta 1$ integrin knockdown using siRNA. They examined the role of $\beta 1$ integrin in transendothelial migration (TEM). They observed the degree of transmigration of tumor cells depending on the position: breached ECs but not laminin, fully transmigrated but no breaching of laminin, simultaneously breaching EC and laminin layer, and fully breached EC and laminin layers. $\beta 1$ integrin was required to invade the endothelial BM; transmigration of a tumor cell was hard if $\alpha 3\beta 1$ and $\alpha 6\beta 1$ integrins could not adhere to endothelial BM laminin.

9.4.4 Trends and Perspectives

Microfluidic devices have been applied to reconstruct *in vitro* disease models. Most models utilized cell lines that have different properties compared to primary cells and patient-derived cells (PDCs). In particular, PDCs show different characteristics in proliferation and metastasis according to personal genetic characteristics [138]. Therefore, clinical translational research through microfluidic devices is emerging as they recapitulate personal disease models. Although clinical translation actually means that clinical approach utilizes *in vitro* data, the current research accepts PDC models or reversely applies clinical data to *in vitro* since *in vitro* models are insufficient in terms of data reliability and model accuracy.

Anti-cancer treatment through chemical and targeted drugs is discussed about side effects and shortcomings. Chemical therapy affects normal cells as well as tumor cells, and target therapy becomes neutralized by the mutant of target cells. Utilization of personal immune system is emerging to overcome obstacles of previous generation drugs. Hence, interests about the dynamics between immune

cells and tumors are increased. Ayuso et al. observed the relativeness between NK cell exhaustion and TME on the microfluidic device [139]. Breast cancer cells and NK cells are seeded in the middle chamber of the device surrounded by collagen matrix with wall-patterned blood vessels. NK cell cytotoxic capacity seemed to be suppressed in TME.

In addition to constructing disease models and drug screening, a novel therapeutic strategy that targets a certain signal is suggested through the observation of biomarkers and signaling pathways of models. Cui et al. showed the performance of a combo therapy of Cilengitide and LY-364947 that inhibit interactions between EC and M2-like tumor-associated macrophage (TAM) through the GBM cell line model [140]. The combo therapy showed better anti-angiogenic effect compared to mono treatment of each drug. Cui et al. also developed a PDC model from GBM patients [121]. They observed GBM regulated TAMs to suppress T cells. They suggested a combo treatment of anti-PD1, immunotherapy to inhibit T cell suppression of TAM, and anti-CSF1R, which inhibits the TAM regulation of GBM, and observed the combo treatment-induced immune recovery.

9.5 Conclusions

Many researchers have used microfluidic devices to mimic and study the functions of each TME integrated with vascular networks. It is hard to supply sufficient nutrients and observe cell–cell interactions if a model is only composed of tumors without a vessel network. Since it is known that the vessel network is critical for the survival of tumors, a vascularized tumor model is required for research [27].

Microfluidic models have been developed and used to reconstruct vascularized tumor models. Such models have ensured high productivity through various manufacturing methods and have been developed to enable more complex reconstruction. In this chapter, we summarized angiogenesis, lymphangiogenesis, and growth factors and related drugs, and introduced related research using microfluidic devices.

The microfluidic model enables relative ease in experimentation compared to xenograft and organoid models. First, it facilitates three-dimensional fluorescent imaging through immunofluorescence. However, several preprocessing steps are required to determine internal events. Second, the microfluidic model helps save time and resources since it is possible to obtain results simultaneously in a short period for various cases, whereas xenograft and organoid models take a long time for each case. In addition, xenografts often show different results in practice due to their heterogeneity, whereas the microfluidic model exhibits homogeneity since it uses human cell lines or patient-derived cells. However, xenograft models are believed to be more reliable because microfluidic models lack peripheral environments such as immune cells. Early PDMS-based microfluidic models were low-throughput due to long fabrication times and large labor requirements; however, the introduction of new methods for mass production, including 3D printing and injection molding, has allowed high-throughput and high-content screening. Moreover, microfluidic

models are compatible with existing instruments following standard “Society of Biomolecular Screening” formats. High throughput allows reproductivity under repetitive experiments. In the future, a human-on-a-chip, the ultimate goal of organ-on-a-chip technology, is expected to be realized through connection and circulation among microfluidic models.

Although the tumor-on-a-chip is a simplified one, it is valuable in biological research about structural and functional units of tumors and TME. Current tumor-on-a-chips are mostly used to evaluate drug performance for the development of new drugs. They can extend their application into studying *in vivo* mechanisms and clinical area through increasing reliability of data. Real-time data from biosensors integrated into tumor-on-a-chip can be one of the means to assist reliability; optical, chemical, and electrical measurements can support the value of data. Latest tumor-on-a-chip research attempted clinical translation that compares clinical and *in vitro* data and recommends an efficient, novel combo therapy based on internal information of cells. Such models are expected to promote personal medicine development, as they can help determine the combination and dose of drugs for each patient. However, novel biological information including unknown physiological mechanisms of tumor dynamics are not explored enough through tumor-on-a-chip models. Thus, it is hoped that the advance in tumor-on-a-chip technology contributes to treating cancer through overcoming existing limitations.

References

1. Kapalczyńska M et al (2018) 2D and 3D cell cultures—a comparison of different types of cancer cell cultures. *Arch Med Sci* 14(4):910–919
2. Fontoura JC et al (2020) Comparison of 2D and 3D cell culture models for cell growth, gene expression and drug resistance. *Mater Sci Eng C* 107
3. Teixeira MI et al (2020) Recent developments in microfluidic technologies for central nervous system targeted studies. *Pharmaceutics* 12(6)
4. van Duinen V et al (2019) Perfused 3D angiogenic sprouting in a high-throughput *in vitro* platform. *Angiogenesis* 22(1):157–165
5. Vaupel P, Kallinowski F, Okunieff P (1989) Blood-flow, oxygen and nutrient supply, and metabolic microenvironment of human-tumors—a review. *Cancer Res* 49(23):6449–6465
6. Fiedler U, Augustin HG (2006) Angiopoietins: a link between angiogenesis and inflammation. *Trends Immunol* 27(12):552–558
7. Folkman J (1984) Angiogenesis. In: *Biology of endothelial cells*. Springer, Boston, pp 412–428
8. Medvedev A, Samsonov V, Fomin V (2006) Rational structure of blood vessels. *J Appl Mech Tech Phys* 47(3):324–329
9. Tucker WD, Arora Y, Mahajan K (2017) Anatomy, blood vessels
10. Gao Y (2017) *Biology of vascular smooth muscle: vasoconstriction and dilatation*, vol 8. Springer
11. Cuenca MV et al (2021) Engineered 3D vessel-on-chip using hiPSC-derived endothelial- and vascular smooth muscle cells. *Stem Cell Rep* 16(9):2159–2168
12. Eble JA, Niland S (2009) The extracellular matrix of blood vessels. *Curr Pharm Des* 15(12): 1385–1400
13. Lee S et al (2020) 3D brain angiogenesis model to reconstitute functional human blood-brain barrier *in vitro*. *Biotechnol Bioeng* 117(3):748–762

14. Osaki T, Serrano JC, Kamm RD (2018) Cooperative effects of vascular angiogenesis and lymphangiogenesis. *Regen Eng Transl Med* 4(3):120–132
15. Cleaver O, Melton DA (2003) Endothelial signaling during development. *Nat Med* 9(6):661–668
16. Chen W et al (2019) The endothelial tip-stalk cell selection and shuffling during angiogenesis. *J Cell Commun Signal* 13(3):291–301
17. Stapor PC et al (2014) Pericyte dynamics during angiogenesis: new insights from new identities. *J Vasc Res* 51(3):163–174
18. Wang WY et al (2020) Functional angiogenesis requires microenvironmental cues balancing endothelial cell migration and proliferation. *Lab Chip* 20(6):1153–1166
19. Abid MR et al (2004) Vascular endothelial growth factor activates PI3K/Akt/forkhead signaling in endothelial cells. *Arterioscler Thromb Vasc Biol* 24(2):294–300
20. Gupta K et al (1999) VEGF prevents apoptosis of human microvascular endothelial cells via opposing effects on MAPK/ERK and SAPK/JNK signaling. *Exp Cell Res* 247(2):495–504
21. Gupta MK, Qin R-Y (2003) Mechanism and its regulation of tumor-induced angiogenesis. *World J Gastroenterol* 9(6):1144
22. Strutz F (2009) The role of FGF-2 in renal fibrogenesis. *Front Biosci (Schol Ed)* 1(1):125–131
23. Cavallaro U et al (2001) Response of bovine endothelial cells to FGF-2 and VEGF is dependent on their site of origin: relevance to the regulation of angiogenesis. *J Cell Biochem* 82(4):619–633
24. Karsan A et al (1997) Fibroblast growth factor-2 inhibits endothelial cell apoptosis by Bcl-2-dependent and independent mechanisms. *Am J Pathol* 151(6):1775
25. Karar J, Maity A (2011) PI3K/AKT/mTOR pathway in angiogenesis. *Front Mol Neurosci* 4:51
26. Kim I et al (2000) Angiopoietin-1 induces endothelial cell sprouting through the activation of focal adhesion kinase and plasmin secretion. *Circ Res* 86(9):952–959
27. Siemann DW, Shi W (2003) Targeting the tumor blood vessel network to enhance the efficacy of radiation therapy. In: *Seminars in radiation oncology*. Elsevier
28. Bergers G, Benjamin LE (2003) Tumorigenesis and the angiogenic switch. *Nat Rev Cancer* 3(6):401–410
29. Hockel M, Vaupel P (2001) Tumor hypoxia: definitions and current clinical, biologic, and molecular aspects. *J Natl Cancer Inst* 93(4):266–276
30. Oka N et al (2007) VEGF promotes tumorigenesis and angiogenesis of human glioblastoma stem cells. *Biochem Biophys Res Commun* 360(3):553–559
31. Jain RK, Martin JD, Stylianopoulos T (2014) The role of mechanical forces in tumor growth and therapy. *Annu Rev Biomed Eng* 16:321–346
32. Schaaf MB, Garg AD, Agostinis P (2018) Defining the role of the tumor vasculature in antitumor immunity and immunotherapy. *Cell Death Dis* 9(2):1–14
33. Fallah A et al (2019) Therapeutic targeting of angiogenesis molecular pathways in angiogenesis-dependent diseases. *Biomed Pharmacother* 110:775–785
34. Kamba T, McDonald D (2007) Mechanisms of adverse effects of anti-VEGF therapy for cancer. *Br J Cancer* 96(12):1788–1795
35. Gardner V, Madu CO, Lu Y (2017) Anti-VEGF therapy in cancer: a double-edged sword, Physiologic and pathologic angiogenesis-signaling mechanisms and targeted therapy, pp 385–410
36. Elice F, Rodeghiero F (2012) Side effects of anti-angiogenic drugs. *Thromb Res* 129:S50–S53
37. Keifer JA et al (2001) Inhibition of NF- κ B activity by thalidomide through suppression of I κ B kinase activity. *J Biol Chem* 276(25):22382–22387
38. Kelly RJ, Rixe O (2010) Axitinib (AG-013736), Small molecules in oncology, pp 33–44
39. Sonpavde G, Hutson TE, Rini BI (2008) Axitinib for renal cell carcinoma. *Expert Opin Investig Drugs* 17(5):741–748
40. Escudier B, Gore M (2011) Axitinib for the management of metastatic renal cell carcinoma. *Drugs R & D* 11(2):113–126

41. Sonpavde G, Hutson TE (2007) Pazopanib: a novel multitargeted tyrosine kinase inhibitor. *Curr Oncol Rep* 9(2):115–119
42. Metzger RJ et al (2013) Pazopanib versus sunitinib in metastatic renal-cell carcinoma. *N Engl J Med* 369(8):722–731
43. Hutson TE et al (2010) Efficacy and safety of pazopanib in patients with metastatic renal cell carcinoma. *J Clin Oncol* 28(3):475–480
44. Adnane L et al (2006) Sorafenib (BAY 43-9006, Nexavar[®]), a dual-action inhibitor that targets RAF/MEK/ERK pathway in tumor cells and tyrosine kinases VEGFR/PDGFR in tumor vasculature. *Methods Enzymol* 407:597–612
45. Zhang J, Gold KA, Kim E (2012) Sorafenib in non-small cell lung cancer. *Expert Opin Investig Drugs* 21(9):1417–1426
46. Capdevila J et al (2012) Sorafenib in metastatic thyroid cancer. *Endocr Relat Cancer* 19(2):209
47. Gan HK, Seruga B, Knox JJ (2009) Sunitinib in solid tumors. *Expert Opin Investig Drugs* 18(6):821–834
48. Lahner H et al (2016) Sunitinib efficacy in patients with advanced pNET in clinical practice. *Horm Metab Res* 48(09):575–580
49. Wells SA Jr et al (2010) Vandetanib for the treatment of patients with locally advanced or metastatic hereditary medullary thyroid cancer. *J Clin Oncol* 28(5):767
50. Parikh R et al (2022) Diagnostic characteristics, treatment patterns, and clinical outcomes for patients with advanced/metastatic medullary thyroid cancer. *Thyroid Res* 15(1):1–14
51. Durán I et al (2022) Exploring the synergistic effects of cabozantinib and a programmed cell death protein 1 inhibitor in metastatic renal cell carcinoma with machine learning. *Oncotarget* 13:237
52. Markham A (2022) Cabozantinib plus Nivolumab: a review in advanced renal cell carcinoma. *Target Oncol*:1–9
53. Arai H et al (2019) Molecular insight of regorafenib treatment for colorectal cancer. *Cancer Treat Rev* 81:101912
54. Waddell T, Cunningham D (2013) Evaluation of regorafenib in colorectal cancer and GIST. *Lancet* 381(9863):273–275
55. Strumberg D, Schultheis B (2012) Regorafenib for cancer. *Expert Opin Investig Drugs* 21(6): 879–889
56. Arrieta O et al (2017) Ramucirumab in the treatment of non-small cell lung cancer. *Expert Opin Drug Saf* 16(5):637–644
57. Casak SJ et al (2015) FDA approval summary: ramucirumab for gastric cancer. *Clin Cancer Res* 21(15):3372–3376
58. Spratlin J (2011) Ramucirumab (IMC-1121B): monoclonal antibody inhibition of vascular endothelial growth factor receptor-2. *Curr Oncol Rep* 13(2):97–102
59. Assoun S et al (2017) Bevacizumab in advanced lung cancer: state of the art. *Future Oncol* 13(28):2515–2535
60. Hainsworth JD et al (2005) Treatment of metastatic renal cell carcinoma with a combination of bevacizumab and erlotinib. *J Clin Oncol* 23(31):7889–7896
61. Hurwitz H et al (2004) Bevacizumab plus irinotecan, fluorouracil, and leucovorin for metastatic colorectal cancer. *N Engl J Med* 350(23):2335–2342
62. Chung C, Pherwani N (2013) Ziv-aflibercept: a novel angiogenesis inhibitor for the treatment of metastatic colorectal cancer. *Am J Health Syst Pharm* 70(21):1887–1896
63. Patel A, Sun W (2014) Ziv-aflibercept in metastatic colorectal cancer. *Biologics* 8:13
64. Choueiri TK et al (2015) Cabozantinib versus everolimus in advanced renal-cell carcinoma. *N Engl J Med* 373(19):1814–1823
65. Hasskarl J (2014) Everolimus, Small molecules in oncology, pp 373–392
66. Royce ME, Osman D (2015) Everolimus in the treatment of metastatic breast cancer., *Breast cancer: basic and clinical research*, vol 9. BCBCR. S29268
67. List A et al (2005) Efficacy of lenalidomide in myelodysplastic syndromes. *N Engl J Med* 352(6):549–557

68. Song K et al (2013) Lenalidomide inhibits lymphangiogenesis in preclinical models of mantle cell lymphoma. *Cancer Res* 73(24):7254–7264
69. Gribben JG, Fowler N, Morschhauser F (2015) Mechanisms of action of lenalidomide in B-cell non-Hodgkin lymphoma. *J Clin Oncol* 33(25):2803
70. Paravar T, Lee DJ (2008) Thalidomide: mechanisms of action. *Int Rev Immunol* 27(3):111–135
71. Gerli R et al (2000) Specific adhesion molecules bind anchoring filaments and endothelial cells in human skin initial lymphatics. *Lymphology* 33(4):148–157
72. Miteva DO et al (2010) Transmural flow modulates cell and fluid transport functions of lymphatic endothelium. *Circ Res* 106(5):920–931
73. Choi K et al (1998) A common precursor for hematopoietic and endothelial cells. *Development* 125(4):725–732
74. Srinivasan RS et al (2007) Lineage tracing demonstrates the venous origin of the mammalian lymphatic vasculature. *Genes Dev* 21(19):2422–2432
75. Gale NW et al (2007) Normal lymphatic development and function in mice deficient for the lymphatic hyaluronan receptor LYVE-1. *Mol Cell Biol* 27(2):595–604
76. Wigle JT et al (2002) An essential role for Prox1 in the induction of the lymphatic endothelial cell phenotype. *EMBO J* 21(7):1505–1513
77. Karkkainen MJ et al (2004) Vascular endothelial growth factor C is required for sprouting of the first lymphatic vessels from embryonic veins. *Nat Immunol* 5(1):74–80
78. Xu Y et al (2010) Neuropilin-2 mediates VEGF-C-induced lymphatic sprouting together with VEGFR3. *J Cell Biol* 188(1):115–130
79. Schacht V et al (2003) T1 α /podoplanin deficiency disrupts normal lymphatic vasculature formation and causes lymphedema. *EMBO J* 22(14):3546–3556
80. Veikkola T et al (2001) Signalling via vascular endothelial growth factor receptor-3 is sufficient for lymphangiogenesis in transgenic mice. *EMBO J* 20(6):1223–1231
81. Salameh A et al (2005) Direct recruitment of CRK and GRB2 to VEGFR-3 induces proliferation, migration, and survival of endothelial cells through the activation of ERK, AKT, and JNK pathways. *Blood* 106(10):3423–3431
82. Hamada K et al (2000) VEGF-C signaling pathways through VEGFR-2 and VEGFR-3 in vasculoangiogenesis and hematopoiesis. *Blood* 96(12):3793–3800
83. Mäkinen T et al (2001) Isolated lymphatic endothelial cells transduce growth, survival and migratory signals via the VEGF-C/D receptor VEGFR-3. *EMBO J* 20(17):4762–4773
84. Paquet-Fifield S et al (2013) Vascular endothelial growth factor-d modulates caliber and function of initial lymphatics in the dermis. *J Invest Dermatol* 133(8):2074–2084
85. Fagiani E et al (2011) Angiopoietin-1 and-2 exert antagonistic functions in tumor angiogenesis, yet both induce lymphangiogenesis. *Cancer Res* 71(17):5717–5727
86. Maula S-M et al (2003) Intratumoral lymphatics are essential for the metastatic spread and prognosis in squamous cell carcinomas of the head and neck region. *Cancer Res* 63(8):1920–1926
87. Lund AW et al (2016) Lymphatic vessels regulate immune microenvironments in human and murine melanoma. *J Clin Invest* 126(9):3389–3402
88. Olmeda D et al (2017) Whole-body imaging of lymphovascular niches identifies pre-metastatic roles of midkine. *Nature* 546(7660):676–680
89. Kodera Y et al (2011) Sunitinib inhibits lymphatic endothelial cell functions and lymph node metastasis in a breast cancer model through inhibition of vascular endothelial growth factor receptor 3. *Breast Cancer Res* 13(3):1–11
90. Saif MW et al (2016) Phase 1 study of the anti-vascular endothelial growth factor receptor 3 monoclonal antibody LY3022856/IMC-3C5 in patients with advanced and refractory solid tumors and advanced colorectal cancer. *Cancer Chemother Pharmacol* 78(4):815–824
91. Escudier B et al (2007) Sorafenib in advanced clear-cell renal-cell carcinoma. *N Engl J Med* 356(2):125–134

92. Sternberg CN et al (2010) Pazopanib in locally advanced or metastatic renal cell carcinoma: results of a randomized phase III trial. *J Clin Oncol* 28(6):1061–1068
93. Albiges L et al (2015) Axitinib in metastatic renal cell carcinoma. *Expert Rev Anticancer Ther* 15(5):499–507
94. Stark DP et al (2017) Quality of life with cediranib in relapsed ovarian cancer: the ICON 6 phase 3 randomized clinical trial. *Cancer* 123(14):2752–2761
95. Kudo M et al (2014) Brivanib as adjuvant therapy to transarterial chemoembolization in patients with hepatocellular carcinoma: a randomized phase III trial. *Hepatology* 60(5):1697–1707
96. Hajrasouliha AR et al (2012) Vascular endothelial growth factor-C promotes alloimmunity by amplifying antigen-presenting cell maturation and lymphangiogenesis. *Invest Ophthalmol Vis Sci* 53(3):1244–1250
97. Yeh Y-W et al (2017) Targeting the VEGF-C/VEGFR3 axis suppresses slug-mediated cancer metastasis and stemness via inhibition of KRAS/YAP1 signaling. *Oncotarget* 8(3):5603
98. Jimenez X et al (2005) A recombinant, fully human, bispecific antibody neutralizes the biological activities mediated by both vascular endothelial growth factor receptors 2 and 3. *Mol Cancer Ther* 4(3):427–434
99. Farré-Guasch E et al (2018) Blood vessel formation and bone regeneration potential of the stromal vascular fraction seeded on a calcium phosphate scaffold in the human maxillary sinus floor elevation model. *Materials* 11(1):161
100. Zhou Z et al (2004) Impaired angiogenesis, delayed wound healing and retarded tumor growth in perlecan heparan sulfate-deficient mice. *Cancer Res* 64(14):4699–4702
101. Hagendoorn J et al (2006) Onset of abnormal blood and lymphatic vessel function and interstitial hypertension in early stages of carcinogenesis. *Cancer Res* 66(7):3360–3364
102. Carnemolla B et al (2002) Enhancement of the antitumor properties of interleukin-2 by its targeted delivery to the tumor blood vessel extracellular matrix. *Blood* 99(5):1659–1665
103. Fujii T (2002) PDMS-based microfluidic devices for biomedical applications. *Microelectron Eng* 61:907–914
104. Van Meer B et al (2017) Small molecule absorption by PDMS in the context of drug response bioassays. *Biochem Biophys Res Commun* 482(2):323–328
105. Shin J et al (2021) Monolithic digital patterning of polydimethylsiloxane with successive laser pyrolysis. *Nat Mater* 20(1):100–107
106. Maines EM et al (2021) Sustainable advances in SLA/DLP 3D printing materials and processes. *Green Chem* (18)
107. Yazdi AA et al (2016) 3D printing: an emerging tool for novel microfluidics and lab-on-a-chip applications. *Microfluid Nanofluidics* 20(3):1–18
108. Soltanian A et al (2019) Generation of functional human pancreatic organoids by transplants of embryonic stem cell derivatives in a 3D-printed tissue trapper. *J Cell Physiol* 234(6):9564–9576
109. Kim IG et al (2020) Transplantation of a 3D-printed tracheal graft combined with iPSC cell-derived MSCs and chondrocytes. *Sci Rep* 10(1):1–14
110. Lim J et al (2021) 3D high-content culturing and drug screening platform to study vascularized hepatocellular carcinoma in hypoxic condition. *Adv Nanobiomed Res* 1(12):2100078
111. Lee S et al (2021) Modeling 3D human tumor lymphatic vessel network using high-throughput platform. *Adv Biol* 5(2):2000195
112. Ko J et al (2019) Tumor spheroid-on-a-chip: a standardized microfluidic culture platform for investigating tumor angiogenesis. *Lab Chip* 19(17):2822–2833
113. Shin N et al (2022) Vascularization of iNSC spheroid in a 3D spheroid-on-a-chip platform enhances neural maturation. *Biotechnol Bioeng* 119(2):566–574
114. Timmins NE, Nielsen LK (2007) Generation of multicellular tumor spheroids by the hanging-drop method. In: *Tissue engineering*. Springer, pp 141–151
115. Datta P et al (2020) 3D bioprinting for reconstituting the cancer microenvironment. *NPJ Precis Oncol* 4(1):1–13

116. Park S-Y et al (2020) Pathologic angiogenesis in the bone marrow of humanized sickle cell mice is reversed by blood transfusion. *Blood* 135(23):2071–2084
117. Abbott NJ et al (2010) Structure and function of the blood–brain barrier. *Neurobiol Dis* 37(1): 13–25
118. Daneman R, Prat A (2015) The blood–brain barrier. *Cold Spring Harb Perspect Biol* 7(1): a020412
119. Chonan Y et al (2017) Endothelium-induced three-dimensional invasion of heterogeneous glioma initiating cells in a microfluidic coculture platform. *Integr Biol* 9(9):762–773
120. Silvani G et al (2021) A 3D-bioprinted vascularized glioblastoma-on-a-chip for studying the impact of simulated microgravity as a novel pre-clinical approach in brain tumor therapy. *Adv Ther* 4(11):2100106
121. Cui X et al (2020) Dissecting the immunosuppressive tumor microenvironments in glioblastoma-on-a-Chip for optimized PD-1 immunotherapy. *Elife* 9:e52253
122. Paek J et al (2019) Microphysiological engineering of self-assembled and perfusable microvascular beds for the production of vascularized three-dimensional human microtissues. *ACS Nano* 13(7):7627–7643
123. Yang X et al (2018) Nanofiber membrane supported lung-on-a-chip microdevice for anti-cancer drug testing. *Lab Chip* 18(3):486–495
124. Hassell BA et al (2017) Human organ chip models recapitulate orthotopic lung cancer growth, therapeutic responses, and tumor dormancy in vitro. *Cell Rep* 21(2):508–516
125. Xu Z et al (2016) Design and construction of a multi-organ microfluidic chip mimicking the in vivo microenvironment of lung cancer metastasis. *ACS Appl Mater Interfaces* 8(39): 25840–25847
126. Lu S et al (2018) Development of a biomimetic liver tumor-on-a-chip model based on decellularized liver matrix for toxicity testing. *Lab Chip* 18(22):3379–3392
127. Jing B et al (2019) Establishment and application of a dynamic tumor-vessel microsystem for studying different stages of tumor metastasis and evaluating anti-tumor drugs. *RSC Adv* 9(30): 17137–17147
128. Kim J et al (2020) Three-dimensional human liver-chip emulating premetastatic niche formation by breast cancer-derived extracellular vesicles. *ACS Nano* 14(11):14971–14988
129. Wufuer M et al (2016) Skin-on-a-chip model simulating inflammation, edema and drug-based treatment. *Sci Rep* 6(1):1–12
130. Jusoh N, Ko J, Jeon NL (2019) Microfluidics-based skin irritation test using in vitro 3D angiogenesis platform. *APL Bioeng* 3(3):036101
131. Businaro L et al (2013) Cross talk between cancer and immune cells: exploring complex dynamics in a microfluidic environment. *Lab Chip* 13(2):229–239
132. Ayuso JM et al (2021) Microfluidic model with air-walls reveals fibroblasts and keratinocytes modulate melanoma cell phenotype, migration, and metabolism. *Lab Chip* 21(6):1139–1149
133. Bourland J, Fradette J, Auger FA (2018) Tissue-engineered 3D melanoma model with blood and lymphatic capillaries for drug development. *Sci Rep* 8(1):1–13
134. Winkler J et al (2020) Concepts of extracellular matrix remodelling in tumour progression and metastasis. *Nat Commun* 11(1):1–19
135. Nguyen D-HT et al (2019) A biomimetic pancreatic cancer on-chip reveals endothelial ablation via ALK7 signaling. *Sci Adv* 5(8):eaav6789
136. Strelez C et al (2021) Human colorectal cancer-on-chip model to study the microenvironmental influence on early metastatic spread. *Iscience* 24(5):102509

137. Chen MB et al (2016) Elucidation of the roles of tumor integrin $\beta 1$ in the extravasation stage of the metastasis cascade. *Cancer Res* 76(9):2513–2524
138. Lee JY et al (2015) Patient-derived cell models as preclinical tools for genome-directed targeted therapy. *Oncotarget* 6(28):25619
139. Ayuso JM et al (2021) Microfluidic tumor-on-a-chip model to evaluate the role of tumor environmental stress on NK cell exhaustion. *Sci Adv* 7(8):eabc2331
140. Cui X et al (2018) Hacking macrophage-associated immunosuppression for regulating glioblastoma angiogenesis. *Biomaterials* 161:164–178

Part III

Cancer Detection and Diagnosis



Biosensors Advances: Contributions to Cancer Diagnostics and Treatment

10

Ana I. Barbosa, Rita Rebelo, Rui L. Reis, and Vitor M. Correlo

Abstract

Cancer is the second leading cause of death worldwide, and its survival rate is significantly affected by early detection and treatment. However, most current diagnostic methods are symptoms oriented, and detecting cancer only in advanced phases. The few existent screening methods, such as mammograms and papanicolaou tests are invasive and not continuous, resulting in a high percentage of non-detected cancers in the early phases. Thus, there is an urgent need to create technologies that make cancer diagnostics more accessible to populations, enabling continuous or semi-continuous, noninvasive, “long-term” screening of cancer in high-risk patients and the whole population. Biosensors are being developed to create technologies that can be applied to point-of-care, wearable, and implantable diagnostics, aiming to fill this important gap in cancer early detection, and, therefore, increase the cancer rate of survival and reduce its morbidity. The versatility of these technologies, due to their miniaturization and diverse detection modes, will enable great advances in cancer early detection, since they can be adapted to the patient and its context, allowing personalized medicine to become a reality.

Keywords

Cancer · Biosensors · Diagnostics · Point-of-care · Wearable · Implantable

A. I. Barbosa · R. Rebelo · R. L. Reis · V. M. Correlo (✉)

3B's Research Group, I3Bs—Research Institute on Biomaterials, Biodegradables and Biomimetics, University of Minho, Headquarters of the European Institute of Excellence on Tissue Engineering and Regenerative Medicine, Guimarães, Portugal

ICVS/3B's—PT Government Associate Laboratory, Braga/Guimarães, Portugal

e-mail: vitorcorrelo@i3bs.uminho.pt

© The Author(s), under exclusive license to Springer Nature Switzerland AG 2022

259

D. Caballero et al. (eds.), *Microfluidics and Biosensors in Cancer Research*,

Advances in Experimental Medicine and Biology 1379,

https://doi.org/10.1007/978-3-031-04039-9_10

10.1 Introduction

Cancer is a world burden being responsible for 9.6 million deaths in 2018, being the second leading cause of death worldwide [1]. It is a group of diverse diseases caused by the uncontrolled growth of abnormal cells that can spread to different organs forming malignant tumors that can affect the organs' function, disturbing the patient's life quality and even causing death if not treated [2].

The survival rate is highly affected by early diagnosis. Studies suggest that 80% of patients survive for at least 10 years after being diagnosed in the early stages of eight of most common cancers, according to Cancer Research UK [3]. Cancers are characterized by development stages depending on the size of the tumor, the spreading in surrounding tissues, and in other parts of the body (metastasis). Early diagnosis implies detecting cancer when it is small and confined to a single part of the body, which typically translates into none or few symptoms to the patient, making it harder to detect [4]. Early diagnosis depends on screening programs that are not currently available for all types of cancers and are typically expensive and invasive [5]. Screening programs are also dependent on the country and their availability of diagnosis facilities and qualified personnel. For example, breast cancer screening relies on mammograms, which expose women to a significant amount of radiation and therefore are usually performed in women after 40 years old every 2 years in most of the countries worldwide. Mammograms rely on X-ray diagnostic technology and professional operators that are not always available in developing countries. Therefore, these screening programs are not usually performed there. The same can be said for cervical and colorectal cancer that rely on the papanicolaou test and in colonoscopy, respectively. Both of these screening tests are invasive and demand highly trained personnel and expensive technology. Consequently, there is an urgent need to create cancer screening tests that are simple, cost-effective, and do not demand highly trained operators. These technologies should be harmless for the patients, and allow automated continuous or semi-continuous cancer detection from body fluids analysis using cancer biomarkers. This easy and accessible diagnosis of cancer is still not a reality due to the lack of specific biomarkers that can have useful clinical use, and the absence of portable, highly sensitive technologies capable of continuous monitoring of physiological conditions and detection of cancer biomarkers in very low concentrations in body fluids, which happens in early cancer stages [6]. Another important factor for increasing patient survival is the treatment monitoring and early detection of cancer recurrence, which can also be significantly improved by the creation of accessible technologies capable of sensitive and specific detection of cancer biomarkers [7].

Biosensors are analytical technologies that use biological recognition agents and different types of transducing systems to specifically quantify a biomarker in a mixture, for example, different types of body fluids (e.g., blood, urine, plasma). They aim to provide improved performance, real-time, label-free, portability, and continuous detection of cancer biomarkers by using point-of-care, wearable, and implantable devices (Fig. 10.1). Therefore, they could close the existent technological gap in cancer early detection and recurrence diagnostic devices. The

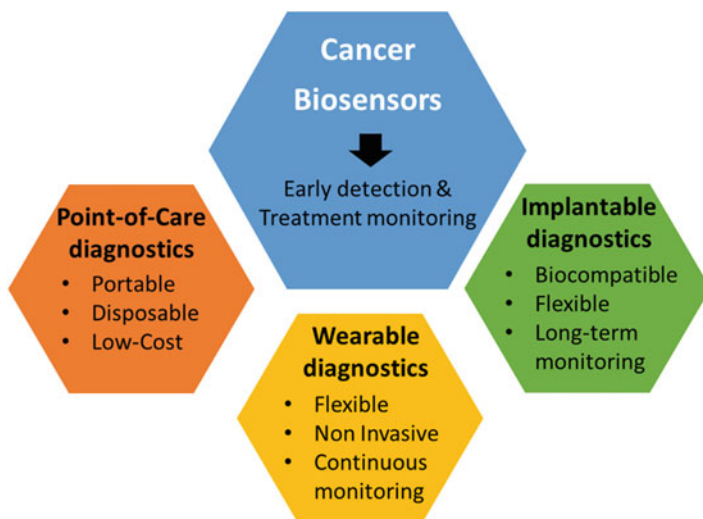


Fig. 10.1 Biosensor technologies that can contribute to cancer early detection and treatment monitoring

development of biosensors happens hand in hand with the choice of a biomarker, since the nature of the late will dictate the bio-recognition layer and the necessary transduction system for reliable signal detection. Proteins are the gold standard of cancer biomarkers, such as CAE (carcinoembryonic antigen), PSA (prostate cancer antigen), or AFP (alpha-fetoprotein); however, these biomarkers are not enough to satisfy the clinical needs of cancer diagnosis, in particular, due to their lack of specificity [8]. New types of cancer biomarkers have been proposed and are waiting clinical validation such as cancer circulating cancer cells and miRNAs [9]. Also, extracellular acidification, caused by lactate accumulation, promotes the evolution of cancer cell phenotypes, which become resistant to acid-induced cytotoxicity. This powerful growth advantage promotes unconstrained proliferation and invasion [10]. Therefore, extracellular pH or lactate concentration can be used as a diagnostic biomarker for tumor aggressiveness [11] and metastases, [12, 13] as long as an extracellular medium can be reached for analysis. Since the single analysis of one cancer biomarker is not always effective, it is important to create technologies capable of simultaneous analysis of several biomarkers that can provide more information for a more accurate diagnosis.

In this chapter, we explain the working principles and present examples of different biosensing technologies for point-of-care (POC), wearable or implantable diagnostics, that can be used for early detection and treatment monitoring of different types of cancer. These technologies aim to achieve a close-to-the-patient diagnostic approach, so that the physiological conditions are continuously or semi-continuously monitored and provide an increase in cancer survival rates in the near future.

10.2 Biosensors Approaches for Cancer Diagnostics and Treatment

10.2.1 Point-of-Care (POC) Technologies

POC diagnostic technologies are portable, usually power-free, user-friendly, disposable, and miniaturized devices that allow rapid results [14]. Qualitative POC diagnostics are widespread technologies; however, POC quantitative devices are still not a reality [15]. Cancer POC diagnostics would significantly contribute to an increase in screening programs which would reflect an overall early detection and therefore decrease of cancer mortality. Simultaneously, POC technologies would allow cancer patients to monitor their treatments and early detect possible recurrences at home or in local health centers, which would simplify the process, increase patient's life quality, and reduce mortality.

The current limitations of cancer POC diagnostics rely on the lack of sensitivity of diagnostic technologies, alongside their cost-effectiveness, as well as the lack of biomarkers with clear clinical meaning [16, 17]. In order to surpass these needs, different biosensing technologies have been developed and further integrated into microfluidic devices, in order to combine the advantages of microfluidic systems with biosensors. Microfluidics allows fast, high-throughput, multiplexed tests, with low sample volumes and reagent consumption [18], while current biosensing technologies can provide high sensitivity, label-free, real-time, and continuous detection [19].

Barbosa et al. (2019) reported AuTiO₂ thin-film composites that exhibit localized surface plasmon resonance (LSPR) detected by a custom-built optical system (Fig. 10.2). These thin films were produced by reactive DC magnetron sputtering, conjugated with a thermal annealing procedure. The combination of these two processes allows the control of AuNPs size and distribution in the TiO₂ metal matrix, producing films with desired sensitivity for LSPR. This is a fast and cost-effective coating technique that allows the deposition of many types of materials onto

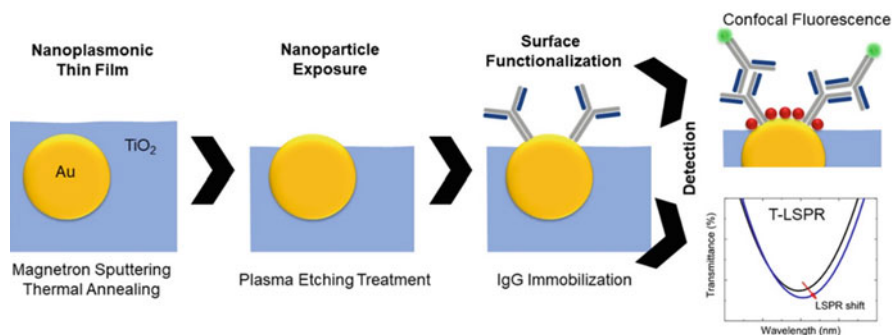


Fig. 10.2 Antibody immobilization on AuTiO₂ thin films and their detection using LSPR and Confocal Microscopy. Figure and legend reproduced with permission from Elsevier [21]

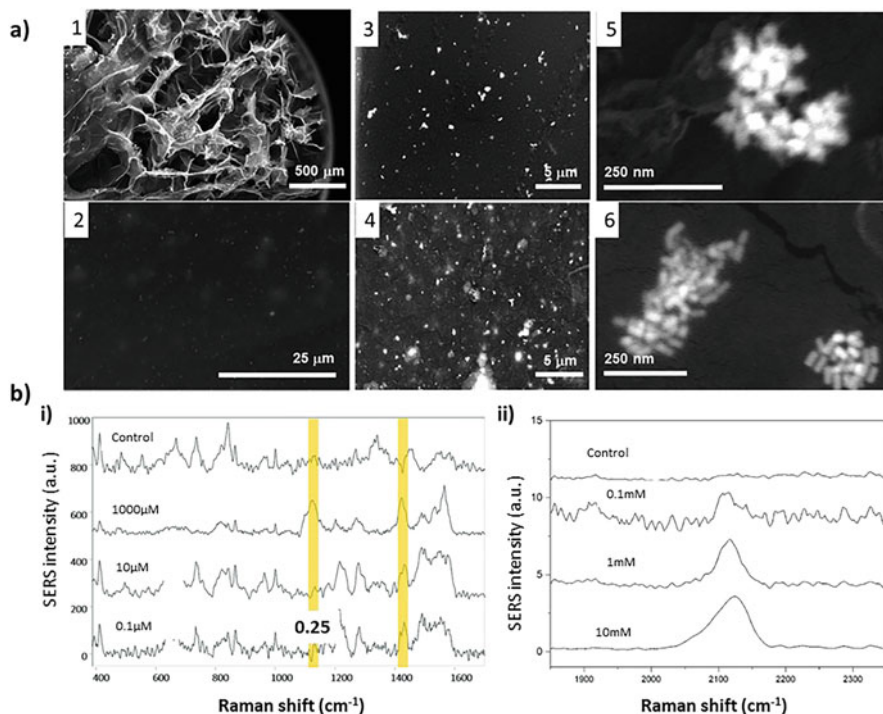


Fig. 10.3 (a) SEM images of GG hydrogels at different magnifications for the AuNSs (1,3 and 5) and Au@AgNRs (2,4 and 6). (b) (i) SERS spectra of the control (GG-SLH–AuNS without analyte) and of the lactate accumulated from lactate solutions at concentrations of 1000, 10, and 0.1 μM (highlighted in yellow two characteristic peaks of lactate at 1127 and 1420 cm^{-1}). (ii) SERS spectra of the control (GG-SLH–Au@AgNR without analyte) and of the thiocyanate accumulated from solutions at concentrations of 10, 1 and 0.1 mM. Images reproduced with permission from the RSC [22]

different substrates by the use of a specially formed magnetic field applied to a diode sputtering target [20]. In order to expose the AuNPs of the films for biomolecule immobilization, the authors had to proceed with further plasma etching treatment, allowing the immobilization of an antibody monolayer that was detected by LSPR, and confirmed by confocal microscopy. These thin film composites allow nanoscale biomolecules real-time, label-free detection of proteins, and can be easily incorporated in microfluidic device arrays for cancer biomarker multiplex detection [21].

In another study, a new biocompatible surface-enhanced Raman scattering (SERS) hybrid material capable of lactate detection was reported (Fig. 10.3). This SERS-based 3D nanobiosensor was produced by embedding gold-based nanostructures into gellan gum “sponge-like” hydrogels. These 3D plasmonic polymeric matrices were able to detect two cancer-cell-related extracellular metabolites, lactate and thiocyanate, and provide stability to the embedded gold-based nanostructures. Due to their mechanical properties, these matrices can be easily

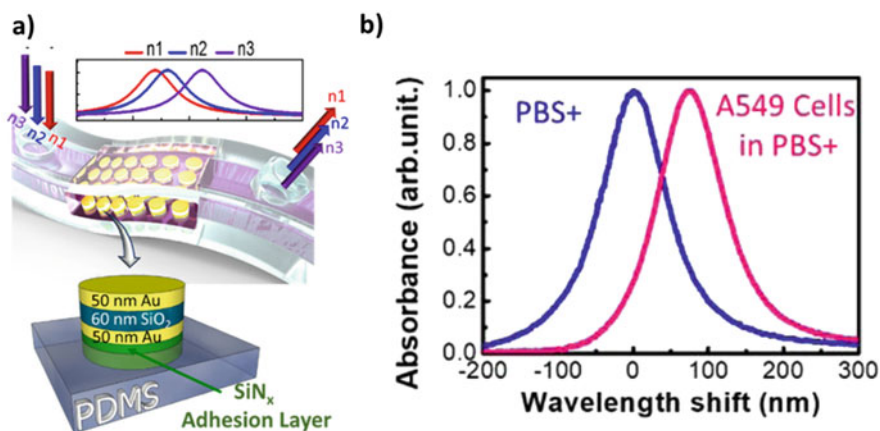


Fig. 10.4 (a) Schematic diagram of the flexible MIM-disk LSPR refractive index sensor integrated into a PDMS fluidic chamber. A single MIM disk on a PDMS substrate is also shown. The MIM structure contains a 50-nm-thick Au disk, a 60-nm-thick SiO₂ disk, a 50-nm-thick Au disk, and a 240-nm-thick SiN_x adhesion layer. (b) Absorption spectra of phosphate-buffered saline solutions with A549 cancer cells and phosphate-buffered saline solution without cells, as detected using MIM-disk LSPR biosensors. The wavelength shift of return-to-zero is based on the absorption spectra of the MIM-disk LSPR biosensors covered with a phosphate-buffered saline solution. Figure and legend reproduced with permission from Spring Nature [23].

deformed for microfluidic incorporation, and recover their shape and properties after 3 h. The production method of the matrices is cost-effective and they are also shelf-stable for 1 year, which are important features for POC diagnostic devices [22].

In a different approach, a flexible LSPR biosensor was reported for the detection of A549 lung cancer cells. This biosensor consisted of a tri-layer of metal–insulator–metal (MIM) nanodisks integrated with biocompatible polydimethylsiloxane (PDMS) substrate. The different geometries and arrangements of embedded nanodisks were studied and optimized to enhance the spatial overlap of the LSPR waves, achieving a sensitivity of 1500 nm/RIU. In addition, the LSPR biosensor was able to distinguish a solution containing PBS and another containing PBS plus A549 (Fig. 10.4). In the future, flexible on-chip microfluidic biosensors can be developed by integrating LSPR sensors on chips capable of having multiple parallel channels on nonflat surfaces [23].

10.2.2 Wearable devices

Wearable diagnostic technologies provide a closer monitoring of a patient's physiological conditions through minimal invasive measurements of biomarkers in biofluids, using devices that are in continuous contact with the human body. These technologies could significantly contribute to cancer early detection and treatment monitoring, since continuous, real-time monitoring can alert users and medical

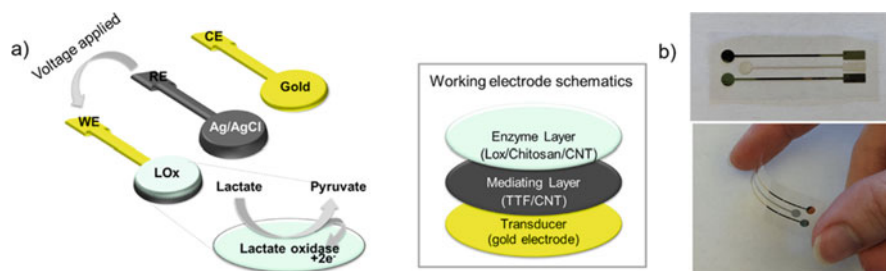


Fig. 10.5 (a) Schematic illustration of a three-electrode “NE” tattoo biosensor for electrochemical epidermal monitoring of lactate. (b) Constituents of the reagent layer of the working electrode which is coated by biocompatible polymer (chitosan). See the text for further details. Figure and legend reproduced with permission from Nature [29].

professionals for abnormal or unforeseen situations in high-risk or on-going treatment patients [24].

Wearable biosensors need to provide direct contact with the sampled biofluids without inducing discomfort to the wearer. Such body compliance can be achieved through the use of advanced materials and smart designs that provide the necessary flexibility and stretchability [25].

The development and commercialization of wearable sensors is more challenging than POC technologies since they need to ensure continuous on-body monitoring for long-duration measurements, on the contrary of POC technologies that provide cost-effective disposable cartridges for punctual measurements. These features interfere with biosensors performance, in particular with their reliability and reproducibility, since it is necessary to maintain the biorecognition elements activity, avoid sensor surface biofouling, overcome the inefficient transport of sample to the sensor surface, and perform complex multistep assays and receptor regeneration [26]. The calibration of on-body sensors is another important aspect of wearable biosensors which presents technical challenges. The long-term measurements also rely on power supplies and data storage processes that need to be miniaturized and integrated into the sensor, which adds complexity and technical challenges to wearable technologies [27]. Commercial wearable platforms perform glucose measurements either on skin through patches, and finger clip, and on eyes through contact lens that measure glucose in tears [28]. Nevertheless, there are still no commercial wearable technologies that monitor cancer biomarkers. Although several have been reported in literature, most of them aim to monitor physiology conditions of sweat and interstitial fluid on the skin, since skin is the largest organ of the human body, and it offers a diagnostic interface rich with vital biological signals from the inner organs, blood vessels, muscles, and dermis/epidermis [26].

A flexible printed temporary-transfer tattoo amperometric biosensor that conforms to the wearer’s skin was developed for lactate detection in sweat (Fig. 10.5). The biosensor showed chemical selectivity toward lactate with linearity up to 20 mM. This biosensor consisted of a printed tattoo made with three electrodes printed onto GORE-TEX textile to simulate the viscoelastic properties of the skin.

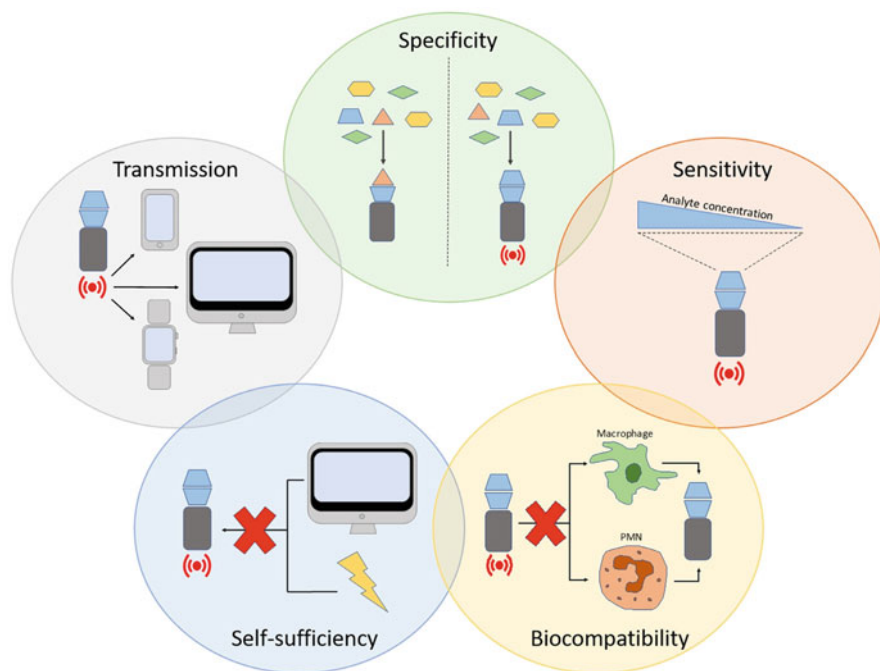


Fig. 10.6 Diagram showing the requirements of implantable biosensors. Figure reproduced with permission from Elsevier [30]

The working and carbon electrodes were made using carbon ink and the reference electrode was prepared with silver/silver chloride ink. The working electrode was set by tetrathiafulvalene (TTF) and multi-walled carbon nanotubes (CNT) functionalization followed by lactase oxidase that was covered by a biocompatible chitosan overlayer. The latter prevents the efflux of the biochemical backbone from the reagent layer onto the underlying epidermis [29].

Implementing a different electrode composition, Payne et al. (2019) also reported a flexible, amperometric sensor made from printed electrodes for lactate enzymatic detection on sweat (Fig. 10.6). However, this sensor uses printed gold as the working electrode and Ag/AgCl as reference electrode, and the electrodes were printed on plastic substrates. The working electrode was modified with chitosan and carbon nanotubes responsible for lactate oxidase (LOX) mediating layer, carbon nanotubes were dispersed in ethanol in the specified concentration. A mediator layer composed of TTF and carbon nanotubes was introduced below the enzyme layer to avoid interference from oxidation of other components of sweat. The optimized sensors show a linear range up to 24 mM lactate and sensitivity of 4.8 $\mu\text{A}/\text{mM}$ which normalizes to 68 $\mu\text{A cm}^{-2}/\text{mM}$ when accounting for the surface area of the sensor [29].

10.2.3 Implantable Devices

Recent innovations in fields like electronics, microfabrication, or nanotechnology led to an increased interest in the development of implantable biosensors. Implantable biosensors present a huge potential for early diagnostics and cancer monitoring, since they have the ability to continuously monitor target analytes and detect change in their levels from inside the human body, which should translate in real-time and accurate data, enabling the detection of physiological events right from the beginning. Therefore, although initially invasive, implantable biosensors would provide long-term sensitive monitoring of cancer development, revolutionizing the way we perceive diagnostics, and significantly contributing to mortality decrease and increment of patient's life quality.

However, fully developed implantable biosensors capable of monitoring and transmitting the data still remains a challenge. In order to achieve that, biosensors should possess some specific requirements (Fig. 10.6) [30, 31]. First, biosensors need to be biocompatible, so that their implantation does not promote any acute immune reaction of the body, which can damage device functionality. This usually happens due to the fibrous encapsulation of devices created by the body's human response. Secondly, biosensors should be specific, enabling monitoring of a specific target in the defined range within complex mixtures, like blood or interstitial fluid. Thirdly, they need to be sensitive, and therefore able to accurately quantify very low biomarkers amounts. Finally, they need to be power self-sufficient and able to transmit the data to the outside of the body. Conventional implantable biosensors usually use an external power source, which can be heavy and discomforting. Consequently, technologies like wireless powering have been used to improve powering methods in implantable biosensors [25, 32]. Wireless technology has also been used in data transmission, since traditional wires can easily be damaged and introduce noise in the data. Implantable biosensors should be able to monitor and remotely send data to an external device, like a computer or smartphone, in a meaningful and easy way for both patients and clinicians [25, 33].

In order to improve biocompatibility and decrease foreign body response, Gray et al. developed an implantable biosensor based on six materials (silicon dioxide, silicon nitride, Parylene-C, Nafion, biocompatible EPOTEK epoxy resin, and platinum) for monitoring the intra-tumoral O_2 and pH [34]. For that, the biocompatibility of the developed biosensor was evaluated up to 7 days post-implantation in a human breast cancer xenograft tumor (Fig. 10.7a). The immunochemistry results did not show the formation of biofouling, variations in tumor necrosis, hypoxic cell number, proliferation, or apoptosis.

In another study, with the intuition of achieving cancer early-stage detection and, consequently, improve survival rate, William et al. (2018) developed an implantable nanosensor able to detect, in a noninvasive way, HE4 (human epididymis protein 4), an ovarian cancer biomarker, and transmit data by near-infrared emission to an external detector. The nanosensor is composed of single-well carbon nanotubes, which present optical properties suitable for in vivo signal transduction. Authors

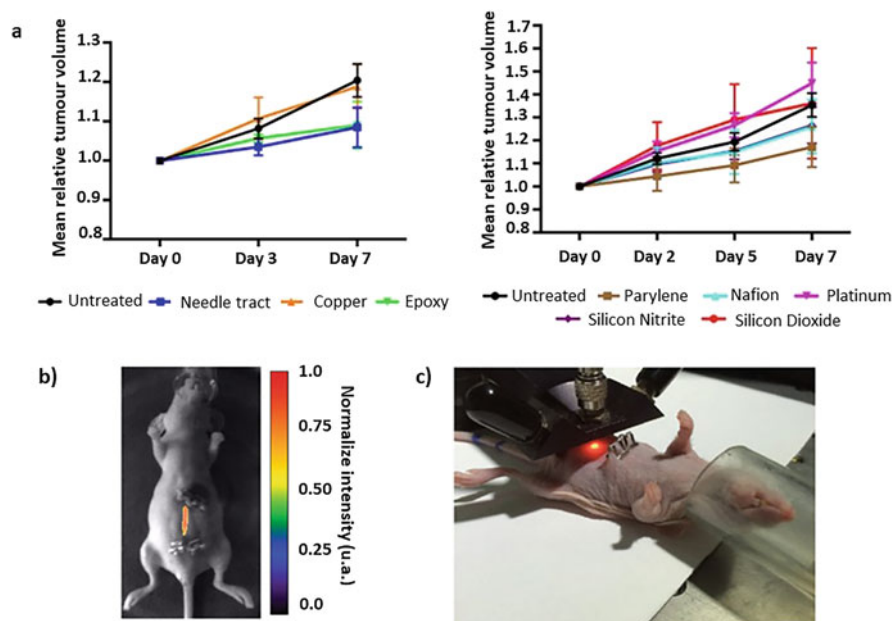


Fig. 10.7 (a) The effects of different biomaterials on mice tumour volumes; (b) near-infrared image of nanosensor emission from the implanted device and (c) photograph of typical data acquisition from the probe-based system used to excite/acquire near-infrared emission from the implanted sensor in mice. Figures reproduced with permission from Wiley and AAAS [34, 35].

implanted the nanosensor in mice, with an antibody for HE4 attached in the probe, and HE4 was detected and measured by photoluminescent methods (Fig. 10.7b, c) [35].

10.3 Limitations of Current Biosensor Approaches

Despite the enormous advances in biosensors for use in cancer diagnostics, their translation to the clinics in the near future is not expectable, since only, a few successful examples are already clinical trials (Table 10.1). Note that in the clinical trials it can only be found POC and wearable biosensors technologies, which implies implantable biosensors, although desirable, still have to overcome serious technological constraints to pass for the clinical trials phase of product development.

The reduced clinical use of cancer biosensors is due to several challenges that they need to overcome, some are specific to POC, wearable and implantable technologies, and some are common to all of these technologies [31, 37, 38]. Common challenges to all biosensors technologies are reliability, cost-effectiveness, and ability to multiplex. Reliability is probably the biggest challenge in biosensors, since it requires intensive study of their reproducibility, sensitivity, and long-term storage. Often, the complex body fluid compositions or non-specific binding can lead to

Table 10.1 Most relevant clinical trials on biosensors for cancer diagnosis [36]

NCT number	Date and status	Title	Comment
NCT02195076	2014–2017 Unknown	Non-Invasive Detection of Lung and Breast Cancer by Odor Signature	A system which uses biosensors that can scent the volatile compounds (VOCs) that lung and breast cancer cells produce, thus distinguishing between healthy control and lung or breast cancer
NCT02659358	2016–2017 Completed	Evaluating the Use of Wearable Biosensors and PROs to Assess Performance Status in Patients With Cancer	To evaluate the association between wearable biosensor data, performance status, and patient-reported outcomes in cancer patients
NCT03173729	2017–2022 Recruiting	Point of Care Test to Diagnosed Colorectal Cancer and Polyps in Low Middle Income Countries	To adapt a 3-metabolite biosensor that identifies patients with colorectal cancer (CRC) and precancerous polyps to Nigerian patients. To evaluate the POC biosensor device in Nigeria
NCT00813878	2001–2012 Terminated	Nipple Secretion Samples in Detecting Breast Cancer in Patients and Healthy Participants Undergoing Breast Cancer Screening, Breast Diagnostic Studies, or Treatment for Benign Breast Disease	Once the feasibility of the nipple blot assay has been determined, an optical biosensor will be developed to detect fluorescent-labeled antibodies directed against CEA found in serum and breast sections
NCT02957370	2015–2021 Recruiting	Molecular Biosensors for Detection of Bladder Cancer	To develop specific and sensitive detectors of biomarker-based signatures associated with diagnosed and recurrent bladder cancer
NCT04518072	2020–2023 Not yet recruiting	Synthetic Metabolic and Genetic Networks for Medical Diagnostics (SynBioDiag)	Develop a scalable, programmable biosensors platform for the multiplexed detection of biomarkers in clinical samples
NCT04260230	2020–2020 Not yet recruiting	Remote Monitoring of Patients at Risk of Sepsis (REACT)	To assess the feasibility of using remote wearable biosensors to record key physiological parameters and transmit this data
NCT03757182	2018–2020 Recruiting	Digitally-Captured Step Counts for Evaluating Performance Status in	To examine the relationships between objectively measured physical activity and provider-assessed and

(continued)

Table 10.1 (continued)

NCT number	Date and status	Title	Comment
		Advanced Cancer Patients (DigiSTEPS)	patient-reported functional outcomes in patients with advanced cancer
NCT03623945	2018–2022 Recruiting	Autoantibodies in Breast Cancer Detection (ABCD)	Collection of blood only to look at circulating autoantibodies that recognize breast cancer proteins to potentially be used as a biosensor for identifying patients with increased risk of having breast cancer
NCT00658658	2008–2015 Completed	Panitumumab in Children with Solid Tumors	To evaluate the safety and pharmacokinetics of up to 3 different dose schedules of panitumumab in pediatric patients with solid tumors
NCT00411450	2006–2010 Completed	Panitumumab Regimen Evaluation in Colorectal Cancer to Estimate Primary Response to Treatment (PRECEPT)	Use of biosensors for the detection of anti-panitumumab antibodies

signal fluctuations, which delay the use of the biosensor in clinics, since for that it is necessary to obtain reliable and quantitative detection results [37, 38]. Another challenge relies on cost-effectiveness of biosensor production, since most of the times biosensors are made for research prototypes without a proper up-scale plan, that contemplates cost, and mass-production manufacturing procedures. Additionally, multiplex is extremely important in cancer's diagnostics and treatment follow-up, since there is not a unique biomarker for cancer screening, which means there is a need to detect a combination of several biomarkers with different thresholds [16, 37, 38]. Finally, biocompatibility is for wearable and implantable technologies a major requirement, since properties like composition, size, shape, charge, among others, can trigger off the foreign body response and lead to an immune reaction of the patient and even damage the biosensor [31, 39].

Although most biosensors are produced in optimized laboratory conditions, there is a long way until they reach the clinics: animal testing and clinical trials [31, 40].

10.4 Conclusions and Future Perspectives

Cancer is a worldwide high rate mortality disease and its early detection and its continuous monitoring could significantly affect cancer's prognosis and treatment. This could be achieved by biosensing technologies able to continuously screen and monitor specific biomarkers at different clinical thresholds. There are mainly three

types of biosensors for cancer diagnostics depending on the local they are applied: POC, wearable, and implantable biosensors. POC technologies allow a quickly and accurately real-time biomarker monitoring. Through the use of portable POC biosensors, the cancer diagnostic process could be improved and patients could be given the most effective and efficient care when and where it is needed. However, limitations such as reliability, sensitivity, and reproducibility need to be overcome. Wearable and implantable biosensors foresee the biomarker detection directly in the human body, which provides a continuous and reliable real-time monitoring of physiological conditions. However, this drastically improves the complexity and technical challenges to the biosensing system, including self-power capability, foreign body response, and data transmission.

Despite the huge development in biosensors, clinical diagnostics still present several challenges that biosensors are not yet able to fulfill. Parameters like portability, precision, reproducibility, sensitivity, and biocompatibility still need to be improved before the biosensor's transition into clinics. Cancer early diagnosis and follow-up treatment could be significantly improved by the monitoring of cancer biomarkers, when biosensing technologies will be capable of meeting clinical demands.

Acknowledgments The authors would like to acknowledge the Portuguese Foundation for Science and Technology (FCT-Fundação para a Ciência e a Tecnologia) for financial support (PTDC/EMD-EMD/31590/2017 and PTDC/BTM-ORG/28168/2017).

References

1. Plummer M, de Martel C, Vignat J, Ferlay J, Bray F, Franceschi S (2016) Global burden of cancers attributable to infections in 2012: a synthetic analysis. *Lancet Glob Heal* 4:e609–e616. [https://doi.org/10.1016/S2214-109X\(16\)30143-7](https://doi.org/10.1016/S2214-109X(16)30143-7)
2. N.I. of H. (US), B.S.C. Study, Understanding Cancer (2007) <https://www.ncbi.nlm.nih.gov/books/NBK20362/>. Accessed 27 Oct 2020
3. Coleman MP, Forman D, Bryant H, Butler J, Rachet B, Maringe C, Nur U, Tracey E, Coory M, Hatcher J, McGahan CE, Turner D, Marrett L, Gjerstorff ML, Johannesen TB, Adolfsson J, Lambe M, Lawrence G, Meechan D, Morris EJ, Middleton R, Steward J, Richards MA (2011) Cancer survival in Australia, Canada, Denmark, Norway, Sweden, and the UK, 1995–2007 (the International Cancer Benchmarking Partnership): an analysis of population-based cancer registry data. *Lancet* 377:127–138. [https://doi.org/10.1016/S0140-6736\(10\)62231-3](https://doi.org/10.1016/S0140-6736(10)62231-3)
4. Hawkes N (2019) Cancer survival data emphasise importance of early diagnosis. *BMJ* 364:l408. <https://doi.org/10.1136/bmj.l408>
5. Wever EM, Draisma G, Heijnsdijk EAM, De Koning HJ (2011) How does early detection by screening affect disease progression?: Modeling estimated benefits in prostate cancer screening. *Med Decis Mak* 31:550–558. <https://doi.org/10.1177/0272989X10396717>
6. Rebelo R, Barbosa AI, Kundu SC, Reis RL, Correlo VM (2020) Biodetection and sensing for cancer diagnostics. In: Biomater 3D tumor model. Elsevier, pp 643–660. <https://doi.org/10.1016/b978-0-12-818128-7.00026-5>
7. Schneble EJ, Graham LJ, Shupe MP, Flynt FL, Banks KP, Kirkpatrick AD, Nissan A, Henry L, Stojadinovic A, Shumway NM, Peoples GE, Setlik RF (2014) Current approaches and challenges in early detection of breast cancer recurrence. *J Cancer* 5:281–290. <https://doi.org/10.7150/jca.8016>

8. Duffy MJ (2001) Clinical uses of tumor markers: a critical review. *Crit Rev Clin Lab Sci* 38: 225–262. <https://doi.org/10.1080/20014091084218>
9. Larrea E, Sole C, Manterola L, Goicoechea I, Armesto M, Arestin M, Caffarel MM, Araujo AM, Araiz M, Fernandez-Mercado M, Lawrie CH (2016) New concepts in cancer biomarkers: circulating miRNAs in liquid biopsies. *Int J Mol Sci* 17. <https://doi.org/10.3390/ijms17050627>
10. Gatenby RA, Gillies RJ (2004) Why do cancers have high aerobic glycolysis? *Nat Rev Cancer* 4:891–899. <https://doi.org/10.1038/nrc1478>
11. Chen M, Chen C, Shen Z, Zhang X, Chen Y, Lin F, Ma X, Zhuang C, Mao Y, Gan H, Chen P, Zong X, Wu R (2017) Extracellular pH is a biomarker enabling detection of breast cancer and liver cancer using CEST MRI. *Oncotarget* 8:45759–45767. <https://doi.org/10.18632/oncotarget.17404>
12. Estrella V, Chen T, Lloyd M, Wojtkowiak J, Cornell HH, Ibrahim-Hashim A, Bailey K, Balagurunathan Y, Rothberg JM, Sloane BF, Johnson J, Gatenby RA, Gillies RJ (2013) Acidity generated by the tumor microenvironment drives local invasion. *Cancer Res* 73:1524–1535. <https://doi.org/10.1158/0008-5472.CAN-12-2796>
13. Martínez-Zaguilán R, Seftor EA, Seftor RE, Chu YW, Gillies RJ, Hendrix MJ (1996) Acidic pH enhances the invasive behavior of human melanoma cells. *Clin Exp Metastasis* 14:176–186. <http://www.ncbi.nlm.nih.gov/pubmed/8605731>. Accessed 28 May 2019
14. Jung W, Han J, Choi JW, Ahn CH (2015) Point-of-care testing (POCT) diagnostic systems using microfluidic lab-on-a-chip technologies. *Microelectron Eng* 132:46–57. <https://doi.org/10.1016/j.mee.2014.09.024>
15. Chin CD, Linder V, Sia SK (2012) Commercialization of microfluidic point-of-care diagnostic devices. *Lab Chip*:2118–2134. <https://doi.org/10.1039/c2lc21204h>
16. Rebelo R, Barbosa A, Reis R, Correlo V (2020) Bio-detection and sensing for cancer diagnostics. In: Kundu S, Reis RL (eds) *Biomater. 3D tumor model*, 1st edn
17. Barbosa AI, Reis NM (2017) A critical insight into the development pipeline of microfluidic immunoassay devices for the sensitive quantitation of protein biomarkers at the point of care. *Analyst* 142:858–882. <https://doi.org/10.1039/c6an02445a>
18. Cui P, Wang S (2019) Application of microfluidic chip technology in pharmaceutical analysis: a review. *J Pharm Anal* 9:238–247. <https://doi.org/10.1016/j.jpha.2018.12.001>
19. Andryukov BG, Besednova NN, Romashko RV, Zaporozhets TS, Efimov TA (2020) Label-free biosensors for laboratory-based diagnostics of infections: current achievements and new trends. *Biosensors* 10:690041. <https://doi.org/10.3390/bios10020011>
20. Rodrigues MS, Costa D, Domingues RP, Apreutesei M, Pedrosa P, Martin N, Correlo VM, Reis RL, Alves E, Barradas NP, Sampaio P, Borges J, Vaz F (2018) Optimization of nanocomposite Au/TiO₂ thin films towards LSPR optical-sensing. *Appl Surf Sci* 438:74–83. <https://doi.org/10.1016/j.apsusc.2017.09.162>
21. Barbosa AI, Borges J, Meira DI, Costa D, Rodrigues MS, Rebelo R, Correlo VM, Vaz F, Reis RL (2019) Development of label-free plasmonic Au-TiO₂ thin film immunosensor devices. *Mater Sci Eng C* 100:424–432. <https://doi.org/10.1016/j.msec.2019.03.029>
22. Abalde-Cel S, Rebelo R, Wu L, Barbosa AI, Rodríguez-Lorenzo L, Krishna Kant RLR, Correlo VM, Diéguez L (2020) A SERS-based 3D nanobiosensor: towards cell metabolite monitoring. *Mater Adv* 1:1613–1621. <https://doi.org/10.1039/D0MA00163E>
23. Chang CY, Lin HT, Lai MS, Shieh TY, Peng CC, Shih MH, Tung YC (2018) Flexible localized surface plasmon resonance sensor with metal–insulator–metal nanodisks on PDMS substrate. *Sci Rep* 8:11812. <https://doi.org/10.1038/s41598-018-30180-8>
24. Darwish A, Hassanien AE (2011) Wearable and implantable wireless sensor network solutions for healthcare monitoring. *Sensors (Basel)* 11:5561–5595. <https://doi.org/10.3390/s110605561>
25. Rodrigues D, Barbosa AI, Rebelo R, Kwon IK, Reis RL, Correlo VM (2020) Skin-integrated wearable systems and implantable biosensors: a comprehensive review. *Biosensors* 10:79. <https://doi.org/10.3390/bios10070079>

26. Liu Y, Pharr M, Salvatore GA (2017) Lab-on-skin: a review of flexible and stretchable electronics for wearable health monitoring. *ACS Nano* 11:9614–9635. <https://doi.org/10.1021/acsnano.7b04898>
27. Heikenfeld J, Jajack A, Rogers J, Gutruf P, Tian L, Pan T, Li R, Khine M, Kim J, Wang J, Kim J (2018) Wearable sensors: modalities, challenges, and prospects. *Lab Chip* 18:217–248. <https://doi.org/10.1039/c7lc00914c>
28. Gonzales WV, Mobashsher AT, Abbosh A (2019) The progress of glucose monitoring—a review of invasive to minimally and non-invasive techniques, devices and sensors. *Sensors* 19. <https://doi.org/10.3390/s19040800>
29. Payne ME, Zamarayeva A, Pister VI, Yamamoto NAD, Arias AC (2019) Printed, flexible lactate sensors: design considerations before performing on-body measurements. *Sci Rep* 9: 13720. <https://doi.org/10.1038/s41598-019-49689-7>
30. Gray M, Meehan J, Ward C, Langdon SP, Kunkler IH, Murray A, Argyle D (2018) Implantable biosensors and their contribution to the future of precision medicine. *Vet J* 239:21–29. <https://doi.org/10.1016/j.tvjl.2018.07.011>
31. Rebelo R, Barbosa AI, Caballero D, Kwon IK, Oliveira JM, Kundu SC, Reis RL, Correlo VM (2019) 3D biosensors in advanced medical diagnostics of high mortality diseases. *Biosens Bioelectron* 130:20–39. <https://doi.org/10.1016/j.bios.2018.12.057>
32. Cadei A, Dionisi A, Sardini E, Serpelloni M (2014) Kinetic and thermal energy harvesters for implantable medical devices and biomedical autonomous sensors. *Meas Sci Technol* 25. <https://doi.org/10.1088/0957-0233/25/1/012003>
33. Cheung CC, Deyell MW (2018) Remote monitoring of cardiac implantable electronic devices. *Can J Cardiol* 34:941–944. <https://doi.org/10.1016/j.cjca.2018.01.003>
34. Gray ME, Meehan J, Blair EO, Ward C, Langdon SP, Morrison LR, Marland JRK, Tsiamis A, Kunkler IH, Murray A, Argyle D (2019) Biocompatibility of common implantable sensor materials in a tumor xenograft model. *J Biomed Mater Res Part B Appl Biomater* 107:1620–1633. <https://doi.org/10.1002/jbm.b.34254>
35. Williams RM, Lee C, Galassi TV, Harvey JD, Leicher R, Sirenko M, Dorso MA, Shah J, Olvera N, Dao F, Levine DA, Heller DA (2018) Noninvasive ovarian cancer biomarker detection via an optical nanosensor implant. *Sci Adv* 4(4):eaq1090
36. National Library of Medicine, Cancer Biosensors Clinical Trials (2021) <https://clinicaltrials.gov/ct2/results?cond=Cancer&term=biosensor&cntry=&state=&city=&dist=>
37. Zhang Y, Li M, Gao X, Chen Y, Liu T (2019) Nanotechnology in cancer diagnosis: progress, challenges and opportunities. *J Hematol Oncol* 12:137. <https://doi.org/10.1186/s13045-019-0833-3>
38. Ming M, Wei Y, Senthilkumaran B, Vigneshvar S, Sudhakumari CC, Prakash H (2016) Recent advances in biosensor technology for potential applications—an overview. *Front Bioeng Biotechnol* 4:3389–3311. <https://doi.org/10.3389/fbioe.2016.00011>
39. Soto RJ, Hall JR, Brown MD, Taylor JB, Schoenfish MH (2017) In vivo chemical sensors: role of biocompatibility on performance and utility. *Anal Chem* 89:276–299. <https://doi.org/10.1021/acs.analchem.6b04251>
40. Higson SPJ (2012) Introduction to biosensors. In: *Biosensors for medical applications*, pp xvii–xviii. <https://doi.org/10.1016/B978-1-84569-935-2.50016-4>



Flexible Sensing Systems for Cancer Diagnostics

11

Anne K. Brooks, Sudesna Chakravarty, and Vamsi K. Yadavalli

Abstract

Practical screening tools and ultrasensitive technologies can play pivotal roles in precision cancer profiling for early diagnosis at asymptomatic stages, as well as for monitoring prognosis, risk stratification, and disease recurrence. While a number of sensors and diagnostic tools continue to be developed for ultrasensitive detection and off-site analysis, there has been an increasing interest in point-of-care devices, particularly those that are mechanically flexible and potentially wearable by the patient. In this chapter, we present a critical insight into the integrated engineering approaches involved in such flexible systems. We consider various aspects in the design of flexible devices, the biomarkers of interest, and the different transduction mechanisms by which mechanically flexible devices can be used in the area of cancer monitoring. We then discuss the different types of flexible biosensing platforms that have been developed to date, including wearables on skin and on clothing, and exhaled breath and implantable sensors. Finally, we discuss the design challenges and future outlook in the development of flexible platforms that can provide comprehensive cancer biomarker panels for patients and clinicians.

Keywords

Biosensors · Wearable · Implantable · Cancer · Biomarkers · Flexible

Anne K. Brooks and Sudesna Chakravarty contributed equally with all other contributors.

A. K. Brooks · S. Chakravarty · V. K. Yadavalli (✉)
Department of Chemical and Life Science Engineering, Virginia Commonwealth University,
Richmond, VA, USA
e-mail: vyadavalli@vcu.edu

11.1 Introduction

Cancers are among the leading causes of mortality arising from noncommunicable diseases. Globally, there were over 19 million new cancer cases, with nearly 10 million fatalities in 2020 [1, 2]. Among the various forms of cancers, the highest mortalities have been associated with conditions affecting the respiratory system (lung), digestive system (stomach, pancreatic, colon, liver), prostate, and breast. High cancer mortality rates can be attributed to several causes, including the lack of timely interventions, and challenges associated with the inherent complexity and heterogeneity of cancers [3]. Current testing modalities and bioassays have been linked with issues of invasiveness, sampling errors, large sample volume requirements, and difficulties in obtaining real-time or continuous data. The high cost of imaging, and complications arising from surgical biopsies, particularly for inaccessible/deep tissue tumors, are among other factors that impede efficient cancer management from a detection, treatment, and recovery perspective [4].

Strategies toward reducing morbidity and mortality are focused on improving early-stage detection via non-invasive/minimally invasive routes, and developing efficient strategies to enable continuous monitoring of patients during and after treatment, to prevent cancer recurrence. It is now known that even individuals with similar cancer types may not respond to the same standards of treatments [5]. Developing scalable platforms for continuous and multiplexed biomarker detection and monitoring the efficacy of therapeutics, can therefore help in forming personalized strategies based on an individual's parameters [6]. While various sensing systems have been studied for the ultrasensitive detection of cancer related biomarkers in diverse formats (conventional assays and point-of-care (POC)) [7–9], mechanically flexible and wearable biosensors have the potential to provide a new paradigm in cancer care. This has been motivated by several factors including increased desire for portability, reducing complex protocols with long assay times, and cost-effectiveness [10, 11]. The ability to obtain high sensitivity, rapid response, small footprint, and multiplexed sensing capabilities makes them suitable for ambulatory usage, with both disease diagnosis and continuous monitoring. Development of such flexible and wearable sensors can lead to enhanced personal monitoring of conditions (often remotely), while potentially enabling implantable systems for the integrated monitoring and treatment of cancers *in vivo*.

In this chapter, we discuss some of the developments and design considerations for the fabrication of flexible platforms used in cancer diagnostics and therapies. The challenges and solutions associated in translating such prototypes to real systems will also be discussed. The reader may note that this is currently a nascent, albeit fast developing field, with a number of devices geared for the consumer market. Several flexible systems have been reported that are usable for a host of healthcare applications [12–15]. We will therefore endeavor to limit our discussion to devices that are either specifically designed for use in cancer biodiagnostics, or those that share vital features that enable them to be adaptable for improving the lives of cancer patients worldwide.

11.2 The Need for Flexible Biosensors in Cancer Detection and Monitoring

At the outset, we consider some of the key driving forces for flexible and wearable systems in cancer detection and monitoring. There is an increased emphasis in healthcare toward patient-centered prevention and early detection of diseases and monitoring of chronic conditions [16]. Rapid, cost-effective, and minimally invasive/non-invasive strategies that can enable monitoring at the bed-side or in a portable fashion, characterize POC devices. These systems have utilized advances in miniaturization such as microfluidics, sample handling, and microelectronics to obtain data in a portable format. They are designed to provide rapid, accurate analysis and often, continuous or automated data via small-footprint devices that may be handheld, or easily transportable. Thus, there is no need for complex sample collection and dispatch to laboratories for testing [17, 18]. Patient samples are used to obtain the parameter of interest—directly and often instantaneously at the site of collection, spurring patient-oriented disease management, reducing the frequency of clinical visits, and providing personalized on-demand interventions [15]. Several POC devices have been demonstrated for the monitoring of targets from biofluids (e.g., blood, urine, saliva). The complex heterogeneity of cancers and the need for personalized treatments therefore, provide the primary motivations to develop and adapt such systems for this aspect of healthcare.

Wearable devices form a subset of POC systems that are designed to be worn on (or positioned within) the physical person [19, 20]. While flexible devices are often designed to be wearable, many currently wearable devices are not necessarily mechanically flexible, providing operation in rigid formats. Thus, flexible systems work on, or inside the body, while conforming to the contours of the body (or clothing) to obtain parameters of interest in a continuous or semi-continuous fashion from an often-ambulatory target (Fig. 11.1). To date, technologies have been developed and even commercialized to monitor diverse physiological parameters, including heart rate, respiration, blood pressure, and locomotion. Sensors have been integrated into everyday wearables such as clothing, footwear, wrist bands, wound dressings, and even tattoos, allowing individuals to continuously monitor physiological signals on-the-go, without the need for expensive equipment or trained professionals. The use of soft, stretchable, and flexible systems is envisioned to further aid in improving human–machine interfaces, as sensors, implantable devices, and theranostics [21, 22].

The early detection of cancers at asymptomatic stages and the monitoring of therapies for patients are examples of areas where flexible platforms can play a pivotal role. Mechanically flexible systems are of interest for on-body diagnostics. Flexible devices are designed to be small, low weight, and portable, making them easy to use in a clinical or outpatient setting, often directly by the end-users themselves. Such devices can intrinsically conform to irregular curvatures, which could include external surfaces such as skin, or internal surfaces such as soft tissues, or even tumors. They are envisioned to directly interface with the target areas, giving them increased sensing capacity and signal transduction compared to other POC

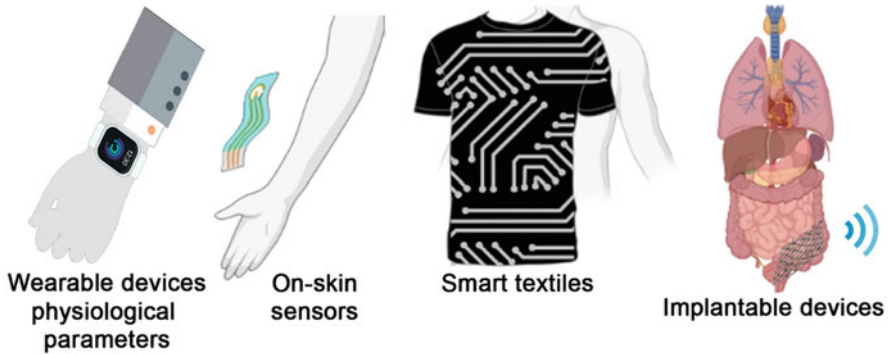


Fig. 11.1 Formats of flexible sensing platforms—wearable devices for monitoring biophysical parameters (e.g., motion, heart rate), bandage-type or tattoo sensors on skin, smart textiles for non-invasive monitoring, and implantable devices that can be placed temporarily or permanently within the body. Wireless transmission of data from implantable devices provides a route for non-invasive data handling

systems. This increases the detection threshold of a given biomarker, and higher sensitivity. Given that many are often thin films, they also could allow for monitoring over an entire surface instead of collecting data at selected points. Thin films also take less material to produce and lead to less waste after use, giving them commercial and ecological advantages over rigid electronic POC systems that are often produced using conventional silicon microelectronics. Small on-body biosensors that are capable of instantaneous and accurate results are desirable, as there is ideally no time lapse between sample preparation, analysis, and the delivery of results to the clinician and patient. Conformable and flexible (bio)sensors can reduce physical discomfort to patients requiring continuous monitoring, while reducing cost per analysis, and providing opportunities for home-based monitoring. The flexible biosensors with potential in cancer management can include a diverse range of integrated medical devices—from smart needles and on skin-wearables to monitor UV exposure, to implantable sensors to monitor tumors. Overall, the benefits include a reduction in the healthcare burden, and an increase in the patient survival rate.

11.3 Target Biomarkers of Interest

Biomarkers are defined as measurable biological indicators of a physiological condition, such as a disease. These can include a variety of types of molecules, such as nucleic acids, proteins, oncogenes or tumor suppressor hormones, metabolites, enzymes, and antibodies [8, 23]. Biomarkers are typically detected in human tissues as well as in biofluids such as blood, serum, urine, or cerebral spinal fluid (Fig. 11.2). While diagnostic biomarkers correspond to detection, prognostic biomarkers help predict outcome and recurrence, and predictive biomarkers estimate responsiveness to treatment [24]. In cancers, some biomarkers may undergo

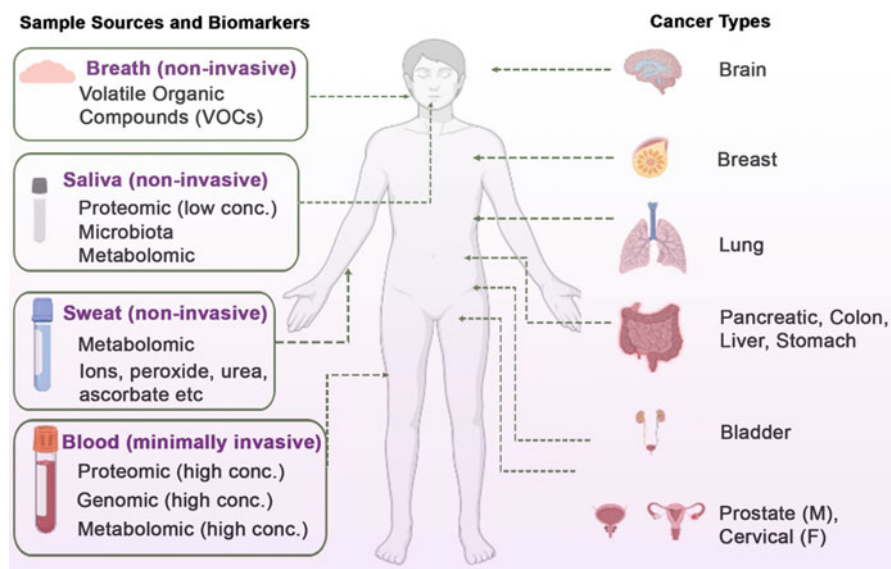


Fig. 11.2 Cancer types and sample source of biomarkers having clinical utility that can be applied to wearable and implantable systems. Biomarkers within the same subtype or across the various subtypes can be used to develop comprehensive biomarker panels for the design of multiplexed flexible assays (“M”—“Male,” “F”—“Female”)

alterations even when phenotypic tumor changes are not observed. Additionally, physically observing changes in tissue and tumors can be invasive, costly, and prone to error and oversight. This makes the analysis of a quantitative biomarker profile useful in the detection of emerging cancer, monitoring progression, and determination of treatment effectiveness. The biomarkers of interest change with different types and stages of cancer making such analysis challenging. We further note that many biomarkers are not easy to adapt to flexible or even POC systems, still requiring off-site assays. In this section, we discuss some types of biomarkers that have been particularly interesting from the perspective of developing flexible systems for cancer. This list is not meant to be exhaustive and the reader is referred to other chapters or references for the various cancer relevant biomarkers [3, 25].

11.3.1 Proteomic Biomarkers

The onset and progression of cancer can be characterized by the changes in numerous proteins within biofluids or tissues. These proteins can play a vital role in the management of cancer. Few important proteomic biomarkers of clinical relevance include Breast (BRCA1, BRCA2, CA 15-3, CA 125, CA 27.29, CEA, NY-BR-1, ING-1, HER2/NEU, ER/PR), Colon (CEA, EGF, p53), Esophageal (SCC), Liver (CEA, AFP), Lung (CEA, CA 19-9, SCC, NSE, NY-ESO-1), Melanoma

(Tyrosinase, NY-ESO-1), Ovarian (CA 125, HCG, p53, CEA, CA 549, CASA, CA 19-9, CA 15-3, MCA, MOV-1, TAG72), Prostate (PSA) [26]. Various systems have been developed targeting one or more of the biomarkers from this list using body fluids such as serum or plasma as the samples of interest.

11.3.2 Genomic Biomarkers

Tumors can acquire mutations through a variety of pathways including changes to the base sequence of DNA (point mutations, deletion or amplification, malfunction of repair genes) or changes in methylation of DNA bases in promoter regions that alter subsequent processes of signal transduction, growth, DNA repair, and apoptosis [27]. Monitoring such genes can shed vital information regarding the onset and progression of cancer. Examples of some important genomic biomarkers of clinical utility for cancer include miRNA-21, miRNA-122, miRNA-223, p53, p62, and circulatory biomarkers (ctDNA, miRNA) [28].

11.3.3 VOC Biomarkers

Cancers associated with the respiratory system such as lung cancer are normally detected at later stages leading to low survival rates. Cancers of the lung are usually accompanied by an increase in oxidative stress leading to the generation of volatile organic compounds (VOCs). VOC biomarkers that can play vital roles in the early detection of such cancers include saturated and unsaturated hydrocarbons, and sulfur containing compounds. Sensors placed in the mouth, or which can measure the VOCs using handheld devices focus on such targets. Other non-volatile compounds can be measured in samples such as exhaled breath condensate as useful indicators for disease [29–31].

11.3.4 Metabolomic Markers

A variety of metabolic pathways are reprogrammed in cancer. For example, the Warburg effect describes changes in glycolysis, wherein cancer cells take up glucose and produce lactate. Changes in amino acid, fatty acid, and cholesterol metabolism are also common. H_2O_2 is another biomarker of interest, as cancer cells secrete larger amounts of H_2O_2 due to their rapid uncontrolled growth. Thus, metabolomic biomarkers such as acetaminophen, uric acid, ascorbic acid, dopamine, and H_2O_2 can contribute to the field of cancer detection and therapy [32, 33].

11.4 Characteristic Properties of Flexible Biosensors for Cancer Diagnostics

In this section, we discuss a few of the salient features of the flexible devices that are pertinent to cancer diagnostics. As discussed above, flexible devices for monitoring physiological parameters typically comprise mechanically compliant supporting substrates with sensing regions that can maintain their function even under physical motion or deformation. In comparison to their rigid counterparts, flexible sensors are typically designed to be functional at non-planar, soft, and non-stationary interfaces. They are designed for continuous or real-time monitoring, which enables operation directly at sites of interest, and without interrupting the normal activities of the wearer. Such systems therefore have the potential to be patient friendly, with a high cost-effectiveness and speed of detection and often, continuous monitoring.

11.4.1 Design Considerations

(Bio)sensors (in both rigid and flexible platforms) are used for the detection and sensitive quantification of specific biomarkers in clinical diagnosis. This can permit evaluation of regular biological and pathological activities, or responses to therapeutic interventions [34–36]. While POC sensors have focused on translating conventional bioassays to miniaturized and portable formats, with easy readouts and reduced sample requirements, flexible sensors are relatively in their infancy. To date, many flexible and wearable sensors have focused on the measurement of *biophysical* parameters such as temperature, pH, heart rate, pressure, motion, etc. [19, 37, 38]. The use of UV monitoring for assessing skin cancer risk is an interesting example of a sensor target that falls outside these boundaries. Such wearable devices can monitor an external parameter (solar exposure) during outdoor activities [39, 40]. Recently, small molecule targets such as ions, glucose, cortisol, and dopamine have been addressed [41, 42]. For various applications in cancer, often multiplexed detection of larger and more complex targets is needed. Examples of such targets and devices are discussed in other sections. Often a broader panel of biomarkers is sought, which necessitates a multi-omics approach featuring similar type biomarkers (e.g., proteomic or genomic) or combinatory biomarkers (proteomic, genomic, metabolic VOCs). Together with the choice of location of the sensors and the target biofluids, the nature of the information sought (e.g., qualitative (yes/no answers) or quantitative (specific concentration)) comprises factors that can determine the design considerations for cancer screening, diagnosis, prognosis, risk stratification, and recurrence monitoring.

Sensors are often designed in terms of accessibility to biomarkers, which can be found in various body fluids at different concentrations. This includes whole blood (typically high biomarker concentrations) or saliva, sweat, urine, and ascites (typically low biomarker concentrations). VOCs in exhaled breath may also act as biomarkers primarily for cancers associated with respiratory systems. The choice of biofluids in turn, dictates the invasiveness of the sensor ranging from non-invasive

sensors (e.g., sweat) to minimally invasive (e.g., blood) or invasive (e.g., subcutaneous or implanted). Though the sampling in biofluids such as sweat, saliva, etc., is easier, the biomarker concentration in such biofluids can be 10-fold lower than that found in blood/serum samples [17]. Therefore, typical sensor issues such as sensitivity, response time, selectivity, reproducibility, and stability are magnified. Based on the biofluid chosen, the location dictates the design vis a vis the interfacing of the sensor with target tissues or fluids. These issues are compounded in the development of multiplexed sensors for the simultaneous detection of many targets on the same platform [17]. There is often a need for enhancement of detection specificity in complex biofluids via the incorporation of antifouling materials and response time acceleration. Multiple biomarkers are often needed for a conclusive outcome in terms of comprehensive profile within a short time frame, which can restrict the development of integrated platforms together with the utilization of minimally invasive/non-invasive sampling approaches.

11.4.2 Material Selection

Depending on their intended application and site of use, material selection may be guided by factors such as mechanical flexibility and/or stretchability, optical transparency, adhesion, hydrophilicity, selective permeability, and biocompatibility [43]. The choice of materials varies depending on the desired properties of both the substrate and the active components, which include functional elements such as conductive electrodes, biomolecules, filters, etc. Conformation with the target area, incorporation of antifouling materials, materials as well as novel engineering approaches are important for reliable performance. Devices must be mechanically strong and durable, yet able to undergo deformations to match the body's motions, or even exhibit self-healing properties [44]. They should ideally match the mechanical stiffness of native tissue, and adhere to soft and wet surfaces. Intrinsically soft materials have been considered for flexible devices, requiring less material modification [45]. However, rigid materials can also be used if fabricated as ultrathin films, altered through shape changes, such as cuts or buckled architecture, or via the inclusion of micro- or nanoarchitectures to impart flexibility [46]. Flexible and biocompatible devices are also of interest for on-body applications, which include considerations such as conformation to wet and soft tissue, and skin curvature. Synthetic, nature-derived, and hybrid materials have found use in flexible electronics, each having their own advantages and disadvantages.

11.4.2.1 Synthetic Materials

Among the most widely used materials in flexible systems are synthetic polymers such as polyethylene terephthalate (PET), polydimethylsiloxane (PDMS), and polyimide (PI) [47]. These are commercially available, while offering benefits such as easy processability, chemical and biological inertness, and thermal stability. Polymers can be easily molded, pressed, or cast into mechanically robust, ultrathin, optically transparent configurations. Active components have typically utilized soft

conductors such as metal nanoparticles and nanowires in inks, conductive polymers such as PEDOT:PSS and PANI, and metal hybrid materials involving carbon and polymers [45]. While incredibly stable, these films are usually not biodegradable, necessitating surgical removal for internal applications, or contributing to non-degradable medical waste. Given the wide interest in developing sensors for cancer, different substrates for the same target have been reported. For instance, biosensors for the human papillomavirus (HPV) responsible for clinical conditions including cervical carcinoma have included pencil graphite surfaces, paper, screen-printed carbon, and interdigitated platinum electrodes [48–50].

11.4.2.2 Nature-Derived and Bioinspired Materials

Nature-derived materials have emerged as attractive alternatives for the development of flexible systems owing to advantages including biocompatibility, biodegradability, and environmental sustainability. Biological materials exploited include proteins, polysaccharides, and specialty materials such as pigments [51]. Salient advantages include transparency, ductility, low weight, high flexibility, and low cost [52]. Commonly used proteins include silk, keratin, and collagen/gelatin. Silk fibroin shows promise in terms of biodegradability, biocompatibility, mechanical robustness, adjustable water solubility, ease of processing, and light weight [53, 54]. Keratin's mechanical strength and durability have made it an ideal substrate [55]. Collagen and its derivative, gelatin, are among the most abundant proteins on earth, and can be processed in different ways to confer different material properties [56]. Polysaccharides include cellulose, chitin, as well as seaweed-based alginate and agarose, and plant-derived starch. Paper, consisting of processed cellulose, is inexpensive and widely available and lightweight. It is thin and porous, making it easy to form composites or incorporate inks through screen printing or inkjet printing. However, its fragility and low stability in wet environments limit its use [57]. Chitin and its partially deacetylated form chitosan have properties such as biodegradability, biocompatibility, antimicrobial properties, and low immunogenicity that have made them ideal for biomedical applications [58]. Naturally derived pigments such as melanin (e.g., derived from squid) and indigo (plant derived) have also found interest owing to unique physical and electrochemical properties [59].

Examples of a few systems and the materials utilized in the substrates therein, are presented in Table 11.1.

Various fabrication technologies have been employed for development of platforms for bioassays. These are dictated by the material choice, feature sizes, and manufacturability, among numerous considerations. Fabrication technologies such as micromolding, photolithography, digital laser processing, etc., enable the fabrication of thin films, fibers, and gels with micro- and nano-scale features [12, 103]. Even if the active devices themselves are thin, soft, or biologically interfaced, external connections to power sources and microelectronics such as data processors and transmission must often be considered in their development. Recent advances in low power wireless technologies such as near-field communications (NFC) or radio frequency identification (RFID), integrated with wireless sensor networks (WSNs) are providing new modalities in data collection

Table 11.1 Examples of different flexible material substrates, sensor configurations and their corresponding cancer biomarkers

Type	Material	Configuration	Biomarker type/cells	Reference	
Synthetic	PDMS	Film	Proteomic	[60]	
	PET	Film	Proteomic, metabolomic, VOCs	[50, 61–64]	
	PMMA	Film	Proteomic, genomic	[65, 66]	
	Polyimide	Film		Proteomic, genomic	[67–69]
		Film wrapped around needle		Various metabolites	[70]
		Layer on carbon electrode		Proteomic	[71–73]
	PVC	Graphene sensor on PVC film	VOCs	[74]	
	Poly (vinylidene fluoride) (PVDF)	Film	Proteomic	[75]	
	Polycarbonate	Film with gold nanobumps	Tumor marker (proteomic)	[76]	
	ITO	Electrode coated in polydopamine	Proteomic	[77]	
		Black phosphorous nanosheets, MOF	Circulatory biomarker (exosomes)	[78]	
	Glass	Sheet with Au electrodes	Proteomic	[79, 80]	
	Optical fiber	Fiber	Proteomic, Endomicroscopy	[81]	
	Carbon	Cloth		Human breast cancer cells (MCF-7) and lung cancer cells (A549)]	[82]
Glassy carbon electrode with conductive layer			CA 19-9, DNA methylation	[83–85]	
Carbon fiber wrapped in conductive material			Metabolite	[86]	
Metal	Gold film/electrode		Proteomic, VOCs, metabolomic	[87–90]	
	Nanowires		Genomic, metabolomic	[91]	
	Cu substrate coated in PPy film		Proteomic	[92]	
PPy	Sandwich film		Proteomic	[93]	
Natural	Chitosan	Film with MWCNTs	Proteomic	[94]	
	Silk	Fiber	pH	[95]	
		Film	Proteomic	[96]	
	Cellulose	Sheet	MCF-7, proteomic	[97–99], [100, 101]	
	Textile	Cloth	Breast tissue imaging	[102]	

and transmission [104]. Device end of life must also be considered; for some applications, it is desired that devices are stable for long-term use while ultimately being biodegradable, as to not contribute to e-waste, while for other applications, it is desired that devices are bioresorbable after short-term use. Degradability includes all parts of a device, such as the substrate, active components, and external connections, all of which depend on the materials of construction [105].

11.5 Sensing Strategies Pertinent to Flexible Devices

Biosensors combine a biological component with a physiochemical transducer to produce a signal quantifying a biological or chemical process [106]. A typical biosensor includes a biorecognition element, a transducer to convert the recognition event into a signal, and a signal processing system to provide the user with a quantitative descriptor of the interaction. There are primarily two approaches for biomarker detection—label-free and labeled. Label-free sensors are able to directly quantify the analyte, while labeled sensors require a recognition element for detection and/or signal amplification [107]. The biorecognition element is usually a macromolecule that interacts with an analyte, the target molecule of interest. This may be an enzyme, aptamer, antibody, oligonucleotide, polysaccharide, cellular structure, etc. The biorecognition element is typically immobilized on a substrate, or physically entrapped in a matrix to facilitate interaction with the target, usually from a biofluid (e.g., blood, serum, sweat, saliva, etc.). Of specific interest for cancer sensing are immunosensors (protein biomarker detection using antigen–antibody interactions), aptasensors (aptamer-based biomarker detection), and genosensors (genomic biomarker detection). It is worth noting that while a number of biomarker sensing strategies have been developed, only a subset of them are transferrable to flexible platforms. This is primarily dictated by the ability for the sampling, transduction, and processing elements to be miniaturized and/or portable. Electrochemical, optical, and transistor-type analytical transduction systems have been adapted to flexible platforms. In this section, we briefly discuss sensing strategies pertaining to flexible cancer biosensors. For a broader discussion on biosensors and various transduction, the reader is referred to a number of excellent reviews on the topic [108, 109].

11.5.1 Electrochemical Sensors

Flexible electrochemical sensing strategy utilizes changes in various electrical parameters for the rapid and timely detection of analytes. Such a strategy holds numerous advantages in personalized cancer therapy owing to its cost-effectiveness, potential for miniaturization (that can be integrated with microfluidics), ease of interfacing with human skin/fabrics due to high conformability, high sensitivity, high selectivity, and in situ monitoring of health condition [110]. Furthermore, such systems can be integrated with smartphones or wireless technologies [111]. This

enables continuous/non-invasive/minimally invasive monitoring of clinically important biomarkers in biofluids by physicians in remote settings [112]. Techniques such as Cyclic Voltammetry (CV), Chronoamperometry, Square Wave Voltammetry (SWV), Electrochemical Impedance Spectroscopy (EIS), and Differential Pulse Voltammetry (DPV) have been employed for proteomic and genomic cancer biomarker detection and quantification [10, 113, 114].

A flexible amperometric sensor based on MnO_2 -nanowires (NWs) on gold nanoparticle modified graphene fibers was employed for the quantification of hydrogen peroxide (H_2O_2) released from live human breast cancer cells with high sensitivity and selectivity [91]. The flexible format allowed for mechanical stability under a variety of deformations without affecting performance. Similarly, a flexible amperometric sensor for H_2O_2 secreted from cancer cells (human breast cancer cells (MCF-7) and lung cancer cells (A549)) in situ was reported. The sensor-carbon cloth supported NiCo-DH/AuPt micro-nano arrays, and exhibited good analytical performance with a limit of detection of $0.145 \mu\text{M}$ and a wide linear range $10 \mu\text{M}$ to 22.08 mM . Woven carbon fibers enabled high surface area for surface modification and cell attachment [82]. A flavin adenine dinucleotide (FAD) immobilized $\text{Ti}_3\text{C}_2\text{T}_x$ flexible electrode was developed for H_2O_2 detection in ovarian cancer cell lines (OVCAR-5 and SKOV-3 cell lines) using CV. It showed good analytical performance for H_2O_2 detection with $0.125 \mu\text{A nM/cm}^2$ sensitivity and a limit of detection of 0.7 nM [115]. A flexible electrochemical sensor composed of gold nanoparticles and polypyrrole (PPy) deposited on polyethylene terephthalate (PET) polymer strip coated with indium tin oxide (ITO) was developed for specific detection of HPV, which has importance in cervical cancer—over 90% of cervical cancer cases can be prevented via early detection of HPV. The electrochemical detection of the HPV16 gene was carried out using CV, and was found to be highly selective, specific, and sensitive (LOD $0.89 \text{ pg}/\mu\text{L}$, LOQ $2.70 \text{ pg}/\mu\text{L}$). The flexible conducting film was conducive to nanoparticle electrosynthesis, with improved electrochemical properties and high surface area compared to rigid alternatives [50]. A flexible, fully organic, biodegradable, label-free impedimetric biosensor for the biomarker, vascular endothelial growth factor (VEGF) was shown on a silk substrate. The biosensor was constructed by photolithographically patterning a conducting ink consisting of a photoreactive silk protein coupled with a conducting polymer and could be interfaced with soft tissue. Electrochemical impedance spectroscopy (EIS) was used to detect low concentrations of VEGF in various fluids (buffer, human serum, and simulated urine, with and without albumin), as well as under conditions of bending [96].

11.5.2 Optical Sensors

Optical biosensors utilize light for the transduction of the recognition event into a signal. Over the years, various types of optical sensing strategies have been used in the field of cancer such as fluorescence, Surface Plasmon Resonance (SPR), Surface Enhanced Raman Scattering (SERS), and optical fibers [116, 117]. While some

optical devices are constrained by size, the portability and non-invasive nature of light is promising for use in *ex vivo*, *in vivo*, and *in vitro* cancer applications. One of the first examples in this regard was a flexible gallium nitride (GaN) light-emitting diode (LED) fabricated on a liquid crystal polymer (LCP) substrate. A water-resistant and biocompatible polytetrafluoroethylene (PTFE) coated flexible white light-emitting phosphor-coated GaN LED was used to detect prostate-specific antigen (PSA). The bending radius and fatigue tests demonstrated the mechanically and optically stable characteristics of the GaN LEDs on the flexible substrates [118].

Magnetically propelled nanomotors have been used for fluorescence-based detection of genomic cancer biomarkers. Au-Ni nanowires as nanomotors were fabricated using a combined electrochemical approach for the preparation of Au with DC magnetron sputtering of the Ni segment. The nanomotors were then modified with a ssDNA as capture probe for the selective and sensitive detection of miRNA-21 (a potential biomarker for colorectal, breast, prostate, lung, pancreatic, and gastric cancers) with a limit of detection of 2.9 pM [119]. A flexible fluorescence sensor based on graphene oxide-modified microfluidic paper was also reported for cancer specific cells such as MCF-7 (Linear range— $180-8 \times 10^7$), K562 ($210-7 \times 10^7$), and HL-60 ($200-7 \times 10^7$ cells mL⁻¹) [120]. In another work, a silk fibroin-coated silica exposed core fiber (ECF) sensor for *in vivo* pH sensing in a mouse model of hypoxia was shown [95]. Such pH sensing enables continuous monitoring of acidity levels in the body, potentially aiding in cancer management.

Exosome detection plays an important role in early-stage cancer detection. Thin silver film coated nanobowl SERS substrates are used to capture exosomes in solution for the biochemical analysis of intact and ruptured exosomes. The active surfaces are fabricated via soft lithography on flexible PDMS substrates on which a thin layer of silver is sputtered [121]. Such encoded exosomes can provide quantitative pH sensing of the intracellular tumor microenvironment which in turn, has implications for intracellular imaging/cancer therapy. The flexibility of the system offers potential for intracellular applications, particularly in advanced stages of cancer. In another work, a flexible nanosilica-integrated PDMS polymer coated interdigitated sensor was fabricated for an endothelial growth factor (EGFR) mutation which accounts for 85% non-small cell lung cancer cases. Here, the PDMS provides a flexible interface for the EGFR mutation detection. The sensor exhibited a limit of detection of 1 aM complementary mutant target [122]. A flexible optical fiber-based surface plasmon resonance was reported for HER 2 biomarker detection with a limit of detection of 10 ng/mL [81]. Probe based endomicroscopy plays a vital role in early-stage *in vivo* detection of cancers associated with GI tract such as gastric, lung, and stomach cancer. A flexible endomicroscope was developed based on fiber Bragg grating sensing for intraoperative gastric endomicroscopy. The sensor was able to perform fast scanning of the target surface (4.4 mm²) in 1 min, demonstrating a high efficiency compared to traditional imaging techniques [123]. Optical techniques can be envisioned to be translated to wearables as shown in Fig. 11.3. Hybridization events of miRNA and other oligonucleotides transiently and *in vivo* could be detected via spectral changes of carbon nanotube photoluminescence. The sensor enables multiplexed detection using different

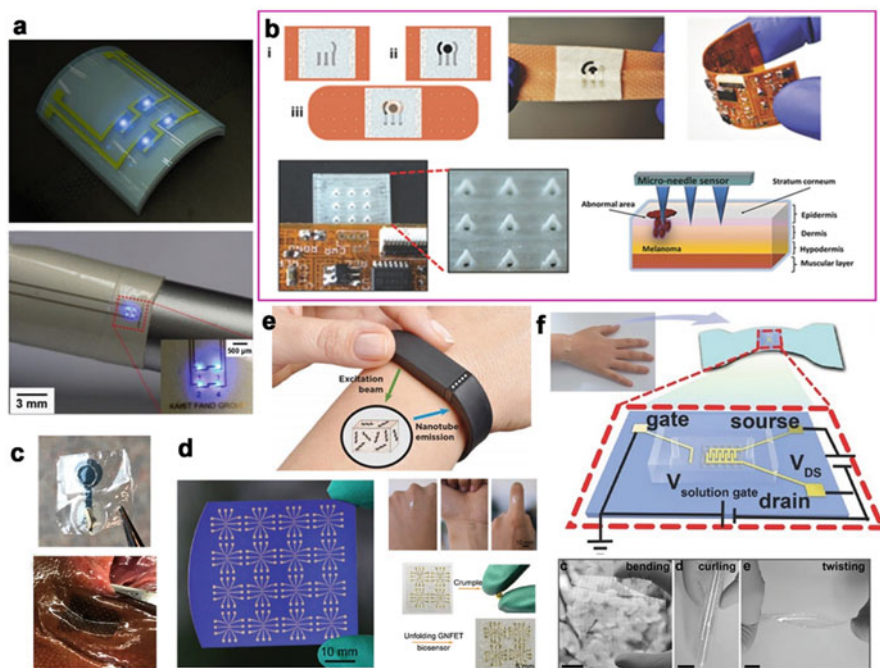


Fig. 11.3 Various sensing modalities in flexible cancer sensors—(a) Optical sensor based on flexible 2×2 GaN LED arrays (each $100 \times 100 \mu\text{m}^2$) on a plastic substrate. The inset indicates electrodes (Au) and active GaN LED devices used to detect PSA [118]. (b) Integrated bandage sensor for epidermal TYR monitoring for melanoma screening. (1) insulator, Ag/AgCl, (2) carbon printing, and (3) casting of agarose gel. The bending and flexibility of wearable bandage sensor and electronic board. The amperometric data is wirelessly transmitted to a smart device. A microneedle sensor is integrated to the soft flexible electronics for transdermal detection of the TYR melanoma biomarker [126]. (c) A flexible silk protein biosensor for impedimetric detection of VEGF. The sensor electrodes are 2–3 μm thick and can be conformable to soft tissue for potentially in situ detection of biomarkers at tissue interfaces [96]. (d) A graphene–Nafion field-effect transistor (GNFET) biosensor for cytokine biomarker detection. Images of the flexible biosensor conformably mounted on the human hand with the ability to be crumpled [125]. (e) Hybridization events of miRNA and other oligonucleotides for urinary bladder cancer or urothelial carcinoma can be detected via spectral changes of carbon nanotube photoluminescence. This can be envisioned as a wearable device that records the emission in response to an excitation signal [134]. (f) Schematic of a GNM FET biosensor integrated on a PDMS film and attached on the human skin. Images of the transparent and flexible GNM FET device arrays under bending, curling, and twisting. Scale bars are 2 cm [62]. (Images used with permission from the respective publishers)

nanotube chiralities and real-time monitoring of DNA-strand displacement, which could be used for detecting miRNA biomarkers for urinary bladder cancer or urothelial carcinoma [124].

11.5.3 Sensors Based on Field-Effect Transistors

Field-Effect Transistor (FET)-based systems utilize electric fields to control the flow of current. Recently, a flexible FET type sensor was utilized for the detection of the ovarian cancer antigen biomarker-CA125. The sensor was fabricated using polymethyl methacrylate (PMMA) functionalized with multiwalled carbon nanotubes—MWCNTs-COOH/rGO. The sensor showed a LOD of 0.5 nU/mL with a wide linear range (10^{-9} to 1 U/mL). It was also able to detect CA125 in human serum samples [65]. Another work showed graphene nanomesh FETs on flexible PET substrates for HER2 detection. It was able to detect breast cancer cells overexpressed with HER 2 down to the single cell level [62]. A flexible and regenerative aptameric field-effect transistor biosensor, consisting of a graphene–Nafion composite film was used for detecting cytokine storm biomarkers in undiluted human biofluids. The composite film enabled the minimization of nonspecific adsorption and reusability. Cytokines (e.g., IFN- γ , an inflammatory and cancer biomarker) could be monitored in undiluted human sweat with a detection range from 0.015 to 250 nM and limit of detection down to 740 fM [125]. Examples of some of the sensing modalities are shown in Fig. 11.3 showing how diverse configurations and devices may be integrated.

11.6 Formats and Configurations of Flexible Sensing/Therapeutic Platforms

In the above sections, we have discussed various sensor design elements and targets of interest for cancer diagnostics. We now present some sensor configurations in flexible formats for health monitoring [52]. These sensors may be integrated with therapeutic platforms as a closed loop system. This offers regulation by means of releasing a therapeutic agent whenever illness biomarkers prevail [127]. By detecting cancers prior to manifestation in biomarkers levels, therapeutic dosing can relate to the severity of such changes. The designs of the devices depend not only on the targets and transduction mechanisms, but also on the way in which the sensors interface with the human body or environment. The application of flexible platforms (biosensors) for cancer can be classified into various formats such as attachments to skin or fabrics, implants, integrated devices for exhaled breath, etc. For instance, skin-mounted electronics systems can assess physiological parameters such as temperature, heart rate, blood pulse, and respiration rate, or chemical constituents in sweat, saliva, and tears.

11.6.1 Wearable on the Human Body

Wearable devices can be mounted directly on the body in order to collect biometric data in a non-invasive fashion. Flexible and wearable platforms can play an important role in cancer therapy, particularly for the care of patients via home-based

monitoring. Such devices can be worn at locations on the skin including the waist, the upper arm/wrist, behind the ear, etc. Other flexible wearables can include patch-type sensors on skin, tattoo-like strips, wristbands, intraocular sensing within contact lenses, and even sensors on tooth enamel [128]. Flexible systems are built on substrates that mimic the flexibility and stretchability of human skin, with low thickness to reduce bending-induced strain. They are designed to be non-irritating and possess the ability to adhere to skin without the need for additional adhesives [129]. While most sensors are typically thin-film devices that aim for enhanced sensing due to increased surface area contact, there are also rigid, small-footprint devices affixed to skin through adhesive pads, penetrating needles, or clamps.

The fabrication of a fully integrated flexible epidermal bandage and a microneedle electrochemical sensing platform was reported for skin melanoma rapid screening. The sensor targets tyrosinase (Tyr) as a biomarker of interest, and the analytical output was investigated using phantom gel, agarose, and porcine skin. The conformable skin wearable sensor has the potential for melanoma screening in decentralized systems, overcoming the issues associated with painful biopsies and the delays/anxiety associated with conventional assays [126]. The concept of using flexible devices integrated with drug delivery can also be explored in this manner. Bioresorbable, miniaturized porous-silicon (p-Si) needles with covalently linked drug cargos were built on a water-soluble film formed from polyvinyl alcohol (PVA). This flexible film can be intimately interfaced with the irregular surface of living tissues, followed by complete dissolution with saline solution within 1 min. Consequently, the p-Si needles remain embedded inside tissues and then undergo gradual degradation, allowing for sustained release of the drug cargos [130]. In another work, a flexible wearable on skin optical device was reported for breast cancer therapy, using continuous monitoring of rapid hemodynamic changes during the patient's chemotherapy infusion. The sensor consists of a flexible substrate with an array of LEDs and optodes which showed high precision in measurement, good thermal stability, high signal-to-noise ratio, and low detector crosstalk [131].

Ultraviolet light radiation (UVR) is one of the primary drivers of skin cancers, one of the most common cancers globally. Devices that accurately measure exposure levels are among the interesting applications in this area. By being flexible and wearable, they can provide real-time, personalized assessments. Figure 11.4 shows exemplary devices that possess these attributes. A spectrally selective colorimetric monitoring of UVR was shown using a photo-electrochromic ink consisting of a multi-redox polyoxometalate and an e-donor. The ink could be combined with simple components such as filter paper and transparency sheets to fabricate low-cost sensors that provide naked-eye monitoring of UVR, even at low doses typically encountered during solar exposure (Fig. 11.4a). Importantly, the diverse UV response of different skin colors demands personalized sensors. Customized design of robust, real-time solar UV dosimeters can meet the specific needs of different skin phototypes [132]. An optical metrology approach combining optoelectronics designs and wireless modes of operation serves as the basis for a miniature, low-cost, and battery-free device for precise dosimetry at multiple wavelengths. The diameter, thickness, and weight of the device are 8 mm, 1.5 mm, and 110 mg,

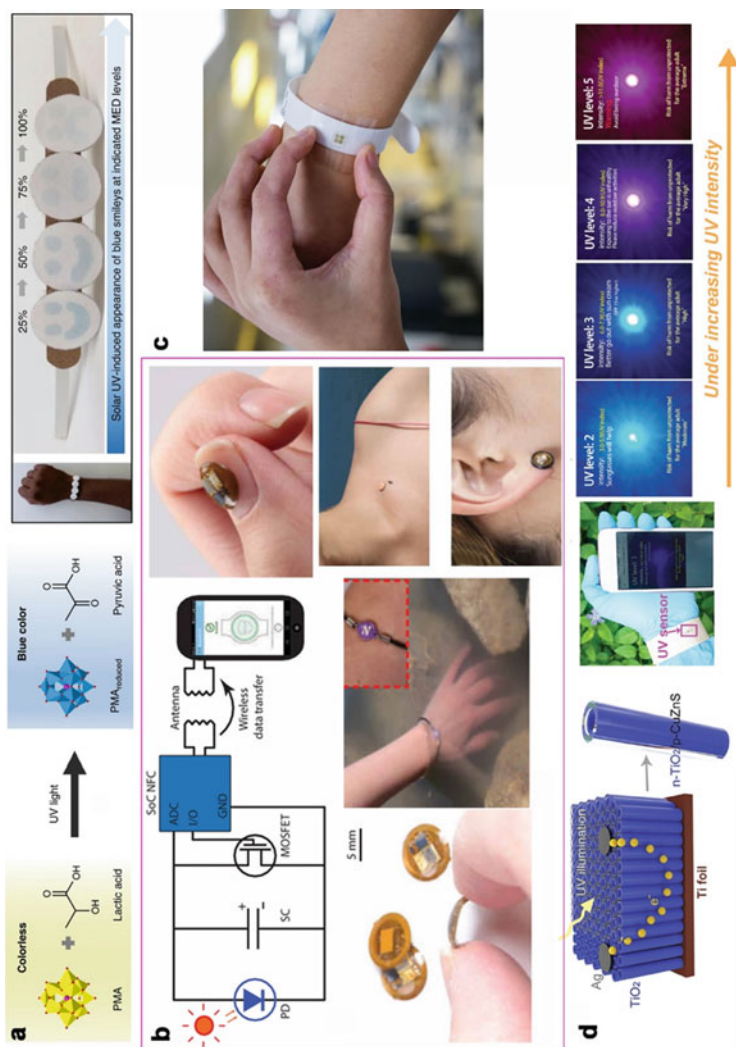


Fig. 11.4 Examples of flexible and wearable sensors designed to be worn on the body to minimize risk of skin cancers. (a) A colorimetric paper-based UV sensor with an aqueous solution containing photo-electrochromic phosphomolybdic acid (PMA) that is reduced by UV radiation in the presence of lactic acid to produce a blue product. This was reported as a prototype device in a wristband format with paper disc-based smileys to allow an easily readable dose-dependent sensor response (adapted from [132]). (b) Millimeter-scale, battery-free, wireless sensors of UVA radiation. Circuit diagram of the system and its wireless

Fig. 11.4 (continued) interface to a smartphone. The NFC chip, the MOSFET, the SC, and the photodetector are labeled NFC, MOS, SC, and PD, respectively. GND indicates ground. Images demonstrating the flexibility of the sensor on various body parts, materials, and form factors (adapted from [39]). (c) AlGaIn/GaN heterostructure membranes used as wearable systems, such as wristbands to measure the UV exposure levels [133]. (d) UV sensitive photodetector device configuration of p-CuZnS/n-TiO₂ NTAs with Ag contacts, and form of the flexible wearable photodetector as a real-time UV monitor with levels reported from a mobile device [40]. (Images used with permission from the respective publishers)

respectively, and use a chip with near-field communication, radio frequency antenna, photodiodes, supercapacitors, and a transistor (Fig. 11.4b) to exploit continuous accumulation for measurement [39]. Flexible UV light sensors using an interdigitated photodetector were created using aluminum gallium nitride (AlGa_N) and free-standing single-crystalline layers of gallium nitride (Ga_N). These membranes are easily bent, allow for use in flexible and wearable sensors (Fig. 11.4c) and operated at high levels of responsivity and sensitivity [133]. Another flexible wearable skin sensor with a p-CuZnS/n-TiO₂ photodetector for skin cancer was reported. The sensor was stable even at a 50° bending angle, high responsivity 640 AW⁻¹, and high quantum efficiency (Fig. 11.4d) [40]. These works show the diverse strategies for the fabrication of flexible skin wearable platforms for skin cancer.

11.6.2 Flexible Sensors Integrated in Textiles

Sensors on fabrics and textiles form an important segment within this category. Functional and “smart” fabrics are becoming increasingly popular, with high conformability to the body profile [134]. Making devices that are wearable and can be incorporated with everyday clothing makes monitoring easy for the patient, as it requires no extra effort, and allow for continuous on-body sensing. Different strategies are considered in developing such fabric-based flexible wearable sensors including the printing of functional electrodes on finished garments via flexible deposition/printing, or modifying fibers/thread to form functional textiles. Modified textiles include sheets woven or knitted from fibers, and non-woven 2D structures. While these have been traditionally made from wool, cotton, or synthetics (nylon, polyester), new materials have been explored for smart textiles [12–15]. Modifications to traditional textile materials, such as treatment to give nanoporous surface morphology and incorporation of functional coatings, can confer properties such as electrochemical conductivity [47]. Considerations include durability, machine wash stability, and biocompatibility to avoid irritation.

Researchers have exploited both forms of flexible wearable electrodes for cancer. A millimeter sized nickel manganate based Negative Temperature Coefficient (NTC) chip thermistor probe was reported for early-stage breast cancer detection. This may be attached to any kind of fabric, with high sensitivity, accuracy, and reliability in terms of analytical performance [135]. As clinicians are accustomed to image interpretation, 2D and 3D thermal imaging systems have been developed to predict hot spots by measuring body surface temperature. A wearable textile antenna was used for the detection of cancerous tumors (xeroderma pigmentosum) in the X-frequency band (8–12 GHz). It showed a reflection coefficient magnitude of -10 dB (between 8 and 12 GHz) in a model of dielectric artificial skin [136]. A flexible wearable ultra-wideband (UWB) antenna was similarly developed for microwave imaging of breast cancer. Specifically, the antenna was composed on three layers of polyimide, with transmission provided by periodic spiral patches. It showed a maximum efficiency of 85%, maximum gain of 3.87 dB, and a wide bandwidth of 3.26–23.37 GHz [137].

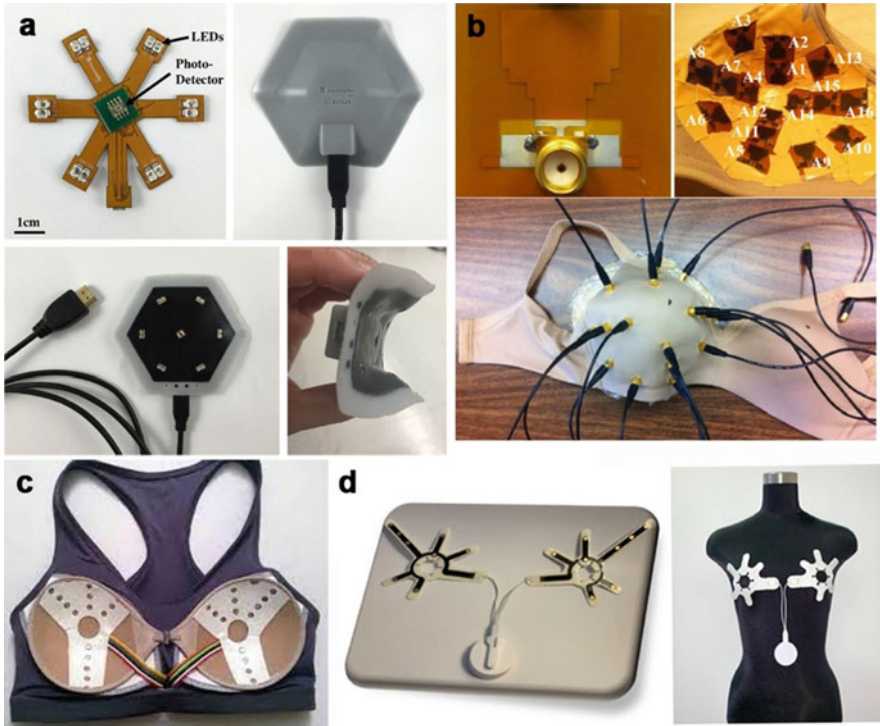


Fig. 11.5 (a) Flexible PCB and optical components. Top and bottom view of the wearable probe and its flexibility under gentle pressure [138]. (b) A wearable prototype showing the connectorized monopole antenna with the array inside the bra-cup. The outside showing the SMA cables that connect to the antennas (the device is sitting on a breast model) [102]. (c) Thermistor sensors integrated into clothing for measuring temperature fluctuations in breast tissue. (d) Wearable biometric patches of the Cyncradia Breast Monitor showing the sensor side of the patches and their placement on skin surface [140]. (Images used with permission from the respective publishers)

An evolution in the design of such flexible and wearable systems can be seen in Fig. 11.5. A continuous-wave wearable diffuse optical probe for investigating the hemodynamic response of locally advanced breast cancer patients during neoadjuvant chemotherapy infusions was developed [138]. The system consisted of a flexible printed circuit board with an array of six dual wavelength surface-mount LED and photodiode pairs (Fig. 11.5a). The probe could be encased in a soft silicone housing that conforms to the natural breast shape in order to explore continuous hemodynamic changes during chemotherapy. A similar flexible wearable on textile sensor was shown with a 20×20 mm 16 antenna array for the microwave detection of breast cancer (Fig. 11.5b). The antenna operated in the range of (2–4) GHz [102]. The proposed biosensor comprised a flexible substrate ($50 \mu\text{m}$ Kapton polyimide) with 16-element 20×20 mm antennas asymmetrically embedded in clothing to provide the wearable interface (Fig. 11.5c). However, the embedded antennas were delicate and required a switching matrix to connect each pair

individually to sensing array ports with a vector network analyzer for measurement, which was somewhat time consuming. In these, the sensor placement was not very comfortable. Figure design changes are seen in Fig. 11.5c, d, which are commercially developed sensors integrated into clothing. The iTBra exploits the relationship between temperature and cancerous cell division, with a heat sensor to track temperature fluctuations in breast tissue [139]. The Cyncadia Breast Monitor (CBM), a non-invasive, non-compressive, and non-radiogenic wearable device for breast cancer detection that can help reduce unnecessary biopsies. The CBM records thermodynamic metabolic data from the breast skin surface over a period of time using two wearable biometric patches consisting of eight sensors each and a data recording device. The acquired multi-dimensional temperature data are analyzed to determine the presence of breast tissue abnormalities [140].

11.6.3 Exhaled Breath Sensors

Exhaled breath analysis is another non-invasive way to measure the physiological status of an individual. There has been interest pertaining to exhaled breath sensors using the detection of various compounds ranging from non-volatile compounds in exhaled breath condensate (EBC) (e.g., cytokines, leukotrienes and hydrogen peroxide) to VOCs such as isoprene, acetone, ethanol, methanol, other alcohols and alkanes [29]. Flexible devices provide a strategy for ambulatory and wearable sensing of these parameters. A flexible chemoresistive sensor was shown for four types of exhaled breath biomarkers—ammonia, isoprene, acetone, and hydrothion. The chemoresistive sensor array was constructed via graphene oxide metal hybrid film deposition on a flexible PET substrate patterned with interdigitated electrodes. It showed 95.8% sensitivity and 96.0% specificity in lung cancer detection in clinical samples [64]. The flexibility of such devices render rapid, non-invasive, and personalized healthcare management. Another work showed the fabrication of a flexible sensor array based on MXene as a sensing layer with a graphene interdigitated electrode for VOC biomarker detection such as alcohol in human exhaled breath [141]. The sensor showed prediction accuracy up to 88.9% in breath samples. Here, owing to attachment of the flexible device to irregular surfaces on the body, the real-time measurement of human breath was enabled. A flexible sensor based on MXene/rGO/CuO hybrid was reported for sensing acetone (a cancer VOC biomarker) [142]. It was found to exhibit 52.09% sensor response toward 100 ppm acetone at room temperature with a fast response and recovery time [142]. Acetone could be detected in human breath using a flexible Pt on Ga–In bimetal oxide nanofiber sensor. It exhibited good analytical performance with low limit of detection (300 ppb), short response time, and a high response to ppm levels of acetone [143]. It also exhibited good stability and moisture insensitivity in the range 40–95%. Flexible sensors can also be used for other forms of analysis. Since lung cancer patients may experience shortness of breath, flexible sensors with the capability of monitoring breath patterns can play a vital role in their treatment and care. In this regard, a multifunctional flexible sensor based on p-NiO/n-CdS on ITO was

fabricated using low temperature solution processed deposition technique. It was shown to have a capability of distinguishing different breath patterns such as deep, fast, and slow [144]. Here, the solution processing enables low-cost fabrication with high throughput.

11.6.4 Implantable Devices

Various devices can be implanted in human bodies/animal models for the continuous monitoring of health conditions. These may include the monitoring of *in vivo* tumor progression, tracking of biological metabolites, and could eventually integrate with feedback controls for tailored drug delivery. With their mechanical conformability, soft and intrinsically flexible devices may be used as subcutaneous sensors or wholly implanted devices. There is the possibility of damage to tissue during insertion of traditional rigid electrodes and implants. Chronic stress in biological environments may also lead to the development of fibrous capsules surrounding the device and eventual failure. Flexible devices made of bioinert or biocompatible materials are therefore designed to avoid these issues, while matching surface softness and shape *in vivo* [22]. Devices match dynamic deformation and elongation of tissue, and adhere to wet surfaces with varied features. Specificity and selectivity in a complex *in vivo* environment are practical considerations. Sensors designed to degrade within the body are attractive options to obviate the need for recovery. Biodegradability and hydrolysis in the aqueous environment must therefore match the timescale of sensing. Degradation byproducts must also be biocompatible. An encapsulation layer of inert material that has tunable degradability can be used; however, this can block sensing and signal transmission. Additionally, devices may need external connections for power and transmission of data, or a wireless alternative [145]. While many *in vivo* flexible implantable devices are of profound utility in cancer detection, integrated delivery of anti-cancer drugs, and therapy in deep-rooted tumors, many are far from deployment in the human body.

An innovative strategy to monitor asymptomatic cancer was shown in the form of a tattoo-based biosensor to detect hypercalcemia, which is associated with various forms of cancer (gastrointestinal, lung, prostate, colon, breast). The applicability of the tattoo was shown in mouse models injected with breast and colon cancer cell lines, with the ability to detect cancer development at asymptomatic stages [146]. A flexible 6 μm thick PET based device (Mylar foil) capped with an encapsulation layer (5 μm thick) was shown. The foil hosted a temperature sensor and a heating unit, and used in the liver tissues of murine cancer models. A 0.1 $^{\circ}\text{C}$ accuracy in temperature was noted at a bending radius of 2.5 mm, showing efficiency in handling exophytic tumor nodules [147]. An example of a flexible therapeutic implant was shown in the form of an implantable self-powered photodynamic therapy system based on a twinning structure piezoelectric nanogenerator encapsulated by parylene-C. It showed a significant antitumor effect (87.46% tumor inhibition) upon irradiation with intermittent continuous simulation of light for 12 days, thus showing potential for clinical cancer treatment [40]. Such implants can be integrated

with sensors to form closed loop therapies. Flexible devices can be integrated with controlled drug release as shown via a noteworthy biodegradable flexible electronic device for controlled paclitaxel delivery. The device was powered by an external alternating magnetic field and showed good inhibitory effect on cancer cell proliferation (MCF-7). The device design comprising Zn and MgO allowed for complete biodegradability, thereby providing relief to breast cancer patients without the need for a second extractive surgery to retrieve the device [148].

Thus, skin and textile-based wearables, implantable and integrated exhaled breath flexible biosensors/platforms can play a pivotal role in cancer management ranging from early detection to long-term monitoring and integrated drug delivery.

11.7 Outlook for Flexible Sensors in Cancer Diagnostics

In conclusion, we note a few of the challenges and opportunities in the future development of clinically relevant flexible systems for cancer diagnostics. Most of these are broadly applicable to the field of wearables and flex systems for human health monitoring, which will also guide the specific area of disease diagnostics. As discussed in this chapter, the goals of personalized cancer detection and therapeutic monitoring are among the primary drivers triggering interest in the field of mechanically flexible systems. While conventional (rigid) electronics and POC devices offer a host of analytical services, flexible systems are designed to enable adherence to novel form factors [149]. Systems that can advance the functionality and compatibility of materials with the body, improve stability, accuracy and reliability, and provide the ability to integrate different components to autonomously gather, analyze, and transfer data, will provide the roadmap for new products and applications.

As noted above, depending on the sample source (e.g., sweat, blood) and nature of biomarkers (e.g., biophysical, biochemical), various categories of mechanically flexible systems (e.g., wearables, implantables) are possible [150]. Typically, the devices are low power, mechanically robust to deformation, low cost, or disposable. From bending and rolling, to conforming onto irregular shapes, folding, twisting, stretching, and deforming, the key performance metrics involve maintaining performance and reliability in the face of mechanical challenges [151]. To promote patient and clinical use, devices need to be compact and comfortable [152]. Flexible and lightweight circuitry design that fits within tight spaces can optimize space and efficiency. The choice of materials for the substrate with the appropriate mechanical properties, the inks, as well as integration with the electronics components are important considerations in addition to manufacturing itself. The material choice in turn, may be dictated by the placement of the flexible device. The rise of biocompatible, synthetic, and naturally biodegradable materials can provide the substrates for soft implantable devices [153]. The requirement for flexibility further necessitates novel technologies for device manufacturing and processing. Methods such as roll-to-roll technologies are ideal for large-scale production of pliant interconnects [154]. Further, devices have to possess interconnects that provide low signal loss and increased mechanical flexibility. Interconnects that can connect

systems without loss of signal, or interfering with the form and fit of the wearables are needed [155]. There often tends to be a mechanical mismatch between the devices and the soft tissue, as well as flexible substrates and microelectronics. These include stiff electronic components including microprocessors, connectors, transmitters, receivers, resistors, capacitors, and power supplies. Smart design and integration of MEMS devices, microcontrollers, and power sources in small and “soft” form factors are needed. Novel ideas such as flexible antennas and flexible energy storage and conversion systems as power sources, batteries, supercapacitors, fuel cells, and even autonomously powered devices powered by the body itself are being developed to form completely soft devices [156, 157]. Low power consumption is important in terms of long-term performance and patient safety. Proximity of the electrical components to living tissues places restrictions on power dissipation for both on-body or implanted systems, in order to minimize cellular damage [158].

In addition to the issues surrounding device design itself, other considerations include, but are not limited to—exploring clinically relevant and appropriate biomarkers, and developing stable and biofriendly interfaces via different biofluids or body parts. Stable interfacing between the analyte of interest and sensor surface tends to be challenging in flexible systems. New strategies must be explored to effectively detect ultralow concentrations, such as circulating tumor cells or nucleotides in μL of fluids. Flexible devices have a higher signal-to-noise ratio than traditional sensors because of better contact and conformability. Thin-film flexible devices reduce the thickness of the diffusion layer, increasing flux. Approaches such as using nanopores for migration, magnetic nanoparticles, and flexible microfluidics are emerging as viable options [159, 160]. Reproducibility consists of precision and accuracy, that is, giving the same value repeatedly over time [159]. The human body is a dynamic environment, so changes in temperature, pH, humidity, and even mechanical bending or stretching for flexible electronics can affect the signal. Biofouling and hysteresis contribute to non-reproducibility over time, necessitating research in temperature and pH-responsiveness, magnetic and acoustic clearing, and self-cleaning [161].

Combinatorial approaches of flexible systems and clinically relevant biomarker panels as potential fingerprints for cancer are still being developed [162]. Many cancers cannot be detected through use of a single biomarker, and are instead, characterized by a host of atypical changes. Further, many different types of cancers or noncancerous conditions can affect the same biomarkers. The development of more accurate biomarker diagnostic panels for different types and stages of cancer is an ongoing challenge not only for conventional assays, but flexible systems as well [163]. This has led to many flexible platforms utilizing chemical to electrical sensing strategies, as to minimize the need for additional equipment and expensive reagents. It is envisioned that the flexible devices work in conjunction with other forms of assays and diagnostic tools to discern multiple biomarkers of interest simultaneously for clinical use. These may include both biophysical and biochemical markers of disease and wellness.

Device design must factor into the end-user demographics and usage settings. Improving access to under-served communities and resource limited countries is equally critical [164]. Flexible platforms offer unique advantages for on-demand care, but may involve different constraints that limit their usability [19]. For at-home use, applying and removing devices consisting of disposable (adhesives, sensors) and reusable components (batteries and circuitry, plastic housings) might not be intuitive. Flexibility oftentimes may lead to increased elasticity but loss of mechanical strength. Micro-/nano-scale thinness can make devices fragile and hard to handle. Developments in wireless technology, micro and nanoelectronics, and functional materials have helped remedy some of these issues. These come with increased costs, which may be prohibitive in terms of wider access. Disposal devices may lead to issues of medical waste. Simultaneously, there is a need for improved ease-of-use of the devices and user-friendly platforms/software to help with data processing and interpretation, both for the patient and clinician [165]. Cybersecurity and secure storage/transmission of patient data is vital [166].

11.8 Conclusion

In summary, this chapter outlines some of the aspects in the design of mechanically flexible devices, sensors, and diagnostic tools that are finding an increasing application in the area of cancer monitoring and therapy. We have discussed various features of such devices, their materials and configurations, areas of application, and the outlook for this stimulating and rapidly growing area of research. We note that given the complexity of cancers and the diverse choices available, devices can adopt different biological, material, and sensing requirements. Not all materials and methods will be applicable to all systems, and not all designs will be clinically and commercially feasible beyond the lab setting. Advances in materials science, nanotechnology, and biosensing strategies are needed to continue to advance the field to a point where convenience and reliability make flexible, on-body, and POC devices worth using in the eyes of a patient compared to current standards. If these are achieved, it is envisioned that development of clinically relevant flexible systems can aid in personalized cancer management ranging from early detection and therapeutic response monitoring, thereby enhancing cancer patient survival and quality of life. The range and diversity of these flexible devices and configurations is remarkable and provides a host of possibilities for the elucidation of different kinds of biomarkers in different environments. The exciting developments in this field, in turn have significant benefits in enhancing patient survival rates, mitigating suffering, and reducing healthcare costs.

Acknowledgements S.C. acknowledges support from the Virginia Commonwealth Cybersecurity Initiative (CCI).

References

1. Ferlay J et al (2021) Cancer statistics for the year 2020: an overview. *Int J Cancer*. <https://doi.org/10.1002/ijc.33588>
2. Siegel RL, Miller KD, Jemal A (2020) Cancer statistics, 2020. *CA Cancer J Clin* 70(1):7–30
3. Wu L, Qu X (2015) Cancer biomarker detection: recent achievements and challenges. *Chem Soc Rev* 44(10):2963–2997
4. Crowley E et al (2013) Liquid biopsy: monitoring cancer-genetics in the blood. *Nat Rev Clin Oncol* 10(8):472–484
5. Lee YT, Tan YJ, Oon CE (2018) Molecular targeted therapy: treating cancer with specificity. *Eur J Pharmacol* 834:188–196
6. Chin L, Andersen JN, Futreal PA (2011) Cancer genomics: from discovery science to personalized medicine. *Nat Med* 17(3):297–303
7. Wang J (2006) Electrochemical biosensors: towards point-of-care cancer diagnostics. *Biosens Bioelectron* 21(10):1887–1892
8. Rusling JF et al (2010) Measurement of biomarker proteins for point-of-care early detection and monitoring of cancer. *Analyst* 135(10):2496–2511
9. Shandilya R et al (2019) Nanobiosensors: point-of-care approaches for cancer diagnostics. *Biosens Bioelectron* 130:147–165
10. Topkaya SN, Azimzadeh M, Ozsoz M (2016) Electrochemical biosensors for cancer biomarkers detection: recent advances and challenges. *Electroanalysis* 28(7):1402–1419
11. Munge BS et al (2016) Multiplex immunosensor arrays for electrochemical detection of cancer biomarker proteins. *Electroanalysis* 28(11):2644–2658
12. Xu M, Obodo D, Yadavalli VK (2018) The design, fabrication, and applications of flexible biosensing devices. *Biosens Bioelectron* 124–125:96–114
13. Wang X, Liu Z, Zhang T (2017) Flexible sensing electronics for wearable/attachable health monitoring. *Small* 13(25)
14. Salim A, Lim S (2019) Recent advances in noninvasive flexible and wearable wireless biosensors. *Biosens Bioelectron* 141:111422
15. Tu J et al (2020) The era of digital health: a review of portable and wearable affinity biosensors. *Adv Funct Mater* 30(29):1906713
16. Vashist SK et al (2015) Emerging technologies for next-generation point-of-care testing. *Trends Biotechnol* 33(11):692–705
17. Li P et al (2021) From diagnosis to treatment: recent advances in patient-friendly biosensors and implantable devices. *ACS Nano* 15(2):1960–2004
18. Feiner R, Dvir T (2018) Tissue-electronics interfaces: from implantable devices to engineered tissues. *Nat Rev Mater* 3(1)
19. Heikenfeld J et al (2018) Wearable sensors: modalities, challenges, and prospects. *Lab Chip* 18(2):217–248
20. Li Y, Chen W, Lu L (2020) Wearable and biodegradable sensors for human health monitoring. *ACS Appl Bio Mater* 4(1):122–139
21. Yang A, Yan F (2021) Flexible electrochemical biosensors for health monitoring. *ACS Appl Electron Mater* 3(1):53–67
22. Rodrigues D et al (2020) Skin-integrated wearable systems and implantable biosensors: a comprehensive review. *Biosensors* 10(7)
23. Bohunicky B, Mousa S (2011) Biosensors: the new wave in cancer diagnosis. *Nanotechnol Sci Appl* 4:1–10
24. Patel J, Patel P (2017) Biosensors and biomarkers: promising tools for cancer diagnosis. *Int J Biosens Bioelectron* 3:313–316
25. Jeffrey SS (2008) Cancer biomarker profiling with microRNAs. *Nat Biotechnol* 26(4):400–401
26. Tothill IE (2009) Biosensors for cancer markers diagnosis. In: *Seminars in cell & developmental biology*. Elsevier

27. Simon E (2010) Biological and chemical sensors for cancer diagnosis. *Meas Sci Technol* 21(11)
28. Jansson MD, Lund AH (2012) MicroRNA and cancer. *Mol Oncol* 6(6):590–610
29. Dent AG, Sutedja TG, Zimmerman PV (2013) Exhaled breath analysis for lung cancer. *J Thorac Dis* 5(Suppl 5):S540
30. Bajtarevic A et al (2009) Noninvasive detection of lung cancer by analysis of exhaled breath. *BMC Cancer* 9(1):1–16
31. Amann A et al (2011) Lung cancer biomarkers in exhaled breath. *Expert Rev Mol Diagn* 11(2):207–217
32. Ishikawa S et al (2016) Identification of salivary metabolomic biomarkers for oral cancer screening. *Sci Rep* 6(1):1–7
33. Kumar N et al (2017) Serum and plasma metabolomic biomarkers for lung cancer. *Bioinformatics* 13(6):202
34. Dehghani S et al (2018) Aptamer-based biosensors and nanosensors for the detection of vascular endothelial growth factor (VEGF): a review. *Biosens Bioelectron* 110:23–37
35. Lin C-W et al (2015) A reusable magnetic graphene oxide-modified biosensor for vascular endothelial growth factor detection in cancer diagnosis. *Biosens Bioelectron* 67:431–437
36. Ferrara N, Gerber H-P, LeCouter J (2003) The biology of VEGF and its receptors. *Nat Med* 9:669
37. Bonato P (2010) Wearable sensors and systems. *IEEE Eng Med Biol Mag* 29(3):25–36
38. Schwartz G et al (2013) Flexible polymer transistors with high pressure sensitivity for application in electronic skin and health monitoring. *Nat Commun* 4:1859
39. Heo SY et al (2018) Wireless, battery-free, flexible, miniaturized dosimeters monitor exposure to solar radiation and to light for phototherapy. *Sci Transl Med* 10(470)
40. Xu X et al (2018) A real-time wearable UV-radiation monitor based on a high-performance p-CuZnS/n-TiO₂ photodetector. *Adv Mater* 30(43)
41. Ray WJ, Joseph W (2013) Wearable electrochemical sensors and biosensors: a review. *Electroanalysis* 25(1):29–46
42. Mahesh KPO et al (2018) Flexible sensor for dopamine detection fabricated by the direct growth of α -Fe₂O₃ nanoparticles on carbon cloth. *Appl Surf Sci* 427(Part B):387–395
43. Wang L et al (2017) New insights and perspectives into biological materials for flexible electronics. *Chem Soc Rev* 46(22):6764–6815
44. Harris K, Elias A, Chung H (2016) Flexible electronics under strain: a review of mechanical characterization and durability enhancement strategies. *J Mater Sci* 51(6):2771–2805
45. Zhou Z et al (2021) Flexible electronics from intrinsically soft materials. *Giant* 6
46. Ning X et al (2018) Assembly of advanced materials into 3D functional structures by methods inspired by origami and Kirigami: a review. *Adv Mater Interfaces* 5(13)
47. Economou A, Kokkinos C, Prodromidis M (2018) Flexible plastic, paper and textile lab-on-a-chip platforms for electrochemical biosensing. *Lab Chip* 18(13):1812–1830
48. Teengam P et al (2017) Electrochemical paper-based peptide nucleic acid biosensor for detecting human papillomavirus. *Anal Chim Acta* 952:32–40
49. Jampasa S et al (2014) Electrochemical detection of human papillomavirus DNA type 16 using a pyrrolidinyI peptide nucleic acid probe immobilized on screen-printed carbon electrodes. *Biosens Bioelectron* 54:428–434
50. Avelino K et al (2021) Flexible sensor based on conducting polymer and gold nanoparticles for electrochemical screening of HPV families in cervical specimens. *Talanta* 226:122118
51. Wang C, Yokota T, Someya T (2021) Natural biopolymer-based biocompatible conductors for stretchable bioelectronics. *Chem Rev* 121(4):2109–2146
52. Wang L, Jiang K, Shen G (2021) Wearable, implantable, and interventional medical devices based on smart electronic skins. *Adv Mater Technol* 6(6):2100107
53. Wen D-L et al (2021) Recent progress in silk fibroin-based flexible electronics. *Microsyst Nanoeng* 7(1):35

54. Shi C et al (2021) New silk road: from mesoscopic reconstruction/functionalization to flexible Meso-electronics/photronics based on cocoon silk materials. *Adv Mater*:e2005910
55. Ko J et al (2017) Human hair keratin for biocompatible flexible and transient electronic devices. *ACS Appl Mater Interfaces* 9(49):43004–43012
56. Meyer M (2019) Processing of collagen based biomaterials and the resulting materials properties. *Biomed Eng Online* 18
57. Pang B et al (2021) Molecular-scale design of cellulose-based functional materials for flexible electronic devices. *Adv Electron Mater* 7(2):2000944
58. Mohebbi S et al (2019) Chitosan in biomedical engineering: a critical review. *Curr Stem Cell Res Ther* 14(2):93–116
59. Pradhan S, Brooks AK, Yadavalli VK (2020) Nature-derived materials for the fabrication of functional biodevices. *Mater Today Bio* 7:100065
60. Pandya HJ, Park K, Desai JP (2015) Design and fabrication of a flexible MEMS-based electro-mechanical sensor array for breast cancer diagnosis. *J Micromech Microeng* 25(7):075025
61. Wang L et al (2016) Flexible, graphene-coated biocomposite for highly sensitive, real-time molecular detection. *Adv Funct Mater* 26(47):8623–8630
62. Yang Y et al (2017) Ultrafine graphene nanomesh with large on/off ratio for high-performance flexible biosensors. *Adv Funct Mater* 27(19)
63. Ibanez-Redin G et al (2020) Screen-printed electrodes modified with carbon black and polyelectrolyte films for determination of cancer marker carbohydrate antigen 19-9. *Microchim Acta* 187(7)
64. Chen Q et al (2020) Constructing an E-nose using metal-ion-induced assembly of graphene oxide for diagnosis of lung cancer via exhaled breath. *ACS Appl Mater Interfaces* 12:17713–17724
65. Majd S, Salimi A (2018) Ultrasensitive flexible FET-type aptasensor for CA 125 cancer marker detection based on carboxylated multiwalled carbon nanotubes immobilized onto reduced graphene oxide film. *Anal Chim Acta* 1000:273–282
66. Lee D et al (2017) Highly selective organic transistor biosensor with inkjet printed graphene oxide support system. *J Mater Chem B* 5(19):3580–3585
67. Carvajal S et al (2018) Disposable inkjet-printed electrochemical platform for detection of clinically relevant HER-2 breast cancer biomarker. *Biosens Bioelectron* 104:158–162
68. Kim HE et al (2019) Solution-gated graphene field effect transistor for TP53 DNA sensor with coplanar electrode array. *Sens Actuators B* 291:96–101
69. Lee D et al (2008) A disposable plastic-silicon micro PCR chip using flexible printed circuit board protocols and its application to genomic DNA amplification. *IEEE Sens J* 8(5–6): 558–564
70. Park J et al (2020) Microscale biosensor array based on flexible polymeric platform toward lab-on-a-needle: real-time multiparameter biomedical assays on curved needle surfaces. *ACS Sens* 5(5):1363–1373
71. Pothipor C et al (2019) Highly sensitive biosensor based on graphene-poly (3-aminobenzoic acid) modified electrodes and porous-hollowed-silver-gold nanoparticle labelling for prostate cancer detection. *Sens Actuators B Chem* 296
72. Jonous Z et al (2019) An electrochemical biosensor for prostate cancer biomarker detection using graphene oxide-gold nanostructures. *Eng Life Sci* 19(3):206–216
73. Shahrokhian S, Salimian R (2018) Ultrasensitive detection of cancer biomarkers using conducting polymer/electrochemically reduced graphene oxide-based biosensor: application toward BRCA1 sensing. *Sens Actuators B* 266:160–169
74. Kovalska E et al (2019) Multi-layer graphene as a selective detector for future lung cancer biosensing platforms†. *Nanoscale* 11:2476–2483
75. Zhu L et al (2021) Digital multimeter-based point-of-care immunoassay of prostate-specific antigen coupling with a flexible photosensitive pressure sensor. *Sens Actuators B* 343:130121
76. Zhu J et al (2020) Low-cost flexible plasmonic nanobump metasurfaces for label-free sensing of serum tumor marker. *Biosens Bioelectron* 150

77. Bahari D, Babamiri B, Salimi A (2020) An eco-friendly MIP-solid surface fluorescence immunosensor for detection of CA 19-9 tumor marker using Ni nanocluster as an emitter labels. *J Iran Chem Soc* 17:2283–2291
78. Sun Y et al (2020) Assembly of black phosphorus nanosheets and MOF to form functional hybrid thin-film for precise protein capture, dual-signal and intrinsic self-calibration sensing of specific cancer-derived exosomes. *Anal Chem* 92:2866–2875
79. Kwon O, Park S, Jang J (2010) A high-performance VEGF aptamer functionalized polypyrrole nanotube biosensor. *Biomaterials* 31(17):4740–4747
80. Pan L et al (2017) An electrochemical biosensor to simultaneously detect VEGF and PSA for early prostate cancer diagnosis based on graphene oxide/ssDNA/PLLA nanoparticles. *Biosens Bioelectron* 89:598–605
81. Lobry M et al (2020) HER2 biosensing through SPR-envelope tracking in plasmonic optical fiber gratings. *Biomed Opt Express* 11(9):4862–4871
82. Zhao J et al (2021) Flexible nickel-cobalt double hydroxides micro-nano arrays for cellular secreted hydrogen peroxide in-situ electrochemical detection. *Anal Chim Acta* 1143:135–143
83. Mo G et al (2021) Spatially-resolved dual-potential sandwich electrochemiluminescence immunosensor for the simultaneous determination of carbohydrate antigen 19-9 and carbohydrate antigen 24-2. *Biosens Bioelectron* 178
84. Yang H et al (2014) Gold-silver nanocomposite-functionalized graphene based electrochemiluminescence immunosensor using graphene quantum dots coated porous PtPd nanochains as labels. *Electrochim Acta* 123:470–476
85. Povedano E et al (2019) Versatile electroanalytical bioplatfroms for simultaneous determination of cancer-related DNA 5-methyl- and 5-hydroxymethyl-cytosines at global and gene-specific levels in human serum and tissues. *ACS Sens* 4(1):227–234
86. Wang L et al (2016) PtAu alloy nanoflowers on 3D porous ionic liquid functionalized graphene-wrapped activated carbon fiber as a flexible microelectrode for near-cell detection of cancer. *NPG Asia Mater* 8:e337
87. Gomes R et al (2018) Sensing CA 15-3 in point-of-care by electropolymerizing O-phenylenediamine (oPDA) on Au-screen printed electrodes. *PLoS One* 13(5)
88. Ahmed AM, Mehaneq A, Elsayed H (2021) Detection of toluene traces in exhaled breath by using a 1D PC as a biomarker for lung cancer diagnosis. *Eur Phys J Plus* 136:626
89. Lee WC et al (2020) Microneedle array sensor for monitoring glucose in single cell using glucose oxidase-bonded polyterthiophene coated on AuZn oxide layer. *Sens Actuators B* 320: 128416
90. Wang M et al (2019) Bimetallic cerium and ferric oxides nanoparticles embedded within mesoporous carbon matrix: electrochemical immunosensor for sensitive detection of carbohydrate antigen 19-9. *Biosens Bioelectron* 135:22–29
91. Zhao A et al (2020) Functionalized graphene fiber modified by dual nanoenzyme: towards high-performance flexible nanohybrid microelectrode for electrochemical sensing in live cancer cells. *Sens Actuators B Chem* 310
92. Kwon O et al (2012) Flexible FET-type VEGF aptasensor based on nitrogen-doped graphene converted from conducting polymer. *ACS Nano* 6(2):1486–1493
93. Song J et al (2021) Free-standing electrochemical biosensor for carcinoembryonic antigen detection based on highly stable and flexible conducting polypyrrole nanocomposite. *Microchim Acta* 188(6)
94. Soares JC et al (2019) Detection of the prostate cancer biomarker PCA3 with electrochemical and impedance-based biosensors. *ACS Appl Mater Interfaces* 11:46645–46650
95. Khalid A et al (2020) Silk: a bio-derived coating for optical fiber sensing applications. *Sens Actuators B* 311:127864
96. Xu M, Yadavalli VK (2019) Flexible biosensors for the impedimetric detection of protein targets using silk-conductive polymer biocomposites. *ACS Sens* 4:1040–1047
97. Hassanpour S et al (2019) A novel paper based immunoassay of breast cancer specific carbohydrate (CA 15.3) using silver nanoparticles-reduced graphene oxide nano-ink

- technology: a new platform to construction of microfluidic paper-based analytical devices (mu ADs) towards biomedical analysis. *Microchem J* 146:345–358
98. Farshchi F, Saadati A, Hasanzadeh M (2020) A novel immunosensor for the monitoring of PSA using binding of biotinylated antibody to the prostate specific antigen based on nano-ink modified flexible paper substrate: efficient method for diagnosis of cancer using biosensing technology. *Heliyon* 6:e04327
 99. Bahavarnia F et al (2019) Paper based immunosensing of ovarian cancer tumor protein CA 125 using novel nano-ink: a new platform for efficient diagnosis of cancer and biomedical analysis using microfluidic paper-based analytical devices (mu PAD). *Int J Biol Macromol* 138:744–754
 100. Li L et al (2018) Editable TiO₂ nanomaterial-modified paper in situ for highly efficient detection of carcinoembryonic antigen by photoelectrochemical method. *ACS Appl Mater Interfaces* 10(17):14594–14601
 101. Kumar S et al (2016) Polyaniline modified flexible conducting paper for cancer detection. *Appl Phys Lett* 108(20)
 102. Porter E et al (2016) A wearable microwave antenna array for time-domain breast tumor screening. *IEEE Trans Med Imaging* 35(6):1501–1509
 103. Yoon J et al (2020) Flexible electrochemical biosensors for healthcare monitoring. *J Mater Chem B* 8(33):7303–7318
 104. Landaluce H et al (2020) A review of IoT sensing applications and challenges using RFID and wireless sensor networks. *Sensors* 20(9)
 105. Corzo D, Tostado-Blázquez G, Baran D (2020) Flexible electronics: status, challenges, and opportunities. *Front Electron* 1
 106. Bhalla N et al (2016) Introduction to biosensors. *Biosens Technol Detection Biomol* 60(1):1–8
 107. Sha R, Badhulika S (2020) Recent advancements in fabrication of nanomaterial based biosensors for diagnosis of ovarian cancer: a comprehensive review. *Microchim Acta* 187(3)
 108. Kim J et al (2019) Wearable biosensors for healthcare monitoring. *Nat Biotechnol* 37(4):389–406
 109. Sharma A et al (2021) Wearable biosensors: an alternative and practical approach in healthcare and disease monitoring. *Molecules* 26(3)
 110. Yu Y et al (2020) Flexible electrochemical bioelectronics: the rise of in situ bioanalysis. *Adv Mater* 32(15)
 111. Kassal P, Steinberg M, Steinberg I (2018) Wireless chemical sensors and biosensors: a review. *Sens Actuators B Chem* 266:228–245
 112. Shin J et al (2018) Mobile diagnostics: next-generation technologies for in vitro diagnostics. *Analyst* 143(7):1515–1525
 113. Campuzano S et al (2021) New challenges in point of care electrochemical detection of clinical biomarkers. *Sens Actuators B* 345:130349
 114. Cho CH et al (2021) Re-engineering of peptides with high binding affinity to develop an advanced electrochemical sensor for colon cancer diagnosis. *Anal Chim Acta* 1146:131–139
 115. Nagarajan R et al (2021) Biocompatible MXene (Ti₃C₂T_x) immobilized with Flavin adenine dinucleotide as an electrochemical transducer for hydrogen peroxide detection in ovarian cancer cell lines. *Micromachines* 12(8)
 116. Zhang L et al (2021) Recent Progress of SERS Nanoprobe for pH detecting and its application in biological imaging. *Biosensors* 11(8)
 117. Carrascosa LG, Calle A, Lechuga LM (2009) Label-free detection of DNA mutations by SPR: application to the early detection of inherited breast cancer. *Anal Bioanal Chem* 393(4):1173–1182
 118. Lee SY et al (2012) Water-resistant flexible GaN LED on a liquid crystal polymer substrate for implantable biomedical applications. *Nano Energy* 1(1):145–151
 119. Karaca G et al (2021) Gold-nickel nanowires as nanomotors for cancer marker biodetection and chemotherapeutic drug delivery. *ACS Appl Nano Mater* 4(4):3377–3388

120. Liang L et al (2016) Aptamer-based fluorescent and visual biosensor for multiplexed monitoring of cancer cells in microfluidic paper-based analytical devices. *Sens Actuators B Chem* 229: 347–354
121. Lee C et al (2015) 3D plasmonic nanobowl platform for the study of exosomes in solution. *Nanoscale* 7(20):9290–9297
122. Abulaiti A et al (2021) Nano-silica embedded polydimethylsiloxane on interdigitated sensor as adhesive polymer for detecting lung cancer mutation. *Biotechnol Appl Biochem*. <https://doi.org/10.1002/bab.2122>
123. Ping Z et al (2021) Miniature flexible instrument with fibre Bragg grating-based Triaxial force sensing for intraoperative gastric endomicroscopy. *Ann Biomed Eng* 49(9):2323–2336
124. Harvey JD et al (2017) A carbon nanotube reporter of microRNA hybridization events in vivo. *Nat Biomed Eng* 1(4):1–11
125. Wang Z et al (2021) A flexible and regenerative aptameric graphene–Nafion biosensor for cytokine storm biomarker monitoring in undiluted biofluids toward wearable applications. *Adv Funct Mater* 31(4):2005958
126. Ciui B et al (2018) Wearable wireless tyrosinase bandage and microneedle sensors: toward melanoma screening. *Adv Healthc Mater* 7(7)
127. Ngoepe M et al (2013) Integration of biosensors and drug delivery technologies for early detection and chronic management of illness. *Sensors* 13(6):7680–7713
128. Yang Y, Gao W (2019) Wearable and flexible electronics for continuous molecular monitoring. *Chem Soc Rev* 48(6):1465–1491
129. Qiao L et al (2020) Advances in sweat wearables: sample extraction, real-time biosensing, and flexible platforms. *ACS Appl Mater Interfaces* 12(30):34337–34361
130. Kim H et al (2020) Bioresorbable, miniaturized porous silicon needles on a flexible water-soluble backing for unobtrusive, sustained delivery of chemotherapy. *ACS Nano* 14(6): 7227–7236
131. Spink SS et al (2021) High optode-density wearable diffuse optical probe for monitoring paced breathing hemodynamics in breast tissue. *J Biomed Opt* 26:062708
132. Zou W et al (2018) Skin color-specific and spectrally-selective naked-eye dosimetry of UVA, B and C radiations. *Nat Commun* 9(1):1–10
133. Zhang Y-Y et al (2021) High performance flexible visible-blind ultraviolet photodetectors with two-dimensional electron gas based on unconventional release strategy. *ACS Nano* 15(5): 8386–8396
134. Ray PP, Dash D, De D (2017) A systematic review of wearable systems for cancer detection: current state and challenges. *J Med Syst* 41(11):1–12
135. Arathy K, Ansari S, Malini K (2020) High reliability thermistor probes for early detection of breast cancer using skin contact thermometry with thermal imaging. *Mater Express* 10(5): 620–628
136. Mersani A, Osman L, Ribero J (2019) Flexible UWB AMC antenna for early stage skin cancer identification. *Prog Electromagn Res M* 80:71–81
137. Saeidi T et al (2020) Miniaturized spiral UWB transparent wearable flexible antenna for breast cancer detection. In: 2020 international symposium on networks, computers and communications (ISNCC). IEEE, Montreal, pp 1–6
138. Teng F et al (2017) Wearable near-infrared optical probe for continuous monitoring during breast cancer neoadjuvant chemotherapy infusions. *J Biomed Opt* 22(1):014001
139. Bhavya G et al (2019) A study on personalized early detection of breast cancer using modern technology. In: *Emerging research in electronics, computer science and technology*. Springer, pp 355–362
140. Royea R et al (2020) An introduction to the Cyncadia breast monitor: a wearable breast health monitoring device. *Comput Methods Programs Biomed* 197:105758
141. Li D et al (2021) A flexible virtual sensor array based on laser-induced graphene and MXene for detecting volatile organic compounds in human breath. *Analyst* 146(18):5704–5713

142. Liu M et al (2021) Flexible MXene/rGO/CuO hybrid aerogels for high performance acetone sensing at room temperature. *Sens Actuators B* 340:129946
143. Zheng J et al (2021) Pt-decorated foam-like Ga-In bimetal oxide nanofibers for trace acetone detection in exhaled breath. *J Alloys Compd* 873:159813
144. Reddy KCS et al (2021) All solution processed flexible p-NiO/n-CdS rectifying junction: applications towards broadband photodetector and human breath monitoring. *Appl Surf Sci* 568:150944
145. Phan H (2021) Implanted flexible electronics: set device lifetime with smart nanomaterials. *Micromachines* 12(2)
146. Tastanova A et al (2018) Synthetic biology-based cellular biomedical tattoo for detection of hypercalcemia associated with. *Sci Transl Med* 10(437)
147. Bermudez G et al (2019) Implantable highly compliant devices for heating of internal organs: toward cancer treatment. *Adv Eng Mater* 21(9)
148. Li H et al (2021) Biodegradable flexible electronic device with controlled drug release for cancer treatment. *ACS Appl Mater Interfaces* 13(18):21067–21075
149. Wang S et al (2016) Flexible substrate-based devices for point-of-care diagnostics. *Trends Biotechnol* 34(11):909–921
150. Gao W et al (2019) Flexible electronics toward wearable sensing. *Acc Chem Res* 52(3): 523–533
151. Baran D, Corzo D, Blazquez G (2020) Flexible electronics: status, challenges and opportunities. *Front Electron* 1(2)
152. Axisa F et al (2005) Flexible technologies and smart clothing for citizen medicine, home healthcare, and disease prevention. *IEEE Trans Inf Technol Biomed* 9(3):325–336
153. Wang P et al (2020) The evolution of flexible electronics: from nature, beyond nature, and to nature. *Adv Sci* 7(20):2001116
154. Luo Y et al (2020) Devising materials manufacturing toward lab-to-fab translation of flexible electronics. *Adv Mater* 32(37):2001903
155. Palavesam N et al (2020) Influence of flexibility of the interconnects on the dynamic bending reliability of flexible hybrid electronics. *Electronics* 9(2):238
156. Park S et al (2018) Self-powered ultra-flexible electronics via nano-grating-patterned organic photovoltaics. *Nature* 561(7724):516–521
157. Inui T et al (2015) A miniaturized flexible antenna printed on a high dielectric constant nanopaper composite. *Adv Mater* 27(6):1112–1116
158. Bazaka K, Jacob MV (2013) Implantable devices: issues and challenges. *Electronics* 2(1): 1–34
159. Naresh V, Lee N (2021) A review on biosensors and recent development of nanostructured materials-enabled biosensors. *Sensors* 21(4)
160. Fallahi H et al (2019) Flexible microfluidics: fundamentals, recent developments, and applications. *Micromachines* 10(12):830
161. Xu J, Lee H (2020) Anti-biofouling strategies for long-term continuous use of implantable biosensors. *Chemosensors* 8:66
162. Ileana Dumbrava E, Meric-Bernstam F, Yap TA (2018) Challenges with biomarkers in cancer drug discovery and development. *Expert Opin Drug Discov* 13(8):685–690
163. Ludwig JA, Weinstein JN (2005) Biomarkers in cancer staging, prognosis and treatment selection. *Nat Rev Cancer* 5(11):845–856
164. World Health Organization (2010) Medical devices: managing the mismatch: an outcome of the priority medical devices project. World Health Organization
165. Paulovich FV, De Oliveira MCF, Oliveira ON Jr (2018) A future with ubiquitous sensing and intelligent systems. *ACS Sens* 3(8):1433–1438
166. Mohan A (2014) Cyber security for personal medical devices internet of things. In: 2014 IEEE international conference on distributed computing in sensor systems. IEEE



Coupling Micro-Physiological Systems and Biosensors for Improving Cancer Biomarkers Detection

12

Virginia Brancato, Rui L. Reis, and Subhas C. Kundu

Abstract

Early cancer detection is still a major clinical challenge. The development of innovative and noninvasive screening approaches for the detection of predictive biomarkers indicating the stage of the disease could save many lives. Traditional *in vitro* and *in vivo* models are not adequate to copycat the native tumor microenvironment and for the discovery of new biomarkers. Recent advances in microfluidics, biosensors, and 3D cell biology speed up the development of micro-physiological bioengineered systems that improve the discovery of new potential cancer biomarkers. This can accelerate the individualization of cancer treatments leading to precision medicine-oriented approaches that could improve patient prognosis. For this reason, it is necessary to develop point-of-care diagnostic tools that can be user-friendly, miniaturized, and easily translated into clinical practice. This chapter describes how far this new generation of cutting-edge technologies, such as microfluidics, label-free detection systems, and molecular diagnostics, are from being applied in the current clinical practice.

Keywords

Cancer diagnosis · Cancer organoids · Cancer modelling · Biosensors · Microfluidics

V. Brancato (✉) · R. L. Reis · S. C. Kundu

3B's Research Group, I3Bs—Research Institute on Biomaterials, Biodegradables and Biomimetics, University of Minho, Headquarters of the European Institute of Excellence on Tissue Engineering and Regenerative Medicine, Guimarães, Portugal

ICVS/3B's, PT Government Associate Laboratory, Braga/Guimarães, Portugal

e-mail: virginia.brancato@i3bs.uminho.pt

© The Author(s), under exclusive license to Springer Nature Switzerland AG 2022

307

D. Caballero et al. (eds.), *Microfluidics and Biosensors in Cancer Research*,

Advances in Experimental Medicine and Biology 1379,

https://doi.org/10.1007/978-3-031-04039-9_12

12.1 Introduction

The World Health Organization (WHO) estimates cancer is among the first two death causes before the age of 70 years in most countries. Cancer incidence and mortality are also increasing because the main risk factors of cancer are related to socio-economic development [1]. Current methods for cancer detection are ultrasounds, magnetic resonance imaging, and biopsy, all based on cancer morphology. These techniques are helpful but not able to capture the genetic and epigenetic landscape of cancer disease [2]. Biomarkers-based technologies are less invasive and aim to improve early cancer diagnosis and increase the life expectancy from the diagnosis. Early diagnoses make a difference in administrating a more personalized therapy in a shorter time [3]. Currently, researchers and pharmaceutical companies are investing their efforts in developing more efficient sensing technologies for the detection of cancer biomarkers in a more precise, fast, and reliable manner for clinical uses. Biosensors can detect nucleic acids, proteins, metabolites, enzymes, or hormones (Fig. 12.1) [4]. The presence, absence, or perturbation of these biomarkers can contribute to predicting the onset, stage, and/or sub-types of cancer, leading to an improvement of the therapy. For this aim, it is necessary to improve the efficiency and reliability of the detection strategy, and the portability of the tests to enable the clinical translation of the biomarkers. Hence, miniaturized biosensors are the key to making point-of-care testing platforms for improved analytical performance [5]. Next, it is fundamental to improve the relevancy of the tumor models employed for the discovery of predictive biomarkers. In this regard, 3D in vitro models, such as organoids and multicellular spheroids, have demonstrated a superior performance compared to conventional platforms to recapitulate the complexity of

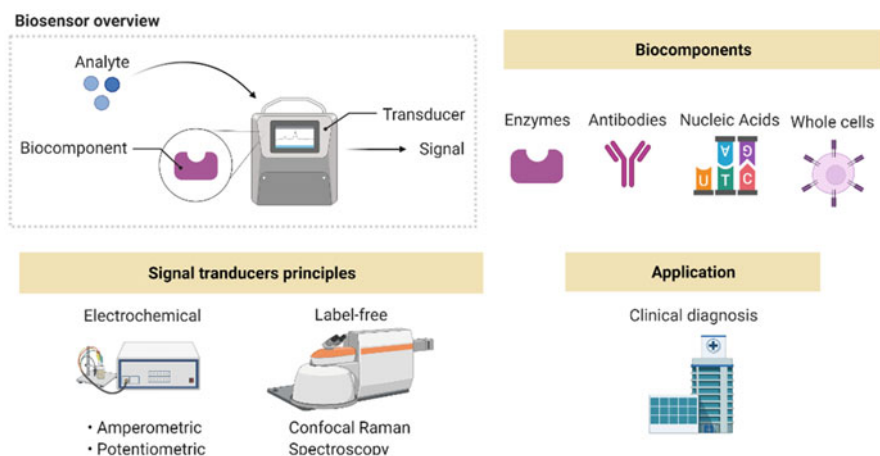


Fig. 12.1 Biosensors overview. A biosensor is a device that measures biochemical reactions by generating a signal that is proportional to the concentration of the analyte of interest. The signal generated is related to metabolites, nucleic acids, pH, and oxygen variation in the biological sample. Created by Biorender

the *in vivo* scenario. As such, they have become the standard for recapitulating human disease or investigating tissue development [6, 7]. When combined with biosensors and dynamic culture platforms, such as microfluidics, these miniaturized physiological systems can expand the discovery of molecules that could be considered as biomarkers in cancer detection [8]. In this chapter, we provide an overview on the integration of 3D tumor models into micro-physiological sensing platforms, and their essential role in the discovery and detection of new cancer biomarkers.

12.2 A New Era of In Vitro Models

Animal models and 2D cell culture have greatly contributed to biomedical research by understanding the key molecular disease pathways. However, they are very limited in reproducing the complexity of the native scenario and the correct response of cells to drugs, besides other bottlenecks. To solve this, micro-physiological systems were developed by combining microfluidic chips with 3D environments made up of natural or biomimetic synthetic matrices encapsulating different cell types. These systems bypass the ethical concerns related to the use of animal models and, at the same time, they copycat cell organization and tissue architecture better than cells culture grown on artificial plastic dishes [9–11]. Indeed, 3D *in vitro* models are replacing 2D culture platforms and animals little by little due to their superior relevance and versatility. Among 3D *in vitro* models, organoids deserve a special mention. They derive from freshly resected human tissues that are processed by mechanical and enzymatic dissociation [12, 13]. Dissociated cells are embedded in hydrogels (mainly Matrigel) and maintained in a growth factors-rich culture medium [14]. The use of organoids in preclinical and clinical trials has increased during the last years, opening new avenues for compound testing *in vitro*. Due to the high correlation between organoids and the original tissue, organoids can play a fundamental role in investigating new biomarkers for cancer detection [15]. Organoids can also be incorporated into a microfluidic chip to mimic the native compartmentalization of different tissue within the human body or to modulate nutrient distribution by the generation of well-controlled gradients [16]. In the following, we highlight several examples on the development and exploitation of organoids, alone and incorporated in microfluidic chips, with particular attention to the strategy for sensing biomarkers that could help cancer detection at an early stage or support the diagnosis.

12.2.1 The Advantage of Miniaturizing Organs in the Microfluidic Chip

Microfluidic technology has been widely exploited for the investigation of a myriad of pathophysiological phenomena. Microfluidic devices represent a versatile platform for studying cell–cell interaction, migration, and drug screening, and importantly, allow precise control over nutrients distribution, pressure, oxygen, and/or

shear stress [17, 18]. Microfluidic devices permit the investigation of the spatial distribution of the cells, and consequently, on the metabolites, ncRNAs, proteins, genes in the cancer tissues, with particular focus on the molecules involved in the mechanisms of extravasation and metastasis [19]. In this section, we briefly highlight how the combination of microfluidics, biosensors, and cancer can contribute to shedding light on the secreted or endogenous molecules. Moreover, the technology exploited to detect these molecules and how microfluidics contributed to this is discussed.

Organoids overcome the oversimplification of the multicellular microenvironment of organs and tissues, as mentioned above. Their physiological relevance allows them to be used as *ex vivo* 3D models that capture partial or complete functions of tissue and organs. Organoids, by definition, are self-organizing 3D cellular structures that copycat the architecture and the cellular composition of an organ or tissue. For almost one century, researchers tried to allow the growth of cells and organs *ex vivo* with some exciting results using sponges, chick embryos, or amphibians. However, in 2009, some researchers managed to grow adult intestinal stem cells in 3D organoids using Matrigel. These cells, expressing that single leucine-rich repeat-containing G protein-coupled receptor 5 (Lgr5), are able to differentiate in crypt-villus structures paving the way for the growth of many other organs and tissue such as stomach, liver, pancreas, lung, kidney, brain, and retina [15]. Organoids have little by little reduced the use of immortalized human cancer cell lines and mouse models, such as patient-derived xenografts since they physiologically resemble tissue heterogeneity and architecture. In addition, when the 3D organoids culture is established in the laboratory, it is cost-effective and less time consuming [20]. For these reasons, in the last decade, tumor organoids, or tumoroids, have exponentially increased their presence in cancer research, starting from colorectal cancer organoids that self-sustain the growth in response to complex and defined culture medium containing growth factors. Nowadays, researchers copycat the morphology and mutational landscape of many cancer types, including breast, gastric, ovarian, bladder, kidney, lung, and prostate. Modern approaches, such as CRISPR-Cas9 and RNA interference, punctual mutations in cancer-driving genes are inserted in wild-type cells in order to recapitulate different stages of cancer progression [21]. When combined with sensing technologies, microfluidic devices enable the continuous monitoring of key metabolic parameters or environmental conditions of the tumor, such as pH, hypoxia, and/or temperature, while controlling the culture conditions and the cellular response to biochemical and biophysical stimuli [22]. Overall, microfluidics provide scalable and reproducible platforms for standardizing the culture, growth, and processing of cancer organoids [23].

12.3 Raman Spectroscopy Application in Biological Samples and In Vitro Organoids-on-Chip Models

Surface-enhanced Raman Spectroscopy (SERS) is an emerging technology for the label-free sensing of molecules obtaining information about their structural and chemical composition [24]. The mechanisms underpinning SERS involve the

amplification of the signal when the molecules are immobilized on metallic nanostructures (typically, gold nanostars), which are illuminated; SERS is generated from the scattered light [25]. One of the challenges in SERS is to drive the molecules in solution to the nanostructures in order to increase the sensitivity. Microfluidics device integrated on a flat silver surface can be employed to increase the sensitivity of the SERS-based detection system. Here, the silver surface with nanoholes is illuminated by mean of a 633-nm laser in order to increase the yields of the SERS signal [26]. This approach could be adopted to grow cells and analyze by SERS their secretome for detecting a transition from normal to tumoral state. Moreover, each molecule in nature can produce its spectral signal. In this way, SERS provides a unique fingerprint for specific molecules [24]. In the last decades, SERS has paved the way for new clinical applications, such as cancer diagnosis, therapy monitoring, and drug screening and testing. The so-called Raman-active molecules can be either lipids, proteins, or nucleic acids that can work as early indicators of a specific physiopathological state. Moreover, when Raman spectroscopy is coupled to patient-derived organoids, it can predict drug efficacy or copycat tumor metabolism and physiology in vitro (Fig. 12.2a) [27]. In the case of 3D tumor models or biological specimens, it is possible to integrate a microscope to the Raman spectroscopy to analyze a specific region of the sample [25]. An interesting example of the clinical application of Raman spectroscopy is the comparison of the blood signatures of healthy and breast cancer patients. It was shown how the spectral bands with higher intensity moved from methionine/tryptophan (amino acids) to phospholipids and guanine. Moreover, it was possible to distinguish the different stages of breast cancer on the basis of the analysis of blood samples [28].

The continuous research addressing the discovery of new targets or compounds in the fight against cancer pushes the improvement of the current technology toward high-throughput screening. For this reason, Raman spectroscopy is a reliable approach for understanding biochemical features of cancer spheroids, in particular, the drug response. The samples do not need pre-treatment, such as fixation or staining that could alter the biochemical profile of the cells. For example, Raman spectroscopy in MCF7 breast cancer spheroids treated with staurosporine, a pro-apoptotic protein kinase inhibitor revealed a significant difference in drug sensitivity when compared to conventional 2D culture. Interestingly, Raman distinguished the presence of microcalcification peaks in spheroids of different ages, showing that this technique can potentially detect the stage of cancer [29].

Raman spectroscopy also supports monitoring the differentiation state of organoids derived from hiPSCs. Changes in glycogen, lipid composition, or cytochrome protein are hallmarks of hiPSCs differentiation that can be detected in fixed samples of these cells to guide the differentiation. Recently, it has been demonstrated that the chromatin status and organization reflect the stage of differentiation of hiPSCs lineage. However, the techniques to analyze chromatin are destructive and not suitable for high-throughput. Liver organoids are made up of a high-throughput system based on an agarose multi-well system. The liver-specific signal pathway is blocked and the differentiation status of the cells is monitored by confocal light absorption and scattering (CLASS) microscopy and Raman spectroscopy that are

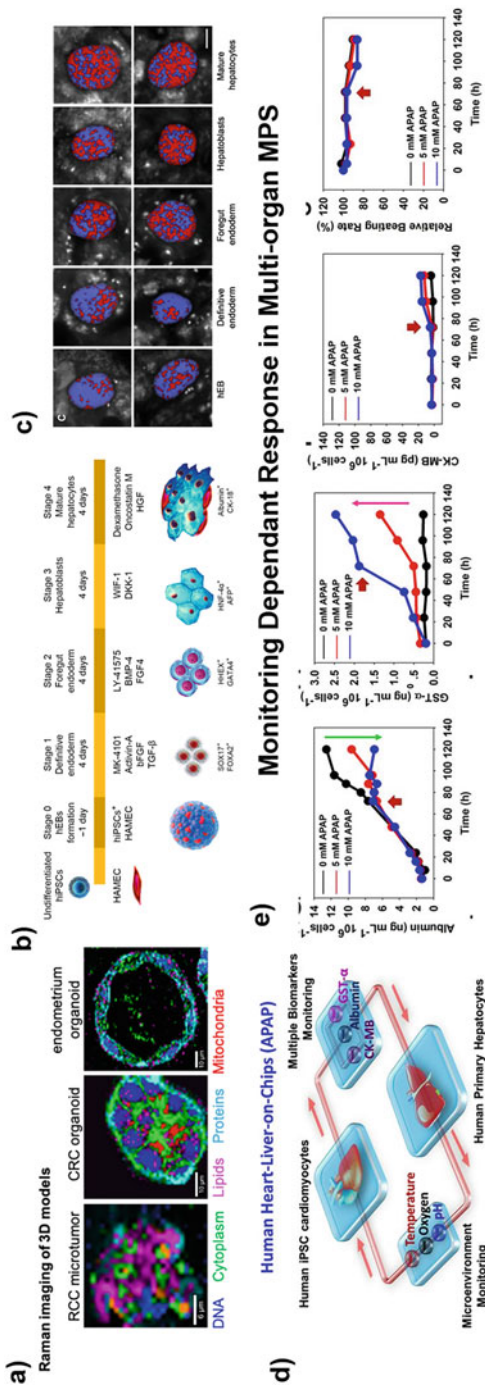


Fig. 12.2 (a) Raman spectroscopy applied to 3D cancer models such as renal cell carcinoma (RCC) microtumors, colorectal cancer (CRC) organoids, and endometrium organoids. The heatmaps are encoded with false color-coded intensity distribution that refers to DNA (blue), cytoplasm (green), lipids (pink), proteins (light blue), and mitochondria (orange/red). Creative common license [27]. (b) Representative graphical protocol of differentiation of hiPSCs to hepatocytes. (c) Representative spatial maps of the chromatin density in live hiPSC organoids at different stages of differentiation. Purple color indicates euchromatin while shades of red indicate heterochromatin. Scale bar, 5 μm. Micrographs (b) and (c) are adapted under Creative common license from [30]. (d) Schematic micrograph of biomimetic human heart-liver-cancer-on-chips with in situ detection of temperature, O₂, and pH. (e) Representative automated electrochemical measurements of albumin and GST-α secreted from hepatocarcinoma organoids, electrochemical measurements of creatine kinase MB from the cardiac tissue, and beat analysis of the cardiac organoids. Adapted under Creative common license from [41]

able to catch the changes in chromatin organization and biochemical composition in the liver organoids in a nondestructive manner (Fig. 12.2b, c) [30].

3D cell cultures, such as spheroids and organoids, are not homogeneous due to the gradient of oxygen and nutrients from the outer to the inner region. It is therefore challenging to map the spatial heterogeneity and predict the differentiation status in 3D. In this regard, microfluidics coupled to Raman can help on promoting and identify the differentiation status of complex tissues. For example, Raman analysis of three peaks corresponding to hydroxyapatite (960 cm^{-1} , an odontogenic differentiation marker), β -carotene ($1156/1528\text{ cm}^{-1}$, precursor of hydroxyapatite), and protein/cellular components (2935 cm^{-1}) helped the recognition of the differentiation status of human dental pulp stem cell spheroids. This study demonstrated that the outer region of the spheroids was mostly subjected to odontogenic differentiation due to the closer and direct exposition to the medium carrying the differentiation factors. Raman spectroscopy allowed the mapping of odontogenic differentiation induced up to 40–50 μm toward the inner part of the spheroids [31].

12.4 Biosensors Integration for Metabolic Read-Out Detection in Organ-on-Chip Platforms

Low cost and short time analysis allow microfluidics to be a valuable approach for detecting metabolites in micro-physiological disease models. However, the complete adoption of these sensor-integrated microfluidic devices will be achieved when they provide user-friendly interfaces that can be utilized by nonspecialized users inside and outside biological laboratories [32, 33]. The first generation of electrochemical biosensors is represented by the analytical devices that transduce biochemical reactions (enzyme–substrate reaction and antigen–antibody ligands) to electrical signals (such as current, voltage, and impedance). In this case, the electrode acts as solid support for the biomolecules' immobilization. It is necessary to maintain the correct orientation of the immobilized enzymes, for example, in order to avoid loss of activity and specificity. One of the challenges is also the choice of the electrode materials that could support this compatibility [34]. The development of biosensors allows the easy monitoring of many different physiological parameters, such as pH, glucose, lactate, oxygen, nitric oxide, and transepithelial electrical resistance. Biosensors can be integrated into 2D and 3D micro-physiological systems enabling static and dynamic detection of single or multiple parameters. Miniaturizing the electrochemical biosensors for on-site analysis with accurate sensitivity and high reproducibility is still a challenge. At this aim, nanomaterials, that present a larger surface area and subsequent higher loading capacity and improved reactants transport, could support the sensor apparatus and increase the performance of the analysis by amplifying the signal. One example of integration between biosensors, 3D cell culture, and bioreactor is given by a model that exploits luminescence-based oxygen sensor beads for the detection of glucose and lactate in spheroids [35]. Another example is provided by a versatile platform relying on tumor spheroids in a microfluidic hanging-drop network with multi-analyte biosensors, where it is

possible to monitor in parallel the temporal evolution of lactate levels and glucose consumption inside the spheroids. The main advantage of this approach is the separation of the sensor unit from the microfluidic chip, offering an easy-to-fabricate modular device [36].

Cell metabolites secretion is altered by extracellular stimuli and by a change in the microenvironmental conditions, such as hypoxia, which could trigger chemotherapy resistance. To better mimic these conditions, a microfluidic chip platform that supports matrix-based organoids culture is integrated into sensitive electrochemical sensors to detect lactate, glucose, and oxygen in response to changes in hypoxia levels. This micro-physiological system allows medium perfusion and continuous parameters monitoring of patient-derived-negative breast cancer cells, a choice that increases the device's physiological impact [37]. One of the main risks of the biosensor-integrated microfluidics platform is the complexity of the fabrication methods and translatability of these devices from the research laboratories to the market. A good example comes from a device that attempts to simplify the detection of toxicology parameters in the cells in response to nanomaterials or nanoparticles stimuli. It is based on a noninvasive optical sensing strategy where luminescent sensor spots (for example, for oxygen and pH) are integrated with a microfluidic chip to detect the changes in cellular response to different stimuli in a dynamic lung cancer environment [38]. The device would replace multi-well plates primarily used in diagnostics to assess cell viability. Another example of how optical sensors facilitate the observation of viable parameters in cancer is given by a microfluidic device able to monitor in real time the oxygen level in hepatocytes for up to 4 weeks. The optical sensor system is based on an immobilized chromophore in polymer beads. The local oxygen concentration is measured using intensity-modulated excitation light since the chromophore phosphofluorescence lifetime is proportional to the oxygen levels. The beads are closely placed into small wells embedded in a collagen matrix inside a dynamic bioreactor for continuous monitoring of oxygen in hepatocytes cell lines and primary cells [39].

Many of the sensors-integrated microfluidic devices can detect biological parameters in 2D that cannot recapitulate some features of cancer progression, such as cell adhesion, growth, and motility. Electrical cell-substrate impedance sensing (ECIS) can detect the electrical alternations between the electrode and the cells in a label-free and not destructive approach. Hence, this technique is gaining much attention in anticancer drug discovery. When ECIS is coupled to microfluidics, it is possible to monitor at a single cell level the 3D migration trajectories. In particular, in a model of breast cancer with invasive MDA-MB-231 or less invasive MCF7 cells, it is possible to follow their migration in real time in Matrigel [40]. Interestingly, an approach integrating electrochemical affinity-based biosensors and microfluidic chips allows the noninvasive quantification of biochemical biomarkers in situ. This approach is possible by sensor regeneration directly in the platform. Usually, the biochemical detection of biomarkers is carried out by ELISA that may not be suitable for miniaturized 3D cell culture, since they use a larger volume of samples in comparison to the microliter volumes of microfluidic chips. Moreover, the advantage of this approach is the possibility to regenerate the

electrochemical sensor up to 25 times [41] (Fig. 12.2d, e). All the reported examples could be translated to clinical routine using primary cells or organoids. Still, one necessary condition should be the simplification of these systems with user-friendly interfaces.

12.5 Future Perspectives and Conclusion

The description of the state-of-the-art approaches in the field of viable biosensing parameters in the cancer microenvironment leads to a critical question: when will these biosensors-integrated devices become portable and routinely used in diagnostic laboratories around the world? The progress in the technology underpinning consumer electronics (e.g., smartphones, tablets, or Google glasses) will positively impact the development of innovative point-of-care devices. The integration of microfluidics and biosensors is still far from reaching a straightforward design due to the need for imaging or optical equipment typically found in an advanced laboratory. We envision that the future of point-of-care devices should rely on platforms that allow sample preparation and analysis *in situ* preferentially in an automated manner. This chapter described how exploiting 3D tumor models, primary spheroids, and organoids, improves the read-outs of biosensor-integrated microfluidic platforms pushing toward more physiological data from *in vitro* screening. This approach shortens the gap between the scientific laboratories and the point-of-care diagnostic market. Moreover, the miniaturization of sensors and the possibility of using them in parallel in microfluidic devices pave the way to adopting electrochemical biosensors as the most interesting integrated micro-physiological system for viable biosensing parameters.

Author Contribution VB: conceptualization, writing original draft, funding acquisition. SCK: supervision; writing-review and editing. RLR: supervision, funding acquisition, writing-review and editing.

Funding This work was supported by EU-Horizon 2020 grant FoReCaST—Forefront Research in 3D Disease Cancer Models as *in vitro* Screening Technologies (H2020-WIDESPREAD-2014-668983). V.B. and S.C.K. also acknowledge the Fundação para a Ciência e a Tecnologia (FCT) for financial support (PTDC/BTM-ORG/28168/2017).

Conflict of Interest The authors declare that the research was conducted without any commercial or financial relationships that could represent a potential conflict of interest.

References

1. Sung H, Ferlay J, Siegel RL, Laversanne M, Soerjomataram I, Jemal A, Bray F (2021) Global cancer statistics 2020: GLOBOCAN estimates of incidence and mortality worldwide for 36 cancers in 185 countries. *CA Cancer J Clin* 71:209–249. <https://doi.org/10.3322/caac.21660>

2. Jayanthi VSPKSA, Das AB, Saxena U (2017) Recent advances in biosensor development for the detection of cancer biomarkers. *Biosens Bioelectron* 91:15–23. <https://doi.org/10.1016/j.bios.2016.12.014>
3. Dwivedi S, Purohit P, Misra R, Pareek P, Goel A, Khattri S, Pant KK, Misra S, Sharma P (2017) Diseases and molecular diagnostics: a step closer to precision medicine. *Indian J Clin Biochem* 32:374–398. <https://doi.org/10.1007/s12291-017-0688-8>
4. Zarei M (2017) Advances in point-of-care technologies for molecular diagnostics. *Biosens Bioelectron* 98:494–506. <https://doi.org/10.1016/j.bios.2017.07.024>
5. Rebelo R, Barbosa AI, Caballero D, Kwon IK, Oliveira JM, Kundu SC, Reis RL, Correlo VM (2019) 3D biosensors in advanced medical diagnostics of high mortality diseases. *Biosens Bioelectron* 130:20–39. <https://doi.org/10.1016/j.bios.2018.12.057>
6. Brancato V, Oliveira JM, Correlo VM, Reis RL, Kundu SC (2020) Could 3D models of cancer enhance drug screening? *Biomaterials* 232:119744. <https://doi.org/10.1016/j.biomaterials.2019.119744>
7. Malik M, Yang Y, Fathi P, Mahler GJ, Esch MB (2021) Critical considerations for the design of multi-organ microphysiological systems (MPS). *Front Cell Dev Biol* 9:1–18. <https://doi.org/10.3389/fcell.2021.721338>
8. Modena MM, Chawla K, Misun PM, Hierlemann A (2018) Smart cell culture systems: integration of sensors and actuators into microphysiological systems. *ACS Chem Biol* 13:1767–1784. <https://doi.org/10.1021/acscchembio.7b01029>
9. Burden N, Chapman K, Sewell F, Robinson V (2015) Pioneering better science through the 3Rs: an introduction to the national centre for the replacement, refinement, and reduction of animals in research (NC3Rs). *J Am Assoc Lab Anim Sci* 54:198–208
10. Antoni D, Burckel H, Josset E, Noel G (2015) Three-dimensional cell culture: a breakthrough in vivo. *Int J Mol Sci* 16:5517–5527. <https://doi.org/10.3390/ijms16035517>
11. Peck Y, Wang D-A (2013) Three-dimensionally engineered biomimetic tissue models for *in vitro* drug evaluation: delivery, efficacy and toxicity. *Expert Opin Drug Deliv* 10:369–383. <https://doi.org/10.1517/17425247.2013.751096>
12. Clevers H (2016) Modeling development and disease with organoids. *Cell* 165:1586–1597. <https://doi.org/10.1016/j.cell.2016.05.082>
13. Sachs N, de Ligt J, Kopper O, Gogola E, Bounova G, Weeber F, Balgobind AV, Wind K, Gracanin A, Begthel H, Korving J, van Boxtel R, Duarte AA, Lelieveld D, van Hoeck A, Ernst RF, Blokzijl F, Nijman IJ, Hoogstraal M, van de Ven M, Egan DA, Zinzalla V, Moll J, Boj SF, Voest EE, Wessels L, van Diest PJ, Rottenberg S, Vries RGJ, Cuppen E, Clevers H (2017) A living biobank of breast cancer organoids captures disease heterogeneity. *Cell*:1–14. <https://doi.org/10.1016/j.cell.2017.11.010>
14. Lancaster MA, Knoblich JA (2014) Organogenesis in a dish: modeling development and disease using organoid technologies. *Science* 345(6194):1247125. <https://doi.org/10.1126/science.1247125>
15. Corrà C, Novellademunt L, Li VSW (2020) A brief history of organoids. *Am J Physiol Cell Physiol* 319:C151–C165. <https://doi.org/10.1152/ajpcell.00120.2020>
16. Benam KH, Dauth S, Hassell B, Herland A, Jain A, Jang K-J, Karalis K, Kim HJ, MacQueen L, Mahmoodian R, Musah S, Torisawa Y, van der Meer AD, Villenave R, Yadid M, Parker KK, Ingber DE (2015) Engineered *in vitro* disease models. *Annu Rev Pathol Mech Dis* 10:195–262. <https://doi.org/10.1146/annurev-pathol-012414-040418>
17. Peela N, Truong D, Saini H, Chu H, Mashaghi S, Ham SL, Singh S, Taviana H, Mosadegh B, Nikkha M (2017) Advanced biomaterials and microengineering technologies to recapitulate the stepwise process of cancer metastasis. *Biomaterials* 133:176–207. <https://doi.org/10.1016/j.biomaterials.2017.04.017>
18. Caballero D, Kaushik S, Correlo VM, Oliveira JM, Reis RL, Kundu SC (2017) Organ-on-chip models of cancer metastasis for future personalized medicine: from chip to the patient. *Biomaterials* 149:98–115. <https://doi.org/10.1016/j.biomaterials.2017.10.005>

19. Ayuso JM, Park KY, Virumbrales-Muñoz M, Beebe DJ (2021) Toward improved in vitro models of human cancer. *APL Bioeng* 5:1–7. <https://doi.org/10.1063/5.0026857>
20. Aberle MR, Burkhardt RA, Tiriak H, Olde Damink SWM, Dejong CHC, Tuveson DA, van Dam RM (2018) Patient-derived organoid models help define personalized management of gastrointestinal cancer. *Br J Surg* 105:e48–e60. <https://doi.org/10.1002/bjs.10726>
21. Zhang YS, Zhang YN, Zhang W (2017) Cancer-on-a-chip systems at the frontier of nanomedicine. *Drug Discov Today* 22:1392–1399. <https://doi.org/10.1016/j.drudis.2017.03.011>
22. Bhatia SN, Ingber DE (2014) Microfluidic organs-on-chips. *Nat Biotechnol* 32:760–772. <https://doi.org/10.1038/nbt.2989>
23. Sontheimer-Phelps A, Hassell BA, Ingber DE (2019) Modelling cancer in microfluidic human organs-on-chips. *Nat Rev Cancer* 19:65–81. <https://doi.org/10.1038/s41568-018-0104-6>
24. Lee H, Xu L, Koh D, Nyayapathi N, Oh KW (2014) Various on-chip sensors with microfluidics for biological applications. *Sensors* 14:17008–17036. <https://doi.org/10.3390/s140917008>
25. Uzunbajakava N, Lenferink A, Kraan Y, Willekens B, Vrensen G, Greve J, Otto C (2003) Nonresonant Raman imaging of protein distribution in single human cells. *Biopolym Biospectroscopy Sect* 72:1–9. <https://doi.org/10.1002/bip.10246>
26. Vlasko-Vlasov V, Joshi-Imre A, Bahns JT, Chen L, Ocola L, Welp U (2010) Liquid cell with plasmon lenses for surface enhanced Raman spectroscopy. *Appl Phys Lett* 96. <https://doi.org/10.1063/1.3429605>
27. Becker L, Janssen N, Layland SL, Mürdter TE, Nies AT, Schenke-Layland K, Marzi J (2021) Raman imaging and fluorescence lifetime imaging microscopy for diagnosis of cancer state and metabolic monitoring. *Cancers (Basel)* 13. <https://doi.org/10.3390/cancers13225682>
28. Nargis HF, Nawaz H, Ditta A, Mahmood T, Majeed MI, Rashid N, Muddassar M, Bhatti HN, Saleem M, Jilani K, Bonnier F, Byrne HJ (2019) Raman spectroscopy of blood plasma samples from breast cancer patients at different stages. *Spectrochim Acta A Mol Biomol Spectrosc* 222: 117210. <https://doi.org/10.1016/j.saa.2019.117210>
29. Jamieson LE, Harrison DJ, Campbell CJ (2019) Raman spectroscopy investigation of biochemical changes in tumor spheroids with aging and after treatment with staurosporine. *J Biophotonics* 12. <https://doi.org/10.1002/jbio.201800201>
30. Pettinato G, Coughlan MF, Zhang X, Chen L, Khan U, Glyavina M, Sheil CJ, Upputuri PK, Zakharov YN, Vitkin E, D'Assoro AB, Fisher RA, Itzkan I, Zhang L, Qiu L, Perelman LT (2021) Spectroscopic label-free microscopy of changes in live cell chromatin and biochemical composition in transplantable organoids. *Sci Adv* 7. <https://doi.org/10.1126/sciadv.abj2800>
31. Kim H, Han Y, Suhito IR, Choi Y, Kwon M, Son H, Kim HR, Kim TH (2021) Raman spectroscopy-based 3D analysis of odontogenic differentiation of human dental pulp stem cell spheroids. *Anal Chem* 93:9995–10004. <https://doi.org/10.1021/acs.analchem.0c05165>
32. Nair MP, Teo AJT, Li KHH (2022) Acoustic biosensors and microfluidic devices in the decennium: principles and applications. *Micromachines* 13. <https://doi.org/10.3390/mi13010024>
33. Signore MA, De Pascali C, Giampetruzzi L, Siciliano PA, Francioso L (2021) Gut-on-chip microphysiological systems: latest advances in the integration of sensing strategies and adoption of mature detection mechanisms. *Sens Bio-Sensing Res* 33:100443. <https://doi.org/10.1016/j.sbsr.2021.100443>
34. Cho IH, Kim DH, Park S (2020) Electrochemical biosensors: perspective on functional nanomaterials for on-site analysis. *Biomater Res* 24:1–12. <https://doi.org/10.1186/s40824-019-0181-y>
35. Bavli D, Prill S, Ezra E, Levy G, Cohen M, Vinken M, Vanfleteren J, Jaeger M, Nahmias Y (2016) Real-time monitoring of metabolic function in liver-onchip microdevices tracks the dynamics of mitochondrial dysfunction. *Proc Natl Acad Sci U S A* 113:E2231–E2240. <https://doi.org/10.1073/pnas.1522556113>

36. Misun PM, Rothe J, Schmid YRF, Hierlemann A, Frey O (2016) Multi-analyte biosensor interface for real-time monitoring of 3D microtissue spheroids in hanging-drop networks. *Microsystems Nanoeng* 2. <https://doi.org/10.1038/micronano.2016.22>
37. Dornhof J, Kieninger J, Muralidharan H, Maurer J, Urban GA, Weltin A (2022) Microfluidic organ-on-chip system for multi-analyte monitoring of metabolites in 3D cell cultures. *Lab Chip*. <https://doi.org/10.1039/d1lc00689d>
38. Zirath H, Spitz S, Roth D, Schellhorn T, Rothbauer M, Müller B, Walch M, Kaur J, Wörle A, Kohl Y, Mayr T, Ertl P (2021) Bridging the academic-industrial gap: application of an oxygen and pH sensor-integrated lab-on-a-chip in nanotoxicology. *Lab Chip* 21:4237–4248. <https://doi.org/10.1039/d1lc00528f>
39. Gehre C, Flechner M, Kammerer S, Küpper JH, Coleman CD, Püschel GP, Uhlig K, Duschl C (2020) Real time monitoring of oxygen uptake of hepatocytes in a microreactor using optical microsensors. *Sci Rep* 10:1–12. <https://doi.org/10.1038/s41598-020-70785-6>
40. Nguyen TA, Yin TI, Reyes D, Urban GA (2013) Microfluidic chip with integrated electrical cell-impedance sensing for monitoring single cancer cell migration in three-dimensional matrixes. *Anal Chem* 85:11068–11076. <https://doi.org/10.1021/ac402761s>
41. Zhang YS, Aleman J, Shin SR, Kilic T, Kim D, Mousavi Shaegh SA, Massa S, Riahi R, Chae S, Hu N, Avci H, Zhang W, Silvestri A, Sanati Nezhad A, Manbohi A, De Ferrari F, Polini A, Calzone G, Shaikh N, Alerasool P, Budina E, Kang J, Bhise N, Ribas J, Pourmand A, Skardal A, Shupe T, Bishop CE, Dokmeci MR, Atala A, Khademhosseini A (2017) Multisensor-integrated organs-on-chips platform for automated and continual in situ monitoring of organoid behaviors. *Proc Natl Acad Sci* 114:E2293–E2302. <https://doi.org/10.1073/pnas.1612906114>



Microfluidic Biosensor-Based Devices for Rapid Diagnosis and Effective Anti-cancer Therapeutic Monitoring for Breast Cancer Metastasis

13

V. S. Sukanya and Subha Narayan Rath

Abstract

Breast cancer with unpredictable metastatic recurrence is the leading cause of cancer-related mortality. Early cancer detection and optimized therapy are the principal determining factors for increased survival rate. Worldwide, researchers and clinicians are in search of efficient strategies for the timely management of cancer progression. Efficient preclinical models provide information on cancer initiation, malignancy progression, relapse, and drug efficacy. The distinct histopathological features and clinical heterogeneity allows no single model to mimic breast tumor. However, engineering three-dimensional (3D) in vitro models incorporating cells and biophysical cues using a combination of organoid culture, 3D printing, and microfluidic technology could recapitulate the tumor microenvironment. These models serve to be preferable predictive models bridging the translational research gap in drug development. Microfluidic device is a cost-effective advanced in vitro model for cancer research, diagnosis, and drug assay under physiologically relevant conditions. Integrating a biosensor with microfluidics allows rapid real-time analytical validation to provide highly sensitive, specific, reproducible, and reliable outcomes. In this manner, the multi-system approach in identifying biomarkers associated with cancer facilitates early detection, therapeutic window optimization, and post-treatment evaluation.

This chapter showcases the advancements related to in vitro breast cancer metastasis models focusing on microfluidic devices. The chapter aims to provide an overview of microfluidic biosensor-based devices for cancer detection and high-throughput chemotherapeutic drug screening.

V. S. Sukanya · S. N. Rath (✉)

Regenerative Medicine and Stem Cell Laboratory (RMS), Department of Biomedical Engineering, Indian Institute of Technology Hyderabad, Sangareddy, Telangana, India
e-mail: subharath@bme.iith.ac.in

Keywords

Breast cancer · Microfluidics · Biosensors · In vitro 3D cancer models · Biomarkers · Therapeutic drug monitoring

13.1 Introduction

Breast cancer (BC) is the most frequently diagnosed cancer, with an estimated 2.3 million new cases worldwide [1]. Metastasis accounts for over 90% of fatality in cancer patients. The differences in tissue origin, the extent of invasiveness, tumor grade, lymph node status, and the presence of known predictive markers are correlated for BC screening, diagnosis, and chemotherapy regimen.

Although there is a plethora of information on breast cancer, the contributing factors for the transformation into invasive form and later into metastasis are still unclear. The profound understanding of cancer progression influences clinical assessments and drug discovery. Traditionally, preclinical studies are based on two-dimensional (2D) in vitro culture models using human breast cancer cell lines and animal models. But they lack the physiological resemblance of human tumor. Microfluidic system is an advanced model incorporating multicellular compartmentalization combined with physio-biochemical factors. Adaptation of biosensors integrated with microfluidics provides highly sensitive and specific quantitative measurements within a clinically relevant time frame.

In this chapter, we first describe the major regulating factors involved in breast cancer metastasis. Followed by a brief description of various in vitro breast tumor model systems, we move on to an elaborate discussion on microfluidic devices. In this section, we look into the recent applications of microfluidic systems in breast cancer metastasis and their implications in anti-cancer drug studies. Next, we will dive into the understanding of biosensors and its applicability integrated with microfluidics. We end the chapter with a brief description of the challenges and future perspectives of biosensor-based microfluidic platforms for advanced cancer diagnostics and chemotherapeutic monitoring.

13.1.1 Key Regulators in Breast Cancer Metastasis

Breast cancer metastasizes to bone, lung, liver, and brain. Paget describes the process of metastasis with the “seed and soil” hypothesis, highlighting the influence of the microenvironment in determining cancer cell fate at the primary or metastatic site [2]. The rate-limiting steps involved in this metastatic cascade are survival of cancer cells in the vasculature (hematogenous or lymphatic) and homing of cells for tumorigenesis in the secondary site [3]. The following section brief the importance of identification and understanding of mediators in the metastatic cascade, which aids in the sequential management of metastatic breast cancer patients.

13.1.1.1 Extracellular Matrix (ECM)

The ECM acts as a scaffold that provides biochemical and mechanical cues for cells. The plethora of ECM proteins alters the cell adhesion, proliferation, apoptosis, dormancy, and stemness of tumor cells. For example, increased levels of glycosaminoglycan hyaluronan are associated with tumor progression and poor prognosis [4]. A case study predicted the risk of breast cancer distant metastasis using tumor microenvironment of metastasis score independent of the histological score [5]. A quantitative mass spectrometric analysis of ECM exhibited distinct ECM-associated proteins in different metastatic organs. This study proved the importance of niche-specific ECM protein in metastatic tropism by knockdown of SERPINB1 (serine protease suicide inhibitor family), leading to a reduction in brain metastasis [6].

13.1.1.2 Intravasation and Extravasation

The epithelial-mesenchymal transition (EMT) mechanisms drive cells toward a migratory phenotype. The master mediators for the EMT notably, the transcription factors TWIST, SNAIL, and SLUG have proven clinical relevance [7]. The cancer cells found in blood samples are called circulating tumor cells (CTCs). Studies indicate the presence of CTCs as a prognostic marker of metastatic advancement and relapse [8]. The clinical validation of CTCs is challenged by its scarcity in the sample (1 CTC/7.5 mL of blood) [9].

13.1.1.3 Colonization or Mesenchymal-Epithelial Transition (MET)

The exact mechanisms underlying metastatic organotropism are still elusive. The reverse of EMT promotes colonization. However, a substantial number of studies reveal the contribution of cytokines, chemokines, metalloproteinases, and angiogenic factors in tissue tropism [10]. The disseminated tumor cells (DTCs) are mostly inefficient to transform into a metastatic lesions. The foreign stroma composition, cytokines, and immune threats challenge DTCs toward their colonization. Bone metastatic breast cancer cells hijack homeostasis of osteoblasts and osteoclasts, resulting in tumor outgrowth and bone resorption. The main players of the vicious cycle of tumor progression include parathyroid hormone-related protein (PTHrP)/RANK-L, insulin-like growth factor-1 (IGF-1), osteopontin (OPN), jagged1 (JAG1) with interleukins (IL-6, IL-8, IL-11) and matrix metalloproteinases (MMPs) [11]. The breast-derived tumor cells on reaching the brain activate astrocytes initiating oncogenic signaling via IL-1, IL-3, IL-6, tumor necrosis factor- α (TNF- α), platelet-derived growth factor (PDGF), and transforming growth factor-beta (TGF- β) [10].

13.1.1.4 Immune System

Successful metastatic derivatives have the potential to overcome the immune regulatory mechanisms. Largely immunology studies focus on primary cancer lesions. Deciphering the complex crosstalk of the immune system and secondary site-specific tumor microenvironment may aid in the development of new immunotherapies and immunoassays targeting metastatic tumors. The assessment of transcriptomic profiles and pathological data revealed the site-specific immune changes from

primary to metastatic tumor [12]. The programmed death protein-1 (PD-1) and its ligand (PDL-1) status difference in primary and metastatic lymph nodes helps to evaluate immunotherapy. The PD-1/PD-L1 positive expression in metastatic lymph nodes shows an association with poor prognostic features including a high Ki-67 index, a high TNM stage, a large number of metastatic lymph nodes, and a high histology grade [13].

13.2 Breast Tumor Modeling

The development of experimental models enhances the understanding of the mechanisms in cancer biology and functions as a platform for testing drugs. A multi-system approach to recapitulate the complexity of the disease condition could improve studies unraveling the molecular mechanisms of breast cancer metastasis. Studies confirm the relevance of using 3D cell cultures over 2D monolayer cultures [14, 15]. Elaborate evidence on the role of stroma influencing the tumor behavior and dissemination of cells necessitated a three-dimensional (3D) model to allow stromal, multicellular interaction within a dynamic extracellular matrix (ECM). After successful in vitro tests, the drugs are subjected to animal models, primarily in rodents despite the inter-species variation. Patient-derived xenograft (PDX) models are generated by transplanting and expanding primary tumor fragments or cells in an immunocompromised murine host. They are used in preclinical settings as they preserve patient-specific tumor characteristics. The standardization, nonhuman matrix components, and unknown effects from immune checkpoints restrict the broad applicability of PDX models [16]. Furthermore, in vivo animal models face challenges in understanding biomechanical cues, visualizing the specific metastatic pathway, and lacking temporal resolution. In vitro 3D cancer models; spheroids or organoids derived from patient cells or commercially available cell lines within ECM/scaffold provide physico-biochemical cues that mimic cancer tissue. The development of microfluidic technology allows multicellular culture incorporating fluid flow, vasculature, mechanical cues within specific ECM under controlled experimental variables.

This section briefly looks into 3D in vitro systems classified as non-microfluidic and microfluidic models (Fig. 13.1). The non-microfluidic system includes spheroids, engineered naturally derived or synthetic scaffolds, ex vivo tissues, and organoids. Further, we detail the application of microfluidic technology in breast cancer biology and therapeutics.

13.2.1 Non-microfluidic 3D Models

Spheroid-based models are the most used 3D tumor system. Spheroids are self-assembled cell aggregates of single tumor cells or co-cultures. Technologies like hanging drop, gel embedding, suspension culture, and nonadherent surface methods are used for spheroid generation [19]. The core of a spheroid contains limited oxygen

[24]. A 3D bioprinted model established using dual hydrogel-based bioinks with adipose-derived mesenchymal stem cells and primary breast cancer cells allowed the examination of doxorubicin (DOX) resistance [25]. A few downsides of employing these materials involve the complexity of preparing compatible materials, batch to batch variation, reproducibility, unpredictable results, and low scalability. Another critical factor is the suitability of the mechanical property of material for cellular compatibility and behavior with the downstream application for drug response [26].

Ex vivo tumor slices represent the direct tumor of a patient. The tissue could be either derived from explanted patient-derived primary and metastatic tumor tissues or patient-derived xenografts. This model contributes to a more personalized therapeutic approach. One drawback of the *ex vivo* culture model is its limited application for functional studies. A recent study proved the feasibility of a functional test for the analysis of homologous recombination status in metastatic biopsy specimens [27]. *Ex vivo* triple-negative breast cancer specimens maintained in the bioreactor system allow cell viability up to 3 weeks. Upon treatment with PDL-1 and anti-cytotoxic T lymphocyte-associated protein (CTLA-4) showed a marked reduction in the number of viable cancer cells after 7 days, whereas the lymphocytes and normal breast tissue were intact [28]. This system lacks reproducible results as all slices will have different compositions of cells and require advanced imaging algorithms for data interpretation. The availability of tumor tissue always remains an issue for conducting detailed studies.

Organoids are 3D cell systems with self-renewal and self-organization capability. Organoids are cultured from biopsy tissue, embryonic body, or pluripotent stem cells using extracellular matrix (such as Matrigel or collagen gel) and the air-liquid interface method [29]. Sachs et al. proved the robust generation of BC organoids from various breast cancer subtypes exhibiting intact histological and genetic heterogeneity. This model can be used for studying patient-specific responses to chemotherapeutic drugs [30]. The standardized organoid culture conditions are still poorly understood.

13.2.2 Microfluidic Model: Breast Cancer-on-Chip

Microfluidic system has microchannels or microchambers (10–1000 μm) dealing with small sample volumes from microliters (10^{-6} L) to femtolitres (10^{-15} L) hence reducing the reagent utilization and supporting automated high-throughput analysis [31, 32]. Microfluidic system offers static and dynamic culture conditions in spatio-temporal manner. In static, growth media is provided once with sufficient intermittent change when there is nutrient depletion. In dynamic, the growth media is perfused in a controlled and continuous manner. Therefore, the devices can generate concentration gradients of drug combination with real-time monitoring [33]. Microfabrication adopts a direct or replica approach. The device manufacturing can involve chemical, mechanical, laser-based processes for low volume production (casting, lamination, laser ablation, 3D printing) and high-volume production (hot embossing, injection molding, and film or sheet operations) elaborated in various review articles [34, 35]. Most of the microfluidic devices used for *in vitro* models are

fabricated by soft lithography. The accessibility and affordability of 3D printing technology allowed the generation of 3D printed microfluidic devices. Here, we explain various applications by classifying microfluidic devices into conventional and 3D printed microchips.

13.2.2.1 Conventional Microchips

Soft lithography involves the fabrication of master and then transfer of master pattern on polymers such as polydimethylsiloxane (PDMS). This technique allows the incorporation of micro-nano scale design with high resolution [36]. Further investigations are needed to explore the use of polymeric materials in microfluidics for better microfabrication output allowing bright-field microscopy of cells [37]. The diverse design patterns allow co-culture of cells which provides insight on invasion, extravasation, micro-metastasis, and mechano-regulation. For example, a recent study induced mechanical stimuli by oscillatory fluid flow (1 Pa, 1 Hz) for osteocytes and proved that loading reduced breast cancer bone metastasis by calculating the distance and percentage of extravasation in a microfluidic device [38]. Microfluidics offers the opportunity to include 3D structures. The devices with 3D lumen embedded in an ECM gel assisted to study the conditioning effect of breast cancer cells on lymphatic vessels [39]. A perfusion-based microfluidic OrganoPlate® platform embedded with ECM allows the simultaneous culture of 96 microtissues to simplify the appropriate therapy selection [40]. A microfluidic device engineered by Nashimoto et al. recapitulates tumor vasculature that enables long-term perfusion culture of the MCF 7 spheroids (>24 h) with drug administration. The authors claimed the importance of continuous nutrients and oxygen support for a drug screening platform [41]. Combination of organoid culture with microfluidics established organs-on-a-chip platforms. Organ-on-a-chip is a promising tool mimicking structural and functional characteristics of native tumor organs with tissue-tissue interactions. A microfluidic device developed using tumor cells or patient-derived tumor organoids with quiescent perfused microvascular network proved the feasibility to assess the impact of chemotherapeutics (paclitaxel) and anti-angiogenics (bevacizumab) within a clinically relevant time period of 1–2 weeks [42].

The requirement of cleanroom facility, high expense, and time required for fabrication of microfluidics limits the mass production required for clinical management.

13.2.2.2 3D Printed Microchips

3D printing of microfluidic devices reduces the fabrication time from several days to hours. The basic manufacturing approaches for 3D printing are direct, mold-based, modular, and hybrid printing. Mehta et al. give a detailed review on these approaches using various additive manufacturing materials [43]. This technology allows rapid, inexpensive, and customized fabrication of functional components with good resolution. For instance, a recent study reported the fabrication of PDMS microchannel scaffolds having 350 μm to 100 μm resolution in width by 3 D printing at a cost less than USD 1.50 for a 5000-piece module library [44]. Bioprinting with microfluidics allows the printing of multiple cells in 3D micropatterns with good spatial resolution

and reproducibility for mapping tumor heterogeneity [24]. A microfluidic device with spatially confined 3D photopatterned mixture of endothelial cells and cancer spheroids within a gelatin methacrylate hydrogel allowed monocyte interaction on T-cell recruitment [45]. 3D printing allows rapid change in design according to the application. The optimization of surface area and fluid flow (optimal rate of 1 mL/h) in the inner design of 3D printed microfluidic device demonstrated an increased capture efficiency of CTCs from blood samples [46]. In another study, a 3D printed microfluidic device enriched CTCs without relying on tumor-specific markers from whole blood samples (Fig. 13.2). The CTC capture efficiency was enhanced by negative depletion of white blood cells through immuno-functionalization of surface with anti-CD45 combined with microfiltration (pore-size 3 μm) [47]. Microparticle and nanoparticles synthesized in microfluidics by taking advantage of precise control over fluid mixing have proven high drug loading with no batch variability and improve anti-cancer drug delivery systems. For instance, an alginate microgel formed by a 3D printed microfluidic chip with a diffusion mixing pattern displayed

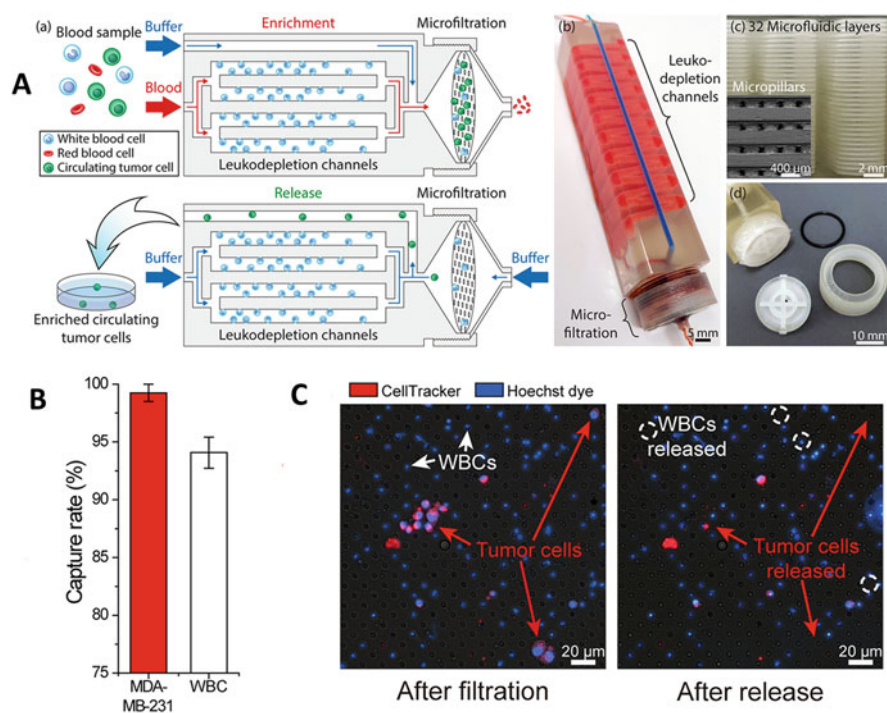


Fig. 13.2 3D-printed microfluidic device for isolation of circulating tumor cells (CTCs) from peripheral blood. (a) Schematics and photo of the microfluidic device depicting the negative enrichment principle. (b) Tumor cell capture efficiency of the microfilter system ($\sim 99\%$). (c) Fluorescence images show retention of white blood cells (WBC) on filter while tumor cells are released with optimal reverse flow. Source: Reprinted from [47] under the Creative Commons Attribution 4.0 International Public License

optimum loading efficiency of DOX [48]. A recent study revealed a novel method to prepare a biomimetic metal-organic nanoparticle formulation for disulfiram-based anti-cancer therapy [49].

The printability of materials and resolution limits the potential of 3D printing microfluidic devices. Unfavorable surface properties of materials post printing (surface roughness, optical transparency, etc.) may perturb specific biological applications. Most of the 3D-printed microfluidic channel sizes are in the millimeters range owing to printer parameters (motor step size, printing speed, nozzle diameter, pixel size, etc.) [43].

13.3 Biosensor Application in Breast Cancer

The early cancer diagnosis is a critical factor for survival rate. Traditionally cancer detection is based on imaging tests through computed tomography (CT), X-ray, positron emission tomography (PET), and nuclear magnetic resonance imaging (NMRI). The widely used diagnosis method is the immune histochemical/compatibility (IHC) analysis of biopsy samples [16]. The microarray gene expression technology and immunoassay (such as enzyme-linked immunosorbent—ELISA) are the two high-throughput diagnosis tools based on the detection of cancer biomarkers [16]. Though, they facilitate a successful outcome; it is a labor-intensive, time-consuming, and expensive procedure. Also, one cannot deny the incorrect interpretation of data due to false-positive results. A platform with rapid sensitivity for the detection of tumor-associated biomolecules would overcome the challenges in early cancer diagnosis.

A biosensor is an analytical device with a biochemical recognition element integrated with a transducer. Previous articles have provided detailed reviews on the evolution of biosensors and its applications in biomedical research and healthcare [50, 51]. A biosensor consists of three main components: a biomarker (target molecule), a bioreceptor (recognition element), and biotransducer components (translates the chemical signal into the measurable physical signal, such as electrical, optical, etc.), together it gives a precise diagnostic output [52]. A biosensor requires sensitivity and selectivity toward the target analyte, optimum response time, linearity, and reproducibility of measured results [53]. One of the critical parameters to check the application of a biosensor is the limit of detection (LOD).

13.3.1 Biomarkers

The widely accepted definition of a biomarker is “a characteristic that is objectively measured and evaluated as an indicator of normal biological processes, pathogenic processes, or pharmacologic responses to a therapeutic intervention” [54]. Biomarkers can be molecular, cellular, and physiological, which can be present in a cell or extracellular. The quantitative variation of the biomarkers between healthy

individuals and cancer patients indicates the disease condition or therapy outcome. The progression in multi-omics (genomics, transcriptomics, proteomics, metabolomics) provided the opportunity of identification and validation of various clinically relevant tumor markers. The conventional clinical scheme checks for the expression of estrogen receptor (ER), progesterone receptor (PR), and human epidermal growth factor receptor 2 (HER-2), Ki-67 allowing to distinguish the three major BrCa phenotypes (luminal A, luminal B, and TNBC) [55]. The relevant breast cancer-related biomolecules include the following [55, 56]:

- *Glycoproteins*—mucin 1 (MUC1), HER2, carcinoembryonic antigen (CEA), epidermal growth factor receptor (EGFR), carbohydrate antigen 15-3 (CA15-3), CA 27-29, mammaglobin (MAM), and epithelial cell adhesion molecule (EpCAM)
- *Genes*—BReast CAncer types (BRCA1, BRCA2)
- *Micro RNAs*—upregulation of miR-16, miR-21, miR-222, and miR-155. downregulation of miR-145, miR-125b, miR-100, miR-10b, and Let-7a-2
- *Circulatory tumor cells (CTC)*
- *Proteins*—ki 67, osteopontin, and tumor Protein 53 (p53)
- *Tumor-Associated Autoantibodies (TAABs)*
- *Antigens*—urokinase plasminogen activator system (uPA), the plasminogen activator inhibitor (PAI)

A single biosensor device allows multi-marker detection combined with high sensitivity and specificity at a fast response rate.

13.3.2 Bioreceptor

High selectivity for an analyte is the major prerequisite for the bioreceptor. The common bioreceptor interactions involve antibody/antigen, enzymes/ligands, nucleic acids/DNA/RNA, cells/tissue, or nanoparticles. Morales and Halpern discuss the characteristics and limitations of each of these biorecognition elements to be considered for designing new biosensors [57].

13.3.3 Biotransducers and Amplification

The transducer or the detector element transforms one signal into another that can be easily observed and quantified [53]. The transducers in biosensors for biomedical applications are based on electrochemical, optical, electronic, piezoelectric, or magnetic properties. The measurable output of gene or protein expression by sensor differentiates cancerous cells from non-cancerous ones.

The following section details the use of regularly used biosensors for breast cancer applications.

Electrochemical biosensor generates quantitative information by converting biochemical signals into electronic signals. Commonly used electrochemical biosensors are voltammetric, amperometric, impedimetric, potentiometric, capacitive/conductometric, and field effect transistor (FET) biosensors. Electric cell-substrate impedance sensing (ECIS) proves to measure cell proliferation, morphology, death, and motility. A recent study reported bioimpedance spectroscopy assisted with magnetic nanoparticles to detect cancer cells in an aqueous medium. The method demonstrated the detection of three pathologically distinct cell lines the early stage (MCF-7), invasive phase (MDA-MB-231), and metastatic (SKBR-3) correlated with the expression of specific cell surface markers EpCAM, MUC-1, and HER-2, respectively [58]. A peptide-functionalized electrode-based capacitive biosensor detects HER 4 protein in serum, which showed a selective measurement in a concentration range of 1 pM to 100 nM [59]. A CRISPR-dCas9 (clustered regularly interspaced short palindromic repeats/deactivated CRISPR associated protein 9) electrochemical impedimetric system provides a label-free tool for detecting circulating tumor DNA in liquid biopsy with a LOD 0.65 nM [60].

Optical biosensors offer real-time and label-free mode detection of a visible signal proportional to the presence of the analyte. Optical biosensors are based on surface-enhanced Raman scattering (SERS), surface plasmon resonance (SPR), chemiluminescence, colorimetric or fluorescence. Nanobiosensors bring a paradigm shift to biosensors owing to the high surface area, biocompatibility, and diverse electromechanical properties of nanomaterials. An ultrasensitive optical biosensor based on gold nanoparticles absorption allows the detection of microRNA-155 with a concentration detection limit of 100 aM is helpful in the diagnosis of early stages of breast cancer [61]. Aptamer (oligonucleotide/peptide) based sensors called aptasensors provide high selectivity and affinity toward the analyte, allowing reaction independent of the transducer used. An optical fiber aptasensor devised against mammaglobin proteins for finding circulating breast cancer cells showed LOD of 49 cells/mL, and with a further coating of gold nanoparticles a LOD of 10 cancer cells/mL was achieved [62]. A nanoplasmonic biosensor developed for real-time monitoring of mutant p53 protein with the growth arrest and DNA damage 45 (GADD45) promoter proved clinical validation with a low detection limit (11.47 fM) [63]. Förster or fluorescence resonance energy transfer (FRET) generates fluorescence emission by the energy transfer between two fluorophores. FRET-based vinculin (a focal adhesion molecule) tension sensor combined with live-cell imaging revealed the altered migratory behavior of MDA-MB 231 cells in the presence of osteocytes. Also, it allowed the quantification of cell tensile forces [64]. A 3D printed immunomagnetic concentrator (3DPIC) with ATP luminescence assay allowed rapid and high detection sensitivity within 30 min, up to 10 cell/mL of CTCs in blood. The sensor claims 10 times more sensitivity than commercial kits for CTC concentration [65].

Electrochemiluminescence/ECL generates the optical output due to high-energy electron-transfer reactions through emitters (luminophores), coreactants, and electrodes. It features near-zero background signal and low power consumption. Motaghi et al. used an aptamer-based bipolar electrode mounted in a 3D printed

microchannel to detect the level of nucleolin on the surface of cancer cells. The luminol intensity of this system is enhanced by the accumulation of gold nanoparticles on secondary aptamer-conjugate on the captured cells in the presence of hydrogen peroxide; this system allows a detection limit of 10 cells [66]. A highly sensitive cytosensor established using luminol/chitosan (attachment biomolecule) as ECL source was applied in the quantification of metastatic cells with a limit of 20 cells/mL [67].

Piezoelectric biosensor generates stable oscillations upon detecting a change in mass of the sample (even nanogram level). A quartz crystal microbalance-based biosensor functionalized with transferrin allowed the detection of highly metastatic breast cancer cells with overexpression of transferrin receptors from low/no metastatic potential with a detection limit of 500 cells/mL [68]. Further, this system was modified with notch-4 receptor and HER2/neu antibodies enabling the detection of metastatic cancer cells with a LOD of 12 cells/mL and 10 cells/mL, respectively [69].

13.4 Biosensor-Based Drug Monitoring

The selection of new or combinations of drug formulations is a tedious process. The commonly used techniques for therapeutic drug monitoring are high-performance liquid chromatography (HPLC), gas chromatography-mass spectrometry (GC-MS/LC-MS-MS), and immunoassays [70]. These techniques require trained personnel for the collection and analysis of the sample and operation of the systems. The accuracy and sensitivity of these analytical methods may produce erroneous drug therapeutic effects. A biosensor is a potential tool in validating the efficacy of therapeutics in a cost-effective, user-friendly approach. From drug development point of view, the sensor can provide a quantitative assessment of pharmacodynamics (PD) and pharmacokinetics (PK) parameters of adsorption, distribution, metabolism, excretion, and toxicity (ADMET). The anti-cancer monitoring is primarily assessed by using electrochemical and optical biosensors.

A fiber-optic apoptosis sensor (<4000 USD) allows *in vivo* monitoring of heterogeneously expressed biomarkers induced by the chemotherapeutic agent. The result is quantified using the ratio of the two fluorescent signals (apoptotic indicator/cell spatial distribution indicator) to modify the drug administration for personalized chemotherapy [71]. Impedance-based biosensor determined the efficacy to overcome the drug resistance using a paclitaxel-loaded nanoemulsion on triple-negative breast cancer cells [72]. An electrochemical biosensor with single-wall carbon nanotubes facilitated monitoring DNA modification (reduction in guanine signal) by anti-cancer drug with a detection limit of 0.6 nM implicates the dose efficacy screening of cancer therapy [73].

13.5 Microfluidics Integrated with Bio-sensing

The biosensor associated with microchips contributes to the emergence of point-of-care (POC) devices. Microfluidics enables the assessment of patient-derived samples which are mostly in short supply. The adaptation of 3D printing into sensor fabrication allows rapid prototyping of geometrically complex elements enabling direct integration with microfluidics. The biosensor can be converted to a wearable biosensor, indicating the ease of integration with microchips to establish portable devices with enhanced sensitivity and detection of trace levels of the analyte. Table 13.1 summarizes the various state-of-the-art microfluidic integrated biosensors developed for breast cancer diagnosis.

Pandya et al. demonstrated the integration of microfluidics and electrical sensing to measure impedance magnitude allowing real-time analysis of the

Table 13.1 Microfluidic integrated biosensors for breast cancer diagnosis

Biosensing specification	Biomarker	Limit of detection	Reference
Immunoarray detection of peptide fragment <ul style="list-style-type: none"> Inkjet printed electrode array 	Parathyroid hormone-related peptide (PTHrP)	150 aM	[74]
Smartphone biosensor with multi-testing-unit <ul style="list-style-type: none"> Surface plasmon resonance (SPR) 	CA125 CA15-3	4.2 U/mL 0.87 U/mL	[75]
Multi-biomarker detection <ul style="list-style-type: none"> Surface enhanced Raman scattering (SERS) immunoassay 	CA153, CA125 CEA	0.01 U/mL 1 pg/mL	[76]
Detection and analysis of cancerous exosomes <ul style="list-style-type: none"> Electrochemical (EC) aptasensor Detachable microfluidic device using a 3D printed magnetic housing 	EpCAM positive exosome	17 exosomes/ μ L	[77]
Multiple biomarkers simultaneous detection <ul style="list-style-type: none"> Graphene oxide quantum dots immunofluorescence assay 	CA125, CA199, CA153 CEA, AFP	0.01–0.05 U/mL 1 pg/mL	[78]
Heart and breast-on-a-chip monitoring of cardiotoxicity <ul style="list-style-type: none"> Electrochemical immunoaptasensors 	Troponin T, CK-MB, HER-2	0.1 pg/mL	[79]
Capturing extracellular vesicle encapsulated microRNAs <ul style="list-style-type: none"> DNA-FET biosensors 	microRNA-195 microRNA-126	84 aM 75 aM	[80]

CA carbohydrate antigen, CEA carcinoembryonic antigen, AFP α -fetoprotein, CK-MB creatine kinase-MB isoenzyme, HER-2 human epidermal growth factor receptor 2, 3D three-dimensional, FET field effect transistor

chemotherapeutic drug. In this study, they delineated the drug-susceptible and tolerant/resistant cells in less than 12 h [81]. A 3D culture microfluidic device embedded with a platinum-based electrochemical microsensor allows the measurement of lactate and oxygen concentrations, which helps to study their influence on cancer treatment [82].

James Rusling's group employed inkjet printing to fabricate sensor electrode arrays for immunodetection of cancer-related biomarkers. They manufactured a low-cost (<USD 0.25) disposable electrochemical sensor platform by patterning silver and gold nanoparticle inks into the 8-electrode array with an insulation layer of poly (amic) acid ink. This sensor array was integrated with a microfluidic device having a chamber where enzyme-labeled magnetic beads equipped with multiple antibodies capture the target molecule. They demonstrated the feasibility of the system for measuring intact parathyroid hormone-related peptide (PTHrP) and circulating peptide fragments in 5 μ L of serum with LOD of 150 aM (\sim 1000-fold lower than immunoradiometric assay) achieved in 30 min [74]. Further, the device was improved for the ultrafast detection of HER-2 in serum within 15 min, having a clinically relevant LOD of 12 pg/mL [83].

Although technically challenging, multiorgan microfluidics with multianalyte assessment paves opportunities to advance translation medicine. A heart-breast cancer-on-a-chip (Fig. 13.3) was developed to monitor chemotherapy-induced cardiotoxicity [79]. Immuno-aptasensors employed with the chip measure cardiac biomarkers (cardiac Troponin T and creatine kinase-MB isoenzyme) and BC marker (HER-2) after treatment with DOX. The sensing modules of this device indicated the limit of detection as low as 0.1 pg/mL for all markers [79]. Further, the model evaluated the cardiotoxicity with a nanoparticle-based drug delivery system. In another research, a DNA-FET-based biosensor integrated with microfluidic system was employed in the quantification of BC biomarkers including microRNA-195 and microRNA-126. This single multimodule microfluidic chip extracts the extracellular vesicle from plasma within 4 h and allows the detection of 84 aM and 75 aM concentrations of microRNA-195 and microRNA-126, respectively [80].

A recent study reported a worm-based microfluidic biosensor (Fig. 13.4) allowing real-time evaluation of biochemical cues associated with metastasis [84]. The analysis of the chemotaxis index (CI) relied on the presence of chemorepellent metabolite (glutamate) secreted by cancer cells. The *Caenorhabditis elegans* in this study displayed a chemotactic preference (high CI) toward malignant phenotype.

13.6 Conclusion and Future Outlook

Breast cancer metastases remain incurable with relapse and complications from conventional therapies. The intertumor and intratumor heterogeneity demands for the treatments tailorable to individual patients. Deciphering the fundamental disease mechanisms employing engineering solutions could help to bring advanced therapies for better outcomes in patients who develop metastases. Biosensors are cost-effective, easy-to-use/make devices with high sensitivity and selectivity

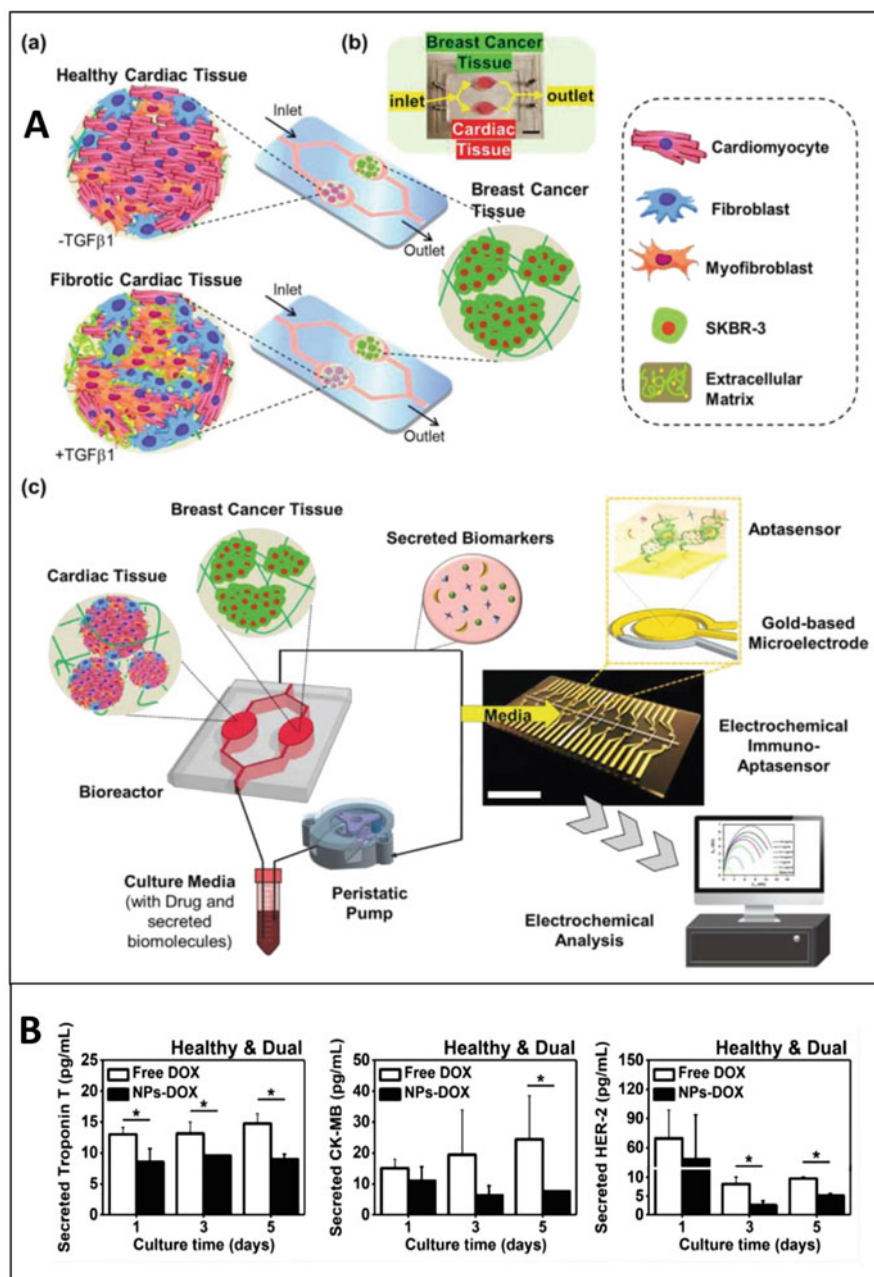


Fig. 13.3 Cardiac-breast cancer-on-a-chip platform. (a) The design and graphic illustration of cardiac-breast cancer-on-a-chip platform with the immuno-aptasensing system comparing healthy cardiac tissues and fibrotic cardiac tissues in presence of transforming growth factor-beta 1 (TGF β 1). (b) Monitoring of biomarkers in healthy cardiac tissue and dual tissues with a supplement of free doxorubicin (DOX) or nanoparticles (NP)-conjugated DOX. * $p < 0.05$. Source: *Reproduced from [79] Wiley Materials*

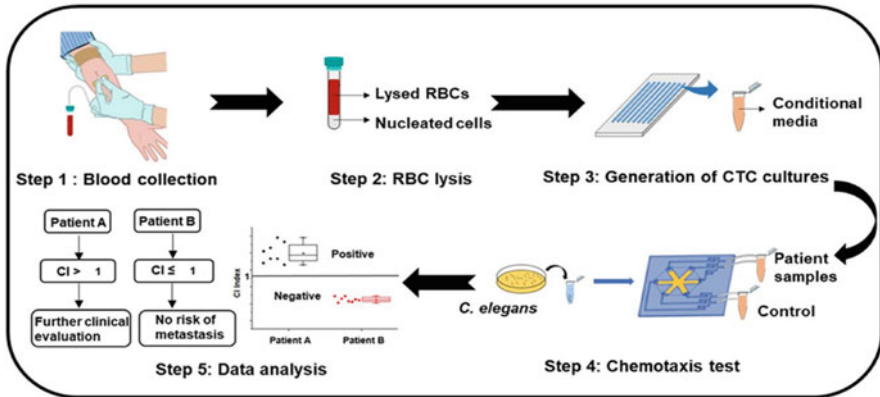


Fig. 13.4 Workflow of the worm-based biosensor. A positive chemotactic index ($CI > 1$) indicates need for further clinical evaluation. A negative index reflects no metastasis risk. *RBC* red blood cells, *CTC* circulating tumor cell. *Reproduced* [84] under the *Creative Commons Attribution 4.0 International Public License*

enabling standardization of cancer biomarkers and anti-cancer monitoring. Metastasis-organ-on-a-chip integrated with a multianalyte biosensor mimics the cancer physiome with the ability to predict treatment efficacy for clinical trials. Innovations in biosensor technology in synchronous with high-throughput microfluidic devices would bring successful and accurate clinical predictions, which aids in the realization of a personalized chemotherapy system.

Acknowledgments This work was supported by the Council of Scientific & Industrial Research (CSIR), Government of India. The authors also like to acknowledge Mr. Dulam Praveen Kumar for providing an oversight on the biosensor part.

References

1. Sung H, Ferlay J, Siegel RL et al (2021) Global cancer statistics 2020: GLOBOCAN estimates of incidence and mortality worldwide for 36 cancers in 185 countries. *CA Cancer J Clin* 71: 209–249. <https://doi.org/10.3322/CAAC.21660>
2. Fidler IJ (2003) The pathogenesis of cancer metastasis: the “seed and soil” hypothesis revisited. *Nat Rev Cancer* 36(3):453–458. <https://doi.org/10.1038/nrc1098>
3. Valastyan S, Weinberg RA (2011) Tumor metastasis: molecular insights and evolving paradigms. *Cell* 147:275–292. <https://doi.org/10.1016/J.CELL.2011.09.024>
4. Chanmee T, Ontong P, Itano N (2016) Hyaluronan: a modulator of the tumor microenvironment. *Cancer Lett* 375:20–30. <https://doi.org/10.1016/J.CANLET.2016.02.031>
5. Rohan TE, Xue X, Lin HM et al (2014) Tumor microenvironment of metastasis and risk of distant metastasis of breast cancer. *J Natl Cancer Inst* 106. <https://doi.org/10.1093/JNCI/DJU136>
6. Hebert JD, Myers SA, Naba A et al (2020) Proteomic profiling of the ECM of xenograft breast cancer metastases in different organs reveals distinct metastatic niches. *Cancer Res* 80:1475–1485. <https://doi.org/10.1158/0008-5472.CAN-19-2961>

7. Martin TA, Goyal A, Watkins G, Jiang WG (2005) Expression of the transcription factors snail, slug, and twist and their clinical significance in human breast cancer. *Ann Surg Oncol* 12:488–496. <https://doi.org/10.1245/ASO.2005.04.010>
8. Banya-Paluchowski M, Schneck H, Blassl C et al (2015) Prognostic relevance of circulating tumor cells in molecular subtypes of breast cancer. *Geburtshilfe Frauenheilkd* 75:232. <https://doi.org/10.1055/S-0035-1545788>
9. Bidard FC, Peeters DJ, Fehm T et al (2014) Clinical validity of circulating tumour cells in patients with metastatic breast cancer: a pooled analysis of individual patient data. *Lancet Oncol* 15:406–414. [https://doi.org/10.1016/S1470-2045\(14\)70069-5](https://doi.org/10.1016/S1470-2045(14)70069-5)
10. Chen W, Hoffmann AD, Liu H, Liu X (2018) Organotropism: new insights into molecular mechanisms of breast cancer metastasis. *NPJ Precis Oncol* 2(1):4. <https://doi.org/10.1038/s41698-018-0047-0>
11. Shupp AB, Kolb AD, Mukhopadhyay D et al (2018) Cancer metastases to bone: concepts, mechanisms, and interactions with bone osteoblasts. *Cancer* 10:182. <https://doi.org/10.3390/CANCERS10060182>
12. Zhu L, Narloch JL, Onkar S et al (2019) Metastatic breast cancers have reduced immune cell recruitment but harbor increased macrophages relative to their matched primary tumors. *J Immunother Cancer* 7(7):1–10. <https://doi.org/10.1186/S40425-019-0755-1>
13. Yuan C, Liu Z, Yu Q et al (2019) Expression of PD-1/PD-L1 in primary breast tumours and metastatic axillary lymph nodes and its correlation with clinicopathological parameters. *Sci Rep* 9:14356. <https://doi.org/10.1038/s41598-019-50898-3>
14. Breslin S, O'Driscoll L (2016) The relevance of using 3D cell cultures, in addition to 2D monolayer cultures, when evaluating breast cancer drug sensitivity and resistance. *Oncotarget* 7:45745–45756. <https://doi.org/10.18632/oncotarget.9935>
15. Fontoura JC, Viezzer C, dos Santos FG et al (2020) Comparison of 2D and 3D cell culture models for cell growth, gene expression and drug resistance. *Mater Sci Eng C* 107:110264. <https://doi.org/10.1016/J.MSEC.2019.110264>
16. Murayama T, Gotoh N (2019) Patient-derived xenograft models of breast cancer and their application. *Cell* 8:621. <https://doi.org/10.3390/CELLS8060621>
17. Monteiro MV, Zhang YS, Gaspar VM, Mano JF (2021) 3D-bioprinted cancer-on-a-chip: level-up organotypic in vitro models. *Trends Biotechnol*. <https://doi.org/10.1016/J.TIBTECH.2021.08.007>
18. Sung KE, Beebe DJ (2014) Microfluidic 3D models of cancer. *Adv Drug Deliv Rev* 79–80:68–78. <https://doi.org/10.1016/J.ADDR.2014.07.002>
19. Han SJ, Kwon S, Kim KS (2021) Challenges of applying multicellular tumor spheroids in preclinical phase. *Cancer Cell Int* 21:152. <https://doi.org/10.1186/S12935-021-01853-8>
20. Crowder SW, Balikov DA, Hwang Y-S, Sung H-J (2014) Cancer stem cells under hypoxia as a chemoresistance factor in breast and brain. *Curr Pathobiol Rep* 2:33. <https://doi.org/10.1007/S40139-013-0035-6>
21. Ham SL, Joshi R, Luker GD, Tavana H (2016) Engineered breast cancer cell spheroids reproduce biologic properties of solid tumors. *Adv Healthc Mater* 5:2788. <https://doi.org/10.1002/ADHM.201600644>
22. Reynolds DS, Tevis KM, Blessing WA et al (2017) Breast cancer spheroids reveal a differential cancer stem cell response to chemotherapeutic treatment. *Sci Rep* 7(7):1–12. <https://doi.org/10.1038/s41598-017-10863-4>
23. Balachander GM, Balaji SA, Rangarajan A, Chatterjee K (2015) Enhanced metastatic potential in a 3D tissue scaffold toward a comprehensive in vitro model for breast cancer metastasis. *ACS Appl Mater Interfaces* 7:27810–27822. https://doi.org/10.1021/ACSAMI.5B09064/SUPPL_FILE/AM5B09064_SI_001.PDF
24. Datta P, Dey M, Ataie Z et al (2020) 3D bioprinting for reconstituting the cancer microenvironment. *NPJ Precis Oncol* 4:18. <https://doi.org/10.1038/s41698-020-0121-2>

25. Wang Y, Shi W, Kuss M et al (2018) 3D bioprinting of breast cancer models for drug resistance study. *ACS Biomater Sci Eng* 4:4401–4411. <https://doi.org/10.1021/ACSBOMATERIALS.8B01277>
26. Bock N, Kryza T, Shokooahmand A et al (2021) In vitro engineering of a bone metastases model allows for study of the effects of antiandrogen therapies in advanced prostate cancer. *Sci Adv* 7. <https://doi.org/10.1126/SCIADV.ABG2564>
27. Meijer TG, Verkaik NS, van Deurzen CHM et al (2019) Direct ex vivo observation of homologous recombination defect reversal after DNA-damaging chemotherapy in patients with metastatic breast cancer. *JCO Precis Oncol*:1–12. <https://doi.org/10.1200/PO.18.00268>
28. Muraro MG, Muenst S, Mele V et al (2017) Ex-vivo assessment of drug response on breast cancer primary tissue with preserved microenvironments. *Onco Targets Ther* 6. <https://doi.org/10.1080/2162402X.2017.1331798>
29. Hofer M, Lutolf MP (2021) Engineering organoids. *Nat Rev Mater* 6(6):402–420. <https://doi.org/10.1038/s41578-021-00279-y>
30. Sachs N, de Ligt J, Kopper O et al (2018) A living biobank of breast cancer organoids captures disease heterogeneity. *Cell* 172:373–386.e10. <https://doi.org/10.1016/J.CELL.2017.11.010>
31. Coluccio ML, Perozziello G, Malara N et al (2019) Microfluidic platforms for cell cultures and investigations. *Microelectron Eng* 208:14–28. <https://doi.org/10.1016/J.MEE.2019.01.004>
32. Dhiman N, Rath SN (2020) Perfusion-based 3D tumor-on-chip devices for anticancer drug testing. *Biomater 3D Tumor Model*:379–398. <https://doi.org/10.1016/B978-0-12-818128-7.00016-2>
33. Sankar S, Mehta V, Ravi S et al (2021) A novel design of microfluidic platform for metronomic combinatorial chemotherapy drug screening based on 3D tumor spheroid model. *Biomed Microdevices* 234(23):1–10. <https://doi.org/10.1007/S10544-021-00593-W>
34. Niculescu A-G, Chircov C, Bîrcă AC, Grumezescu AM (2021) Fabrication and applications of microfluidic devices: a review. *Int J Mol Sci* 22:2011. <https://doi.org/10.3390/IJMS22042011>
35. Scott SM, Ali Z (2021) Fabrication methods for microfluidic devices: an overview. *Micromachines* 12:319. <https://doi.org/10.3390/MI12030319>
36. Qin D, Xia Y, Whitesides GM (2010) Soft lithography for micro- and nanoscale patterning. *Nat Protoc* 5(5):491–502. <https://doi.org/10.1038/nprot.2009.234>
37. Tsao C-W, Li W, Tan SH, Nguyen N-T (2016) Polymer microfluidics: simple, low-cost fabrication process bridging academic lab research to commercialized production. *Micromachines* 7:225. <https://doi.org/10.3390/MI7120225>
38. Mei X, Middleton K, Shim D et al (2019) Microfluidic platform for studying osteocyte mechanoregulation of breast cancer bone metastasis. *Integr Biol* 11:119–129. <https://doi.org/10.1093/INTBIO/ZYZ008>
39. Ayuso JM, Gong MM, Skala MC et al (2020) Human tumor-lymphatic microfluidic model reveals differential conditioning of lymphatic vessels by breast cancer cells. *Adv Healthc Mater* 9:1900925. <https://doi.org/10.1002/ADHM.201900925>
40. Lanz HL, Saleh A, Kramer B et al (2017) Therapy response testing of breast cancer in a 3D high-throughput perfused microfluidic platform. *BMC Cancer* 17. <https://doi.org/10.1186/S12885-017-3709-3>
41. Nashimoto Y, Okada R, Hanada S et al (2020) Vascularized cancer on a chip: the effect of perfusion on growth and drug delivery of tumor spheroid. *Biomaterials* 229:119547. <https://doi.org/10.1016/J.BIOMATERIALS.2019.119547>
42. Shirure VS, Bi Y, Curtis MB et al (2018) Tumor-on-a-chip platform to investigate progression and drug sensitivity in cell lines and patient-derived organoids. *Lab Chip* 18:3687–3702. <https://doi.org/10.1039/C8LC00596F>
43. Mehta V, Rath SN (2021) 3D printed microfluidic devices: a review focused on four fundamental manufacturing approaches and implications on the field of healthcare. *Bio-Design Manuf* 42(4):311–343. <https://doi.org/10.1007/S42242-020-00112-5>

44. Felton H, Hughes R, Diaz-Gaxiola A (2021) Negligible-cost microfluidic device fabrication using 3D-printed interconnecting channel scaffolds. *PLoS One* 16:e0245206. <https://doi.org/10.1371/JOURNAL.PONE.0245206>
45. Aung A, Kumar V, Theprungsirikul J et al (2020) An engineered tumor-on-a-chip device with breast cancer-immune cell interactions for assessing T-cell recruitment. *Cancer Res* 80:263–275. <https://doi.org/10.1158/0008-5472.CAN-19-0342>
46. Chen J, Liu CY, Wang X et al (2020) 3D printed microfluidic devices for circulating tumor cells (CTCs) isolation. *Biosens Bioelectron* 150:111900. <https://doi.org/10.1016/J.BIOS.2019.111900>
47. Chu C-H, Liu R, Ozkaya-Ahmadov T et al (2021) Negative enrichment of circulating tumor cells from unmanipulated whole blood with a 3D printed device. *Sci Rep* 11:20583. <https://doi.org/10.1038/s41598-021-99951-0>
48. Cai S, Shi H, Li G et al (2019) 3D-printed concentration-controlled microfluidic chip with diffusion mixing pattern for the synthesis of alginate drug delivery microgels. *Nanomaterials (Basel)* 9. <https://doi.org/10.3390/NANO9101451>
49. Chang Y, Jiang J, Chen W et al (2020) Biomimetic metal-organic nanoparticles prepared with a 3D-printed microfluidic device as a novel formulation for disulfiram-based therapy against breast cancer. *Appl Mater Today* 18:100492. <https://doi.org/10.1016/J.APMT.2019.100492>
50. Mohankumar P, Ajayan J, Mohanraj T, Yasodharan R (2021) Recent developments in biosensors for healthcare and biomedical applications: a review. *Measurement* 167:108293. <https://doi.org/10.1016/J.MEASUREMENT.2020.108293>
51. Nares V, Lee N (2021) A review on biosensors and recent development of nanostructured materials-enabled biosensors. *Sensors* 21:1109. <https://doi.org/10.3390/S21041109>
52. Tothill IE (2009) Biosensors for cancer markers diagnosis. *Semin Cell Dev Biol* 20:55–62. <https://doi.org/10.1016/J.SEMCDB.2009.01.015>
53. Bhalla N, Jolly P, Formisano N, Estrela P (2016) Introduction to biosensors. *Essays Biochem* 60:1. <https://doi.org/10.1042/EBC20150001>
54. Atkinson AJ, Colburn WA, DeGruttola VG et al (2001) Biomarkers and surrogate endpoints: preferred definitions and conceptual framework. *Clin Pharmacol Ther* 69:89–95. <https://doi.org/10.1067/MCP.2001.113989>
55. Pereira A, Sales M, Rodrigues L (2019) Biosensors for rapid detection of breast cancer biomarkers. *Adv Biosens Heal Care Appl*:71–103. <https://doi.org/10.1016/B978-0-12-815743-5.00003-2>
56. Mittal S, Kaur H, Gautam N, Mantha AK (2017) Biosensors for breast cancer diagnosis: a review of bioreceptors, biotransducers and signal amplification strategies. *Biosens Bioelectron* 88:217–231. <https://doi.org/10.1016/J.BIOS.2016.08.028>
57. Morales MA, Halpern JM (2018) Guide to selecting a biorecognition element for biosensors. *Bioconjug Chem* 29:3231. <https://doi.org/10.1021/ACS.BIOCONJCHEM.8B00592>
58. Huerta-Núñez LFE, Gutierrez-Iglesias G, Martinez-Cuazitl A et al (2019) A biosensor capable of identifying low quantities of breast cancer cells by electrical impedance spectroscopy. *Sci Rep* 9(1):1–12. <https://doi.org/10.1038/s41598-019-42776-9>
59. Zhuravski P, Arya SK, Jolly P et al (2018) Sensitive and selective Affimer-functionalised interdigitated electrode-based capacitive biosensor for Her4 protein tumour biomarker detection. *Biosens Bioelectron* 108:1–8. <https://doi.org/10.1016/J.BIOS.2018.02.041>
60. Uygun ZO, Yeniay L, Girgin Sağın F (2020) CRISPR-dCas9 powered impedimetric biosensor for label-free detection of circulating tumor DNAs. *Anal Chim Acta* 1121:35–41. <https://doi.org/10.1016/J.ACA.2020.04.009>
61. Hakimian F, Ghourchian H, Hashemi AS et al (2018) Ultrasensitive optical biosensor for detection of miRNA-155 using positively charged Au nanoparticles. *Sci Rep* 8:2943. <https://doi.org/10.1038/s41598-018-20229-z>
62. Loyez M, Hassan EM, Lobry M et al (2020) Rapid detection of circulating breast cancer cells using a multiresonant optical fiber aptasensor with plasmonic amplification. *ACS Sens* 5:454–463. <https://doi.org/10.1021/ACSSENSORS.9B02155>

63. Song S, Lee JU, Kang J et al (2020) Real-time monitoring of distinct binding kinetics of hot-spot mutant p53 protein in human cancer cells using an individual nanorod-based plasmonic biosensor. *Sens Actuators B* 322:128584. <https://doi.org/10.1016/J.SNB.2020.128584>
64. Li F, Chen A, Reeser A et al (2019) Vinculin force sensor detects tumor-osteocyte interactions. *Sci Rep* 9(9):1–11. <https://doi.org/10.1038/s41598-019-42132-x>
65. Park C, Abafogi AT, Ponnuvelu DV et al (2021) Enhanced luminescent detection of circulating tumor cells by a 3D printed Immunomagnetic concentrator. *Biosensors* 11. <https://doi.org/10.3390/BIOS11080278>
66. Motaghi H, Ziyae S, Mehrgardi MA et al (2018) Electrochemiluminescence detection of human breast cancer cells using aptamer modified bipolar electrode mounted into 3D printed microchannel. *Biosens Bioelectron* 118:217–223. <https://doi.org/10.1016/J.BIOS.2018.07.066>
67. Nasrollahpour H, Mahdipour M, Isildak I et al (2021) A highly sensitive electrochemiluminescence cytosensor for detection of SKBR-3 cells as metastatic breast cancer cell line: a constructive phase in early and precise diagnosis. *Biosens Bioelectron* 178:113023. <https://doi.org/10.1016/J.BIOS.2021.113023>
68. Atay S, Pişkin K, Yılmaz F et al (2015) Quartz crystal microbalance based biosensors for detecting highly metastatic breast cancer cells via their transferrin receptors. *Anal Methods* 8: 153–161. <https://doi.org/10.1039/C5AY02898A>
69. Yılmaz M, Bakhshpour M, Göktürk I et al (2021) Quartz crystal microbalance (QCM) based biosensor functionalized by HER2/neu antibody for breast cancer cell detection. *Chemosensors* 9:80. <https://doi.org/10.3390/CHEMOSENSORS9040080>
70. Kang J-S, Lee M-H (2009) Overview of therapeutic drug monitoring. *Korean J Intern Med* 24:1. <https://doi.org/10.3904/KJIM.2009.24.1.1>
71. Liao KC, Chiu HS, Fan SY et al (2016) Percutaneous fiber-optic biosensor for immediate evaluation of chemotherapy efficacy in vivo (part I): strategy of assay design for monitoring non-homogeneously distributed biomarkers. *Sens Actuators B* 222:544–550. <https://doi.org/10.1016/J.SNB.2015.08.067>
72. Attari F, Hazim H, Zandi A et al (2021) Circumventing paclitaxel resistance in breast cancer cells using a nanoemulsion system and determining its efficacy via an impedance biosensor. *Analyst* 146:3225–3233. <https://doi.org/10.1039/D0AN02013C>
73. Moghadam FH, Taher MA, Karimi-Maleh H (2021) Doxorubicin anticancer drug monitoring by ds-DNA-based electrochemical biosensor in clinical samples. *Micromachines* 12:808. <https://doi.org/10.3390/M12070808>
74. Otieno BA, Krause CE, Jones AL et al (2016) Cancer diagnostics via ultrasensitive multiplexed detection of parathyroid hormone-related peptides with a microfluidic Immunoarray. *Anal Chem* 88:9269–9275. <https://doi.org/10.1021/ACS.ANALCHEM.6B02637>
75. Fan Z, Geng Z, Fang W et al (2020) Smartphone biosensor system with multi-testing unit based on localized surface Plasmon resonance integrated with microfluidics chip. *Sensors* 20. <https://doi.org/10.3390/S20020446>
76. Zheng Z, Wu L, Li L et al (2018) Simultaneous and highly sensitive detection of multiple breast cancer biomarkers in real samples using a SERS microfluidic chip. *Talanta* 188:507–515. <https://doi.org/10.1016/J.TALANTA.2018.06.013>
77. Kashefi-Kheyabadi L, Kim J, Chakravarty S et al (2020) Detachable microfluidic device implemented with electrochemical aptasensor (DeMEA) for sequential analysis of cancerous exosomes. *Biosens Bioelectron* 169:112622. <https://doi.org/10.1016/J.BIOS.2020.112622>
78. Wang C, Zhang Y, Tang W et al (2021) Ultrasensitive, high-throughput and multiple cancer biomarkers simultaneous detection in serum based on graphene oxide quantum dots integrated microfluidic biosensing platform. *Anal Chim Acta* 1178:338791. <https://doi.org/10.1016/J.ACA.2021.338791>
79. Lee J, Mehrotra S, Zare-Eelanjeh E et al (2021) A heart-breast cancer-on-a-chip platform for disease modeling and monitoring of cardiotoxicity induced by cancer chemotherapy. *Small* 17: 2004258. <https://doi.org/10.1002/SMLL.202004258>

80. Huang C-C, Kuo Y-H, Chen Y-S et al (2021) A miniaturized, DNA-FET biosensor-based microfluidic system for quantification of two breast cancer biomarkers. *Microfluid Nanofluidics* 25(25):1–12. <https://doi.org/10.1007/S10404-021-02437-8>
81. Pandya HJ, Dhingra K, Prabhakar D et al (2017) A microfluidic platform for drug screening in a 3D cancer microenvironment. *Biosens Bioelectron* 94:632. <https://doi.org/10.1016/J.BIOS.2017.03.054>
82. Dornhof J, Kieninger J, Muralidharan H et al (2021) Oxygen and lactate monitoring in 3D breast cancer organoid culture with sensor-integrated microfluidic platform. In: 21st international conference on solid-state sensors, actuators microsystems, transducers, pp 703–706. <https://doi.org/10.1109/TRANSDUCERS50396.2021.9495557>
83. Carvajal S, Fera SN, Jones AL et al (2018) Disposable inkjet-printed electrochemical platform for detection of clinically relevant HER-2 breast cancer biomarker. *Biosens Bioelectron* 104: 158–162. <https://doi.org/10.1016/J.BIOS.2018.01.003>
84. Zhang J, Chua SL, Khoo BL (2021) Worm-based microfluidic biosensor for real-time assessment of the metastatic status. *Cancer* 13:873. <https://doi.org/10.3390/CANCERS13040873>



Vincent Hyenne, Jacky G. Goetz, and Naël Osmani

Abstract

Metastatic dissemination accounts for most of the death in patients during cancer progression. There is thus an urge to identify specific biomarkers as proxies for cancer progression and assessment of treatment efficiency. Cancer is a systemic disease involving the shuttling of tumor cells and tumor secreted factors to distant organs, mostly via biofluids. During this transfer, these factors are accessible for easy sampling and therefore constitute a unique source of information witnessing the presence and the evolution of the disease. Hence, liquid biopsies offer multiple advantages, including simple and low-invasive sampling procedures, low cost, and higher compliance. Importantly, liquid biopsies are adapted to personalized medicine allowing a longitudinal follow-up to monitor treatment efficiency or resistance, and risk of relapse.

V. Hyenne

INSERM UMR_S1109, Strasbourg, France

Université de Strasbourg, Strasbourg, France

Fédération de Médecine Translationnelle de Strasbourg, Strasbourg, France

Equipe Labellisée Ligue Contre le Cancer, Paris, France

CNRS, SNC5055, Strasbourg, France

J. G. Goetz · N. Osmani (✉)

INSERM UMR_S1109, Strasbourg, France

Université de Strasbourg, Strasbourg, France

Fédération de Médecine Translationnelle de Strasbourg, Strasbourg, France

Equipe Labellisée Ligue Contre le Cancer, Paris, France

e-mail: osmani@unistra.fr

© The Author(s), under exclusive license to Springer Nature Switzerland AG 2022

341

D. Caballero et al. (eds.), *Microfluidics and Biosensors in Cancer Research*,

Advances in Experimental Medicine and Biology 1379,

https://doi.org/10.1007/978-3-031-04039-9_14

The evolution of methodologies to isolate circulating tumor cells (CTCs) and extracellular vesicles (EVs) from blood samples associated with the characterization of their membrane surface repertoire and content have been instrumental in the emergence of liquid biopsies as an easy and non-invasive alternative as opposed to classical surgery-mediated tumor biopsies.

In this chapter, we comment on CTCs and EVs carrying features with great potential as cancer biomarkers. More specifically, we focus on the adhesive and mechanical properties of CTCs as metastatic markers. We also consider the recent development of EVs isolation methods and the identification of new biomarkers. Finally, we discuss their relevance as cancer prognosis tools.

Keywords

Liquid biopsy · Biomarker · CTC (circulating tumor cell) · Extracellular vesicle · Metastasis

14.1 Introduction

Metastatic cancer is a systemic disease involving the transfer of tumor cells and tumor secreted factors between organs. This transfer often requires a transition in biofluids which are then accessible for easy sampling and therefore constitute a unique source of information regarding the presence and the evolution of the disease. Hence, liquid biopsy presents multiple advantages, including simple sampling and low invasive procedures, low cost, and higher compliance, thereby partially addressing the risks induced by over-diagnosis [1]. Importantly, liquid biopsy is adapted to personalized medicine as it allows a longitudinal follow-up to monitor treatment efficiency or resistance and risk of relapse. Establishing specific and reliable biomarkers for liquid biopsies is essential since the overall decrease in the mortality rate of cancer patients (29% in 30 years in the United States [2]) is now limited by relapse, individual tumor heterogeneity and therapy resistance. For these reasons, the past decades witnessed an explosion in methods available for liquid biopsies and in the number of biomarkers identified from various nature and sources, in most cancer types. However, their routine use in clinics still requires significant adaptations and standardizations [3]. While other sources of biomarkers (such as soluble seric markers or ctDNA) have been developed [4], we will focus on cell-derived markers which might reflect much accurately tumor heterogeneity. These include circulating tumor cells (CTCs) and extracellular vesicles (EVs) for which new isolation and analysis methods, including microfluidics and biosensor technologies, recently emerged. We will describe these novel approaches and highlight some of the most trustful or promising biomarkers. An exhaustive listing of all discovered biomarkers in CTCs or EVs has been provided elsewhere [5].

As metastatic dissemination accounts for most of the death in patients during cancer progression [6], there is an urge to identify specific biomarkers as proxies for cancer progression. Metastasis starts as transformed cells acquire invasive

properties, breach through the basement membrane of their organ of origin and invade the surrounding stroma [7, 8]. Cancer cells are then able to reach nearby vessels and enter either lymphatic or blood circulation in a process named intravasation and become circulating tumor cells (CTCs). This opens access to the major hematogenous circulatory system for cancer cells' hematogenous dissemination which can then travel to distant organs either as single cells, homo or hetero-clusters [9]. Once they reach the capillary beds of those organs, CTC arrest either by occlusion or direct adhesion and enter the perivascular niche using extravasation [10]. Depending on the fitness to the newly colonized environment, disseminated cancer cells will either form metastatic colonies, die or enter dormancy [11–13]. Cancer cell identity and phenotypic properties are also not set in stone adding an additional layer of complexity. Cancer cells are able to plastically evolve between their differentiated identity of origin and a more mesenchymal identity, reflecting the developmental programs being hijacked, depending on both cell autonomous and environmental cues, in a process known as epithelial-mesenchymal plasticity [14–16]. Among this continuum of cellular states lies steps where cancer cells reach a higher tumor-initiating potential which is highly related to a more cancer stem cell (CSC) identity, although this is still debated [17, 18].

Recently, it has become obvious that primary tumors permanently release high levels of factors in the circulation, including soluble proteins, cell-free DNA or RNA and EVs. Among these factors, EVs present a unique and complex combination of lipids, proteins, RNAs (mRNAs, miRNAs, lncRNAs, Y-RNAs, tRNAs, piRNAs, ciRNAs, etc.), and sometimes DNA, conferring them a high potential for liquid biopsies [19–23]. EVs are extremely heterogenous in sizes (with diameters ranging from a few nanometers to a couple of microns), molecular content and nomenclature, with two main families exosomes and microvesicles, distinguished by their sub-cellular origin [20]. In addition, EVs are present in all body fluids (blood, lymph, urine, cerebrospinal fluids, saliva, milk, and others) and carry factors representative of their secreting cell. Therefore, since all cells secrete EVs carrying a molecular signature of their pathophysiological status, it could theoretically be possible to identify EV-related markers specific of any tumor progression step [24]. This would include early transformation stages and pre-metastatic stages, as tumor EVs are most likely released at the initiation of the disease and potentially before tumor cells escape the primary tumor. Functionally tumor EVs were shown to contribute to multiple aspects of tumor progression by mediating the communication between tumor cells themselves and between tumor cells and surrounding stromal cells present in the microenvironment [25, 26]. This can result in the horizontal transfer of proliferative, migratory, metabolic or drug resistance properties and to the indoctrination of several types of stromal cells. Importantly, tumor EVs can travel to distant organs through lymphatic or hematogenous dissemination and induce important modifications of the microenvironment. This can result in the formation of pre-metastatic niches, a favorable microenvironment in organs distant from the primary tumor before the arrival of metastatic cells [27, 28]. Altogether, the early and massive presence of EVs in biofluids (10^7 to 10^{12} EVs/ml of plasma [29, 30]), combined with the stability and diversity of their cargoes propelled them as an ideal

source of biomarkers for the early detection of cancer, therapy resistance and risk of relapse prediction.

Over the past decades, a large amount of work has been made to understand primary tumor growth, cancer genetics and clonal evolution, but also the processes underlying the colonization of secondary sites by disseminated tumor cells until the emergence of clinically detectable metastatic foci [31–33]. However, the mechanisms driving the dissemination of circulating tumor cells (CTC) through the vasculature toward specific organs, i.e., organotropism, remain elusive. In particular, the role of mechanics and adhesive properties are emerging as important factors during cancer progression and more specifically during the hematogenous dissemination of CTCs and EVs [10]. There is thus an urge in developing new markers to assess the potential of dissemination in cancer-diagnosed patients in order to fine-tune the therapeutical strategies [34–36]. The evolution of methodologies to isolate CTCs and EVs from blood samples associated with the characterization of their membrane surface repertoire and content have been instrumental in the emergence of liquid biopsies as an easy and non-invasive alternative as opposed to classical surgery-mediated tumor biopsies [37, 38].

In this chapter, we highlight the role of several features of CTCs and EVs as potential cancer biomarkers. More specifically, we focus on the adhesive and mechanical properties of CTCs as metastatic markers. We also consider the role of the molecular content of EVs in cancer progression. Finally, we discuss their relevance as cancer prognosis tools.

14.1.1 CTC Biomarkers

The cell surface of cancer cells which is the most easily accessible has become a major center of interest. Hence, it is not surprising that much effort has been put into using membrane-associated molecular components as either aim for targeted therapies or prognostic markers. Cell surface-associated biomolecules have thus emerged as obvious targets either for CTC capture or their characterization [38].

14.1.1.1 Surface Markers

One major cell surface difference between native blood cells and some CTCs is the presence of epithelial markers (Fig. 14.1). Epithelial cell adhesion molecule (EpCAM/CD326) has emerged as an important target since it was shown to be highly expressed by cancer cells [39]. Much attention was devoted toward using EpCAM not only to identify CTCs but more importantly to capture them in liquid biopsies. This led to the development of the CellSearch system which is based on the isolation of CTCs using EpCAM coated magnetic beads coupled to the validation of the epithelial identity with a pan-keratin antibody—a family of epithelial-specific intermediate filaments—and a negative staining for CD45, a classic pan-leukocyte marker [40, 41]. Likewise, isolation approaches are being developed to capture melanoma CTC relying on the marker melanoma cell adhesion molecule (MCAM/CD146) [42]. Recent reports also suggest that the combination of EpCAM and

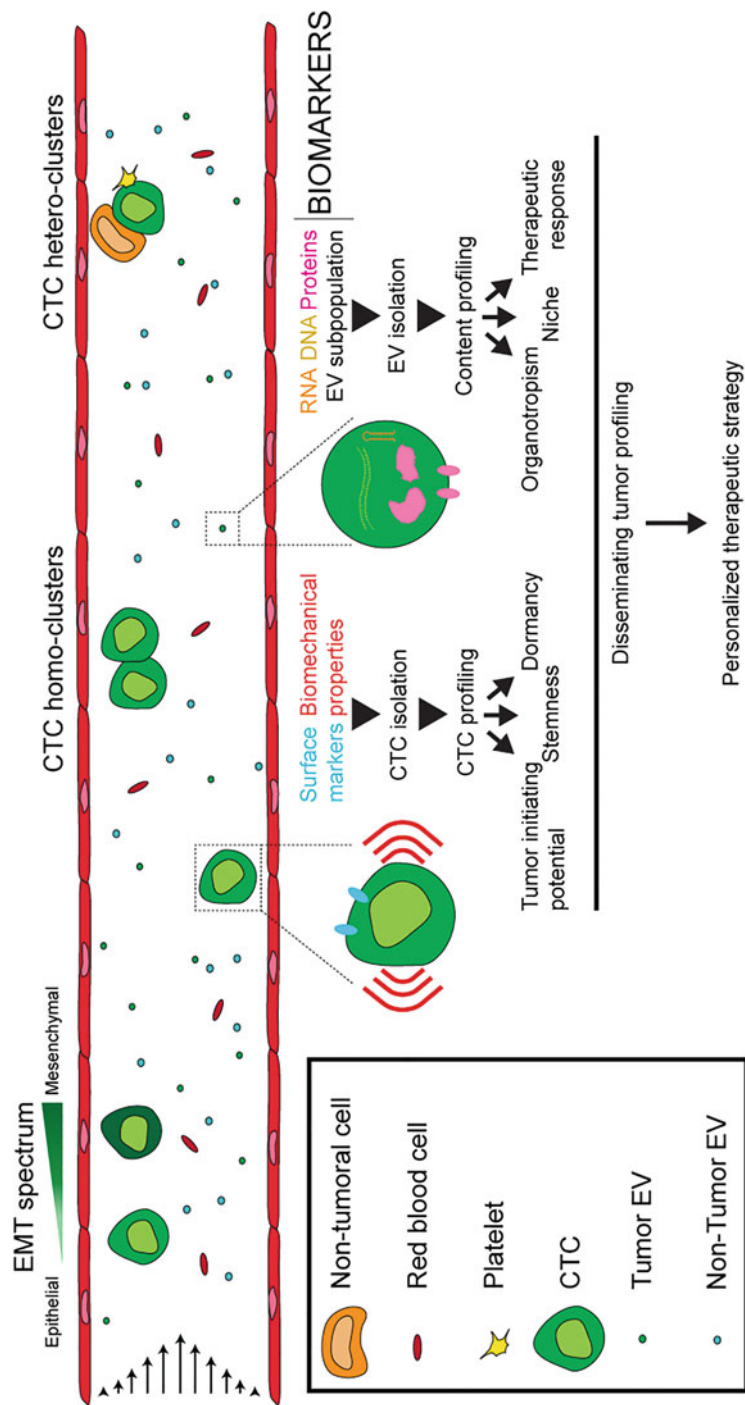


Fig. 14.1 CTCs and EVs are biomarkers accessible through liquid biopsies for cancer phenotyping. EVs and CTCs are released within blood by the primary tumor through and reach distant organs. CTCs are found with different EMT phenotype as single or clusters, either with CTCs or non-tumoral cells such as immune cells, cancer-associated fibroblasts, or platelets. CTCs can be isolated through their surface markers or mechanical properties for metastatic tumor profiling. EVs convey important molecular information from the tumor including RNA and proteins. EVs can be purified from liquid biopsies for subsequent analysis of their content. This deep profiling of tumor dissemination will favor the personalization of the therapeutical strategy selected for each specific patient

MCAM might even further improve breast cancer CTC detection [43, 44]. The CellSearch is so far the only FDA-approved CTC isolation device being used for the diagnostic purpose to monitor metastatic cancers. The EpCAM immunopurification methods have been successfully combined to microfluidic microfabrication with EpCAM antibody-coated structures such as microposts (CTC chip) or grooves inducing microvortex driven mixing (HB-Chip) in order to improve throughput and sensitivity [45, 46].

It appears that the simple numeration of CTC might not be the most accurate proxy for disease progression [40]. Furthermore, it is now well accepted that cancer cells do not always harbor such epithelial features. They plastically shuttle between their differentiated identity of origin and a mesenchymal state similar to their developmental origin using a transdifferentiation-like process—similar to the EMT for epithelial-derived cancer [17, 47]. The input of developmental and stem cell biology concepts has been instrumental in understanding the plastic continuum, among which some hybrid states may uphold phenotypic features of stemness, which are essential for CTC survival and tumor initiating potential [14, 15, 48]. It has been now well demonstrated that metastasis initiating CTCs are present in a myriad of states along the EMT continuum [48, 49]. This explains why detecting and capturing CTCs solely on markers expressed by differentiated cells could induce a bias toward a subpopulation of CTCs likely suboptimal in setting up distant colonies [50–52]. Consequently, there has been an urge in identifying new CTC markers which could be used complementary or alternatively to EpCAM/MCAM markers. For instance, the Epispot technique which is based on the use of cytokeratin 19 after Ficoll based purification [53] was efficiently used to characterize colon cancer CTCs [54].

As mentioned previously, the switch of cancer cells toward phenotypes yielding stemness-like properties might boost up their metastatic potential. Identifying and using such markers might thus turn out to be highly relevant and provide important potential therapeutic tools. The surface expression of several well-described stemness markers has been assessed in circulating cancer cells [55]. For instance, CD24, which among others binds to p-selectin expressed by platelets and endothelial cells, was demonstrated to be a major marker for CSC in disseminating from small cell lung cancer—of note, these cells are also overexpressing EpCAM [56]. CD24 was also observed in some subtypes of breast cancers but has not been retained as a CSC marker since CD24+ are often found to be non-tumorigenic [50, 51, 57]. CD44 is an adhesion receptor for several extracellular matrix components such as hyaluronan, collagen and fibronectin as well as several endothelial cell surface receptors including selectins. It is well accepted that CD44+ cancer cells yield a high metastatic potential [51, 57, 58]. ICAM1, an adhesion receptor that is expressed by leukocytes and endothelial cells, was recently shown to be expressed by CTCs and promote their clustering, correlating with a higher metastatic potential [59]. CD97, a G protein-coupled adhesion receptor, was shown to be expressed by CTCs promoting their interaction with platelets promoting efficient extravasation and metastatic colonization [60]. However, these receptors are also expressed by several blood cell types including leukocytes and hematopoietic progenitors [61–

63], suggesting they should be used in combination with other markers. Therefore, attention was put toward the integrin family of adhesion receptors since epithelial and mesenchymal cells express integrins that are significantly different from those of blood cells [64]. Integrin $\beta 1$ expression was shown to correlate with increased colony formation ability [65, 66]. A very promising integrin pair in the epithelial-specific integrin $\alpha 6\beta 4$ which is the main adhesion receptor found in hemidesmosomes [67]. These integrins can be efficiently used to isolate CD44+ breast CTC with tumor-initiating properties thus undergoing at least partly EMT [68, 69]. A recent study showed that EpCAM purified breast CTC expressed integrin $\alpha 6\beta 4$ [70]. These markers could be used in combination with CD44 to very efficiently characterized CTC with tumor-initiating properties [71].

It has been suggested that tumor-initiating properties do not correlate with stemness properties but rather with a regenerative-like phenotype which is associated with the expression of the neuronal-specific adhesion receptor L1CAM [72]. This provides an interesting and highly specific metastasis initiating marker although it remains to be formally demonstrated that this receptor is expressed on CTCs.

As discussed previously, the paradigm of highly motile mesenchymal cancer cells driving metastatic progression has been challenged for the past decade. This has been allowed by the evolution of mouse intravital imaging leading to the striking observation of disseminating cancer cells expressing E-cadherin and driving CTC clustering in mouse metastasis experimental models [73]. However, the fine-tuning of E-cadherin seems elemental as E-cadherin activation led to a decrease in metastasis [74] suggesting a complex relationship between E-cadherin expression and activation and CTC metastatic potential. It was recently shown that E-cadherin expression was observed in clustered CTCs from patient liquid biopsies and correlated with survival [75]. Besides adhesion receptors, other stem cell markers were assessed for their expression in cancer cells with tumor-initiating potentials. CD133 (Prom1) was shown to be expressed in CD44+ tumor-initiating cells [68, 76]. The use of glycosphingolipids gangliosides was efficiently demonstrated as potent markers to identify cancer cells with tumor-initiating abilities [77–80]. The transition from an epithelial toward a mesenchymal phenotype include among other a switch in the expression of intermediate filaments with a downregulation of cytokeratin and the upregulation of vimentin (a major mesenchymal marker). It appears that cancer cells express cell surface vimentin through a mechanism that remains elusive but was shown to be efficient at capturing EpCAM-negative CTCs [81–83]. The use of ganglioside and cell surface vimentin was efficiently used to isolate osteosarcoma CTC [80].

The aldehyde dehydrogenase (ALDH), a detoxifying enzyme required for the oxidation of intracellular aldehydes, is highly expressed in cancer cells with stemness properties [84]. Breast CTCs with hybrid EMT phenotypes can be efficiently identified in liquid biopsies from patients [85]. One important drawback is that this is an intracellular marker and is thus less compatible with a high-throughput clinically oriented strategy. However, the identification of ALDH^{high} cells can now be achieved using fluorescence cytometry [86].

14.1.1.2 Biomechanical Features

As mentioned above, the use of molecular markers in order to specifically capture CTCs with tumor-initiating properties requires the use of a combination of them and might thus limit the throughput. An alternative approach to isolate CTCs lies in their different biophysical properties compared to blood cells or even their non-transformed counterparts (Fig. 14.1). Indeed, biomechanical properties are now emerging as important features driving cancer progression either within the primary tumor during the growth [87–89], the invasive switch [90, 91] or during metastatic colonization [10, 92, 93]. Cancer cells are bigger than most blood cells [46, 94]. Furthermore, there are an increasing amount of data suggesting that cancer cells are biomechanically softer than their non-transformed counterparts at least within the primary tumor [95, 96].

Size

The first attempts to purify CTC from native blood cell relied on the use of porous membrane [97]. With the idea to increase throughput, the engineering of microfluidic devices to purify CTCs based on their biophysical properties has been pioneered since the early 2000s by several groups [98]. Early designs were microfabricated sieving device with parallel columns creating channels of narrower width [99]. Likewise, other size separation microfluidic device took advantage of critical gaps with cross-section preventing CTC passage [100]. Another family of devices depends on the use of centrifugational separation of CTCs based on a spiral architected microfluidic device [101]. These designs led to the commercialization of devices like the Parsotix, which is based on size-exclusion through critical gaps [102] and the ClearCell FX on the other hand relies on centrifugal forces separation with a spiral design [103] among others. However, these remain to be formally approved for clinical use. An alternate design uses hydrodynamic-driven size separation. For instance, the CTC-iChip relies on a dual-chip technology with a hydrodynamic size-based separation that is combined with EpCAM immunomagnetic selection of CTC and CD45-driven leukocyte depletion [94]. Such technology was further developed into a high-throughput device, the LP CTC-iChip which is compatible with clinically-performed leukapheresis (a procedure where leukocytes are separated from blood) [104]. Another strategy relies on 3D imprinted chips which take advantage of centrifugation to filter out CTCs using fluid-assisted separation technology (FAST). It allows fast size-based isolation of CTCs from whole blood and is also commercially available [105].

CTC hetero and homo clusters, although rarer in blood, have been shown to yield a much higher metastatic potential [9, 106–108]. While few clusters could be captured with non-specific devices such as the Parsotix [107, 108], there has been a large amount of work aiming at creating devices to target circulating clusters [109–111]. Using capillary vessel-mimicking microfluidic channels, it was shown that CTC clusters could squeeze to pass through narrow capillary vessels by individual cell deformation and remodeling of intercellular adhesion between CTCs [110]. This suggests that size exclusion might not be the most relevant approach in such a context. On the other hand, isolation of CTCs by cell sizes does not always provide

enough specificity in particular in cases where CTCs are smaller (in small cell lung cancer for instance) and may be lost, while conversely larger leukocytes may be retained.

Deformability

Optical deformation, a microfluidic device that uses a two-beam laser trap to serially deform single suspended cells, was able to discriminate subtle mechanical changes between non-transformed, tumoral, and metastatic breast cancer lines [112]. This early work suggested that single-cell mechanical phenotyping through deformation could be a relevant marker to assess the metastatic potential of CTCs. The implementation of microfluidic-driven cell perfusion makes optical stretching reaching 50–100 cells/h compatible with higher throughput requirements for clinical use [113]. In a recent study, optical stretching was efficiently used to discriminate CTCs from CD45⁻ cells isolated from liquid biopsies of breast cancer patients [114]. In a surrogate approach, deformability cytometry allows rapid high throughput compatible mechanical phenotyping of circulating cells on the fly. It relies on cells entering a small constriction and data acquisition through different means (imaging, electrical resistance or suspended microchannel resonator) with throughput ranging from few cells to thousands of cells per second [115–119]. A deeper review and comparison of the different deformability cytometry modalities has been published recently [120]. Deformability cytometry is able to discriminate between transformed and metastatic cell lines from lung or breast cancer [117, 121]. In a configuration where deformability cytometry is coupled to a suspended microchannel resonator, it could discriminate between CTCs and blood cells and detected mild mechanical differences between different EMT phenotypes with cells having a more mesenchymal phenotype being softer [122]. Real-time deformability cytometry could differentiate low and high metastatic potentials of osteosarcoma cell lines [123]. A recent development of this technic includes the combination of mechanical profiling with fluorescence flow cytometry to sort CD34⁺ hematopoietic stem cells [124]. This suggests it might be combined with any relevant cell surface marker making it thus a relevant method for clinical diagnosis purposes on CTCs. Indeed, deformability cytometry morpho-rheological phenotyping of blood cells was successfully used to enumerate and characterize the different cell types with high throughput efficiency. It was also able to discriminate between normal red blood cells and spherocytosed red blood cells after malaria infection, between leukocytes that are either non-activated or activated after infection and between normal white blood cells or leukemic cells [125].

Perfusable deformation-based microfluidic chips were implemented with channels of different cross-sections where CTC will be retained depending on their deformability [126]. Similarly, high throughput microfluidic-based methods for CTC isolation from liquid biopsies rely on a single row of anisotropic micropillars as a size exclusion and deformability cell filter as the CROSS chip [127] and RUBY chip [128]. An alternate design is the flexible micro spring array (FMSA) which is based on highly porous and flexible micro-spring structures compatible with a high throughput of liquid biopsies [129]. In a quite different

method, microfluidics combined with the use of acoustic waves were successfully used to sort CTCs. The separation is also mainly driven by size and mechanical parameters such as compressibility and density [130, 131]. We provide a non-exhaustive list of recent methods to isolate CTCs to highlight different biophysical-based strategies but refer the readers to excellent recent reviews which cover in detail the latest advances in biophysical-based CTC isolation [132–134].

14.2 Extracellular Vesicles Biomarkers

While CTCs constitute the ultimate evidence of the presence of a (pre-)metastatic tumor, their scarcity makes their clinical use challenging and their presence might not accurately correlate with disease progression [40]. Two recent studies show that tumor secreted EVs might be much more abundant than CTCs in patients plasma. Indeed, in patients with castration-resistant prostate cancer, metastatic breast cancer, metastatic colorectal cancer, or non-small cell lung cancer, the number of large tumor EVs in plasma is 20 times higher than the number of CTCs [135, 136]. In addition to these large EVs ($>1 \mu\text{m}$) co-isolated with CTCs and defined as DNA and CD45 negative and EpCAM and CK positive, there might be even more small tumor EVs present in the plasma and containing numerous potential biomarkers (Fig. 14.1).

14.2.1 EVs Isolation and Characterization

The large amounts of EVs present in body fluids can be isolated by different methods relying on EV properties (size, density, solubility) or on the presence of specific EV surface markers. The former methods include historically and most popular ultracentrifugation-based protocols, but also density gradient, size exclusion chromatography (SEC), ultrafiltration (tangential flow filtration and asymmetric flow field-flow fractionation) and polymer-based precipitation, while the later are mostly based on immunocapture [137]. Importantly, the choice of the isolation method directly impacts the identification of EV cargoes by proteomics or RNA sequencing and needs to be optimized depending on the sample origin [138–140]. Therefore, the identification of low expression EVs biomarkers requires considering both EV purity and EV yield when performing EV isolation. On one hand, with low purity, EV's signature will be hidden by contaminants. On the other hand, a low yield will require higher sample volumes which might be inadequate for patients. For instance, in plasma, the major source of EVs biomarkers so far, lipoproteins and chylomicrons contaminants excess by far the number of EVs ($>10^5$ to 10^7) and have similar ranges of size and density which complicates their separation from EVs [30, 141, 142]. Therefore a proper separation of EVs and lipoproteins from plasma might require the use of a combination of methods such as SEC and density gradients [140], SEC and ultrafiltration [143] or EV precipitation, density gradients and SEC [144]. Alternatively, novel approaches, which might be more suited to diagnosis are emerging. This is the case for instance of the ultrafiltration-based Exodus method,

which was shown to improve the yield and purity of urine EVs for transcriptomics [145]. Yet, the appropriate set of methods adapted to routine use in clinics still needs to be defined [146]. Once isolated, EVs size and concentration can be analyzed using classical methods of detection such as nanoparticle tracking analysis (NTA) and resistive pulse sensing (RPS). However, these approaches require a minimal concentration (10^6 – 10^7 particle/ml) and lack specificity as they cannot distinguish EVs from other objects of similar sizes (lipoproteins, ribonucleoproteic complexes, virus, etc.). Therefore, additional analyses are required, including electron microscopy to prove the presence of lipid bi-layered vesicles and molecular analysis to assess the presence of EV markers (among the most common ones: the 3 tetraspanins CD63, CD9, CD81, but also AnnexinA1, syntenin-1, Alix...) and the absence of contaminants [147, 148]. The molecular content of EVs can be analyzed as a bulk by looking at the global EV signature using conventional proteomic, lipidomic or RNA sequencing approaches or by looking at specific markers using targeted approaches (by western-blot, ELISA, RT-PCR) [137]. These approaches are instrumental in identifying novel EV biomarkers [149], but they do not take into account EVs heterogeneity since they rely on the bulk analysis of global EV content.

Therefore, the past years witnessed the emergence of alternative methods, allowing to characterize individual vesicles and the use of specific EV subpopulations as biomarkers [150]. In particular, consequent progresses were made in adapting flow cytometry to the detection of nanoscale objects, allowing to quantify specific subpopulation of EVs isolated from body fluids [151]. For instance, tetraspanin and EpCAM positive EVs can be efficiently detected from urine by flow cytometry with 10 times less urine volume than conventional detection [152]. Besides flow cytometry, several methods of EVs immunocapture have been developed and can be used in diagnosis [150]. EVs are first captured on a slide or on a bead using an antibody directed against an EV surface protein and then one (or more) other surface protein is detected using specific antibody(ies). Revelation of the antibody labeling can be achieved through various methods such as quantum dots [153] or biotin/streptavidin affinity [154, 155]. Importantly, those methods were reported to function on crude plasma without EV isolation. As an alternative to secondary antibodies, aptamers (short nucleic acid oligomers exhibiting specific protein-binding affinity) can be used to detect proteins at the surface of EVs with high sensitivity, using fluorescence [156, 157] or electrochemical detection [158, 159]. Another method of detection of immuno-captured EVs, based on surface-enhanced Raman spectroscopy appears promising. For instance, three markers CD63, Glypican-1 and CD44v6 could be detected with high sensitivity on pancreatic cancer cell lines EVs using surface-enhanced Raman spectroscopy [160]. Besides, a similar method was used to track changes in the composition of four markers in plasma EVs during the treatment of melanoma patients [161]. Finally, microfluidic chips can be used to analyze specific mRNA levels enriched in tumor EVs present in blood from patients with glioblastoma [162].

Overall, the boom in new methods of EVs isolation and analysis tends to provide more sensitivity and specificity to EVs detection and to decrease sample volumes. However, the best method for clinical translation, allowing fast and quantitative

analysis of circulating EVs at high throughput and low cost remains to be determined.

14.2.2 Global EVs Levels and EVs Subpopulations as Cancer Biomarkers

Over the past years, several types of EV-related parameters were proposed as tumor biomarkers. They include the total number of circulating EVs, specific sub-populations of circulating EVs, individual EV proteins or RNAs, combination of EV molecules or other emerging EV characteristics. The simplest EV-related biomarker is probably the possibility that the global number of circulating EVs, or the amount of circulating EV proteins, might reflect the presence and the evolution of a tumor and could therefore be used in diagnosis [163]. Indeed, several reports observed such an increase in lymph and blood circulation of melanoma or glioblastoma patients [164–167]. This could be explained by the fact that several parameters related to tumor growth (hypoxia, acidity, nutrients availability, inflammation..) or treatment (irradiation, chemotherapy) modulate EV secretion rates [168–171]. However, the accurate rate of EV secretion by tumors during their evolution is unknown. Animal models allowing to confidently identify circulating tumor EVs have recently been described and might be instrumental to address this question [172]. Importantly, the increase of circulating EVs in cancer patients could also be due to non-tumor EVs. Indeed, circulating EVs levels are also varying depending on immune-related disorders and on multiple physiologic factors, such as age, fasting, or exercise [173–175]. These variations make the use of global EV levels more complex and suggest that measuring specific EV subpopulation might be more relevant biomarkers to assess tumor progression. Several studies identified an increase in specific EV subpopulations in plasma from patients with particular cancer types, as for instance CD81-EpCAM and CD81-EPHA2 EVs in pancreatic cancer [153], CD9-CD63 and EpCAM-CD63 EVs in colorectal cancer [154], CD9/CD147 EVs in colorectal cancer [155], CD63-PTK7 EVs in lymphoblastic leukemia [156] or CD9-CD63-EpCAM-MUC1 EVs in breast cancer patients [157].

14.2.3 EVs Proteins as Cancer Biomarkers

A hunt for EV-associated cancer biomarkers was launched over the past years. It allowed the identification of tens of novel potential diagnosis targets, which can either be single RNAs or proteins or more complex molecular signatures [149, 176–178]. The molecules isolated from cancer patients biofluids are not necessarily originating from EVs secreted by cancer cells but could be present on EVs secreted by non-tumor cells when the organism harbors a tumor. Past studies allowed the identification of single molecules which could be used to monitor either the presence and/or status of a given tumor or to predict treatment response and clinical outcome. Among them, the protein glypican-1 (GPC1) received much attention. EV-bound

GPC1 was initially shown to be enriched in plasma from patients with early pancreatic cancer and, to a lesser extent from patients with breast cancer [177]. Highly debated [179, 180], it has then been suggested that GPC1 mRNA [181], GPC1 regulatory miRNA [182] or GPC1 protein combined with other EV proteins [183, 184] could be more efficient in pancreatic or colorectal cancer diagnosis. In addition to GPC1, EV-bound PD-L1, which contributes to immunosuppression by exhausting T-cells [185, 186] can also be used for cancer diagnosis, in particular to distinguish responders from non-responders patients with metastatic melanoma [186, 187]. Many other EV protein markers were described over the past years [188, 189]. They include, among others, MIF in metastatic pancreatic cancer [190], MET in melanoma [163], CD5L as a potential serum EV biomarker in lung cancer patients [191], Del-1 or fibronectin in EVs from breast cancer patients [192, 193], Survivin in EVs from breast or prostate cancer patients [194, 195] or PKG1, RALGAP2, NFX1, TJP2 in breast cancer EVs patients [196] or HSP70 in breast and lung cancer patients [197].

While each of these markers might be promising, their validation by independent groups in independent cohorts, a prerequisite for translation toward clinics, is often awaited. As an alternative to single EV proteins, it might be more efficient to monitor multiple EV proteins in the same time. A recent and massive study analyzed the EV proteome of 426 human samples and proposed pan-cancer or cancer-specific EVs multi-protein signatures which could help to identify and classify cancer in patients [149]. Although promising, the clinical validation of such signatures remains to be demonstrated.

14.2.4 EVs RNAs and DNA as Cancer Biomarkers

In addition to proteins, circulating EVs also contain important amounts of RNAs. EVs miRNAs in particular were proposed as cancer biomarkers potentially outperforming cell-free plasma miRNA as shown for colon cancer patients [198]. Many individual EVs miRNAs have been described. This is the case for instance of plasma EVs miRNAs miR-1246 and miR-21 in breast cancer patients [199] or miR-10b, miR-21, miR-30c and miR-181 in pancreatic cancer patients [179]. In addition to plasma, EVs miRNAs biomarkers were also identified in urine [200], as for instance miR-21-5p, miR-4454, and miR-720-3007a in bladder cancer patients [201, 202]. Similarly to protein biomarkers, multiple miRNAs could be more sensitive and specific than single miRNAs and miRNA combination were proposed to improve breast cancer [203–205] or sarcoma [206] diagnosis. However, miRNAs constitute a minority of total RNAs present in EVs [207] and other RNA types might constitute relevant cancer biomarkers, as proposed for coding mRNAs in breast [178] and prostate cancer [208], piRNAs in prostate cancer [209], circRNAs in gastric cancer [210] or lncRNA in breast cancer [211]. In addition to RNA, DNA fragments were identified in circulating EVs from cancer patients [22, 23, 212]. Importantly, several recent studies showed that DNA EVs is more abundant and more efficient to detect mutations than cell-free DNA [213–215]. This

EVs DNA corresponds to double-stranded fragments up to 17 kb long covering the whole genome, which can be used to detect mutations reflecting the genetic status of the tumor. EVs DNA sequencing reveals mutations in oncogenes or tumor suppressor genes, such as KRAS, EGFR or P53 [22, 23, 212]. It can therefore help to analyze the status of the primary tumor in order to choose the appropriate treatment. For instance, the EGFR T790M mutation, which confers resistance to anti-EGFR therapy, was shown to be detectable in EVs with an improved sensitivity compared to cell-free DNA alone [216]. While EV proteins, RNAs and DNA provide valuable diagnosis tools, their combination might be even more powerful. For instance, measuring the levels of a set of EVs miRNAs could be combined with immunocapture of specific EVs subpopulations and significantly improves sensitivity and specificity in breast cancer [203] or pancreatic cancer diagnosis [217].

14.2.5 Alternative EV Biomarkers

In addition to proteins and nucleic acids, understudied components or properties of EVs might also constitute valid cancer biomarkers. Indeed, lipid profiles as well as protein post-translational modifications of EV proteins were shown to differ between tumor and non-tumor EVs [218–220]. Besides, EVs metabolic signature, which was recently proposed as tuberculosis biomarkers [221], could also be meaningful in cancer that are known to have alternative metabolism. More generally, global differences in EVs biochemical composition could be identified through Raman spectroscopy, defining a specific signature for patients with Parkinson's disease [222]. Similarly, tumor EVs could be distinguished from red blood cell EVs and lipoproteins [223], opening the door to the establishment of a tumor EV signature. Indeed, EVs from tumor cells could be differentiated from non-cancer EVs using an automated Raman trapping analysis [224]. Finally, the mechanical properties of EVs can now be measured [225] and could potentially be used similarly to those of CTCs.

14.3 Discussion

Liquid biopsies are now accepted as an important diagnostic tool in order to adapt the therapeutic strategy to each specific patient [37]. There is thus an urgent need for the development of fast, efficient and clinically compatible strategies to purify CTCs as well as EVs from blood samples.

Marker-based CTC isolation is so far the most efficient in a clinical context, as demonstrated by the fact that the CellSearch, an EpCAM-immunoisolation device, is for now the only clinically approved device. However, these strategies are challenged by the growing observation they are biasing capture toward specific phenotypes along the EMT spectrum. Biophysical-based strategies should undoubtedly gain momentum in clinics with Parsotix being CE marked for use as an *in vitro* diagnostic device in Europe. Given the heterogeneity in size among a single CTC population and the small size of CTCs observed in some cancer types such as small

cell lung cancer, the use of biomarker versus biophysical properties should be adapted to cancer clinical specificities. The combination of both methods might be a promising solution in an attempt to design a first intention universal device and is currently being tested [94, 104]. Although still debated, it appears that cancer cells within the primary tumor are mechanically softer than their normal counterpart [95]. An emerging concept is also that the mechanical state of cells is not set in stone and that the different steps of the metastatic cascade might act as bottlenecks to specifically select the most mechanically fitted state at each step [92]. CTCs are more resistant to shear stress than first thought. Shear resistance requires plasma membrane repair [226] and nucleoskeleton integrity [227]. Recent work has suggested that cytoskeletal remodeling is essential in CTC mechanoadaptation to shear stress [228]. Deformability cytometry given its high throughput at the single cell level seems compatible with large-scale mechanical phenotyping of CTCs from liquid biopsies. Interestingly it was able to detect that CTC in a more mesenchymal state were softer and CTC covered with platelets were stiffer [122]. Improving the sensibility of these device seems essential for efficient cancer targeting personalized medicine. Single cell-oriented methods might be relevant in a clinical context to monitor CTC mechanical plasticity along the course of the metastatic progression, although it remains unknown what are the best mechanically fitted cell states at each step of the metastatic cascade [92].

As for now, cancer diagnosis relying on circulating EVs lags behind CTCs in clinics. However, given the growing number of published EV biomarkers candidates and the number (>50) of undergoing clinical trials on the matter (<https://clinicaltrials.gov>), it is likely that EVs will close the gap in the coming years. However, for this to happen, significant challenges will have to be addressed. Obviously, the first one will be to identify the appropriate markers or set of markers for each cancer type, for specific stages and to predict treatment efficiency or resistance. Most studies describing novel EV biomarkers rely on small number of patients and need to be validated in independent cohorts [189]. Importantly, the sensitivity and specificity of those EV biomarkers will have to be compared to existing non-EVs circulating biomarkers and to conventional diagnosis methods. This has recently been done for the most advanced EV biomarker to date, the ExoDx Prostate (Intelliscore) (EPI) test, which relies on the quantification of three EVs RNAs to diagnose prostate cancer from urine samples [229]. A pooled meta-analysis from 3 independent studies revealed superior performances of the EPI test compared to standard diagnosis (including classical prostate-specific antigen (PSA) levels) to discriminate high-grade prostate cancer.

The transition toward clinics will require standardized sample preparation procedures following precise guidelines for sensitive and reproducible detection [146, 230]. Pre-analytical variables, such as sampling time, rapid separation from cells to avoid secretion, storage, transport, and processing were shown to affect EV measurement and will therefore have to be defined and standardized [189, 231]. The optimal method to isolate circulating EVs in clinics might differ from the methods used in marker discovery phases. For instance, ultracentrifugation, which is widely used in fundamental EV research (alone or in combination with other isolation

methods), is time-consuming, has low throughput and reproducibility and is therefore not adapted to clinical use. Similarly, other methods such as SEC, density gradient, or immunocapture exhibit significant drawbacks for clinical use [189]. Hence, EV isolation methods and readouts will have to be improved or optimized for clinical translation by taking into account time requirement, standard equipment, throughput, and cost.

Dual isolation of both CTCs and EVs is a seducing emerging strategy that has recently been applied to blood samples from melanoma and pancreatic ductal adenocarcinoma [42, 232]. This could allow a deeper characterization of the metastatic context including the profiling of disseminating cancer cells and the identification of potential preferential sites of colonization with already established premetastatic niches from a single patient sample. Liquid biopsies-oriented metastatic cancer analysis has been a major center of interest in both cancer biology as well as clinics. However, there are several other alternative approaches that have been implemented recently with the aim of monitoring cancer progression using non-invasive methods. This includes the use of *in vivo* cytometry which might be a promising imaging-based complementary tool to liquid biopsies for diagnosing and monitoring purposes [233].

Acknowledgments We thank the Tumor Biomechanics lab (www.goetzlab.fr), for support and discussions. This work has been supported by Plan Cancer, INCa, Cancéropôle Grand-Est and La Ligue Contre le Cancer and by institutional funds from INSERM and the University of Strasbourg.

References

1. Srivastava S, Koay EJ, Borowsky AD et al (2019) Cancer overdiagnosis: a biological challenge and clinical dilemma. *Nat Rev Cancer* 19:349–358. <https://doi.org/10.1038/S41568-019-0142-8>
2. Siegel RL, Miller KD, Jemal A (2020) Cancer statistics, 2020. *CA Cancer J Clin* 70:7–30. <https://doi.org/10.3322/CAAC.21590>
3. Alix-Panabières C (2020) The future of liquid biopsy. *Nature* 579:S9. <https://doi.org/10.1038/D41586-020-00844-5>
4. Alix-Panabières C, Pantel K (2021) Liquid biopsy: from discovery to clinical application. *Cancer Discov* 11:858–873. <https://doi.org/10.1158/2159-8290.CD-20-1311>
5. Zhou E, Li Y, Wu F et al (2021) Circulating extracellular vesicles are effective biomarkers for predicting response to cancer therapy. *EBioMedicine* 67:103365. <https://doi.org/10.1016/j.ebiom.2021.103365>
6. Lambert AW, Pattabiraman DR, Weinberg RA (2017) Emerging biological principles of metastasis. *Cell* 168:670–691. <https://doi.org/10.1016/j.cell.2016.11.037>
7. Friedl P, Wolf K, Lammerding J (2011) Nuclear mechanics during cell migration. *Curr Opin Cell Biol* 23:55–64
8. Eddy RJ, Weidmann MD, Sharma VP, Condeelis JS (2017) Tumor cell invadopodia: invasive protrusions that orchestrate metastasis. *Trends Cell Biol* 27:595–607. <https://doi.org/10.1016/j.tcb.2017.03.003>
9. Ozimski LL, Gremmelspacher D, Aceto N (2021) A fatal affair: circulating tumor cell relationships that shape metastasis. *iScience* 24:103073. <https://doi.org/10.1016/j.isci.2021.103073>

10. Follain G, Herrmann D, Harlepp S et al (2020) Fluids and their mechanics in tumour transit: shaping metastasis. *Nat Rev Cancer* 20:107–124. <https://doi.org/10.1038/s41568-019-0221-x>
11. Obenauf AC, Massagué J (2015) Surviving at a distance: organ-specific metastasis. *Trends Cancer* 1:76–91. <https://doi.org/10.1016/j.trecan.2015.07.009>
12. Klein CA (2020) Cancer progression and the invisible phase of metastatic colonization. *Nat Rev Cancer* 20:681–694. <https://doi.org/10.1038/s41568-020-00300-6>
13. Phan TG, Croucher PI (2020) The dormant cancer cell life cycle. *Nat Rev Cancer* 20:398–411. <https://doi.org/10.1038/s41568-020-0263-0>
14. Dongre A, Weinberg RA (2019) New insights into the mechanisms of epithelial–mesenchymal transition and implications for cancer. *Nat Rev Mol Cell Biol* 20:69. <https://doi.org/10.1038/s41580-018-0080-4>
15. Pastushenko I, Blanpain C (2019) EMT transition states during tumor progression and metastasis. *Trends Cell Biol* 29:212–226. <https://doi.org/10.1016/j.tcb.2018.12.001>
16. Brabletz S, Schuhwerk H, Brabletz T, Stemmler MP (2021) Dynamic EMT: a multi-tool for tumor progression. *EMBO J* 40. <https://doi.org/10.15252/embj.2021108647>
17. Lambert AW, Weinberg RA (2021) Linking EMT programmes to normal and neoplastic epithelial stem cells. *Nat Rev Cancer* 21:325–338. <https://doi.org/10.1038/s41568-021-00332-6>
18. Massagué J, Ganesh K (2021) Metastasis-initiating cells and ecosystems. *Cancer Discov* 11: 971–994. <https://doi.org/10.1158/2159-8290.CD-21-0010>
19. Fabbiano F, Corsi J, Gurrieri E et al (2020) RNA packaging into extracellular vesicles: an orchestra of RNA-binding proteins? *J Extracell Vesicles*. <https://doi.org/10.1002/jev2.12043>
20. van Niel G, D’Angelo G, Raposo G (2018) Shedding light on the cell biology of extracellular vesicles. *Nat Rev Mol Cell Biol*. <https://doi.org/10.1038/nrm.2017.125>
21. Skotland T, Hessvik NP, Sandvig K, Llorente A (2019) Exosomal lipid composition and the role of ether lipids and phosphoinositides in exosome biology. *J Lipid Res* 60:9–18. <https://doi.org/10.1194/jlr.R084343>
22. Balaj L, Lessard R, Dai L et al (2011) Tumour microvesicles contain retrotransposon elements and amplified oncogene sequences. *Nat Commun*. <https://doi.org/10.1038/ncomms1180>
23. Kahlert C, Melo SA, Protopopov A et al (2014) Identification of double-stranded genomic DNA spanning all chromosomes with mutated KRAS and p53 DNA in the serum exosomes of patients with pancreatic cancer. *J Biol Chem* 289:3869–3875. <https://doi.org/10.1074/jbc.C113.532267>
24. Möller A, Lobb RJ (2020) The evolving translational potential of small extracellular vesicles in cancer. *Nat Rev Cancer* 20:697–709. <https://doi.org/10.1038/s41568-020-00299-w>
25. Kalluri R, LeBleu VS (2020) The biology, function, and biomedical applications of exosomes. *Science* 367. <https://doi.org/10.1126/science.aau6977>
26. Sheehan C, D’Souza-Schorey C (2019) Tumor-derived extracellular vesicles: molecular parcels that enable regulation of the immune response in cancer. *J Cell Sci* 132(20):jcs235085
27. Ghoroghi S, Mary B, Asokan N et al (2021) Tumor extracellular vesicles drive metastasis (it’s a long way from home). *FASEB BioAdvances* 3:930–943. <https://doi.org/10.1096/FBA.2021-00079>
28. Peinado H, Zhang H, Matei IR et al (2017) Pre-metastatic niches: organ-specific homes for metastases. *Nat Rev Cancer* 17:302–317. <https://doi.org/10.1038/nrc.2017.6>
29. Arraud N, Linares R, Tan S et al (2014) Extracellular vesicles from blood plasma: determination of their morphology, size, phenotype and concentration. *J Thromb Haemost* 12:614–627. <https://doi.org/10.1111/JTH.12554>
30. Sódar BW, Kittel Á, Pálóczi K et al (2016) Low-density lipoprotein mimics blood plasma-derived exosomes and microvesicles during isolation and detection. *Sci Rep* 6:1–12. <https://doi.org/10.1038/srep24316>
31. Klein CA (2013) Selection and adaptation during metastatic cancer progression. *Nature* 501: 365–372. <https://doi.org/10.1038/nature12628>

32. Naxerova K, Jain RK (2015) Using tumour phylogenetics to identify the roots of metastasis in humans. *Nat Rev Clin Oncol* 12:258–272. <https://doi.org/10.1038/nrclinonc.2014.238>
33. Hu Z, Curtis C (2020) Looking backward in time to define the chronology of metastasis. *Nat Commun* 11:3213. <https://doi.org/10.1038/s41467-020-16995-y>
34. Steeg PS (2016) Targeting metastasis. *Nat Rev Cancer* 16:201–218. <https://doi.org/10.1038/nrc.2016.25>
35. Esposito M, Ganesan S, Kang Y (2021) Emerging strategies for treating metastasis. *Nat Cancer* 2:258–270. <https://doi.org/10.1038/s43018-021-00181-0>
36. Ganesh K, Massagué J (2021) Targeting metastatic cancer. *Nat Med* 27:34–44. <https://doi.org/10.1038/s41591-020-01195-4>
37. Bardelli A, Pantel K (2017) Liquid biopsies, what we do not know (yet). *Cancer Cell* 31:172–179. <https://doi.org/10.1016/j.ccell.2017.01.002>
38. Keller L, Pantel K (2019) Unravelling tumour heterogeneity by single-cell profiling of circulating tumour cells. *Nat Rev Cancer* 19:553–567. <https://doi.org/10.1038/s41568-019-0180-2>
39. Stahel RA, Gilks WR, Lehmann H-P, Schenker T (1994) Third international workshop on lung tumor and differentiation antigens: overview of the results of the central data analysis. *Int J Cancer* 57:6–26. <https://doi.org/10.1002/ijc.2910570704>
40. Cristofanilli M, Budd GT, Ellis MJ et al (2004) Circulating tumor cells, disease progression, and survival in metastatic breast cancer. *N Engl J Med* 351:781–791. <https://doi.org/10.1056/NEJMoa040766>
41. Allard WJ, Matera J, Miller MC et al (2004) Tumor cells circulate in the peripheral blood of all major carcinomas but not in healthy subjects or patients with nonmalignant diseases. *Clin Cancer Res* 10:6897–6904. <https://doi.org/10.1158/1078-0432.CCR-04-0378>
42. Kang Y-T, Hadlock T, Lo T-W et al (2020) Dual-isolation and profiling of circulating tumor cells and cancer exosomes from blood samples with melanoma using immunoaffinity-based microfluidic interfaces. *Adv Sci* 7:2001581. <https://doi.org/10.1002/advs.202001581>
43. Mostert B, Kraan J, Bolt-de Vries J et al (2011) Detection of circulating tumor cells in breast cancer may improve through enrichment with anti-CD146. *Breast Cancer Res Treat* 127:33–41. <https://doi.org/10.1007/s10549-010-0879-y>
44. Onstenk W, Kraan J, Mostert B et al (2015) Improved circulating tumor cell detection by a combined EpCAM and MCAM CellSearch enrichment approach in patients with breast cancer undergoing neoadjuvant chemotherapy. *Mol Cancer Ther* 14:821–827. <https://doi.org/10.1158/1535-7163.MCT-14-0653>
45. Nagrath S, Sequist LV, Maheswaran S et al (2007) Isolation of rare circulating tumour cells in cancer patients by microchip technology. *Nature* 450:1235–1239. <https://doi.org/10.1038/nature06385>
46. Stott SL, Hsu C-H, Tsukrov DI et al (2010) Isolation of circulating tumor cells using a microvortex-generating herringbone-chip. *Proc Natl Acad Sci* 107:18392–18397. <https://doi.org/10.1073/pnas.1012539107>
47. Diener J, Sommer L (2021) Reemergence of neural crest stem cell-like states in melanoma during disease progression and treatment. *Stem Cells Transl Med* 10:522–533. <https://doi.org/10.1002/sctm.20-0351>
48. Mani SA, Guo W, Liao M-J et al (2008) The epithelial-mesenchymal transition generates cells with properties of stem cells. *Cell* 133:704–715. <https://doi.org/10.1016/j.cell.2008.03.027>
49. Yu M, Bardia A, Wittner BS et al (2013) Circulating breast tumor cells exhibit dynamic changes in epithelial and mesenchymal composition. *Science* 339:580–584. <https://doi.org/10.1126/science.1228522>
50. Sieuwerts AM, Kraan J, Bolt J et al (2009) Anti-epithelial cell adhesion molecule antibodies and the detection of circulating normal-like breast tumor cells. *J Natl Cancer Inst* 101:61–66. <https://doi.org/10.1093/jnci/djn419>

51. Chaffer CL, Brueckmann I, Scheel C et al (2011) Normal and neoplastic nonstem cells can spontaneously convert to a stem-like state. *Proc Natl Acad Sci* 108:7950–7955. <https://doi.org/10.1073/pnas.1102454108>
52. Zhang L, Ridgway LD, Wetzel MD et al (2013) The identification and characterization of breast cancer CTCs competent for brain metastasis. *Sci Transl Med* 5:180ra48. <https://doi.org/10.1126/scitranslmed.3005109>
53. Alix-Panabières C, Vendrell J-P, Slijper M et al (2009) Full-length cytokeratin-19 is released by human tumor cells: a potential role in metastatic progression of breast cancer. *Breast Cancer Res* 11:1–10. <https://doi.org/10.1186/bcr2326>
54. Denève E, Riethdorf S, Ramos J et al (2013) Capture of viable circulating tumor cells in the liver of colorectal cancer patients. *Clin Chem* 59:1384–1392. <https://doi.org/10.1373/clinchem.2013.202846>
55. Donati G, Watt FM (2015) Stem cell heterogeneity and plasticity in epithelia. *Cell Stem Cell* 16:465–476. <https://doi.org/10.1016/j.stem.2015.04.014>
56. Jahchan NS, Lim JS, Bola B et al (2016) Identification and targeting of long-term tumor-propagating cells in small cell lung cancer. *Cell Rep* 16:644–656. <https://doi.org/10.1016/j.celrep.2016.06.021>
57. Al-Hajj M, Wicha MS, Benito-Hernandez A et al (2003) Prospective identification of tumorigenic breast cancer cells. *Proc Natl Acad Sci* 100:3983–3988. <https://doi.org/10.1073/pnas.0530291100>
58. Chaffer CL, Marjanovic ND, Lee T et al (2013) Poised chromatin at the ZEB1 promoter enables breast cancer cell plasticity and enhances tumorigenicity. *Cell* 154:61–74. <https://doi.org/10.1016/j.cell.2013.06.005>
59. Taftaf R, Liu X, Singh S et al (2021) ICAM1 initiates CTC cluster formation and trans-endothelial migration in lung metastasis of breast cancer. *Nat Commun* 12:4867. <https://doi.org/10.1038/s41467-021-25189-z>
60. Ward Y, Lake R, Faraji F et al (2018) Platelets promote metastasis via binding tumor CD97 leading to bidirectional signaling that coordinates transendothelial migration. *Cell Rep* 23:808–822. <https://doi.org/10.1016/j.celrep.2018.03.092>
61. Eibl RH (2012) Single-molecule studies of integrins by AFM-based force spectroscopy on living cells. In: *Scanning probe microscopy in nanoscience and nanotechnology*, vol 3. Springer, pp 137–169
62. Oatley M, Bölükbası ÖV, Svensson V et al (2020) Single-cell transcriptomics identifies CD44 as a marker and regulator of endothelial to haematopoietic transition. *Nat Commun* 11:1–18. <https://doi.org/10.1038/s41467-019-14171-5>
63. Wang T, Ward Y, Tian L et al (2005) CD97, an adhesion receptor on inflammatory cells, stimulates angiogenesis through binding integrin counterreceptors on endothelial cells. *Blood* 105:2836–2844. <https://doi.org/10.1182/blood-2004-07-2878>
64. Humphries JD, Byron A, Humphries MJ (2006) Integrin ligands at a glance. *J Cell Sci* 119:3901–3903. <https://doi.org/10.1242/jcs.03098>
65. Vishnoi M, Peddibhotla S, Yin W et al (2015) The isolation and characterization of CTC subsets related to breast cancer dormancy. *Sci Rep* 5:17533. <https://doi.org/10.1038/srep17533>
66. Boral D, Vishnoi M, Liu HN et al (2017) Molecular characterization of breast cancer CTCs associated with brain metastasis. *Nat Commun* 8:196. <https://doi.org/10.1038/s41467-017-00196-1>
67. Osmani N, Labouesse M (2015) Remodeling of keratin-coupled cell adhesion complexes. *Curr Opin Cell Biol* 32:30–38. <https://doi.org/10.1016/j.ceb.2014.10.004>
68. Meyer MJ, Fleming JM, Lin AF et al (2010) CD44posCD49fhiCD133/2hi defines xenograft-initiating cells in estrogen receptor–negative breast cancer. *Cancer Res* 70:4624–4633. <https://doi.org/10.1158/0008-5472.CAN-09-3619>

69. Bierie B, Pierce SE, Kroeger C et al (2017) Integrin- $\beta 4$ identifies cancer stem cell-enriched populations of partially mesenchymal carcinoma cells. *Proc Natl Acad Sci* 114:E2337–E2346. <https://doi.org/10.1073/pnas.1618298114>
70. Sharifi M, Zarrin B, Najafi MB et al (2021) Integrin $\alpha 6 \beta 4$ on circulating tumor cells of metastatic breast cancer patients. *Adv Biomed Res* 10:16. https://doi.org/10.4103/abr.abr_76_21
71. Kröger C, Afeyan A, Mraz J et al (2019) Acquisition of a hybrid E/M state is essential for tumorigenicity of basal breast cancer cells. *Proc Natl Acad Sci* 116:7353–7362. <https://doi.org/10.1073/pnas.1812876116>
72. Ganesh K, Basnet H, Kaygusuz Y et al (2020) L1CAM defines the regenerative origin of metastasis-initiating cells in colorectal cancer. *Nat Cancer* 1:28–45. <https://doi.org/10.1038/s43018-019-0006-x>
73. Padmanaban V, Krol I, Suhail Y et al (2019) E-cadherin is required for metastasis in multiple models of breast cancer. *Nature* 573:439–444. <https://doi.org/10.1038/s41586-019-1526-3>
74. Na T-Y, Schecterson L, Mendonsa AM, Gumbiner BM (2020) The functional activity of E-cadherin controls tumor cell metastasis at multiple steps. *Proc Natl Acad Sci* 117:5931–5937. <https://doi.org/10.1073/pnas.1918167117>
75. Hapach LA, Carey SP, Schwager SC et al (2021) Phenotypic heterogeneity and metastasis of breast cancer cells. *Cancer Res* 81:3649–3663. <https://doi.org/10.1158/0008-5472.CAN-20-1799>
76. Fang C, Fan C, Wang C et al (2016) CD133 + CD54 + CD44 + circulating tumor cells as a biomarker of treatment selection and liver metastasis in patients with colorectal cancer. *Oncotarget* 7:77389–77403. <https://doi.org/10.18632/oncotarget.12675>
77. Battula VL, Shi Y, Evans KW et al (2012) Ganglioside GD2 identifies breast cancer stem cells and promotes tumorigenesis. *J Clin Invest* 122:2066–2078. <https://doi.org/10.1172/JCI59735>
78. Liang Y-J, Ding Y, Lavery SB et al (2013) Differential expression profiles of glycosphingolipids in human breast cancer stem cells vs. cancer non-stem cells. *Proc Natl Acad Sci* 110:4968–4973. <https://doi.org/10.1073/pnas.1302825110>
79. Chiu CG, Nakamura Y, Chong KK et al (2014) Genome-wide characterization of circulating tumor cells identifies novel prognostic genomic alterations in systemic melanoma metastasis. *Clin Chem* 60:873–885. <https://doi.org/10.1373/clinchem.2013.213611>
80. Fasanya HO, Dopico PJ, Yeager Z et al (2021) Using a combination of gangliosides and cell surface vimentin as surface biomarkers for isolating osteosarcoma cells in microfluidic devices. *J Bone Oncol* 28:100357. <https://doi.org/10.1016/j.jbo.2021.100357>
81. Satelli A, Mitra A, Brownlee Z et al (2015) Epithelial–mesenchymal transitioned circulating tumor cells capture for detecting tumor progression. *Clin Cancer Res* 21:899–906. <https://doi.org/10.1158/1078-0432.CCR-14-0894>
82. Satelli A, Batth I, Brownlee Z et al (2017) EMT circulating tumor cells detected by cell-surface vimentin are associated with prostate cancer progression. *Oncotarget* 8:49329–49337. <https://doi.org/10.18632/oncotarget.17632>
83. Xie X, Wang L, Wang X et al (2021) Evaluation of cell surface vimentin positive circulating tumor cells as a diagnostic biomarker for lung cancer. *Front Oncol* 11:1712. <https://doi.org/10.3389/fonc.2021.672687>
84. Ginestier C, Hur MH, Charafe-Jauffret E et al (2007) ALDH1 is a marker of normal and malignant human mammary stem cells and a predictor of poor clinical outcome. *Cell Stem Cell* 1:555–567. <https://doi.org/10.1016/j.stem.2007.08.014>
85. Papadaki MA, Stoupis G, Theodoropoulos PA et al (2019) Circulating tumor cells with stemness and epithelial-to-mesenchymal transition features are chemoresistant and predictive of poor outcome in metastatic breast cancer. *Mol Cancer Ther* 18:437–447. <https://doi.org/10.1158/1535-7163.MCT-18-0584>
86. Leng Z, Yang Z, Li L et al (2017) A reliable method for the sorting and identification of ALDHhigh cancer stem cells by flow cytometry. *Exp Ther Med* 14:2801–2808. <https://doi.org/10.3892/etm.2017.4846>

87. Northcott JM, Dean IS, Mouw JK, Weaver VM (2018) Feeling stress: the mechanics of cancer progression and aggression. *Front Cell Dev Biol* 6. <https://doi.org/10.3389/fcell.2018.00017>
88. Levayer R (2020) Solid stress, competition for space and cancer: the opposing roles of mechanical cell competition in tumour initiation and growth. *Semin Cancer Biol* 63:69–80. <https://doi.org/10.1016/j.semcancer.2019.05.004>
89. Stylianopoulos T, Munn LL, Jain RK (2018) Reengineering the physical microenvironment of tumors to improve drug delivery and efficacy: from mathematical modeling to bench to bedside. *Trends Cancer* 4:292–319. <https://doi.org/10.1016/j.trecan.2018.02.005>
90. Wei SC, Yang J (2016) Forcing through tumor metastasis: the interplay between tissue rigidity and epithelial–mesenchymal transition. *Trends Cell Biol* 26:111–120. <https://doi.org/10.1016/j.tcb.2015.09.009>
91. Kai F, Laklai H, Weaver VM (2016) Force matters: biomechanical regulation of cell invasion and migration in disease. *Trends Cell Biol* 26:486–497. <https://doi.org/10.1016/j.tcb.2016.03.007>
92. Gensbittel V, Kräter M, Harlepp S et al (2021) Mechanical adaptability of tumor cells in metastasis. *Dev Cell* 56:164–179. <https://doi.org/10.1016/j.devcel.2020.10.011>
93. Wirtz D, Konstantopoulos K, Searson PC (2011) The physics of cancer: the role of physical interactions and mechanical forces in metastasis. *Nat Rev Cancer* 11:512–522. <https://doi.org/10.1038/nrc3080>
94. Ozkumur E, Shah AM, Ciciliano JC et al (2013) Inertial focusing for tumor antigen–dependent and –independent sorting of rare circulating tumor cells. *Sci Transl Med* 5:179ra47. <https://doi.org/10.1126/scitranslmed.3005616>
95. Alibert C, Goud B, Manneville J-B (2017) Are cancer cells really softer than normal cells? *Biol Cell* 109:167–189. <https://doi.org/10.1111/boc.201600078>
96. Plodinec M, Loparic M, Monnier CA et al (2012) The nanomechanical signature of breast cancer. *Nat Nanotechnol* 7:757–765. <https://doi.org/10.1038/nnano.2012.167>
97. Vona G, Sabile A, Louha M et al (2000) Isolation by size of epithelial tumor cells: a new method for the immunomorphological and molecular characterization of circulating tumor cells. *Am J Pathol* 156:57–63. [https://doi.org/10.1016/S0002-9440\(10\)64706-2](https://doi.org/10.1016/S0002-9440(10)64706-2)
98. Toner M, Irimia D (2005) Blood-on-a-chip. *Annu Rev Biomed Eng* 7:77–103. <https://doi.org/10.1146/annurev.bioeng.7.011205.135108>
99. Mohamed H, McCurdy LD, Szarowski DH et al (2004) Development of a rare cell fractionation device: application for cancer detection. *IEEE Trans Nanobiosci* 3:251–256. <https://doi.org/10.1109/TNB.2004.837903>
100. Xu L, Mao X, Imrali A et al (2015) Optimization and evaluation of a novel size based circulating tumor cell isolation system. *PLoS One* 10:e0138032. <https://doi.org/10.1371/journal.pone.0138032>
101. Hou HW, Warkiani ME, Khoo BL et al (2013) Isolation and retrieval of circulating tumor cells using centrifugal forces. *Sci Rep* 3:1259. <https://doi.org/10.1038/srep01259>
102. Miller MC, Robinson PS, Wagner C, O’Shannessy DJ (2018) The Parsortix™ cell separation system—a versatile liquid biopsy platform. *Cytometry A* 93:1234–1239. <https://doi.org/10.1002/cyto.a.23571>
103. Lee Y, Guan G, Bhagat AA (2018) ClearCell® FX, a label-free microfluidics technology for enrichment of viable circulating tumor cells. *Cytometry A* 93:1251–1254. <https://doi.org/10.1002/cyto.a.23507>
104. Mishra A, Dubash TD, Edd JF et al (2020) Ultrahigh-throughput magnetic sorting of large blood volumes for epitope-agnostic isolation of circulating tumor cells. *Proc Natl Acad Sci* 117:16839–16847. <https://doi.org/10.1073/pnas.2006388117>
105. Kim T-H, Lim M, Park J et al (2017) FAST: size-selective, clog-free isolation of rare cancer cells from whole blood at a liquid–liquid interface. *Anal Chem* 89:1155–1162. <https://doi.org/10.1021/acs.analchem.6b03534>

106. Aceto N, Bardia A, Miyamoto DT et al (2014) Circulating tumor cell clusters are oligoclonal precursors of breast cancer metastasis. *Cell* 158:1110–1122. <https://doi.org/10.1016/j.cell.2014.07.013>
107. Gkoutela S, Castro-Giner F, Szczerba BM et al (2019) Circulating tumor cell clustering shapes DNA methylation to enable metastasis seeding. *Cell* 176:98–112.e14. <https://doi.org/10.1016/j.cell.2018.11.046>
108. Szczerba BM, Castro-Giner F, Vetter M et al (2019) Neutrophils escort circulating tumour cells to enable cell cycle progression. *Nature* 566:553. <https://doi.org/10.1038/s41586-019-0915-y>
109. Sarioglu AF, Aceto N, Kojic N et al (2015) A microfluidic device for label-free, physical capture of circulating tumor cell clusters. *Nat Methods* 12:685–691. <https://doi.org/10.1038/nmeth.3404>
110. Au SH, Storey BD, Moore JC et al (2016) Clusters of circulating tumor cells traverse capillary-sized vessels. *Proc Natl Acad Sci* 113:4947–4952. <https://doi.org/10.1073/pnas.1524448113>
111. Jiang X, Wong KHK, Khankhel AH et al (2017) Microfluidic isolation of platelet-covered circulating tumor cells. *Lab Chip* 17:3498–3503. <https://doi.org/10.1039/C7LC00654C>
112. Guck J, Schinkinger S, Lincoln B et al (2005) Optical deformability as an inherent cell marker for testing malignant transformation and metastatic competence. *Biophys J* 88:3689–3698. <https://doi.org/10.1529/biophysj.104.045476>
113. Lincoln B, Schinkinger S, Travis K et al (2007) Reconfigurable microfluidic integration of a dual-beam laser trap with biomedical applications. *Biomed Microdevices* 9:703–710. <https://doi.org/10.1007/s10544-007-9079-x>
114. Nel I, Morawetz EW, Tschodu D et al (2021) The mechanical fingerprint of circulating tumor cells (CTCs) in breast cancer patients. *Cancers* 13:1119. <https://doi.org/10.3390/cancers13051119>
115. Gossett DR, Tse HTK, Lee SA et al (2012) Hydrodynamic stretching of single cells for large population mechanical phenotyping. *Proc Natl Acad Sci* 109:7630–7635. <https://doi.org/10.1073/pnas.1200107109>
116. Adamo A, Sharei A, Adamo L et al (2012) Microfluidics-based assessment of cell deformability. *Anal Chem* 84:6438–6443. <https://doi.org/10.1021/ac300264v>
117. Byun S, Son S, Amodei D et al (2013) Characterizing deformability and surface friction of cancer cells. *Proc Natl Acad Sci* 110:7580–7585. <https://doi.org/10.1073/pnas.1218806110>
118. Lange JR, Steinwachs J, Kolb T et al (2015) Microconstriction arrays for high-throughput quantitative measurements of cell mechanical properties. *Biophys J* 109:26–34. <https://doi.org/10.1016/j.bpj.2015.05.029>
119. Otto O, Rosendahl P, Mietke A et al (2015) Real-time deformability cytometry: on-the-fly cell mechanical phenotyping. *Nat Methods* 12:199–202. <https://doi.org/10.1038/nmeth.3281>
120. Urbanska M, Muñoz HE, Shaw Bagnall J et al (2020) A comparison of microfluidic methods for high-throughput cell deformability measurements. *Nat Methods* 17:587–593. <https://doi.org/10.1038/s41592-020-0818-8>
121. Nyberg KD, Hu KH, Kleinman SH et al (2017) Quantitative deformability cytometry: rapid, calibrated measurements of cell mechanical properties. *Biophys J* 113:1574–1584. <https://doi.org/10.1016/j.bpj.2017.06.073>
122. Bagnall JS, Byun S, Begum S et al (2015) Deformability of tumor cells versus blood cells. *Sci Rep* 5:18542. <https://doi.org/10.1038/srep18542>
123. Hostenstein CN, Horvath A, Schär B et al (2019) The relationship between metastatic potential and in vitro mechanical properties of osteosarcoma cells. *Mol Biol Cell* 30:887–898. <https://doi.org/10.1091/mbc.E18-08-0545>
124. Rosendahl P, Plak K, Jacobi A et al (2018) Real-time fluorescence and deformability cytometry. *Nat Methods* 15:355–358. <https://doi.org/10.1038/nmeth.4639>
125. Toepfner N, Herold C, Otto O et al (2018) Detection of human disease conditions by single-cell morpho-rheological phenotyping of blood. *Elife* 7:e29213. <https://doi.org/10.7554/eLife.29213>

126. Hakim M, Khorasheh F, Alemzadeh I, Vossoughi M (2021) A new insight to deformability correlation of circulating tumor cells with metastatic behavior by application of a new deformability-based microfluidic chip. *Anal Chim Acta* 1186:339115. <https://doi.org/10.1016/j.aca.2021.339115>
127. Ribeiro-Samy S, Oliveira MI, Pereira-Veiga T et al (2019) Fast and efficient microfluidic cell filter for isolation of circulating tumor cells from unprocessed whole blood of colorectal cancer patients. *Sci Rep* 9:8032. <https://doi.org/10.1038/s41598-019-44401-1>
128. Lopes C, Piairol P, Chfcharo A et al (2021) HER2 expression in circulating tumour cells isolated from metastatic breast cancer patients using a size-based microfluidic device. *Cancers* 13:4446. <https://doi.org/10.3390/cancers13174446>
129. Harouaka RA, Zhou M-D, Yeh Y-T et al (2014) Flexible micro spring array device for high-throughput enrichment of viable circulating tumor cells. *Clin Chem* 60:323–333. <https://doi.org/10.1373/clinchem.2013.206805>
130. Ding X, Li P, Lin S-CS et al (2013) Surface acoustic wave microfluidics. *Lab Chip* 13:3626–3649. <https://doi.org/10.1039/C3LC50361E>
131. Li P, Mao Z, Peng Z et al (2015) Acoustic separation of circulating tumor cells. *Proc Natl Acad Sci* 112:4970–4975. <https://doi.org/10.1073/pnas.1504484112>
132. Bankó P, Lee SY, Nagygyörgy V et al (2019) Technologies for circulating tumor cell separation from whole blood. *J Hematol Oncol* 12:48. <https://doi.org/10.1186/s13045-019-0735-4>
133. Lei KF (2020) A review on microdevices for isolating circulating tumor cells. *Micromachines* 11:531. <https://doi.org/10.3390/mi11050531>
134. Belotti Y, Lim CT (2021) Microfluidics for liquid biopsies: recent advances, current challenges, and future directions. *Anal Chem* 93:4727–4738. <https://doi.org/10.1021/acs.analchem.1c00410>
135. Nanou A, Miller MC, Zeune LL et al (2020) Tumour-derived extracellular vesicles in blood of metastatic cancer patients associate with overall survival. *Br J Cancer* 122:801–811. <https://doi.org/10.1038/s41416-019-0726-9>
136. Nanou A, Coumans FAW, van Dalum G et al (2018) Circulating tumor cells, tumor-derived extracellular vesicles and plasma cytokeratins in castration-resistant prostate cancer patients. *Oncotarget* 9:19283–19293. <https://doi.org/10.18632/ONCOTARGET.25019>
137. Gurunathan S, Kang M-H, Jeyaraj M et al (2019) Review of the isolation, characterization, biological function, and multifarious therapeutic approaches of exosomes. *Cell* 8:307. <https://doi.org/10.3390/CELLS8040307>
138. Van Deun J, Mestdagh P, Sormunen R et al (2014) The impact of disparate isolation methods for extracellular vesicles on downstream RNA profiling. *J Extracell Vesicles* 3:1–14. <https://doi.org/10.3402/jev.v3.24858>
139. Veerman RE, Teeuwen L, Czarzewski P et al (2021) Molecular evaluation of five different isolation methods for extracellular vesicles reveals different clinical applicability and subcellular origin. *J Extracell Vesicles* 10. <https://doi.org/10.1002/JEV2.12128>
140. Karimi N, Cvjetkovic A, Jang SC et al (2018) Detailed analysis of the plasma extracellular vesicle proteome after separation from lipoproteins. *Cell Mol Life Sci*. <https://doi.org/10.1007/s00018-018-2773-4>
141. Simonsen JB (2017) What are we looking at? Extracellular vesicles, lipoproteins, or both? *Circ Res* 121:920–922. <https://doi.org/10.1161/CIRCRESAHA.117.311767>
142. Johnsen KB, Gudbergsson JM, Andresen TL, Simonsen JB (2019) What is the blood concentration of extracellular vesicles? Implications for the use of extracellular vesicles as blood-borne biomarkers of cancer. *Biochim Biophys Acta Rev Cancer* 1871:109–116. <https://doi.org/10.1016/j.bbcan.2018.11.006>
143. Nordin JZ, Lee Y, Vader P et al (2015) Ultrafiltration with size-exclusion liquid chromatography for high yield isolation of extracellular vesicles preserving intact biophysical and functional properties. *Nanomed Nanotechnol Biol Med* 11:879–883. <https://doi.org/10.1016/J.NANO.2015.01.003>

144. Zhang X, Borg EGF, Liaci AM et al (2020) A novel three step protocol to isolate extracellular vesicles from plasma or cell culture medium with both high yield and purity. *J Extracell Vesicles* 9. <https://doi.org/10.1080/20013078.2020.1791450>
145. Chen Y, Zhu Q, Cheng L et al (2021) Exosome detection via the ultrafast-isolation system: EXODUS. *Nat Methods* 18:212–218. <https://doi.org/10.1038/S41592-020-01034-X>
146. Xu R, Greening DW, Zhu HJ et al (2016) Extracellular vesicle isolation and characterization: toward clinical application. *J Clin Invest* 126:1152–1162. <https://doi.org/10.1172/JCI81129>
147. Jeppesen DK, Fenix AM, Franklin JL et al (2019) Reassessment of exosome composition. *Cell* 177:428–445.e18. <https://doi.org/10.1016/j.cell.2019.02.029>
148. Kugeratski FG, Hodge K, Lilla S et al (2021) Quantitative proteomics identifies the core proteome of exosomes with syntenin-1 as the highest abundant protein and a putative universal biomarker. Springer
149. Hoshino A, Kim HS, Bojmar L et al (2020) Extracellular vesicle and particle biomarkers define multiple human cancers. *Cell* 182:1044–1061.e18. <https://doi.org/10.1016/j.cell.2020.07.009>
150. Liang Y, Lehrich BM, Zheng S, Lu M (2021) Emerging methods in biomarker identification for extracellular vesicle-based liquid biopsy. *J Extracell Vesicles*:10. <https://doi.org/10.1002/jev2.12090>
151. Welsh JA, Van Der Pol E, Arkesteijn GJA et al (2020) MIFlowCyt-EV: a framework for standardized reporting of extracellular vesicle flow cytometry experiments. *J Extracell Vesicles* 9. <https://doi.org/10.1080/20013078.2020.1713526>
152. Campos-Silva C, Suárez H, Jara-Acevedo R et al (2019) High sensitivity detection of extracellular vesicles immune-captured from urine by conventional flow cytometry. *Sci Rep* 9:1–12. <https://doi.org/10.1038/s41598-019-38516-8>
153. Rodrigues M, Richards N, Ning B et al (2019) Rapid lipid-based approach for normalization of quantum-dot-detected biomarker expression on extracellular vesicles in complex biological samples. *Nano Lett* 19:7623–7631
154. Wei P, Wu F, Kang B et al (2020) Plasma extracellular vesicles detected by single molecule array technology as a liquid biopsy for colorectal cancer. *J Extracell Vesicles* 9:1809765. <https://doi.org/10.1080/20013078.2020.1809765>
155. Yoshioka Y, Kosaka N, Konishi Y et al (2014) Ultra-sensitive liquid biopsy of circulating extracellular vesicles using ExoScreen. *Nat Commun* 5:3591. <https://doi.org/10.1038/ncomms4591>
156. He D, Ho SL, Chan HN et al (2019) Molecular-recognition-based DNA nanodevices for enhancing the direct visualization and quantification of single vesicles of tumor exosomes in plasma microsamples. *Anal Chem* 91:2768–2775. https://doi.org/10.1021/ACS.ANALCHEM.8B04509/SUPPL_FILE/AC8B04509_SI_001.PDF
157. Zhang J, Shi J, Zhang H et al (2020) Localized fluorescent imaging of multiple proteins on individual extracellular vesicles using rolling circle amplification for cancer diagnosis. *J Extracell Vesicles* 10:e12025. <https://doi.org/10.1002/JEV2.12025>
158. Mathew DG, Beekman P, Lemay SG et al (2020) Electrochemical detection of tumor-derived extracellular vesicles on nanointerdigitated electrodes. *Nano Lett* 20:820–828. <https://doi.org/10.1021/ACS.NANOLETT.9B02741>
159. Huang R, He L, Xia Y et al (2019) A sensitive aptasensor based on a hemin/G-quadruplex-assisted signal amplification strategy for electrochemical detection of gastric cancer exosomes. *Small Weinhe Bergstr Ger*:15. <https://doi.org/10.1002/SMLL.201900735>
160. Zhang W, Jiang L, Diefenbach RJ et al (2020) Enabling sensitive phenotypic profiling of cancer-derived small extracellular vesicles using surface-enhanced Raman spectroscopy nanotags. *ACS Sens* 5:764–771. <https://doi.org/10.1021/ACSSENSORS.9B02377>
161. Wang J, Wuethrich A, Sina AAI et al (2020) Tracking extracellular vesicle phenotypic changes enables treatment monitoring in melanoma. *Sci Adv* 6. <https://doi.org/10.1126/SCIADV.AAX3223>

162. Shao H, Chung J, Lee K et al (2015) Chip-based analysis of exosomal mRNA mediating drug resistance in glioblastoma. *Nat Commun* 6:1–9. <https://doi.org/10.1038/ncomms7999>
163. Cappello F, Logozzi M, Campanella C et al (2017) Exosome levels in human body fluids: a tumor marker by themselves? *Eur J Pharm Sci* 96:93–98. <https://doi.org/10.1016/j.ejps.2016.09.010>
164. García-Silva S, Benito-Martín A, Sánchez-Redondo S et al (2019) Use of extracellular vesicles from lymphatic drainage as surrogate markers of melanoma progression and BRAF V600E mutation. *J Exp Med*. <https://doi.org/10.1084/jem.20181522>
165. Osti D, Del Bene M, Rappa G et al (2019) Clinical significance of extracellular vesicles in plasma from glioblastoma patients. <https://doi.org/10.1158/1078-0432.CCR-18-1941>
166. Peinado H, Alečković M, Lavotshkin S et al (2012) Melanoma exosomes educate bone marrow progenitor cells toward a pro-metastatic phenotype through MET. *Nat Med* 18:883–891. <https://doi.org/10.1038/nm.2753>
167. Sabbagh Q, André-Grégoire G, Alves-Nicolau C et al (2021) The von Willebrand factor stamps plasmatic extracellular vesicles from glioblastoma patients. *Sci Rep* 11:1–11. <https://doi.org/10.1038/s41598-021-02254-7>
168. Venturella M, Criscuoli M, Carraro F et al (2021) Interplay between hypoxia and extracellular vesicles in cancer and inflammation. *Biology* 10. <https://doi.org/10.3390/BIOLOGY10070606>
169. Keklikoglou I, Cianciaruso C, Güç E et al (2019) Chemotherapy elicits pro-metastatic extracellular vesicles in breast cancer models. *Nat Cell Biol* 21:190–202. <https://doi.org/10.1038/s41556-018-0256-3>
170. Federici C, Petrucci F, Caimi S et al (2014) Exosome release and low pH belong to a framework of resistance of human melanoma cells to cisplatin. *PLoS One* 9. <https://doi.org/10.1371/journal.pone.0088193>
171. Mutschelknaus L, Peters C, Winkler K et al (2016) Exosomes derived from squamous head and neck cancer promote cell survival after ionizing radiation. *PLoS One*:11. <https://doi.org/10.1371/JOURNAL.PONE.0152213>
172. Zaborowski MP, Lee K, Na YJ et al (2019) Methods for systematic identification of membrane proteins for specific capture of cancer-derived extracellular vesicles. *Cell Rep* 27:255–268.e6. <https://doi.org/10.1016/j.celrep.2019.03.003>
173. Whitham M, Parker BL, Friedrichsen M et al (2018) Extracellular vesicles provide a means for tissue crosstalk during exercise. *Cell Metab* 27:237–251.e4. <https://doi.org/10.1016/j.cmet.2017.12.001>
174. Eitan E, Green J, Bodogai M et al (2017) Age-related changes in plasma extracellular vesicle characteristics and internalization by leukocytes. *Sci Rep* 7:1342. <https://doi.org/10.1038/s41598-017-01386-z>
175. Newman LA, Fahmy A, Sorich MJ et al (2021) Importance of between and within subject variability in extracellular vesicle abundance and cargo when performing biomarker analyses. *Cell* 10:1–18. <https://doi.org/10.3390/CELLS10030485>
176. Laurenzana I, Trino S, Lamorte D et al (2021) Analysis of amount, size, protein phenotype and molecular content of circulating extracellular vesicles identifies new biomarkers in multiple myeloma. *Int J Nanomed* 16:3141–3160. <https://doi.org/10.2147/IJN.S303391>
177. Melo SA, Luecke LB, Kahlert C et al (2015) Glypican-1 identifies cancer exosomes and detects early pancreatic cancer. *Nature* 523:177–182. <https://doi.org/10.1038/nature14581>
178. Keup C, Mach P, Aktas B et al (2018) RNA profiles of circulating tumor cells and extracellular vesicles for therapy stratification of metastatic breast cancer patients. <https://doi.org/10.1373/clinchem.2017.283531>
179. Lai X, Wang M, McElyea SD et al (2017) A microRNA signature in circulating exosomes is superior to exosomal glypican-1 levels for diagnosing pancreatic cancer. *Cancer Lett* 393:86–93. <https://doi.org/10.1016/J.CANLET.2017.02.019>

180. Lucien F, Lac V, Billadeau DD et al (2019) Glypican-1 and glycoprotein 2 bearing extracellular vesicles do not discern pancreatic cancer from benign pancreatic diseases. *Oncotarget* 10: 1045–1055. <https://doi.org/10.18632/ONCOTARGET.26620>
181. Hu J, Sheng Y, Kwak KJ et al (2017) A signal-amplifiable biochip quantifies extracellular vesicle-associated RNAs for early cancer detection. *Nat Commun* 8. <https://doi.org/10.1038/S41467-017-01942-1>
182. Li J, Chen Y, Guo X et al (2017) GPC1 exosome and its regulatory miRNAs are specific markers for the detection and target therapy of colorectal cancer. *J Cell Mol Med* 21:838–847. <https://doi.org/10.1111/JCMM.12941>
183. Xiao D, Dong Z, Zhen L et al (2020) Combined exosomal GPC1, CD82, and serum CA19-9 as multiplex targets: a specific, sensitive, and reproducible detection panel for the diagnosis of pancreatic cancer. *Mol Cancer Res* 18:1300–1310. <https://doi.org/10.1158/1541-7786.MCR-19-0588>
184. Buscaill E, Chauvet A, Quincy P et al (2019) CD63-GPC1-positive exosomes coupled with CA19-9 offer good diagnostic potential for resectable pancreatic ductal adenocarcinoma. *Transl Oncol* 12:1395–1403. <https://doi.org/10.1016/J.TRANON.2019.07.009>
185. Poggio M, Hu T, Pai CC et al (2019) Suppression of exosomal PD-L1 induces systemic anti-tumor immunity and memory. *Cell* 177:414–427.e13. <https://doi.org/10.1016/j.cell.2019.02.016>
186. Chen G, Huang AC, Zhang W et al (2018) Exosomal PD-L1 contributes to immunosuppression and is associated with anti-PD-1 response. *Nature* 560:382–386
187. Cordonnier M, Nardin C, Chanteloup G et al (2020) Tracking the evolution of circulating exosomal-PD-L1 to monitor melanoma patients. *J Extracell Vesicles* 9:1–11. <https://doi.org/10.1080/20013078.2019.1710899>
188. Zhou B, Xu K, Zheng X et al (2020) Application of exosomes as liquid biopsy in clinical diagnosis. *Signal Transduct Target Ther* 5. <https://doi.org/10.1038/s41392-020-00258-9>
189. Hu T, Wolfram J, Srivastava S (2021) Extracellular vesicles in cancer detection: hopes and hypes. *Trends Cancer* 7:122–133. <https://doi.org/10.1016/j.trecan.2020.09.003>
190. Costa-Silva B, Aiello NM, Ocean AJ et al (2015) Pancreatic cancer exosomes initiate pre-metastatic niche formation in the liver. *Nat Cell Biol*:1–7. <https://doi.org/10.1038/ncb3169>
191. Choi ES, Al Faruque H, Kim JH et al (2021) CD5L as an extracellular vesicle-derived biomarker for liquid biopsy of lung cancer. *Diagnostics (Basel)* 11. <https://doi.org/10.3390/DIAGNOSTICS11040620>
192. Moon PG, Lee JE, Cho YE et al (2016) Identification of developmental endothelial Locus-1 on circulating extracellular vesicles as a novel biomarker for early breast cancer detection. *Clin Cancer Res Off J Am Assoc Cancer Res* 22:1757–1766. <https://doi.org/10.1158/1078-0432.CCR-15-0654>
193. Moon PG, Lee JE, Cho YE et al (2016) Fibronectin on circulating extracellular vesicles as a liquid biopsy to detect breast cancer. *Oncotarget* 7:40189–40199. <https://doi.org/10.18632/ONCOTARGET.9561>
194. Khan S, Jutzy JMS, Valenzuela MMA et al (2012) Plasma-derived exosomal survivin, a plausible biomarker for early detection of prostate cancer. *PLoS One* 7. <https://doi.org/10.1371/JOURNAL.PONE.0046737>
195. Khan S, Bennit HF, Turay D et al (2014) Early diagnostic value of survivin and its alternative splice variants in breast cancer. *BMC Cancer* 14. <https://doi.org/10.1186/1471-2407-14-176>
196. Warmoes M, Lam SW, van der Groep P et al (2016) Secretome proteomics reveals candidate non-invasive biomarkers of BRCA1 deficiency in breast cancer. *Oncotarget* 7:63537–63548. <https://doi.org/10.18632/ONCOTARGET.11535>
197. Chanteloup G, Cordonnier M, Isambert N et al (2020) Monitoring HSP70 exosomes in cancer patients' follow up: a clinical prospective pilot study. *J Extracell Vesicles* 9:1766192. <https://doi.org/10.1080/20013078.2020.1766192>
198. Min L, Zhu S, Chen L et al (2019) Evaluation of circulating small extracellular vesicles derived miRNAs as biomarkers of early colon cancer: a comparison with plasma total

- miRNAs. *J Extracell Vesicles* 8. https://doi.org/10.1080/20013078.2019.1643670/SUPPL_FILE/ZJEV_A_1643670_SM8506.ZIP
199. Ogata-Kawata H, Izumiya M, Kurioka D et al (2014) Circulating exosomal microRNAs as biomarkers of colon cancer. *PLoS One* 9. <https://doi.org/10.1371/JOURNAL.PONE.0092921>
 200. Bryant RJ, Pawlowski T, Catto JWF et al (2012) Changes in circulating microRNA levels associated with prostate cancer. *Br J Cancer* 106:768–774. <https://doi.org/10.1038/BJC.2011.595>
 201. Matsuzaki K, Fujita K, Jingushi K et al (2017) MiR-21-5p in urinary extracellular vesicles is a novel biomarker of urothelial carcinoma. *Oncotarget* 8:24668–24678. <https://doi.org/10.18632/ONCOTARGET.14969>
 202. Armstrong DA, Green BB, Seigne JD et al (2015) MicroRNA molecular profiling from matched tumor and bio-fluids in bladder cancer. *Mol Cancer* 14. <https://doi.org/10.1186/S12943-015-0466-2>
 203. Kim MW, Park S, Lee H et al (2021) Multi-miRNA panel of tumor-derived extracellular vesicles as promising diagnostic biomarkers of early-stage breast cancer. *Cancer Sci*. <https://doi.org/10.1111/CAS.15155>
 204. Hannafon BN, Trigoso YD, Calloway CL et al (2016) Plasma exosome microRNAs are indicative of breast cancer. *Breast Cancer Res* 18. <https://doi.org/10.1186/S13058-016-0753-X>
 205. Worst TS, Previti C, Nitschke K et al (2020) miR-10a-5p and miR-29b-3p as extracellular vesicle-associated prostate cancer detection markers. *Cancers* 12. <https://doi.org/10.3390/CANCERS12010043>
 206. Asano N, Matsuzaki J, Ichikawa M et al (2019) A serum microRNA classifier for the diagnosis of sarcomas of various histological subtypes. *Nat Commun* 10:1–10. <https://doi.org/10.1038/s41467-019-09143-8>
 207. Chevillet JR, Kang Q, Ruf IK et al (2014) Quantitative and stoichiometric analysis of the microRNA content of exosomes. *Proc Natl Acad Sci U S A* 111:14888–14893. <https://doi.org/10.1073/pnas.1408301111>
 208. McKiernan J, Donovan MJ, O'Neill V et al (2016) A novel urine exosome gene expression assay to predict high-grade prostate cancer at initial biopsy. *JAMA Oncol* 2:882–889. <https://doi.org/10.1001/JAMAONCOL.2016.0097>
 209. Peng Q, Chiu PKF, Wong CYP et al (2021) Identification of piRNA targets in urinary extracellular vesicles for the diagnosis of prostate cancer. *Diagnostics (Basel)* 11. <https://doi.org/10.3390/DIAGNOSTICS11101828>
 210. Lu L, Fang S, Zhang Y et al (2021) Exosomes and exosomal circRNAs: the rising stars in the progression, diagnosis and prognosis of gastric cancer. *Cancer Manag Res* 13:8121–8129. <https://doi.org/10.2147/CMAR.S331221>
 211. Zhao X, Guo X, Jiao D et al (2021) Analysis of the expression profile of serum exosomal lncRNA in breast cancer patients. *Ann Transl Med* 9:1382. <https://doi.org/10.21037/ATM-21-3483>
 212. Thakur BK, Zhang H, Becker A et al (2014) Double-stranded DNA in exosomes: a novel biomarker in cancer detection. *Cell Res* 24:766–769. <https://doi.org/10.1038/cr.2014.44>
 213. Lee JS, Hur JY, Kim IA et al (2018) Liquid biopsy using the supernatant of a pleural effusion for EGFR genotyping in pulmonary adenocarcinoma patients: a comparison between cell-free DNA and extracellular vesicle-derived DNA. *BMC Cancer* 18:1–8. <https://doi.org/10.1186/s12885-018-5138-3>
 214. Fernando MR, Jiang C, Krzyzanowski GD, Ryan WL (2017) New evidence that a large proportion of human blood plasma cell-free DNA is localized in exosomes. *PLoS One* 12:1–15. <https://doi.org/10.1371/journal.pone.0183915>
 215. Wan Y, Liu B, Lei H et al (2018) Nanoscale extracellular vesicle-derived DNA is superior to circulating cell-free DNA for mutation detection in early-stage non-small-cell lung cancer. *Ann Oncol* 29:2379–2383. <https://doi.org/10.1093/ANNONC/MDY458>

216. Castellanos-Rizaldos E, Grimm DG, Tadigotla V et al (2018) Exosome-based detection of EGFR T790M in plasma from non-small cell lung cancer patients. *Clin Cancer Res Off J Am Assoc Cancer Res* 24:2944–2950. <https://doi.org/10.1158/1078-0432.CCR-17-3369>
217. Madhavan B, Yue S, Galli U et al (2015) Combined evaluation of a panel of protein and miRNA serum-exosome biomarkers for pancreatic cancer diagnosis increases sensitivity and specificity. *Int J Cancer* 136:2616–2627. <https://doi.org/10.1002/IJC.29324>
218. Brzozowski JS, Jankowski H, Bond DR et al (2018) Lipidomic profiling of extracellular vesicles derived from prostate and prostate cancer cell lines. *Lipids Health Dis* 17:1–12. <https://doi.org/10.1186/S12944-018-0854-X/FIGURES/4>
219. Zhang Y, Wu X, Tao WA (2018) Characterization and applications of extracellular vesicle proteome with post-translational modifications. *Trends Anal Chem* 107:21–30. <https://doi.org/10.1016/J.TRAC.2018.07.014>
220. Chen I-H, Xue L, Hsu C-C et al (2017) Phosphoproteins in extracellular vesicles as candidate markers for breast cancer. *Proc Natl Acad Sci* 114:3175–3180. <https://doi.org/10.1073/pnas.1618088114>
221. Luo P, Mao K, Xu J et al (2020) Metabolic characteristics of large and small extracellular vesicles from pleural effusion reveal biomarker candidates for the diagnosis of tuberculosis and malignancy. *J Extracell Vesicles* 9:1790158. <https://doi.org/10.1080/20013078.2020.1790158>
222. Gualerzi A, Picciolini S, Carlomagno C et al (2019) Raman profiling of circulating extracellular vesicles for the stratification of Parkinson’s patients. *Nanomed Nanotechnol Biol Med* 22. <https://doi.org/10.1016/J.NANO.2019.102097>
223. Enciso-Martinez A, Van Der Pol E, Hau CM et al (2020) Label-free identification and chemical characterisation of single extracellular vesicles and lipoproteins by synchronous Rayleigh and Raman scattering. *J Extracell Vesicles* 9. <https://doi.org/10.1080/20013078.2020.1730134>
224. Penders J, Nagelkerke A, Cunnane EM et al (2021) Single particle automated Raman trapping analysis of breast cancer cell-derived extracellular vesicles as cancer biomarkers. *ACS Nano*. <https://doi.org/10.1021/acsnano.1c07075>
225. LeClaire M, Gimzewski J, Sharma S (2021) A review of the biomechanical properties of single extracellular vesicles. *Nano Select* 2:1–15. <https://doi.org/10.1002/nano.202000129>
226. Barnes JM, Nauseef JT, Henry MD (2012) Resistance to fluid shear stress is a conserved biophysical property of malignant cells. *PLoS One* 7:e50973. <https://doi.org/10.1371/journal.pone.0050973>
227. Mitchell MJ, Denais C, Chan MF et al (2015) Lamin A/C deficiency reduces circulating tumor cell resistance to fluid shear stress. *Am J Physiol Cell Physiol* 309:C736–C746. <https://doi.org/10.1152/ajpcell.00050.2015>
228. Moose DL, Krog BL, Kim T-H et al (2020) Cancer cells resist mechanical destruction in circulation via RhoA/actomyosin-dependent mechano-adaptation. *Cell Rep* 30:3864–3874.e6. <https://doi.org/10.1016/j.celrep.2020.02.080>
229. Margolis E, Brown G, Partin A et al (2021) Predicting high-grade prostate cancer at initial biopsy: clinical performance of the ExoDx (EPI) prostate intelliscore test in three independent prospective studies. *Prostate Cancer Prostatic Dis*. <https://doi.org/10.1038/S41391-021-00456-8>
230. Ayers L, Pink R, Carter DRF, Nieuwland R (2019) Clinical requirements for extracellular vesicle assays. *8(1):1593755*. <https://doi.org/10.1080/20013078.2019.1593755>
231. Coumans FAW, Brisson AR, Buzas EI et al (2017) Methodological guidelines to study extracellular vesicles. *Circ Res* 120:1632–1648. <https://doi.org/10.1161/CIRCRESAHA.117.309417>
232. Buscaill E, Alix-Panabières C, Quincy P et al (2019) High clinical value of liquid biopsy to detect circulating tumor cells and tumor exosomes in pancreatic ductal adenocarcinoma patients eligible for up-front surgery. *Cancers (Basel)* 11:1656. <https://doi.org/10.3390/CANCERS11111656>
233. Suo Y, Gu Z, Wei X (2020) Advances of in vivo flow cytometry on cancer studies. *Cytometry A* 97:15–23. <https://doi.org/10.1002/cyto.a.23851>



From Exosomes to Circulating Tumor Cells: Using Microfluidics to Detect High Predictive Cancer Biomarkers **15**

Catarina M. Abreu, David Caballero, Subhas C. Kundu, and Rui L. Reis

Abstract

Early cancer screening and effective diagnosis is the most effective form to diminish the number of cancer-related deaths. Liquid biopsy constitutes an attractive alternative to tumor biopsy due to its non-invasive nature and sample accessibility, which permits effective screening and patient monitoring. Within the plethora of biomarkers present in circulation, liquid biopsy has mainly been performed by analyzing circulating tumor cells, and more recently, extracellular vesicles. Tracking these biological particles could provide valuable insights into cancer origin, progression, treatment efficacy, and patient prognosis. Microfluidic devices have emerged as viable solutions for point-of-care cancer screening and monitoring due to their user-friendly operation, low operation costs, and capability of processing, quantifying, and analyzing these bioparticles in a single device. However, the size difference between cells and exosomes (micrometer vs nanometer) requires an adaptation of microfluidic isolation approaches, particularly in label-free methodologies governed by particle and fluid mechanics. This chapter will explore the theory behind particle isolation and sorting in different microfluidic techniques necessary to guide researchers into the design and development of such devices.

C. M. Abreu (✉) · D. Caballero · S. C. Kundu · R. L. Reis

3B's Research Group, I3Bs—Research Institute on Biomaterials, Biodegradables and Biomimetics, University of Minho, Headquarters of the European Institute of Excellence on Tissue Engineering and Regenerative Medicine, AvePark, Parque de Ciência e Tecnologia, Zona Industrial da Gandra, Barco, Guimarães, Portugal

ICVS/3B's—PT Government Associate Laboratory, Braga/Guimarães, Portugal
e-mail: catarina.abreu@i3bs.uminho.pt

KeywordsExosomes · Circulating tumor cells · Cancer · Microfluidics · Diagnosis

15.1 Introduction

Cancer is a leading cause of death worldwide, accounting for nearly 10 million deaths per year [1]. From these, over 90% of cancer-related deaths are due to the metastatic form of the disease [2]. Hence, early diagnosis remains the most effective tool in the fight against cancer. Liquid biopsy has emerged as a valuable alternative to solid tumor biopsies due to its non-invasive nature, low cost, and accessibility, which allows patient monitoring during treatment, enabling personalized medicine. Several studies have shown that the number of circulating tumor cells (CTCs) detected in circulation could predict therapy response in cases of metastatic cancer [3–5].

Moreover, the molecular characterization of these cells by analyzing the genetic and proteomic signatures can offer valuable insights into the mechanisms of disease progression and assist in the development of personalized medicine [6–8]. Due to its predictive value, CTC isolation and detection as a form of liquid biopsy has been explored over the past years. Alongside CTCs, a new type of player has attracted the interest of the medical and scientific community. Extracellular vesicles, small lipidic vesicles released by cells, contain molecular information (proteins, lipids, DNA, and RNA) from the cell of origin and can provide critical information about the primary tumor, formation of pre-metastatic niches, and mechanisms of metastasis [9–12]. Thus, the isolation of these bioparticles permits the identification of the probable metastatic sites and act as indicators of patient prognosis and recurrence.

Despite the value of CTC and exosome liquid biopsies, they have yet to be employed in standard clinical practice, mainly due to the technical challenges associated with their isolation [13, 14]. The applicability of liquid biopsy relies on the development of well-established protocols and high-throughput dependable technologies that can easily be operated within a clinical setting with minimal and automated sample pre-processing steps. Microfluidic platforms are promising technologies capable of bridging the gap between the lab and the clinic by providing a methodology that permits particle and fluid manipulation in a simple setup. Even though many microfluidic devices have been described for CTC isolation at high recovery rates and purity, the application of these techniques to extracellular vesicles (EVs) remains a challenge. The size difference between CTCs and EVs requires an adaptation of microfluidic isolation approaches, particularly in label-free methodologies governed by particle and fluid mechanics.

This chapter discusses the theory behind bioparticle isolation and sorting in microfluidic devices and highlights the most relevant and recent studies, acting as a guide for researchers interested in the field.

15.2 The Theory Behind Microfluidic Bioparticle Isolation: From the Micro to the Nanoscale

Bioparticle isolation approaches are generally classified into affinity-based and label-free approaches. The first considers the isolation of CTCs or EVs according to the recognition of specific markers, while the latter uses the differential physical properties of the bioparticles. In the following sections, we will discuss the main strategies used in microfluidic-based isolation, with particular highlights in label-free technologies: inertial microfluidics, microfluidic filtration, acoustofluidics, deterministic lateral displacement, and ferrohydrodynamics.

15.2.1 Affinity-Based Isolation

Affinity-based isolation relies on the use of capture probes capable of recognizing and binding to a specific molecular target in the bioparticle of interest, for instance, taking advantage of the antigen–antibody/aptamer, substrate–enzyme, or receptor–ligand interaction.

Although the theory behind the development of surface-biofunctionalized microfluidic platforms may appear simplistic when compared with label-free isolation, it is necessary to ensure the operating conditions (e.g., flow rate, antibody concentration, incubation time) are favorable for target binding [15]. For instance, low flow rates are frequently used to ensure enough time is provided for antigen–antibody binding, which results in lower throughput systems when compared with label-free approaches. Despite this, several features can strategically be designed to enhance the interaction between the probe and the marker of interest. Mixers can be incorporated to promote these interactions and increase the capture efficiency and throughput of the system [16–18].

CTC isolation platforms frequently use antibodies to target epithelial surface markers (e.g., EpCAM, EGFR, HER2, and MUC1) to recover circulating cells that present an epithelial phenotype [19, 20]. In the case of melanoma-derived CTCs, EpCAM is downregulated, and therefore its use as a biomarker is not useful in the clinic. Recent work has shown that the combined use of melanoma specific cell adhesion molecule (MCAM), also known as CD146 or MUC18, and melanoma-associated chondroitin sulfate proteoglycan (MCSP) is capable of high CTC recovery from the whole blood of melanoma patients [21]. The proposed microfluidic immunoaffinity device allowed the distinction between cancer and healthy patients based on the number of isolated CTCs and exosomes. Despite this, the detection of epithelial markers does not account for CTCs that exhibit a more mesenchymal phenotype and that have shown to be correlated with higher invasiveness and metastasis [19, 20]. For instance, the presence of the CD133 in CTCs isolated from patients with metastatic lung cancer is indicative of a worse prognosis [22]. Alternatively, negative enrichment methods, which target leukocyte-specific surface markers (e.g., CD45 and CD66b), could be used to deplete circulating immune cells and permit the recovery of CTCs independently of their phenotype.

EV isolation from clinical samples is often based on the targeting of surface markers associated with EV biogenesis (CD81⁺, CD9⁺, CD63⁺) [23]. More recently, the targeting of the lipidic contents of the membrane has been proposed as an alternative approach [24]. For instance, phosphatidylserine has been recently used for the directed targeting of vesicles and phosphatidylserine⁺ cells in a microfluidic device with structures functionalized with annexin V [25].

Although affinity-based strategies can achieve high purity samples, bioparticle isolation and fractionation can be accomplished based on the differentiation of their physical properties, such as size, deformation, electric/dielectric properties. As microfluidic CTC and EV isolation platforms have been extensively reviewed in previous works [26–29], the following sections will be dedicated to the principles and fundamental theory of label-free techniques, used to avoid the initial targeting of specific subpopulations and loss of potentially relevant biological information.

15.2.2 Inertial Microfluidics

In a straight channel, besides gravity and buoyancy, which produce no alteration in the lateral migration profile, particles are subjected to inertial forces that direct lateral migration perpendicularly to the main flow until equilibrium is reached. Lateral particle migration within a straight channel, in a Newtonian fluid, is dominated by the inertial lift force (F_L), defined as the net force between the shear-gradient-induced lift force (F_{LS}) and the wall-induced lift force (F_{LW}).

In a microfluidic channel with a Poiseuille flow distribution, F_{LS} will direct the particles from the center of the channel toward the walls, producing asymmetric wave around the particle due to its spinning. Once the particles reach the vicinity of the wall, the wake created by the particles will be disturbed, inducing a force that propels the particles away from the wall, F_{LW} (Fig. 15.1i). As these forces are position-dependent, once a particle is near the centerline of the stream, the F_{LS} will direct particle migration, whereas the F_{LW} will dominate close to the walls. The resulting net force, F_L , can be given by Eq. (15.1) [30, 31]:

$$F_L = f_L \rho_f U^2 d_p^4 / D_h^2 \quad (15.1)$$

where f_L is the lift coefficient (a dimensionless number that depends on the Reynolds number and specific particle position along the cross-section of the channel), ρ_f , U , and d_p correspond to the fluid density [kg.m⁻³], maximum velocity of the fluid [m.s⁻¹], which can be estimated as twice the average characteristic velocity, and particle diameter [m], respectively. The D_h is defined as the hydraulic diameter and is calculated based on the geometry of the channel. For instance, for a rectangular channel, as is the case of most microfluidic channels, D_h is given by Eq. (15.2) [31, 32]:

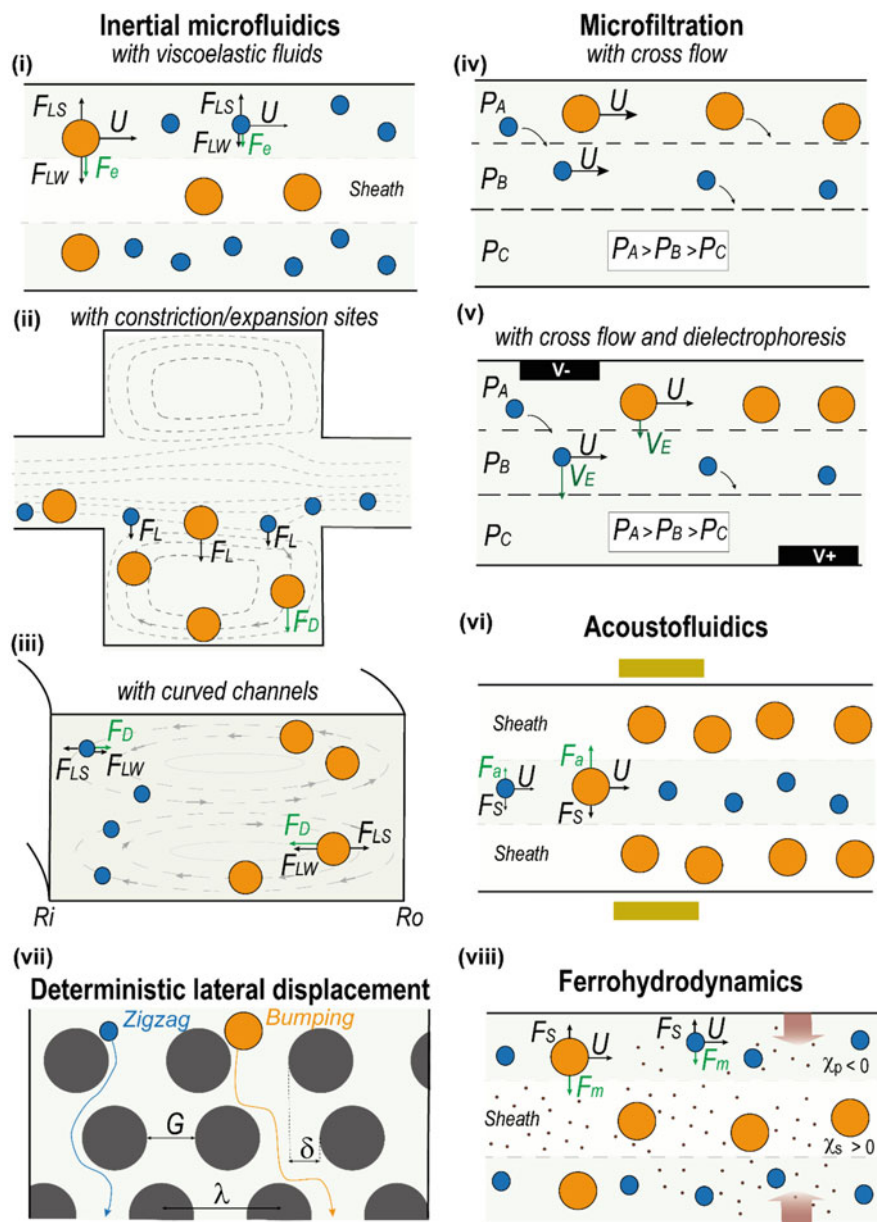


Fig. 15.1 Schematic representation of the label-free strategies for EV sorting. (i–iii) Inertial microfluidics, (iv, v) Microfiltration. (vi) Acoustofluidics. (vii) Deterministic lateral displacement. (viii) Ferrohydrodynamics

$$D_h = 2wh/(w + h) \quad (15.2)$$

where w and h refer to the channel cross-section width and height, respectively.

The control of the flow regime, performed by the Reynolds number (Re), is particularly relevant to modulate the contribution of the inertial and viscous forces within a fluid (Eq. 15.3).

$$\text{Re} = \frac{\rho U D_h}{\mu} = \frac{2\rho Q}{\mu(w + h)} \quad (15.3)$$

where μ is the dynamic viscosity [Pa s].

15.2.2.1 Dean Flow Fractionation

A microchannel with a Newtonian fluid that presents constriction and expansion sites, curvatures and localized microstructures will not follow the standard velocity profile of the Poiseuille flow [30–32]. Instead, these structures will induce a secondary flow, named the Dean flow, where two vortices with opposite directions are created (Fig. 15.1ii-iii). The use of the secondary Dean flow for particle separation has several advantages. Firstly, the vortices generated by the Dean flow assist in particle stirring, contributing to lateral particle displacement and reducing the time required for particles to achieve equilibrium [31–33]. With this, the length of the focusing channel can be significantly reduced when compared with a device without the action of Dean forces. Secondly, the existence of secondary Dean flow will enhance particle distributions along the cross-section of the channel, enabling the fractionated collection of particles with different sizes [31].

The Dean drag force (F_D), perpendicular to the main stream, can be expressed by (Eq. 15.4) [30, 31]. However, for simplicity, it is often approximated to the Stokes drag force (F_S).

$$F_D = \rho_f U_D^2 d_p D_h^2 R^{-1} \tilde{3} \pi \eta d_p (\nu_f - \nu_p) = F_S \quad (15.4)$$

where μ , d_p , and ν represent the dynamic viscosity of the liquid [Pa.s], the diameter of the particle [m], and relative velocity of the particle with respect to the liquid [m.s^{-1}], respectively.

The flow velocity in a Dean vortex, U_D , is often estimated applying the expression developed by Ookawara et al. (Eq. 15.5) [30]:

$$U_D = 1.8 \times 10^{-4} \text{De}^{1.63} \quad (15.5)$$

where De is the dimensionless Dean number given by Eq. (15.6) [32]:

$$\text{De} = \text{Re} \sqrt{\frac{D_h}{2R}} \quad (15.6)$$

where R is the radius of the curvature.

For spiral microfluidics, as the radius of the channel gradually increases from the inlet to the outlet, the average of Dean number from the innermost (R_i) and outermost (R_o) radius is typically considered [32].

Inertial microfluidics has been intensively used for particle manipulation, particularly for the isolation of CTCs [34, 35]. Typically, these devices require a sample pre-processing step to permit a higher separation resolution and purity in CTC recovery. This can be done either by sample dilution, removal/lysis of red blood cells (RBCs), or the addition of a sheath buffer. A recent work published by Smith et al., reported a microfluidic device capable of enriching CTCs from the whole blood by the sequential use of inertial microfluidic strategies [36]. The CTCKey device makes use of microstructures in the first section to direct CTCs toward the periphery of the channel (Fig. 15.2a). In the following segment, the cells are processed in two outer channels and four inner channels with curvatures. The CTCs, previously concentrated in the first segment, are directed towards the two outer external channels and exposed to Dean forces. Here, they become focused on the center of the streamline and permit the recovery of 75% of CTCs. The presence of four inner channels allowed the recovery of approximately 20% of CTCs that have escaped to the waste in the first section. This process permitted the concentration of CTCs through the reduction of blood volume by 78% at a flow rate of 2.4 mL/min.

Expansion–contraction reservoirs have also been used to enrich CTCs and microvesicles [37, 40]. In this strategy, larger particles are trapped in center of the microvortices due to the experienced shear lift force, while smaller particles flow through the central channel (Fig. 15.1ii). This principle has been applied in the Vortex HT device for the isolation of CTCs from advanced prostate cancer patients at a high throughput (8 mL/min) (Fig. 15.2b) [37]. Since the CTCs are trapped in the microvortices, the recovery of these cells requires complete sample processing with posterior interruption of vortex formation in the expansion sites. This strategy renders the integration of these devices in subsequent in-line processing or detection troublesome. On the other hand, spiral microdevices allow the continuous collection of the fractionated population by incorporating multiple outlets and retrieving the CTCs from the inner outlet of the device [22, 41, 42].

Although inertial microfluidics has been extensively applied for the separation of micrometer-sized bioparticles, such as blood cells and CTCs, separation of exosomes from larger EVs by inertial microfluidics comprises a challenge as the contribution of the inertial lift becomes trivial once the particle diameter decreases to the nanoscale [33, 38, 39]. Hence, for the isolation of sub-micrometer and nanometer-sized bioparticles, additional forces are required to modulate particle separation, such as the Dean drag force and elastic lift force.

15.2.2.2 Elastic Lift Force

The use of non-Newtonian viscoelastic fluids will exert an additional force on the moving particles, the elastic lift force, that will enable the modulation of the particle's equilibrium position within a microfluidic channel [38, 39] (Fig. 15.1i). Different synthetic polymer solutions can be used to produce a biocompatible

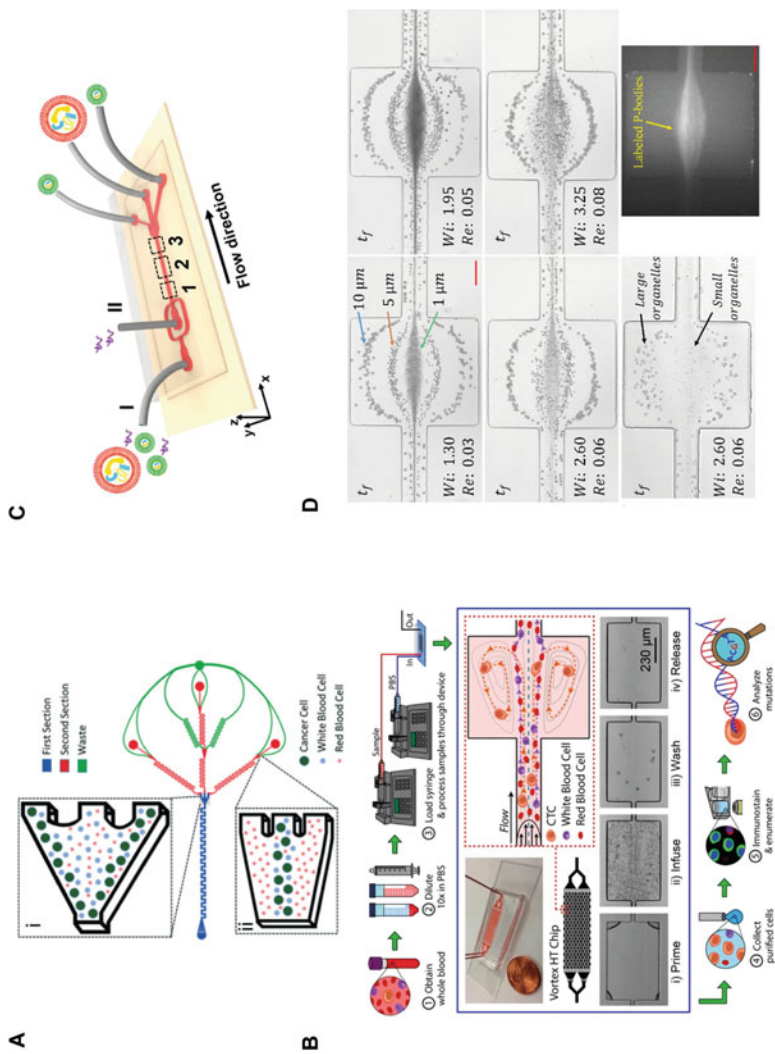


Fig. 15.2 Inertial microfluidic devices. (a) Circulating tumor cell enrichment using the CTCKey device. Republished with permission of the Royal Society of Chemistry, from Smith et al. [36]. (b) Enrichment of circulating tumor cells using Vortex microfluidic technology. Adapted with permission from Renier et al. [37]. (c) Exosome isolation from EVs using viscoelastic flow microfluidics. Adapted with permission from Liu et al. [38]. Copyright 2017 American Chemical Society. (d) Oscillatory Viscoelastic Microfluidics for the enrichment of bioparticles. Adapted with permission from Asghari et al. [39]. Copyright 2020 American Chemical Society

viscoelastic fluid with similar properties to blood, namely poly(ethylene oxide) (PEO) [43], polyvinylpyrrolidone (PVP) [44], and polyacrylamide (PAA) [45].

In a Poiseuille flow with a viscoelastic solution, the elastic lift forces (Eq. 15.7) arise from variations of the first normal stress (N_1) over the particle volume [38]:

$$F_e = C_e d_p^3 \nabla N_1 \quad (15.7)$$

where C_e is the elastic coefficient, and N_1 can be defined according to the Oldroyd-B model for a viscoelastic fluid in a rectangular channel (Eqs. 15.8, 15.9, and 15.10) [32, 38]:

$$N_1 = Wi \dot{\gamma}^2 \quad (15.8)$$

$$\dot{\gamma} = \frac{2Q}{hw^2} \quad (15.9)$$

$$Wi = \lambda \dot{\gamma} = \frac{2\lambda Q}{hw^2} \quad (15.10)$$

where $\dot{\gamma}$ represents the characteristic shear rate [s^{-1}], Wi is the Weissenberg number that measures the viscoelastic effect on the particle, and λ is the relaxation time of non-Newtonian fluids [s].

A study conducted in 2017 demonstrated that the interplay between the inertial, elastic lift and viscous drag forces allows the targeted recovery of exosomes (>90%) from the cell culture medium and serum samples [38]. While larger EVs experience a more significant elastic lift force ($\propto d_p^3$) and thus migrate faster to the centerline of the stream, exosomes, which require higher migration times to reach the centerline, are collected on the outlets near the walls (Fig. 15.2c). Despite promising, these approaches require channel lengths of a few centimeters to provide enough time to achieve sub-micrometer particle separation. Once the particles fall within the nanometer range, increased channel lengths are required to overcome the associated Brownian motion [39]. To overcome this, Asghari et al. developed a simple microfluidic system composed of a single channel with constriction and expansion sites to focus and separate EVs of distinct dimensions by an oscillatory viscoelastic flow. With this system, it was possible to separate p-bodies (300 nm to 1 μ m) from a mammalian cell lysate and λ -DNA (\approx 500 nm) and small EVs (<200 nm) from the cell culture medium (Fig. 15.2d).

15.2.3 Microfluidic Filtration

One of the most widely used techniques for particle isolation is membrane-based filtration. These systems allow the straightforward isolation of particles of interest from clinical samples with minimal sample processing, based on pressure-driven approaches or combined with electrophoresis to enhance particle isolation. In pressure-driven microfluidic systems, filtration occurs due to a pressure gradient

generated between two channels separated by a semipermeable membrane (Fig. 15.1iv).

The transmembrane pressure drop (Eq. 15.11) can be calculated by multiplying the flow rate by the membrane resistance.

$$\Delta P = QR_{\text{membrane}} = QN_{\text{pore}}R_{\text{pore}} \quad (15.11)$$

The total membrane resistance is determined by the addition in parallel of the resistance of each pore (R_{pore}) given by the Dagan equation [46] (Eq. 15.12):

$$R_{\text{pore}} = \frac{\mu}{r^3} \left[3 + \frac{8}{\pi} \left(\frac{L}{r} \right) \right] \quad (15.12)$$

where μ is the fluid viscosity [$\text{Pa}\cdot\text{s}^{-1}$], r is the pore radius [m], and L is the pore length [m].

In these systems, cross-flow filtration is preferred to dead-end flow filtration as the tangential flow will disrupt the formation of the filter cake, which reduces the permeate flux and filtration efficiency [46].

Recently, tangential flow filtration has been used for the isolation and concentration of EVs above 80 nm in a nanoporous polycarbonate track-etch (nPCTE) and nanoporous silicon-nitride (NPN) membranes [46]. In this model, the EVs are retained in the membrane pores and posteriorly recovered when the transmembrane pressure is reversed. Notably, the authors found that greater membrane thickness resulted in a higher transmembrane pressure drop which renders EV recovery more complex. Moreover, NPN membranes enable the direct optical detection of the retained EVs, in contrast to the conventional track-etch membranes, which lack optical transparency [46]. In a different work, microfluidic filtration has been used for the isolation of CTs from the blood of metastatic pancreatic cancer patients using a lateral flow microfiltration device in which the posts are functionalized with anti-EpCAM antibodies, enhancing CTC retention in the device while WBCs and RBCs are depleted [47].

To further enhance particle separation and processing time, combining microfiltration systems with electrophoretic separation or immunoaffinity is also possible. Electrophoresis is an electrokinetic phenomenon in which a force is exerted on a charged particle when it is subjected to an electrical field. In these systems, particles with different sizes are exposed to the same flow rate but experience different electrophoretic forces. Particles with smaller hydrodynamic radius (R_h), such as proteins and exosomes, possess a higher electrophoretic velocity (V_E) (Eq. 15.13) and thus, migrate faster to the electrode than microvesicles and larger particles for the same electrical field.

$$V_E = \frac{qE}{6\pi\mu R_h} \quad (15.13)$$

where q is the particle's surface charge [$\text{C}\cdot\text{m}^{-2}$], which can be calculated according to the Grahame equation [48], E is the applied electric field [$\text{V}\cdot\text{m}^{-1}$].

The negatively charged particles, such as EVs [49, 50], migrate toward the anode, with varying velocities depending on their size, while the positively charged particles move toward the cathode. The inclusion of nanoporous membranes will ensure that specific populations can be directed and recovered in certain channels (Fig. 15.1v). One of the first reports of the use of electrophoresis-based filtration dates from 2012, where the system was used to separate EVs from whole blood with higher purity and throughput when compared with the standard pressure-driven filtration [51].

15.2.4 Acoustofluidic Isolation

Acoustofluidic separation is a label-free, biocompatible, and contactless method that can be used to separate biological particles such as cells and EVs. Since acoustofluidic isolation relies on the interplay between the acoustic radiation force generated by a piezoelectric material and the drag force arising from acoustic streaming, particles of different sizes and physical properties (*p.e.* size, density, and compressibility) will experience distinct resulting forces, and consequentially separation profiles (Fig. 15.1vi).

The acoustic radiation force on a spherical particle is given by Eq. (15.14):

$$F_a = -\frac{\pi^2 p_0^2 d_p^3 \beta_f}{12\lambda} \phi(\beta, \rho) \sin\left(\frac{4\pi x}{\lambda}\right) \quad (15.14)$$

where p_0 is the acoustic pressure [Pa], d_p is the particle diameter [m], β_f represents the compressibility of the fluid [Pa^{-1}]. ϕ , λ , and x represent the acoustic contrast factor, the wavelength of the acoustic waves [nm], and the distance from a pressure node [nm], respectively.

The acoustic pressure is determined from the device characteristics (Eq. 15.15),

$$p_0 = \sqrt{\frac{PZ}{A}} \quad (15.15)$$

where Z represents the acoustic impedance [Ohm] of the substrate, A is the area [m^2] of the interdigitated transducers (IDT), and P is the input signal power [W].

The acoustic contrast factor is given by (Eq. 15.16):

$$\phi(\beta, \rho) = \frac{5\rho_p - 2\rho_f}{2\rho_p + \rho_f} - \frac{\beta_p}{\beta_f} \quad (15.16)$$

where ρ_p and β_p represent the density [$\text{kg}\cdot\text{m}^{-3}$] and compressibility of the particle [$\text{m}^2 \text{N}^{-1}$], respectively, and ρ_m and β_m depict the density and compressibility of the fluid. Positive and negative acoustic contrast factors determine whether the force will be directed toward pressure nodes or antinodes, respectively.

Suspended particles experiencing acoustic streaming are subject to a drag force given by Stokes equation (Eq. 15.4). While the motion of micrometer-sized particles is dominated by the acoustic radiation force (Eq. 15.14), which scales with particle volume ($\propto d_p^3$), the acoustic streaming force scales with the particle diameter. In this sense, as the particle diameter decreases to the nanoscale, the acoustic streaming force becomes preponderant, dictating the particle's trajectory. The empowerment of the acoustic radiation force could be achieved by increasing the operating frequency of the acoustic waves to the MHz. For this, only surface acoustic wave (SAW) and not bulk acoustic wave (BAW) devices can be used for the isolation of sub-micrometer particles as they can operate within 1 MHz to 1 GHz [52]. In SAW devices, two interdigitated transducers (IDTs) patterned on a piezoelectric substrate are placed parallel or orthogonally to a microfluidic channel. Once a radiofrequency (RF) signal is applied, the IDTs generate two series of SAWs that propagate through the microfluidic channel, forming a standing wave that causes pressure fluctuations in the liquid and moves the particles to the pressure nodes or antinodes.

Acoustophoresis has been applied for the isolation of CTCs [53, 54] and bacteria [55] and more recently for the recovery of erythrocyte-derived exosomes [56]. By tuning the RF power of the IDTs and the flow rates, it was possible to adjust the filter size cut-off, with higher frequencies and smaller flow rates contributing to the better fractionation of smaller vesicles. These experimental conditions allowed the collection of 200 nm vesicles in the central channel while the larger vesicles were isolated towards the outer outlets. In a different work, tilted angle standing SAW devices were combined with two microfluidic separation units for the initial removal of blood cells, allowing the posterior fractionation of exosomes from microvesicles present in the sample [57]. By using two sheath inlets, the particle mixture was forced to form a narrow straight stream, ensuring all particles were subjected to the same initial separation condition. Upon applying tilted angle SAWs, nanoscale particles, in which the drag force dominates, continue in the streamline. In contrast, cells and microvesicles are sequentially removed in each of the purification modules as they move toward the pressure nodes. This work was the first report of successful exosome recovery from whole blood samples.

15.2.5 Deterministic Lateral Displacement

Deterministic lateral displacement (DLD) is a size-based particle sorting technique that makes use of an array of pillars displaying an offset configuration to displace particles in predetermined paths [58] (Fig. 15.1vii).

Each row of posts is horizontally shifted concerning the previous by a distance defined as a fraction (δ) of the center-to-center pillar distance (λ). The design geometry, shift fraction, and gap between adjacent pillars (G) will determine the critical diameter (D_c) and a maximum angle (θ_{\max}), which will dictate the particle migration path (Eqs. 15.17 and 15.18) [58, 59].

$$D_c = 2\beta = 2\eta G\delta \quad (15.17)$$

$$\theta_{\max} = \tan^{-1}\left(\frac{\delta}{\lambda}\right) \quad (15.18)$$

Particles with a diameter equal to or larger than the critical cut-off will be laterally displaced by the bumping with the pillar arrays at a migration angle equal to θ_{\max} . In contrast, particles with diameters smaller than D_c will follow the fluid streamline (β) through a zigzag mode with a mean angle of 0° with respect to the array [59]. Device clogging is particularly significant when these parameters are approximate, and particle density is high. Thus, the designed gap must be larger than the diameter of the largest particle to separate within the system. The smallest particle to be separated is given by the critical diameter of the section with the smallest δ .

Since this separation technology relies on a deterministic phenomenon, it is necessary to ensure that fluid dynamics follow a laminar flow regime driven by advection and not by diffusional processes. For this, two dimensionless numbers, Re (Eq. 15.3) and Péclet (Pe) need to be adjusted. The Pe number is given by Eq. (15.19), where the characteristic length is replaced by $\delta\lambda$ [58].

$$\text{Pe} = \frac{\delta\lambda v}{D} \quad (15.19)$$

Previous studies have reported the use of DLD for CTC enrichment and recovery [60, 61]. Recent work described the enrichment of CTCs from whole blood by the sequential use of filter-DLD modules with different critical diameters (Zongbin [62]). In the first module, larger cells, including CTCs and WBCs, are recovered and directed to the cell-size separation module, while smaller cells, such as RBCs, are depleted from the sample (Fig. 15.3a). In the second module, the critical diameter gradually increases from 8 to 22 μm , allowing the fractionation of CTCs and WBCs due to their size differences. This device permitted high separation efficacy (>96%) and throughput (1 mL/min) with elevated levels of purity (>99%).

Although particle isolation can easily be accomplished for micrometer-sized particles at high high-throughput, experimental limitations arise from sub-micrometer particle fractionation, as small δ require longer channel lengths to achieve significant particle separation due to the increasing contribution of Brownian motion and diffusion [58]. Computational simulations have shown that the tuning of the ionic strength of the buffer solution can modulate particle trajectory [64]. Buffer solutions with lower ionic strengths increase the thickness of the electrical double layer of the particles, increasing their apparent size and contributing to the lateral displacement of significantly smaller particles [64]. The first successful DLD exosome fractionation system consisted of a silicon nanoscale array with gap sizes between 25 and 235 nm [59]. The authors showed that by conducting experiments at low Pe numbers, where diffusion and DLD compete, it is possible to sort particles with diameters between 20 and 110 nm. Additionally, it was reinforced the importance of accounting for particle–particle interactions and fluid-flow distortion at the

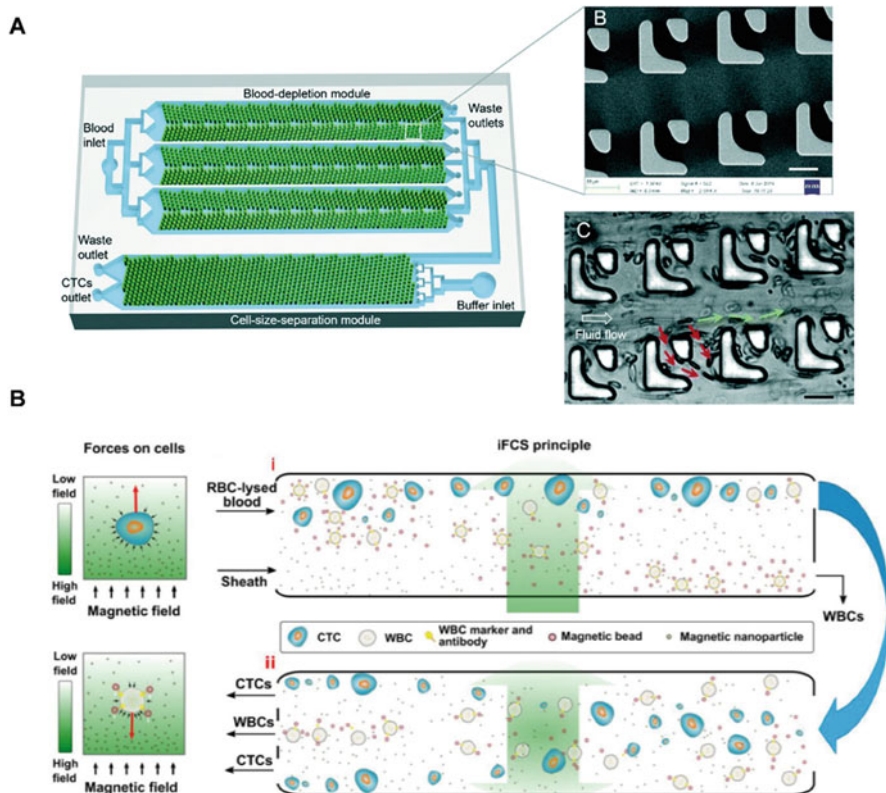


Fig. 15.3 Deterministic lateral displacement and ferrohydrodynamic particle separation. (a) Cascaded filter DLD device for the isolation of circulating tumor cells. Republished with permission of the Royal Society of Chemistry, from Zongbin Liu et al. [62]. Permission conveyed through Copyright Clearance Center, Inc. (b) Ferrohydrodynamic isolation of circulating tumor cells by cell diamagnetophoresis and white blood cell depletion by the action of magnetophoresis. Republished with permission of the Royal Society of Chemistry, from Zhao et al. [63]. Permission conveyed through Copyright Clearance Center, Inc

nanoscale as single particles can influence particle displacement, even in highly diluted samples for $D_p \sim 0.5G$ [59].

15.2.6 Ferrohydrodynamics

Ferrohydrodynamics allows the label-free size-sorting of diamagnetic particles immersed in a magnetizable fluid through the modulation of the magnetic field (Fig. 15.1viii). Under the exposure of a magnetic field gradient, the suspended magnetic nanoparticles present in the ferrofluid will be polarized while the

diamagnetic particles will move in the opposite direction of the magnetic field gradient, in a phenomenon entitled “diamagnetophoresis.”

A diamagnetic particle in suspension in a magnetic nanoparticle colloidal suspension is subject to the ferrohydrodynamic force (Eq. 15.20) and the hydrodynamic drag force (Eq. 15.4). Hence, the balance between these two forces will dictate the particles’ trajectory.

$$F_m = -\mu_0 V_p (M \nabla) H \quad (15.20)$$

where μ_0 is the permeability of the free space [$\text{N}\cdot\text{A}^{-2}$], V_p is the particle volume [m^3], and M and H represent the non-linear magnetization [$\text{A}\cdot\text{m}^2$] and magnetic field strength [$\text{A}\cdot\text{m}^{-1}$], respectively.

The ferrohydrodynamic force is predominant at room temperature for particles in the micrometer and sub-micrometer range; however, once the diameter decreases to the nanoscale, the hydrodynamic drag force will become dominant [65]. Hence, ferrohydrodynamics has been mainly used for the enrichment of CTCs. Zhao and colleagues developed a microfluidic device capable of enriching low concentrations of CTCs in RBC-lyzed blood samples of patients with non-small cell lung cancer [66]. Upon cell debris removal, processed blood samples are focused on a straight channel by a ferrofluid sheath flow and exposed to a permanent magnet on its bottom. Larger diamagnetic bioparticles, including CTCs and some WBCs, experience a more significant repulsive force when exposed to the non-uniform magnetic field when compared to smaller bioparticles. This causes them to migrate faster in the opposite direction permitting their separation with a CTC recovery rate of 92.9% and a throughput of 6 mL/h. In a posterior work, the authors included a second processing step to ensure higher CTC purity upon recovery [63]. In this work, WBCs were labeled with magnetic beads, causing them to experience both diamagnetophoresis (owing to its cell surface) and magnetophoresis (owing to the attached magnetic beads) (Fig. 15.3b). Once the WBCs flew through the straight channel, subjected to a magnetic field with its maximum in the center of the channel, the labeled WBCs migrated toward the middle of the streamline as the magnetic force outweighed the diamagnetic effect. This permitted a high recovery rate (99.08%) and sample throughput (12 mL/h) with minimal WBC contamination.

On the other hand, to achieve successful EV fractionation, the balance between the ferrohydrodynamic force and the hydrodynamic drag force must be modulated to ensure the ferrohydrodynamic force produces a weak effect on exosomes and significant contribution to the microvesicle movement. In recent work, this methodology has been applied toward isolating EVs and sorting microvesicles and exosomes from the blood serum of healthy individuals. This was accomplished by adjusting the geometry of the device, the magnetic field, and fluid operating conditions. To achieve vesicle sorting, samples pre-mixed with ferrofluid were flown near the vicinity of the microchannel, where the magnetic field was higher, inducing the migration of the microvesicles toward the center of the microchannel [65].

15.3 Conclusion

Microfluidic devices have demonstrated great applicability in isolating circulating biomarkers in the laboratory, with high potential to be applied in the clinic. However, before these platforms are implemented in current clinical practice, it is imperative to develop standardized protocols that enable the selection of the adequate platform based on the intended downstream application. For instance, if the intention is to determine the total number of particles within a system, label-free isolation methods allow the highest recovery, but sample purity may be compromised. On the other hand, if the purpose of bioparticle isolation is the analysis of the molecular cargo, affinity-based isolation platforms will allow the highest purity for further downstream processing. In the future, the ideal platform will include multiple processing modules that enable particle isolation, quantification, and analysis in a single high-throughput platform with minimal pre-processing steps sample volume requirements.

Acknowledgements D.C. acknowledges the financial support from the Portuguese Foundation for Science and Technology (FCT) under the program CEEC Individual 2017 (CEECIND/00352/2017). C.M.A., S.C.K., and D.C. also thank the support from the FCT under the scope of the projects 2MATCH (PTDC/BTM-ORG/28070/2017) and BREAST-IT (PTDC/BTM-ORG/28168/2017) funded by the Programa Operacional Regional do Norte supported by European Regional Development Funds (ERDF). The authors also thank the financial support from the European Union Framework Program for Research and Innovation Horizon 2020 on the FoReCaST project under (Grant Number: 668983).

Conflicts of Interest None.

References

1. Bray F, Ferlay J, Soerjomataram I et al (2018) Global cancer statistics 2018: GLOBOCAN estimates of incidence and mortality worldwide for 36 cancers in 185 countries. *CA Cancer J Clin* 68:394–424. <https://doi.org/10.3322/caac.21492>
2. Guan X (2015) Cancer metastases: challenges and opportunities. *Acta Pharm Sin B* 5:402–418
3. Abdalla TSA, Meiners J, Riethdorf S et al (2021) Prognostic value of preoperative circulating tumor cells counts in patients with UICC stage I-IV colorectal cancer. *PLoS One* 16:e0252897. <https://doi.org/10.1371/journal.pone.0252897>
4. Lee CH, Hsieh JCH, Wu TMH et al (2019) Baseline circulating stem-like cells predict survival in patients with metastatic breast cancer. *BMC Cancer* 19:1–10. <https://doi.org/10.1186/s12885-019-6370-1>
5. Moreno JG, Miller MC, Gross S et al (2005) Circulating tumor cells predict survival in patients with metastatic prostate cancer. *Urology* 65:713–718. <https://doi.org/10.1016/j.urology.2004.11.006>
6. Aaltonen KE, Novosadová V, Bendahl PO et al (2017) Molecular characterization of circulating tumor cells from patients with metastatic breast cancer reflects evolutionary changes in gene expression under the pressure of systemic therapy. *Oncotarget* 8:45544–45565. <https://doi.org/10.18632/oncotarget.17271>
7. Bredemeier M, Edimiris P, Tewes M et al (2016) Establishment of a multimarker qPCR panel for the molecular characterization of circulating tumor cells in blood samples of metastatic

- breast cancer patients during the course of palliative treatment. *Oncotarget* 7:41677–41690. <https://doi.org/10.18632/oncotarget.9528>
8. De Luca F, Rotunno G, Salvianti F et al (2016) Mutational analysis of single circulating tumor cells by next generation sequencing in metastatic breast cancer. *Oncotarget* 7:26107–26119. <https://doi.org/10.18632/oncotarget.8431>
 9. Colombo M, Raposo G, Théry C (2014) Biogenesis, secretion, and intercellular interactions of exosomes and other extracellular vesicles. *Annu Rev Cell Dev Biol* 30:255–289
 10. Hoshino A, Costa-Silva B, Shen T-L et al (2015) Tumour exosome integrins determine organotropic metastasis. *Nature* 527:329–335. <https://doi.org/10.1038/nature15756>
 11. Thakur BK, Zhang H, Becker A et al (2014) Double-stranded DNA in exosomes: a novel biomarker in cancer detection. *Cell Res* 24:766–769. <https://doi.org/10.1038/cr.2014.44>
 12. Xu R, Rai A, Chen M et al (2018) Extracellular vesicles in cancer – implications for future improvements in cancer care. *Nat Rev Clin Oncol* 15:617–638
 13. Russano M, Napolitano A, Ribelli G et al (2020) Liquid biopsy and tumor heterogeneity in metastatic solid tumors: the potentiality of blood samples. *J Exp Clin Cancer Res* 39:95. <https://doi.org/10.1186/s13046-020-01601-2>
 14. Zhou B, Xu K, Zheng X et al (2020) Application of exosomes as liquid biopsy in clinical diagnosis. *Signal Transduct Target Ther* 5:1–14. <https://doi.org/10.1038/s41392-020-00258-9>
 15. Squires TM, Messinger RJ, Manalis SR (2008) Making it stick: convection, reaction and diffusion in surface-based biosensors. *Nat Biotechnol* 26:417–426. <https://doi.org/10.1038/nbt1388>
 16. Dorayappan KDP, Gardner ML, Hisey CL et al (2019) A microfluidic chip enables isolation of exosomes and establishment of their protein profiles and associated signaling pathways in ovarian cancer. *Cancer Res* 79:3503–3513. <https://doi.org/10.1158/0008-5472.CAN-18-3538>
 17. Hisey CL, Dorayappan KDP, Cohn DE et al (2018) Microfluidic affinity separation chip for selective capture and release of label-free ovarian cancer exosomes. *Lab Chip* 18:3144–3153. <https://doi.org/10.1039/c8lc00834e>
 18. Lo TW, Zhu Z, Purcell E et al (2020) Microfluidic device for high-throughput affinity-based isolation of extracellular vesicles. *Lab Chip* 20:1762–1770. <https://doi.org/10.1039/c9lc01190k>
 19. Barriere G, Fici P, Gallerani G et al (2014) Circulating tumor cells and epithelial, mesenchymal and stemness markers: characterization of cell subpopulations. *Ann Transl Med* 2:109
 20. Cho HY, Choi JH, Lim J et al (2021) Microfluidic chip-based cancer diagnosis and prediction of relapse by detecting circulating tumor cells and circulating cancer stem cells. *Cancers (Basel)* 13:1–17
 21. Kang YT, Hadlock T, Lo TW et al (2020) Dual-isolation and profiling of circulating tumor cells and cancer exosomes from blood samples with melanoma using Immunoaffinity-based microfluidic interfaces. *Adv Sci* 7:2001581. <https://doi.org/10.1002/advs.202001581>
 22. Hou HW, Warkiani ME, Khoo BL et al (2013) Isolation and retrieval of circulating tumor cells using centrifugal forces. *Sci Rep* 3:1–8. <https://doi.org/10.1038/srep01259>
 23. Willms E, Cabañas C, Mäger I et al (2018) Extracellular vesicle heterogeneity: subpopulations, isolation techniques, and diverse functions in cancer progression. *Front Immunol* 9:1. <https://doi.org/10.3389/fimmu.2018.00738>
 24. Skotland T, Sandvig K, Llorente A (2017) Lipids in exosomes: current knowledge and the way forward. *Prog Lipid Res* 66:30–41. <https://doi.org/10.1016/j.plipres.2017.03.001>
 25. Kang YT, Purcell E, Palacios-Rolston C et al (2019) Isolation and profiling of circulating tumor-associated exosomes using extracellular vesicular lipid–protein binding affinity based microfluidic device. *Small* 15. <https://doi.org/10.1002/sml.201903600>
 26. Cho H, Kim J, Song H et al (2018) Microfluidic technologies for circulating tumor cell isolation. *Analyst* 143:2936–2970
 27. Contreras-Naranjo JC, Wu HJ, Ugaz VM (2017) Microfluidics for exosome isolation and analysis: enabling liquid biopsy for personalized medicine. *Lab Chip* 17:3558–3577
 28. Iliescu FS, Vrtačnik D, Neuzil P, Iliescu C (2019) Microfluidic technology for clinical applications of exosomes. *Micromachines* 10

29. Lei KF (2020) A review on microdevices for isolating circulating tumor cells. *Micromachines*:11
30. Gou Y, Jia Y, Wang P, Sun C (2018) Progress of inertial microfluidics in principle and application. *Sensors (Basel)*:18
31. Zhou Y, Ma Z, Tayebi M, Ai Y (2019) Submicron particle focusing and exosome sorting by wavy microchannel structures within viscoelastic fluids. *Anal Chem* 91:4577–4584. <https://doi.org/10.1021/acs.analchem.8b05749>
32. Xiang N, Zhang X, Dai Q et al (2016) Fundamentals of elasto-inertial particle focusing in curved microfluidic channels. *Lab Chip* 16:2626–2635. <https://doi.org/10.1039/c6lc00376a>
33. Tay HM, Kharel S, Dalan R et al (2017) Rapid purification of sub-micrometer particles for enhanced drug release and microvesicles isolation. *NPG Asia Mater* 9:e434–e434. <https://doi.org/10.1038/am.2017.175>
34. Razavi Bazaz S, Mashhadian A, Ehsani A et al (2020) Computational inertial microfluidics: a review. *Lab Chip* 20:1023–1048
35. Zhang J, Yan S, Yuan D et al (2016) Fundamentals and applications of inertial microfluidics: a review. *Lab Chip* 16:10–34
36. Smith KJ, Jana JA, Kaehr A et al (2021) Inertial focusing of circulating tumor cells in whole blood at high flow rates using the microfluidic CTCKey™ device for CTC enrichment. *Lab Chip* 21:3559–3572. <https://doi.org/10.1039/D1LC00546D>
37. Renier C, Pao E, Che J et al (2017) Label-free isolation of prostate circulating tumor cells using vortex microfluidic technology. *npj Precis Oncol* 1:15. <https://doi.org/10.1038/s41698-017-0015-0>
38. Liu C, Guo J, Tian F et al (2017) Field-free isolation of exosomes from extracellular vesicles by microfluidic viscoelastic flows. *ACS Nano* 11:6968–6976. <https://doi.org/10.1021/acsnano.7b02277>
39. Asghari M, Cao X, Mateescu B et al (2020) Oscillatory viscoelastic microfluidics for efficient focusing and separation of nanoscale species. *ACS Nano* 14:422–433. <https://doi.org/10.1021/acsnano.9b06123>
40. Lemaire CA, Liu SZ, Wilkerson CL et al (2018) Fast and label-free isolation of circulating tumor cells from blood: from a research microfluidic platform to an automated fluidic instrument, VTX-1 liquid biopsy system. *SLAS Technol* 23:16–29. <https://doi.org/10.1177/2472630317738698>
41. Guglielmi R, Lai Z, Raba K et al (2020) Technical validation of a new microfluidic device for enrichment of CTCs from large volumes of blood by using buffy coats to mimic diagnostic leukapheresis products. *Sci Rep* 10:1–9. <https://doi.org/10.1038/s41598-020-77227-3>
42. Warkiani ME, Khoo BL, Wu L et al (2016) Ultra-fast, label-free isolation of circulating tumor cells from blood using spiral microfluidics. *Nat Protoc* 11:134–148. <https://doi.org/10.1038/nprot.2016.003>
43. Xu Z, Wang S, Li Y et al (2014) Covalent functionalization of graphene oxide with biocompatible poly(ethylene glycol) for delivery of paclitaxel. *ACS Appl Mater Interfaces* 6:17268–17276. <https://doi.org/10.1021/am505308f>
44. Kaneda Y, Tsutsumi Y, Yoshioka Y et al (2004) The use of PVP as a polymeric carrier to improve the plasma half-life of drugs. *Biomaterials* 25:3259–3266. <https://doi.org/10.1016/j.biomaterials.2003.10.003>
45. Nguyen MK, Lee DS (2010) Bioadhesive PAA-PEG-PAA triblock copolymer hydrogels for drug delivery in oral cavity. *Macromol Res* 18:284–288. <https://doi.org/10.1007/s13233-010-0315-5>
46. Dehghani M, Lucas K, Flax J et al (2019) Tangential flow microfluidics for the capture and release of nanoparticles and extracellular vesicles on conventional and ultrathin membranes. *Adv Mater Technol* 4:1900539. <https://doi.org/10.1002/admt.201900539>
47. Chen K, Amontree J, Varillas J et al (2020) Incorporation of lateral microfiltration with immunoaffinity for enhancing the capture efficiency of rare cells. *Sci Rep* 10:14210. <https://doi.org/10.1038/s41598-020-71041-7>

48. Lyklema J (2005) *Fundamentals of interface and colloid science*, 1st edn. Elsevier
49. Chen Z, Yang Y, Yamaguchi H et al (2020) Isolation of cancer-derived extracellular vesicle subpopulations by a size-selective microfluidic platform. *Biomicrofluidics* 14. <https://doi.org/10.1063/5.0008438>
50. Cho S, Jo W, Heo Y et al (2016) Isolation of extracellular vesicle from blood plasma using electrophoretic migration through porous membrane. *Sens Actuators B* 233:289–297. <https://doi.org/10.1016/j.snb.2016.04.091>
51. Davies RT, Kim J, Jang SC et al (2012) Microfluidic filtration system to isolate extracellular vesicles from blood. *Lab Chip* 12:5202–5210. <https://doi.org/10.1039/c2lc41006k>
52. Shilton RJ, Travagliati M, Beltram F, Cecchini M (2014) Nanoliter-droplet acoustic streaming via ultra high frequency surface acoustic waves. *Adv Mater* 26:4941–4946. <https://doi.org/10.1002/adma.201400091>
53. Liu H, Ao Z, Cai B et al (2018) Size-amplified acoustofluidic separation of circulating tumor cells with removable microbeads. *Nano Futur* 2:025004. <https://doi.org/10.1088/2399-1984/aabf50>
54. Wu Z, Jiang H, Zhang L et al (2019) The acoustofluidic focusing and separation of rare tumor cells using transparent lithium niobate transducers. *Lab Chip* 19:3922–3930. <https://doi.org/10.1039/c9lc00874h>
55. Li S, Ma F, Bachman H et al (2017) Acoustofluidic bacteria separation. *J Micromech Microeng* 27:015031. <https://doi.org/10.1088/1361-6439/27/1/015031>
56. Lee K, Shao H, Weissleder R, Lee H (2015) Acoustic purification of extracellular microvesicles. *ACS Nano* 9:2321–2327. <https://doi.org/10.1021/nn506538f>
57. Wu M, Ouyang Y, Wang Z et al (2017) Isolation of exosomes from whole blood by integrating acoustics and microfluidics. *Proc Natl Acad Sci U S A* 114:10584–10589. <https://doi.org/10.1073/pnas.1709210114>
58. Inglis DW, Davis JA, Austin RH, Sturm JC (2006) Critical particle size for fractionation by deterministic lateral displacement. *Lab Chip* 6:655–658. <https://doi.org/10.1039/b515371a>
59. Wunsch BH, Smith JT, Gifford SM et al (2016) Nanoscale lateral displacement arrays for the separation of exosomes and colloids down to 20nm. *Nat Nanotechnol* 11:936–940. <https://doi.org/10.1038/nnano.2016.134>
60. Liu Z, Huang F, Du J et al (2013) Rapid isolation of cancer cells using microfluidic deterministic lateral displacement structure. *Biomicrofluidics* 7. <https://doi.org/10.1063/1.4774308>
61. Liu Z, Zhang W, Huang F et al (2013) High throughput capture of circulating tumor cells using an integrated microfluidic system. *Biosens Bioelectron* 47:113–119. <https://doi.org/10.1016/j.bios.2013.03.017>
62. Liu Z, Huang Y, Liang W et al (2021) Cascaded filter deterministic lateral displacement microchips for isolation and molecular analysis of circulating tumor cells and fusion cells. *Lab Chip* 21:2881–2891. <https://doi.org/10.1039/D1LC00360G>
63. Zhao W, Liu Y, Jenkins BD et al (2019) Tumor antigen-independent and cell size variation-inclusive enrichment of viable circulating tumor cells. *Lab Chip* 19:1860–1876. <https://doi.org/10.1039/c9lc00210c>
64. Zeming KK, Thakor NV, Zhang Y, Chen CH (2016) Real-time modulated nanoparticle separation with an ultra-large dynamic range. *Lab Chip* 16:75–85. <https://doi.org/10.1039/c5lc01051a>
65. Liu Y, Zhao W, Cheng R et al (2020) Label-free ferrohydrodynamic separation of exosome-like nanoparticles. *Lab Chip* 20:3187–3201. <https://doi.org/10.1039/d0lc00609b>
66. Zhao W, Cheng R, Jenkins BD et al (2017) Label-free ferrohydrodynamic cell separation of circulating tumor cells. *Lab Chip* 17:3097–3111. <https://doi.org/10.1039/c7lc00680b>



Microfluidics for the Isolation and Detection of Circulating Tumor Cells

16

Jessica Sierra-Agudelo, Romen Rodriguez-Trujillo,
and Josep Samitier

Abstract

Nowadays, liquid biopsy represents one of the most promising techniques for early diagnosis, monitoring, and therapy screening of cancer. This novel methodology includes, among other techniques, the isolation, capture, and analysis of circulating tumor cells (CTCs). Nonetheless, the identification of CTC from whole blood is challenging due to their extremely low concentration (1–100 per ml of whole blood), and traditional methods result insufficient in terms of purity, recovery, throughput and/or viability of the processed sample. In this context, the development of microfluidic devices for detecting and isolating CTCs offers a wide range of new opportunities due to their excellent properties for cell manipulation and the advantages to integrate and bring different laboratory processes into the microscale improving the sensitivity, portability, reducing cost and time. This chapter explores current and recent microfluidic approaches that have been

J. Sierra-Agudelo

Nanobioengineering Group, Institute for Bioengineering of Catalonia (IBEC), Barcelona Institute of Science and Technology (BIST), Barcelona, Spain

R. Rodriguez-Trujillo (✉)

Nanobioengineering Group, Institute for Bioengineering of Catalonia (IBEC), Barcelona Institute of Science and Technology (BIST), Barcelona, Spain

Department of Electronics and Biomedical Engineering, University of Barcelona, Barcelona, Spain
e-mail: romen.rodriguez@ub.edu

J. Samitier

Nanobioengineering Group, Institute for Bioengineering of Catalonia (IBEC), Barcelona Institute of Science and Technology (BIST), Barcelona, Spain

Department of Electronics and Biomedical Engineering, University of Barcelona, Barcelona, Spain

Centro de Investigación Biomédica en Red en Bioingeniería, Biomateriales y Nanomedicina (CIBER-BBN), Madrid, Spain

© The Author(s), under exclusive license to Springer Nature Switzerland AG 2022

389

D. Caballero et al. (eds.), *Microfluidics and Biosensors in Cancer Research*,

Advances in Experimental Medicine and Biology 1379,

https://doi.org/10.1007/978-3-031-04039-9_16

developed for the analysis and detection of CTCs, which involve cell capture methods based on affinity binding and label-free methods and detection based on electrical, chemical, and optical sensors. All the exposed technologies seek to overcome the limitations of commercial systems for the analysis and isolation of CTCs, as well as to provide extended analysis that will allow the development of novel and more efficient diagnostic tools.

Keywords

Microfluidics · Liquid biopsy · Circulating tumor cells · Cancer detection · Cancer diagnosis

16.1 Introduction

One of the big challenges in cancer is achieving an early-stage diagnosis. Currently tumors are not found until symptoms appear or by chance when the patient undergoes a medical test which in both situations can be too late for the patient. Many analysts now argue that the development of efficient methods for screening, early diagnosis, and monitoring, are promising technologies to achieve a high-efficiency therapy and to reduce cancer mortality [1]. As has been reported, several biological body fluids like blood, urine, and saliva contain biomarkers, which could be DNA, RNA, proteins, or whole cells [1, 2]. In recent years, interest has arisen in the development of new technologies to detect those biomarkers from body fluids, such as liquid biopsies [1]. The emergence of liquid biopsies has been useful for the diagnosis of physiological conditions, inflammatory processes and specially represents a good alternative tool for non-invasive analysis of tumor-derived materials.

Currently, tissue biopsies represent the gold standard for tumor profiling. Nonetheless, this method displays many limitations that include the invasiveness, risk and depending on some anatomical locations is not easy (or even impossible) to obtain [3]. In fact, it provides a limited vision of the tumor profile, considering that tumors are heterogeneous composed of different subpopulations of cells, which display a variability of genetic and epigenetic changes. In addition to differences between primary and metastatic lesions [3]. Therefore, the tissue biopsies fail to represent the overall tumor profile, capture the alterations in different parts, and monitor the diseases progression [4].

On the other hand, liquid biopsies could be done through routine blood extraction and analysis, a procedure that is much easier and less invasive than a tumor biopsy. In this context, liquid biopsies are a cheaper, faster, non-invasive alternative to conventional biopsies, that can be used for personalized cancer therapy [1, 3]. In a broad sense, liquid biopsy is based on the isolation of biomarkers from blood that can be used for cancer diagnostic and monitoring. This definition englobes circulating tumor cells (CTCs), circulating tumor DNA (ctDNA), and exosomes [1, 2, 5].

16.1.1 What Are the Circulating Tumor Cells?

Since 1869, Ashworth discovered the tumor cells in the peripheral blood and proposed the concept of a CTC [6]. These CTCs are cancer cells, which leave the primary tumor and enter the bloodstream initiating a process called metastasis that is responsible for almost 90% of cancer deaths [7]. From the biological point of view, these cells do not bind to the extracellular matrix (ECM) and survive in the bloodstream because of their resistance to apoptotic process known as “anoikis” [8], as well as factors associated with epithelial and mesenchymal plasticity or stem cell-like properties.

Metastasis is a biological complex process, which involves cell migration, invasion, arrest at secondary and primary parts, intrusion of tumor cells in bloodstream, dissemination, extravasation at distant parts, colonization and finally, the formation of a metastatic secondary tumor clinically detectable (Fig. 16.1) [7, 10]. Recent studies indicate the high heterogeneity of CTC population, including CTCs clusters, individual CTCs, epithelial CTCs, hybrid epithelial-mesenchymal CTCs, mesenchymal CTCs and stem-like CTCs [11]. In fact, it has been found that CTCs clusters show distinct features regarding to individual CTCs, such as phenotype, sign of gene

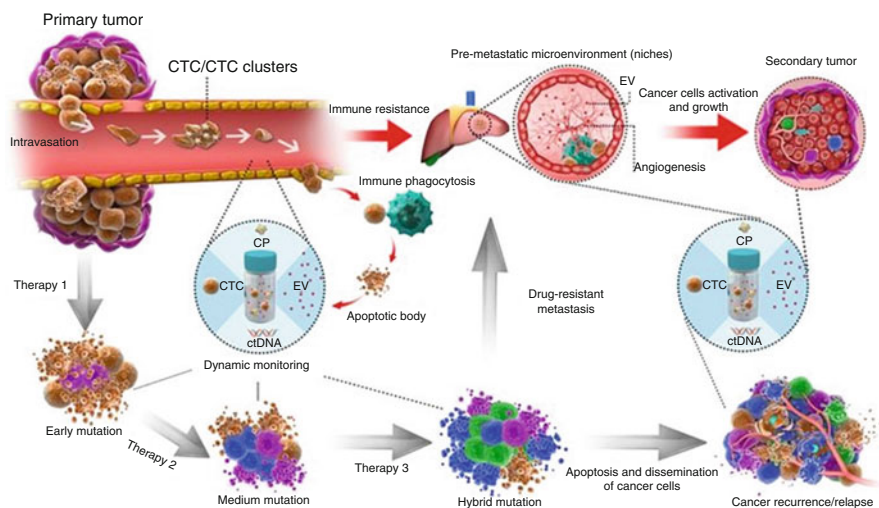


Fig. 16.1 Liquid biopsy and CTCs origin and progression under therapeutic application. Circulating proteins (CPs), circulating tumor DNA (ctDNA), circulating tumor cells (CTCs) and extracellular vesicles (EVs) enter the circulation and can be used to detect minimal tumor generation and monitor tumor heterogeneity. CTCs will be generated by the primary tumor and cooperate with TEPs (tumor-educated blood platelets) to survive and enter in circulation as single CTCs or CTCs clusters. Furthermore, EVs represent pre-metastatic scavengers that resist to immune damage and allow metastasis in secondary areas. After target therapy is applied, the drug-resistant cancer cells will proliferate by adaptive evolution. Thus, liquid biopsy allows to predict metastasis or relapse. Natural cancer development is represented by the red arrows, meanwhile the development of tumors after therapy is shown by the black arrows. **Licensed under CC-BY 4.0 International License. The Final, Published Version of This Article Is Available at [9]**

expression and nature [12, 13]. Moreover, other studies have revealed that CTCs clusters may have 100 times more metastatic potential than single CTCs [14]. The presence of CTCs in blood has been recognized in many types of cancer, such as breast cancer, colon cancer, lung, prostate among others [14]. In fact, previous clinical studies in patients with breast cancer have correlated the presence of CTCs with an increase in tumor burden, aggressiveness, as well as decreased time to relapse [10].

In these circumstances, isolation and detection of CTCs that are circulating into the bloodstream could be used for early cancer metastasis detection as well as for monitoring tumor's responsiveness to radio/chemotherapy and developing personalized patient treatments. Some of the diagnostic possibilities that CTCs detection would offer can be summarized as follows [15].

- The presence of CTCs in blood is highly associated with metastatic risk but also indicates primary tumor existence. As it is known that CTCs are present in blood from very early stages of the disease and prior to the appearance of symptoms, a device that allows the detection of CTCs could be used for both determining metastatic risk and early cancer detection.
- It is also known that the number of CTCs present in the blood sample is related to the stage of the patient's disease. Thus, another advantage could be to monitor tumor's responsiveness to therapy. This would be done by running routine blood analysis and comparing the number of CTCs prior and after the treatment.
- Another important issue is tumor heterogeneity, both within a tumor and between the primary tumor and its metastases, which cannot be captured by a simple tissue biopsy. This heterogeneity accounts for the genotypic differences between different regions of the tumor or between the primary and the secondary tumors. It is known that almost all tumors treated with any therapy acquire resistance because of tumor heterogeneity, clonal evolution, and selection [16]. Therefore, CTCs isolation and analysis would enable to understand better the phenomena of metastatic drug resistance.
- Tumors are very prone to suffer mutations in their genome, so their molecular profile changes frequently, and so does the effective treatment required. Thus, liquid biopsy would allow monitoring the molecular profile of the tumor just by taking periodic blood samples from the patient. Therefore, according to the results obtained the clinicians can find out if the treatment is correct or if it must be adjusted due to mutations.

It is therefore clear that the development of a platform allowing CTCs isolation and detection from blood samples would be a major improvement in the study and treatment of cancer. Nevertheless, the identification of CTC from whole blood is challenging, as the number of CTCs in 1 mL of blood from a cancer patient is only 1–100, in comparison with 10^9 hematologic cells [17]. Hence, the traditional methods to isolate cells, like flow cytometry, density gradient centrifugation, and immunocapture by magnetic beads do not have enough sensitivity to detect rare cells like CTCs [18].

Despite the high number of scientific publications related to CTCs detection, there is only one CTC test approved by the FDA, the CellSearch[®] system by Menarini Silicon Biosystems [19]. This system uses magnetic particles coated with antibodies that bind to the protein EpCAM (epithelial cell adhesion molecule) for quantifying the CTCs in metastatic breast, prostate, and colon [20]. In the last few decades, EpCAM was considered as universal tumor biomarker for epithelial-derived cancer types [21]. Nevertheless, several studies indicate that some CTCs can be EpCAM-negative [22] such as those which had an epithelial-to-mesenchymal transition and mesenchymal origin. Moreover, CTCs isolated from patients display a wide range of EpCAM expression, where a part of these cells are EpCAM-negative [23, 24] for instance in some advanced lung cancer [23, 25, 26]. This represents one of the main drawbacks of this platform as well as, it requires expensive equipment and allows neither 100% purity nor isolation of viable cells for further culture and studies.

To overcome these limitations, several microfluidic platforms have also been developed. Indeed, Lab-on-a-Chip (LOC) technologies have been exploited in the recent decades for several biomedical applications such as diagnostics, biochemical assays, and drug discovery among others. Microfluidics and LOC technologies are directly correlated terms since LOC technologies aim to integrate and bring different laboratory processes into the microscale to exploit the advantages that working at this length scale provides. Therefore, these devices are frequently composed of microfluidic elements like microchannels, micropumps, microvalves, etc. to enable processing small (micro scaled) amounts of liquid.

Nowadays, most of the analytical and diagnostic assays are done with benchtop equipment in hospitals and/or centralized laboratories, which are either operated by trained personnel or composed of chains of automated pipetting robots with the associated increment of power consumption and space demand. Microfluidic LOC platforms arise as an alternative to the present model of diagnostics since these offer a wide range of new opportunities that can be summarized as: [27, 28].

- Portability due to its reduced dimensions.
- Higher sensitivity.
- Faster results obtaining.
- Reduced laboratory space.
- Lower cost per test due to less quantity of reagent required.

In addition, apart from those advantages stated above, working at the microscale allows taking advantage of the unique phenomena taking place at such scale:

- Gravitational force loses importance.
- Well-defined laminar flow.
- Controllable diffusion.
- High degree of parallelization.

Therefore, all the characteristics mentioned before, together with the fact that microfluidic LOC devices have the perfect size for cell manipulation and that they have the possibility to play with well-defined particle forces related to inertial effects [29, 30], make them ideal for building CTCs isolation devices that can be used for liquid biopsies.

16.2 Microfluidic-Based Isolation of CTCs

The application of microfluidic devices to the detection and isolation of circulating tumor cells is quite recent, the firsts scientific works arising towards 2005. The first scientist to create a considerable impact in the field was Prof. Toner and his group at Harvard Medical School with the publishing in 2007 of a research paper [31] in which they obtained promising results concerning the isolation of CTCs on a microchip capable of efficient and selective separation of viable CTCs from peripheral whole blood samples, mediated by the interaction of target CTCs with antibody (EpCAM)-coated microposts under precisely controlled laminar flow conditions, and without requisite pre-labeling or processing of samples. At that moment, this was revolutionary and encouraged a lot of scientists, all with the same purpose of developing a lab-on-chip device to detect and isolate CTCs. If we now look back on that paper, it has become the most cited paper regarding CTCs isolation using microfluidics with almost 3000 citations up to date.

Since then, many other microfluidic devices have been proposed for the separation of CTC from blood. They can be based in microfiltration, deterministic lateral displacement, centrifugation, inertial focusing, affinity-based methods, among others [29, 32–35]. They separate according to cell properties like size, density, shape, deformability, or biomarkers expression [27, 36, 37]. The parameters used to evaluate the performance of this technology include **purity**, **throughput**, **recovery rate** and **cell viability**. The purity is associated to the blood cells depletion, which indicates the number of CTCs compared to blood cells. Meanwhile, recovery rate reflects the ratio of targeted cells collected in the CTCs outlet to the total number of CTCs, throughput refers to the amount of blood sample (usually in milliliters) that can be processed in the device per unit of time and thus the number of cells that can be captured and, finally, cell viability indicates if the cells recovered are alive [29, 36]. Considering the low concentration of CTCs on the blood, it is important to guarantee that all the CTCs are being recovered by the device and that they are viable. Thus, the cells recovered could be used in personalized drug screening [38, 39]. Overall, with the emergence of personalized medicine the latest developed devices for CTCs separation are focused on the detection of CTCs via label-independent methods, low pre-treatment, large volume of sample processing in a short time, high purity, and possibility to propagate the isolated CTCs [40, 41].

16.2.1 Affinity-Based Methods

The affinity-based microfluidic devices are based on the use of specific antibodies attached on the channels walls to capture target cells. These devices have been developed as positive enrichment techniques when the antibodies are used to directly capture CTCs and negative enrichment techniques if antibodies are used to target blood cells. The first positive enrichment platforms were devices composed of series of posts functionalized with EpCAM antibodies as explained before [31]. Nevertheless, the cells follow the fluid streamlines of the laminar flow, which limit the interaction between the CTCs and the antibody modified surface. To overcome this, herringbone-like structures were proposed [35, 37, 42–44] that promotes fluid mixing in the channel, thus increasing particle-surface interaction. Figure 16.2 presents a representation of particles trajectories in a rectangular channel and in a channel with a herringbone structure. In Fig. 16.2a, the particles follow the fluid streamlines in a rectangular straight channel, while in Fig. 16.2b, the herringbone structure promotes a mixing, so the particles move transversally on the channel with more probability to reach the functionalized channel walls.

Different herringbone chips were studied for positive enrichment, including the surface functionalization with different antibodies (Fig. 16.4b) [46], specific for some cell lines. Some of them have two opposed surfaces with herringbone structures to increase the mixing [35, 37, 42, 44]. Moreover, to decrease the non-specific cell adherence, Wang et al. proposed a wavy herringbone structure [35]. However, one of the major disadvantages of this system is associated with the difficulty of eluding CTCs after being captured, this process could have an impact on their viability [34].

Recently, new methods have been developed for improving positive enrichment methods such as hydrogel microparticles (MP) functionalized with EpCAM antibodies, which have the advantages of water-like reactivity, biologically compatible materials, and synergy with various analysis platforms (Fig. 16.3) [35]. In this method the hydrogel particles are synthesized using degassed mold lithography (DML), as a result, the porosity and functionality of the MPs increase achieving an effective conjugation with antibodies [48]. In addition, the MPs functionalization is based on carbodiimide cross-link chemistry conjugated to antibodies through carboxyl groups. Also, NHS and EDC chemistry was used to covalently attach Neutravidin protein to the carboxyl groups. Finally, biotinylated anti-EpCAM

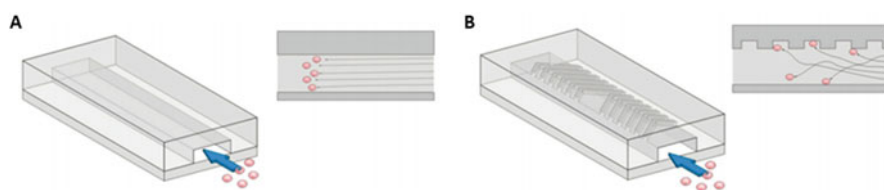


Fig. 16.2 Graphic representation of the particles trajectories in (a) traditional rectangular channel and in a (b) herringbone device. Figure from [42] Copyright 2010 National Academy of Sciences

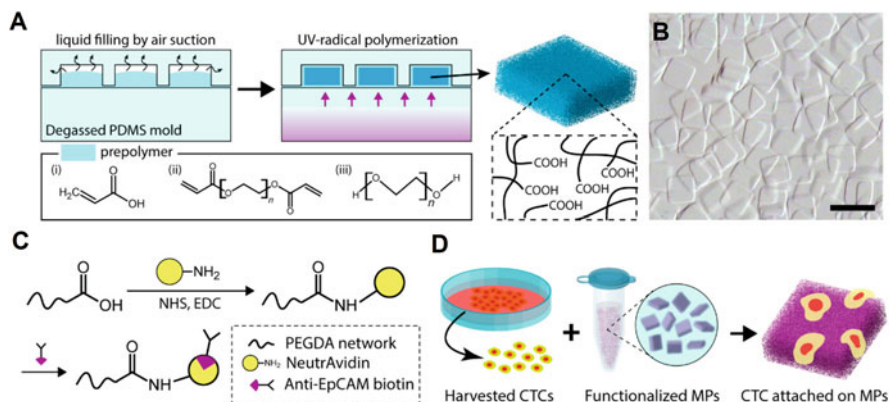


Fig. 16.3 Positive enrichment methods based on hydrogel microparticles (MP) and EpCAM antibodies. (a) Hydrogel microparticles synthesized by degassed mold Lithography (DML). Thus, UV-induced radical polymerization with prepolymers (i) acrylic acid (ii), polyethylene glycol diacrylate (PEGDA) and (iii) polyethylene glycol (PEG), hydrogel microparticles containing carboxyl groups are synthesized. (b) Image of polymerized hydrogel microparticles (MP). Scale bar 200 μm . (c) Interaction between avidin protein and biotin allows the anti-EpCAM–biotin conjugation. This principle is based on the reaction between carboxyl groups in the particles and primary amines in NeutraAvidin with the help of N-hydroxysuccinimide (NHS) and N-(3-dimethylaminopropyl)-N'-ethylcarbodiimide hydrochloride (EDC). (d) Circulating tumor cells (CTCs) captured by functionalized hydrogel microparticles with EpCAM antibody. **Licensed under CC-BY 4.0 International License. The final, published version of this article is available at [47]**

antibodies were used for avidin–biotin reaction [47]. Moreover, other methods based on Immunofunctionalized hydrogels have been successfully developed for capturing CTCs (Fig. 16.4c).

Other studies were focused on increasing the capture efficiency of CTCs, such as the GEDI chip [49]. In this case, the optimization was based on the displacement, size, and shape of microposts, as well as the use of a specific prostate antigen (PSMA). On the other hand, among the commercial methods available, CEETM microfluidic chip is characterized by randomly located microposts functionalized with streptavidin, which allow to capture targeted CTCs with biotinylated antibodies [50]. Meanwhile, The NanoVelcro CTC chip is composed of silicon (Fig. 16.4a) nanowire substrates (SiNWs) functionalized with EpCAM for CTCs capture [35, 51].

All the previous methods have a limitation, though. As mentioned before, not all CTC express a specific membrane marker. Potentially important CTCs subpopulations like mesenchymal and stem cell like CTCs would be missed [52]. Besides, the CTCs would need to be eluted after being captured, and this process might have an impact on the CTC viability [14, 24]. So that, affinity-based techniques based on negative enrichment were proposed.

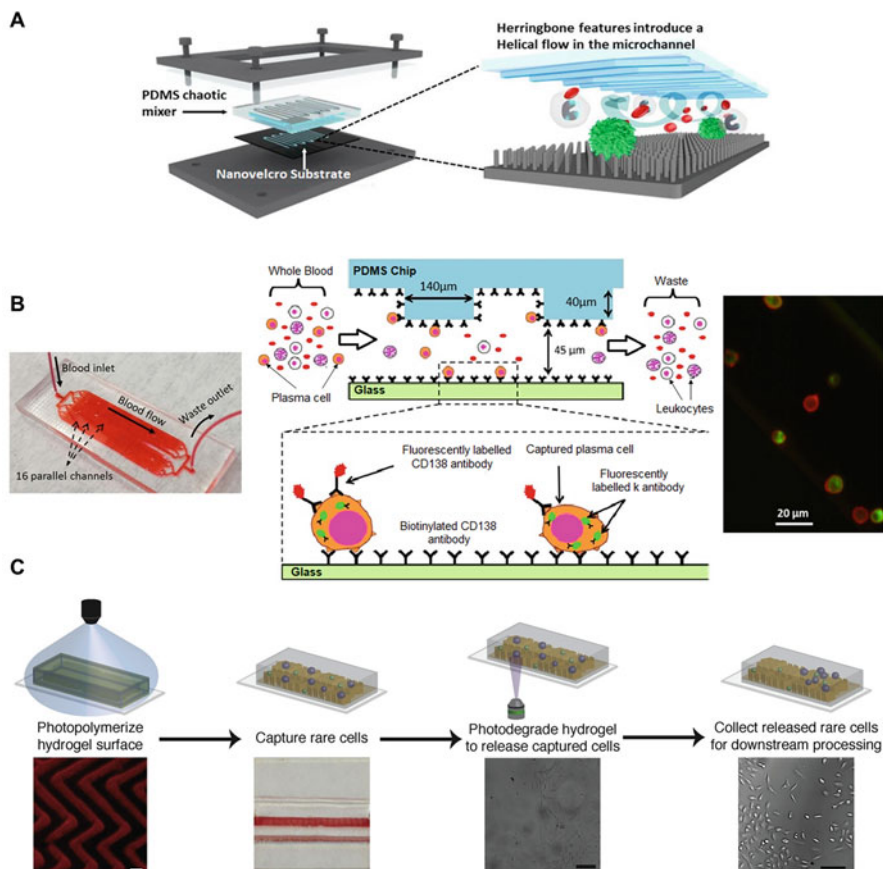


Fig. 16.4 (a) NanoVelcro CTC Chip is composed of a patterned silicon nanowire (SiNW) substrate and herringbone features which promote the helical flow in the microchannel improving the interaction between CTCs and anti-EpCAM coated SiNW substrate. **Licensed under Creative Commons Attribution 3.0 License (CC BY 3.0). The final, published version of this article is available at [45].** (b) Herringbone microfluidic device composed of 16 parallel microchannels for cells capture (left image). The center image is a Schematic representation for capture and analysis of plasma cells in microfluidic device. In this technology, the microchannels are coated with biotinylated CD138 antibodies, which capture the cells from the flow. Finally, capture cells are staining with anti- κ immunoglobulin for their identification. Fluorescence image shows the cells captured from a clinical sample. Red represents the CD138 and green anti- κ immunoglobulin (Right image). **Licensed under Creative Commons Attribution 3.0 License (CC BY 3.0). The final, published version of this article is available at [46].** (c) Schematic representation of fabrication and degradation of patterned photodegradable hydrogel films. Thus, a PDMS master is covered with hydrogel and irradiated at 405 nm light. Subsequently, a microfluidic herringbone channel is bonded on the top of the hydrogel film. The hydrogel can be degraded under flow condition using irradiation of 365 nm light. Finally, the CTCs can be collected for further processing [38]. **Copyright (2018), Elsevier**

Negative enrichment of CTCs is an affinity-based method that has the purpose of removing hematopoietic cells by targeting specific antigens that are not expressed by the CTCs as, for instance, CD45 (leukocyte common antigen) [53]. For example, CTC-iChip was developed by Ozkumur et al., which eliminate the blood cells based on physical properties and CD45/CD15 expression [54]. Hyun et al., proposed a herringbone device for negative enrichment by targeting of leukocytes with the surface immobilized with CD45 after the blood lysis or centrifugation for eliminating the erythrocytes [17]. Moreover, other technology known as the geometrically activated surface interaction (GASI) chip was fabricated, which was similar to the Herringbone chip but with microvortexing features aimed at increasing the number of captured leukocytes [54]. On the other hand, a novel work was reported by Fatih Sarioglu and colleagues, they developed a method for negative enrichment of CTCs using whole blood. This method is composed by 3D microfluidic device which captures the leukocytes based on immuno-enhanced microfiltration, also allows the depletion of erythrocytes, and remains the CTCs in suspension [55]. Overall, negative enrichment allows the capture of CTCs with low or no expression of EpCAM and the CTCs can be collected intact and viable for subsequently clinical analysis [56]. However, as the population of leukocytes in the sample is usually very high, even large depletion rates are not always ensuring good results concerning the purity of the sample. In addition, negative enrichment is used to capture the leukocytes after the blood sample has been already processed to eliminate the erythrocytes, so that, this methodology has the potential to be used to complement other techniques by enriching their results in terms of purity.

Recent evidence suggests, however, that the entire CD45+ population should not be considered as a discriminant for isolating CTCs from a population of leukocytes, due to some CTCs displaying expression levels of CD45 and some leukocytes subpopulation such as non-lymphocytes, which show low expression of CD45. To overcome the limitations of employing antibodies, aptamers have emerged as a potential alternative for the isolation of CTCs. These are single-stranded oligonucleotides such as RNA, DNA, or peptides that bind to targets such as proteins with a high specificity and sensitivity [50]. Moreover, it was also discovered that an *in vitro* process called “systematic evolution of ligands by exponential enrichment” (SELEX) allows the synthesis and selection of aptamers in a straightforward manner. In fact, the potential use of aptamers for isolating CTCs has been successfully evaluated with samples spiked with different cancer cell lines and in patients’ samples [57]. Based on the previous findings, the key advantage of using aptamers for the isolation of CTCs is that they can be prepared in different panels targeting several proteins expressed on available cancer cells, for which it is not necessary to know the precise targets [58, 59].

Finally, both negative and positive enrichment methods can be combined with magnetic-activated cell sorting. In this case, magnetic microbeads are coated with the antibodies and a magnetic field is used to attract the target cells bounded to the microbeads [29, 60]. However, these devices have limited throughput due to the time needed for the force to act on the particles [30].

16.2.2 Label-Free Methods

The devices discussed within the previous section have, as a main drawback, the fact that they rely on the expression of a certain biomarker present on the cell membrane. However, this condition is not always satisfied, and this might lead to a loss of CTCs and affect the performance of the device in terms of the recovery rate. As an alternative, several microfluidic devices have been proposed for the enrichment of CTCs from blood based exclusively on physical properties of the CTCs, such as size, density, mechanical plasticity, and dielectric properties [61]. Among these methods, the ones that have been more exploited are size-based methods [62, 63].

16.2.2.1 Size-Based Methods

This methodology considers the difference on size between CTCs, erythrocytes, and leukocytes. As was previously indicated, the diameter of CTCs usually ranges from 15 μm to 20 μm [18], erythrocytes are between 6 μm and 8 μm , meanwhile, the leukocytes go from 6 μm to 20 μm , where neutrophils represent between 40% and 75% with diameters that go from 10 μm to 12 μm [64]. Among size-based methods, one can basically find filters, in which the sample flow through an array of micro-scale constrictions and inertial microfluidic sorting devices, in which the cells are separated due to size-dependent inertial fluid forces.

Filtering Microfluidic Sorting Devices

Normally, these kinds of devices capture the CTCs as they are bigger in size, allowing to pass the other cellular components. Depending on the filtering principle, they can use either chromatography columns, pillars, or pores [65].

Chromatography is a classical technique for separating components of a mixture based on their ability to pass through a column with a porous material. This method is used for separating molecules in a label-free manner [65, 66]. In 2011, Hongshen Ma et al. used this principle, but in an opposite behavior for CTCs separation. Thus, dynamic microstructures have the advantages of filtration and hydrodynamic manipulation, wherewith is possible to discriminate cells based in size and deformability, meanwhile the cells are in a continuous flow [65].

On the other hand, an outstanding device designed in the low Reynolds number regime is known as deterministic lateral displacement (DLD) (Fig. 16.5a and b). In this technology, the smaller cells follow the streamlines and pass through a series of posts without net lateral displacement. Meanwhile, the bigger cells change to a different streamline when enter in contact with the pillars and are laterally moved from the original streamline [69]. The evidence from previous studies has shown the potential of this technology in separating cancer cells from blood with a performance of 80% [67]. In general, devices based on pillars use an array of microposts that form constrictions. Mohamed et al. developed a microfluidic device composed by pillars of four successively decreasing clearances from 20 μm to 5 μm (Fig. 16.5c) [65, 68].

On the other hand, technology based on pores consist of a membrane with holes which demonstrated a recovery rate higher than 85%. In fact, there are some commercial devices based on this principle, such as Rarecells[®], Screencell[®], and

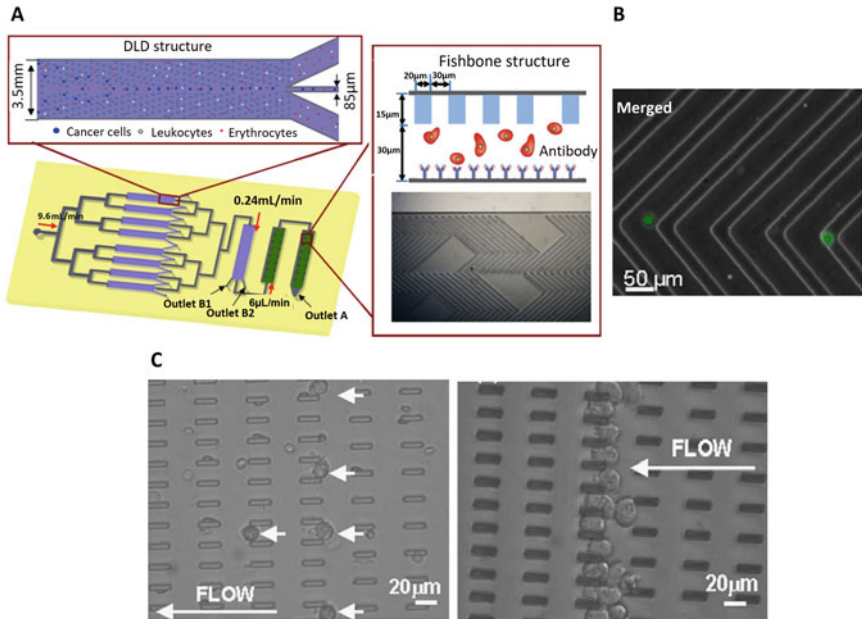


Fig. 16.5 (a) Microfluidic chip composed of a deterministic lateral displacement (DLD) channel with mirrored triangular micropost array. Thus, bigger cells like cancer cells and some leukocytes were concentrated in the middle of the channel, meanwhile the smaller cell such as the erythrocytes and most of the leukocytes follow the streamlines flow direction. Finally, the capture channel is a PDMS layer with herringbone structures modified with EpCAM. These structures promoting the capture of CTCs. **Copyright (2013), Elsevier [67].** (b) Fluorescent images of cancer cells captured on the chip surface. Cells were stained with Vybrant[®] DyeCycle[™] Green. **Copyright (2013), Elsevier [67].** (c) Microfluidic devices for cancer isolation based on cell size and deformability. The images show blood samples spiked with MDA231 cells, where all the blood cells flow freely through the device, but the MDA231 cells were retained between the gaps. **Copyright (2009), Elsevier [68]**

Clearcells[®] [32]. The principle of this technology is based on the force applied to the cells, which depends on the flow rate and is related with the deformability of the cells. Thus, the flow rates and the cross-section of the membrane constrictions are the key parameters that define the efficiency of this kind of devices. Nonetheless, the major disadvantage of this method is the clogging, when it is used with whole blood sample and as a result, the flow rate changes. The flow rate modification triggers a low throughput and change in the limit separation size. Moreover, these microfluidic technologies do not allow recover the CTCs from the membrane for further clinical analysis [65].

Inertial Microfluidic Devices

Among the systems proposed in the literature, microfluidic devices based on the inertial focusing are promising, which could overcome the limitations of other

methods that use pillars, pores, or labeling approaches with the advantage of achieving a high throughput [67]. Several studies have revealed that in a Reynolds number between stokes flow ($Re \ll 1$) and inviscid flow, namely, in a range from 1 to approximately 100, forces from inertial effects appear such as drag forces from Dean flows, shear gradient lift forces, and wall effect lift forces, which are balanced for achieving the size-based separation [30, 70].

Overall, the system can be described by the channel Reynolds number (Re) and the particles Reynolds number (Re_p) by the following equations, where ρ_f and μ are the fluid density and dynamic viscosity, U_m is the maximum fluid velocity in the channel, D_h represents the hydraulic diameter and a the particle diameter. In a rectangular channel $D_h = 2WH/(W + H)$, in which W is the channel width and H the channel height.

$$Re = \frac{\rho_f U_m D_h}{\mu} \quad (16.1)$$

$$Re_p = Re_c \frac{a^2}{D_h^2} = \frac{\rho_f U_m a^2}{\mu D_h} \quad (16.2)$$

In 2007, Di Carlo et al. published a pioneer work, in which the inertial focusing was used to control the particles position in microfluidics devices with curved channels according to the particles size. They demonstrated that particles did not follow the fluid streamlines but migrated across them as the inertial forces became significant. The particle's position in the microchannel was related to the particle's diameter [30].

Traditionally, the inertial lift forces and drag forces are orthogonally on a particle [71], but in a curved channel a secondary cross-sectional flow start to appear (Dean flows). Then, the Dean flow triggers the particles experience a drag force on the same axis as the shear gradient and the wall effect lift forces [30]. Hence, the balance between these forces cause different equilibrium positions of particles depending on their size. Thus, small particles follow the Dean flow while big particles are under a stronger lift force.

The Dean flow can be described by the Dean number through the Eq. (16.3), in which r is the radius of channel curvature [30, 72]. Moreover, inertial lift forces and drag forces can be calculated as indicate the Eqs. (16.4 and 16.5).

$$De = Re \sqrt{\frac{D_h}{2r}} \quad (16.3)$$

$$F_L = \frac{f_L(Re, x, \rho) \rho U_F^2 a_p^4}{D_h^2} \quad (16.4)$$

In Eq. (16.4) Re represents the channel Reynolds number, μ is the fluid dynamic viscosity, ρ is the fluid density, U_F is the average velocity of the fluid and a_p is the

particles diameter. Meanwhile, f_L is the lift coefficient that corresponds to a complex function of the Re and the cross-sectional positions of particles x_p .

As previously mentioned, Dean Drag Force can be expressed as Eq. (16.5). Where ρ is the fluid density, U_F is the average velocity of the fluid and a_p is the particles diameter. Meanwhile, D_h is the cross-sectional hydraulic diameter and R is the radius of the microchannel [71, 72].

$$F_D \propto \rho U_F^2 a_p D_h^2 / R \quad (16.5)$$

Up to now, several spiral devices have been reported for isolating CTCs from the blood applying inertial forces [36]. As explained before, the separation is based on the difference of size. Thus, the lift force is important for bigger cells like CTCs, meanwhile is not significant for smaller cells such as erythrocytes and small leukocytes. The blood cells mainly follow the Dean flow due to the Drag force, and do not focus on certain positions. Finally, by carefully designing the device geometry, the blood cells will leave the system using one device outlet, according to the Dean cycle and the CTCs are focused on another outlet [51], thus obtaining separation.

Some devices developed by previous researchers included a sheath flow inlet to initially confine the blood cells in one wall, so all of them can follow the Dean cycle [29, 36, 51, 55, 73]. Sun et al. proposed a double spiral device with 6 loops and alternation of the flow direction due to an S-turn. The device has 20 a low aspect ratio compared to other devices in the literature ($H/W = 0.167$) and present one inlet and three outlets [18]. Moreover, spiral design with a trapezoidal cross-section was also proposed to generate stronger Dean flow than in a traditional rectangular cross-section; this Device is composed of 3 loops and a recovery rate of 80% was obtained [29, 36]. Some years ago, devices with multiplexed setup were proposed to increase the throughput [29, 73], which are composed of 4 spirals in parallel that were stacked forming a multiplexed device with 40 spirals, reaching a throughput of ~ 500 mL/min. The system was tested for the separation of Chinese hamster ovary cells (CHO) and yeast [29]. Also, cascade microfluidic devices were proposed including the integration of more than one spiral [70, 74]. These technologies demonstrated a recovery rate between 80% and 90% and a throughput up to 2 mL/min [70]. Figure 16.6 represents different spiral microfluidic technologies.

16.2.2.2 Dielectrophoresis

The dielectrophoresis (DEP) represents a label-free, precise, and low-cost diagnostic method [78]. This method is based on the dielectric cell properties, due to the cells are electrically neutral but they can be polarized, which depends on their polarity and conductivity. Thus, when the cells are subjected to a non-uniform electric field, a dielectrophoretic force (FDEP) starts to appear, whose magnitude and direction depend on the dielectric properties of the cells, the medium, their size and shape, as well as the frequency of the electric field [78]. It has been reported two types of

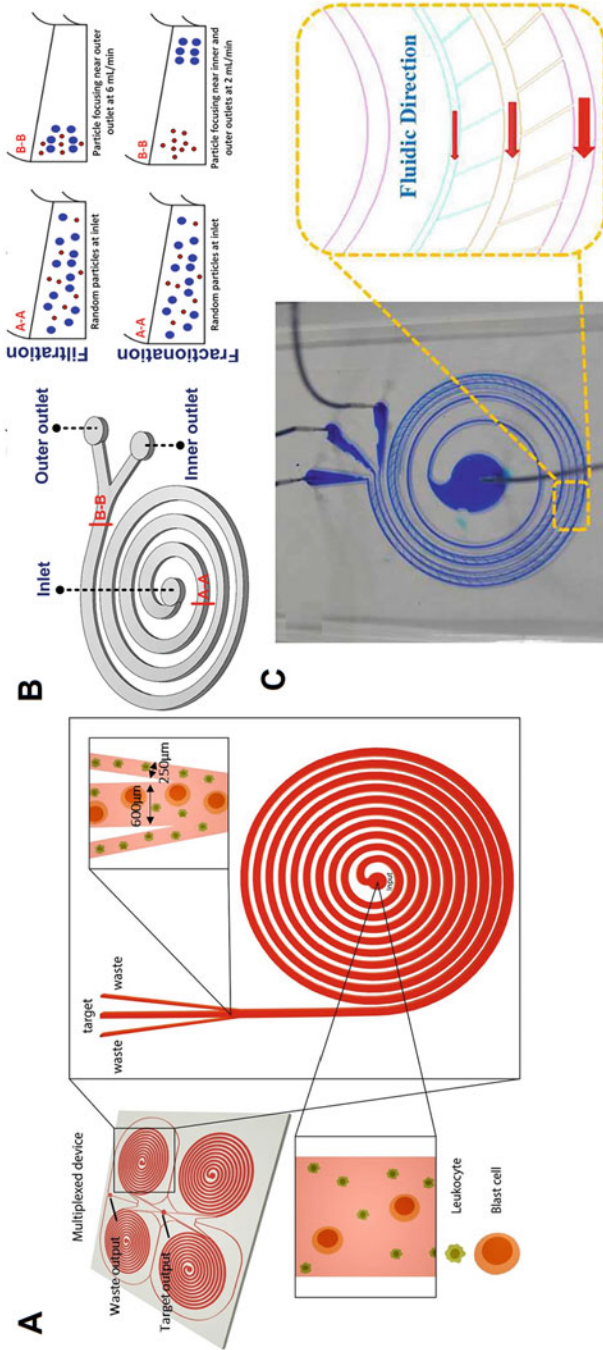


Fig. 16.6 (a) Multiplexed spiral device. The device is composed by four inputs in the middle of the sorting unit. The figure shows the CTCs outlet and waste outlets are indicated. **Licensed under CC BY 4.0 International License. The final, published version of this article is available at [75]** (b) Spiral microfluidic device with trapezoidal cross-section microchannels. The device has two modes: filtration and fractionation. In filtration mode, the particles suspended are trapped and focused near the outer wall under strong vortices. Meanwhile, in the fractionation mode, smaller particles (red) are trapped in Dean vortices and keep near the outer wall, but the bigger particles (blue) are focused near the inner wall. Thus, the particle separation by size is achieved. Basically, changing from one mode to other depends on the magnitude of the hydrodynamic forces inside the microchannels. **Licensed under CC BY 4.0 International License. The final, published version of this article is available at [76]** (c) Representation of triple-microchannel spiral microfluidic chip composed by slits for isolation of CTCs. The three microchannels are interconnected by arrays of slits, which allow that the cells pass from one main microchannel to other through the flow direction. **Licensed under CC BY 4.0 International License. The final, published version of this article is available at [77]**

FDEP, a positive dielectrophoresis (PDEP) which appears when the cell polarization is bigger than the medium. Thus, the cells move towards the strong electric field region. On the other hand, there is a negative dielectrophoresis (nDEP) that appears if the polarization of the cells is smaller than the medium and therefore the cells move in the opposite direction [79]. This method allows that cells can be differentiated depending on the polarizability [80].

Currently, microfluidic devices with electrodes embedded that produce the AC electric field have been developed (Fig. 16.7a and b). The benchtop device in the literature presents a recovery rate between 70% and 90% [83]. Alazzam et al. [84] demonstrated a yield of 95% by applying this methodology. The main drawback is the low throughput. Therefore, this methodology is used as a complement to the other ones, as the sized based methods. This has been explored by Moon et al. [85] who combines hydrodynamic focusing with dielectrophoresis and obtained 162-fold enrichment of the MCF-7 cells—CTCs cells model over RBCs at a 7.6 mL/h flow rate [86].

In contrast with traditional technologies reported, microfluidics-integrated separation method combined with ODEP (Optically Induced Dielectrophoresis) represent a novel strategy for complex cell manipulation, which involve suspension, transportation, collection, and purification of cancer cell. This method was validated with 8 mL of blood samples with H209 cancer cell clusters, as result an excellent recovery rate up to $91.5\% \pm 5.6\%$ was achieved [56].

16.3 Microfluidic-Based Detection of CTCs

In general, the CTC separation methods described so far have in common the absence of integrated detection of the isolated tumor cells into the microdevice. Most of the systems, to elucidate the presence of the CTCs, use fluorescent-labeled antibodies specifically attached to the CTC, and the fluorescence label is detected with an external microscope. However, some authors have gone one step further and have combined microfluidic isolation techniques with integrated sensors for CTCs analysis in situ. We have summarized here some representative examples using either electrical, optical, or chemical sensors.

Field effect transistors (FET) are semiconductor components with three terminals (gate (G), source (S) and drain (D)) [87]. One of the major challenges of using FETs as biosensors is achieving the immobilization of affinity reagents such as antibodies or aptamers on the open gates [88]. Furthermore, Yi-Hong Chen and their colleagues developed a microfluidic device composed by CTC-specific aptamers functionalized on a FET surface and it is composed of a dual-layer with two inlets and 14 individual trapping chambers. The chip was tested with human colon cancer cell lines (HCT-8), as a CTC model and blood samples were spiked with HCT-8 cells. As result, the device was able to capture a maximum of 42 from a total of 1000 cancer cells [52].

Some years ago, Pulikkathodia and colleagues developed a high electron mobility transistor (HEMT), which is composed of a multiplexed sensor integrated into a microfluidic channel to detect colorectal cancer cells (HTC-8) [42]. Besides, the rise

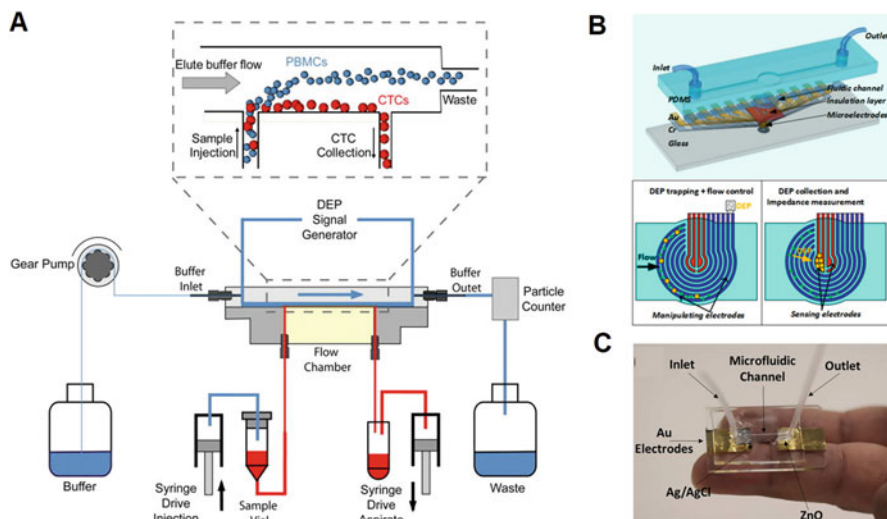


Fig. 16.7 (a) Schematic representation of ApoStream flow chamber. This device applies an AC electric field to the sample and is composed of electroplated copper and gold electrodes on the bottom part of the flow chamber. The sample was introduced into the flow chamber, and the cancer cells are collected in the other rectangular port. The principle of separation is based on the DEP forces, which pull the cancer cells through the bottom chamber and repel the other cells [80]. **Reprinted from, with the permission of AIP Publishing.** (b) Microfluidic device composed of electrodes, which allow the isolation of cancer cells due to the DEP effect and the difference in cell size. Thus the target cells were trapped onto the sensing electrodes. Finally, the impedance measurements allow to identify the presence of cancer cells. **Copyright (2018), Elsevier [81].** (c) Microfluidic pH Sensor for detection of cancer cells based on the measurements between a silver-silver chloride and zinc oxide electrodes for CTCs recognition in blood. The device detects the cancer cells based on changes of pH in the extracellular environment [82]. **Copyright © 2017, American Chemical Society**

of impedance spectroscopy represents an excellent tool for label-free characterization of cells, which provides information about electrical cell parameters [89]. Some devices were developed based on this principle, such as the microfluidic device with circular electrodes designed by Nguyen and Jen. This Device was validated with A549 lung CTCs and blood, which was able to discern between the two cell populations based on their different resistivity [87]. It is worth also mentioning that in 2014, Hywel Morgan and colleagues used a single-cell microfluidic impedance cytometry to determine the dielectric features of MCF-7 cells and discriminate them from leukocytes. Moreover, it was demonstrated that the combination of the impedance cytometry with magnetic beads conjugated with antibodies enables to detect very low amount of MCF-7 (~100 in 1 ml blood) [90].

To date, some optically read-out methods and their integration into microfluidic devices have been designed, which include reflectance spectroscopy, surface plasmon resonance, and evanescent wave sensing, among others. In 2012, Kumeria

and colleagues reported a microfluidic nanopore reflectometric interference spectroscopy (RIFS) device composed of microchannels and Anodic Aluminum Oxide (AAO) substrate modified with anti-EpCAM for detecting CTCs [91]. Thus, when the CTCs binding to the EpCAM antibody on AAO Surface, a wavelength shift in the Fabry-Perot interference fringe appears [91].

With respect to the chemical-based sensing devices, according to the study provided by Tzu-Keng Chiu et al., the metabolic performance of cancer cells as, for example, the production of lactic acid by CTCs represents a promising approach. This technology can count the cells by the formation of a micro-droplet and optical transduction of lactic acid for cell single detection. Unfortunately, the device cannot detect the presence of similar cells like leukocytes [92].

Finally, the metabolic change produced by the CTC that produces a reduction in the surrounding pH was also used as a method for differentiating cancer cell lines. The PH studies were performed by potentiometric methods with Ag/AgCl reference electrode and a ZnO working electrode. Nonetheless, the proposed device was not tested with blood samples (Fig. 16.7c) [82].

16.4 Conclusions

Microfluidic technologies have emerged as high-impact technologies in the field of circulating tumor cells isolation and detection, which represent a novel method for early cancer diagnosis, as well as an excellent tool for monitoring the disease evolution and treatment efficiency. There has been a great advance in the isolation and detection of circulating tumor cells using microfluidic devices within the past 15 years as they offer a high-throughput, compact, and economic alternative to the presently established methods. Many of the developed devices have indeed tried to overcome the limitations of commercial technologies such as CellSearch.

This chapter provided a compilation of literature related to the developed microfluidic technologies and the principles behind them for detection and separation of CTCs from others blood components. Also, it was defined the potential of introducing sensors, physical, chemical, and biological principles in the separation, detection, and analysis of CTCs through microfluidic devices.

With respect to the isolation of CTCs, many different methods have been proposed up to date, which we can classify into affinity-based methods, when a target molecule is used to capture the cells and label-free methods if the cells are sorted based on their physical characteristics without the need for labeling.

The affinity-based methods have the main drawback that they rely on a specific interaction between the microfluidic system walls and the cells membrane. However, this condition is not always satisfied and might lead to the miss of cancer cells and then affect the recovery rate. In addition, positive enrichment methods directly capture CTCs and so this result in not trustable cells for further analysis. Besides, affinity-based methods work better at low cell concentration, which is not the case for blood samples. Nevertheless, they have proved to be a good alternative to use as a

complementary method, after a previous purification to remove high cell contamination.

On the other hand, with respect to label-free methods, the devices based on lateral displacement and microfiltration are more prone to clogging, so they cannot process high volume of samples. The devices based on dielectrophoretic forces present very good selectivity, but they have low throughput due to the weak electrical forces compared to the hydrodynamic drag. Inertial microfluidic devices offer a good alternative that solves some of the previous limitations as they can deal with high cell concentration without clogging, have proven an excellent cell recovery and offer very high throughput. However, high sample concentration leads to increased cell-cell interaction, which lower the purity and the inherent overlapping in size between leukocytes and CTCs also lowers purity.

As an overall conclusion, we can therefore state that microfluidic lab-on-a-chip devices have the potential to make a breakthrough for the isolation and detection of CTCs from blood samples. Nevertheless, after a careful reviewing of the available literature, there is no device with the necessary standard for parameters like purity, recovery rate, throughput, and cell viability as it is needed for its use in clinical settings. A convenient strategy would probably be to prioritize a high (or full) cell recovery and a good quality of the isolated cells (viability) to have a representative population for further studies. Indeed, CTCs are very scarce, and we cannot afford to lose any information about the tumor.

Acknowledgments CIBER-BBN is an initiative funded by the VI National R&D&i Plan 2008–2011, Iniciativa Ingenio 2010, Consolider Program, CIBER Actions and financed by the Instituto de Salud Carlos III with assistance from the European Regional Development Fund. The Nanobioengineering group in the Institute of Bioengineering of Catalonia (IBEC) has support from the Commission for Universities and Research of the Department of Innovation, Universities, and Enterprise of the Generalitat de Catalunya (2017 SGR 1079) and is part of the CERCA Program/ Generalitat de Catalunya. This work is partially supported by Obra Social “La Caixa” project “Understanding and measuring mechanical tumor properties to improve cancer diagnosis, treatment, and survival: Application to liquid biopsies”.

References

1. Martins I et al (2021, Feb) Liquid biopsies: applications for cancer diagnosis and monitoring. *Genes* 12(3):349. <https://doi.org/10.3390/genes12030349>
2. Mattox AK, Bettegowda C, Zhou S, Papadopoulos N, Kinzler KW, Vogelstein B (2019, Aug) Applications of liquid biopsies for cancer. *Sci Transl Med* 11(507):eaay1984. <https://doi.org/10.1126/scitranslmed.aay1984>
3. Heitzer E, Ulz P, Geigl JB (2015, Jan) Circulating tumor DNA as a liquid biopsy for cancer. *Clin Chem* 61(1):112–123. <https://doi.org/10.1373/clinchem.2014.222679>
4. Xie F, Li P, Gong J, Tan H, Ma J (2018, May) Urinary cell-free DNA as a prognostic marker for KRAS-positive advanced-stage NSCLC. *Clin Transl Oncol* 20(5):591–598. <https://doi.org/10.1007/s12094-017-1754-7>
5. Michela B (2021, Jul) Liquid biopsy: a family of possible diagnostic tools. *Diagnostics* 11(8): 1391. <https://doi.org/10.3390/diagnostics11081391>
6. “25806217”

7. Guan X (2015, Sep) Cancer metastases: challenges and opportunities. *Acta Pharm Sin B* 5(5): 402–418. <https://doi.org/10.1016/j.apsb.2015.07.005>
8. Li S et al (2019, Apr) Shear stress promotes anoikis resistance of cancer cells via caveolin-1-dependent extrinsic and intrinsic apoptotic pathways. *J Cell Physiol* 234(4):3730–3743. <https://doi.org/10.1002/jcp.27149>
9. Qiu J et al (2020) Refining cancer management using integrated liquid biopsy. *Theranostics* 10(5):2374–2384. <https://doi.org/10.7150/thno.40677>
10. Chaffer CL, Weinberg RA (2011, Mar) A perspective on cancer cell metastasis. *Science* 331(6024):1559–1564. <https://doi.org/10.1126/science.1203543>
11. Aktas B, Tewes M, Fehm T, Hauch S, Kimmig R, Kasimir-Bauer S (2009, Aug) Stem cell and epithelial-mesenchymal transition markers are frequently overexpressed in circulating tumor cells of metastatic breast cancer patients. *Breast Cancer Res* 11(4):R46. <https://doi.org/10.1186/bcr2333>
12. Fabisiewicz A, Grzybowska E (2017, Jan) CTC clusters in cancer progression and metastasis. *Med Oncol* 34(1):12. <https://doi.org/10.1007/s12032-016-0875-0>
13. Geethadevi A, Parashar D, Bishop E, Pradeep S, Chaluvally-Raghavan P (2017, Dec) ERBB signaling in CTCs of ovarian cancer and glioblastoma. *Genes Cancer* 8(11–12):746–751. <https://doi.org/10.18632/genesandcancer.162>
14. Plaks V, Koopman CD, Werb Z (2013, Sep) Circulating tumor cells. *Science* 341(6151): 1186–1188. <https://doi.org/10.1126/science.1235226>
15. Woestemeier A et al (2020, Mar) Clinical relevance of circulating tumor cells in esophageal cancer detected by a combined MACS enrichment method. *Cancers* 12(3):718. <https://doi.org/10.3390/cancers12030718>
16. Gerlinger M et al (2012, Mar) Intratumor heterogeneity and branched evolution revealed by multiregion sequencing. *N Engl J Med* 366(10):883–892. <https://doi.org/10.1056/NEJMoa1113205>
17. Hyun K-A, Jung H-I (2014) Advances and critical concerns with the microfluidic enrichments of circulating tumor cells. *Lab Chip* 14(1):45–56. <https://doi.org/10.1039/C3LC50582K>
18. Sun J et al (2012) Double spiral microchannel for label-free tumor cell separation and enrichment. *Lab Chip* 12(20):3952. <https://doi.org/10.1039/c2lc40679a>
19. Menairini Silicon Biosystems. CellSearch - circulating tumor cell test. <https://www.cellsearchctc.com/>, 2022
20. Miller MC, van Doyle G, Terstappen LWMM (2010) Significance of circulating tumor cells detected by the cellsearch system in patients with metastatic breast colorectal and prostate cancer. *J Oncol* 2010:1–8. <https://doi.org/10.1155/2010/617421>
21. Eslami-S Z, Cortés-Hernández LE, Alix-Panabières C (2020, Aug) Epithelial cell adhesion molecule: an anchor to isolate clinically relevant circulating tumor cells. *Cell* 9(8):1836. <https://doi.org/10.3390/cells9081836>
22. Woo D, Yu M (2018, Nov) Circulating tumor cells as ‘liquid biopsies’ to understand cancer metastasis. *Transl Res* 201:128–135. <https://doi.org/10.1016/j.trsl.2018.07.003>
23. Mikolajczyk SD et al (2011) Detection of EpCAM-negative and cytokeratin-negative circulating tumor cells in peripheral blood. *J Oncol* 2011:1–10. <https://doi.org/10.1155/2011/252361>
24. de Wit S et al (2015, Dec) The detection of EpCAM+ and EpCAM– circulating tumor cells. *Sci Rep* 5(1):12270. <https://doi.org/10.1038/srep12270>
25. Gabriel MT, Calleja LR, Chalopin A, Ory B, Heymann D (2016, Apr) Circulating tumor cells: a review of non-EpCAM-based approaches for cell enrichment and isolation. *Clin Chem* 62(4): 571–581. <https://doi.org/10.1373/clinchem.2015.249706>
26. Krebs MG et al (2012, Feb) Analysis of circulating tumor cells in patients with non-small cell lung cancer using epithelial marker-dependent and -independent approaches. *J Thorac Oncol* 7(2):306–315. <https://doi.org/10.1097/JTO.0b013e31823c5c16>
27. Sajeesh P, Sen AK (2014, Jul) Particle separation and sorting in microfluidic devices: a review. *Microfluid Nanofluid* 17(1):1–52. <https://doi.org/10.1007/s10404-013-1291-9>

28. Mark D, Haeberle S, Roth G, von Stetten F, Zengerle R (2010) Microfluidic lab-on-a-chip platforms: requirements, characteristics and applications. *Chem Soc Rev* 39(3):1153. <https://doi.org/10.1039/b820557b>
29. Warkiani ME, Wu L, Tay AKP, Han J (2015, Dec) Large-volume microfluidic cell sorting for biomedical applications. *Annu Rev Biomed Eng* 17(1):1–34. <https://doi.org/10.1146/annurev-bioeng-071114-040818>
30. di Carlo D, Irimia D, Tompkins RG, Toner M (2007, Nov) Continuous inertial focusing, ordering, and separation of particles in microchannels. *Proc Natl Acad Sci* 104(48):18892–18897. <https://doi.org/10.1073/pnas.0704958104>
31. Nagrath S et al (2007, Dec) Isolation of rare circulating tumour cells in cancer patients by microchip technology. *Nature* 450(7173):1235–1239. <https://doi.org/10.1038/nature06385>
32. Vona G et al (2000, Jan) Isolation by size of epithelial tumor cells. *Am J Pathol* 156(1):57–63. [https://doi.org/10.1016/S0002-9440\(10\)64706-2](https://doi.org/10.1016/S0002-9440(10)64706-2)
33. Jiang X et al (2017) Microfluidic isolation of platelet-covered circulating tumor cells. *Lab Chip* 17(20):3498–3503. <https://doi.org/10.1039/C7LC00654C>
34. Lin Z, Luo G, Du W, Kong T, Liu C, Liu Z (2020, Mar) Recent advances in microfluidic platforms applied in cancer metastasis: circulating tumor cells' (CTCs) isolation and tumor-on-A-Chip. *Small* 16(9):1903899. <https://doi.org/10.1002/smll.201903899>
35. Wang S, Thomas A, Lee E, Yang S, Cheng X, Liu Y (2016) Highly efficient and selective isolation of rare tumor cells using a microfluidic chip with wavy-herringbone micro-patterned surfaces. *Analyst* 141(7):2228–2237. <https://doi.org/10.1039/C6AN00236F>
36. Al-Faqheri W, Thio THG, Qasaimeh MA, Dietzel A, Madou M, Al-Halhouli A (2017, Jun) Particle/cell separation on microfluidic platforms based on centrifugation effect: a review. *Microfluid Nanofluid* 21(6):102. <https://doi.org/10.1007/s10404-017-1933-4>
37. Xue P, Zhang L, Guo J, Xu Z, Kang Y (2016, Dec) Isolation and retrieval of circulating tumor cells on a microchip with double parallel layers of herringbone structure. *Microfluid Nanofluid* 20(12):169. <https://doi.org/10.1007/s10404-016-1834-y>
38. LeValley PJ et al (2019, Feb) Immunofunctional photodegradable poly(ethylene glycol) hydrogel surfaces for the capture and release of rare cells. *Colloids Surf B: Biointerfaces* 174:483–492. <https://doi.org/10.1016/j.colsurfb.2018.11.049>
39. Zhang X, Ju S, Wang X, Cong H (2019, Aug) Advances in liquid biopsy using circulating tumor cells and circulating cell-free tumor DNA for detection and monitoring of breast cancer. *Clin Exp Med* 19(3):271–279. <https://doi.org/10.1007/s10238-019-00563-w>
40. Zhou J, Kulasinghe A, Bogseth A, O'Byrne K, Punyadeera C, Papautsky I (2019, Dec) Isolation of circulating tumor cells in non-small-cell-lung-cancer patients using a multi-flow microfluidic channel. *Microsyst Nanoeng* 5(1):8. <https://doi.org/10.1038/s41378-019-0045-6>
41. Kulasinghe A et al (2017, Mar) Enrichment of circulating head and neck tumour cells using spiral microfluidic technology. *Sci Rep* 7(1):42517. <https://doi.org/10.1038/srep42517>
42. Stott SL et al (2010, Oct) Isolation of circulating tumor cells using a microvortex-generating herringbone-chip. *Proc Natl Acad Sci* 107(43):18392–18397. <https://doi.org/10.1073/pnas.1012539107>
43. Xue P et al (2014, Mar) Isolation and elution of Hep3B circulating tumor cells using a dual-functional herringbone chip. *Microfluid Nanofluid* 16(3):605–612. <https://doi.org/10.1007/s10404-013-1250-5>
44. Xue P, Wu Y, Guo J, Kang Y (2015, Apr) Highly efficient capture and harvest of circulating tumor cells on a microfluidic chip integrated with herringbone and micropost arrays. *Biomed Microdevices* 17(2):39. <https://doi.org/10.1007/s10544-015-9945-x>
45. He W et al (2016, Mar) Detecting ALK-rearrangement of CTC enriched by nanovelcro chip in advanced NSCLC patients. *Oncotarget*. <https://doi.org/10.18632/oncotarget.8305>
46. Qasaimeh MA et al (2017, May) Isolation of circulating plasma cells in multiple myeloma using CD138 antibody-based capture in a microfluidic device. *Sci Rep* 7(1):45681. <https://doi.org/10.1038/srep45681>

47. Lee NJ et al (2020, Jan) Affinity-enhanced CTC-capturing hydrogel microparticles fabricated by degassed Mold lithography. *J Clin Med* 9(2):301. <https://doi.org/10.3390/jcm9020301>
48. Kim HU, Lim YJ, Lee HJ, Lee NJ, Bong KW (2020) Degassed micromolding lithography for rapid fabrication of anisotropic hydrogel microparticles with high-resolution and high uniformity. *Lab Chip* 20(1):74–83. <https://doi.org/10.1039/C9LC00828D>
49. Gleghorn JP et al (2010) Capture of circulating tumor cells from whole blood of prostate cancer patients using geometrically enhanced differential immunocapture (GEDI) and a prostate-specific antibody. *Lab Chip* 10(1):27–29. <https://doi.org/10.1039/B917959C>
50. Turetta M et al (2018, Dec) Emerging Technologies for Cancer Research: towards personalized medicine with microfluidic platforms and 3D tumor models. *Curr Med Chem* 25(35): 4616–4637. <https://doi.org/10.2174/0929867325666180605122633>
51. Hou S et al (2013, Mar) Polymer nanofiber-embedded microchips for detection, isolation, and molecular analysis of single circulating melanoma cells. *Angew Chem Int Ed* 52(12): 3379–3383. <https://doi.org/10.1002/anie.201208452>
52. Yu M et al (2013, Feb) Circulating breast tumor cells exhibit dynamic changes in epithelial and mesenchymal composition. *Science* 339(6119):580–584. <https://doi.org/10.1126/science.1228522>
53. Ferreira MM, Ramani VC, Jeffrey SS (2016, Mar) Circulating tumor cell technologies. *Mol Oncol* 10(3):374–394. <https://doi.org/10.1016/j.molonc.2016.01.007>
54. Ozkumur E et al (2013, Apr) Inertial focusing for tumor antigen-dependent and -independent sorting of rare circulating tumor cells. *Sci Transl Med* 5(179):179ra147. <https://doi.org/10.1126/scitranslmed.3005616>
55. Guglielmi R et al (2020, Dec) Technical validation of a new microfluidic device for enrichment of CTCs from large volumes of blood by using buffy coats to mimic diagnostic leukapheresis products. *Sci Rep* 10(1):20312. <https://doi.org/10.1038/s41598-020-77227-3>
56. Hyun K-A, Lee TY, Jung H-I (2013, May) Negative enrichment of circulating tumor cells using a geometrically activated surface interaction Chip. *Anal Chem* 85(9):4439–4445. <https://doi.org/10.1021/ac3037766>
57. Zhao Z, Xu L, Shi X, Tan W, Fang X, Shangguan D (2009) Recognition of subtype non-small cell lung cancer by DNA aptamers selected from living cells. *Analyst* 134(9):1808. <https://doi.org/10.1039/b904476k>
58. Song Y et al (2013, Apr) Selection of DNA aptamers against epithelial cell adhesion molecule for cancer cell imaging and circulating tumor cell capture. *Anal Chem* 85(8):4141–4149. <https://doi.org/10.1021/ac400366b>
59. Racila E et al (1998, Apr) Detection and characterization of carcinoma cells in the blood. *Proc Natl Acad Sci* 95(8):4589–4594. <https://doi.org/10.1073/pnas.95.8.4589>
60. Mishima Y et al (2017, Apr) The mutational landscape of circulating tumor cells in multiple myeloma. *Cell Rep* 19(1):218–224. <https://doi.org/10.1016/j.celrep.2017.03.025>
61. Esmailsabzali H, Beischlag TV, Cox ME, Parameswaran AM, Park EJ (2013, Nov) Detection and isolation of circulating tumor cells: principles and methods. *Biotechnol Adv* 31(7): 1063–1084. <https://doi.org/10.1016/j.biotechadv.2013.08.016>
62. Burger R, Ducrée J (2012, May) Handling and analysis of cells and bioparticles on centrifugal microfluidic platforms. *Expert Rev Mol Diagn* 12(4):407–421. <https://doi.org/10.1586/erm.12.28>
63. Warkiani ME et al (2016, Jan) Ultra-fast, label-free isolation of circulating tumor cells from blood using spiral microfluidics. *Nat Protoc* 11(1):134–148. <https://doi.org/10.1038/nprot.2016.003>
64. Smerage JB, Hayes DF (2006, Jan) The measurement and therapeutic implications of circulating tumour cells in breast cancer. *Br J Cancer* 94(1):8–12. <https://doi.org/10.1038/sj.bjc.6602871>
65. Jin C et al (2014) Technologies for label-free separation of circulating tumor cells: from historical foundations to recent developments. *Lab Chip* 14(1):32–44. <https://doi.org/10.1039/C3LC50625H>

66. Gerhardt T, Woo S, Ma H (2011) Chromatographic behaviour of single cells in a microchannel with dynamic geometry. *Lab Chip* 11(16):2731. <https://doi.org/10.1039/c1lc20092e>
67. Liu Z et al (2013, Sep) High throughput capture of circulating tumor cells using an integrated microfluidic system. *Biosens Bioelectron* 47:113–119. <https://doi.org/10.1016/j.bios.2013.03.017>
68. Mohamed H, Murray M, Turner JN, Caggana M (2009, Nov) Isolation of tumor cells using size and deformation. *J Chromatogr A* 1216(47):8289–8295. <https://doi.org/10.1016/j.chroma.2009.05.036>
69. Inglis DW (2009, Jan) Efficient microfluidic particle separation arrays. *Appl Phys Lett* 94(1):013510. <https://doi.org/10.1063/1.3068750>
70. Zhang Z, Ramnath N, Nagrath S (2015, Sep) Current status of CTCs as liquid biopsy in lung cancer and future directions. *Front Oncol* 5:209. <https://doi.org/10.3389/fonc.2015.00209>
71. Amini H, Lee W, di Carlo D (2014) Inertial microfluidic physics. *Lab Chip* 14(15):2739. <https://doi.org/10.1039/c4lc00128a>
72. di Carlo D (2009) Inertial microfluidics. *Lab Chip* 9(21):3038. <https://doi.org/10.1039/b912547g>
73. Warkiani ME et al (2014) Slanted spiral microfluidics for the ultra-fast, label-free isolation of circulating tumor cells. *Lab Chip* 14(1):128–137. <https://doi.org/10.1039/C3LC50617G>
74. Abdulla A, Liu W, Gholamipour-Shirazi A, Sun J, Ding X (2018, Apr) High-throughput isolation of circulating tumor cells using cascaded inertial focusing microfluidic channel. *Anal Chem* 90(7):4397–4405. <https://doi.org/10.1021/acs.analchem.7b04210>
75. Khoo BL, Shang M, Ng CH, Lim CT, Chng WJ, Han J (2019, Dec) Liquid biopsy for minimal residual disease detection in leukemia using a portable blast cell biochip. *NPJ Precis Oncol* 3(1):30. <https://doi.org/10.1038/s41698-019-0102-5>
76. Warkiani ME, Tay AKP, Guan G, Han J (2015, Sep) Membrane-less microfiltration using inertial microfluidics. *Sci Rep* 5(1):11018. <https://doi.org/10.1038/srep11018>
77. Chen H (2018, Dec) A triplet parallelizing spiral microfluidic Chip for continuous separation of tumor cells. *Sci Rep* 8(1):4042. <https://doi.org/10.1038/s41598-018-22348-z>
78. Gascoyne PRC, Wang X-B, Huang Y, Becker FF (1997, May) Dielectrophoretic separation of cancer cells from blood. *IEEE Trans Ind Appl* 33(3):670–678. <https://doi.org/10.1109/28.585856>
79. Lee D, Hwang B, Kim B (2016, Dec) The potential of a dielectrophoresis activated cell sorter (DACS) as a next generation cell sorter. *Micro Nano Syst Lett* 4(1):2. <https://doi.org/10.1186/s40486-016-0028-4>
80. Gupta V et al (2012, Jun) ApoStream™, a new dielectrophoretic device for antibody independent isolation and recovery of viable cancer cells from blood. *Biomicrofluidics* 6(2):024133. <https://doi.org/10.1063/1.4731647>
81. Nguyen N-V, Jen C-P (2018, Dec) Impedance detection integrated with dielectrophoresis enrichment platform for lung circulating tumor cells in a microfluidic channel. *Biosens Bioelectron* 121:10–18. <https://doi.org/10.1016/j.bios.2018.08.059>
82. Mani GK, Morohoshi M, Yasoda Y, Yokoyama S, Kimura H, Tsuchiya K (2017, Feb) ZnO-based microfluidic pH sensor: a versatile approach for quick recognition of circulating tumor cells in blood. *ACS Appl Mater Interfaces* 9(6):5193–5203. <https://doi.org/10.1021/acsami.6b16261>
83. Low WS, Wan Abas WAB (2015) Benchtop technologies for circulating tumor cells separation based on biophysical properties. *Biomed Res Int* 2015:1–22. <https://doi.org/10.1155/2015/239362>
84. Alazzam A, Stiharu I, Bhat R, Meguerditchian A-N (2011, Jun) Interdigitated comb-like electrodes for continuous separation of malignant cells from blood using dielectrophoresis. *Electrophoresis* 32(11):1327–1336. <https://doi.org/10.1002/elps.201000625>
85. Moon H-S et al (2011) Continuous separation of breast cancer cells from blood samples using multi-orifice flow fractionation (MOFF) and dielectrophoresis (DEP). *Lab Chip* 11(6):1118. <https://doi.org/10.1039/c0lc00345j>
86. Liao C-J et al (2018, Oct) An optically induced Dielectrophoresis (ODEP)-based microfluidic system for the isolation of high-purity CD45neg/EpCAMneg cells from the blood samples of

- cancer patients—demonstration and initial exploration of the clinical significance of these cells. *Micromachines* 9(11):563. <https://doi.org/10.3390/mi9110563>
87. Tietze U, Schenk C, Gamm E (2008) Field effect transistor. In: *Electronic circuits*. Springer, Berlin, Heidelberg, pp 169–268. https://doi.org/10.1007/978-3-540-78655-9_3
88. Han K-H, Han A, Frazier AB (2006, Apr) Microsystems for isolation and electrophysiological analysis of breast cancer cells from blood. *Biosens Bioelectron* 21(10):1907–1914. <https://doi.org/10.1016/j.bios.2006.01.024>
89. Gu W, Zhao Y (2010, Nov) Cellular electrical impedance spectroscopy: an emerging technology of microscale biosensors. *Expert Rev Med Devices* 7(6):767–779. <https://doi.org/10.1586/erd.10.47>
90. Spencer D, Hollis V, Morgan H (2014, Nov) Microfluidic impedance cytometry of tumour cells in blood. *Biomicrofluidics* 8(6):064124. <https://doi.org/10.1063/1.4904405>
91. Kumeria T, Kurkuri MD, Diener KR, Parkinson L, Losic D (2012, May) Label-free reflectometric interference microchip biosensor based on nanoporous alumina for detection of circulating tumour cells. *Biosens Bioelectron* 35(1):167–173. <https://doi.org/10.1016/j.bios.2012.02.038>
92. Chiu T-K, Lei K-F, Hsieh C-H, Hsiao H-B, Wang H-M, Wu M-H (2015, Mar) Development of a microfluidic-based optical sensing device for label-free detection of circulating tumor cells (CTCs) through their lactic acid metabolism. *Sensors* 15(3):6789–6806. <https://doi.org/10.3390/s150306789>



Evolution in Automatized Detection of Cells: Advances in Magnetic Microcytometers for Cancer Cells

17

Alexandre Chícharo, Diogo Miguel Caetano, Susana Cardoso, and Paulo Freitas

Abstract

Flow cytometers are well-established tools with fundamental importance in biology and medicine to examine and identify cell populations, density, size distributions, compositions, and disease diagnosis and monitoring. Still, these devices are expensive with a low level of integration for sample preparation. Miniaturized microfluidic cytometers, i.e., microcytometers, for monitoring cells in a wide range of biological samples are currently being developed, providing more affordable and integrated solutions. Several detection methods have been developed and applied in microcytometers such as electrical, optical, and magnetic sensing techniques, which are integrated with microfluidic technology. Magnetic microcytometers present several advantages when compared to optical systems such as the fact that these devices provide more stable labeling by using magnetic nanoparticles (MNPs) or beads (MBs) instead of fluorophores. In this chapter, we explore the evolution of the automation of whole cell detection and enumeration that led to the development of microcytometers and particularly examine the anatomy of magnetic microcytometers applied to cancer research. We then give an overview of the challenges of Circulating Tumor Cells

A. Chícharo (✉)

International Iberian Nanotechnology Laboratory, Braga, Portugal
e-mail: alexandre.chicharo@inl.int

D. M. Caetano · S. Cardoso

Instituto de Engenharia de Sistemas e Computadores – Microsistemas e Nanotecnologias, INESC-MN, Lisbon, Portugal

P. Freitas

International Iberian Nanotechnology Laboratory, Braga, Portugal

Instituto de Engenharia de Sistemas e Computadores – Microsistemas e Nanotecnologias, INESC-MN, Lisbon, Portugal

© The Author(s), under exclusive license to Springer Nature Switzerland AG 2022

413

D. Caballero et al. (eds.), *Microfluidics and Biosensors in Cancer Research*,

Advances in Experimental Medicine and Biology 1379,

https://doi.org/10.1007/978-3-031-04039-9_17

enrichment and enumeration, and the progress of magnetic microcytometers in this field.

Keywords

Magnetic sensors · Microfluidics · Magnetic Nanoparticles · Microcytometers · Circulating Tumor Cells

17.1 Introduction

Cell enumeration has shown its huge impact on the extensive areas of biological sciences [1]: from the food industry to clinical diagnostics. In this fast-growing era of cells as biomarkers [2, 3], a variety of techniques have been developed in the past decades to enumerate and classify single cells. Cells can be identified by the proteins expressed on their surface membrane for instance which comprise approximately 30% of total human proteins [4]. Therefore cell counting and the proteins expressed on their membrane serve as valuable prognostic and predictive biomarkers in many diseases [5], e.g. the enumeration of cancer cells.

Succeeding several approaches for manual cell counting, current innovations led to the development of automatic cell counters based on numerous sensing methods. These new automatized methods were the consequence of technological advances in new materials, fabrication techniques and new sensory techniques. The current gold standard device for single-cell analysis at high throughput is the well-established optical flow cytometers. Today, these prominent tools have a imperative impact on modern biology and medicine. They are extensively used daily to examine and identify cell populations, density, size distributions, compositions, and, monitoring of diseases [5, 6]. Still, these benchtop devices are expensive, require operation specialists and present low levels of integration for sample preparation [7]. This limits its application in challenging cases of complex specimens such as on the enumeration of Circulating Tumor Cells (CTCs) from blood patient samples [8].

Flow cytometers are nowadays being miniaturized on more compact equipment, also called microcytometers [9]. The microcytometers combine microfluidics and innovative sensing techniques to detect single cells. Compared with the classic, large-scale flow cytometers, microcytometers provide a more affordable alternative and present the opportunity of being integrated as point-of-care (POC) devices [7, 10]. Several detection methods have been developed and applied in microcytometers, such as electrical detection [11], photodiodes [10, 12], surface-enhanced Raman spectroscopy (SERS) [13], and magnetic sensing techniques [14, 15].

Magnetic microcytometers have paved the way in this field and more, allowing selective cell biomarkers detection and enumeration in complex specimens. Magnetic microcytometers, are generally developed by solid-state processes and are integrated with microfluidic channels to present the cells one-by-one closely to the sensor [14, 16]. The magnetic detection is performed locally without the need of

integrating complex equipment, such as micro-lenses used in optical approaches and provide ultra-fast detection. Furthermore, magnetic microcytometers present some advantages when compared to optical systems such as the fact that these devices rely on a more stable labeling by using magnetic nanoparticles (MNPs) or beads (MBs) instead of fluorophores, which may suffer from photobleaching. Moreover, the use of magnetic labels enables magnetic cell separation and pre-concentration [17, 18] which is a very useful technique in some applications.

In the next sections, we present the importance of cell counting, its significance in many biology fields, and describe a general historical evolution of cell counting and cell labeling methods employed to discriminate cells. We overview the progress of automated cell counters in the cancer research, and highlight a particular type of these microcytometers: the magnetic microcytometer.

17.2 Whole Cell Enumeration Techniques: From Manual to Automatized to Miniaturized

17.2.1 Manual Cell Detection Techniques

The invention of the microscope led to the discovery and investigation of the most basic life unit, the cell [19]. With the development of better microscopes and new techniques to quantify these microorganisms, cell counting was performed manually and became important in biological sciences [20], for cell culturing and fundamental research, such as the monitoring of environmental microorganisms, viability studies in toxicity and drug development, and, in-process controls on industrial bioprocesses.

The hemocytometer or Neubauer chamber was designed in the nineteenth century to estimate blood cells under a microscope [20] and has been widely used globally until today. The concentration of cells in a suspension can be calculated by counting the number of cells in a known volume. Though, the lowest limit for accurate counting of cells using a hemocytometer is usually considered to be 2.5×10^5 /mL. To help discern different types of cells, the first labeling methods were developed, which improved the cell counting systems, e.g. to distinguish between live and dead cells. These stain labeling techniques consisted on the incorporation of coloring dyes by the porous membrane of cells, such as Trypan blue, neutral red [21], Turk solution [22], and Luciferase [23]. These labeling methods become a routine technique to differentiate and quantify cells to the present-day.

One of the major breakthroughs in microscopy and cell enumeration was the fluorescent labeling together with the development of fluorescence microscopes in the early twentieth century [24]. By substituting the white transmitted light in microscopes with UV-light and treating living organisms with fluorescent substances, cells were able to emit light and microscopes become much more complex equipments [24]. Examples of initial fluorescence dyes are nucleic acid stains, calcein, and other esterases. In the 1940s, fluorescent antibody labeling was developed [25], making way to an ever-growing number of methodologies to

differentiate cell populations and different compartments within cells. Microscopes' evolved to increase image contrast and spatial resolution and were coupled to computers and image processing techniques. Some examples of modern microscopes specialized in cells imaging include laser scanning confocal microscopy, two-photon microscopy, scanning disk confocal microscopy, total internal reflection, and super-resolution microscopy [25]. All these technological advances led to devices able to manually identify, count and differentiate cells more easily. Further on, in the next sections, the automatization of cell counting using optical methods is described in more detail.

17.2.2 Automatized Cell Detection Methods

While cell counting with manual microscopic techniques is a time-demanding process, subject to poor reproducibility and inter-observer variability, automated cell analyzers have raised great interest. Benchtop and portable devices have been developed for the automatic counting of cells such as analyzing digital images obtained by microscopy, flow cytometer that detect cells flowing in a capillary tube, and, the coulter counter method, that detects electric changes when cells flow through a small aperture.

With the access to computers, in the 1980s, and image processing techniques led to automated cell counting based on high-quality microscopy images through photographs of all or a portion of the cells and using statistical classification algorithms [20, 26, 27]. A large range of image classification techniques arose according to the microscopy technique and labeling used in the image capture: bright-field, bioluminescence, fluorescence, etc. Nowadays this method is easy to implement also using microfluidic channels that trap cells for instance [28, 29] but also using other image capturing equipment such as smartphones, or digital cameras [26, 30]. Common drawbacks include complex algorithms [31], lack of image capture reproducibility due to light exposure and focus, manual adjustment of algorithm parameters [20], and more importantly, the low throughput for diluted or low concentrated samples.

With the invention of the photodiode, a new method was developed by detecting cells in flow rather than static images and that could analyze large volumes: the flow cytometer. The first concept in flow cytometry was demonstrated by coupling a laser beam and a method for aligning and moving the cells towards a detection region, and successfully demonstrated the first use of fluorescence-based flow cytometry [5]. These fluorescence labels [32] enabled the identification of many types of cells by deconvolution algorithms. Indeed, high-throughput automated blood cells' counting became a reality where thousands of cells are detected per second, one by one, through a laser beam [33]. Later on, another technique, the image-based flow cytometry [34], combines the high-throughput of flow cytometry and capability of attaining high-speed microscopic imaging of each detected cell. The flow cytometer field will remain vigorous with the ever-growing evolving features [6], however, some drawbacks are well-known, such as the size of bulky devices (generally

restricted to centralized laboratories), very high cost to purchase and maintenance, the prerequisite of specialized personnel to operate the equipment, and, the manual sample preparation and labeling [6]. For these reasons, they are rarely used for general cell counting applications but then to obtain qualitative and quantitative analysis on the proportions of cell populations in complex samples.

In contrast to optical approaches, another method for cell detection and counting can be performed by the cells' intrinsic electric properties. The Coulter effect [5, 35] is based on the changes in the electrical-impedance when cells flow through an aperture and an electric current is applied. Cells are detected with current drops as they are poor electrical conductors and their size can be discriminated by the measured signal [5]. Coulter counters rapidly became standard apparatus in cell counting leveraging from a label-free technique and considerable cheaper than flow cytometers [36]. Though, the specificity in these devices is decreased, unable to differentiate live from dead cells and cells that form clusters, thus limiting its application for complex specimens.

17.2.3 Miniaturized and Automatized Cell Detection Methods: Microcytometers

In the past two decades, the integration and miniaturization of devices were made possible with the advances in materials, microfluidics, optics, electronics, and computers. The demand to deliver miniaturized less expensive devices for specific cell enumeration has been the main motivation of these developments. Further on, these miniaturized system facilitates the integration of automated sample preparation which could be used for POC home testing or by unspecialized personnel in low-resource areas [5]. Additionally, these devices can bypass clogging issues experienced in benchtop flow cytometry, by making microfluidic cartridges disposable and quickly replaceable fluidic modules [12]. Sample preparation can be simplified and integrated by the use of other microfluidic devices, such as the ones presented in the context of CTCs, explored further in this chapter (section 17.4.).

Contrary to standard fluorescent-based flow cytometers, microcytometers were developed using a panoply of sensing methods, such as optical, electrical-impedance, and magnetic approaches. In this section, we present an overview of each of these techniques in microcytometers, how the diferent detection strategy were designed and what type or if a labeling step was employed.

1. Optical microcytometers

The same level of cell information of benchtop flow cytometers or more is compulsory in optical microcytometers. Thus several components such as optical fibers and lenses need to be incorporated into these miniaturized systems. Examples of additional optical components are waveguides [37], in-plane lenses [38], beam stops and apertures to suppress stray light, diffractive elements such as prisms and gratings, optical filters, and power dividers [7, 12, 37]. Typical optical

microcytometers tend to mimic benchtop flow cytometers but also improve in the finer detection strategies such as adding two photodiodes for the cell detection [39], which could also be used to discriminate mechanical cell properties. Other label-free approaches were proposed that employ distinctive optical detectors such as photonic crystals [40], allowing the recognition of different blood cells and information on the cell shape and size.

Label-free methods are very advantageous in cell detection, as they do not require labeling protocols or sample manipulation. They are particularly useful for cell specimens with low complexity, such as *in vitro* cell cultures. For more complex cell samples, careful labeling strategies are employed, allowing discrimination of different subpopulations. Examples of labeling methods to detect cells using optical approaches are fluorescence [12, 41–44], optical scattering [38], and surface-enhanced Raman spectroscopy (SERS) [45].

The most common approach in optical microcytometers is through multicolor fluorescence detection. This allows cell recognition through fluorescent-tagged antibodies that target specific membrane molecules of cells. Such a procedure is capable of distinguishing morphologically identical cells and of classifying them according to their biological function [46]. Detection of cells flowing in a microchannel mounted on top of a microscope was also performed using fluorescence, in addition to multi-parametric information like bright-field, and dark-field [47]. Additionally, this study showed high-throughput discrimination of cell cycle phases of cells in large cellular populations specimens [47]. Other works [41, 44] measure fluorescence and scattering through fiber optics integrated into microfluidics to detect particles and cells. These systems were developed with two pairs of fiber optics (excitation and reception) to redundantly identify positive CTCs by the simultaneous identification of signal belonging to two membrane receptors [41]. More detailed developments in the field of optical microcytometry is presented in recent literature reviews [12, 13, 45, 48].

Although fluorescence dye labeling is very common, they present inherent constraints such as photobleaching, saturation, low intensity, and the limitation number on broad emission spectra that can be distinctly collected within the visible wavelength region. Thus, other optical labeling techniques are being combined in microcytometers, such as SERS. For e.g., labeling cells with gold nanoparticles the simultaneous detection of three cell surface markers of cancer cells could be obtained [45]. New advances in the miniaturization of these components are being addressed [7, 49], such as a miniaturization system based on a confocal Raman probe using a fiber optics.

2. Electrical-impedance microcytometers

Electrical-impedance microcytometers, inspired from label-free Coulter counters, present many advantages in cell enumeration as electrical signals are the most straightforward form for recording and processing [50]. They are less complex devices when compared to optical microcytometers that require optical converter systems to obtain electrical signals. Also the sensing components, such metal

electrodes, are easily microfabricated, aligned, and integrated with microfluidic systems, when compared to other components such as objective lenses, fiber optics, laser beam, etc. Therefore, electrical-impedance cytometry has great potential for biomedical applications and diagnostics [11].

While the integration of these sensors is more straightforward than optical microcytometers, a huge variety of configurations electrodes can be devised for the electrical characterization of cells. The layout and number of electrodes could be configured in coplanar electrodes, parallel electrodes, and constriction channel [11, 51]. Further on, whereas DC-impedance signals found on Coulter counters depend on the volume of a cell, AC-impedance gives additional information about membrane capacity and resistance, cytoplasm conductivity, and permittivity [46]. An example on the capabilities of electrical-impedance microcytometers is the discrimination of platelets, red blood cells (RBCs), monocytes, granulocytes, and lymphocytes from whole blood samples [46]. More recent literature reviews on electrical-impedance microcytometers highlight the developments on the electrical detection and characterization of single cells [11, 36, 52, 53].

Further on, optical and electrical-impedance microcytometers can be combined, allowing the simultaneous measurement of four parameters of cells in the same device, namely fluorescence, large-angle side scatter, and dual-frequency electrical-impedance (electrical volume and opacity) [42]. Finally, although the label-free approaches has been successfully demonstrated to discriminate cells, other innovative labeling methods can increase the system sensitivity. An example is the quantification of rare CTCs using graphene nanoplates (GNPs) bound to the cell surface [54]. These increase the conductivity of the detected CTCs and signal signatures from other cells. Additionally, other methods could increase the sensitivity of these devices after the cell pre-enrichment using MBs [54–56].

3. Magnetic microcytometers

Analogous to electrical-impedance microcytometers, magnetic microcytometers are fully compatible with standard complementary metal-oxide semiconductor (CMOS) processing, enabling low-cost production and easy integration with auxiliary electronics. In fact, magnetic sensors are used in our daily lives, such as computers, smartphones, and automobiles. Examples of these sensors [15, 57] are micro-Hall [58], Giant Magneto-Impedance (GMI) [59], magnetic nuclear resonance (MNR) [60, 61], inductive microcoils [62], and magnetoresistive sensors [63, 64].

More recently, magnetic sensors are being translated into biomedical applications [15, 65–67]. Magnetic biosensing offers many advantages for cell enumeration as typically biological materials are devoid of magnetic properties [15, 68–70]. They also present low and stable background when compared to fluorescence labeling systems, and these sensors cannot pick up the electrical properties of the saline solutions from cell suspensions observed in the electrical-impedance sensing techniques [71]. To put it simply, cell detection is obtained by first labeling the surface of cells with magnetic reporting agents, such MNPs or MBs, or by their internalization. Typically, the reporting agents are functionalized with antibodies

specific to the proteins expressed on the outer cell surface. When cells flow over the magnetic sensor, they are detected by the magnetic fields emitted from the reporting agents. Indeed, magnetic labeling and separation [17, 55] have gained much interest in the past years, enabling minimal sample processing when compared to other techniques (e.g., fluorescent labeling). It also provides magnetophoresis techniques that attract MBs to a specific location, and the possibility to capture and concentrate cells, proteins, exosomes, etc.

The first proposed prototype of the magnetic microcytometer was demonstrated in 2011 with the detection of single magnetically labeled K_g1-a leukemia cells flowing over spin valve (SV) sensors [14]. Cells were magnetically labeled with 50 nm MNPs and flowed through a 150 μm wide and 14 μm high straight microchannels. There was good agreement between the numbers of cells counted by the prototype when compared to a hemocytometer. A magnetophoresis technique with current lines was also demonstrated for a pre-enrichment strategy of these cells [14, 16, 64].

Then, a different type of magnetic sensor, a miniaturized Hall sensor (μHall sensor) was successfully implemented, showing the immunomagnetically labeled cancer cells in whole blood [68]. Enumeration of CTCs was performed at high throughput (10^7 cells/min) in the presence of vast numbers of blood cells and without the need for any washing or purification steps. It demonstrated the potential application of real-time multiplexing analysis of three membrane cancer biomarkers of CTCs.

Following this work, a new magnetic microcytometer for the quantification of cancer cells was demonstrated and integrated with a new magnetophoresis technique to present cells closer to the sensors [72]. Cancer cells were detected in whole blood, and cell diameters were assessed using time-of-flight measurements between magnetoresistive sensors. Later on, the same group presented a quantitative magnetic flow cytometer with reproducible rolling of RBCs over giant magnetoresistance sensing elements [73]. This study demonstrated measurements of hydrodynamic diameter of cells, quantification of the binding capacity of immunomagnetic labels, and discrimination of cell morphology. Following this, a new prototype was proposed also based on a Wheatstone bridge configuration of four magnetoresistive sensor discs [74].

Other works followed with new improvements and applications, for example, in the rapid and phenotype-specific enumeration of pathogens [75], capable of measuring single, magnetically labeled bacteria directly in clinical specimens. This clinical utility of the μHall chip was assessed to diagnose infectious diseases by enumerating Gram-positive bacteria. Following this, a magnetic counter that identifies and quantifies bacteria *Streptococcus agalactiae* and *Group B Streptococci* in milk samples was developed to diagnose bovine mastitis [76–79], a costly disease for dairy farmers. Studies used in vitro cultured cells together with 44 milk field samples from 11 Portuguese dairy farms were demonstrated with this method and correlated with PCR analysis. In addition, due to the fact that bacterial cells can form clusters producing different signal signatures, numerical simulation was performed to evaluate correct bacterial enumeration [80].

Soon after, a new type of magnetic microcytometer was demonstrated for the detection of cancer cells using an inductive micro-coil [81, 82]. The chip detects cells labeled with MBs by demodulating the change in coupling between an excitation coil and a pickup coil of a differential spiral transformer. Magnetic labels of different materials were investigated, showing their suitability for multiplexing assays. And finally, a new magnetic microcytometer presented a new strategy to present cells closer to the sensors using a versatile 3D hydrodynamic focusing feature. By adjusting parameters, cancer cells could effectively be focused on the bottom of the microchannels achieving at least a two-fold increase in signal [83].

In summary, magnetic microcytometers present several advantages such as the use of stable magnetic labels to obtain selective cell detection while minimizing background noise. In this new research field, many advances and configurations have been demonstrated, such as the use of the different types of sensors, sensor architecture, and microfluidic channels, enabling these small devices to discriminate cells on different specimens. Table 17.1 presents a compilation of the state-of-the-art of magnetic microcytometers for the particular application of cancer cells. Several configurations of these systems are discriminated such as the type of sensor or sensor architecture used, targeted cells, type of labels, specimen, microfluidic channel feature, recognition of specific targets, magnetization level, and output signal amplitude. This shows that these systems work with different configurations, which can be customized for a particular application or extract different information on the biological samples. In the next section, we deepen the details on different architectures, sensing strategies, and signal amplification methods that have been applied in the cancer field.

17.3 Anatomy of Magnetic Microcytometers for Cancer Cells

Magnetic microcytometers are a particular class of biosensors designed to detect the presence or enumeration of whole cells. Their recognition occurs when cells labeled with MNPs or MBs flow over a magnetic sensor, an example is depicted Fig. 17.1. The sensor picks up the stray magnetic field of the MNPs labeling the cells. This labeling is typically achieved through the functionalization of antibodies on the surface of the MNPs. These antibodies are specific to the extracellular protein expressed on the surface of the cells, thus conferring a selective labeling to target the cells under investigation. Alternative recognizing molecules [86] other than antibodies can also be coupled such as aptamers, phages, etc.

Figure 17.1 depicts a schematic representation of the anatomy of a magnetic microcytometer. A sensing element, such as spin valve (SV), is typically at the bottom of a microfluidic channel. Cells flow in a horizontal trajectory over the sensors. The cells are covered with MNPs or MBs via specific recognition of antibodies functionalized on the surface of these micro or nanoparticles. Typically, superparamagnetic MBs, i.e., that do not present magnetic field at 0 mT, are selected to label cells as opposed to other types of MBs, such as ferromagnetic, which could form clumps. Depending on the sensor type, a strategy used to magnetize

Table 17.1 Compilation of representative publications in magnetic microcytometers for cancer cells

Reference/ Year	Sensor	Microfluidic channel	Cell type	Labeling type	Sample Specimen	Multiplex? Recognition molecule	Additional features
Loureiro et al. [14] 2011	GMR sensor $3 \mu\text{m} \times 40 \mu\text{m}$	Microfluidic channel	Cancer cells	50 nm CD34 MBs	In vitro culture cells	No, CD34 antibody	Detection and counting method
Issadore et al. [68] 2012	$\mu\text{Hall } 8 \times 8 \mu\text{m}^2$ and 2×4 array	Microfluidic channel with hydrodynamic lateral and vertical focusing	Cancer cells, CTCs	MNPs 10, 12, and 16 nm	In vitro culture cells and clinical cancer samples	Yes: EpCAM, HER2/neu, EGFR	Multiplex detection
Helou et al. [72] 2013	GMR Wheatstone bridge	Microfluidic channel with magnetophoretic focusing	Cancer cells	MBs <200 nm	In vitro culture cells in whole blood	No, CD326 antibody	Magnetophoretic enrichment, discrimination of cell size
Lee et al. [84] 2014	Wheatstone bridge GMR magnetic discs $250 \mu\text{m}$	Microfluidic channel with hydrodynamic lateral focusing	Macrophage and cancer cells	MNPs 10 nm	In vitro culture cells	No, internalized MNPs	Cell sorting with magnetic field gradient
Murali et al. [82] 2017	Spiral transformer in CMOS $270 \mu\text{m}$	Microfluidic channel	Cancer cells	MBs 800 nm , $1 \mu\text{m}$, $4.5 \mu\text{m}$	In vitro culture cells	No, CD326 antibody	Integration with CMOS technology, no external magnet
Chicharo et al. [83] 2018	Up to 12 GMR sensors $3 \mu\text{m} \times 200 \mu\text{m}$	Microfluidic channels with hydrodynamic lateral and vertical focusing	Cancer cells	MBs 500 nm	In vitro culture cells	No, EpCAM antibody	Multichannel microchip and signal amplification method

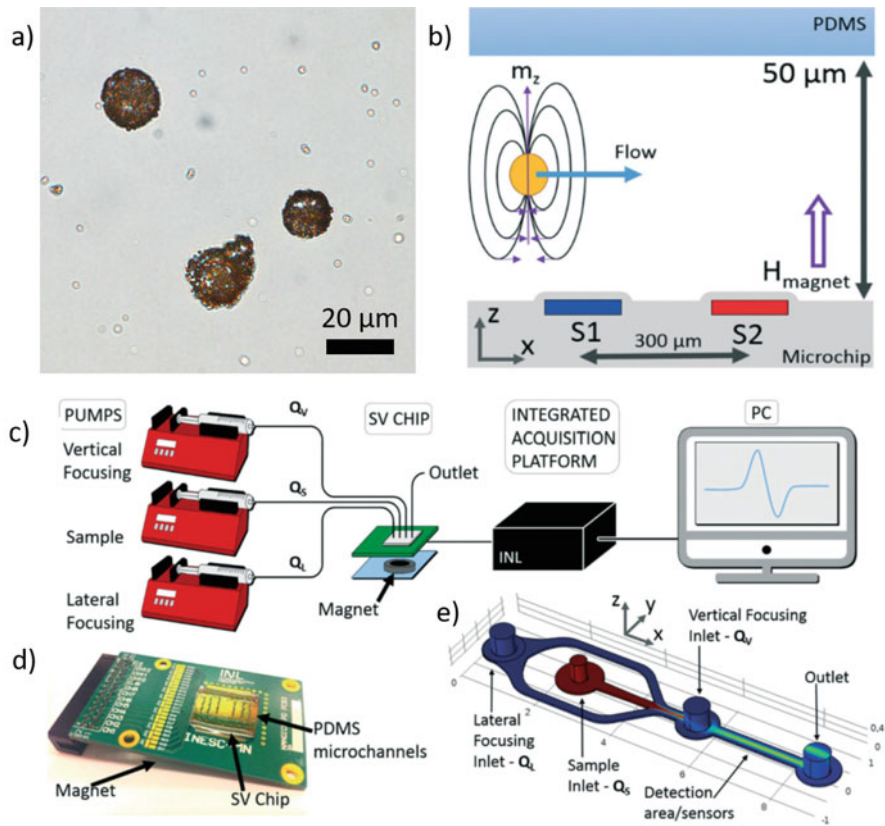


Fig. 17.1 Anatomy of a magnetic microcytometer [83, 85]. (a) SW480 cancer cells labeled with 1 μm diameter magnetic beads. (b) Schematic representation of a magnetized cell flowing over two sensors S1 and S2. (c) Schematic diagram of the prototype, incorporating a sensor microchip, a permanent magnet, the electronic setup, syringe pumps, and computer for processing signals. (d) A microchip composed of spin valve sensors integrated with the PDMS microchannels on top. The microchip is on top of a printed circuit board (PCB) for electrical connections, and a permanent magnet (PM) is positioned underneath. (e) Representation of the 3D hydrodynamic focusing microchannel with combined lateral and vertical focusing. Figures reproduced with permission

superparamagnetic MNPs consists of placing a permanent magnet (PM) below the sensors. This way, labeled cells present a magnetic moment proportional to the amount of MNPs loaded on the surface, the properties of magnetic material of MBs, and the magnetic field intensity. Cells are typically loaded with a syringe and microtubing, and pressure is applied with syringe pumps at selected flow rates. Last and not least, sensors are connected to an electronic setup that amplifies signals, filters, and records signals on a computer. Typical signals from magnetic microcytometers are composed of the characteristic shape of peak and valley as described further in the chapter [85]. The recorded signals are then post-processed by

different algorithms to discriminate signals, count cells, or extract other information on the cell, such as size.

In the following sections, we give an overview of the architectures behind the magnetic microcytometers from published works presented in Table 17.1 and give more detail on how cancer cells are detected with magnetic microcytometers. First, we give a brief summary of how different magnetic sensors operate and the detection strategy used in these works, according to the type of sensor used. Then, we give an overview of how microfluidic integration with the magnetic sensors is obtained, and how functionalization of MBs and labeling of cells were performed. Finally, we overview the electronic equipment employed, and what type of signal processing was devised to automatically enumerate cancer cells on these devices.

17.3.1 Magnetic Sensors and Magnets

There are many different types of magnetic sensors, examples are magnetoresistive sensors, Hall sensors, fluxgate sensors, superconducting quantum interference device (SQUID), induction magnetometer, inductosyn, sychros, and resolvers, Eddy current sensors, magnetic encoders, magnetic force and torque sensors, magnetic flowmeters [87]. These sensors have been developed for many different applications. Only a small portion of these sensors can be miniaturized to cell dimensions (below 200 μm) which are compatible with standard photolithography methods and the semiconductor industry. These are the magnetoresistive sensors, μHall sensors, inductors, GMI, and atomic magnetometers. The sensors used in Table 17.1 are magnetoresistive sensors, μHall , and μCoils . In this section, we give an overview of these particular sensors and how they were applied for the detection of cancer cells.

1. Giant magnetoresistive sensors

Magnetoresistive sensors are a class of spintronic devices [88, 89] a field that has seen a significant developments in the past decades [90]. It was in the late 70s, with the progress of thin films technology [63] that new classes of materials composed of multilayers arose and exhibiting new proprieties. Together with new fabrication processes at the micro and nano-scale, new devices were developed, such as the magnetoresistive sensors, based on the magnetoresistance (MR) effect [88]. The MR is the property of which a material changes its electrical resistance when an external magnetic field is applied. Different configurations of MR sensors were developed, such as the anisotropic (AMR), giant (GMR), and tunneling (TMR) [88, 91]. The MR ratio (%) is defined by the maximum variation of resistance of the material or device:

$$\text{MR} = \frac{R_{\max} - R_{\min}}{R_{\min}} \quad (17.1)$$

In 1991, IBM® invented a device called spin valve (SV) based on the GMR effect [92]. A SV is also composed of multistacks of nanometer-thick layers. Typically, two ferromagnetic (FM) layers: a free layer and a pinned layer, are separated by a conductive layer. An additional layer (the pinning layer) composed of an antiferromagnetic (AFM) material is deposited in direct contact with one FM layer, the pinned layer. The magnetization of the pinned layer is held locked in a defined orientation by the strong exchange interaction of the AFM, thus acting as a reference layer. The other FM layer—the free layer—rotates the orientation of its magnetic moment as a response to an external field, acting as the sensing layer. Typical MR ratios in SV are between 6 and 20% [88]. In order to measure small magnetic fields, the linear region of the sensors is centered around 0 mT, where the change in resistance of the sensor is proportional to the applied field (typically ± 15 mT). In this configuration, the sensor is sensitive to the magnetic fields in the direction along with its height (h) (easy axis of the pinned layer). The output voltage of the sensor can be described by [63, 88]:

$$\Delta V = MR I_{bias} R_{sq} \frac{W}{h} \frac{1}{2} \langle \cos(\theta_f - \theta_p) \rangle \quad (17.2)$$

where W represents the sensor's width, h is the SV height, I_{bias} is the current applied, R_{sq} is the unit resistance of the SV stack, and, the average difference between the angles of the magnetization of the free (θ_f) and pinned (θ_p) layers with respect to the current direction.

The GMR sensors are the most popular and widely explored in magnetic microcytometers. Since most works use superparamagnetic MNPs, a PM is positioned below the chip in order to magnetize these MNPs directly over the sensors. The magnetic field generated is perpendicular to the plane of sensors, conferring a vertical magnetic moment to the MNPs and consequently the labeled cells. The shape of the signal obtained from single cells in this configuration is composed of a characteristic peak and valley, presented in Fig. 17.1c.

The first prototype demonstrated used a set of three individual $3 \mu\text{m} \times 40 \mu\text{m}$ SVs biased with 1 mA each [14]. A PM was positioned below the chip with a vertical magnetic field of 190 mT. The SV sensor presented a multilayer stack deposited by ion beam deposition of 2 Ta/2.5 Ni₈₀Fe₂₀/2.5 Co₈₀Fe₂₀/2 Cu/2.5 Co₈₀Fe₂₀/6 Mn₇₆Ir₂₄/2 Ta/15 TiW(N₂) (thickness in nm, compositions in at %) and patterned by ion milling. Contacts (300 nm thick sputtered Al) were then patterned by liftoff. The SVs presented an MR of 7.69% and sensitivity of 4.8 V T^{-1} .

Helou et al. used a different configuration of a sensor for cell detection composed of four single SVs in a Wheatstone bridge [72]. The GMR Wheatstone bridge had an MR of 6.6% and a sensitivity of $1.4\% \text{ mT}^{-1}$. The configuration of four SV resulted in a different signature detected signals shape, resulted by the superimpose amplitudes of the balancing SVs in this configuration. The authors also achieved a method to predict the cell diameter by measuring the time-of-flight between each SV when the cells flowed over them.

Lee et al. also developed a GMR sensor in the Wheatstone bridge configuration [84]. Each of the four elements consisted of circular 250 μm diameter GMR discs with a multistack of 10 IrMn/3 NiFe/1 Co/2.5 Cu/1 Co/3 NiFe (thickness in nm). The authors employed this Wheatstone bridge to enhance the sensing sensitivity and reduce noise or signal shifts. Since the linear region of these sensors is far from 0 mT, the authors applied an in-plane magnetic field H_y to shift to the linear range and applied an out-of-plane magnetic field with an AC coil, instead of a PM.

Indeed, the magnets positioned below the microchip need to be carefully placed in a region below the 0.5 mm^2 . This feature often requires meticulous alignment of the PM, which could induce small magnetic fields transversally to the sensors (H_x) and decrease their sensitivity [83]. Chicharo et al. designed a custom-made PM with high out-of-plane magnetic field (>100 mT) and low transverse in-plane field (<1 mT) over a large area (30.2 mm^2). The device developed consisted of 6 independent microfluidic channels each with four individual SV sensors of 3 Ta/2.5 Ni₈₀Fe₂₀/8 Mn₇₆Ir₂₄/1.5 Co₈₀Fe₂₀/NOL/3 Co₈₀Fe₂₀/2.6 Cu/2.5 Co₈₀Fe₂₀/2.8 Ni₈₀Fe₂₀/3 Ta (target compositions in %, thicknesses in nm). Using two SVs in the same microchannel, authors were able to measure linear velocities of MBs of up to 7 cm s^{-1} . The magnetoresistance ratio and sensitivity for sensors were around 8.15% and 7.1 $\Omega \text{ mT}^{-1}$, respectively. Further on, signal amplitudes depend on several factors such size of SV, number of MBs, and electronic amplification system, however, numerical simulated work to predict signals from labeled cells using different sizes of SVs resulted that signal amplitudes are higher with SV sizes closer to cells diameter [85].

2. μHall sensors

Another type of magnetic sensor used in magnetic microcytometers was the μHall sensor. Hall sensors are widely used in consumer electronic products, the automotive industry, magnetic field measurement devices, etc. They can be miniaturized to the size of cells, named micron-Hall or μHall [93–95]. Contrary to SV sensors that sense the in-plane magnetic fields, μHall sensors are sensitive to the out-of-plane magnetic fields. The μHall is based on the Hall effect, where a voltage difference is observed on an electrical conductor to an applied magnetic field perpendicular to the electric current applied. A Lorentz force is generated in the direction perpendicular to the direction of the electric charge movement resulting in different output voltages to the applied magnetic field. A μHall sensor converts an external magnetic field into a voltage or current output signal. This output Hall voltage (V_H) is given by [94]:

$$V_H = R_H \left(\frac{I}{t} B \right)$$

where R_H is the Hall Effect co-efficient depending on the materials used and dimensions, I is the current flow through the sensor, t is the thickness of the sensor and B is the Magnetic Flux density perpendicular to the sensor. These sensors have typical sensitivities up to 175 V/(T.A) 15 and linear response over a large range of magnetic fields. Microfabrication of μHall sensors is performed by standard

photolithography methods, good spatial resolution, are compatible with CMOS technology, and very good performance/cost ratio, however, they present higher noise than MR sensors.

One significant work with magnetic microcytometers was demonstrated using μ Hall sensors [68]. The size of the sensor design was obtained by numerical simulations of the type of cells labeled with MNPs when subjected to an external magnetic field. Electrodes were photolithographically patterned, and metal layers were deposited with a multilayer of 5 Ni/5 Au/25 Ge/40 Au/10 Ni/40 Au (thickness in nm). Then, passivation layers to protect from biological solutions were obtained with 30 Al₂O₃/100 nm Si₃N₄/100 nm SiO₂ (thickness in nm). Eight sensor configurations (overlapping 2 × 4 arrays) ensured that individual cells pass directly over at least two μ Hall elements. Then the signals from all eight μ Hall sensors were processed by an algorithm to measure the magnetic moment of each cell. The same prototype was demonstrated for the rapid and phenotype-specific enumeration of pathogens [75] capable of measuring single, magnetically labeled bacteria directly in clinical specimens with minimal sample processing.

3. μ Coils

Another type of magnetic sensing strategy used rely on inductors. These are typically composed of coils that store energy in a magnetic field when electric current flows through. Contrary to GMR and μ Hall sensors, which measure the magnetic field, inductors rely on Faraday's law. Briefly, a voltage is generated in a coil upon an out-of-plane alternating magnetic flux. The sensitivity of inductors increases with the frequency, and therefore large frequencies (gigahertz range) are typically used to measure small magnetic flux.

This type of sensor, using an inductive micro-coil, was employed to a new class of magnetic microcytometers [81, 82]. The system detects cells labeled with MBs by demodulating the change in coupling between an excitation coil and a pickup coil of a differential spiral transformer. Magnetic labels of different materials were examined, showing their suitability for multiplexing assays. The system does not require an external PM, like in the case of GMR and μ Hall, to magnetize the superparamagnetic MBs and was integrated into CMOS technology.

17.3.2 Microfluidic Channels and Cell Flow Handling

All these micron-sized sensors are compatible with microfluidic technology for cell flow. Microfluidic channels deliver the cells on a high-throughput in a single cell at the time manner, so signals acquired correspond precisely to one cell. Undoubtedly, the size, shape, and enhanced features in these microfluidic channels have a large impact on magnetic microcytometers. The first demonstrated magnetic microcytometer used a straight microchannel, with a rectangular cross-section of 150 μ m wide and 14 μ m thick, made using standard soft lithography of PDMS [14]. An irreversible bond was achieved through activation of O₂ plasma of the microchip and the microfluidic module composed of PDMS. This is important since

pressure is applied to move cell suspension solutions inside the microfluidic channel and a securing bonding mitigates possible leaks resulting from input pressure. Bonding is performed under the microscope for the alignment of both structures: the SV sensors and the microfluidic channel. A syringe pump is typically used to load the cell suspensions into the magnetic microcytometers. The small thickness of the microchannel allows cells to be more confined in height and close to sensors, however, they are also subjected to known parabolic velocity in the microchannel cross-section. Most subsequent works followed the processes presented in the work, such as the irreversible bonding and pumping methods; however, different arrangements of the microfluidic channel sizes and features were further explored.

The μ Hall system used a curved microfluidic channel and two new features to align the cell flowing over the sensors [68]. The first feature consisted of lateral hydrodynamic focusing by inserting two adjacent channels on the sides of the cell flow. This feature constricts the cells to the center of the microchannel, increasing the velocity uniformity of cells and decreasing the effects of the parabolic velocity features near the sidewalls of the microchannel. A second feature was the incorporation of chevron patterns on the bottom of the channel before the sensing elements. These structures induce inertial forces on the cells flowing and confine these cells on the bottom of the channel, closer to the sensors.

Another work [72], employed a different strategy to confine cell movement over the sensors using an in situ cell pre-enrichment feature. It consisted of a magnetophoretic guiding mechanism of a ferromagnetic Ni chevron pattern. In the presence of an external field of a NdFeB magnet, it produces a magnetophoretic force in the labeled cells with MNPs. Labeled cells migrate to the bottom of the channel, and with equilibrium with hydrodynamic drag forces from flowing cells, these are presented to closer the sensing elements. Cells that are not labeled do not get attracted to the bottom of the microchannel. The microfluidic channel is large (700 μm width 200 μm height) to avoid clogging, minimize pressure drops and to increase throughput for large volumes.

Other following works also employed a microfluidic channel (60 μm wide and 47 μm thick) with hydrodynamic lateral focusing to ensure a single cell size focusing at the time over the sensor [84]. Lee et al. additionally added a downstream feature for cell separation at the end of the microchannel. Here the microchannel was divided into two output channels, one of which attracts magnetically labeled cells to the selected outlet, since they are sensitive to magnetic field gradient by a nearby PM.

Opposit to most magnetic microcytometers, where an irreversible bonding is made between the PDMS and the microchip, a work employed a compression fixing system to seal microfluidic channels over the sensors [79]. The PDMS microfluidic channel has features of 200 μm in width and 100 μm thick channels and is held together with a glass cover slide and a compression fit.

Finally, another work developed an adaptable 3D hydrodynamic focusing system that confines the cells towards the bottom of the microchannel, closer to the sensors [83]. This was performed using both lateral and vertical hydrodynamic focusing features on a 300 μm wide and height of 50 μm microchannels. It uses three syringe

pumps with a set of different flow rates to obtain the high control flow of cells over the sensors. To calibrate focusing features, numerical simulations on the flow profile were obtained, which were verified with fluorescent dyes on each of the flows sheaths. Optimal flow rates were obtained down to the size of cancer cells detected. Similar to the works above, it also demonstrated the importance of the vertical focusing feature to increase the signal from detected cells, as cells flow much closer with a more uniform velocity profile.

17.3.3 Magnetic Nanoparticles, Beads and Cell Labeling

Magnetic microcytometers leverage from stable labels of MNPs or MBs [96]. The selection of MBs is of extreme importance since they are the reporting agents being detected by the sensors. Furthermore, MBs size and functionalization need to be selected for different cell sizes and types. The specificity of this recognition is achieved by functionalizing MNPs' surfaces. Typically, antibodies are used to attach to specifically expressed membrane proteins on the target cancer cells presented in Table 17.1.

For the detection of myeloid leukemia cell lines, which present an average of 5 μm in diameter, Loureiro et al. employed 50 nm diameter MBs for their detection [14]. Since these cells highly express the CD34 antigen, the authors choose CD34 MicroBeads (MACS, Miltenyi), estimating around 2880 MNPs per cell.

For the clinical evaluation of CTCs, the authors employed three different MNPs to obtain a multiplexed analysis of three membrane proteins at the single-cell level [68]. Simultaneous detection of the biomarkers EpCAM, HER2/neu, and EGFR on individual cells were attained. To achieve efficient cellular labeling with MNPs, the authors used a two-step bioorthogonal procedure that increased the number of nanoparticle loading by three-fold, using modified TCO-antibodies with three MNPs each. Manganese-doped ferrite (MnFe_2O_4) MNPs of different diameters (10, 12, and 16 nm) were used for each of the targeted biomarkers. Each MNP has a unique magnetization response owing to their size differences which were decomposed to evaluate the expression of cells after signal acquisition.

Helou et al. employed a magnetophoretic pre-enrichment and focusing of labeled FaDu head and neck cancer cell line [72]. These cell lines have an average diameter of 16 μm and high expression of EpCAM (epithelial cell adhesion molecule). The FaDu cells were incubated with superparamagnetic MNPs with a diameter below 200 nm, previously functionalized with anti-EpCAM antibodies. The size of nanoparticles was selected to obtain a favorable amount of magnetic retention force over the fluidic drag force in laminar flow conditions of the microfluidic channel.

Opposite to other works, Lee et al. did not functionalize MNPs and instead, they co-cultured cells with a water-based ferrofluid (EMG705, Ferrotec) containing 10 nm Fe_3O_4 for 24 h [84]. Cells used in this study were mouse monocyte-macrophage cells (RAW264.7) and nasopharyngeal carcinoma cells (NPC-TW01).

In this work, the MNPs entered the cells by endocytosis, and labeled cells were pre-concentrated with a PM.

Murali et al. demonstrated the detection of SKBR-3 cancer cells with a μ Coil sensor [82]. These cells present over-expression of EpCAM antigen on their membrane and have a typical diameter of 15 μm . The labeling of these cells is carried out in a two-step process. First, with biotinylated anti-EpCAM (CD326) antibody followed by incubation of large magnetic beads of 4.5 μm diameter (Dynabeads). These MBs consist of single domain (5–20 nm) ferromagnetic nanoparticles embedded in a polymer matrix.

Chicharo et al. demonstrated the detection of SW80 cancer cell lines derived from colon adenocarcinoma with diameters of ca. 20 μm [83]. This cell line also had over-expression of EpCAM proteins on their membrane. The authors selected larger streptavidin-MBs of 500 nm diameter beads (Masterbeads Streptavidin, Ademtech) and functionalized them with biotinylated anti-human antibody CD326 (EpCAM). An average loading of 1700 MBs per cell was estimated with a cell surface coverage area of 21%.

17.3.4 Signal Acquisition, Amplification, and Data Analysis

In magnetic microcytometers, most sensors need electrical biasing and are necessary to convert the output signal of the sensor/transducer to a measurable quantity, which can be subsequently processed in the signal chain. An example of a generic sensor interface can be seen in Fig. 17.2. The output of the sensor goes through an analog front-end (AFE) where amplification and filtering are performed followed by a digitalization stage. Regardless of the chosen implementation, there are several characteristics of fluidics, sensors, electronic signal processing that are correlated and must be well established. This section summarizes different approaches in hardware and signal processing for different systems presented in Table 7.1.

To design an efficient interface and configure the electronics biasing and acquisition of magnetic microcytometers, at least two essential characteristics of the signal must be determined. First, one needs to determine the necessary signal bandwidth, and consequently, the acquisition rate. Second and deeply tied to the first, is the SNR at the output of the sensor, the actual amplitude of the signal. These parameters are influenced by the overall characteristics of the system, such as flow speed, the shape and size of the sensor, sensitivity of the sensor, magnet strength used to magnetize

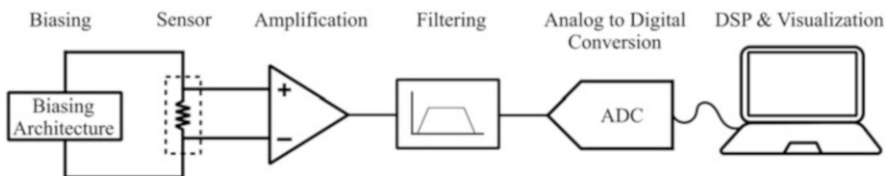


Fig. 17.2 General architecture for resistive sensor interfaces, used in most magnetic microcytometers

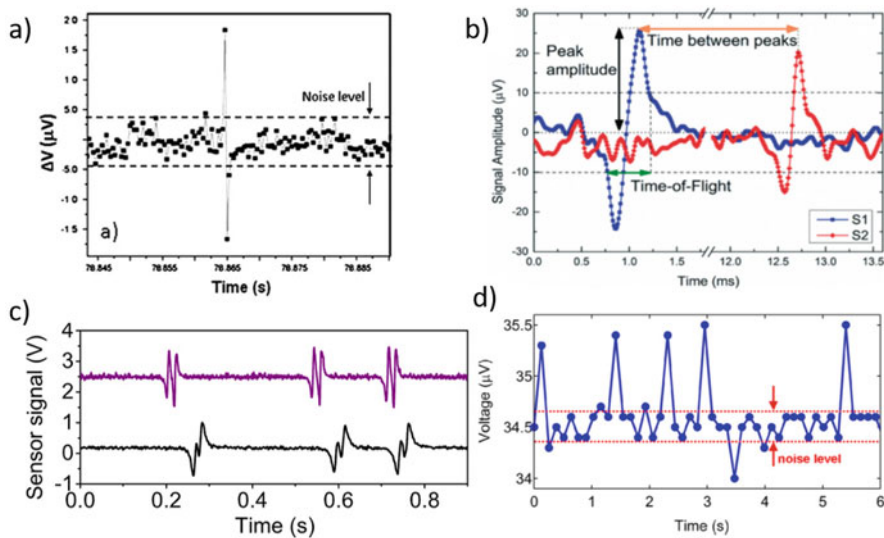


Fig. 17.3 Signal examples from different systems, illustrating differences and similarities of the signals produced by the systems in (a) [14], (b) [83], (c) [72], (d) [84]. Figures reproduced with permission

MNPs, MNPs size, cell size, number of events, and event frequency. MNP conjugated with cells, for instance, produce small signals in the order of units to hundreds of micro-volts [15].

On the system side, the quality of the acquired signal depends first and foremost on the sensor. The GMR sensors tend to be popular choice for magnetic microcytometers, since they have the best compromise between noise, signal, and fabrication simplicity. GMR sensors are also simple to bias and read, either in alternate or direct current mode. Thus, they have been consistently used in the works presented in Table 17.1.

Furthermore, one must consider the noise contribution of the reading electronics. After the sensor, the most important contributor to signal quality are the biasing architecture, which directly adds to the sensors noise; the biasing is followed by the first amplification stage, which is the front-end component that contributes the most to the sensor referred noise. For the resistive/impedance sensors, most of the works use very simple and reliable biasing schemes [97] like the Wheatstone bridge [14, 16, 72] or half-bridge [73, 76, 98], or benchtop current sources [68, 75]. The amplification/acquisition of the signal is, in most cases, performed with ultralow noise benchtop lock-in amplifiers (reducing the bandwidth with programmable filters), high precision voltmeters, or with custom build discrete electronics [68, 75, 78, 97, 99, 100]. For inductive sensors such as flux gates [101] or microcoils [81, 82], each author designs a specific biasing and reading scheme, and an alternate current source is usually used for biasing. In [101] a lock-in amplifier is used as a readout stage. In [81, 82] the architecture of an RF receiver is used. The interfacing

systems for inductive sensors are usually more complicated than that of resistive sensors. However, they have the advantage of conveying the targets information also in the signal phase depending on the materials used in the labeling particles. According to the authors Murali et al. [82], this property is similar to the different colors in an optical system. Thus, the phase information allows them to differentiate among at least three differently marked cells.

Examples of the signals produced by some the systems compiled in Table 17.1, can be seen in Fig. 17.3. Most of the authors design the system to produce bipolar signals, and some use compound data from at least two sensors to compute the time-of-flight of the cells. This can be done with separate signals [83, 100] or with summed signals [73], depending on if one needs to keep the information of each sensor separable or not. In this figure, it is also noticeable that signals can be very weak and with amplitudes in the same range as overall system noise.

As stated before, the signal quality depends on the overall noise contribution of the system, the signal shape, and the relation between the system bandwidth and the signal's band with the most energy/information. Regarding the sampling rate, most works measure the sensor signal in the base-band, sampling at low rates (<200 kSps) [73, 78, 100, 15]. Other works use larger sampling frequencies [68, 75] (<2.5 MSps), allowing for lower test times at the cost of the noise performance. Some works measure the signal in the radio frequency range [81, 82] due to the increased performance of inductive sensors at those frequencies. The most demanding signals for the system are also associated with particles traveling at highest speeds. In [68, 75] it is recommended that at least 10 samples are necessary to fully reconstruct and characterize a pulse. Thus, the sampling rate should be at least $10/T_p$, where T_p is the overall duration of the pulse. Regarding the signal processing and filtering techniques, very little is mentioned in the existing literature. Most works only employ digital or analog band-pass filtering technique to reduce noise and then employ simple threshold-based heuristics for detection.

17.4 Circulating Tumor Cells in Liquid Biopsies

Cancer remains among the leading causes of death worldwide and constitutes a growing global society risk and a major obstacle to human development and well-being [103]. According to the World Health Organization (WHO) [103], there is more than eight million people dying from cancer worldwide each year, a prediction of a 70% increase in new cases in the next 20 years. More than 90% of these cancer-related deaths are due to the progression of a systemic metastatic disease. These figures mirror our narrow knowledge of the key processes that drive to human cancer metastasis [103, 104].

Cancer is the outcome of a complex, multi-step evolutionary process during which normal cells acquire aberrant features that enable them to become tumorigenic and ultimately malignant [105, 106]. Metastasis is the spread of cancer to several distant organs. The process comes from cancer cells intravasating from the primary site into the circulatory system and then extravasating and propagating at distant

sites, eventually leading to metastatic disease [107]. Thomas Ashworth was the first scientist to report this, back in 1869 during an autopsy of a metastatic patient, that microscopically observed cells found in the blood resembled cancer cells [107]. These cell, circulating tumor cells (CTCs) are cancer cells that detach from a solid tumor mass and flow through the blood circulatory system, and may begin colonization processes in distant organs [107–109].

The detection and molecular characterization of CTCs are currently one of the most active areas of translational cancer research, offering new grounds for liquid biopsies [110]. Detailed investigation into CTCs remains exceptionally challenging [107]. They are present in extremely rare numbers, ranging from one to a few hundred in a 7.5 mL tube of blood. This is very low number when compared against a background of billions of subpopulations of blood cells. Furthermore, the number of CTCs found is highly correlated with the patient outcome and survival rate [111, 112]. An ever-growing methods and techniques for CTC purification and isolation emerged together with implementation for clinical diagnostic output. Most of these techniques take advantage of the distinct molecular biomarker profiles and the physical traits of CTCs [107].

Typical methods for discriminating CTCs are based on the molecular biomarker epithelial cell adhesion molecule (EpCAM) recognition. The ubiquitous expression of the EpCAM in epithelial tumor cells allows to differentiate CTCs from blood cells, as the latter presents little or no expression. Nonetheless, it appears unquestionable that EpCAM is not a universal biomarker of cancer, and alternative methods able to recognize a broader spectrum of phenotypes are undeniably desired [111, 113]. Several works have already demonstrated that the expression of epithelial surface markers can be transiently lost during the epithelial to mesenchymal transition (EMT) process [112, 114, 115]. This process enables the detachment of tumor cells from primary tumor, which then lead to circulation in the bloodstream. Likewise, epithelial traits might be reacquired during the reverse process of mesenchymal to epithelial transition (MET), to allow cell to cell interactions and cancer cell colonization in distant organs [113, 114].

In the following section, we provide the reader with the current conjuncture of commercial devices for CTC quantification as well as innovative demonstrated detection methods for purification, detection, characterization, and quantification with microcytometers of these rare cells.

17.4.1 Circulating Tumor Cell Enrichment and Enumeration

Currently, there is the fundamental technical challenge to efficiently enrich CTCs from the normal hematopoietic cells of blood. CTC-enrichment methods are divided into two major categories: (i) physical properties (e.g., density, size, deformability, electric charges) and (ii) biological properties (e.g., surface protein expression and invasion capacity) [107, 116]. Recent review articles can provide the reader with a deeper look of current technologies used to capture and enumerate CTCs [107, 112, 116–118].

Separation methods based on physical properties allow CTCs enrichment with no additional labeling steps [119, 120]. Several companies already commercialize these type of technologies, examples are: (i) density gradient centrifugation (Ficoll®, OncoQuick™, RosetteSep™, CyteSealer™), presenting losses of CTCs; (ii) filtration through distinguishing filters (ISET®, ScreenCell®, CellSieve™) or novel three-dimensional microfilters, also presenting losses of cells as small CTCs can be lost and large hematopoietic cells can be retained by the pores of the filters; (iii) inertial separation based on size (ClearCell™ FX); and, (iv) electrophoresis based separation (ApoStream®, DEPArray™) which discriminates CTCs based on their electrical signature. Nevertheless, new combined methods and geometry innovations in microfluidics channels will continue being explored throughout, such as: a microfluidic filter to trap CTCs by size (larger) and deformability (stiffer) from blood cells [121]; a microfluidic device combining multi-orifice flow fractionation and dielectrophoretic cell separation technique [122]; a system composed of two porous Parylene-C layers with hexagonally arranged 8 μm pores and 40 μm pores for filtration by size [123]; a microchannel with triangular pillars for efficient capture of CTC clusters that showed the impact of in the metastasis process [124]; and an acoustic-based separation method that separates CTCs based on their size, density, compressibility, or a combination thereof [125].

Within the methods targeting direct biological biomarkers of CTCs, immunoaffinity-based enrichment is the most widely used strategy [107]. Affinity-based enrichment technologies can be divided into two categories: (i) positive enrichment techniques, which target tumor-associated antigens to capture CTCs specifically, or (ii) negative enrichment techniques that target hematopoietic cells and thus depletion of the unwanted cells is performed. Typically, higher cell purity is obtained from positive enrichment techniques (which rely on the antibody's specificity, mostly used is anti-EpCAM) at the cost of not expressed targets being recognized by the antibodies. Negative enrichment technologies overcome some drawbacks of positive enrichment such as not being limited to the specified antibody subpopulation of cells and CTCs are obtained without attached antibodies that can affect downstream applications, such as flow cytometry. Examples of these types of enrichment technologies are: (i) modified-surface capture through antibodies (PE or NE) [126–129], which capture cells flowing based on antibodies on the surface of the device, such as a functionalized guidewire for in vivo capture of CTCs [130]; (ii) microfluidic micro-post arrays to increase surface exposure [131–133] with multiple immunoaffinity-type of antibodies; and (iii) immunomagnetic methods as previously explained that isolate CTCs using antibody-conjugated MBs to concentrate them using a PM [134–137]. The strategies above summarize the basic principles of the methodology for enriching CTCs from a complex sample of whole blood.

The cells recovered can undergo either: (i) subsequent analysis such as immunostaining for specific markers or fluorescence in situ hybridization (FISH) techniques for microscope inspection of biomarkers expression or presence of specific DNA mutations on chromosomes; analyzed through flow cytometry [138]; DNA and RNA extraction for sequencing, quantitative RT-PCR (qRT-PCR), and potential expression profile analysis; or viable cells can be released and propagated

in cell culture [138]; or (ii) combination of different technologies, which are able to purify CTCs based on more than one technology or integrate these with detection systems/sensors for automatic quantification or analysis. Examples of these combined technologies that leverage from tumor-associated physical and biological properties are: for instance, microfluidic devices for cell separation by size and immunomagnetic selection with MBs [136]; and, the combination of immunomagnetic selection of CTCs and image modules to quantify and analyze CTCs or sensor such as electrical-impedance sensor [54] or μ Hall sensors [139, 140].

CellSearch® is the only technology approved by the FDA to aid in monitoring patients with metastatic breast, prostate, and colorectal cancers [141]. A high prognostic value using these combined technologies has been demonstrated by CellSearch®, licensed by Janssen Diagnostics. The CellSearch® system uses MBs functionalized with an EpCAM antibody, performs RBCs lysis and centrifugation, immunostains for the expression of Cytokeratin (CK 8, 18, 19), DAPI and CD45, and then uses magnetic separation gradients of the EpCAM positive cells onto the surface of a glass slide. All the surface area of the glass slide is scanned in bright-field and optimized fluorescent channels, and an image algorithm detects the cells. As white blood cells may also be present, a specialized technician then manually selects and counts all CK+, DAPI+ and CD45- cells of previously enriched EpCAM positive cells. Although the advances in the clinical settings have been driven by this technology and serve as gold standard for comparison with newer technologies, several drawbacks have been identified. Namely, the low sensitivity and versatility of the system to capture variable expression EpCAM—subpopulations of CTCs, expensive and bulk equipment, lengthy process for sample processing and microscope scanning, and in particular, the need for specialized personnel to manually identify and count CTCs from acquired images.

More recently, other commercially available devices were demonstrated to obtain direct image analysis by improved high-speed imaging and efficient imaging processing. Some examples may include the need for pre-enriched methods [142, 143] or not [144–146]. In addition, other emerging technologies [147, 148] are pioneering ideas such in vivo flow cytometry of CTCs [149].

17.4.2 Circulating Tumor Cell Enumeration Using Microcytometers

Some microcytometers have been developed for CTC automatic cell detection. These have been demonstrated using different detection systems such as electrical-impedance, optical, and magnetic detection. An example is the CTC-eChip [54], depicted in Fig. 17.4 a), which electrically discriminates CTCs from human peripheral blood cells. The system also features a lateral magnetophoresis of magnetically labeled CTCs to enrich them in an outlet and graphene nanoparticles (GNPs) for labeling and enhanced electrical detection. Amplitude and phase discrimination of different cell population was achieved using GNPs to increase their conductivity, and quantification of cancer cell lines spiked in blood was performed. The enrichment efficiency was 37%, with discrimination efficiency of 94%.

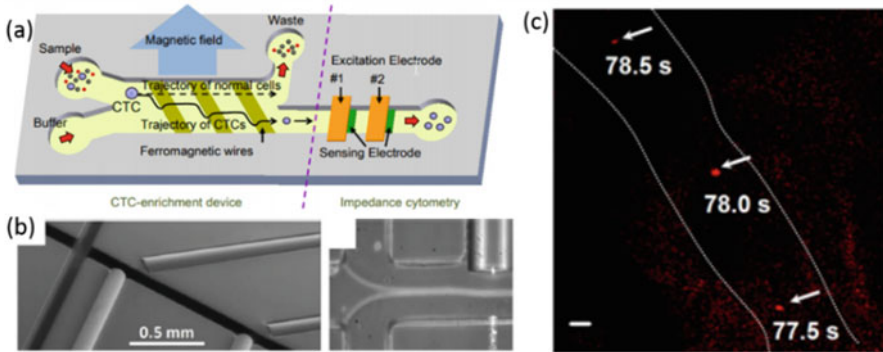


Fig. 17.4 Microcytometers for CTC enumeration. (a) Schematic diagram of the CTC-eChip composed of the CTC-enrichment device and impedance cytometry [54]. (b) SEM image of Optofluidic Chip with integrated fiber optics and bright-field hydrodynamic focused sample and laser excitation [150]. (c) Overlay image of three consecutive frames showing an in vivo cell flowing in a blood vessel [150]. Copyright (2007) National Academy of Sciences, USA Figures reproduced with permission

Another tool to quantify the number of CTCs was proposed by presenting a hydrodynamic optofluidic chip with integrated optical fibers [150], depicted in Fig. 17.4 b). The device is able to confine the cells in the sample fluid and screen CTCs simultaneously with two detectors. Two membrane receptors, HER2 and EpCAM were fluorescence labeled for quantification of CTCs in patient samples in comparison with healthy patients. Initial volume of 8 mL was reduced from collection of peripheral blood mononuclear cells (PBMCs) or buffy coat by density gradient centrifugation.

Another breakthrough in the field was proposed for intravital flow cytometry [150], depicted in Fig. 17.4 c). First, injection of tumor-specific fluorescent ligand labels the CTCs in blood vessels and then multiphoton fluorescence imaging of superficial blood vessels quantifies the CTCs in vivo in flow. The system demonstrated the capability to quantify CTCs weeks before metastatic disease is detected by other methods using mice models and subsequently CTC quantification in whole blood cancer patients at very low concentration of 2 CTCs per ml.

Finally, as mentioned previously, a miniaturized μ Hall sensor was shown to quantify immunomagnetically tagged cancer cells in whole blood [68], with no enrichment or dilution. As the use of a single biomarkers is generally inadequate to identify a cell type, they developed a bar-code method to detect three biomarkers and demonstrate CTC quantification compared to CellSearch with clinical standards of 20 ovarian cancer patients. The μ Hall achieved a diagnosis accuracy of 96%, compared to 15% from CellSearch.

17.4.3 Outlook on magnetic microcytometers

The need to deliver accurate but less expensive devices for the selective count of cells in different specimens have posed new challenges to scientists and engineers. Microcytometers are able to miniaturize benchtop devices, such as flow cytometers, and can be automated or easily integrated with different sample-handling modules due to advances in microfluidics, optics, electronics, and computers in the past decades. Several detection methods have been demonstrated to monitor cells in suspension—such as the ones based on optical, electrical-impedance, and magnetic transducers.

Magnetic microcytometers present several advantages, such as the use of stable labels—MBs—to obtain selective cell detection while minimizing background noise, due to the inherently magnetic-free background of biological samplings. Although this is a new field in research, many progress has been observed, and new configurations of devices are retrieving important information on samples and in particular a more detailed analysis of cells. Examples of different configuration are the type of sensors, sensor architecture and microfluidic channels, enabling these small devices to discriminate cells. New advances on this new research field are being made by several group as this technology is still maturing before being applied in the clinical or diagnostic settings.

References

1. Vembadi A, Menachery A, Qasaimeh MA (2019) Cell cytometry: review and perspective on biotechnological advances. *Front Bioeng Biotechnol* 7. <https://doi.org/10.3389/fbioe.2019.00147>
2. Strimbu K, Tavel JA (2011) What are biomarkers? *Curr Opin HIV AIDS* 5:463–466. <https://doi.org/10.1097/COH.0b013e32833ed177>
3. Xu W, Mezencev R, Kim B et al (2012) Cell stiffness is a biomarker of the metastatic potential of ovarian cancer cells. *PLoS One* 7. <https://doi.org/10.1371/journal.pone.0046609>
4. Várady G, Cserepes J, Németh A et al (2013) Cell surface membrane proteins as personalized biomarkers: where we stand and where we are headed. *Biomark Med* 7:803–819. <https://doi.org/10.2217/bmm.13.90>
5. Green R, Wachsmann-Hogiu S (2015) Development, history, and future of automated cell counters. *Clin Lab Med*. <https://doi.org/10.1016/j.cll.2014.11.003>
6. Chattopadhyay PK, Roederer M (2012) Cytometry: today's technology and tomorrow's horizons. *Methods*. <https://doi.org/10.1016/j.ymeth.2012.02.009>
7. Ateya DA, Erickson JS, Howell PB et al (2008) The good, the bad, and the tiny: a review of microflow cytometry. *Anal Bioanal Chem*
8. Cohen SJ, Punt CJA, Iannotti N et al (2008) Relationship of circulating tumor cells to tumor response, progression-free survival, and overall survival in patients with metastatic colorectal cancer. *J Clin Oncol* 26:3213–3221. <https://doi.org/10.1200/JCO.2007.15.8923>
9. Yang RJ, Fu LM, Hou HH (2018) Review and perspectives on microfluidic flow cytometers. *Sensors Actuators B Chem* 266:26–45. <https://doi.org/10.1016/j.snb.2018.03.091>
10. Piyasena ME, Graves SW (2014) The intersection of flow cytometry with microfluidics and microfabrication. *Lab Chip* 14:1044–1059. <https://doi.org/10.1039/C3LC51152A>
11. Petchakup C, Li H, Hou HW (2017) Advances in single cell impedance cytometry for biomedical applications. *Micromachines*. <https://doi.org/10.3390/mi8030087>

12. Godin J, Chen C-H, Cho SH et al (2008) Microfluidics and photonics for Bio-System-on-a-Chip. *J Biophotonics* 1:355–376. <https://doi.org/10.1002/jbio.200810018>
13. Smith R, Wright KL, Ashton L (2016) Raman spectroscopy: an evolving technique for live cell studies. *Analyst* 141:3590–3600. <https://doi.org/10.1039/C6AN00152A>
14. Loureiro J, Andrade PZ, Cardoso S et al (2011) Magneto-resistive chip cytometer. *Lab Chip* 11:2255–2261. <https://doi.org/10.1039/C0LC00324G>
15. Soares R, Martins VC, Macedo R, Cardoso FA, Martins SAM, Caetano DM, Fonseca PH, Silvério V, Cardoso S, Freitas PP (2019) *Anal Bioanal Chem* 411:1839–1862
16. Loureiro J, Fermon C, Pannetier-Lecoœur M et al (2009) Magneto-resistive detection of magnetic beads flowing at high speed in microfluidic channels. *IEEE Trans Magn* 45:4873–4876. <https://doi.org/10.1109/TMAG.2009.2026287>
17. Mohammed L, Gomaa HG, Ragab D, Zhu J (2017) Magnetic nanoparticles for environmental and biomedical applications: a review. *Particuology*. <https://doi.org/10.1016/j.partic.2016.06.001>
18. Silverio V, López-Martínez MJ, Franco F et al (2017) On-chip magnetic nanoparticle manipulation and trapping for biomedical applications. *IEEE Trans Magn* 53:11–16. <https://doi.org/10.1109/TMAG.2017.2715848>
19. Mazzarello P (1999) A unifying concept: the history of cell theory. *Nat Cell Biol* 1:E13–E15. <https://doi.org/10.1038/8964>
20. Cadena-Herrera D, Esparza-De Lara JE, Ramírez-Ibañez ND et al (2015) Validation of three viable-cell counting methods: manual, semi-automated, and automated. *Biotechnol Rep* 7:9–16. <https://doi.org/10.1016/j.btre.2015.04.004>
21. Kim SI, Kim HJ, Lee HJ et al (2016) Application of a non-hazardous vital dye for cell counting with automated cell counters. *Anal Biochem* 492:8–12. <https://doi.org/10.1016/j.ab.2015.09.010>
22. Bio-RAD (2009) Cell counting-cell viability and cytotoxicity. 10–11. https://www.bio-rad.com/webroot/web/pdf/lsr/literature/Bulletin_6234.pdf
23. Meisenheimer PL, O'Brien MA, Cali JJ (2008) Luminogenic enzyme substrates: the basis for a new paradigm in assay design. *Cell Notes*:10–14. https://businessdocbox.com/Biotech_and_Biomedical/115263487-Luminogenic-enzyme-substrates-the-basis-for-a-new-paradigm-in-assay-design.html
24. Renz M (2013) Fluorescence microscopy—a historical and technical perspective. *Cytom Part A* 83:767–779. <https://doi.org/10.1002/cyto.a.22295>
25. Sanderson MJ, Smith I, Parker I, Bootman MD (2016) Fluorescence microscopy. *Cold Spring Harb Protoc* 2014:36. <https://doi.org/10.1101/pdb.top071795>
26. Tholudur A, Giron L, Alam K et al (2006, October) Comparing automated and manual cell counts for cell culture applications. *Bioprocess Int*:28–34. https://bioprocessintl.com/wp-content/uploads/bpicontent/06049ar04_76381a.pdf
27. Sandhaus LM (2015) Body fluid cell counts by automated methods. *Clin Lab Med* 35:93–103. <https://doi.org/10.1016/j.cll.2014.10.003>
28. Piairo P, Chicharo A, Abalde-cela S et al (2019) Expression of HER2 in circulating tumour cells from metastatic breast cancer patients isolated using a size-based microfluidic device. 1–22. <https://doi.org/10.3390/cancers13174446>
29. Carneiro A, Piairo P, Teixeira A et al (2022) Discriminating epithelial to mesenchymal transition phenotypes in circulating tumor cells isolated from advanced gastrointestinal cancer patients. <https://doi.org/10.3390/cells11030376>
30. Roy M, Jin G, Seo D et al (2014) A simple and low-cost device performing blood cell counting based on lens-free shadow imaging technique. *Sensors Actuators B Chem* 201:321–328. <https://doi.org/10.1016/j.snb.2014.05.011>
31. Xue Y, Ray N (2017) Cell detection with deep convolutional neural network and compressed sensing. 1–28
32. Telford WG, Hawley T, Subach F et al (2012) Flow cytometry of fluorescent proteins. *Methods* 57:318–330. <https://doi.org/10.1016/j.ymeth.2012.01.003>

33. Maher KJ, Fletcher MA (2005) Quantitative flow cytometry in the clinical laboratory. *Clin Appl Immunol Rev* 5:353–372. <https://doi.org/10.1016/j.cair.2005.10.001>
34. McFarlin BK, Gary MA (2017) Flow cytometry what you see matters: enhanced clinical detection using image-based flow cytometry. *Methods* 112:1–8. <https://doi.org/10.1016/j.ymeth.2016.09.001>
35. Davis BH, Barnes PW (2012) Automated cell analysis: principles. *Lab Hematol Pract*:26–32. <https://doi.org/10.1002/9781444398595.ch3>
36. Xu Y, Xie X, Duan Y et al (2016) A review of impedance measurements of whole cells. *Biosens Bioelectron* 77:824–836. <https://doi.org/10.1016/j.bios.2015.10.027>
37. Bin LG, Lin CH, Chang GL (2003) Micro flow cytometers with buried SU-8/SOG optical waveguides. *Sensors Actuators A Phys* 103:165–170. [https://doi.org/10.1016/S0924-4247\(02\)00305-9](https://doi.org/10.1016/S0924-4247(02)00305-9)
38. Zhao Y, Li Q, Hu X, Lo Y (2016) Microfluidic cytometers with integrated on-chip optical systems for red blood cell and platelet counting. *Biomicrofluidics* 10. <https://doi.org/10.1063/1.4972105>
39. Ji QQ, Du S, Van Uden MJ et al (2013) Microfluidic cytometer based on dual photodiode detection for cell size and deformability analysis. *Talanta* 111:178–182. <https://doi.org/10.1016/j.talanta.2013.03.004>
40. Stewart J, Pyatt A (2014) Photonic crystal based microscale flow cytometry. *Opt Express* 22:12853. <https://doi.org/10.1364/OE.22.012853>
41. Hashemi N, Erickson JS, Golden JP, Ligler FS (2011) Optofluidic characterization of marine algae using a microflow cytometer. *Biomicrofluidics* 5:1–9. <https://doi.org/10.1063/1.3608136>
42. Spencer D, Elliott G, Morgan H (2014) A sheath-less combined optical and impedance micro-cytometer. *Lab Chip* 14:3064–3073. <https://doi.org/10.1039/C4LC00224E>
43. Yang SY, Lien KY, Huang KJ et al (2008) Micro flow cytometry utilizing a magnetic bead-based immunoassay for rapid virus detection. *Biosens Bioelectron* 24:855–862. <https://doi.org/10.1016/j.bios.2008.07.019>
44. Etcheverry S, Faridi A, Ramachandraith H et al (2017) High performance micro-flow cytometer based on optical fibres. *Sci Rep*. <https://doi.org/10.1038/s41598-017-05843-7>
45. MacLaughlin CM, Mullaithilaga N, Yang G et al (2013) Surface-enhanced raman scattering dye-labeled Au nanoparticles for triplexed detection of leukemia and lymphoma cells and SERS flow cytometry. *Langmuir* 29:1908–1919. <https://doi.org/10.1021/la303931c>
46. Simon P, Frankowski M, Bock N, Neukammer J (2016) Label-free whole blood cell differentiation based on multiple frequency AC impedance and light scattering analysis in a micro flow cytometer. *Lab Chip* 16:2326–2338. <https://doi.org/10.1039/C6LC00128A>
47. Rane AS, Rutkauskaitė J, deMello A, Stavrakis S (2017) High-throughput multi-parametric imaging flow cytometry. *Chem* 3:588–602. <https://doi.org/10.1016/j.chempr.2017.08.005>
48. Huh D, Gu W, Kamotani Y et al (2005) Microfluidics for flow cytometric analysis of cells and particles. *Physiol Meas* 26. <https://doi.org/10.1088/0967-3334/26/3/R02>
49. Roy M, Seo D, Oh S et al (2017) A review of recent progress in lens-free imaging and sensing. *Biosens Bioelectron* 88:130–143. <https://doi.org/10.1016/j.bios.2016.07.115>
50. Trujillo-Rodriguez R. High speed microfluidic devices for particle counting on a chip. <https://dialnet.unirioja.es/servlet/tesis?codigo=254730>
51. Tahsin Guler M, Bilican I, Agan S, Elbuken C (2015) A simple approach for the fabrication of 3D microelectrodes for impedimetric sensing. *J Micromech Microeng* 25:095019. <https://doi.org/10.1088/0960-1317/25/9/095019>
52. Chen J, Xue C, Zhao Y et al (2015) Microfluidic impedance flow cytometry enabling high-throughput single-cell electrical property characterization. *Int J Mol Sci* 16:9804–9830. <https://doi.org/10.3390/ijms16059804>
53. Cheung K, Gawad S, Renaud P (2005) Impedance spectroscopy flow cytometry: on-chip label-free cell differentiation. *Cytom Part A* 65:124–132. <https://doi.org/10.1002/cyto.a.20141>

54. Han S-I, Han K-H (2015) Electrical detection method for circulating tumor cells using graphene nanoplates. *Anal Chem* 87:10585–10592. <https://doi.org/10.1021/acs.analchem.5b03147>
55. Liu F, Pawan KC, Zhang G, Zhe J (2016) Microfluidic magnetic bead assay for cell detection. *Anal Chem* 88:711–717. <https://doi.org/10.1021/acs.analchem.5b02716>
56. Spencer D, Hollis V, Morgan H (2014) Microfluidic impedance cytometry of tumour cells in blood. *Biomicrofluidics* 8. <https://doi.org/10.1063/1.4904405>
57. Lin G, Makarov D, Schmidt OG (2017) Magnetic sensing platform technologies for biomedical applications. *Lab Chip* 17:1884–1912. <https://doi.org/10.1039/C7LC00026J>
58. Boero G, Demierre M, Besse PA, Popovic RS (2003) Micro-Hall devices: performance, technologies and applications. *Sensors Actuators A Phys* 106:314–320. [https://doi.org/10.1016/S0924-4247\(03\)00192-4](https://doi.org/10.1016/S0924-4247(03)00192-4)
59. Wang T, Zhou Y, Lei C et al (2017) Magnetic impedance biosensor: a review. *Biosens Bioelectron* 90:418–435. <https://doi.org/10.1016/j.bios.2016.10.031>
60. Lee H, Sun E, Ham D, Weissleder R (2008) Chip-NMR biosensor for detection and molecular analysis of cells. *Nat Med* 14:869–874. <https://doi.org/10.1038/nm.1711>
61. Ghazani AA, Castro CM, Gorbатов R et al (2012) Sensitive and direct detection of circulating tumor cells by multimarker μ -nuclear magnetic resonance. *Neoplasia* 14:388–395
62. Tumanski S (2007) Induction coil sensors – a review. *Meas Sci Technol* 18. <https://doi.org/10.1088/0957-0233/18/3/R01>
63. Freitas PP, Ferreira R, Cardoso S, Cardoso F (2007) Magnetoresistive sensors. *J Phys Condens Matter* 19:165221. <https://doi.org/10.1088/0953-8984/19/16/165221>
64. Freitas PP, Cardoso FA, Martins VC et al (2012) Spintronic platforms for biomedical applications. *Lab Chip* 12:546–557. <https://doi.org/10.1039/C1LC20791A>
65. Martinkova P, Kostelnik A, Valek T, Pohanka M (2017) Main streams in the construction of biosensors and their applications. *Int J Electrochem Sci* 12:7386–7403. <https://doi.org/10.20964/2017.08.02>
66. Giouroudi I, Kokkinis G (2017) Recent advances in magnetic microfluidic biosensors. *Nanomaterials* 7:171. <https://doi.org/10.3390/nano7070171>
67. Freitas PP, Martins VC, Cardoso FA et al (2017) Spintronic biochips. In: *Nanomagnetism: applications and perspectives*. Wiley-VCH Verlag GmbH & Co. KGaA, Weinheim, pp 165–200. <https://doi.org/10.1002/9783527698509.ch9>
68. Issadore D, Chung J, Shao H et al (2012) Ultrasensitive clinical enumeration of rare cells ex vivo using a micro-hall detector. *Sci Transl Med*. <https://doi.org/10.1126/scitranslmed.3003747>
69. Chicharo A, Cardoso F, Cardoso S, Freitas PP (2014) Dynamical detection of magnetic nanoparticles in paper microfluidics with spin valve sensors for point-of-care applications. *IEEE Trans Magn* 50. <https://doi.org/10.1109/TMAG.2014.2325813>
70. Chicharo A, Cardoso F, Cardoso S, Freitas PJP (2015) Real-time monitoring of magnetic nanoparticles diffusion in lateral flow microporous membrane using spin valve sensors. *IEEE Trans Magn* 51:1–4. <https://doi.org/10.1109/TMAG.2014.2358645>
71. Shao H, Chung J, Issadore D (2016) Diagnostic technologies for circulating tumour cells and exosomes. *Biosci Rep* 36:e00292–e00292. <https://doi.org/10.1042/BSR20150180>
72. Helou M, Reisbeck M, Tedde SF et al (2013) Time-of-flight magnetic flow cytometry in whole blood with integrated sample preparation. *Lab Chip* 13:1035–1038. <https://doi.org/10.1039/C3LC41310A>
73. Reisbeck M, Helou MJ, Richter L et al (2016) Magnetic fingerprints of rolling cells for quantitative flow cytometry in whole blood. *Sci Rep*. <https://doi.org/10.1038/srep32838>
74. Lee CP, Lai MF, Huang HT et al (2014) Wheatstone bridge giant-magnetoresistance based cell counter. *Biosens Bioelectron* 57:48–53. <https://doi.org/10.1016/j.bios.2014.01.028>
75. Issadore D, Chung HJ, Chung J et al (2013) μ Hall chip for sensitive detection of bacteria. *Adv Healthc Mater* 2:1224–1228. <https://doi.org/10.1002/adhm.201200380>

76. Fernandes AC, Duarte CM, Cardoso FA et al (2014) Lab-on-chip cytometry based on magnetoresistive sensors for bacteria detection in milk. *Sensors* (Switzerland). <https://doi.org/10.3390/s140815496>
77. Duarte CM, Fernandes AC, Cardoso FA et al (2015) Magnetic counter for Group B Streptococci detection in milk. *IEEE Trans Magn* 51:1–4. <https://doi.org/10.1109/TMAG.2014.2359574>
78. Duarte C, Costa T, Carneiro C et al (2016) Semi-quantitative method for streptococci magnetic detection in raw milk. *Biosensors* 6:19. <https://doi.org/10.3390/bios6020019>
79. Loureiro J, Andrade PZ, Cardoso S et al (2011) Spintronic chip cytometer. *J Appl Phys* 109:2255–2261. <https://doi.org/10.1063/1.3559503>
80. Jitariu A, Duarte C, Cardoso S et al (2017) Numerical evaluation of bacterial cell concentration by magnetoresistive cytometry. *IEEE Trans Magn* 53. <https://doi.org/10.1109/TMAG.2016.2623675>
81. Boser BE, Murali P (2014) Flow cytometer-on-a-chip. In: *IEEE 2014 Biomedical Circuits and Systems Conference BioCAS 2014 – Proceedings*, pp 480–483. <https://doi.org/10.1109/BioCAS.2014.6981767>
82. Murali P, Niknejad AM, Boser BE (2017) CMOS microflow cytometer for magnetic label detection and classification. *IEEE J Solid State Circuits* 52:543–555. <https://doi.org/10.1109/JSSC.2016.2621036>
83. Chicharo A, Martins M, Barnsley LC et al (2018) Enhanced magnetic microcytometer with 3D flow focusing for cell enumeration. *Lab Chip* 18:2593–2603. <https://doi.org/10.1039/c8lc00486b>
84. Lee C-P, Lin C-W, Lai M-F (2014) Wheatstone bridge giant-magnetoresistance based cell counter. *Biosens Bioelectron*. <https://doi.org/10.1016/j.bios.2014.01.028>
85. Chicharo A (2018) Design and optimization of a magnetic microcytometer for cell detection and enumeration. Ph.D. Thesis. Universidade de Lisboa, Instituto Superior Técnico
86. Turner GS, Anthony PF, Wilson GS (1989) *Biosensors fundamentals and applications*, vol 53. Oxford University Press, Oxford. ISBN: 0198547242
87. Kuang K (2012) *Magnetic sensors – principles and applications*. InTec. ISBN 978-953-51-0232-8
88. Freitas PP, Ferreira R, Cardoso S (2016) Spintronic sensors. *Proc IEEE*. <https://doi.org/10.1109/JPROC.2016.2578303>
89. Duine R (2011) Spintronics: an alternating alternative. *Nat Mater* 10:344–345. <https://doi.org/10.1038/nmat3015>
90. Chicharo A (2012) Spintronic lateral flow biochip platform. Instituto Superior Técnico, University of Lisbon, M.Sc. Thesis
91. Cardoso S, Leitao DC, Dias TM et al (2017) Challenges and trends in magnetic sensor integration with microfluidics for biomedical applications. *J Phys D Appl Phys* 50. <https://doi.org/10.1088/1361-6463/aa66ec>
92. Diény B, Speriosu VS, Parkin SSP et al (1991) Giant magnetoresistive in soft ferromagnetic multilayers. *Phys Rev B*. <https://doi.org/10.1103/PhysRevB.43.1297>
93. Lee JY, Oh Y, Oh S, Chae H (2020) Low power CMOS-based hall sensor with simple structure using double-sampling delta-sigma ADC. *Sensors* (Switzerland) 20:1–13. <https://doi.org/10.3390/s20185285>
94. Ramsden E (2011) *Hall-effect sensors: theory and application* hardcover. ISBN: 9780750679343
95. Ahmed H, Destgeer G, Park J et al (2018) Vertical hydrodynamic focusing and continuous acoustofluidic separation of particles via upward migration. *Adv Sci* 5. <https://doi.org/10.1002/advs.201700285>
96. Vila A, Martins VC, Chicharo A et al (2014) Customized design of magnetic beads for dynamic magnetoresistive cytometry. *Magn IEEE Trans* 50:1–4
97. Caetano DM (2021) *Circuits and signal processing for magnetoresistive sensor arrays* [Doctoral Dissertation]. Universidade de Lisboa, Instituto Superior Técnico

98. Aledealat K, Mihajlović G, Chen K et al (2010) Dynamic micro-Hall detection of superparamagnetic beads in a microfluidic channel. *J Magn Magn Mater* 322:L69–L72. <https://doi.org/10.1016/j.jmmm.2010.08.006>
99. Caetano DM, Kuntz T, Silva J, Tavares G, Fernandes J (2021) WO2021125987A1. PT Patent No. PT116012A
100. Chicharo A, Barnsley LC, Martins M et al (2018) Custom magnet design for a multi-channel magnetic microcytometer. *IEEE Trans Magn* 54:1–5. <https://doi.org/10.1109/TMAG.2018.2835369>
101. Sun X, Feng Z, Zhi S et al (2017) An integrated microfluidic system using a micro-fluxgate and micro spiral coil for magnetic microbeads trapping and detecting. *Sci Rep* 7:1–8. <https://doi.org/10.1038/s41598-017-13389-x>
102. Stewart BW, Wild CP (2014) World cancer report 2014. *World Heal Organ*:1–2. <https://doi.org/9283204298>
103. Chaffer CLW (2011) A perspective on cancer cell metastasis. *Science* 331:1559–1564. <https://doi.org/10.1126/science.1203543>
104. Gkoutela S, Aceto N (2016) Stem-like features of cancer cells on their way to metastasis. *Biol Direct* 11:1–14. <https://doi.org/10.1186/s13062-016-0135-4>
105. Hanahan D, Weinberg RA (2011) Hallmarks of cancer: the next generation. *Cell* 144:646–674. <https://doi.org/10.1016/j.cell.2011.02.013>
106. Rawal S, Yang Y-P, Cote R, Agarwal A (2017) Identification and quantitation of circulating tumor cells. *Annu Rev Anal Chem* 10:321–343. <https://doi.org/10.1146/annurev-anchem-061516-045405>
107. Massagué J, Obenauf AC (2016) HHS Public Access 529:298–306. <https://doi.org/10.1038/nature17038.Metastatic>
108. Talmadge JE, Fidler IJ (2010) AACR centennial series: the biology of cancer metastasis: historical perspective. *Cancer Res* 70:5649–5669. <https://doi.org/10.1158/0008-5472.CAN-10-1040>
109. Alix-Panabières C, Pantel K (2013) Circulating tumor cells: liquid biopsy of cancer. *Clin Chem* 59:110–118. <https://doi.org/10.1373/clinchem.2012.194258>
110. de Wit S, van Dalum G, Lenferink ATM et al (2015) The detection of EpCAM+ and EpCAM–circulating tumor cells. *Sci Rep* 5:12270. <https://doi.org/10.1038/srep12270>
111. Joosse SA, Gorges TM, Pantel K (2015) Biology, detection, and clinical implications of circulating tumor cells. *EMBO Mol Med* 7:1–11. <https://doi.org/10.15252/emmm.201303698>
112. Raimondi C, Nicolazzo C, Gradilone A (2015) Circulating tumor cells isolation: the “post-EpCAM era”. *Chin J Cancer Res* 27:461–470. <https://doi.org/10.3978/j.issn.1000-9604.2015.06.02>
113. Apostolou P, Papadimitriou M, Papatotiriou I (2017) Stemness gene profiles of circulating tumor cells. *J Cancer Ther* 08:155–167. <https://doi.org/10.4236/jct.2017.82013>
114. Mitra A, Mishra L, Li S (2015) EMT, CTCs and CSCs in tumor relapse and drug-resistance. *Oncotarget* 6:10697–10711. <https://doi.org/10.18632/oncotarget.4037>
115. Alix-Panabières C, Pantel K (2014) Technologies for detection of circulating tumor cells: facts and vision. *Lab Chip* 14:57–62. <https://doi.org/10.1039/C3LC50644D>
116. Neoh KH, Hassan AA, Chen A et al (2018) Rethinking liquid biopsy: microfluidic assays for mobile tumor cells in human body fluids. *Biomaterials* 150:112–124. <https://doi.org/10.1016/j.biomaterials.2017.10.006>
117. Bottos A, Hynes NE (2014) Cancer: staying together on the road to metastasis. *Nature* 514:309–310. <https://doi.org/10.1038/514309a>
118. Lei KF (2020) A review on microdevices for isolating circulating tumor cells. *Micromachines* 11:1–19. <https://doi.org/10.3390/mi11050531>
119. Bankó P, Lee SY, Nagygyörgy V et al (2008) Technologies for circulating tumor cell separation from whole blood. In: *Encyclopedia of microfluidics and nanofluidics*. Springer US, Boston, MA, pp 216–216

120. Tan SJ, Lakshmi RL, Chen P et al (2010) Versatile label free biochip for the detection of circulating tumor cells from peripheral blood in cancer patients. *Biosens Bioelectron* 26:1701–1705. <https://doi.org/10.1016/j.bios.2010.07.054>
121. Moon H-S, Kwon K, Kim S-I et al (2011) Continuous separation of breast cancer cells from blood samples using multi-orifice flow fractionation (MOFF) and dielectrophoresis (DEP). *Lab Chip* 11:1118. <https://doi.org/10.1039/c0lc00345j>
122. Lin HK (2011) 3D microfilter devise for viable circulating tumor cell (CTC) enrichment from blood. *Biomed Microdevices* 13:1–22. <https://doi.org/10.1007/s10544-010-9485-3.3D>
123. Sarioglu AF, Aceto N, Kojic N et al (2015) A microfluidic device for label-free, physical capture of circulating tumor cell clusters. *Nat Methods* 12:685–691. <https://doi.org/10.1038/nmeth.3404>
124. Li P, Mao Z, Peng Z et al (2015) Acoustic separation of circulating tumor cells. *Proc Natl Acad Sci* 112:4970–4975. <https://doi.org/10.1073/pnas.1504484112>
125. Stott SL, Hsu C-H, Tsukrov DI et al (2010, October) Isolation of circulating tumor cells using a microvortex-generating herringbone-chip. 107:18392–18397. <https://doi.org/10.1073/pnas.1012539107>
126. Sheng W, Ogunwobi OO, Chen T et al (2014) Capture, release and culture of circulating tumor cells from pancreatic cancer patients using an enhanced mixing chip. *Lab Chip* 14:89–98. <https://doi.org/10.1039/C3LC51017D>
127. Yoon HJ, Kim TH, Zhang Z et al (2013) Sensitive capture of circulating tumour cells by functionalised graphene oxide nanosheets. *Nat Nanotechnol* 8:735–741. <https://doi.org/10.1038/nnano.2013.194>
128. Diéguez L, Winter MA, Pocock KJ et al (2015) Efficient microfluidic negative enrichment of circulating tumor cells in blood using roughened PDMS. *Analyst* 140:3565–3572. <https://doi.org/10.1039/C4AN01768D>
129. Cho H, Kim J, Jeon C-W, Han K-H (2017) A disposable microfluidic device with a reusable magnetophoretic functional substrate for isolation of circulating tumor cells. *Lab Chip* 17:4113–4123. <https://doi.org/10.1039/C7LC00925A>
130. Mikolajczyk SD, Millar LS, Tsinberg P et al (2011) Detection of EpCAM-negative and cytokeratin-negative circulating tumor cells in peripheral blood. *J Oncol* 2011. <https://doi.org/10.1155/2011/252361>
131. Galletti G, Sung MS, Vahdat LT et al (2014) Isolation of breast cancer and gastric cancer circulating tumor cells by use of an anti HER2-based microfluidic device. *Lab Chip* 14:147–156. <https://doi.org/10.1039/C3LC51039E>
132. Nagrath S, Sequist LV, Maheswaran S et al (2007) Isolation of rare circulating tumour cells in cancer patients by microchip technology. *Nature* 450:1235–1239. <https://doi.org/10.1038/nature06385>
133. Miltenyi S, Müller W, Weichel W, Radbruch A (1990) High gradient magnetic cell separation with MACS. *Cytometry* 11:231–238. <https://doi.org/10.1002/cyto.990110203>
134. Talasz AH, Powell AA, Huber DE et al (2009) Isolating highly enriched populations of circulating epithelial cells and other rare cells from blood using a magnetic sweeper device. *Proc Natl Acad Sci* 106:3970–3975. <https://doi.org/10.1073/pnas.0813188106>
135. Liu Z, Fusi A, Klopocki E et al (2011) Negative enrichment by immunomagnetic nanobeads for unbiased characterization of circulating tumor cells from peripheral blood of cancer patients. *J Transl Med* 9:70. <https://doi.org/10.1186/1479-5876-9-70>
136. Karabacak NM, Spuhler PS, Fachin F et al (2014) Microfluidic, marker-free isolation of circulating tumor cells from blood samples. *Nat Protoc* 9:694–710. <https://doi.org/10.1038/nprot.2014.044>
137. Vishnoi M, Peddibhotla S, Yin W et al (2015) The isolation and characterization of CTC subsets related to breast cancer dormancy. *Sci Rep* 5:1–14. <https://doi.org/10.1038/srep17533>
138. Liang YC, Chang L, Qiu W et al (2017) Ultrasensitive magnetic nanoparticle detector for biosensor applications. *Sensors (Switzerland)* 17:1–10. <https://doi.org/10.3390/s17061296>

139. Kamande JW, Hupert ML, Witek MA et al (2013) Modular microsystem for the isolation, enumeration, and phenotyping of circulating tumor cells in patients with pancreatic cancer. *Anal Chem* 85:9092–9100. <https://doi.org/10.1021/ac401720>
140. Ferreira MM, Ramani VC, Jeffrey SS (2016) Circulating tumor cell technologies. *Mol Oncol* 10:374–394. <https://doi.org/10.1016/j.molonc.2016.01.007>
141. López-Riquelme N, Minguela A, Villar-Permy F et al (2013) Imaging cytometry for counting circulating tumor cells: comparative analysis of the CellSearch vs ImageStream systems. *APMIS* 121:1139–1143. <https://doi.org/10.1111/apm.12061>
142. Casavant BP, Mosher R, Warrick JW et al (2013) A negative selection methodology using a microfluidic platform for the isolation and enumeration of circulating tumor cells. *Methods* 64:137–143. <https://doi.org/10.1016/j.ymeth.2013.05.027>
143. Das M, Riess JW, Frankel P et al (2012) ERCC1 expression in circulating tumor cells (CTCs) using a novel detection platform correlates with progression-free survival (PFS) in patients with metastatic non-small-cell lung cancer (NSCLC) receiving platinum chemotherapy. *Lung Cancer* 77:421–426. <https://doi.org/10.1016/j.lungcan.2012.04.005>
144. Marrinucci D, Bethel K, Kolatkar A et al (2012) Fluid biopsy in patients with metastatic prostate, pancreatic and breast cancers. *Phys Biol* 9. <https://doi.org/10.1088/1478-3975/9/1/016003>
145. Hillig T, Horn P, Nygaard AB et al (2015) In vitro detection of circulating tumor cells compared by the CytoTrack and CellSearch methods. *Tumor Biol* 36:4597–4601. <https://doi.org/10.1007/s13277-015-3105-z>
146. Yu M, Stott S, Toner M et al (2011) Circulating tumor cells: approaches to isolation and characterization. *J Cell Biol* 192:373–382. <https://doi.org/10.1083/jcb.201010021>
147. Qian W, Zhang Y, Chen W (2015) Capturing cancer: emerging microfluidic technologies for the capture and characterization of circulating tumor cells. *Small* 11:3850–3872. <https://doi.org/10.1002/smll.201403658>
148. Georgakoudi I, Solban N, Novak J et al (2004) In vivo flow cytometry: a new method for enumerating circulating cancer cells, pp 5044–5047. <https://doi.org/10.1158/0008-5472.CAN-04-1058>
149. Pedrol E, Garcia-Algar M, Massons J et al (2017) Optofluidic device for the quantification of circulating tumor cells in breast cancer. *Sci Rep* 7:1–9. <https://doi.org/10.1038/s41598-017-04033-9>
150. He W, Wang H, Hartmann LC et al (2007) In vivo quantitation of rare circulating tumor cells by multiphoton intravital flow cytometry. *Proc Natl Acad Sci* 104:11760–11765. <https://doi.org/10.1073/pnas.0703875104>



Droplet-Based Microfluidic Chip Design, Fabrication, and Use for Ultrahigh-Throughput DNA Analysis and Quantification

18

Stéphanie Baudrey, Roger Cubi, and Michael Ryckelynck

Abstract

DNA is widely used as a biomarker of contamination, infection, or disease, which has stimulated the development of a wide palette of detection and quantification methods. Even though several analytical approaches based on isothermal amplification have been proposed, DNA is still mainly detected and quantified by quantitative PCR (qPCR). However, for some analyses (e.g., in cancer research) qPCR may suffer from limitations arising from competitions between highly similar template DNAs, the presence of inhibitors, or suboptimal primer design. Nevertheless, digitalizing the analysis (i.e., individualizing DNA molecules into compartments prior to amplifying them in situ) allows to address most of these issues. By its capacity to generate and manipulate millions of highly similar picoliter volume water-in-oil droplets, microfluidics offers both the required miniaturization and parallelization capacity, and led to the introduction of digital droplet PCR (ddPCR). This chapter aims at introducing the reader to the basic principles behind ddPCR while also providing the key guidelines to fabricate, set up, and use his/her own ddPCR platform. We further provide procedures to detect and quantify DNA either purified in solution or directly from individualized cells. This approach not only gives access to DNA absolute concentration with unrivaled sensitivity, but it may also be the starting point of more complex in vitro analytical pipelines discussed at the end of the chapter.

Keywords

DNA quantification · Biomarker detection · PCR · Droplet-based microfluidics · Microfabrication

S. Baudrey · R. Cubi · M. Ryckelynck (✉)

Université de Strasbourg, CNRS, Architecture et Réactivité de l'ARN, Strasbourg, France

e-mail: m.ryckelynck@unistra.fr

© The Author(s), under exclusive license to Springer Nature Switzerland AG 2022

445

D. Caballero et al. (eds.), *Microfluidics and Biosensors in Cancer Research*,

Advances in Experimental Medicine and Biology 1379,

https://doi.org/10.1007/978-3-031-04039-9_18

18.1 Introduction

DNA is widely used as a biomarker of contamination (e.g., in the food industry), infection (e.g., detection of pathogenic bacteria or viruses), or disease (e.g., cancer or genetic disease) and many techniques have been developed to specifically detect a given sequence and even quantify it. Several isothermal methods allowed to set-up point-of-care assays [10], sometimes with a simple qualitative result like color change [12]. Whereas these assays are highly portable, they may also be sometimes limited by moderate sensitivity and specificity. Besides, very high specificity and sensitivity (down to single molecule) can be reached with Polymerase Chain Reaction (PCR), a method consisting in performing iterative cycles of primer annealing, extension, and strand denaturation orchestrated by temperature change. Though the requirement of a thermal-cycling equipment increases the cost of the method and limits its portability, the temperature dependence of each step also enables synchronizing amplification cycles, a feature easing the access to a reliable read-out especially in quantitative PCR approach (qPCR). qPCR, also known as real-time PCR, consists in monitoring DNA amplification reaction through the apparition of fluorescence resulting either from the intercalation of a non-specific fluorogenic dye (e.g., SYBR Green, EvaGreen) into amplified DNA or from sequence-specific probes (e.g., TaqMan, molecular beacon being the most widely used) that specifically anneal to target amplicons [9]. The fluorescent signal is then used to determine a threshold cycle, Ct (Fig. 18.1a), that is directly correlated with target DNA concentration (the more concentrated the DNA, the lower the Ct) by comparison to a standard (either internal or external). Yet, this relative quantification is also an

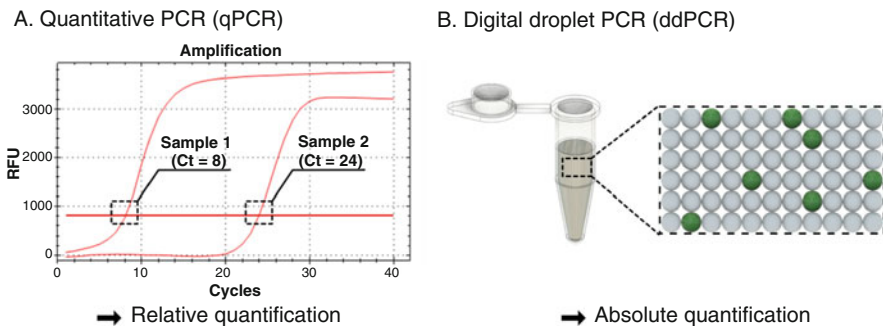


Fig. 18.1 Comparison of qPCR and ddPCR DNA quantification concepts. (a) DNA quantification by quantitative PCR (qPCR). DNA is quantified by monitoring DNA amplification in real time and the number of cycles required to cross a fluorescence threshold (horizontal red line) is determined as being the threshold cycle (Ct). Note that for illustration purposes the threshold was placed much higher than where it should normally be. In the shown example, Sample 1 would contain ~65,500-fold (2^{24-8} , assuming both PCR reactions being 100% efficient) more target DNA than Sample 2. (b) DNA quantification by digital droplet PCR (ddPCR). DNA is quantified by counting the number of fluorescent compartments at the end of PCR amplification. In the shown example, 7 out of 66 compartments are positive (in green), so the absolute concentration in DNA would be ~0.1 (7/66) DNA molecule per volume of compartment

Achilles' heel that may challenge qPCR accuracy in case of differential amplification efficiency between different targets or samples. Such imbalance can be due to a suboptimal primer design or simply result from the presence of inhibitors introduced during sample preparation (e.g., heparin during blood collection). In any case, proper quantification would be flawed. Furthermore, qPCR sensitivity can be limited when searching for specific point mutants contained in large fraction of wild-type molecules; a scenario typically encountered, for instance, when analyzing tumor content or circulating DNA [14].

Many limitations of qPCR can be addressed by digitalizing the assay, i.e. by individualizing DNA molecules into independent compartments prior to amplifying them using the same molecular tools developed for qPCR. First introduced by Vogelstein et al using microtiter plates [19], the so-called digital PCR has recently benefited from the strong miniaturization made possible using droplet-based microfluidics. In this technology, highly homogeneous emulsion made of picoliter (pL) water-in-oil droplets is generated using dedicated microfluidic devices [16]. Diluting DNA molecules into typical qPCR reaction mixture prior to emulsifying it allows, upon thermocycling and droplet fluorescence analysis, to easily discriminate those droplets initially occupied by a DNA molecule (highly fluorescent droplets in which each starting DNA molecule was converted into hundreds of thousands of copies) from those initially empty droplets that stayed poorly fluorescent (Fig. 18.1b). Since DNA molecules distribute within droplets according to Poisson statistics [13], droplet occupancy can easily be computed from a known DNA concentration and vice versa using Eq. (18.1):

$$P_{(x=k)} = \frac{e^{-\lambda} \lambda^k}{k!} \quad (18.1)$$

where λ is the average number of DNA molecule per compartment, k is the exact number of DNA molecule per compartment, and $P_{(x=k)}$ is the probability of having k DNA molecule per compartment. Being able to directly count the DNA molecules contained in a sample gives access to an absolute quantification of the target, making the approach less exposed to qPCR limitations. The robustness of this digital droplet PCR (ddPCR) approach led to the development of several commercial platforms making the technologies widely accessible. Yet, to be robust, these platforms are also locked systems with low versatility in their use and are therefore difficult to be repurposed for other applications. Building on this statement, we present in this chapter a general strategy allowing everyone to build, set up, and use his/her own digital droplet PCR analysis platform that can easily be upgraded to perform more complex analyses discussed at the end of this chapter and that may use ddPCR as starting point.

18.2 Setting-up the Stage: Design and Preparation of Microfluidic Device and Workstation

At the heart of the technology, the microfluidic devices can be fabricated in any clean-room facility using the procedure described below or ordered from a specialized company. Moreover, droplet production and fluorescence analysis using these devices require a custom workstation that can easily be assembled from commercially available parts.

18.2.1 Preparation of Microfluidic Device

The microfluidic chips used in this chapter (see below) are typically made of polydimethyl-siloxane (PDMS), a soft elastomer that can be molded (note that commercial devices are usually rather made of hard plastic). Prior to being able to fabricate a chip, the blueprint of the device should be designed using a vector graphic design software like AutoCAD (AutoDesk) prior to being printed as a high resolution (50,800 dpi) photomask in negative mirror by a specialized company (e.g., Selba S.A.). Note that the key distances of the designs used to perform ddPCR as presented in this chapter are given below. This photomask is then used to prepare a master mold by photolithography (Fig. 18.2, left column), later replicated into microfluidic chips using soft lithography (Fig. 18.2, right column).

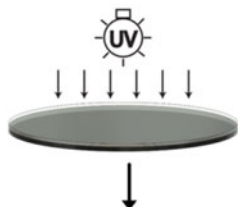
18.2.1.1 Preparation of a Mold Using Photolithography

The surface of a 3-inch silicon wafer (Si-Mat, Silicon Materials) is first activated for 30 seconds using a plasma cleaner (e.g., Femto device Diener, 40 kHz, 100 Watts) connected to an oxygen gas source set at 0.5 mbar with power set to 25%. Then, a 0.5 μm layer of SU8 2000.5 photoresist (MicroChem) is spread onto the surface of the activated wafer using a spin coater (e.g., Laurell WS-650MZ-23NPP) following manufacturer instructions (Table 18.1). The wafer was then prebaked for 1 min at 95 °C prior to being UV-exposed for 15 seconds (corresponding to an exposure energy of 60 mJ/cm^2). Though no photomask is used at this step, the exposure can be performed on a mask aligner (see below). The precoated and UV-exposed wafer is then post-baked for 3 min at 95 °C. This sub-layering step is optional but was found to help the good adhesion of printed mold structures during the photolithography step per se.

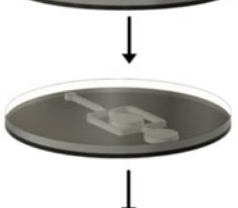
A 10–40 μm thick layer of SU8-20xx (xx should be adapted to the desired depth) photoresist (MicroChem Corp.) is then spread onto the prepared wafer using a spin coater following supplier recommendations (Table 18.1). The coated wafer is prebaked for 5 min at 95 °C (for 10–15 μm deep molds), or 3 min at 65 °C followed by 6 min at 95 °C (for the 40 μm deep molds). The wafer is then installed on a mask aligner (e.g., CP 200 mask-aligner, SUSS Microtec ReMan) together with the photomask. The montage is then exposed to UV illumination for 60 seconds (here, an exposure of 240 mJ/cm^2). Note that exposure time may have to be adjusted to the thickness of the resist layer following manufacturer recommendations. Upon

A. Photolithography

1. Preparation of a sub-layer of photoresist on the wafer



2. UV irradiation of the photoresist through a photomask



3. Mold development



Mold ready to be used

B. Soft lithography

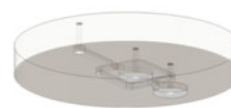
4. PDMS casting and curing on the mold



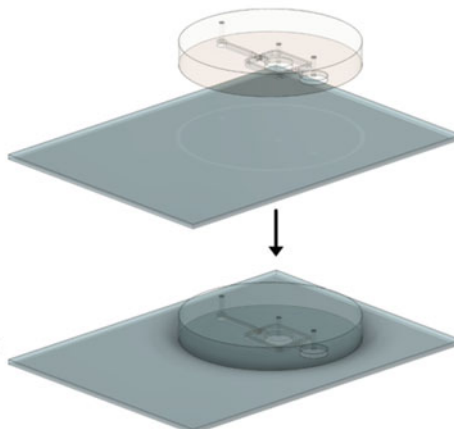
5. Cutting the PDMS replica off the mold



6. Punching inlets and outlets in PDMS replica



7. Bonding of PDMS replica on a glass slide



Microfluidic device ready to be used

Fig. 18.2 Main steps of the fabrication of a microfluidic device. (a) A mold is first fabricated by photolithography. During this step, a sub-layer of $0.5\ \mu\text{m}$ of photoresist is first deposited on the surface of the wafer (**step 1**) and activated by UV irradiation. A second layer is then spread onto the sub-layer and the drawing of the microfluidic device, printed as a negative mirrored photomask, is patterned by UV irradiation (**step 2**). The uncured resin is removed by development and a mold is obtained (**step 3**). (b) The master mold is then replicated into PDMS microfluidic devices by soft lithography (**step 4 and 5**). Upon PDMS curing, the replica is cut off the mold (**step 5**), the inlets

exposure, 10 μm and 15 μm molds are post-baked for 1 min at 65 $^{\circ}\text{C}$ and 5 min at 95 $^{\circ}\text{C}$, whereas 40 μm molds are post-baked for 1 min at 65 $^{\circ}\text{C}$ and 6 min at 95 $^{\circ}\text{C}$. Imprinted structures should be readily distinguishable at the end of this baking step.

Unreacted photoresist is then removed by placing the imprinted wafer onto a spin coater, covering it with SU8 developer (MicroChem) and incubating for 3 min prior to removing the developer by spinning the wafer for 25 sec at 2500 rpm. The treatment should be repeated 3 times before washing the wafer with an excess of isopropyl alcohol followed by 25 sec of spinning at 2500 rpm. Finally, the mold is hard baked for 10 min at 200 $^{\circ}\text{C}$ to cure cracks that may have appeared at the surface of the resist.

18.2.1.2 Molding the PDMS Chip by Soft Lithography

The wafer prepared before is transferred into a 9 cm Petri dish and covered by 30 g of a thoroughly mixed 10/1 PDMS/curing agent solution (Sylgard 184 PDMS kit, Dow Corning). The mixture is degassed using a vacuum dessicator until no bubble forms. It is then baked for at least 1 h 30 at 65 $^{\circ}\text{C}$. Upon curing, PDMS replica is cut with a surgical blade and peeled off the mold before punching inlets and outlets using a 1 mm biopsy punch (Harris Uni-Core™). A glass slide and the PDMS slab should then be activated with an oxygen plasma (e.g., Femto device Diener, 40 kHz, 100 Watts) for 30 sec at a power of 25% and 0.5 mbar of oxygen prior to putting the activated glass and molded PDMS faces into physical contact and placing them on a hot plate for 15 min at 65 $^{\circ}\text{C}$. Finally, the surface of the channels is passivated using a 1% solution of 1H,1H,2H,2H-Perfluorodecyltrichlorosilane (ABCR) diluted in Novec 7500 (3 M), injected through a 0.45 μm PTFE filter (Merck-Millipore) into the channels and flushed out with pressurized air. Note that the molding procedure presented here can be repeated 50 to 100 times with the same mold.

18.2.1.3 Preparation of Emulsion Collection and Incubation Devices

An emulsion can be collected and incubated in any sort of container, possibly covered by mineral oil to prevent evaporation and to limit damage to the emulsion. Yet, we recommend using collection devices prepared as described below (Fig. 18.3) as we found them to allow gentle handling of the emulsion, which prevents unwanted coalescence.

An 8 mm thick slab of cured PDMS (corresponding to ~36 g of cross-linked PDMS) should be prepared and cured in a 9 cm Petri dish. PDMS plugs are then punched off the slab using a 6 mm biopsy punch (Harris Uni-Core™) and two 1 mm diameter holes are punched into each plug using a 1 mm biopsy punch (Harris Uni-Core™). A length of PTFE tubing (I.D. 0.56 mm, O.D. 1.07 mm, Thermo Scientific) is inserted through each hole and the montage is inserted into a 200 μL tube. The tube is finally filled with Novec 7500 fluorinated oil (3 M) using a syringe

Fig. 18.2 (continued) and outlets are punched (**step 6**), and channels are closed by binding the PDMS replica to a glass slide (**step 7**)

Table 18.1 Spin coating parameters used to spread the desired thickness of photoresist

Photoresist	Thickness	1st spinning step	2nd spinning step
SU8-2000.5	0.5 μm	5 sec at 100 rpm	30 sec at 500 rpm
SU8-2007	10 μm	5 sec at 500 rpm	30 sec at 1500 rpm
SU8-2010	15 μm	5 sec at 500 rpm	30 sec at 1600 rpm
SU8-2025	40 μm	5 sec at 500 rpm	30 sec at 2000 rpm

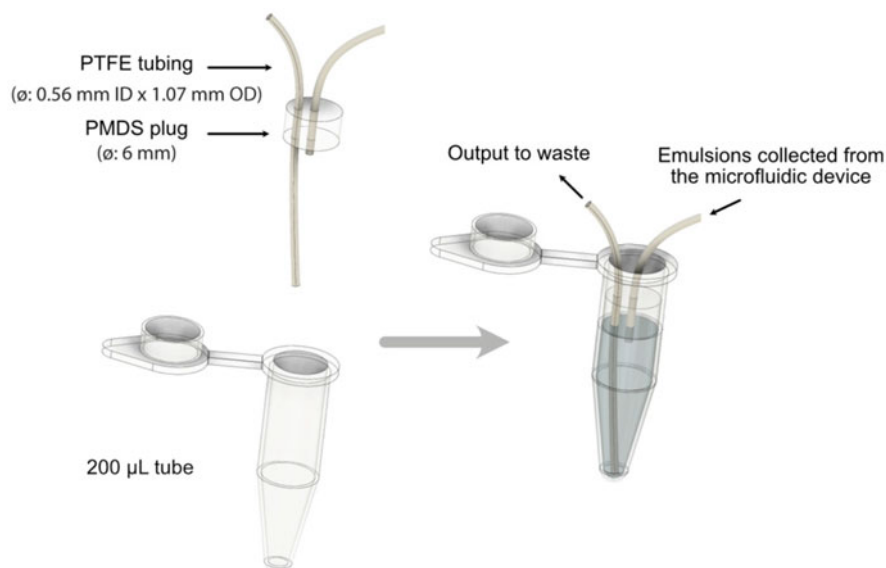


Fig. 18.3 Preparation of an emulsion collection tube. Two PTFE tubings are inserted into a plug of PDMS. The tubing at the bottom of the tube is connected to the waste exhaust while the tubing near the PDMS plug is connected to the microfluidic device to collect emulsion. The entrance of the emulsion in the collection tube pushes out the excess of oil towards the waste

connected to the shortest tubing while purging the air out of the system through the other one.

18.2.2 Design and Set-up of a Custom Microfluidic Workstation

Besides the microfluidic chips, the workstation is an instrumental piece of equipment that can easily be assembled from commercially available parts. A schematic of the typical prototype we use is shown in Fig. 18.4 and is assembled on a vibration dampening platform (Thorlabs B75150AX), the optical set-up being assembled on the breadboard. In this setting, two lasers (a 638 nm laser, Cobolt 06-MLD 180 mW and a 488 nm laser, CrystaLaser DL488-050-O) are merged using a dichroic mirror (Semrock FF495-DiO3-25x36; **D1**) and spots are shaped as a line by a pair of lenses

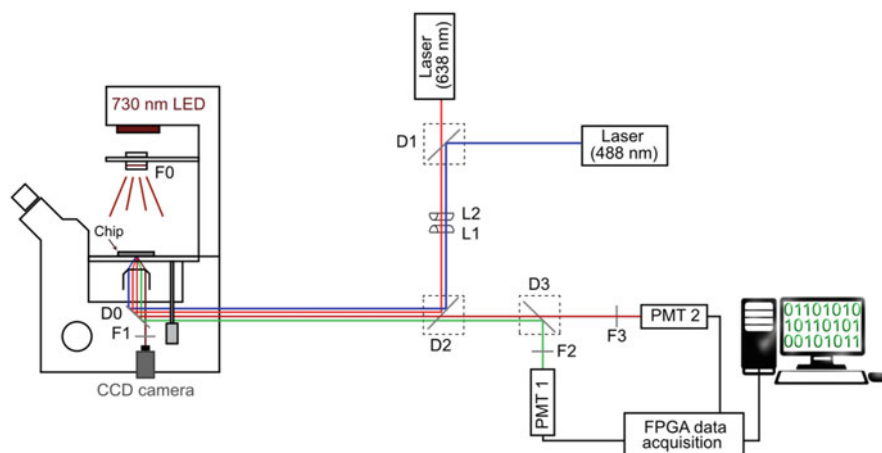


Fig. 18.4 Schematic of a microfluidic workstation. The main parts are shown together with a detailed schematic of the optical set-up including lasers, photomultiplier tubes (PMT), filters (F), dichroic mirrors (D), and lenses (L). The features of each component are given in the main text

(Semrock LJ1567L1-A and LJ1878L2-A, **L1** and **L2**). Excitation lights are then reflected using a multi-edges dichroic mirror (Semrock Di01-R405/488/561/635-25x36; **D2**) and the combined beams enter an inverted Nikon Eclipse Ti-S microscope in which they are reflected by a dichroic mirror (Semrock FF665-Di02-25x36; **D0**) located below the microscope objective lenses. Excitation lights are then focused into microfluidic channel while passing through a Nikon Super Plan Fluor 20x (or possibly a 40x) ELWD objective, and both green (EvaGreen or TaqMan probe) and red (Cy5) emitted lights are collected through the same path, reflected by **D0** and transmitted through **D2** before being resolved by a dichroic mirror (Semrock FF562-Di03-25x36, **D3**). Green and red fluorescence are then measured by two photomultiplier tubes (PMT, Hamamatsu H10722-20) equipped with bandpass filters (Semrock FF03-525/50-25 and FF01-679/41-25 for green and red detection, respectively, **F2** and **F3**) to clean the signal. PMT signal is collected, recorded, and analyzed in real time by an intelligent data acquisition (DAQ) module featuring a user-programmable FPGA electronic card (National Instruments PCIe 7852R) installed on the computer and driven by internally developed firmware and software written in LabView 2019 (National Instrument).

The operations on the microfluidic chip can be visualized in real time using a CCD camera (e.g., Guppy device from Allied Vision) connected onto the camera side port of the microscope via a C-mount. To this end, the halogen light-source was exchanged for a collimated 730 nm LED equipped with a long path filter (Semrock FF01-715/LP-25, **F0**). Moreover, the camera was protected from lasers reflection (wavelength > 665 nm) by a long-pass filter (Semrock, BLP01-664R-25, **F1**) mounted in front of the camera. Finally, liquids can be infused into the chips using a 7-bar MFCS™ pressure-driven flow controller (Fluigent) equipped with S Flowmeters and driven by MAESFLO software.

18.3 Digital Droplet PCR Quantification of DNA

As highlighted in the introduction, DNA is widely used as a biomarker of contamination, infection, and disease. In the case of cancer, for instance, the target DNA can either be free (e.g., a purified DNA sample originating from a molecular biology process, a liquid biopsy, or extracted from solid tumors) or contained into cells (e.g., from cultured cells, dissociated tissues or tumors). Moreover, PCR amplification can be detected using either a non-specific intercalating dye or a sequence-specific probe. As an attempt to address these different possibilities, we will consider two scenarios of DNA quantification by digital droplet PCR (ddPCR) of which the detection modes (i.e., intercalating dye and sequence-specific probe) are readily exchangeable.

18.3.1 Scenario 1: ddPCR Quantification of Purified DNA Using an Intercalating Dye

18.3.1.1 Consideration on the Choice of the Dye

Whereas several intercalating dyes have been developed, they are not all compatible with ddPCR. Indeed, after having tested several of them, we found that, while some dyes rapidly partition in the oil phase (personal communication, unpublished data) and others modified ones (e.g., PEGylated PicoGreen) readily exchange between droplets [13], EvaGreen (Biotium) is particularly well suited for droplet applications as it stays properly confined within the droplets where it allows to reliably detect DNA amplification [17]. Therefore, we highly recommend using either a commercial qPCR mixture already formulated with EvaGreen or to supplement a homemade PCR mixture with this dye.

18.3.1.2 ddPCR Mixture Preparation

According to MIQE guidelines [7], the PCR mixture should be prepared using DNA/RNA PCR laminar flow workstation to avoid contamination of stock reagents with airborne DNA molecules. For a typical ddPCR experiment, 100 μL of reaction mixture is prepared by mixing 50 μL of SsoFast™ EvaGreen® Supermix (Bio-Rad), 0.5 μM of each primer, 10 μM Cyanine 5 carboxylic acid (Lumiprobe) used as droplet tracker, 0.1% Pluronic F68 (Sigma Aldrich), and a dilution of DNA to quantify prepared in 200 $\mu\text{g}/\mu\text{L}$ solution of yeast total RNA (Thermo Scientific). Pluronic F68 and total RNA are important to limit the loss of DNA by adsorption on plastic surfaces. Importantly, the solution containing template DNA should never be introduced in the PCR laminar flow workstation and should rather be added to the mixture at another location. Moreover, several dilutions of the solution to quantify should be tested to reach partial droplet occupancy, a non-saturating condition required for being able to perform a digital quantification.

18.3.1.3 ddPCR Mixture Emulsification and Thermocycling

The PCR mixture is emulsified into 2.5 pL droplets using a 10 μm deep droplet generator (Fig. 18.5A) prepared using the procedure presented above (see § 18.2.1.1

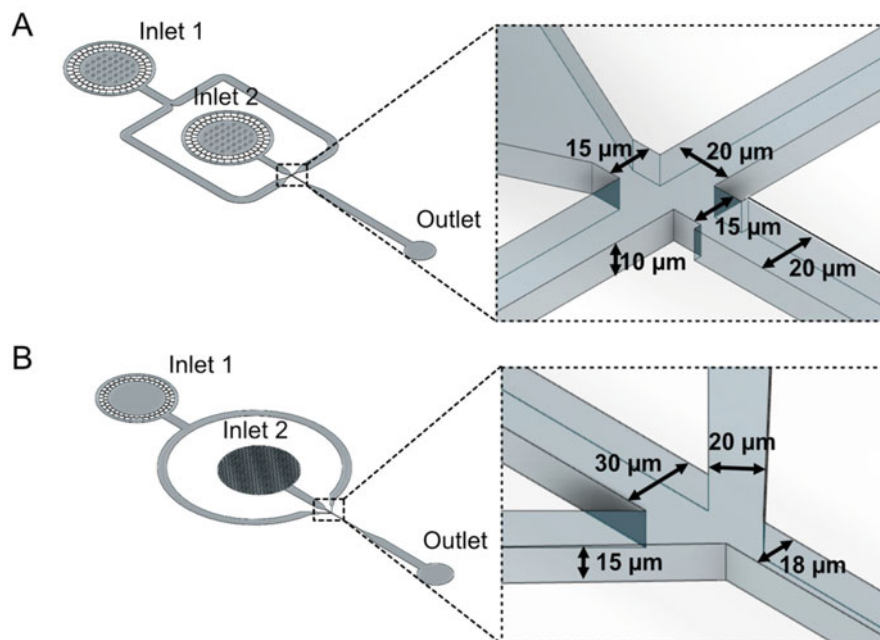


Fig. 18.5 Microfluidic devices used for the ddPCR quantification of purified DNA. (a) Droplet generation microfluidic device. An aqueous phase is infused through Inlet 2 and pinched by two orthogonal flows of fluorinated oil supplemented with surfactant and infused through Inlet 1 to generate 2.5 pL droplets. The produced emulsion is collected at the Outlet of the chip. (b) Droplet fluorescence analysis device. The emulsion to analyze is infused through Inlet 2 and the droplets are spaced by a fluorinated oil stream infused through Inlet 1. Finally, the emulsion leaves the device through the Outlet. The key dimensions of each device are given in the corresponding box

and 18.2.1.2). The aqueous phase is loaded into a length of PTFE tubing connected to the Inlet 2 of the device, whereas the other end of the tubing is connected to a flowmeter. Droplets are then generated by infusing a stream of Novec 7500 fluorinated oil (3 M) supplemented with 3% fluorosurfactant [11] connected to Inlet 1 of the chip. 2.5 pL droplets are then produced at a frequency of $\sim 13,000$ droplets per second and their volume adjusted by tuning the flow rate of each inlet. The emulsion is recovered from the Outlet into a collection device (see § 18.2.1.3.).

At the end of the production, PTFE tubings are removed from the collection tube and the holes are sealed by plugs of melted poly-ethylene tubing (PE-20, Intramedic). Finally, the tube is placed into a thermocycler (e.g., T100 thermocycler, Bio-Rad) and subjected to the adapted program (Table 18.2).

18.3.1.4 Droplet Fluorescence Analysis and Digital Quantification

Upon thermocycling, the emulsion is reinjected into a 15 μm deep droplet analysis device (Fig. 18.5B) prepared using the procedure presented above (see § 18.2.1.1 and 18.2.1.2). Sealing plugs are removed from the collection tube and exchanged for

Table 18.2 ddPCR thermocycling conditions used with purified DNA

Step	Temperature	Time	Cycles
Initial denaturation	98 °C	2 min	Not repeated
Denaturation	98 °C	10 sec	
Annealing	60 °C	30 sec	Repeated 29 times
Extension	72 °C	30 sec	
Final hold	4 °C	Forever	Not repeated

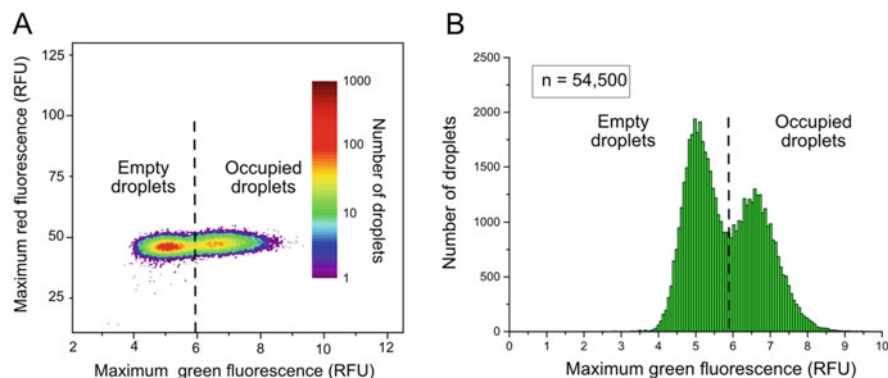


Fig. 18.6 Typical droplet fluorescence analysis profiles. (a) Red and green fluorescence distribution. The red and the green fluorescence of each droplet are measured. Whereas the fluorescence of the droplet tracker (red Cy5) is identical for all the droplets, those droplets in which PCR amplification took place have a strongly increased green fluorescence (6–8 RFUs emitted by intercalated EvaGreen) with respect to empty ones (4–6 RFUs). (b) Green fluorescence distribution. Only the distribution of the green fluorescence is shown and both droplet populations (empty and occupied) are labeled. Both representations allow to appreciate a 42% droplet occupancy

lengths of PTFE tubing filled with surfactant-free Novec 7500 fluorinated oil. One of the tubing is connected to Inlet 2 of the device, whereas the other one is connected to a flowmeter. A stream of surfactant-free Novec 7500 fluorinated oil is used to push the emulsion and infuse it into the microfluidic device. Another stream of surfactant-free Novec 7500 fluorinated oil is infused into the chip through Inlet 1 and used to space the reinjected droplets to make them distinguishable during fluorescence analysis.

The green (DNA content) and red (droplet detection) fluorescence of each droplet is recorded while it passes in front of the laser line of the optical set-up (see § 18.2.2) and the data are collected and analyzed in real time using a firmware operated by a user-programmable FPGA electronic card. Measuring the maximal green fluorescence intensity of each droplet (detected as red fluorescent objects) allows two populations to be observed (Fig. 18.6): a first population displaying a low green fluorescence (4–6 RFUs on Fig. 18.6) corresponding to droplets initially free of template DNA (empty droplets) and a second population displaying an increased

fluorescence (6–8 RFUs on Fig. 18.6) due to EvaGreen intercalation into amplified DNA and corresponding to occupied droplets.

Considering Poisson statistics, the fraction of occupied droplets directly gives access to the absolute DNA concentration using Eq. (18.2):

$$\lambda = -\ln(1 - \text{Occupancy}) \quad (18.2)$$

In the example shown on Fig. 18.6, 42% droplet occupancy allows to compute a λ value of ~ 0.55 target DNA molecule per 2.5 pL droplet, so an absolute concentration of ~ 0.22 target DNA molecule per pL.

18.3.2 Scenario 2: ddPCR Quantification of DNA Contained in Cells Using Sequence-Specific Probes

ddPCR can also be used to detect a target DNA (e.g., point mutations in cell genome or viral DNA inserted into host genome) contained in cells. Cells may have various origins but for the sake for simplicity we will consider the case of in vitro cultured cells in which GAPDH gene is detected using sequence-specific TaqMan probes.

18.3.2.1 Cells Preparation

HEK-293 cells (ATCC® CRL-1573) are prepared in a cell culture room in compliance with cell culture room rules. Cells are cultured in 75 cm² flask (BD Falcon) containing DMEM(1X) + GlutaMAX™-I (Gibco) supplemented with 10% of FBS (Gibco) and incubated at 37 °C and 5% CO₂. When reaching 80–90% confluence, cells are recovered through a 2–5 min incubation with 2 mL of 0.25% trypsin-EDTA in a CO₂ incubator until they start to detach from the flask. Then 8 mL of DMEM (1X) + GlutaMAX™-I supplemented with 10% of FBS are immediately added to inactivate trypsin, and cells are pelleted 5 min at 1000 rpm. Cells are washed with 7 mL of DPBS 1X prior to being counted using an automated cell counter (e.g., Luna™ Automated Cell Counter, Logos Biosystems).

18.3.2.2 Cells Emulsification

Cells are then individualized in large 100 pL droplets allowing to accommodate them. Moreover, to ease access to DNA, the cells are usually lysed upon encapsulation. To prevent unwanted prematured lysis, the cell-containing aqueous phase is combined on-chip with the lysis solution just prior to droplets production (Fig. 18.7a and b).

Cells are resuspended at a concentration of 16.10^6 cell/mL into DPBS 1X supplemented with 14% OptiPrep™ (a densifier allowing to keep cells in suspension during the encapsulation process), 2 μ M of Cyanine 5 carboxylic acid (to track droplets), and “ddPCR supermix for probes (no dUTP)” (Bio-Rad) to a 1x final concentration. The mixture is loaded into a length PTFE tubing and connected on one side to a flowmeter and, on the other side, to Inlet 1 of a 40 μ m deep cell encapsulation device (Fig. 18.7a) prepared as described above (see § 18.2.1.1 and

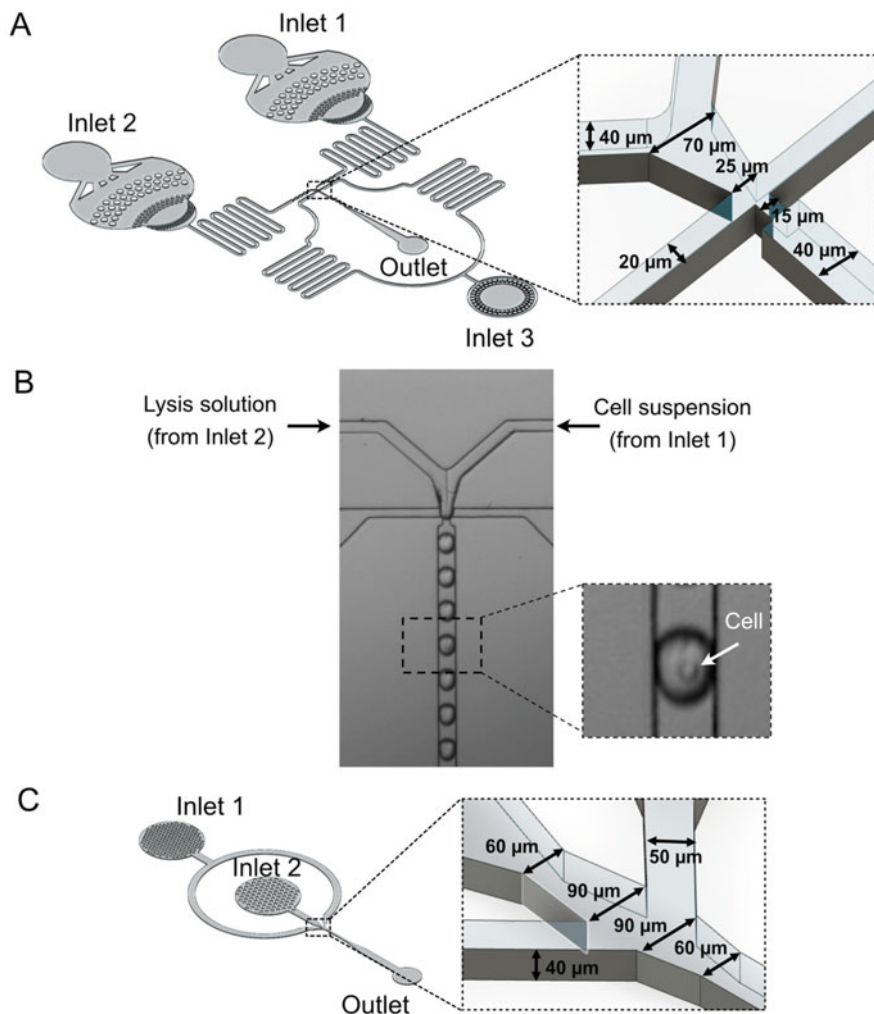


Fig. 18.7 Microfluidic devices used for the ddPCR quantification of DNA contained in cells. (a) Droplet generation microfluidic device. An aqueous phase containing cell suspension is infused through Inlet 1, whereas a lysis solution is infused through Inlet 2. Both solutions are briefly co-flow prior to being dispersed into 100 pL droplets upon pinching by two orthogonal flows of fluorinated oil supplemented with surfactant and infused through Inlet 3. The produced emulsion is collected at the Outlet of the chip. (b) Micrographs of the droplet generator in action. Difference in refractive index of each aqueous solution allows the co-flow to be visualized. Moreover, careful observation allows encapsulated cells to be distinguished (white arrow in the insert). (c) Droplet fluorescence analysis device. The emulsion to analyze is infused through Inlet 2 and the droplets are spaced by a fluorinated oil infused through Inlet 1. Finally, the emulsion leaves the device through the Outlet. The key dimensions of each device are given in the corresponding box

Table 18.3 Thermocycling conditions used for gene specific ddPCR amplification

Step	Temperature	Time	Cycle repeats
Initial denaturation/enzyme activation	95 °C	10 min	Not repeated
Denaturation	95 °C	10 sec	Repeated 44 times
Annealing/extension	60 °C	30 sec	
Enzyme deactivation	98 °C	10 min	Not repeated

18.2.1.2). In parallel, a lysis solution containing 1% Triton™ X-100, “ddPCR supermix for probes (no dUTP)” (Bio-Rad) to a 1x final concentration and GAPDH-specific primers/TaqMan probe mixture (PRIME-PCR probe assay qHsaCEP0041396-FAM, Bio-Rad) added to the recommended concentration is loaded into a length PTFE tubing and connected on one side to a flowmeter and, on the other side, to Inlet 2 of the microfluidic device. Both aqueous phases are infused at the same flow rate to mix both solutions one-to-one (Fig. 18.7b) prior to dispersing it into 100 pL by a stream of Novec 7500 fluorinated oil containing 3% fluorosurfactant infused in the chip through Inlet 3. As before, droplet production can be monitored thanks to Cy5 red fluorescence, and the emulsion is recovered in a collection device prepared before (see § 18.2.1.3). Upon collection, tubes are sealed as before (see § 18.3.1.3) and placed in a thermocycler in which the emulsion is subjected to the appropriate thermal-cycling program (Table 18.3).

18.3.2.3 Droplet Fluorescence Analysis and Quantification of Cells of Interest

As before (see § 18.3.1.4), upon thermocycling, the emulsion is reinjected from the collection tubing to a 40 µm deep droplet fluorescence analysis device (Fig. 18.7c) prepared as described above (see § 18.2.1.1 and 18.2.1.2). The emulsion is infused through Inlet 2 and droplets are spaced by a surfactant-free Novec 7500 fluorinated oil infused into the chip through Inlet 1. Droplets are detected by their red fluorescence and the presence of a cell containing the DNA of interest (in our example, every cell fulfills this condition as we choose to target a wild-type cellular gene) will be associated with an increased green fluorescence resulting from the degradation of the TaqMan probe during specific amplification. Therefore, simply measuring the fraction of droplet displaying high green fluorescence allows to immediately access to the absolute concentration of cells containing the DNA of interest using Eq. (18.2).

18.4 Conclusions: ddPCR for DNA Quantification and More

Since its introduction a few years ago, digital droplet PCR (ddPCR) appeared to be a powerful alternative to the more conventional qPCR when high accuracy and/or the capacity of detecting rare variants are required, as this might typically be the case in cancer-related studies [16]. For instance, searching for the early apparition of mutants in a complex population of cells/molecules typically requires to be able to

detect a low number of mutated DNA molecules diluted into a large excess of wild-type ones. In such scenario, qPCR would be rapidly saturated by the latter (e.g., by titration of amplification primers) and display a limited sensitivity. ddPCR does not suffer from such a limitation since each template DNA is individualized prior to being amplified, so that no competition occurs between templates. Therefore, ddPCR sensitivity is directly dictated by the number of compartments that can be analyzed; the more compartments can be analyzed, the better the sensitivity. Early developments established that, indeed, such digitalization allowed to increase the detection sensitivity of KRAS-coding gene mutants (an oncogene involved in the apparition of many cancers) from 5% using qPCR to 1/200,000 with ddPCR [14]. Such sensitivity makes it theoretically feasible to detect circulating free DNA or even to identify rare cells contained in a complex mixture (e.g., a tumor), since ddPCR can be performed on DNA from both origins.

ddPCR is now made broadly accessible by the commercialization of benchtop devices (e.g., QX series platforms from Bio-Rad). However, even though efficient and robust, such equipment usually handles a low number (i.e., tens of thousands) of large (nanoliter) droplets. Therefore, should a much higher number of droplets (i.e., millions) needed to be produced and analyzed (e.g., to detect ultra rare events or to amplify DNA while limiting PCR artifacts linked to unwanted recombination events), this chapter intends to provide the reader with the main guidelines to fabricate, set up, and use his/her own ddPCR platform and possibly widen its application scope with minor modifications. Using small pL droplets like those presented here, also makes it possible to further manipulate them in microfluidic-assisted manners, for instance, to modify their content on demand by liquid addition via droplet-droplet fusion [8, 13] or picoinjection [1]. This makes possible, for instance, to *in vitro* express (transcribe and possibly translate) the information carried by the previously amplified piece of DNA [13, 17]. Moreover, the measured droplet fluorescence can be used as a signal to trig droplet deflection in a sorting device [20], like the Fluorescence-Activated Droplet Sorter we developed [4]. Combining the use of these different devices enables to perform serial operations on droplets and doing so to set up ultrahigh-throughput functional screening pipelines like the microfluidic-assisted *In Vitro* Compartmentalization (μ IVC) and its derivative [6, 17]. Such pipelines allowed us, for instance, to develop optimized synthetic RNAs [3, 5, 18] or improved catalysts [2, 17] or even to characterize complex biological mechanisms like ribosome decoding [15]; a set of possible applications that all began with a ddPCR step.

Acknowledgments This work of the Interdisciplinary Thematic Institute “IMCBio,” as part of the ITI 2021-2028 program of the University of Strasbourg, CNRS, and Inserm, was supported by IdEx Unistra (ANR-10-IDEX-0002), by SFRI-STRAT’US project (ANR-20-SFRI0012) and EUR IMCBio (ANR-17-EURE-0023) under the framework of the French Investments for the Future Program as well as from the previous LabEx NetRNA (ANR-10-LABX-0036). This work was also supported by the “Centre National de la Recherche Scientifique” (CNRS), the “Université de Strasbourg,” and its Initiative of Excellence (IdEx).

References

1. Abate AR, Hung T, Mary P, Agresti JJ, Weitz DA (2010) High-throughput injection with microfluidics using picoinjectors. *Proc Natl Acad Sci U S A* 107:19163–19166
2. Autour A, Ryckelynck M (2017) Ultrahigh-throughput improvement and discovery of enzymes using droplet-based microfluidic screening. *Micromachines-Basel* 8:128
3. Autour A, Jeng SCY, Cawte AD, Abdolazadeh A, Galli A, Panchapakesan SSS, Rueda D, Ryckelynck M, Unrau PJ (2018) Fluorogenic RNA mango aptamers for imaging small non-coding RNAs in mammalian cells. *Nat Commun* 9:656
4. Baret JC, Miller OJ, Taly V, Ryckelynck M, El-Harrak A, Frenz L, Rick C, Samuels ML, Hutchison JB, Agresti JJ et al (2009) Fluorescence-activated droplet sorting (FADS): efficient microfluidic cell sorting based on enzymatic activity. *Lab Chip* 9:1850–1858
5. Bouhedda F, Fam KT, Collot M, Autour A, Marzi S, Klymchenko A, Ryckelynck M (2020) A dimerization-based fluorogenic dye-aptamer module for RNA imaging in live cells. *Nat Chem Biol* 16:69–76
6. Bouhedda F, Cubi R, Baudrey S, Ryckelynck M (2021) μ IVC-Seq: a method for ultrahigh-throughput development and functional characterization of small RNAs. *Methods Mol Biol* 2300:203–237
7. Bustin SA, Benes V, Garson JA, Hellemans J, Huggett J, Kubista M, Mueller R, Nolan T, Pfaffl MW, Shipley GL et al (2009) The MIQE guidelines: minimum information for publication of quantitative real-time PCR experiments. *Clin Chem* 55:611–622
8. Chabert M, Dorfman KD, Viovy JL (2005) Droplet fusion by alternating current (AC) field electrocoalescence in microchannels. *Electrophoresis* 26:3706–3715
9. Ginzinger DG (2002) Gene quantification using real-time quantitative PCR: an emerging technology hits the mainstream. *Exp Hematol* 30:503–512
10. Glokler J, Lim TS, Ida J, Frohme M (2021) Isothermal amplifications - a comprehensive review on current methods. *Crit Rev Biochem Mol Biol* 56:543–586
11. Holtze C, Rowat AC, Agresti JJ, Hutchison JB, Angile FE, Schmitz CHJ, Koster S, Duan H, Humphry KJ, Scanga RA et al (2008) Biocompatible surfactants for water-in-fluorocarbon emulsions. *Lab Chip* 8:1632–1639
12. Ma C, Wang W, Mulchandani A, Shi C (2014) A simple colorimetric DNA detection by target-induced hybridization chain reaction for isothermal signal amplification. *Anal Biochem* 457:19–23
13. Mazutis L, Araghi AF, Miller OJ, Baret JC, Frenz L, Janoshazi A, Taly V, Miller BJ, Hutchison JB, Link D et al (2009) Droplet-based microfluidic systems for high-throughput single DNA molecule isothermal amplification and analysis. *Anal Chem* 81:4813–4821
14. Pekin D, Skhiri Y, Baret JC, Le Corre D, Mazutis L, Salem CB, Millot F, El Harrak A, Hutchison JB, Larson JW et al (2011) Quantitative and sensitive detection of rare mutations using droplet-based microfluidics. *Lab Chip* 11:2156–2166
15. Pernod K, Schaeffer L, Chicher J, Hok E, Rick C, Geslain R, Eriani G, Westhof E, Ryckelynck M, Martin F (2020) The nature of the purine at position 34 in tRNAs of 4-codon boxes is correlated with nucleotides at positions 32 and 38 to maintain decoding fidelity. *Nucleic Acids Res* 48:6170–6183
16. Quan PL, Sauzade M, Brouzes E (2018) dPCR: a technology review. *Sensors* 18
17. Ryckelynck M, Baudrey S, Rick C, Marin A, Coldren F, Westhof E, Griffiths AD (2015) Using droplet-based microfluidics to improve the catalytic properties of RNA under multiple-turnover conditions. *RNA* 21:458–469
18. Trachman RJ 3rd, Autour A, Jeng SCY, Abdolazadeh A, Andreoni A, Cojocar R, Garipov R, Dolgosheina EV, Knutson JR, Ryckelynck M et al (2019) Structure and functional reselection of the mango-III fluorogenic RNA aptamer. *Nat Chem Biol* 15:472–479
19. Vogelstein B, Kinzler KW (1999) Digital PCR. *Proc Natl Acad Sci U S A* 96:9236–9241
20. Xi HD, Zheng H, Guo W, Ganan-Calvo AM, Ai Y, Tsao CW, Zhou J, Li W, Huang Y, Nguyen NT et al (2017) Active droplet sorting in microfluidics: a review. *Lab Chip* 17:751–771



Emerging Microfluidic and Biosensor Technologies for Improved Cancer Theranostics

19

David Caballero, Catarina M. Abreu, Rui L. Reis,
and Subhas C. Kundu

Abstract

Microfluidics and biosensors have already demonstrated their potential in cancer research. Typical applications of microfluidic devices include the realistic modeling of the tumor microenvironment for mechanistic investigations or the real-time monitoring/screening of drug efficacy. Similarly, point-of-care biosensing platforms are instrumental for the early detection of predictive biomarkers and their accurate quantification. The combination of both technologies offers unprecedented advantages for the management of the disease, with an enormous potential to contribute to improving patient prognosis. Despite their high performance, these methodologies are still encountering obstacles for being adopted by the healthcare market, such as a lack of standardization, reproducibility, or high technical complexity. Therefore, the cancer research community is demanding better tools capable of boosting the efficiency of cancer diagnosis and therapy. During the last years, innovative microfluidic and biosensing technologies, both individually and combined, have emerged to improve cancer theranostics. In this chapter, we discuss how these emerging—and in some cases unconventional—microfluidics and biosensor technologies, tools, and concepts can enhance the predictive power of point-of-care devices and the development of more efficient cancer therapies.

D. Caballero (✉) · C. M. Abreu · R. L. Reis · S. C. Kundu (✉)

3B's Research Group, I3Bs – Research Institute on Biomaterials, Biodegradables and Biomimetics, University of Minho, Headquarters of the European Institute of Excellence on Tissue Engineering and Regenerative Medicine, Barco, Guimarães, Portugal

ICVS/3B's – PT Government Associate Laboratory, Braga/Guimarães, Portugal

e-mail: dcaballero@i3bs.uminho.pt; kundu@i3bs.uminho.pt

© The Author(s), under exclusive license to Springer Nature Switzerland AG 2022

461

D. Caballero et al. (eds.), *Microfluidics and Biosensors in Cancer Research*,

Advances in Experimental Medicine and Biology 1379,

https://doi.org/10.1007/978-3-031-04039-9_19

Keywords

Biosensors · Cancer diagnosis · Cancer therapeutics · Microfluidics · Personalized medicine · Point-of-care

19.1 Introduction

Early cancer diagnosis is fundamental for selecting the adequate therapeutic approach and improving patients' prognosis. Traditionally, tissue biopsy has been the gold standard for diagnosing and profiling the tumor [1]. This method is reasonably efficient and provides valuable information about the tumor's genetic profile helping physicians take decisions. However, tissue biopsy is highly invasive since it relies on the physical sampling of the tumor for pathologic analysis. Additionally, the high heterogeneity of the tumor can make that the gathered data is not representative of the actual tumor, which may lead to a wrong diagnosis and, consequently, to a non-effective treatment. This situation has generated the need for more sensitive, reliable, and efficient diagnostic, modeling, and screening technologies that are also predictive and simple.

During the last decade, a new paradigm has emerged in the field of in vitro models capable to emulate the complex physiology (e.g., cellular, biological, and biochemical content), hydrodynamic events (e.g., fluid flow, shear stress), and mechanical properties (e.g., physical forces, matrix rigidity) of the native tumor microenvironment (TME), as well as the functionality of human tissues and organs, within a microfluidic device. This new technology was coined *organ-on-a-chip* (OoC), and has revolutionized the field of disease modeling, diagnosis, and drug screening. OoC overcomes the limitations of traditional cell culture methods based on static and flat platforms, which fail in reproducing the complexity of the in vivo scenario [2], and importantly, using minute volumes of sample and reagents, making this methodology highly efficient compared to traditional approaches based on solid biopsies. Microfluidic OoC can further be employed to detect and isolate tumor biomarkers, which are present in peripheral blood, such as circulating tumor cells (CTCs), extracellular vesicles, antibodies, or DNA/RNA (ctDNA/RNA). Compared to conventional methods, such as tumor biopsy mentioned above, microfluidics can accelerate the early detection and diagnosis of the disease and evaluating treatments prior to testing them on patients.

Throughout the last years, a large plethora of microfluidic OoC has been developed, such as the lung [3–5], heart [6], spleen [7], gut [8], liver [9], kidney [10], brain [11], or vasculature [12, 13], among many others [14]. Significantly, tumor-on-a-chip models have also been developed to investigate the mechanism of action of drugs or the etiology of the disease. This type of microfluidic model of tumors has been extensively reviewed [15], and it is the focus of a specifically-dedicated chapter in the book (see Chap. 6—Das and Fernández). An essential feature of organ- or tumor-on-a-chip technology is integrating one or several tissues. Therefore, they can

be employed to investigate the efficacy of treatments and side effects (e.g., toxicity) in other distant tissues.

The interest in OoC has increased upon the integration of miniaturized sensors on-chip for the real-time and continuous monitoring of critical physiological (physical, chemical, and biological) parameters. This cutting-edge technology has already demonstrated its potential for investigating critical factors involved in tumorigenesis or for the accurate evaluation of pharmacological compounds' efficacy (or toxicity). In this regard, they are pivotal for monitoring tumor evolution and therapy response, being an essential tool for the cancer research community [15, 16]. Additionally, microfluidic-integrated biosensors can also contribute to gaining new insights into the effect of metabolic products.

Overall, the combination of innovative microfluidics and biosensor technologies provides a unique opportunity to advance in cancer theranostics by enhancing the reliable detection of tumor biomarkers and the evaluation of anti-cancer drugs' effects. In this chapter, we discuss the latest advances and emerging technologies in microfluidics and biosensors for the development of point-of-care devices capable of providing novel therapeutic solutions and improving the prognosis of cancer patients.

19.2 Biosensor Technologies for Cancer Diagnosis and Therapy Monitoring

Biosensors are (bio-) analytical devices employed in healthcare-related applications to quantify biological and biochemical processes by converting a biorecognition event of interest into a readable electronic signal proportional to the analyte content [17, 18]. Biosensors have experienced enormous growth during the last decades due to their high utility in healthcare and disease management. Figure 19.1 shows the evolution of biosensors since the invention of the glucose sensor pioneered by Clark and Lyons in 1962 [19]. Biosensors have improved their miniaturization and portability capacity over the years [21], boosting their use in the clinics and pharmaceutical/biotechnology industry. Biosensors emerged to replace the traditional analytical assays used in research and clinical laboratories, such as the widely utilized enzyme-linked immunosorbent assay (ELISA). Despite their efficiency, these conventional methods can be time-consuming and laborious, and more importantly, they lack the needed automation and continuous and real-time quantification as demanded by modern medical approaches. New biosensing technologies and methods can provide multiple advantages for the detection of specific analytes in solution, such as a faster response time and higher sensitivity.

The final performance of biosensors is determined by several key parameters that affect their sensitivity and selectivity, including their size, architecture, and (bio-) recognition elements. Other attributes of a suitable biosensor include high specificity, reproducibility, and stability. Altogether, the successful accomplishment of these characteristics depends on the type of transducer and method employed to detect the pathophysiological event. Typical transducer methods include *optical*,

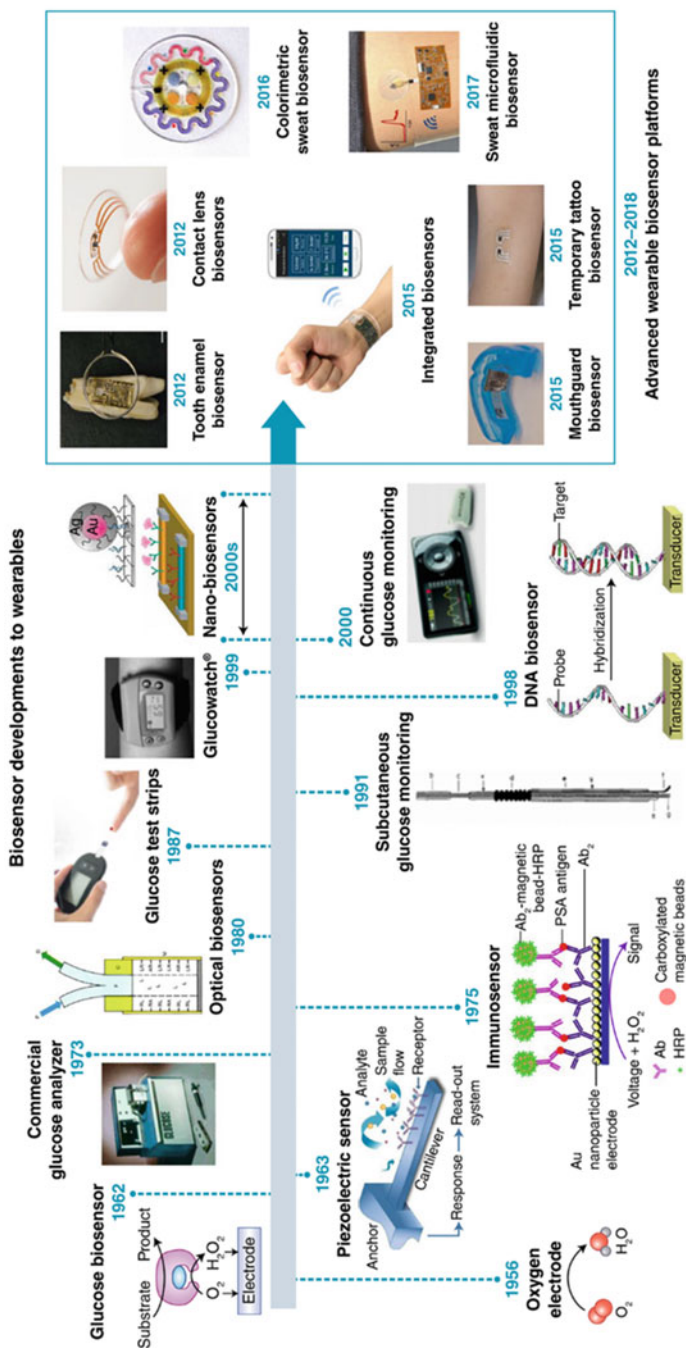


Fig. 19.1 Biosensor development panorama. (Left) Time-frame of biosensor development since the invention of the glucose biosensor by Clark and Lyons in 1962 [19]. (Right) Advanced wearable biosensors. Reproduced with permission from the publisher [20]

electrochemical, magnetic, thermal, or mass sensitive. Optical and electrochemical detections are undoubtedly preferred for their simple integration within microfluidic devices. This is due to their easy miniaturization capability and compatibility with microfabrication procedures [22–24]. Regarding optical biosensors, and in addition to traditional fluorescence characterization of the cellular state, methods based on surface plasmon resonance (SPR) and evanescent waves have been widely explored. The main reason is their efficacy, simplicity, and high capacity of miniaturization of the electrodes and other sensing elements. For electrochemical sensors, their miniaturization and compatibility with microfabrication technologies also facilitate for their integration within microfluidic devices. Both types of sensing methods provide similar outcomes, even though the electrochemical ones have, in general, a superior performance considering their specificity, response time, and low cost, among other advantages.

In the following, we describe the current and emerging field of biosensors in cancer research, including classical approaches and more sophisticated trends. The objective of this section is not to describe in detail all the available (electrochemical and optical) sensing techniques applied to cancer theranostics but to give a brief overview of some of the available methods, technologies, and possibilities. For more information, the readers may consult the chapter(s) specifically dedicated to biosensors within the book (see Chap. 1—Barreiros dos Santos et al.) or specialized reviews on the topic [22, 25].

19.2.1 Current Trends in Biosensors

19.2.1.1 Electrochemical-Based Methods

Most of the 3D biosensors devices used in cancer diagnosis are based on electrochemical transducers. The main reason behind this preference is their improved sensitivity, selectivity, and efficiency compared to other transduction methods. Their simplicity and low production cost also make electrochemical biosensors the preferred option for cancer researchers.

In electrochemical-based biosensors, the specific molecular recognition of the analyte of interest by the immobilized biorecognition element changes the interfacial charge, capacitance, resistance, mass, and thickness at the sensor surface. This change can be measured by different electrochemical techniques to quantitate the amount of target analyte detected. Different measurement methods are available within electrochemical transducers, but the most utilized ones include the following:

- *Electrochemical impedance spectroscopy* is a powerful technique that measures small changes in the resistive and capacitive properties in a liquid media and/or in the electrode surface by perturbing the system. It analyzes the impedance ($Z = V/I$) of the observed system as a function of the frequency and excitation signal to provide quantitative information about the conductance, the dielectric coefficient, and the static properties of the interfaces of a system, and its dynamics change due to adsorption or change-transfer phenomena. The electrochemical impedance Z is

usually measured by applying an AC—sinusoidal—potential V (of frequency ω) to an electrochemical cell using a three-electrode potentiostat then measuring the current I through it. Impedimetric detection is primarily used to develop affinity biosensors to, e.g., monitor binding events, such as antibody–antigen-specific interactions on an electrode surface. In this case, the small changes in impedance are proportional to the concentration of the measured antigen.

- *Voltammetry/Amperometry* techniques are based on applying a potential to a working electrode vs a reference electrode and measuring the resulting current, which occurs from the electrochemical oxidation/reduction reactions at the working electrode of a given electroactive species, typically dissolved in an electrolyte solution. In voltammetry, the potential is scanned over a set potential range (e.g., cyclic voltammetry, differential pulse voltammetry, square-wave voltammetry, and others). In amperometry, changes in the current I produced by the oxidation/reduction are monitored directly with time at a constant potential at the working electrode with respect to the reference one. The current is proportional to the concentration of the electroactive species in the sample [25].
- *Potentiometry* measures the potential between two electrodes (a working and a reference electrode) in an electrochemical cell at a negligible current. The glass pH and the ion-selective electrodes (K^+ , Ca^{2+} , Na^+ , Cl^-) are examples of potentiometric sensors that can be turned into biosensors by coating them with a biological element, such as an enzyme, that catalyzes a reaction that forms the ion [25].

Despite their inherent advantages, electrochemical biosensors can suffer from certain drawbacks, such as cross-reactivity with interfering species, particularly for potentiometric methods. In contrast, electrochemical biosensors are compatible with a high miniaturization capacity that enables the integration of microelectrodes within microfluidic devices for the continuous monitoring of target analytes, as already mentioned [26]. Such integration capacity also enables their use as actuators, e.g. the manipulation and capture of rare cancer cells [27, 28].

19.2.1.2 Optical-Based Biosensors

Optical biosensors have been massively utilized in different research fields and sectors, including (bio) medicine, biotechnology, pharmacology, food safety, and environmental monitoring, among others. Some examples of daily-used optical biosensors include pH test strips, pregnancy tests, or the recently developed COVID-19 test. This high applicability results from their small dimensions, low LoD, and high sensitivity, which make them ideal tools for the rapid, multiplexing, and real-time detection of cancer biomarkers [22]. Optical-based biosensors offer some advantages when compared to their electrochemical counterparts. In particular, certain optical-based methods enable the label-free detection of analytes of many biological and chemical compounds remotely. Additionally, other type of optical components, such as laser diodes or lenses, can be scaled down and miniaturized, which enables their integration within microfluidic devices [29].

Optical biosensors can be divided into two main categories, namely *label-free* and *label-based*. The former is based on detecting the signal generated directly by the interaction of the analysed substance with the transducer [30]. The latter is based on using a label to generate an optical signal (fluorescent, colorimetric, luminescent) that can be detected, such as a fluorescently-labeled antibody. Biorecognition elements can be very heterogeneous, and besides antibodies, other types of elements can be utilized, such as antigens, nucleic acids, cells, or tissues, among others. Next, the detection is performed by analyzing the interaction of the optical signal with the element, substance, or compound of interest. Typical optical transducer methods include evanescent waves (e.g., surface plasmon resonance—SPR, optical waveguide lightmode spectroscopy—OWLS), interference (e.g., Mach–Zehnder interferometer), resonators (e.g., atomic force microscopy cantilevers), fluorescence (e.g., confocal microscopy), absorbance (e.g., UV/vis absorbance), or chemo/bio-luminescence, among others. These methods are straightforward, and the optical signal is captured by sensitive detection methods, such as a standard CCD camera or a photomultiplier device. In the following, we briefly comment on the most predominant optical-based biosensors:

- *Surface plasmon resonance* is one of the most typical optical-based biosensing methods that allow the direct, label-free, and real-time detection of analytes. The working mechanism of SPR biosensors is based on the illumination with polarized light (typically, a laser beam) of a thin metal surface (the sensor electrode), normally gold, at a specific angle and at the interface of two media (e.g., metal and fluid). This generates surface plasmons in the metal, which reduces the intensity of the reflected light at a specific resonance angle and is proportional to the adhered mass [30]. The analyte can be detected by measuring the shift in the refractive index, angle, or wavelength in a kinetic analysis (i.e., as a function of time). Typically, the metal surface of an SPR chip is functionalized with a biorecognition element, such as an antibody. Then, the chip is inserted into a fluidic system for analyte-ligand detection. SPR is very popular in optical biosensing methods, and indeed, commercial instruments are available, such as the well-known Biacore™. One key feature of SPR is that it can also be employed for “imaging” by using a microarray chip (typically, an array of circular metallic spots), thus allowing simultaneous imaging and quantification of the biosensing events. Finally, the performance of standard SPR can be enhanced using metallic nanostructures resulting in *Localized SPR (LSPR)*. The main difference between traditional SPR and LSPR is that the induced plasmons resulting from the incident light oscillate locally on the nanostructures and not at the metal/fluid interface. In LSPR, the absorbance occurs within the ultraviolet-visible band. In this case, the biosensing event using functionalized nanostructures is based on spectral shifts, that is, color change and absorption peak shifts.
- *Evanescent waves*: This method exploits the biological recognition between the analyte and the ligand within the limited specimen region of an evanescent wave (or field). The incidence of the light at the interface of a substrate and a surrounding medium with a lower refraction index generates the evanescence

wave. This wave has a limited penetration depth from the surface, typically 100–200 nm, and therefore, only events occurring near the surface can be detected/imaged. This has an associated advantage, since it reduces significantly the background noise (only the molecules/binding events at the surface are excited/detected). Evanescent wave sensing methods can be label-free or label-based. Examples of these two modes are, respectively, the *optical waveguide lightmode spectroscopy* (OWLS) or the *total interference reflection fluorescence* (TIRF) microscopy.

The intrinsic properties of the above-mentioned electrochemical- and optical-based sensing systems enable their faithful integration into microfluidic devices to exploit the analytical improvement associated with reducing size. This is in addition to other intrinsic benefits of microfluidics by itself, such as the well-known reduced consumption of reagents or the possibility of automation (see Sect. 19.3.1). However, despite some successful examples, this type of biosensors displays some limitations and bottlenecks in terms of miniaturization, integration, and performance. In the following section, we describe novel trends in this field to enhance biosensor sensitivity and signal-to-noise ratio, and therefore, reduce the detection limit.

19.2.2 Emerging Biosensor Methods

Currently, there is a myriad of innovative biosensing methodologies being developed for cancer research applications. Among all of them, a few have encountered particular attention by the cancer research community due to their high performance and clinical potential. These include three-dimensional (3D), wearable, implantable, and flexible biosensors (Fig. 19.2). In the following, we briefly discuss their main characteristics and applications, describing some representative examples of each technique.

19.2.2.1 Three-Dimensional Biosensors

Current cancer diagnostic and screening assays used in the clinics mainly rely on imaging and tissue biopsy. These methods typically require the use of complex and expensive technologies or tedious procedures. In some instances, these methodologies lack the needed sensitivity and specificity to detect the tumor at an early stage. Importantly, these procedures cannot evaluate continuously the health condition of the patient and their response to therapy. As aforementioned, biosensors offer advanced capabilities for the constant monitoring of patient condition through the accurate screening of predictive biomarkers that may help to evaluate the efficacy of anti-cancerous drugs.

Traditional biosensors rely on two-dimensional (2D) surfaces decorated with the biorecognition layer. However, such planar surfaces are typically associated with poor analytical performance, such as a low limit of detection or a narrow dynamic range, resulting from the limited amount of analyte that can be captured. Other

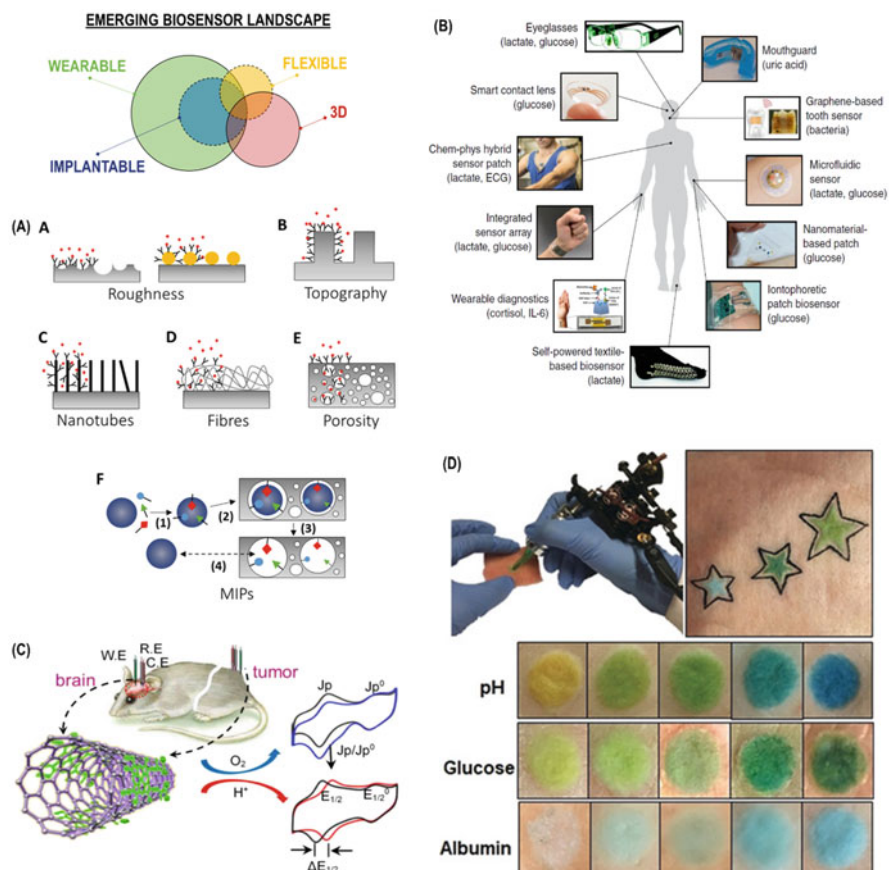


Fig. 19.2 Emerging biosensor technologies. (a) Three-dimensional biosensors and the typical architectures used for their build-up [1]; (b) wearable biosensors and specific examples reported [20]; (c) implantable biosensor for the intravital detection of predictive pH and O₂ tumor biomarkers [31]; and (d) flexible biosensors and an example based on a tattoo system [32]. *Figures reproduced with permission from the publishers*

typical limitations of 2D biosensors include a lack of flexibility (i.e., they are mainly based on rigid surfaces) that limits their capability to be implanted or used as a wearable device (see below) [33]. Next, a significant limitation of planar (micro-) electrodes when integrated within microfluidic devices is the effect of shear stress. The magnitude of these hydrodynamic forces can detach (or inhibit) the binding between the biorecognition element and the analyte of interest. To solve this, a new generation of biosensors has emerged to improve their performance in capture efficiency and sensitivity. These are 3D biosensors, which typically display a 3D architecture with a larger roughness, porosity, and/or topographic features, which enhances the electrode area and the amount of immobilized (captured) biorecognition elements (analyte), and therefore, the overall sensitivity of the sensor

(Fig. 19.2a) [1]. Some examples of 3D biosensor platforms fitting within this category include topographically-structured materials, vertically-aligned nanotubes, electrodeposited fibrillary networks, hydrogel and polymers, nanocomposites, or molecular-imprinted polymers. These 3D structures can be fabricated through a diversity of micro/nano/bio-fabrication methods (e.g., UV-photolithography and physical/chemical etching—for structured materials; bioprinting—for hydrogels; freeze-drying—for scaffolds; electrospinning—for fibrillary networks; and others). Typically, hydrogels and/or polymers are used for manufacturing 3D biosensors because they provide a native-like environment for maintaining the activity of the biorecognition elements, such as antibodies. The integration of sensing micro- and nanostructures into the 3D biomaterials can significantly enhance the performance of biosensors due to the larger active surface area that results in a superior electrochemical or photonic behavior. Probe-free biosensors, such as molecular-imprinted polymers (MIPs), have also been reported with the advantage of not relying on biomolecules that lose their activity over time (Fig. 19.2a). An advantageous feature of MIPs is that they can mimic the natural recognition entities (e.g., antibodies, proteins, and others). However, probe-free biosensors display reduced sensitivity/specificity compared to their immobilized counterparts. Finally, the enhanced analytical performance of 3D biosensors made them ideal candidates for being integrated within microfluidic devices resulting in more efficient point-of-care systems. This combination may provide more advanced tools to measure clinically-relevant parameters with ultrahigh precision in a fast, selective, and quantitative way, and therefore, with the potential to revolutionize the field of medical diagnostics. However, the translation of 3D biosensors to the clinics is still unrealistic. This is because it is not yet clear whether 3D biosensors integrated within microfluidic chips can actually solve the limitations of traditional analytical technologies. One of the main reasons is that most tests for *in vitro* biomarker detection are typically based on blood extraction and analysis. Therefore, it is not envisioned how 3D biosensors and microfluidics can overcome this. One solution may be to fabricate these 3D structures with biocompatible and flexible materials, making them especially interesting as implantable point-of-care devices. Other bottlenecks may include a limited multiplex capability, reproducibility, assay duration, or stability. Multiplex capability can easily be achieved using multiple microfluidic chips with the 3D sensing entities in parallel for the simultaneous detection of several analytes [34]. In any case, 3D biosensors are expected to establish a new paradigm in clinical settings despite these limitations. For this, though, they may have to display advanced features, such as wearable, implantable, and/or flexible characteristics, as described below.

19.2.2.2 Wearable Biosensors

Wearable biosensors have tremendously progressed during the last years due to the advances in microelectronics, nanotechnology, and the growing health awareness from the population. As described in recent excellent reviews [35–38], wearable biosensors can monitor in real time health status, such as vital signs (e.g., heart rate) or exercise activity (e.g., calorie consumption) of patients. Indeed, some of these

wearable biosensors are already well-established medical products, providing a portable alternative to traditional analytical instruments [35–37]. Following the success of minimally-invasive—transdermal—glucose sensors [39], wearable biosensors have now focused their efforts toward clinical applications for monitoring predictive biomarkers of health condition, thus avoiding the need for painful (and invasive) procedures of periodic blood sampling [20]. The main objective of advanced biosensing systems is to alert the user and medical team of an abnormal situation early in advance. In this regard, wearable biosensors are expected to revolutionize the management of certain chronic diseases, particularly cancer.

To date, a multitude of wearable biosensors has been reported for the detection of analytes in body fluids, including tears (ocular biosensors), saliva (oral biosensors), or sweat and interstitial fluid (epidermal biosensors), among others (Fig. 19.2b) [20, 38, 40–43]. These body fluids are a valuable source of—predictive—molecular disease biomarkers, such as ions, small molecules, and proteins. Body fluids may be a valuable “supplier” of clinically-useful information for cancer diagnosis and therapy monitoring. Among all the types of wearable biosensors, epidermal ones have received a larger attention due to the superior accessibility and availability of skin in the body. The working mechanism of these sensors is typically based on using—hollow and solid—micro/nano-needle patches for the sampling of sweat or dermal interstitial fluid in contact with the sensing biorecognition element [44–46]. In general, the interstitial fluid provides more systemic (and relevant) information due to its blood origin, even though its sampling is slightly more invasive than that for sweat. Typically, needles-based sensors are fabricated using rigid materials that penetrate the dermis, such as metals and polymers, even though hydrogels-based needles have also been utilized [45]. The needles can also be combined with more flexible and stretchable materials to reproduce the skin’s mechanical properties and better accommodate the sensing patch on-site. Interestingly, micro/nano-needles have already demonstrated their utility as a wearable for cancer biosensing applications. For example, they have recently been employed for the *in situ* detection and quantification of miRNA-210, a circulating molecule that correlates with melanoma recurrence [47]. The detection of this marker was performed by the incubation of the patch with DNA intercalator solution, which produced a detectable fluorescence signal proportional to the DNA concentration. However, for this application, a microscope was needed to detect the signal. Thus, its wearable applicability is limited. Similarly, a micro-needles wearable biosensor was also used to rapidly screen melanoma [48]. In this pioneering work, the sensor was capable of detecting the presence of tyrosinase enzyme, a cancer biomarker, in the presence of its catechol substrate immobilized on the surface of the sensor transducer. Upon detection, catechol rapidly converted to benzoquinone and electrochemically detected with a signal proportional to the biomarker level. The sensor was interfaced with a conformal flexible electronic board, thus enabling their use as a wearable device with wireless data transmission. Typically, for this type of flexible board, soft materials are preferred to integrate electronics. On many occasions, the sensing part is also fabricated with biocompatible conductive polymers, which are also flexible [49–51]. In this regard, the use of the traditional PDMS (Sylgard 184, 10:1 w/w

pre-polymer/crosslinker) typically used in lab-on-a-chip applications is not appropriate due to its high rigidity (Young modulus— $Y \sim 3$ MPa). A softer elastomer, such as Ecoflex™ displaying a rigidity reminiscent of the human skin ($Y \sim 125$ kPa) could alternatively be used to fabricate soft sensing entities, and importantly, be tailored with electrochemical, optical, or mechanical properties [35]. Finally, some needle-free sampling methods of interstitial fluid have also been proposed, being the so-called reversed iontophoresis the most popular one due to its simplicity. In brief, a low electric current is applied across the skin, promoting the transmigration of biomarkers across the blood vasculature and to the skin surface [52]. Despite its efficacy, this approach may induce skin irritation and pain.

Wearable epidermal biosensors have also been combined with soft and flexible microfluidic channels [53–55]. This type of approach enables the transport (and accumulation) through capillary forces of the target analyte present in sweat or interstitial fluid toward the sensing area for its *in situ* analysis, preventing fluid evaporation or contamination. As a representative example, these cutting-edge systems have been recently employed to capture and analyze the levels of lactate, glucose, chloride ion concentrations, or pH present in sweat during physical activity [54]. This revolutionary device integrates a colorimetric transducer with wireless communication electronics to transmit information about the result of the chemical analyses. Importantly, this device was validated in human studies, demonstrating the functionality of the microfluidic-integrated biosensor.

Similarly, a soft microfluidic chip integrating an electrochemical biosensor was mounted on the skin for real-time patient-driven sweat analysis of critical metabolites (lactate and glucose) levels [46]. This biosensing chip merged microfluidics and electrochemical detection technologies in a flexible electronic board to transmit the gathered on-body measurements from a patient to a mobile phone via a wireless connection. This type of approach is an area of special interest in the clinics, particularly in oncology, and to all the healthcare industry [56]. Indeed, some proof-of-concept results have illustrated its potential as a non-invasive method for detecting and screening excreted biomarkers and discriminating between healthy and non-healthy patients [57, 58]. In some cases, though, the biomarkers' detection and profiling was performed off-chip by standard analytical approaches to distinguish between controls, primary tumor, or metastasis using a panel of volatile organic compounds [57].

One of the main challenges of wearable biosensors is to guarantee the stability of the affinity capture probes over prolonged exposure periods within an environment that is mechanically active and whose composition evolve, such as for sweat. Other challenges include (i) the biocompatibility of all the sensing elements in contact with the body to avoid biofilm formation at the sensing interface, (ii) guarantee an efficient transport of sample over the sensor area (in particular for microfluidics-integrated biosensors), (iii) to ensure the proper calibration of the biosensor, and (iv) to engineer miniaturized power supplies, in particular for electrochemical-based sensors [20]. For the latter, the energy can be scavenged from the body movement by using, e.g., non-toxic piezoelectric materials [59]. Indeed, modern piezoelectric biomaterials for clinical applications avoid the toxicity of conventional piezoelectric

materials, being additionally biodegradable eliminating the need for surgical extraction in case of implantation. Next, modern wearable biosensors must be capable of monitoring different types of clinically-valuable signals to provide more accurate information of patient condition. For this, different sensing modalities (e.g., optical, electrochemical, and others) may be combined in hybrid wearable biosensor patches, as recently reported [43]. Finally, and as discussed in ref. [35], future commercial biosensors may need to address the problem of attachment (and detachment) of the disposable components (e.g., sensing elements, adhesives) in a region exposed to movement, bathing, non-desired sweating, or irritation.

19.2.2.3 Implantable Biosensors

Implantable biosensors are defined as those sensing devices implanted within the human body. They share some similarities with wearable biosensors, and actually, they are considered a sub-group of them (Fig. 19.2) [60]. This type of sensor also allows the real-time and continuous monitoring of the vital signs and health status of individual (cancer) patients. They can provide valuable information about the effect of a therapeutic compound without the need for invasive biopsies or laborious imaging/analytical procedures; only an initial surgery may be needed for their implantation. In general, implantable biosensors also show flexible characteristics to accommodate their morphologies to the region around tissues or organs where they are implanted (see Sect. 19.2.2.4). However, there are several examples of non-flexible implantable biosensors, such as the pacemaker or the glucose level pump. In this case, the miniaturization of the sensing device is sufficient for their operational purpose without producing any discomfort or pain. A particular feature of implantable biosensors that distinguishes them from wearable ones is that they are localized (i.e., implanted) within the human body. This is associated with specific requirements that all implantable biosensors must accomplish. In particular, they must be highly biocompatible to avoid (i) the foreign body immune response; (ii) inflammation; (iii) the formation of fibrotic tissue around the sensor; and (iv) the formation of biofouling around the sensing area.

Additionally, it is desirable to design biosensors that maintain their proper functionality over long periods and, eventually, display biodegradable properties to ensure its clearance when they are not anymore needed. Other key features of implantable biosensors are the need for reliable data transmission and power supply. For the former, in some instances, this is done by physical means (e.g., transcutaneous cables), but this can produce discomfort to the patient, or there is the risk of infection/rupture, among other potential issues [61]. In this regard, wireless transmission is preferred to communicate the data through electromagnetic induction (remote powering) by radio frequency, typically at a high-ultrahigh MHz frequency band. Usually, this method is based on integrating miniaturized antennas and transceiver units, among other miniaturized components, to transmit outside the body. Regarding the power supply, an external system can be employed for powering the implantable devices. These are located either outside or inside the body. The formers are typically very bulky and the latter may require invasive surgeries to recharge them; both situations are obviously undesirable. To solve

this, advances in materials science, microelectronics, and nanotechnology have resulted in the development of more advanced power supply systems, such as piezoelectric materials that can scavenge the energy generated by body motion.

Implantable biosensors have an enormous potential for the early detection of predictive tumor biomarkers (for a more detailed list of tumor biomarkers for each type of tumor, the readers are referred to Chap. 4 by Caballero et al., within the book, or to specialized literature). These biomarkers can be of different types, such as cellular (i.e., detection of disseminated tumor cells by using smart cancer traps [62]) or biochemical (i.e., detection of specific compounds released by the tumor or perturbed levels of particular markers). For the latter, low pH and O₂ levels (i.e., hypoxia) are characteristic of the tumor microenvironment, and are considered well-established markers. Therefore, implantable biosensors targeting pH and O₂ levels may work as “sentinels” to detect the onset of the tumor in real-time and provide valuable information before the tumor starts disseminating. Indeed, this approach was followed using a simple electrochemical biosensor for the simultaneous detection of these two parameters and implanted *in vivo* in a mice model [31]. The sensing electrodes were based on carbon nanotube fibers functionalized with specific molecules (Hemin-Fc) whose electrochemical behavior changed when exposed to pH and O₂ concentration differences. These changes were monitored (and quantified) by measuring the shift in the oxidation and reduction peaks of the cyclic voltammetry (current vs potential) plots (Fig. 19.2c). Despite the simplicity of the approach, this biosensor demonstrated an unprecedented spatiotemporal resolution, selectivity, and stability.

Overall, implantable biosensors are an emerging technology with very promising possibilities in cancer research due to their high performance, including a fast response time, a miniaturized size, and a low detection limit, among others. Together with their low manufacturing costs, this type of technology is desirable for the healthcare industry for developing innovative point-of-care systems to be employed in cancer patients to monitor their health status and response to therapy.

19.2.2.4 Flexible Biosensors

Bioelectronic devices with flexible and stretchable properties have been postulated as the new generation of point-of-care devices to monitor *in situ* the vital signs of patients (heart rate, blood pressure, or body temperature, among others) [63]. This is because flexible biosensors combine the advantages of classical biosensing technologies with the intrinsic characteristics of certain types of elastic materials and fabrication methods that provide the biosensors with advanced stretchable properties. In contrast to their rigid counterparts, flexible biosensors can be easily integrated on the skin or implanted inside the body adjusted to the complex 3D morphologies of human tissues and organs [36, 64, 65]. Further, flexible biosensors can also be fabricated on stretchable membranes enabling the development of multiplexing devices to detect multiple analytes [66].

Like implantable ones, flexible biosensors are also a sub-group within the more generic field of wearable biosensing devices (Fig. 19.2). To date, the great majority of flexible biosensors are based on epidermal electronic patches or dermal tattoos

[67]. This type of sensors enables the monitoring of proteins, saccharides, or metabolites confined in the interstitial fluid. Tattoo-based biosensors typically involve a change in color in response to variations in pH, compounds levels, or protein concentration (Fig. 19.2d) [32]. In this work, three colorimetric chemical sensors were used, which produced a color change in the visible spectrum in response to the aforementioned biomarkers reversibly and quantitatively. The first sensor detected changes in pH using standard methyl red, bromothymol blue, and phenolphthalein dyes as pH indicators, whereas the second and third ones detected changes in the levels of glucose (by enzymatic reactions of glucose oxidase and peroxidase) and albumin (using a yellow dye turning green upon its association with albumin). This simple colorimetric biosensing approach could be extended to cancer diagnostics applications by detecting specific biomarkers in the skin or interstitial fluid. In particular, it is very amenable for the continuous monitoring of patients suffering (or at high risk to suffer) from melanoma. Finally, an additional advantage of tattoos is the possibility of real-time and quantitative measurements of multiple markers by using, e.g., a smartphone camera, which enables self-diagnoses and telemedicine.

Similarly, epidermal biosensor patches can also be employed as screening tools to analyze sweat and interstitial fluid constituents and detect cancer-specific compounds [57]. Despite the described advantages of this type of sensor, they are also associated with certain drawbacks that limit their practical clinical application. These include, but are not limited to, the need for constant calibration, signal drift, non-representative results (e.g., the sensor may be affected by photobleaching or degradation), or cutaneous allergy (e.g., bio-incompatibility) [32]. In this regard, tattoo-based biosensors may offer better performance than epidermal ones due to enhanced protection of skin.

Overall, flexible biosensors may significantly improve the management of high-risk cancer patients by monitoring the efficacy of treatments or by the early detection of predictive biomarkers. This is undoubtedly one step further toward the implantation of personalized medicine, from which cancer patients may benefit. For more detailed information, the readers are invited to check other chapters focused on this type of biosensors (e.g., Chap. 11—Yadavalli et al.) or specialized reviews on the topic [67].

19.3 Microfluidic Technologies for Cancer Modeling and Drug Screening

19.3.1 Current Trends in Microfluidics

During the last decades, many advanced cell culture platforms have emerged for cancer research applications. In particular, three-dimensional (3D) models, such as hydrogels, scaffolds, spheroids, or microcarriers, have been employed to culture—cancer—cells in an environment that copycat the *in vivo* habitat of cells. However, despite reproducing the native structural (mechanical and architecture) and

biochemical properties, these models still lack a critical physiological aspect: the fluid flow. This is fundamental for the continuous delivery of nutrients and gases and removing the waste products generated by cells. Pre-clinical *in vitro* models have evolved toward the design, fabrication, and implementation of microfluidic-based systems. Microfluidics can solve the limitations mentioned above by perfusing tiny amounts of culture media or other types of fluids (e.g., blood, serum, air) through microchannels at physiological flow rates. These biomimetic devices are capable of improving the efficiency and predictability of point-of-care platforms, particularly relevant for drug discovery/screening and diagnostics. Microfluidics has indeed revolutionized the *in vitro* modeling of cancer and drug discovery/screening efficiency. This is partly because they can efficiently recapitulate relevant physiological features of the dynamic native scenario at the microscale, such as the formation of biochemical gradients, co-culture of cells, or shear stress stimuli, in a robust and reproducible manner. Additionally, fundamental operations, such as transport of compounds, molecules, cells, mixing of substances or fluids, or detection of analytes can also be performed within the microfluidic chip, thus boosting their analytical potential. Microfluidic organ-on-a-chip devices have already shown their potential, and a myriad of tissue/organ models have been reported, as introduced above in Sect. 19.1.

The exponential growth experienced by microfluidics and OoC can be attributed to the technology employed for their fabrication (developed by the microelectronics industry to manufacture printed circuit boards) that allow miniaturization, automatization, and parallelization of assays. Typically, a microfluidic device is fabricated by UV-photolithography following well-standardized procedures; these can be summarized as follows: (i) CAD design of the chip; (ii) printing of a photomask containing the microfluidic structures in a transparent-dark format; (iii) photolithography patterning and etching to generate a 3D mold of the chip (Note: Alternatively to UV-photolithography, higher resolution Direct Write Laser Lithography—DWL can be employed using a laser beam instead of UV light); (iv) replica molding of the mold using an elastomer, typically PDMS (Sylgard 184, Dow Corning); (v) drilling of the inlet/outlet(s) to allow the connection of tubing for fluid perfusion; and (vi) bonding the PDMS replica mold with a glass slide or thin cover slip by plasma activation. Overall, this fabrication process allows a broad control over the fabrication parameters (e.g., architecture, mechanical properties, biocompatibility, scalability, and others), and a diverse variety of designs can be generated. In this case, though, and in general, all the events occur in the same optical plane, even though more complex configurations can be obtained. Finally, the inner channels of the microfluidic chips are typically coated with adhesive proteins from the ECM, such as fibronectin, to promote the adhesion of cells (e.g., endothelial cells to mimic the vasculature). Similarly, chambers within the chip are filled with cell-laden hydrogels to reproduce the *in vivo* habitat. Both the microfluidic channels and the chambers are typically interconnected through micro-slits to permit their interaction and the migration of cells from one region to the other. Finally, the chip can be located within a microscope to monitor the behavior of cells.

As previously mentioned, this approach has been widely utilized to investigate critical events of cancer, and meaningful insights have been obtained so far. However, the typical planar configuration and rigid properties of this type of chips are also associated with certain limitations, such as the appearance of non-physiological cell responses. In this regard, novel microfluidic technologies have emerged to address these issues and are described below.

19.3.2 Emerging Microfluidics Technologies

19.3.2.1 Three-Dimensional Microfluidic Chips

The combination of several layers during fabrication or the stacking/sandwiching of different 2D constructs can lead to the development of 3D microfluidic systems that better recapitulate the complicated 3D architecture and active mechanical/biological functions of human tissues. A descriptive example is the lung-on-a-chip, where two apposed microchannels were interconnected through a thin porous membrane made of PDMS [3]. This configuration permitted the culture of human alveolar epithelial cells and pulmonary microvascular endothelial cells on opposite sides of the membrane, thus obtaining a 3D representation of the native human alveolus. However, this approach is still limited in its ability to generate complex 3D structures, and in some cases, the cells are still grown on planar and relatively rigid surfaces. Additionally, it lacks the needed complexity to copycat the tortuous and dense architecture of the native vascular networks, impacting the reproduced tissue's biological function [68]. To partially solve this, and as previously mentioned, the microfabricated chambers or reservoirs can be filled with cell-laden synthetic or natural-based hydrogels to reproduce the extracellular matrix. This way, the cells can be grown in a precisely-engineered 3D microenvironment with controlled mechanochemical properties that can be further tuned in terms of architecture and chemical moieties to support the growth of different cell types and complex tissues.

Recent advances in nanotechnology, micro-/nano-/bio-fabrication tools, and modern tissue engineering methods have permitted the development of a new generation of microfluidic devices that account for the non-planar and soft nature of the native habitat of cells. For this, cutting-edge technologies, such as *3D (bio-) printing* [69], *microthermoforming* [70], *sacrificial micromolding* [71], or *laser photoablation* [55], have been employed. In the following, we briefly describe the working mechanism of these techniques (for more details, the reader is referred to the cited references).

- *3D (bio-) printing*: This is a layer-by-layer fabrication technique that emerged to solve the limitation of traditional—planar—microfabrication methods. This technology has already been used to fabricate many natural and synthetic structures (e.g., complex 3D scaffolds). Importantly, it has the potential to revolutionize the field of microfluidics by manufacturing the entire chip with embedded complex 3D structures in a single step [72]. 3D (bio) printing includes various methods, including *inkjet printing*, *extrusion printing*, *stereolithography*, or *two-photon*

polymerization, among others [16]. Microfluidic channels as small as 25 μm can be printed (even though two-photon printing can print features and channels in the nm range). Some limitations of 3D (bio-) printing include the limited scope of printable materials and their cytocompatibility (for stereolithography) that may prevent the proliferation of cells, and the fabrication of channels with uncontrolled rough surfaces (for extrusion of thermopolymers) that may hinder the optical observation within the chip. As a result, bioprinted-based microfluidics can be considered still in its infancy, and many improvements in its performance are still needed. Among them, the fabrication of enclosed 3D microchannels and structures down to 10 μm must be ensured and the integration of different types of (bio) materials with other physicochemical properties [72].

- *Microthermoforming*: This method uses the principles of hot embossing, which employs a thin thermoplastic film firmly clamped and heated up to its glass transition temperature to replicate 3D micro-/nano-structures from a mold. In microthermoforming, the thin film, typically polystyrene, is 3D stretched using vacuum or compressed air replicating the surface morphology of the mold [73]; after cooling, the 3D structured sheet can be safely demolded. This approach enables the fabrication of microstructures (e.g., chambers) with spherical bottoms. In the context of microfluidics, this technique is very attractive for the fabrication of hollow vascular-like microfluidic structures. The fabrication process is straightforward: after the preparation of the thermoformed microchannel, the film is bound to a thicker plastic sheet containing fluidic inlet/outlet ports by heat sealing, micro-pressure forming process, or other sealing methods, such as solvent vapor fusion [74]. Microthermoforming has been successfully employed to fabricate microfluidic chips containing complex micro-/nano-structures [75, 76]. Another advantage is the use of porous materials, or the in situ generation of micro-pores, allowing the study of many biological processes or reproducing tissue-tissue interactions. Despite its simplicity, this method is still limited to the use of rigid thermoplastics, which may generate artificial phenotypes on cells. Additionally, there is a limitation of the aspect ratio of the molded structures, an important factor for 3D microfluidics. Finally, the generated structures are typically located along a single plane, even though several patterned sheets can be stacked to create more complex architectures.
- *Sacrificial micromolding*: This is a simple fabrication approach where a sacrificial material, typically gelatin, is employed to form complex 3D microfluidic-like structures. The melting (and subsequent flushing) of the gelatin results in the production of interconnected channels.
- *Laser photoablation*: Laser-based etching of hydrogels has shown remarkable potential for fabricating well-defined hollow microchannels within 3D biocompatible hydrogels. Typically, laser photoablation has been dedicated to modifying 2D surfaces. Still, this technique has attracted significant interest during the last years for its potential to fabricate more complex 3D hydrogel-embedded microfluidic channels mimicking the microvascular network [77]. This approach typically employs an image-guided femtosecond-pulsed laser (usually infrared) [55, 78, 79]. The large intensities generated induce the degradation of the

hydrogel through non-specific chemical bond photolysis, extreme local heating, or microcavitation [78]. The resolution of the generated microchannels depends on a bunch of parameters, including the numerical aperture of the objective and the focusing angle that also determines the working distance, that is, the depth that can be achieved inside the hydrogel (high NA \rightarrow high focusing angle \rightarrow short working distance). One of the main advantages of laser photoablation is directing cell functions by locally manipulating the cell microenvironment. Further, using an extensive portfolio of synthetic and natural biomaterials, including soft hydrogels (e.g., collagen, silk fibroin, hyaluronic acid, poly(ethylene glycol)) and hard polymers (e.g., PDMS, PMMA, and others), opens new opportunities for the development of the next generation of fully-organic 3D microfluidic devices. This includes the possibility to create large endothelial channels within the hydrogel. On the other hand, one general concern in cellular integrity as a result of the effect of the high-energy laser.

19.3.2.2 Modular Microfluidics

Organs-on-a-chip systems have emerged as model devices with unprecedented possibilities in cancer research to predict drug efficiency or toxicology within a microfluidic device. Organ-on-a-chip can be divided into single and multi-organ platforms [80]. Single-based chips present serious limitations: they are static in terms of assembly and either too specific (tailored to the needs of a certain tissue) or too generic (one-size-fits-all design). Multi-organ devices solve some of these limitations, allowing the study of inter-organ interactions (e.g., metabolites), off-target toxicity, or organ-specific metastasis [81]. However, this type of chip suffers from a high degree of personalization because every laboratory develops its own customized chip, threatening the comparison of results among different laboratories. Some generic and versatile designs have been reported to solve this. These designs are typically based on several microfluidic channels interconnected by micro-slits, allowing the injection of cell-laden hydrogels and the fluid flow. Indeed, the high versatility of these generic chips have resulted that some of them are commercially available. In some other cases though, this unique and generic design is not appropriate and more standardized designs are needed. In this regard, it has been proposed the use of standardized and reconfigurable individual modules (or units), having each of them a specific function. These modules can be fabricated by high precision additive manufacturing techniques giving a high degree of freedom for their design. Alternatively, more standard replica molding methods can be utilized. Then, the fabricated units can be interconnected in a LEGOTM-like manner. Applied to cancer research, only a reduced set of pre-fabricated and standardized modules may be needed (e.g., endothelial module, tumor module, sensor modules, and others) [82–86]. The different modules can be either interconnected laterally or stacked in 3D (Fig. 19.3a and b). Either way, this strategy provides design flexibility difficult to achieve by other standard means. Next, as mentioned before, the modules can contain channels or tissue reservoirs/chambers (Fig. 19.3b and c) [87].

Customized 3D chip designs can be achieved by interconnecting the desired modules following a plug & play configuration. One or more modules can be

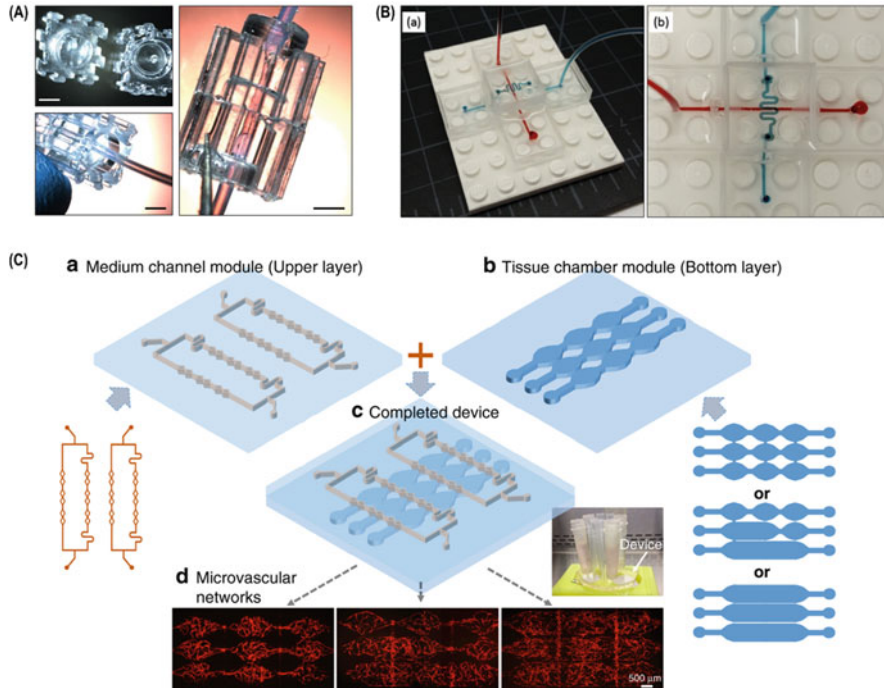


Fig. 19.3 Modular microfluidics. (a) Images showing the building blocks of a modular microfluidic system and their interconnection (lateral and vertical) to enable fluid flow and interface modeling (Images provided by the 3B's Research Group—University of Minho). (b) Two-layers microfluidic blocks for the 3D flow of fluids. A LEGO™-like planar platform is used as physical support to seal the microfluidic channels [84] (Reproduced with permission from the publisher). (c) More complex microfluidic modular systems containing a medium channel and a tissue culture module to form in vivo-like vascular networks [87] (Creative Commons Attribution 4.0 International License)

reconfigured, removed, or replaced by others containing specific compounds or cells. As an example, simple modules were arranged rationally to generate droplets. Sensing units were also connected to detect the flow and distribution of the generated drops [82]. Notably, the modules can be fabricated in different (bio) materials to reproduce tissue interfaces with different in vivo properties (composition, rigidity, etc.). Following this idea, any organ/tissue of the human body may be mimicked by interconnecting a reduced number of modules following a simple “recipe,” defined as the number and types of modules and their interconnection order needed to build that specific tissue. Further, these modules may be assembled onto a board containing an array of micro/nano-electrodes to “microfluidically” connect the different units and provide the microfluidic platform with sensory detection properties, enabling the monitoring of critical clinical (e.g., metabolic) parameters in real time.

This standardization can be employed to model several key aspects occurring in the metastatic cascade. For example, two different modules mimicking different organs can be interconnected to investigate the effect of the tumor toward the other organs, enabling the field of *modular multi-organ-on-a-chip*. This includes standard metastatic studies or more complex cancer-related pathological events, such as cachexia (i.e., the wasting of the muscular mass due to the tumor). Additionally, the different modules may be perfused with various cell culture media and flow rates to mimic the different conditions of the native scenario.

Finally, another advantage of modular microfluidics is that each module can be tested independently before being interconnected to a larger system. The fabrication of the modules is also compatible with mass production, and therefore, cheap to produce. It is envisioned that the final users may select pre-fabricated parts from a portfolio and assemble them to construct a microfluidic chip. Considering all these advantages, one may ask why researchers and the market have not yet adopted microfluidics with standardized modules? The main limiting factor is the proper interconnection of the modules to ensure that the high pressure needed to flow the fluid in extensive and complicated assemblies does not generate leakage. Similarly, the interconnection of the modules with a sensing board is also challenging to accomplish reliably. Additionally, there is the complexity of its monitoring using traditional optical microscopy, where certain events that occur within the stacked modules may not be visible. However, despite these drawbacks, modular microfluidics still has a high potential and is a valuable tool to democratize the field of microfluidics and expand their use to non-specialized users.

19.3.2.3 Biologically-Inspired Hydrogel-Based Microfluidics

Typically, poly(dimethylsiloxane) (PDMS) has been utilized in developing microfluidic devices due to its unique properties, namely its high transparency, fairly good biocompatibility, and gas permeability, among others. Unfortunately, PDMS displays certain limitations, such as high rigidity, a strong hydrophobicity that causes the absorption of hydrophobic molecules, challenging surface treatment, and the restriction of culturing cells in a planar monolayer. The latter makes that spatial orientation and cell-cell/ECM cannot be well mimicked perturbing cell phenotype, morphodynamics, viability, or gene expression, among other features. Together with the lack of standardization and integration, this has threatened the adoption of PDMS-based microfluidics by the market. Hydrogels, both natural- and synthetic-derived, have become an indispensable tool to culture cells in a native-like microenvironment due to their high degree of biomimicry and the possibility to retain tissue-specific function. Their controlled physicochemical composition, structural properties (e.g., architecture, porosity, rigidity), advanced functionality (e.g., cell adhesion properties, diffusion of small molecules), and cell biocompatibility have made hydrogels the preferred option for performing cell culture experiments. Typically, hydrogels have been utilized as a functional 3D region integrated within a microchip fabricated in a rigid polymeric material (e.g., PDMS or PMMA). This approach is preferred due to the advantages of using a solid material for manipulation and a soft one to mimic the cellular environment. Typically, several rigid

chambers are interconnected to microchannels through micro-slits and then filled with a hydrogel. The surface tension of the hydrogel before its polymerization avoids its spreading toward the adjacent channels. This approach is very versatile for pre-clinical studies, but cells may be still exposed to rigid surfaces.

Due to their advanced performance, hydrogels have already been used as a manufacturing material to build fully hydrogel-based 3D microfluidic chips, originating the field of the so-called *soft microfluidics*. In this case, hydrogels such as collagen [88], gelatin [89], gelatin methacrylate [90], alginate [91], silk fibroin [92], chitosan [93], and other extracellular matrix proteins have been utilized. Hydrogels also enable the generation of 3D gradients of chemokines across the hydrogel [94], or the possibility of being implanted in vivo. However, natural-origin hydrogels may lead to very soft structures due to their limited range of mechanical rigidity and degradability, which may collapse and block the channels. For this reason, under certain circumstances, the use of synthetic hydrogels is preferred; these are simpler to synthesize, offer a higher flexibility in material tunability, and in general, have a better imaging quality. In general, a limiting factor of synthetic hydrogels is their non-degradability, which threatens the mimicking of the natural environment of cells, and therefore, may compromise their viability and function. An additional drawback of hydrogel-based microfluidics is their tendency to swell and shrink due to their high water content. To minimize this, the degree of crosslinking can be adjusted, but this might impact the mechanical properties and structure of the material.

Different microfabrication approaches have been reported to fabricate a fully hydrogel-based microfluidic chip, including the well-known *replica molding* (i.e., replicate the chip from a mold typically fabricated by UV-photolithography), *sacrificial materials* or *templates* (e.g., removal of a thin wire after gel casting or digestion of a biomaterial template), *self-organization*, and *3D (bio) printing*. However, and in general, these approaches only allow the fabrication of planar microfluidic systems. More sophisticated techniques capable of fabricating more realistic 3D microfluidic networks include *microscopy-guided laser ablation microscopy*. This innovative fabrication approach allows the removal of material, such as a hydrogel, by irradiating with a pulsed laser beam that increases the temperature at the focal point until the material vaporizes [55]. This technique enables the precise modification of biomaterials with a high degree of control, allowing the fabrication of perfusable 3D hydrogel-embedded microfluidic channels [77, 79, 95] (Fig. 19.4a and b). This technique is compatible with a myriad of hydrogels (besides other rigid materials, such as glass, PDMS, PMMA, etc.), including collagen, silk fibroin, hyaluronic acid, poly(ethylene glycol), gelatin, fibrin, alginate, or agar/agarose [55, 79]. This approach has gained increasing interest in tissue engineering for the generation of embedded channels reproducing the architecture of native capillary beds within cell-laden hydrogels (Fig. 19.4c) [79]. A key advantage of laser ablation microscopy is that the localized degradation of the hydrogel does not affect the viability of the encapsulated cells within $\sim 20\ \mu\text{m}$ of the laser beam. This allows unprecedented control over the formation of microfluidic channels needed to deliver nutrients or other compounds, such as drugs. Finally, this method is especially

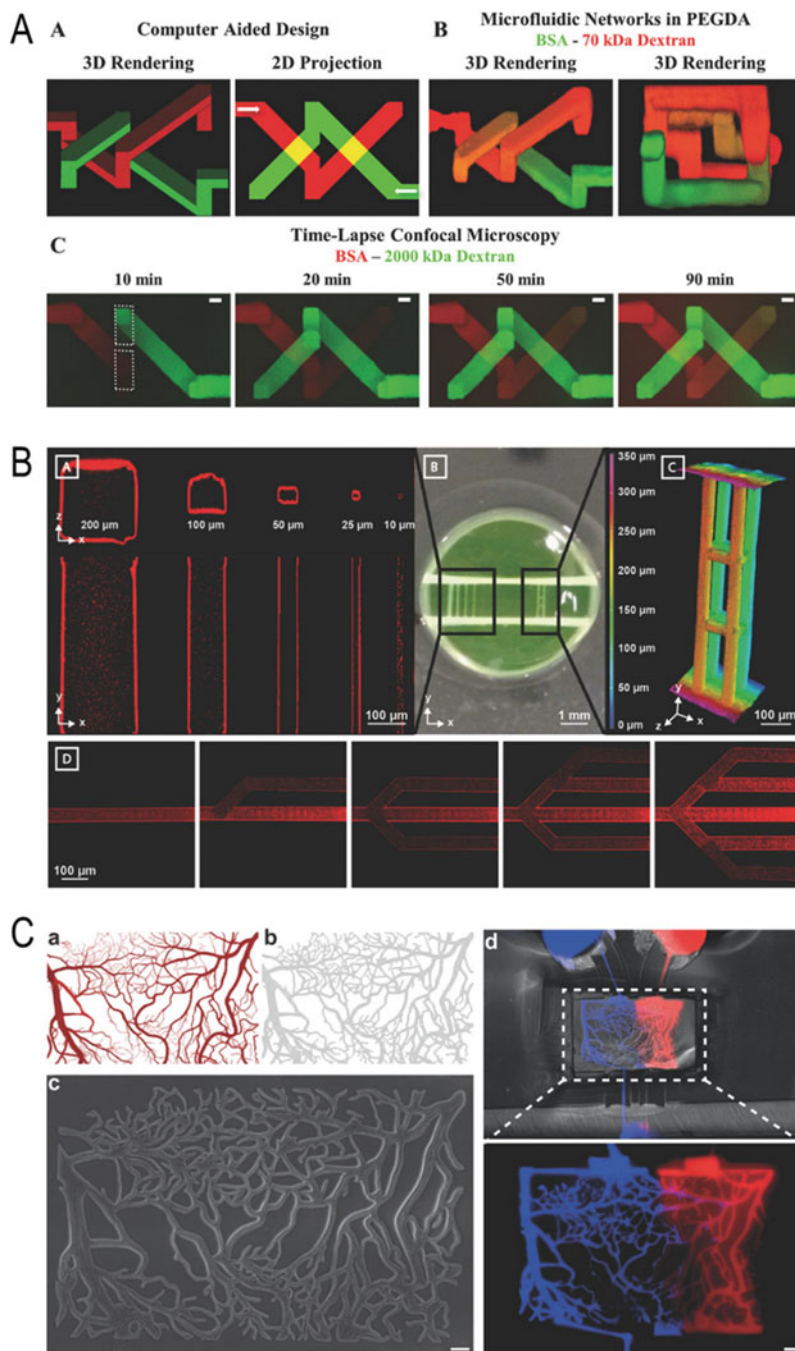


Fig. 19.4 Laser ablation hydrogel-based microfluidic networks. (a) (a) 3D computer-aided design, and (b) ablated 3D microchannels (20 $\mu\text{m} \times 20 \mu\text{m}$) in PEGDA hydrogel exposed to 70 kDa dextran (in red) and BSA (in green). The orange region illustrates the mixing by diffusion of both dyes. (c)

appealing for developing more realistic microfluidic in vitro models to elucidate the mechanisms of cancer metastasis or for drug screening applications [92].

Interestingly, soft microfluidics devices integrating biosensors have already been reported [96]. However, the biosensing assays are predominantly based on optical microscopy due to the incompatibility to integrate traditional metallic electrodes within the hydrogel. One option might be using a stand-alone board over which the hydrogel chip is deposited, thus sealing the channels and providing sensing properties to the device. Another option would be to benefit from the softness of the gel and inject/introduce a sensing wire within the area of interest and detect clinically-relevant parameters (e.g., pH, O₂, H₂O₂, secreted compounds, and others). Finally, the hydrogel can be designed to display specific sensitivity/reactivity to the surrounding environment. Therefore, it can be employed as an endogenous/exogenous stimuli-responsive transducer, providing a promising approach for both fluid actuation and biosensing [62]. The latter can be achieved by encapsulating a biologically active component that produces a measurable signal [33]. Indeed, this approach was already followed some time ago to capture small groups of cancer cells and sense cell-secreted proteases. The sensing was performed by incorporating MMP9-cleavable peptides that contained a donor/acceptor FRET pair (FITC and DABCYL) inside the microfluidic device integrating PEG hydrogel photopatterned microstructures. The capture of the cancer cells caused the appearance of a detectable fluorescence signal. The chip was used for the detection of lymphoma-secreted MMP9, which play a key role in ECM reorganization and are typically overexpressed in cancer cells [97]. Overall, the use of stimuli-responsive materials has attracted a lot of interest during the last years, boosting the use of soft microfluidics for a wide range of applications, including cancer research [62].

19.4 Emerging Trends in Microfluidics-Integrated Biosensors for Cancer Research

Large pharmaceutical and biotechnology companies are investing a significant amount of resources in developing innovative pre-clinical models to efficiently predict the outcome of a specific therapy, including microfluidics-based platforms [98]. As already mentioned, traditional in vitro (2D and 3D) and in vivo (animal)

Fig. 19.4 (continued) Time sequence showing the flow of the dyes [77]. **(b)** Perfusable microvessel generation. **(a)** Fluorescence microscopy image showing the fabricated channels with different dimensions. **(b)** Image of the channels-embedded hydrogel device. **(c)** Magnified 3D image showing interconnected microchannels, **(d)** Time sequence showing the flow of fluorescent beads along the channels [78]. **(c)** Capillary bed microfabrication in poly(ethylene glycol) hydrogel. **(a-b)** Thresholded and laser mask images of the capillary bed. **(c)** Microscopy image showing the reproduced microfluidic capillary bed network. **(d)** Perfusion of fluorescent dyes (Alexa 647-labeled PEG, in red; 2000 kDa FITC-dextran, in blue), mimicking arteriovenous circulation [79]. *Figures reproduced with permission from the publishers*

models are becoming obsolete because they cannot recapitulate the complexity of the human body, thus questioning the relevancy of the obtained data. Microfluidics-based organ-on-a-chip technology has become a powerful alternative to faithfully model human organs and their associated diseases, such as cancer. However, despite this potential, microfluidics technology is still mainly restricted to research laboratories with access to a cleanroom facility where highly skilled personnel use complex micro- and nano-fabrication techniques for chips fabrication. It also lacks the standardization and personalization needed for clinical applications and demanded by the healthcare market. In this regard, new strategies have emerged to mimic human organs and tissues using novel microfluidic design concepts, bioengineering approaches, and cutting-edge ICT technologies, which are simpler, more straightforward, and less expensive. In the following, we discuss some of these new trends that may boost the applicability of microfluidic systems into the clinic.

19.4.1 Generic Microfluidic Systems

Microfluidics and lab-on-a-chip devices are robust tools for investigating the etiology of diseases and improving the efficiency of (cancer) disease diagnosis and therapy evaluation, reducing the turnaround times and costs of conventional medical devices. Despite this potential, microfluidics has a reduced customer acceptance yet. This is in part related to the “tedious” procedure of traditional PDMS-based chip fabrication and the associated high manufacturing cost and time of academic proof-of-concept devices. Similarly, there is a significant chip-to-chip variability and a high incompatibility with existing imaging and analytical—biosensing—technologies. This is indeed a bottleneck for non-specialized researchers who lack access to microfabrication facilities and the necessary skills to manipulate the associated hardware, such as external fluid handling items (e.g., pumps) [99]. During the last years, several microfluidic companies, such as Mimetas™, Emulate™, or AIM Biotech™, have developed very versatile, robust, reproducible, and affordable single-use microfluidics devices that have democratized the field of microfluidics with user-friendly chips. These chips are so versatile that they can indeed be applied for a large plethora of applications [16], integrating some of them sensing units (e.g., Micronit™, Darwin Microfluidics™, MicruX™); in others, the sensing is located outside the chip, which may be enough for specific applications (e.g., Elveflow™, Dropsens™, and others). Typically, these generic chips are manufactured using cost-effective materials widely utilized in the medical device industry, such as PMMA or polycarbonate, and already approved by regulatory agencies [99]. However, certain dynamic or flexible parts, such as valves or membranes, typically made of PDMS in prototype chips, cannot be integrated on this type of generic rigid chip. Therefore, simpler static architectures must be employed.

The use of these generic chips has experienced a significant increase during the last years, in particular for point-of-care diagnosis and disease modeling. Some microfluidics companies have gathered significant funds from governmental organizations (e.g., FDA in the USA) and established agreements with large

pharmaceutical companies, such as AstraZeneca™, Roche™, or Merck™, among others, for using their microfluidic devices for their research. Applied to cancer research, this type of generic chips has been utilized to investigate many fundamental and clinical aspects, including 3D cancer cell migration and invasion, angiogenesis and vascularization, intra/extravasation assays, immunotherapy studies, and more. Significantly, these devices have been scaled up to standard well-plates enabling experimental high-throughput screening tests. Therefore, they are compatible with standard analytical and characterization techniques, such as plate readers. Finally, it is worth mentioning that some of these chips come with accessories that further automatize the manipulation and reading of the system, such as culture platform integrating incubator conditions and media flow and sampling.

19.4.2 Smart Biomaterials for Microfluidics Development

There is indeed a wide variety of biomaterials that can be utilized as 3D culture system to support the growth of—cancer—cells within microfluidic chips, such as rigid scaffolds or softer hydrogels [100]. These biomaterials provide the needed biochemical and architectural support to cells, such as spheroids, organoids, or vascular networks. Integrating these cells within a microfluidic chip typically requires their encapsulation within a biomimetic 3D matrix. For this, a rich portfolio of biomaterials can be chosen, whose selection will depend on the type of cells utilized and the experiment's aim. Typical examples include the widely utilized Matrigel™ or collagen, among others (Table 19.1). The advantage of these biomaterials is their biocompatibility, biodegradability, bioavailability, and similarity to the native matrix. However, they also display critical drawbacks, such as batch-to-batch variability, complex molecular composition, uncontrolled degradation, or limited capacity to tune their mechanical properties. In contrast, synthetic materials, such as polyethylene glycol (PEG), poly(lactic-co-glycolic) acid (PLGA), poly(acrylamide) (PA), poly(vinyl alcohol), or poly ϵ -caprolactone (PCL), among others, display better mechanical properties, are simple to synthesize, and provide a high experimental control over the biochemical and mechanical properties of the gel,

Table 19.1 Traditional and emerging natural-based biomaterials used in microfluidics cancer research

Traditional biomaterials		Emerging biomaterials	
<i>Agarose</i>	Polysaccharide	<i>Cell-derived matrices</i>	Protein (multiple)
<i>Alginate</i>	Polysaccharide	<i>(Nano-) cellulose</i>	Polysaccharide
<i>Chitosan</i>	Polysaccharide	<i>Fucoidan</i>	Polysaccharide
<i>Collagen I</i>	Protein	<i>Gellan gum</i>	Polysaccharide
<i>Fibrin/fibrinogen</i>	Protein	<i>Platelet lysate</i>	Bioactive molecules cocktail
<i>Gelatin</i>	Protein	<i>Silk fibroin</i>	Protein
<i>Hyaluronic acid</i>	Polysaccharide		
<i>Matrigel™</i>	Protein (multiple)		

with low batch-to-batch variability. However, this type of biomaterials typically lacks natural cell adhesion sites. Additionally, they cannot be remodeled by cells. New biomaterials have emerged displaying advanced properties for the culture of cells within microfluidic devices to solve all these limitations (Table 19.1) [100]. These biomaterials offer a myriad of advantages when compared to traditional materials, such as superior biocompatibility (e.g., cell-derived matrices), xeno-free conditions (e.g., platelet lysate), or controlled mechanical and degradation properties (e.g., silk fibroin), among others. Recent excellent works have extensively reviewed the use of this type of biomaterials for precision cancer medicine applications [62]. Indeed, the combination of precision biomaterials and microfluidics can result in a new generation of microfluidic devices displaying unique functional capabilities [62]. These new properties can be exploited to integrate remotely-triggered actuators (e.g., valves, pumps) and sensors (e.g., electrodes) on-chip eliminating external equipment typically employed to control the fluidic functions. Some attempts have already been reported to integrate these functional elements in microfluidic devices, such as the use of contactless piezoelectric or electrokinetic micropumps [101], chip-integrated sensing elements [102] or hydrogel-based valves [103]. Chip-integrated and contactless (bio) sensors are typically based on the use of miniaturized optical detection elements, usually photonic-based (e.g., grating-coupled, interferometric, photonic crystal, and microresonators [102]) that reduce the need for external optical components. Among all the optical-based sensing methods, the use of waveguides offers many advantages, such as high-throughput characteristics or a simple waveguide fabrication process in different type of materials, such as hydrogels [104, 105]. The detection of the analyte of interest can be based on standard binding-induced fluorescence or on changes in the refractive index next to the waveguide, where the evanescent field decays exponentially from the sensor surface. Alternative to waveguides, SPR chips can also be utilized (see Sect. 19.2.1.2) [106]. These two sensing approaches can be easily integrated and combined with a microfluidic system, and therefore, offer a unique opportunity for the development of contactless point-of-care analytical devices.

Similarly, valves can remotely be activated by a diverse variety of extrinsic stimuli, such as light, temperature, electric or magnetic fields, depending on the material chemical composition, or intrinsic stimuli, such as pH or enzymes, which can also induce valve actuation [103]. In general, the valves can be switched on/off at a fast response rate (1–2 s.) by adjusting the stimuli intensity [107], therefore compatible with microfluidics' dynamic requirements. Overall, these miniaturized valves and pumps' small size and easy fabrication enable their on-chip integration for automated and remote fluid manipulation.

19.4.3 Other Emerging Biosensor and Microfluidic Approaches

Traditional clinical assays for cancer detection are performed through classical laboratory analytical technologies (e.g., image-based examination, sequencing, mass spectrometry, and others), which under certain circumstances may be very

laborious and limited in terms of sensitivity and selectivity [108]. During the last decade, several innovative technologies and microfluidics-based approaches have appeared for the detection of cancer biomarkers, including liquid biopsy methods [109], electronic noses [110], or optoelectronic sensors, among others [111]. This is because the combination of sensing technologies with microfluidics can further boost detection efficiency. Liquid biopsy has largely attracted the interest of the cancer research community due to its superior ability to early diagnose the presence of a tumor in a non-invasive manner through the detection of specific biomarkers from the body fluids, in particular, the presence of CTCs, ctDNA/RNA, or exosomes in peripheral blood, and widely reviewed in the literature [112–114]. Similarly, the combination of microfluidics and surface-enhanced Raman spectroscopy (SERS)-based biosensing is emerging as an increasingly popular technology for developing automated, high-throughput, multiplexing, and highly sensitive point-of-care devices [115]. This is mainly due to its simplicity, selectivity, ultrasensitivity, and multiplexing capability, which allows their easy integration within lab-on-a-chip devices. Indeed, SERS-integrated microfluidic biosensors have already shown their potential for the detection of tiny amounts of cancer biomarkers and multiple point DNA mutations in heterogeneous tumors as a liquid biopsy approach [116]. The use of computational algorithms for cancer classification is particularly relevant for analyzing the Raman fingerprints, an essential feature for precision and personalized medicine. This approach has been validated with patient DNA samples and well-established analytical techniques, such as PCR, showing a high clinical potential as a “smart” pre-clinical diagnostic tool for the stratification of cancer patients. However, the use of PDMS to manufacture the chip threatens its practical translation to the clinics. To solve this, the same group proposed using paper as a low-cost sensing substrate for disease diagnosis and monitoring [64]. In this case, the microfluidic PDMS-based device was used solely to deliver sensing SERS nanoparticles (gold nanostars and nanorods) on the paper substrate. As a proof of concept, the lysed products of two different cell lines (human peripheral blood mononuclear cells and SW480 colorectal cancer cells) were analyzed. The obtained data allowed to distinguish the spectral fingerprints from both cell types, suggesting the feasibility of paper-based substrates and SERS for cancer-related point-of-care applications.

As discussed, PDMS displays a limited performance that impacts not only on cell behavior, but also on fluid dynamics, in particular in highly miniaturized channels. The solid walls of this elastomeric material affect the proper flow of fluid. Hydrophobic coatings, electrowetting, or liquid-infused porous surface, among other approaches, can partially solve this enhanced friction. Similarly, hydrogel-based channels or sheath flow can mask the effect of solid walls but are also associated with certain drawbacks, such as an uncontrolled diffusion toward the hydrogel bulk or the need for a continuous flow. Recently, a new revolutionary microfluidics technology emerged based on “liquid tubes” to manage the flow of fluids. This technology employs an immiscible and non-toxic magnetic fluid stabilized by a magnetic field to stably coat the walls of the channel, obtaining a near frictionless liquid-in-liquid microfluidic channel (Fig. 19.5a) [117]. Interestingly, this approach is not merely a static coating, but manipulating the magnetic field enables the valving, splitting,

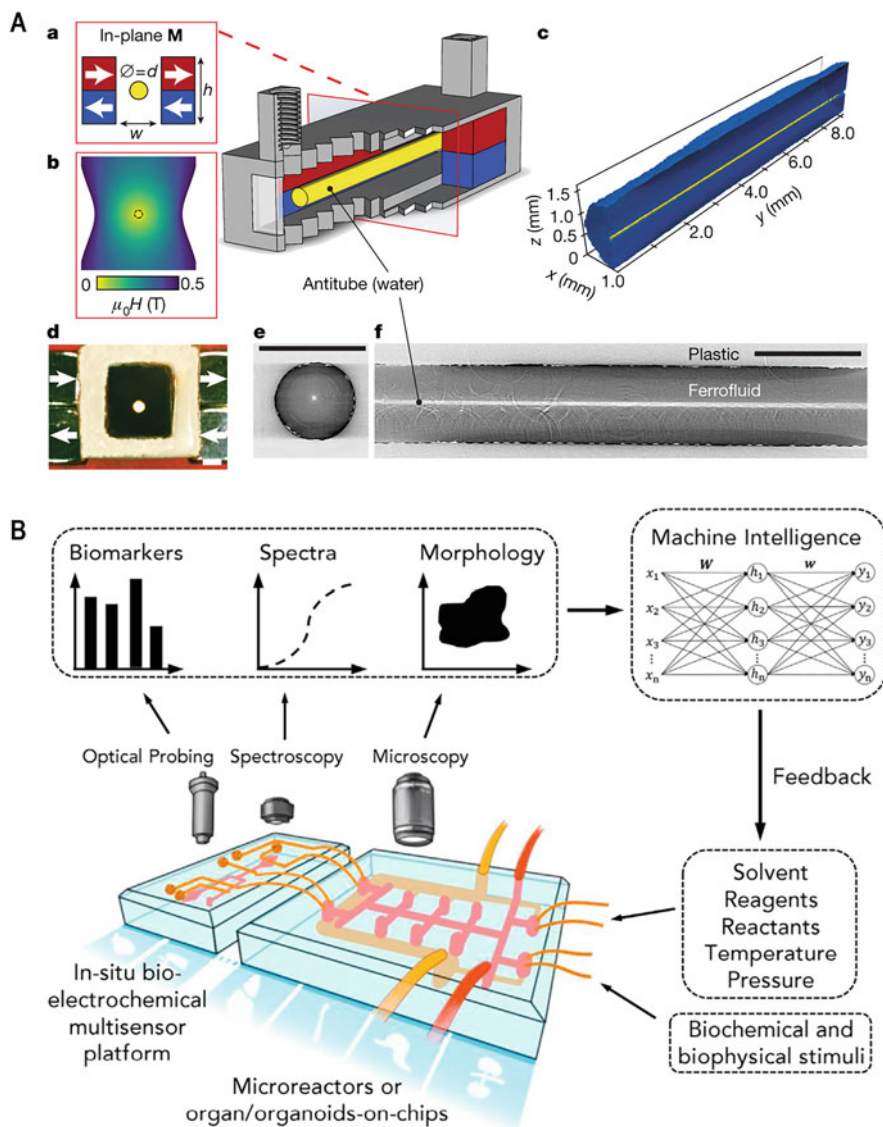


Fig. 19.5 Other emerging microfluidic and biosensor-integrated microfluidic technologies. (a) Microfluidic with magnetic liquid tube channels for the frictionless perfusion of fluids [117]. (b) Intelligent microfluidic (microreactors or organ-on-a-chip) platform based on computational modeling and machine learning tools [118]. The scheme shows a microfluidic chip coupled to a multi-biosensing platform. (Reproduced with permission from the publishers)

merging, and/or pumping of fluids, such as human blood. A limitation of this method is the lack of transparency of the ferrofluids (Fe_3O_4) employed, but this can be solved by using optically-transparent magnetic oil coined “Magoil” similar to those employed for magnetic resonance imaging. This revolutionary method opens new

possibilities for the transport and manipulation of biological fluids and establishes a novel paradigm in microfluidics.

Finally, computational modeling and machine learning tools are expected to play a fundamental role in improving the performance of future microfluidic and biosensors technologies, in particular, to reduce the consumption of reagents further, to extract more significant amounts of valuable datasets, or to boost their automatization degree, among others (Fig. 19.5b) [118]. This type of platform uses the collected data to analyze by machine learning critical experimental (e.g., reagents, reactants, temperature, pressure), biochemical (e.g., reagents, drugs, growth factors), and/or biophysical parameters (e.g., shear forces, electrical/optogenetic stimulation) and the ways to optimize them. This approach will univocally provide more powerful predictive tools learning from the generated data, thus opening new avenues and opportunities in drug discovery, screening, cancer modeling, or precision medicine, thus boosting the field of intelligent cancer research.

19.5 Conclusions

During the last years, incredible progress in microfluidics and biosensors both from a technological and application perspective has been achieved as a result of the synergy between different multidisciplinary fields, including nanotechnology, biomedicine, materials science, tissue engineering, (bio-) chemistry, and electronics, for developing new engineering strategies and high-performance systems. Indeed, microfluidic platforms have demonstrated their enormous potential for more efficient drug screening, point-of-care diagnostics, and biological studies. Applied to cancer research, microfluidics has proved to be instrumental for personalized medicine to assess the efficacy of (new) therapeutic compounds. When integrated with biosensing technologies, it enables the detection of critical biomarkers or monitoring therapy efficacy. This significant potential has been boosted by the development of new emerging microfluidic and biosensing technologies that are expected to revolutionize the field and reduce the premature death of cancer. Further, integrating computational tools and other revolutionary technologies will boost the use of biosensors and microfluidics in cancer diagnosis and therapeutics [119]. However, more progress is still needed to expand the applications of microfluidics outside research labs, particularly in clinical settings. For this, the collaboration between biomedical researchers (e.g., nanotechnologists, cell biologists, materials scientists, and others) and the end-users (e.g., oncologists, regulatory agents, and others) will be fundamental.

Acknowledgements D.C. acknowledges the financial support from the Portuguese Foundation for Science and Technology (FCT) under the program CEEC Individual 2017 (CEECIND/00352/2017). D.C., C.M.A, and S.C.K. thank the support from the FCT under the scope of the project 2MATCH (PTDC/BTM-ORG/28070/2017) funded by the Programa Operacional Regional do Norte supported by European Regional Development Funds (ERDF). S.C.K. also acknowledges the FCT for the support provided through the BREAST-IT project (PTDC/BTM-ORG/28168/2017). Finally, all the authors thank the financial support from the EU Framework Programme

for Research and Innovation Horizon 2020 on Forefront Research in 3D Disease Cancer Models as in vitro Screening Technologies (FoReCaST—no. 668983).

Conflicts of Interest None.

References

1. Rebelo R et al (2019) 3D biosensors in advanced medical diagnostics of high mortality diseases. *Biosens Bioelectron* 130:20–39
2. Mirbagheri M et al (2019) Advanced cell culture platforms: a growing quest for emulating natural tissues. *Mater Horiz* 6(1):45–71
3. Huh D et al (2010) Reconstituting organ-level lung functions on a chip. *Science* 328(5986):1662–1668
4. Benam, K.H., et al., Human lung small airway-on-a-chip protocol, 3D cell culture: methods and protocols, Z. Koledova, 2017, Springer New York 345–365
5. Hassell BA et al (2017) Human organ Chip models recapitulate Orthotopic lung cancer growth, therapeutic responses, and tumor dormancy in vitro. *Cell Rep* 21(2):508–516
6. Gaudriault P, Fassini D, Homs-Corbera A (2020) Chapter 8 - heart-on-a-chip. In: Hoeng J, Bovard D, Peitsch MC (eds) *Organ-on-a-chip*. Academic Press, Cambridge, pp 255–293
7. Rigat-Brugarolas LG et al (2014) A functional microengineered model of the human splenon-on-a-chip. *Lab Chip* 14(10):1715–1724
8. Kim HJ et al (2016) Contributions of microbiome and mechanical deformation to intestinal bacterial overgrowth and inflammation in a human gut-on-a-chip. *Proc Natl Acad Sci U S A* 113(1):E7–E15
9. Ma L-D et al (2018) Design and fabrication of a liver-on-a-chip platform for convenient, highly efficient, and safe in situ perfusion culture of 3D hepatic spheroids. *Lab Chip* 18(17):2547–2562
10. Wilmer MJ et al (2016) Kidney-on-a-chip Technology for drug-induced nephrotoxicity screening. *Trends Biotechnol* 34(2):156–170
11. Kilic O et al (2016) Brain-on-a-chip model enables analysis of human neuronal differentiation and chemotaxis. *Lab Chip* 16(21):4152–4162
12. Llenas M et al (2021) Versatile vessel-on-a-chip platform for studying key features of blood vascular tumors. *Bioengineering* 8(6):81
13. Luque-González MA et al (2020) Human microcirculation-on-chip models in cancer research: key integration of lymphatic and blood vasculatures. *Adv Biosys* 4(7):2000045
14. Ronaldson-Bouchard K, Vunjak-Novakovic G (2018) Organs-on-a-chip: a fast track for engineered human tissues in drug development. *Cell Stem Cell* 22(3):310–324
15. Caballero D et al (2017) Organ-on-chip models of cancer metastasis for future personalized medicine: from chip to the patient. *Biomaterials* 149:98–115
16. Caballero D et al (2020) Chapter 15 - Microfluidic systems in cancer research. In: Kundu SC, Reis RL (eds) *Biomaterials for 3D tumor modeling*. Elsevier, Amsterdam, pp 331–377
17. Grieshaber D et al (2008) Electrochemical biosensors - sensor principles and architectures. *Sensors (Basel, Switzerland)* 8(3):1400–1458
18. Bhalla N et al (2016) Introduction to biosensors. *Essays Biochem* 60(1):1–8
19. Clark LC Jr, Lyons C (1962) Electrode systems for continuous monitoring in cardiovascular surgery. *Ann N Y Acad Sci* 102:29–45
20. Kim J et al (2019) Wearable biosensors for healthcare monitoring. *Nat Biotechnol* 37(4):389–406
21. Barreiros Dos Santos M et al (2019) Portable sensing system based on electrochemical impedance spectroscopy for the simultaneous quantification of free and total microcystin-LR in freshwaters. *Biosens Bioelectron* 142(111550):30

22. Kaur B, Kumar S, Kaushik BK (2022) Recent advancements in optical biosensors for cancer detection. *Biosens Bioelectron* 197:113805
23. Hasan MR et al (2021) Recent development in electrochemical biosensors for cancer biomarkers detection. *Biosens Bioelectron X* 8:100075
24. Chen C, Wang J (2020) Optical biosensors: an exhaustive and comprehensive review. *Analyst* 145(5):1605–1628
25. Ronkainen NJ, Halsall HB, Heineman WR (2010) Electrochemical biosensors. *Chem Soc Rev* 39(5):1747–1763
26. Rackus DG, Shamsi MH, Wheeler AR (2015) Electrochemistry, biosensors and microfluidics: a convergence of fields. *Chem Soc Rev* 44(15):5320–5340
27. Engel L et al (2018) Local electrochemical control of hydrogel microactuators in microfluidics. *J Micromech Microeng* 28(10):105005
28. Pratt ED et al (2011) Rare cell capture in microfluidic devices. *Chem Eng Sci* 66(7):1508–1522
29. Kuswandi B et al (2007) Optical sensing systems for microfluidic devices: a review. *Anal Chim Acta* 601(2):141–155
30. Damborský P, Švitel J, Katrlík J (2016) Optical biosensors. *Essays Biochem* 60(1):91–100
31. Liu L et al (2017) An electrochemical biosensor with dual signal outputs: toward simultaneous quantification of pH and O₂ in the brain upon ischemia and in a tumor during cancer starvation therapy. *Angew Chem Int Ed* 56(35):10471–10475
32. Yetisen AK et al (2019) Dermal tattoo biosensors for colorimetric metabolite detection. *Angew Chem Int Ed* 58(31):10506–10513
33. Herrmann A, Haag R, Schedler U (2021) Hydrogels and their role in biosensing applications. *Adv Healthc Mater* 10(11):2100062
34. Misun PM et al (2016) Multi-analyte biosensor interface for real-time monitoring of 3D microtissue spheroids in hanging-drop networks. *Microsyst Nanoeng* 2(1):16022
35. Heikenfeld J et al (2018) Wearable sensors: modalities, challenges, and prospects. *Lab Chip* 18(2):217–248
36. Yang Y, Gao W (2019) Wearable and flexible electronics for continuous molecular monitoring. *Chem Soc Rev* 48(6):1465–1491
37. Piwek L et al (2016) The rise of consumer health wearables: promises and barriers. *PLoS Med* 13(2):e1001953
38. Park H, Park W, Lee CH (2021) Electrochemically active materials and wearable biosensors for the in situ analysis of body fluids for human healthcare. *NPG Asia Mater* 13(1):23
39. Chuang H et al (2008) Pilot studies of transdermal continuous glucose measurement in outpatient diabetic patients and in patients during and after cardiac surgery. *J Diabetes Sci Technol* 2(4):595–602
40. Gao W et al (2016) Fully integrated wearable sensor arrays for multiplexed in situ perspiration analysis. *Nature* 529(7587):509–514
41. Terse-Thakoor T et al (2020) Thread-based multiplexed sensor patch for real-time sweat monitoring. *NPJ Flex Electron* 4(1):18
42. Wang Z et al (2021) A flexible and regenerative aptameric graphene–nafion biosensor for cytokine storm biomarker monitoring in undiluted biofluids toward wearable applications. *Adv Func Mater* 31(4):2005958
43. Imani S et al (2016) A wearable chemical–electrophysiological hybrid biosensing system for real-time health and fitness monitoring. *Nat Commun* 7(1):11650
44. Kolluru C et al (2019) Recruitment and collection of dermal interstitial fluid using a microneedle patch. *Adv Healthc Mater* 8(3):1801262
45. Madden J et al (2020) Biosensing in dermal interstitial fluid using microneedle based electrochemical devices. *Sens Bio-Sens Res* 29:100348
46. Martín A et al (2017) Epidermal microfluidic electrochemical detection system: enhanced sweat sampling and metabolite detection. *ACS Sensors* 2(12):1860–1868

47. Al Sulaiman D et al (2019) Hydrogel-coated microneedle arrays for minimally invasive sampling and sensing of specific circulating nucleic acids from skin interstitial fluid. *ACS Nano* 13(8):9620–9628
48. Ciui B et al (2018) Wearable wireless Tyrosinase bandage and microneedle sensors: toward melanoma screening. *Adv Healthc Mater* 7(7):1701264
49. Caballero D et al (2013) Directing polypyrrole growth by chemical micropatterns: a study of high-throughput well-ordered arrays of conductive 3D microrings. *Sens Act B: Chem* 177: 1003–1009
50. Errachid A et al (2007) Electropolymerization of nano-dimensioned polypyrrole micro-ring arrays on gold substrates prepared using submerged micro-contact printing. *Nanotechnology* 18(48):485301
51. Gerard M, Chaubey A, Malhotra BD (2002) Application of conducting polymers to biosensors. *Biosens Bioelectron* 17(5):345–359
52. Chen Y et al (2017) Skin-like biosensor system via electrochemical channels for noninvasive blood glucose monitoring. *Sci Adv* 3(12):e1701629
53. Reeder JT et al (2019) Waterproof, electronics-enabled, epidermal microfluidic devices for sweat collection, biomarker analysis, and thermography in aquatic settings. *Sci Adv* 5(1): eaau6356
54. Koh A et al (2016) A soft, wearable microfluidic device for the capture, storage, and colorimetric sensing of sweat. *Sci Transl Med* 8(366):366ra165
55. Pradhan S, et al (2017) Fundamentals of laser-based hydrogel degradation and applications in cell and tissue engineering. *Adv Healthc Mater* 6(24):10.1002/adhm.201700681. <https://doi.org/10.1002/adhm.201700681>
56. Jadoon S et al (2015) Recent developments in sweat analysis and its applications. *Intl J Anal Chem* 2015:164974
57. Monedeiro F et al (2020) Investigation of sweat VOC profiles in assessment of cancer biomarkers using HS-GC-MS. *J Breath Res* 14(2):1752–7163
58. Calderón-Santiago M et al (2015) Human sweat metabolomics for lung cancer screening. *Anal Bioanal Chem* 407(18):5381–5392
59. Chorsi MT et al (2019) Piezoelectric biomaterials for sensors and actuators. *Adv Mater* 31(1): 1802084
60. Siontorou CG et al (2017) Point-of-care and implantable biosensors in cancer research and diagnosis. In: Chandra P, Tan YN, Singh SP (eds) *Next generation point-of-care biomedical sensors Technologies for Cancer Diagnosis*. Springer, Singapore, pp 115–132
61. Rodrigues D et al (2020) Skin-integrated wearable systems and implantable biosensors: a comprehensive review. *Biosensors* 10(7):79
62. Caballero D et al (2022) Precision biomaterials in cancer theranostics and modelling. *Biomaterials* 280:121299
63. Wang C et al (2016) Carbonized silk fabric for Ultrastretchable, highly sensitive, and wearable strain sensors. *Adv Mater* 28(31):6640–6648
64. Gray M et al (2018) Implantable biosensors and their contribution to the future of precision medicine. *Vet J* 239:21–29
65. Kim D-H et al (2011) Epidermal Electronics. *Science* 333(6044):838–843
66. Kokkinos C et al (2016) Lab-on-a-membrane foldable devices for duplex drop-volume electrochemical biosensing using quantum dot tags. *Anal Chem* 88(13):6897–6904
67. Takaloo S, Moghimi Zand M (2021) Wearable electrochemical flexible biosensors: with the focus on affinity biosensors. *Sens Bio-Sens Res* 32:100403
68. Baptista D et al (2019) Overlooked? Underestimated? Effects of substrate curvature on cell behavior. *Trends Biotechnol* 37(8):838–854
69. Zhu W et al (2016) 3D printing of functional biomaterials for tissue engineering. *Curr Opin Biotechnol* 40:103–112
70. Baptista D et al (2021) 3D alveolar in vitro model based on epithelialized biomimetically curved culture membranes. *Biomaterials* 266(120436):10

71. Cerchiari A et al (2015) Formation of spatially and geometrically controlled three-dimensional tissues in soft gels by sacrificial micromolding. *Tissue Eng Part C Methods* 21(6):541–547
72. Waheed S et al (2016) 3D printed microfluidic devices: enablers and barriers. *Lab Chip* 16(11):1993–2013
73. Truckenmüller R et al (2011) Thermoforming of film-based biomedical microdevices. *Adv Mater* 23(11):1311–1329
74. Truckenmüller R et al (2002) Low-cost thermoforming of micro fluidic analysis chips. *J Micromech Microeng* 12(4):375–379
75. Focke M et al (2011) Microthermoforming of microfluidic substrates by soft lithography (μ TSL): optimization using design of experiments. *J Micromech Microeng* 21(11):115002
76. Truckenmüller R et al (2008) Flexible fluidic microchips based on thermoformed and locally modified thin polymer films. *Lab Chip* 8(9):1570–1579
77. Heintz KA et al (2016) Fabrication of 3D biomimetic microfluidic networks in hydrogels. *Adv Healthc Mater* 5(17):2153–2160
78. Arakawa CK et al (2017) Multicellular vascularized engineered tissues through user-programmable biomaterial Photodegradation. *Adv Mater* 29(37):24
79. Brandenberg N, Lutolf MP (2016) In situ patterning of microfluidic networks in 3D cell-laden hydrogels. *Adv Mater* 28(34):7450–7456
80. Rogal J, Probst C, Loskill P (2017) Integration concepts for multi-organ chips: how to maintain flexibility?! *Future Sci OA* 3(2):FSO180
81. Loskill P et al (2015) μ Organo: a Lego®-like Plug & Play System for modular multi-organ-chips. *PLoS One* 10(10):e01139587
82. Bhargava KC, Thompson B, Malmstadt N (2014) Discrete elements for 3D microfluidics. *Proc Natl Acad Sci U S A* 111(42):15013–15018
83. Chen Y-W et al (2012) Modular microfluidic system fabricated in thermoplastics for the strain-specific detection of bacterial pathogens. *Lab Chip* 12(18):3348–3355
84. Vittayarukskul K, Lee AP (2017) A truly Lego®-like modular microfluidics platform. *J Micromech Microeng* 27(3):035004
85. Hsieh Y-F et al (2014) A Lego®-like swappable fluidic module for bio-chem applications. *Sens Act B: Chem* 204:489–496
86. Owens CE, Hart AJ (2018) High-precision modular microfluidics by micromilling of interlocking injection-molded blocks. *Lab Chip* 18(6):890–901
87. Yue T et al (2021) A modular microfluidic system based on a multilayered configuration to generate large-scale perfusable microvascular networks. *Microsyst Nanoeng* 7(1):4
88. Buchanan CF et al (2014) Three-dimensional microfluidic collagen hydrogels for investigating flow-mediated tumor-endothelial signaling and vascular organization. *Tissue Eng Part C Methods* 20(1):64–75
89. Liu J et al (2015) Hydrogels for engineering of Perfusable vascular networks. *Int J Mol Sci* 16(7):15997–16016
90. Lee Y et al (2015) Photo-crosslinkable hydrogel-based 3D microfluidic culture device. *Electrophoresis* 36(7–8):994–1001
91. Johann RM, Renaud P (2007) Microfluidic patterning of alginate hydrogels. *Biointerphases* 2(2):73–79
92. Rodrigues de Carvalho M, et al Enzymatically crosslinked silk fibroin hydrogel microfluidic platform, methods of production and uses thereof, 2021, Association for the Advancement of tissue engineering and cell based technologies & therapies (A4TEC), Portugal
93. He J et al (2013) Bottom-up fabrication of 3D cell-laden microfluidic constructs. *Mater Lett* 90:93–96
94. Kobel S, Lutolf MP (2011) Biomaterials meet microfluidics: building the next generation of artificial niches. *Curr Opin Biotechnol* 22(5):690–697
95. Arakawa CK et al (2017) Multicellular vascularized engineered tissues through user-programmable biomaterial Photodegradation. *Adv Mater* 29(37):1703156
96. Pinelli F, Magagnin L, Rossi F (2020) Progress in hydrogels for sensing applications: a review. *Mater Today Chem* 17:100317

97. Son KJ et al (2013) Micropatterned sensing hydrogels integrated with reconfigurable microfluidics for detecting protease release from cells. *Anal Chem* 85(24):11893–11901
98. Guan A et al (2017) Medical devices on chips. *Nat Biomed Eng* 1(3):0045
99. Volpatti LR, Yetisen AK (2014) Commercialization of microfluidic devices. *Trends Biotechnol* 32(7):347–350
100. Caballero D, Reis RL, Kundu SC (2020) Chapter 1 - Trends in biomaterials for three-dimensional cancer modeling. In: Kundu SC, Reis RL (eds) *Biomaterials for 3D tumor modeling*. Elsevier, Amsterdam, pp 3–41
101. Fu X et al (2015) Microfluidic pumping, routing and metering by contactless metal-based electro-osmosis. *Lab Chip* 15(17):3600–3608
102. Washburn AL, Bailey RC (2011) Photonics-on-a-chip: recent advances in integrated waveguides as enabling detection elements for real-world, lab-on-a-chip biosensing applications. *Analyst* 136(2):227–236
103. Obst F et al (2020) Hydrogel microvalves as control elements for parallelized enzymatic Cascade reactions in microfluidics. *Micromachines* 11(2):167
104. Darwish N et al (2010) Multi-analytical grating coupler biosensor for differential binding analysis. *Sens Act B: Chem* 144(2):413–417
105. Diéguez L et al (2012) Optical gratings coated with thin Si₃N₄ layer for efficient Immunosensing by optical waveguide Lightmode spectroscopy. *Biosensors* 2(2):114–126
106. Masson J-F (2017) Surface Plasmon resonance clinical biosensors for medical diagnostics. *ACS Sensors* 2(1):16–30
107. Jadhav AD et al (2015) Photoresponsive microvalve for remote actuation and flow control in microfluidic devices. *Biomicrofluidics* 9(3):034114–034114
108. Wang W et al (2017) Laboratory analytical methods applied in the early detection of cancers by tumor biomarker. *Anal Meth* 9(21):3085–3093
109. Chen M, Zhao H (2019) Next-generation sequencing in liquid biopsy: cancer screening and early detection. *Hum Genomics* 13(1):34
110. Baldini C et al (2020) Electronic nose as a novel method for diagnosing cancer: a systematic review. *Biosensors* 10(8):84
111. Zilberman Y, Sonkusale SR (2015) Microfluidic optoelectronic sensor for salivary diagnostics of stomach cancer. *Biosens Bioelectron* 67:465–471
112. Ferrara F et al (2022) Beyond liquid biopsy: toward non-invasive assays for distanced cancer diagnostics in pandemics. *Biosens Bioelectron* 196(113698):12
113. Peng Y et al (2021) Circulating tumor DNA and minimal residual disease (MRD) in solid tumors: current horizons and future perspectives. *Front Oncologia* 11:763790
114. Akgönüllü S et al (2021) Microfluidic systems for cancer diagnosis and applications. *Micromachines* 12(11):1349
115. Langer J et al (2020) Present and future of surface-enhanced Raman scattering. *ACS Nano* 14(1):28–117
116. Wu L et al (2020) Profiling DNA mutation patterns by SERS fingerprinting for supervised cancer classification. *Biosens Bioelectron* 165:112392
117. Dunne P et al (2020) Liquid flow and control without solid walls. *Nature* 581(7806):58–62
118. Galan EA et al (2020) Intelligent microfluidics: the convergence of machine learning and microfluidics in materials science and biomedicine. *Matter* 3(6):1893–1922
119. Zhang YS et al (2017) Multisensor-integrated organs-on-chips platform for automated and continual in situ monitoring of organoid behaviors. *Proc Natl Acad Sci U S A* 114(12):E2293–E2302

Part IV

Clinical Applications: Towards Personalized Medicine



Microfluidics for Cancer Biomarker Discovery, Research, and Clinical Application

20

Justina Žvirblytė and Linas Mažutis

Abstract

Currently, cancer is the leading cause of death and its incidence and mortality is growing rapidly all over the world. One of the confounding factors contributing to the failure of conventional cancer diagnostics and treatment strategies is a high degree of intratumoral and intertumoral heterogeneity at the single-cell and molecular levels. Recent innovations in microfluidic techniques have revolutionized single-cell and single-molecule research and challenged the conventional definition of a “biomarker.” Alongside classic cancer biomarkers such as circulating tumor DNA or circulating tumor cells (CTC), tumor cell heterogeneity, transcriptional and epigenetic cell states and their abundance in the tumor microenvironment have been demonstrated to impact disease progression and treatment response. Utilizing high-throughput, robust microfluidic techniques for the detection, isolation, and analysis of various cancer biomarkers, valuable information about the tumor can be obtained for clinical decision-making. This chapter presents clinically relevant advances of cancer biomarker research using microfluidics technology and identifies the emerging applications for disease diagnosis, monitoring, and personalized treatment.

Keywords

Microfluidics · Cancer diagnosis · Personalized medicine · Clinical applications · Cancer biomarkers

J. Žvirblytė · L. Mažutis (✉)

Institute of Biotechnology, Life Sciences Center, Vilnius University, Vilnius, Lithuania

e-mail: linas.mazutis@bti.vu.lt

© The Author(s), under exclusive license to Springer Nature Switzerland AG 2022

499

D. Caballero et al. (eds.), *Microfluidics and Biosensors in Cancer Research*,

Advances in Experimental Medicine and Biology 1379,

https://doi.org/10.1007/978-3-031-04039-9_20

20.1 Introduction

Cancer comprises a large group of complex disease processes and is now the leading cause of death worldwide with nearly ten million deaths in 2020 [1]. The most common cancer diagnoses in 2020 were breast cancer, followed by lung, prostate, skin, and colon malignancies, while most deaths were caused by lung, colon, liver, stomach, and breast cancers, respectively. Cancer incidence and mortality are growing rapidly around the world, with an estimated global 47% rise in new cases worldwide by 2040 based on demographic projections [1]. These data highlight the inadequacy of current disease management and the need for advanced early detection protocols, disease monitoring, and personalized treatment strategy development.

One of the confounding factors contributing to the failure of conventional cancer diagnostics and treatment strategies is a high degree of intratumoral and intertumoral heterogeneity at the single-cell and molecular levels [2]. As a tumor progresses, the diversity of its cells and cell states steadily increases, enabling further tumor progression, relapse, and resistance to therapy. Deciphering tumor heterogeneity and understanding the role of individual clones within a tumor are crucial for identifying the most effective treatment strategies and for preventing further progression and metastasis. Recent innovations in single-cell omics technologies that enable genome transcriptome and epigenome profiling have opened new avenues for tackling populational heterogeneity and delineating the gene-regulatory mechanisms that govern cancer phenotypes and disease progression [3, 4]. Single-cell transcriptomics have been particularly instrumental in this quest, enabling discoveries of new cell types in human tissues [5–7] and the reconstruction of cell developmental trajectories and tumorigenesis [8–11], and providing a foundation for human organ cell atlases [12], to name a few advances. Analysis of single-cell gene expression has shown that in many biological contexts, cells do not exist in clearly defined, stable states, but operate on a phenotypic continuum [13, 14], which perhaps reflects the natural plasticity of living systems, enabling them to adapt and acquire different phenotypes. Single-cell omics is a rapidly growing new field that provides many advantages over traditional “bulk” tissue profiling techniques, such as the ability to decipher intra-tissue heterogeneity in cell types, profile the disease microenvironments, and study rare subpopulations [15–17]. These techniques have revealed an intricate tumor mutational [18] and epigenetic-plasticity landscape [19] as well as cellular interactions in primary and metastatic tumor microenvironments [14, 20, 21] that can impact disease progression and patients’ response to therapies [22–24]. Although single-cell genomic and transcriptomic methods have greatly impacted many areas of biomedical research, other “omics” approaches such as chromatin profiling [25], DNA methylation [26, 27], and proteomics [28–30] have been under rapid development. Together, these single-cell omics technologies are becoming essential tools and revolutionizing many diverse fields of biomedical and biological research [31, 32].

However, while single-cell omics methods paved the way for a comprehensive disease characterization at the single-cell and molecular levels, most methods are not

suitable for everyday use in clinical-based cancer diagnostics and monitoring because translational approaches are needed to transfer the fundamental research findings into a clinical milieu. Initiatives such as the Human Tumor Atlas Network of the National Cancer Institute can help with this transfer as they aim to integrate single-cell omics and clinical characteristics into an interactive longitudinal 3D cancer atlas across various stages, cancer types and treatment outcomes. The effort is expected to make a profound impact on translational medicine by accelerating the discoveries of therapeutically relevant novel biomarkers, cell types, states and cellular interactions that would advance clinical research [33].

Despite academia's substantial progress in cancer research, the clinical gold standard for cancer diagnosis, stage/grade classification and treatment guidance remains solid tissue biopsy. Although critical in certain disease contexts, direct tissue examination has several inherent limitations. First, malignant tissue might be unavailable for sampling due to limited tumor size or localization, especially for a metastatic disease. Second, tissue biopsy is an invasive procedure, making it unfeasible and overly invasive for continuous disease monitoring and treatment response over extended course of treatment [34]. Third, biopsied tissue samples are typically too small for broader analytical procedures such as drug screening and treatment effectiveness analysis. Lastly, due to the spatial, cellular, molecular, and temporal heterogeneity of a tumor, tissue biopsy represents only a snapshot of a tumor's ecosystem, providing a limited and often inaccurate picture for treatment decision-making [35].

Over the past decade, the use of liquid biopsy has gained increasing attention as a less invasive alternative to solid tissue sampling [36–39]. A broad range of cancer biomarkers, such as circulating tumor and tumor-associated cells, cell-free DNA, cell-free RNAs (mRNAs, miRNAs, and lncRNAs), tumor-secreted exosomes, proteins, and metabolites have been found in various bodily fluids (urine, saliva, blood, plasma, etc.). These biomarkers contain valuable information for disease diagnosis, monitoring, prognosis and treatment response, and hold untapped possibilities for future discoveries [40]. However, accurate detection and quantification of tumor biomarkers are often challenging tasks due to the limited amount of biomaterial available for analysis as well as the limited sensitivity and specificity of commonly used analytical techniques (e.g., RT-PCR, FACS). In this context, microfluidic technologies offer several advantages over conventional biochemical and molecular biology approaches [41, 42]. The ability to perform enzymatic reactions in microfluidic compartments of nano- to femto-liter scale reaction volumes not only offers an improved analytical sensitivity but also requires lower quantities of input biomaterial. Furthermore, parallelization of thousands or even millions of individual reactions increases throughput while enabling laboratory automation. Finally, microfluidic approaches are continuously evolving, improving, and expanding into different branches of biomedicine, such as complex disease modeling or drug screening [43–45]. This chapter presents clinically relevant advances of cancer biomarker research using microfluidics technology and identifies the emerging applications for disease diagnosis, monitoring, and personalized treatment.

20.2 Tumor, Immune and Non-Immune Cells as Biomarkers of Cancer Progression Using Microfluidics

Microfluidics broadly encompasses the handling, manipulation, and analysis of liquids in microchannels or microcompartments. At microscales ($\leq 100 \mu\text{m}$), viscous forces and interfacial effects become dominant, forcing the liquids to behave very differently than at the macroscale, thus offering new analytical capabilities. To achieve desirable microscale features tailored to a specific application, lithography techniques are commonly used to manufacture microfluidic devices, chips, and systems. Four major microfluidic systems (Fig. 20.1) are used to isolate and process individual biological species (e.g., cells, nucleic acids): (i) microchannels engraved in solid or elastic materials, (ii) microchambers separated by pressure-driven valves, (iii) micro wells, and (iv) microdroplets (as reviewed in [46]). Each of these systems has pros and cons. For example, continuous-flow microfluidics is primarily used for cell culture applications such as perfusion or organ-on-a-chip systems [43], but is not suitable for high-throughput screening applications. Valve-based microfluidics offers automated workflows of single-cell analytics [47], but its relatively high operational costs and limited throughput often restrict its use in clinical settings. In contrast, applications based on microdroplets offer unmatched ultra-high-throughput possibilities, but do not work well in multi-step and heterogeneous reactions on compartmentalized biological species.

The BEST (Biomarkers, EndpointS, and other Tools) glossary by the US Food and Drug Administration defines a biomarker as a “defined characteristic that is measured as an indicator of normal biological processes, pathogenic processes, or responses to an exposure or intervention, including therapeutic interventions. Molecular, histologic, radiographic, or physiologic characteristics are types of biomarkers” [48]. In cancer research and treatment, the most exploited biomarkers are genetic alterations; classic examples include the BCRA1/2 mutation testing for breast and ovarian cancer risk assessment [49], EGFR mutation testing for lung cancer treatment with tyrosine kinase inhibitors [50] and BCR-ABL translocation detection in chronic myeloid leukemia for diagnosis and targeted therapy with tyrosine kinase inhibitors [51].

Historically biomarker research has focused primarily on various nucleic acids and proteins present in tumorous tissues or bodily fluids [52, 53], but rapid technological advances in microfluidics and next-generation sequencing have opened new possibilities to identify disease-specific signatures beyond the classical definition of “biomarker” (Fig. 20.2). Today, we recognize that non-tumor cells such as immune, endothelial, and stromal cell populations residing in a tumor’s microenvironment modulate disease progression and response to therapy. Therefore, specific tumor, immune and stromal cells or their phenotypes, subpopulations, and their abundance in the tumor microenvironment or circulating blood can be utilized as “biomarkers” for disease progression, prognosis, and therapy response.

Tumor Cells Generally, tumor cells are highly heterogeneous at genetic, epigenetic, and transcriptional levels and this heterogeneity not only reduces the efficacy of

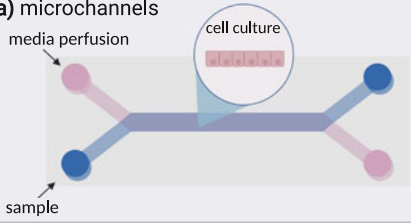
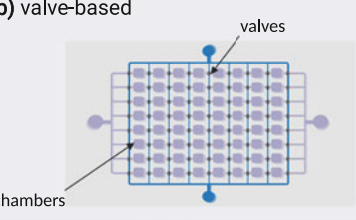
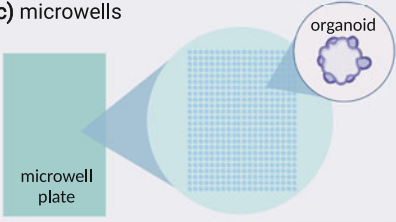
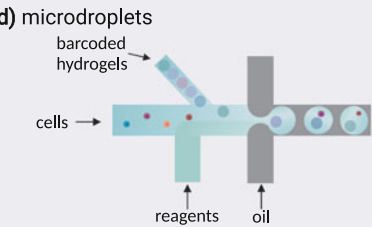
Microfluidic approaches	Applications
<p>a) microchannels</p> 	<ul style="list-style-type: none"> • organ-on-a-chip • tumor-on-a-chip • drug development and screening • CTC isolation • 2D/3D cell culture <p><i>Throughput: 1-10 reactions per chip</i></p>
<p>b) valve-based</p> 	<ul style="list-style-type: none"> • sc-omics • sc-functional assays • digital PCR • personalized drug screening • 2D cell culture <p><i>Throughput: 10-10³ reactions per chip</i></p>
<p>c) microwells</p> 	<ul style="list-style-type: none"> • sc-functional assays • sc-omics • cell culture • organoids <p><i>Throughput: 10²-10⁴ reactions per chip</i></p>
<p>d) microdroplets</p> 	<ul style="list-style-type: none"> • digital droplet PCR • sc-omics • sc-functional assays • sc-FACS <p><i>Throughput: 10⁴-10⁷ reactions per chip</i></p>

Fig. 20.1 Major microfluidic approaches and their applications. **(a)** Microchannels engraved in elastic or solid materials are used primarily for complex tumor or organ system cultivation and analysis. Various microfluidic chip designs can be used for analyte isolation based on its size or biophysical properties. **(b)** Valve-based microfluidic platforms consisting of microchambers and precisely controlled pressure-driven valves are used to control the delivery of reagents to the microchambers. **(c)** Microwell-based microfluidics are a miniaturized version of conventional microtiter plates. Nanoliter volume wells can be used to isolate and assay hundreds to thousands of single cells. **(d)** Droplet-based microfluidics are used for biological sample (e.g., cells, nucleic acids) compartmentalization in monodisperse aqueous microdroplets. Various assays on millions of single cells or single molecules can be performed inside microdroplets in a massively parallel fashion. *sc* single cell. Figure was created with BioRender

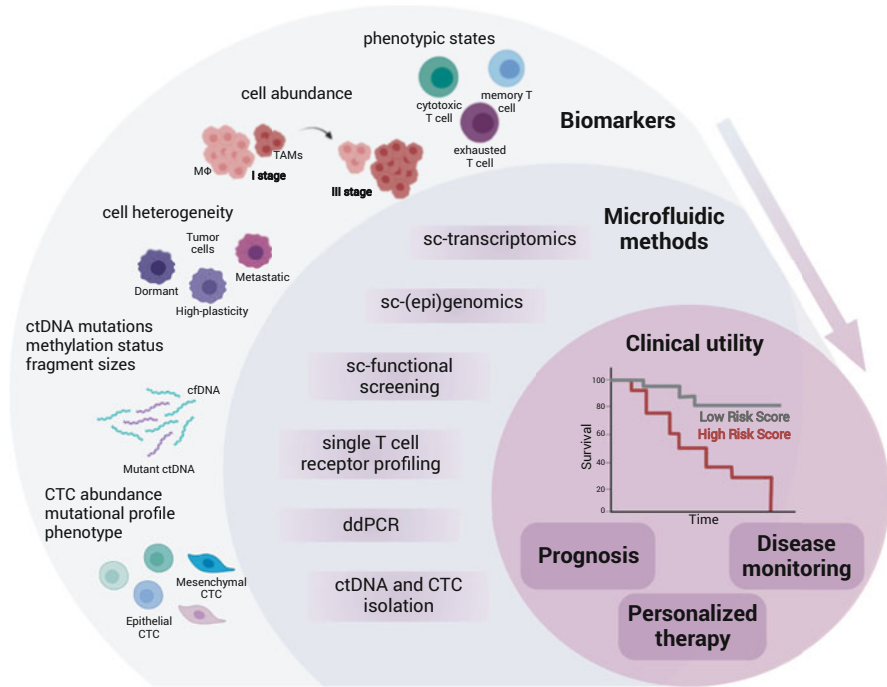


Fig. 20.2 Cancer biomarkers for clinical application using microfluidics. Microfluidic techniques have revolutionized cancer biomarker research and changed the conventional definition of a “biomarker.” Alongside classic cancer biomarkers such as circulating tumor DNA or circulating tumor cells (CTC), tumor cell heterogeneity, transcriptional and epigenetic cell states and their abundance in the tumor microenvironment have been demonstrated to impact disease progression and treatment response. Therefore, using a set of microfluidic techniques (e.g., single-cell omics, T cell receptor profiling, ddPCR), valuable genotype or phenotype information can be obtained for clinical decision-making. Various biomarkers and characteristics such as changes in the tumor microenvironment cell composition, tumor heterogeneity, CTC phenotype, ctDNA mutations and epigenetic status can be utilized for prognosis and personalized treatment decisions. Moreover, biomarkers obtained via liquid biopsy (e.g., CTCs and ctDNA) offer a minimally invasive disease monitoring option. Abbreviations: *CTCs* cell-free DNA, *ctDNA* circulating tumor DNA, *ddPCR* digital droplet PCR, *MΦ* macrophages, *sc* single cell, *TAMs* tumor-associated macrophages. Figure was created with BioRender

therapy, but also provides a tumor the selective advantage in various biological contexts such as metastatic dissemination or circumvention of immune system surveillance [18, 19, 54–56]. The functional selective advantage of tumor cells is often driven by transcriptional heterogeneity, as was recently demonstrated in leptomeningeal metastasis [54]. In this lethal condition, tumor cells disseminate into the cerebrospinal fluid (an environment without nutrients), where the cells adapt by turning on the genes of the high-affinity iron collection system (*LCN2/SCL22A17*), and by doing so outcompete the immune cells (e.g., macrophages) for essential metal ion. In a model experiment, inoculated recipient mice treated with

iron chelator conferred the survival benefit and inhibited tumor cell growth, suggesting a possible therapeutic target. Another noteworthy example, a high-plasticity cell state (HPCS) expressing high levels of the marker gene *TIGIT* (T cell immunoreceptor with IgG and ITIM domains) was recently discovered using the droplet microfluidic scRNA-seq approach in lung adenocarcinoma. The HPCS harbored a high tumorigenic capacity, and was drug resistant and associated with a poor prognosis [55]. In a small cell lung cancer, HPCS that overexpressed *PLCG2* demonstrated a pro-metastatic and a stem-like phenotype [57]. Very likely, similar types of treatment-resistant, highly plastic transcriptional and/or epigenetic cell states [25] could be present in a spectrum of human cancers and could be exploited as a novel therapeutic target. Hence, microfluidics-enabled discovery of transcriptional tumor cell states not only deepens our understanding of fundamental cancer development mechanisms, but can also be utilized to pinpoint specific drug-resistant or metastatic cell states as relevant disease biomarkers. As our understanding of transcriptional and epigenetic cell states deepens, these novel biomarkers could soon be transferred to the clinic for treatment decision-making and exploration of novel therapeutic targets.

Immune Cells Continually growing evidence suggests that certain immune cell populations may serve as useful biomarkers for disease progression and prognosis in multiple cancers, albeit this remains in the research phase. For instance, in clear cell renal cell carcinoma, the abundance of tumor-associated macrophages and exhausted T cells has been linked to the advanced cancer stage and associated with poor prognosis [20]. In triple-negative breast cancer (TNBC), single-cell profiling revealed a specific resident memory T cell population, associated with improved prognosis [58]. An interesting study utilizing genotyping, single-cell RNA sequencing and machine learning discovered a primitive acute myeloid leukemia population expressing stemness-related genes (i.e., *MEIS1*, *NRIP1*, *MSI2*) that were associated with poor outcomes [59]. Moreover, single-cell profiling of the immune compartment has shown great potential in predicting the patient's response to immunotherapy. For example, using scRNA-seq and T cell receptor profiling in lung, endometrial, colorectal, and renal cancers, a clonally expanded effector T cell population predicted clinical responsiveness to anti-PDL1 immunotherapy [60]. Notably, this population was evident not only in tumor tissues, but also in circulation, thus offering a possibility for minimally invasive patient screening. Similarly, two distinct CD8+ T cell states were discovered in metastatic melanoma that correlated with the patient's response or resistance to immune checkpoint blockade (ICB): in non-responders, the T cells were in an exhausted state, while in the responder group, the T cells expressing genes associated with memory and activation were more abundant [23]. Importantly, these T cell states were found in both pre- and post-treatment samples, suggesting a predictive potential. Conversely, in clear cell renal carcinoma, ICB treatment remodeled the tumor microenvironment so that macrophages shifted towards the pro-inflammatory phenotype and T cells exhibited characteristics of a terminally exhausted phenotype [22]. The immune evasion signature (e.g., *VSIR*, *VSIG4*, *PD-L1*, *PDCD1LG2*, etc.) expressed by these

populations were associated with poor overall survival rates and hinted at a possible ICB-resistance mechanism.

Non-Immune Tumor-Associated Cells Non-immune cells in the tumor microenvironment can also hold clinically relevant information. For example, heterogenous populations of cancer-associated fibroblasts (CAFs), found in primary and metastatic tumors, hold potential therapeutic and prognostic value [61]. In breast cancer, vascular and matrix subpopulations of CAFs were associated with metastatic dissemination and promoted cancer cell invasion in vitro [62]. Furthermore, the stromal subtype marker ratio (S100A4/PDPN) in immuno-stained breast tumor tissue specimens positively correlated with progression-free and overall survival [63]. In bladder urothelial carcinoma, an inflammatory CAF signature correlated with a poor prognosis [64]. Similar findings were reported for intrahepatic cholangiocarcinoma [65]. However, the CAF effect seems to be cancer dependent based on various studies on both CAF tumor-promoting and tumor-restraining functions [61]. For instance, the secretion of type-1 collagen by alpha-smooth muscle actin (α -SMA)-expressing fibroblasts impairs cancer progression, and in mouse models, deletion of type-1 collagen in pancreatic tumors promoted cancer progression via recruitment of myeloid-derived suppressor cells and T cell inhibition [66]. Noteworthy, distinct stromal populations are evident not only in the tumor microenvironment, but in the blood circulation as well. Using the droplet microfluidics approach, the detection and sorting of highly metabolically active circulating stromal cells based on single-cell extracellular pH have recently been reported [67]. In this proof-of-concept study, the authors demonstrated that an abundance of circulating, highly metabolically active tumor-associated stromal cells is a strong biomarker for poor survival of metastatic prostate cancer patients. Evidently, because fibroblast subpopulations have varying impact on cancer progression, more research is needed before specific fibroblast-derived markers are ready for clinical use. Nevertheless, non-tumor, non-immune cell populations of the tumor microenvironment could potentially improve prognosis and treatment decisions, and simultaneously enable the development of novel therapeutic approaches.

Presently, single-cell profiling of solid or liquid biopsies is not yet financially and analytically feasible for patient screening, however, in cases where therapeutic options are uncertain or extremely costly, the detailed analyses of transcriptional biomarkers may provide useful insights into putative drug-resistance mechanisms and guide therapeutic strategies with the best chances to prevail. Indeed, tumor-promoting cells could also serve as a diagnostic marker of disease and as a therapeutic target: in fact, numerous clinical trials are in progress for TAM depletion, dendritic cell expansion and CAF activation [68]. These and a growing number of other examples illustrate that single-cell profiling holds a great promise for improving disease prognosis and personalized treatment decisions.

20.3 Circulating Tumor Cells

Circulating tumor cells (CTCs), present in the blood of primary and metastatic cancer patients, are often considered tumor seeds. Even though metastasis is now understood as a very complex process, and the presence of CTCs in the blood does not always translate into metastasis, nonetheless, the CTC count serves as a valuable prognostic marker, and a strong indicator of an increased probability of metastasis. Overall, a high CTC count is linked to poor prognosis for various cancer types across various disease stages [69].

The first evidence of CTCs in a metastatic cancer patient was published in 1869 [70], but it took nearly a century for this discovery to be recognized following the first CTC detection techniques reported in the 1960s [71]; interest in CTC research grew with the rise of immunomagnetic separation techniques in late 1990s [72]. Due to their extreme rarity—approximately 1 CTC per billion blood cells in cancer patients—the capture and isolation of CTCs is challenging and most methods rely on specific cellular markers. CTCs are thought to originate from the tumor mass and exhibit an epithelial phenotype. Thus, the most common strategies for separating and isolating these cells are based on anti-EpCAM and anti-cytokeratin antibodies. For example, the CellSearch[®] system, approved by the US FDA for detection of CTCs in metastatic breast, colorectal, or prostate cancers, counts CTCs in 7.5 ml of whole blood using ferrofluid particles coated with anti-EpCAM antibodies and subsequently detects cytochrome positive cells using fluorescently labeled antibodies [73].

The CTC count has proven to be a clinically valid predictor of prognosis and therapy success in both non-metastatic [74] and metastatic [75, 76] diseases. To date, it is the only FDA-approved CTC detection system, although as fundamental understanding of CTC has grown, it has become clear that simple enumeration of CTCs is not sufficient to guide treatment as it does not convey much information about the tumor itself. Combining microfluidics, antibody cocktails and fluorescence in situ hybridization (FISH), researchers have demonstrated that the CTC population is highly heterogeneous [77, 78], and that epithelial-marker (EpCAM) expressing cells represent only a fraction of CTCs. Current research supports a continuum model: CTCs exhibit a range of phenotypes across the epithelial-to-mesenchymal transition, where CTC subpopulations are considered epithelial, partly epithelial-mesenchymal or mesenchymal [36, 79]. Therefore, much current effort is dedicated to developing reliable and sensitive marker-independent CTC isolation systems, preferably compatible with downstream molecular and phenotypic characterization techniques (e.g., scRNA-Seq).

Development of label-free and high-throughput cell isolation methods using microfluidic chips has accelerated the progress in CTC research. Label-free isolation can be achieved either by depleting the blood cells from the sample using known markers, or by exploiting the biophysical differences between blood cells and CTCs. A classic example of the former is the CTC-iChip [80] system that enables both positive and negative selection of CTCs based on magnetic bead labeling whereby anti-EpCAM-labeled beads are used for positive enrichment, while anti-CD45- and anti-CD15-labeled particles are used for leukocyte and granulocyte depletion. In the

microfluidic device, small blood components such as red blood cells (RBCs) are depleted based on size-dependent lateral displacement, and the leftover nucleated cells are positioned using inertial focusing and finally, magnetically labeled cells are separated using a magnetic field. The CTC-iChip offers high-throughput (ten million cells per second) and highly efficient (97% for spiked-in cancer cells) capture of cancer cells. This system can also be used for downstream analysis of CTCs [81]. Recently, the system was further improved when PDMS chips were replaced with industrial plastic chips, and the workflow was fully automated, greatly reducing hands-on time and improving technology accessibility [82]. The CTC-iChip system has been widely accepted by the research community [83–87], but the clinical utility of this device has yet to be established.

Other microfluidic techniques for separating and capturing CTCs based on cells' biophysical properties are being actively pursued. For example, Warkiani et al. introduced an elegant system for separating cells based on size using a microfluidics chip with a spiral-shaped channel with a trapezoidal cross-section [88]. The cells are separated when the Dean drag force is coupled with inertial microfluidics phenomena. This method has demonstrated 80–90% capture efficiency with model cancer cell lines, and it successfully captured CTCs derived from the blood of metastatic breast and lung cancer patients [88]. However, cancer cells are not uniform in size and the size range of white blood cells and CTCs can overlap, resulting in reduced capture efficiency, which can compromise the downstream analysis. Antibody-independent separation of CTCs was also examined using continuous flow and dielectrophoresis (DEP), which distinguishes cells based on cell membrane area and the morphological differences that influence dielectric properties [89]. Even though relatively low capture efficiencies of 70–80% were achieved for model cell lines, the design concepts were applied to develop a commercial instrument ApoStream[®] that separates CTCs based on DEP properties, albeit this has not yet been approved by the FDA. Other CTC capture techniques are also slowly moving towards the clinic. For example, the FDA labeled two more CTC capture systems, Vortex VTX-1 Liquid Biopsy System by Vortex Biosciences [90] and ClearCell[®] FX1 System[™] by Biolidics, as Class 1 medical devices for diagnostic use. Also, the “Parsortix[®] technology by Angle is seeking FDA approval for diagnostics for metastatic breast cancer [91].

While the diagnostic value of the CTC count is well reported, and its current path into the clinic is promising, it faces several roadblocks. The biological action and prevalence of CTCs remain poorly understood. CTCs are not detected in all metastatic or primary cancer patients, and CTC counts differ widely and this inter-patient variability hinders broader application of CTC use in diagnostics. For example, the CellSearch[®] system established threshold for prognostication is 5 CTCs in 7.5 ml blood for metastatic disease, but the values for different patients vary from a few cells to several hundred [73]. Another important biological consideration is CTC clustering. The aforementioned strategies generally target single CTCs, but CTC clusters are generally present in cancer patients' blood and could potentially have hold more clinical value than just a CTC count. CTC clusters have been found to have up to 100 fold greater metastatic potential than individual CTCs, regardless of

treatment method [92]. Thus, several microfluidic techniques have been introduced to capture CTC clusters. For instance, thermosensitive 3D scaffolds coated with anti-EpCAM antibodies [93] and a deterministic lateral displacement approach that assesses and utilizes differences in cluster size and asymmetry for separation [94] have been developed. Another research group has proposed a label-free microfluidic system of bifurcating traps with a set of microscale triangular pillars for the physical capture of CTC clusters [95]. Using this system, the researchers detected CTC clusters in 30–40% of patients with melanoma, metastatic breast or prostate cancer, and did so without needing to pre-process blood samples (such as RBC lysis). With growing evidence of critical CTC cluster involvement in cancer disease progression and metastasis establishment, development of such detection systems are crucial. Overall, single and clustered CTC detection systems could potentially be used for diagnostics and prognostics and some have already made their way into the clinic.

In conjunction with improved isolation techniques, there is noticeable progress in comprehensive characterization methods for downstream CTC analysis [42]. CTCs convey valuable information about the fundamental properties of the tumor, which can be utilized for prognosis or informed treatment decisions. An excellent example is the androgen receptor splice variant 7 (AR-V7) detection for metastatic castration-resistant prostate cancer. In a multicenter clinical PROPHECY study, AR-V7 detected in CTCs was validated as a predictor of shorter progression-free and shorter overall survival in patients treated with androgen receptor inhibitors [96]. It was concluded that patients with AR-V7 positive CTCs should be offered alternative treatments. CTC-derived gene expression signatures were predictive of therapy response in multiple cancers, including melanoma [83] and in localized and metastatic, prostate, [85] and breast [84] cancers. More advanced microfluidics-based single-cell profiling methods also benefit CTC biomarker research. For instance, breast cancer CTC and clustered CTC DNA methylation profiling revealed specific hypomethylation signatures in CTC clusters leading to enhanced metastatic potential [97]. Interestingly, an *in vitro* and *in vivo* (in mice models) Na^+/K^+ ATPase inhibition enabled breakup of the clusters and suppressed metastasis, highlighting a potential therapeutic target in metastatic disease. In another study, using a PDX model of TNBC and lung metastases, transcriptomic analysis revealed increased expression of ICAM1 in metastases and in patient-derived CTC clusters [98]. Importantly, ICAM1 expression blocking inhibited CTC cluster formation, trans-endothelial migration and metastasis, revealing a fundamental and targetable mechanism in metastasis. Since CTCs are the cells extravasating into the bloodstream, an interesting microfluidics assay for phenotype determination and migration potential evaluation has been recently developed [99]. In this system, CTCs are first sorted by surface markers using labeled aptamers, and then these subsets are separated based on migration potential in response to chemotactic stimuli. Another interesting development worth mentioning is a microfluidic western blotting system for protein detection in single (nonclustered) CTCs [100].

The non-invasive tumor characterization methods using microfluidics offer novel high-throughput therapeutic target identification and treatment monitoring for personalized therapy. The techniques reviewed in this section have brought the

CTC research closer to clinical use, however, efforts are needed to strengthen the link between CTC characteristics and clinical applications, plus, the implementation of standardization and quality assurance measures is necessary for assay reproducibility and robustness.

20.4 Circulating Tumor DNA

Cell-free DNA (cfDNA), first described more than 70 years ago in 1948 [101], consists of various forms of partly degraded double-stranded DNA found in the blood and other bodily fluids. The majority of cfDNA is released from dying cells and is present in the bloodstream of healthy individuals. However, in cancer patients, a small fraction of cfDNA originates from the tumor, which is termed *circulating tumor DNA* (ctDNA). This biomarker has received enormous attention in the cancer biomarkers field, owing to its non-invasive nature and promising clinical applications [102, 103].

ctDNA profiling provides an appealing alternative to tumor tissue sampling, and has already proven to be useful for fundamental cancer research, such as in the detection of druggable targets and in identifying novel resistance mechanisms [104], as well as for diagnostic and clinical prognostic purposes [103]. For instance, ctDNA was utilized as a predictor of relapse in colorectal carcinoma, where 93% of patients with detectable, patient-specific, mutated ctDNA post-surgery (where the surgery had a curative intent) had relapsed within a year [105]. Furthermore, ctDNA mutation profiling coupled with protein detection in a liquid biopsy was proposed for early breast cancer detection and successfully detected malignancies across all disease stages [106]. Importantly, ctDNA characterization is not limited to DNA mutational profiling, which is the most popular strategy for diagnostics, but diverse features of ctDNA can be analyzed, such as fragment sizes, methylation status, nucleosome positioning and even transcription factor binding sites; these analyses reveal valuable information about the tumor. For example, in colon cancer, transcription factor binding sites inferred from ctDNA predicted tumor subtypes and were used to detect early-stage cancer with >70% specificity [107]. In colorectal cancer, a methylated marker set was used to detect cancer with 95% specificity, and the abundance of methylated ctDNA correlated with disease stage [108]. Impressive phylogenetic ctDNA analysis in lung cancers depicted tumor evolution and associated ctDNA with clinical variables (e.g., tumor volume). Moreover, the subclonal analysis using ctDNA provided insight into possible causes of disease relapse and even predicted the site of relapse [109].

Despite the potential versatility of ctDNA testing, currently cell-free DNA assays are approved only for companion diagnostic purposes for several specific cancers and targeted therapies. For instance, in 2016, the FDA approved the cobas[®] EGFR mutation test v2 as a companion diagnostic for plasma ctDNA EGFR mutations in advanced-stage, non-small cell lung cancer (NSCLC) patients considered for treatment with tyrosine kinase inhibitors (TKI) [110]. In 2019, the theascreen[®] PIK3CA RGQ PCR Kit for detecting mutations in the PIK3CA gene in tumor tissue or plasma

of advanced-stage breast cancer patients considered for treatment with alpelisib was approved [111]. In 2020, the FDA approved the comprehensive genomic profiling test Guardant360[®] CDx for NSCLC patients to predict the benefit to the drug osimertinib [112]. The same year the FDA also approved FoundationOne[®] Liquid CDx for personalized treatment in NSCLC, breast, ovarian, and metastatic castration-resistant prostate cancers [113]. All of these tests are limited to mutational profiling; furthermore, if a patient tests negative for the mutations in ctDNA, additional tumor tissue profiling is necessary. Hence, the full potential of the ctDNA biomarker is yet to be implemented in clinical settings, along with robust techniques for diagnosis, prognosis, and treatment selection utilizing ctDNA.

Microfluidics has greatly advanced the field of cfDNA research, where digital droplet PCR (ddPCR) has been the enabling technology for high-sensitivity and specificity targeted DNA analysis. Using a microfluidic device, highly diluted DNA is isolated into microdroplets together with PCR reagents and fluorescent probes for mutation detection. The emulsion of droplets is then thermocycled after which the fluorescence of each droplet is measured [114]. By counting the number of positive and/or negative droplets, the absolute copy number of nucleic acids in a sample can be precisely quantified. For instance, in a prospective phase II Unicancer ProdigE-14 Trial, the ddPCR detected specific KRAS mutations in colorectal cancer patients with 91% sensitivity [75] compared to other PCR-based assays with a mean sensitivity of 67% [115]. The ddPCR assays are commercially available (i.e., the fully automated BioRad QX ONE ddPCR system that launched in 2019), making them readily accessible to researchers and clinicians. In addition, several *in vitro* diagnostic tests utilizing the ddPCR technology (e.g., SAGAsafe[®] EGFR T790M mutation detection kit for lung cancer diagnostics) offer an unprecedented detection limit of 0.0037% mutant allele frequency. Another droplet microfluidics system built on the Bio-Rad QXDx BCR-ABL %IS kit, showed 1–2 log improved sensitivity in chronic myeloid leukemia as compared to the standard RT-qPCR assay. Thus, ddPCR technology can be applied for diagnostics [108], prognostics [116] and treatment selection [75]. It is expected that this microfluidic technique will soon become a routine clinical evaluation procedure for cancer patients.

Notwithstanding the sensitivity and applicability of ctDNA analysis techniques such as ddPCR, the performance of these assays relies on the quality of the sample, which is heavily influenced by the collection and isolation methods. ctDNA is particularly difficult to isolate efficiently due to its very low quantities (typically a few ng/ml), the masking of rare mutant molecules by non-tumor cfDNA (ctDNA comprises only about 0.1–5% cfDNA depending on stage and type of tumor [102]) and the short fragment size (for cancer patients approximately 50–170 bp [117, 118]). The standard DNA isolation techniques, which involve many manual handling steps, increase the risk of sample loss, contamination, and technical biases. Thus, microfluidic isolation approaches that offer easy automation, low-volume sample processing, reduced reagent costs and operation times are being actively developed [119–122]. For instance, a solid phase extraction microfluidic device consisting of micropillar beds with photoactivated surface carboxylic groups, recovered over 70% of 50 bp DNA fragments, significantly outperforming commercial

DNA extraction kits [119]. Another promising system is the microfluidic vortex and gradient magnetic-activated cfDNA sorter for on-chip cfDNA isolation using magnetic beads in only 19 minutes [120].

Importantly, microfluidic platforms combining ctDNA extraction with downstream analysis such as ddPCR are also under active development. For example, an integrated DNA extraction and detection workflow was built on two microfluidic chips: the first was for capturing ctDNA on the surface of positively charged beads and the second, for direct emulsification of eluted ctDNA with ddPCR reagents [123]. This system detected mutations in breast and colon cancer patients' ctDNA, although the DNA extraction efficiency was only 64%, and mutations were not detected in all patients with known somatic variants in tumor tissue. A promising integrated droplet digital PCR device (ddPCR) consisting of macroscale liquid compartments; macro-, meso-, and micro-mixers; a microfluidic chip; heater and fluorescence-detection optics has been developed [124]. In this device, a 2 ml plasma sample is mixed with magnetic beads for ctDNA isolation; next, the eluted sample plus the ddPCR reagents are subjected to droplet generation on-chip, after which the emulsion is thermocycled directly in the device; lastly, the droplets containing the amplified DNA are passed through a detection channel for on-chip fluorescence readout. The device was shown to detect known biomarkers (mutations) in samples with as low as 1% mutant DNA spiked-in healthy-donor plasma, although clinical cancer patient samples were not analyzed. These integrated "sample-to-answer" approaches offer minimal manual sample processing and high throughput, thus, with considerable improvements expected in the near future, they hold much potential for clinical applications.

For ctDNA screening to become a standard practice, certain biological and technical challenges must be overcome. For instance, the current screening practice focuses on known tumor, tissue-derived mutations, but not all patients have detectable ctDNA with recognizable mutations, or detectable ctDNA at all [109]. Also, as demonstrated previously, the mutated cfDNA can be released not only by a tumor, but also by hematopoietic cells, a phenomenon known as clonal hematopoiesis of indeterminate potential (CHIP) [125]. Ultra-deep sequencing of cfDNA and WBCs from healthy donors and cancer patients show that more than 53% of cfDNA mutations in cancer patients are due to CHIP, thus highlighting the importance of implementing matched cfDNA-WBC controls for accurate data interpretation in future studies [126]. Important prerequisites for clinical ctDNA analysis application include proof of clinical validity and utility in large cohorts as well as pre-analytical and analytical variable standardization. Initiatives such as the CANCER-ID consortium, a public-private partnership supported by Europe's Innovative Medicines Initiative (IMI), have been established to resolve these challenges [127] and will hopefully fuel the translation of ctDNA research.

20.5 Microfluidics for Personalized Medicine

The advent of immunotherapies and targeted therapies has revolutionized cancer treatment. However, cancer therapy success varies between patients, even those with the same disease type and stage, mainly due to tumor heterogeneity [128]. Thus, the concept of personalized medicine has come into focus. Precisely tailored treatment regimens, adjusted over a course of disease could maximize the efficacy of existing therapies. Current biomarker profiling strategies, such as assessment of specific mutations in tumor tissue, CTCs, or ctDNA, have demonstrated great utility for treatment selection, yet only for a small fraction of cancers and only for specific treatments.

Therefore, fast and robust approaches to determine tumor sensitivity to specific drugs directly on patient biospecimens are of great interest and hold great promise. Microfluidics offers a platform for drug screening using very limited patient material such as tissue biopsy or primary cells. For example, Stevens et al. presented a microfluidic system to determine the therapeutic sensitivity of single cancer cells by using a microchannel resonator that measures cell mass and mass accumulation rate (MAR) [129]. Decreased MAR indicated positive reaction to therapeutics in acute myeloid leukemia patient cells, although the measurement was not direct because primary cells underwent a period of *in vitro* culture. Another interesting example of personalized drug screening is a fully automated plug-based microfluidic platform developed by Eduati et al. [130]. In this system, cells are encapsulated into droplets termed “plugs” in a density of about 100 cells per plug together with a drug (or combination of drugs) and fluorescent apoptosis reporter compound. Tubing containing the plugs is then incubated for 16 hours at 37 °C after which the cell death fluorescent readout is measured. The system’s utility was demonstrated using biopsies from pancreatic cancer patients, and the results underscored inter-patient variability, which further emphasized the importance of personalized drug screening approaches. The authors claim that the entire workflow can be completed within 48 hours for less than US \$150 per patient, thus opening a path for the translation of the technology to clinical applications.

The complex tumor microenvironment can alter the patient’s response to therapeutic agents, therefore, systems mimicking the *in vivo* conditions are also desired. Microfluidics are particularly suited for such application; numerous studies are ongoing on organoid, tumoroid and even multi-organ *in vitro* systems have been reported [43, 44, 131] that can be utilized not only to advance the fundamental knowledge of cellular interactions and behavior, but also various compounds in exploratory (e.g., drug development) and applied (e.g., personalized medicine) settings. Tumor organoids have been widely used for personalized testing of available and emerging therapies such as various chemotherapies [45, 132–134], immunotherapies [135, 136] and chemoradiation [137], but most methods used lack standardization and reproducibility required for wider applications. Microfluidic techniques could help resolve these issues. For instance, Ruppen et al. developed a microfluidic system for generating highly homogeneous cancer spheroids trapped in microwells for drug testing [133]. They generated co-culture

spheroids from primary lung cancer cells and pericytes, and demonstrated that pericytes act as a barrier to cancer cells, ostensibly protecting them from the negative effects of chemotherapy. Recently Schuster et al. presented a fully automated, high-throughput microfluidic organoid culture system for individual, combinatorial, or sequential drug screening with real-time fluorescent imaging [45]. The system consists of 200 well chambers that enable culturing organoids for ten different patients simultaneously in up to 20 different conditions. The robustness of this system was demonstrated by generating patient-derived pancreatic tumor organoids, and the results once more underscored significant inter-patient response variability to various treatments.

As in any other model system, cancer organoids have several limitations that hinder further application in biomedicine. The protocols of tissue handling and culture environment are ill-defined; homogeneity of organoids is difficult to achieve, especially since most protocols rely on cell self-organization. The culture poorly resembles the tumor microenvironment and lacks stromal cell populations and an immune compartment; extracellular matrices and media formulations need standardization; success in creating throughput, robustness, and reproducibility, despite several research attempts, has been low. An interesting attempt to overcome these limitations was presented recently: a multi-well microfluidic platform to culture tissue pieces called *cuboids* [138]. In a proof-of-concept study, mouse liver tissue was cut into uniform-sized cubical pieces that were immobilized in a microfluidic chip for culture with cancer drugs. The system preserved the unique tissue architecture and maintained the original cellular composition, however, it remains to be determined whether such an approach could be applied to tumor tissue culture.

Nonetheless, the personalized drug testing strategies have much potential to revolutionize cancer treatment. Microfluidic approaches that offer high-throughput, rapid clinically relevant analysis, highly controlled conditions, robustness, and reproducibility are likely to be employed, however, interdisciplinary effort from clinicians, bioengineers, and biologists is necessary for further implementation and transfer to clinical settings.

20.6 Challenges for Application of Microfluidics

Despite the major advancements in applying microfluidic techniques for cancer biomarker research, several technical challenges need to be addressed prior to transfer to clinical applications.

Standardization Currently, the majority of microfluidic systems are prototypes developed primarily by academic labs for a broad range of applications, each of which requires specific materials such as coatings, beads, surfactants, oils, and so on. The versatility of microfluidics technology is what makes it so applicable to different fields, but also what hinders the transition from the proof-of-concept stage to broader applications following commercialization. All aspects of microfluidics

remain to be standardized—from material selection to manufacturing, device operation, measurable system parameters for different applications, testing methods and even the most basic processes such as long-term storage requirements and shelf life [139]. A non-profit organization, the Microfluidics Association [140] promotes microfluidics standardization focusing on the interoperability of microfluidic devices. Another entity, the International Organization for Standardization, launched an initiative “ISO/PRF 22916 Microfluidic devices—Interoperability requirements for dimensions, connections and initial device classification” [141], which aims to create certified microfluidic standards useful for both academic labs and established companies to help accelerate the commercialization and development of the microfluidic devices.

Failure Modes and Performance To address microfluidics standardization, failure modes and assessment of device performance first need to be determined. Failure modes can relate to fabrication, design, usage or even the environment [139]. Regardless of the many issues related to the biological side of assays, currently, most failure modes for microfluidic devices are related to clogging, bubble formation, leakage, cross-contamination, coating, cracking, and delamination. The major barrier to establishing methods to avoid these complications is that, generally, such issues remain under-reported, especially in academia. Similarly, certain performance parameters need to be established to reliably compare the assays.

Materials and Manufacturing The majority of microfluidic devices used for the novel biomarker assays are manufactured in research laboratories using sophisticated techniques (e.g., soft photolithography) that require many hours of skilled hands-on labor. Also, the materials used are compatible with a small-scale production only. For instance, the standard material for microfluidics chip fabrication is polydimethylsiloxane (PDMS), which is not suitable for mass production. Moreover, it comes with some technological caveats, such as leeching of uncured oligomers and absorption of hydrophobic molecules [142], which might compromise the biological assay performed.

Cost Microfluidic systems generally are very cost efficient in term of the reagents and biological material used. However, chips are designed to be disposable, thus, for in vitro diagnostic purposes and clinical accessibility, stringent cost targets must be met.

Sample Quality Even the best analytical systems will not deliver reliable results if sample quality is low. In all biological assays, high sample quality is of extreme importance as is a degree of standardization for sample collection and processing. For instance, effort was put into creating a whole blood stabilization method for preserving viable rare cells (e.g., CTCs) for up to 72 h [86], but to be useful, such efforts must be widely accepted by the research and clinical communities.

The FDA’s Center for Devices and Radiological Health ensures patient access to safe and effective innovative devices. The Office of Science and Engineering

Laboratories has launched a Microfluidics Program that focuses on regulatory science research in preclinical testing, device quality and performance. The program's goal is to fill the regulatory gaps by fostering microfluidic device development, innovation and assessment, as well as to prepare regulatory agencies to address challenges specific to microfluidic devices throughout the medical device lifecycle [143] and across the industry. Hopefully, the regulatory aspects of microfluidic devices and standardization issues will be resolved soon, opening up the era for microfluidic technology for clinical purposes.

20.7 Future Prospects

Innovative microfluidic methods enabling single-cell and single-molecule analysis have substantially advanced our understanding of fundamental mechanisms of tumorigenesis, metastasis, cellular diversity and interactions in the tumor microenvironment, immune evasion and therapy resistance. Using this knowledge, therapies directed at novel targets such as tumor-associated cells are being developed, and new biomarkers for disease progression and therapy responses are under active exploration. Microfluidics-based technologies will remain instrumental in advancing single-cell biomarkers and analytics for the foreseeable future. In particular, the innovations in single-cell isolation methods, molecular indexing, computational algorithms and sequencing will expand our ability to detect and analyze multiple genomic modalities at the individual cellular level and to do so in a high-throughput fashion [31, 32, 144]. As multi-omics techniques will continue to advance they will further deepen our understanding of the fundamental processes behind cancer biology, from disease initiation to metastasis, and will greatly enhance translational medicine.

The exploration of non-invasive biomarkers such as CTCs and ctDNA using microfluidic techniques is on the brink of widespread clinical application. Due to the minimally invasive nature of liquid biopsies, especially when combined with fast, high-throughput robust analysis offered by microfluidics, circulating biomarker screening will likely become standard practice for patient stratification and disease monitoring. Since certain tumor biomarkers such as ctDNA, RNAs, and exosomes can be detected beyond the blood, in other bodily fluids such as saliva and urine, we expect that microfluidic technologies for analyte detection in these samples will emerge soon.

Another interesting prospect that is gaining increased attention is the integration of computational techniques such as artificial intelligence and machine learning into biological sample analysis [11]. Some impressive examples have emerged, such as the PanSeer, the ctDNA methylation test and machine learning classification method that can detect malignancy even up to four years prior to conventional cancer diagnosis [145]. However, the clinical utility of such systems remains to be established.

Low-cost, high-throughput, sensitive, and robust microfluidic solutions, combined with computational advances have great potential to fuel personalized medicine and shape the future of clinical practice.

Acknowledgments This work has received funding from European Regional Development Fund (project No 01.2.2-LMT-K-718-04-0002) under grant agreement with the Research Council of Lithuania.

References

1. Sung H, Ferlay J, Siegel RL, Laversanne M, Soerjomataram I, Jemal A et al (2021) Global cancer statistics 2020: GLOBOCAN estimates of incidence and mortality worldwide for 36 cancers in 185 countries. *CA Cancer J Clin* 71(3):209–249
2. McGranahan N, Swanton C (2017 Feb 9) Clonal heterogeneity and tumor evolution: past, present, and the future. *Cell* 168(4):613–628
3. Stubbington MJT, Rozenblatt-Rosen O, Regev A, Teichmann SA (2017 Oct 6) Single-cell transcriptomics to explore the immune system in health and disease. *Science* 358(6359):58–63
4. Tanay A, Regev A (2017 Jan) Scaling single-cell genomics from phenomenology to mechanism. *Nature* 541(7637):331–338
5. Villani A-C, Satija R, Reynolds G, Sarkizova S, Shekhar K, Fletcher J et al (2017 Apr 21) Single-cell RNA-seq reveals new types of human blood dendritic cells, monocytes, and progenitors. *Science* 356(6335):eaah4573
6. Plasschaert LW, Žilionis R, Choo-Wing R, Savova V, Knehr J, Roma G et al (2018 Aug) A single-cell atlas of the airway epithelium reveals the CFTR-rich pulmonary ionocyte. *Nature* 560(7718):377–381
7. Keren-Shaul H, Spinrad A, Weiner A, Matcovitch-Natan O, Dvir-Szternfeld R, Ulland TK et al (2017 Jun 15) A unique microglia type associated with restricting development of Alzheimer’s disease. *Cell* 169(7):1276–1290.e17
8. Paul F, Arkin Y, Giladi A, Jaitin DA, Kenigsberg E, Keren-Shaul H et al (2015 Dec 17) Transcriptional heterogeneity and lineage commitment in myeloid progenitors. *Cell* 163(7):1663–1677
9. Tirosh I, Izar B, Prakadan SM, Wadsworth MH, Treacy D, Trombetta JJ et al (2016 Apr 8) Dissecting the multicellular ecosystem of metastatic melanoma by single-cell RNA-seq. *Science* 352(6282):189–196
10. Briggs JA, Weinreb C, Wagner DE, Megason S, Peshkin L, Kirschner MW et al (2018 Jun 1) The dynamics of gene expression in vertebrate embryogenesis at single-cell resolution. *Science* 360(6392):eaar5780
11. Wagner A, Regev A, Yosef N (2016 Nov) Revealing the vectors of cellular identity with single-cell genomics. *Nat Biotechnol* 34(11):1145–1160
12. Regev A, Teichmann SA, Lander ES, Amit I, Benoist C, Birney E et al (2017 Dec 5) The human cell atlas. *eLife* 6:e27041
13. Velten L, Haas SF, Raffel S, Blaszkiewicz S, Islam S, Hennig BP et al (2017 Apr) Human haematopoietic stem cell lineage commitment is a continuous process. *Nat Cell Biol* 19(4):271–281
14. Azizi E, Carr AJ, Plitas G, Cornish AE, Konopacki C, Prabhakaran S et al (2018 Aug) Single-cell map of diverse immune phenotypes in the breast tumor microenvironment. *Cell* 174(5):1293–1308.e36
15. Klein AM, Mazutis L, Akartuna I, Tallapragada N, Veres A, Li V et al (2015 May 21) Droplet barcoding for single-cell transcriptomics applied to embryonic stem cells. *Cell* 161(5):1187–1201
16. Ng AHC, Peng S, Xu AM, Noh WJ, Guo K, Bethune MT et al (2019) MATE-Seq: microfluidic antigen-TCR engagement sequencing. *Lab Chip* 19(18):3011–3021
17. Satpathy AT, Granja JM, Yost KE, Qi Y, Meschi F, McDermott GP et al (2019 Aug) Massively parallel single-cell chromatin landscapes of human immune cell development and intratumoral T cell exhaustion. *Nat Biotechnol* 37(8):925–936

18. Morita K, Wang F, Jahn K, Hu T, Tanaka T, Sasaki Y et al (2020 Oct 21) Clonal evolution of acute myeloid leukemia revealed by high-throughput single-cell genomics. *Nat Commun* 11(1):5327
19. Gaiti F, Chaligne R, Gu H, Brand RM, Kothen-Hill S, Schulman RC et al (2019 May) Epigenetic evolution and lineage histories of chronic lymphocytic leukaemia. *Nature* 569(7757):576–580
20. Braun DA, Street K, Burke KP, Cookmeyer DL, Denize T, Pedersen CB et al (2021 May) Progressive immune dysfunction with advancing disease stage in renal cell carcinoma. *Cancer Cell* 39(5):632–648.e8
21. Zheng C, Zheng L, Yoo J-K, Guo H, Zhang Y, Guo X et al (2017 Jun) Landscape of infiltrating T cells in liver cancer revealed by single-cell sequencing. *Cell* 169(7):1342–1356.e16
22. Bi K, He MX, Bakouny Z, Kanodia A, Napolitano S, Wu J et al (2021 May) Tumor and immune reprogramming during immunotherapy in advanced renal cell carcinoma. *Cancer Cell* 39(5):649–661.e5
23. Sade-Feldman M, Yizhak K, Bjorgaard SL, Ray JP, de Boer CG, Jenkins RW et al (2018 Nov 1) Defining T cell states associated with response to checkpoint immunotherapy in melanoma. *Cell* 175(4):998–1013.e20
24. Yost KE, Satpathy AT, Wells DK, Qi Y, Wang C, Kageyama R et al (2019 Aug) Clonal replacement of tumor-specific T cells following PD-1 blockade. *Nat Med* 25(8):1251–1259
25. LaFave LM, Kartha VK, Ma S, Meli K, Priore ID, Lareau C et al (2020 Aug 10) Epigenomic state transitions characterize tumor progression in mouse lung adenocarcinoma. *Cancer Cell* 38(2):212–228.e13
26. Argelaguet R, Clark SJ, Mohammed H, Stapel LC, Krueger C, Kapourani C-A et al (2019 Dec) Multi-omics profiling of mouse gastrulation at single-cell resolution. *Nature* 576(7787):487–491
27. Clark SJ, Argelaguet R, Kapourani C-A, Stubbs TM, Lee HJ, Alda-Catalinas C et al (2018 Feb 22) scNMT-seq enables joint profiling of chromatin accessibility DNA methylation and transcription in single cells. *Nat Commun* 9(1):781
28. Peterson VM, Zhang KX, Kumar N, Wong J, Li L, Wilson DC et al (2017 Oct) Multiplexed quantification of proteins and transcripts in single cells. *Nat Biotechnol* 35(10):936–939
29. Stoeckius M, Hafemeister C, Stephenson W, Houck-Loomis B, Chattopadhyay PK, Swerdlow H et al (2017 Sep) Simultaneous epitope and transcriptome measurement in single cells. *Nat Methods* 14(9):865–868
30. Mimitou EP, Cheng A, Montalbano A, Hao S, Stoeckius M, Legut M et al (2019 May) Multiplexed detection of proteins, transcriptomes, clonotypes and CRISPR perturbations in single cells. *Nat Methods* 16(5):409–412
31. Leonavicius K, Nainys J, Kuciauskas D, Mazutis L (2019 Feb 1) Multi-omics at single-cell resolution: comparison of experimental and data fusion approaches. *Curr Opin Biotechnol* 55:159–166
32. Zhu C, Preissl S, Ren B (2020 Jan) Single-cell multimodal omics: the power of many. *Nat Methods* 17(1):11–14
33. Rozenblatt-Rosen O, Regev A, Oberdoerffer P, Nawy T, Hupalowska A, Rood JE et al (2020 Apr 16) The human tumor atlas network: charting tumor transitions across space and time at single-cell resolution. *Cell* 181(2):236–249
34. Ilić M, Hofman P. Pros: Can tissue biopsy be replaced by liquid biopsy? *Transl Lung Cancer Res* [Internet]. 2016 Aug [cited 2021 Sep 6];5(4). Available from: <https://tlcr.amegroups.com/article/view/8950>
35. Bedard PL, Hansen AR, Ratain MJ, Siu LL (2013 Sep) Tumour heterogeneity in the clinic. *Nature* 501(7467):355–364
36. Lim SB, Di Lee W, Vasudevan J, Lim W-T, Lim CT (2019 Dec) Liquid biopsy: one cell at a time. *Npj Precis Oncol*. 3(1):23

37. Pantel K, Alix-Panabières C (2019 Jul) Liquid biopsy and minimal residual disease — latest advances and implications for cure. *Nat Rev Clin Oncol* 16(7):409–424
38. Pinzani P, D’Argenio V, Re MD, Pellegrini C, Cucchiara F, Salvianti F et al (2021 Jun 1) Updates on liquid biopsy: current trends and future perspectives for clinical application in solid tumors. *Clin Chem Lab Med CCLM* 59(7):1181–1200
39. Siravegna G, Marsoni S, Siena S, Bardelli A (2017 Sep) Integrating liquid biopsies into the management of cancer. *Nat Rev Clin Oncol* 14(9):531–548
40. Ignatiadis M, Sledge GW, Jeffrey SS (2021 May) Liquid biopsy enters the clinic — implementation issues and future challenges. *Nat Rev Clin Oncol* 18(5):297–312
41. Garcia-Cordero JL, Maerkl SJ (2020 Oct) Microfluidic systems for cancer diagnostics. *Curr Opin Biotechnol* 65:37–44
42. Mathur L, Ballinger M, Utharala R, Merten CA (2020 Mar) Microfluidics as an enabling technology for personalized cancer therapy. *Small* 16(9):1904321
43. Hofer M, Lutolf MP (2021 May) Engineering organoids. *Nat Rev Mater* 6(5):402–420
44. Liu X, Fang J, Huang S, Wu X, Xie X, Wang J et al (2021 Jun 21) Tumor-on-a-chip: from bioinspired design to biomedical application. *Microsyst Nanoeng* 7(1):1–23
45. Schuster B, Junkin M, Kashaf SS, Romero-Calvo I, Kirby K, Matthews J et al (2020 Oct 19) Automated microfluidic platform for dynamic and combinatorial drug screening of tumor organoids. *Nat Commun* 11(1):5271
46. Heath JR, Ribas A, Mischel PS (2016 Mar) Single-cell analysis tools for drug discovery and development. *Nat Rev Drug Discov* 15(3):204–216
47. Thorsen T, Maerkl SJ, Quake SR (2002 Oct 18) Microfluidic Large-Scale Integration. *Science* 298(5593):580–584
48. U.S. Food and Drug Administration. About biomarkers and qualification [internet]. FDA. FDA; 2021 [cited 2021 Sep 8]. Available from: <https://www.fda.gov/drugs/biomarker-qualification-program/about-biomarkers-and-qualification>
49. Wooster R, Bignell G, Lancaster J, Swift S, Seal S, Mangion J et al (1995 Dec) Identification of the breast cancer susceptibility gene BRCA2. *Nature* 378(6559):789–792
50. Pao W, Chmielecki J (2010 Nov) Rational, biologically based treatment of EGFR-mutant non-small-cell lung cancer. *Nat Rev Cancer* 10(11):760–774
51. Druker BJ, Talpaz M, Resta DJ, Peng B, Buchdunger E, Ford JM et al (2001 Apr 5) Efficacy and safety of a specific inhibitor of the BCR-ABL tyrosine kinase in chronic myeloid leukemia. *N Engl J Med* 344(14):1031–1037
52. La Thangue NB, Kerr DJ (2011 Oct) Predictive biomarkers: a paradigm shift towards personalized cancer medicine. *Nat Rev Clin Oncol* 8(10):587–596
53. Srinivas PR, Kramer BS, Srivastava S (2001) Trends in biomarker research for cancer detection. *Lancet Oncol* 2:698–704
54. Chi Y, Remsik J, Kiseliovas V, Derderian C, Sener U, Alghader M et al (2020 Jul 17) Cancer cells deploy lipocalin-2 to collect limiting iron in leptomeningeal metastasis. *Science* 369(6501):276–282
55. Marjanovic ND, Hofree M, Chan JE, Canner D, Wu K, Trakala M et al (2020 Aug) Emergence of a high-plasticity cell state during lung cancer evolution. *Cancer Cell* 38(2):229–246.e13
56. Lawson DA, Kessenbrock K, Davis RT, Pervolarakis N, Werb Z (2018 Dec) Tumour heterogeneity and metastasis at single-cell resolution. *Nat Cell Biol* 20(12):1349–1360
57. Chan JM, Quintanal-Villalonga Á, Gao VR, Xie Y, Allaj V, Chaudhary O, et al. Signatures of plasticity, metastasis, and immunosuppression in an atlas of human small cell lung cancer. *Cancer Cell* [Internet]. 2021 Oct 14 [cited 2021 Oct 15]; Available from: <https://www.sciencedirect.com/science/article/pii/S1535610821004979>
58. Savas P, Virassamy B, Ye C, Salim A, Mintoff CP, Caramia F et al (2018 Jul) Single-cell profiling of breast cancer T cells reveals a tissue-resident memory subset associated with improved prognosis. *Nat Med* 24(7):986–993

59. van Galen P, Hovestadt V, Wadsworth MH II, Hughes TK, Griffin GK, Battaglia S et al (2019 Mar) Single-cell RNA-Seq reveals AML hierarchies relevant to disease progression and immunity. *Cell* 176(6):1265–1281.e24
60. Wu TD, Madireddi S, de Almeida PE, Banchereau R, Chen Y-JJ, Chitre AS et al (2020 Mar) Peripheral T cell expansion predicts tumour infiltration and clinical response. *Nature* 579(7798):274–278
61. Chen Y, McAndrews KM, Kalluri R (2021 Sep) Clinical and therapeutic relevance of cancer-associated fibroblasts. *Nat Rev Clin Oncol* 6:1–13
62. Bartoschek M, Oskolkov N, Bocci M, Lövrot J, Larsson C, Sommarin M et al (2018 Dec 4) Spatially and functionally distinct subclasses of breast cancer-associated fibroblasts revealed by single cell RNA sequencing. *Nat Commun* 9(1):5150
63. Friedman G, Levi-Galibov O, David E, Bornstein C, Giladi A, Dadiani M et al (2020 Jul) Cancer-associated fibroblast compositions change with breast cancer progression linking the ratio of S100A4+ and PDPN+ CAFs to clinical outcome. *Nat Cancer* 1(7):692–708
64. Chen Z, Zhou L, Liu L, Hou Y, Xiong M, Yang Y et al (2020 Oct 8) Single-cell RNA sequencing highlights the role of inflammatory cancer-associated fibroblasts in bladder urothelial carcinoma. *Nat Commun* 11(1):5077
65. Affo S, Nair A, Brundu F, Ravichandra A, Bhattacharjee S, Matsuda M et al (2021 Jun 14) Promotion of cholangiocarcinoma growth by diverse cancer-associated fibroblast subpopulations. *Cancer Cell* 39(6):866–882.e11
66. Chen Y, Kim J, Yang S, Wang H, Wu C-J, Sugimoto H et al (2021 Apr 12) Type I collagen deletion in α SMA+ myofibroblasts augments immune suppression and accelerates progression of pancreatic cancer. *Cancer Cell* 39(4):548–565.e6
67. Rivello F, Matula K, Piruska A, Smits M, Mehra N, Huck WTS (2020 Sep 30) Probing single-cell metabolism reveals prognostic value of highly metabolically active circulating stromal cells in prostate cancer. *Sci Adv* 6(40):eaaz3849
68. Bejarano L, Jordão MJC, Joyce JA (2021 Apr 1) Therapeutic targeting of the tumor microenvironment. *Cancer Discov* 11(4):933–959
69. Vasseur A, Kiavue N, Bidard F-C, Pierga J-Y, Cabel L (2021) Clinical utility of circulating tumor cells: an update. *Mol Oncol* 15(6):1647–1666
70. Ashworth TR (1869) A case of cancer in which cells similar to those in the tumours were seen in the blood after death. *Australas Med J* 14:146–147
71. Salgado I, Hopkirk JF, Long RC, Ritchie AC, Ritchie S, Webster DR (1959 Oct 15) Tumour cells in the blood. *Can Med Assoc J* 81(8):619–622
72. Racila E, Euhus D, Weiss AJ, Rao C, McConnell J, Terstappen LW et al (1998 Apr 14) Detection and characterization of carcinoma cells in the blood. *Proc Natl Acad Sci U S A* 95(8):4589–4594
73. Riethdorf S, Fritsche H, Müller V, Rau T, Schindlbeck C, Rack B et al (2007 Feb 1) Detection of circulating tumor cells in peripheral blood of patients with metastatic breast cancer: a validation study of the cellsearch system. *Clin Cancer Res* 13(3):920–928
74. Riethdorf S, Müller V, Loibl S, Nekljudova V, Weber K, Huober J et al (2017 Sep 15) Prognostic impact of circulating tumor cells for breast cancer patients treated in the neoadjuvant “Geparquattro” trial. *Clin Cancer Res* 23(18):5384–5393
75. Bidard F-C, Kiavue N, Ychou M, Cabel L, Stern M-H, Madic J et al (2019 Jun) Circulating tumor cells and circulating tumor DNA detection in potentially Resectable metastatic colorectal cancer: a prospective ancillary study to the Unicancer Prodiges-14 trial. *Cell* 8(6):516
76. Bidard F-C, Peeters DJ, Fehm T, Nolé F, Gisbert-Criado R, Mavroudis D et al (2014 Apr) Clinical validity of circulating tumour cells in patients with metastatic breast cancer: a pooled analysis of individual patient data. *Lancet Oncol* 15(4):406–414
77. Mikolajczyk SD, Millar LS, Tsinberg P, Coutts SM, Zomorodi M, Pham T et al (2011) Detection of EpCAM-negative and cytokeratin-negative circulating tumor cells in peripheral blood. *J Oncol* 2011:252361

78. Pecot CV, Bischoff FZ, Mayer JA, Wong KL, Pham T, Bottsford-Miller J et al (2011 Dec 1) A novel platform for detection of CK+ and CK- CTCs. *Cancer Discov* 1(7):580–586
79. Wu S, Liu S, Liu Z, Huang J, Pu X, Li J et al (2015 Apr 24) Classification of circulating tumor cells by epithelial-mesenchymal transition markers. *PLoS One* 10(4):e0123976
80. Ozkumur E, Shah AM, Ciciliano JC, Emmink BL, Miyamoto DT, Brachtel E et al (2013 Apr 3) Inertial focusing for tumor antigen-dependent and -independent sorting of rare circulating tumor cells. *Sci Transl Med* 5(179):179ra47
81. Karabacak NM, Spuhler PS, Fachin F, Lim EJ, Pai V, Ozkumur E et al (2014 Mar) Microfluidic, marker-free isolation of circulating tumor cells from blood samples. *Nat Protoc* 9(3):694–710
82. Fachin F, Spuhler P, Martel-Foley JM, Edd JF, Barber TA, Walsh J et al (2017 Sep 7) Monolithic Chip for high-throughput blood cell depletion to Sort rare circulating tumor cells. *Sci Rep* 7(1):10936
83. Hong X, Sullivan RJ, Kalinich M, Kwan TT, Giobbie-Hurder A, Pan S et al (2018 Mar 6) Molecular signatures of circulating melanoma cells for monitoring early response to immune checkpoint therapy. *Proc Natl Acad Sci* 115(10):2467–2472
84. Kwan TT, Bardia A, Spring LM, Giobbie-Hurder A, Kalinich M, Dubash T et al (2018 Oct 1) A digital RNA signature of circulating tumor cells predicting early therapeutic response in localized and metastatic breast cancer. *Cancer Discov* 8(10):1286–1299
85. Miyamoto DT, Lee RJ, Kalinich M, LiCausi JA, Zheng Y, Chen T et al (2018 Mar 1) An RNA-based digital circulating tumor cell signature is predictive of drug response and early dissemination in prostate cancer. *Cancer Discov* 8(3):288–303
86. Wong KHK, Tessier SN, Miyamoto DT, Miller KL, Bookstaver LD, Carey TR et al (2017 Nov 23) Whole blood stabilization for the microfluidic isolation and molecular characterization of circulating tumor cells. *Nat Commun* 8(1):1733
87. Yu M, Bardia A, Aceto N, Bersani F, Madden MW, Donaldson MC et al (2014 Jul 11) Ex vivo culture of circulating breast tumor cells for individualized testing of drug susceptibility. *Science* 345(6193):216–220
88. Warkiani ME, Guan G, Luan KB, Lee WC, Bhagat AAS, Kant Chaudhuri P et al (2014) Slanted spiral microfluidics for the ultra-fast, label-free isolation of circulating tumor cells. *Lab Chip* 14(1):128–137
89. Shim S, Stemke-Hale K, Tsimberidou AM, Noshari J, Anderson TE, Gascoyne PRC (2013 Jan 16) Antibody-independent isolation of circulating tumor cells by continuous-flow dielectrophoresis. *Biomicrofluidics* 7(1):011807
90. Lemaire CA, Liu SZ, Wilkerson CL, Ramani VC, Barzanian NA, Huang K-W et al (2018 Feb 1) Fast and label-free isolation of circulating tumor cells from blood: from a research microfluidic platform to an automated fluidic instrument, VTX-1 liquid biopsy system. *SLAS Technol Transl Life Sci Innov* 23(1):16–29
91. Kitz J, Goodale D, Postenka C, Lowes LE, Allan AL (2021 Feb 1) EMT-independent detection of circulating tumor cells in human blood samples and pre-clinical mouse models of metastasis. *Clin Exp Metastasis* 38(1):97–108
92. Schuster E, Taftaf R, Reduzzi C, Albert MK, Romero-Calvo I, Liu H. Better together: circulating tumor cell clustering in metastatic cancer. *Trends Cancer* [Internet]. 2021 Sep 1 [cited 2021 Sep 8];0(0). Available from: [https://www.cell.com/trends/cancer/abstract/S2405-8033\(21\)00146-1](https://www.cell.com/trends/cancer/abstract/S2405-8033(21)00146-1)
93. Cheng S-B, Xie M, Chen Y, Xiong J, Liu Y, Chen Z et al (2017 Aug 1) Three-dimensional scaffold Chip with thermosensitive coating for capture and reversible release of individual and cluster of circulating tumor cells. *Anal Chem* 89(15):7924–7932
94. Au SH, Edd J, Stoddard AE, Wong KHK, Fachin F, Maheswaran S et al (2017 May 26) Microfluidic isolation of circulating tumor cell clusters by size and asymmetry. *Sci Rep* 7(1):2433

95. Sarioglu AF, Aceto N, Kojic N, Donaldson MC, Zeinali M, Hamza B et al (2015 Jul) A microfluidic device for label-free, physical capture of circulating tumor cell clusters. *Nat Methods* 12(7):685–691
96. Armstrong AJ, Halabi S, Luo J, Nanus DM, Giannakakou P, Szmulewitz RZ et al (2019 May 1) Prospective multicenter validation of androgen receptor splice variant 7 and hormone therapy resistance in high-risk castration-resistant prostate cancer: the PROPHECY study. *J Clin Oncol* 37(13):1120–1129
97. Gkountela S, Castro-Giner F, Szczerba BM, Vetter M, Landin J, Scherrer R et al (2019 Jan 10) Circulating tumor cell clustering shapes DNA methylation to enable metastasis seeding. *Cell* 176(1):98–112.e14
98. Taftaf R, Liu X, Singh S, Jia Y, Dashzeveg NK, Hoffmann AD et al (2021 Aug 11) ICAM1 initiates CTC cluster formation and trans-endothelial migration in lung metastasis of breast cancer. *Nat Commun* 12(1):4867
99. Poudineh M, Labib M, Ahmed S, Nguyen LNM, Kermanshah L, Mohamadi RM et al (2017 Jan 2) Profiling functional and biochemical phenotypes of circulating tumor cells using a two-dimensional sorting device. *Angew Chem Int Ed* 56(1):163–168
100. Sinkala E, Sollier-Christen E, Renier C, Rosàs-Canyelles E, Che J, Heirich K et al (2017 Mar 23) Profiling protein expression in circulating tumour cells using microfluidic western blotting. *Nat Commun* 8(1):14622
101. Mandel P, Métais P (1948) Les acides nucléiques du plasma sanguin chez l'homme. *C R Seances Soc Biol Fil* 142:241–243
102. Keller L, Pantel K (2019 Oct) Unravelling tumour heterogeneity by single-cell profiling of circulating tumour cells. *Nat Rev Cancer* 19(10):553–567
103. Kilgour E, Rothwell DG, Brady G, Dive C (2020 Apr 13) Liquid biopsy-based biomarkers of treatment response and resistance. *Cancer Cell* 37(4):485–495
104. Misale S, Yaeger R, Hobor S, Scala E, Janakiraman M, Liska D et al (2012 Jun) Emergence of KRAS mutations and acquired resistance to anti-EGFR therapy in colorectal cancer. *Nature* 486(7404):532–536
105. Diehl F, Schmidt K, Choti MA, Romans K, Goodman S, Li M et al (2008 Sep) Circulating mutant DNA to assess tumor dynamics. *Nat Med* 14(9):985–990
106. Lennon AM, Buchanan AH, Kinde I, Warren A, Honushefsky A, Cohain AT et al (2020 Jul 3) Feasibility of blood testing combined with PET-CT to screen for cancer and guide intervention. *Science* 369(6499):eabb9601
107. Ulz P, Perakis S, Zhou Q, Moser T, Belic J, Lazzeri I et al (2019 Oct 11) Inference of transcription factor binding from cell-free DNA enables tumor subtype prediction and early detection. *Nat Commun* 10(1):4666
108. Cho N-Y, Park J-W, Wen X, Shin Y-J, Kang J-K, Song S-H et al (2021 Jan) Blood-based detection of colorectal cancer using cancer-specific DNA methylation markers. *Diagnostics* 11(1):51
109. Abbosh C, Birkbak NJ, Wilson GA, Jamal-Hanjani M, Constantin T, Salari R et al (2017 May) Phylogenetic ctDNA analysis depicts early-stage lung cancer evolution. *Nature* 545(7655):446–451
110. U.S. Food and Drug Administration. cobas EGFR Mutation Test v2 [Internet]. FDA. FDA; 2016 [cited 2021 Sep 23]. Available from: <https://www.fda.gov/drugs/resources-information-approved-drugs/cobas-egfr-mutation-test-v2>
111. U.S. Food and Drug Administration. The theascreen PIK3CA RGQ PCR Kit - P190001 and P190004 [Internet]. FDA. FDA; 2019 [cited 2021 Sep 23]. Available from: <https://www.fda.gov/medical-devices/recently-approved-devices/therascreen-pik3ca-rgq-pcr-kit-p190001-and-p190004>
112. U.S. Food and Drug Administration. Guardant360 CDx – P200010 [Internet]. FDA. FDA; 2020 [cited 2021 Sep 23]. Available from: <https://www.fda.gov/medical-devices/recently-approved-devices/guardant360-cdx-p200010>

113. U.S. Food and Drug Administration. FoundationOne[®] Liquid CDx (F1 Liquid CDx) [Internet]. FDA. 2020 [cited 2021 Sep 23]. Available from: <https://www.accessdata.fda.gov/scripts/cdrh/cfdocs/cfpma/pma.cfm?id=p200016>
114. Pekin D, Skhiri Y, Baret J-C, Le Corre D, Mazutis L, Ben Salem C et al (2011) Quantitative and sensitive detection of rare mutations using droplet-based microfluidics. *Lab Chip* 11(13): 2156
115. Hao Y-X, Fu Q, Guo Y-Y, Ye M, Zhao H-X, Wang Q et al (2017 Feb 16) Effectiveness of circulating tumor DNA for detection of KRAS gene mutations in colorectal cancer patients: a meta-analysis. *Oncotargets Ther* 10:945–953
116. Garcia-Murillas I, Chopra N, Comino-Méndez I, Beaney M, Tovey H, Cutts RJ et al (2019 Oct 1) Assessment of molecular relapse detection in early-stage breast cancer. *JAMA Oncol* 5(10): 1473
117. Moulriere F, Chandrananda D, Piskorz AM, Moore EK, Morris J, Ahlborn LB et al (2018 Nov 7) Enhanced detection of circulating tumor DNA by fragment size analysis. *Sci Transl Med* 10(466):eaat4921
118. Snyder MW, Kircher M, Hill AJ, Daza RM, Shendure J (2016 Jan) Cell-free DNA comprises an in vivo nucleosome footprint that informs its tissues-of-origin. *Cell* 164(1–2):57–68
119. Campos CDM, Gamage SST, Jackson JM, Witek MA, Park DS, Murphy MC et al (2018 Nov 6) Microfluidic-based solid phase extraction of cell free DNA. *Lab Chip* 18(22):3459–3470
120. Gwak H, Kim J, Cha S, Cheon Y, Kim S-I, Kwak B et al (2019 Mar) On-chip isolation and enrichment of circulating cell-free DNA using microfluidic device. *Biomicrofluidics* 13(2): 024113
121. Lee H, Park C, Na W, Park KH, Shin S (2020 Dec) Precision cell-free DNA extraction for liquid biopsy by integrated microfluidics. *NPJ Precis Oncol* 4(1):3
122. Zhou R, Wang C, Huang Y, Huang K, Wang Y, Xu W et al (2021 Sep) Label-free terahertz microfluidic biosensor for sensitive DNA detection using graphene-metasurface hybrid structures. *Biosens Bioelectron* 188:113336
123. Perez-Toralla K, Pereiro I, Garrigou S, Di Federico F, Proudhon C, Bidard F-C et al (2019 May 1) Microfluidic extraction and digital quantification of circulating cell-free DNA from serum. *Sens Actuators B Chem* 286:533–539
124. Geng Z, Li S, Zhu L, Cheng Z, Jin M, Liu B et al (2020 May 19) “Sample-to-answer” detection of rare ctDNA mutation from 2 mL plasma with a fully integrated DNA extraction and digital droplet PCR microdevice for liquid biopsy. *Anal Chem* 92(10):7240–7248
125. Steensma DP, Bejar R, Jaiswal S, Lindsley RC, Sekeres MA, Hasserjian RP et al (2015 Jul 2) Clonal hematopoiesis of indeterminate potential and its distinction from myelodysplastic syndromes. *Blood* 126(1):9–16
126. Razavi P, Li BT, Brown DN, Jung B, Hubbell E, Shen R et al (2019 Dec) High-intensity sequencing reveals the sources of plasma circulating cell-free DNA variants. *Nat Med* 25(12): 1928–1937
127. Lampignano R, Neumann MHD, Weber S, Klotten V, Herdean A, Voss T et al (2020 Jan 1) Multicenter evaluation of circulating cell-free DNA extraction and downstream analyses for the development of standardized (pre)analytical work flows. *Clin Chem* 66(1):149–160
128. Dagogo-Jack I, Shaw AT (2018 Feb) Tumour heterogeneity and resistance to cancer therapies. *Nat Rev Clin Oncol* 15(2):81–94
129. Stevens MM, Maire CL, Chou N, Murakami MA, Knoff DS, Kikuchi Y et al (2016 Nov) Drug sensitivity of single cancer cells is predicted by changes in mass accumulation rate. *Nat Biotechnol* 34(11):1161–1167
130. Eduati F, Utharala R, Madhavan D, Neumann UP, Longerich T, Cramer T et al (2018 Jun 22) A microfluidics platform for combinatorial drug screening on cancer biopsies. *Nat Commun* 9(1):2434
131. LeSavage BL, Suhar RA, Broguiere N, Lutolf MP, Heilshorn SC (2021 Aug) Next-generation cancer organoids. *Nat Mater* 12:1–17

132. Kopper O, de Witte CJ, Löhmußaar K, Valle-Inclan JE, Hami N, Kester L et al (2019 May) An organoid platform for ovarian cancer captures intra- and interpatient heterogeneity. *Nat Med* 25(5):838–849
133. Ruppen J, Wildhaber FD, Strub C, SRR H, Schmid RA, Geiser OT et al (2015) Towards personalized medicine: chemosensitivity assays of patient lung cancer cell spheroids in a perfused microfluidic platform. *Lab Chip* 15(14):3076–3085
134. Vlachogiannis G, Hedayat S, Vatsiou A, Jamin Y, Fernández-Mateos J, Khan K et al (2018 Feb 23) Patient-derived organoids model treatment response of metastatic gastrointestinal cancers. *Science* 359(6378):920–926
135. Neal JT, Li X, Zhu J, Giangarra V, Grzeskowiak CL, Ju J et al (2018 Dec 13) Organoid modeling of the tumor immune microenvironment. *Cell* 175(7):1972–1988.e16
136. Schnalzer TE, Groot MH, Zhang C, Mosa MH, Michels BE, Röder J, et al. 3D model for CAR-mediated cytotoxicity using patient-derived colorectal cancer organoids. *EMBO J* [Internet] 2019 Jun 17 [cited 2021 Sep 27];38(12). Available from: <https://onlinelibrary.wiley.com/doi/10.15252/embj.2018100928>
137. Ganesh K, Wu C, O'Rourke KP, Szeglin BC, Zheng Y, Sauvé C-EG et al (2019 Oct) A rectal cancer organoid platform to study individual responses to chemoradiation. *Nat Med* 25(10):1607–1614
138. Horowitz LF, Rodriguez AD, Au-Yeung A, Bishop KW, Barner LA, Mishra G et al (2021) Microdissected “cuboids” for microfluidic drug testing of intact tissues. *Lab Chip* 21(1):122–142
139. Reyes DR, van Heeren H, Guha S, Herbertson L, Tzannis AP, Ducrée J et al (2021) Accelerating innovation and commercialization through standardization of microfluidic-based medical devices. *Lab Chip* 21(1):9–21
140. Microfluidics Association [Internet]. Microfluidics Association. [cited 2021 Sep 29]. Available from: <https://microfluidics-association.org/>
141. ISO/PRF 22916 [Internet]. ISO. [cited 2021 Sep 29]. Available from: <https://www.iso.org/cms/render/live/en/sites/isoorg/contents/data/standard/07/41/74157.html>
142. Regehr KJ, Domenech M, Koepsel JT, Carver KC, Ellison-Zelski SJ, Murphy WL et al (2009 Aug 7) Biological implications of polydimethylsiloxane-based microfluidic cell culture. *Lab Chip* 9(15):2132–2139
143. Center for Devices and Radiological Health. Microfluidics program: research on microfluidics-based medical devices [internet]. FDA FDA; 2021 [cited 2021 Sep 28]. Available from: <https://www.fda.gov/medical-devices/medical-device-regulatory-science-research-programs-conducted-osel/microfluidics-program-research-microfluidics-based-medical-devices>
144. Perkel JM (2021 Jul 19) Single-cell analysis enters the multiomics age. *Nature* 595(7868):614–616
145. Chen X, Gole J, Gore A, He Q, Lu M, Min J et al (2020 Jul 21) Non-invasive early detection of cancer four years before conventional diagnosis using a blood test. *Nat Commun* 11(1):3475



Methods for the Detection of Circulating Biomarkers in Cancer Patients

21

Patricia Mondelo-Macía, Ana María Rodríguez-Ces,
María Mercedes Suárez-Cunqueiro, and Laura Muínelo Romay

Abstract

Liquid biopsy has emerged as one of the main pillars for personalized oncology. The term englobes body-fluid samples which contain tumor-derived material such as circulating tumor DNA (ctDNA), circulating tumor cells (CTCs), and circulating extracellular vesicles (cEVs). Potential clinical application of liquid biopsy analyses includes cancer screening, detection of minimal residual disease and recurrence, therapy selection, and evaluation of acquired resistance. Despite the great developments of technology focused on circulating biomarkers characterization only cfDNA testing is nowadays implemented for the therapy selection in some advanced tumors. This can be partially explained by the fact that there is still a lack of global standardization of procedures both in the pre-analytical and analytical steps. In the present chapter, we summarize the different strategies for addressing the study of liquid biopsy taking into account their pros and cons to be

P. Mondelo-Macía · A. M. Rodríguez-Ces

Translational Medical Oncology Group (Oncomet), Health Research Foundation Institute of Santiago (IDIS), Complejo Hospitalario Universitario de Santiago de Compostela (SERGAS), Santiago de Compostela, Spain

Department of Surgery and Medical-Surgical Specialties, Medicine and Dentistry School, Universidade de Santiago de Compostela (USC), Santiago de Compostela, Spain

Centro de Investigación Biomédica en Red en Cáncer (CIBERONC), Instituto de Salud Carlos III, Madrid, Spain

M. M. Suárez-Cunqueiro · L. M. Romay (✉)

Translational Medical Oncology Group (Oncomet), Health Research Foundation Institute of Santiago (IDIS), Complejo Hospitalario Universitario de Santiago de Compostela (SERGAS), Santiago de Compostela, Spain

Centro de Investigación Biomédica en Red en Cáncer (CIBERONC), Instituto de Salud Carlos III, Madrid, Spain

applied in a clinical context and we also discuss the main technical and clinical challenges in the field of circulating biomarkers and personalized oncology.

Keywords

Circulating tumor biomarkers · Liquid biopsy · Personalized oncology · Circulating tumor cells · Extracellular vesicles

21.1 Introduction: Clinical Relevance of Liquid Biopsy for Personalized Oncology

Advances in molecular biology have clearly changed the way to manage cancer, allowing us to coin the term “personalized oncology.” This term refers to the individualized diagnosis, treatment and disease monitoring based on the specific molecular characteristics of each tumor [1]. In this context, the analysis of tissue remains the gold standard for making cancer diagnosis and characterization, but this procedure has limitations such as access difficulty, mainly to biopsy metastasis, the lack of representativity of the tumor heterogeneity and the possibility of follow-up the clonal evolution under the therapy pressure [2]. Therefore, the analysis of circulating biomarkers has emerged as a key tool reaching more personalized management of cancer patients [3].

The term “liquid biopsy” was first used by Pantel and Panabières in 2010 to refer to the analysis of circulating tumor cells (CTCs) in blood from cancer patients [4]. Currently, the concept is generally employed to talk about the sampling and analysis of tumor-derived material present in different body-fluids, mainly blood, but also other body fluids such as saliva, urine, cerebrospinal fluid, ascites, or pleural effusions [3]. Circulating biomarkers present in fluid biopsies comprise CTCs, circulating tumor DNA (ctDNA), circulating cell-free RNA (cfRNA), circulating extracellular vesicles (cEVs), and other circulating elements such as immune cells or tumor-educated platelets, among others. These circulating biomarkers have shown great potential for cancer screening, molecular diagnosis, predicting the patients’ prognosis, assessing minimal residual disease after surgery, the therapy selection/monitoring and for characterizing the mechanisms of resistance in different tumor types [3].

In the clinical setting, ctDNA has been recently implemented to analyze driver mutations that condition the response to targeted therapies and some molecular tests have been approved as a companion diagnostic in the context of advanced breast, non-small-cell lung (NSCLC), prostate and ovarian tumors. NSCLC was the first tumor in which the analysis of ctDNA for tumor phenotyping was included in the guidelines. Thus, genomic alterations in *EGFR*, *ALK*, *ROS1*, *BRAF*, *MET*, and *RET* must be analyzed in tissue or ctDNA to determine the appropriate treatment [5] (National Comprehensive Cancer Network (NCCN). Non-Small Cell Lung Cancer. Version 4.2020. NCCN Clinical Practice Guidelines in Oncology. Accessed January 6, 2020. nccn.org/professionals/physician_gls/pdf/nscl.pdf). In advanced breast cancer, NCCN guidelines recommend the analysis of *PIK3CA* status using tissue

samples or ctDNA to guide the administration of Alpelisib [6] (National Comprehensive Cancer Network (NCCN). Invasive Breast Cancer. Version 4.2020. NCCN Clinical Practice Guidelines in Oncology. Accessed January 6, 2020. [nccn.org/professionals/physician_gls/pdf/breast.pdf](https://www.nccn.org/professionals/physician_gls/pdf/breast.pdf)). Also, in advanced colorectal cancer, several studies have highlighted the feasibility of interrogating *RAS* and *BRAF* status to guide anti-EGFR therapy [7, 8]. The value of ctDNA analyses for the response assessment has been reported in many tumors such as melanomas or breast cancer, and for different targeted and non-targeted therapies [9–12]. Plasma ctDNA has been also explored as a prognostic biomarker to stratify the risk of recurrence in localized tumors after curative surgery, indicating those patients with a need of more intensive adjuvant therapy [13, 14]. In the same line, cfDNA studies have shown value as diagnostic tools. For this purpose, the identification of methylated patterns has been successfully applied to detect the presence of different tumor types [15]. Actually, the detection of methylation in the promoter region of the *SEPT9* gene in plasma cfDNA (Epi proColon test) represents the first blood-based test approved by the FDA for the screening of CRC [16, 17].

CTC research is considered the start-point of the liquid biopsy field. Early in the formation and growth of a primary tumor, cells are released into the bloodstream. Several groups are studying the clinical benefit of CTC monitoring [18]. CTCs have been validated as a prognostic marker in metastatic breast cancer and other solid tumors such as prostate, colorectal, and lung cancer, showing even more accuracy than conventional imaging methods for response evaluation [19]. However, there are still technical challenges to using CTC monitoring to detect minimal residual disease in patients at early stages. On the other hand, the molecular characterization of CTCs is of great interest to guide the selection of targeted therapies since it allows clinicians to have a dynamic view of different molecular targets such as ERBB2, EGFR, AR or PD-L1, among others [19, 20].

On the other hand, the field of cEVs and miRNAs is continuously increasing due to their relevant function during the process of carcinogenesis and tumor spread. They can be detected in different body fluids and have shown great potential as cancer biomarkers for diagnostic and prognostic purposes. In particular, EVs contain both proteins and nucleic acids that can serve to increase tumor detection sensitivity [21, 22]. However, one of the main limitations for cEVs based approaches is the absence of tumor-specific markers to identify the tumor-derived EVs. Only hot shot protein 60 (HSP60) and Glypican-1 (GPC1) have been identified as potential identifiers for detecting EVs from colorectal, pancreatic, and breast cancer detection [23]. Thus, studies based on cEVs and in fluid samples are still in an infancy stage and further validation in clinical studies is required to clarify their impact on precision oncology.

Finally, other blood elements such as tumor-educated platelets (TEPs) or the different circulating immune cells have been evaluated as liquid biopsy biomarkers for prediction or monitoring of therapy responses, but their application is still far from the clinical routine [24, 25].

In the present chapter, we summarize the analytical strategies developed to interrogate the presence of CTCs, ctDNA, and cEVs as the main type of circulating markers with clinical interest for personalized oncology.

21.2 Strategies for CTCs Isolation and Characterization

Circulating tumor cells are present in the bloodstream at a low proportion, about 1 CTC per 10^6 – 10^7 leukocytes [26] and with a very short half-life (1–2.4 h) [27, 28]. Due to the low concentration in blood, CTCs identification and characterization require methods with high analytical sensitivity and specificity [28], being their isolation technically challenging. In the last years, a high number of promising CTC-detection technologies have been developed, focused on the differential features between CTCs and the surrounding normal blood cells, including physical properties (size, density, electric charges, deformability) and biological properties (cell surface protein expression, viability) [29]. Here, we divide the different methods to enrich CTCs into two main principles: antigen-dependent methods and antigen-independent methods (Fig. 21.1).

21.2.1 CTCs Isolation Strategies

21.2.1.1 Antigen-Dependent

Antigen-dependent isolation approaches are the most common methods employed and they are based on the presence of specific surface markers by CTCs (called positive enrichment) or by blood cells (negative enrichment).

Positive enrichment, the most employed strategy is usually carried out using antibodies that recognize epithelial cell adhesion molecule (EpCAM) [29] conjugated with magnetic nanoparticles. Among the current EpCAM-based technologies, CellSearch® system (Menarini, Silicon Biosystem, Bologna, Italy) [30] has become the “gold standard” for the CTC-detection methods. CellSearch® system employs anti-EpCAM-coated ferrofluid nanoparticles for the selection of EpCAM positive cells. Next, an immunostaining step discriminates CTCs from leukocytes based on the positive expression of cytokeratins and the absence of CD45 staining together with morphologic criteria. Although a high number of alternatives that employ magnetic nanoparticles conjugated with anti-EpCAM antibodies are also available [31], until now CellSearch® system is the unique method approved by the Food and Drug Administration (FDA) for clinical use in metastatic breast, prostate and colorectal cancer [32–34].

Recently, new positive enrichment methods are being developed, in which the specific surface markers are immobilized on the surface of microfluidic chips [31] to increase the contact between the cells and, therefore, to enhance capture efficiency. However, the isolation in all these approaches is based on the EpCAM expression, therefore they are not able to detect CTCs that show no EpCAM expression, for example, CTCs of non-epithelial tumors such as sarcomas or CTC that have undergone epithelial-to-mesenchymal (EMT) transition [35, 36].

Negative enrichment methods employ magnetic nanoparticles conjugated with antibodies against the common leukocyte antigen CD45 [37] or other antigens expressed in blood cells and represent a good alternative to avoid the limitations of the EpCAM-dependent isolation. They allow isolating CTCs independently of any CTC surface marker expression however due to the low proportion of CTCs and

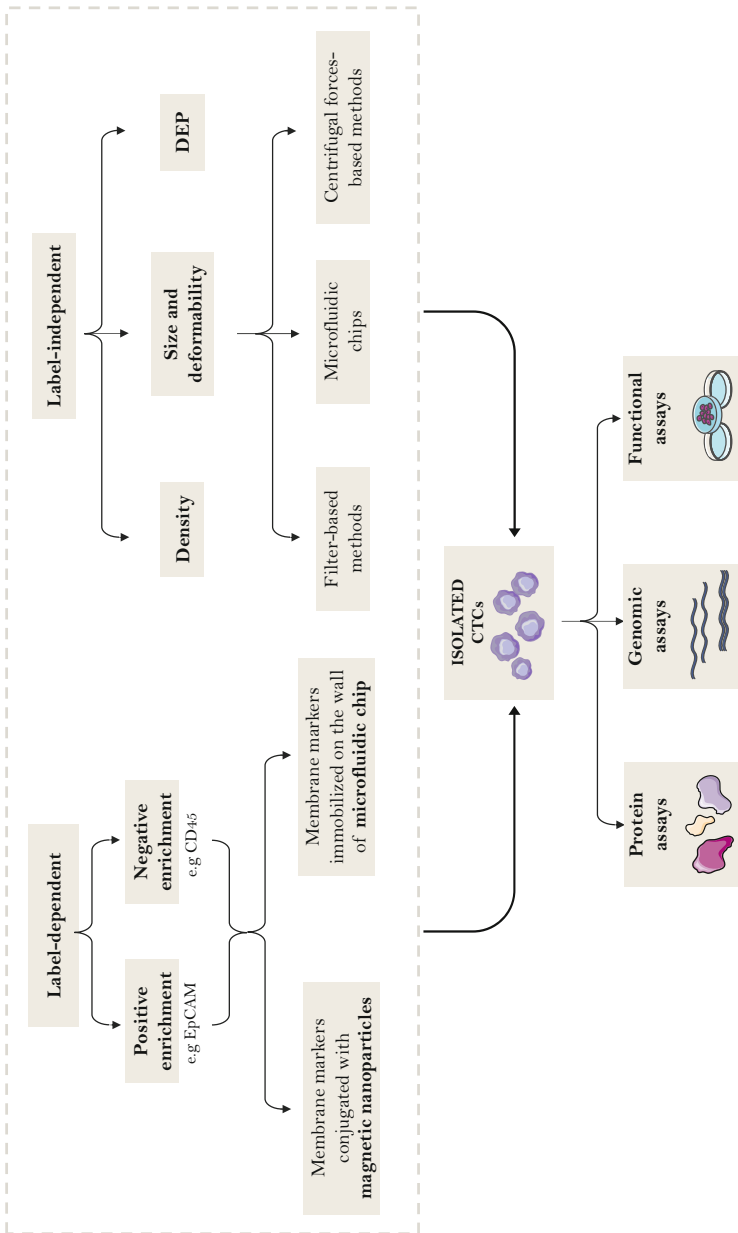


Fig. 21.1 Different strategies for CTCs isolation and characterization. DEP, dielectrophoresis

the recent observation that CTCs travel into the bloodstream coated with blood cells [38], the resulted recovery rate is often relatively low [31].

21.2.1.2 Antigen-Independent

Antigen-independent methods are based on physical properties of CTCs such as density, electric charges (DEP, dielectrophoresis), size, and deformability, among others. The principal advantage and difference with the antigen-dependent methods are that they do not require specific surface markers on CTCs, so they also allow the isolation of CTCs with a low epithelial phenotype. Density-based methods were the first techniques developed. These methods allow to processing of high volumes of blood (about 25 mL) with a quick processing time; however, they generally show a low efficiency and purity of the sample obtained [31]. The size-based methods are the most common. They are based on the fact that tumor cells are larger than blood cells [39, 40] and, therefore, they can be isolated using filter-based strategies (such as ISET assay (Rarecells Diagnostics, Paris, France) [41]), microfluidic chips (such as Parsortix system (Angle, UK) [42]) and methods based on centrifugal forces [43]. The different charges between blood cells and CTCs can also be employed in their isolation. DEP field forces are employed to move CTCs independently to other blood cells, being a highly specific method [44].

Antigen-independent methods are generally easy to implement, however they depend on the availability of advanced materials or assistive engineering technologies for better clinical application [20]. Interestingly, new methods combining antigen-based capture with the advantages of microfluidics methods, such as CTC-iChip are being developed for increasing the isolation efficacy [45]; however, nowadays a robust and standardized platform to capture CTCs for clinical application remains a challenge.

Finally, it is important to remark that small volumes processed with the methods here described may be a serious limitation for the detection of these rare events, especially in cancer patients without metastases, in which the number of CTCs is expected to be very low. To solve this problem, some “in vivo” approaches such as GILUPI Nanodetector® [46] or Diagnostic leukapheresis (DLA) can be employed [47].

21.2.1.3 Single CTCs Isolation

After enrichment, the CTC fraction usually still contains a substantial number of leukocytes [29]. This background of leukocytes is seen in all CTC enrichment platforms being the posterior molecular analyses of CTCs a challenge. Therefore, after the detection of CTCs, there are some platforms that allow the isolation of pure CTCs at a single level by the use of micromanipulation or via dielectron force manipulation (such as the DEPArray system (Menarini, Silicon Biosystem, Bologna, Italy), among other strategies [48].

21.2.2 CTCs Characterization

After enrichment, a variety of approaches can be employed to distinguish and characterize the CTCs. Analysis of CTCs at the proteome, genome, and transcriptome level provides valuable information about the molecular heterogeneity of these cells and more precise characterization of the disease [49]. Furthermore, CTCs can also be used for functional studies “in vitro” and “in vivo” models, allowing to study the biological process and characteristics of CTCs as well as test the response to different therapies.

21.2.2.1 Protein Expression

After enrichment, immunohistochemical or immunofluorescent (IHC or IF) assays can be used to distinguish CTCs from nonspecifically captured cells. The most commonly used antibodies are cytokeratins combined with markers such as CD45 that identify the background blood cells [50]. In addition, other surface proteins can be analyzed by IF that could be key candidates for targeted therapies. Thus, certain protein expression in CTCs has been studied, such as PD-L1 in lung cancer patients [51] and ER and HER2 in breast cancer, among others [52]. In addition, a microfluidic western blot technology for proteomic phenotyping of CTCs has also been developed, however, the number of proteins included is scarce [53].

21.2.2.2 Genomic Analyses

Genomic analyses at the DNA level allow for the detection of driver mutations in enriched CTCs samples [54]. Real-time polymerase chain reaction (RT-PCR), digital droplet PCR (ddPCR), and next-generation sequencing (NGS) are the most employed methods; however, results obtained present a low sensitivity because of “masking” the tumor profile by wild-type DNA from leukocytes [55].

More comprehensive analyses can be carried out using CTCs isolated at a single level followed by amplification of the whole genome, providing a valuable tool in order to know more about the heterogeneity of the tumor [55], as well as to predict the response of therapy. For example, the genomic profile of single CTCs can be employed to generate a copy number abnormalities (CNA)-based classification that can differentiate chemosensitive from chemorefractory patients in small cell lung cancer [56]. In contrast, technical limitations of CTCs isolation efficiency and the difficulties of performing whole-genome analyses on rare cells have limited the number of CTCs genomic profile studies [50] in comparison with cfDNA studies.

In another hand, gene-expression analyses in CTCs could be useful to know the nature and extent of tumor heterogeneity, linking phenotypic differences with genetic and epigenetic aberrations [57]. However, RNA is less stable and more difficult to preserve in comparison to DNA. Hence, RNA degradation constitutes a major challenge for CTCs analyses in multicenter clinical studies. Until now few single-CTCs transcriptome studies have been performed.

21.2.2.3 Functional Analyses

CTCs can also be characterized in functional studies. Some strategies for CTCs isolation offer the possibility to isolate viable CTCs and apply innovative culturing technologies to study fundamental characteristics of CTCs such as invasiveness, kinetic activity, and responses to different therapies [28]. In vitro models have been successfully reported, however, to obtain a cell culture high number of CTCs are required, and few patients have the CTCs number required. So far, it has been possible to obtain a short-term and long-term expansion of CTCs from breast, colorectal, lung, and prostate cancer, among others [58]. These cell lines can be used for drug screening, but the process of establishing these cell lines is not yet rapid enough to enable studies to inform treatment decisions for the donor patient [59].

In another hand, CTC-derived explant (CDX) models have emerged recently. For their generation, CTCs are enriched from the blood of patients and injected into immunocompromised mice to generate tumors and expand the initial material. Thus, CDXs constitute a valuable tool for clinical drug development [60]. These CDXs have been successfully generated in small cell lung [61], colorectal [62], breast [63], and prostate cancer [64], among others. Their main limitation is the time required to develop the CDXs models, usually several months.

21.3 Strategies for cfDNA/ctDNA Characterization

Although the mechanisms by which this tumor DNA reaches the circulation are not fully described, there are currently two accepted processes to explain its release. The passive mechanism implies that cells release DNA into the circulation as a consequence of cell death phenomena (necrosis or apoptosis). In this sense, the usual size of ctDNA is 167 bp, in line with the size of nucleosomal DNA that normally appears in apoptotic phenomena, but fragments that represent nucleosomal dimers or trimers can also appear. The second mechanism that allows the appearance of DNA in circulation is associated with an active release by tumor cells and may constitute a communication mechanism, although this process is not known in detail [65, 66]. Once in circulation, cfDNA is eliminated in the liver, kidney, and spleen, with an approximate half-life in the circulation of 16 min [66]. In cancer patients, ctDNA is found in a variable but normally very low (1–0.01%) percentage in relation to all cfDNA, which is usually less than 1 ng/ μ L. As already mentioned, this fraction varies depending on the stage, location, or degree of vascularization of the tumor, but also other physiological conditions such as tissue damage or marked exercise. Thus, tumors with multiple metastatic locations and highly vascularized will have higher levels of ctDNA [67].

21.3.1 cfDNA Isolation and Quantification

Before describing detection techniques, it is important to focus on cfDNA isolation methods. For plasma isolation, the most recommended protocol includes double

centrifugation: the first centrifugation at $1200/1600\times g$ for 10 min and then the second centrifugation at $5000/6000\times g$ for another 10 min to ensure the elimination of any cellular debris. Once the plasma is isolated, it must be stored at -80°C until its use and avoid several processes of freezing and thawing of the sample [51, 68]. For cfDNA isolation, we can use traditional extraction methods such as phenol-chloroform or alcoholic precipitation, which normally have very high yields. However, these approaches require more processing time than commercial extraction kits, which are mainly based on affinity columns, magnetic particle capture, capture by filtration, and methods based on the phenol-chloroform strategy. There are several studies that have compared the efficiency of different commercial isolation kits [68, 69]. The main differences observed between them are the recovery efficiency and the size of the isolated fragments. In some studies, the recovery results have been favorable to kits that use magnetic particles, such as MagNA Pure (Roche Diagnostics, Basel, Switzerland), compared to those that use affinity columns. One of the most widely used column-based isolation kits is the QIAamp DNA Blood Mini Kit (Qiagen, Hilden, Germany), which has shown cfDNA recoveries of 80–90%. Another column kit that has shown good results is the NucleoSpin Plasma XS (Marcherey Nagel, Düren, Germany), which is capable of recovering DNA fragments >50 bp in very small volumes [70].

Four main strategies are commonly used to characterize the concentration and size of isolated cfDNA: spectrometry, fluorometry, electrophoresis, and PCR-based techniques. The most specific and sensitive of the four options is the assessment of cfDNA quantity by PCR-based strategies to detect conserved sequences in the genome [71].

21.3.2 ctDNA Characterization

CfDNA analyses allow to identify mutations of interest (including resistance mutations) to guide the therapeutic decisions in several cancer types [72], the detection of cancer at early stages and the presence of minimal residual disease [59, 73, 74] as well as the assessment of the tumor mutational burden [75].

Thus, after isolation, ctDNA can be assessed to investigate for molecular alterations by two different approaches: single-gene analysis (PCR-based methods) or genome-wide analysis (through NGS strategies) (Table 21.1). During the last years, the development and improvement of these technologies has allowed the implementation of ctDNA analyses into the clinical routine. Thus, four tests have been approved by the FDA for clinical use. Two PCR-based assays, the theascreen® *PIK3CA* PCR Kit (Qiagen, Hilden, Germany) for breast cancer patients [76] and the Cobas® *EGFR* Mutation Test v2 (Roche Molecular Systems, Inc., Basel, Switzerland) for NSCLC patients [77] and two NGS-based assays, the FoundationOne Liquid CDx test (Foundation Medicine, Inc., MA, EEUU) for patients with solid malignant neoplasm [78] and the Guardant360 CDx (Guardant Health, Inc., CA, EEUU) for NSCLC patients [79]. All of the kits allow identifying patients who may benefit from treatments based on specific targeted therapies.

Table 21.1 Summary of the most common strategies for the ctDNA analysis

Method	Platform	Sensitivity	Specificity	Limitations
PCR-based	RT-PCR	1–0.1%	99%	Detects only known mutations; medium sensitivity
	ddPCR	0.01–0.1%	100%	Detects only known mutations; limited in multiplexing
	BEAMing	0.01%	100%	Detects only known mutations
Genome wide analyses	NGS panels	> 0.4	> 99%	High ctDNA input; bioinformatic interpretation
	WGS/WES	0.02%	80–90%	High ctDNA input; bioinformatic interpretation; higher risk of false positives

However, due to the low concentration of ctDNA in total cfDNA, ctDNA analyses involve a challenge for detecting genetic alterations (point mutations, CNAs or small indels) at the early stages of tumor development [80]. Epigenetic analyses on cfDNA have increased relevance to improving ctDNA detection in the early phases of the disease.

21.3.2.1 PCR-Based Techniques

PCR-based techniques were the first assays that allow to detect single or a low number of point mutations using highly sensitive and specific techniques with a rather fast and cost-effective rate. Real-time PCR (RT-PCR) was the first assay employed, reporting specific known mutations, but with a limited sensitivity (0.1–1%) [81]. In the last years, new technologies such as digital PCR (dPCR) methods, which include droplet digital PCR (ddPCR) and BEAMing (beads, emulsions, amplification and magnetics), showed high concordance with results obtained in tumor tissue [8, 82], and improved the sensitivity (0.01–0.1%) and specificity (100%).

Nevertheless, the main limitation of ctDNA analyses using PCR-based techniques is the requirement of previous information about the tumor type and the mutations characterizing this tumor. Therefore, PCR-based techniques are commonly employed to select targeted therapies, monitor the patients' evolution or detect resistant mutations during the treatment.

21.3.2.2 NGS

The second approach is focused on a genome-wide analysis of CNAs or point mutations through next-generation sequencing (NGS) strategies. Based on the assay panel size, there are single-locus/multiplexed assays, targeted sequencing, and genome-wide sequencing [83]. Genome-wide characterization allows a more complete and patient-specific genotyping to assess tumor heterogeneity and to follow the clonal evolution across the treatment [83]. The principal limitations of NGS-based strategies are the high cfDNA input requirement and general present lower specificity (80–99%) [67, 81].

Among these approaches, ctDNA can be analyzed by specific panels covering a high number of targeted genes (by NGS panels) or analyzing the total genome by whole-genome sequencing (WGS) or whole-exome sequencing (WES). WES and WGS based methods allow the detection of all possible aberrations in DNA, although it has limited analytical sensitivity in cfDNA applications. This phenomenon could be due to the efficiency by which the genetic regions of interest can be captured/enriched from cfDNA and the higher error rate of sequencing reactions [84].

21.3.2.3 Epigenetic Alterations

In addition to genetic alterations, different types of epigenetic marks have been explored in cancer as specific to the malignant process. These marks have been mainly explored in tissue samples but their interest in cancer diagnosis and monitoring using liquid biopsy has increased exponentially during the last 5 years [85].

DNA methylation is the most studied epigenetic modification. This covalent modification consists of the incorporation of a methyl group to the 5' carbon of cytosines in cytosine-phosphate-guanine (CpG) dinucleotides to generate 5-methylcytosine (5mC) [86]. The detection strategies of DNA methylation patterns can be divided into sodium bisulfite conversion dependent or independent [87]. The most used are the bisulfite conversion dependent and are based on the fact that after sodium bisulfite treatment, 5mC cannot be converted into uracils [88].

For interrogating DNA of both CTCs or cfDNA different techniques have been successfully applied such as methylation-specific PCR (MSP), methylation-sensitive high-resolution melting (MS-HRM), quantitative methylation-specific PCR (qMSP) and digital PCR (dPCR) such as methyl-BEAMing and droplet digital PCR (ddPCR) [89–92]. These PCR based approaches are directed to analyze a low number of CpG, while other strategies like methylation microarrays [93, 94] or genome-wide bisulfite-based approaches based on NGS provide a more comprehensive view of the methylome using both cfDNA from cancer patients or DNA isolated from CTCs, even at the single-cell level [95, 96].

21.4 Advances in Circulating Extracellular Vesicles Analyses

The extracellular environment contains a large number of mobile membrane-limited vesicles secreted from different cells called “extracellular vesicles” (EVs) [97–99]. Although current research focuses primarily on two major types of EVs (exosomes and microvesicles (MVs)), EVs also include other vesicular structures such as large apoptotic bodies (Abs) as well as retrovirus-like particles (RLPs), exosome-like vesicles and membrane particles [97, 99, 100].

EVs represent a tool for intercellular communication in the body [97, 101–104] being present in a variety of body fluids including blood, urine, saliva, cerebrospinal fluid, lymphatics, tears, saliva and nasal secretions, ascites, and semen [101, 105, 106], which make EVs an interesting cancer biomarker. They carry different types of cellular content such as lipids, proteins, metabolites, receptors, effector molecules,

and nucleic acids like DNA and RNA (mRNA and microRNA) [107, 108]. This content can be translated to another cell [107–110] promoting different mechanisms including tumor progression by favoring angiogenesis and tumor cell migration in metastases [111–113]. Actually, EVs have shown to be valuable tools as biomarkers for longitudinal monitoring, defining tumor type, stage, progression, and treatment response [114, 115].

Exosomes are small EVs that generally possess a diameter of ~40–100 nm and a buoyant density of 1.13–1.19 g/mL [101, 116–118]. They are generated through a double invagination of the plasma membrane and the following formation of intracellular multivesicular bodies (MVBs) containing intraluminal vesicles (ILVs) [119]. These vesicular bodies are sorted by the endosomal network to their appropriate destinations, including lysosomal degradation, recycling, or exocytosis, releasing his ILVs content as exosomes [98, 106, 120, 121]. On the other hand, microvesicles arise through direct outward budding and fission of the plasma membrane, in a process called ectocytosis which produces microvesicles, microparticles, and large vesicles in the size range of ~50 nm to 1 μ m in diameter [106, 113].

21.4.1 Isolation Methods

Currently, available purification methods are not capable of fully discriminating between exosomes and MVs [97, 122]. This lack of sufficient specificity and sensitivity makes more challenging their implementation in routine clinical practice [123, 124]. In fact, nowadays, there is no consensus on a “gold standard” method for EV isolation and purification [125]. Therefore, it is of utmost importance to improve and establish guidelines for EV isolation and analysis [125, 126], since depending on the method employed the amount, type and purity of the EVs recovered is different. Here we summarize some of the options for their isolation and characterization (Fig. 21.2).

21.4.1.1 Ultracentrifugation Techniques

Differential Ultracentrifugation

This is the most commonly employed EVs isolation method [127–129]. It is based on a succession of differential centrifugal forces to separate the particles: firstly, a low centrifugal force (300–400 \times g) to sediment a main portion of the cells, a 2000 \times g to remove cell debris, a 10,000 \times g to remove the aggregates with a buoyant density higher than the EVs and a final high force (100,000 \times g) that concentrate EVs in the resulting supernatant [126, 130]. However, this protocol is not unified and can vary depending on the volume and viscosity of the sample, which can affect the speed of centrifugation and the time needed for the obtention of the EVs [130, 131]. This strategy needs costly instrumentation, is time-consuming, requires a large amount of sample, and the recovery is normally low and contaminated with non-vesicular

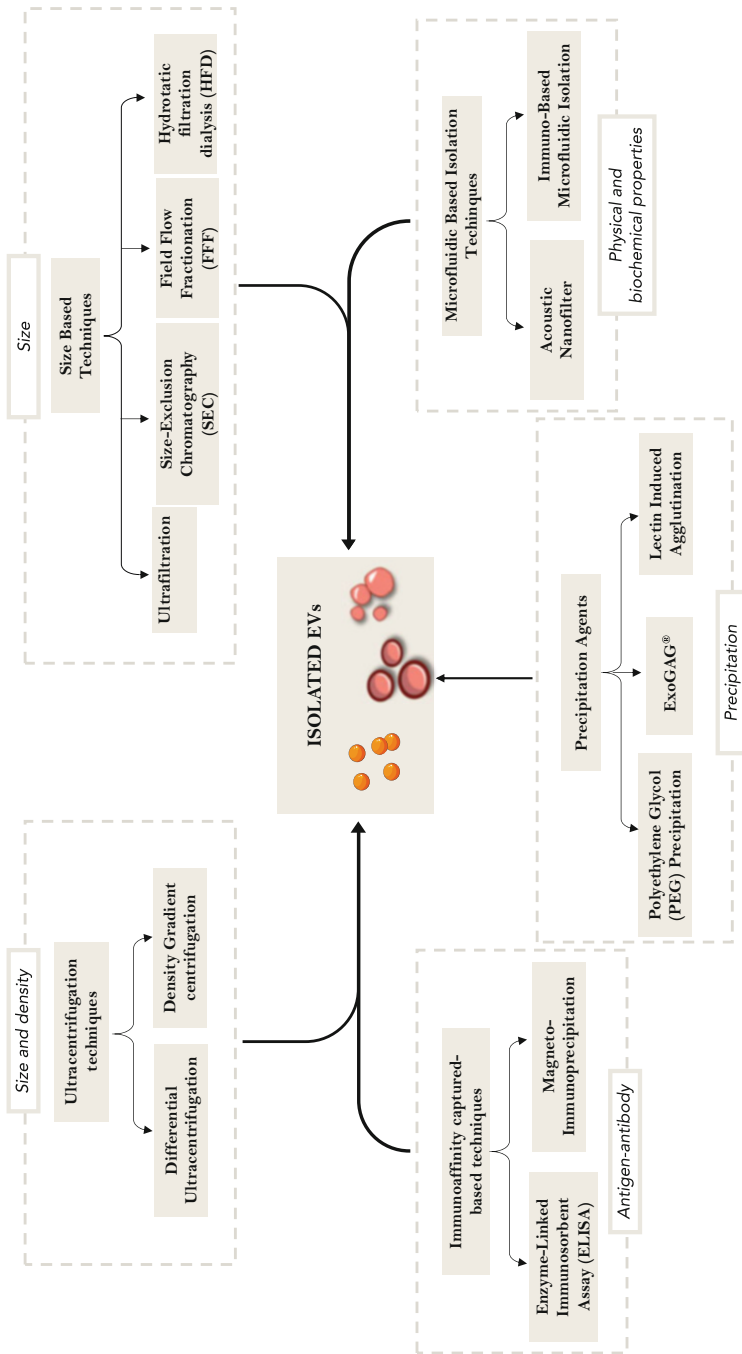


Fig. 21.2 Different strategies for EVs isolation and characterization

materials [132], which affect the purity of the samples in terms of the omics, RNA, and functional EVs analysis [133].

Density Gradient Centrifugation

This is a stricter strategy based on size and density [126] where the separation occurs in the presence of a preconstructed density gradient, typically made of sucrose or iodixanol [134], resulting in differences in the osmotic pressure which can potentially affect the EVs [134, 135]. Density Gradient centrifugation is very effective in separating EVs from protein aggregates and non-membranous particles. Although it reports higher purity, it counts with limitations associated with ultracentrifugation [136] such as low recovery [137].

21.4.1.2 Size-Based Techniques

Ultrafiltration

This is the most commonly used size-based technique and consists of the separation of particles using semipermeable membranes with defined pore size or molecular weight cut [134]. While the larger particles are retained, the smaller ones passed through the filter into the filtrate [138]. Ultrafiltration is less time-consuming than ultracentrifugation and does not require special equipment [139]. However, the use of shear force may result in the deformation, clogging, or trapping in the unit or breaking up of large vesicles which may potentially skew the results of downstream analysis [139–141].

Size-Exclusion Chromatography (SEC)

This technique lies in sorting vesicles and other molecules based on their size by filtration through a gel. The gel is composed of spherical beads which contain pores of a specific size distribution through which small particles can penetrate. When the sample enters the gel, small molecules slow down the movement into the pores, causing them to elute later, while large molecules are excluded from entering the pores [142, 143]. Despite SEC methods enabling more accurate EVs purification [144] and preserving vesicle integrity and biological activity, they require run times of several hours, are not easily scalable, and cannot be used for high throughput applications [145].

Field-Flow Fractionation (FFF)

In this separation technique, a force field is applied perpendicular to a sample flow, to enable separation based on different sizes and molecular weights. When the perpendicular force field is applied, analytes in the sample are driven toward the boundary. Brownian motion creates a counteracting motion such that smaller particles tend to reach an equilibrium position further away from the boundary. This type of separation spans a broad size range and could be applied to a wide variety of eluents [136].

Hydrostatic Filtration Dialysis (HFD)

In HFD, based on the traditional dialysis separation method, the sample is forced through a dialysis tube with a mesh of membrane with a molecular weight cutoff of 1000 kDa by hydrostatic pressure. As a result, larger particles like exosomes and other EVs remain in the tube where they can be collected. Apart from showing an efficient enrichment of the vesicles in comparison with the differential centrifugation protocol, it counts with a superior cost-efficiency with a faster workflow too [146].

21.4.1.3 Precipitation Agents

Polyethylene Glycol (PEG) Precipitation

By introducing a water-excluding polymer, such as polyethylene glycol (PEG) into the sample, exosomes can be settled out of biological fluids [139]. The water molecules “tides-up” causing exosomes, and the rest of the less soluble molecules, to precipitate out the solution [139]. This isolation method is quick, easy to use, requiring little technical expertise or any specialized equipment [134, 141]. Furthermore, it is compatible with a large number of samples. However, although it could be an easy option to integrate into clinical usage, its lack of selectivity, causes PEG polymers to be not exclusive to EVs and have other contamination substances [128, 133, 141].

Lectin Induced Agglutination

As an alternative to PEG, lectins are a family of proteins that bind carbohydrate moieties of other particles at a very high specificity [122]. Like PEG precipitation methods, the lectin precipitation methods are not time-consuming and do not need much expertise but have the problem of other soluble components. Hence, Lectin-induced exosome agglutination was explored for urinary exosome isolation [147].

It is also important to remark that several commercially available kits based on precipitation agents have been produced like ExoQuick (System Biosciences, CA, EEUU) [148] and ExoSpin (Cell Guidance System, Cambridge, UK) [149], which are based on PEG precipitation or ExoGAG (NasasBiotech, A Coruña, Spain) [123] that is a reactive that bonds with the glycosaminoglycans (GAGs) presented in the surface of EVs.

21.4.1.4 Immunoaffinity Captured-Based Techniques

They rely on the use of antibodies to capture the EVs based on the presence of lipids, proteins, and polysaccharides exposed on their surface [138, 150]. The fact that these techniques are primarily marker-dependent could be a constraint because the specificity of the assay relies on the specificity of the antibody used and thus tend to underestimate counts [134]. On the other hand, it presents a higher EVs purity than other methods based on other techniques [141]. Some examples of immunoaffinity capture-based techniques not exclusive to EVs are the Enzyme-Linked Immunosorbent Assay (ELISA) used to isolate exosomes from urine, plasma, and serum and Magneto-Immuno-precipitation that in comparison with ELISA has a higher isolation efficiency [122].

21.4.1.5 Microfluidic Based Isolation Techniques

Microfluidic-based isolation techniques are presented as a way to establish the use of EVs in clinical practice; however, its implementation is obstructed by issues such as scalability, validation, and standardization. They consist of the isolation of EVs based on their physical and biochemical properties simultaneously [134]. With their use, significant reductions in sample volume, reagent consumption, and isolation time are obtained because they can reproduce numerous laboratory processes on a microscale with high accuracy and specificity [149].

21.4.2 cEVs Cargo Profiling

EVs have a tremendous potential to be used in the field of liquid biopsy due to the molecules enclosed in them, which turn them into a useful circulating biomarker [117]. These molecules are basically DNAs, RNAs, multiple proteins, and metabolites [151] (Fig. 21.3). The identification of EVs-RNAs has been improved in the last years. The RNA cargo includes protein-coding transcripts (mRNAs) and many types of non-coding RNAs, including miRNA, long non-coding RNAs (LncRNAs), circular RNAs (circRNAs), small nucleolar RNA (snoRNAs), small nuclear RNAs (snRNAs), transfer RNA (tRNAs), ribosomal RNAs (rRNAs), and piwi-interacting RNAs (piRNAs) [152, 153]. Besides, EVs harbor different types of DNA, including single-stranded (ssDNA), double-stranded (dsDNA), mitochondrial DNA (mtDNA), and even viral DNA [154]. Importantly, the analysis of dsDNA in exosomes reflects the mutational status of parental tumor cells, thus is potentially

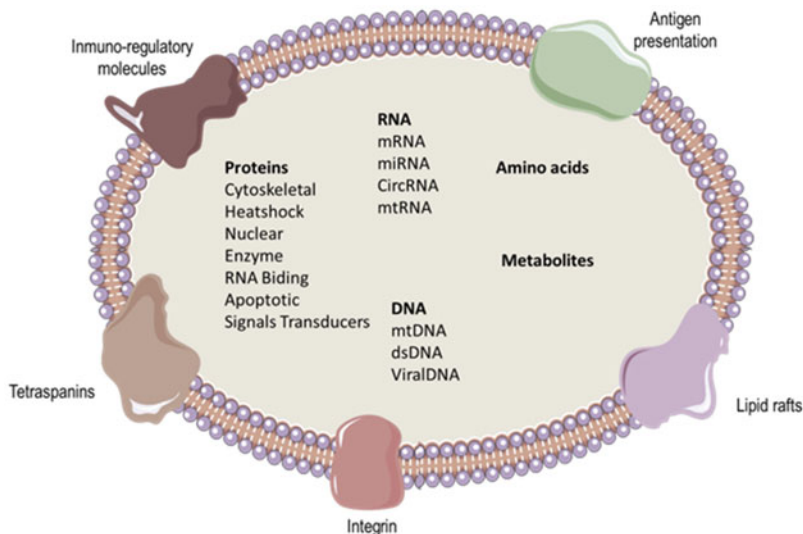


Fig. 21.3 Representation of EVs structure and molecular content

useful for early detection of cancer and metastasis and also for tumor phenotyping [155, 156].

The protein content of cEVs has been also explored to find diagnostic and prognostic biomarkers. Current tools used to study EV-proteins include Western blot, enzyme-linked immunosorbent assays (ELISA), flow cytometry, and mass spectrometry, among others. Thus, for example, higher levels of ANXA2 were described in cEVs isolated from plasma samples of patients with EC than healthy controls. The presence of therapeutic targets such as PD-L1 is also feasible in the fraction of cEVs although its clinical meaning is not totally understood [157, 158]. Also, Melo et al. demonstrated the interest of Glypican-1 (GPC1) positive exosomes for identifying early and late-stage pancreatic cancer from healthy individuals or patients with benign disease [23].

21.5 Alternative Circulating Biomarkers

In recent years the potential of tumor-educated blood platelets as a non-invasive tumor biomarker has been demonstrated [159, 160]. Platelets are involved in the progression and spread of various solid cancers, and their RNA molecular signatures can provide specific information about the presence, location, and molecular characteristics of the tumors [161]. Preliminary studies indicate that platelet RNA may complement the information obtained with other non-invasive biomarkers for cancer diagnosis, potentially improving early-tumors detection and facilitating dynamic monitoring of the disease [161]. In fact, recent advances in the characterization of platelet-mRNA using high-throughput techniques revealed that, in the presence of malignant disease, there was an increase from 10 to more than 1000 altered mRNAs in platelets. In fact, clinically relevant fusions such as *EML4-ALK* rearrangements have been described in platelets from patients with non-small cell lung carcinoma (NSCLC) [162]. Besides platelets can intake plasma proteins that promote tumor growth and vascularization, such as basic fibroblast growth factor (FGF) or vascular endothelial growth factor (VEGF) [163, 164].

For platelets isolation, there are some important points that should be taken into account. Many drugs can interfere with platelet studies (for example, antihistamines, aspirin, non-steroidal anti-inflammatory drugs). Furthermore, systemic factors such as chronic or transient inflammatory diseases, or cardiovascular events and other noncancerous diseases, can also influence the platelet mRNA profile. Therefore, for blocking platelet activation during the isolation procedure, strong mechanical forces should be avoided and platelet inhibitors such as Citrate or HEPES can be also used. The recommended isolation method is double centrifugation. The first centrifugation at $150\text{--}300\times g$ to obtain platelet-rich plasma and the second to collect the platelet fraction is generally performed at $300\text{--}800\times g$.

On the other hand, in the era of immunotherapy, several works have described the interest of analyzing the immune cells present in the bloodstream. The isolation and characterization of these cells are preferentially performed by flow cytometry and the selected cell fraction can be analyzed by different strategies to characterize the

proteins and DNA/RNA content. Of note, a correlation between the neutrophil to lymphocyte ratio has been described as a mark of the immunotherapy activity in terms of survival rates [165, 166]. Besides, the T-cell receptor (TCR) repertoire, which consists of the number of T cells with specific TCRs, has also been described as a predictor biomarker in patients under immunotherapy treatment [167]. The analysis of PD-1 expression on circulating lymphocytes has been linked to better immune responses in melanoma and renal cell carcinoma [168]. Among the different subpopulations of immune cells CD8+/CD73+ subset of lymphocytes has been associated with worse survival and poor clinical benefits in patients with melanoma under immunotherapy [169]. Also, in melanoma low levels of myeloid-derived suppressor cells were associated with better response to immunotherapy [170].

21.6 Challenges for the Clinical Application

The possibility of finding non-invasive circulating biomarkers that provide comprehensive information about the molecular characteristics of each tumor is of incredible interest for oncologists [171]. However, 20 years after the field of liquid biopsy started to grow only ctDNA analyses are being used in a clinical context. Numerous studies have shown the potential of new technologies for detecting genetic alterations associated with ctDNA, with promising preliminary clinical results. However, the implementation of liquid biopsy analyses is being slow due to the need for very high-sensitive technologies and more economic sources to cover the PCR or NGS-based studies. Besides, liquid biopsy tests lack standardized workflows, and this impacts reproducibility and, therefore, on the robustness of the tests [171]. Preanalytical steps, including sample collection, processing, and storage, are important factors conditioning this reproducibility [172, 173]. The specificity is also a critical point, since, for example, the detection of mutations in cancer-associated genes is not a guarantee of their tumoral origin. Thus, the existence of clonal hematopoiesis should be taken into consideration when interpreting NGS results on cfDNA analysis in order to avoid false positives [174]. In addition to genetic alterations, epigenetic marks will play an important role to translate the cfDNA analyses to diagnosis or screening scenarios [85]. Besides, fragmentomics also appears as a promising strategy to identify tumors specific patterns in cfDNA from cancer patients [175].

Although ctDNA has emerged as the leading circulating biomarker, the analysis of other circulating biomarkers such as CTCs and cEVs can provide more biological information about tumor dissemination and the development of resistance mechanisms. In addition, the field of CTCs should go behind the enumeration and validate the CTC phenotyping as a surrogate of the solid tumor. For that, techniques should improve their versatility and sensitivity to be able to have more CTCs numbers for molecular characterization [18]. In this context, single-CTCs characterization is opening new perspectives for the definition and interpretation of tumor heterogeneity and its biological impact on tumor aggressiveness. For advancing in cEVs validation as a clinical tool the implementation of easy and reproducible

techniques is a clear challenge in the close future [176]. Besides, the development of novel strategies for cEVs isolation which cover EV subgroups in a pure fraction will be also a key point for the field development [21, 176].

Overall, the incorporation of liquid biopsy analyses into the clinical context requires the generation of guidelines and harmonized procedures. This will allow the development of interventional clinical trials to demonstrate the clinical benefit of including liquid biopsy for the management of cancer patients.

21.7 Conclusions

The application of liquid biopsy-based biomarkers is being broadly explored in many clinical contexts to manage cancer patients due to its minimal invasiveness and its value to obtain comprehensive and dynamic information about tumors. Several technologies have been developed during the last 20 years to address the study of different circulating elements, mainly CTCs, cfDNA, and cEVs. Sensitivity and reproducibility are two of the most valuable characteristics which are mandatory to characterize the tumoral material present in body fluids. The analysis of CTCs needs still improvement in these two aspects, and for this reason, CTCs studies are mainly focused on translational research to understand the dissemination process although different clinically relevant markers can be characterized in this tumor circulation population. Fortunately, cfDNA analyses, through PCR or NGS-based approaches, are nowadays being incorporated into the clinical practice to select targeted therapies in advanced tumors opening new avenues for personalized treatments. Other circulating elements such as cEVs or educated platelets represent promising biomarkers to complement the current alternatives to address the study of liquid biopsies in oncology.

References

1. Letai A (2017 Sep 8) Functional precision cancer medicine-moving beyond pure genomics. *Nat Med* 23(9):1028–1035
2. Parikh AR, Leshchiner I, Elagina L, Goyal L, Levovitz C, Siravegna G et al (2019) Liquid versus tissue biopsy for detecting acquired resistance and tumor heterogeneity in gastrointestinal cancers. *Nat Med* 25(9):1415–1421
3. Siravegna G, Marsoni S, Siena S, Bardelli A (2017 Sep) Integrating liquid biopsies into the management of cancer. *Nat Rev Clin Oncol* 14(9):531–548
4. Pantel K, Alix-Panabières C (2010 Sep) Circulating tumour cells in cancer patients: challenges and perspectives. *Trends Mol Med* 16(9):398–406
5. Leighl NB, Page RD, Raymond VM, Daniel DB, DIVERS SG, Reckamp KL et al (2019 Aug 1) Clinical utility of comprehensive cell-free DNA analysis to identify genomic biomarkers in patients with newly diagnosed metastatic non-small cell lung cancer. *Clin Cancer Res* 25(15):4691–4700
6. André F, Ciruelos EM, Juric D, Loibl S, Campone M, Mayer IA et al (2021) Alpelisib plus fulvestrant for PIK3CA-mutated, hormone receptor-positive, human epidermal growth factor

- receptor-2-negative advanced breast cancer: final overall survival results from SOLAR-1. *Ann Oncol* 32(2):208–217
7. Vidal J, Muinelo L, Dalmases A, Jones F, Edelstein D, Iglesias M et al (2017 June 1) Plasma ctDNA RAS mutation analysis for the diagnosis and treatment monitoring of metastatic colorectal cancer patients. *Ann Oncol* 28(6):1325–1332
 8. García-Foncillas J, Taberner J, Élez E, Aranda E, Benavides M, Camps C et al (2018) Prospective multicenter real-world RAS mutation comparison between OncoBEAM-based liquid biopsy and tissue analysis in metastatic colorectal cancer. *Br J Cancer* 119(12):1464–1470
 9. Hrebien S, Citi V, Garcia-Murillas I, Cutts R, Fenwick K, Kozarewa I et al (2019) Early ctDNA dynamics as a surrogate for progression-free survival in advanced breast cancer in the BEECH trial. *Ann Oncol* 30(6):945–952
 10. Lee JH, Menzies AM, Carlino MS, McEvoy AC, Sandhu S, Weppler AM et al (2020) Longitudinal monitoring of ctDNA in patients with melanoma and brain metastases treated with immune checkpoint inhibitors. *Clin Cancer Res* 26(15):4064–4071
 11. Moss EL, Gorsia DN, Collins A, Sandhu P, Foreman N, Gore A et al (2020 Aug 10) Utility of circulating tumor DNA for detection and monitoring of endometrial cancer recurrence and progression. *Cancers* 12(8):2231
 12. Muinelo-Romay L, Casas-Arozamena C, Abal M (2018 Aug 7) Liquid biopsy in endometrial cancer: new opportunities for personalized oncology. *Int J Mol Sci* 19:2311
 13. Tie J, Cohen JD, Lo SN, Wang Y, Li L, Christie M et al (2021) Prognostic significance of postsurgery circulating tumor DNA in nonmetastatic colorectal cancer: individual patient pooled analysis of three cohort studies. *Int J Cancer* 148(4):1014–1026
 14. Radovich M, Jiang G, Hancock BA, Chitambar C, Nanda R, Falkson C et al (2020) Association of circulating tumor DNA and circulating tumor cells after neoadjuvant chemotherapy with disease recurrence in patients with triple-negative breast cancer: preplanned secondary analysis of the BRE12-158 randomized clinical trial. *JAMA Oncol* 6(9):1410–1415
 15. Liu X, Ren J, Luo N, Guo H, Zheng Y, Li J et al (2019) Comprehensive DNA methylation analysis of tissue of origin of plasma cell-free DNA by methylated CpG tandem amplification and sequencing (MCTA-Seq). *Clin Epigenetics* 11(1):93
 16. Pickhardt PJ (2016) Emerging stool-based and blood-based non-invasive DNA tests for colorectal cancer screening: the importance of cancer prevention in addition to cancer detection. *Abdom Radiol (New York)* 41(8):1441–1444
 17. Issa IA, Nouredine M (2017 July 28) Colorectal cancer screening: an updated review of the available options. *World J Gastroenterol* 23(28):5086–5096
 18. Habli Z, AlChamaa W, Saab R, Kadara H, Khraiche ML (2020 Jul) Circulating tumor cell detection technologies and clinical utility: challenges and opportunities. *Cancers* 17:12(7)
 19. Vasseur A, Kiavue N, Bidard F-C, Pierga J-Y, Cabel L (2021) Clinical utility of circulating tumor cells: an update. *Mol Oncol* 15(6):1647–1666
 20. Zhong X, Zhang H, Zhu Y, Liang Y, Yuan Z, Li J et al (2020) Circulating tumor cells in cancer patients: developments and clinical applications for immunotherapy. *Mol Cancer* 19(1):15
 21. Herrero C, Abal M, Muinelo-Romay L (2020) Circulating extracellular vesicles in gynecological tumors: realities and challenges. *Front Oncol* 10:565666
 22. Liang Y, Lehrich BM, Zheng S, Lu M (2021) Emerging methods in biomarker identification for extracellular vesicle-based liquid biopsy. *J Extracell Vesicles* 10(7):e12090
 23. Melo SA, Luecke LB, Kahlert C, Fernandez AF, Gammon ST, Kaye J et al (2015 Jul 9) Glypican-1 identifies cancer exosomes and detects early pancreatic cancer. *Nature* 523(7559):177–182
 24. Int Veld SGJG, Wurdinger T (2019) Tumor-educated platelets. *Blood* 133(22):2359–2364
 25. Griffiths JL, Wallet P, Pflieger LT, Stenehjem D, Liu X, Cosgrove PA et al (2020) Circulating immune cell phenotype dynamics reflect the strength of tumor-immune cell interactions in patients during immunotherapy. *Proc Natl Acad Sci U S A* 117(27):16072–16082

26. Allan AL, Vantighem SA, Tuck AB, Chambers AF, Chin-Yee IH, Keeney M (2005 May) Detection and quantification of circulating tumor cells in mouse models of human breast cancer using immunomagnetic enrichment and multiparameter flow cytometry. *Cytometry A* 65(1):4–14
27. Alix-Panabières C, Pantel K (2016) Clinical applications of circulating tumor cells and circulating tumor DNA as liquid biopsy. *Cancer Discov* 6(5):479–491
28. Pantel K, Speicher MR (2016 Mar 10) The biology of circulating tumor cells. *Oncogene* 35(10):1216–1224
29. Alix-Panabières C, Pantel K (2013 Jan) Circulating tumor cells: liquid biopsy of cancer. *Clin Chem* 59(1):110–118
30. Riethdorf S, O’Flaherty L, Hille C, Pantel K (2018) Clinical applications of the CellSearch platform in cancer patients. *Adv Drug Deliv Rev* 125:102–121
31. Rushton AJ, Nteliopoulos G, Shaw JA, Coombes RC (2021 Feb 26) A review of circulating tumour cell enrichment technologies. *Cancers* 13:13(5)
32. Hayes DF, Cristofanilli M, Budd GT, Ellis MJ, Stopeck A, Miller MC et al (2006 Jul 15) Circulating tumor cells at each follow-up time point during therapy of metastatic breast cancer patients predict progression-free and overall survival. *Clin Cancer Res* 12(14 Pt 1):4218–4224
33. de Bono JS, Scher HI, Montgomery RB, Parker C, Miller MC, Tissing H et al (2008 Oct 1) Circulating tumor cells predict survival benefit from treatment in metastatic castration-resistant prostate cancer. *Clin Cancer Res* 14(19):6302–6309
34. Cohen SJ, Punt CJA, Iannotti N, Saidman BH, Sabbath KD, Gabrail NY et al (2008 Jul 1) Relationship of circulating tumor cells to tumor response, progression-free survival, and overall survival in patients with metastatic colorectal cancer. *J Clin Oncol* 26(19):3213–3221
35. Grover PK, Cummins AG, Price TJ, Roberts-Thomson IC, Hardingham JE (2014 Aug) Circulating tumour cells: the evolving concept and the inadequacy of their enrichment by EpCAM-based methodology for basic and clinical cancer research. *Ann Oncol* 25(8):1506–1516
36. Kowalik A, Kowalewska M, Góźdz S (2017) Current approaches for avoiding the limitations of circulating tumor cells detection methods-implications for diagnosis and treatment of patients with solid tumors. *Transl Res* 185:58–84.e15
37. Liu Z, Fusi A, Klopocki E, Schmittel A, Tinhofer I, Nonnenmacher A et al (2011 May 19) Negative enrichment by immunomagnetic nanobeads for unbiased characterization of circulating tumor cells from peripheral blood of cancer patients. *J Transl Med* 9:70
38. Szczerba BM, Castro-Giner F, Vetter M, Krol I, Gkoutela S, Landin J et al (2019) Neutrophils escort circulating tumour cells to enable cell cycle progression. *Nature* 566(7745):553–557
39. Vona G, Sabile A, Louha M, Sitruk V, Romana S, Schütze K et al (2000 Jan) Isolation by size of epithelial tumor cells: a new method for the immunomorphological and molecular characterization of circulating tumor cells. *Am J Pathol* 156(1):57–63
40. Hao S-J, Wan Y, Xia Y-Q, Zou X, Zheng S-Y (2018) Size-based separation methods of circulating tumor cells. *Adv Drug Deliv Rev* 125:3–20
41. Farace F, Massard C, Vimond N, Drusch F, Jacques N, Billiot F et al (2011 Sep 6) A direct comparison of CellSearch and ISET for circulating tumour-cell detection in patients with metastatic carcinomas. *Br J Cancer* 105(6):847–853
42. Miller MC, Robinson PS, Wagner C, O’Shannessy DJ (2018) The Parsortix™ cell separation system: a versatile liquid biopsy platform. *Cytometry A* 93(12):1234–1239
43. Hou HW, Warkiani ME, Khoo BL, Li ZR, Soo RA, Tan DS-W et al (2013) Isolation and retrieval of circulating tumor cells using centrifugal forces. *Sci Rep* 3:1259
44. Gascoyne PRC, Shim S (2014 Mar 12) Isolation of circulating tumor cells by dielectrophoresis. *Cancers* 6(1):545–579
45. Nagrath S, Sequist LV, Maheswaran S, Bell DW, Irimia D, Ulkus L et al (2007 Dec 20) Isolation of rare circulating tumour cells in cancer patients by microchip technology. *Nature* 450(7173):1235–1239

46. Dizdar L, Fluegen G, van Dalum G, Honisch E, Neves RP, Niederacher D et al (2019) Detection of circulating tumor cells in colorectal cancer patients using the GILUPI CellCollector: results from a prospective, single-center study. *Mol Oncol* 13(7):1548–1558
47. Fischer JC, Niederacher D, Topp SA, Honisch E, Schumacher S, Schmitz N et al (2013 Oct 8) Diagnostic leukapheresis enables reliable detection of circulating tumor cells of nonmetastatic cancer patients. *Proc Natl Acad Sci U S A* 110(41):16580–16585
48. Valihrach L, Androvic P, Kubista M (2018 Mar) Platforms for single-cell collection and analysis. *Int J Mol Sci* 11:19(3)
49. Lawson DA, Kessenbrock K, Davis RT, Pervolarakis N, Werb Z (2018) Tumour heterogeneity and metastasis at single-cell resolution. *Nat Cell Biol* 20(12):1349–1360
50. Agarwal A, Balic M, El-Ashry D, Cote RJ (2018 Mar) Circulating tumor cells. *Cancer J* 24(2):70–77
51. Mondelo-Macia P, García-González J, León-Mateos L, Anido U, Aguín S, Abdulkader I et al (2021) Clinical potential of circulating free DNA and circulating tumour cells in patients with metastatic non-small-cell lung cancer treated with pembrolizumab. *Mol Oncol* 15(11):2923–2940
52. Cortés-Hernández LE, Eslami-S Z, Pantel K, Alix-Panabières C (2020) Molecular and functional characterization of circulating tumor cells: from discovery to clinical application. *Clin Chem* 66(1):97–104
53. Sinkala E, Sollier-Christen E, Renier C, Rosàs-Canyelles E, Che J, Heirich K et al (2017) Profiling protein expression in circulating tumour cells using microfluidic western blotting. *Nat Commun* 8:14622
54. Maheswaran S, Sequist LV, Nagrath S, Ulkus L, Brannigan B, Collura CV et al (2008 Jul 24) Detection of mutations in EGFR in circulating lung-cancer cells. *N Engl J Med* 359(4):366–377
55. Punnoose EA, Atwal S, Liu W, Raja R, Fine BM, Hughes BGM et al (2012 Apr 15) Evaluation of circulating tumor cells and circulating tumor DNA in non-small cell lung cancer: association with clinical endpoints in a phase II clinical trial of pertuzumab and erlotinib. *Clin Cancer Res* 18(8):2391–2401
56. Carter L, Rothwell DG, Mesquita B, Smowton C, Leong HS, Fernandez-Gutierrez F et al (2017) Molecular analysis of circulating tumor cells identifies distinct copy-number profiles in patients with chemosensitive and chemorefractory small-cell lung cancer. *Nat Med* 23(1):114–119
57. Krebs MG, Metcalf RL, Carter L, Brady G, Blackhall FH, Dive C (2014 Mar 21) Molecular analysis of circulating tumour cells—biology and biomarkers. *Nat Rev Clin Oncol* 11(3):129–144
58. Guo T (2016 Aug 31) Culture of circulating tumor cells - holy grail and big challenge. *Int J Cancer Clin Res* 3:63
59. Pantel K, Alix-Panabières C (2019) Liquid biopsy and minimal residual disease - latest advances and implications for cure. *Nat Rev Clin Oncol* 16(7):409–424
60. Lallo A, Schenk MW, Frese KK, Blackhall F, Dive C (2017 Aug) Circulating tumor cells and CDX models as a tool for preclinical drug development. *Transl Lung Cancer Res* 6(4):397–408
61. Hodgkinson CL, Morrow CJ, Li Y, Metcalf RL, Rothwell DG, Trapani F et al (2014 Aug) Tumorigenicity and genetic profiling of circulating tumor cells in small-cell lung cancer. *Nat Med* 20(8):897–903
62. Schölich S, García SA, Iwata N, Niemietz T, Betzler AM, Nanduri LK et al (2016 May 10) Circulating tumor cells exhibit stem cell characteristics in an orthotopic mouse model of colorectal cancer. *Oncotarget* 7(19):27232–27242
63. Pereira-Veiga T, Abreu M, Robledo D, Matias-Guiu X, Santacana M, Sánchez L et al (2019) CTCs-derived xenograft development in a triple negative breast cancer case. *Int J Cancer* 144(9):2254–2265

64. Faugeron V, Pailler E, Oulhen M, Deas O, Brulle-Soumare L, Hervieu C et al (2020) Genetic characterization of a unique neuroendocrine transdifferentiation prostate circulating tumor cell-derived eXplant model. *Nat Commun* 11(1):1884
65. Jahr S, Hentze H, Englisch S, Hardt D, Fackelmayer FO, Hesch RD et al (2001 Feb 15) DNA fragments in the blood plasma of cancer patients: quantitations and evidence for their origin from apoptotic and necrotic cells. *Cancer Res* 61(4):1659–1665
66. Kustanovich A, Schwartz R, Peretz T, Grinshpun A (2019) Life and death of circulating cell-free DNA. *Cancer Biol Ther* 20(8):1057–1067
67. Keller L, Belloum Y, Wikman H, Pantel K (2021) Clinical relevance of blood-based ctDNA analysis: mutation detection and beyond. *Br J Cancer* 124(2):345–358
68. Meddeb R, Pisareva E, Thierry AR (2019) Guidelines for the preanalytical conditions for analyzing circulating cell-free DNA. *Clin Chem* 65(5):623–633
69. van der Leest P, Boonstra PA, Ter Elst A, van Kempen LC, Tibbesma M, Koopmans J et al (2020 May 13) Comparison of circulating cell-free DNA extraction methods for downstream analysis in cancer patients. *Cancers* 12:1222
70. Franczak C, Filhine-Tresarrieu P, Gilson P, Merlin J-L, Au L, Harlé A (2019 Feb 1) Technical considerations for circulating tumor DNA detection in oncology. *Expert Rev Mol Diagn* 19(2):121–135
71. Mauger F, Dulary C, Daviaud C, Deleuze J-F, Tost J (2015 Sep) Comprehensive evaluation of methods to isolate, quantify, and characterize circulating cell-free DNA from small volumes of plasma. *Anal Bioanal Chem* 407(22):6873–6878
72. Kilgour E, Rothwell DG, Brady G, Dive C (2020) Liquid biopsy-based biomarkers of treatment response and resistance. *Cancer Cell* 37(4):485–495
73. Cohen JD, Li L, Wang Y, Thoburn C, Afsari B, Danilova L et al (2018 Feb 23) Detection and localization of surgically resectable cancers with a multi-analyte blood test. *Science (New York, NY)*. 359(6378):926–930
74. Abbosh C, Birkbak NJ, Swanton C (2018) Early stage NSCLC - challenges to implementing ctDNA-based screening and MRD detection. *Nat Rev Clin Oncol* 15(9):577–586
75. Wang Z, Duan J, Cai S, Han M, Dong H, Zhao J et al (2019 May 1) Assessment of blood tumor mutational burden as a potential biomarker for immunotherapy in patients with non-small cell lung cancer with use of a next-generation sequencing cancer gene panel. *JAMA Oncol* 5(5):696–702
76. Martínez-Sáez O, Chic N, Pascual T, Adamo B, Vidal M, González-Farré B et al (2020) Frequency and spectrum of PIK3CA somatic mutations in breast cancer. *Breast Cancer Res* 22(1):45
77. Malapelle U, Sirera R, Jantus-Lewintre E, Reclusa P, Calabuig-Fariñas S, Blasco A et al (2017) Profile of the Roche cobas® EGFR mutation test v2 for non-small cell lung cancer. *Expert Rev Mol Diagn* 17(3):209–215
78. Woodhouse R, Li M, Hughes J, Delfosse D, Skoletsky J, Ma P et al (2020) Clinical and analytical validation of FoundationOne liquid CDx, a novel 324-gene cfDNA-based comprehensive genomic profiling assay for cancers of solid tumor origin. *PLoS One* 15(9):e0237802
79. Laufer-Geva S, Rozenblum AB, Twito T, Grinberg R, Dvir A, Soussan-Gutman L et al (2018) The clinical impact of comprehensive genomic testing of circulating cell-free DNA in advanced lung cancer. *J Thoracic Oncol* 13(11):1705–1716
80. Ren AH, Fiala CA, Diamandis EP, Kulasingam V (2020) Pitfalls in cancer biomarker discovery and validation with emphasis on circulating tumor DNA. *Cancer Epidemiol Biomarker Prev* 29(12):2568–2574
81. Elazezy M, Joesse SA (2018) Techniques of using circulating tumor DNA as a liquid biopsy component in cancer management. *Comput Struct Biotechnol J* 16:370–378
82. Bando H, Kagawa Y, Kato T, Akagi K, Denda T, Nishina T et al (2019) A multicentre, prospective study of plasma circulating tumour DNA test for detecting RAS mutation in patients with metastatic colorectal cancer. *Br J Cancer* 120(10):982–986

83. Chen M, Zhao H (2019) Next-generation sequencing in liquid biopsy: cancer screening and early detection. *Hum Genomics* 13(1):34
84. Szilágyi M, Pös O, Márton É, Buglyó G, Soltész B, Keserű J et al (2020 Sep 17) Circulating cell-free nucleic acids: main characteristics and clinical application. *Int J Mol Sci* 21:6827
85. Rodriguez-Casanova A, Costa-Fraga N, Bao-Caamano A, López-López R, Muínelo-Romay L, Diaz-Lagares A (2021) Epigenetic landscape of liquid biopsy in colorectal cancer. *Front Cell Dev Biol* 9:622459
86. Portela A, Esteller M (2010 Oct) Epigenetic modifications and human disease. *Nat Biotechnol* 28(10):1057–1068
87. Huang J, Wang L (2019 Nov) Cell-free DNA methylation profiling analysis-technologies and bioinformatics. *Cancers* 6:11(11)
88. Frommer M, McDonald LE, Millar DS, Collis CM, Watt F, Grigg GW et al (1992 Mar 1) A genomic sequencing protocol that yields a positive display of 5-methylcytosine residues in individual DNA strands. *Proc Natl Acad Sci U S A* 89(5):1827–1831
89. Li M, Chen W-D, Papadopoulos N, Goodman SN, Bjerregaard NC, Laurberg S et al (2009 Sep) Sensitive digital quantification of DNA methylation in clinical samples. *Nat Biotechnol* 27(9):858–863
90. Chimonidou M, Strati A, Tzitzira A, Sotiropoulou G, Malamos N, Georgoulis V et al (2011 Aug) DNA methylation of tumor suppressor and metastasis suppressor genes in circulating tumor cells. *Clin Chem* 57(8):1169–1177
91. Boeckx N, Op de Beeck K, Beyens M, Deschoolmeester V, Hermans C, De Clercq P et al (2018) Mutation and methylation analysis of circulating tumor DNA can be used for follow-up of metastatic colorectal cancer patients. *Clin Colorectal Cancer* 17(2):e369–e379
92. Barault L, Amatu A, Bleeker FE, Moutinho C, Falcomatà C, Fiano V et al (2015 Sep) Digital PCR quantification of MGMT methylation refines prediction of clinical benefit from alkylating agents in glioblastoma and metastatic colorectal cancer. *Ann Oncol* 26(9):1994–1999
93. Gallardo-Gómez M, Moran S, Páez de la Cadena M, Martínez-Zorzano VS, Rodríguez-Berrocal FJ, Rodríguez-Girondo M et al (2018) A new approach to epigenome-wide discovery of non-invasive methylation biomarkers for colorectal cancer screening in circulating cell-free DNA using pooled samples. *Clin Epigenetics* 10:53
94. Friedlander TW, Ngo VT, Dong H, Premasekharan G, Weinberg V, Doty S et al (2014 May 15) Detection and characterization of invasive circulating tumor cells derived from men with metastatic castration-resistant prostate cancer. *Int J Cancer* 134(10):2284–2293
95. Li W, Li Q, Kang S, Same M, Zhou Y, Sun C et al (2018) CancerDetector: ultrasensitive and non-invasive cancer detection at the resolution of individual reads using cell-free DNA methylation sequencing data. *Nucleic Acids Res* 46(15):e89
96. Gkoutela S, Castro-Giner F, Szczerba BM, Vetter M, Landin J, Scherrer R et al (2019) Circulating tumor cell clustering shapes dna methylation to enable metastasis seeding. *Cell*. 176(1–2):98–112.e14
97. Raposo G, Stoorvogel W (2013 Feb 18) Extracellular vesicles: exosomes, microvesicles, and friends. *J Cell Biol* 200(4):373–383
98. György B, Szabó TG, Pásztói M, Pál Z, Misják P, Aradi B et al (2011 Aug) Membrane vesicles, current state-of-the-art: emerging role of extracellular vesicles. *Cell Mol Life Sci* 68(16):2667–2688
99. Colombo M, Raposo G, Théry C (2014) Biogenesis, secretion, and intercellular interactions of exosomes and other extracellular vesicles. *Annu Rev Cell Dev Biol* 30:255–289
100. Théry C, Ostrowski M, Segura E (2009 Aug) Membrane vesicles as conveyors of immune responses. *Nat Rev Immunol* 9(8):581–593
101. van der Meel R, Krawczyk-Durka M, van Solinge WW, Schiffelers RM (2014 Jun) Toward routine detection of extracellular vesicles in clinical samples. *Int J Lab Hematol* 36(3):244–253
102. Raposo G, Nijman HW, Stoorvogel W, Liejendekker R, Harding CV, Melief CJ et al (1996 Mar 1) B lymphocytes secrete antigen-presenting vesicles. *J Exp Med* 183(3):1161–1172

103. Zitvogel L, Regnault A, Lozier A, Wolfers J, Flament C, Tenza D et al (1998 May) Eradication of established murine tumors using a novel cell-free vaccine: dendritic cell-derived exosomes. *Nat Med* 4(5):594–600
104. Yáñez-Mó M, Siljander PR-M, Andreu Z, Zavec AB, Borràs FE, Buzas EI et al (2015) Biological properties of extracellular vesicles and their physiological functions. *J Extracell Vesicles* 4:27066
105. Kalluri R (2016 Apr 1) The biology and function of exosomes in cancer. *J Clin Invest* 126(4):1208–1215
106. Akers JC, Gonda D, Kim R, Carter BS, Chen CC (2013 May) Biogenesis of extracellular vesicles (EV): exosomes, microvesicles, retrovirus-like vesicles, and apoptotic bodies. *J Neuro-Oncol* 113(1):1–11
107. Ratajczak J, Miekus K, Kucia M, Zhang J, Reca R, Dvorak P et al (2006 May) Embryonic stem cell-derived microvesicles reprogram hematopoietic progenitors: evidence for horizontal transfer of mRNA and protein delivery. *Leukemia* 20(5):847–856
108. Valadi H, Ekström K, Bossios A, Sjöstrand M, Lee JJ, Lötvall JO (2007 Jun) Exosome-mediated transfer of mRNAs and microRNAs is a novel mechanism of genetic exchange between cells. *Nat Cell Biol* 9(6):654–659
109. Lai RC, Yeo RWY, Tan KH, Lim SK (2013) Exosomes for drug delivery: a novel application for the mesenchymal stem cell. *Biotechnol Adv*. 31(5):543–551
110. Zaborowski MP, Balaj L, Breakefield XO, Lai CP (2015 Aug 1) Extracellular vesicles: composition, biological relevance, and methods of study. *Bioscience* 65(8):783–797
111. Hood JL, San RS, Wickline SA (2011 Jun 1) Exosomes released by melanoma cells prepare sentinel lymph nodes for tumor metastasis. *Cancer Res* 71(11):3792–3801
112. Rak J (2010 Nov) Microparticles in cancer. *Semin Thromb Hemost* 36(8):888–906
113. Cocucci E, Racchetti G, Meldolesi J (2009 Feb) Shedding microvesicles: artefacts no more. *Trends Cell Biol* 19(2):43–51
114. Zhang H-G, Grizzle WE (2011 Mar 1) Exosomes and cancer: a newly described pathway of immune suppression. *Clin Cancer Res* 17(5):959–964
115. Logozzi M, de Milito A, Lugini L, Borghi M, Calabrò L, Spada M et al (2009 Apr 17) High levels of exosomes expressing CD63 and Caveolin-1 in plasma of melanoma patients. *PLoS One* 4(4):e5219
116. Ciardiello C, Cavallini L, Spinelli C, Yang J, Reis-Sobreiro M, de Candia P et al (2016 Feb 6) Focus on extracellular vesicles: new Frontiers of cell-to-cell communication in cancer. *Int J Mol Sci* 17(2):175
117. Carvalho J, Oliveira C (2014) Extracellular vesicles - powerful markers of cancer EVolution. *Front Immunol* 5:685
118. Nosova VP, Alekseeva LM, Bobkov II, Mumladze RB, Popova OA (1989) Changes in the rheologic properties of the blood in peptic ulcer. *Sov Med*. 4:87–90
119. Théry C, Zitvogel L, Amigorena S (2002 Aug) Exosomes: composition, biogenesis and function. *Nat Rev Immunol* 2(8):569–579
120. Kahlert C, Kalluri R (2013 Apr) Exosomes in tumor microenvironment influence cancer progression and metastasis. *J Mol Med (Berlin, Germany)* 91(4):431–437
121. van Niel G, D'Angelo G, Raposo G (2018) Shedding light on the cell biology of extracellular vesicles. *Nat Rev Mol Cell Biol* 19(4):213–228
122. Doyle LM, Wang MZ (2019) Overview of extracellular vesicles, their origin, composition, purpose, and methods for exosome isolation and analysis. *Cells* 8(7):727
123. Herrero C, de la Fuente A, Casas-Arozamena C, Sebastian V, Prieto M, Arriuebo M et al (2019 Dec 12) Extracellular vesicles-based biomarkers represent a promising liquid biopsy in endometrial cancer. *Cancers* 11:2000
124. Mathai RA, Vidya RVS, Reddy BS, Thomas L, Udupa K, Kolesar J et al (2019 Mar) Potential utility of liquid biopsy as a diagnostic and prognostic tool for the assessment of solid tumors: implications in the precision oncology. *J Clin Med* 18:8(3)

125. Lötvall J, Hill AF, Hochberg F, Buzás EI, di Vizio D, Gardiner C et al (2014) Minimal experimental requirements for definition of extracellular vesicles and their functions: a position statement from the International Society for Extracellular Vesicles. *J Extracell Vesicles* 3:26913
126. Théry C, Amigorena S, Raposo G, Clayton A (2006 Apr) Isolation and characterization of exosomes from cell culture supernatants and biological fluids. *Curr Protoc Cell Biol Chapter 3: Unit 3.22*
127. Hiemstra TF, Charles PD, Gracia T, Hester SS, Gatto L, Al-Lamki R et al (2014 Sep) Human urinary exosomes as innate immune effectors. *J Am Soc Nephrol* 25(9):2017–2027
128. Zarovni N, Corrado A, Guazzi P, Zocco D, Lari E, Radano G et al (2015 Oct 1) Integrated isolation and quantitative analysis of exosome shuttled proteins and nucleic acids using immunocapture approaches. *Methods (San Diego, Calif)*. 87:46–58
129. Gardiner C, di Vizio D, Sahoo S, Théry C, Witwer KW, Wauben M et al (2016) Techniques used for the isolation and characterization of extracellular vesicles: results of a worldwide survey. *J Extracell Vesicles* 5:32945
130. Momen-Heravi F, Balaj L, Alian S, Mantel P-Y, Halleck AE, Trachtenberg AJ et al (2013 Oct) Current methods for the isolation of extracellular vesicles. *Biol Chem* 394(10):1253–1262
131. Livshits MA, Livshits MA, Khomyakova E, Evtushenko EG, Lazarev VN, Kulemin NA et al (2015 Nov 30) Isolation of exosomes by differential centrifugation: theoretical analysis of a commonly used protocol. *Sci Rep* 5:17319
132. Webber J, Clayton A (2013) How pure are your vesicles? *J Extracell Vesicles* 2
133. van Deun J, Mestdagh P, Sormunen R, Cocquyt V, Vermaelen K, Vandesompele J et al (2014) The impact of disparate isolation methods for extracellular vesicles on downstream RNA profiling. *J Extracell Vesicles* 3
134. Li P, Kaslan M, Lee SH, Yao J, Gao Z (2017) Progress in exosome isolation techniques. *Theranostics* 7(3):789–804
135. Kowal J, Arras G, Colombo M, Jouve M, Morath JP, Prindal-Bengtson B et al (2016 Feb 23) Proteomic comparison defines novel markers to characterize heterogeneous populations of extracellular vesicle subtypes. *Proc Natl Acad Sci U S A* 113(8):E968–E977
136. Shao H, Im H, Castro CM, Breakefield X, Weissleder R, Lee H (2018) New technologies for analysis of extracellular vesicles. *Chem Rev* 118(4):1917–1950
137. Tauro BJ, Greening DW, Mathias RA, Ji H, Mathivanan S, Scott AM et al (2012 Feb) Comparison of ultracentrifugation, density gradient separation, and immunoaffinity capture methods for isolating human colon cancer cell line LIM1863-derived exosomes. *Methods (San Diego, Calif)*. 56(2):293–304
138. Zhang M, Jin K, Gao L, Zhang Z, Li F, Zhou F et al (2018 Sep) Methods and technologies for exosome isolation and characterization. *Small Methods* 2(9):1800021
139. Zeringer E, Barta T, Li M, Vlassov A (2015 Apr 1) v. Strategies for isolation of exosomes. *Cold Spring Harb Protoc* 2015(4):319–323
140. Liga A, Vliegenthart ADB, Oosthuyzen W, Dear JW, Kersaudy-Kerhoas M (2015 Jun 7) Exosome isolation: a microfluidic road-map. *Lab Chip* 15(11):2388–2394
141. Batrakova EV, Kim MS (2015 Dec 10) Using exosomes, naturally-equipped nanocarriers, for drug delivery. *J Control Release*. 219:396–405
142. Grubisic Z, Rempff P, Benoit H (1967 Sep) A universal calibration for gel permeation chromatography. *J Polym Sci B Polym Lett* 5(9):753–759
143. Feng Y, Huang W, Wani M, Yu X, Ashraf M (2014) Ischemic preconditioning potentiates the protective effect of stem cells through secretion of exosomes by targeting Mecp2 via miR-22. *PLoS One* 9(2):e88685
144. Roura S, Gámez-Valero A, Lupón J, Gálvez-Montón C, Borràs FE, Bayes-Genis A (2018) Proteomic signature of circulating extracellular vesicles in dilated cardiomyopathy. *Lab Investig*. 98(10):1291–1299

145. Gámez-Valero A, Monguió-Tortajada M, Carreras-Planella L, Franquesa M, Beyer K, Borràs FE (2016) Size-exclusion chromatography-based isolation minimally alters extracellular vesicles' characteristics compared to precipitating agents. *Sci Rep* 6:33641
146. Musante L, Tataruch D, Gu D, Benito-Martin A, Calzaferrì G, Aherne S et al (2014 Dec 23) A simplified method to recover urinary vesicles for clinical applications, and sample banking. *Sci Rep* 4:7532
147. Samsonov R, Shtam T, Burdakov V, Glotov A, Tsyrlina E, Berstein L et al (2016 Jan) Lectin-induced agglutination method of urinary exosomes isolation followed by mi-RNA analysis: application for prostate cancer diagnostic. *Prostate* 76(1):68–79
148. Hu JL, Wang W, Lan XL, Zeng ZC, Liang YS, Yan YR et al (2019) CAFs secreted exosomes promote metastasis and chemotherapy resistance by enhancing cell stemness and epithelial-mesenchymal transition in colorectal cancer. *Mol Cancer* 18(1):91
149. Matys MSS, Aigner C, Schulz SMM, Schachner H, Rees AJJ, Kain R (2021 Apr 28) Isolation of small extracellular vesicles from human sera. *Int J Mol Sci* 22(9):4653
150. Konoshenko MY, Lekchnov EA, Vlassov AV, Laktionov PP (2018) Isolation of extracellular vesicles: general methodologies and latest trends. *BioMed Res Int.* 2018:8545347
151. Huang T, Song C, Zheng L, Xia L, Li Y, Zhou Y (2019) The roles of extracellular vesicles in gastric cancer development, microenvironment, anti-cancer drug resistance, and therapy. *Mol Cancer* 18(1):62
152. Nolte-'t Hoen ENM, Buermans HPJ, Waasdorp M, Stoorvogel W, Wauben MHM, 't Hoen PAC (2012 Oct) Deep sequencing of RNA from immune cell-derived vesicles uncovers the selective incorporation of small non-coding RNA biotypes with potential regulatory functions. *Nucleic Acids Res* 40(18):9272–9285
153. Kim KM, Abdelmohsen K, Mustapic M, Kapogiannis D, Gorospe M (2017) RNA in extracellular vesicles. *Wiley Interdiscip Rev RNA* 8(4):10.1002/wrna.1413
154. Elzanowska J, Semira C, Costa-Silva B (2021) DNA in extracellular vesicles: biological and clinical aspects. *Mol Oncol* 15(6):1701–1714
155. Kahlert C, Melo SA, Protopopov A, Tang J, Seth S, Koch M et al (2014 Feb 14) Identification of double-stranded genomic DNA spanning all chromosomes with mutated KRAS and p53 DNA in the serum exosomes of patients with pancreatic cancer. *J Biol Chem* 289(7):3869–3875
156. Thakur BK, Zhang H, Becker A, Matei I, Huang Y, Costa-Silva B et al (2014 Jun) Double-stranded DNA in exosomes: a novel biomarker in cancer detection. *Cell Res* 24(6):766–769
157. Ricklefs FL, Alayo Q, Krenzlin H, Mahmoud AB, Speranza MC, Nakashima H et al (2018) Immune evasion mediated by PD-L1 on glioblastoma-derived extracellular vesicles. *Sci Adv.* 4(3):eaar2766
158. Wu F, Gu Y, Kang B, Heskia F, Pachot A, Bonneville M et al (2021 Jun) PD-L1 detection on circulating tumor-derived extracellular vesicles (T-EVs) from patients with lung cancer. *Transl Lung Cancer Res* 10(6):2441–2451
159. Nilsson RJA, Balaj L, Hulleman E, van Rijn S, Pegtel DM, Walraven M et al (2011 Sep 29) Blood platelets contain tumor-derived RNA biomarkers. *Blood* 118(13):3680–3683
160. Luo C-L, Xu Z-G, Chen H, Ji J, Wang Y-H, Hu W et al (2018) LncRNAs and EGFRvIII sequestered in TEPs enable blood-based NSCLC diagnosis. *Cancer Manag Res* 10:1449–1459
161. Best MG, Vancura A, Wurdinger T (2017) Platelet RNA as a circulating biomarker trove for cancer diagnostics. *J Thromb Haemost* 15(7):1295–1306
162. Park C-K, Kim J-E, Kim M-S, Kho B-G, Park H-Y, Kim T-O et al (2019 Aug) Feasibility of liquid biopsy using plasma and platelets for detection of anaplastic lymphoma kinase rearrangements in non-small cell lung cancer. *J Cancer Res Clin Oncol* 145(8):2071–2082
163. Roweth HG, Battinelli EM (2021) Lessons to learn from tumor-educated platelets. *Blood* 137(23):3174–3180
164. Klement GL, Yip T-T, Cassiola F, Kikuchi L, Cervi D, Podust V et al (2009 Mar 19) Platelets actively sequester angiogenesis regulators. *Blood* 113(12):2835–2842

165. Jiang T, Bai Y, Zhou F, Li W, Gao G, Su C et al (2019) Clinical value of neutrophil-to-lymphocyte ratio in patients with non-small-cell lung cancer treated with PD-1/PD-L1 inhibitors. *Lung Cancer (Amsterdam, Netherlands)* 130:76–83
166. Bryant AK, Sankar K, Strohbehn GW, Zhao L, Elliott D, Qin A et al (2022) Prognostic and predictive value of neutrophil-to-lymphocyte ratio with adjuvant immunotherapy in stage III non-small-cell lung cancer. *Lung Cancer (Amsterdam, Netherlands)* 163:35–41
167. Gibney GT, Weiner LM, Atkins MB (2016 Dec) Predictive biomarkers for checkpoint inhibitor-based immunotherapy. *Lancet Oncol* 17(12):e542–e551
168. Kim CG, Hong MH, Kim KH, Seo I-H, Ahn B-C, Pyo K-H et al (2021 Jan) Dynamic changes in circulating PD-1+ CD8+ T lymphocytes for predicting treatment response to PD-1 blockade in patients with non-small-cell lung cancer. *Eur J Cancer* 143:113–126
169. Capone M, Fratangelo F, Giannarelli D, Sorrentino C, Turiello R, Zanotta S et al (2020) Frequency of circulating CD8+CD73+T cells is associated with survival in nivolumab-treated melanoma patients. *J Transl Med* 18(1):121
170. Meyer C, Cagnon L, Costa-Nunes CM, Baumgaertner P, Montandon N, Leyvraz L et al (2014 Mar) Frequencies of circulating MDSC correlate with clinical outcome of melanoma patients treated with ipilimumab. *Cancer Immunol Immunother* 63(3):247–257
171. De Mattos-Arruda L, Siravegna G (2021) How to use liquid biopsies to treat patients with cancer. *ESMO Open* 6(2):100060
172. Gerber T, Taschner-Mandl S, Saloberger-Sindhöringer L, Popitsch N, Heitzer E, Witt V et al (2020) Assessment of pre-analytical sample handling conditions for comprehensive liquid biopsy analysis. *J Mol Diagn* 22(8):1070–1086
173. Fleischhacker M, Schmidt B (2020 Jun 25) Pre-analytical issues in liquid biopsy – where do we stand? *J Lab Med* 44(3):117–142
174. Hu Y, Ulrich BC, Supplee J, Kuang Y, Lizotte PH, Feeney NB et al (2018) False-positive plasma genotyping due to clonal hematopoiesis. *Clin Cancer Res* 24(18):4437–4443
175. YMD L, DSC H, Jiang P, RWK C (2021 Apr 9) Epigenetics, fragmentomics, and topology of cell-free DNA in liquid biopsies. *Science* 372(6538):eaaw3616
176. Ayers L, Pink R, Carter DRF, Nieuwland R (2019) Clinical requirements for extracellular vesicle assays. *J Extracell Vesicles* 8(1):1593755



Advances in Microfluidics for the Implementation of Liquid Biopsy in Clinical Routine

22

Alexandra Teixeira, Adriana Carneiro, Paulina Piairol, Miguel Xavier, Alar Ainla, Cláudia Lopes, Maria Sousa-Silva, Armando Dias, Ana S. Martins, Carolina Rodrigues, Ricardo Pereira, Liliana R. Pires, Sara Abalde-Cela, and Lorena Diéguez

Abstract

In recent years, we have seen major advances in the field of liquid biopsy and its implementation in the clinic, mainly driven by breakthrough developments in the area of molecular biology. New developments have seen an integration of microfluidics and also biosensors in liquid biopsy systems, bringing advantages in terms of cost, sensitivity and automation. Without a doubt, the next decade will

Alexandra Teixeira, Adriana Carneiro and Paulina Piairol as joint first authors that contributed equally to the preparation of the chapter.

A. Teixeira

International Iberian Nanotechnology Laboratory, Braga, Portugal

Life and Health Sciences Research Institute (ICVS), School of Health Sciences, University of Minho, Braga, Portugal

A. Carneiro

International Iberian Nanotechnology Laboratory, Braga, Portugal

IPO Experimental Pathology and Therapeutics Group, Research Center of IPO Porto (CI-IPOP)/RISE@CI-IPOP (Health Research Network), Portuguese Oncology Institute of Porto (IPO Porto)/Porto Comprehensive Cancer Center (Porto.CCC), Porto, Portugal

P. Piairol · M. Xavier · A. Ainla · C. Lopes · S. Abalde-Cela · L. Diéguez (✉)

International Iberian Nanotechnology Laboratory, Braga, Portugal

e-mail: lorena.dieguez@inl.int

M. Sousa-Silva · A. Dias · A. S. Martins · C. Rodrigues · R. Pereira

International Iberian Nanotechnology Laboratory, Braga, Portugal

Escola de Ciências, Campus de Gualtar, Universidade do Minho, Braga, Portugal

L. R. Pires

RUBYnanomed Lda, Braga, Portugal

© The Author(s), under exclusive license to Springer Nature Switzerland AG 2022

553

D. Caballero et al. (eds.), *Microfluidics and Biosensors in Cancer Research*,

Advances in Experimental Medicine and Biology 1379,

https://doi.org/10.1007/978-3-031-04039-9_22

bring the clinical validation and approval of these combined solutions, which is expected to be crucial for the wide implementation of liquid biopsy systems in clinical routine.

Keywords

Liquid biopsy · Microfluidics · Cancer diagnosis · Precision medicine · Personalized treatment

22.1 Introduction

Bodily fluids, whether scarce or abundantly available, can be sampled and analysed in a minimally invasive way using liquid biopsy, this procedure can be applied to not only blood and urine but also saliva, cerebrospinal fluid and pleural effusions. Such specimens are valuable sources of tumour cells and tumour-derived biomolecules such as circulating tumour cells (CTCs), circulating tumour DNA (ctDNA) and circulating tumour RNA (ctRNA), which are among the most widely analysed tumour biomarkers, while numerous others have gradually attracted increasing attention, including extracellular vesicles (EVs), cell-free microRNAs (cfmiRNAs), circulating cell-free proteins and tumour-educated platelets (TEPs) [1, 2]. Over the past decade, we have witnessed some of these analytes being established as relevant biomarkers to inform cancer management, which in turn elevated liquid biopsy to a promising precision oncology tool [3].

Liquid biopsy is a much safer and less invasive procedure than standard tumour biopsy, which consists of direct sampling of tissue through a surgical procedure involving varying degrees of instrumentation and invasiveness. Despite common, tissue biopsy is not without risk of complication for the patient. Besides being resource intensive, access barriers to the tissue may also exist depending on the tumour localization. Moreover, contrary to the conventional biopsy, an additional advantage of liquid biopsy resides in its high repeatability. Serial testing over time is an unmatched opportunity to obtain a detailed picture of the dynamic behaviour of tumours as well as chance to monitor therapeutic responses in real time [4, 5]. Taken together, these advantages render liquid biopsy particularly appealing to modern oncology as it predominantly lies on the molecular profiling of tumours to identify targetable alterations to support treatment decision and patient management.

Circulating biomarkers are central to diagnosis and prognosis in precision oncology, and search for improved biomarkers is at an unprecedented high demand [6]. Still making its way into routine clinical practice entails rigorous scientific demonstrations of analytical validation, clinical validation and clinical utility to be incrementally pursued in preclinical and clinical settings. This evidence-based journey has been the focal point of the field of research that begun by describing centrifugation-based methods to isolate circulating tumour cells in the 1960s

[7, 8]. Since then, many new strategies to isolate and detect CTCs have been reported in the literature, based on negative enrichment, magnetic sorting, microfiltration, size-based separation and magnetophoretic mobility separation to name a few [9–11].

Technological advancements greatly contributed to overcome the main challenges of blood-based biomarker detection. These are rare events in circulation [12]. An efficient separation of CTCs or ctDNA retrieves very low concentrations from an extremely high background of unsought normal circulating content, either erythrocytes and leukocytes or circulating DNA. Adding complexity to its detection, ctDNA is highly fragmented and CTCs are largely heterogeneous in morphology and phenotype [13, 14].

The past decade has been the most prolific in the development of technologies to isolate and detect CTCs, dozens of platforms using different approaches for CTCs isolation have been reported in the literature [9, 15], while several of these methods are successful in achieving high specificity and sensitivity combined, most result in non-viable cells. Capturing viable CTCs poses unique prospects in pursuing functional studies, for instance drug testing directly on patient's cells [1, 16, 17]. While the intrinsic complexity of some challenges slows down the pace of progress, others have already been successfully tackled and present exceptional developments. Microfluidics has been broadly explored for this purpose and more importantly offered valuable advances enabling high purity, accuracy and throughput in the analysis of liquid biopsy components. It offers researchers unprecedented control over fluid volumes and flow rates, as well as several other physical parameters of the substrate, additionally it enables miniaturization and can be easily combined with basic or advanced bioimaging techniques [18, 19]. Liquid biopsy platforms have benefited from incorporation of microfluidics and improved translation of biomarkers to the clinical setting as a result.

In this direction, the development of sensitive molecular assays drove and supported the analytical and clinical validity of CTC and ctDNA in cancer [20]. The prognostic significance of CTCs in early and metastatic cancer, particularly breast cancer has been widely reported [21]. CTCs can be detected in peripheral blood from early to late-stage breast cancer patients and the meta-analysis provides evidence that the presence of CTCs in peripheral blood is significantly associated with poorer prognosis and represents a significant risk factor for both progression free survival and overall survival. Similarly, additional meta-analysis provided strong evidence for the prognostic significance of CTCs detection in gastrointestinal malignancies, correlating the presence of CTCs with poor patient prognosis and unfavourable clinicopathological factors, both in gastric and colorectal cancer, regardless of the detection method [22]. A plethora of significant correlations between CTC enumeration and metastatic diseases have been reported in oesophageal cancer [23, 24], bladder cancer [25, 26], liver cancer [27], renal cancer [28, 29] and prostate cancer [30].

As for ctDNA, prior evidences demonstrated its potential clinical use in metastatic settings [31–33], as higher concentration of ctDNA is detected in advanced cancers compared with localized ones. Still, recently, new ultrasensitive

technologies have emerged that are able to detect the smallest amounts of ctDNA, which is critical to address early detection of cancer or minimal residual disease [34]. It was only recently, in 2016, that the FDA approved the first ctDNA test in NSCLC (Cobas v2; Roche Molecular Diagnostics) to determine EGFR mutational status in liquid biopsies when tumour tissue testing is not feasible [35]. It represented an important step towards clinical implementation of liquid biopsy and, indeed, to date, the number of regulatory approvals of ctDNA liquid biopsy solutions for single cancer indications continues to grow, fuelling the clinical translational trajectory of liquid biopsies in oncology.

22.2 Microfluidic Techniques for Biomarker Isolation

Microfluidic sorting techniques can be broadly categorized as relying on passive or active mechanisms. While passive sorting uses specific channel structures, hydrodynamic forces or steric hindrances to sort particles, active sorting mechanisms rely on the use of external forces, typically an electric or a magnetic field, or acoustic or pneumatic actuation. In addition, sorting can be label-free meaning that particles are separated based on their intrinsic physical properties, including but not limited to size, stiffness, shape, dielectric properties or intrinsic magnetic susceptibility; or use antibodies to target specific markers at the cell membrane or cytoplasm for detection and separation. Generally, label-free sorting is advantageous for minimizing cell/particle damage and for avoiding costly and labour-intensive processing steps. However, when a known marker is specific and unique to a target population, high purity can be achieved using immune-based sorting. The ideal sorting approach will ultimately depend on the particle of interest and particularly on the established application.

22.2.1 CTCs and CTC Clusters

Early detection of metastases is complicated as it currently relies on the sensitivity of traditional clinical imaging methods such as magnetic resonance imaging and positron emission tomography. Also, these tools do not provide updated molecular information about the tumour that is crucial to guide and personalize patient's treatment. Thus, there is an urgent unmet need to develop technologies that are able to efficiently isolate CTCs from the blood of cancer patients. However, capturing CTCs from blood samples is technically challenging since CTCs are extremely rare (1 to a few 10 s per mL), being obscured by billions of peripheral blood cells [36].

The principles of CTC isolation can be generally divided into two approaches—biochemical and biophysical. Biochemical isolation is based on the identification of unique biomarkers while biophysical approaches rely on the differentiation between intrinsic physical properties of CTCs and blood cells. Regardless of the approach chosen, to evaluate performance it is important to consider the capture efficiency and

isolation purity, and critically high-throughput, given the need to process large volumes of whole blood in reasonably short periods of time [36].

The most common techniques for CTC isolation use antibody-based methods, mostly through the identification of epithelial markers, such as EpCAM, as there is no ubiquitous cancer biomarker. In fact, the only analytically valid and FDA-approved platform for prognostic use in advanced breast, colorectal and prostate cancers is CellSearch®. This technology operates through immunomagnetic-conjugated antibodies against EpCAM, a transmembrane glycoprotein present on the surface of some CTCs but absent in blood cells. Following this enrichment step, the captured cells are immunostained with antibodies against cytokeratin (CK), to demonstrate the epithelial origin of the cell, and CD45 to exclude cells of the hematopoietic lineage. Another commercially available technology for CTC capture is the AdnaTest® from AdnaGen. Similarly to CellSearch®, the AdnaTest is based on magnetic enrichment of EpCAM-expressing cells, but detection is achieved by RT-PCR of putative tumour-associated transcripts [10]. Both of these biochemical approaches are based on detecting epithelial surface markers of CTCs (EpCAM and CK). However, some CTCs, especially those of a highly invasive and metastatic capacity, can lose their epithelial phenotype via the epithelial to mesenchymal transition (EMT) process, and upregulate instead mesenchymal markers. Altogether, this may result in significant CTC loss during the enrichment step and biased analysis in biochemical-based methodologies [37].

Alternatively, several technologies have been developed to isolate CTCs based on the premise that these cells are physically distinct from most normal blood cells. For example, CTCs are on average larger than most white blood cells (WBCs; 8–20 μm) [38], and based on this, approaches like size/deformation-based microfluidic devices, and size-based membrane filters and hydrodynamic methods have been proposed. However, the simplicity of these procedures, added to their label-free character, can also become a limitation, since isolation is often non-specific thus potentially affecting capture efficiency [39]. In fact, some morphological data regarding CTCs have highlighted the heterogeneity typical of these cells since their shape can vary significantly and their size has often been reported to vary from 4 to 30 μm [40]. In addition, CTCs are typically deformable, which could also affect their isolation efficiency by changing their apparent size. Indeed, the selection of a specific capture size may yield reliable CTC isolation in most patient samples, yet inadequate overall performance across a large patient set [41, 42].

Notwithstanding, the use of microfluidics for the capture and detection of CTCs has been associated with multiple advantages such as enabling cost-effective, simple and automated operation using small quantities of samples and reagents to carry out highly sensitive detection. Additionally, it allows a one-step process of sample loading, separation and capture of living rare cells that can be later analysed through microscopy or downstream molecular techniques [41, 43]. Furthermore, microfluidics offers an opportunity to combine isolation and detection methods into a single device, paving the way for the development of real point-of-care diagnostic CTC devices [41].

One of the advantages of microfluidic cell sorting, either using a labelled or label-free approach, is that the small features of these devices provide extraordinarily high surface area to volume ratios. Hence, antibody-based CTC isolation can be enhanced by coating the device surface with capture molecules that specifically bind to CTC surface markers [41]. Naturally, the flow parameters require optimization to maximize the probability of attachment—the flow rate should be slow enough to ensure cell-surface attachment, but reasonably fast to generate enough shear, thus preventing non-specific attachment of blood cells [44]. The CTC-chip was designed to accommodate 78,000 anti-EpCAM functionalized microposts providing an abundance of sites for CTC capture, with the authors reporting over 60% CTC recovery. Aiming for higher efficiency, a second-generation device used grooves on the device surface to disrupt laminar flow streamlines, thus maximizing collisions between target cells and the antibody-coated surface [45]. The device, coined ‘herringbone-chip’, overcame its predecessor in several aspects since it increased throughput and improved both CTC capture efficiency and purity. It also improved CTC imaging and scaled up device production [45]. However, it should be noted that the same limitation regarding the loss of epithelial markers may compromise the efficiency of microfluidic antibody-based isolation of CTCs from certain cancer phenotypes.

On the other hand, many size-based microfluidic systems for CTC isolation have been developed aiming to achieve superior results. Examples include, but are not limited to, the Parsortix® System from Angle [46], the VTX-1 from Vortex Biosciences [47] and the RUBYchip™ from RUBYnanomed [48, 49]. These size-based methods are label-free, avoiding the bias created by the expression of epithelial antigens. However, smaller CTCs may be missed and the capture of large leukocytes can result in lower sample purities.

Combinatory approaches also exist relying on size selection and negative enrichment. This is the case of the CTC-iChip, that combines size-based separation of nucleated cells from RBCs, platelets and plasma, with depletion of WBCs tagged with magnetic beads, using CD45 and CD66b antibodies [50]. Despite its success, the applicability of the CTC-iChip could be questioned due to long set-up and processing times, hindering its clinical translation [51].

Several technologies have been developed for the capture of individual CTCs, but they are only rarely capable of capturing CTC clusters, which have an increased metastatic potential when compared to single CTCs [52]. The survival advantage of CTC clusters is associated with the cooperation between cells within the cluster, providing a shielding effect from shear forces, environmental or oxidative stresses, and immune assault [53]. CTCs are frequently associated with stromal or immune cells forming heterotypic clusters, which may provide additional advantages [53]. Like CTCs, CTC clusters can also be captured by positive selection or based on their larger size or different shape. However, due to the large variability reported for cluster capture efficiencies and the large shear rates inherent to many devices, the current methodologies for the isolation of single CTCs are mostly not applicable. This is because escape or dissociation of CTC clusters into single cells or smaller clusters is likely to occur during blood processing [54]. The Cluster-chip is a microfluidic device that uses triangular micropillars to specifically isolate CTC

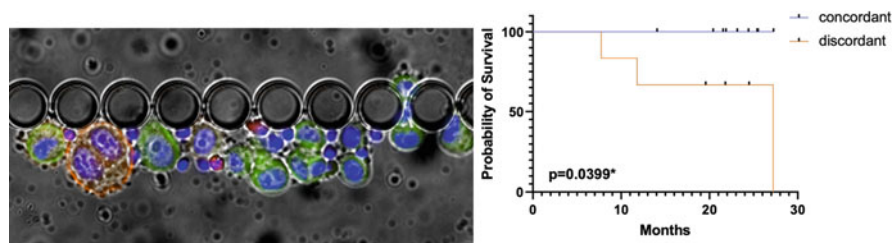


Fig. 22.1 (left) CTCs are isolated in the RUBYchip™ (DAPI in blue, CK in green, CD45 in red and HER2 in orange), (right) Overall survival plot, where populations are selected according to analysis of HER2 being concordant or discordant between CTCs and the tissue biopsy (modified from [48])

clusters from unprocessed patient blood samples with high sensitivity [55]. Although high efficiencies for cluster capture were reported, some limitations included the physical capture mechanism, which relied on batch processing, thus resulting in long on-chip residence times; and elevated shear stresses, which were needed to release the majority of clusters from micropillars, potentially resulting in changes or damage to cellular structures and/or content [54]. Thus, to overcome these constraints the Cluster-chip was updated to a new version that used a two-stage deterministic lateral displacement (DLD) strategy. Briefly, the first stage was designed to allow size-based separation of larger clusters from smaller clusters and single cells. Larger particles were separated by continuously bumping on a series of micropillars while smaller particles were able to zigzag through the device to arrive at the second stage, where an asymmetrical pillar array design and reduced channel height isolated the smaller clusters [54]. This device was able to isolate CTC clusters that experienced low shear stress rates and on-chip residence times on the order of seconds, minimizing damage or processing bias. Another device specifically developed for the capture and reversible release of individual CTC and CTC clusters is based on a thermosensitive three-dimensional scaffold system [56]. The device can efficiently capture clusters while assuring high viability for downstream applications, including cell culture. The scaffold is uniformly coated with a thermosensitive gelatin hydrogel, which dissolves at 37° C, triggering a gentle release of the captured cells [56]. However, clinical feasibility as well as validation by confirming the prognostic value of CTC clusters in cancer patients will be required for clinical translation of a CTC cluster capture platform.

Detection and analysis of CTCs, as well as the integration of viable CTCs in functional studies can provide valuable information for the understanding of cancer onset and progression. Indeed, prognostic indications can already be made based on the enumeration of CTCs in blood and the study of CTCs can lead to discovery of new cancer biomarkers. Recent publications also hint on the clinical utility of CTCs, as increased CTC numbers might predict disease recurrence and resistance to treatment. Furthermore, downstream analysis of CTCs can be used as a Companion Diagnostic strategy to evaluate therapeutic targets and select personalized treatment

options. For instance, in a recent report, CTCs isolated from a cohort of metastatic breast cancer patients were used to evaluate the expression of the HER2 protein and compare against the phenotype from the primary tumour [48]. Patients who had concordant HER2 expression had 100% survival after 27 months, while patients with discordant expression had 0% survival (Fig. 22.1). Despite the promising results, interventional clinical trials are needed to assess the real value of CTCs to guide therapeutic decisions.

22.2.2 EVs

Extracellular vesicles (EVs) are cell-derived particles present in body fluids, which originate from both healthy and pathological cells, and play key roles in a variety of cellular processes including cell-to-cell communication, inflammation, cellular homeostasis, survival, transport and regeneration [57, 58]. In cancer, it is postulated that EVs contribute to the formation of a tumour-supporting stroma by activating cancer-associated fibroblasts, promoting tumour angiogenesis, supporting the formation of pre-metastatic niches and suppressing anti-tumour immune responses [59–62]. Thus, it comes as no surprise that EVs have garnered significant interest for their potential use as cancer biomarkers in the past few decades. In addition, EVs are more abundant in liquid biopsies when compared to CTCs and offer protection from degradation to nucleic acids (DNA, mRNA, microRNA and long noncoding RNAs) and proteins encapsulated within their lipid shell, effectively extending their half-life. On the downside, EVs span a wide range of particle sizes, hampering the applicability of a variety of isolation and purification strategies, and it is often difficult to discriminate EVs from other particles of similar size and composition [58].

The size of EVs is intrinsically associated with their mechanism of formation, which also divides EVs into three main categories. Exosomes range from 30 to 150 nm and originate from endocytic multivesicular bodies, which release their content upon fusion with the cell membrane; microvesicles (MVs) range from 100 to 1000 nm and originate via budding of the plasma membrane; and apoptotic bodies are a form of MVs that originate during programmed cell death and can measure as much as 5000 nm. The size heterogeneity, ranging from the nanometre to the micrometre scale, added to the difficulty of assigning an EV to a particular biogenesis pathway, unless EVs are caught red-handed in the act of release, has led to a recent recommendation to use nomenclature based on physical characteristics, such as size, rather than biogenesis [63].

Strategies for EV separation are typically based on biophysical properties such as size, density, morphology, deformability (membrane rigidity) and surface chemistry, some of which depend on the cell type that they were produced from. Conventional techniques include differential ultracentrifugation (UC), density gradients, precipitation, filtration, size exclusion chromatography (SEC) and immuno-isolation—with the first being by far the most common [63]. These techniques can be ranked by five key figures of merit: (i) recovery rate or yield, (ii) purity, (iii) throughput,

(iv) processing time and complexity and (v) cost of equipment and consumables. EVs can be extracted from a variety of sources ranging from *in vitro* cell cultures to patient-derived samples. Blood is an attractive source for containing EVs in abundance (0.5–1.5 billion/mL) [64]. However, it poses an added challenge due to the presence of other components such as lipoproteins, protein complexes, viruses and microparticles, with overlapping physical properties. Thus, relying on a single method might be insufficient to isolate EVs with both high yield and purity, and using a combination of techniques is customary aiming for higher specificity.

UC is capable of processing large sample volumes and does not require any chemical treatment thus allowing for downstream analysis. However, it offers low recovery efficiency and purity, is time-consuming, requires bulky equipment and the high centrifugal forces may lead to rupture, aggregation and compaction of EVs [57, 58]. Density gradient centrifugation increases purity and yield but is more complex and requires longer processing times. Ultrafiltration uses nano-porous membranes with pore sizes ranging from 1 to 100 nm to retain EVs. The basic filtration scheme is simple but suffers from disadvantages such as clogging, extrusion effects and a typically lower yield associated with irreversible bonding of EVs to the filtration membranes. These advantages can be tackled by using tangential flow filtration methods [65], which are gentler, but require more elaborate set-ups. SEC uses columns of porous beads to elute fractions of liquid biopsies based on size. It preserves EV structure, prevents aggregation and significantly reduces the sample protein content. However, it is non-specific, sample volumes are reduced, and leads to sample dilution, thus usually requiring an additional concentration step. Precipitation methods include a variety of commercially available kits like ExoQuick®, mirCURY®, ExoGAG® and others. The process is simple and preserves EV structure. It is though non-specific leading to low purity, and the addition of reagents may compromise downstream analysis. Immuno-isolation in its turn is highly specific, resulting in higher purities. The disadvantages are that it requires previous knowledge about the targeted EVs, sample volumes are low frequently requiring pre-concentration, and antibodies may hamper further analysis [57, 58].

Harnessing the unique properties of microfluidics and fluid dynamics at the microscale has been the object of extensive research targeting the separation of multiple particles from biofluids, including animal cells, yeasts, bacteria, viruses, proteins and nucleic acids. Microfluidic-based sorting is typically classified as passive or active depending on whether it relies on channel structures and hydrodynamic phenomena, or on the actuation of external forces including electric, magnetic, acoustic or others.

An example of passive microfluidic-based sorting of EVs is the nanoDLD device from IBM [66, 67]. The principles are based on the original deterministic lateral displacement (DLD) technology introduced in 2004, which uses arrays of micro (or nano)-metre sized pillars to sort particles of different sizes and/or deformability, with resolutions down to tens of nanometres. The latest development includes over 30,000 parallel devices capable of handling 17 millilitres per hour and of achieving a 30-fold enrichment, approximating clinically relevant volumes and processing times [66]. Inertial microfluidics and viscoelastic flows have been demonstrated to achieve

high purity (>90%) and high recovery (>80%) when sorting exosomes from other EVs present in cell culture media [68, 69]. Separation is achieved by balancing elastic and inertial lift forces and viscous drag. Though a promising proof-of-principle and with great potential, it should be noted that not only the EVs used in this study were obtained from culture media, but were also pre-processed by differential centrifugation and filtration. Another approach, also using EVs from pre-processed culture media, used a λ -DNA mediated viscoelastic flow and aptamers targeting EpCAM and HER2 to simultaneously separate and detect exosomes, MVs and apoptotic bodies from a series of breast and mammary cancer cell lines (including HER-positive and negative cells) [70]. Aiming to reduce the long channel lengths typically used in viscoelastic microfluidics, Asghari et al. recently introduced an oscillatory flow and demonstrated separation of small EVs [71]. Another microfluidics-based approach is asymmetric field-flow fractionation (AF4) [72], which uses a semi-permeable membrane and two perpendicular flows to separate EVs based on hydrodynamic size. It was reported to achieve high recovery yields in reduced periods of time (1 h) but it is limited to small amounts of samples and, yet again, this demonstration was done with EVs obtained from cell cultures and pre-processed by differential UC.

From active microfluidic-based approaches, nanoFACS offers a powerful solution, being able to sort particles at high throughput (nearly 100,000/s) and with high purity yields. However, it is label-dependent and with that derive all the shortcomings associated with immuno-dependent methods [73, 74]. Acoustofluidics uses ultrasound waves to separate particles based on size, density or compressibility differences. By exploiting a two-stage device, Wu et al. [75] showed separation of exosomes from unprocessed blood with both yield and purity superior to 98%. The first stage of the device decluttered the sample from larger microscale cells while the second stage purified exosomes from other EVs of different sizes. On the downside, the device throughput was just 4 microlitres per minute. AC electrokinetics, such as field gradients, can be used to transport particles. For example, Ibsen et al. [76] isolated exosomes from undiluted human plasma by using an AC field that concentrated EVs at the edges of an electrode array, allowing their subsequent washing and isolation. To process 50 μ L of plasma the device needed 15 min.

In sum, EVs offer tremendous hope as cancer biomarkers to be used for diagnostics, prognostics, treatment monitoring and to direct revolutionary personalized medicine from non-invasive liquid biopsies. However, EV isolation and analysis is hindered by their size heterogeneity, which overlaps with a variety of other particles that are abundant in liquid biopsies—particularly whole blood. This renders conventional sorting methods incapable of providing satisfactory EV sorting in isolation, thus leading to the use of combinatorial approaches that contribute to lengthy and inadequate protocols. Microfluidics has shown great potential to overcome the challenges faced by conventional methods. Addressing the current difficulties related to throughput, standardization and reproducibility will be key to drive clinical translation with significant therapeutic implications.

22.2.3 ctDNA

The presence of cfDNA in human plasma derived from patients with systemic lupus erythematosus was first reported by Mandel and M \acute{e} ttais, in 1948 [77]. Three decades later, several publications reported that the levels of cfDNA in cancer patients were higher than in healthy individuals [78], since high levels of tumour DNA (called circulating tumour DNA, ctDNA) are released by tumours at advanced stages, due to the increased cell death [79, 80]. This genetic material found in the circulation of cancer patients has demonstrated to reflect the mutations found in the primary or metastatic tumour and, as such, ctDNA has emerged as a novel sensitive biomarker in cancer research [81, 82]. Despite it being intensively studied, the mechanisms of release of ctDNA are not fully understood [83]. Many mechanisms have been identified, and the two main ones are active DNA release and cellular breakdown [84]. As such, ctDNA can be released from tumour cells by apoptosis, necrosis, phagocytosis and active secretion [83–85].

After the suggestion that the increased cfDNA fragments in tumour patients could have a tumoural origin [86], mutated K-Ras sequences were detected in the plasma of pancreatic cancer patients, confirming the theory [87]. Later, it was shown that the length of the strands could be related to the DNA origin, as ctDNA has shown to be smaller than cfDNA originated from healthy cells [88]. cfDNA from healthy individuals ranges from 200 to 10000 bp, while cfDNA originating from tumours is more fragmented with an average size of 160 bp, and some fragments are even smaller than 100 bp [89, 90]. The concentration of cfDNA in the plasma of cancer patients can be up to 1000 ng/mL, while in healthy individuals it ranges from 0 to 100 ng/mL [84]. Differences were observed not only between healthy individuals and cancer patients, but also between patients at different disease stages. In patients with metastatic cancer, ctDNA concentrations were found to be higher than in patients with localized tumours, 86%–100% against 49%–78%, respectively [91, 92].

The interest in ctDNA increased further with the ability to detect specific mutations from certain tumours [79, 81] that could be used for precise diagnosis and patient subtyping and be correlated with treatment resistance. Nonetheless, the quality of the analysis depends heavily on the quality of the isolation and extraction protocols to recover the ctDNA, and commonly used techniques require mutant copy abundance [13, 79]. Actually, due to the fragmented nature of ctDNA and its short half-life in circulation, between 16 and 90 min, depending on the multiple factors such as tumour stage, standard processes for solid phase extraction (SPE) of DNA are largely inefficient, limiting their use in the clinic [79].

Most of the commercial kits for ctDNA extraction come together with kits for mutation analysis by real-time PCR, such as the TherascreenTM EGFR plasma RGQ PCR kit (Qiagen), with a reasonable recovery of 56.49%, according to Sorber et al. [81] and the Cobas EGFR Mutation Test v2 (Roche Molecular Diagnostics) [93]. Those extraction kits normally use silica beads to bind the plasma-borne cfDNA fragments onto their surface upon induction by a chaotropic salt [94]. Despite the reasonable recovery that these kits can achieve, multiple studies have

demonstrated significant variability among laboratories, which may be due to bias introduced by different operators [95, 96]. Another disadvantage of using this type of kits is the extensive sample handling and processing, leading to samples loss [97].

Microfluidic devices are a new attractive approach for clinical use when compared to benchtop methods, as they offer unique technical features that may overcome the limitations of the aforementioned methods, such as reduced processing time, cost-effectiveness, closed systems to avoid sample loss or contamination, and mostly, simple workflow [79, 98]. Despite its potential, there is still a small amount of literature regarding the extraction of ctDNA using microfluidics. This is mostly due to the difficulty in detecting low concentrations of ctDNA in the presence of high concentrations of nonmutated DNA, and also due to the small size of ctDNA fragments [99].

The first studies using microfluidics were mostly based on the size and properties of cfDNA. Consequently, electrokinetic trapping on microchannels was developed, in which charged ions accumulate by applied electric field forming the drain of targeted analytes [100]. Indeed, microfluidic solid phase extraction (SPE) tools have been used successfully for extraction of free DNA in environmental and food samples [101, 102]. Size-based micropillar structures, microcolumn-packed separation and electrophoretic system on microchannel were developed, for cfDNA extraction based on its size [103, 104]. However, these methods could not further purify the cfDNA for specific ctDNA detection. Another approach was based on the qPCR technique applied in a microfluidic platform. The authors used thermal amplification of a single DNA copy and fluorescence was used to monitor the concentration with the help of DNA fluorescent probes [105, 106]. These microfluidic systems were reported without sensitivity specification.

A seven droplet-based digital PCR microfluidic system to identify specific mutations detecting ctDNA was reported by Pekin and colleagues [107]. The device functionalized with probes was used to isolate mutated DNA, from the wild-type with fluorescence signal. The authors demonstrated accurate and sensitive quantification of mutated KRAS oncogene, but the platform is limited by the number of droplets for analysis [107]. Furthermore, Bahga et al. came up with a microfluidic device to isolate ctDNA using dielectrophoretic capture electrodes, reporting high capture efficiency, without details of sensitivity [108]. Koboldt and colleagues, in 2017, developed a microfluidic multiplex PCR technology for sensitive quantification of ctDNA [109]. Plasma from ovarian and pancreatic patients was used, and the authors reported ctDNA mutation detection, with a sensitivity of 92% and specificity of 100% [109]. Campos et al. demonstrated a low-cost plastic microfluidic surface based on SPE for ctDNA extraction, with more than 90% purity noticed. This device detected successfully KRAS mutation gene from plasma samples of colorectal and NSCLC cancer patients, proving its utility for clinical disease detection [79]. Gwak et al. designed a microfluidic platform capable of cfDNA extraction in 19 min, combining multi-vortex mixing modules to increase the binding between the cfDNA and the silica magnetic particles used, along with a gradient magnetic-activated cfDNA sorter module for the capture of the MPs [110].

Despite recent advances in the development of microfluidic platforms for ctDNA extraction and detection, these remain limited and inconsistent among different studies. Lack of standardization is currently the biggest limitation to implement microfluidic SPE tools in the clinic [18].

22.3 Techniques for Downstream Analysis

The molecular analysis of liquid biopsy biomarkers is obviously interesting to retrieve information about cell phenotype, mutational landscape and gene expression, but cancer cells can also be used to perform functional analysis. Beyond this, the simple quantification of tumour material, ctDNA or CTCs, can be correlated with the tumour burden. As such many microfluidic tools have been developed for the enumeration of cancer cells. Some of these tools are summarized in the chapter from Chícharo et al.

22.3.1 Cell Phenotyping and Gene Expression

22.3.1.1 Flow Cytometry

Flow cytometry assays are mainly done to measure antigen expression, using fluorescently labelled antibodies, and providing multi-dimensional analysis of the different cell types contained in a complex sample [109]. As such, flow cytometers are an invaluable tool used in cell biology, biotechnology, biomedical research, and also in the clinic [111], promoting the analysis of body fluid samples including bone marrow, cerebrospinal fluid and pleural fluid, for the diagnosis and monitoring of diseases like leukaemia and HIV [112, 113]. Nevertheless, research has advanced in recent years in the field of microfluidic flow cytometry, to create cheaper, faster, portable, more autonomous, less prone to contamination and smaller alternatives to the traditional flow cytometry, while providing a simplified operation and a reduction of resource consumption in the assays [11]. Major developments in microfluidic flow cytometry have been reported including the different subsystems: sample pumping, sorting, focusing, detection and data analysis; all of them tuneable depending on the requirements of the desired application [114].

The strategies mostly described for sample pumping are based on peristaltic, piezoelectric, absorbent, electroosmotic and pressure driven mechanisms. To reduce cell rupture during pumping of biological samples, various efforts have been made to improve and implement new strategies including electrophoresis and high-frequency piezoelectric activated peristaltic pumps [114–119]. With the same goal, Lee et al. demonstrated an absorbent microflow cytometer chip, in which the solution was driven by the absorbing force of superabsorbent materials [120]. Or a more recent approach, microfluidic sample pumping was done using a simple T-shaped microchannel with electric field-effect flow control [121].

Sample focusing is also critical in a conventional flow cytometer as the cells need to pass through a specific zone to ensure the appropriate detection accuracy and

throughput [114]. This means that the location of the cells in the microchannel could affect the detection accuracy greatly. Thus, in microfluidic flow cytometry, the major focusing methods used are based on sheath flow and sheathless flow [122, 123]. For example, Mao and collaborators demonstrated a microfluidic flow cytometer that combines hydrodynamic sheath and dean flows to control the axial position of the cells within a microfluidic channel [124]. This system is based on inducing dean flow in a curved microfluidic channel, where the microfluidic deflection can be used to hydrodynamically focus cells in the vertical direction and allows 3D hydrodynamic focusing on a single plane. Additionally, this system was then successfully integrated into the laser-induced fluorescence detection system to provide effective high-throughput flow cytometry measurements at a rate of over 1700 cells/s [124].

Many different microchip sorting systems are already described and conventionally divided into active and passive methods. In microfluidic flow cytometry, the sorting methods described are optical, magnetic, electric or acoustic fields or piezoelectric actuators (active methods), and electrophoresis as specific geometric structures (passive sorting) [125–127].

Lastly, the strategies used to improve the selectivity and sensitivity of microfluidic flow cytometers for the analysis/detection of different samples include the use of conventional optical detection and other powerful detection techniques such as impedance spectroscopy and electrochemical detection. In addition, ultrasound and photoacoustic-based detection methods have been gradually also applied in microfluidic flow cytometry [111, 128]. For example, a multi-channel parallel microfluidic cytometer that is based on analogue detection combined with parallel microfluidics was developed with the capacity to reduce data load and increase throughput, simplifying the classification algorithm to a fraction of a microsecond. Furthermore, the system presented a slow-flow regime, providing a better and more careful quantitation of fluorescence than conventional flow cytometry systems [129].

The versatility of microfluidic cytometers has been demonstrated in several works. For example, Göröcs and co-workers fabricated an image-based microfluidic flow cytometer for the detection of toxic algae in water samples [130]. Cho and collaborators used their microflow cytometer and included a fluorescence-activated cell sorter (FACS) for the isolation of *E. coli* [131]. This microfluidic FACS strategy was also applied for the determination of apoptosis and necrosis in HeLa cells [132]. Also, microfluidic flow cytometers have also been applied for the purification and detection of viral sample, or even for single-cell analysis [133].

Many microfluidic flow cytometers are already in the market, including GigaSort™ (Cytonome, Inc, USA), MACSQuant Tyto™ (Owl Biomedical, Inc, Germany), SH 800 (Sony Biotechnology, Inc, USA), Wolf™ (Nanocollect Biomedical, Inc, USA) and Moxi Go II™ (ORFLO, Inc, USA) [111, 134]. In summary, the implementation of microfluidics in flow cytometry is in continuous optimization and it is expected to achieve major improvements in diagnostics and biomedical research.

22.3.1.2 FISH

Fluorescence In Situ Hybridization (FISH) is a molecular technique consisting in the hybridization of a labelled probe with a target nucleic acid sequence within a cell or tissue section to produce a measurable fluorescence signal. FISH assays have been extensively used during recent years, with a wide range of nucleic acid and mimic probes being commercially available for the assessment of specific sequences of genes, RNAs or even entire chromosomes, making a tremendous impact in the fields of genomics, biotechnology and bioinformatics. This technique can precisely localize and quantify molecules of interest at single-cell resolution in a cell sample or tissue slice. As such, FISH has many applications for diagnostic purposes, such as assessing the presence or absence of specific genes, chromosomal abnormalities or gene expression, relevant in many areas, namely for haematological analysis, identification of microorganisms, prenatal diagnosis and cancer prognosis and therapeutic selection [135, 136]. However, FISH presents as all techniques some disadvantages, such as the complexity of their protocols, being time-consuming, and needing skilled dedicated personnel. This consequently means that this technique is costly, which has affected the fast and wide adoption of FISH in the laboratories. The integration of FISH protocols into microfluidic systems offers a streamline solution to these challenges, by including and automating all steps into one single device while reducing assay time, reagent volumes and enabling operation by non-skilled personnel even at the point-of-care.

Several microfluidic FISH assays have been developed in recent years and demonstrated in a variety of proof-of-concept applications. With the aim to decrease probe consumption, Nguyen et al. reported a microfluidic-assisted FISH (MA-FISH), capable to reduce the hybridization time to 4 h and reagent volume by a factor of 5 concerning the conventional protocol and also the reaction rate and reported on their extra-short incubation microfluidics-assisted FISH (ESIMA-FISH) [137]. Microfluidic FISH has been reported as a high-throughput method for single-cell analyses and detection of chromosomal abnormality in haematological diseases. Different strategies have been developed for immobilization and analysis of hematopoietic cells from peripheral blood or bone marrow samples [138]. Also, a strategy to immobilize circulating plasma cells and circulating leukaemic cells for cytogenetic analysis of TEL/AML1 translocation and BCR/ABL1 fusion aberrations allowed to evaluate MRD in multiple myeloma and leukaemia was also developed [139].

The use of FISH is also very popular to assess genetic alterations in CTCs. Their analysis enables the real-time assessment of disease evolution, as well as the design of personalized treatments. In 2012 was reported for the first time a device for microfluidic isolation and FISH analysis of CTCs [140]. In 2015, the potential of microfluidic FISH for molecular diagnostics was proven. The authors demonstrated the capability of their on-chip FISH system for the evaluation of ERBB2 in cells captured from pleural fusion samples from breast cancer patients [141].

In summary, the applications of microfluidic FISH are multiple, being also used for chromosomal DNA analysis [142], including telomer length and chromosomal aneuploidy assessment, applied to prenatal [143] and cancer [142] diagnosis.

Furthermore, this technique has also been reported for the diagnosis of Alzheimer's disease [144] and malaria [145]. Recent works have reported on novel developments to integrate microfluidic FISH in co-culture systems [146] and in microdroplets [147], and for real-time monitoring of FISH kinetics [148].

22.3.1.3 Immunofluorescence

Immunofluorescence uses fluorescent dyes to label biomarkers in cells. It takes advantage of the specificity of antibodies to target antigens present in different parts/compartments of cells of interest. Since immunofluorescence is one of the most broadly spread techniques for the analysis of cells in traditional biological protocols, it has also been applied to the analysis of cells within microfluidic devices. Microfluidics however brings an inherent added value in terms of minimizing the volume of the fluorescently labelled antibodies, as well as providing a platform where to immobilize the cells to analyse. These microfluidic devices containing the labelled cells can then be analysed easily under the microscope, with the advantage of protecting the biological sample in an isolated chamber, as well as ensuring reproducible and controlled conditions during the labelling protocols.

Immunofluorescence combined with microfluidics has been applied in the context of different scientific fields including environmental and food analyses, viral studies or cancer. For example, the immunofluorescence detection of the dengue virus using dielectrophoretic microfluidic platform was proposed by Chang and co-workers [149]. Beyond the standard use of microfluidics in combination with immunofluorescence for capture and immunostaining of target cells, microfluidic immunofluorescence was also applied for cell reprogramming. Interestingly, the micro-confined environment showed a 50-fold increase in the efficiency of the overall reprogramming outcome [150, 151].

In the context of cancer diagnosis and liquid biopsy, the HER2 expression in breast cancer cells from 25 cancer patients was also studied, with a microfluidic device that provided the needed precision required for protocols that aim at being implemented in the clinic [152]. Hung et al. integrated a set of microfluidic modules for the capture of cells from cholangiocarcinoma (CCA) samples, the subsequent immunostaining using two specific CCA biomarkers, and a detection module for visualization [153]. Several other examples may be provided for other cancer settings and research challenges such as lung adenocarcinoma, in situ mapping of immune cells or the widely spread molecular analysis of circulating tumour cells (CTCs) isolated in microfluidic devices or even for detection of two different cholangiocarcinoma biomarkers from captured cells, using different modules [154].

Despite the extended combination of immunofluorescence with microfluidics, it has been restricted to the qualitative molecular analysis of those cells. It is still needed to implement strategies that allow the quantitative determination of the expression of those antigens, and in that sense using robust platforms may be the way to move forward to have an efficient implementation in the clinic.

22.3.1.4 SERS

Surface-enhanced Raman scattering spectroscopy (SERS) is commonly used to promote the enhancement of the weak Raman signal of a target molecule, more precisely in cases where high sensitivity is desired, and detection is limited by the low concentration of the analyte. SERS is considered an ultrasensitive and powerful analytical tool, and its potential has already been demonstrated in various fields, such as biology, environmental, food, pharmacology and medicine. However, it can be difficult to maintain the reproducibility and consistency of SERS-based techniques, but this drawback can be easily overcome by integrating SERS detection into a microfluidic platform, which promotes a continuous flow condition for highly reproducible SERS measurements [155, 156]. In addition, this combination of technologies offers new opportunities for multiplexed nanoparticle-based assays, which are highly selective and specific. This strategy has been studied, improved and applied for the detection of biological and chemical molecules [156], contaminants in food [157] or water [158] or even for analysis of single cells and cancer biomarkers.

The integration of SERS with droplet microfluidics has demonstrated potential for single-cell analysis [159], more precisely in the work developed by Willner et al., where was demonstrated intracellular variability in the expression of glycans on the cell membrane of prostate cancer cells and detection of sialic acid on single-cell level in cancer cell lines (MCF-7, HepG2, SGC and BNL.CL2) [160]. These studies promote a better understanding of cellular systems [159]. This strategy was also applied for the detection of *Escherichia coli* [161], *Staphylococcus aureus* [162] and eukaryotic cell lysate [163].

On the other hand, for detection of cancer subpopulations, Zhang et al. developed a strategy that integrates microfluidics, for size-based cell isolation, with SERS used for in situ reporting of cell membrane proteins. Also, a reliable SERS immunosensor was developed on a microfluidic chip for the simultaneous detection of multiple breast cancer biomarkers in real samples and demonstrated a successful performance compared with standard techniques [164]. More recently, Kapara et al. demonstrated that multiplexing capabilities of SERS can be successfully used to understand more about nanoparticle uptake in tumour spheroids (cultured in a microfluidic device) and also to identify and classify live ER α -positive MCF-7 breast cancer spheroids [165].

In summary, SERS-microfluidic sensors promote fast analysis, high sensitivity and even high throughput using a small sample volume, while being portable, inexpensive and miniaturized, so these sensors are in line with the development trend of modern analytical technology [156].

22.3.2 DNA Mutations

Nowadays, genetic profiling of tumours has become common both for researchers in oncobiology and for clinical diagnosis and treatment [166–168]. The analysis of DNA mutations is extremely important for tumour profiling and to discover genetic

signatures in oncology with a direct impact in diagnosis, prognosis and therapeutic selection for cancer patients [169, 170]. For the molecular analysis of DNA in clinical samples, several techniques are currently used, including polymerase chain reaction (PCR), digital droplet PCR (ddPCR), microarrays and fluorescence in situ hybridization (FISH). Additionally, new technologies have been developed, namely next generation sequencing (NGS) which can provide rapid detection of thousands of cancer-related genes with a high degree of analytic accuracy [171, 172].

Traditionally, tumour mutations are analysed directly in the tumour tissue obtained either through biopsy or surgery but, over the last years, non-invasive mutational analysis of the tumour can be performed through liquid biopsy assays, either analysing cfDNA or tumour cells that appear in body fluids. Indeed, the analysis of mutations in CTCs can be an effective tool to predict disease aggressiveness and to monitor therapeutic response [173], ultimately contributing to a better understanding of the metastatic process and to the design of personalized treatment in a simple and non-invasive way [174].

The conventional techniques are reproducible, capable to detect multiple mutations at the same time, and present high specificity and sensitivity. Nevertheless, the specificity is dependent on many factors, such as the design of the primers and probes. Additionally, the sensitivity is very variable, being the qPCR, ddPCR and NGS, the most sensitive among all. Thus, conventional techniques used to detect DNA mutations are not perfect and have disadvantages associated with their complexity, data analytics and the time required from sample preparation to results.

In that sense, highly specific technologies have been developed for the efficient detection of ctDNA. Beyond PCR, currently used techniques include Scorpion Amplification Refractory Mutation System (ARMS); Beads, Emulsions, Amplification and Magnetic analysis (BEAMing); and NGS [18, 20, 175, 176]. The ddPCR technique is based on water-oil emulsions, small DNA fragments are encapsulated into thousands of droplets for amplification and analysis of genetic alterations and specific mutations with high sensitivity [99, 177–179]. However, this method is considered to be insensitive to detect a low amount of the mutant allele, working only when the required amount of targeted mutation is present [99, 180]. So, researchers developed Scorpion ARMS, to detect low amounts of mutations and reduce false-negative rates [99, 178, 179]. Similar to ddPCR, BEAMing binds DNA to magnetic beads before preparing the emulsion in droplets, and sorting the beads that contain cell mutations by flow cytometry [99]. The sensitivity of this method is 1 mutated DNA fragment for 10000 normal fragments [181].

Ischi and colleagues collected plasma from non-small-cell lung cancer (NSCLC) and conducted a study using ddPCR, in which a drug resistance mechanism in epidermal growth factor receptor (EGFR) tyrosine kinase inhibitor treatment was detected [182]. The EGFR mutation in this type of cancer was observed by other authors, with high levels of sensitivity and specificity [99]. Other studies detected ctDNA in breast cancer [183] and colorectal cancer [184]. For instance, van Ginkel and colleagues detected ctDNA and specific mutations by ddPCR and BEAMing, from whole blood samples [96]. There is no doubt that these methods are sensitive and efficient in ctDNA detection and helpful in monitoring cancer progression,

however, they remain expensive, time-consuming, require innovative and costly systems, and it is technically difficult to standardize them for routine clinical use [185, 186].

Several efforts have been done to promote improvements in this area, developing smaller portable platforms, that consume lower amounts of reagents and need smaller volume samples, with lower costs, and providing faster results while maintaining the sensitivity and specificity required [187]. In this line, many microfluidic technologies have emerged, such as microfluidic PCR systems [188–190], universal arrays placed in polymer-based microfluidic channels [191, 192], and others based on a combination of two complementary technologies, microfluidics and SERS have been developed [193, 194], all aiming to overcome the shortcomings of the conventional techniques.

From all the microfluidic strategies developed, microfluidic PCR devices are the most common approach, in either of two possible configurations: stationary, where the sample is kept in a microchamber in which the temperature is cycled; or in-flow, in which the sample flows through different thermal zones, so that the different processes of denaturation, annealing and extension can occur [190]. These innovative strategies combine the requirements needed for a wider implementation of tumour mutation analysis for precision diagnosis and personalized treatment.

22.3.3 RNAs

The analysis of gene expression in tumour material has been used more frequently, to improve the area of precision medicine in cancer. Although the analysis of DNA alterations (such as mutations) is the most commonly used, the study of RNA and their eventual modifications has increased tremendously in the last few years [195]. Particularly, a set of small, endogenous, highly conserved, noncoding RNAs that control the expression of genes, called micro RNAs (miRNAs), can harbour mutations that are linked with diverse human cancers, however RNAs are not stable free in circulation [196]. On the other hand, living cancer cells release extracellular vesicles (EVs) into the circulation, containing tumour-derived RNA within their cargo, and enabling the analysis of tumour-derived miRNAs, messenger RNAs (mRNAs) and long noncoding RNAs (lncRNAs) [197].

One of the most attractive aspects of studying these EVs is how the biomolecular contents of tumour-derived EVs (TEVs) mirror those of the parental tumour cells, providing key insights into the disease progression and its mechanisms [198]. The content of the circulating TEVs can indeed be used in the context of liquid biopsies for early detection of cancer, for monitoring disease burden in patients and for assessing recurrence in the post-resection setting. Nonetheless, isolating sufficient TEVs by ultracentrifugation-based approaches can be an arduous, time-consuming process and is inconsistent in the context of yield and purity. As discussed earlier, microfluidic platforms can enable high-throughput EV isolation for posterior analysis of genomic content, reliably identifying mutations present in the patient plasma. This possible application of microfluidic techniques demonstrates its potential for

the development of point-of-care platforms to monitor, for example, a residual or recurrent tumour presence in a cancer patient undergoing therapy.

As such, tumour RNAs can be utilized as diagnostic and prognostic biomarkers. Compared to DNA amplification and analysis using qPCR, RNA amplification requires an additional step in reverse transcriptase which originated the widely used qRT-PCR technology. This genomic analysis technique can be greatly assisted with its implementation in microfluidic devices which provide miniaturization, integration, parallelization and automation of the biochemical assay, speeding up the whole process while reducing the consumption of sample and required reagents [199, 200].

22.3.4 Sequencing

Sequencing is a technique that allows the determination of the sequence of nucleic acids. It was firstly described in the early seventies and became increasingly popular with the development of Sanger sequencing method which allowed automation and the development of DNA sequencers [201]. Sanger DNA sequencing was the gold standard for many years and was replaced in the last two decades by ‘next generation sequencing’ (NGS). NGS runs many sequencing reactions in parallel, providing a high-throughput automated process and ultimately bringing the opportunity to sequence the entire genome at once. The appearance of NGS boosted biological and medical research, namely in the field of liquid biopsy making ctDNA sequencing accessible and detecting multiple mutations simultaneously [99].

Moreover, NGS enabled whole-genome sequencing (WGS), a technique that provides the whole genomic profile of tumour DNA. This technique demonstrated to be instrumental to characterize mutations and monitor disease progression [202]. Whole-exome sequencing (WES) is a popular alternative of WGS. Although WGS provides abundant information, it is expensive. By only sequencing the exons, WES simplifies the analysis (exome makes up only 1.5% of the whole human genome) and still provides valuable information in a disease scenario, as all protein coding genes are in the exome [203]. WGS and WES require high input sample volume, what has been limiting their application for early cancer diagnosis when levels of ctDNA are low.

In parallel with the NGS, the development of amplification techniques supports the growth of genomics and opened the opportunity for single-cell analysis. In liquid biopsy, the importance of circulating tumour cells (CTCs) for the characterization of metastasis and understanding the metastatic process is clear. However, the cells are rare and the very low number limited their full characterization. With these techniques it is now possible to probe patient-derived CTCs at the single-cell level [204]. In these cases, DNA amplification is performed by digital PCR (dPCR). The technique provides more sensitivity than classical PCR and absolute quantification. Examples of methods available for digital PCR include digital droplet, spinning disc microfluidics or microfluidic dPCR chips [205]. dPCR provides high sensitivity, precision and absolute quantification, allowing nucleic acid analysis beyond the

reach of other methods in a number of applications such as liquid biopsy. In case of transcriptome analysis, single cell is also enabled by Smart-Seq (Illumina) technology.

These technological advances were paramount not only for biomarker detection, but also for the development of innovative diagnostic, prognostic and predictive tools to better detect or monitor of cancer patients and to effectively assist in clinical decisions [206]. Some of these existing products in the clinic that use NGS for biomarker analysis are detailed below, according to the type of biomarker.

22.3.4.1 Genome and Epigenome

Cobas® EGFR Mutation Test v2 (Roche) is one of the most successful products in the field of liquid biopsy. It consists in a PCR test that identifies specific mutations in the epidermal growth factor receptor (EGFR) gene. The test is approved for clinical use in the 1st and 2nd line EGFR TKI therapy in patients with advanced non-small cell lung cancer (NSCLC). The test is used in ctDNA as well as in DNA extracted from solid biopsies. Cobas® was the first companion diagnostic product approved in liquid biopsy.

A similar approach is proposed by Guardant360®, an FDA-approved comprehensive liquid biopsy test for all advanced solid tumours. It provides genomic profiling for advanced cancer patients. In the context of NSCLC, the company claims to be able to detect disease 1-3 weeks earlier than tissue biopsy. Additionally, the test covers other genomic alterations which may be relevant in other types of cancer too.

Early detection of cancer is also the claim of Galleri® (Grail). The Galleri test uses NGS and machine-learning algorithms to analyse methylation patterns of cfDNA in blood to detect cancer and predict its origin with high accuracy. The test is not FDA-approved yet, but clinical trials are ongoing.

Towards personalized treatment and complete understanding of cancer heterogeneity, the Cancer Personalized Profiling by Deep Sequencing (CAPP-Seq) test has been developed by Roche. It provides for the detection of a wide array of mutations in ctDNA from patient blood. This is a high-throughput technique that combines NGS and informatic algorithms to precisely identify and quantify mutations. Signatera™ (Natera) is a commercially available test focused on the detection of ctDNA for molecular residual disease (MRD) assessment. Instead of being based on well-characterized mutation, the test is personalized based on the primary tumour mutation signature of the patient.

22.3.4.2 Transcriptome

Biomarkers of mRNA are also target for the early detection of cancer in body fluids. SelectMDx® test (MDxHealth) measures the expression of two mRNA cancer-related biomarkers (HOXC6 and DLX1) in urine samples. Combined with patient clinical risk factors, this test is meant to help the clinician to determine whether the patient should undergo a tissue biopsy or not, in the context of prostate cancer.

Similarly, the Progenesa™ PCA3 (Gen-Probe Inc) is a specific assay to detect PCA3, a prostate-specific mRNA biomarker. The biomarker is also detected in urine

and is used as support for clinical decision to determine if tissue biopsy is needed. Progensa™ assay is FDA approved and CE marked.

A similar test is available for the detection of bladder cancer. Cxbladder™ is a urine-based laboratory test to quantify mRNA levels of five biomarkers. The test can also be used to support clinicians to rule out the need of cystoscopy.

22.3.5 Beyond NGS: Proteome and Metabolome

The proteome refers to all the proteins present in a cell or organism at a specific time point. The study of proteome has been conducted mainly using mass spectrometry and more recently protein arrays that together with bioinformatics became a robust tool in proteomics.

Biodesix is a company specialized in lung cancer and offers multiple testing. The VeriStrat® blood-based immune profiling proteomic test provides a personalized view of each patient's immune response to their lung cancer and predict the benefit of treatment with EGFR inhibitors. IMMray™ PanCan-d (Immunovia) is a blood test developed for early detection of pancreatic cancer (PDAC stage I & II). The test is offered exclusively as a laboratory developed test (LDT). IMMray™ is an antibody-based microarray technology that creates a snapshot of the immune system response from a blood sample.

The metabolome is defined as small-molecule analytes (<2000 Da) found within a biological sample. These can be blood, plasma, urine, faeces and also exhaled breath and exhaled breath condensate. Metabolomics is studying this type of compounds by using techniques such as nuclear magnetic resonance (NMR) and mass spectrometry (MS) to determine metabolic profiles in biological samples.

Breathomics is a specific branch of metabolomics. The field evolved significantly in the last few years and biomarker volatile organic compounds (VOCs) have been associated with inflammatory diseases, infectious diseases and cancer [207]. Analysis of breath brought however several difficulties due to the very low concentration of compounds that were frequently below the detection limit of the current techniques. To circumvent this issue, new forms of collecting breath were developed in order to concentrate these metabolites. Owlstone Medical Breath Biopsy® platform is such an example that is currently under clinical trial to discriminate VOC biomarkers for six different types of cancer. This area is still in early phase of development, however the establishment of databases such as Human Breathomics databases is accelerating development. The incorporation of automation in these data analysis is needed to bring this knowledge to clinical setting.

22.3.6 Functional Assays

The development of cell-based assays emerged as a tool to provide representative data of higher-level biological responses and interactions that are not possible to obtain with other type of analysis. The implementation of microfluidics improves the

throughput and quality of these assays in a variety of fundamental biological research topics, such as understanding of metastasis, cell proliferation and drug testing [208].

Metastasis is known to be the cumulative result of several changes in tumour cells and their microenvironment. The understanding of molecular and cellular processes underlying this multistep event is crucial to predict cancer progression, develop suitable treatments, as well as to discover key mechanisms that ignite metastasis [209]. For this reason, experimental metastatic models can provide a clear view of the mechanisms of metastasis and serve as a platform for biomarker discovery and anti-metastatic drug testing. However, the aggressive and invasive processes of metastasis are a consequence of a bi-directional communication of cancer cells and their surrounding tumour environment that 2D traditional cell-based assays, such as the Transwell® system, cannot represent due to their static nature [210]. On the other hand, broadly used animal models serve as testing platforms of higher complexity compared to 2D models, but involve complicated, time-consuming and expensive procedures that eventually lead to a delay in the development of new drugs [211]. Microfluidic technology has enormous potential in the field of advanced 3D models due to its ability for spatial and temporal control of cell growth, chemical and physical stimuli. Microfluidic organ-on-a-chip models enable the reconstitution of the body tissues and dynamics found *in vivo*, in one simple and controllable microdevice. Due to this fact, various microfluidic devices have been developed to assess different stages of the metastatic cascade including cell dissemination from the primary tumour [212], influence of the tumour microenvironment [213], intra- and extra-vasation [214] and the influence of chemical gradients in cancer cell migration [215]. As such, these biomimetic models enable the development of functional assays that can be carried out for a better understanding of metastases and that allow the collection of valuable data that can be used to discover new cancer biomarkers, critical for cancer prediction and new drug development.

The assessment of tumour cell proliferation and differentiation is also essential to understand the formation of cancer. Traditionally, cell culture studies are performed in 2D flasks, petri dishes or microtiter plates containing cell culture media that allow cell growth for limited time periods. However, as mentioned above, the impact that the dynamic physiological conditions of the human body and the interactions of cells with their microenvironment can have on their functionalities and phenotype cannot be monitored by using these traditional methods [216]. With this regard, microfluidic devices are great candidates for cell culture and differentiation assays since they mimic *in vivo* systems, enabling the precise control of culture conditions and the replication of microcultures and their cellular interactions [217]. Likewise, they also present several attractive features such as a continuous supply of nutrients, removal of waste and high automation capability [216]. For instance, Justin Cooper-White et al. were able to trap single cells in a two-layered microfluidic device and promote their proliferation for multiple generations over extended periods of time (>7 days) under media perfusion [218].

Regarding drug development, animal testing platforms can be crucial when predicting the efficacy and toxicity of anti-cancer drugs in the human body.

Nevertheless, differences in species can lead to errant pharmacokinetic predictions and rejections of promising compounds, which also occurs when performing said studies with *in vitro* cell line models that lack basic physiologic functions. Fortunately, microfluidics can overcome these limitations as stated before, since they can replicate physiologic dynamics, being better suited to represent *in vivo* situations and as such prove to be attractive when assessing drug effectiveness, as mentioned for the case of the metastatic cascade. Finally, low-cost microfluidic systems can be fast prototyped to enable multiplexed and automated drug screening assays with high control and precision. For instance, CTCs isolated from the blood of cancer patients are a prime candidate to perform chemoresistance assays for personalized drug development, however, these assays require the manipulation of small sample volumes without the loss of rare cells [219, 220]. A study by Bithi et al. demonstrated that this problem could be overcome by manufacturing microfluidic devices capable of performing this task, and not only reducing the loss of rare CTCs, but also having a reproducible sample discretization, heterogeneity assessment at single-cell level and an easy identification of the drug response [219].

Microfluidic devices represent a new era of testing platforms that take functional assays accuracy to a higher level, narrowing the gap between *in vitro* and *in vivo* conditions and further enhancing drug discovery research and reducing the ‘bottle-neck effect’ in preclinical testing.

22.4 Outlook

So far, only a handful of liquid biopsy methods have been cleared to be used in the clinic. However, for the liquid biopsy biomarkers reviewed above a different success in terms of successful transfer into the clinic should be remarked. As per ctDNA, several methods have been cleared by the different regulatory bodies in different geographies. The fact that the clinical utility of ctDNA has been demonstrated enabled the FDA and CE-IVD approval and thus the clinical implementation of liquid biopsy tests starting by Cobas (Roche) [221] and followed by Target Selector (Biocept), Therascreen (Qiagen) or Idylla (Biocartis) among others [222]. These tests allow the detection of the presence of specific mutations in breast, prostate, colorectal, NSCLC, ovarian, bladder, HCC or NMIBC. The results of the analysis may be used, depending on each specific test, for diagnosis, prognosis, monitoring and surveillance and/or companion diagnostics. The implementation of these tests in the clinic was a breakthrough for liquid biopsy, demonstrating that there is a whole range of possibilities when analysing body fluids, which may impact the quality of the care for cancer patients. Very recently in 2020, two additional ctDNA-based tests were approved, the FoundationOne Liquid CDx [223, 224] and the Guardant360 CDx [225]. Unlike the previous approved tests based on ctDNA which tested just for a single mutation, these newly approved technologies are NGS-based and capable of detecting multiple mutations. Furthermore, the initial approval was later in the same year expanded to include more cancer types than initially approved. As a whole, the Guardant360 CDx [226] and the FoundationOne Liquid CDx [227] target 55 and

324 tumour genes, respectively. These approvals will further boost the use of liquid biopsy in the clinic, demonstrating how the use of liquid biopsy may provide information on the benefit of a specific targeted therapy. The assays can also be used for general tumour profiling, enhancing the applicability and potential uptake by clinicians and pathology laboratories.

Regarding CTCs and EVs, there is still a long road ahead when compared to ctDNA technologies achievements. In the case of CTCs, only the CellSearch® system, initially developed by Johnson and Johnson and later acquired by Menarini, has FDA clearance. The implementation of this CTC assay in the clinic has not been as effective as those of ctDNA, mainly due to its inability of demonstrating clinical utility, as it only relates CTC counts with prognosis. Ever since the approval of CellSearch® [228], many other technologies made their appearance in the research arena. Some of these technologies take indeed benefit of microfluidic approaches for the isolation of the very scarce CTCs that may be found in the body fluids. For example, the Parsortix® System from Angle [46], the VTX-1 from Vortex Biosciences [47] and the RUBYchip™ from RUBYnomed [48].

As per the EVs, they have been traditionally explored mainly in relation to their potential as drug delivery systems [229]. However, with the recent advances in liquid biopsy they are now being explored as potential biomarkers to be used in diagnostics [230, 231]. Nevertheless, despite the huge amount of relevant information EVs contain, the challenge to achieve an efficient isolation, as well as the classification of the EV subpopulations is hindering their clinical translation. Despite the majority of the ongoing clinical trials based on EVs are related to therapy, already some are trying to demonstrate the clinical applicability and utility in diagnosis [232]. For example, the ExoColon clinical trial run by the Centre Hospitalier Universitaire Dijon aims at demonstrating the hypothesis of the potential of using miRNAs contained in circulating EVs as biomarkers of early prognosis in colorectal cancer [233].

Besides the crucial role of microfluidic devices for the handling of liquid biopsy biomarkers, the use of these platform as organ-on-a-chip (OoC) models to study liquid biopsy is perhaps one of the most promising synergetic applications of both fields. Currently, the limiting factor for the extended application of this technology is the difficulty on developing robust OoC microfluidic platforms that can mimic the tumour environment. In this sense, the manufacturing of microfluidic devices must pursue standardized approaches in order to offer the cancer research and clinical communities reproducible and unbiased results. Companies such as Emulate, InSphero or Mimetas [234] lead the market traction providing platforms that can mimic different types of organs such as colon, brain, lung or kidney among others. The applications of OoC are endless and have been reviewed elsewhere in this book. As per the liquid biopsy field, an OoC model that can be translated into the clinic is still depending on the capacity of microfluidic manufacturers to produce reliable, robust and integrated systems. Several and meaningful advances can still be found in the literature, mainly for the development of 3D cancer models that may shed light in the metastatic process [235], on the 3D cell culture [236], metabolism of tumours [237] and drug development and dose testing [238].

We may conclude that microfluidic platforms are key for the implementation of a personalized management of cancer in connection with liquid biopsies. From the diagnostics point of view these microfluidic platforms offer an efficient isolation of circulating biomarkers enabling patient stratification, tumour profiling and monitoring. From a therapeutic perspective both companion diagnostic developments and the application of OoC models will certainly enable a personalized and continuously updated course of treatment for cancer patients. Hopefully once and for all, when these approaches are fully translated and implemented into the clinic the heterogenic and dynamic nature of cancer may finally be fully considered, making cancer a chronic disease and ensuring a good quality of life for cancer patients.

References

1. Mader S, Pantel K (2017) Liquid biopsy: current status and future perspectives. *Oncol Res Treat* 40:404–408. <https://doi.org/10.1159/000478018>
2. Wu J, Hu S, Zhang L et al (2020a) Tumor circulome in the liquid biopsies for cancer diagnosis and prognosis. *Theranostics* 10:4544–4556. <https://doi.org/10.7150/thno.40532>
3. Palmirotta R, Lovero D, Cafforio P et al (2018) Liquid biopsy of cancer: a multimodal diagnostic tool in clinical oncology. *Ther Adv Med Oncol* 10:1758835918794630. <https://doi.org/10.1177/1758835918794630>
4. Hofman P, Popper HH (2016) Pathologists and liquid biopsies: to be or not to be? *Virchows Arch* 469:601–609
5. Pantel K, Alix-Panabières C (2010) Circulating tumour cells in cancer patients: challenges and perspectives. *Trends Mol Med* 16:398–406. <https://doi.org/10.1016/j.molmed.2010.07.001>
6. Slikker W Jr (2018) Biomarkers and their impact on precision medicine. *Exp Biol Med* (Maywood) 243:211–212. <https://doi.org/10.1177/1535370217733426>
7. Alexander RF, Spriggs AI (1960) The differential diagnosis of tumour cells in circulating blood. *J Clin Pathol* 13:414–424. <https://doi.org/10.1136/jcp.13.5.414>
8. Salgado I, Hopkirk JF, Long RC et al (1959) Tumour cells in the blood. *Can Med Assoc J* 81: 619–622
9. Ferreira MM, Ramani VC, Jeffrey SS (2016) Circulating tumor cell technologies. *Mol Oncol* 10:374–394. <https://doi.org/10.1016/j.molonc.2016.01.007>
10. Millner LM, Linder MW, Valdes R Jr (2013) Circulating tumor cells: a review of present methods and the need to identify heterogeneous phenotypes. *Ann Clin Lab Sci* 43:295–304
11. Yap TA, Lorente D, Omlin A et al (2014) Circulating tumor cells: a multifunctional biomarker. *Clin Cancer Res* 20:2553. <https://doi.org/10.1158/1078-0432.CCR-13-2664>
12. Yu M, Stott S, Toner M et al (2011) Circulating tumor cells: approaches to isolation and characterization. *J Cell Biol* 192:373–382. <https://doi.org/10.1083/jcb.201010021>
13. Neumann MHD, Bender S, Krahn T, Schlange T (2018) ctDNA and CTCs in liquid biopsy - current status and where we need to progress. *Comput Struct Biotechnol J* 16:190–195. <https://doi.org/10.1016/j.csbj.2018.05.002>
14. Stoecklein NH, Fischer JC, Niederacher D, Terstappen LWMM (2016) Challenges for CTC-based liquid biopsies: low CTC frequency and diagnostic leukapheresis as a potential solution. *Expert Rev Mol Diagn* 16:147–164. <https://doi.org/10.1586/14737159.2016.1123095>
15. Paoletti C, Hayes DF (2016) Circulating tumor cells. Springer, Cham, pp 235–258
16. Paterlini-Brechot P, Benali NL (2007) Circulating tumor cells (CTC) detection: clinical impact and future directions. *Cancer Lett* 253:180–204. <https://doi.org/10.1016/j.canlet.2006.12.014>
17. Poulet G, Massias J, Taly V (2019) Liquid biopsy: general concepts. *Acta Cytol* 63:449–455. <https://doi.org/10.1159/000499337>

18. Belotti Y, Lim CT (2021) Microfluidics for liquid biopsies: recent advances, current challenges, and future directions. *Anal Chem* 93:4727–4738. <https://doi.org/10.1021/acs.analchem.1c00410>
19. Iliescu FS, Poenar DP, Yu F et al (2019) Recent advances in microfluidic methods in cancer liquid biopsy. *Biomicrofluidics* 13:41503. <https://doi.org/10.1063/1.5087690>
20. Alix-Panabières C, Pantel K (2016) Clinical applications of circulating tumor cells and circulating tumor DNA as liquid biopsy. *Cancer Discov* 6:479. <https://doi.org/10.1158/2159-8290.CD-15-1483>
21. Zhang L, Riethdorf S, Wu G et al (2012) Meta-analysis of the prognostic value of circulating tumor cells in breast cancer. *Clin Cancer Res* 18:5701. <https://doi.org/10.1158/1078-0432.CCR-12-1587>
22. Yang C, Chen F, Wang S, Xiong B (2019) Circulating tumor cells in gastrointestinal cancers: current status and future perspectives. *Front Oncol* 9:1427. <https://doi.org/10.3389/fonc.2019.01427>
23. Li Y, Wu G, Yang W et al (2020) Prognostic value of circulating tumor cells detected with the CellSearch system in esophageal cancer patients: a systematic review and meta-analysis. *BMC Cancer* 20:581. <https://doi.org/10.1186/s12885-020-07059-x>
24. Wang S, Du H, Li G (2017) Significant prognostic value of circulating tumor cells in esophageal cancer patients: a meta-analysis. *Oncotarget* 8(15815–15826):10.18632/oncotarget.15012
25. Busetto GM, Ferro M, Del Giudice F et al (2017) The prognostic role of circulating tumor cells (CTC) in high-risk non-muscle-invasive bladder cancer. *Clin Genitourin Cancer* 15:e661–e666. <https://doi.org/10.1016/j.clgc.2017.01.011>
26. Jiang H, Gu X, Zuo Z et al (2021) Prognostic value of circulating tumor cells in patients with bladder cancer: a meta-analysis. *PLoS One* 16:e0254433
27. Chen F, Zhong Z, Tan H-Y et al (2020) The significance of circulating tumor cells in patients with hepatocellular carcinoma: real-time monitoring and moving targets for cancer therapy. *Cancers* 12:1734
28. Basso U, Facchinetti A, Rossi E et al (2021) Prognostic role of circulating tumor cells in metastatic renal cell carcinoma: a large, multicenter, prospective trial. *Oncologist* 26:740–750. <https://doi.org/10.1002/onco.13842>
29. Guan Y, Xu F, Tian J et al (2021) The prognostic value of circulating tumour cells (CTCs) and CTC white blood cell clusters in patients with renal cell carcinoma. *BMC Cancer* 21:826. <https://doi.org/10.1186/s12885-021-08463-7>
30. Goldkorn A, Ely B, Quinn DI et al (2014) Circulating tumor cell counts are prognostic of overall survival in SWOG S0421: a phase III trial of docetaxel with or without atrasentan for metastatic castration-resistant prostate cancer. *J Clin Oncol* 32:1136–1142. <https://doi.org/10.1200/JCO.2013.51.7417>
31. Muendlein A, Geiger K, Gaenger S et al (2021) Significant impact of circulating tumour DNA mutations on survival in metastatic breast cancer patients. *Sci Rep* 11:6761. <https://doi.org/10.1038/s41598-021-86238-7>
32. Tie J, Kinde I, Wang Y et al (2015) Circulating tumor DNA as an early marker of therapeutic response in patients with metastatic colorectal cancer. *Ann Oncol Off J Eur Soc Med Oncol* 26:1715–1722. <https://doi.org/10.1093/annonc/mdv177>
33. Vandekerkhove G, Lavoie J-M, Annala M et al (2021) Plasma ctDNA is a tumor tissue surrogate and enables clinical-genomic stratification of metastatic bladder cancer. *Nat Commun* 12:184. <https://doi.org/10.1038/s41467-020-20493-6>
34. Vidal J, Taus A, Montagut C (2020) Dynamic treatment stratification using ctDNA. Springer, Cham, pp 263–273
35. Douillard J-Y, Ostoros G, Cobo M et al (2014) First-line gefitinib in Caucasian EGFR mutation-positive NSCLC patients: a phase-IV, open-label, single-arm study. *Br J Cancer* 110:55–62. <https://doi.org/10.1038/bjc.2013.721>

36. Lei KF (2020) A review on microdevices for isolating circulating tumor cells. *Micromachines* 11:531. <https://doi.org/10.3390/mi11050531>
37. Andree KC, van Dalum G, Terstappen LWMM (2016) Challenges in circulating tumor cell detection by the CellSearch system. *Mol Oncol* 10:395–407. <https://doi.org/10.1016/j.molonc.2015.12.002>
38. Prinyakupt J, Pluempitiriwiyawej C (2015) Segmentation of white blood cells and comparison of cell morphology by linear and naïve Bayes classifiers. *Biomed Eng Online* 14:1–19. <https://doi.org/10.1186/s12938-015-0037-1>
39. Esmaeilsabzali H, Beischlag TV, Cox ME et al (2013) Detection and isolation of circulating tumor cells: principles and methods. *Biotechnol Adv* 31:1063–1084. <https://doi.org/10.1016/j.biotechadv.2013.08.016>
40. Allard WJ (2004) Tumor cells circulate in the peripheral blood of all major carcinomas but not in healthy subjects or patients with nonmalignant diseases. *Clin Cancer Res* 10:6897–6904. <https://doi.org/10.1158/1078-0432.CCR-04-0378>
41. Dong Y, Skelley AM, Merdek KD et al (2013) Microfluidics and circulating tumor cells. *J Mol Diagn* 15:149–157. <https://doi.org/10.1016/j.jmoldx.2012.09.004>
42. Marrinucci D, Bethel K, Bruce RH et al (2007) Case study of the morphologic variation of circulating tumor cells. *Hum Pathol* 38:514–519. <https://doi.org/10.1016/j.humpath.2006.08.027>
43. Myung JH, Hong S (2015) Microfluidic devices to enrich and isolate circulating tumor cells. *Lab Chip* 15:4500–4511. <https://doi.org/10.1039/C5LC00947B>
44. Nagrath S, Sequist LV, Maheswaran S et al (2007) Isolation of rare circulating tumour cells in cancer patients by microchip technology. *Nature* 450:1235–1239. <https://doi.org/10.1038/nature06385>
45. Stott SL, Hsu C-H, Tsukrov DI et al (2010) Isolation of circulating tumor cells using a microvortex-generating herringbone-chip. *Proc Natl Acad Sci* 107:18392–18397. <https://doi.org/10.1073/PNAS.1012539107>
46. Xu L, Mao X, Imrali A et al (2015) Optimization and evaluation of a novel size based circulating tumor cell isolation system. *PLoS One* 10:e0138032
47. Renier C, Pao E, Che J et al (2017) Label-free isolation of prostate circulating tumor cells using Vortex microfluidic technology. *NPJ Precis Oncol* 1:15. <https://doi.org/10.1038/s41698-017-0015-0>
48. Lopes C, Piai P, Chícharo A et al (2021) HER2 expression in circulating tumour cells isolated from metastatic breast cancer patients using a size-based microfluidic device. *Cancers* 13:4446
49. Carneiro A, Piai P, Teixeira A, Ferreira D, Cotton S, Rodrigues C, Chícharo A, Abalde-Cela S, Santos LL, Lima L, Diéguez L (2022) Discriminating epithelial to mesenchymal transition phenotypes in circulating tumor cells isolated from advanced gastrointestinal cancer patients. *Cells* 11(3):376. <https://doi.org/10.3390/cells11030376>
50. Ozkumur E, Shah AM, Ciciliano JC et al (2013) Inertial focusing for tumor antigen-dependent and -independent sorting of rare circulating tumor cells. *Sci Transl Med* 5:179ra47. <https://doi.org/10.1126/scitranslmed.3005616>
51. Fachin F, Spuhler P, Martel-Foley JM et al (2017) Monolithic chip for high-throughput blood cell depletion to sort rare circulating tumor cells. *Sci Rep* 7:10936. <https://doi.org/10.1038/s41598-017-11119-x>
52. Kapeleris J, Zou H, Qi Y et al (2020) Cancer stemness contributes to cluster formation of colon cancer cells and high metastatic potentials. *Clin Exp Pharmacol Physiol* 47:838–847. <https://doi.org/10.1111/1440-1681.13247>
53. Giuliano M, Shaikh A, Lo HC et al (2018) Perspective on circulating tumor cell clusters: why it takes a village to metastasize. *Cancer Res* 78:845. <https://doi.org/10.1158/0008-5472.CAN-17-2748>
54. Au SH, Edd J, Stoddard AE et al (2017) Microfluidic isolation of circulating tumor cell clusters by size and asymmetry. *Sci Rep* 7:2433. <https://doi.org/10.1038/s41598-017-01150-3>

55. Sarioglu AF, Aceto N, Kojic N et al (2015) A microfluidic device for label-free, physical capture of circulating tumor cell clusters. *Nat Methods* 12:685–691. <https://doi.org/10.1038/nmeth.3404>
56. Cheng S-B, Xie M, Chen Y et al (2017) Three-dimensional Scaffold chip with thermosensitive coating for capture and reversible release of individual and cluster of circulating tumor cells. *Anal Chem* 89:7924–7932. <https://doi.org/10.1021/acs.analchem.7b00905>
57. Gholizadeh S, Shehata Draz M, Zarghooni M et al (2017) Microfluidic approaches for isolation, detection, and characterization of extracellular vesicles: current status and future directions. *Biosens Bioelectron* 91:588–605. <https://doi.org/10.1016/j.bios.2016.12.062>
58. Weng J, Xiang X, Ding L et al (2021) Extracellular vesicles, the cornerstone of next-generation cancer diagnosis? *Semin Cancer Biol* 74:105–120. <https://doi.org/10.1016/j.semcancer.2021.05.011>
59. Becker A, Thakur BK, Weiss JM et al (2016) Extracellular vesicles in cancer: cell-to-cell mediators of metastasis. *Cancer Cell* 30:836–848. <https://doi.org/10.1016/j.ccell.2016.10.009>
60. Ko SY, Lee W, Kenny HA et al (2019) Cancer-derived small extracellular vesicles promote angiogenesis by heparin-bound, bevacizumab-insensitive VEGF, independent of vesicle uptake. *Commun Biol* 2:386. <https://doi.org/10.1038/s42003-019-0609-x>
61. Kuriyama N, Yoshioka Y, Kikuchi S et al (2020) Extracellular vesicles are key regulators of tumor neovasculature. *Front Cell Dev Biol* 8:611039. <https://doi.org/10.3389/fcell.2020.611039>
62. Marar C, Starich B, Wirtz D (2021) Extracellular vesicles in immunomodulation and tumor progression. *Nat Immunol* 22:560–570. <https://doi.org/10.1038/s41590-021-00899-0>
63. Théry C, Witwer KW, Aikawa E et al (2018) Minimal information for studies of extracellular vesicles 2018 (MISEV2018): a position statement of the International Society for Extracellular Vesicles and update of the MISEV2014 guidelines. *J Extracell Vesicles* 7:1535750. <https://doi.org/10.1080/20013078.2018.1535750>
64. Gandham S, Su X, Wood J et al (2020) Technologies and standardization in research on extracellular vesicles. *Trends Biotechnol* 38:1066–1098. <https://doi.org/10.1016/j.tibtech.2020.05.012>
65. Busatto S, Vilanilam G, Ticer T et al (2018) Tangential flow filtration for highly efficient concentration of extracellular vesicles from large volumes of fluid. *Cells* 7:273. <https://doi.org/10.3390/cells7120273>
66. Wunsch BH, Hsieh KY, Kim S-C et al (2021) Advancements in throughput, lifetime, purification, and workflow for integrated nanoscale deterministic lateral displacement. *Adv Mater Technol* 6:2001083. <https://doi.org/10.1002/admt.202001083>
67. Wunsch BH, Smith JT, Gifford SM et al (2016) Nanoscale lateral displacement arrays for the separation of exosomes and colloids down to 20 nm. *Nat Nanotechnol* 11:936–940. <https://doi.org/10.1038/nnano.2016.134>
68. Liu C, Guo J, Tian F et al (2017) Field-free isolation of exosomes from extracellular vesicles by microfluidic viscoelastic flows. *ACS Nano* 11:6968–6976. <https://doi.org/10.1021/acsnano.7b02277>
69. Zhou Y, Ma Z, Tayebi M, Ai Y (2019) Submicron particle focusing and exosome sorting by wavy microchannel structures within viscoelastic fluids. *Anal Chem* 91:4577–4584. <https://doi.org/10.1021/acs.analchem.8b05749>
70. Liu C, Zhao J, Tian F et al (2019) λ -DNA- and Aptamer-mediated sorting and analysis of extracellular vesicles. *J Am Chem Soc* 141:3817–3821. <https://doi.org/10.1021/jacs.9b00007>
71. Asghari M, Cao X, Mateescu B et al (2020) Oscillatory viscoelastic microfluidics for efficient focusing and separation of nanoscale species. *ACS Nano* 14:422–433. <https://doi.org/10.1021/acsnano.9b06123>
72. Zhang H, Lyden D (2019) Asymmetric-flow field-flow fractionation technology for exomere and small extracellular vesicle separation and characterization. *Nat Protoc* 14:1027–1053. <https://doi.org/10.1038/s41596-019-0126-x>

73. Morales-Kastresana A, Musich TA, Welsh JA et al (2019) High-fidelity detection and sorting of nanoscale vesicles in viral disease and cancer. *J Extracell Vesicles* 8:1597603. <https://doi.org/10.1080/20013078.2019.1597603>
74. Morales-Kastresana A, Telford B, Musich TA et al (2017) Labeling extracellular vesicles for nanoscale flow cytometry. *Sci Rep* 7:1878. <https://doi.org/10.1038/s41598-017-01731-2>
75. Wu M, Ouyang Y, Wang Z et al (2017) Isolation of exosomes from whole blood by integrating acoustics and microfluidics. *Proc Natl Acad Sci* 114:10584. <https://doi.org/10.1073/pnas.1709210114>
76. Ibsen SD, Wright J, Lewis JM et al (2017) Rapid isolation and detection of exosomes and associated biomarkers from plasma. *ACS Nano* 11:6641–6651. <https://doi.org/10.1021/acsnano.7b00549>
77. Mandel P, Metais P (1948) Nuclear acids in human blood plasma. *C R Seances Soc Biol Fil* 142:241–243
78. Leon SA, Shapiro B, Sklaroff DM, Yaros MJ (1977) Free DNA in the serum of cancer patients and the effect of therapy. *Cancer Res* 37:646
79. Campos CDM, Gamage SST, Jackson JM et al (2018) Microfluidic-based solid phase extraction of cell free DNA. *Lab Chip* 18:3459–3470. <https://doi.org/10.1039/C8LC00716K>
80. Kustanovich A, Schwartz R, Peretz T, Grinshpun A (2019) Life and death of circulating cell-free DNA. *Cancer Biol Ther* 20:1057–1067. <https://doi.org/10.1080/15384047.2019.1598759>
81. Sorber L, Zwaenepoel K, Deschoolmeester V et al (2017) A comparison of cell-free DNA isolation kits: isolation and quantification of cell-free DNA in plasma. *J Mol Diagn* 19:162–168. <https://doi.org/10.1016/j.jmoldx.2016.09.009>
82. van Dessel LF, Vitale SR, Helmijr JCA et al (2019) High-throughput isolation of circulating tumor DNA: a comparison of automated platforms. *Mol Oncol* 13:392–402. <https://doi.org/10.1002/1878-0261.12415>
83. Aucamp J, Bronkhorst AJ, Badenhorst CPS, Pretorius PJ (2018) The diverse origins of circulating cell-free DNA in the human body: a critical re-evaluation of the literature. *Biol Rev* 93:1649–1683. <https://doi.org/10.1111/brv.12413>
84. Pessoa LS, Heringer M, Ferrer VP (2020) ctDNA as a cancer biomarker: a broad overview. *Crit Rev Oncol Hematol* 155:103109. <https://doi.org/10.1016/j.critrevonc.2020.103109>
85. Thierry AR, El Messaoudi S, Gahan PB et al (2016) Origins, structures, and functions of circulating DNA in oncology. *Cancer Metastasis Rev* 35:347–376. <https://doi.org/10.1007/s10555-016-9629-x>
86. Stroun M, Anker P, Maurice P et al (1989) Neoplastic characteristics of the DNA found in the plasma of cancer patients. *Oncology* 46:318–322. <https://doi.org/10.1159/000226740>
87. Sorenson GD, Pribish DM, Valone FH et al (1994) Soluble normal and mutated DNA sequences from single-copy genes in human blood. *Cancer Epidemiol Biomarkers Prev* 3:67
88. Yang J, Selvaganapathy PR, Gould TJ et al (2015) A microfluidic device for rapid quantification of cell-free DNA in patients with severe sepsis. *Lab Chip* 15:3925–3933. <https://doi.org/10.1039/C5LC00681C>
89. Deutsch TM, Riethdorf S, Fremd C et al (2020) HER2-targeted therapy influences CTC status in metastatic breast cancer. *Breast Cancer Res Treat* 182:127–136. <https://doi.org/10.1007/s10549-020-05687-2>
90. Moulriere F, Robert B, Arnau Peyrotte E et al (2011) High fragmentation characterizes tumour-derived circulating DNA. *PLoS One* 6:e23418
91. Chetan B, Mark S et al (2014) Detection of circulating tumor DNA in early- and late-stage human malignancies. *Sci Transl Med* 6:224ra24. <https://doi.org/10.1126/scitranslmed.3007094>
92. Han X, Wang J, Sun Y (2017) Circulating tumor DNA as biomarkers for cancer detection. *Genom Proteomics Bioinform* 15:59–72. <https://doi.org/10.1016/j.gpb.2016.12.004>
93. Keppens C, Palma JF, Das PM et al (2018) Detection of EGFR variants in plasma: a multilaboratory comparison of a real-time PCR EGFR mutation test in Europe. *J Mol Diagn* 20:483–494. <https://doi.org/10.1016/j.jmoldx.2018.03.006>

94. Quiagen QIAamp Circulating Nucleic Acid Kit (handbook). <https://www.qiagen.com/ca/products/top-sellers/qiaamp-circulating-nucleic-acid-kit/#resources/>
95. Mauger F, Dulary C, Daviaud C et al (2015) Comprehensive evaluation of methods to isolate, quantify, and characterize circulating cell-free DNA from small volumes of plasma. *Anal Bioanal Chem* 407:6873–6878. <https://doi.org/10.1007/s00216-015-8846-4>
96. van Ginkel JH, van den Broek DA, van Kuik J et al (2017) Preanalytical blood sample workup for cell-free DNA analysis using Droplet Digital PCR for future molecular cancer diagnostics. *Cancer Med* 6:2297–2307. <https://doi.org/10.1002/cam4.1184>
97. Malentacchi F, Pizzamiglio S, Verderio P et al (2015) Influence of storage conditions and extraction methods on the quantity and quality of circulating cell-free DNA (ccfDNA): the SPIDIA-DNAplax external quality assessment experience. *Clin Chem Lab Med* 53:1935–1942. <https://doi.org/10.1515/cclm-2014-1161>
98. Dittrich PS, Manz A (2006) Lab-on-a-chip: microfluidics in drug discovery. *Nat Rev Drug Discov* 5:210–218. <https://doi.org/10.1038/nrd1985>
99. Gauri S, bin Ahmad MR (2020) ctDNA detection in microfluidic platform: a promising biomarker for personalized cancer chemotherapy. *J Sensors* 2020:8353674
100. Hahn T, O'Sullivan CK, Drese KS (2009) Microsystem for field-amplified electrokinetic trapping preconcentration of DNA at poly(ethylene terephthalate) membranes. *Anal Chem* 81:2904–2911. <https://doi.org/10.1021/ac801923d>
101. Carvalho J, Diéguez L, Ipatov A et al (2021) Single-use microfluidic device for purification and concentration of environmental DNA from river water. *Talanta* 226:122109. <https://doi.org/10.1016/j.talanta.2021.122109>
102. Carvalho J, Puertas G, Gaspar J et al (2018) Highly efficient DNA extraction and purification from olive oil on a washable and reusable miniaturized device. *Anal Chim Acta* 1020:30–40. <https://doi.org/10.1016/j.aca.2018.02.079>
103. Barry A, Cohen S (2013) Quality assessment of genomic DNA degradation. *Genet Eng Biotechnol News* 33:28. <https://doi.org/10.1089/gen.33.16.12>
104. Sun M, Lin JS, Barron AE (2011) Ultrafast, efficient separations of large-sized dsDNA in a blended polymer matrix by microfluidic chip electrophoresis: a design of experiments approach. *Electrophoresis* 32:3233–3240. <https://doi.org/10.1002/elps.201100260>
105. Baker M (2012) Digital PCR hits its stride. *Nat Methods* 9:541–544. <https://doi.org/10.1038/nmeth.2027>
106. Vogelstein B, Kinzler KW (1999) Digital PCR. *Proc Natl Acad Sci* 96:9236. <https://doi.org/10.1073/pnas.96.16.9236>
107. Pekin D, Skhiri Y, Baret J-C et al (2011) Quantitative and sensitive detection of rare mutations using droplet-based microfluidics. *Lab Chip* 11:2156–2166. <https://doi.org/10.1039/C1LC20128J>
108. Bahga SS, Han CM, Santiago JG (2013) Integration of rapid DNA hybridization and capillary zone electrophoresis using bidirectional isotachopheresis. *Analyst* 138:87–90. <https://doi.org/10.1039/C2AN36249J>
109. Guan Y, Mayba O, Sandmann T et al (2017) High-throughput and sensitive quantification of circulating tumor DNA by microfluidic-based multiplex pcr and next-generation sequencing. *J Mol Diagn* 19:921–932. <https://doi.org/10.1016/j.jmoldx.2017.08.001>
110. Gwak H, Kim J, Cha S et al (2019) On-chip isolation and enrichment of circulating cell-free DNA using microfluidic device. *Biomicrofluidics* 13:24113. <https://doi.org/10.1063/1.5100009>
111. Shrirao AB, Fritz Z, Novik EM et al (2018) Microfluidic flow cytometry: the role of microfabrication methodologies, performance and functional specification. *Technology* 6:1–23. <https://doi.org/10.1142/S2339547818300019>
112. Laerum OD, Farsund T (1981) Clinical application of flow cytometry: a review. *Cytometry* 2: 1–13
113. Virgo PF, Gibbs GJ (2012) Flow cytometry in clinical pathology. *Ann Clin Biochem* 49:17–28. <https://doi.org/10.1258/acb.2011.011128>

114. Gong Y, Fan N, Yang X et al (2019) New advances in microfluidic flow cytometry. *Electrophoresis* 40:1212–1229. <https://doi.org/10.1002/elps.201800298>
115. Chiou C-H, Yeh T-Y, Lin J-L (2015) Deformation analysis of a pneumatically-activated polydimethylsiloxane (PDMS) membrane and potential micro-pump applications. *Micromachines* 6:216
116. Gao M, Gui L (2014) A handy liquid metal based electroosmotic flow pump. *Lab Chip* 14: 1866–1872. <https://doi.org/10.1039/C4LC00111G>
117. Lu Y, Liu T, Lamanda AC et al (2015) AC electrokinetics of physiological fluids for biomedical applications. *J Lab Autom* 20:611–620. <https://doi.org/10.1177/2211068214560904>
118. Ma HK, Chen RH, Yu NS, Hsu YH (2016) A miniature circular pump with a piezoelectric bimorph and a disposable chamber for biomedical applications. *Sensors Actuators A Phys* 251:108–118. <https://doi.org/10.1016/j.sna.2016.10.010>
119. Yu F, Horowitz MA, Quake SR (2013) Microfluidic serial digital to analog pressure converter for arbitrary pressure generation and contamination-free flow control. *Lab Chip* 13:1911–1918. <https://doi.org/10.1039/C3LC41394B>
120. Lee Y-C, Hsieh W-H (2014) Absorbent-force-driven microflow cytometer. *Sensors Actuators B Chem* 202:1078–1087. <https://doi.org/10.1016/j.snb.2014.05.117>
121. Jiang H, Fan N, Peng B, Weng X (2017) Characterization of an induced pressure pumping force for microfluidics. *Appl Phys Lett* 110:184102. <https://doi.org/10.1063/1.4982969>
122. Asghari M, Serhatlioglu M, Ortaç B et al (2017) Sheathless microflow cytometry using viscoelastic fluids. *Sci Rep* 7:12342. <https://doi.org/10.1038/s41598-017-12558-2>
123. Hur SC, Tse HTK, Di Carlo D (2010) Sheathless inertial cell ordering for extreme throughput flow cytometry. *Lab Chip* 10:274–280. <https://doi.org/10.1039/B919495A>
124. Mao X, Lin S-CS, Dong C, Huang TJ (2009) Single-layer planar on-chip flow cytometer using microfluidic drifting based three-dimensional (3D) hydrodynamic focusing. *Lab Chip* 9:1583–1589. <https://doi.org/10.1039/B820138B>
125. Lenshof A, Laurell T (2010) Continuous separation of cells and particles in microfluidic systems. *Chem Soc Rev* 39:1203–1217. <https://doi.org/10.1039/B915999C>
126. Reece A, Xia B, Jiang Z et al (2016) Microfluidic techniques for high throughput single cell analysis. *Curr Opin Biotechnol* 40:90–96. <https://doi.org/10.1016/j.copbio.2016.02.015>
127. Shields CW IV, Ohiri KA, Szott LM, López GP (2017) Translating microfluidics: cell separation technologies and their barriers to commercialization. *Cytom Part B Clin Cytom* 92:115–125. <https://doi.org/10.1002/cyto.b.21388>
128. Gnyawali V, Strohm EM, Wang J-Z et al (2019) Simultaneous acoustic and photoacoustic microfluidic flow cytometry for label-free analysis. *Sci Rep* 9:1585. <https://doi.org/10.1038/s41598-018-37771-5>
129. McKenna BK, Evans JG, Cheung MC, Ehrlich DJ (2011) A parallel microfluidic flow cytometer for high-content screening. *Nat Methods* 8:401–403. <https://doi.org/10.1038/nmeth.1595>
130. Göröcs Z, Tamamitsu M, Bianco V et al (2018) A deep learning-enabled portable imaging flow cytometer for cost-effective, high-throughput, and label-free analysis of natural water samples. *Light Sci Appl* 7:66. <https://doi.org/10.1038/s41377-018-0067-0>
131. Cho SH, Chen C-H, Lo Y-H (2011) Optofluidic biosensors: miniaturized multi-color flow cytometer and fluorescence-activated cell sorter (microFACS). *Proc SPIE* 2011:80990F
132. Yao B, Luo G, Feng X et al (2004) A microfluidic device based on gravity and electric force driving for flow cytometry and fluorescence activated cell sorting. *Lab Chip* 4:603–607. <https://doi.org/10.1039/B408422E>
133. Mazutis L, Gilbert J, Ung WL et al (2013) Single-cell analysis and sorting using droplet-based microfluidics. *Nat Protoc* 8:870
134. uFluidix Cell Characterization Using Microfluidic Flow Cytometry. <https://www.ufluidix.com/microfluidics-research-reviews/microfluidic-flow-cytometry-principles-and-commercial-review/>

135. Huber D, Voith von Voithenberg L, Kaigala GV (2018) Fluorescence in situ hybridization (FISH): history, limitations and what to expect from micro-scale FISH? *Micro Nano Eng* 1: 15–24. <https://doi.org/10.1016/j.mne.2018.10.006>
136. Rodriguez-Mateos P, Azevedo NF, Almeida C, Pamme N (2020) FISH and chips: a review of microfluidic platforms for FISH analysis. *Med Microbiol Immunol* 209:373–391
137. Nguyen HT, Trouillon R, Matsuoka S et al (2017) Microfluidics-assisted fluorescence in situ hybridization for advantageous human epidermal growth factor receptor 2 assessment in breast cancer. *Lab Investig* 97:93–103. <https://doi.org/10.1038/labinvest.2016.121>
138. Zanardi A, Bandiera D, Bertolini F et al (2010) Miniaturized FISH for screening of onco-hematological malignancies. *Biotechniques* 49:497–504. <https://doi.org/10.2144/000113445>
139. Weerakoon-Ratnayake M, Vaidyanathan S, Larky N et al (2020) Microfluidic device for on-chip immunophenotyping and cytogenetic analysis of rare biological cells. *Cells* 9:519. <https://doi.org/10.3390/cells9020519>
140. Lim LS, Hu M, Huang MC et al (2012) Microsieve lab-chip device for rapid enumeration and fluorescence in situ hybridization of circulating tumor cells. *Lab Chip* 12:4388–4396. <https://doi.org/10.1039/c2lc20750h>
141. Perez-Toralla K, Mottet G, Guneri ET et al (2015) FISH in chips: turning microfluidic fluorescence in situ hybridization into a quantitative and clinically reliable molecular diagnosis tool. *Lab Chip* 15:811–822. <https://doi.org/10.1039/c4lc01059k>
142. Wang X, Takebayashi SI, Bernardin E et al (2012) Microfluidic extraction and stretching of chromosomal DNA from single cell nuclei for DNA fluorescence in situ hybridization. *Biomed Microdevices* 14:443–451. <https://doi.org/10.1007/s10544-011-9621-8>
143. Ho SSY, Chua C, Gole L et al (2012) Same-day prenatal diagnosis of common chromosomal aneuploidies using microfluidics-fluorescence in situ hybridization. *Prenat Diagn* 32:321–328. <https://doi.org/10.1002/pd.2946>
144. Devadhasan JP, Kim S, An J (2011) Fish-on-a-chip: a sensitive detection microfluidic system for Alzheimer's disease. *J Biomed Sci* 18:1–11
145. Walzer KA, Fradin H, Emerson LY, Corcoran DL, Chi J-T (2019) Latent transcriptional variations of individual *Plasmodium falciparum* uncovered by single-cell RNA-seq and fluorescence imaging. *PLoS Genet* 15:e1008506
146. Day JH et al (2020) Injection molded open microfluidic well plate inserts for user-friendly coculture and microscopy. *Lab Chip* 20:107–119
147. Guo S et al (2018) Ultrahigh-throughput droplet microfluidic device for single-cell miRNA detection with isothermal amplification. *Lab Chip* 18:1914–1920
148. Ostromohov N, Huber D, Bercovici M, Kaigala GV (2018) Real-time monitoring of fluorescence in situ hybridization kinetics. *Anal Chem* 90:11470–11477. <https://doi.org/10.1021/acs.analchem.8b02630>
149. Iswardy E, Tsai TC, Cheng IF et al (2017) A bead-based immunofluorescence-assay on a microfluidic dielectrophoresis platform for rapid dengue virus detection. *Biosens Bioelectron* 95:174–180. <https://doi.org/10.1016/j.bios.2017.04.011>
150. Gagliano O, Luni C, Qin W et al (2019) Microfluidic reprogramming to pluripotency of human somatic cells. *Nat Protoc* 14:722–737. <https://doi.org/10.1038/s41596-018-0108-4>
151. Luni C, Giulitti S, Serena E et al (2016) High-efficiency cellular reprogramming with microfluidics. *Nat Methods* 13:446–452. <https://doi.org/10.1038/nmeth.3832>
152. Dupouy DG, Ciftlik AT, Fiche M et al (2016) Continuous quantification of HER2 expression by microfluidic precision immunofluorescence estimates HER2 gene amplification in breast cancer. *Sci Rep* 6:1–10. <https://doi.org/10.1038/srep20277>
153. Hung LY, Chiang NJ, Tsai WC et al (2017) A microfluidic chip for detecting cholangiocarcinoma cells in human bile. *Sci Rep* 7:1–10. <https://doi.org/10.1038/s41598-017-04056-2>
154. Brajkovic S, Pelz B, Procopio M-G et al (2018) Microfluidics-based immunofluorescence for fast staining of ALK in lung adenocarcinoma. *Diagn Pathol* 13:79. <https://doi.org/10.1186/s13000-018-0757-1>

155. Teixeira A, Hernández-Rodríguez J, Wu L et al (2019) Microfluidics-driven fabrication of a low cost and ultrasensitive SERS-based paper biosensor. *Appl Sci* 9:1387. <https://doi.org/10.3390/app9071387>
156. Wu Y, Jiang Y, Zheng X et al (2019b) Facile fabrication of microfluidic surface-enhanced Raman scattering devices via lift-up lithography. *R Soc Open Sci* 5:172034. <https://doi.org/10.1098/rsos.172034>
157. Pu H, Xiao W, Sun D-W (2017) SERS-microfluidic systems: a potential platform for rapid analysis of food contaminants. *Trends Food Sci Technol*. <https://doi.org/10.1016/j.tifs.2017.10.001>
158. Krafft B, Tycova A, Urban RD et al (2021) Microfluidic device for concentration and SERS-based detection of bacteria in drinking water. *Electrophoresis* 42:86–94. <https://doi.org/10.1002/elps.202000048>
159. Willner MR, McMillan KS, Graham D et al (2018) Surface-enhanced raman scattering based microfluidics for single-cell analysis. *Anal Chem* 90:12004–12010. <https://doi.org/10.1021/acs.analchem.8b02636>
160. Cong L, Liang L, Cao F et al (2019) Distinguishing cancer cell lines at a single living cell level via detection of sialic acid by dual-channel plasmonic imaging and by using a SERS-microfluidic droplet platform. *Microchim Acta* 186:367. <https://doi.org/10.1007/s00604-019-3480-z>
161. Walter A, März A, Schumacher W et al (2011) Towards a fast, high specific and reliable discrimination of bacteria on strain level by means of SERS in a microfluidic device. *Lab Chip* 11:1013–1021. <https://doi.org/10.1039/C0LC00536C>
162. Lu X, Samuelson DR, Xu Y et al (2013) Detecting and tracking nosocomial methicillin-resistant staphylococcus aureus using a microfluidic SERS biosensor. *Anal Chem* 85:2320–2327. <https://doi.org/10.1021/ac303279u>
163. Hassoun M, Rüger J, Kirchberger-Tolstik T et al (2017) A droplet-based microfluidic chip as a platform for leukemia cell lysate identification using surface-enhanced Raman scattering. *Anal Bioanal Chem* 2017:1–8. <https://doi.org/10.1007/s00216-017-0609-y>
164. Zheng Z, Wu L, Li L et al (2018) Simultaneous and highly sensitive detection of multiple breast cancer biomarkers in real samples using a SERS microfluidic chip. *Talanta* 188:507–515. <https://doi.org/10.1016/j.talanta.2018.06.013>
165. Kapara A, Findlay Paterson KA, Brunton VG et al (2021) Detection of estrogen receptor alpha and assessment of fulvestrant activity in MCF-7 tumor spheroids using microfluidics and SERS. *Anal Chem* 93:5862–5871. <https://doi.org/10.1021/acs.analchem.1c00188>
166. Farshidfar F, Zheng S, Gingras M-C et al (2017) Integrative genomic analysis of cholangiocarcinoma identifies distinct IDH-mutant molecular profiles. *Cell Rep* 18:2780–2794. <https://doi.org/10.1016/j.celrep.2017.02.033>
167. Raphael BJ, Hruban RH, Aguirre AJ et al (2017) Integrated genomic characterization of pancreatic ductal adenocarcinoma. *Cancer Cell* 32:185–203
168. Wheeler DA, Roberts LR, Network CGAR (2017) Comprehensive and integrative genomic characterization of hepatocellular carcinoma. *Cell* 169:1327
169. Goossens N, Nakagawa S, Sun X, Hoshida Y (2015) Cancer biomarker discovery and validation. *Transl Cancer Res* 4:256–269. <https://doi.org/10.3978/j.issn.2218-676X.2015.06.04>
170. Von Hoff DD, Stephenson JJ, Rosen P et al (2010) Pilot Study using molecular profiling of patients' tumors to find potential targets and select treatments for their refractory cancers. *J Clin Oncol* 28:4877–4883. <https://doi.org/10.1200/JCO.2009.26.5983>
171. Narrandes S, Xu W (2018) Gene expression detection assay for cancer clinical use. *J Cancer* 9: 2249–2265. <https://doi.org/10.7150/jca.24744>
172. Obradovic J, Jurisic V (2012) Evaluation of current methods to detect the mutations of epidermal growth factor receptor in non-small cell lung cancer patients. *Multidiscip Respir Med* 7:52. <https://doi.org/10.1186/2049-6958-7-52>

173. Pantel K, Alix-Panabières C (2019) Liquid biopsy and minimal residual disease—latest advances and implications for cure. *Nat Rev Clin Oncol* 16:409–424. <https://doi.org/10.1038/s41571-019-0187-3>
174. Micalizzi DS, Maheswaran S, Haber DA (2017) A conduit to metastasis: circulating tumor cell biology. *Genes Dev* 31:1827–1840. <https://doi.org/10.1101/gad.305805.117>
175. Abou Daya S, Mahfouz R (2018) Circulating tumor DNA, liquid biopsy, and next generation sequencing: A comprehensive technical and clinical applications review. *Meta Gene* 17:192–201. <https://doi.org/10.1016/j.mgene.2018.06.013>
176. Li H, Jing C, Wu J et al (2019) Circulating tumor DNA detection: a potential tool for colorectal cancer management. *Oncol Lett* 17:1409–1416. <https://doi.org/10.3892/ol.2018.9794>
177. Chaudhuri AA, Binkley MS, Osmundson EC et al (2015) Predicting radiotherapy responses and treatment outcomes through analysis of circulating tumor DNA. *Semin Radiat Oncol* 25:305–312. <https://doi.org/10.1016/j.semradonc.2015.05.001>
178. Liu J, Zhao R, Zhang J, Zhang J (2015) ARMS for EGFR mutation analysis of cytologic and corresponding lung adenocarcinoma histologic specimens. *J Cancer Res Clin Oncol* 141:221–227. <https://doi.org/10.1007/s00432-014-1807-z>
179. Shaozhang Z, Ming Z, Haiyan P et al (2014) Comparison of ARMS and direct sequencing for detection of EGFR mutation and prediction of EGFR-TKI efficacy between surgery and biopsy tumor tissues in NSCLC patients. *Med Oncol* 31:926. <https://doi.org/10.1007/s12032-014-0926-3>
180. Zhang BO, Xu C-W, Shao Y et al (2015) Comparison of droplet digital PCR and conventional quantitative PCR for measuring EGFR gene mutation. *Exp Ther Med* 9:1383–1388. <https://doi.org/10.3892/etm.2015.2221>
181. Postel M, Roosen A, Laurent-Puig P et al (2018) Droplet-based digital PCR and next generation sequencing for monitoring circulating tumor DNA: a cancer diagnostic perspective. *Expert Rev Mol Diagn* 18:7–17. <https://doi.org/10.1080/14737159.2018.1400384>
182. Ishii H, Azuma K, Sakai K et al (2015) Digital PCR analysis of plasma cell-free DNA for non-invasive detection of drug resistance mechanisms in EGFR mutant NSCLC: correlation with paired tumor samples. *Oncotarget* 6(30850–30858):10.18632/oncotarget.5068
183. Chu D, Paoletti C, Gersch C et al (2016) ESR1 mutations in circulating plasma tumor DNA from metastatic breast cancer patients. *Clin Cancer Res* 22:993. <https://doi.org/10.1158/1078-0432.CCR-15-0943>
184. Denis JA, Patroni A, Guillerme E et al (2016) Droplet digital PCR of circulating tumor cells from colorectal cancer patients can predict KRAS mutations before surgery. *Mol Oncol* 10:1221–1231. <https://doi.org/10.1016/j.molonc.2016.05.009>
185. Crowley E, Di Nicolantonio F, Loupakis F, Bardelli A (2013) Liquid biopsy: monitoring cancer-genetics in the blood. *Nat Rev Clin Oncol* 10:472–484. <https://doi.org/10.1038/nrclinonc.2013.110>
186. García-Foncillas J, Alba E, Aranda E et al (2017) Incorporating BEAMing technology as a liquid biopsy into clinical practice for the management of colorectal cancer patients: an expert taskforce review. *Ann Oncol Off J Eur Soc Med Oncol* 28:2943–2949. <https://doi.org/10.1093/annonc/mdx501>
187. Slatko BE, Gardner AF, Ausubel FM (2018) Overview of next-generation sequencing technologies. *Curr Protoc Mol Biol* 122:e59–e59. <https://doi.org/10.1002/cpmb.59>
188. Chiu DT, deMello AJ, Di Carlo D et al (2017) Small but perfectly formed? Successes, challenges, and opportunities for microfluidics in the chemical and biological sciences. *Chem* 2:201–223. <https://doi.org/10.1016/j.chempr.2017.01.009>
189. Fu Y, Zhou H, Jia C et al (2017) A microfluidic chip based on surfactant-doped polydimethylsiloxane (PDMS) in a sandwich configuration for low-cost and robust digital PCR. *Sensors Actuators B Chem* 245:414–422. <https://doi.org/10.1016/j.snb.2017.01.161>
190. Ying L, Wang Q (2013) Microfluidic chip-based technologies: emerging platforms for cancer diagnosis. *BMC Biotechnol* 13:76. <https://doi.org/10.1186/1472-6750-13-76>

191. Situma C, Wang Y, Hupert M et al (2005) Fabrication of DNA microarrays onto poly(methyl methacrylate) with ultraviolet patterning and microfluidics for the detection of low-abundant point mutations. *Anal Biochem* 340:123–135. <https://doi.org/10.1016/j.ab.2005.01.044>
192. Wang Y, Vaidya B, Farquar HD et al (2003) Microarrays assembled in microfluidic chips fabricated from poly(methyl methacrylate) for the detection of low-abundant DNA mutations. *Anal Chem* 75:1130–1140. <https://doi.org/10.1021/ac020683w>
193. Wu L, Garrido-Maestu A, Guerreiro JRL et al (2019a) Amplification-free SERS analysis of DNA mutation in cancer cells with single-base sensitivity. *Nanoscale*. <https://doi.org/10.1039/C9NR00501C>
194. Wu L, Teixeira A, Garrido-Maestu A et al (2020b) Profiling DNA mutation patterns by SERS fingerprinting for supervised cancer classification. *Biosens Bioelectron* 112392. <https://doi.org/10.1016/j.bios.2020.112392>
195. Malone ER, Oliva M, Sabatini PJB et al (2020) Molecular profiling for precision cancer therapies. *Genome Med* 12:8. <https://doi.org/10.1186/s13073-019-0703-1>
196. Budakoti M, Panwar AS, Molpa D et al (2021) Micro-RNA: the darkhorse of cancer. *Cell Signal* 83:109995. <https://doi.org/10.1016/j.cellsig.2021.109995>
197. Kosaka N, Kogure A, Yamamoto T et al (2019) Exploiting the message from cancer: the diagnostic value of extracellular vesicles for clinical applications. *Exp Mol Med* 51:1–9. <https://doi.org/10.1038/s12276-019-0219-1>
198. Kamyabi N, Abbasgholizadeh R, Maitra A et al (2020) Isolation and mutational assessment of pancreatic cancer extracellular vesicles using a microfluidic platform. *Biomed Microdev* 22: 23. <https://doi.org/10.1007/s10544-020-00483-7>
199. Chung Y-D, Liu T-H, Liang Y-L et al (2021) An integrated microfluidic platform for detection of ovarian clear cell carcinoma mRNA biomarker FXYD2. *Lab Chip* 21:2625–2632. <https://doi.org/10.1039/D1LC00177A>
200. Gao Y, Qiang L, Chu Y et al (2020) Microfluidic chip for multiple detection of miRNA biomarkers in breast cancer based on three-segment hybridization. *AIP Adv* 10:45022. <https://doi.org/10.1063/1.5137784>
201. Heather JM, Chain B (2016) The sequence of sequencers: the history of sequencing DNA. *Genomics* 107:1–8. <https://doi.org/10.1016/j.ygeno.2015.11.003>
202. Hudson TJ, Anderson W, Aretz A et al (2010) International network of cancer genome projects. *Nature* 464:993–998. <https://doi.org/10.1038/nature08987>
203. Bailey MH, Meyerson WU, Dursi LJ et al (2020) Retrospective evaluation of whole exome and genome mutation calls in 746 cancer samples. *Nat Commun* 11:4748. <https://doi.org/10.1038/s41467-020-18151-y>
204. Lim SB, Di Lee W, Vasudevan J et al (2019) Liquid biopsy: one cell at a time. *NPJ Precis Oncol* 3:23. <https://doi.org/10.1038/s41698-019-0095-0>
205. Quan P-L, Sauzade M, Brouzes E (2018) dPCR: a technology review. *Sensors (Basel)* 18: 1271. <https://doi.org/10.3390/s18041271>
206. Aravanis AM, Lee M, Klausner RD (2017) Next-generation sequencing of circulating tumor DNA for early cancer detection. *Cell* 168:571–574. <https://doi.org/10.1016/j.cell.2017.01.030>
207. Khoubnasabjafari M, Mogaddam MRA, Rahimpour E et al (2021) Breathomics: review of sample collection and analysis, data modeling and clinical applications. *Crit Rev Anal Chem* 1–27. <https://doi.org/10.1080/10408347.2021.1889961>
208. Pihl J, Sinclair J, Karlsson M, Orwar O (2005) Microfluidics for cell-based assays. *Mater Today* 8:46–51. [https://doi.org/10.1016/S1369-7021\(05\)71224-4](https://doi.org/10.1016/S1369-7021(05)71224-4)
209. Fares J, Fares MY, Khachfe HH et al (2020) Molecular principles of metastasis: a hallmark of cancer revisited. *Signal Transduct Target Ther* 5:28. <https://doi.org/10.1038/s41392-020-0134-x>
210. Dominiak A, Chelstowska B, Olejarz W, Nowicka G (2020) Communication in the cancer microenvironment as a target for therapeutic interventions. *Cancers (Basel)* 12:1232. <https://doi.org/10.3390/cancers12051232>

211. Ma Y-HV, Middleton K, You L, Sun Y (2018) A review of microfluidic approaches for investigating cancer extravasation during metastasis. *Microsyst Nanoeng* 4:17104. <https://doi.org/10.1038/micronano.2017.104>
212. Kim SH, Hwang SM, Lee JM et al (2013) Epithelial-to-mesenchymal transition of human lung alveolar epithelial cells in a microfluidic gradient device. *Electrophoresis* 34:441–447. <https://doi.org/10.1002/elps.201200386>
213. Yu T, Guo Z, Fan H et al (2016) Cancer-associated fibroblasts promote non-small cell lung cancer cell invasion by upregulation of glucose-regulated protein 78 (GRP78) expression in an integrated bionic microfluidic device. *Oncotarget* 7. <https://doi.org/10.18632/oncotarget.8232>
214. Riahi R, Yang YL, Kim H et al (2014) A microfluidic model for organ-specific extravasation of circulating tumor cells. *Biomicrofluidics* 8:24103. <https://doi.org/10.1063/1.4868301>
215. Zou H, Yue W, Yu W-K et al (2015) Microfluidic platform for studying chemotaxis of adhesive cells revealed a gradient-dependent migration and acceleration of cancer stem cells. *Anal Chem* 87:7098–7108. <https://doi.org/10.1021/acs.analchem.5b00873>
216. Coluccio ML, Perozziello G, Malara N et al (2019) Microfluidic platforms for cell cultures and investigations. *Microelectron Eng* 208:14–28. <https://doi.org/10.1016/j.mee.2019.01.004>
217. Luo T, Fan L, Zhu R, Sun D (2019) Microfluidic single-cell manipulation and analysis: methods and applications. *Micromachines* 10:104. <https://doi.org/10.3390/mi10020104>
218. Chen H, Sun J, Wolvetang E, Cooper-White J (2015) High-throughput, deterministic single cell trapping and long-term clonal cell culture in microfluidic devices. *Lab Chip* 15:1072–1083. <https://doi.org/10.1039/C4LC01176G>
219. Bithi SS, Vanapalli SA (2017) Microfluidic cell isolation technology for drug testing of single tumor cells and their clusters. *Sci Rep* 7:41707. <https://doi.org/10.1038/srep41707>
220. Smit DJ, Pantel K, Jücker M (2021) Circulating tumor cells as a promising target for individualized drug susceptibility tests in cancer therapy. *Biochem Pharmacol* 188:114589. <https://doi.org/10.1016/j.bcp.2021.114589>
221. Kwapisz D (2017) The first liquid biopsy test approved. Is it a new era of mutation testing for non-small cell lung cancer? *Ann Transl Med* 5(46):10.21037/atm.2017.01.32
222. Baldacchino S (2021) Current advances in clinical application of liquid biopsy. In: *Histopathology and liquid biopsy*. IntechOpen, London
223. Takeda M, Takahama T, Sakai K et al (2021) Clinical application of the FoundationOne CDx assay to therapeutic decision-making for patients with advanced solid tumors. *Oncologist* 26:e588–e596. <https://doi.org/10.1002/onco.13639>
224. Woodhouse R, Li M, Hughes J et al (2020) Clinical and analytical validation of FoundationOne Liquid CDx, a novel 324-Gene cfDNA-based comprehensive genomic profiling assay for cancers of solid tumor origin. *PLoS One* 15:e0237802. <https://doi.org/10.1371/journal.pone.0237802>
225. Leighl NB, Page RD, Raymond VM et al (2019) Clinical utility of comprehensive cell-free DNA analysis to identify genomic biomarkers in patients with newly diagnosed metastatic non-small cell lung cancer. *Clin Cancer Res* 25:4691. <https://doi.org/10.1158/1078-0432.CCR-19-0624>
226. Guardant Health Inc (2021) Summary of safety and effectiveness data (SSED) - next generation sequencing oncology panel, somatic or germline variant detection system. https://www.accessdata.fda.gov/cdrh_docs/pdf20/P200010S002B.pdf. Accessed 20 Jan 2011
227. Foundation Medicine Inc (2020) FoundationOne®CDx Technical Information. https://www.accessdata.fda.gov/cdrh_docs/pdf17/P170019S013C.pdf. Accessed 20 Jan 2011
228. Sarah McManus Summary Information - CellSearch Circulating Tumor Cell Kit. https://www.accessdata.fda.gov/cdrh_docs/pdf10/k103502.pdf
229. Wiklander OPB, Brennan MÁ, Jan L et al (2019) Advances in therapeutic applications of extracellular vesicles. *Sci Transl Med* 11:eaav8521. <https://doi.org/10.1126/scitranslmed.aav8521>

230. Trino S, Lamorte D, Caivano A et al (2021) Clinical relevance of extracellular vesicles in hematological neoplasms: from liquid biopsy to cell biopsy. *Leukemia* 35:661–678. <https://doi.org/10.1038/s41375-020-01104-1>
231. Yekula A, Muralidharan K, Kang KM et al (2020) From laboratory to clinic: translation of extracellular vesicle based cancer biomarkers. *Methods* 177:58–66. <https://doi.org/10.1016/j.ymeth.2020.02.003>
232. Zhou B, Xu K, Zheng X et al (2020) Application of exosomes as liquid biopsy in clinical diagnosis. *Signal Transduct Target Ther* 5:144. <https://doi.org/10.1038/s41392-020-00258-9>
233. Centre Hospitalier Universitaire Dijon (2020) Contents of circulating extracellular vesicles: biomarkers in colorectal cancer patients (ExoColon). <https://clinicaltrials.gov/ct2/show/NCT04523389#contacts>
234. Mauriac H, Casquillas GV. Organ-on-chip companies developping innovative technologies. <https://www.elflow.com/microfluidic-reviews/organs-on-chip-3d-cell-culture/organ-chip-companies/>
235. Tadmety A, Syed A, Nie Y et al (2017) Liquid biopsy on chip: a paradigm shift towards the understanding of cancer metastasis. *Integr Biol (Camb)* 9(1):22
236. Mattei F, Andreone S, Mencattini A et al (2021) Oncoimmunology meets organs-on-chip. *Front Mol Biosci* 8:192
237. Wan L, Neumann CA, LeDuc PR (2020) Tumor-on-a-chip for integrating a 3D tumor microenvironment: chemical and mechanical factors. *Lab Chip* 20:873–888. <https://doi.org/10.1039/C9LC00550A>
238. Liu X, Fang J, Huang S et al (2021) Tumor-on-a-chip: from bioinspired design to biomedical application. *Microsyst Nanoeng* 7:50. <https://doi.org/10.1038/s41378-021-00277-8>



Correction to: Sensors and Biosensors in Organs-on-a-Chip Platforms

Gerardo A. Lopez-Muñoz, Sheeza Mughal, and Javier Ramón-Azcón

Correction to:
Chapter 3 in: D. Caballero et al. (eds.),
Microfluidics and Biosensors in Cancer Research,
***Advances in Experimental Medicine and Biology* 1379,**
https://doi.org/10.1007/978-3-031-04039-9_3

This book was inadvertently published with an incorrect spelling of the author's name in Chapter 3 as Sheeza Mugal whereas it should be Sheeza Mughal.

The updated original version for this chapter can be found at
https://doi.org/10.1007/978-3-031-04039-9_3

© The Author(s), under exclusive license to Springer Nature Switzerland AG 2022
D. Caballero et al. (eds.), *Microfluidics and Biosensors in Cancer Research,*
Advances in Experimental Medicine and Biology 1379,
https://doi.org/10.1007/978-3-031-04039-9_23

C1